A11100 985925
NAT'L INST OF STANDARDS & TECH R.I.C.
A1110098592S
International Specia/Neutron standa
QC100 .U57 V493;1977 C.1 NBS-P

NBS SPECIAL PUBLICATION 493

U.S. DEPARTMENT OF COMMERCE / National Bureau of Standards

NEUTRON STANDARDS AND APPLICATIONS

PROCEEDINGS OF A SYMPOSIUM

AUTHENTICATED
U.S. GOVERNMENT
INFORMATION
GPO

DATE DUE

4-27-90 IUL	5768462		

Demco, Inc. 38-293

Neutron Standards and Applications

1977
780308
QC100
.U57
NO.493
1977
C.2
Special publication, no.493

Proceedings of the
International Specialists Symposium on
Neutron Standards and Applications
Held at the National Bureau of Standards
Gaithersburg, MD, March 28-31, 1977

Edited by

C.D. Bowman and A.D. Carlson

Center for Radiation Research
Institute for Basic Standards
National Bureau of Standards
Washington, D.C. 20234

H.O. Liskien

Central Bureau of Nuclear Measurements
Commission of European Communities
B-2440 Geel
Steenweg Naar Retie
BELGIUM

and

L. Stewart

Los Alamos Scientific Laboratory
Los Alamos, NM 87545

Sponsored by

National Bureau of Standards
U.S. Department of Commerce

Central Bureau of Nuclear Measurements
Commission of European Communities

U.S. Energy Research and Development Administration

Electric Power Research Institute (U.S.A.)

American Nuclear Society

American Physical Society

Nuclear Energy Agency (Europe)

International Union of Pure and Applied Physics

with the Cooperation of the
International Atomic Energy Agency

U.S. DEPARTMENT OF COMMERCE, Juanita M. Kreps, Secretary

Dr. Sidney Harman, Under Secretary

Jordan J. Baruch, Assistant Secretary for Science and Technology

NATIONAL BUREAU OF STANDARDS, Ernest Ambler, Acting Director

Issued October 1977

Library of Congress Cataloging in Publication Data

International Specialists Symposium on Neutron Standards and Applications, National Bureau of Standards, 1977. Neutron standards and applications.

(NBS special publication ; 493)

Supt. of Docs. no.: C13.10:493

1. Neutrons--Standards--Congresses. I. Bowman, Charles D., 1935- II. United States. National Bureau of Standards. III. Title. IV. Series: United States. National Bureau of Standards. Special publication ; 493

QC100.U57 no. 493 [QC793.5.N4622] 602'.1s 77-14317
[539.7'213'021]

National Bureau of Standards Special Publication 493

Nat. Bur. Stand. (U.S.), Spec. Publ. 493, 379 pages (Oct. 1977)

CODEN: XNBSAV

For sale by the Superintendent of Documents, U.S. Government Printing Office
Washington, D.C. 20402 - Price $8.50

Stock No. 003-003-01847-3

PREFACE

These are the proceedings of an International Specialists' Symposium on Neutron Standards and Applications held at the National Bureau of Standards, Gaithersburg, Md. from March 28 - 31, 1977. The field of neutron standards now spreads across a rather broad range of subjects including absolute neutron source strength, differential and integral standards for reaction cross sections, and standards for neutron dosimetry for nuclear reactor core and containment, personnel protection, cancer therapy, and fission reactor design. The purpose of the Symposium was to bring together workers from this spectrum of fields for the purpose of reviewing the present status, tying the different branches more closely together, and planning for a more coordinated international program in the future.

In order to achieve the broad and even coverage of the field, the papers were presented by invitation only although the conference was open to anyone. In spite of this and its billing as a symposium for specialists, 142 registrants were recorded with 34 participants from 13 foreign countries. The symposium closed with a summary session which was recorded and is reproduced in full in these proceedings for those interested in comments and review of the full conference.

The papers are printed in the proceedings as they were received from the authors and in the order in which they were presented in the sessions. For convenience we have preserved the conference notation for the sessions. To speed the publication of the proceedings, all papers were submitted by the authors in camera-ready form. We are greatly indebted to the authors and all those who assisted in the preparation of the manuscripts. Their efforts have made it possible to get the proceedings in print much more rapidly than would otherwise be the case. To make the proceedings more useful we include, as well as a table of contents, an author index, a list of participants, and a CINDA index of subject matter. We would like to thank Dr. Charles Dunford of Brookhaven National Laboratory for the preparation of the CINDA index.

When commercial equipment, instruments and materials are mentioned or identified in this proceedings it is intended only to adequately specify experimental procedure. In no case does such identification imply recommendation or endorsement by the National Bureau of Standards, nor does it imply that the material or equipment identified is necessarily the best available for the purpose.

We wish to express our appreciation for the financial support from the U. S. Energy Research and Development Administration, The Central Bureau of Nuclear Measurements and the National Bureau of Standards which made the publication possible.

The Editors gratefully acknowledge the assistance of the National Bureau of Standards Office of Technical Publications in the preparation of these proceedings and of Mrs. Sara Torrence and Mrs. Lynn Boggs of the Office of Information Activities for help in the arrangements for the Symposium. We are appreciative also of the advice and suggestions of Dr. Bryan Patrick, Harwell and of the excellent secretarial assistance of Mrs. Julia Marks, Mrs. Gracie Wood, and Mrs. Sarah Stewart.

C. D. Bowman and A. D. Carlson
NBS

H. O. Liskien
CBNM

L. Stewart
LASL

PROGRAM COMMITTEE

M. R. Bhat, BNL

J. B. Czirr, LLL

F. Gabbard, Univ. of Kentucky

W. W. Havens, Jr., Columbia University

B. R. Leonard, Jr., BNW

H. Liskien, CBNM

R. W. Peelle, ORNL

A. B. Smith, ANL

P. G. Young, LASL

C. D. Bowman, NBS, Chairman

ABSTRACT

These proceedings contain forty-seven papers, which were presented at the International Specialists Symposium on Neutron Standards and Applications held at the National Bureau of Standards on March 28-31, 1977. The topics addressed at the Symposium include light-element cross section standards, capture and fission cross section standards, integral neutron standards, flux measuring techniques, and medical and personnel dosimetry.

Key words: Cross section standards; dosimetry; fission; flux; measuring techniques; neutrons; standards.

TABLE OF CONTENTS

*The session on ^{6}Li was planned for the program committee by the Nuclear Energy Agency Nuclear Data Committee as a consequence of its strong interest in this standard and its associated uncertainties.

INTRODUCTORY REMARKS

Session A:

Dr. Ernest Ambler, Acting Director
National Bureau of Standards

It is indeed a pleasure for me to welcome you to the National Bureau of Standards for this Symposium. I understand that 15 countries are represented and that about one-third of you are from outside of the United States. I strongly believe that almost every aspect of basic standards requires close international cooperation and collaboration and that such interactions will be established and strengthened at this meeting.

I might add that here at NBS we place emphasis on the international aspect of all our work. I am proud of the strong line of communication that we maintain around the world through conference sponsorship and participation, laboratory visits, corroborative activities and committee work in international organizations in setting standards. Dr. Charles Bowman's fine service as chairman of this Symposium is just one example - an example that I am very proud of - of our activity in this area.

The international flavor and significance of improved neutron standards are clearly reflected in the endorsements which this Symposium has received. I note the endorsements of four international organizations - The Central Bureau of Nuclear Measurements, The Nuclear Energy Agency (Europe), The International Union of Pure of Applied Physics, and the International Atomic Energy Agency. Within the United States, the Symposium has been endorsed by four divisions of the Energy Research and Development Administration, the industry-operated Electric Power Research Institute, the American Physical Society, the American Nuclear Society, and of course by the National Bureau of Standards.

These endorsements reflect the importance and diversity of the field of neutron standards. For energy production by fission, a knowledge of neutron cross sections to high accuracy is central. In fusion-energy sources, at least in the near term, nearly all of the energy is carried by neutrons. Fuel for both fission and fusion systems is bred using neutrons.

Many medical specialists believe that high-energy neutrons provide an effective modality for cancer therapy. Neutrons are now commonly used in activation analysis and radiography. The need for safe working conditions, in all of these fields, requires accurate neutron personnel dosimetry.

The National Bureau of Standards has long been aware of the need for standards in the field of neutron based technology. Our program goes back more than 20 years to the NBS initiative in developing the radium-beryllium neutron source standard widely known as NBS-I. Increased efforts in this field during the late fifties and early sixties led to the first symposium in this country on the subject of neutron standards. Sponsored by the European-American Nuclear Data Committee, the meeting took place in 1970 at the Argonne National Laboratory. This was followed by the IAEA-sponsored panel which met in Vienna, Austria in 1972 and further delineated the challenges in this field.

Here at NBS we were increasingly recognizing the importance of this field. While Director of the Institute of Basic Standards of NBS, I strongly encouraged a growing program in neutron standards within our Center for Radiation Research.

Our work has broadened into a program in both differential and integral neutron standards carried out using such major facilities as our 3-MeV positive ion Van de Graaff accelerator, our 10-MW reactor, our 100-MeV electron linac, and several other specialized facilities.

Our program now spans nine decades of neutron energy from subthermal to 20 MeV. We can count eight calibrated neutron fields which are available as flux standards for outside use. We have on-going, active programs in support of the full spectrum of neutron applications including fission nuclear energy programs, fusion energy, medical and personnel neutron dosimetry. I hope that you will be able to get an opportunity to visit our experiments and facilities in spite of the busy schedule of the Symposium.

I am justifiably proud of our commitment at NBS to neutron standards, but I strongly believe that our program should be a partnership with other neutron standards activities both within and outside the U.S. Neutron work in general is perhaps the most technically difficult area of work in ionizing radiation. Progress in neutron standards often comes slowly and after much intercomparison and corroboration.

Therefore, I believe that we all recognize a unique opportunity here to advance the field. Let us hope that some problems will be laid to rest, that progress in international coordination and collaboration can be made in others, and that the new problems in neutron standard will be recognized. You now face a very full four-day schedule. Let me again welcome you here and wish you much success.

Dr. H. Liskien, Chairman
INDC Subcommittee on
Standard Reference Data

There are still many scientific/technical fields where essential effort has to be devoted to the change of units and the harmonization of standards. This is due to regionally independent approaches in the past with results which are insufficient for the international interchanges of today. In contrast to this, a modern field like neutron technology - and especially the data aspect of it - has been an international enterprise nearly from the beginning. Today we have WRENDA, an international request list for neutron data, we have CINDA, an international index to literature containing information on microscopic neutron data, and we have under the EXFOR agreement an international network for the compilation, exchange and retrieval of experimental neutron data.

It is therefore not at all astonishing that also the task to establish a set of neutron data standards has seen an international approach. In a month's time it will be ten years since the IAEA convened a panel on "Nuclear Standards for Neutron Measurements" in Brussels. In 1970, the European-American Nuclear Data Committee organized a symposium on "Neutron Standards and Flux Normalization", while the 2nd IAEA panel on "Neutron Standard Reference Data" was held in Vienna four and a half years ago. In this sense we are here celebrating the opening of the fourth international meeting on this subject.

In such a meeting, we try to compare critically our established set of standards with the real needs, to assess the progress in methods and accuracy and, to identify weaknesses to be eliminated in the future. The progress itself is of course achieved between the meetings in our home laboratories by improving detectors, performing accurate measurements and evaluating best values. But also this work should see more international cooperation. In this respect two good examples are taken from the recent past: 1)the first round of comparing results on fluence determinations between various laboratories organized by the Bureau International des Poids et Mesures and 2)the work of an INDC ad-hoc group to establish a set of neutron energy standards. I think it would be most fruitful if this symposium could initiate more such common attacks on crucial points in the field of "Neutron Standards and Applications".

SURVEY OF RECENT EXPERIMENTS FOR THE ^{7}Li-SYSTEM

H. -H. Knitter
Central Bureau for Nuclear Measurements
B-2440 Geel, Belgium

Recent experiments on reactions relevant to the ^{7}Li-system are described. It concerns the reactions ^{6}Li(n,t)^{4}He, ^{6}Li(n,n)^{6}Li, ^{4}He(t,n)^{6}Li and ^{4}He(t,t)^{4}He, for which differential cross sections $\sigma_i(E,\Theta)$, angle integrated cross sections $\sigma_i(E)$ and neutron total cross sections $\sigma_T(E)$ were measured. Also polarization experiments yielding the analyzing power $A_i(E,\Theta)$ are described.

(measurements review; polarization; ^{3}H(α,^{6}Li)n, ^{4}He(t,t)^{4}He; ^{6}Li neutron cross sections; ^{7}Li system)

Introduction

The ^{6}Li(n,t)^{4}He reaction cross section is used in many situations as a standard and it is also of importance in tritium breeding calculations for thermo-nuclear fusion reactors.

Since from the theoretical point of view the reaction data from different entrance and/or exit channels of the same nuclear system are interconnected with each other, it seems reasonable to use the experimental information contained in all the experiments made on the ^{7}Li-system for a quantitative description of the ^{6}Li(n,t)^{4}He standard cross section. The most pertinent reactions of the ^{7}Li-system which are of interest for the ^{6}Li(n,t)^{4}He standard cross section are displayed in table 1. They are put together in two groups of reactions. The upper part of the table gives the ^{6}Li(n,t)^{4}He reaction itself and its inverse reaction ^{4}He(t,n)^{6}Li as well as the scattering processes to the respective entrance channels. The lower part of the table shows reactions of less importance. Besides the capture process, which has only a very small cross section[1], they are energetically possible only above that excitation energy region of the ^{7}Li-nucleus which is of direct interest for the application of the ^{6}Li(n,t)^{4}He reaction as a standard. However in a complex analysis the second group of reactions can provide useful information too, especially on the characterization of the ^{7}Li-level scheme, at high excitation energies.

Table 1 : Most pertinent reactions leading to the ^{7}Li-system

Reaction	Q-Value (MeV)	Reaction
^{6}Li(n,t)^{4}He	+ 4.787	^{4}He(t,n)^{6}Li
^{6}Li(n,n)^{6}Li	0.000	^{4}He(t,t)^{4}He
^{6}Li(n,γ)^{7}Li	+ 7.252	^{7}Li(γ,n)^{6}Li
^{6}Li(n,n'd)^{4}He	- 1.471	
^{6}Li(n,n')^{6}Li*	- 2.184	
^{6}Li(n,p)^{6}He	- 2.727	
^{6}Li(n,d)^{5}He	- 2.36	

Due to short coming in time, only recent experiments performed on the reactions displayed in the upper part of table 1 will be discussed. Since contributions to this symposium will be given which deal with the experimental data base of the ^{7}Li-system and also with their theoretical interpretation only experimental methods and techniques are presented.

Measurements of the ^{6}Li(n,t)^{4}He cross section

There are several recent measurements of the integrated ^{6}Li(n,t)^{4}He reaction cross section. The two experiments performed by Lamaze et al.[2] and by Gayther[3] cover the neutron energy range from some keV to several hundreds of keV. The measurements of Bartle[4] and Bartle et al.[5] cover the neutron energy range from 2 to 10 MeV and 10 to 14 MeV respectively.

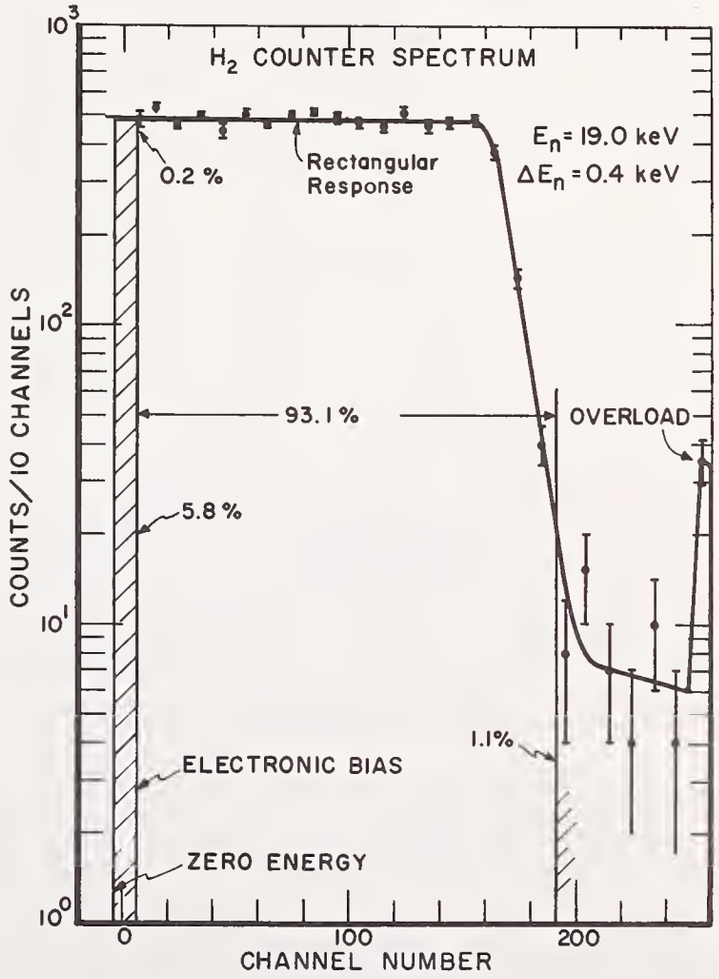

Fig. 1 : Hydrogen proportional counter pulse height spectrum for 19 keV neutrons[6].

The experiment of Lamaze et al.[2] uses the NBS-linac neutron time-of-flight facility. In the neutron energy range from 3 to 600 keV the $^6Li(n,t)^4He$ events were detected in a 0.5 mm thick ^6Li loaded glass scintillator of type NE 912 coupled to a photomultiplier tube. The shape of the cross section was measured relative to the energy dependence of the n-p scattering cross section. The recoil protons were detected with a hydrogen-filled proportional counter of 5.08 cm diameter and 60.96 cm length positioned at the end of a 200 m beam line. A collimated beam of 2.5 cm diameter was incident on the front face of the proportional counter. The output signals were sorted simultaneously according to both, time-of-flight and pulse height. A pulse height spectrum obtained with this proportional counter is shown in fig. 1[6]. The normalization of the relative cross section curve was done in the keV-range with respect to the $^6Li(n,t)^4He$ cross section itself, in a region where it is known pretty well. This cross section was obtained with an accuracy of better than $\pm$ 3 % in the region of the resonance.

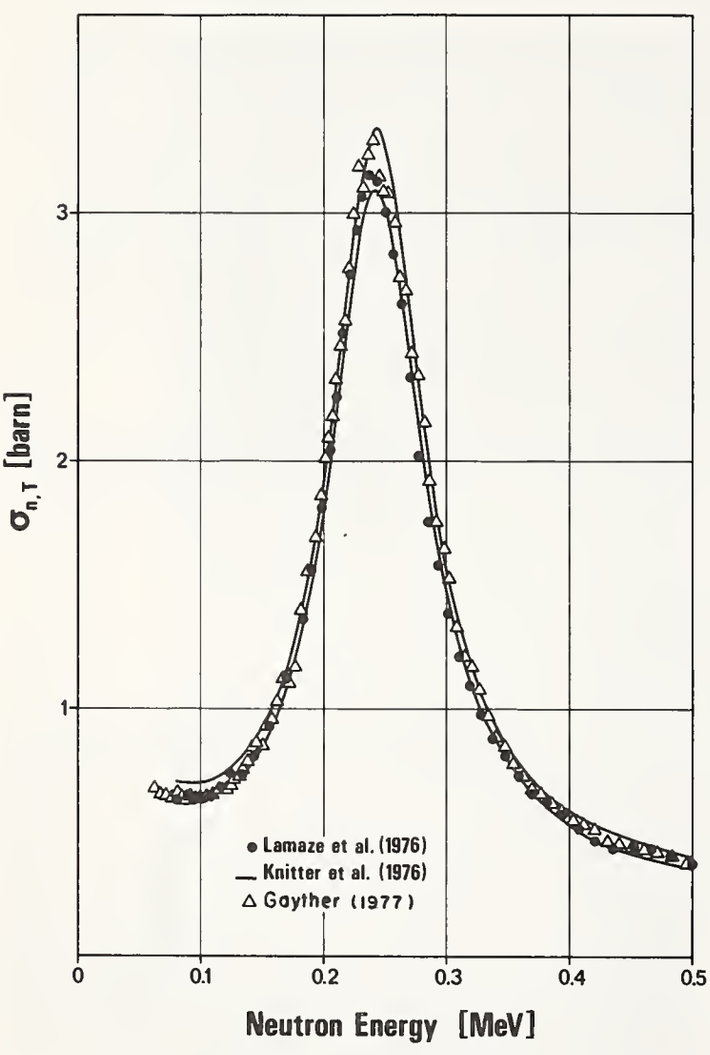

Fig. 2 : $^6Li(n,t)^4He$ cross section is plotted versus incident neutron energy. •, - and △ are results of Lamaze et al.[2], Knitter et al.[18] and Gaythor[3] respectively.

Another recent and similar measurement of the integrated $^6Li(n,t)^4He$ cross section was made by Gaythor[3] in almost the same neutron energy range from some keV to 800 keV, using the Harwell-Linac. The detector and sample was a 1 mm thick ^6Li glass scintillator. The shape of the $^6Li(n,t)^4He$ cross section was measured relative to the $^{235}U(n,f)$ cross section using the numerical values as evaluated by Sowerby[7]. Then, as in the case of Lamaze et al.[2] the relative cross sections were normalized in the 2-10 keV range to the $^6Li(n,t)^4He$ cross section itself. An error of $\pm$ 3 % was assigned to the evaluated $^{235}U(n,f)$ cross section. Across the resonance the two measurements are compared with each other in fig. 2.

The experimental set-up of an absolute measurement, based on the associated particle method as used by Bartle[4], is shown in fig. 3 and is discussed in detail in ref. 8. The deuteron beam, produced by the EN tandem accelerator of the University of Wisconsin, is well collimated for reaction kinematical reasons. In the energy range from 2 to 10 MeV the neutrons are produced by the $^2D(d,n)^3He$ reaction. The neutron producing targets are made of deuterated polyethylene foils, 0.5 μm thick. Besides ^3He-particles also Coulomb scattered deuterons and α-particles from the $^{12}C(d,\alpha)^{10}B$ reaction are incident on the ^3He associated particle detector. This is just thick enough to stop the ^3He-ions and it is followed by a veto detector. Since the scattered deuterons have a longer range than the ^3He particles, they are stopped in the veto detector. An anti-coincidence circuit prevents the deuteron signals from being present in the ^3He-spectrum. The collimation of the ^3He particles together with the reaction kinematics defines the associated neutron cone and determines also the energy of the neutrons. In the present experiment the energy spread of the neutron beam varied with neutron energy from 80 keV at 2 MeV to 500 keV at 10 MeV.

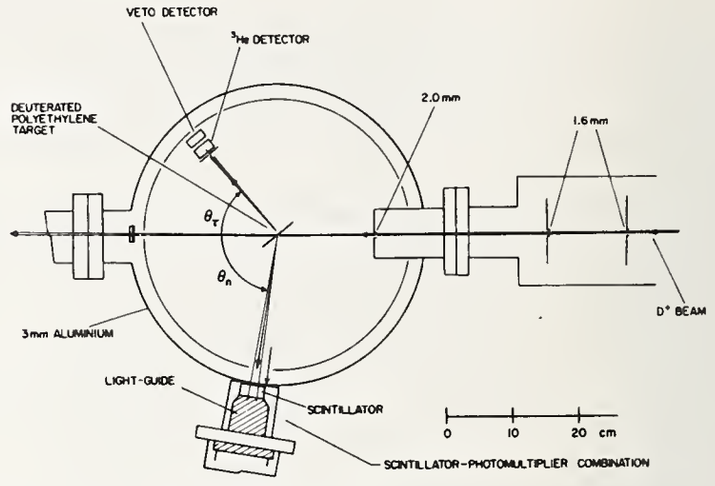

Fig. 3 : Experimental set-up for the associated particle method of Bartle et al.[4].

As a ^6Li target and detector served a ^6Li I (Eu) scintillator crystal of 2.5 cm in diameter and 1.3 cm thick viewed via a light guide by a photomultiplier. This crystal is positioned such that it encompasses the associated neutron beam. The cross section determination is possible with a typical uncertainty of $\pm$ 3 %. The results are shown in fig. 4[4]. The ^6Li I (Eu) crystal has different responses for α-particles and tritons. In the case of fast neutrons this property permits to obtain information about the angular distribution of the $^6Li(n,t)^4He$ reaction, since the centre-of-mass motion causes the emitted tritons and α-particles to have

a range of energies in the laboratory system. The energy of each product particle is a known function of the emission angle of e. g. the triton. Since each product particle gives different response, also the total response of the two particles is an unambigious func-

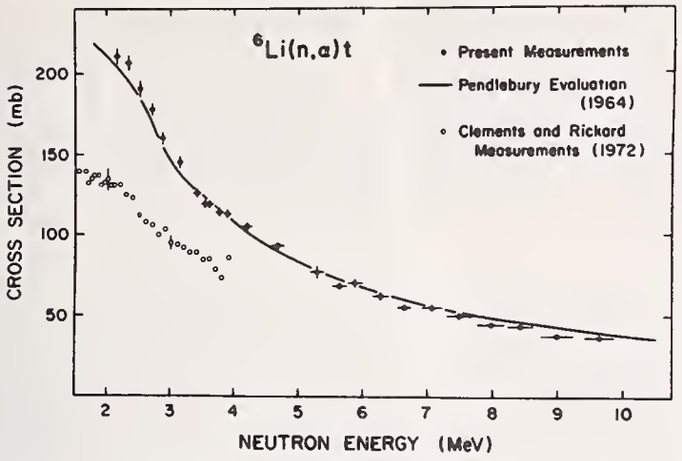

Fig. 4 : ^{6}Li(n,t)^{4}He cross section versus neutron energy. •, - and o are results of Bartle et al.[4], Pendlebury[9] and Clements and Rickard[10].

tion of the angle. Fig. 5 shows some of the pulse height spectra obtained by Bartle[4]. Both response functions are needed to unfold the spectra to obtain angular distributions. They were obtained from the total widths of the distributions. Although in general the measurements are done with polarized neutrons one obtains angular distributions which are the same as for an unpolarized neutron beam, since the experiment makes an inherent integration over the whole azimuthal angle.

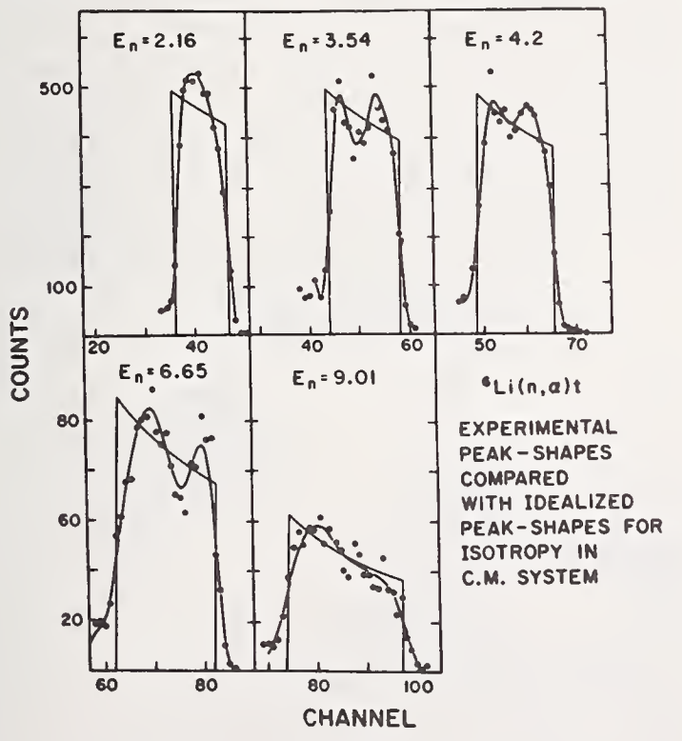

Fig. 5 : Pulse height spectra of triton plus α-particles as obtained by Bartle et al. [4].

A new and similar system was recently set up by Bartle et al. [5] at the cyclograaff of the Australian National University in Canberra. Due to the higher deuteron energy available, an associated neutron energy range from 2 to 20 MeV can be covered. The measurement of the ^{6}Li(n,t)^{4}He cross section was reported up to 14 MeV incident neutron energy [5].

Rather extensive angular distribution measurements for the ^{6}Li(n,t)^{4}He reaction below 2 MeV were done already some years ago by Overley et al.[11]. Besides the above mentioned measurements of Bartle there are angular distribution measurements by Rosario-Garcia et al. [12] at five incident neutron energies between 4. 71 and 7. 25 MeV. They produced neutrons by the D(d,n)^{4}He reaction, utilizing the deuteron beam from the dynamitron of the State University of New York in Albany. The charged particles were detected with a counter telescope consisting of three proportional counters and one silicon detector. The sum signal of the proportional counters served as ΔE signal whereas the silicon detector was the E detector. Particle identification was accomplished using an Ortec 423 particle identifier module. This particle identifier uses the method of Goulding et al. [13] in which E and ΔE signals are used to produce an empirical identification function[14] which has a nearly unique value for each particle type regardless of energy. Absolute differential cross sections were obtained by comparison with neutron proton elastic scattering from a 9. 7 mg/cm^2 thick polyethylene target placed inside the telescope instead of the ^{6}Li target. However, the angular distributions measured by Bartle[4] and by Rosario-Garcia[12] show evidently different shapes.

The anisotropy of angular distributions of the ^{6}Li(n,t)^{4}He reaction at 25 keV neutron energy was measured by Schroeder et al. [15] using an iron-filtered beam and a solid state detector device. S. Raman et al. [16] measured the α to triton ratio at 180° from 0. 5 eV to 25 keV using a diffused junction silicon detector. This ratio deviates from unity by 0. 005 $E^{0.54}$ where E is the neutron energy in eV. These measurements will be treated in a separate contribution to this symposium.

Neutron total cross section measurements of ^{6}Li

Recent neutron total cross section measurements were performed by Harvey et al. [17], Knitter et al. [18] and are being made by Smith[19].

The transmission measurement of Harvey was done in the energy range from 10 eV to 10 MeV using the ORELA as a neutron source and employing time-of-flight spectrometry for the energy determination. At several discrete energies the total cross section was measured in a separate experiment employing iron filtered beam technique. The results obtained with the two techniques agreed. The total cross section for the sample material (0. 9875 (^{6}Li) + 0. 0135 (^{7}Li)) is given and reaches a maximum value of (10. 97 ± 0. 10)b at an energy of 246 keV. A correction for the ^{7}Li content is not made, but can reach in certain energy ranges values near to 1 %.

The total cross section measurement of Knitter et al. [18] was made at the Van de Graaff accelerator of the CBNM in the energy range from 0. 08 to 3. 0 MeV using monoenergetic neutrons. The neutrons were detected with a time-of-flight spectrometer. The cross sections were corrected for the ^{7}Li content in the samples and for the energy spread of the incident neutron beam. A peak value of (11. 27 ± 0. 12)b was obtained at

an incident neutron energy of (247 ± 3)keV.

The preliminary total cross section data of Smith et al.[19] were measured using a 200 keV broad band of pulsed neutrons centered around the energy of 250 keV produced by the Argonne National Laboratory dynamitron accelerator. An interesting energy calibration method was applied. At distances of 6.5, 7.0 and 7.5 meters, between neutron producing target and time-of-flight detector the γ-rays associated with the subsequent (~ 1000 nsec later) neutron burst fall just below, about at, and just above the resonances at 250 keV. These associated γ-ray peaks provide sharp energy calibration markers. The according neutron energies depend essentially only from the frequency of the crystal oscillator of the accelerator. The shape of the cross section curve, however, was measured at a shorter distance of about 4 m distance, because here the transmission spectra are not disturbed by the peak of the γ-flash. The energy scale transfer to the shorter distance was made by the five major iron resonances in the range 170 to 270 keV. The energetic positions were measured also with the above mentioned vernier method. The data are preliminary and, therefore, they are not displayed here.

Neutron scattering experiments

Recent neutron scattering angular distribution measurements were made by Knitter et al.[18] in the energy range from 0.2 to 3.0 MeV, by Lane et al.[20] from 4.0 to 7.5 MeV, and by Bilpuch et al.[21] from 7.5 to 14 MeV. The gap between 3.0 and 4.0 MeV is being closed by Smith[19] with a good overlap at the low energy side. All measurements are done employing conventional nanosecond time-of-flight technique using pulsed beams from electrostatic accelerators. The measurements of Knitter et al. and Bilpuch et al. are made relative to the n-p scattering cross section, the ones of Smith et al. are relative to the carbon scattering cross section and the ones of Lane et al. are relative to the zero degree differential cross section of the $T(p,n)^3He$ reaction. Fig. 6 shows the results of Lane et al.[20] in terms of Legendre polynomial expansion coefficients and some representative angular distributions.

Fig. 7 was taken from ref. 18 and shows experimental values of the total cross section and the integrated elastic cross section. The two upper full lines are obtained from a simultaneous fit to the experimental total cross sections and integrated elastic cross sections by a single level Breit-Wigner formula. The two lowest full lines give the limits for the $^6Li(n,t)^4He$ cross section resulting from the fit. Fig. 2 shows the data of the most recent $^6Li(n,t)^4He$ cross section of Lamaze et al.[2] and of Gayther [3]. The two full lines have the same meaning as in fig. 7.

The reaction $^3H(\alpha, ^6Li)n$

It is evident that the inverse reaction $^3H(\alpha, ^6Li)n$ will have a large weight in the evaluation of the $^6Li(n,t)^4He$ cross section. Recently, the excitation function at zero degree in the laboratory system was measured by a group of the Los Alamos Van de Graaff facility and this work will be published soon[24]. Alpha-particles are incident on a tritium target. The threshold α-particle energy is 11.136 MeV, and, at the laboratory energy of 11.61 MeV one reaches the $5/2^-$ level in the ^7Li compound system which is visible in the inverse reaction channel at about 240 keV laboratory neutron energy. Due to the large negative Q-value, the ^6Li-recoils are kinematically collimated to a cone of about ± 4 degrees. The ^6Li particles are separated spatially from the incident beam and from the Coulomb scattered particles by a magnetic field. The zero and 180° centre-of-mass cross sections were obtained from the two kinematic groups present at zero degree in the laboratory system. Their difference in energy is about 1.6 MeV. The reaction data were normalized by measuring simultaneously the yield of elastically recoiling tritons. More details can not be given, since this work is not yet published.

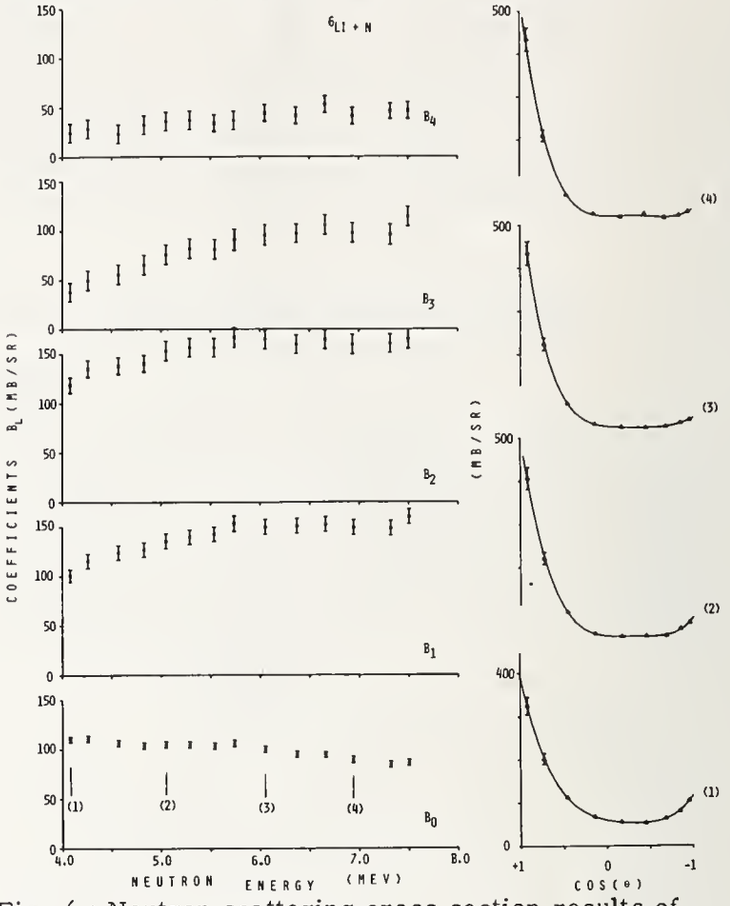

Fig. 6 : Neutron scattering cross section results of Lane et al.[20] in terms of Legrendre polynomial expansion coefficients and some representative angular distributions.

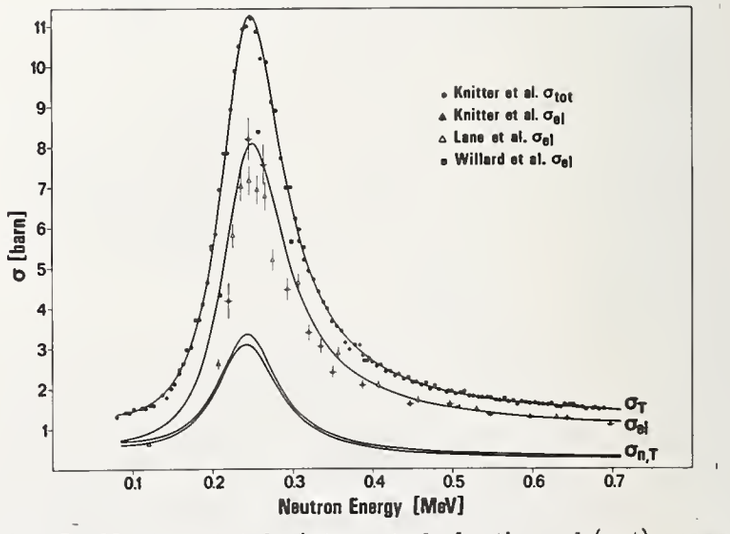

Fig. 7 : Neutron total, integrated elastic and (n,t) cross sections of ^6Li versus incident neutron energy[18]. Δ and ■ are data of ref. 22 and 23 respectively.

The $^4He(t,t)^4He$ scattering experiments

This entrance channel to the ^7Li-system consists of a spin-zero and a spin-$1/2$ particle and therefore the interpretation of the data is rather easy. Earlier studies of the triton - α scattering process have contributed considerably to the understanding of the ^7Li-system[25,26,27]. Recent measurements did not come to my knowledge. There are unpublished data in the triton energy range from 7 to 14 MeV from the Los Alamos tandem Van de Graaff facility displayed in graphical form in the work of Hale[28] on the R-matrix analysis of light element standards. However, these data will be published soon[24] under ref. [29].

Experiments using polarized projectiles

Studies of polarization effects can provide information of a basic nature, which can be obtained only indirectly or sometimes not at all using traditional experimental methods[30]. This was demonstrated already in the first nuclear polarization experiment which was made by Heusinkveld and Freier in 1951 at the University of Minnesota[31]. This ^4He-proton double scattering experiment gave the level sequence for the P-state doublet of the $^5Li^*$ nucleus, an information which could not be obtained by conventional scattering experiments[32].

The polarization power of ^6Li or neutrons was measured at the electron Linac of the Yale University [33,34]. Fig. 8 shows the schematics of the experimental set-up. A beam of unpolarized neutrons is produced at the (γ,n)-target of the Linac. The neutrons become partially polarized by the first scattering on carbon. In a second scattering the analysing power $A(\Theta)$ of ^6Li and of other nuclei were measured in the energy range from 2 to 5 MeV. The polarization of the incident neutrons was obtained from a separate scattering experiment in which the polarizer and the analyzer consisted of the same material of spin zero nuclei, in which case the analyzing power is equal to the polarization power[32]. The solenoid which is positioned in the flight path served to precess the neutron spin,

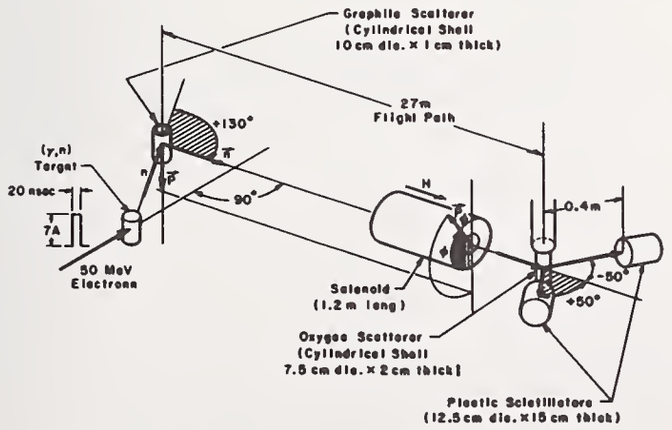

Fig. 8 : Experimental arrangement for measuring the analyzing power in neutron scattering experiments at the Yale-University[32].

and the analyzing power could be obtained from the count rate ratios with and without magnetic field and from the spin precession angle. Firk et al. [33,34] made a R-matrix analysis for the ^7Li system, using the scattering cross section data of Lane et al.[22] and their own polarization results. The differential scattering cross section for unpolarized neutrons $\sigma(\theta)$ and the polarization can be given in form of expansions

$$\sigma(\theta) = \lambda^2 \sum_L B_L P_L(\cos\theta)$$

$$\sigma(\theta) \cdot p(\theta) = \lambda^2 \sum_L C_L P_L^1(\cos\theta)$$

where $P_L(\cos\theta)$ and $P_L^1(\cos\theta)$ are the Legendre and associated Legendre polynomials. The B_L's as functions of the collision matrix are derived by Blatt and Biedenharn[35] with the phase correction of Huby[36] and the C_L's are given as function of the collision matrix by Simon and Welton[37].

The analysing power for the $^4He(t,t)^4He$ reaction was measured by a team of the Los Alamos tandem Van de Graaff facility[38,39] at centre-of-mass angles

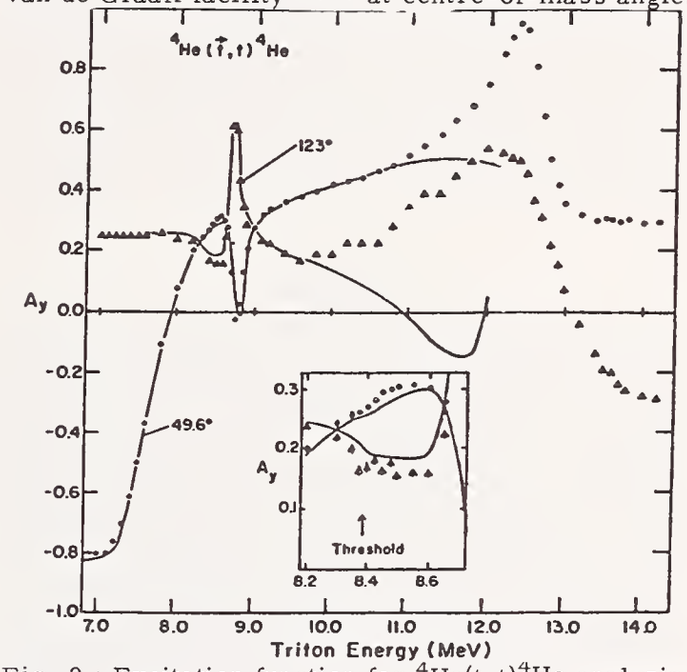

Fig. 9 : Excitation function for $^4He(t,t)^4He$ analyzing power[38].

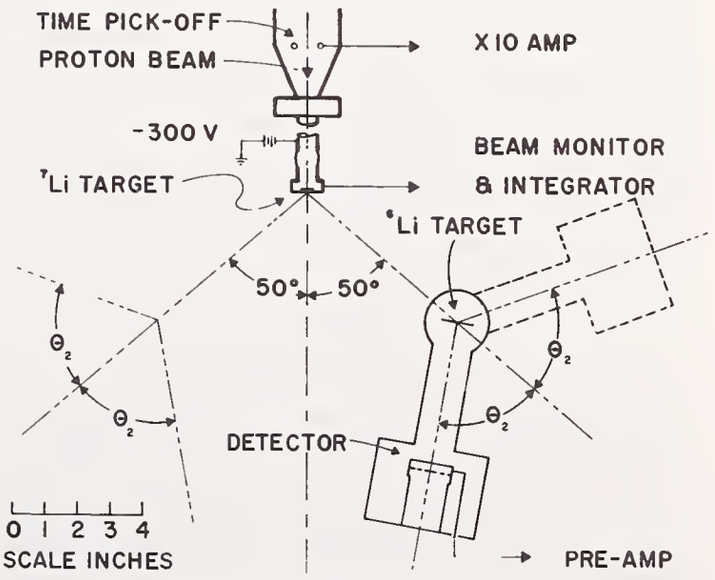

Fig. 10 : A plan view of the experimental arrangement to measure the analyzing power of the $^6Li(n,t)^4He$ reaction.

of 49.6° and 123° in the energy range from 7 to 14 MeV. In addition angular dependence of the polarization power at 8.79 MeV, 10.82 MeV and 12.25 MeV was obtained. The polarized tritons were produced with the Los Alamos Lambshift polarizing ion source for tritium[40]. At the target of the accelerator a beam current of 80 nA with a polarization of 0.8 has been obtained. Fig. 9 shows a part of the results. The resonance near 8.8 MeV is of particular interest, since it corresponds to the resonance near 240 keV in the $^6Li(n,t)^4He$ reaction.

The analyzing powers of the $^6Li(n,t)^4He$ reaction was measured by Karim and Overley[41] with the University of Oregon pulsed Van de Graaff accelerator in the neutron energy range from 0.2 to 1.4 MeV. Fig. 10 shows the experimental arrangement. With a thick metalic lithium target polarized neutrons are produced in the energy range between 0.2 and 1.4 MeV at the angles of $\pm$ 50 degrees with respect to the proton beam. The α and triton particles were detected in a solid state detector and two dimensional spectra were recorded in energy and flight time. This allowed to determine the neutron energy and to make a particle identification. The results compare also favourably with previous results[42] at two energies near the 240 keV resonance.

Conclusion

Recent measurements of the $^6Li(n,t)^4He$ cross section were done in the incident neutron energy range from some keV to several hundreds of keV[2,3] and from 2 to 14 MeV[4,5]. Neutron total cross section measurements were made[17,18] and are being made[19] in the neutron energy range from 10 eV to 10 MeV, where special emphasis has been paid to the region of the 250 keV resonance. Recent neutron scattering cross section measurements were performed in different experiments from 0.2 to 3.0 MeV[18], from 4.0 to 7.5 MeV[20] and from 7.5 to 14 MeV[21]. The gap between 2 and 3 MeV is being closed[19] such that the whole energy range from 200 keV to 14 MeV is being covered by recent scattering experiments. Zero and 180° degree centre-of-mass cross sections of the reaction $^3H(\alpha,^6Li)n$ are measured and will be available soon[24]. Similar is the situation with $^4He(t,t)^4He$ scattering experiments [24,29]. Also analyzing power measurements for the $^6Li(n,n)^6Li$, $^4He(t,t)^4He$ and $^6Li(n,t)^4He$ were done in the laboratory energy ranges from 2 to 5 MeV[33,34], from 7 to 14 MeV[38,39] and from 0.2 to 1.4 MeV[41] respectively. All this recent experimental results represent a large and valuable body of data for understanding of the ^7Li-system.

References

1. F. C. Barker, Phil. Mag. 2 (1957) 780
2. G. P. Lamaze, O. A. Wasson, R. A. Schrack and A. D. Carlson, Proc. of the Int. Conf. on the Interactions of Neutrons with Nuclei, Lowell, Massachusetts, 6-9 July, 1976, Vol. 2, p. 1341
3. D. B. Gayther, AERE-Harwell, private communication 12. 1. 1977, will be published as report AERE-8556 (1977)
4. C. M. Bartle, Proc. of the Conf. on Neutron Cross Sections and Technology, Washington D. C., 1975, Vol. 2, p. 688, NBS Special Publication 425
5. C. M. Bartle, D. W. Gibbie and C. Hollas, Proc. of the Int. Conf. on the Interactions of Neutrons with Nuclei, Lowell, Massachusetts, 6-9 July, 1976, Vol. 2, p. 1342
6. O. A. Wasson, Proc. of the NEANDC/NEACRP Specialists Meeting on Fast Fission Cross Sections, 28-30 June 1976, held at Argonne National Laboratory, ANL-76-90 p. 183
7. M. G. Sowerby, B. H. Patrick and D. S. Mather, Ann. Nucl. Sci. Eng. 1 (1974) 409
8. C. M. Bartle and P. A. Quin, Nucl. Instr. Meth. 121 (1974) 119
9. E. D. Pendlebury, AWRE 0-60/64 (1964)
10. P. J. Clements and I. C. Rickard, AERE-R 7075 (1972)
11. J. C. Overley, R. M. Sealock and D. H. Ehlers, Nucl. Phys. A 221 (1974) 573
12. E. Rosario-Garcia and R. E. Benenson, Nucl. Phys. A 275 (1977) 453
13. F. S. Goulding, D. A. Landis, J. Cerny III and R. H. Pehl, IEEE Trans. Nucl. Sci. 11 (1964) 388
14. H. Bichsel and C. Tschalaer, UCRL-17663 (1967)
15. I. G. Schroder, E. D. McGarry, G.de Leeuw-Gierts and S. de Leeuw, Proc. of the Conf. on Neutron Cross Sections and Technology, Washington D. C., 1975, Vol. 1, p. 240
16. S. Raman, N. W. Hill, J. Halperin and J. A. Harvey, Proc. of the Int. Conf. on Interactions of Neutrons with Nuclei, Lowell, Massachusetts, 6-9 July, 1976, Vol. 2, p. 1340
17. J. A. Harvey and N. W. Hill, Proc. of the Conf. on Neutron Cross Sections and Technology, Washington D. C., 1975, Vol. 1, p. 244
18. H. -H. Knitter, C. Budtz-Jørgensen, M. Mailly and R. Vogt, Report EUR-5726e (1977)
19. A. B. Smith, private communication January 24, 1977 Argonne National Laboratory
20. R. O. Lane, R. M. White and H. D. Knox, Proc. of the Int. Conf. on the Interactions of Neutrons with Nuclei, Lowell, Massachusetts, 6-9 July, 1976, Vol. 2, p. 1043
21. E. G. Bilpuch, D. H. Epperson, D. W. Glasgow, S. G. Glendinning, C. R. Gould, H. H. Hogue, P. W. Lisowski, C. E. Nelson, H. W. Newson, F. O. Purser, L. S. Seagondollar, T. Tornow and P. von Behren, Proc. of the Int. Conf. on the Interactions of Neutrons with Nuclei, Lowell, Massachusetts, 6-9 July, 1976, Vol. 2, p. 1309
22. R. O. Lane, A. S. Langsdorf Jr., J. E. Monahan and A. J. Elwyn, Report-ANL-6172, and Ann. Phys. 12 (1961) 135
23. H. B. Willard, J. D. Bair, J. D. Kington and H. O. Cohn Phys. Rev. 101 (1956) 765
24. N. Jarmie, Los Alamos Scientific Laboratory, private communication, January 10, 1977
25. T. A. Tombrello and L. S. Senhouse, Phys. Rev. 129 (1963) 2252
26. R. J. Spiger and T. A. Tombrello, Phys. Rev. 163 (1967) 964
27. M. Ivanovich, P. G. Young and G. G. Ohlsen, Nucl. Phys. A 110 (1968) 441

28. G. H. Hale, Proc. of the Conf. on Neutron Cross Sections and Technology, Washington D. C., 1975, Vol. 1, p. 302

29. R. A. Hardekopf, N. F. Jarmie, G. G. Ohlsen, R. V. Poore, R. F. Haglund Jr., R. E. Brown, P. A. Schmelzbach, D. B. Anderson, D. M. Stupin and P. A. Lovoi, to be published LA-6188 (1977)

30. F. W. K. Firk, Proc. of the Int. Conf. on the Interactions of Neutrons with Nuclei, Lowell, Massachusetts, July 6-9, 1976, p. 389

31. M. Heusinkveld and G. Freier, Phys. Rev. 85 (1952) 80

32. H. Faissner, Ergebnisse der Exakten Naturwissenschaften 22 (1959) 180

33. R.J. Holt, F. W. K. Firk, G. T. Hickey and R. Nath Nucl. Phys. A 237 (1975) 111

34. F. W. K. Firk, J. E. Bond, G. T. Hickey, R. J. Holt, R. Nath and H. L. Schuttz, Proc. of the Conf. on Neutron Cross Sections and Technology, Washington D. C., 1975, Vol. 2, p. 875, NBS Special publication 425

35. J. M. Blatt and L. C. Biedenharn, Rev. Mod. Phys. 24 (1952) 258

36. R. Huby, Proc. Phys. Soc. 67A (1954) 1103

37. A. Simon and T. A. Welton, Phys. Rev. 90 (1953) 1036

38. R. A. Hardekopf, N. Jarmie, G. G. Ohlsen and R. V. Poore, Proc. of the Fourth International Symposium on Polarization Phenomena in Nuclear Reactions, Zürich, Switzerland, 25-29 August, 1975

39. R. A. Hardekopf, G. G. Ohlsen, R. V. Poore and N. Jarmie, Proc. of the Fourth International Symposium on Polarization Phenomena in Nuclear Reactions, Zürich, Switzerland, 25-29 August, 1975

40. R. A. Hardekopf, G. G. Ohlsen, R. V. Poore and N. Jarmie, Phys. Rev. C13 (1975) 2127

41. M. Karim and J. C. Overley, Proc. of the Conf. on Neutron Cross Sections and Technology, Washington D. C., 1975, Vol. 2, p. 788, NBS Special publication 425

42. H. Wäffler and G. Walch, Direct Interactions and Nuclear Reaction Mechanisms, Gordon and Breach, New York, 1964, p. 633

ANGULAR ANISOTROPY IN THE $^6Li(n,\alpha)^3H$ REACTION BELOW 100 keV

J. A. Harvey
Oak Ridge National Laboratory
Oak Ridge, Tennessee 37830

and

I. G. Schröder
National Bureau of Standards
Washington, D.C. 20234

The data on the differential (n,α) cross section of ^6Li has been reviewed below a neutron energy of 100 keV. Measurements in this region, compared to that above 100 keV, have been few. Only recently has interest increased as large and unsuspected anisotropies have been observed in this energy region. Thus, at 25 keV an anisotropy amounting to 67% in the forward-to-backward direction has been observed; while in the region between 1 eV and 10 keV measurements indicate that in the forward-to-backward 66° cone the asymmetry has an energy dependence, in the laboratory system, which can be expressed analytically as $1 + 0.0055 \sqrt{E_n(eV)}$. These angular anisotropies seem to arise from interference between the large p-wave resonance at 247 keV and many s-wave resonances which account for the large 1/v (n,α) thermal cross section. New and detailed measurements of the differential (n,α) cross section are needed not only to be able to account analytically for these interference effects but also because it is necessary to consider these anisotropies when the $^6Li(n,\alpha)^3H$ cross section is used as a standard.

(Angular distribution; fast neutrons; linac; reactor filtered beam; $^6Li(n,\alpha)T$; standard)

Introduction

The $^6Li(n,\alpha)^3H$ reaction has been increasingly used as a standard in partial cross section measurements, for flux normalization, for neutron detection and in neutron spectroscopy. The suitability of this reaction as a standard rests in its Q-value (+ 4.784 MeV) and large thermal cross section (940 barns); in the smooth 1/v behaviour of its cross section to within 1% below 10 keV, and that above this energy and up to 100 keV the cross section varies smoothly though no longer following the 1/v behaviour. This is due to a large p-wave resonance (5/2⁻) at 247 keV which dominates the region between 100 and 500 keV.

The $^6Li(n,\alpha)^3H$ reaction has been extensively studied both experimentally[1] and theoretically.[1] Most of these studies, however, have centered in the region above 100 keV. Below this energy very little data exists. In particular, differential (n,α) measurements in the region below 100 keV have been few and mainly unpublished.[2,3] This is regrettable as large and unsuspected anisotropies have been recently observed in this energy region. The present review will try to give a summary of these recent experimental results and some of their implications.

Early Measurements

The first attempt to measure the $^6Li(n,\alpha)^3H$ differential cross section below 100 keV was made by G. de Leeuw-Gierts in 1963[2] using ultra fine grain nuclear emulsions loaded with ^6Li at an incident neutron energy of 20 keV. The angular distribution obtained is shown on Fig. 1 together with a theoretical fit arising from a single-level S-matrix analysis made by Mahaux and Robaye.[4] This experiment was followed by that of Beets et al.[3] who used a thick tritium target (60 keV) and measured the (n,α) angular distribution in the energy region between 60 and 100 keV. Two different experimental set-ups were used. The first consisted of a circular multiplate nuclear emulsion chamber with a central ^6Li target. The second experiment used the same type of ^6Li loaded fine grain emulsion as in the 20 keV experiment. The angular distributions obtained from the two arrangements are shown in Fig. 2 together with a theoretical fit from the S-matrix analysis of

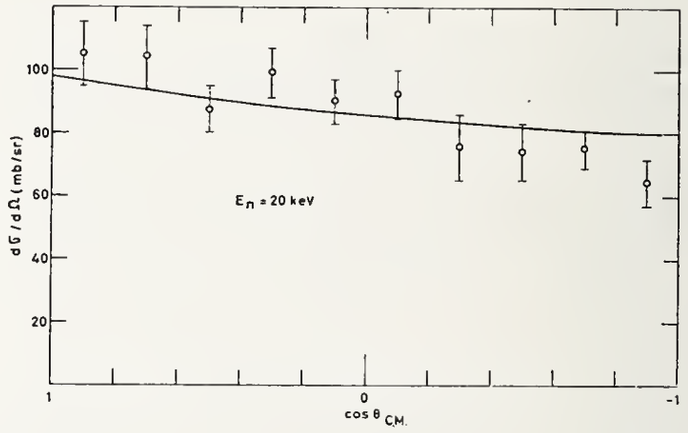

Fig. 1. Differential cross section at 20 keV from the data of reference 2. Solid curve is theoretical fit of Mahaux and Robaye.[4]

Mahaux and Robaye.[4] The discrepancies between the two distributions can be attributed to the slightly different energy composition of the neutron beams, the non-uniformity of the epicadmium neutrons in the emulsion experiment and the presence of neutrons > 150 keV that could not be properly accounted for in the camera arrangement. Furthermore, both the 20 and 80 keV experiments using loaded emulsions were subject to rather large thermal backgrounds of ~ 20%.

Angular Anisotropy at 25 keV and 2 keV Using Filtered Beams

The installation of both a 25 keV iron-filtered[5] and a 2 keV scandium-filtered[6] beam facility at the NBS reactor, the fact that unexplained results were being obtained with ^6Li semiconductor spectrometers in the region below 100 keV,[7] and the paucity of data on the behaviour of the differential (n,α) cross section in this region prompted the study of the angular anisotropy of the $^6Li(n,\alpha)^3H$ reaction at 25 keV[8] and to later look for similar effects at 2 keV.

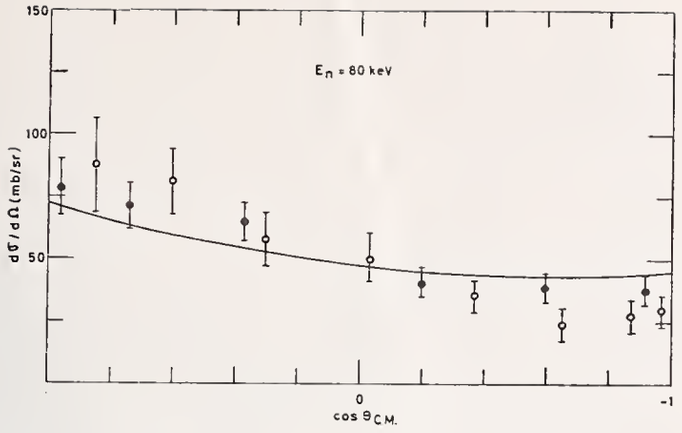

Fig. 2. Differential cross section at 80 keV obtained by Beets et al.[3] The circles represent the values obtained with the ^{6}Li loaded nuclear emulsion, while the dots represent the values obtained with the emulsion chamber. Solid curve is from fit of Mahaux and Robaye.[4]

To measure the angular anisotropy in the ^{6}Li(n,α)^{3}H reaction at 25 keV a surface-barrier detector was coated with 80 μg/cm^2 of ^{6}LiF (front face) and used as a 2π detector. This detector was placed in two different angular positions with respect to the neutron beam: front face at 90° and back face 90° to the beam. The pulse-height distribution of both α-particles and tritons were recorded for these two positions (Fig. 3). In a subsequent set of measurements a second surface barrier detector was placed coaxially with the first (at 90° to the beam) and in such a way as to subtend a 45° cone. Coincidence measurements that simultaneously recorded the energy distribution in both detectors allowed a measure of the angular asymmetry in the backward-to-forward 45° cone (Fig. 4). Lastly, thermal calibration runs were performed before and after the 25 keV measurements to calibrate the system and to insure that spurious anisotropies were not introduced electronically.[8]

Subsequently a similar set of experiments were performed with the same detectors and electronic system at the 2 keV filtered beam facility. The results obtained together with those at 25 keV are summarized in Table I.

TABLE I

Ratio	25 keV	2 keV
R (180°)	1.67 ± 0.11	1.07 ± 0.06
R (45°)	1.96 ± 0.06	1.24 ± 0.02

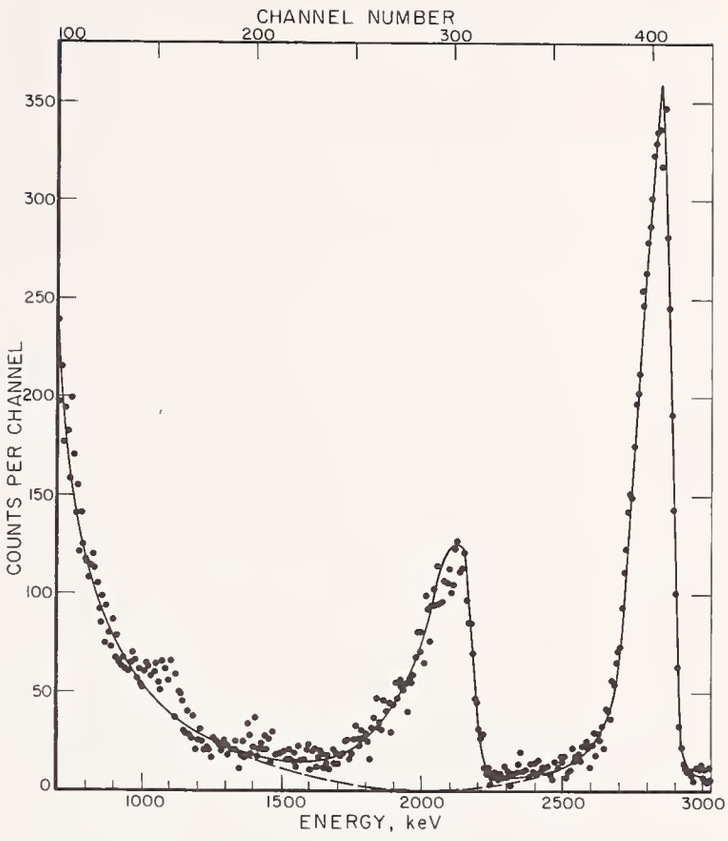

Fig. 3. Experimental pulse-height distribution obtained in the forward 2π measurements made at 25 keV. (Reference 8)

Angular Distribution of the ^{6}Li(n,α)^{3}H Reaction at 25 keV

The results obtained at 25 keV using the 2π detector were complemented by a set of two other measurements: front face at 45° to the neutron beam and back face 45° to the neutron beam. From these four 2π measurements and from the coincidence experiments a coarse-grided angular distribution was obtained. (The details of the method are explained in reference 8.) The results are shown in Fig. 5. This figure shows the angular distribution in both the laboratory and center-of-mass system. The two dashed lines in these distributions represent the errors arising from the uncertainty in the determination of the background (see Fig. 3). The dotted lines in the laboratory distribution correspond to an isotropic distribution in the center-of-mass system.

Angular Anisotropy in the ^{6}Li(n,α)^{3}H Reaction in the 1 eV to 10 keV Energy Region

The determination of the energy dependence of the angular anisotropy of the ^{6}Li(n,α)^{3}H reaction in the energy region between 1 eV and 10 keV was performed at ORELA using a thin (101 μg/cm^2) ^{6}LiF target.[9] The measurements were made with a diffused-junction silicon detector which subtended an average angle of 66°

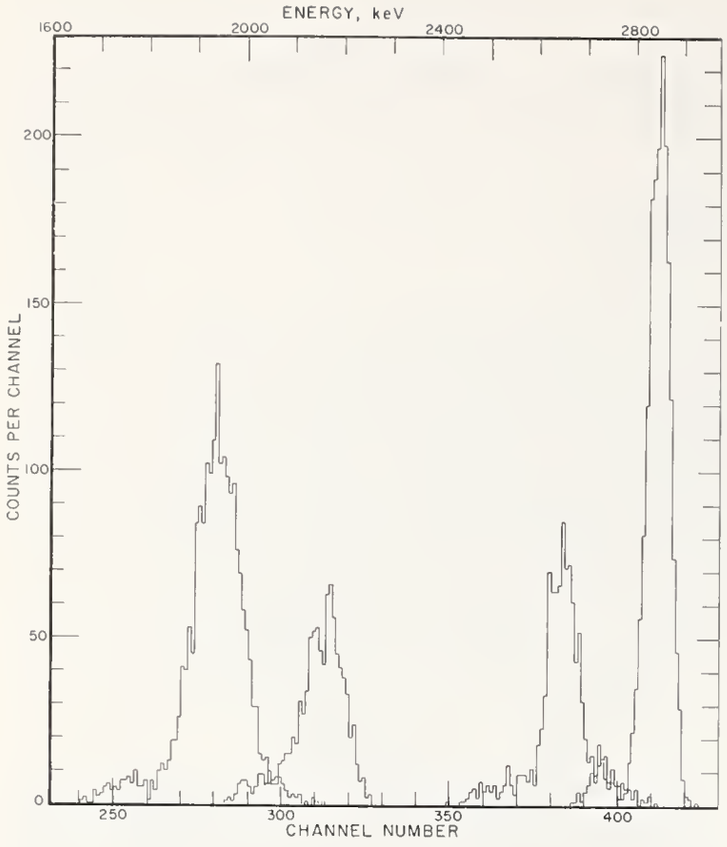

Fig. 4. Composite picture showing the pulse-height distribution obtained in the coincidence experiment of Schröder et al.[8] performed at 25 keV.

to the lithium target. The detector resolution was such that both the triton and alpha groups were well resolved so that an accurate ratio of their intensities could be obtained as a function of energy. In the 1 eV to 10 keV energy region the ORNL results give an energy dependence for the asymmetry in the forward-to-backward 66° cone (in the laboratory system) of the form

$$A = 1 + 0.0055 \sqrt{E_n}$$

where E_n is the neutron energy in electron-volts. This energy dependence is shown graphically in Fig. 6.

Conclusions

The differential (n,α) cross section of ^{6}Li in the region above 100 keV has been extensively studied, most recently by Overley et al.[10] No such detailed work exists yet below 100 keV. Thus all one can say is that the existence of the angular anisotropy below 100 keV seems to arise from interference between the large p-wave (5/2$^-$) resonance at 247 keV and the many s-wave resonances which account for the large 1/v (n,α) thermal cross section.

The theoretical analysis of the ^{6}Li(n,α) cross section which ranges from the single-level, single-channel R-matrix and S-matrix calculations of Mahaux and Robaye[4] to the multilevel, multichannel R-matrix computations of Hale[11] does not have the input which is available above 100 keV. In order to fill this gap it is necessary to obtain detailed angular

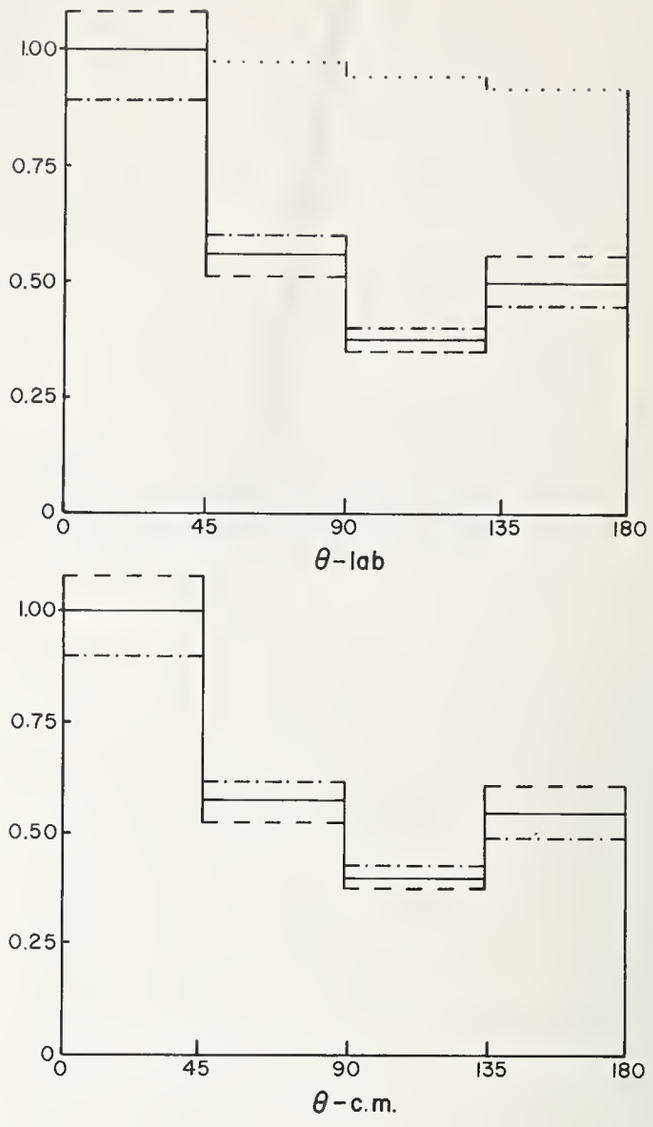

Fig. 5. Angular anisotropy of the ^{6}Li(n,α)^{3}H reaction at 25 keV in the lab and center-of-mass systems (reference 8).

distributions in the energy range from 1 to 100 keV. Below this energy the differential (n,α) cross section should be of the form a + b cosθ and therefore the ORNL data as it stands seems adequate.

At present only a few experiments are contemplated. The filtered beam work at NBS using solid state detectors will be completed at 2 keV and a measurement made at 144 keV (silicon filtered beam).[12] Lastly, two groups, one from the University of Michigan[13] and one from HEDL[14] are planning to perform a series of differential measurements using track-etch detectors.

Bibliography

1. See papers on ^{6}Li in this conference and references therein.
2. G. de Leeuw-Gierts, PhD Thesis, Faculte de Sciences, Universite Libre de Bruxelles (1968).

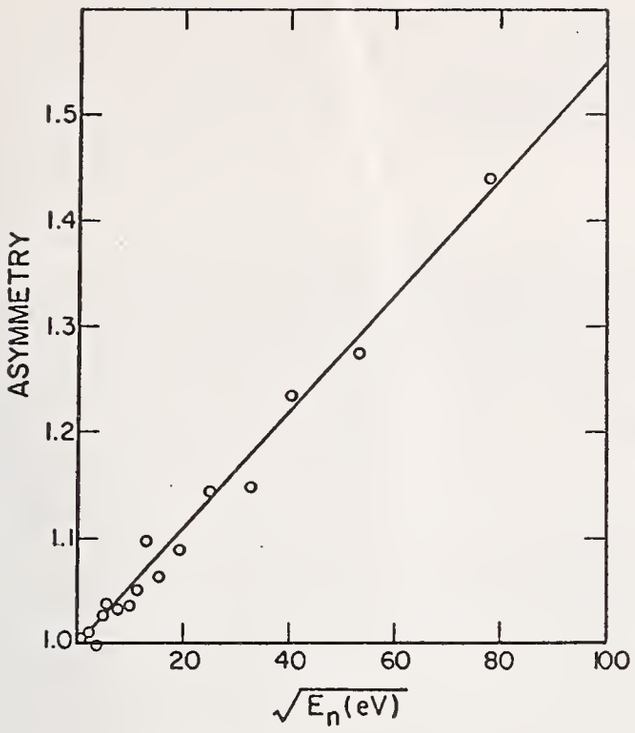

Fig. 6. Asymmetry in the forward-to-backward 66° cone (in the laboratory system) of the $^6Li(n,\alpha)^3H$ reaction between 1 eV and 10 keV. Data of Harvey et al.[9]

3. C. Beets, G. de Leeuw-Gierts, S. de Leeuw, Y. Baudinet-Robinet, G. Robaye, and L. Winand, Nucl. Phys., 69, 145 (1965).
4. C. Mahaux and G. Robaye, Nucl. Phys., 74, 161 (1965).
5. E. D. McGarry and I. G. Schröder, Proceedings of a Conference on Nuclear Cross Sections and Technology, Washington, D.C. March 3-7, 1975. NBS Special Publication 425, Vol. 1, p. 116.
6. I. G. Schröder, R. B. Schwartz, and E. D. McGarry, Proceedings of a Conference on Nuclear Cross Sections and Technology, Washington, D.C. March 3-7, 1975. NBS Special Publication 425, Vol. 1, p. 89.
7. G. de Leeuw-Gierts and S. de Leeuw (private communication).
8. I. G. Schröder, E. D. McGarry, G. de Leeuw-Gierts, and S. de Leeuw. Proceedings of a Conference on Nuclear Cross Sections and Technology, Washington, D.C. March 3-7, 1975. NBS Special Publication 425, Vol. 1, p. 240.
9. J. A. Harvey, J. Halperin, N. W. Hill and S. Raman, ORNL/TM-5450, p. 14, May 1976.
10. J. C. Overley, R. M. Sealock, and D. H. Ehlers, Nucl. Phys., A221, 573 (1974).
11. G. M. Hale, Proceedings of a Conference on Nuclear Cross Sections and Technology, Washington, D.C. March 3-7, 1975. NBS Special Publication 425, Vol. 1, p. 302.
12. R. B. Schwartz, this conference.
13. John C. Engdahl, private communication.
14. Raymond Gold, private communication.

EXPERIMENTAL DATA BASE FOR THE Li-7 SYSTEM

H. Derrien and L. Edvardson
Centre de Compilation de Données Neutroniques
de l'Agence pour l'Energie Nucléaire (OCDE)
B.P. No.9
91190 GIF SUR YVETTE
FRANCE

A review of the experimental data available for the Li-7 system is given, including reactions induced by neutrons and those induced by He-4 on H-3 or by H-3 on He-4. For reactions induced by neutrons only, the energy range up to about 5 MeV has been considered. Some recommendations are given concerning possible future measurements and the validity of the recent evaluations for the Li-6(n,α) cross section.

(Elastic scattering; ^{6}Li(n,α); ^{6}Li total; ^{7}Li system; neutrons; review of measurements).

Introduction

The most recent international meetings on neutron standards were held in October, 1970 at Argonne (organised by Argonne National Laboratory and sponsored by the EANDC), and in Vienna in November, 1972, organised by the IAEA. The problem of the Li-6(n,α) cross section was examined during these meetings. A complete review of the Li-6 neutron cross section in the energy range from Thermal to 1.7 MeV was presented by C.A. Uttley at the Argonne meeting (1) for all the data available in 1970, but no such review was presented at Vienna in 1972. Since this date, a great effort has been made to try to explain the large discrepancies existing in the Li-6(n,α) cross section, particularly in the vicinity of the 250 keV resonance and beyond. The investigations have been made in the following directions :

1. The energy calibration. The important differences in the location of the resonance peak do not permit a direct comparison of the cross section from several measurements. The problem of the energy standard has been studied in several laboratories by the time-of-flight method using linacs and cyclotrons (Columbia, Harwell, Geel, Karlsruhe and Saclay). The results of these investigations will be presented by G.D. James at this meeting.

2. The content of Li-6 in the Lithium glasses. The content given by the manufacturers has been questioned for some glasses used in absolute measurements; precise measurements have been made, for instance, by a non-destructive method : measurement of the neutron transmission of the glasses and determination of the Li-6 content from the 1/v variation of the total cross section at low energy.

3. Further measurements of the Li-6(n,α) cross section. The results have not been any more encouraging; for instance, a new method used by Friesenhahn in 1974 led to a cross section which is in disagreement with all the previous results (61).

4. Analysis of the experimental data using the nuclear reaction theories. At the present stage, a choice has to be made amongst the disparate experimental results; a way in which to make this choice is to try to predict the cross section values by using a formalism which permits the calculation of the Li-6(n,α) cross section from other experimental results considered as accurate or from a set of experimental results as diverse as possible. This problem was envisaged as early as 1969 by K.M. Diment and C.A. Uttley, (2) who calculated the (n,α) cross section at the resonance by using the parameters obtained from the scattering and total cross sections. We know that the cross sections obtained at the peak of the resonance was about 1 barn higher than the values measured by Schwarz (46). At this time, the one-level Breit-Wigner formula used by Diment and Uttley was suspected : for instance, it does not take into account the interference due to a $5/2^-$ level which lies below the neutron threshold. As a consequence, a solution to the problem which could be considered with high confidence, should be obtained by using a complete R-matrix formalism which takes into account the interferences between all the levels of same spin in all the open channels. This kind of analysis has recently been performed by G.M. Hale et al. (3) for the ENDF/B data files and the results are presented at this session by the author.

In fact, in the R-matrix formalism, one must consider all the reactions leading to Li-7 compound nucleus and all the possibilities of de-excitation of this system, i.e., all the possible entrance and exit channels. A complete compilation of the Li-7 levels and reaction channels has recently been performed by F. Ajzenberg-Selove (4); the data in Figure 1 have been extracted from this compilation; they show the $5/2^-$ levels at 6.68 and 7.47 MeV excitation energy (the neutron binding energy is 7.2506 MeV). The nuclear reactions energetically available for our purpose are the following :

Li-6 total neutron
Li-6(n,γ)Li-7
Li-6(n,n)Li-6
Li-6(n,α)t
α-t scattering
t(α,n)Li-6

The reaction Li-6(n,γ)Li-7 has very little importance; the corresponding cross section is smaller than 50 mb at thermal energy and is negligible at higher energies and then the neutron absorption cross section is nearly equal to the (n,α) cross section. The α-t scattering is of great importance because it corresponds to the exit channel of the Li-6(n,α)t reaction. G.M. Hale et al. have particularly shown that the calculated cross sections for Li-6(n,α)t are very sensitive to the α-t scattering angular distributions. The same remark applies to the α(t,n)Li-6 reaction which is the inverse reaction of Li-6(n,α)t.

In this paper, we will review the experimental data available for the reactions listed above, except for the Li-6(n,γ)Li-7 reaction. The neutron data are available in the EXFOR international files on request from the 4 Neutron Data Compilation Centres (NNCSC, Brookhaven; CCDN, Saclay; NDS, Vienna,

and CJD, Obninsk). The references given at the end of this review are sorted following the corresponding reactions. For the neutron entrance channel reactions, some details concerning the experiments are also given and the references are coded according to the procedure used in CINDA 76/77. For the other reactions, the references and some mixed references are given in the usual manner.

α-t Scattering and t(α,n)Li-6 Reactions

The experimental data available correspond to the references 8-13. They include differential cross section, angular distribution and polarization measurements. Some important theoretical analyses have been done on α-t scattering and the results have been published in the references 14-17; we think that these works should not be ignored when trying to solve the Li-6(n,α) problem by a nuclear reaction formalism.

The differential cross sections and angular distributions for α-t scattering have been measured by M. Ivanovich et al. (9) in the 3-11 MeV α energy range; by R.J. Spiger et al. (10) for α energies between 4 and 18 MeV and by L.S. Chuang (11) for triton bombarding energy in the range 2-3 MeV. Phase shift analyses have been performed by these authors and parameters for the Li-7 levels have been obtained. The polarization of tritons scattered by He-4 have been measured by P.W. Keaton et al. (8) for incident triton energy equal to 6.0; 6.9; 9.5; 10.2 and 10.25 MeV and for several angles; concerning the phase shift analyses, their results are in agreement with those of Spiger et al. More recently, R.A. Harde Kopf et al. (12), at Los Alamos, have obtained the excitation function and angular distribution for the He-4($\vec{t}$,t)He-4 analysing power in the triton energy range 7-14 MeV for 8 incident energies; they have also measured the angular distribution of the He-4(t,t)He-4 scattering for 6 energies and 17 angles in the energy range 8.23-12.00 MeV; the results have been used by Hale et al. for an R-matrix analysis.

Several theoretical analyses were performed on the above-mentioned data by different authors. The resonating method has been used by R.E. Brown et al. (14) to calculate the phase shifts and the results are in good agreement with the experimental results of Spiger and those of Ivanovich. An optical potential analysis was performed by V.G. Neudatchin (16), which happens to be as good as the resonating method when applied to the results of Spiger or Ivanovich. The shell treatment of separable interactions made by L.M. Kuznetsova (15) is also in agreement with the experimental results of Spiger. An R-matrix analysis was also performed by R.C. Baker (17) on the Spiger data. The interesting feature of these theoretical analyses is that no inconsistencies in the experimental data have been pointed out.

Concerning the H-3(α,n)Li-6 reaction, only two results are known. Firstly, the measurement of Spiger et al. (10) for α incident energy 11.0-12.4 MeV with the dominant effect of the 7.47 MeV Li-7 resonance; the results were normalized to the Schwarz Li(n,α)t results (inverse reaction). Secondly, the results of R.E. Brown et al. (13) not yet published : the 0^0 cross sections have been obtained at 15 α energies from 11.3 to 12.0 MeV (range of En=0.08 to 3.9 MeV for the inverse reaction); 2 to 5% accuracy is expected and the results could be of great importance for solving the problem of the Li-6(n,α) reaction.

Concerning the α-t scattering, we have not compared the 3 most important results, i.e., Spiger et al., Ivanovitch et al. and Harde Kopf et al. A direct comparison is not easily possible because the measurements were not done at the same angles and energies. The R-matrix analysis should be applied simultaneously to the three sets of data to verify their consistency.

The Total Neutron Cross Section

The total cross section is generally obtained from transmission measurements using samples of appropriate thicknesses. If the resolution is good enough, which is always the case in the Li-6 measurements, the transmission is an absolute measurement of the total cross section : the measurement of the incident and transmitted neutron flux is done with the same detector in the same geometry. If the Li-6 content of the sample is well known, the total cross section is generally obtained with an accuracy better than 2% and can be considered as a basic measurement for testing the coherence of partial cross sections which are more difficult to measure with high accuracy. A precise knowledge of the total cross section is particularly important at low energies in order to determine the 1/v variation of the absorption cross section, i.e., the (n,α) cross section and the thermal values can also be obtained by extrapolating the 1/v law.

The references 18-26 correspond to the total cross section measurements performed between 1954 and 1976 in the energy range from 70 eV to about 10 MeV. One notes that there is only one measurement at low energy : that of Diment and Uttley (24) for neutron energies above 72 eV. However, J. Harvey (25) announced, at the 1975 Washington conference, a measurement from 10 eV neutron energy; unfortunately, the lower part of the results have not been published and the data present in the EXFOR files begin at 24.6 keV. There is no measurement at very low energy, and the only way in which to obtain the total cross section below 72 eV is to extrapolate the 1/v law obtained by Diment and Uttley, i.e.:

$$\sigma_T(\text{barn}) = (149.5\pm0.3)/\sqrt{E} + (0.70\pm0.01);$$

however, the extrapolation gives a thermal absorption cross section equal to (940±2) barn, in agreement with direct measurements at thermal energy.

The experimental total cross sections are compared in Figures 2 and 3 over the whole energy range. The data of Diment and Uttley are present in the total energy range and are used in Table I as an element of comparison. In Figure 2, the energies have been adjusted to obtain the peak of the resonance at 246 keV for all sets of data; for a given set, the corrections are constant in relative values. However, this method of adjustment could be inexact. For instance, in the case of a linac time-of-flight measurement, the part of the error due to a poor evaluation of the so-called t^0 increases relatively when the time-of-flight decreases. One example of this kind of effect is given in Figure 4 which shows the superposition of the results of Diment and Uttley (chosen as reference data) and those of Meadows (23); in Meadows' results the resonance seems to be wider than in that of Diment's results. This is probably due to an under-estimation of the energy correction in the high energy range of Meadow's data (relative to Diment's data).

Table I shows that, with the exception of the old values of Johnson (18) and those of Farrell (19), the measured cross sections agree within 3% over the resonance. However, in the low energy part of the

resonance, the values of Harvey and Meadows have a tendency to be higher than those of Diment and Uttley. Again, if one accepts the values of Johnson, the agreement is rather good between the different measurements in the high energy range (0.5 to 10 MeV); but there is a tendency for the Diment and Uttley values to be lower than the others. A careful evaluation of the data should lead to an evaluated total cross section with an accuracy better than 3%; in particular, one should reach an accuracy of 2% at the peak of the resonance.

Neutron Elastic Scattering

The experimental results available in the experimental data files correspond to references 27-35. These data contain angular distributions, polarization measurements and integrated cross sections. The integrated cross sections are plotted in Figure 5 with the Hale et al. R-matrix evaluation. Above about 0.5 MeV no severe discrepancies exist between the different results. But the 250 keV resonance is not well defined and it is difficult to evaluate the energy of the maximum $\sigma(n,n)$ cross section. There are only 9 points between 200 and 500 keV in the recent results of Knitter (35); 14 points between 100 and 500 keV in Lane's (28) data and only 3 points in Villard's data (27); the values are generally given with a large error bar in the resonance. At low energy (from 1 to 100 keV), there is only one measurement by Asami and Moxon (32) giving a constant $\sigma(n,n)$ cross section equal to (0.752±0.043) b up to about 50 keV. This value is about 0.05 b higher than the one obtained in the Hale et al. R-matrix analysis (0.71 b at thermal energy). The thermal value obtained by Uttley et al. (1) by analysing the Diment and Uttley total cross section is equal to 0.724 barn.

The Li-6(n,α)t Reaction

The experimental data available, including angular distribution and polarization measurements correspond to the references 36-69. Everyone knows that the main feature of the data is the important discrepancies existing in the experimental results for all energy ranges above about 100 keV. Between 1950 and 1960, nine measurements were performed with a discrepancy of about 25% at the peak of the 250 keV resonance; 7 measurements between 1960 and 1970 give approximately the same discrepancy; 13 measurements have been performed since 1970 and the inconsistency is still 25% in this period of time. If we consider all the measurements between 1950 and 1977, the difference between the lower and higher values in the peak of the resonance is about 40% relative to the mean value. Apparently no improvement has been obtained in 27 years, and the evident conclusion drawn by the unbiased observer would be that we do not know how to measure the Li-6(n,α) cross section with high accuracy in the vicinity of the 250 keV resonance and at higher energies. Thus the question to be answered is : Is it possible and reasonable to use the Li-6(n,α) cross section as a standard above 100 keV neutron energy? Perhaps at the end of this session we will be able to answer this question.

The thermal absorption cross section has been measured by Meadows (53) using the pulsed neutron method. He obtained a value of (936±4) barn. From the measurement of the total cross section of a Li_2SO_4 sample, using the BR2 chopper facility at Geel (Belgium), Becker and Deruytter (51) obtained the value of (944±19) barn for the absorption. In this experiment the accuracy was limited by the difficulty in obtaining the accurate value of the Li-6 content of the sample. The value obtained by Uttley and Diment by extrapolating the 1/v law is equal to (939±2) barn. The value proposed by Hale et al. from the R-matrix evaluation is equal to 935.89 barn. One can see that there is an agreement within less than 1% in the different values proposed for the (n,α) cross section at thermal.

The 1/v law established by Diment and Uttley from the total cross section measurement has been confirmed to be valid by Coates' et al. (59) measurement with an approximation of ±1% up to 10 keV. Unfortunately, there are no other measurements at low energy to confirm the Harwell results. However, the Hale et al. evaluation is also in agreement with Coates' results as shown in Figure 6.

Figure 7 illustrates the large discrepancies existing at the 250 keV resonance for some selected results. It is not necessary to comment on this Figure. In Figure 8, we have shown the most recent measurements and evaluations :

1) the new values of Fort et al. (69) which correspond to the earlier Helsinki values corrected by a factor of 1.117 due to the re-evaluation of the Li-6 content of the glasses (by transmission measurement at the Saclay Linac (5)).

2) the values obtained by Lamaze et al. (65) from a measurement relative to (n,p) scattering;

3) the values obtained by Gayther et al. (67) from a measurement relative to U-235(n,f) cross section using the U-235(n,f) standard of the Sowerby evaluation;

4) the R-matrix evaluation by Hale et al.;

5) the value calculated by Knitter (68) from a fit of his measured total and scattering cross sections using a single level Breit-Wigner formula.

The Lamaze data have been included in the Hale et al. R-matrix analysis and it is worth mentioning that the discrepancy between the experimental and calculated values is still 3% at the peak of the resonance, whereas the evaluation of Knitter is in agreement with the values of Lamaze.

We have also plotted, in Figure 8, the data from Poenitz (60) and Coates which are not too far from the above results at the peak of the resonances. The integral cross section between 0.100 and 0.500 MeV corresponding to some sets of data in Figure 8 are given in the following Table :

	Area in b-MeV
Lamaze	0.481
Gayther 77	0.492
Knitter 77	0.488
Hale	0.486
Poenitz 74	0.471

One can see that :

1) there is only a 0.4% difference between the area of the resonance calculated from the Knitter and Hale et al. values (Knitter's area is 0.4% higher than Hale's, whereas Knitter's values are 2.5% lower at the peak of the resonance);

2) the area calculated from the Poenitz values is only 3% smaller than the one calculated from Hale et al. whereas the peak cross section is about 10% smaller; perhaps there is an effect of resolution in the results of Poenitz;

3) the resonance in Fort's results seems to be wider than in the others. It is difficult to know if this is due to an effect of resolution or to the correction on the energy scale. However, the Fort measurement is the only one which is purely absolute and it is comforting to see that his final value agrees, at the peak of the resonance, with the recent measurements and the recent evaluations.

Figure 9 shows the dispersion of the results in the energy range 0.5 - 5 MeV. A series of six different measurements corresponds to high values of the cross section and one measurement gives very low cross sections (about two times smaller). Between these extremes, in the energy range 0.5 - 1 MeV, we find in quite good agreement the values of Poenitz, the recent values of Lamaze and Gayther and the Hale et al. evaluation. It is also important to note that Stephany et al. (63) have tried to resolve the discrepancy in the MeV energy range by an absolute cross section measurement at 964 keV. They found a value of 0.356 b which falls into the high series of values mentioned above. However, in the last ERDA Progress Report (7.b) the authors recognize that this value is 12 or 15% too high and they are now investigating a new method for a more accurate absolute measurement at 964 keV and at other available energies.

Conclusion

In this review we have not tried to examine or criticise the measurement methods and the possible sources of error in view of eliminating some results which could be doubtful. This was done by C.A. Uttley et al. at the 1970 Argonne meeting for the measurements before 1970 and will probably be done at this meeting by Knitter for the most recent measurements. We have only tried to gather the maximum of experimental data in the energy range up to about 5 MeV; these data are available to any evaluator who wishes to make a definitive point on the Li-6(n,α) cross section. However, from a simple examination of the data, it is possible to make some recommendations for the future :

1. There is a lack of measurements in some of the energy ranges for some reactions :

(a) the total neutron cross section has not been measured at low energy; a recommendation for such a measurement was also made by Uttley at the 1970 ANL meeting; the Harvey measurement has not fulfilled the recommendation because the results in the low energy range have not been published. So, the 1/v law is still established only from the Harwell measurement;

(b) according to Deruytter (7) more measurements need to be done at thermal energy; although the few results available agree within better than 1%, these results cannot be trusted with more than 2% accuracy (problems of the Li-6 content in the samples used);

c) a better definition of the resonance in the elastic scattering needs to be obtained; that was also a recommendation of Uttley at the 1970 ANL meeting; only one measurement has been done, by Knitter et al., since the ANL meeting.

2. Concerning the (n,α) reaction, a lot of experiments have been performed since 1970, and we have already pointed out that the discrepancies are still unacceptable. We should not recommend that more experiments be performed unless the reason for the discrepancies has been clearly established and the new experiments could be undertaken with a high degree of confidence. The attempt of Stephany et al. to resolve the discrepancy in the MeV region is an example of what could be done : they realized that the cross section value at 964 keV announced at the last Washington Conference is 12 to 15% too high due to the underestimation of some experimental effect (7.b) and they are investigating a new method which will be used only if the preliminary results are sufficiently encouraging.

3. The problem of energy calibration should also be examined carefully. According to the calculation of Hale et al. and Knitter et al. there is a difference of about 4 keV between the maximum values in the total and the (n,α) cross section for the resonance near 240-250 keV. This difference, which is a function of the resonance parameters and the channel radii, needs to be verified experimentally. On the other hand, energy adjustment of the data for a point per point comparison cannot be done precisely if one ignores how to perform the correction; this means that each author should give the law of variation of the error on energy versus the energy, if possible.

4. Nevertheless, we should not be too pessimistic at the present time. The R-matrix evaluation done by Hale et al. has shed a supplement of light on to the Li-6(n,α) cross section, by using the α-t scattering data; the parameters of this reaction channel should be the same as those of the exit channel of the Li-6(n,α)t reaction. However, Knitter has also shown that the parameters obtained from a single level Breit-Wigner analysis of the total and scattering cross section give, for the Li-6(n,α)t cross section, values which are in quite good agreement with the evaluation of Hale et al. Consequently, it appears that the interferences between the two 5/2$^-$ levels in Li-7 are not very strong. It is comforting to note the consistency which now exists between the evaluations and the very recent sets of experimental data (Lamaze, Gayther, Knitter), including the re-evaluated data of Fort et al., and a recommendation should be made to use those sets of evaluated and experimental data as a basis for the definition of the Li-6(n,α) standard cross section.

Acknowledgement

The authors wish to thank Miss Lynette Truran for her help in correcting the English and the material realisation of this document.

Mixed References

1. C.A. Uttley et al., Neutron Standards and Normalization, p.80, ANL, 21-23 October, 1970.

2. K.M. Diment et al., AERE-PR/NP 16 (1969), p.3

3. G.M. Hale et al.
   (a) Nuclear Cross Sections & Technology, Washington, March, 1975, p.302;
   (b) LA-6518-MS;
   (c) private communication.

4. F. Ajzenberg-Selove et al. Nucl. Phys. A 227 (1974), 54.

5. H. Derrien, not published.
   M. Moxon, private communication.

6. E. Fort et al., to be published.

7. A.J. Deruytter, private communication.

7.b J.C. Engdahl et al., BNL-NCS-2151, p.143

References for α-t Entrance Channel

8. P.W. Keaton, et al., Phys. Rev. Let. 20 (1968) 1392

9. M. Ivanovich et al., Nucl. Phys. A 110 (1968) 441

10. R.J. Spiger and T.A. Tombrello, Phys. Rev. 163 (1970) 964

11. L.S. Chuang, Nucl. Phys. A 174 (1971) 399

12. R.A. Harde Kopf et al., LA-6188 (1977)

13. R.E. Brown et al., BNL-NCS-21501 (1976)

14. R.E. Brown and Y.C. Tang, Phys. Rev. 176 (1968) 1235

15. L.M. Kuznetsova et al., Sov. Jour. Nucl. Phys. 13 (1971) 394

16. V.G. Neudatchin et al., Lettere al Nuovo Cimento 5 (1972) 834

17. F.C. Barker, Aust. Jour. of Phys. 25 (1972) 341

References for Total cross section measurements

No.	Author	Reference(*)	Year	Energy Range	Machine	No. of Points
18	JOHNSON+	PR 96 985	54	33-4150 keV	VDG	232
19	FARRELL+	68 WASH 153	68	44-646 keV	VDG	125
20	HIBDON+	68 WASH 159	68	10-1360 keV	VDG	704
21	FOSTER+	PR/C 3 576	71	2-15 MeV	VDG	237
22	GOULDING+	GOULDING 72	72	0.7-30 MeV	Linac	507
23	MEADOWS+	NSE 48 221	72	0.1-15 MeV	VDG	987
24	UTTLEY+	UTTLEY 74	74	0.07-7000 keV	Linac	3260
25	HARVEY+	75 WASH 244	75	0.025-10 MeV	Linac	185
26	KNITTER+	EUR-5726e	77	0.084-3 MeV	VDG	233

References for elastic scattering measurements

No.	Author	Reference(*)	Year	Energy Range	No. of Integrated values
27	VILLARD+	PR 101 765	56	210-300 keV	Only $d\sigma/d\theta$.
28	LANE+	AP 12 135	61	0.05-2.25 MeV	25
29	BATCHELOR+	NP 47 385	63	3.35-4.64 MeV	6
30	KNITTER+	EUR-3454e	67	1.0-2.3 MeV	14
31	HOPKINS+	NP/A 107 139	68	4.8-7.5 MeV	
32	ASAMI+	7OHELS 153	70	1.0-110 keV	1
33	DEMANINS+	INFN-73 2	73	2.0-4.7 MeV	8
34	HOLT+	NP/A 237 111	75	2.0-5.0 MeV	Analyzing power
35	KNITTER+	EUR-5726e	77	0.1-3.0 MeV	40

References for Li-6(n,α)t Measurements

No.	Reference(*)	Year	Author	Energy Range	Comments	No. of points
36	ANL-4515	50	BLAIR+	142-624 keV	relative to U-235(n,f)	13
37	PR 90 1049	53	DARLINGTON+	200-600 keV	only angular distribution	1

References for Li-6(n,α)t Measurements Cont/d

No.	Reference(*)	Year	Author	Energy Range	Comments	No. of points
38	PR 95 117	54	WEDDELL+	1.5 and 2.0 MeV	Nuc. emulsion, normalized 0.42b at 0.6 MeV	2
39	DOK 111 791	56	GORLOV+	9.1-730 keV	absolute	24
40	PR 103 741	56	RIBE.	0.88-6.52 MeV	absolute	10
41	PR 112 926	58	KERN+	12.6-17.9 MeV	absolute	23
42	PR 114 1580	59	BAME+	9.0-342 keV	Relative to U5(n,f) also $d\sigma/d\theta$.	29
43	PR 114 201	59	GABBARD+	0.025-4.07 MeV	Absolute value determined at 0.255 and 0.600 MeV	123
44	PR 115 1707	59	MURRAY+	1.20-7.93 MeV	relative to U8(n,f)	11
45	ZN/A 15 200	60	BORMAN.	2.5 and 14.1 MeV	relative to I-127(n,2n)	2
46	NP 63 593	65	SCHWARZ+	2.9-588 keV	Relative to H(n,p) for E>150 keV normalized 945 b at thermal	
47	AF 29 45	65	CONDE+	100 keV	absolute	1
48	66 WASH 763	66	BARRY.	25-100 keV	Normalized 950 b at 0.025 eV; standard U5(n,f)=577b at 0.025 eV	3
49	JNE 21 271	67	COX+	10.7-102 keV	absolute (absorption measur.)	7
50	ZFK-130 143	67	RENDIC+	2.7 and 14.4 MeV	Diff. sig. int. relative to H(n,p)	2
51	70 ANL 125	70	BECKER+	0.0253 eV	absorption = (944±19) barns	1
52	JNE 24 323	70	SOWERBY+	10 eV - 74 keV	relative to B-10(n,α)	86
53	NSE 40 12	70	MEADOWS+	0.0253 eV	absorption = (936±4) barns	1
54	70 HELS 1 253	70	FORT+	82-517 keV	absolute	40
55	71 KNOX 2 611	71	PHERSON+	10-287 keV	Peak normalized at 2.8 b; flux calibration with Pu-Be	31
56	AERE-7075	72	CLEMENT+	0.16-3.9 MeV	Normalized between 0.3-0.5 MeV on previous Uttley, Coates, Fort.	68
57	EANDC(E)-148	72	FORT+	0.021-1.7 MeV	absolute	118
58	NP/A 221 573	74	OVERLEY+	0.1-1.8 MeV	diff. sig. int.	25
59	COATES 74	74	COATES+	1.04-327 keV	Normalized at $149.5/\sqrt{E}$ in the range 1.5-10 keV	159
60	ZP 268 359	74	POENITZ.	91 keV - 1.50 MeV	Normalized to absolute meas. by the same author	67
61	INT 7011	74	FRIESENHAHN+	1.03 keV - 1.7 MeV	Relative to (n,p) scatt.; normalized $148.9/\sqrt{E}$ in 3.5-4.5 keV	331
62	BAP 20 163	75	BARTLE.	2.16-9.66 MeV	absolute	24
63	75 WASH 236	75	STEPHANY+	964 keV	absolute	1
64	75 WASH 240	75	SHRODER+	25 keV	angular anisotropy	
65	LAMAZE 76	76	LAMAZE+	3.34-945 keV	relative to (n,p) scattering	88
66	76 LOWELL 1340	76	RAMAN+	0.5 eV - 25 keV	angular anisotropy	

References for Li6(n,α)t Measurements Cont/d

No.	Reference(*)	Year	Author	Energy Range	Comments	No. of points
67	GAYTHER 77	77	GAYTHER+	3-809 keV	Relative to U-235(n,f); U5(n,f) from Sowerby evaluation	
68	EUR-57262	77	KNITTER+	85-500 keV	calculated from σ_T and σ(n,n)	
69	FORT	77	FORT+	82-517 keV	Helsinki values re-evaluated	

(*) See the codes for references in CINDA 76/77; the name followed by the year corresponds to a private communication.

TABLE I

COMPARISON BETWEEN THE Li-6 EXPERIMENTAL TOTAL CROSS SECTIONS

The values given are the ratio to the DIMENT and UTTLEY values

ENERGY RANGE (MeV)	JOHNSON ORL,1954	FARREL DKE,1968	HIBDON ANL,1968	FOSTER BNW,1971	MEADOWS ANL,1972	GOULDING RPI,1972	KNITTER GEL,1974	HARVEY ORL,1975
0.06-0.08		1.018	1.00					1.022
0.08-0.10		1.047	1.018				1.000	1.059
0.10-0.12		0.968	1.003		1.065		0.974	1.000
0.12-0.50	0.967	0.979	1.003		1.033		1.020	1.007
0.50-1.0			1.042		1.053			0.989
1.0-1.5	1.143				1.037	1.060		1.033
1.5-2.0	1.031					1.059		1.043
2.0-2.5	1.025					1.041		1.016
2.5-3.0	1.073			1.054		1.060		1.033
3.0-3.5	1.005			1.010		1.024		1.006
3.5-4.0	0.979			0.996		1.017		0.986
4.0-4.5				1.002		1.020		1.013
4.5-5.0				0.995		1.010		0.993

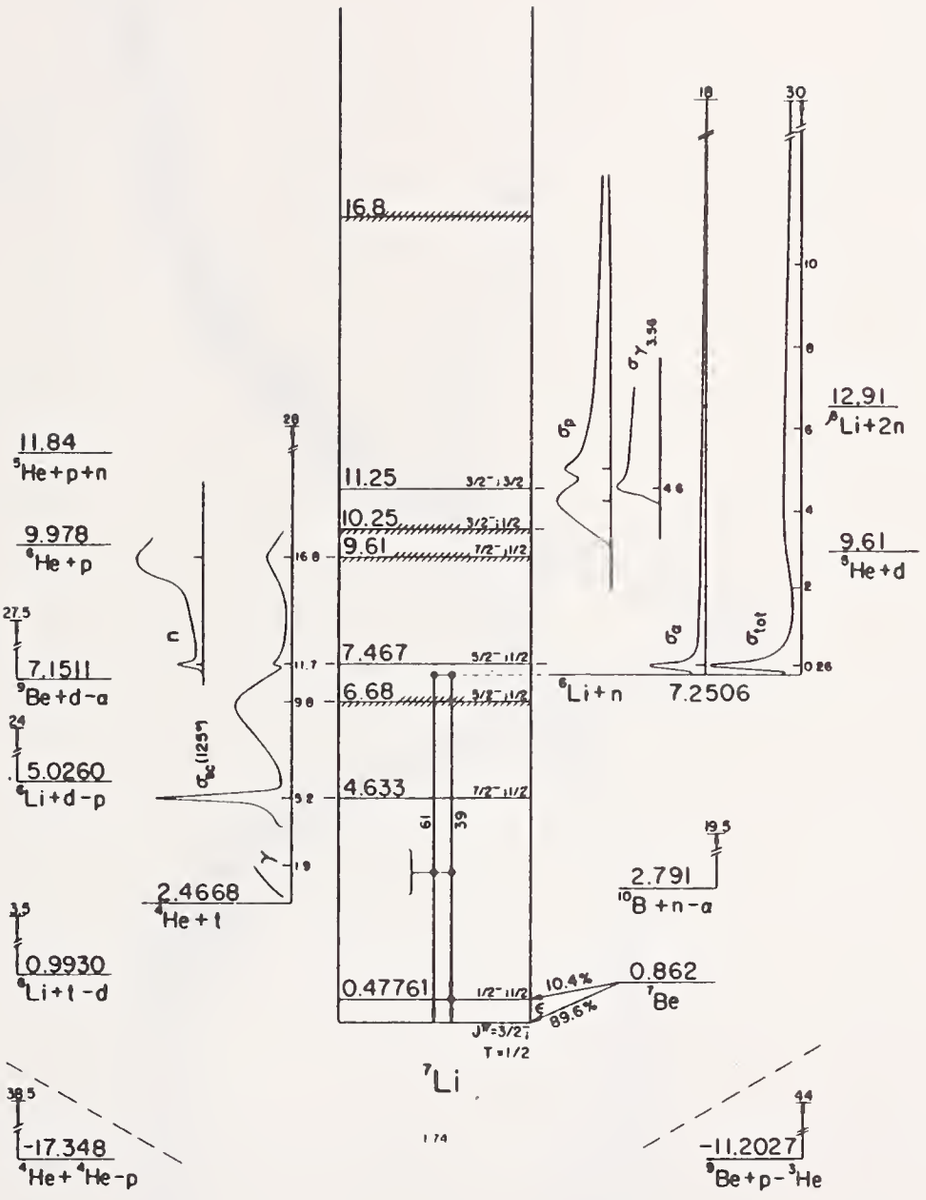

Figure 1 Energy levels of the Li-7 System (From F. Ajzenberg-Selove (4)).

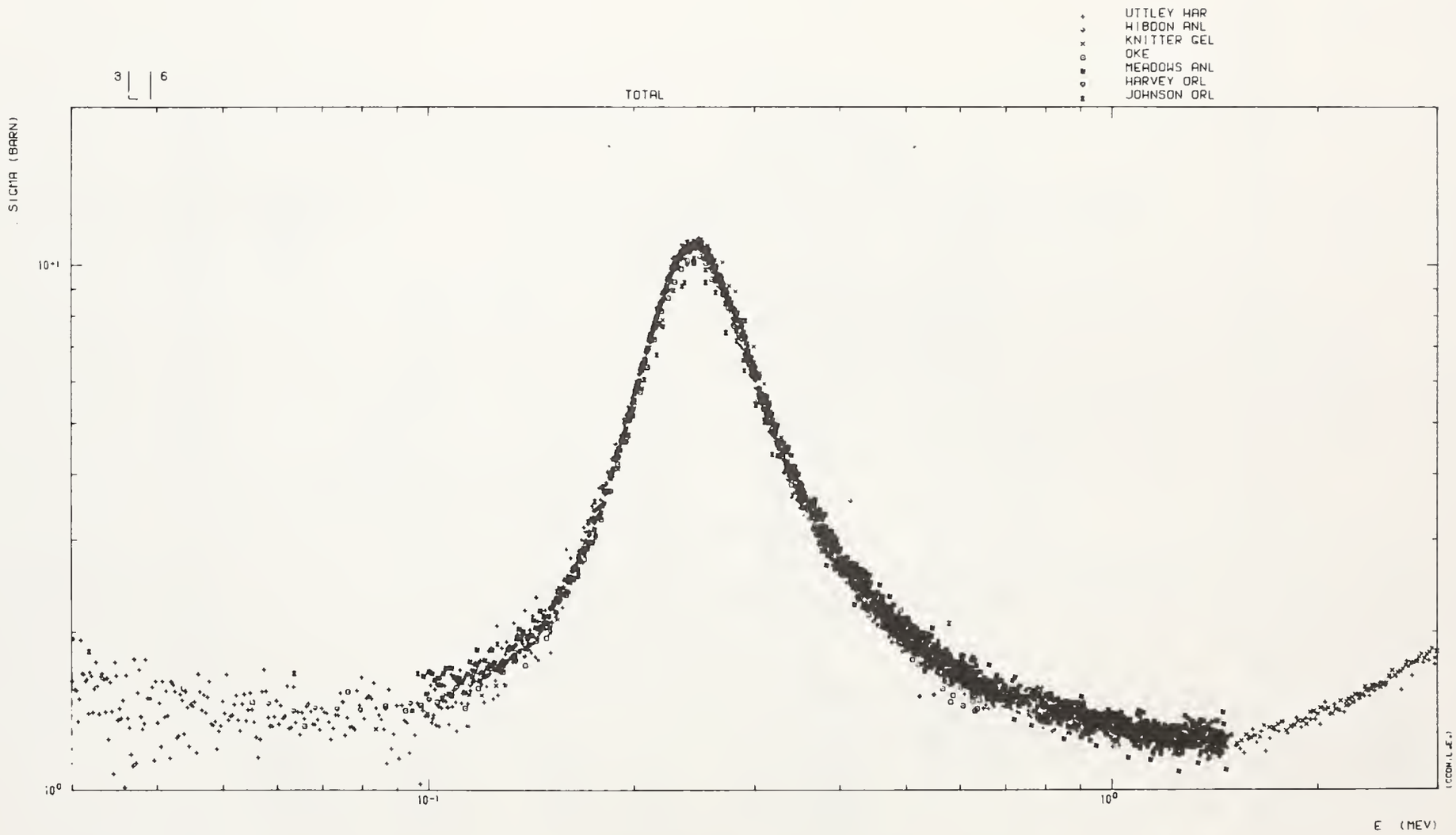

Figure 2 Li-6 total neutron cross sections in the energy range 10 keV - 3 MeV.

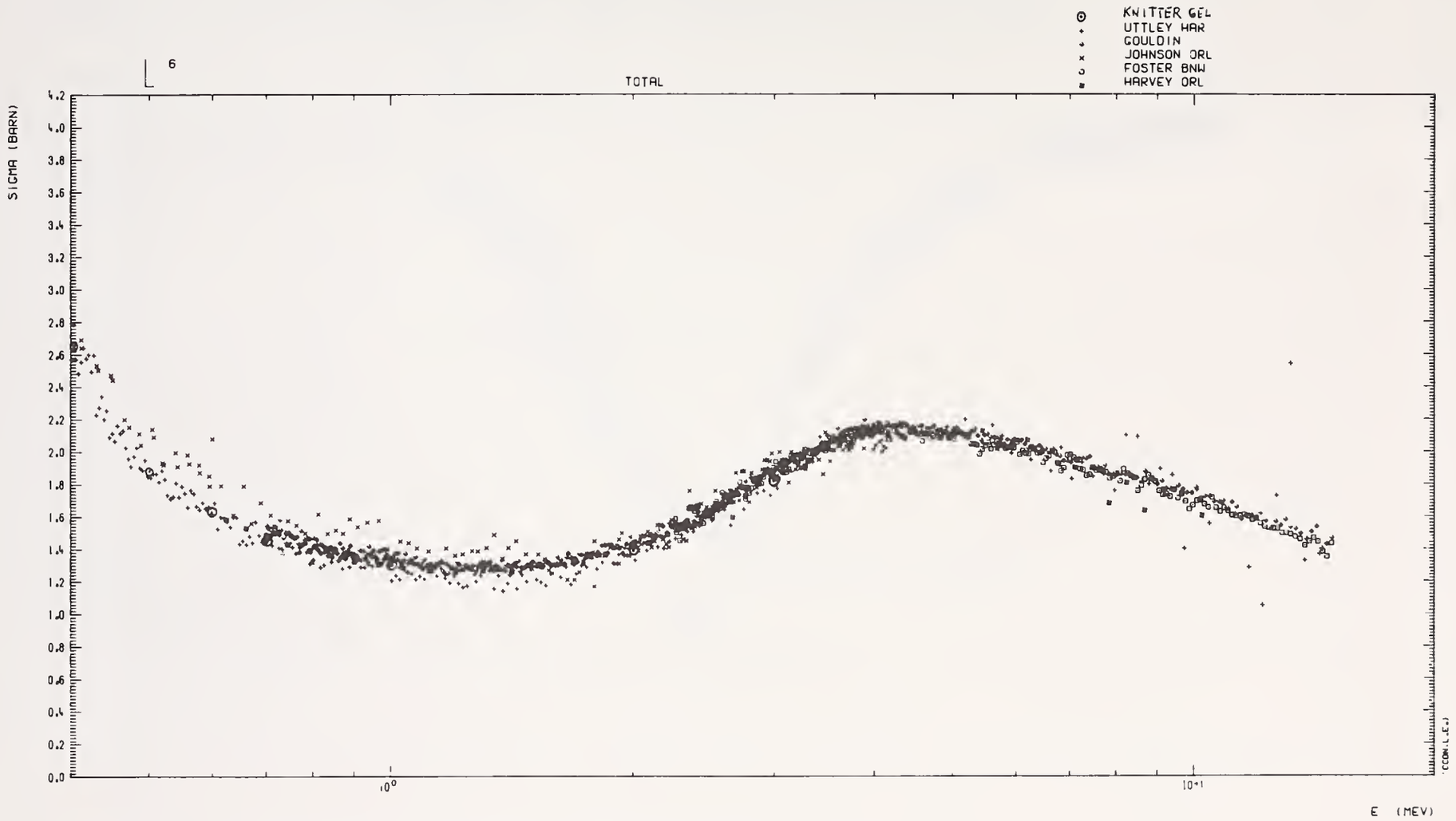

Figure 3 Li-6 total neutron cross sections in the energy range 0.5 - 15 MeV.

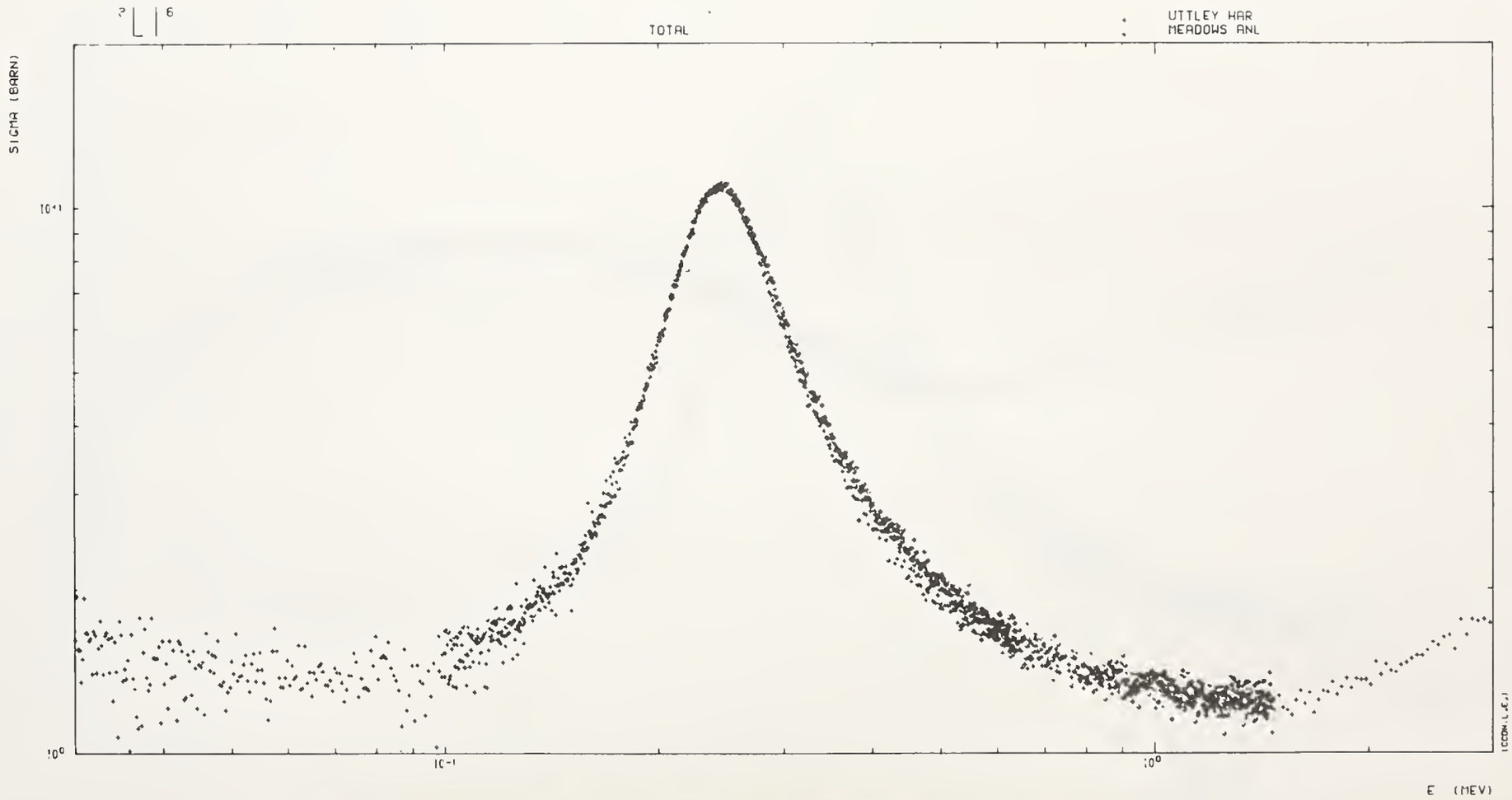

Figure 4 Li-6 total neutron cross sections : UTTLEY and MEADOWS results over the resonance.

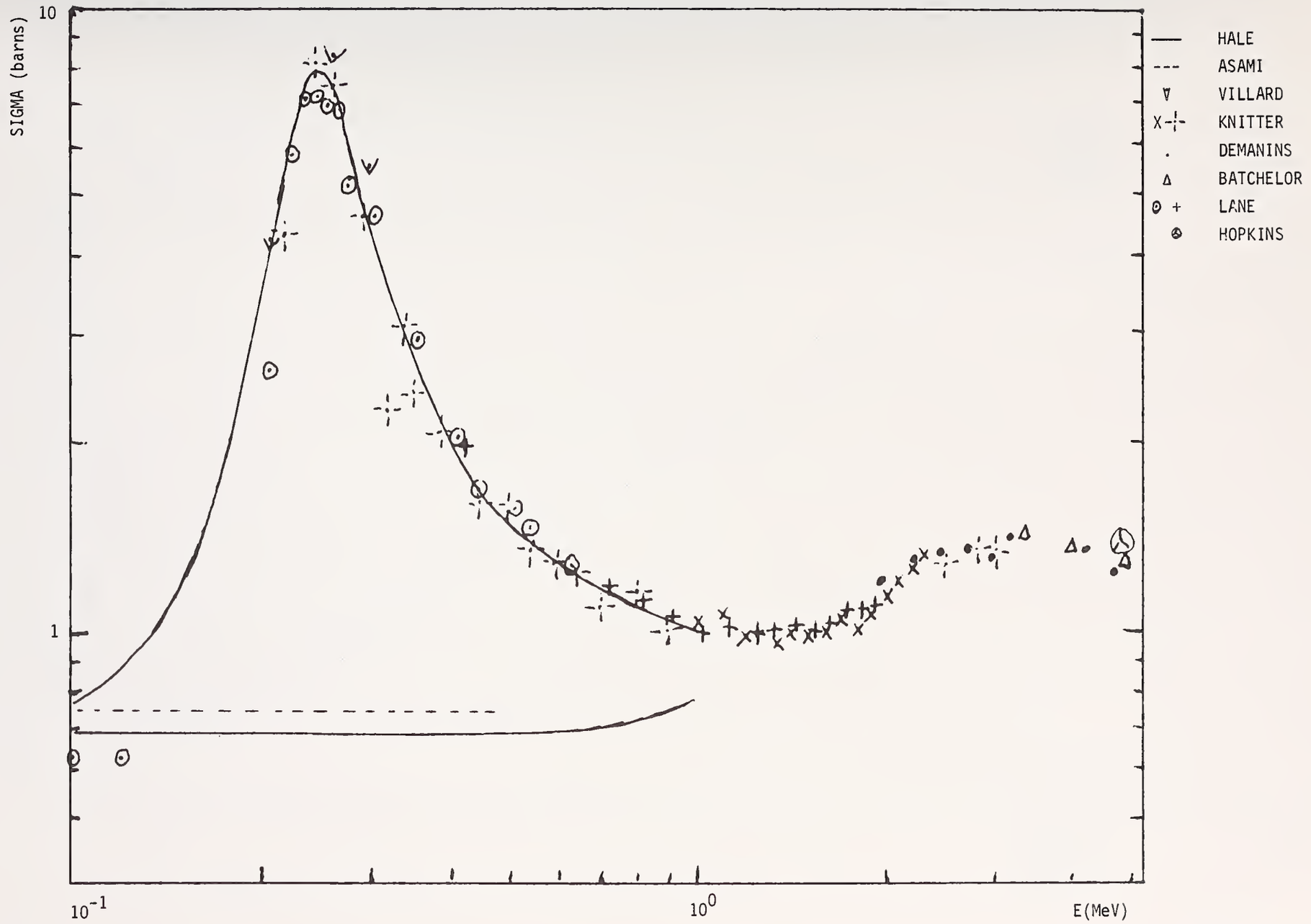

Figure 5 **Li-6 neutron** scattering cross section. The lines at the lower end of the figure represent the results of ASAMI and HALE between 10 and 100 keV.

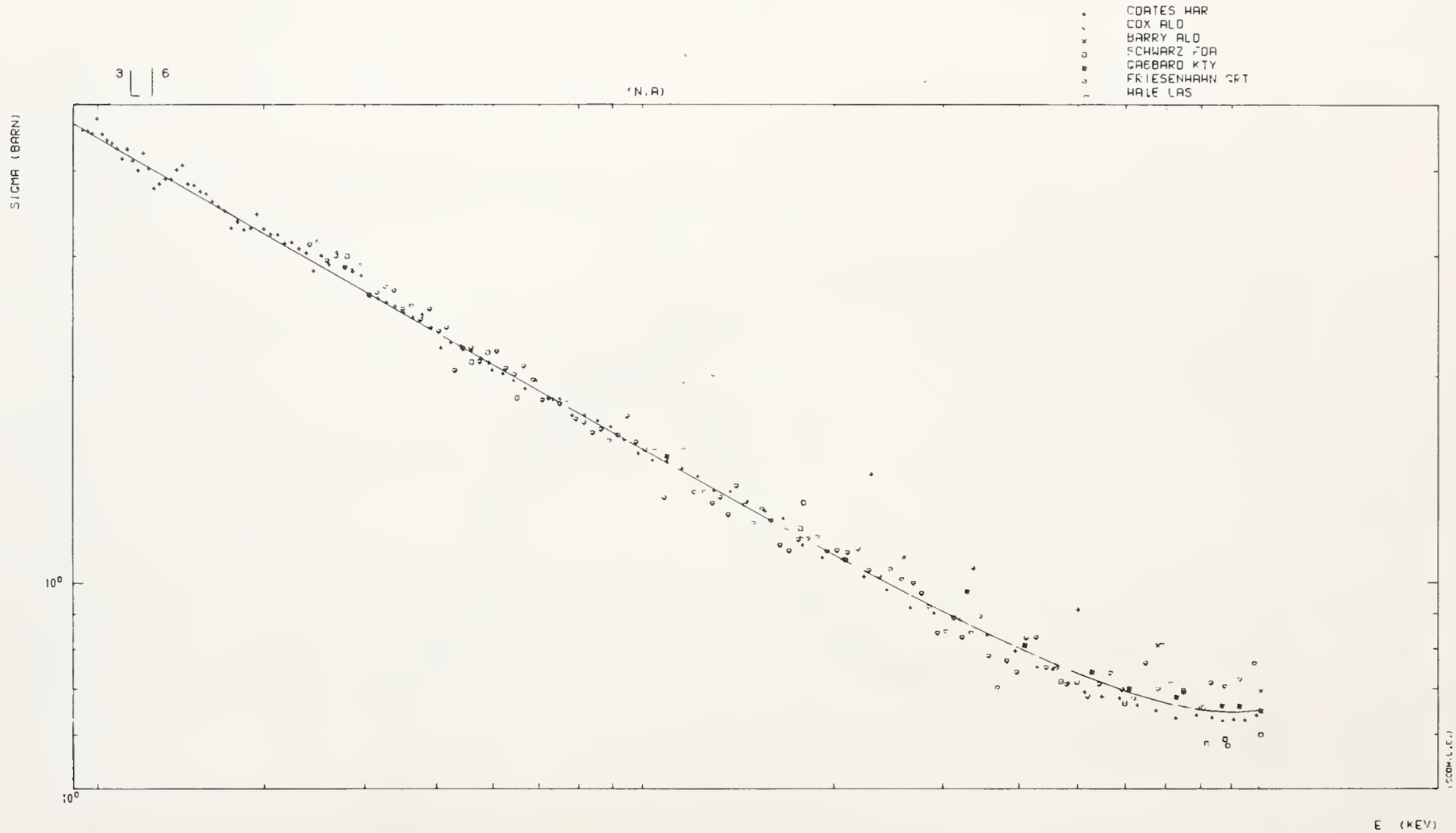

Figure 6 Li-6(n,α) cross sections in the energy range 1 - 100 keV.

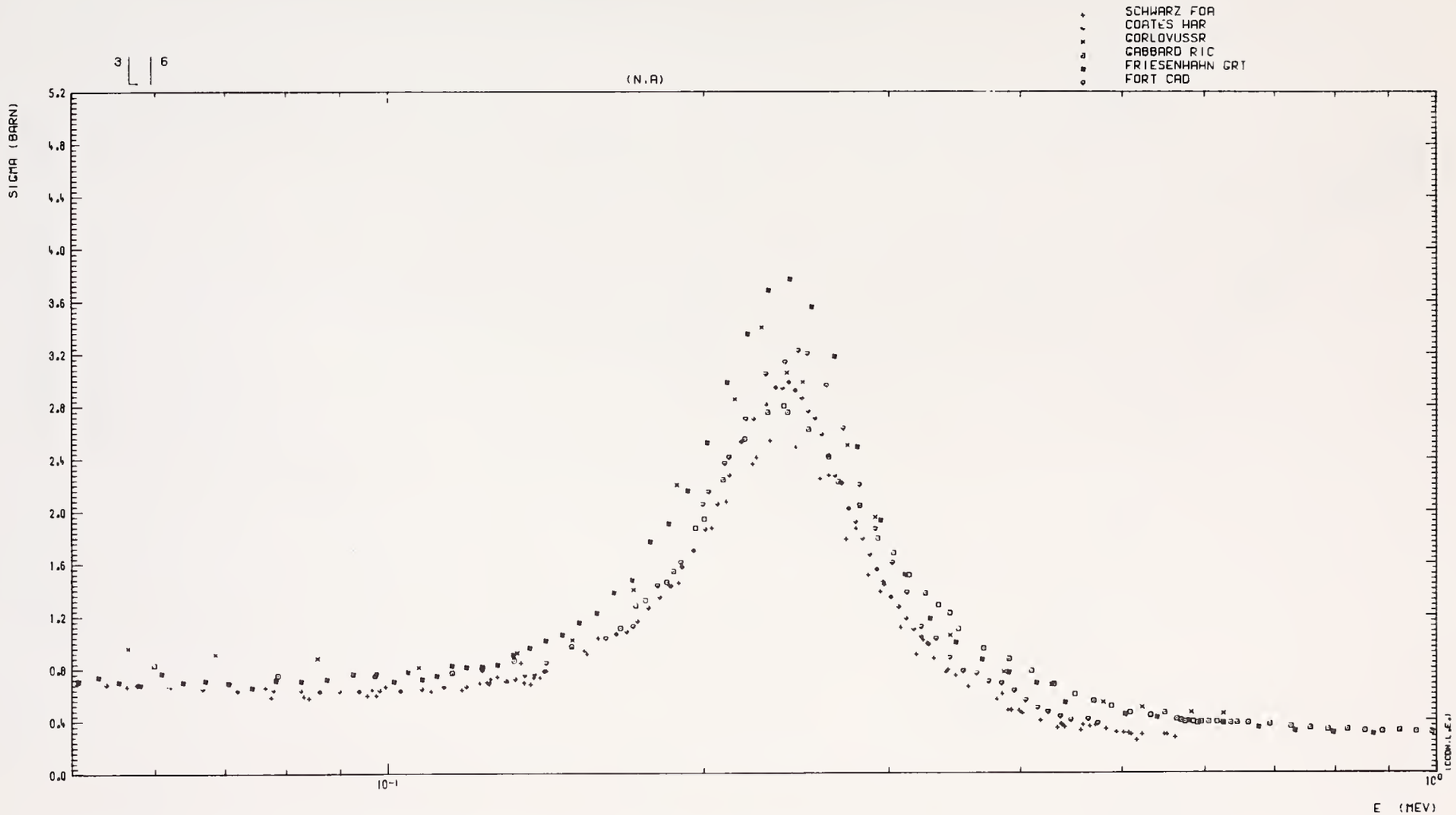

Figure 7 Li-6(n,α) cross sections in the energy range 0.05 - 1.00 MeV.

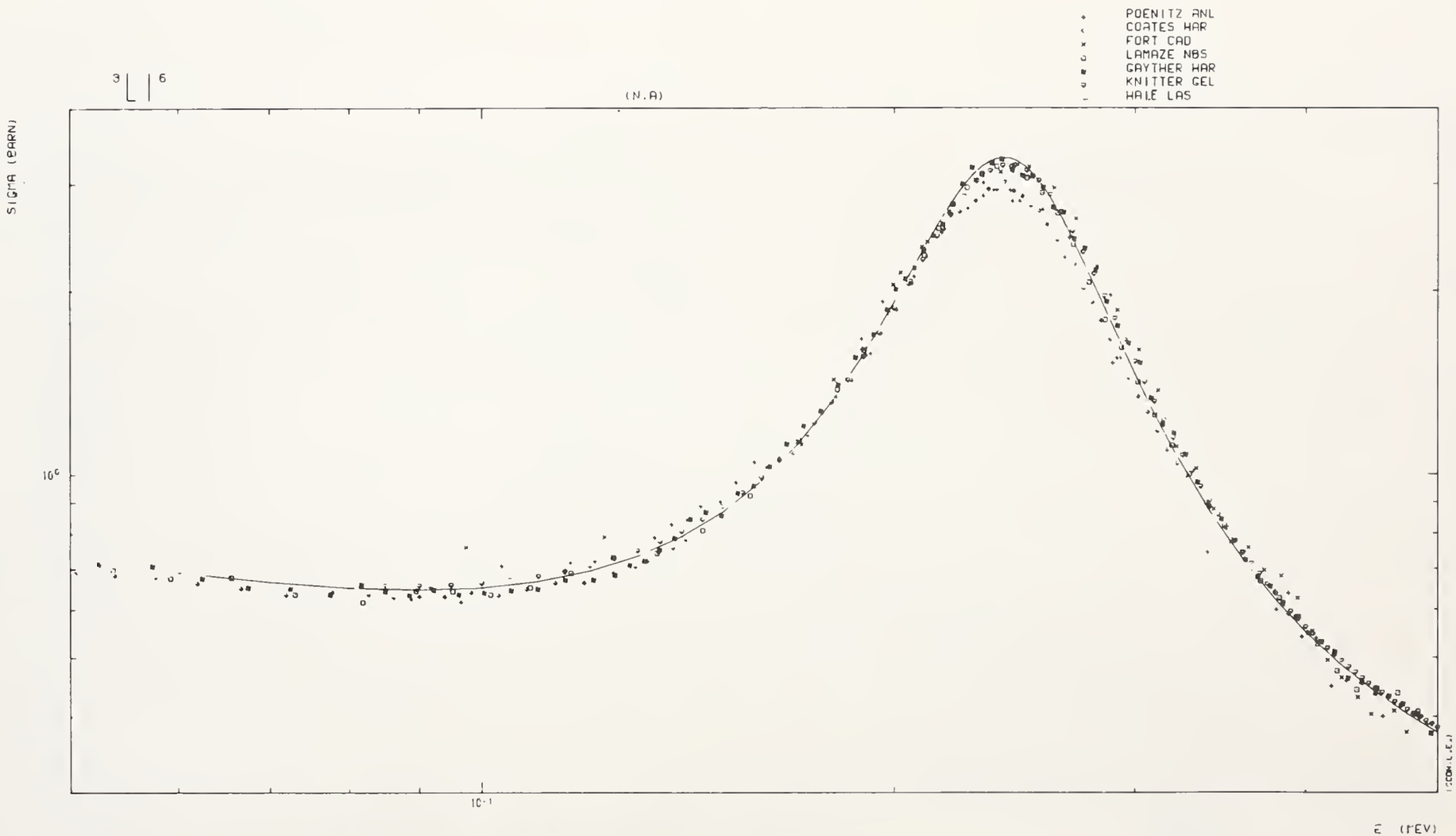

Figure 8 Li-6(n,α) cross sections; recent measurements and evaluations.

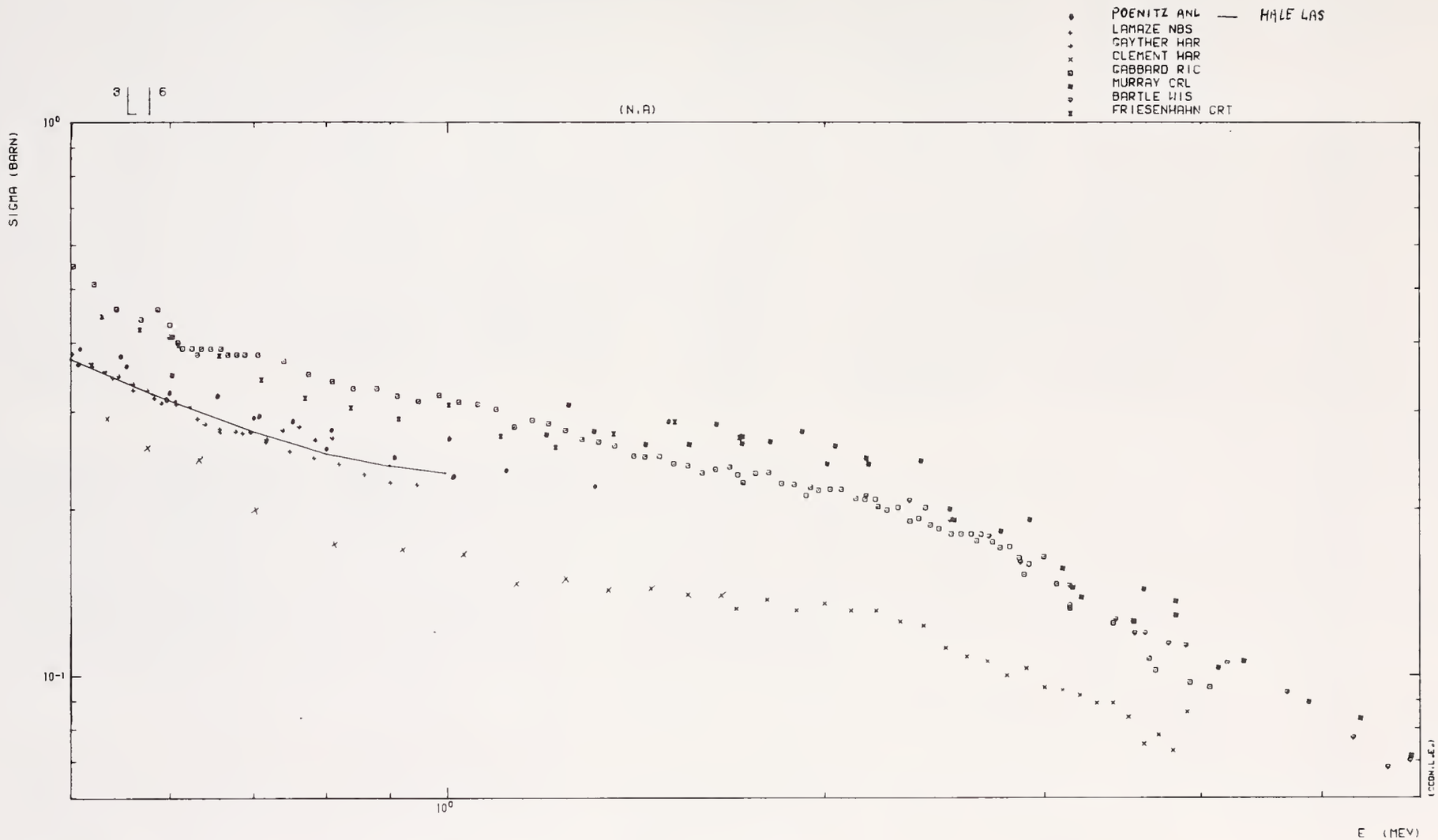

Figure 9 Li-6(n,α) cross sections in the energy range 0.5 - 6.0 MeV.

R-MATRIX ANALYSIS OF THE ^{7}Li SYSTEM*

G. M. Hale
Los Alamos Scientific Laboratory, University of California
Theoretical Division
Los Alamos, New Mexico 87545

ABSTRACT

We describe a multichannel, multilevel, R-matrix analysis of reactions in the ^{7}Li system which was used to provide the ENDF/B-V neutron cross sections for ^{6}Li at low energies. Resonance parameters obtained from the R-matrix levels are presented. Various features of the data are interpreted in terms of these resonances.

(^{7}Li System; ^{6}Li(n,t); R-Matrix; resonance parameters; standard)

Introduction

Discrepant measurements is a problem one almost always faces in the evaluation of neutron cross sections, but in the case of a standard cross section, the problem intensifies the difficulty of obtaining evaluated cross-section values of the desired accuracy. However, one knows from general considerations of nuclear reaction theory that the standard cross section is linked by unitarity to data for other reactions in the same compound system, and thus one has the prospect of reducing the uncertainty of the evaluated standard cross section by analyzing it simultaneously with these other data in a unitary framework. R-matrix theory[1] is a particularly appropriate unitary framework for such analyses, as was discussed in Ref. 2.

We have used multichannel, multilevel R-matrix analyses of reactions in the ^{7}Li system to provide evaluated cross sections for the neutron-induced reactions on ^{6}Li at low energies for versions IV and V of the Evaluated Nuclear Data File (ENDF/B). At the time of the version IV analysis,[2,3] the data set dominating the fit was the neutron total cross section measurement from Harwell,[4] both because of its quoted precision and number of points. The resulting ^{6}Li(n,t) cross section (the "standard" in this system) was not much different from that obtained in Version III, which had been largely based on the Harwell measurement.

The value of the calculated ^{6}Li(n,t) cross section at the peak of the 240 keV resonance was 3.5 b, some 16% higher than the value indicated by a contemporary group of direct measurements.[5-7] However, we noticed, as had the Harwell group, that unitary constraints forced the total cross section unacceptably high above Diment's measurements in the peak when the (n,t) cross section was lowered to better agree with the direct measurements. It is emphasized that this discrepancy between the cross section measurements was indicated by attempts to fit them unitarily. The common practice of evaluating the total and (n,t) cross sections separately, then obtaining the elastic cross section by subtraction, would not necessarily have signaled a problem.

We noticed in performing the Version IV analysis that in addition to this strong unitary link to the total cross section in the region of the resonance, the (n,t) cross section was also quite sensitive to the differential cross section for t + α elastic scattering. At that time, however, measurements of this cross section[8] had not been made with accuracy comparable to that of the Harwell total cross section measurements. Precise measurements of the t + α differential cross section[9] were later made at Los Alamos, and these were incorporated in the analysis, along with new measurements of the total cross section from Oak Ridge.[10] Preliminary results of this analysis, reported at the Conference on Nuclear Cross Sections and Technology[2] two years ago, indicated the effect of the new data was to lower the calculated (n,t) cross section in the peak of the resonance (to 3.4 b) and raise the calculated peak total cross section (to 11.1 b). This trend has continued in subsequent analyses, including that used recently to provide ENDF/B-V neutron cross sections for ^{6}Li at energies below 2 MeV.

The Version V analysis will be described briefly in the following section, indicating the types of data included, and the fits obtained to representative data sets from each reaction. The third section presents resonance parameters corresponding to R-matrix levels required for the fit, and the concluding section discusses the interpretation of specific features in the data for reactions in the ^{7}Li system in terms of these resonances.

Version V Analysis

The 3 arrangement channels considered in this analysis were t + ^{4}He, n + ^{6}Li, and n + ^{6}Li* (2.18). Various quantities specifying the channel configuration are given in Table I.

TABLE I

Channel Configuration for ^{7}Li Analysis

Arrangement	Channel Radius	ℓ_{max}	Channel Spins(s)
t + ^{4}He	4.02 fm	5	1/2
n + ^{6}Li	4.20 fm	1	3/2, 1/2
n + ^{6}Li*	4.50 fm	1	7/2, 5/2

Data for all possible reactions were considered at triton energies below 14 MeV, and at neutron energies below 2 MeV. Although specific references to all the data included will not be given, the different types of data analyzed for each reaction are listed in Table II.

TABLE II

Types of Data Included in ^{7}Li Analysis

Reaction	Total Cross Section	Reaction Cross Section	Integrated Cross Section	Differential Cross Section	Polarization
^{4}He(t,t)^{4}He				X	X
^{6}Li(n,t)^{4}He			X	X	
^{6}Li(n,n)^{6}Li			X	X	X
α + t		X			
n + ^{6}Li	X				

*Work performed under the auspices of the United States Energy Research and Development Administration.

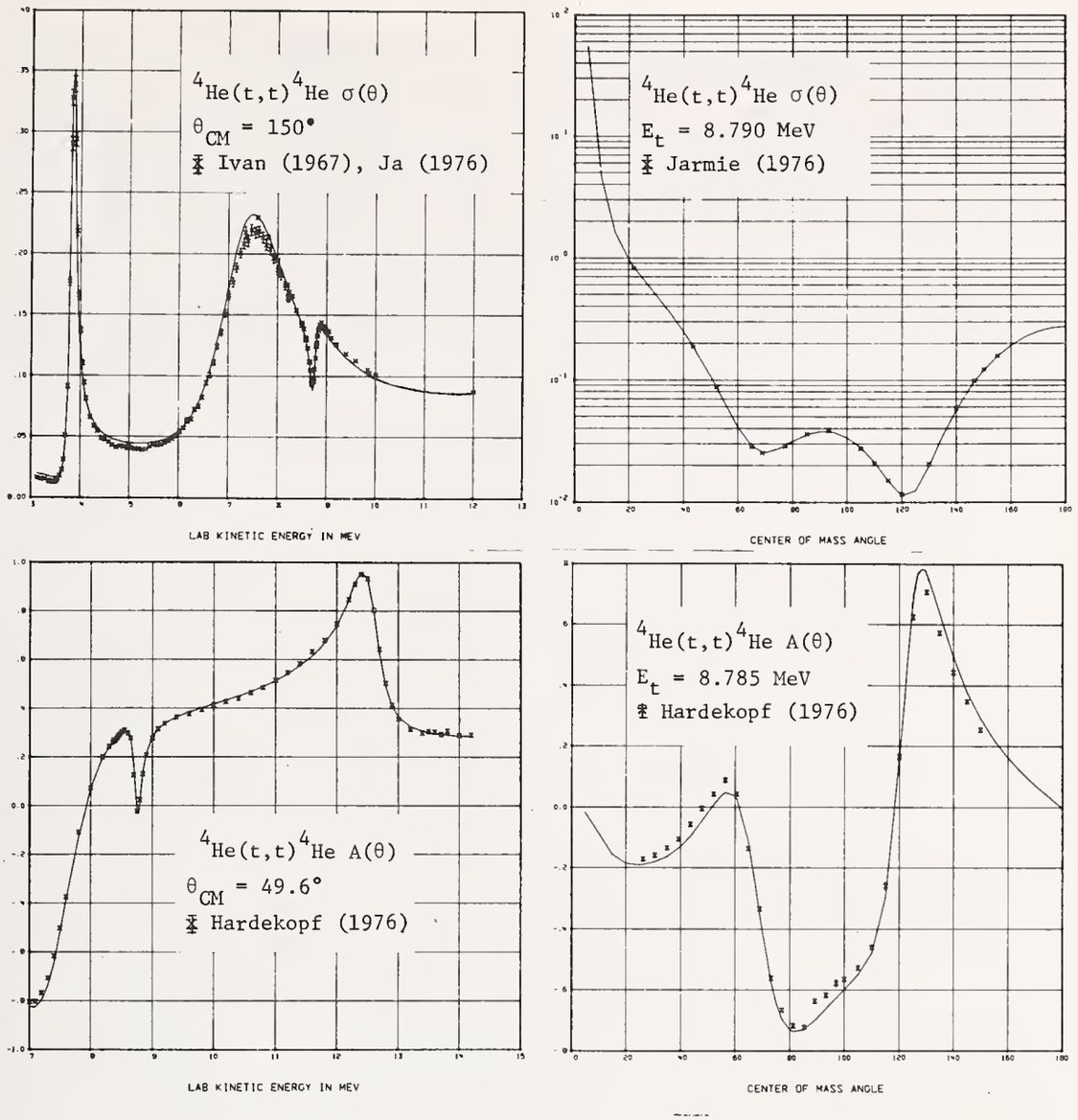

Fig. 1. Calculated and measured observables for ^{4}He(t,t)^{4}He. The cross section data are from Refs. 9 and 12; the analyzing power data are from Ref. 13.

The data were fitted in the usual least-squares sense by the R-matrix analysis code EDA.[11] Renormalizations and energy shifts were allowed for some of the data sets; in these cases, the deviations from the original experimental scales contributed to the overall χ^2 of the fit.

The resulting fits to some of the t + α elastic scattering measurements are shown in Fig. 1. Anomalies occurring in the differential cross section and analyzing power excitation curves (left side of the figure) at triton energies of approximately 3.9, 7.3, 8.8, and 12.4 MeV correspond to the first 4 resonances in ^{7}Li above the t + α threshold. Parameters for these resonances, which have total angular momentum and parity (J^P) assignments of $7/2^-$, $5/2^-$, $5/2^-$, and $7/2^-$, respectively, are given in the next section. The third resonance is the $J^P = 5/2^-$ level which shows up prominantly in the neutron cross sections at E_n = 250 keV. Angular distributions of the cross section and analyzing power are shown on the right side of the figure at triton energies close to this resonance. The low-energy measurements of the cross-section excitation are those of Ivanovich,[12] while those at overlapping energies and higher are of Jarmie.[9] The calculated curve follows the newer, more precise Jarmie data in the region of the overlap. The differential cross section data shown are also those of Jarmie,[9,13] while the analyzing power excitation and angular distributions were measured by Hardekopf.[13]

Figure 2 compares the R-matrix calculation with selected data for the ^{6}Li(n,t)^{4}He reaction. On the left are shown recent measurements[14] of the ^{6}Li(n,t) cross section over the $5/2^-$ resonance at center-of-mass angles of 0 and 180°. These measurements became available after the Version V analysis was completed, so that the curves represent a prediction, rather than a fit. The right side of the figure shows the fits to Overley's measurements[15] of the ^{6}Li(n,t) angular distributions at E_n = .1 and 1.0 MeV. The pronounced asymmetry in the cross section evident at 100 keV persists down to energies as low as 25 keV.[16] These low-energy asymmetry effects in the cross section are well reproduced by the calculations, and can be explained in terms of resonance interference, as discussed in the concluding section.

Representative fits to the ^{6}Li(n,n)^{6}Li angular distributions measured by Lane[17] and Knitter[18] are shown in Fig. 3. The Lane angular distributions required substantial renormalizations at energies near the peak of the 240 keV resonance, with the result that our calculated integrated elastic cross section lies somewhat above Lane's points over the peak. This agrees with recent results of Knitter[19] for the elastic cross sec-

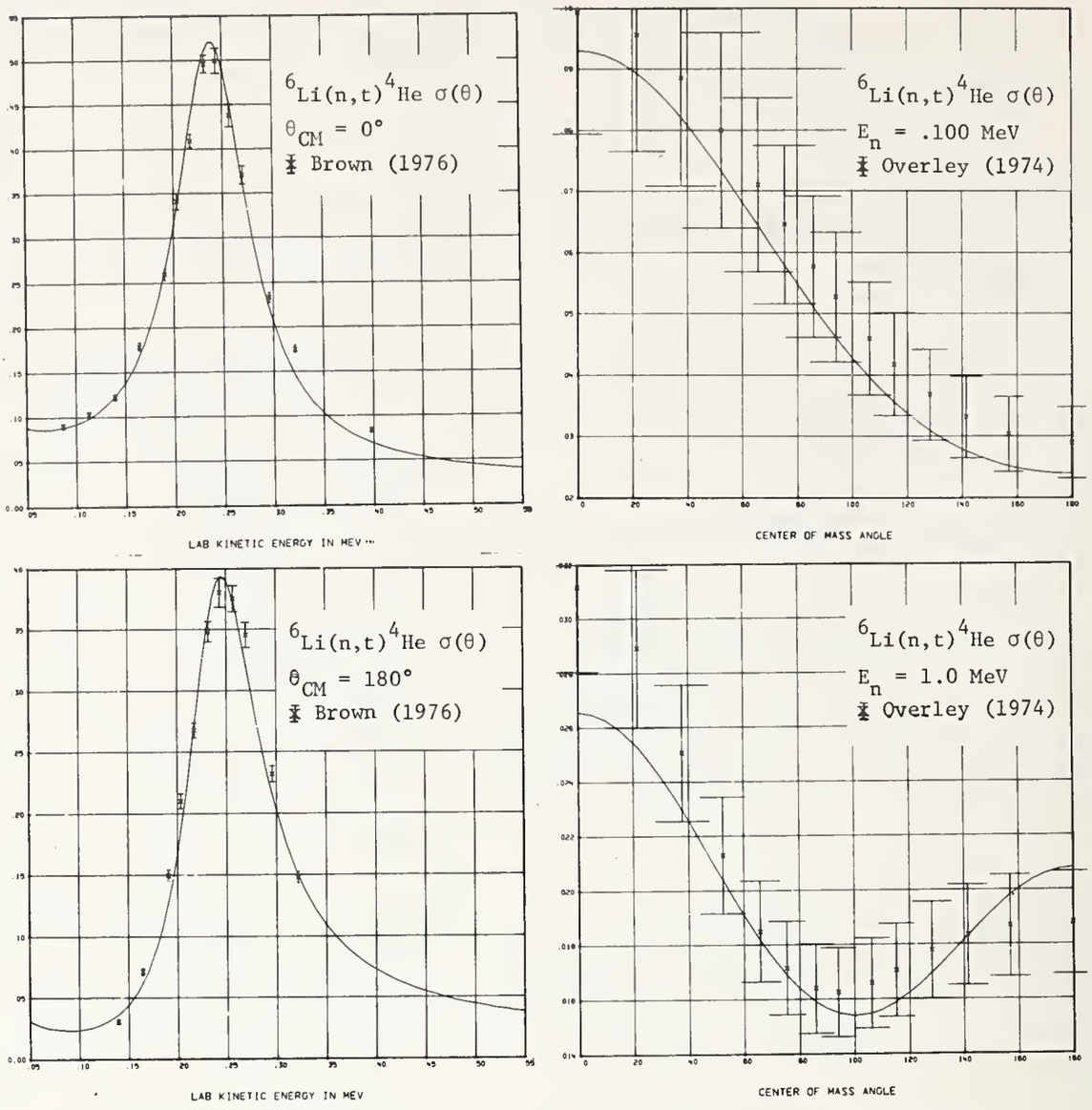

Fig. 2. Calculated and measured observables for ^{6}Li(n,t)^{4}He. Data for the excitation curves are from Ref. 14. Data for the angular distributions are from Ref. 15.

tion over the resonance. Calculated values of the polarization (not shown) for elastically scattered neutrons also agree well with measurements by Lane. [20]

Figure 4 shows the fits to the total cross sections of primary interest in this discussion, the neutron total and ^{6}Li(n,t) integrated cross section. Of course, the latter cross section is the standard and is, at that, only recommended for use at energies below the 240 keV resonance. But because of the strong influence of the resonance on the ^{6}Li(n,t) cross section as it begins to deviate from 1/v behavior (at about 20 keV), and because of the close unitary connection (already mentioned), it has with the neutron total cross section, an isolated discussion of the standard cross section would not suffice.

We see that the calculated ^{6}Li(n,t) cross section is generally in very good agreement with recent measurements made at the National Bureau of Standards [21] (NBS) up to ~600 keV. In the region of the resonance, the calculated cross section has come down by roughly half the difference between the Version IV results and the earlier direct measurements, [5-7] and still exceeds the NBS data by about 2.5% in the peak of the resonance. The data shown are those that were used in the analysis. Corrections to the data since that time have raised the experimental values in the minimum around 90 keV to agree even better with the calculation, but have reduced somewhat the experimental values in the peak. The largest uncertainty of the calculated cross section in the standards region (below 150 keV) occurs in the vicinity of the 90 keV minimum. At lower energies, the thermal value of 935.9 b is in excellent agreement with Meadows' value, [22] and the cross section is quite consistent with Sowerby's ratio measurements [23] below 80 keV, when considered in conjunction with the Version V ^{10}B(n,α) cross section.

The calculated total cross section agrees well with measurements of Diment [4] and Harvey, [10] except for a systematic tendency to overshoot the experimental values in the peak of the resonance and undershoot them in the preceeding minimum. These differences are of the order of 2-6%, and may be within the bounds of realistic uncertainties on the total cross sections in these regions, if not within the stated errors. The energy scale of these total cross section measurements [4,10] essentially determined the position of the 5/2$^-$ resonance, with the calculated peak total cross section occurring at 245 keV, and the calculated peak (n,t) cross section at 240 keV, in agreement with most of the measurements using time-of-flight neutron energy determination.

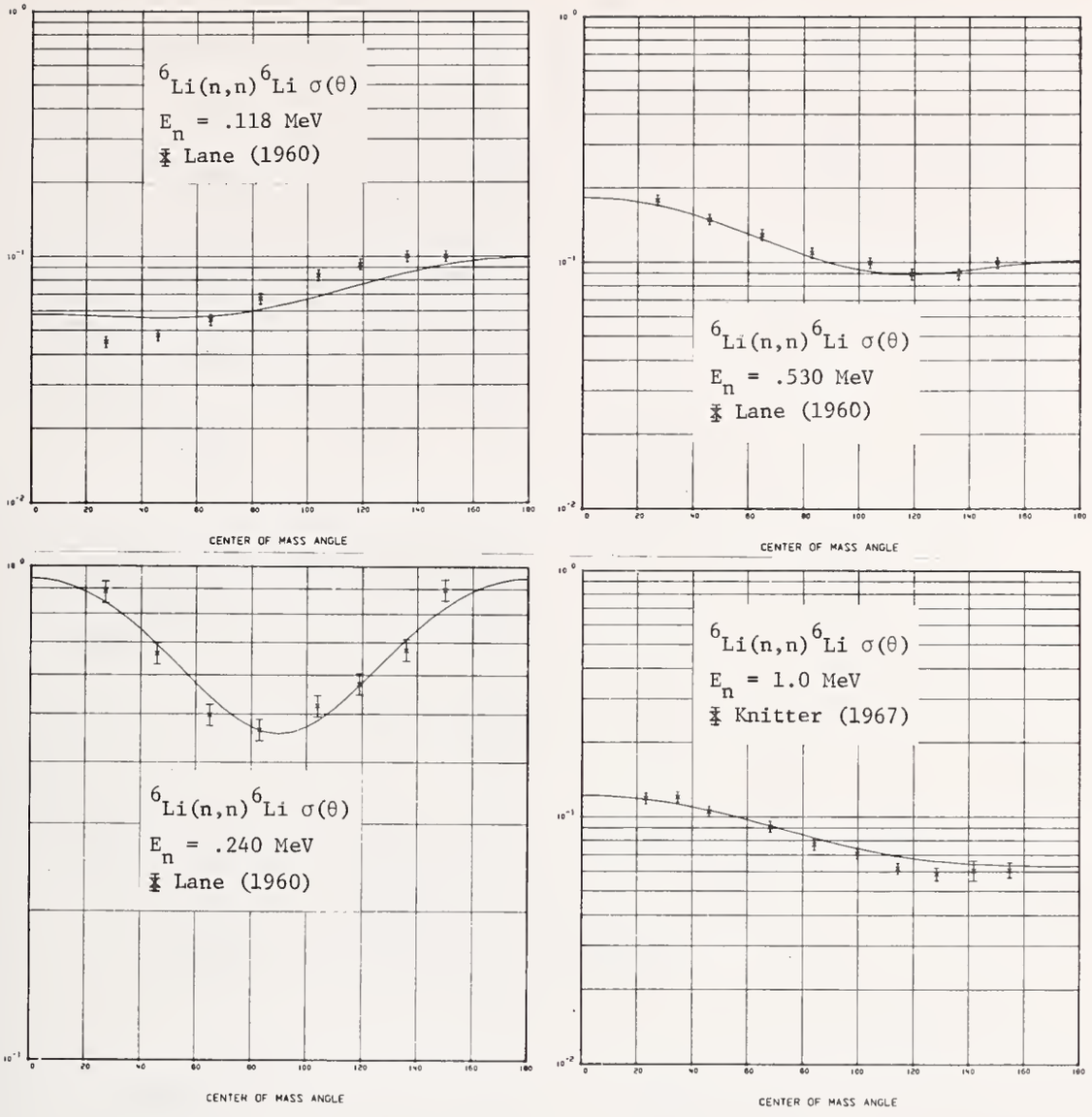

Fig. 3. Calculated and measured angular distributions for ^{6}Li(n,n)^{6}Li. The data are from Refs. 17 and 18.

Resonance Parameters

Since experimental data for nuclear reactions are most directly related to matrices (such as the S-matrix) of amplitude ratios for asymptotic wavefunctions, it is appropriate that resonance parameters for asymptotic measurements be related to the poles and residues of such matrices. The R-matrix is not, of course, an asymptotic quantity, and its poles and residues depend on the boundary conditions imposed at the nuclear surface to define the R-matrix, and upon the channel radii which define the nuclear surface. However, one can always transform the R-matrix to an asymptotic form having poles and residues which, although energy-dependent, no longer depend on boundary conditions at the nuclear surface, or upon radial distances outside that surface.[24]

We choose the asymptotic form to be the S-matrix so that our specification of resonance parameters corresponds with the prescription given by Humblet.[25] The transformed R-matrix in that case has the form

$$R_L = \sum_\mu \frac{g_\mu g_\mu^T}{E_\mu - E} \quad ,$$

where the g_μ and E_μ are known, complex (energy-dependent) functions of the parameters $\gamma_\lambda, E_\lambda$ of the original R-matrix. If, for some complex energy E_0,

$$E_\mu(E_0) - E_0 = 0 \quad ,$$

then E_0 is a pole of R_L and thus, of the S-matrix as well. The resonant energy and total width associated with the pole are

$$E_R = R_e(E_0)$$

$$\Gamma = -2\ \mathrm{Im}(E_0),$$

while the partial widths are given by

$$\Gamma_c = \Gamma \frac{|g_{\mu c}(E_0)|^2 P_c(E_0)}{\sum_c |g_{\mu c}(E_0)|^2 P_c(E_0)} \quad ,$$

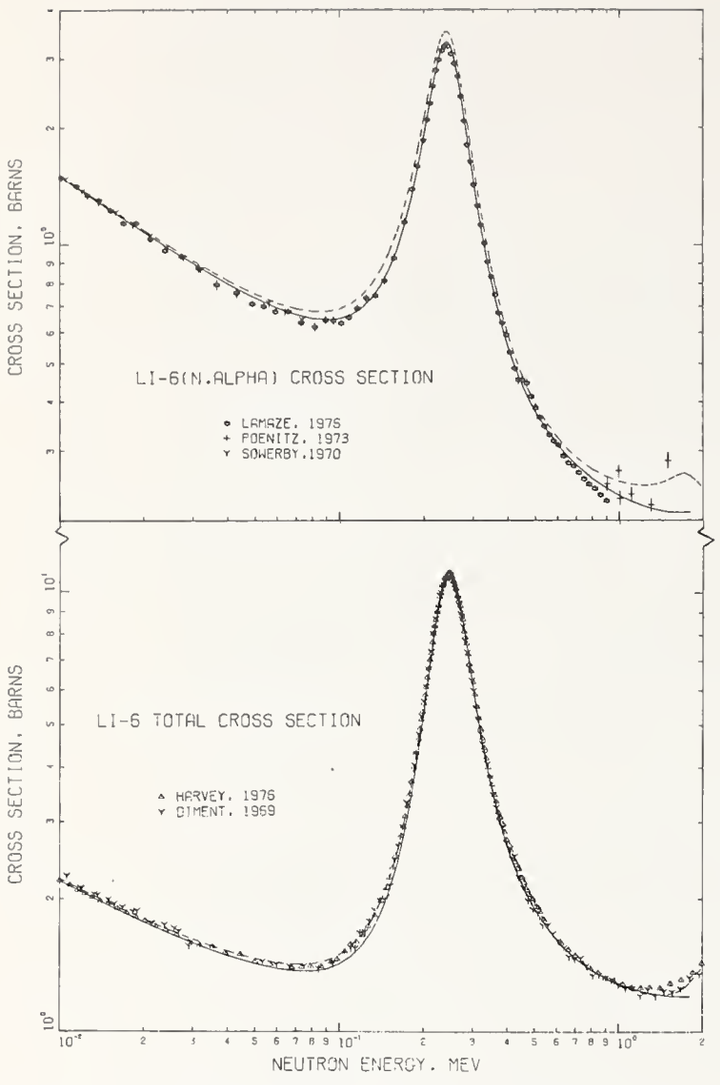

Fig. 4. The $^{6}Li(n,t)^{4}He$ integrated cross section and n + ^{6}Li total cross section for E_n between .01 and 2 MeV. The solid curves are the ENDF/B-V results, and the dashed curves are ENDF/B-IV. Data for the upper curve are from Refs. 5, 21, and 23; data for the lower curves are from Refs. 4 and 10.

with

$$P_c(E_0) = \frac{Re(\rho_c)}{|O_c|^2} \quad ,$$

where ρ_c is the product of the channel radius with the channel wave number, and O_c is the channel outgoing-spherical-wave function, all evaluated at the complex energy E_0.

Resonance parameters obtained in this way from the Version V R-matrix parameters are presented in Table III, along with widths and resonance positions from F. Selove's latest compilation for ^{7}Li.[26] The first 4 resonances listed are those visible in the excitation curves shown in Fig. 1. The agreement of our calculated parameters for those resonances with values taken from the compilation[26] is satisfactory, although not always within the errors assigned by Selove.

The last two resonances lie above the highest energy at which experimental data were included, and their parameters are therefore quite uncertain. They do correspond roughly with the levels found by Holt et al.[27] in their analysis of n + ^{6}Li elastic polarizations at neutron energies between 2 and 5 MeV, except that our calculated widths are somewhat narrower.

It should be mentioned in this connection that the prescription we use can result in resonance parameters that are quite different from those obtained from the usual expressions[28] relating R-matrix parameters to external widths and resonance positions at real energies. This is particularly true at higher excitation energies, where the complex pole prescription tends to give smaller widths which appear to correspond more closely with the widths of the experimentally observed anomolies. We also note that the complex poles and partial widths defined above are formally radius-independent in the external region, while those resulting from the usual R-matrix relations are not.

Conclusions

This analysis indicates that many of the features observed in the measurements for reactions in the ^{7}Li system can be interpreted in terms of the resonances identified. In addition to the obvious structure in the cross sections and polarizations due to the presence of the first 4 levels above the t + α threshold, one can ascribe the behavior of the low-energy $^{6}Li(n,t)$ cross section to broader, more distant states. Near-background levels having $J^P = 1/2^+$ (one of which may be associated with the broad structure at E_x = 16.8 MeV in ^{7}Li), and the broad $3/2^+$ resonance tentatively identified in this analysis seem to be mainly responsible for the large 1/v integrated cross sections at low energies. Interference terms, arising from the presence of the prominant $5/2^-$ resonance at 7.46 MeV excitation energy and of the $3/2^+$ level higher up, cause most of the asymmetry in the differential cross sections at low energies, with interference between the $1/2^+$ and negative parity levels having non-zero $^{2}P_n$ widths contributing to a lesser extent. More recent extensions of this analysis to somewhat higher energies[29] indicate that the $3/2^-$ level is responsible for the broad structure seen in both the neutron elastic and total cross sections at $E_n \sim 3.5$ MeV, and at the same time, produces a "shoulder" in the $^{6}Li(n,t)$ integrated cross section at $E_n \sim 2.2$ MeV.

Recent measurements for reactions in this system appear to be approaching unitary consistency. At this stage, however, the precise experimental determination of the total cross section below and over the resonance seems to be most elusive, both in terms of the magnitude of the cross section near the peak, and the energy of the peak. New measurements of the total cross section by Knitter[19] and by Smith[30] agree well in magnitude with the Version V calculations, but not in energy scale. Questions about the $^{6}Li(n,t)$ cross section persist in relation to ratio measurements. While Gayther's[31] new ratio measurement of $^{235}U(n,f)$ relative to $^{6}Li(n,t)$ appears quite consistent with the Version V results, Macklin's[32] ratio of $^{197}Au(n,\gamma)$ relative to $^{6}Li(n,t)$ does not. The resolution of these differences will doubtless require further (but hopefully, small) changes in the neutron cross sections for ^{6}Li. We feel, however, that the utility of this approach, and the importance of analyzing standard cross sections in a unitarily consistent way with other data from the same system, have been demonstrated by the Version V results.

TABLE III

Resonance Parameters for the ^{7}Li System

J^P	E_x[a]	E_x[b]	State	Partial Width[a]	Total Width[a]	Total Width[b]
$7/2^-$	4.672	4.633±.008	^2F_t	.071	.071	.093±.008
$5/2^-$	6.596	6.675±.054	^2F_t	.944	.945	$.875^{+.2}_{-.1}$
			^4P_n	.001		
$5/2^-$	7.455	7.467±.004	^2F_t	.023	.077	.089±.007
			^4P_n	.054		
$7/2^-$	9.568	9.61±.81	^2F_t	.294	.412	- - -
			$^8P_{n*}$	.118		
$3/2^-$	9.853[c]	10.25±.1	^2P_t	.182[c]	1.171[c]	1.4±.1
			^4P_n	.969[c]		
			^2P_n	.020[c]		
$3/2^+$	11.279[c]		^2D_t	1.360[c]	2.517[c]	
			^4S_n	1.157[c]		

a. Values (in MeV) derived from the Version V R-matrix parameters.

b. Values (in MeV) tabulated in Ref. 26.

c. Values given for resonances above the range of the analysis, which are therefore quite uncertain.

Acknowledgments

This analysis is an outgrowth of work begun by D. C. Dodder and K. Witte. The effort still benefits from collaboration with them on many aspects of the problem. I am grateful to N. Jarmie, R. Brown, L. Stewart, and P. Young for their help in collecting and reviewing the experimental data.

References

1. E. P. Wigner and L. Eisenbud, Phys. Rev. 72, 29 (1947), and A. M. Lane and R. G. Thomas, Rev. Mod. Phys. 30, 257 (1958).

2. G. M. Hale, "R-Matrix Analysis of the Light Element Standards," Proceedings of a Conference on Nuclear Cross Sections and Technology, Vol. 1, 302 (1975).

3. G. M. Hale, L. Stewart, and P. G. Young, Los Alamos Scientific Laboratory report LA-6518-MS (1976).

4. K. M. Diment and C. A. Uttley, Harwell report AERE-PR/NP 15, p 12 (1969).

5. W. P. Poenitz, Z. Phys. 268, 359 (1974).

6. W. Fort and J. P. Marquette, "Experimental Methods Used at Cadarache to Determine the ^{6}Li(n,α)T Cross Section between 200 keV and 1700 keV," Proceedings of a Panel on Neutron Standard Reference Data, November 20-24 (1972), IAEA, Vienna. Note: Fort expects to renormalize his data upward by ~11%.

7. M. S. Coates, G. J. Hunt, and C. A. Uttley, "Measurements of the Relative ^{6}Li(n,α) Cross Sections in the Energy Range 1 keV to 7500 keV," Neutron Standards Reference Data, IAEA, Vienna, p. 105 (1974).

8. R. J. Spiger and T. A. Tombrello, Phys. Rev. 163, 964 (1970).

9. N. Jarmie et al., Bull. Am. Phys. Soc. 20, 596 (1975).

10. J. A. Harvey and N. W. Hill, Proc. Conf. on Nuclear Cross Sections and Technology, Vol. I, 244 (1975).

11. D. C. Dodder, K. Witte, and G. M. Hale, "The LASL Energy-Dependent Analysis Code EDA," unpublished.

12. M. Ivanovich, P. G. Young, and G. G. Ohlsen, Nucl. Phys. A110, 441 (1968).

13. R. A. Hardekopf et al., Los Alamos Scientific Laboratory report LA-6188 (1977).

14. R. E. Brown, G. G. Ohlen, R. F. Haglund, Jr., and N. Jarmie, LA-UR-77-407 (1977) (Submitted to Phys. Rev. C).

15. J. C. Overley, R. M. Sealock, and D. H. Ehlers, Nucl. Phys. A221, 573 (1974).

16. I. G. Schröder, E. D. McGarry, G. de Leeuw-Gierts, and S. de Leeuw, Proc. Conf. on Nuclear Cross Sections and Technology, Vol. I, 240 (1975).

17. R. O. Lane, Ann. Phys. 12, 135(1961).

18. H. H. Knitter and A. M. Coppola, EANDC report (E) 57(U) (1967).

19. H. H. Knitter, C. Budtz-Jorgensen, M. Mailly, and R. Vogt, CBNM-VG (1976).

20. R. O. Lane, A. J. Elwyn, and A. Langsdorf, Jr., Phys. Rev. 136, B 1710 (1964).

21. G. P. Lamaze, O. A. Wasson, R. A. Schrack, and A. D. Carlson, Proc. International Conference on the Interactions of Neutrons with Nuclei, Vol. 2, 1341 (1976).

22. J. W. Meadows, Neutron Standards and Flux Normalization (AEC23), 129 (1971).

23. M. G. Sowerby, B. H. Patrick, C. A. Uttley, and K. M. Diment, J. Nucl. Energy 24, 323 (1970).

24. G. M. Hale, Nuclear Theory in Neutron Nuclear Data Evaluation, Vol. II (IAEA-190) 1 (1976).

25. J. Humblet and L. Rosenfeld, Nucl. Phys. 26, 529 (1961).

26. F. Selove and T. Lauritsen, Nucl. Phys. A227, 54 (1974).

27. R. J. Holt, F. W. K. Firk, G. T. Hickey, and R. Nath, Nucl. Phys. A237, 111 (1975).

28. See, for instance, Lane and Thomas (Ref. 1), p. 295.

29. G. M. Hale and D. C. Dodder, Proc. International Conf. on the Interactions of Neutrons with Nuclei, Vol. 2, 1459 (1976).

30. A. B. Smith, P. Guenther, D. Havel, and J. F. Whalen, ANL/NDM-29 (1977).

31. D. B. Gayther, AERE-R 8556 (1977).

32. R. L. Macklin, J. P. Halperin, and R. R. Winters, Phys. Rev. C11, 1270 (1975).

SPECIAL PROBLEMS WITH ^{6}Li GLASSES

G. P. Lamaze
National Bureau of Standards
Washington, D.C. 20234

Properties of Ce activated Li loaded glass scintillators are discussed as well as their applications as neutron detectors. Three special problems that may arise in their use for neutron detection are non-uniformity of the ^{6}Li content, multiple scattering, and after pulsing of the photomultiplier. These problems and their consequences are discussed as well as some possible solutions.

(glass scintillators; ^{6}Li(n,α)T; Monte Carlo; multiple scattering; neutron detection; photomultipliers)

Introduction

Before I discuss the problems with the use of ^{6}Li glass, let me point out some of its advantages. As we have seen in the earlier talks, the ^{6}Li(n,α)T reaction has a very large cross section with a value of ∿940 b at thermal and a very nice 1/V behavior up to about 10 keV. Figure 1 shows a result of a recent NBS measurement.[2] The straight line is the ENDF/B-V evaluation that Gerry Hale talked about previously.[2] One can see that at 10 keV, the deviation from 1/V is less than 1% and at 30 keV it is already about 6% and rising rapidly. Figure 2 compares the NBS results with ENDF/B-V in the region of 2 to 800 keV. Not only does the ^{6}Li(n,α) reaction have a large cross section (∿3.15 b at the peak) but it also has a very high Q-value (∿4.79 MeV). This combination of features has led many investigators to search for a fast scintillator to take advantage of these two attractions.

Early investigations[3] centered on ^{6}LiI(Eu), but the Iodine introduces a great deal of structure in the response function and ^{6}LiI(Eu) is also reported to undergo changes in its scintillation properties as it ages. In 1958, Ginther and Schulman[4] reported on Cerium activated glass scintillators. In that same year, Voitovetskii, Tolmacheva, and Arsaev[5] reported the first ^{6}Li loaded, Ce activated glass scintillators suitable for neutron detection. Much work has been done in the ensuing years and a wide variety of glasses are now commercially available.

In fact, to get in the neutron detection business today is pretty simple; all you need is a photomultiplier, a piece of ^{6}Li glass and a can of beer. Figure 3 shows a schematic of the mounting scheme used at NBS with a "typical" pulse height spectrum. The glass is mounted into an aluminum 7 oz. beer can and viewed edge on by a photomultiplier about 2 cm away. No light pipe or optical coupling compound is used in order to minimize the scattering material in the beam. The simplicity and low cost of this apparatus makes it a very attractive neutron detector.

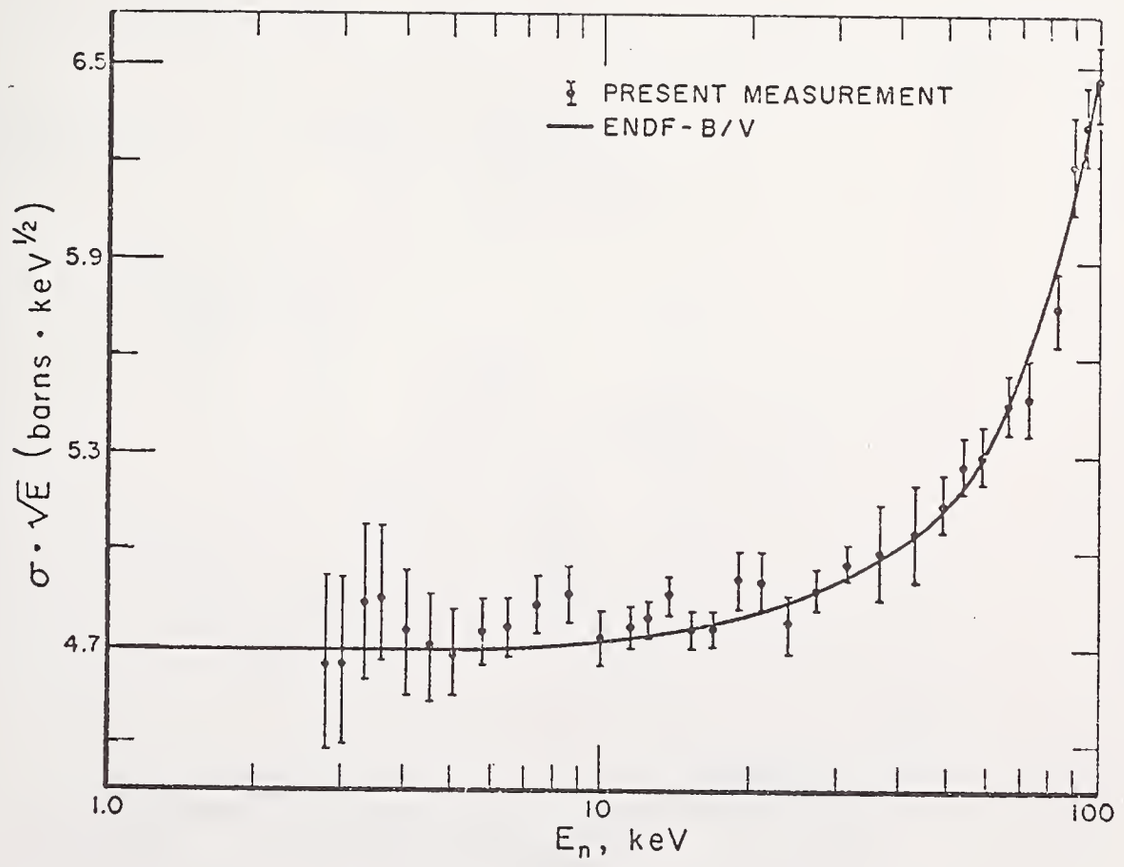

Fig. 1. Results of a recent NBS measurement[1] of the ^{6}Li(n,α)T cross section. Error bars shown include systematic errors.

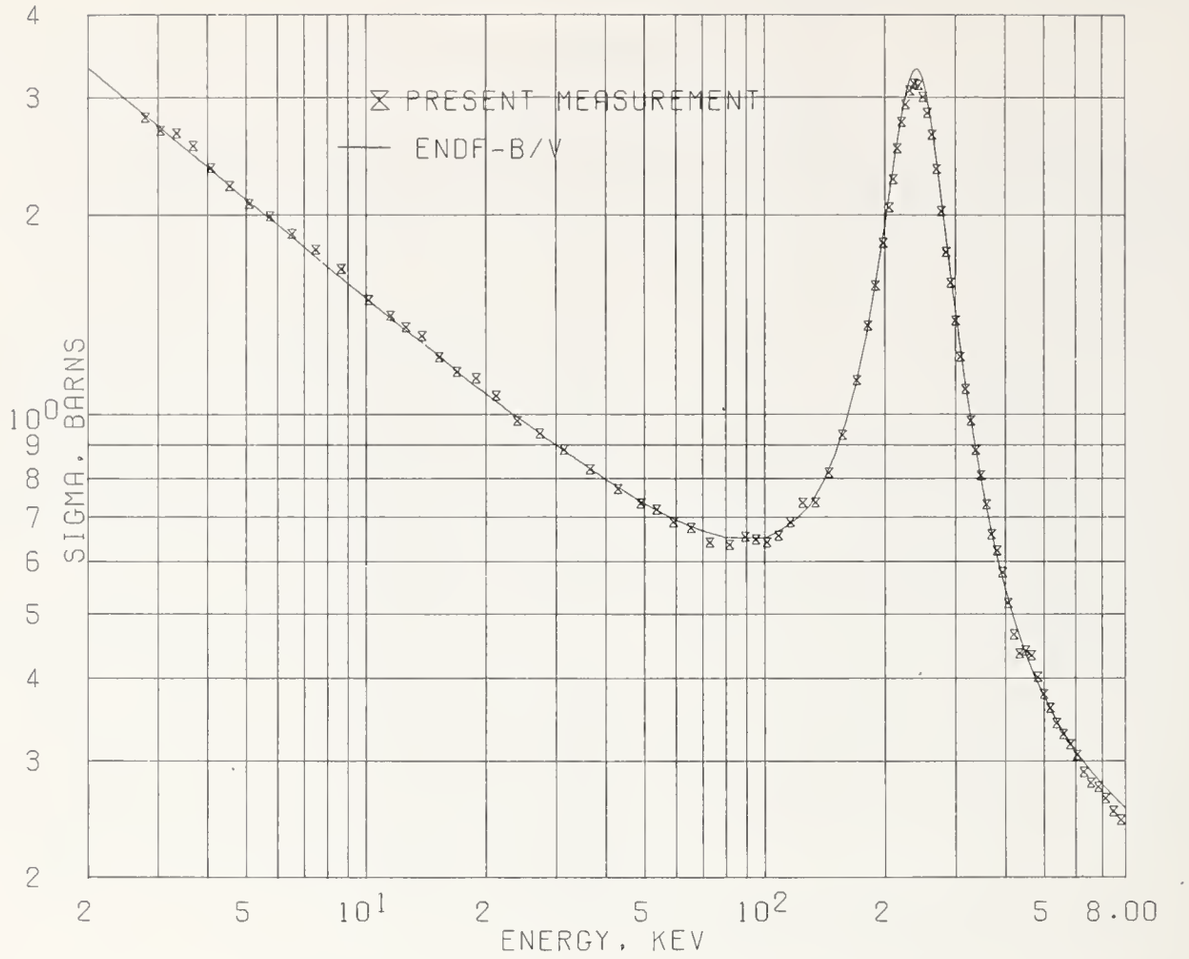

Fig. 2. Results of a recent NBS measurement of the $^{6}Li(n,\alpha)T$ cross section compared with ENDF-B/V.

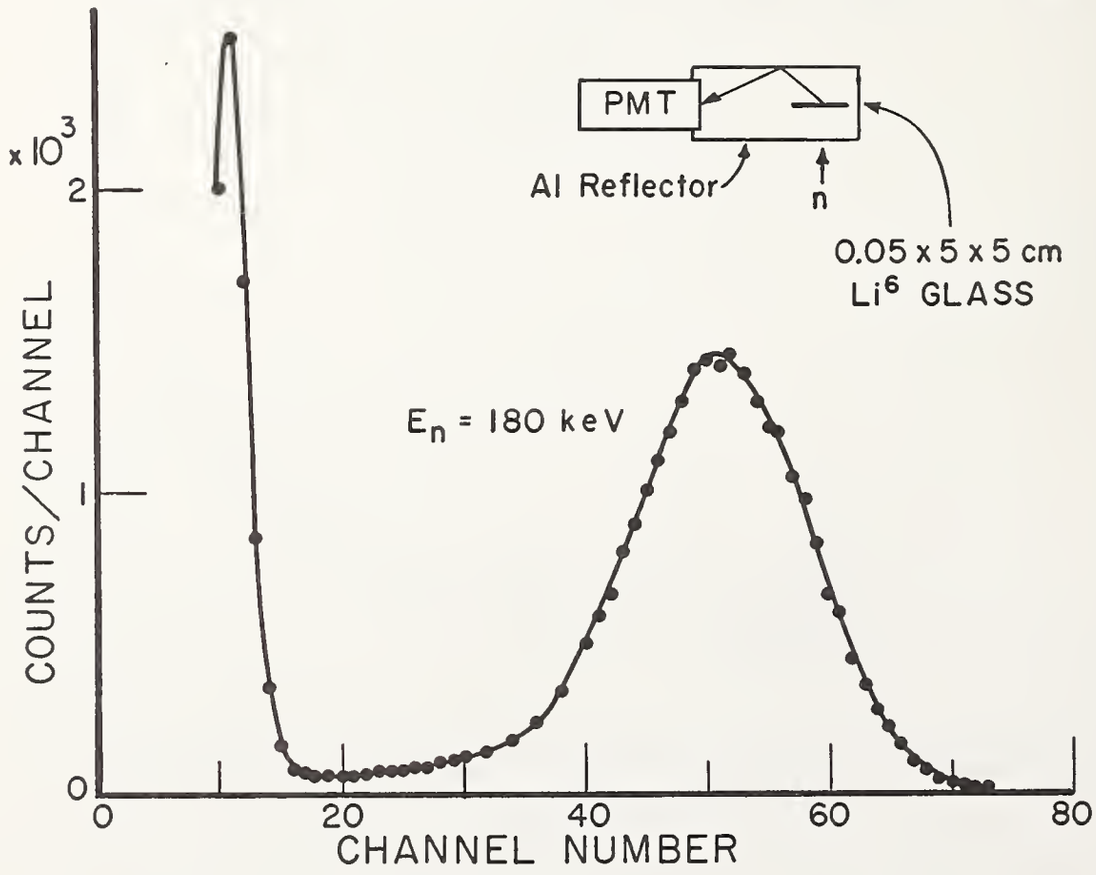

Fig. 3. Method employed at NBS to couple ^{6}Li glass to phototube shown with typical pulse height response to Linac neutrons.

I will now describe an interesting series of measurements by Spowart[6,7] in Scotland on the properties of ^{6}Li glass. Spowart presents an excellent review of the physics of Lithium glasses and is certainly worthwhile reading for those who might be interested in developing better glass scintillators. What Spowart has done is to take the full range of commercially available glasses and measure the response of the glasses as a function of Li content. Figure 4 shows the pulse height vs Li content for thermal neutron capture. It is interesting that there is a minimum light output for about 7.5% Li content. The response of glass scintillators to monoenergetic electrons is shown in Figure 5. This too shows a minimum light output for 7.5% Li content. It is not clear that this effect is due to the change in Li content or perhaps to a difference in the Ce content of the different glasses. Although the Ce content of NE907, NE908, and NE912 is nominally the same, Spowart has not measured them accurately as he did with the Li content. As will be shown later, the glasses suffer from non-uniformity problems.

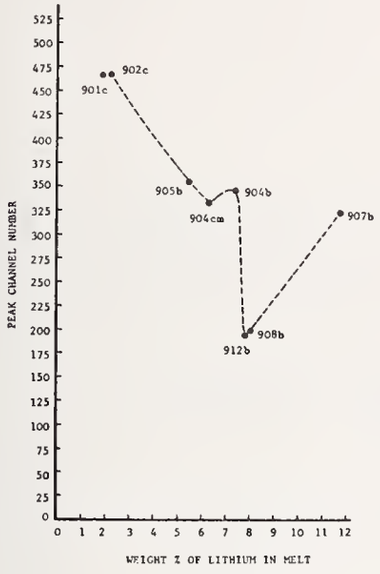

Fig. 4. Pulse height vs Lithium content using thermal neutron beam activation.

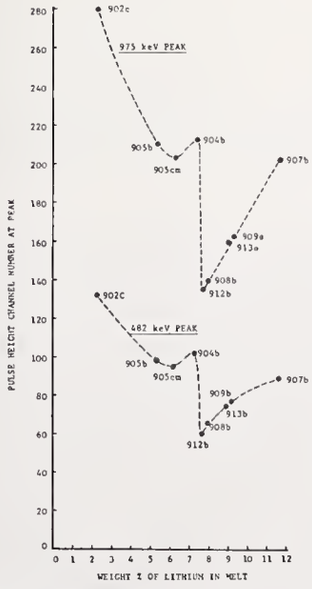

Fig. 5. Peak pulse height vs Li content using ^{207}Bi EC beta activation.

Figure 6 gives a measure of the resolution function obtained by Spowart. As expected, the glasses with the lowest pulse height also have the poorest resolution. This indicates that the NE912 and NE908 glasses are producing fewer photons per unit energy deposited than the other glasses.

Spowart has also investigated the effect of temperature on the pulse height and resolution of Li loaded glass scintillators. Figure 7 shows a plot of the variation of the $^{6}Li(n,\alpha)$ peak pulse height as a function of temperature. As can be seen, the light output of the scintillator increases as a function of temperature from 100 to 450°K. Near room temperature a difference of 50°K changes the pulse height by about 10%. The mechanism of this increase in light output is apparently an increase in the phonon population with temperature which assists the energy transfer to the Ce^{3+}

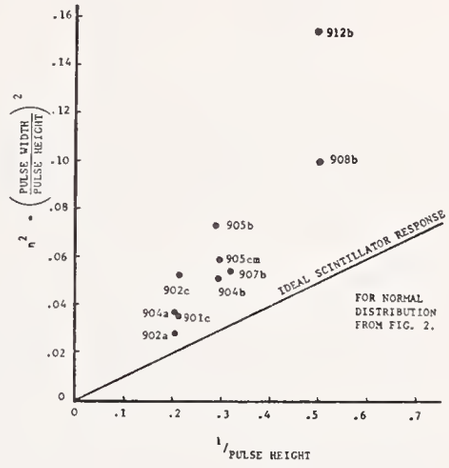

Fig. 6. Analysis of scintillator performance, activation by thermal neutrons from Am/Be moderated source.

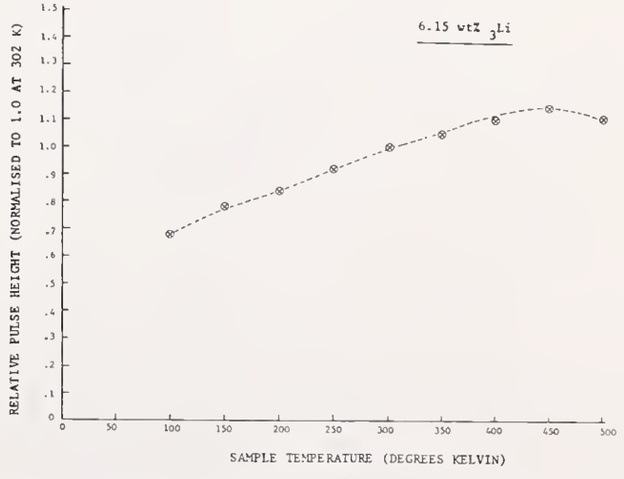

Fig. 7. Variation of $^{6}Li(n,\alpha)$ peak pulse height with temperature for medium lithium glass.

luminescent centers. This increased efficiency of energy transfer also improves the resolution as shown in Figure 8. For most applications, the experimenter won't bother controlling the temperature; however, one should be aware of this characteristic and take proper precautions against large temperature variations during an experiment. This also presents the experimenter with the interesting option of cooling the photomultiplier while heating the Li glass to maximize the system performance.

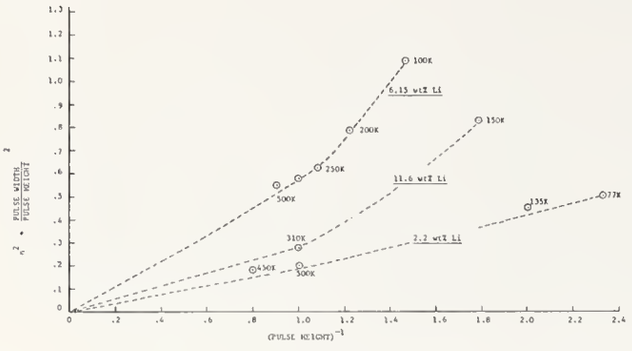

Fig. 8. The effect of temperature on pulse height statistics.

The next major problem I would like to discuss is the non-uniformity of the Li glasses. This can be a serious problem for many measurements, especially certain types of Van de Graaff measurements where the neutron flux might not be uniform over the face of the scintillator. Figure 9 shows the Li content of a 9 mm Harwell glass as measured by Moxon.[8] The content was obtained by measuring the transmission of the glass as a function of energy and position. By fitting the results to a formula of $\sigma_T = a + b/\sqrt{E}$, the 1/V and constant components of the cross section could be determined. The 1/V component (i.e., ^{6}Li) of the glass seems to be very uniform except at the edges where some depletion of the Li has occurred. The constant component on the other hand does seem to have some variation in density across the diameter. Moxon concludes that this glass as well as a 9 mm thick Cadarache glass were very uniform in Li content, except at the edges. He speculates that the Li might be leached out in the cutting and the polishing of individual pieces. Tests performed by the Analytical Chemistry Section at Harwell indicate that Li could easily be leached out if the glass were to come into contact with slightly acidic water solutions.

Figure 10 shows the result of transmission measurements on a 0.5 mm thick piece of NE 912 using the NBS Reactor thermal column. As you traverse the glass from one edge to the other, a 4% variation in ^{6}Li content is observed.

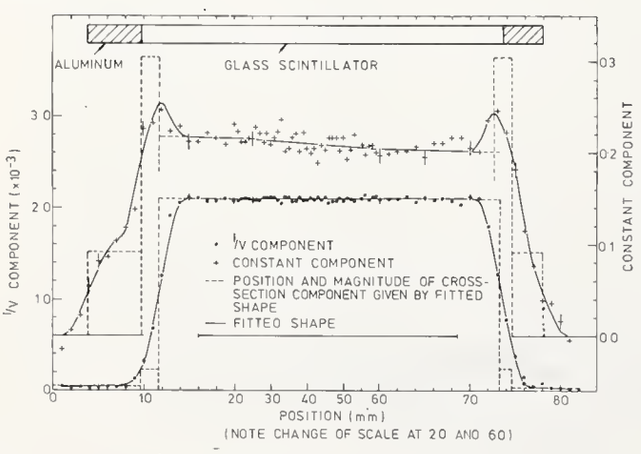

Fig. 9. A least square fit to one of the spatial distribution measurements for the AERE glass.

Figure 11 shows the transmission of the same glass with a traversal made at 90° to the first traversal. In this direction the glass seems to be fairly uniform. The non-uniformity of a particular glass sample raises several experimental problems. First, the ^{6}Li content cannot be determined by chemical analysis of a part of the glass, or by transmission of part of the glass. In fact, the absolute determination of the ^{6}Li content may be impossible to obtain with any precision. Even in relative measurements, the experimenter must be careful to always illuminate the same portion of the glass and take care that the neutron flux is uniform over the used portion.

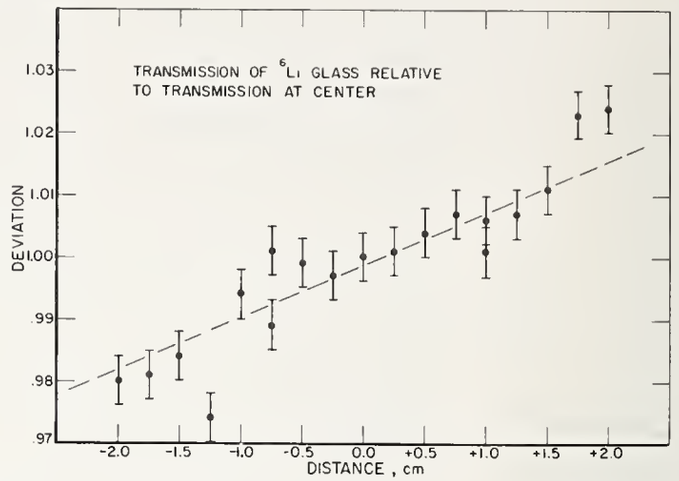

Fig. 10. Transmission of a 0.5 mm piece of NE912 as measured with thermal neutrons.

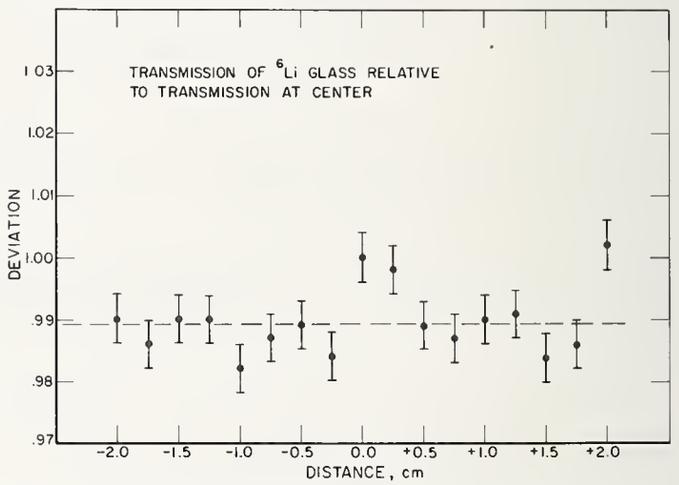

Fig. 11. Transmission of the same glass as Figure 10 but with a traversal perpendicular to the first traversal.

Let me now turn to the one unavoidable problem found in any experiment with ^{6}Li glass: multiple scattering. NE912 which has one of the highest percentages of ^{6}Li contains 21% silicon, 55% oxygen, 22.5% ^{6}Li, 1% ^{7}Li, and 0.5% cerium. Scattering resonances in these elements can cause significant errors in the measure of the neutron flux. Figure 12 shows the multiple scattering correction factor for a 5.08 cm diameter and 0.5 mm thick NE912 scintillator. With the exception of a very narrow Si resonance at 55 keV, the correction is very flat from 2 keV to 250 keV. At that point, the influence of the ^{6}Li resonance is seen. At 440 keV, the effect of the oxygen resonance is very dramatic and requires a rather large correction for even a very thin glass. As the glass thickness is increased, the corrections become even larger, as seen in Figure 13. The correction is shown for three representative energies. For an 8 mm thick glass, a ∿ 15%

correction must be made at 250 keV and a ~45% correction must be made at 440 keV. The error bars shown are only the statistical errors for the MonteCarlo calculation. There are obvious systematic errors involved, such as the actual composition of the glass and the accuracies of the scattering cross sections and angular distributions used in the program. Clearly, high precision measurements in the 400 to 500 keV region with ^{6}Li glass detectors are almost impossible due to the multiple scattering problem.

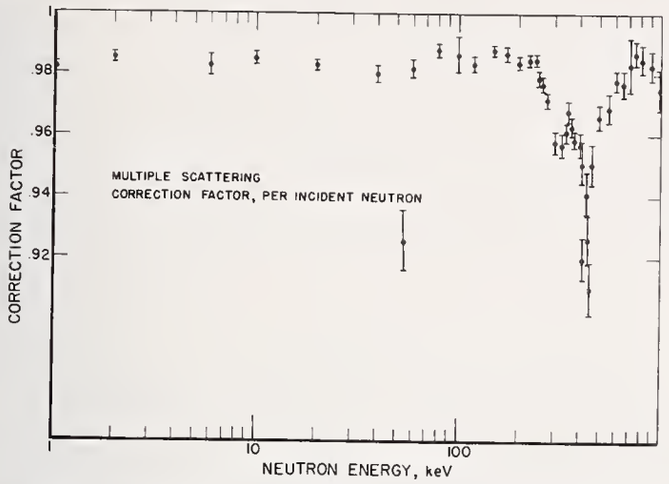

Fig. 12. Multiple scattering correction factor for a 5.08 cm diameter by 0.05 cm thick piece of NE912.

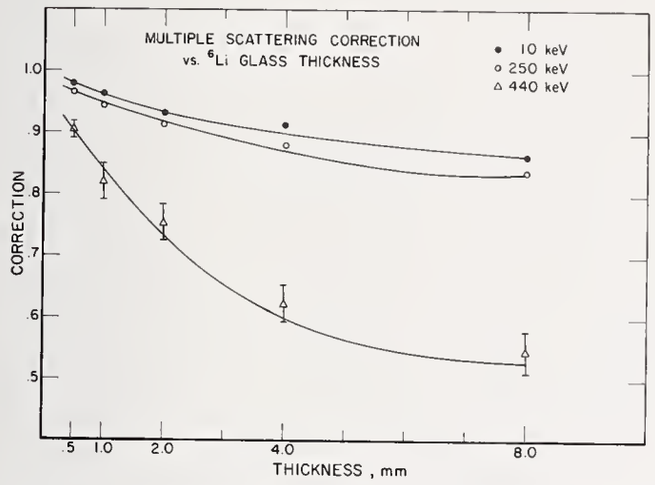

Fig. 13. Variation of the multiple scattering correction factor as a function of glass thickness.

Another problem in the use of Li glass in Linac T-o-F experiments is the γ-flash. The glasses are very sensitive to γ-radiation and this can lead to total saturation of the photo multiplier and amplifiers as well as after pulsing of the photomultiplier. The large electron pulse in the photomultiplier ionizes residual gases in the tube. These ions are accelerated back to the photocathode and will excite further bursts of electrons. These signals come from 0.4 μS to 60 μS after the γ-flash and can look like valid events. At NBS we solve this problem by offgating the photomultiplier during the γ-flash.[9] This has the double feature of keeping the photo multiplier from saturating as well as preventing the after pulsing. The after pulse suppression works by pulsing a fine mesh grid that is placed over the front face of the photomultiplier tube. During the γ-flash a +300 volt pulse is placed on the grid, suppressing the photoelectrons and preventing them from striking the first dynode. Figure 14 shows the after pulses after a large light source hits the photocathode. The upper scope trace shows two after pulse groups at about 0.6 and 1.0 μS after the light flash. The lower trace shows the effect of off gating; the light flash has been reduced by a factor of about 15 and the after pulses have been completely eliminated. Figure 15 shows the after pulsing at long times. The after pulsing peaks at about 40μS after the flash and gradually dies away so that no after pulsing is observed after about 100 μS. The after pulse suppression system completely eliminates this long term component also. Although this system can solve the problem of the after pulsing of the photomultiplier, the glass scintillator itself seems to after pulse after a strong γ-flash. Additionally the experimenter is faced with the γ-decay of the neutron producing targets. These effects make neutron detection at short times after the γ-flash very difficult and seems to indicate that two parameter data taking (i.e., time-of-flight and pulse height) may be necessary to separate γ-rays from neutron events.

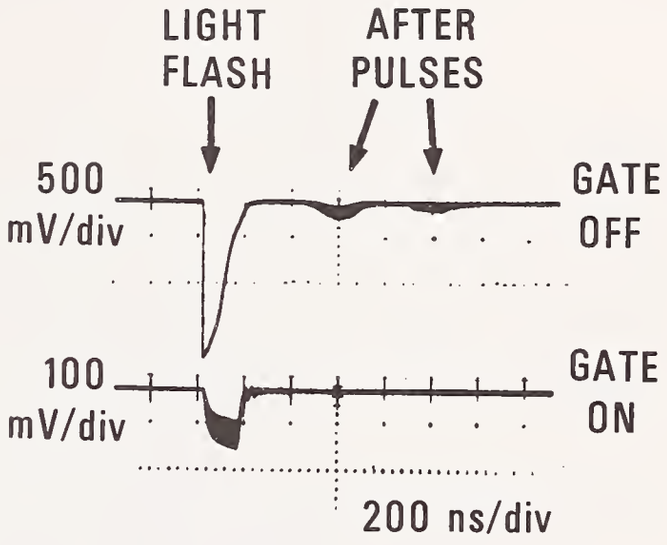

Fig. 14. Observed phototube output. Top trace is with no after-pulse suppression; bottom trace is with 300 volt pulse applied to wire mesh.

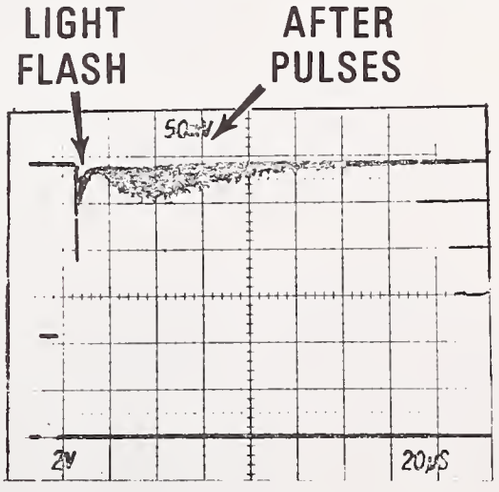

Fig. 15. Observed phototube output for long times (20 μS/div). When gating is applied, these pulses are completely suppressed.

To summarize, the work of Spowart demonstrates that both improved scintillation properties and increased efficiency of ^{6}Li glass scintillators is possible. Above 200 keV, uncertainties in the ^{6}Li (n,α)T cross section and multiple scattering corrections reduce the desirability of ^{6}Li glass as a flux monitor. Below 200 keV, the cross section is relatively well known, γ-flash and after pulsing is not a problem (except at short flight paths), and the multiple scattering corrections are smooth and relatively small. If nonuniformity of the scintillator is not a problem or if a very uniform scintillator is being used, ^{6}Li glass makes a very nice flux monitor below 200 keV.

Acknowledgements

I would like to thank R. B. Schwartz for his assistance in the transmission measurements of the NBS ^{6}Li glasses and M. C. Moxon for advance copies of his results and figures.

References

1. G. P. Lamaze, R. A. Schrack, O. A. Wasson, To be published.

2. G. Hale, See these proceedings.

3. James Schenck, Nature 171(1953) 518.

4. R. J. Ginther and J. H. Schulman, I.R.E. Trans. NS-5(1958) 92.

5. Voitovetskii, Tolmacheva, and Arsaev, Atomnaya En. 6 (1959) 321.

6. A. R. Spowart, Nucl. Instr. and Meth. 135 (1976) 441.

7. A. R. Spowart, Nucl. Instr. and Meth. 140 (1977) 19.

8. M. C. Moxon, J. D. Downes, and D.A.J. Endacott, UKAEA Report, AERE-R8409, Harwell, Oxfordshire (1976).

9. G. P. Lamaze, J. K. Whittaker, R. A. Schrack and O. A. Wasson, Nucl. Instr. and Meth. 123 (1975) 403.

INSTRUMENTS FOR USE OF ^{6}Li AS A STANDARD*

L. W. Weston
Oak Ridge National Laboratory
Oak Ridge, Tennessee 37830

A review is given of the instruments which use the $^{6}Li(n,\alpha)^{3}H$ reaction as a standard in the measurement of neutron flux. These instruments consist of scintillation detectors, gaseous ionization detectors, and external particle detectors. The Li glass scintillator is the most versatile because of minimized effects of the angular distribution of the reaction products and simplicity. The gaseous ionization detector has lower gamma-ray sensitivity than does the scintillation detector. Surface-barrier diodes may be used to detect the reaction products when a neutron spectrometer is desired. A choice of instruments to use this reaction must consider gamma-ray sensitivity, effects of the angular distribution of the reaction, and the range of the triton in the detector.

(Instruments: $^{6}Li(n,\alpha)^{3}H$, scintillation detectors, gaseous ionization detectors, external particle detectors)

Introduction

Instruments which use the $^{6}Li(n,\alpha)^{3}H$ reaction for the measurement of neutron flux must use the advantages and minimize the disadvantages of this reaction. The Q value of the reaction is 4.78 MeV, which is high enough to make the reaction relatively easily detectable for all incoming neutron energies; however, this high Q value makes the reaction difficult for use as a neutron spectrometer except for very high resolution detectors such as silicon surface-barrier detectors. The cross section of the reaction is large with relatively smooth variations except near the large resonance at about 244 keV. This p-wave resonance makes the reaction difficult to use as a standard cross section in the neutron energy range from about 150 to 350 keV and causes the angular distribution to be anisotropic in the center-of-mass system above a few eV neutron energy. The tritons show forward peaking of about 5% at 100 eV, 18% at 1000 eV, 55% at 10 keV, and anisotropies which do not vary monotonically at higher neutron energies.[1-3] Any detector using this reaction for the measurement of neutron flux must be independent of this angular distribution or must be understood well enough that corrections can be made. The energy of the alpha particle from the reaction is 2.05 MeV for zero incoming neutron energy. The range of the alpha particle in Argon at atmospheric pressure is 1.1 cm for zero energy neutrons and 2.0 cm for 1-MeV neutron absorption. These ranges create no problem in most detectors. The energy of the emitted triton is 2.73 MeV for zero incoming neutron energy. The corresponding ranges of the triton in Argon are 6 cm and 11 cm for zero and 1 MeV neutron absorption and this rather long range creates problems and limitations in most detectors using this reaction.

There are three basic methods by which to detect the $^{6}Li(n,\alpha)$ reaction: 1. ^{6}Li embedded in a scintillation detector; 2. a gaseous ionization detector; and 3. external charged-particle detectors such as silicon surface-barrier detectors. There is no convenient gaseous form of Li such as in the case of $^{10}BF_3$.

At the present time the scintillation detector is the most popular because of high efficiency, accurate time determination of the event, insensitivity to angular distribution, and low mass in the neutron beam. The advantages and disadvantages of the three methods of detection will be discussed.

Scintillation Detectors

There are three practical forms of scintillation detectors available which may use the ^{6}Li reaction. These are the ^{6}Li loaded glass scintillator, a LiF layer sandwiched between two very thin plastic scintillators, and ^{6}LiI scintillators. The glass scintillator is most popular because it is commercially available and easily used. The ^{6}LiI crystal scintillator[4,5] is not practical for the measurement of neutron flux because the iodine has a high capture cross section with many large resonances. The plastic sandwich detector developed by Dabbs et al.[6] is an innovation which is relatively unproven.

The advantages of the Li glass scintillator are that it has a high efficiency, fast timing, and may perturb the neutron beam to only a small extent. The principal disadvantage of the Li glass detector is its sensitivity to gamma-rays. Because of the gamma sensitivity, the optimum thickness for a Li glass detector is about 0.5 mm if the corresponding efficiency is acceptable. At this thickness the loss of tritons from the surface is <10% and the gamma sensitivity is minimized. If the glass is made thinner, a large fraction of the reaction products is lost from the surface of the glass because of the rather long range of the triton. If an appreciable fraction of the tritons is lost from the surface of the glass, one no longer obtains a peak in the pulse-height spectrum which is well above most gamma-ray induced pulses. Also if part of the tritons are lost from the glass, the efficiency becomes sensitive to the angular distribution of the reaction products.

Since Li glass can be obtained[7] with a concentration of ^{6}Li of up to 7.3%, the efficiency of 1/2-mm glass can be as high as 93% for thermal neutrons and 0.46% for 1-keV neutrons. For higher efficiency the glass is available up to 2.54 cm in thickness. Such thick detectors of Li glass are used for measurements such as total cross sections; however, one pays a price in gamma-ray sensitivity. For this reason the volume of glass scintillitor should always be kept at a minimum for a given application.

The gamma-ray sensitivity of Li glass has been discussed in detail elsewhere.[4,8] The maximum value of the peak created by the $^{6}Li(n,\alpha)^{3}H$ reaction corresponds to an equivalent electron of 1.6 MeV energy created by

a gamma ray. The pulse-height resolution (FWHM) of the peak is 20-30%. Gamma rays which deposit less than about 1 MeV energy in the scintillator can be effectively discriminated against by means of pulse-height selection. With an electron linear accelerator, the use of Li glass usually requires the equivalent of 2 cm or more of Pb in the beam to reduce the effects of the gamma flash for neutron flight times of less than about 10 μsec.

In time-of-flight experiments the timing of a detector is important. From Li glass a time resolution of about 2 ns can be obtained. This is a good match to many other detectors such as fission chambers and capture-gamma-ray detectors and thus is an attractive feature of the Li glass detector.

The mounting of Li glass scintillators so they can be viewed by photomultipliers is not very critical. In most applications it is preferable to mount the PM tubes outside the neutron beam. Such a mounting minimizes neutron scattering corrections and gamma-flash problems if a LINAC is used. Tests at Oak Ridge indicated that coupling the Li glass optically at the edges to two PM tubes gives equivalent results to mounting the Li glass in a light reflecting box with no direct light coupling. Both methods[9,10] of mounting Li glass are used at ORELA in Oak Ridge.

The plastic sandwich detector has most of the characteristics of the Li glass detector. This detector, as used by J. W. T. Dabbs,[6] consists of a layer of 96 μgms of LiF per cm^2 which is vacuum evaporated on a 0.01-cm thick NE-110 plastic scintillator. A similar layer of plastic scintillator is placed over the LiF layer. The LiF layer is 2 cm in diameter and the plastic 2.5 cm in diameter. The sandwich is viewed by two photomultipliers in a light-reflecting box. The principal advantage of this detector is a faster recovery from a "gamma flash" such as is characteristic of a LINAC. The plastic does not exhibit long-term phosphorescence as does Li glass, which can exhibit a pulse of several microseconds in width under such conditions. Another advantage is the smooth cross section of the plastic components. There are no resonances in silicon and oxygen to contend with. Because the reaction products must be allowed to escape from the LiF layer, it is limited to about 200 $\mu g/cm^2$. The maximum efficiency of a single detector is thus limited to about 0.45% for thermal neutrons and 2.3 x 10^{-3}% for 1-keV neutrons. A disadvantage of this detector is the light output is lower than Li glass so that electronic noise is more of a problem. Also, the "gamma flash" response of the detector is greater than that of Li glass even though the recovery is faster. This is not a serious problem for beams of the order of 2 cm in diameter, but presents electronic recovery problems for beams of greater dimensions. The hydrogen in the plastic of the detector scatters about 2.2% of the neutron beam and a correction must be applied for neutron scattering in the hydrogen and carbon and subsequent absorption in the ^6Li.

Gaseous Ionization Detectors

The general advantage of gaseous ionization detectors is low gamma-ray sensitivity. In applications where the gamma-ray intensity accompanying the neutron flux cannot be effectively reduced to tolerable levels this can be very important. The ^6Li reaction has not been used as extensively in gaseous ionization chambers because of the popularity of the use of the $^{10}B(n,\alpha)$ reaction. Chambers using BF_3 gas have been used extensively in the form of cylindrical proportional counters as well as parallel plate ionization chambers. Since the $^6Li(n,\alpha)$ reaction is becoming more popular as a standard relative to the $^{10}B(n,\alpha)$ reaction, there may be increased use of the Li reaction in gaseous ionization counters. The $^6Li(n,\alpha)$ reaction has the advantage of a less complex cross section above about 80 keV and the absence of two groups of alpha particles as occurs in the ^{10}B reaction.

The gaseous ionization detector must detect the alpha and triton from the ^6Li reaction. Since the range of the alpha particle in Argon is from 1.1 cm for thermal neutrons to 2.0 cm for 1-MeV neutrons, a detector of about 2 cm thickness will transfer all the energy of the alpha particle to the gas. Unfortunately the triton range is correspondingly about 6 and 11 cm, which is too long for normal thickness chambers because of electron drift time and voltage gradient problems. An example of a gaseous ionization chamber using ^6Li is that of Friesenhahn et al.[11] which was a gridded ion chamber with a spacing of 2 cm between the grid and the Li metal coated plate. The pulse-height spectrum was complex as can be seen in Figure 1, because the tritons which were emitted at 90° with respect to the foil gave a much larger pulse than those emitted at 0°. This effect was caused by the fact that the triton range was long compared to the spacing of the chamber. Examples

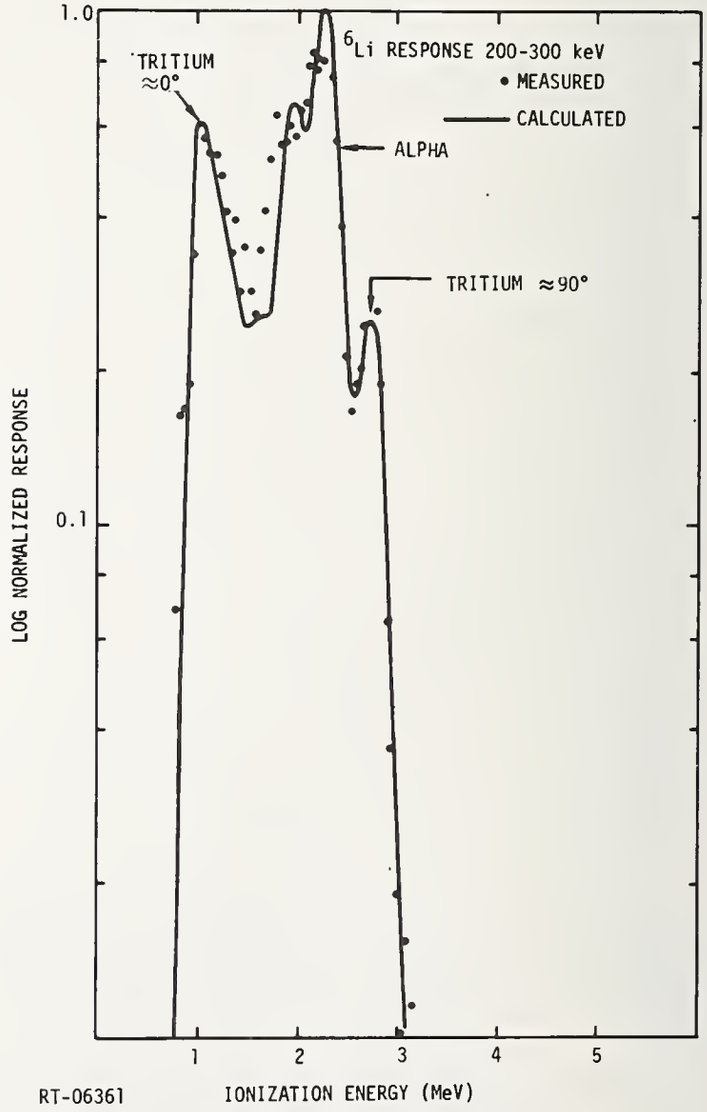

Figure 1. Calculated versus measured ^6Li gridded ion chamber response. Chamber constructed by Friesenhan et al.[11]

of non-gridded parallel plate ionization chambers are those used by Macklin[12] and Poenitz.[13] With non-gridded chambers the pulse-height spectrum is very broad because of the dependence on the track orientation of the particle. With these chambers it is important that either the lowest energy triton pulses are counted or that corrections be made for the tritons not counted; otherwise the efficiency of the chamber becomes sensitive to changes in the angular distribution of the ^{6}Li reaction versus neutron energy.

With present day electronics the time resolution of a gaseous parallel plate ionization chamber is limited to a minimum of about 10 ns with about 30 ns being achieved with relative ease. This limitation is imposed by the low energy release of the reaction as compared to fission fragments and the long range of the reaction products.

The efficiency of a single gaseous ionization detector is limited by the thickness of the Li layer in the chamber. Since 200 $\mu g/cm^2$ of LiF is about the limit, this efficiency is about $2.3 \times 10^{-3}\%$ for 1-keV neutrons. The effective area of such a chamber may be many square centimeters. Proportional counters with amplification of the ionizing events in the gas could be constructed, but would have no obvious advantages.

External Particle Detectors

There are two forms of external particle detectors which have been used with the ^{6}Li reaction. Both these systems used commercially available surface-barrier diodes to detect the reaction products from the ^{6}Li reaction. One system is when the Li layer is placed very close to the surface of the silicon diode[1,2,14-16] and the other is when the diode is placed outside the neutron beam in low solid angle geometry.[17-19] When the Li layer is placed on or very close to the diode, a second diode may be placed on the other side to form a sandwich detector.

The use of surface-barrier detectors has two advantages: very good energy resolution of the reaction products and high stopping power. Surface-barrier detectors are capable of timing resolution of about 25 ns. The ^{6}Li sandwich detector has one characteristic which is unique relative to the other discussed detectors. This characteristic is that the energy resolution of the surface-barrier detectors is sufficient that the detector can determine neutron energy as well as the occurrence of an absorption and thus can be used as a neutron spectrometer. The uncertainty in neutron energy determination (FWHM) is about 300 keV.[14] The efficiency of the Li sandwich detectors is comparable to other detectors using a layer of LiF; however, the area is restricted to a few cm^2 in this case because of the size of available surface-barrier detectors.

The sandwich detector has a disadvantage which has prohibited its use except in special cases. The surface-barrier detectors must be very close to the LiF layer. Thus there is a relatively large mass of silicon in the neutron beam and high backgrounds are caused by neutron-induced charged-particle reactions in the silicon and gold of the detectors. This problem is severe for neutrons of greater than about 5 MeV energy. Figure 2 illustrates pulse-height spectra obtained at neutron energies of 1.99 MeV and 14 MeV. Proposals[20] have been made to construct such a spectrometer using silicon enriched in ^{30}Si to construct the surface-barrier detectors. This would reduce the charged-particle backgrounds by more than an order of magnitude; however, this proposal has not been carried out because of the expense. Because of the high background from charged-particle reactions, the ^{6}Li sandwich detector will probably be retained for specialized use.

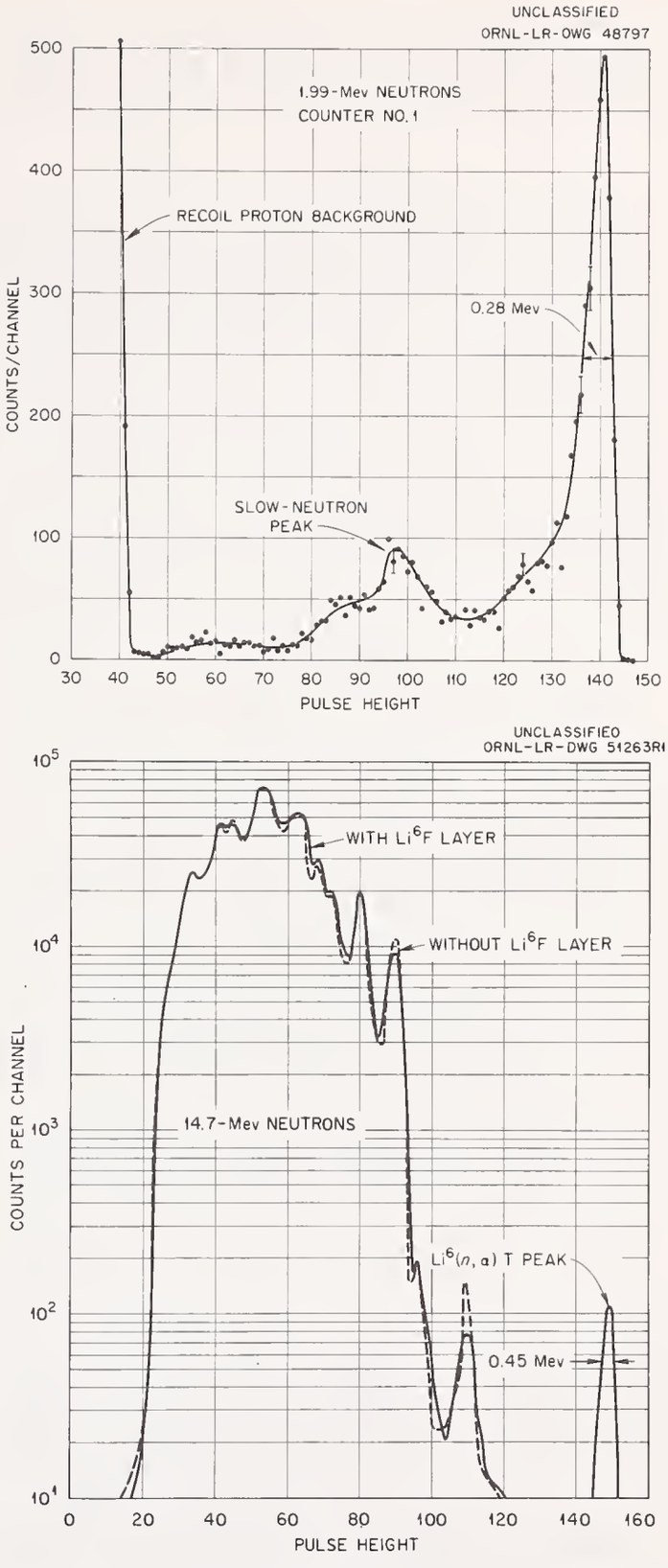

Figure 2. Pulse-height spectra for Li sandwich detector[14] using surface-barrier diodes.

Surface-barrier detectors outside the neutron beam to detect the ^{6}Li reaction have been used by several experimentalists.[17-19] This method has the disadvantages of very low efficiency and sensitivity

to the angular distribution of the reaction. Because of these disadvantages this form of detection is suitable only when there is a very high intensity of neutrons and other means of detection are not suitable.

Summary

The characteristics of the various detectors of the $^{6}Li(n,\alpha)^{3}H$ reaction have been discussed. Even though it is far from an ideal detector because of its gamma-ray sensitivity and the large resonance in ^{6}Li at about 244 keV, the ^{6}Li glass scintillator is widely applicable and a good choice of a detector for the measurement of neutron flux. Ionization chambers may present an attractive choice when the gamma-ray sensitivity of the glass detector is prohibitive. The surface-barrier sandwich may be attractive when a determination of the interacting neutron energy is desirable and the intensity of neutrons above about 5 MeV is low. The plastic sandwich detector requires further test and evaluation. The other forms of detectors are desirable only for specialized cases.

References

*Research sponsored by the Energy Research and Development Administration under contract with the Union Carbide Corporation.

1. S. Raman, N. W. Hill, J. Halperin and J. A. Harvey, "Angular Anisotropy in the $^{6}Li(n,\alpha)^{3}H$ Reaction in the eV and keV Energy Region," *Proc. Int. Conf. on Interactions of Neutrons with Nuclei*, Lowell, Mass., p. 1340, CONF-760715-72, Tech. Info. Center, ERDA (1976).

2. I. Schröder et al., *Proc. Conf. Nuclear Cross Sections and Technology*, p. 240, National Bureau of Standards Special Publication 425, Vol. I, U.S. Gov. Printing Office, Washington, D.C. (1975).

3. D. I. Garber et al., "Angular Distributions in Neutron-Induced Reactions," BNL 400, Third Edition, Vol. I, p. 3-6-1, Clearinghouse for Federal Scientific and Technical Information, NBS, U.S. Dept. Commerce, Springfield, Va. (1970).

4. F. D. Brooks, "Neutron Time-of-Flight Methods," p. 389, European Atomic Energy Community, Brussels (1961).

5. R. B. Murray, IRE Trans. on Nucl. Sci., p. 159, Vol. NS-5, No. 3 (1958).

6. J. W. T. Dabbs et al., Phys. Div. Ann. Prog. Rept., Dec. 31, 1975, ORNL-5137, p. 3 (1975).

7. Nuclear Enterprises Inc., Scintillator Division, Scintillator Catalogue, 935 Terminal Way, San Carlos, Calif. 94070.

8. G. G. Slaughter, F. W. K. Firk, and R. J. Ginther, "Neutron Time-of-Flight Methods," p. 425, European Atomic Energy Community, Brussels (1961).

9. R. L. Macklin, N. W. Hill, and B. J. Allen, Nucl. Inst. and Methods 96, 509 (1971).

10. R. B. Perez et al., Nucl. Sci. Eng. 55, 203 (1974).

11. S. J. Friesenhahn et al., "The (n,α) Cross Sections of ^{6}Li and ^{10}B Between 1 and 1500 keV," INTEL-RT 7011-001, Intelcom Rad. Tech., P.O. Box 80817, San Diego, Calif. (1974); see also GULF-RT-A12210, Gulf Radiation Tech., San Diego, Calif. (1972); see also *Proc. Conf. Nuclear Cross Sections and Technology*, p. 232, NBS Special Publication 425, Vol. I, U.S. Gov. Printing Office, Washington, D.C. (1975).

12. R. L. Macklin and N. W. Hill, private communication.

13. W. P. Poenitz, private communication.

14. T. A. Love et al., Nuclear Electronics I (IAEA Vienna, 1962) p. 415.

15. I. C. Rickard, Nucl. Inst. Methods 105, 397 (1972).

16. P. J. Clements et al., Nucl. Inst. Methods 125, 61 (1975).

17. V. V. Verbinski and M. S. Bokhari, Nucl. Inst. Methods 46, 309 (1967).

18. J. R. Lemley, G. A. Keyworth, and B. C. Diven, Nucl. Sci. Eng. 43, 281 (1971).

19. C. Wagemans and A. J. Deruytter, Annals of Nuclear Energy, Vol. 3, p. 437 (1976).

20. T. A. Love, private communication.

EXPERIMENTS AND THEORY FOR DIFFERENTIAL n-p SCATTERING

C. A. Uttley
Atomic Energy Research Establishment
Harwell

The present status of the n-p differential scattering cross section is presented over the energy range below 30 MeV. This energy range covers the application of this cross section for the flux or relative flux spectrum measurements which are used to produce differential cross section data for fission and fusion reactor systems. Recent neutron-proton scattering experiments between 20 and 30 MeV have improved the isospin-zero phase shifts, particularly $\delta(^1P_1)$, which largely determine the anisotropy and the asymmetry about $\pi/2$ in neutron-proton scattering below 20 MeV.

[Nuclear Reactions np scattering E ≤ 30 MeV; experimental σ(θ), calculated σ(θ), phase shift analyses, model predictions].

Introduction

The differential neutron-proton scattering cross-section is used as a standard relative to which other elastic cross sections are measured in the MeV region of neutron energies. It is also the primary cross section for neutron flux or flux spectrum measurements above about 0.5 MeV. In these applications of the cross section a knowledge of the angular distribution in both hemispheres is required.

The detection of proton recoils from hydrogeneous radiators to determine, for example, the neutron spectrum from a linac target, requires the angular distribution at backward angles in the centre-of-mass, and neutron flux measurements using a proton recoil telescope usually utilize the cross section near 180°. The angular distribution predominantly in the forward hemisphere is needed on the other hand for relative scattering cross section measurements, and for the determination of the relative response of organic scintillators to neutron energy by scattering monoenergetic neutrons from hydrogenous samples.

Over the last few years most neutron-proton scattering experiments below 30 MeV have been made in the energy range 20-30 MeV using Van de Graaff or Tandem accelerators and the $^3H(d,n)^4He$ reaction as the neutron source. Indeed, apart from total cross sections and some differential scattering data at 14.1 MeV[1] few n-p measurements exist below 20 MeV compared with proton-proton scattering experiments. Thus the determination of the neutron-proton differential scattering at energies below 30 MeV has relied on calculation[2] using the phase shifts obtained from continuous energy phase shift analyses[3][4] of all nucleon-nucleon scattering data up to about 350 MeV. The isospin-one phases obtained from these analyses are accurate and unambiguous due to the accuracy of proton-proton experiments and the variety of observables which have been measured. The relatively inaccurate and sparse neutron-proton scattering data prior to 1970, however, resulted in difficulties in achieving a unique set of isospin-zero phases, especially below 80 MeV, which were theoretically acceptable unless some constraint was imposed on the analysis.[3]

A phase shift analysis of nucleon-nucleon scattering data, which includes several new neutron-proton scattering experiments, has recently been carried out in the energy range 20-30 MeV.[5] These new data comprise neutron-proton polarization measurements at 21.1 MeV[6] and 21.6 MeV[7] and neutron-proton angular distribution measurements at 24 and 27.2 MeV[8] as well as cross section measurements at two angles at 24 MeV.[9] Between them the measurements have considerably improved the accuracy of the data set of neutron-proton scattering observables available in this energy range, and the effect has been to provide a unique set of isospin-zero phases for partial waves $\ell = 0,1,2$ which is independent of model predictions or other constraints.

Angular Distribution and Differential Scattering Cross Section Measurements

Two different experimental techniques are necessary to measure the angular distribution of neutron-proton scattering over a wide angular range in the centre-of-mass (C.M.) system for energies below 50 MeV. Recoil protons from a thin polyethylene radiator exposed to an incident neutron beam can be detected with a counter telescope over an angular range 0° to more than 45° before the recoils have insufficient energy to be distinguished from increasing background events. This angular range corresponds to the whole of the backward hemisphere for n-p scattering in the C.M. system.

In order to extend the angular distribution to more forward angles the neutrons scattered by a hydrogenous target must be detected. This technique enables the angular distribution to be measured from some limiting forward angle to beyond 90°. Thus an angular region of overlap exists between the two methods which enables the data to be normalized.

The conversion of the relative cross section onto an absolute scale is usually achieved by fitting a Legendre polynomial expansion to the relative data and normalizing to the total cross section which has been measured to an accuracy of better than 1% below 30 MeV. However phase shift analysts prefer their own freedom to normalise relative data.

Detection of recoil protons

The most recent angular distribution measurements employ a counter telescope in which one or more thin solid state transmission detectors are placed between the hydrogenous radiator and a detector, usually a plastic scintillator or cesium iodide crystal, sufficiently thick to stop the most energetic recoil protons. The advantages of fast rise times and fast coincidence circuits were exploited by Rothenberg[10] to measure the angular distribution of neutron-proton scattering at 24 MeV to an accuracy of better than 2% between 164° and 89° in the centre-of-mass. A schematic diagram of Rothenberg's counter telescope is shown in fig. 1. The hydrogenous radiator is a polyethylene foil mounted on a thin platinum backing and supported on a target wheel which also has positions for a

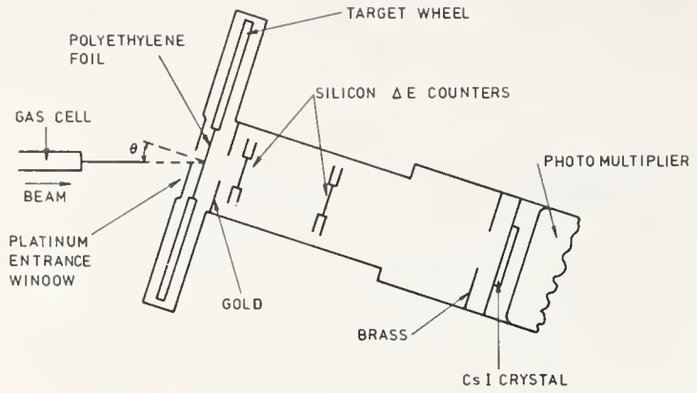

Fig. 1 Proton recoil detector for angular distribution measurements.

platinum blank, and a carbon target which can be centred on the telescope axis for background measurements. A modified version employing only one ΔE detector and with the CsI crystal replaced by an NE102 scintillator as the total energy detector was used by Burrows[8] to measure the angular distributions at 24 and 27.2 MeV over the angular range 158° to 71°. Burrows also made use of a particle identification programe to select the recoil protons which allowed his measurements to be extended into the forward hemisphere.

The 24 MeV data of Rothenberg and Burrows, converted into the C. of M. were fitted by least squares to a two parameter expression $A_0 + A_2P_2(\cos\theta)$ and normalized to the same total cross section of 397 mb. The values of $\sigma(180/\sigma(90)$ obtained by Rothenberg and by Burrows were 1.146 ± 0.017 and 1.135 ± 0.014 respectively.

Montgomery[11] et al. have recently reported an angular distribution measurement at 25.8 MeV in which backward angle data between 90° and 178° were obtained using a similar ΔE - E telescope. The half-angle subtended by the telescope at the polyethylene foil is smaller (2.55°) in this measurement than in the case of Rothenberg (3.3°) and of Burrows (6.2°) so that the correction to the angle of the telescope axis to obtain the mean laboratory proton recoil angle is also less.

Few attempts have been made to measure the cross section at or near 180° using counter telescopes due to the difficulty of measuring the neutron flux incident on the polyethylene target with an accuracy comparable to that of the angular distribution data. An exception was the measurement of Shirato and Saitoh[1] at 14.1 MeV in which the flux was determined by the associated particle method.

Recently Drosg[12] has reported measurements which give information on the 180° neutron-proton scattering cross section in the energy range 20 - 30 MeV. In these measurements, Drosg compared the zero-degree $^3H(d,n)^4He$ cross sections at 5 deuteron energies between 6 and 11 MeV (E_n = 23.1 to 28.5 MeV) obtained by time-of-flight and an NE213 liquid scintillator with those obtained with a proton recoil counter telescope. The efficiency of the scintillator over this neutron energy range was calibrated relative to the differential cross section of the $^3H(d,n)^4He$ reaction at 13.36 MeV between neutron emission angles θ(n) of 29° and 90°. The latter cross section was obtained from charged particle measurements of the $D(t,^4He)n$ reaction at 20 MeV. The zero-degree $^3H(d,n)^4He$ cross sections using the proton recoil telescope and the Hopkins and Breit[2] (YALE) calculation of the 180° neutron-proton cross sections were (5.7 ± 3.3)% lower than those obtained with the calibrated time-of-flight system.

In another experiment using both detectors, Drosg compared the zero-degree yield of 11.23 MeV neutrons from the $^3H(p,n)^3He$ reaction with that of 25.3 MeV neutrons from the $^3H(d,n)^4He$ reaction. Thus only the relative efficiencies of the detectors are required, and an independent check of the relative efficiencies of the scintillator was carried out at these two energies using the $^3H(d,n)^4He$ and $D(t,n)^4Ho$ reactions. A comparison of the telescope yields at 11.23 MeV and 25.3 MeV with those for the scintillator at these energies determines the ratio $\sigma(180°, 11.23)/\sigma(180°, 25.3)$ of the neutron-proton scattering cross sections. The measured ratio of 2.22 ± 0.06 is (6.7 ± 2.9)% higher than the value of 2.08 from the Hopkins and Breit (YALE) calculation and supports the previous experiment.

Detection of Scattered neutrons

Three recent experiments have been reported at energies below 30 MeV in which the angular distribution of neutrons scattered from an incident monoenergetic beam by a hydrogenous target has been measured. In two of these measurements, by Masterson[9] at 24 MeV and by Cookson et al.[13] at 27.3 MeV, the monoenergetic neutrons were produced by the $^3H(d,n)^4He$ reaction at zero-degrees, while in the measurement by Montgomery et al.[11] at 25.8 MeV using the Davis cyclotron the incident neutron beam was selected by time-of-flight.

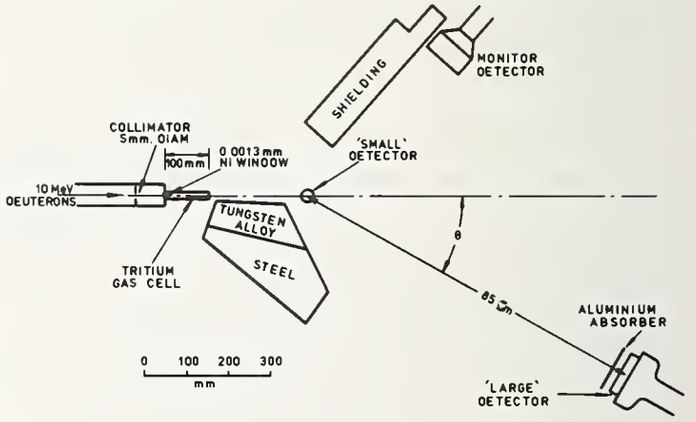

Fig. 2 Experimental layout for angular distribution measurements by detecting scattered neutrons.

The principle of the experiments is illustrated in Fig. 2 which refers specifically to the measurement of Cookson et al. Neutrons in the incident beam are scattered by protons in the small target scintillator and are detected at a laboratory angle ψ by a larger scintillator placed about 1m from the target. A scattered event is defined by a coincidence between pulses from the two detectors occurring within a narrow time interval ≃ 100 nsec. A second organic scintillator at a fixed angle to the incident beam is used as a monitor. Each event is characterized by three parameters: the scattered neutron time-of-flight and the pulse amplitudes from the target scintillator and neutron detector. The first of these parameters is required to separate scattered neutrons arising from the primary beam from those of lower energies produced in the source and from γ-rays. The pulse amplitude distributions help to identify the type of

events producing peaks in the time-of-flight spectra for the different scattering angles.

Two potentially important sources of error in the relative cross section measurements by this method are: (a) scattered events due to fast recoil protons produced near the edge of the target and reaching the neutron detector; (b) scattered events due to neutron reactions in carbon in the target scintillator. The effect of fast recoil protons can be eliminated by placing a thin counter in anticoincidence between the target and neutron detectors as in the experiment of Montgomery et al. Alternatively a thin aluminium plate shielding the neutron detector will suffice as indicated in Fig. 2. The reactions in carbon which can simulate a neutron-proton scattered event are $^{12}C(n,n')3\alpha$ and $^{12}C(n,n'\gamma)^{12}C$. For all situations when the first reaction gives neutrons which could fall within the time-of-flight limits of the n-p elastically scattered peak, the light output of the alpha particles is lower than the discriminator level on the target scintillator and so the events are not recorded. The second reaction is significant, however, and must be investigated experimentally.

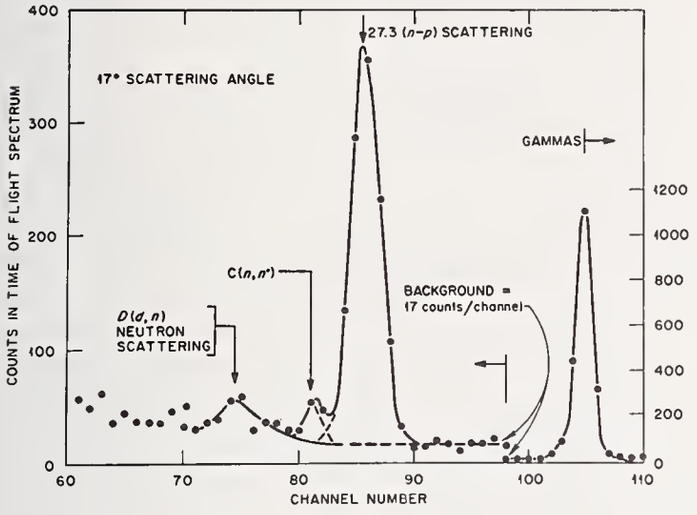

Fig. 3 Time-of-flight spectrum of scattered events at a laboratory angle of 17°. (Cookson et al.)

A time-of-flight spectrum is shown in fig. 3 for the scattering of 27.3 MeV neutrons through a laboratory angle of 17° in the experiment of Cookson et al. The small peak to the left (low energy end) of the main peak was ascribed to the $^{12}C(n,n'\gamma)$ reaction in which the 4.44 MeV γ-ray is detected in the target and the inelastic neutron in the neutron detector. This assignment was confirmed in a separate experiment in which the NE102A target scintillator was replaced by an NE213 cell of similar dimensions used with an (n-γ) pulse shape discrimination circuit. A peak was observed at the same position in the TOF spectrum, independent of scattering angle, when γ-ray events in the target scintillator were selected. A correction for the effect of this reaction is necessary because the inelastic neutrons are not resolved from the main elastic peaks at intermediate scattering angles.

Calculated corrections are also necessary for: (a) the loss of events due to scattering collisions close to the walls of the target in which the recoil protons lose too little energy to be detected, (b) multiple scattering in the target in which the net contribution is calculated for the attenuation of neutrons initially scattered at the correct angle and for those scattered into the detector by subsequent collisions in carbon or hydrogen. Scattering events from carbon atoms alone are not detected. The size of these corrections in the experiment of Cookson et al. is shown in Table 1.

Relative efficiency of the neutron detector

The wide energy range of the scattered neutrons to be detected requires that a measurement of the efficiency of the detector scintillator be made. In the experiments of Montgomery et al. and of Cookson et al., the efficiency measurements over the required energy range were carried out using the associated particle method which gives the absolute efficiency for neutron detection. Although the absolute efficiency is not required even for absolute cross section measurements, this method has the essential feature of being independent of other cross section data.

The associated particle technique adopted by Cookson et al.[14] utilized the $^{3}H(p,n)^{3}He$, $^{2}H(d,n)^{3}He$ and $^{3}H(d,n)^{4}He$ reactions in order to measure the efficiency of a 10 cm. diameter by 2.54 cm thick NE102A. detector over the energy range 5 - 25 MeV which corresponds to the scattering of 27.3 MeV neutrons over a laboratory angular range from 17° to 57.9°, and

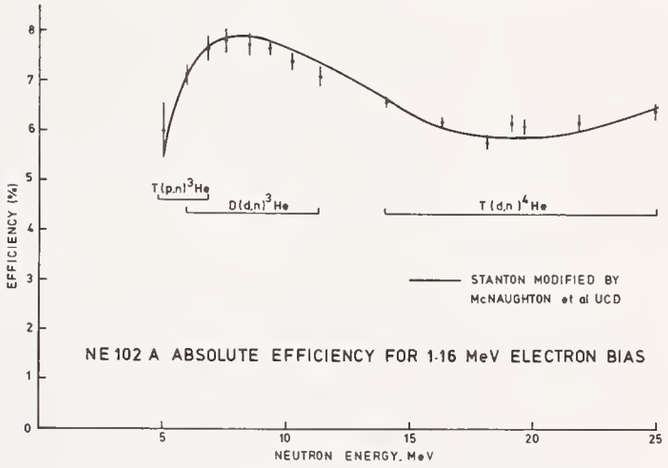

Fig. 4 The absolute efficiency of a 10 cm diameter by 2.54 cm thick NE102A plastic scintillator for a bias of 1.16 MeV electron energy.

allowing for an angular spread of scattering events at each detector angle of $\pm$ 6.6°. The efficiency of their detector is shown in Fig. 4 for the 1.16 MeV electron energy bias used in their angular distribution measurement. The curve which is compared with the measured data is the efficiency predicted by the Monte Carlo code of Stanton in which some of the input data for the carbon reaction cross sections and the electron-proton light output relationship have been modified by McNaughton et al.[15] The agreement between measured and predicted efficiencies observed by the Davis group for their 7.1 cm diameter by 15.2 cm long plastic scintillators, used in the angular distribution measurement at 25.8 MeV, is similar to that indicated in Fig. 4. In the latter case, the difference in the angular distribution between using the relative efficiency predicted by the Stanton code and that given by a freehand curve through the experimental efficiency points is small except for the energy region round 11 MeV, where an additional uncertainty was included to the data of Cookson et al. for the two largest scattering angles in Table 1.

Table 1

Corrections to angular distribution data in which scattered neutrons are detected (Cookson et al.)

Lab Scattering angle (degrees)	proton bias on target MeV	Loss of proton recoils	$^{12}C(n,n'\gamma)$	Net relative multiple scattering	C-of-mass Relativistic Correction
17	0.5	1.001	0.950	1.000	0.989
26.6	2.3	1.011	0.974	1.001	0.992
33.2	4.0	1.023	0.979	1.002	0.995
39.2	5.4	1.041	0.985	1.003	0.998
45.0	6.5	1.058	0.990	1.005	0.999
50.8	7.8	1.08	0.995	1.006	1.004
57.9	7.8	1.10	0.996	1.007	1.011

Differential neutron-proton cross sections

To measure the absolute cross section by detecting the scattered neutrons requires the measurement of the neutron flux incident on the target scintillator using the same neutron detector. It is achieved by removing the target scintillator and measuring the incident neutron flux relative to unit charge collected on the neutron source. Thus the scattering cross section at laboratory angle ψ depends only on the ratio of the neutron detector efficiencies at incident energy E_o and at scattered neutron energy $E_o \cos^2 \psi$, and not on the absolute detector efficiency.

The absolute 24 MeV neutron-proton scattering cross sections at laboratory angles of 19.5° and 25.1° were measured by Masterson[9] to an accuracy of better than 2% using this procedure. It is applicable only when a detector is employed capable of discriminating between neutrons and gamma-rays since, unless a pulsed accelerator is used, no time-of-flight discrimination is available for the zero-degree flux measurement. In principle the accuracy of the differential cross section will be worse than the angular distribution data due to the additional uncertainty in the absolute correction for multiple scattering and flux attenuation in the target.

Normalization of relative cross section data

It is common practice for angular distribution data to be normalized to the total cross section by fitting a legendre polynomial expansion $\sum_{o}^{n} a_i P_i (\cos\theta)$ to the data after a relativistic conversion to the centre-of-mass system. However, little is to be gained by this procedure if the data are to be included in a phase shift analysis since all measurements are then separately normalized to the most recent total cross section data. A comparison can be made with existing evaluations of n-p differential scattering based on different phase shift analyses by normalizing the relative data to unity at 90°. Such a comparison is shown in fig. 5 of the 27.3 MeV data of Cookson et al. and the 27.2 MeV proton recoil data of Burrows with the predicted values of $\sigma(\theta)/\sigma(90)$ using the Yale phase shifts and those from the parametrization of Binstock.[16] The latter is based on calculations from phase shifts predicted by the Bryan-Gersten[17]

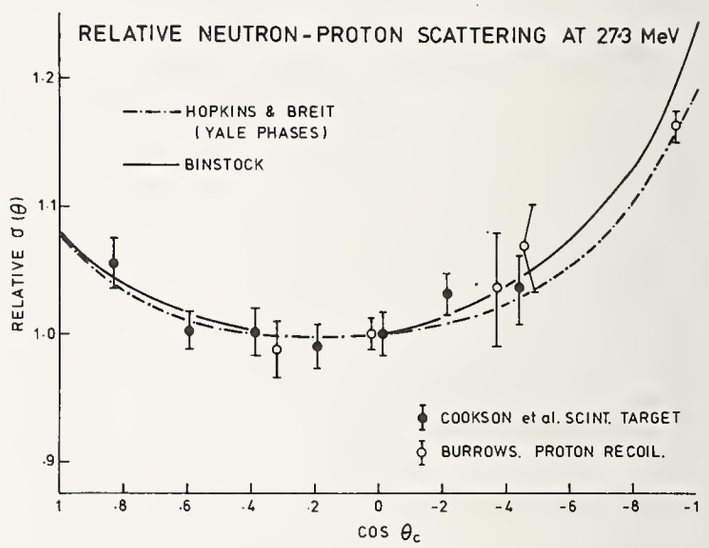

Fig. 5 Relative scattering cross section at 27.3 MeV compared with predictions from a model calculation (Binstock) and from phase shift analyses.

model. The data appear to be in better agreement with the Yale phase shifts due largely to the datum at the most backward angle.

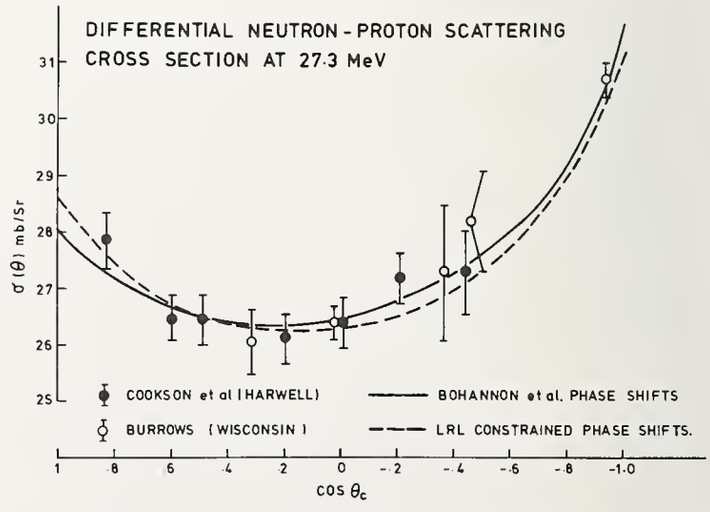

Fig. 6 Differential scattering cross sections at 27.3 MeV from relative data normalized to total cross section and compared with predictions from phase shift analyses.

The angular distribution measurement of Burrows was included in the data set used in the phase shift analysis of Bohannan et al.[15] referred to in the Introduction. The differential scattering cross section resulting from the normalization of Burrows data in this analysis is shown in fig. 6 along with the cross sections predicted by Bohannan at 27.3 MeV (the effect of 0.1 MeV difference in energy < ½% in cross section). The Livermore (constrained) prediction is also shown in fig. 6.

Phase Shift Analyses

The continuous energy phase shift analyses of MacGregor, Arndt and Wright[3] (Livermore) and of Seaman et al.[4] (Yale) were made to nucleon-nucleon scattering data available prior to 1970 and form the basis for the evaluation of the H(n,n)H scattering observables up to 30 MeV by Hopkins and Breit.[2]

The simultaneous fitting of all p-p and n-p scattering observables over a wide energy range gave the energy dependence of all the significant phase parameters which improved the determination of the lower partial wave phases of importance below 30 MeV. The analysis by the Livermore group without any imposed constraints on the data showed that the isospin-zero phases were relatively poorly determined due to an inadequate set of n-p scattering observables and particularly differential scattering measurements at energies below 100 MeV. They observed a strong correlation between the $^3S_1$-$^3D_1$ mixing parameter, ε_1, and the singlet p-wave phase shift, $\delta(^1P_1)$, such that when the former was constrained to be positive at low energies, as suggested by its relationship to the deuteron quadrupole moment[18], the value of $\delta(^1P_1)$ decreased to a value more in accord with model predictions. The Livermore group also demonstrated that the solution obtained by forcing an exact fit to the ratio $\sigma(165^o)/\sigma(8^o)$ at 24 MeV measured by Rothenberg resulted in a positive ε_1 at low energies and an equally acceptable value of $\delta(^1P_1)$. The solution arising from this experimental constraint is shown in Table 2.

The Livermore group also reported a single energy phase shift analysis at 25 MeV which included all p-p and n-p data in the energy range 20-30 MeV. The phase parameters obtained from this search are also shown in Table 2. Evidently the accuracy of the angular distribution data of Rothenberg at 24 MeV is not sufficient to outweigh the earlier neutron-proton angular distribution data included in the analysis, since the sign of ε_1 is still negative and the value of $\delta(^1P_1)$ larger than for the Yale and Livermore constrained set.

Recently Bohannan, Burt and Signell[5] have published the results of a phase shift analysis of p-p and n-p data in the energy range 20-30 MeV which include the results of several n-p scattering experiments made since the Livermore analysis. The precision of the new data has meant that many of the earlier measurements included in the Livermore analysis at 25 MeV could be removed from the data set because they had no significant effect on the deduced phase parameters.

The new high precision data now available and used by Bohannon et al. consists of neutron-proton polarization measurements at 21.1 MeV by Morris et atl.[6] and at 21.6 MeV by Jones and Brooks[7] in addition to the angular distribution measurements of Burrows at 24 MeV and 27.2 MeV[8] and the differential scattering cross sections at 24 MeV of Masterson.[9]

The analysis includes charge splitting of all the p-p and n-p isospin-one phase shifts and is not confined to separate p-p and n-p values of ^1S_o. In fact the charge splitting of ^1S_o was included as a separate parameter. The low orbital angular momentum phase parameters obtained from this analysis are shown in Table 2 although calculated higher partial wave phase shifts were also included.

A comparison of the phase parameters listed in Table 2 shows that: (a) the isospin-one phases, largely determined by p-p scattering experiments, are in good agreement; (b) discrepancies in the isospin-zero phases are largely confined to $\delta(^1P_1)$ and ε_1 and arise from the inadequacy of the earlier n-p differential scattering data. In the case of ε_1 no neutron-proton scattering observable has been measured which is particularly sensitive to this parameter, and the range of the values of ε_1 noted in Table 2 has a negligible influence on the neutron-proton differential scattering cross section below 30 MeV compared with that for $\delta(^1P_1)$.

The significance of $\delta(^1P_1)$ below 20 MeV

It was suggested by Macgregor et al.[3] that the neutron-proton scattering observable most sensitive to $\delta(^1P_1)$ which could readily be measured was the differential scattering cross section. This was confirmed in a sensitivity analysis carried out at 50 MeV by Binstock and Bryan.[19] The importance of this phase parameter to n-p differential scattering at low energies is shown in fig. 7(a). The summed contribution from the three triplet S-P terms to the coefficient of $P_1(\cos\theta)$ in the n-p differential scattering cross section decreases more rapidly with energy than the singlet S-P term. The calculation was carried out using the tabulated phase shifts of Seaman et al. down to 10 MeV and the constrained set of Macgregor et al. below 10 MeV for partial waves $\ell = 0,1,2$. It is clear that most of the coefficient below 20 MeV, and therefore the asymmetry in scattering, is determined by $\delta(^1P_1)$. The reason for the suppression of the triplet S-P terms is indicated in Fig. 7(b). In addition to a cancellation due to the sign of one ^3P phase being opposite, the individual ^3S-^3P terms are reduced by $^3S_1$ passing through $\pi/2$ near 18 MeV.

The importance of the recent neutron-proton scattering experiments between 20 and 30 MeV is that, when included in the data set for a phase shift analysis by Bohannon et al., they produce unambiguous isospin-zero phases with no external constraints. The accurate neutron-proton polarization measurements of Jones and Brooks[7] at 21.1 MeV over the C.of M. angular range 50^o to 170^o have determined the spin-orbit combination of the ^3D phases ($9^3D_1 + 5^3D_2 - 14^3D_3$)

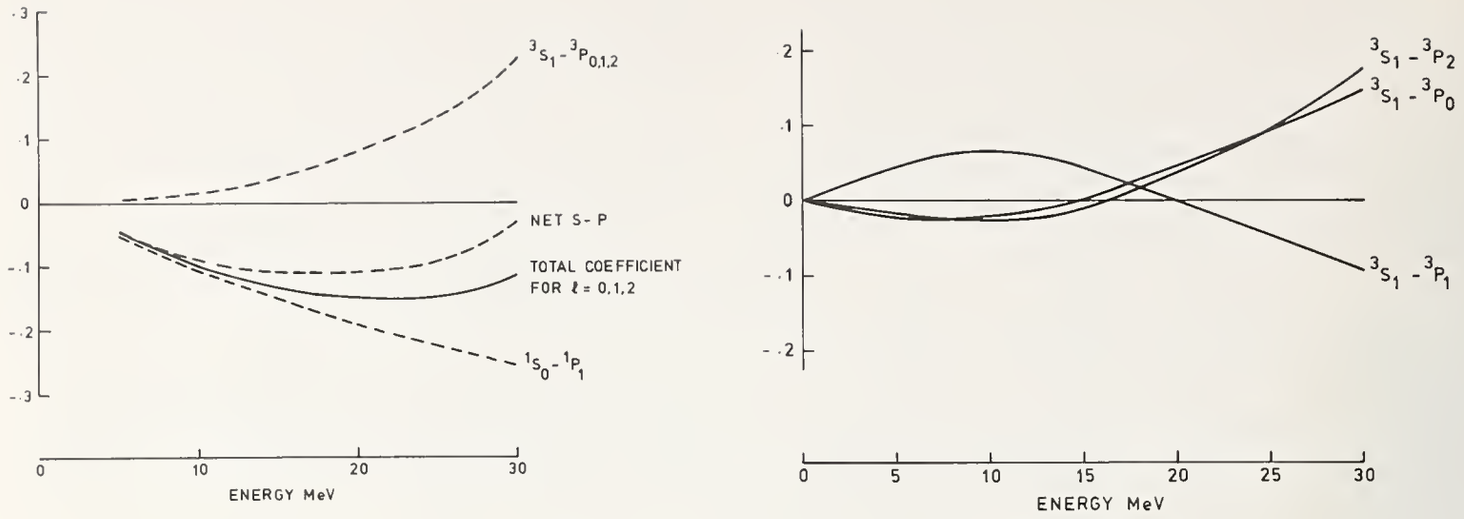

Fig. 7 (a) Components of coefficient A_1 of P_1 (cos θ) in differential n-p scattering below 30 MeV; (b) energy dependence of individual triplet S-P components of A_1.

Table 2

Phase shifts in degrees at 25 MeV from analyses of (p,p) and (n,p) scattering data

Phase Shift	Livermore (Experimental)	Livermore (Constrained)	Livermore (Single Energy)	Yale	Bohannon et al.
T = 1					
^1S_o(n,p)	52.96 ± 0.62	52.31 ± 0.62	48.84 ± 1.75	50.51 ± 0.01	51.0 ± 1.5
^3P_o	8.21 ± 0.11	8.21 ± 0.11	8.52 ± 0.31	8.15 ± 0.17	7.95 ± 0.68
$^3P_1$	-5.08 ± 0.03	-5.08 ± 0.03	-5.04 ± 0.15	-4.96 ± 0.06	-5.06 ± 0.16
$^3P_2$	2.59 ± 0.04	2.59 ± 0.04	2.54 ± 0.08	2.63 ± 0.05	2.64 ± 0.12
$^1D_2$	0.72 ± 0.01	0.72 ± 0.01	0.74 ± 0.03	0.915 ± 0.017	0.751 ± 0.029
T = 0					
$^3S_1$	79.48 ± 0.38	79.18 ± 0.37	84.49 ± 2.70	80.19 ± 0.14	81.0 ± 1.6
$^1P_1$	-1.85 ± 0.39	-4.61 ± 0.08	-4.0 ± 0.69	-4.90 ± 0.48	-5.18 ± 0.47
ε_1	-0.68 ± 0.42	1.29 ± 0.32	-0.34 ± 0.731	1.82 ± 0.49	1.03 ± 0.58
$^3D_1$	-2.60 ± 0.09	-2.42 ± 0.08	-3.21 ± 0.18	-3.00 ± 0.42	-2.91 ± 0.09
$^3D_2$	4.16 ± 0.05	4.08 ± 0.05	-	3.99 ± 0.42	3.89 ± 0.10
$^3D_3$	0.18 ± 0.03	0.23 ± 0.03	-	0.14 ± 0.20	0.038 ± 0.023

from the shape of $P(\theta)_{n,p}$ with angle. The differential scattering data also involve the separate ^3D phases and the two types of measurements together evidently produce a solution yielding a unique value of $\delta(^1P_1)$.

Model predictions of $\delta(^1P_1)$

Binstock and co-workers[19][20][21] have carried out an extensive analysis of experimental nucleon-nucleon data near 50 MeV to determine the value of $\delta(^1P_1)$ at this energy and to compare it with predictions of various meson-theoretical and phenomenological models. They find from their phase shift analysis that the value of $\delta(^1P_1)$ depends strongly on the n-p differential scattering data included in the data set, with less significant changes in the other isospin-zero phase parameters. Bryan and

Binstock have compared the values of $\delta(^1P_1)$ from their analyses with those predicted by models in which the coupling constants for π and heavier meson exchange have been obtained by fitting nucleon-nucleon data from 0 to 450 MeV. One such model is that of Bryan and Gersten[17] referred to earlier as the model used by Binstock to parametrize the total, differential scattering and polarization for (n-p) elastic scattering above 25 MeV. The predicted values of $\delta(^1P_1)$ at 50 MeV only agree with those deduced from analysis when selected n-p differential scattering data are included.

The value of $\delta(^1P_1)$ at 25 MeV predicted by the Bryan-Gersten model is -6.25^o which is more than two standard deviations smaller than the value of $(-5.18 \pm 0.47)^o$ from the analysis of Bohannon in Table 2. This accounts at least in part for the increased asymmetry observed in fig. 5 for the Binstock angular distribution compared with those for the Yale and Livermore (constrained) phase shifts which have values of $\delta(^1P_1)$ closer to Bohannon's. It should be pointed out, however, that the $\delta(^1P_1)$ of Bohannon et al. at 25 MeV is in agreement with the value of -5.12^o predicted by the phenomenological potential model of Hamada and Johnston.[22]

The latter model has been recommended by Lomon and Wilson[23] as giving phase parameters which best represent the n-p scattering observables at low energies. The phase shifts below 5 MeV vary with energy as $k^{(2\ell+1)}$, where ℓ is the orbital angular momentum and k is the neutron wave number. This threshold behaviour was used in the evaluation of Hopkins and Breit. Lomon and Wilson have discussed the deviation from the threshold behaviour which occurs with increasing energy due to the influence of the long range part of the interaction potential arising from one-pion-exchange (OPEP). They have found from a comparison of several models with experimental data that the Hamada - Johnston potential, which includes OPEP and is adjusted to reproduce the deuteron data (binding energy, triplet scattering length and quadrupole moment), gives the best agreement at low energies.

Discussion

The phase shift analysis of Bohannon et al. centered at 25 MeV neutron energy and motivated by recent accurate n-p polarization data can be updated shortly by the inclusion of the angular distribution data of McNaughton et al. at 25.8 MeV and those of Cookson et al. at 27.3 MeV. A comparison with existing evaluations at 25 MeV may indicate the need to recalculate the observables $\sigma(\theta)$, σ_T and $P(\theta)$ up to 30 MeV in a convenient format similar to that adopted by Hopkins and Breit. In this event, the energy dependence of the phase shifts prescribed by the Hamada-Johnston potential could be used and normalized if necessary to those of the phase shift analyses.

One problem posed by the measurements of Drosg is the accuracy with which the 180^o neutron-proton scattering cross section can be specified, since this limits the accuracy of flux measurements above 20 MeV using proton recoil counter telescopes. The 180^o cross sections in mb/sr at 27.3 MeV predicted from available phase shift analyses are: Yale 31.27, Livermore (constrained) 31.16, Bohannon 31.68 and Binstock 32.35, representing a total spread of 3.7%. The value indicated by Drosg's measurements is (5.7 ± 3.3)% lower than the Yale and Livermore (constrained) predictions and about two standard deviations lower than the arithmetic mean value of the predicted cross sections. However Drosg[24] has shown that the Yale and Livermore predictions of $\sigma(180^o)$ over the energy range 8 to 16 MeV, when applied to counter telescope measurements of the 0^o excitation function of the $^2H(d,n)^3He$ reaction of other workers, agree very well with his measurement using the calibrated time-of-flight system discussed earlier.

Acknowledgements

Much of the material presented in this paper was produced by my colleagues Drs. J.A. Cookson (Harwell), J.L. Fowler (ORNL), M. Hussain (Dacca University) and R.B. Schwartz (NBS Washington) to whom I am indebted. Communications with Dr. P. Signell (Michigan State University) and Dr. M. Drosg (Vienna University) are gratefully acknowledged.

References

(1) Shirato, S. and Saitoh, K. Journal of Phys. Soc. Japan 36, 331 (1974).
(2) Hopkins, J.C. and Breit, G. Nucl. Data Tables A9, 137 (1971).
(3) Macgregor, M.H., Arndt, R.A. and Wright, R.H. Phys. Rev. 182, 1714 (1969).
(4) Seaman, R.E., Friedman, K.A., Breit, G., Haracz, R.D., Holt, J.M. and Pratkash, A. Phys. Rev. 165, 1579 (1968).
(5) Bohannon, G.E., Burt, T. and Signell, P. Phys. Rev. C13, 1816 (1976).
(6) Morris, C.L., O'Malley, T.K., Hay, J.W. and Thornton, S.T. Phys. Rev. C9, 924 (1974).
(7) Jones, D.T.L. and Brooks, F.D. Nucl. Phys. A222, 79 (1974).
(8) Burrows, T.W. Phys. Rec. C7, 1306 (1973).
(9) Masterson, T.G. Phys. Rev. C6, 690 (1972).
(10) Rothenberg, L.N. Phys. Rev. C1, 1226 (1970).
(11) Montgomery, T.C., Bonner, B.E., Brady, F.P., Broste, W.B. and McNaughton, M.W. Annual Report, Crocker Nucl. Lab. UCD-CNL786.
(12) Drosg, M. Proc. of Int. Conf. on the Int. of Neutrons with Nuclei, P.1383, Lowell 1976.
(13) Cookson, J.A., Hussain, M., Fowler, J.L., Schwartz, R.B. and Uttley, C.A. INDC(UK)-28U also Fowler, J.L. et al. Bulletin of the Amer. Phys. Soc. 22, 53 (1977).
(14) Cookson, J.A., Hussain, M., Uttley, C.A., Fowler, J.L. and Schwartz, R.B. Proc. of Conf. on Nuclear Cross Sections and Technology, Washington, 1975, ed. R.A. Schrack and C.D. Bowman.
(15) McNaughton, M.W., et al. Nucl. Instr. and Meth. 116, 25 (1974) and ref. 11.
(16) Binstock, J. Phys. Rev. C 10, 19 (1974).
(17) Bryan, R. and Gersten, A. Phys. Rev. D 6, 341 (1972).
(18) Signell, P. Advances in Nuclear Physics, ed. H. Baramger and E. Vogt (Plenum) 1969 vol. 2.
(19) Binstock, J. and Bryan, R. Phys. Rev. D9 2528 (1974).
(20) Arndt, R.A., Binstock, J. and Bryan, R. Phys. Rev. D8, 1397 (1973).
(21) Bryan, R. and Binstock, J. Phys. Rev. D10, 72 (1974).
(22) Hamada, T. and Johnston, I.D. Nucl. Phys. 34, 382 (1962).
(23) Lomon, E. and Wilson, R. Phys. Rev. C, 1329 (1974).
(24) Drosg, M. Private communication.

USE OF THE n,p SCATTERING REACTION FOR NEUTRON FLUX MEASUREMENTS*

J. B. Czirr
Lawrence Livermore Laboratory
University of California
Livermore, California 94550

Several contemporary proton-recoil detectors are described and compared. These detectors have been used for neutron-spectrum measurements over various portions of the 10-keV-to-20-MeV energy range. Several factors which limit the accuracy of the results are compared quantitatively. General suggestions are given for setting and using standard cross sections and for future developments using the n,p scattering reaction.

(Detectors; flux; neutrons; proton-recoil; scattering; standards)

Introduction

For a neutron-induced reaction to be considered as a first-class standard, we require that the cross section be known to better than ±1%. Even with this requirement met, experimental difficulties may preclude the use of the reaction in certain energy regions of interest. Such considerations have led to the use of the $^{6}Li(n,\alpha)$ and $^{10}B(n,\alpha)$ or $^{10}B(n,\alpha\gamma)$ reactions as standards for neutron energies below 10 or 20 keV. Above these energies, high-precision flux-measurement techniques (involving a neutron cross section) make use of the n,p scattering reaction. Other techniques of comparable accuracy involve totally absorbing detectors or associated-particle systems.

The present paper will describe techniques for neutron flux measurements in the 10-keV-to-20-MeV energy range which use the n,p scattering reaction. Figure 1 gives an example of the use of this reaction to obtain the fission cross section of ^{239}Pu. This paper describes methods of obtaining the rate R_1 of Figure 1. Implicit in this figure is the suggestion that the n,p scattering reaction is not suitable for everyday use by those interested in off-the-shelf flux monitors.

Contemporary Proton Detectors

A classification scheme is given in Table 1 for five contemporary proton-recoil detectors and Figure 2 shows the geometrical arrangement for each system.[1-5]

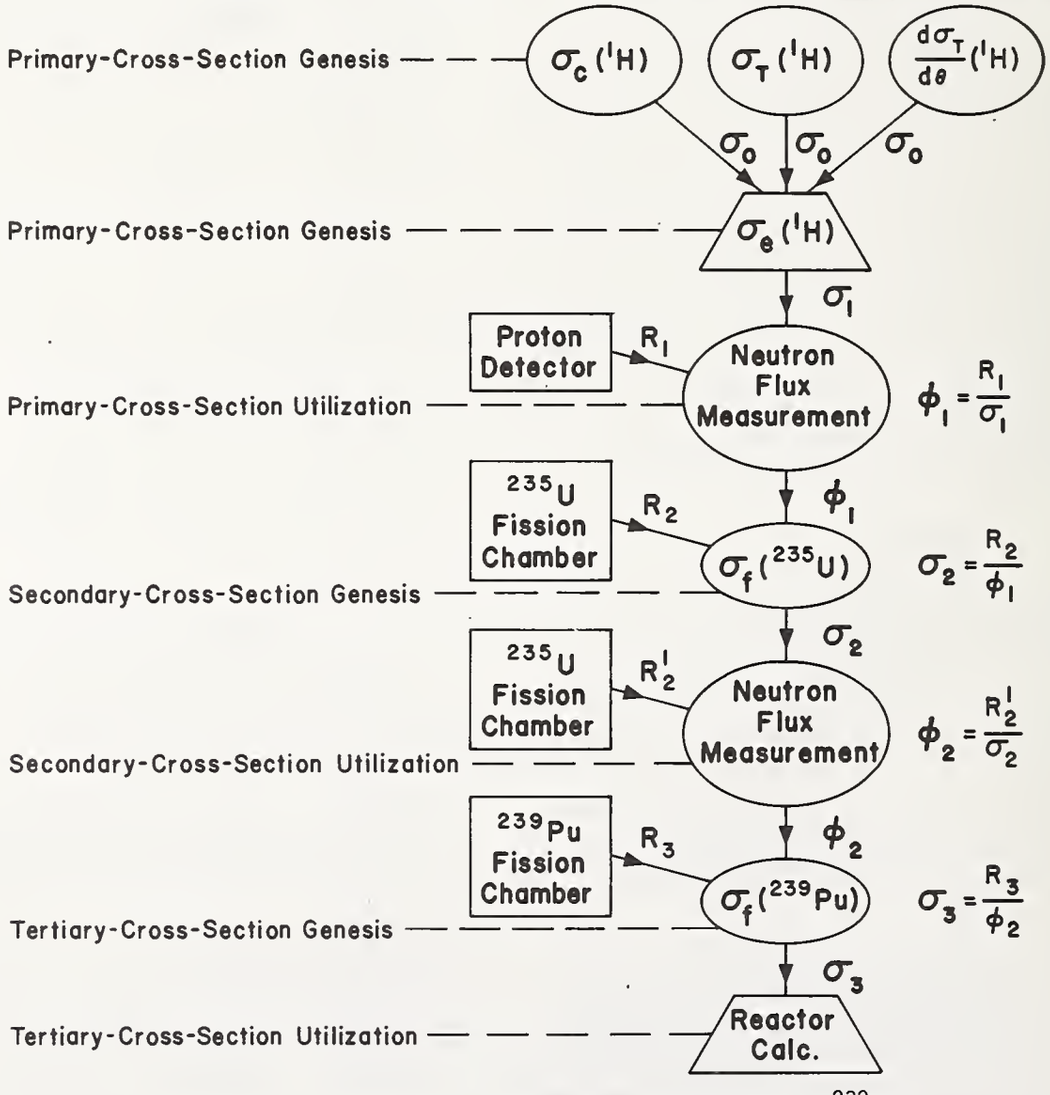

Fig. 1. Schematic outline of the use of standard cross sections to obtain σ_f (^{239}Pu).

* Work performed under the auspices of the U.S. Energy Research and Development Administration. W-7405-Eng-48

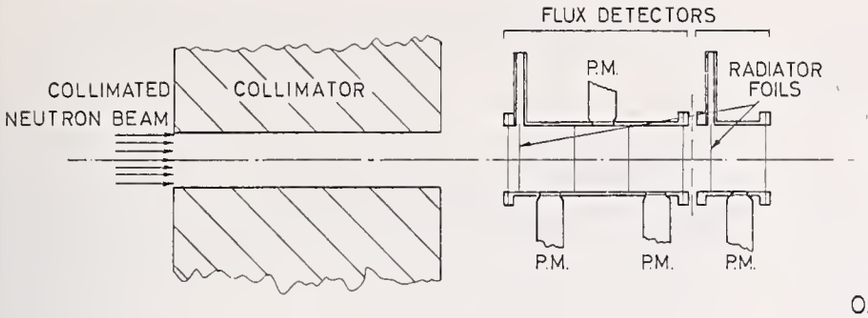

KFK PROTON-RECOIL TELESCOPE

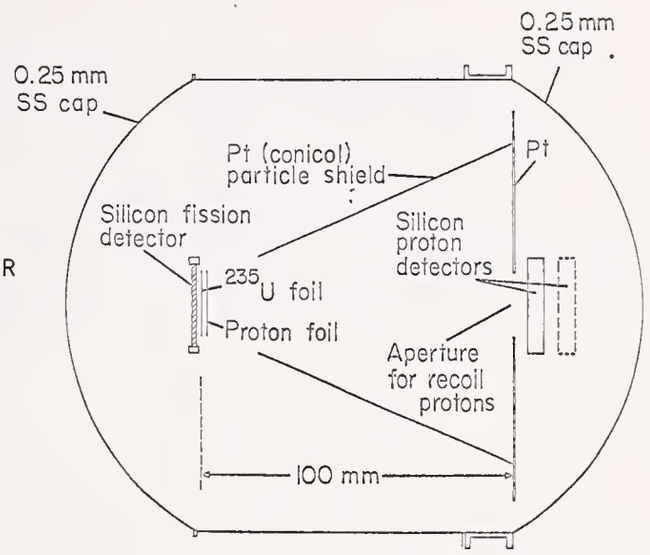

LASL PROTON-RECOIL DETECTOR

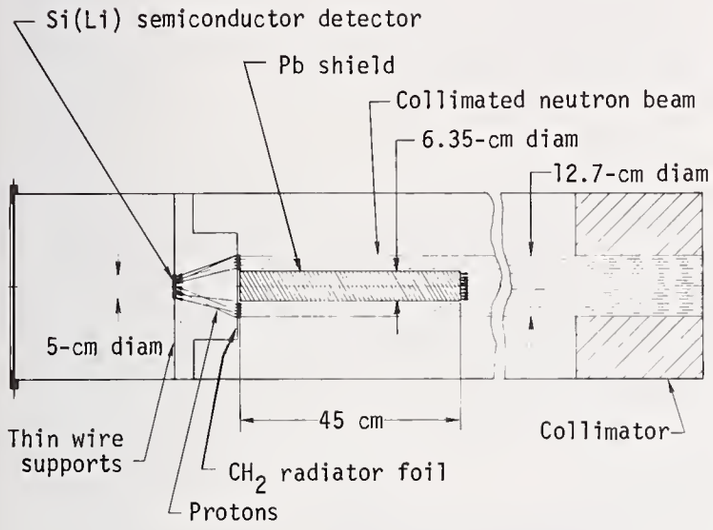

LLL PROTON-RECOIL DETECTOR

NBS HYDROGEN-FILLED PROPORTIONAL COUNTER

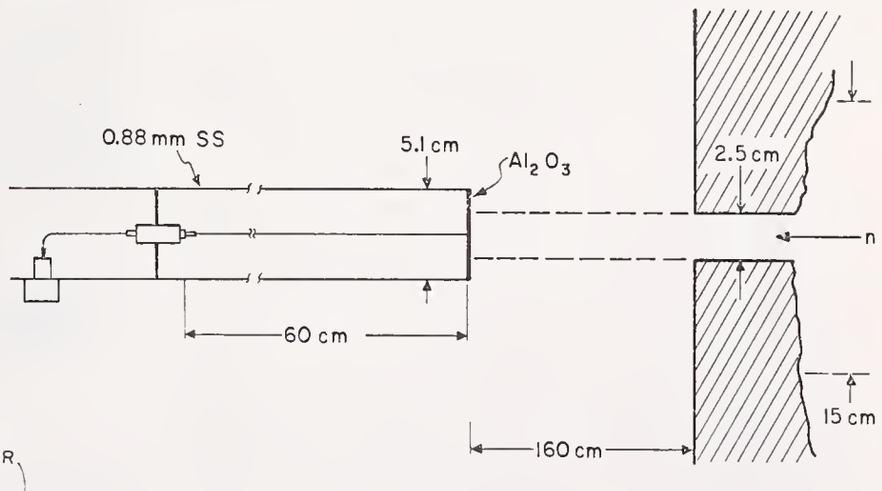

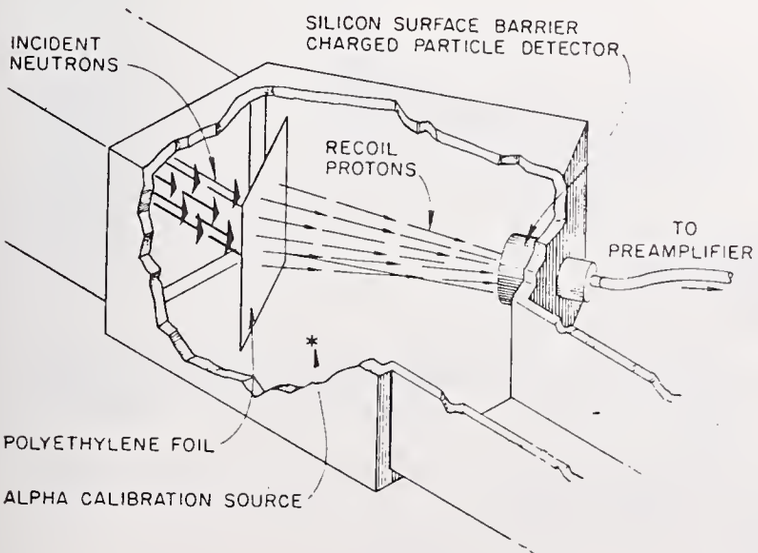

ORNL PROTON-RECOIL DETECTOR

Fig. 2. Geometrical arrangements for five contemporary proton-recoil-detector systems.

It is interesting that none of these modern detectors rely on a precise neutron-energy-measurement capability.† This feature permits an important increase in proton-detection efficiency. It is also to be noted that none of the five systems match the ideal detector listed in the last column of Table I.

A quantitative comparison of several detectors is shown in Table II. Each of these detectors was chosen to perform with a particular accelerator and they are not necessarily to be compared with each other for use with a single neutron source. For this reason, the information must be used judiciously as a starting point for future developments or for evaluating past results. Fortunately, most of these systems were used to obtain the fission cross section of ^{235}U, a circumstance which allows us to make valid comparisons. For this purpose, we show in Figure 3 the total error quoted for several ^{235}U fission-cross-section measurements as a function of neutron energy.[1-4] Because the error in measuring the fission rate is usually smaller than that of the flux measurement, these results serve as a rough figure of merit for the several proton detectors.

Limitations on Accuracy

I will attempt to evaluate those factors which limit the accuracy of the various detector systems. Eight such factors have been identified and are listed in Table III.

1. Cross Section Errors

The n,p total-cross-section error is less than 1% below 30 MeV and will be ignored. Only the effect of uncertainties in the angular distributions will be compared in Table III. The listed percentages are the published uncertainty in $\sigma_H(\theta)$ at the appropriate angle.[6] The numbers in parentheses refer to the neutron energy at which the uncertainty applies.

2. Background

The typical percentage background over the useful energy range is listed. If it can be assumed that the fractional error in the background is the same for each system (±10% of the background, for example), then a relative uncertainty can be estimated from Table III.

3. Neutron-Energy Resolution

Because of the widely different energy ranges and accelerators involved, only a crude characterization of energy resolution will be given. The values of $\Delta E/E$ are listed near the midrange of the appropriate energy region for each system. In most cases, the cross-section accuracy illustrated in Figure 3 was achieved by summing over several high-resolution time-of-flight channels. For these cases, the practical resolution is taken to be the fractional separation between adjacent published energies. For the NBS proportional counter, a timing uncertainty of 0.6 μsec was used and for the ORNL system, a beam width of 50 nsec was the limiting factor.

4. Counting Rate

I will assume that each investigator was free to place his proton detector at the optimum flight-path distance. The appropriate counting rates can then be computed directly from Table II. The resulting rates are listed in Table III, where only the thick-foil rates are included. The high rate for the LASL detector is a result of the short flight path (10 cm.) employed with a monoenergetic neutron source. A

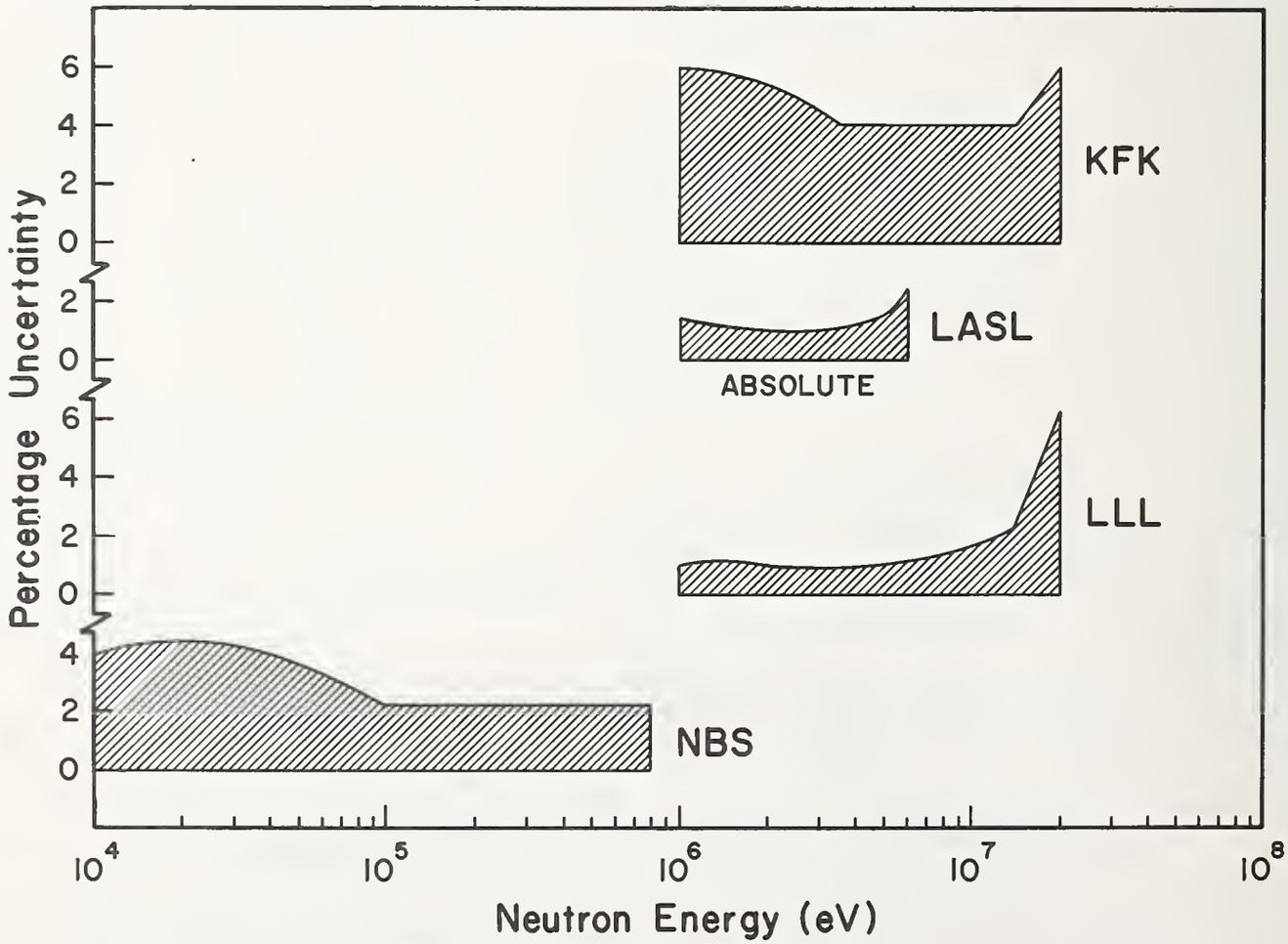

Fig. 3. Figure of merit for four contemporary systems vs. neutron energy.

† Neutron energy is measured by time of flight or is inferred from the source reaction.

further efficiency factor of approximately 10^{-2} must be applied to this system because of the necessity of obtaining each data point separately. The rate in parentheses reflects this added factor.

5. Pulse-Height Extrapolation

An error is incurred in extrapolating the measured portion of the pulse-height distribution to zero pulse height for two of the detector types. The electronic threshold for the NBS proportional counter is set at 1.1 keV and this results in an extrapolation error of less than 0.5% for neutron energies above 10 keV.[4] This estimate is based on a 5% uncertainty in the threshold energy and a constant value for energy loss per ion pair (W) above 1.1 keV. However, variations of 10% in W have been observed in the 1-to-10-keV region by Bennett and Yule.[7] These latter results would imply the necessity of a small correction to the NBS data below 20 keV.

The low-energy KFK telescope relies on calculated efficiencies to obtain the effect of a 300 keV electronic threshold. The calculated efficiency drops rapidly below 2.5 MeV and limits the accuracy below this energy.[1] A ±5% uncertainty in the calculated efficiency seems reasonable for energies below 2.5 MeV. Above this energy the efficiency is more slowly varying and less affected by bias uncertainties.

6. Spurious Reactions

A portion of the observed background rates is due to neutron-induced reactions in the proton detectors. Although an absolute calculation of these rates would be difficult, it is instructive to compare relative rates. For this purpose, we will list the ratio of the neutron flux to the proton flux impinging on the various proton detectors. All ratios were calculated at an incident neutron energy of 1 MeV. It is evident that there is a poor correlation between ϕ_n/ϕ_p and the observed background rates.

7. and 8. Unwanted Neutron Scattering

The fraction of neutrons which strike the neutron "radiator" after a prior collision is listed as "Inscatter" in Table III. These estimates are based upon calculations and indicate a negligible error from this source.

An estimate of the uncertainties caused by scattering materials in the neutron beam may be obtained from the row labeled "Outscatter." The listed quantities are the total atoms/cm^2 of material in front of the proton radiator.

In addition to the eight sources of error discussed above, there are several effects which are not routinely reported on a quantitative basis. These include 1) effective-volume changes for gas-filled counters and 2) timing errors caused by variations in pulse height at the input of fixed-level discriminators. In the absence of published data concerning the magnitude of these effects, a quantitative error estimate is impossible.

General Rules for Setting Standards

I would like to summarize five personal observations concerning the demanding business of setting standards for world-wide use.

1. Do not push your luck. (Avoid strong statements about accuracy near the ends of your useful range.)

2. Never allow your systematic errors to exceed your random uncertainty. (Statistical precision is often achieved at high cost by incurring large corrections in the process.)

3. Do not feel obligated to build "the universal detector" when measuring standards. (Tailor the detector to your source since it need not be used elsewhere.)

4. It is easy to measure the signal--the hard part is measuring the background. (Think ahead as to what can be changed to obtain the background rate.)

5. Avoid extrapolations into unmeasured regions. (Keep the signal away from zero pulse height.)

These statements may not be ratified by everyone involved in standards work, but I feel that they would go a long way toward preventing "down stream pollution."

Suggestions for Using Standards

What can the measurer of a tertiary cross section (in the spirit of Fig. 1) do to take full advantage of contemporary standard cross sections?

Include a measurement of a standard cross section with a reaction similar to the desired quantity. For example, when measuring the fission cross section of ^{239}Pu relative to ^{10}B(n,α) below 10 keV, include a measurement of $\sigma_f(^{235}U)$, to provide a "parallel" standard in addition to using the ^{10}B "vertical" standard as a spectrum monitor. This added information can be very useful even at energies where rapid fluctuations in the standard cross section (^{235}U) preclude its use as a spectrum monitor.

Future Developments

I will now propose two new detector systems, one a direct descendant of the LLL system described above,[3] and the other a more general detector type not currently in use in standards work.

One possible disadvantage of the current LLL system is the presence of a massive lead shield in the central portion of the neutron beam. Any detector--such as a fission chamber--which is placed a short distance in front of this shield would be subject to sizable backscattering corrections. An alternate geometry with an order of magnitude greater efficiency is illustrated in Figure 4. A thin proton radiator is placed a few cm in front of a 19-cm-diameter photomultiplier (PM) tube, with the entire assembly contained in a vacuum chamber. Protons are detected in a 1-mm-thick ^{7}Li-glass scintillator which covers only an outer ring on the PM tube face. A massive collimator prevents exposure of the scintillator to the incident beam but exposes the full radiator area. The spacing may be adjusted so that the minimum proton energy is approximately 50% of the incident neutron energy and the fraction of recoil protons detected is 14%. If (n,α) or (n,p) reactions in the glass scintillator present background problems, the newly-developed BaF_2(Ce) scintillators[8] may be used instead, with an order of magnitude reduction in the troublesome cross sections. This sytem is listed as number 6 in Table II and should be useful throughout the 1-to-20-MeV range.

Turning now to entirely new systems, we notice that the very convenient organic scintillators have never been used--in a manner which takes advantage of the accurate n,p cross section--for standards-quality

spectrum measurements. This unfortunate circumstance is probably based on the striking non-linearity in the pulse-height vs proton energy[9] and in large surface losses for thin scintillators. I would like to suggest that the second effect could be eliminated by backing a thin(~0.5 mm)plastic scintillator with enough ^{7}Li-glass scintillator to stop maximum-energy protons (~1.5 mm). The resulting pulse-height spectrum for mono-energetic neutrons would be similar to that observed in proportional counters, for the top 90% of the spectrum. Monte Carlo calculations indicate that the light output from recoil carbon nuclei and alpha particles [from $^{12}C(n,\alpha)$ reactions] are confined to less than 10% of that from protons, at a fixed incident-neutron energy.[10] It seems reasonable that with appropriate effort, the pulse-height spectrum could be extrapolated to zero with an accuracy approaching 1-2% of the total area. Scattering from the photomultiplier tube can be eliminated by viewing the scintillators edge on. Table II, number 7, lists the characteristics of this detector.

These proposals do not describe finished products, but may suggest fruitful avenues for investigation. Undoubtedly, other schemes will arise to permit continued future use of the all-important n,p reaction.

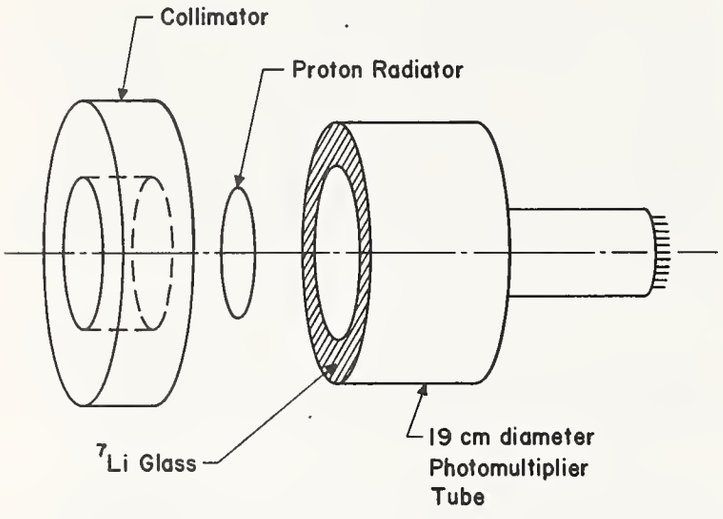

Fig. 4. Geometrical arrangement for proposed proton-recoil detector.

Appendix

A brief historical survey will be given for proton-recoil detectors which predate the systems described in Table I. Four basic types have been employed and the geneology of each will be traced back a generation or two.

1. Gas-filled proportional counters

The NBS counter is similar to the detector described by Bennett and Yule in Ref. 7, a system in use for many years at ANL. The NBS system achieved improved timing resolution by restricting the incident neutron beam to the central one-fourth of the detector volume.

2. Multiple-component proton telescopes

The high-energy KFK system followed historically the early proportional-counter telescopes described in Ref. 11. Improved timing resolution was achieved by using gas scintillators.

3. Single-component in-beam detectors

The LASL detector is similar to the system described by Johnson,[11] with solid-state detectors replacing the inorganic scintillators. This technique was also suggested by E. Pfletschinger and employed by Käppeler and Fröhner at KFK.[12]

4. Single-component out-of-beam detectors

The improved shielding arrangement of the ORNL system was first employed by Jaszczak and Macklin.[5] The LLL detector took advantage of this concept and included an improved proton-detection efficiency.[1]

References

1. I. Schouky, S. Cierjacks, P. Brotz, D. Gröschel, B. Leugers, Proceedings of the Conference on Nuclear Cross Sections and Technology, Washington, D.C., March 3-7, 1975, p. 277.
2. D. M. Barton, B. C. Diven, G. E. Hansen, G. A. Jarvis, P. G. Koontz, R. K. Smith, Nucl. Sci. Engin. 60, 369 (1976).
3. G. S. Sidhu and J. B. Czirr, Nucl. Instr. and Methods, 120, 251 (1974).
4. O. A. Wasson, Proceedings of the NEANDC/NEACRP Specialists Meeting on Fast Neutron Fission Cross Sections of U-233, U-235, U-238 and Pu-239, Argonne National Laboratory, June 28-30, 1976, p. 183.
5. R. J. Jaszczak and R. L. Macklin, Rev. Sci. Instr., 42, 240 (1971).
6. J. C. Hopkins and G. Breit, Nuclear Data Tables, A9, 137 (1971).
7. E. F. Bennett and T. J. Yule, Proceedings of the Conference on Neutron Standards and Flux Normalization, Argonne National Laboratory, October 21-23, 1970, p. 385.
8. J. B. Czirr and E. Catalano, "Cerium-activated BaF_2 and CaF_2 Scintillators," to be published in Nucl. Instr. and Methods.
9. J. B. Czirr, D. R. Nygren and C. D. Zafirators, Nucl. Instr. and Methods, 31, 226 (1964).
10. R. Batchelor, W. B. Gilboy, J. B. Parker and J. H. Towle, Nucl. Instr. and Methods, 13, 70 (1961).
11. C. H. Johnson, Chapter II. C in Fast-Neutron Physics, Part I, edited by J. B. Marion and J. L. Fowler (Interscience Publishers, Inc. N.Y., 1960), p. 247.
12. F. Käppeler and F. H. Fröhner, Proceedings of the Conference on Nuclear Data for Reactors, Helsinki, June 15-19, 1970, p. 221.

Table I

Proton-Detector Classification

	1 KFK	2 LASL	3 LLL	4 NBS	5 ORNL	Ideal
Proton detector in neutron beam	YES	YES	⊖	YES	⊖	⊖
Neutron energy measurement	⊖	⊖	⊖	⊖	⊖	YES
Extrapolation to zero proton pulse height	YES	⊖	⊖	YES	⊖	⊖
Solid radiator	YES	YES	YES	⊖	YES	⊖
Multiple-element detector	YES	⊖	⊖	⊖	⊖	⊖
100% proton efficiency	⊖	⊖	⊖	YES	⊖	YES

⊖ = NO

Ref. Detector Code

1. KFK - Telescope
2. LASL - One-element telescope
3. LLL - One-element telescope
4. NBS - Proportional counter
5. ORNL - One-element telescope

Table II

Detector System Comparison

System	H Atoms per cm^2 ($X10^{20}$)	Proton Eff. (%)	Neutrons E_{min} (MeV)	Neutrons E_{max} (MeV)	Flight Path (m)	Radiator Area (Cm^2)	Proton $\frac{E_{min}}{E_{max}}$ (%)
1-KFK(LOW)	0.4	∿ 60	2	6	57	75	0
" (HIGH)	0.8	∿ 3	5	30	57	75	∿10
2-LASL	0.41-2.2	1.0	1	>15	0.10	3.1	99
3-LLL	0.26-2.8	1.7	1	>15	60	95	60
4-NBS	65	100	0.005	0.8	200	4.9	0
5-ORNL	0.16-2.2	0.26	0.2	> 6	40	18	75
6-Proposed	0.3-3.0	14	∿ 1	>15	--	75	50
7-Proposed	5-10	100	∿ 0.1	>15	--	100	0

Table III

Sources of Error

		1 KFK (LOW)	1 KFK (HIGH)	2 LASL	3 LLL	4 NBS	5 ORNL
1)	Error in $\sigma(\theta)$ H	~ 0 (all E_n)	0.6% (5MeV) 1.1% (20MeV)	0.6% (5MeV) 1.1% (20MeV)	0.4% (5MeV) 0.3% (20MeV)	0 (all E_n)	0.3% (5MeV) 0.1% (20MeV)
2)	Background	3%	1%	10%	3%	3%	30%
3)	Neutron-energy resolution Energy	3% (3MeV)	2% (15MeV)	3% (3MeV)	4% (3MeV)	2.5% (0.1 MeV)	6% (3MeV)
4)	Counting rate (relative)	85	8	10^5 (1000)	20	1200	1.0
5)	Pulse-height-extrapolation error	5% (<2MeV)	--	--	--	< 0.5%	--
6)	ϕ_n/ϕ_p	10^4	10^5	10^5	2	36	~ 2
	Detector material	85% Ar 15% N_2	85% Ar 15% N_2	Si	Si	0.8%C 99%H	Si
7)	Inscatter (Typical)	<0.1%	<0.1%	2%	1%	1/2%	?
8)	Outscatter ($Atom/cm^2$) Material	negligible	negligible	negligible	7×10^{21} Al	8×10^{21} Al 11×10^{21} O	?

SURFACE BARRIER SPECTROMETERS FOR CALIBRATION OF FAST NEUTRONS IN MeV RANGE

O. P. Joneja, R. V. Srikantaiah*, M. R. Phiske, J. S. Coachman
and M. P. Navalkar
Neutron Physics Section
Bhabha Atomic Research Centre
Trombay, Bombay 400 085
India

At present there are very few methods available for calibrating fast neutrons in the MeV range. In the present paper methods employing Li^6 sandwich and proton recoil spectrometers using surface barrier detectors for calibration of neutron energies and fluxes have been described. The results obtained with mono-energetic neutron sources in the energy range of 1-4 MeV are given. The accuracies for energy and flux calibrations are also discussed.

(Energy and flux calibration, fast neutrons, isotropic neutrons, Li^6 sandwich surface barrier spectrometer, proton recoil surface barrier spectrometer)

Introduction

At present there are very few methods available for calibration of neutrons from 1 MeV to 4 MeV, both in terms of energy and flux. The standard methods such as time of flight or proton recoil spectrometers using gas for ionization involve either elaborate instrumentation or strong neutron sources or unfolding procedure which have to take into account wall effects or end corrections. Surface barrier spectrometers, on the other hand, are free from some of the above disadvantages and cover a wide range of energy. Moreover sandwich spectrometers such as Li^6 or He^3, can be used for calibrations with both beam and isotropic neutron sources. This aspect of calibration in isotropic neutron distribution as exist in reactors or moderating assemblies is very important since the other methods cannot be used in such a situation. In this paper, the use of surface barrier spectrometers for calibrating neutrons in the energy range of 1.0 to 4 MeV is discussed with some of the experimental results.

Description of the Spectrometers and the Experiment

A Li^6 sandwich spectrometer using two surface barrier detectors (250 mm^2 active area with a depletion depth of about 400 microns) in coincident mode was assembled [1]. A block diagram of the electronics set-up is shown in Fig. (1). A thin layer of Li^6F with thickness of 150 μgm/cm^2 was deposited on a VYNS film to act as radiator. This method was prefered to vacuum deposition of Li^6F directly on the surface barrier detector since the same detecting head could be used for background corrections.

A similar type of proton recoil spectrometer using single surface barrier detector and hydrogenous radiator (200 μgm/cm^2) deposited on VYNS film was assembled [2].

The spectrometers were subjected to mono-energetic neutrons in the energy range of 1.0 MeV to 4 MeV obtained from p-t reaction using 5.5 MeV Van de Graaff accelerator. The output of the accelerator was monitored by a calibrated long counter.

Results and Discussions

a) Li^6 Sandwich Spectrometer

A typical response of a sandwich Li^6 spectrometer for neutron energy of 2.23 MeV is shown in Fig. (2). The time integrated counts in a channel 'i' corresponding to energy E is given by

$$C(E) = N_T \int \eta(E)\,\sigma(E)\,\phi_{in}(E)\,dt \int_{E_i}^{E_{i+1}} R(E')\,dE' \quad \text{---(1)}$$

where N_T = Total number of Li^6 atoms

$\phi_{in}(E)$ = Incident flux of neutrons of energy E falling on the radiator

$R(E)$ = Normalised resolution function

$\eta(E)$ = Total efficiency

In order to calculate both energy and flux of the incident neutrons falling on the radiator, it is necessary to calibrate channel number and efficiency 'η' which is energy dependent. The method of doing such a calibration involving both experimental and theoretical calculations is explained in APPENDIX. The results of energy calibration which is linear with channel number is given in Fig. (3), thereby showing that neutrons of unknown energy can be calibrated.

---

* Technical Physics Division, BARC

The time integrated incident neutron flux can be obtained using eqn. (1) if η (E) can be calculated. In the present case, the method of calculations for η (E) which is given in APPENDIX was tested using four neutron energies which gave same time integrated flux within errors of 10%.

b) Proton Recoil Surface Barrier Spectrometer

A typical response of surface barrier spectrometer for neutron energy of 2.73 MeV is shown in Fig. (4).

The proton recoil spectrum is given by

$$\frac{dD(E)}{dE} = N_T \int \sigma(E) \phi_{in}(E) \frac{1}{E} dt \quad \cdots (2)$$

where $D(E)$ is the proton recoil spectrum for neutrons of energy E. Fig. (5) gives the energy calibration of the spectrometer with channel number which is linear, thereby showing that any unknown neutron energy can be calibrated.

For determining the time integrated incident flux, the following equation is used

$$\int \phi_{in}(E) dt = \frac{1}{N_T \sigma(E)} \sum_{i=1}^{max} C_i \quad \cdots (3)$$

Where C_i are the proton counts in i^{th} channel. The time integrated flux for neutron energies in the energy range of 1 to 4 MeV was obtained and the results gave a flux value within 10%.

Conclusions

Using the mono-energetic neutrons in the energy range of 1.0 MeV to 4 MeV and with Li^6 sandwich and proton recoil surface barrier spectrometers, it is shown that it is possible to calibrate the neutron energy with an accuracy better than 2% and flux within 10%. The advantage of Li^6 sandwich spectrometer is that it can be used for calibrations on isotropic neutron distribution.

References

[1] DAE Symposium on Reactor Physics, Bombay, 1975, Coachman, J. C., Joneja, O. P. and Navalkar, M. P.

[2] National Symposium on Radiation Physics, Mysore, 1976, Srikantiah, R. V., Joneja, O. P., Coachman, J. C. and Navalkar, M. P.

APPENDIX

Calibration of Li^6 Sandwich and Proton Recoil Surface Barrier Spectrometers

Absolute calibration of neutron energy as well as flux demands stringent conditions as regards energy loss mechanisms and overall efficiency of the system under consideration.

Energy Calibration

The absolute energy calibration can be effectively determined from the following relation

$$E_a = E_d + \Delta E_c - Q \quad \cdots (4)$$

where E_a = Actual energy

E_d = Average energy deposited in the detector system

ΔE_c = Average energy lost by secondary charged particles in the radiating material

The only unknown factor, ΔE_c can be accurately calculated by simulating the energy lost for a given geometry using Monte-Carlo method. In this method, a fictitious calibrated analyser is constructed and the events after emerging from the radiating material are distributed as per their energy. The difference in peak position from the actual channel gives the average energy lost in the radiating material. An average energy loss curve can therefore be calculated for a desired energy range and the correction can be suitably applied. The energy calibration without energy loss considerations in the radiating material is obtained with a thermal neutron source in the case of Li^6 sandwich system and with a double α source in the case of proton recoil system.

Flux Calibration

The flux calibration requires an overall efficiency of the system which in general can be defined as

$$\eta(E) = \frac{N_D(E)}{N_T(E)} = \frac{N_T(E) - N_n(E)}{N_T(E)} \quad \cdots (5)$$

where N_T = Total number of events

N_D = Number of events detected

N_n = Number of events not registered

In the case of a sandwich system the event is not registered if the secondary charged particles do not satisfy the coincidence conditions and under the circumstances, the unregistered terms consist of

$$N_n = N_L + N_{DT} + N_{REL} \quad \cdots (6)$$

where N_L = Events leaked through finite separation between the detectors

N_{DT} = Events in which both the secondary particles are detected by the same detector

N_{BBL} = Either or both the secondary particles do not exceed the experimental bias level

A Monte Carlo code COINCID is developed to take into account all factors associated for a particular system for a selected energy range. Thus using this code absolute efficiency which is a function of energy and the system under consideration can be calculated. The calculations can be experimentally verified using various neutron energies.

For proton recoil spectrometer, the total proton recoils give the absolute incident flux.

BLOCK DIAGRAM OF ELECTRONIC SYSTEM

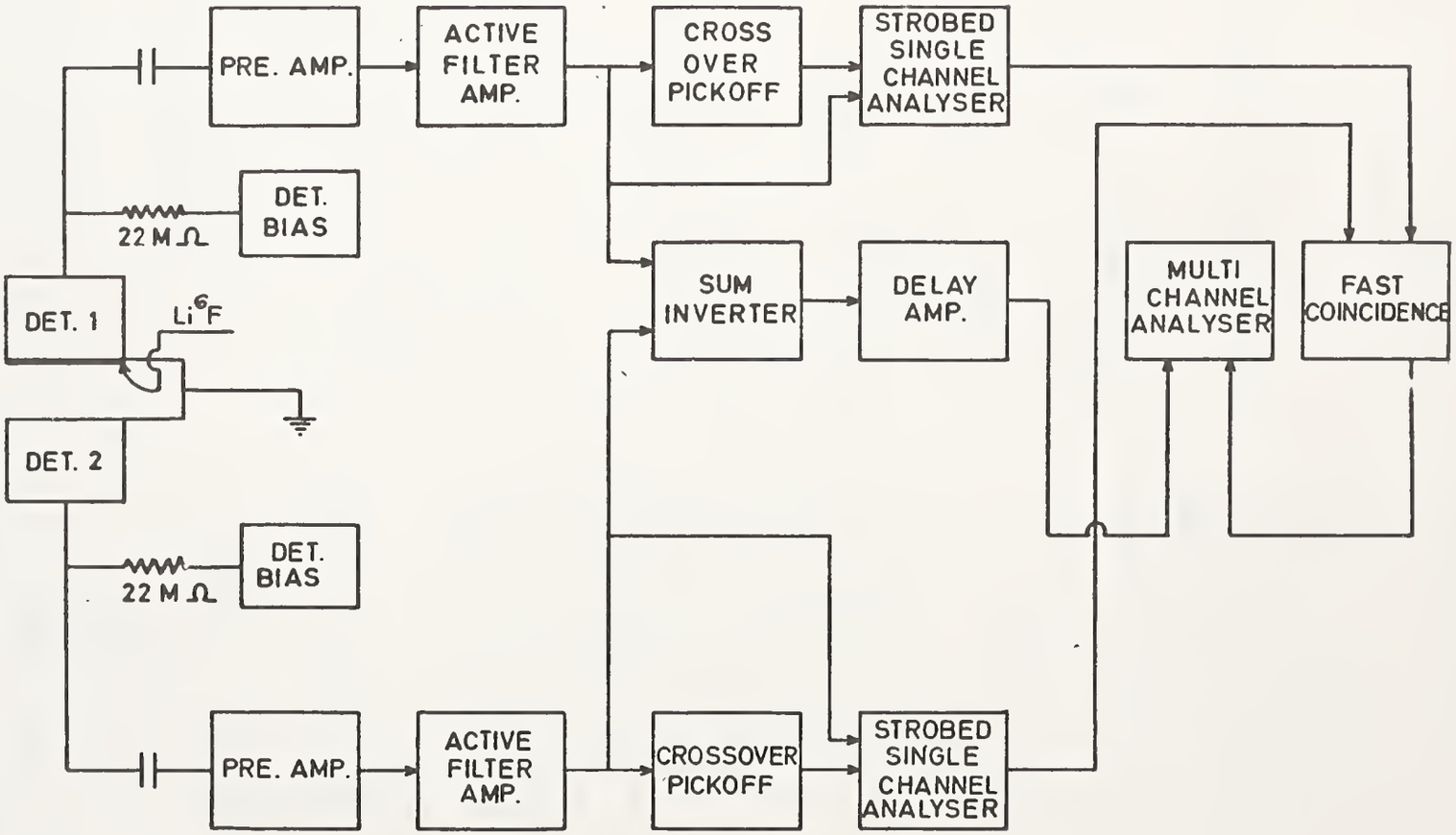

FIG. (1)

TYPICAL RESPONSE OF A SANDWICH SYSTEM (Li^6)

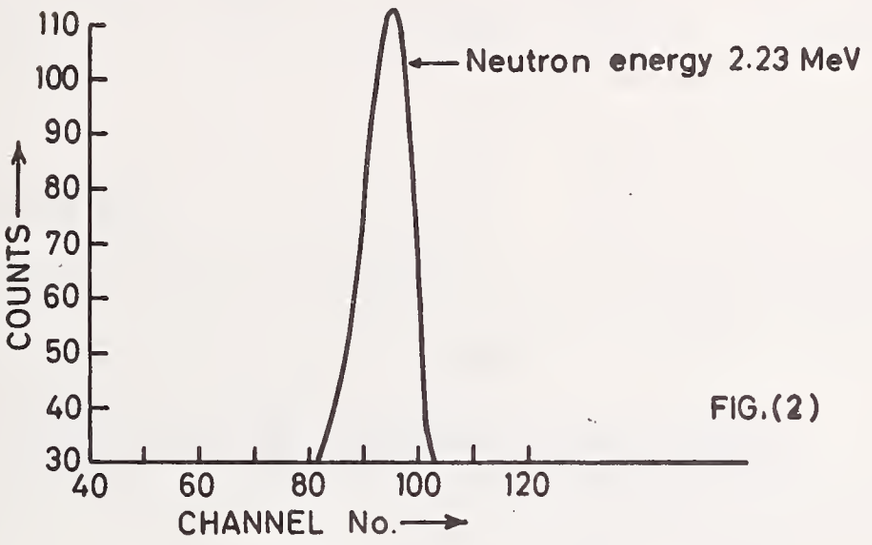

FIG. (2)

FIG. 2

ENERGY LINEARITY OF SPECTROMETER (Li^6)

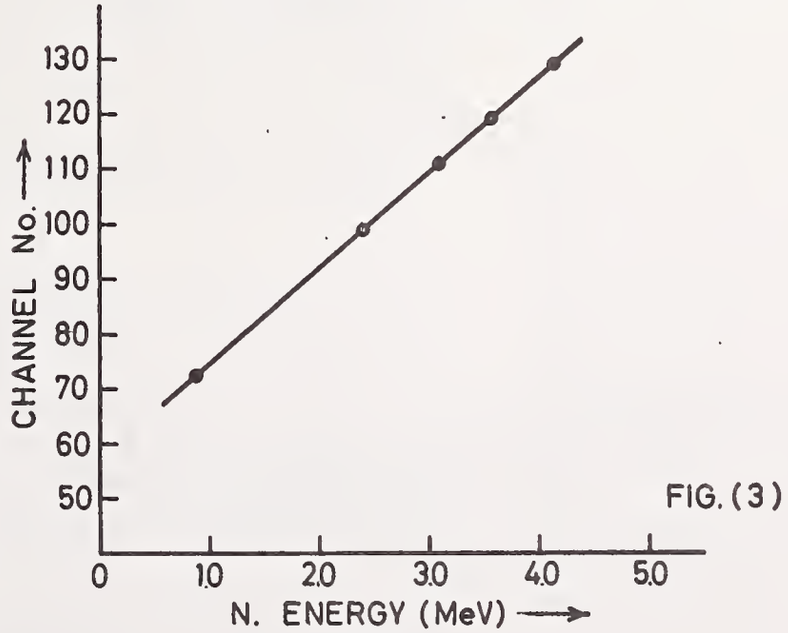

FIG. (3)

FIG. 3

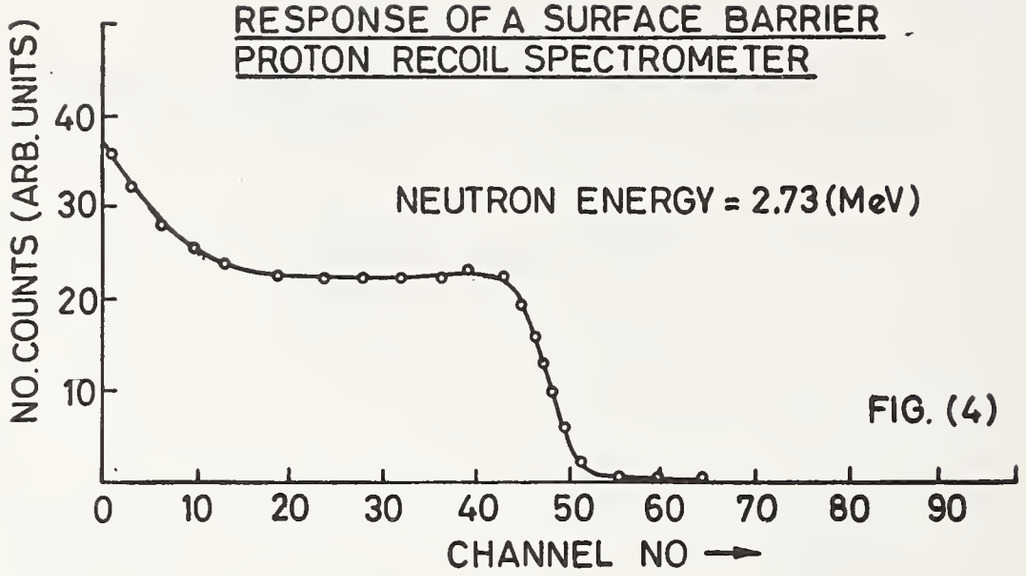
RESPONSE OF A SURFACE BARRIER
PROTON RECOIL SPECTROMETER
NEUTRON ENERGY = 2.73 (MeV)
NO. COUNTS (ARB. UNITS)
40
30
20
10
0
10
20
30
40
50
60
70
80
90
CHANNEL NO →

FIG. (4)

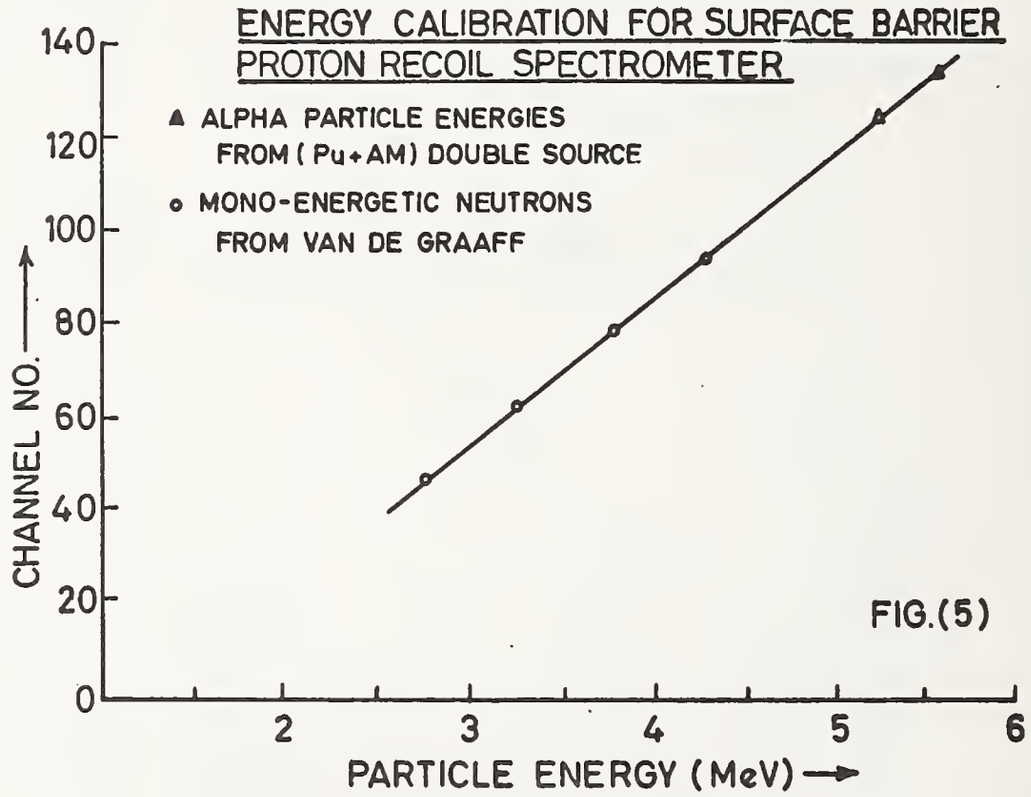
ENERGY CALIBRATION FOR SURFACE BARRIER
PROTON RECOIL SPECTROMETER
▲ ALPHA PARTICLE ENERGIES
FROM (Pu+AM) DOUBLE SOURCE
o MONO-ENERGETIC NEUTRONS
FROM VAN DE GRAAFF
CHANNEL NO. →
140
120
100
80
60
40
20
0
2
3
4
5
6
PARTICLE ENERGY (MeV) →

FIG.(5)

REVIEW OF $^{10}B(n,\alpha)^{7}Li$ CROSS-SECTION MEASUREMENTS IN THE ENERGY RANGE FROM 10 keV TO 1 MeV

E. Wattecamps
Central Bureau for Nuclear Measurements
B-2440 Geel, Belgium

Cross-section data of the $^{10}B(n,\alpha)^{7}Li$ and of the $^{10}B(n,\alpha_1)^{7}Li^{*}$ reaction are compiled together with related cross-section data such as $\sigma(n,\alpha_0)$, σ_{tot}, $\sigma_{n,n}$, branching ratio and the ratio of $\sigma(n,\alpha)$ of ^{6}Li to ^{10}B. For each type of cross-section a characterisation of the measurements and some comments are listed in a table. The data are illustrated in plots together with ENDF/B-IV data. Measurements of different origin are compared, agreement or disagreement is discussed. Qualitative statements on accuracies that recommendable sets might achieve are made, and motivation for some new measurements is argued.

(Abstract: alpha; boron; branching ratio; compilation; cross-section; elastic; lithium; neutron; measurements; total).

Introduction

Detectors relying on the $^{10}B(n,\alpha)^{7}Li$ reaction are widely used for flux determination of thermal, epithermal or fast neutrons. The cross-section underlying the neutron flux determinations is $\sigma(n,\alpha)$ with $\sigma(n,\alpha) = \sigma(n,\alpha_0) + \sigma(n,\alpha_1)$.
The α_0 refers to the emission of an α-particle of about 1.8 MeV for a neutron interaction at thermal energy, leaving the ^{7}Li nucleus in its ground state. The α_1 refers to the emission of an α-particle of about 1.5 MeV for a neutron interaction at thermal energy, leaving the residual nucleus in its first excited state, which decays by prompt 478 keV gamma ray emission. Some detectors rely on the detection of this gamma ray, and therefore $\sigma(n,\alpha_1)$ data are requested as well as $\sigma(n,\alpha)$ data.

How large is the uncertainty of present experimental data for $\sigma(n,\alpha)$ and $\sigma(n,\alpha_1)$ and how do measurements of different origin compare with each other? These questions will be discussed together with related cross-section measurements such as σ_{tot}, $\sigma_{n,n}$, branching ratio $R = \sigma(n,\alpha_1) / (\sigma(n,\alpha_0) + \sigma(n,\alpha_1))$ and the $\sigma(n,\alpha)$ ratio of ^{6}Li to ^{10}B. The related experimental data have been compiled also since any subsequent evaluation and recommendation for $\sigma(n,\alpha)$ or $\sigma(n,\alpha_1)$ data must be consistent with the present knowledge of some related cross-sections which might be even more accurately known, for instance σ_{tot} or the $\sigma(n,\alpha)$ ratio of ^{6}Li to ^{10}B.

Some data sets of $\sigma(n,\alpha)$ or $\sigma(n,\alpha_1)$ are deduced from measurements of R and $\sigma(n,\alpha_0)$ or from $\sigma(n,\alpha)$ ratio of ^{6}Li to ^{10}B and $\sigma(n,\alpha)$ of ^{6}Li. In an attempt to deal with independent observations related cross-section data are added to this compilation, but illustrated in separate plots.

Many reviews and evaluations have already been made. See for instance [IRVING D.C. (1967), DERUYTTER A.J. (1967), GUBERNATOR K. (1968), SOWERBY M.G.(1970), STEWART L. (1972), HALE G.M. (1976) and LISKIEN H. (1976)]

The 2200 m/s values of $\sigma(n,\alpha)$ and R are 3835 ± 5 barn [DERUYTTER A.J.(1973)] and 0.93692 ± 0.00006 [DERUYTTER A.J. (1967)] and therefore $\sigma(n,\alpha_1)$ = 3593 ± 5 barn. From thermal energy up to 1 keV the recommended fit of $\sigma(n,\alpha)$ of SOWERBY M.G. et al (1970)is claimed to be accurate within ±1%, within ± 2% up to 10 keV and within ± 3% up to 100 keV. According to SOWERBY M.G. (1965) the branching ratio below 150 keV is constant 0.935 ± 0.005. Thus, below 10 keV the $^{10}B(n,\alpha)^{7}Li$ reaction is a well established and accepted standard. Although the cross-section above 10 keV is not particularly smooth and large and although $\sigma(n,n)$ of hydrogen is an accepted standard, boron 10 is often used in detectors even in that higher energy range because of the positive Q-value and ease of application in various detectors. To get well overlapping results in broad energy ranges between $^{10}B(n,\alpha)^{6}Li$ and H(n,n)H normalised data, the $\sigma(n,\alpha)$ cross-section should be known to within less or equal 2 per cent up to 1 MeV.

The emphasis of the present review is put on the energy range from 10 keV to 1 MeV where most of the recent contributions deal with, and where the requested accuracy is still not achieved. A typical request for $\sigma(n,\alpha)$ data in the range of energy from 10 keV to 1 MeV is 2% and similar requests have been formulated by eleven laboratories with unanimous priority I in WRENDA 76/77.

Presentation and Discussion of Cross-Section Data

General Information

The status of experimental data for each cross-section type is drawn in Fig. 1 to 11. The essential features or particularities of each measurement are briefly summarized in Tables 1 to 7 in Annex 1. The compilation deals with about 5000 pairs of energy and cross-section values. Most of the data have been obtained on magnetic tape from the CCDN, Centre de Compilation de Données Neutroniques, Paris; some data were taken from publications and in some very few cases numerical data have been extracted from published graphs. All data were put on cards in the same format in a single set of units [eV, barn]. Some data sets with high resolution but poor statistical accuracy were summed into groups with improved statistical accuracy. Plots were made at the CBNM computer with the code ANGELA. The scale of the plots was adapted individually to get a clear picture even if a drawing comprises thousand data points. Together with the experimental data a continuous curve is drawn which is the ENDF/B-IV evaluated data, see MAGURNO B.A.(1975), made available by CCDN, and IRVINGS D.C. (1967) evaluated data for the branching ratio R.

This compilation, together with some qualitative arguments on accuracies is part of CBNM's contribution to the INDC and NEANDC meetings on standards and discrepancies. An investigation of assessable accuracies of fits on the basis of a quantitative analysis is in progress now for some selected cross-section types and began with the compilation of an error file.

Data of σ_{tot}

Data from 100 eV to 20 MeV are illustrated in Fig. 2. Detailed plots of small energy regions are given in Fig. 1, 3 and 4. A brief characterisation of the measurements and some comments are listed in Table 1 of Annex 1.

The measurements of MOORING F. (1966) and DIMENT K. (1967) agree well and they are the basic data for the evaluation of this cross-section. Measurements prior to those suffer from poor accuracy of sample composition. The data of SPENCER R. (1973) were obtained with 0.2 ns/m resolution from 90 keV to 420 keV and do not show a suspected narrow resonance. Spencer's data are shown in their original high resolution fashion, namely 538 points, in Fig. 3, but in condensed fashion, with improved statistical accuracy, in Fig. 2. The promising data of AUCHAMPAUGH G. (1976) are claimed to have an uncertainty less than 1.5%.

Below 10 keV DIMENT's data and fit are accurate to within 0.5%, and fulfil the requested accuracy. From 10 keV up to 400 keV new data of SPENCER R. (1973) make it senseful to investigate fits up to 400 keV to get a recommendable curve with properly defined accuracies. Additional measurements are needed from 400 keV to 1.5 MeV to fulfil the 1% request up to 1 MeV, (see WRENDA 1977, CASWELL R.S. n° 691016) since the available data sets are scarce, DIMENT K. (1967) and BOCKELMAN C. (1951), and differ by 10% in that particular energy range. Above 1.5 MeV five resonances are apparent and the ENDF/B-IV evaluation does not fit too well the experimental data as it is illustrated in Fig. 4.

Data of $\sigma(n,\alpha)$, $\sigma(n,\alpha_1)$ and $\sigma(n,\alpha_0)$

These data are illustrated in Fig. 5, 5 bis, 6 and 7. Characteristics of the measurements with some comments are listed in Tables 2, 3 and 4 of Annex 1. Below 10 keV the recommended data of SOWERBY M.G.(1970), with an accuracy of 2% at 10 keV, are commonly accepted. Above 10 keV much effort is still devoted to accurate measurements and many different methods have been and are still applied. Recent experiments by FRIESENHAHN J. (1974) and SEALOCK R. (1976) have been performed with refined and new techniques but their data did not solve the problems as such. By detailed consideration of Fig. 5 and in particular Fig. 5 bis, in the range of energy from 30 keV to 1 MeV, the data can be split into three groups: "high", "low" and "medium". The "low" group comprises the results of DAVIS E. (1961), BICHSEL H. (1957) and MACKLIN R. (1968), the "high" group comprises the data of FRIESENHAHN J. (1974), BOGART D. (1968), COX S. (1966), MOORING F. (1966) and BILPUCH E. (1960), and the "medium" group comprises data of SOWERBY M.G. (1970), SEALOCK R. (1975) and ENDF/B-IV, HALE G. (1973).
Handdrawn curves through the "low" and through the "high" group, with all data considered of equal weight, yield two distinct curves which differ by 10, 23, 30 and 25 per cent at 100, 250, 500 and 750 keV respectively. The data of SEALOCK R. (1975) coincide with the "low" group at 200 and above 600 keV, but with the "high" group at about 400 keV.

The data of SOWERBY M.G. (1970) are not the result of an independent observation. The $^{10}B(n,\alpha)^7Li$ cross-section was deduced from a measured ratio of (n,) of ^6Li to ^{10}B and $^6Li(n,\alpha)$ T cross-section which is not numerically documented. As a matter of test the author of this paper has used the well documented and accurate ratio measurements of SOWERBY M.G. (1970) together with $^6Li(n,\alpha)T$ data of the ENDF/B-IV evaluation. It turns out that this $^{10}B(n,\alpha)^7Li$ cross-section is 2, 3.4, 3.3, 7.5 and 15.4 per cent higher than the recommended data of Sowerby at 20, 40, 60, 80 and 100 keV respectively.

This and previous arguments illustrate that $\sigma(n,\alpha)$ of ^{10}B still does not have the status of a standard cross-section with an accuracy of 2% as requested in the energy range from 40 keV to 1 MeV.

The peculiar $\sigma(n,\alpha)$ data of ENDF/B-IV above 1 MeV (see Fig. 5) are to be explained by the evaluation of $\sigma(n,\alpha_1)$ data in Fig. 6. Above 1 MeV there are only two measurements, DAVIS E. (1961) and NELLIS D. (1969), the shape is similar but the amplitude differs by a factor 1.4. Evaluators have preferred the $\sigma(n,\alpha_1)$ data of NELLIS and have renormalized the data of DAVIS. The latter did also measure $\sigma(n,\alpha)$ but NELLIS did not, consequently the recommended $\sigma(n,\alpha)$ data float about 40% above the results of DAVIS.

The overall status of $\sigma(n,\alpha_1)$ data is much more favorable than for $\sigma(n,\alpha)$ data. Below 100 keV all data, except FRIESENHAHN J. (1974), agree reasonably well and a fit might achieve the ± 2% accuracy level. In the range of energy from 100 keV to 1 MeV the ENDF/B-IV values, established previously to the measurements of SCHRACK R. (1976) and SEALOCK R. (1976) are reasonably well confirmed by the latter though a slight decrease of about 4% might be suggested from 350 to 600 keV. The data of SEALOCK R. (1976) agree with the data of DAVIS E. (1969), in the region of overlap from 700 to 1000 keV, and this is an argument against the data of NELLIS. SEALOCK's data agree also with SCHRACK's results in the region of overlap from 300 to 600 keV. Below 300 keV SEALOCK's data indicate a trend towards lower values similar to SEALOCK's $\sigma(n,\alpha)$ data and in both cases in contrast with the other data. The data of FRIESENHAHN would compare much closer if a renormalisation by 0.85 might be applied. The data of COATES M. (1972) seem 10% low at 150 keV and so do MACKLIN's data. A recommended data set would hardly get ± 5% accuracy from 100 keV to 1 MeV, even if renormalisation of some measurements were allowed, and new measurements should be undertaken.

For the sake of completeness, the $\sigma(n,\alpha_0)$ have been compiled in Fig. 7. SEALOCK's data show a bump at 350 keV. MACKLIN's data, unique results obtained by the inverse reaction $^7Li(\alpha,n)^{10}B$, and the cause of low $\sigma(n,\alpha_1)$ data, unfortunately have no other experiment of comparable quality to compare with.

All data of σ_{tot}, $\sigma(n,\alpha)$, $\sigma(n,\alpha_1)$ and $\sigma(n,\alpha_0)$ are illustrated in a single plot, Fig. 8. Data of a definite cross-section type but of different origins carry the same symbol and this might erroneously suggest equal weight to the different results. Lines A/v, B/v and C/v were drawn through $\sigma(n,\alpha)$, $\sigma(n,\alpha_1)$ and $\sigma(n,\alpha_0)$. It is seen that $\sigma(n,\alpha)$ roughly has a 1/v dependence up to 400 keV, whereas $\sigma(n,\alpha_1)$ and $\sigma(n,\alpha_0)$ deviate in opposite directions from ~ 1/v already at 200 keV and 20 keV, respectively. The $\sigma(n,\alpha)$ line on top of Fig. 8 stresses that $\sigma(n,\alpha)$at 400 keV is only 12% of σ_{tot}.

Data of $\sigma_{n,n}$

Elastic scattering cross-section data from 400 eV to 20 MeV are illustrated in Fig. 9. Characteristics and comments to these experiments are listed in Table 5 of Annex 1. The largest data sets are those of LANE R. (1971), ASAMI A. (1969) and MOORING F. (1966). The agreement among those is fairly good. The data of LANE R. and ASAMI A. are taken as input data for the ENDF/B-IV evaluation but MOORING's data are not.

The recommended ENDF/B-IV data agree fairly well (±10%) with the measured data, though this accuracy is still insufficient to use $\sigma_{n,n}$ data together with σ_{tot} as a means to obtain σ_{abs} with the help of $\sigma_{tot} - \sigma_{n,n} = \sigma_{abs} \cong \sigma_{n,\alpha}$. At 400 keV $\sigma_{n,n}$ amounts to 4 b, whereas $\sigma_{n,\alpha}$ is 1 b. Since 2% accuracy is requested for $\sigma_{n,\alpha}$ this would imply a relative error of less or equal 0.5 per cent on $\sigma_{n,n}$ which is not likely to be achieved above 10 keV, neither by experiment, nor by theoretical analyses.
The most recent measurement of LANE R. together with angular distributions and polarisation experiments have been performed primarily to determine resonance parameters for use in R-matrix analysis.

Data of branching ratio R.

Many different measurements of R have been made, as illustrated in Fig. 10 and Table 6. Below 100 keV the branching ratio might be defined to within 1% and the emphasis of this discussion is put on the less accurate data from 100 to 1000 keV.

The uncertainty of PETREE B. (1951) data is difficult to estimate, though the energy dependence of R is smooth and consistent with more recent data. The data of BICHSEL H. (1952) and DAVIS E. (1961) suffer from large uncertainties of 10 to 20%. Data of SOWERBY M. (1965) scatter but nevertheless indicate lower values than any other experiment. The first experiment with surface barrier semi-conductor detectors, see MACKLIN R. (1967), did separate more clearly a_0 from a_1 than any former measurement with BF_3-proportional counting devices. The absolute error claimed by MACKLIN R. is 0.003 which is extremely small and never achieved so far. MACKLIN's data should heavily determine recommendable values but a smooth handdrawn curve through the bulk of the data does hardly fit likewise MACKLIN's value at 500 keV and the LAMAZE G. (1974) value at 790 keV which is claimed to within a standard deviation of 0.03. The data of FRIESENHAHN J. (1974) have been deduced from separate measurements of $\sigma(n,a_1)$ and $\sigma(n,a)$. The results scatter and are systematically high as compared to others. The recent measurements by SEALOCK R. (1976) are made with a complex but promising method which essentially relies on surface barrier semiconductor detectors. The experiment was not primarily designed for R determination. The data suffer from poor statistical accuracy, though a general trend towards low values is present.

A critical appraisal of R-values from 100 to 1000 keV shows that 3 to 5% accuracy for a recommendable curve might hardly be achieved with existing data.

Data of $\sigma(n,a)$ of ^{6}Li to ^{10}B

As seen in Fig. 11 and Table 7 there are five ratio measurements and one calculated ratio. The latter was obtained from $\sigma(n,a)$ data of ^{6}Li and ^{10}B of ENDF/B-IV. The measurement of SOWERBY M. (1970) from 10 eV to 80 keV illustrates the 1/v range and the departure from 1/v from 500 eV on. Particular attention must be drawn to these measurements since they are the basis of all recommended $^{10}B(n,a)^{7}Li$ cross-section sets below 100 keV. See also comments on $\sigma(n,a)$ in previous paragraph . The data of BERGMAN A. (1961) are claimed to be within 0.4% accuracy and are systematically lower than SOWERBY's data. The difference amounts to 3% at 30 keV. The data of FRIESENHAHN S. scatter considerably in the range of energy from 1 keV to 100 keV. Above 100 keV there is no other measurement to compare with, and a shift of 12 keV is observed between their results and the ENDF/B-IV data. The data of PEREZ (1974) were deduced by the author of this paper from published flux ratios and more accurate cross-section ratios, taking into account self absorption and other corrections, should be acquired. These preliminary data of PEREZ nevertheless indicate a slight tendency towards low ratios. Recent measurements of σ_f of ^{235}U relative to $\sigma(n,a)$ of ^{6}Li and to ^{10}B, by WAGEMANS C. (1971), claimed to be accurate within ± 3%, are in favour of ratios that are 9% lower at 30 keV than the presently recommended ratios.

Below 1 keV the ratios are well established, from 1 keV to 100 keV the accuracy gradually decreases with increasing energy and hardly gets ± 3% at 100 keV. Above 100 keV experimental data are too scarce to draw significant conclusions.

Conclusions

The compilation of $\sigma(n,a)$ and $\sigma(n,a_1)$ cross-section data shows that data requests from 10 keV to 1 MeV are not fulfilled. To define recommendable data with assessable accuracies a new evaluation is recommended. The evaluation ought to take full account of and be consistent with related and available accurate cross-section data, such as branching ratios and $\sigma(n,a)$ ratios of ^{6}Li to ^{10}B.

It is questionable whether new measurements of σ_{tot} from 400 keV to 1 MeV would reduce the error margins of $\sigma(n,a)$.

New measurements of $\sigma(n,a_1)$ or $\sigma(n,a)$ are inevitable if one has to achieve 2% accuracy up to 1 MeV. The large scattering of present $\sigma(n,a)$ data and the common use of $\sigma(n,a_1)$ for flux determination in cross-section measurements tends to recommend primarily new $\sigma(n,a)$ and branching ratio measurements.

Cross-section ratio measurements above 10 keV of $\sigma(n,a)$ of ^{6}Li to ^{10}B with a single detector are recommended. Evaluations of ^{10}B and ^{6}Li cross-section data should yield data sets which are consistent with the measured ratio of $\sigma(n,a)$ of ^{6}Li to B.

Acknowledgement

I should like to thank Dr. C. BASTIAN, Mr. R. BUYL and Mr. J. VAN GILS for providing and running the plotting programs and Mrs. P. DAEMS-LUYPAERTS for her diligent help in preparing the drawings.

REFERENCES

ASAMI A., J.Nucl.Energy 24 (1970) 85

AUCHAMPAUGH G.F. et al., to be published

BECKER R. et al., Phys.Rev. 102, n° 5 (1956) 1384

BERGMAN A.A. et al., Soviet Phy. JETP 13, n° 5 (1961) 895

BICHSEL H. et al., Phys.Rev. 108, n° 4 (1957) 1025

BILPUCH E., Ann. Phys. 10 (1960) 455

BOCKELMAN C., Phys.Rev. 80, n° 6 (1950) 1011

BOGART D. et al., Nucl.Phys. A 125 (1969) 463

COATES M.S. et al., Conf. Vienna "Neutron Standards and Reference Data" IAEA-STI/PUB/371, p. 129,(1972)

COOK C.F. et al., Phys.Rev. 94, n° 3 (1954) 651

COOKSON J.A., Nucl.Phys. A 146 (1970) 417

COON J.H. et al., Phys.Rev. 88, n° 3 (1952) 562

COX S.A. et al., J.Nucl.Energy 21 (1967) 271

DAVIS E.A. et al., Nucl.Phys. 27 (1961) 448

DE PANGHER J. et al., Rept. BNWL-260 (1966)

DERUYTTER A. et al., J.Nucl. Energy 21 (1967)

DERUYTTER A.J. et al. J.Nucl.Energy 27 (1973) 645

DIMENT K.M., Rept. AERE-R-5224 (1967)

FOSSAN D.B. et al., Phys.Rev. 123, n° 1 (1961) 209

FRIESENHAHN S.J. et al., Rept. GULF-RT-A 12210 (1972)

FRIESENHAHN S.J. et al., Rept. INTEL-RT 7011-001 (1974)

GUBERNATOR K. et al., Rept. EUR 3950 e (1968)

HALE G.M. et al., see MAGURNO B.A. (1975)

HALE G.M. et al., Rept. LA-6518-MS or NEANDC(US)-200/U (1976)

HAUSLADEN S.L., Dr. Thesis COO-1717-5, Ohio University

HIBDON C. et al., Rept. ANL-4552 (1950) 6

HOPKINS J.L., see MAGURNO B.A., p. 73

IRVING D.C., Rept. ORNL-TM-1872 (1967)

LAMAZE G.P. et al., Nucl.Sci. and Eng. 56 (1975) 94

LANE R.O. et al., Phys.Rev. C 4 n° 2 (1971) 380
see also HAUSLADEN S.L.

LISKIEN H., Conf."Interactions of Neutrons with Nuclei" Lowell (1976) 1110

MACKLIN R.L. et al., Phys.Rev. 165 n° 4 (1968) 1147

MAGURNO B.A., Rept. BNL-NCS-50464 or NEANDC(US)-196/L or INDC(US)-73L or NEACRP-L-148 (1975)

MOORING F.P. et al., Rept. ANL-6877 (1964)

MOORING F.P. et al., Nucl.Phys. 82 (1966) 16

NELLIS D.O. et al., Phys.Rev. C 1, n° 3 (1969) 847

NERESON, Rept. LA-1655 (1954)

PEREZ R.B. et al., Nucl.Sci. and Eng. 55 (1974) 203

PETREE B. et al., Phys.Rev. 83, n° 6 (1951) 1148

PORTER D. et al., Rept. AWRE O 45/70 (1970)

ROHRER, see BILPUCH E.(1960)

SCHRACK R. et al., priv. communication and Rept. ERDA/NDC 3/U (1976) 148

SEALOCK R.M. et al., Phys.Rev. C 13 n° 6 (1976) 2149

SOWERBY M.G., J.Nucl.Energy A/B 20 (1966) 135

SOWERBY M.G. et al., J.Nucl.Energy 24 (1970) 323

SPENCER R. et al., Rept. KFK 1518 and EANDC(E)147"AL" (1973)

STEWART L., Conf.Neutron Standard Reference Data IAEA-Vienna (1972) 149

TESCH K., Nucl.Phys. 37 (1962) 412

TSUKADA K. et al., J.Phys.Soc. of Jpn 18 n° 5 (1962) 610

VALKOVIC V. et al., Phys.Rev. 139 (1965) 331

VAUCHER B. et al., Helv.Phys.Acta 43 (1970) 237

WAGEMANS C. et al., Ann.Nucl.Energy 3 (1976) 437

WILLARD H.B., Phys.Rev. 98 n° 3 (1954) 669

WRENDA World Request List for Nuclear Data INDC(SEC)-55/URSF(1976)

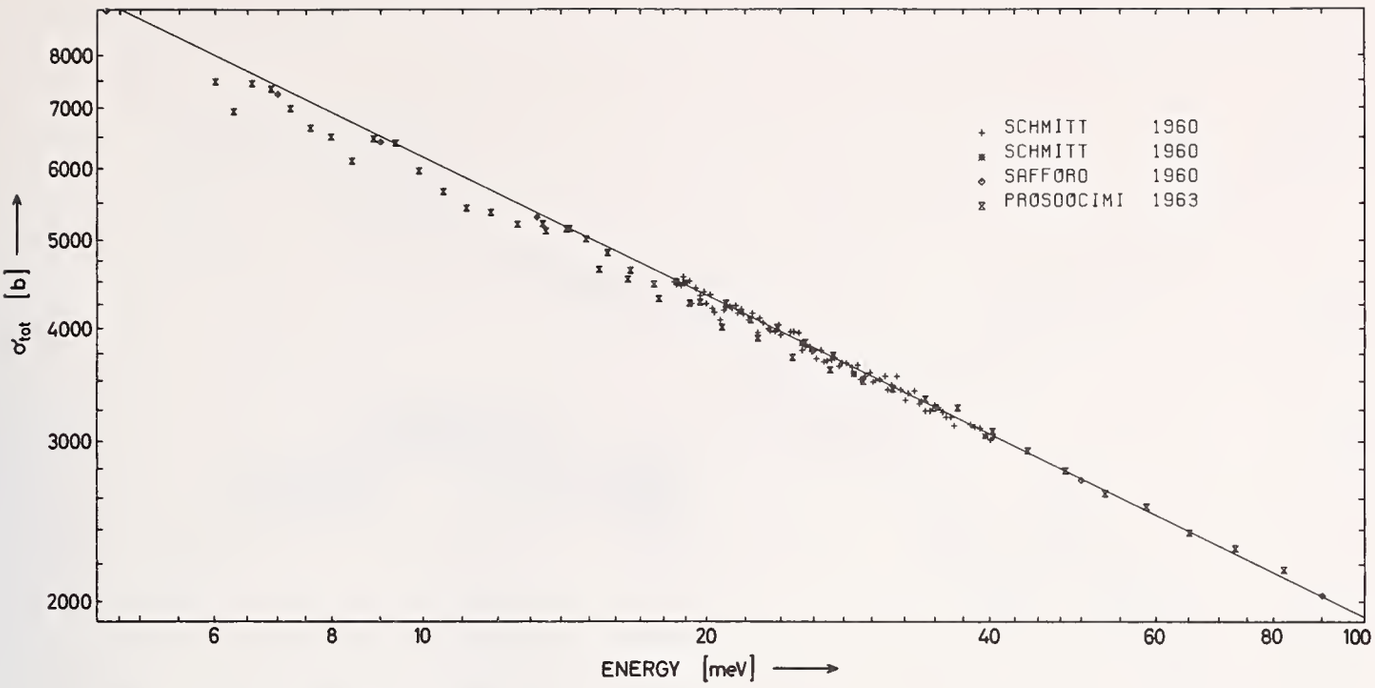

Fig.1 σ_{tot} from 5 meV to 100 meV.

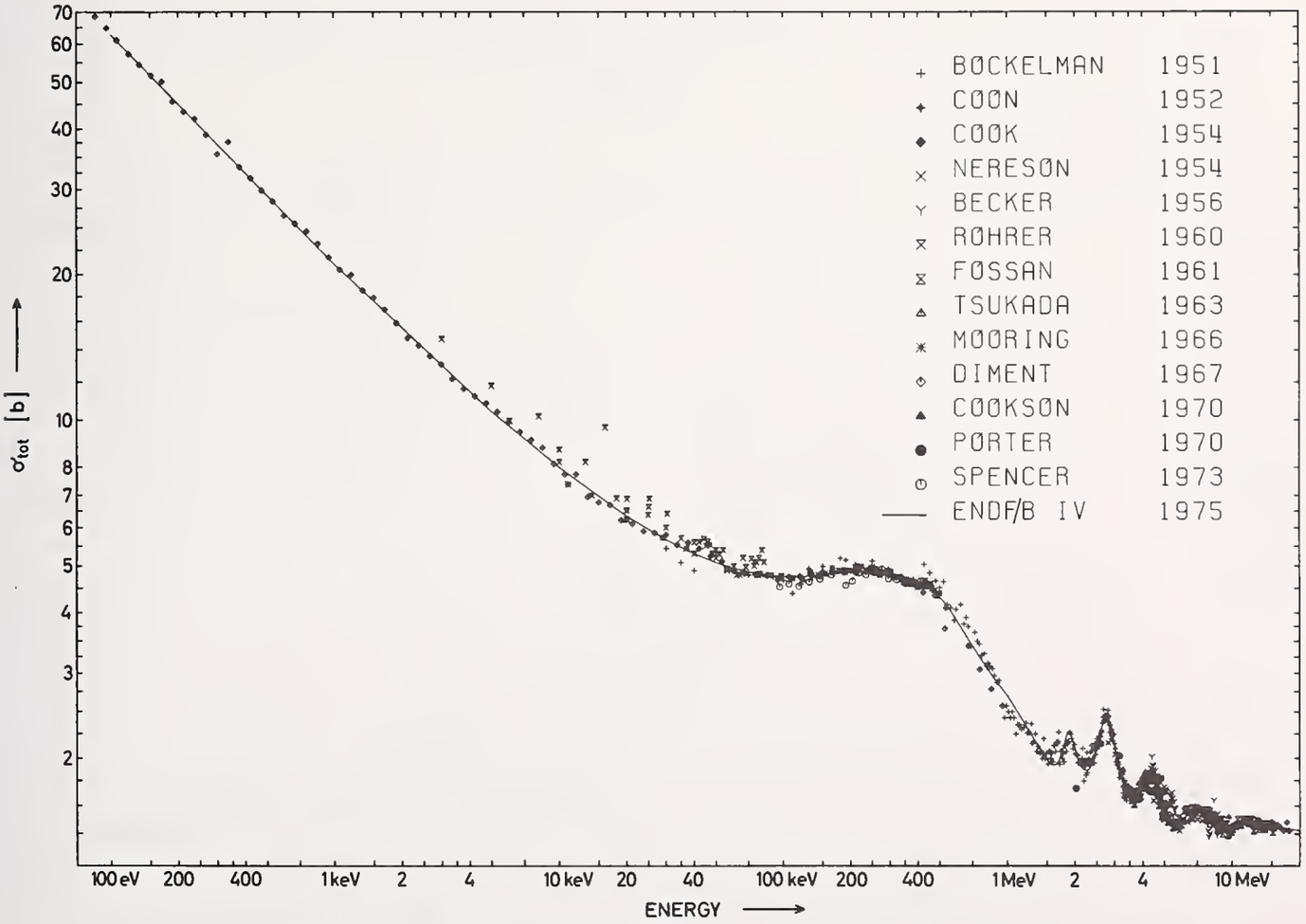

Fig.2 σ_{tot} from 100 eV to 20 MeV.

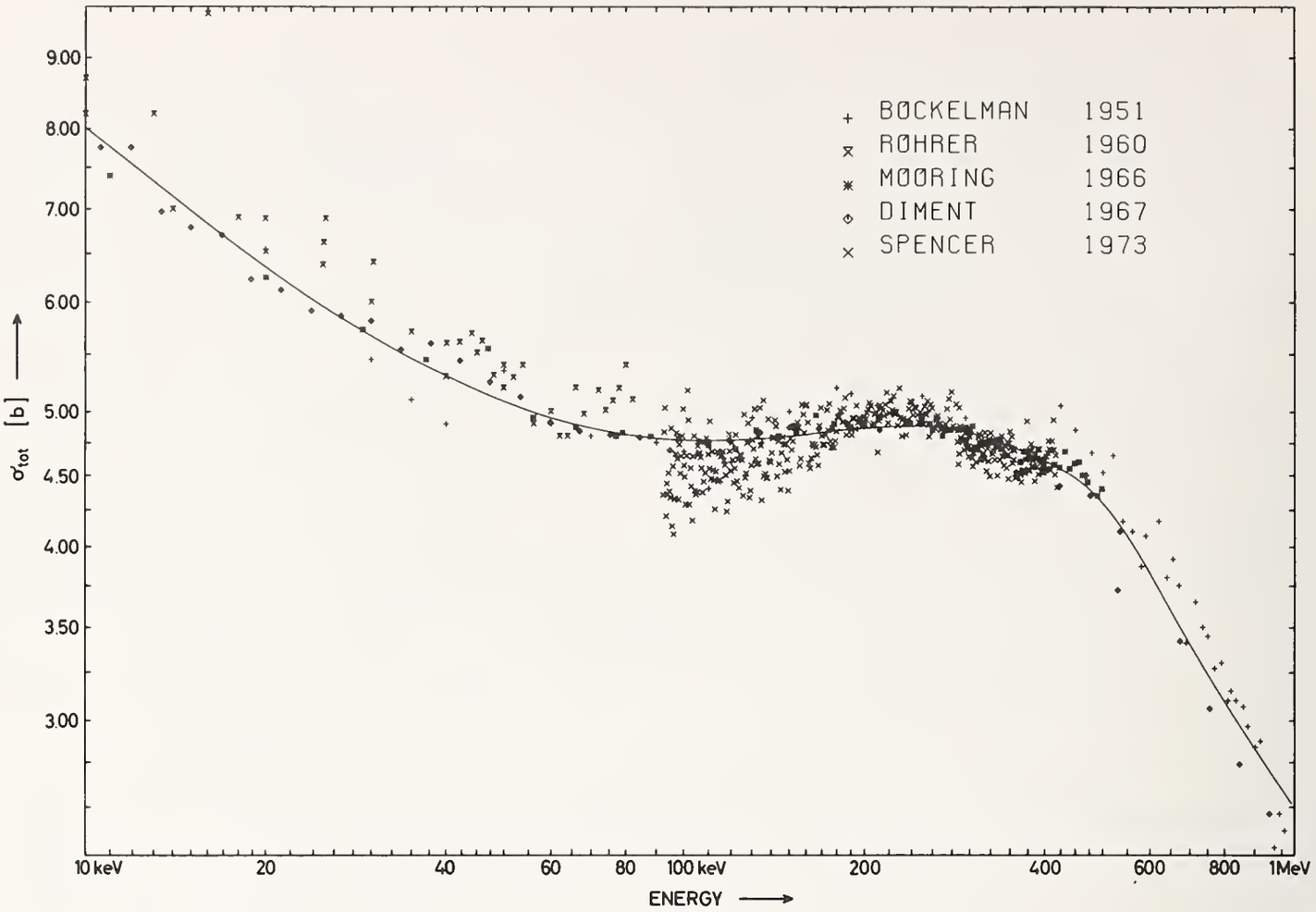

Fig.3 σ_{tot} from 10 keV to 1 MeV.

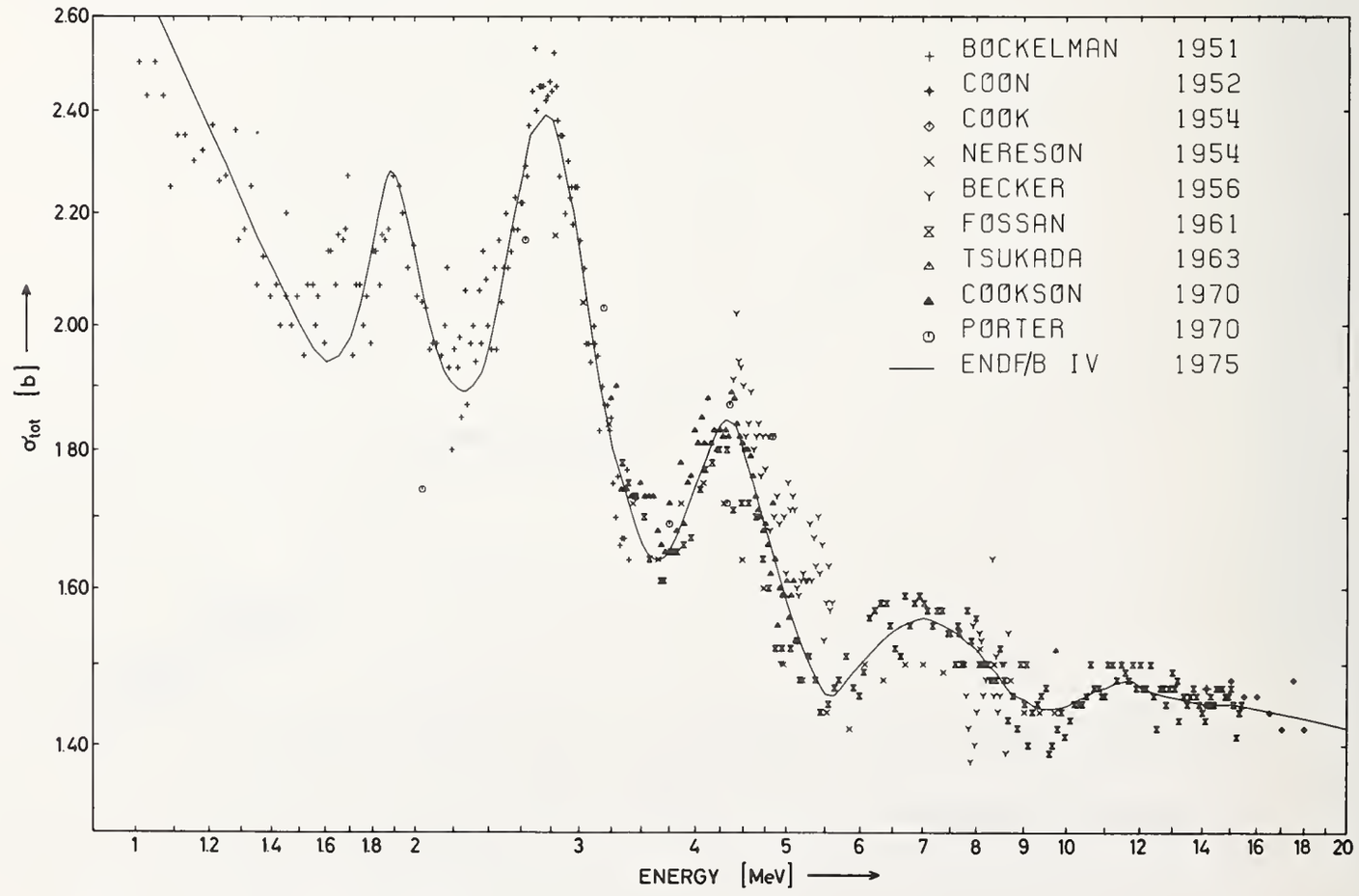

Fig.4 σ_{tot} from 1 MeV to 20 MeV.

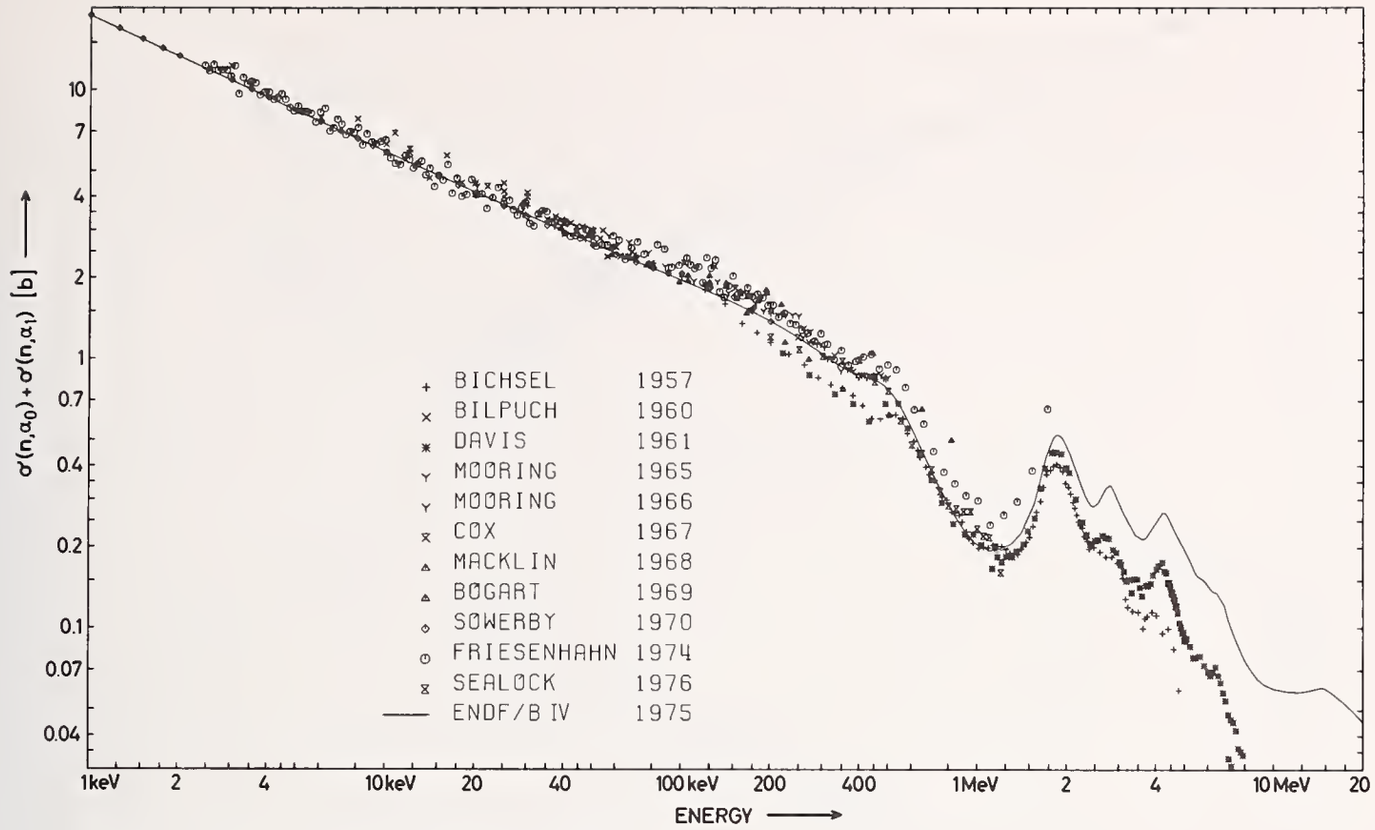

Fig.5 $\sigma'(n,\alpha_0) + \sigma'(n,\alpha_1)$ from 1keV to 20MeV.

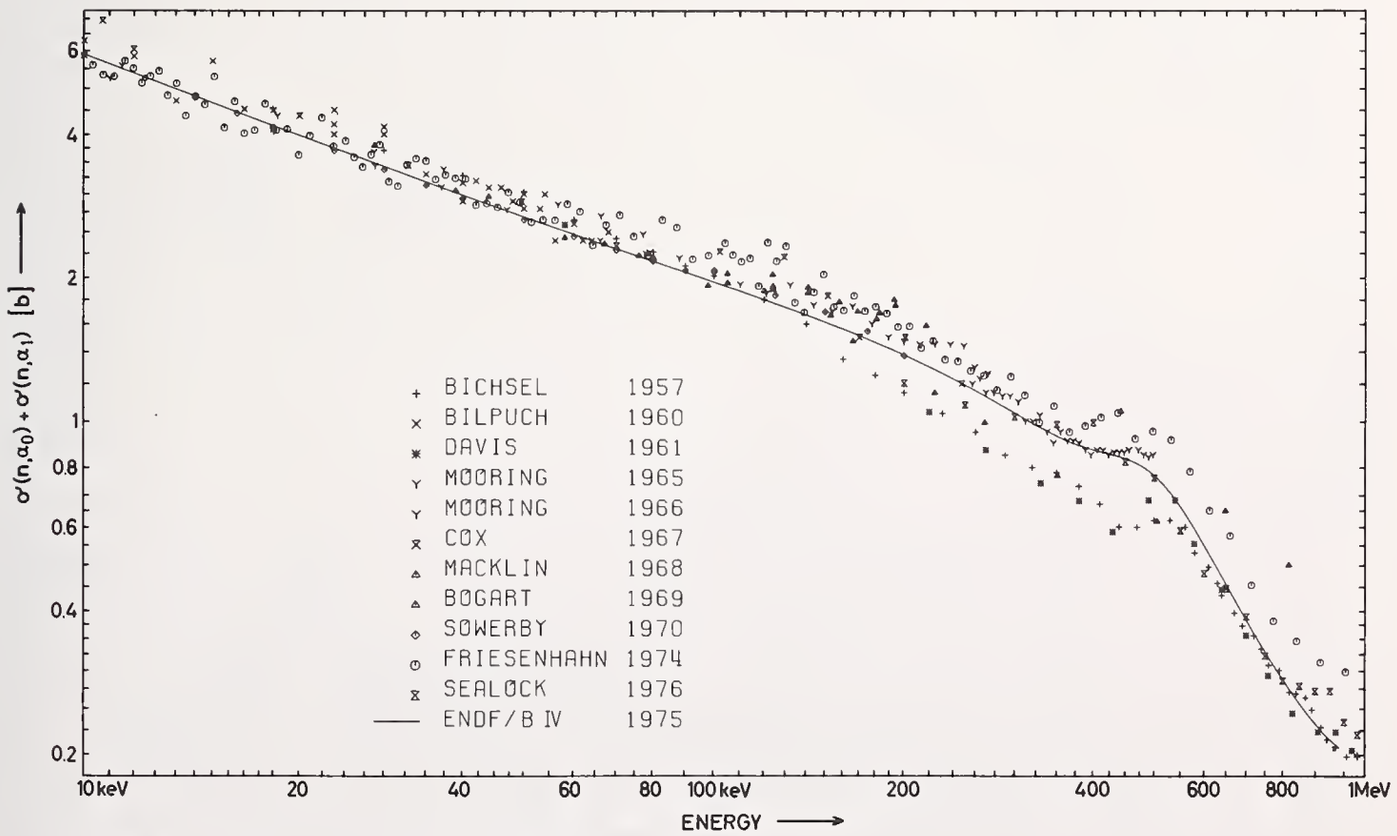

Fig.5bis $\sigma'(n,\alpha_0) + \sigma'(n,\alpha_1)$ from 10keV to 1MeV.

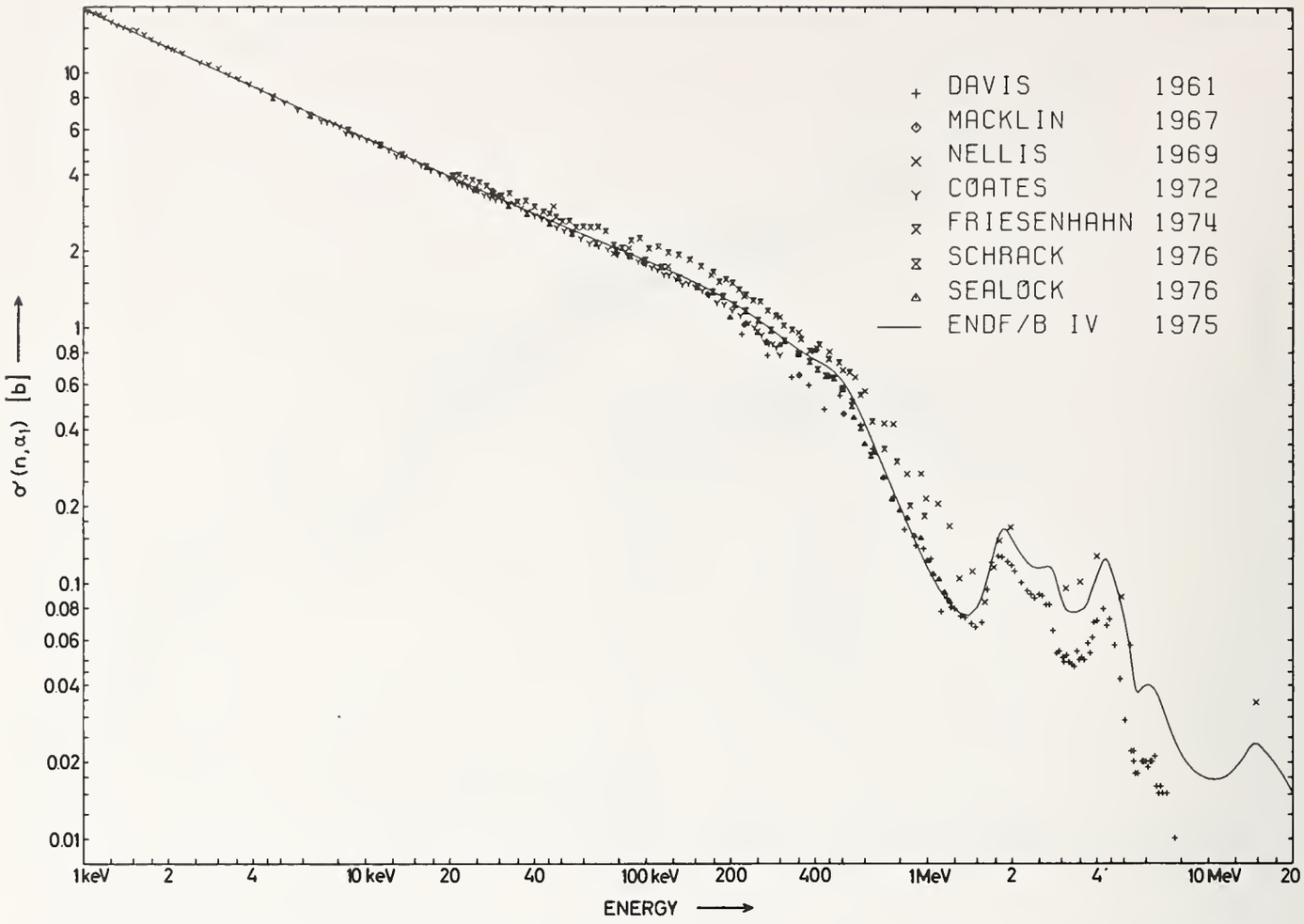

Fig.6 $\sigma'(n,\alpha_1)$ from 1keV to 20 MeV.

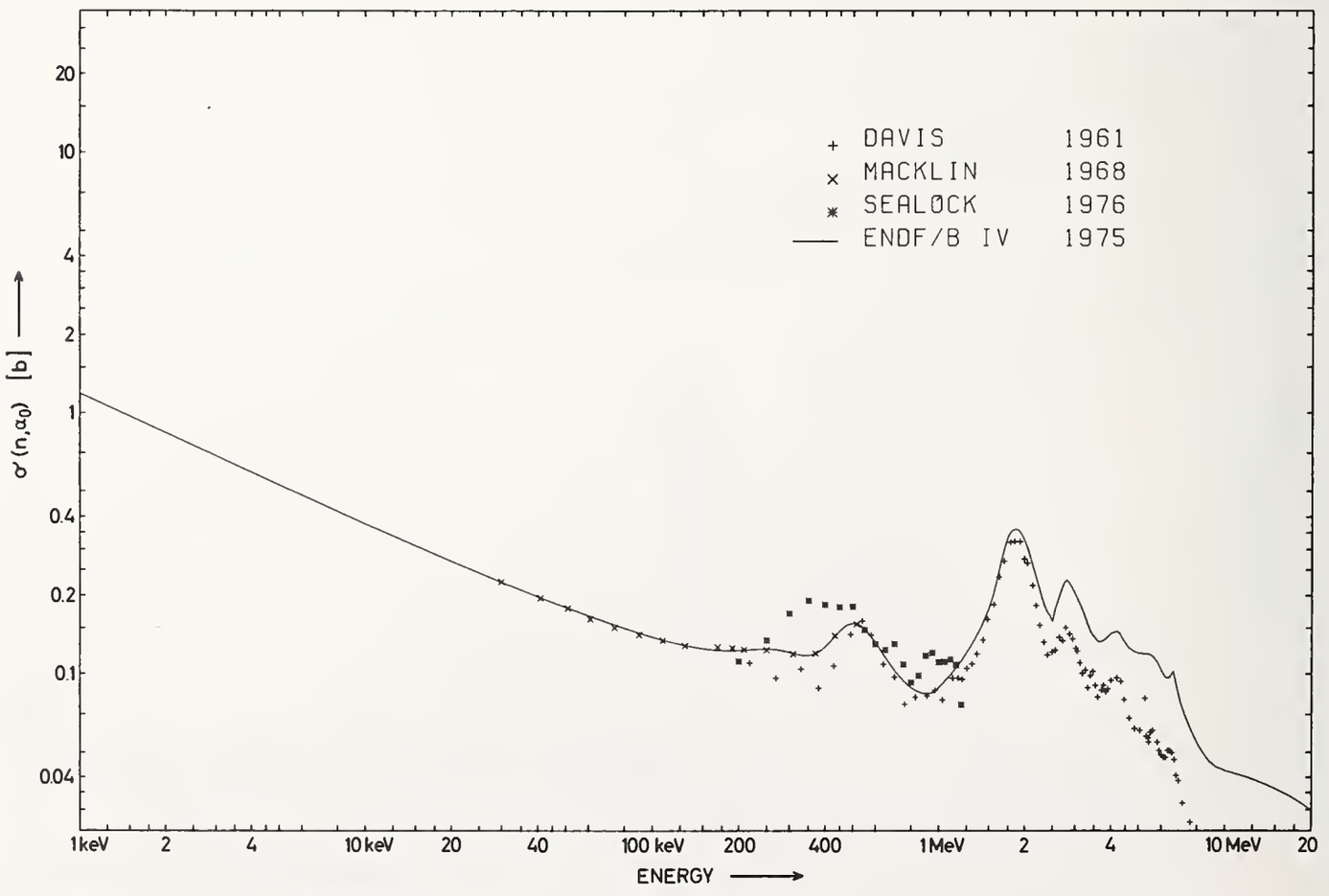

Fig.7 $\sigma'(n,\alpha_0)$ from 1keV to 20 MeV.

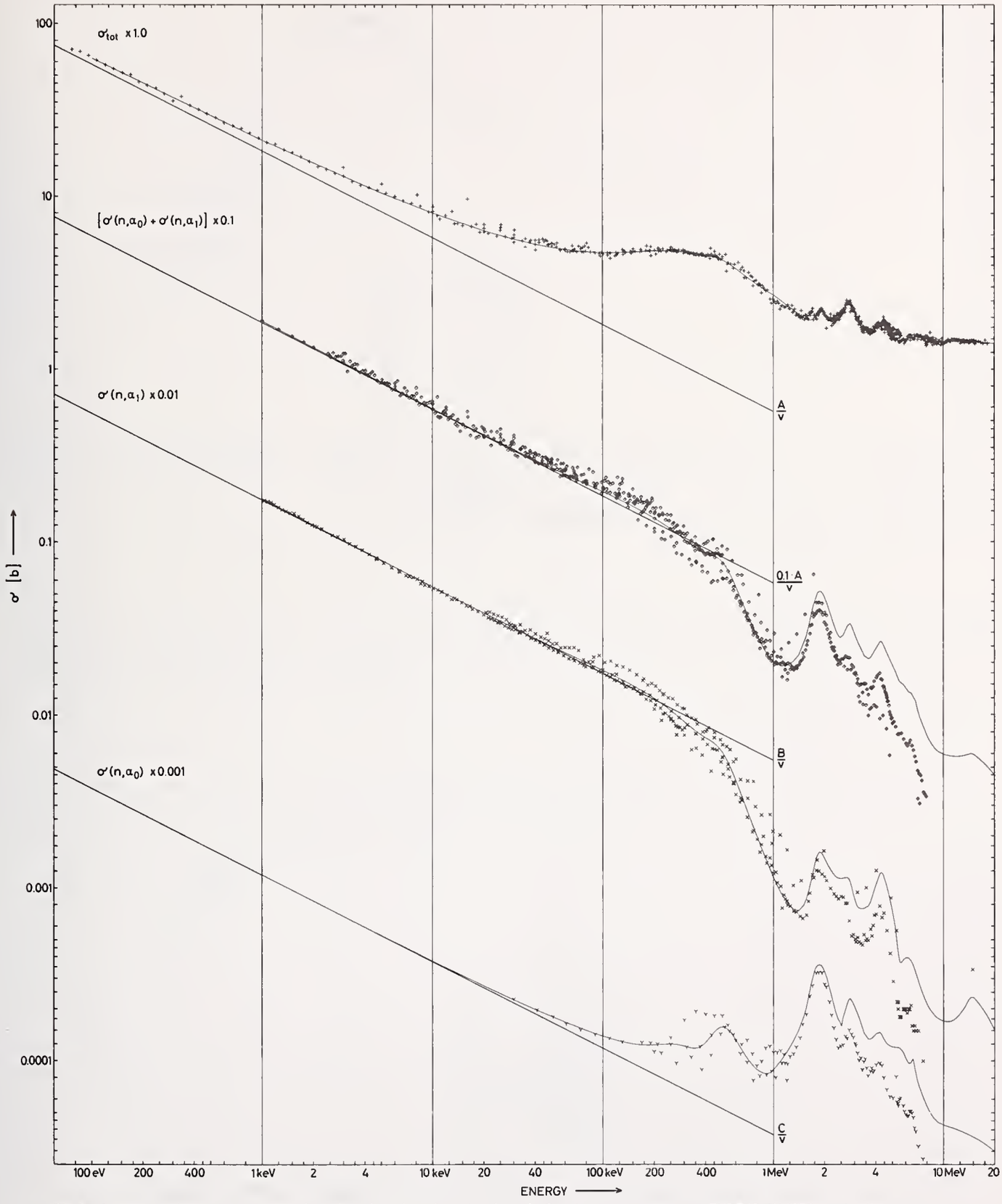

Fig.8 Cross-sections: σ'_{tot}, $\sigma'(n,\alpha_0)+\sigma'(n,\alpha_1)$, $\sigma'(n,\alpha_1)$ and $\sigma'(n,\alpha_0)$. Continuous curves are ENDF/B IV 1975 evaluation.

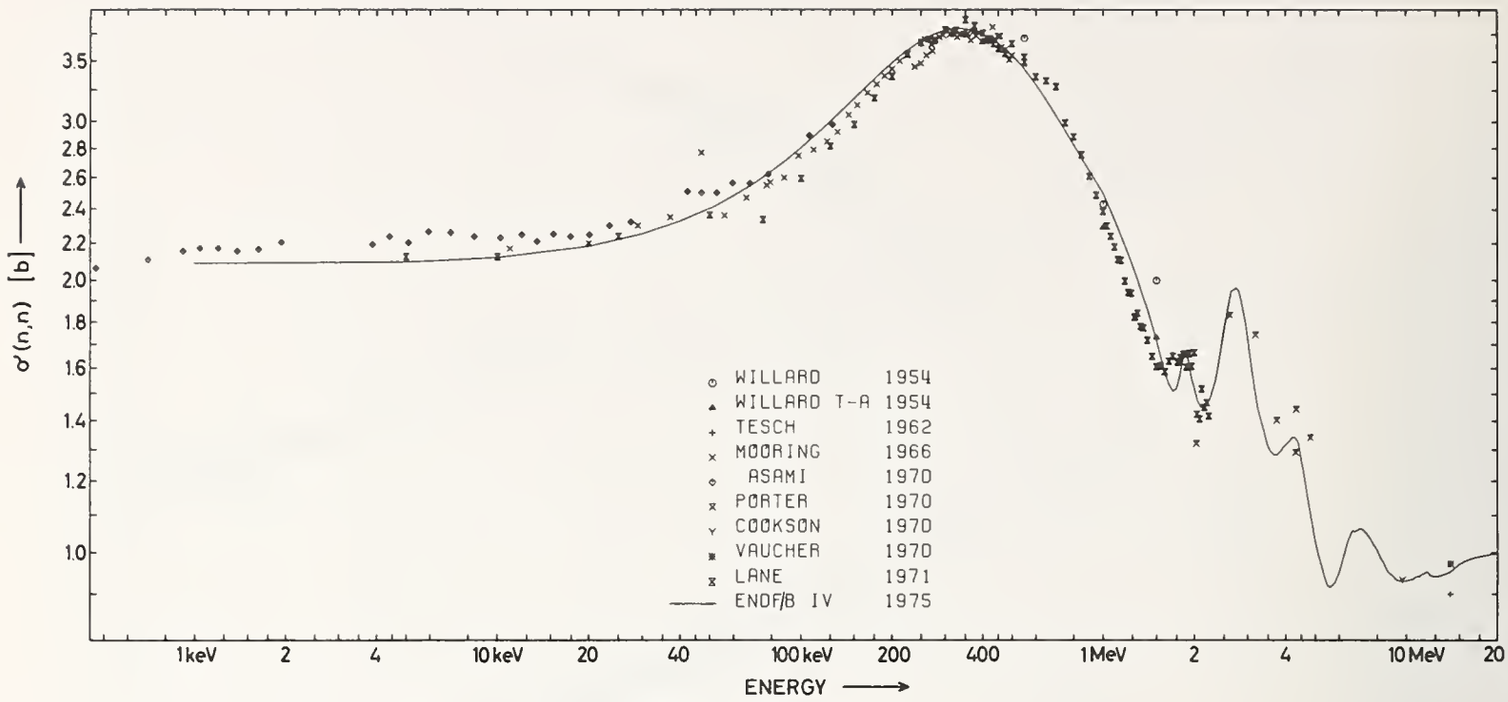

Fig.9 Elastic scattering cross-section from 500 eV to 20 MeV.

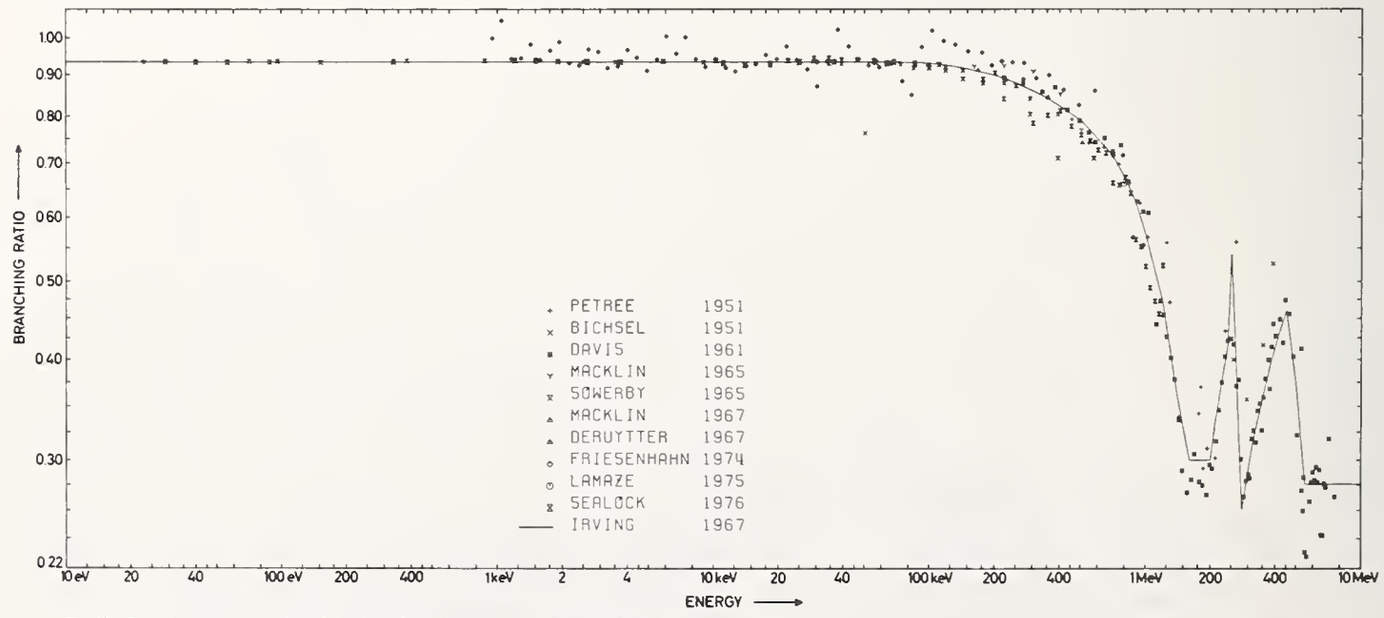

Fig.10 Branching ratio $\sigma(n,\alpha_1) / \sigma(n,\alpha_0) + \sigma(n,\alpha_1)$ from 10 eV to 10 MeV.

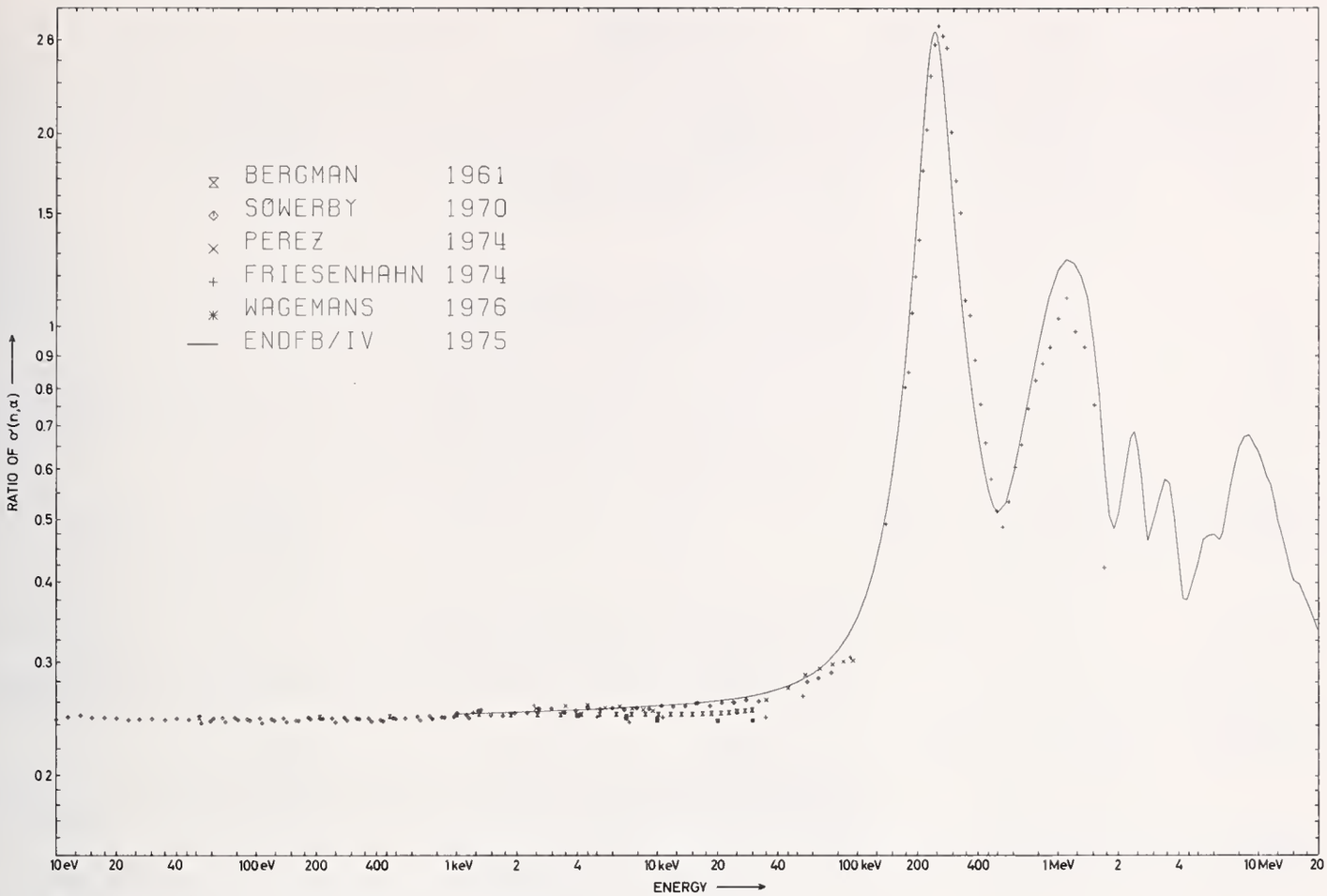

Fig.11 Ratio of $^{6}Li(n,\alpha)T$ to $^{10}B(n,\alpha)^{7}Li$ from 10 eV to 20 MeV.

ANNEX 1.

Table 1. Summary of σ_{tot} cross-section measurements of ^{10}B in keV and low MeV energy range

Investigator Name Date - Laboratory	Data Energy min.-max. Number of points	Experiment Source - spectrum - resolution sample	Comments
BOCKELMAN C. 1951 - WIS	20 keV - 3.4 MeV 197	V.d.G. - mono - ΔE = 20 keV determination isotopic composition might be in error	cross-sections about 15% greater than those of BARSCHALL-1946
COON J. 1952 - LAS	14 MeV 1	D(T,n)α - mono - ΔE = 40 keV accuracy of sample composition not documented	1.47 $\pm$ 0.03 barns
COOK C. 1954 - RIC	14.1 MeV - 18.0 MeV 7	V.d.G. D(T,n)α - 8 energies - $\Delta E \leq$ 40 keV accuracy of sample composition not documented.	accuracy 0.03 barns
NERESON 1954 - LAS	2.8 MeV - 9.7 MeV 26	Reactor - fission spec. - continuous E=10% p.recoil spectrom. - sample at least 98% pure	Statistical accuracy $\pm$ 3% at 3 MeV, $\pm$ 8% at 13 MeV
BECKER R. 1956 - WIS	4.4 MeV-8.6 MeV 66	V.d.G. mono - E_n = 40 keV, no indication on accuracy of determination of sample composition	statistical accuracy single point about 5%.
ROHRER 1960 - DKE	3 keV - 82 keV 41		unpublished, but see BILPUCH E. 1960 $\sigma_{tot} = 642\ E^{-\frac{1}{2}} + 2.43$
FOSSAN A. 1961 - WIS	3.3 MeV - 15 MeV 138	V.d.G. - mono - ΔE = 30 keV 5% impurities of uncertain composition	$\leq$3% statistical accuracy
TSUKADA K. 1963 - JAE	3.2 MeV - 5.1 MeV 59	V.d.G. - mono - $\Delta E \leq$ 20 keV - 93% enriched ^{10}B from ORNL no indication on accuracy of composition	statistical error $\leq$ 2% overall error estimated $\leq$ 3%
MOORING F. 1966 - ANL	10 keV - 500 keV 55	V.d.G. - mono - ΔE = 10 keV same experiment yields also $\sigma_{n,n'}/\sigma_{tot}$ composition of samples known to within 0.01 atom-percent.	accuracy 5% $\sigma_{abs} - \sigma_{n\alpha} \leq$ 100 mb below 500 keV
DIMENT K. 1967 - HAR	76 eV - 953 keV 83	Linac - white - 0.5 ns/m sample ^{10}B content (93.0 $\pm$ 0.2)% corrections made for impurities	fit yields $\sigma_{tot} = (630.3 \pm 3.1)E^{-\frac{1}{2}} + (1.95 \pm 0.10)$ for $E \leq$ 10 keV and σ_{tot}(DIMENT) - $\sigma_{n,n'}$(MOORING) yields $\sigma_{abs} \sim E^{-\frac{1}{2}}$ up to 300 keV
COOKSON J. 1969 - ALD	9.72 MeV 1	V.d.G. - mono - ΔE = 40 keV elast.& inelastic scatt. angular cross section is measured	σ_{tot} = 1597 mb whereas FOSSAN measured 1430 mb
PORTER D. 1970 - ALD	2.0 Mev - 4.8 MeV 7	V.d.G. - mono - ΔE = 30 keV - elastic and inelast.scatt. cross section measurement relative to H(n,n)H B-sample composition given to within 0.01%	integration over angle and known efficiency of calibrated scintillator yields $\sigma_{tot} = \sigma_{el.} + \sigma_{non\text{-}el.}$
SPENCER R. 1973 - KFK	90 keV - 420 keV 538	V.d.G. - white - 0.2 ns/m. Up to 5% uncertainty in σ_{tot} by deviations in chemical analyser.	agreement with BOCKELMAN C. 1951 - MOORING F. 1966 and DIMENT K. 1967, if chemical analysis of IMF Frankfurt is taken. No narrow resonance.
AUCHAMPAUGH G. 1976 - LAS	1.5 MeV - 11 MeV ?	V.d.G. - white - 25 ps/m - agreement with ENDF/B-IV better than 1%. Previously unknown resonances in σ_{tot} are revealed - numerical data not available yet but expected soon.	No indication of narrow resonance structure. Error $\leq$ 1.5%
HALE G. Nov. 73 - BNL	Evaluation ENDF/B-IV		
	0 to 1 MeV	R-matrix calculation plus σ_{tot} data of DIMENT K. - 67.	
	1 to 20 MeV	smooth curve through DIMENT K.-67, BOCKELMAN C.-51, TSUKADA K.-62, FOSSAN D.-61, COON J.-52, and COOK C.-54.	

Table 2. Summary of $^{10}B(n,\alpha_0+\alpha_1)^{7}Li$ cross-section measurements in keV and low MeV energy range

Investigator Name Date - Laboratory	Data Energy min.-max. Number of points	Experiment Source - spectrum - detector flux shape - normalisation	Comments
BICHSEL H. 1957 - RIC	20 keV - 5 MeV 98	V.d.G. - mono - BF_3 tubes - long counter assumed flat - norm. at 20 keV on $1/v$ from thermal 4010 b.	Long counter not documented but see later BOGART D.-68 accuracy: 25%
BILPUCH E. 1960 - DKE	3 keV - 70 keV 32	no experimental determination of $\sigma_{n,\alpha}$	σ_{tot} of ROHRER R. minus σ_{nn} of HIBDON C.
DAVIS E. 1961 - RIC	200 keV - 8 MeV 100	V.d.G. - mono - BF_3 grid ion. $E < 4.5$ MeV long counter, $E > 4.5$ MeV known $^{7}Li(p,n)$yield - long counter abs. by Pu-Be source	Accuracy: 20 - 30%
MOORING F. 1964 - ANL	11 keV - 77 keV 8	not well documented in ANL-6877, but probably preliminary results of type in MOORING F.-66	see Mooring F.-66
MOORING F. 1966 - ANL	10 keV - 500 keV 55	V.d.G. - mono - σ_{tot} and ratio σ_{nn} over σ_{tot} measured with transmission sample and scattering detector. No flux shape - no calibration needed.	Upper limit for $\sigma_{n,t} + \sigma_{n\gamma} + \sigma_{n,p} \leq 100$ mb, thus $\sigma_{n,\alpha} \approx \sigma_{abs}$, $\sigma_{tot} - \sigma_{abs}$ fits well with $\sigma_{n,n}$ of LANE R.-67
COX S. 1966 - ALD	11 keV - 250 keV 12	V.d.G. - mono - spherical shell transmission method - no flux shape - no calib. needed	accuracy : 10%
DIMENT K. 1967 - HAR	100 eV - 10 MeV 83	Linac - white - σ_{tot} measured	data for $\sigma_{n,\alpha}$ given, but obtained by calculation from σ_{tot} of DIMENT K. 1967 minus $\sigma_{n,n}$ of MOORING F. - 1966.
MACKLIN R. 1968 - ORL	30 keV - 500 keV 6	V.d.G. - n,α_0 determination by inverse reaction $^{7}Li(\alpha,n)^{10}B$ - long counter "4π graphite sphere" - additional $\sigma_{n,\alpha_0}/\sigma_{n,\alpha}$ ratio measurement with SBSC.	accuracy: 2% small standard deviation and particular type of method used make results attractive.
BOGART D. 1968 - LRC	30 keV - 800 keV 27	V.d.G. - mono - BF_3 - "Precision long counter" see DE PANGHER J.; norm. at 80 keV with $1/v$ from thermal 3840	calibration of BICHSEL H.-57 long counter by "precision long counter" yields revised BICHSEL data in good agreement.
SOWERBY M. 1970 - HAR	10 eV - 80 keV 33	Linac - white - ratio measured σ of $^{6}Li(n,\alpha)$ to $^{10}B(n,\alpha)$	The $\sigma_{n,\alpha}$ of ^{10}B is deduced from measured $\sigma(n,\alpha)$ ratio of ^{10}B to ^{6}Li and by assuming $\sigma_{n,\alpha}$ of ^{6}Li to be known. The latter deduced from $\sigma_{tot}-\sigma_{n,n}$ but no numerical data given. Cross-section given by an equation and uncertainty at 1, 10, 100 and 200 keV respectively is 1, 2, 3 and 5%.
FRIESENHAHN J. 1974 - IRT	1 keV - 1.5 MeV 152	Linac - white - B ion.ch. but also BF_3 - flux shape by CH_4 prop. counter, norm. at 4 keV by $1/v$ from thermal 3843,8	cross-checks ion ch. with BF_3-counter results deviate by 20%.
SEALOCK R. 1975 - ORE	200 keV - 1.2 MeV 21	V.d.G. - white - SBSC-known $^{7}Li(p,n)$ yield gives absolute energy dependent flux and other quantities absolute also, therefore absolute cross-sections	detailed measurements of n,α_0 ; n,α_1 ; $n,\alpha_0+\alpha_1$; $\sigma(\vartheta)$ and similar measurements for $^{6}Li(n,\alpha)t$. Accuracy ± 12%, but σ_{n,α_0} at 350 keV is about 1.8 times value of DAVIS E. or MACKLIN R.

HALE G. Nov. 1973 - BNL	Evaluation ENDF/B-IV	$\sigma_{n,\alpha}$ is sum of σ_{n,α_0} and σ_{n,α_1}
	σ_{n,α_0} - below 1 MeV	R-matrix calculation and experimental data of MACKLIN-68, DAVIS-61 and VAN DER ZWAN-72
	- 1 MeV to 20 MeV	based on DAVIS-67, but above 2 MeV renormalised by 1.4
	σ_{n,α_1} - below 1 MeV	R-matrix calculation and experimental data of FRIESENHAHN-72
	- 1 MeV to 20 MeV	smooth curve through DAVIS-61 and NELLIS-70 , data of DAVIS-61 above 2 MeV renormalised by 1.4

Table 3. Summary of $^{10}B(n,\alpha_1\gamma)^{7}Li$ cross-section measurements in keV and low MeV energy range

Investigator Name Date - Laboratory	Data Energy min.max. number of points	Experiment Source - spectrum - detector flux shape - normalisation	Comments
DAVIS E. 1961-RIC	200 keV - 2 MeV 82	V.d.G. - mono - $\Delta E \geqslant 25$ keV - BF_3 grid ion ch. - $E < 4.5$ MeV long counter $E > 4.5$ MeV known $^{7}Li(p,n)$ yield Long counter absolute by Pu Be-source	error: 20 - 30%
MACKLIN R. 1968 - ORL	30 keV - 800 keV 7	V.d.G. - n,α_0 determination by inverse reaction $^{7}Li(\alpha,n)^{10}B$ - long counter "4π graphite sphere" - additionally $\sigma_{n,\alpha_0}/\sigma_{n,\alpha_1}$ measurement by SBSC. n,α_0 and n,α_1 normalised at 30 keV on 1/v from thermal $\sigma_{n,\alpha}$ = 3843.2 b and use of own measured ratio n,α_0 to n,α_1 equal to 0.0689 ± 0.0006	Standard deviation estimates 2 to 2.5 % Small error and type of method used makes results attractive.
NELLIS D. 1969 - TNC	50 keV - 15 MeV 31	V.d.G. - mono - $\Delta E \geqslant 40$ keV NaI and/or GeLi - flux shape and flux by long counter - γ-ray efficiency also known!	error: ± 6%
COATES M. 1972 - HAR	1 keV - 300 keV 63	Linac - white - 1 ns/m - B_2O_3 and NaI - flux shape by spherical B-vaseline long counter - normalisation to SOWERBY at 1 keV	σ_{n,α_1} lower than values of Sowerby: 2% at 10 keV and up to 10% lower at 150 keV
FRIESENHAHN J. 1974 - IRT	1 keV - 1.5 MeV 56	Linac - white - ΔE = 3 keV at 250 keV ^{10}B slab Ge(Li) flux shape methane proport. counter - normalised on 1/v at 4 keV from 3601,7 at thermal.	error on shape of $\sigma_{n,\alpha_1}(E)$ is 2.5 to 4.6% from 2 keV to 1 MeV. - Data of report FRIESENHAHN 1972 are superseded by rept. FRIESENHAHN 1974. In both reports $\sigma(n,\alpha_1)$ data are identical.
SCHRACK R. 1976 - NBS	5 keV - 600 keV 36	Linac - white - 0.6 ns/m - ^{10}B slab NaI and Ge(Li) - hydrogen proportional counter relative units normalised at 4 keV on 3459,8 at thermal.	results NaI and Ge(Li) agree within 5% - most accurate results with Ge(Li) error 3% between 8 and 400 keV, 5% between 5 and 700 keV.
SEALOCK R. 1976 - ORU	.2 MeV - 1.2 MeV 21	V.d.G. - white - SBSC - absolute data by known $^{7}Li(p,n)$ yield and known geometry - angular distribution also measured.	error ranges from 5% at .2 MeV to 10% at 1.1 MeV.
HALE G. et al. 1975 - BNL	Evaluation ENDF/B - IV		
	below 1 MeV - calculated from R-matrix parameters and experimental data of FRIESENHAHN 1972.		
	1 to 20 MeV - smooth curve through measurements of DAVIS 1961 and NELLIS 1970 with smooth extrapolation from 15 to 20 MeV. The data of DAVIS 1961 above approximately 2 MeV were renormalised by a factor of 1.4.		

Table 4. Summary of $^{10}B(n,\alpha_0)^{7}Li$ cross-section measurements in keV and low MeV energy range

Investigator Name Date - Laboratory	Data Energy min.-max. number of points	Experiment Source - spectrum - detector flux shape - normalisation	Comments
DAVIS E. 1961 - RIC	200 keV - 8 MeV 82	V.d.G. - mono - $\Delta E \geq 25$ keV - BF_3 grid ion. chamber - $E < 4.5$ MeV long counter $E > 4.5$ MeV known $^{7}Li(p,n)$ yield - long counter abs. by Pu-Be source	error: 20 - 30%
MACKLIN R. 1968 - ORL	30 keV - 800 keV 7	V.d.G. - n,α determination by inverse reaction $^{7}Li(\alpha,n)^{10}B$ - long counter "4π graphite sphere" and $\sigma_{n,\alpha_0}/\sigma_{n,\alpha_1}$ ratio measurement by SBSC. n,α_0 and n,α_1 normalised at 30 keV on $1/v$ from $\sigma(n,\alpha)$ equal to 3843.2 b and use of own measured ratio $\sigma(n,\alpha_0)$ to $\sigma(n,\alpha_1)$ equal to 0.0689± 0.006.	standard deviation estimates 2 à 2.5%. Small error and type of method used makes results attractive.
SEALOCK R. 1976 - ORL	2 MeV - 1.2 MeV 21	V.d.G. - white - SBSC - absolute data by known $^{7}Li(p,n)$ yield and known geometry - angular distribution also measured.	error: 200 keV - 15%, 600 keV - 5%, 1.1 MeV - 9%.
HALE G. 1975 - BNL	Evaluation ENDF/B-IV below 1 MeV	- calculated from R-matrix analysis and experimental n,α_0 data input for the fit were those of MACKLIN 1968 and DAVIS 1961. In addition, the angular distributions of VAN DER ZWAN 1972 for the inverse reaction were included in the analysis.	
	from 1 to 20 MeV	- based on DAVIS-61 measurements with smooth extrapolation from 8 to 20 MeV, DAVIS-61 measurement above approx. 2 MeV was normalised by a factor of 1.4.	

Table 5. Summary of measured elastic scattering cross-section data in keV and low MeV energy range

Investigator Name Date - Laboratory	Data Energy min.-max. number of points	Experiment Source - Spectrum - Resolution Detector	Comments
WILLARD H.B. 1955 - ORL	0.5, 1 and 1.5 MeV + angular distribution measured from 30° to 120° at 9 angles additionally 3 points given for $\sigma_{tot} - \sigma_{abs}$	V.d.G. - mono - hydrogen proportional counter - E dependent efficiency determined by calib. with long counter results claimed in absolute units	$\sigma_{n,n}$ deduced by integration of measured $d\sigma(\vartheta)/d\omega$ which over-all error is ±15% $\sigma_{n,n}$ values deviate by 16% from $\sigma_{tot} - \sigma_{abs}$; might be due to non-uniform density of the samples.
TESCH K. 1962 - AAC	14 MeV - 1 point angular distrib. from 20 to 155° at 15 angles	$H^3(d,n)\alpha$ - mono - associated α-particle technique: NE 102 and Pilot chemicals scintillator - absolute efficiency known by previous associated particle technique in non-scattered beam	$\sigma_{n,n}$ deduced by integration of measured $d\sigma(\vartheta)d\omega$ $\sigma_{n,n}$ is 900 mb ± 50
MOORING F.P. 1966 - ANL	10 keV - 500 keV 55 points no angular distrib.	V.d.G. - mono - σ_{tot} and ratio $\sigma_{n,n}$ over σ_{tot} measured with transmission sample and 4π scattering detector no flux shape needed - no normalisation needed	$\sigma_{n,n}$ deduced from published values, namely $\sigma_{tot} - \sigma_{abs}$
ASAMI A. 1969 - HAR	1-120 keV, 30 points angular distrib. measured at 39°, 65°, 120° and 144°	Linac - white - 1 ns/m - ^{6}Li glasses - $\sigma_{n,n}$ of ^{10}B relative to $\sigma_{n,n}$ of C	no significant difference between $\sigma_{n,n}$ at four angles total uncertainty ranges from 1.1% at 120 keV to 3.7% at 1 keV
PORTER D. 1970 - ALD	2 - 5 MeV, 7 points ang.distr. measured at 10 angles from 30° to 135°	V.d.G. - mono - ΔE = 30 keV - elast. and inelastic angular scatt. cross-section - measurement relative to H(n,n)H. ^{10}B sample composition given to within 0.01%	uncertainty ⩽ 3.8% angular distributions well fitted by optical model calculations
COOKSON J. 1970 - ALD	9.72 MeV, 1 point ang.distr. meas. at 9 angles	V.d.G. - mono - ΔE = 40 keV - 0.5 ns/m NE 213 liq.scint. ^{10}B sample composition characterised to 0.1%- inelast.scatt.cross-section also measured.	uncertainty 7.3% angular distribution well fitted by optical model calculations
VAUCHER B. 1970 - LAU	14.1 MeV, 1 point ang.distr. measured at 14 angles	$D(T,n)\alpha$ - mono - ΔE = 100 keV - associated particle technique - NE 213 liq. scint. - angular distrib. of inelast. scatt. cross section to nine levels also available	$\sigma_{n,n}$ = 972 ±35 mb very detailed measurement in angle and in number of levels
LANE R. 1971-ANL	75 keV - 2.2 MeV, 67 points, angular distrib. measured at 5 angles and polarization experiments	V.d.G. - mono - ΔE from 30 to 100 keV BF_3 in oil - efficiency known by calib. with Ra-Be Source - energy dependent shape known by H(n,n)H	uncertainty ⩽ 2.5% $\sigma(\vartheta) \cdot P(\vartheta)$ polynomial expansion.
ENDFB/IV 1975 - BNL	0 to 1 MeV	calculated from R-matrix analysis - experimental data included in fit are those of ASAMI F. et al. 1966 and LANE R. et al. 1971	
	1 to 7 MeV	smooth curve through measurements of LANE R. et al. 1971, PORTER et al., 1970 and HOPKINS, 1969. Constrained to be consistent with σ_{tot} and reactions σ_x.	
	7 to 14 MeV	smooth curve through measurements of HOPKINS 1969, COOKSON J. et al. 1970, TESCH K. 1962, VAUCHER B. et al. 1970, and VALKOVIC et al. 1965.	
	14 to 20 MeV	optical model extrapolation from 14 MeV data.	

Table 6. Summary of branching ratio $R = \sigma_{n,a_1} / \sigma_{n,a_0} + \sigma_{n,a_1}$ measurements in keV and low MeV energy range

Investigator Name Date - Laboratory	Data Energy min.-max. number of points	Experiment source - spectrum - detector	Comments
PETREE B. 1951 - WIS	.3 - 2.6 MeV 18	V.d.G. - mono - BF_3 prop. counter	numerical values deduced from drawing - uncertainty on R difficult to estimate
BICHSEL H. 1952 - BAS	th - 0.5 - 3.5 - 3.9 MeV 8	1 MeV cascade - mono - BF_3 ion. chamber	neutron spectrum broad $\frac{\Delta E}{E} \cong 1\%$ uncertainty R ranges from 0.6% at E_{th} to 10% at 3.9 MeV
DAVIS E. 1961 - RIC	.2 - 8.0 MeV 83	V.d.G. - mono - BF_3 grid ion - chamber	R was deduced from published numerical data of σ_{n,a_0} and σ_{n,a_1} error of which is 20 to 30%
MACKLIN R. 1965 - ORL	30 - 700 keV 8	V.d.G. - mono - SBSC	below 200 keV error $\leqslant 0.005$ above 200 keV error $\leqslant 0.05$
SOWERBY M. 1965 - HAR	23 eV - 0.5 MeV 42	Linac - white - $^{10}BF_3$ low gas mult.	abs.error $\leqslant 0.015$ up to 600 keV
MACKLIN R. 1967 - ORL	30 - 500 keV 7	V.d.G. - mono - SBSC	abs. error 0.003
DERUYTTER A. 1967 - GEL	E_{th} 1	reactor - Maxw. - SBSC	R = 0.93692 ± 0.00006 high quality $a_0 - a_1$ resolution
FRIESENHAHN J. 1974 - IRT	1 - 1500 keV 62	Linac - white - Ge(Li) for a_1 and BF_3 for $a_0 + a_1$	abs.error on E-dependent shape of R is 2 keV - 0.010; 50 keV - 0.006; 500 keV - 0.031
LAMAZE G. 1974 - NBS	790 keV 1	V.d.G. - Mono - BF_3 prop. counter	R = 0.66 ± 0.03
SEALOCK R. 1976 - ORU	.2 - 1.2 MeV 27	V.d.G. - white - SBSC	R was deduced from published numerical data of σ_{n,a_0} and σ_{n,a_1} error of which is 4 to 15%
IRVING D. 1967 - ORL	Evaluation, smooth curve through experimental points of SOWERBY M.-65, MACKLIN R.-65, DAVIS E.-61 and PETREE B.-51		

Table 7. Summary of measured ratios of $\sigma_{n,a}$ of $^6Li(n,a)T$ to $^{10}B(n,a)^7Li$ in keV and low MeV energy range

Investigator Name Date - Laboratory	Data Energy min.-max. number of points	Experiment Source - Spectrum - Resolution Detector Li, detector B	Comments
BERGMAN A. 1961 - LEB	50 eV - 40 keV 20	Slowing down time spectrometer - ΔE 14% around the mean at best - Ar prop. counter with ^{10}B and ^6LiF layer of .22 and 1.13 mg/cm^2 respectively	corrections small - total error on ratio about 0.4% - numerical data were deduced from drawing on p. 898 of publication
SOWERBY M. 1970 - HAR	10 eV - 80 keV 86	Linac - white - 2.5 ns/m - 0.3 cm thick Li glass scint. - BF_3 counter below 1 keV boron plug + NaI above 50 eV up to 74 keV - multiple scattering correct. for ^6Li up to 15%	both measurements in relative units and normalised at 10-20 eV on the 1/v value deduced from thermal of 3839 ± 20 and 940 ± 4 barns for ^{10}B and ^6Li respect. Uncertainty in ratio $\leqslant 0.0030$ i.e. $\leqslant 1.2$ %.
PEREZ 1974 - ORL	2 - 100 keV 17	Linac - white - 0.2 ns/m - 1 mm thick ^6Li-glass and BF_3 ionization chamber	ratio of neutron flux spectra as published on page 206 were multiplied by ratio of Li to B cross-sections of Sowerby et al. to get original ratio of counting rates. This ratio in turn is proportional to $\sigma_{n,a}$ of Li to B. This procedure is crude and more accurate data are expected from the authors.

Table 7. (continued)

Investigator Name Date - Laboratory	Data Energy min.-max. Number of points	Experiment Source - Spectrum - Resolution Detector Li, Detector B	Comments
FRIESENHAHN S. 1974 - IRT	1 - 1500 keV 179	Linac - white - ^{6}Li ion chamber ^{10}B ion chamber and BF_3-proport. counter.	Systematic uncertainty in ratio amounts to 4.6%, 1.2%, 0.2% and 0.1% at 1 MeV, 0.5 MeV, 0.1 MeV and 50 keV respectively
WAGEMANS C. 1976 - GEL	1 - 30 keV 5	Linac - white - 0.7 ns/m - SBSC thin LiF and B layers of 220 and and 176 $\mu g/cm^2$ respectively. SBSC detectors are located outside the collimated neutron beam and detect those α-particles emerging at about 90° on neutron flight direction.	error about 3% - ratio is normalised at 1 keV at 0.2479 value of Sowerby et al.
MAGURNO B. 1975 - BNL	Evaluation of ENDF/B-IV of $^{6}Li(n,\alpha)T$ and $^{10}B(n,\alpha)^{7}Li$ cross-section data were used to calculate ratios for comparison with experiments.		

INSTRUMENTS FOR USE OF ^{10}B AS A STANDARD

A. D. Carlson
National Bureau of Standards
Washington, D.C. 20234

The interaction of neutrons with ^{10}B provides two commonly used neutron cross section standards. The $^{10}B(n,\alpha_1\gamma)^7Li$ reaction is implemented with detectors such as NaI or Ge(Li) to detect the 478-keV gamma ray emitted in this reaction. The $^{10}B(n,\alpha_0+\alpha_1\gamma)^7Li$ (commonly referred to as $^{10}B(n,\alpha)^7Li$) reaction is used with proportional counters, ionization chambers, solid-state detectors and boron scintillators. A discussion of the use of these detectors for implementing these cross sections will be presented.

(Boron scintillators; Ge(Li); ionization chambers; NaI; neutron flux determination; proportional counters; solid-state detectors; standard cross section; $^{10}B(n,\alpha_1\gamma)^7Li$; $^{10}B(n,\alpha_0+\alpha_1\gamma)^7Li$)

Introduction

The measurements of neutron cross sections are greatly simplified when the data are obtained relative to standard neutron cross sections. The neutron flux is then essentially determined with the standard cross section and the basic flux measuring techniques need not be employed. The $^{10}B(n,\alpha)^7Li$ reactions are often used as cross section standards. These reactions and Q values are outlined in Fig. 1 along with the energy level diagram for ^{11}B. There are two basic reactions of interest. For the $^{10}B(n,\alpha_0)^7Li$ reaction, the ^7Li nucleus is left in its ground state and the total energy shared by the reaction products is 2.792 MeV plus the kinetic energy of the incident neutron. For the $^{10}B(n,\alpha_1)^7Li^*$ reaction, the ^7Li nucleus is left in its first-excited state and the total energy shared by the reaction products is 2.314 MeV plus the kinetic energy of the incident neutron. The ^7Li nucleus promptly decays to its ground state with the emission of a 0.478-MeV gamma ray. The products of these reactions can be detected by a number of techniques which will be the subject of this paper. In Fig. 2 the two cross sections which are used as standards, $^{10}B(n,\alpha_1\gamma)^7Li$ and $^{10}B(n,\alpha_0+\alpha_1\gamma)^7Li$, are shown. At the higher neutron energies these cross sections are not considered standards due to the large cross section uncertainties. It will be assumed that with further improvements in these cross sections, the upper limit of their usefulness as standards may approach 1 MeV. Measurements made relative to these standards which are not well defined at this time can be resurrected at a later time when the standards have been improved. However, fundamental problems may arise above ~500 keV where the cross sections are falling very rapidly with neutron energy.

The only detectors which will be considered in this paper are those for which the efficiency is directly proportional to a ^{10}B standard cross section, neglecting small correction factors. Thus, detectors such as the ^{10}B vaseline ball[1] used at Harwell for which the efficiency is almost independent of the ^{10}B standard will not be discussed.

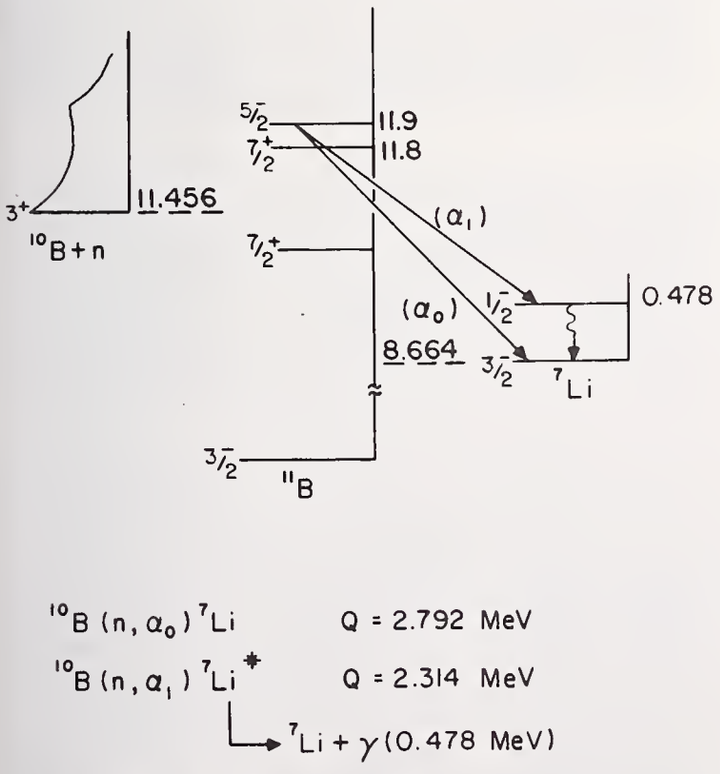

Figure 1. Energy level diagram for ^{11}B showing the decay modes of a level in ^{11}B to states in ^7Li by emission of an α particle.

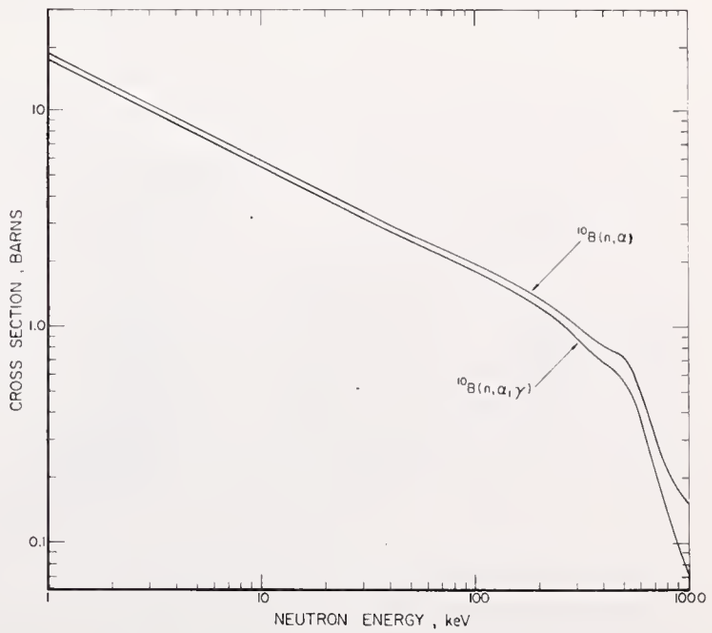

Figure 2. The $^{10}B(n,\alpha_1\gamma)$ and $^{10}B(n,\alpha)$ cross sections from 1 to 1000 keV.

$^{10}B(n,\alpha_1\gamma)^7Li$

Cross section measurements relative to the $^{10}B(n,\alpha_1\gamma)^7Li$ cross section have been made only with detectors which record the 478-keV gamma ray from this reaction. This technique is convenient to implement since the energy of the gamma ray produced is independent of the neutron energy. Thus, response functions which are dependent on neutron energy are not required in analyzing these data. In principle it should be possible to implement this cross section by detecting the charged particle(s) produced when ^7Li is left in its first excited state. This is not practical except possibly at low neutron energies due to difficulties in separating these events from those leaving ^7Li in its ground state.

Gamma-Ray Detectors

NaI and Ge(Li) detectors have been employed in using this cross section. Fig. 3 shows an experimental layout for making these measurements. Both a NaI and a Ge(Li) detector are shown but only one of these detectors would be used for a given experiment. The neutron beam is collimated to a size larger than the size of the ^{10}B sample yet small enough so that the beam does not strike the gamma-ray detector. The detector-sample geometry shown here is particularly appropriate for linac experiments. Having the detector at back angles reduces the effect of the scattered gamma-flash photons. The background from scattered neutrons is determined by replacing the ^{10}B sample with carbon or ^{11}B. This measurement is important since scattered neutrons can interact with the detector materials and produce a gamma-ray background. Also shown in this Fig. is the detector employed for the measurement of the cross section to be determined. The positioning of the two detectors is dependent on a number of factors which must be evaluated for each given experiment, i.e. relative counting rates in the two detectors, materials in the beam for each detector, relative time resolution of each detector for white-source measurements, etc. Fig. 4 shows the pulse-height distributions for a NaI detector for 510-keV neutrons as obtained by Schrack.[2] The upper curve are data obtained with the ^{10}B sample in place. The lower curve is obtained with a carbon scatterer replacing the ^{10}B sample. This Fig. shows the importance of making scattered-neutron background measurements. In addition to the prominent 478 keV line, 203-keV and 417-keV gamma-rays from iodine and 438-keV gamma rays from sodium can be seen. The resolution of NaI detectors limits the usefulness of this technique particularly at high neutron energies where many background gamma-rays from neutron interactions in sodium and iodine can produce a significant background near the 478-keV line.

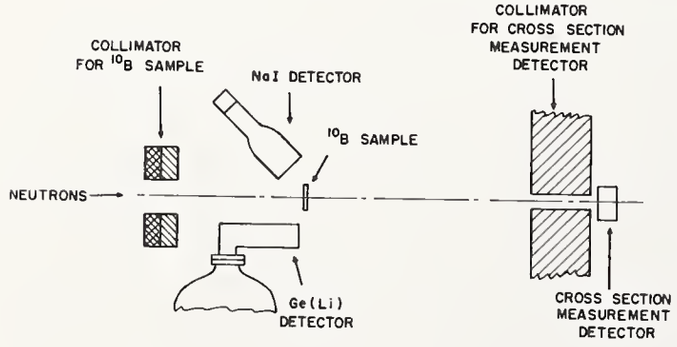

Figure 3. Simplified experimental setup for implementing the $^{10}B(n,\alpha_1\gamma)$ cross section.

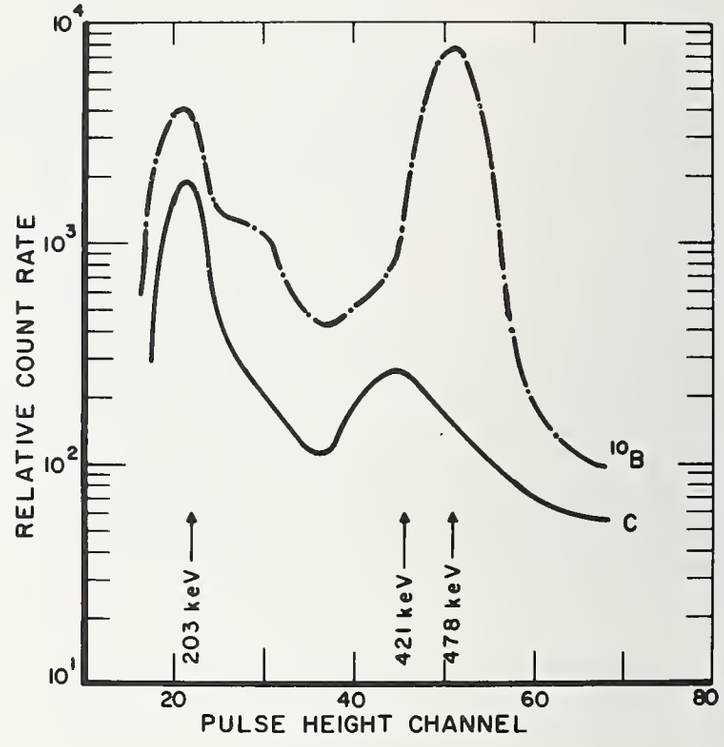

Figure 4. Pulse-height distributions for 510-keV neutrons for a NaI detector system used in implementing the $^{10}B(n,\alpha_1\gamma)$ cross section. The upper curve was obtained with a ^{10}B sample. The lower curve was obtained with a carbon scatterer. The arrow labeled 203 keV shows the position of the (n,n') gamma-ray from iodine. The arrow labeled 421 keV shows the position of a peak which is a mixture of 438-keV gamma-rays from sodium and 417-keV gamma-rays from iodine.

The use of Ge(Li) detectors significantly simplifies this problem as a result of the intrinsically better resolution compared with NaI and since the gamma-rays from inelastic scattering in germanium are well separated from the 478-keV line. Fig. 5 shows measurements by Orphan[3] of the pulse-height distribution for a Ge(Li) detector for neutron energies near 1 MeV. The 596-keV gamma-rays from ^{74}Ge and the 695-keV gamma-rays from ^{72}Ge are well resolved from the 478-keV gamma-ray peak. The Ge(Li) detector technique does suffer from reduced efficiency due to limitations in the size of Ge(Li) detectors. Both NaI and Ge(Li) detectors have good time resolution, the Ge(Li) detector being somewhat better, so they can be used conveniently for white source neutron time-of-flight measurements. Throughout the useful region for this cross section (up to ~300 keV), the systematic errors are probably ~1%

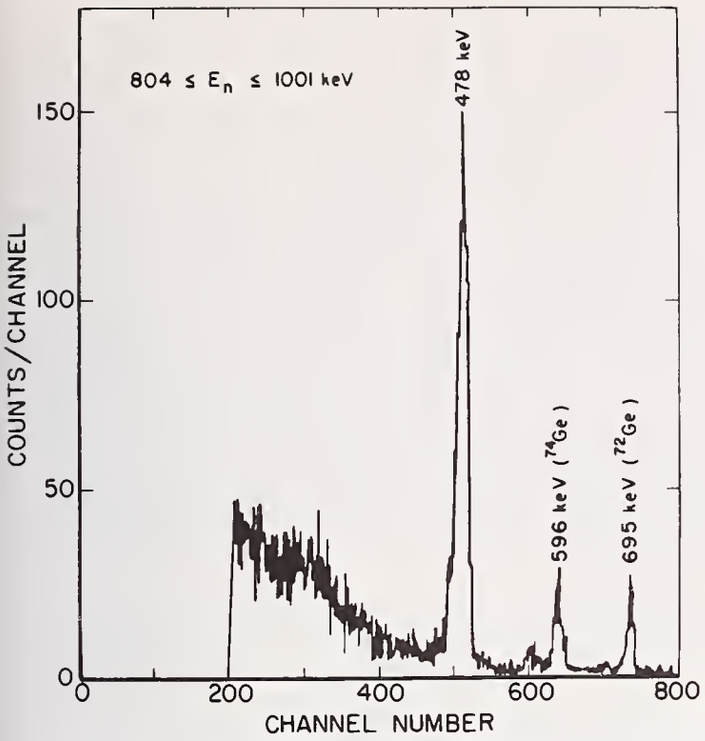

Figure 5. The pulse height distribution for a Ge(Li) detector used in implementing the $^{10}B(n,\alpha_1\gamma)$ cross section for neutron energies from 804 to 1001 keV.

for the Ge(Li) detector and somewhat larger for NaI detectors. These systematic errors are primarily a result of uncertainties in the background and small uncertainties in the self shielding and multiple scattering in the sample. In addition to these systematic errors which are appropriate to relative measurements, a solid angle and detector efficiency uncertainty must be included for absolute measurements. A convenient method for determining the product of solid angle and detector efficiency involves replacing the ^{10}B sample with a disk of equal area containing a uniform calibrated source of ^{7}Be. ^{7}Be decays by electron capture to produce the 478-keV excited state of ^{7}Li.

$^{10}B(n,\alpha_o + \alpha_1\gamma)^{7}Li$

This reaction is implemented by employing detectors which will detect either the α_o or α_1 particles (and also possibly the ^{7}Li nuclei). The energies of these particles change with neutron energy thus causing some complication in the interpretation of data where the neutron energy is a significant fraction of the Q value. Historically this has limited the use of this cross section at higher neutron energies. The cross section has been implemented with proportional counters, ionization chambers, solid-state detectors and boron scintillators. The use of each of these detectors will be discussed below.

Proportional Counters

The simplicity of these detectors has led to extensive use of these counters in neutron experiments. Fig. 6 shows a typical simplified experimental set-up. Typically the counter gas employed is $^{10}BF_3$. Neutrons incident upon the counter can interact with ^{10}B and the reaction products, ^{7}Li and an α-particle, will produce ionization in the counter as they come to rest. Consider an event which occurs near the center of the counter. Then for low enough neutron energies the reaction products lose all their energy before striking the walls. The total ionization will be closely proportional to the total energy of the reaction products,

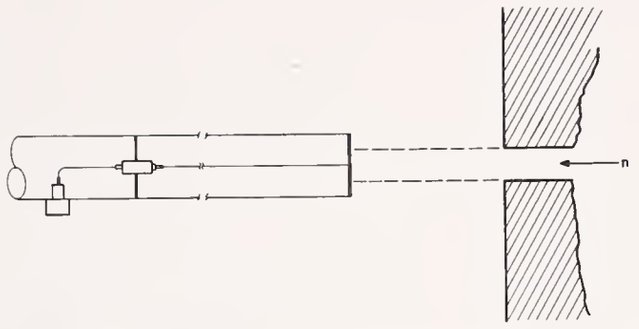

Figure 6. Simplified experimental set-up for the use of a $^{10}BF_3$ gas proportional counter.

$(Q + E_n)$. Thus, aside from resolution effects, a sharp peak should be observed for the $^{10}B(n,\alpha_o)^{7}Li$ reaction and a separate peak for the $^{10}B(n,\alpha_1\gamma)^{7}Li$ reaction. These two peaks will be separated in energy by 478 keV since the ^{7}Li gamma ray will not generally be detected. If this entire counter were being irradiated with neutrons, some of the reaction products would strike the walls of the counter before losing all their energy by ionization. This "wall effect" gives rise to a low energy tail in the pulse-height distribution. In Fig. 6 the neutron beam is collimated to a size smaller than the diameter of the counter. If the beam diameter is small enough (and the counter dimensions are great enough), the wall effect can be removed. The reduction in counting rate is very large for a moderate size counter if the collimator is designed to entirely eliminate the wall effect. The collimator also removes the background resulting from direct beam neutrons striking the walls of the counter. An added benefit for linac measurements is that the gamma flash is significantly reduced by this collimator since much of this problem is a result of photons which interact with the walls of the counter.

The time jitter of proportional counters is worse than that of the other detectors under discussion. This results from the fact that multiplication in these counters only occurs very near the central anode wire. So electrons must drift in a moderate field (i.e. slow-electron velocity) until they are essentially at the center of the counter. Thus the time between the reaction (and formation of ionization) and the formation of the signal at the anode varies from $\sim$ zero for ionization concentrated near the wire to a maximum for ionization concentrated near the walls of the counter. The collimator which was described previously has the further advantage of reducing the time jitter by reducing the effective radius of the counter (note the effective radius is somewhat larger than the diameter of the collimator due to the reaction products which are directed toward the walls of the counter). The timing of the counter can also be improved by employing various gas mixtures.

The proportional counter necessarily will have effects associated with distortion of the field near the ends of the counter (end effect) however, with modern counter geometries having reasonable lengths, this effect is small, $\Delta L/L \sim 1$-2% (uncertainty in length/length). In Fig. 7, the energy spectrum from a 5-cm

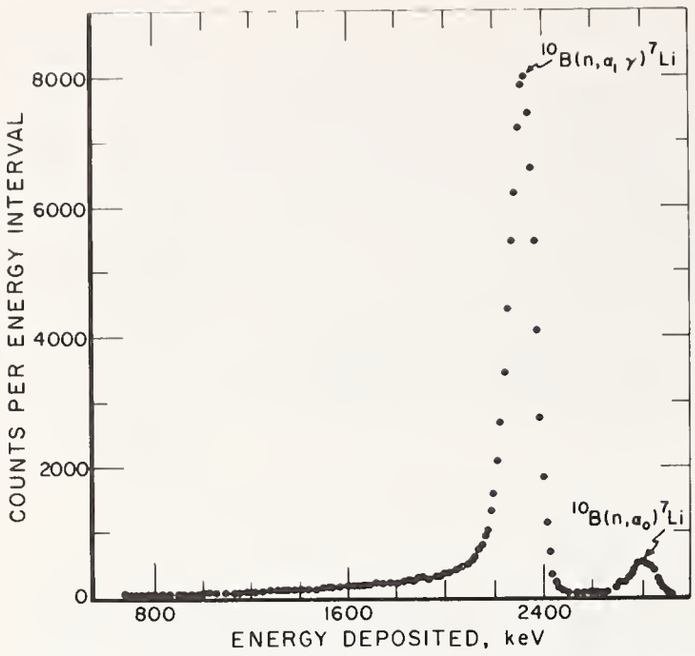

Figure 7. Pulse height distribution for a $^{10}BF_3$ gas proportional counter for thermal neutrons.

diameter proportional counter[4] exposed to thermal neutrons is shown. The two groups associated with $^{10}B(n,\alpha,\gamma)^7Li$ and $^{10}B(n,\alpha_o)^7Li$ are well resolved. This resolution (~5%) was made possible by operating the counter with 10% $^{10}BF_3$ and 90% argon. The argon was used to reduce wall effects by increasing the stopping power of the gas. It also reduced the time jitter of the counter. The long tail at low energies is a result

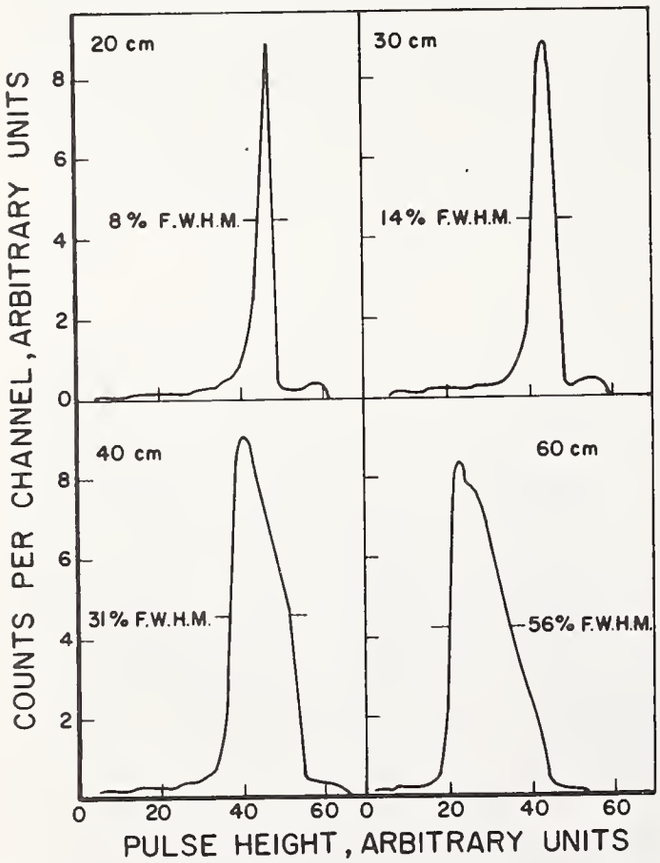

Figure 8. Pulse height distributions for $^{10}BF_3$ gas proportional counters for fillings of 20, 30, 40 and 60 cm Hg pressure for thermal neutrons.

of wall and end effects. The low ^{10}B content in this detector limits its usefulness. Fig. 8 shows the effect of increasing the pressure of $^{10}BF_3$ in a gas proportional counter.[5] The larger the pressure the poorer the separation of the two groups. This results from electron attachment to the $^{10}BF_3$ molecules. However it is not necessary to resolve the groups. All that is needed is the total number of counts above a bias which is appreciably above the noise pulses. Thus useful counters can be made with ~ one atmosphere of $^{10}BF_3$. However the higher pressures lead to poorer time jitter (See Ref. 6). The rather poor timing is perhaps the worst limitation in the use of these counters. As the neutron energy increases the wall effect can become important. Also at high neutron energies, pulses from ^{10}B nuclei which have been scattered by neutrons are large enough so that the discrimination level must be increased. Thus a possible systematic error in the spectrum fraction can be introduced. The pulse-height distribution for a gas proportional counter with one atmosphere of $^{10}BF_3$ for neutron energies of about 500 keV is shown in Fig. 9. The low-energy pulses in

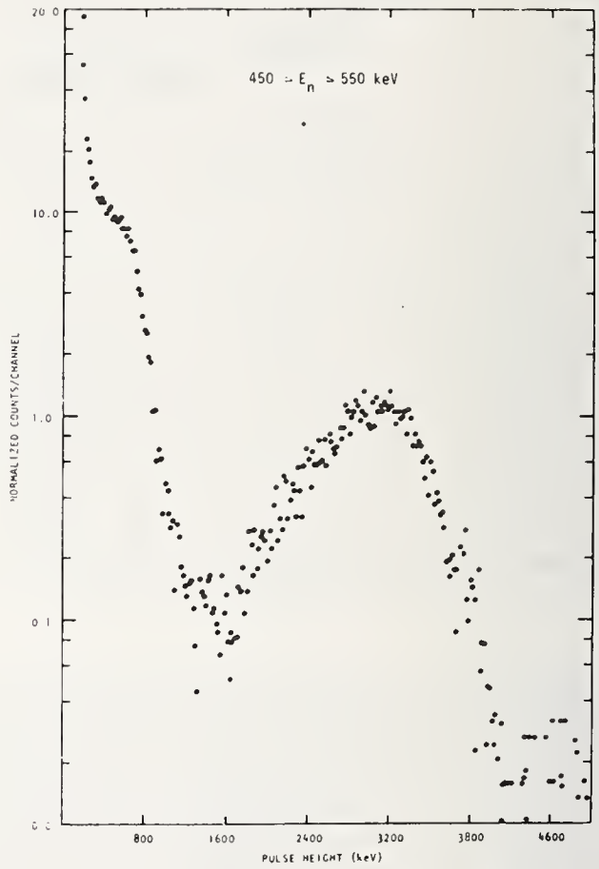

Figure 9. Pulse height distribution for a one atmosphere $^{10}BF_3$ gas proportional counter for neutrons from 450 to 550 keV.

this Fig. are ^{10}B recoils. These recoils are present in all ^{10}B counters which detect charged particles. The total systematic errors (mainly from room return neutrons, spectrum fraction and end window scattering) are in the 1 to 3% range for this type of detector. This detector is most easily implemented in a cross-section measurement as the counter located further from the source so that transmission corrections for the constituents of the counter need not be applied to the cross-section measuring counter. In white source experiments this reduces the effect of the time jitter of the counter also.

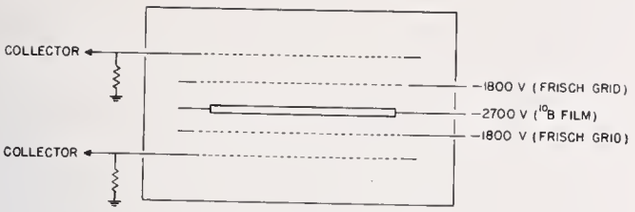

Figure 10. Schematic layout of the Frisch gridded ion chamber used by Friesenhahn.

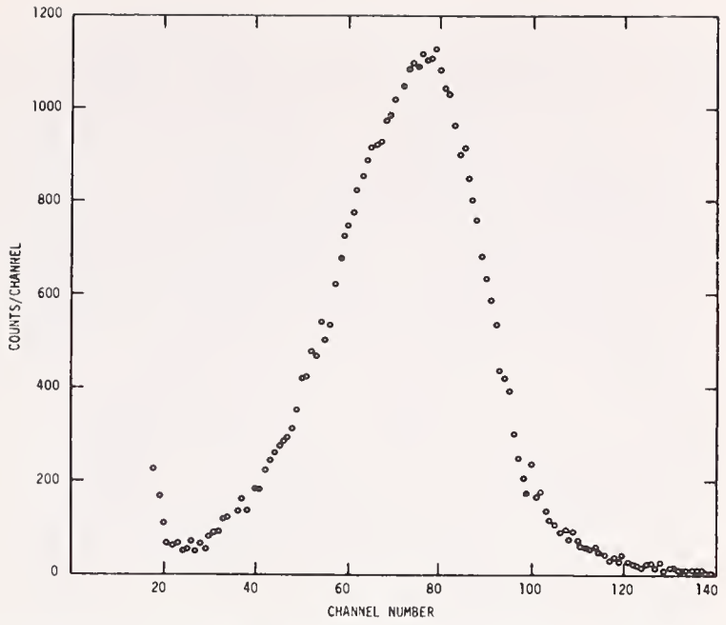

Figure 11. The sum pulse height distribution for the gridded ion chamber designed by Friesenhahn for neutron energies from 1 - 10 keV.

Ionization Chambers

Ionization chambers containing $^{10}BF_3$ or solid ^{10}B deposits can be fabricated so that scattering from the chamber is small and the transmission corrections for the constituents of the chamber are easily calculated. A $^{10}BF_3$ ungridded gas ionization chamber has been used by Weston[7] for low-neutron energies. A 20% $^{10}BF_3$ + 80% argon gas mixture is used to reduce the range of the reaction products and to improve the timing of the detector. A timing of 35 ns has been obtained. Summing of the reaction products occurs but for ungridded chambers the pulse size depends on the track orientations of the α particle and ^{7}Li ion. Thus the pulse height distribution is very broad and the chamber is limited in usefulness to low-neutron energies where the pulse height distribution is essentially constant with neutron energy (i.e., the spectrum fraction is approximately constant). The use of gridded chambers removes this problem.

Fig. 10 shows the layout for a detector with Frisch grids used by Friesenhahn.[3] In this chamber a self supporting ^{10}B film was employed which is a colloidal suspension of ^{10}B in a thin plastic film. The thickness of the film is $\sim$ 200 $\mu g/cm^2$. This is thin enough so that both reaction products can escape from the film. The spacing between the film and the Frisch grid is 2 cm which is slightly greater than the range of the most energetic reaction products for the counting gas (10% CO_2 + 90% A). The electrons are drawn through the Frisch grid to the collector, all moving through the same potential difference to the collector. A fast pulse proportional to the ionization appears between the grid and the collector. Thus by summing the pulses at the two collectors shown here, a pulse proportional to the Q value of the reaction plus the neutron energy is produced. The principal disadvantage of this detector is the low counting rate due to the thin ^{10}B deposits. To increase the counting rate, Friesenhahn employed eleven modules of this type separated by suppressor grids to prevent cross talk between adjacent modules. The complete ion chamber is more than 1 m long and the frames are 25 cm x 25 cm. It is the largest ion chamber of which I am aware. Fig. 11 shows the sum pulse height distribution for this detector for neutron energies from 1 to 10 keV. The greatest difficulty with the use of this detector is the determination of the spectrum fraction. At low-

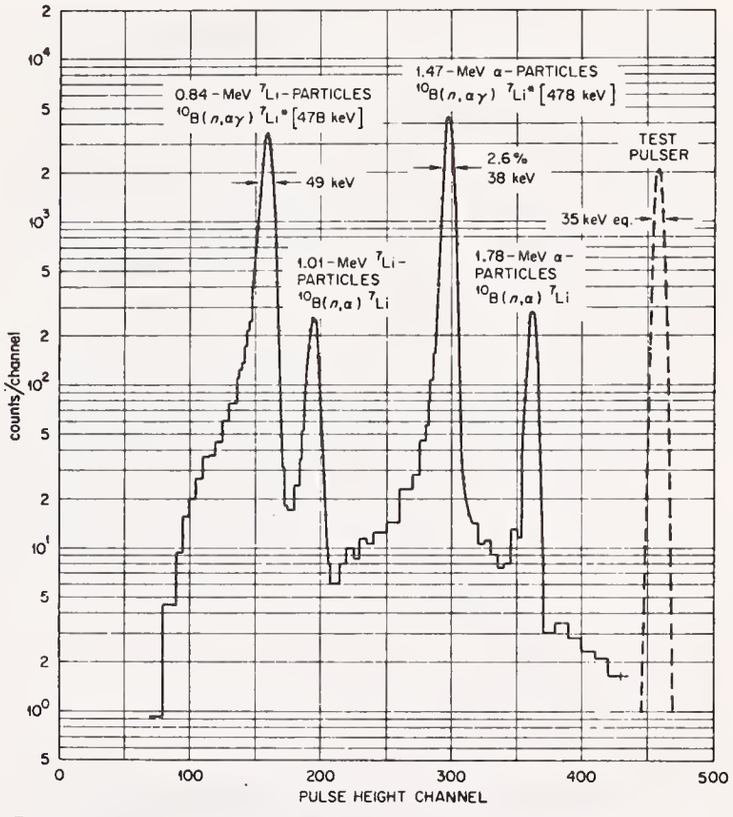

Figure 12. The pulse height distribution of the gridded ion chamber designed by Peelle for neutron energies less than 2 keV.

neutron energies, as in this Fig., the fraction of the events below a reasonable pulse-height bias is quite small. However, at high neutron energies the bias must be increased to eliminate proton recoils from hydrogen in the plastic binder. In principal the spectrum fraction can be calculated however some of the input data which are needed are not known accurately enough, such as dE/dx of the film at low ion energies. The calculation must take into account such effects as the neutron kinetic energy, the branching ratio and the angular distribution of the reaction products. The spectrum fraction correction was 15% at 700 keV. The systematic uncertainty with this detector is $\sim$ 2%.

In Fig. 12 the pulse-height distribution for a gridded ^{10}B ionization chamber designed by Peelle[8] is shown. This chamber was designed to be used with gridded fission chambers for cross section measurements on a linac. The timing of this detector should be $\sim$ 30 ns. This chamber contains thin deposits of ^{10}B evaporated onto a mylar backing. Only one of the reaction products is then observed except at very high neutron energies where the incoming momentum of the neutron in a fraction of the events permits both reaction products to go in the forward direction. Four peaks are observed since there is no summing. These spectra were obtained for neutron energies below 2 keV. In normal practice the pulse-height bias would be placed just above the ^{7}Li particles. The pulse height resolution is seen to be excellent. At high neutron energies, however, the spectra are more complicated than those shown in Fig. 12 as a result of kinematic effects. Then the separation between the α particles and ^{7}Li ions is not as clear and corrections must be made for the α particles lost below the bias. This is not the most important complication, however. The low count rate at high-neutron energies due to the thin film is the real problem.

Solid-State Detectors

The reaction products from the $^{10}B(n,\alpha)^{7}Li$ reaction can also be detected with any charged-particle detector. Solid-state detectors are convenient and the demands on these detectors are quite minimal compared with the state of the art. The depletion layer need not be very thick since the maximum energies of the reaction products are relatively low. The energy resolution of the detector can be fairly poor since the thickness of the ^{10}B film will dictate the resolution of the system. It is preferable however to have large area detectors to increase the solid angle for counting rate considerations.

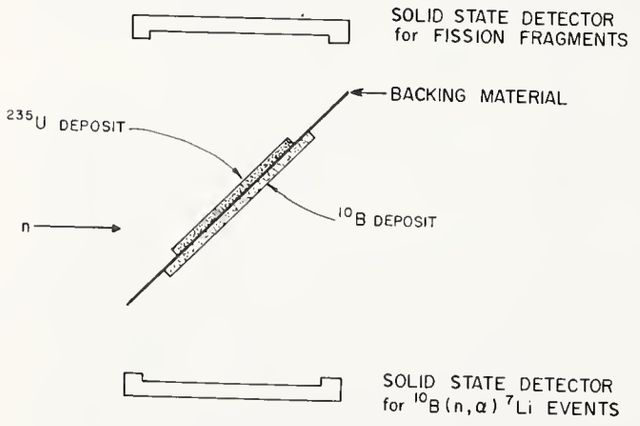

Figure 13. The detector geometry employed by Wagemans and Deruytter for a measurement of the ^{235}U fission cross section relative to $^{10}B(n,\alpha)^{7}Li$.

Fig. 13 shows the detector geometry employed by Wagemans and Deruytter[9] for measurements of the ^{235}U fission cross section relative to the $^{10}B(n,\alpha)^{7}Li$ standard. The solid-state detectors are shielded from the direct neutron beam by a collimator. Fundamentally this is the same geometry as that involved in a double ionization chamber set-up. The nearly equivalent environments for the two films reduce the systematic errors in the cross section measurement. This chamber is evacuated so that the reaction products do not lose energy when passing from the foil to the detector.

For the geometry of Fig. 13 the reaction products must pass through a thicker deposit of material than the areal density before they are detected in the solid-state detector. This worsens the pulse-height resolution of the system relative to an ion chamber of equivalent areal density. Also the solid angle must be determined with the solid-state detector system whereas an ion chamber detects all reaction products which are emitted from the foil which have energies greater than the bias energy. It is then obvious that the counting rate will be higher for the ion chamber than for a solid-state detector system of equivalent areal density. The limited angular range over which particles are detected for the solid state detector has one virtue. The kinematic effects which worsen the separation of the particle groups are reduced if the range of angles for which particles are detected is limited.

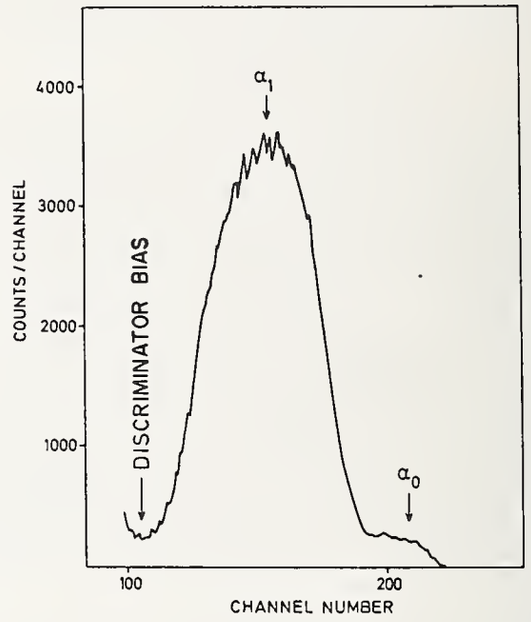

Figure 14. Pulse height distribution for the solid-state detector system employed by Wagemans and Deruytter.

In Fig. 14 the pulse height distribution observed by Wagemans and Deruytter is shown. This distribution should be compared with that observed by Peelle (Fig. 12). The resolution of the solid-state detector system is much worse due to the greater effective thickness of the ^{10}B film. The measurements of Wagemans and Deruytter only extend to 30 keV so the shape of the pulse height distribution should be essentially the same for the full energy region.

The timing with solid-state detectors is very good (in the ns region). In particular, for this experiment it was not a limitation to the time resolution. The solid angle for the solid state detector can be deduced by calculation or by replacing the ^{10}B film with a uniform calibrated alpha source having the same area as the ^{10}B deposit. In the Wagemans experiment the systematic errors in the use of the $^{10}B(n,\alpha)^{7}Li$ reaction are small, $\lesssim$ 1%.

^{10}B Scintillators

In the late 1950's and early 1960's a considerable effort was expended looking for a satisfactory method for implementing scintillators containing ^{10}B. Good timing should be possible with scintillator-photomultiplier tube combinations. The kinetic energy of the reaction products would be summed and should produce a convenient response function. The objective was to obtain high concentrations of ^{10}B so that high efficiency could be achieved. For some uses high concentrations of ^{10}B would allow smaller scintillator thicknesses so that the multiple scattering corrections (and therefore their uncertainties) could be reduced. Scintillators which are loaded with ^{10}B compounds unfortunately poison the scintillator so that the greater the concentration of ^{10}B the lower the pulse height from ^{10}B(n,α)^{7}Li reactions. In Fig. 15 the

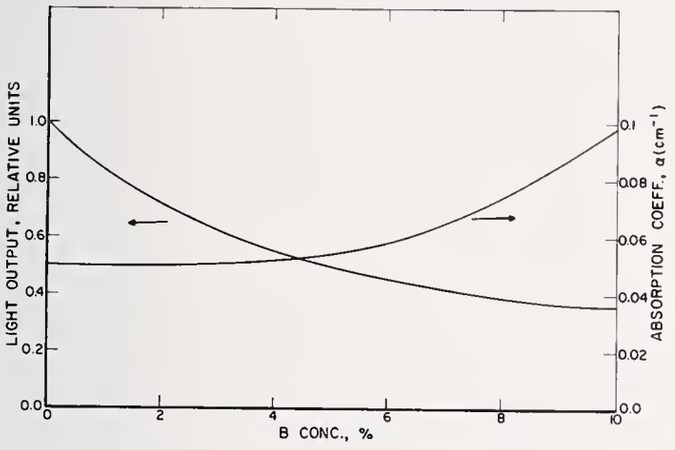

Figure 15. Dependence of the light output and light absorption on boron concentration for a boron-loaded plastic scintillator.

light output[10] as a function of boron concentration for a plastic scintillator is shown. To obtain usable efficiencies the pulses were so small that photomultiplier tube noise was an important factor. Various techniques were employed to handle these problems. For example, Bollinger[11] coupled two photomultiplier tubes to one scintillator and by requiring a coincidence between the pulses from these tubes, he significantly reduced the noise rate. Also cooled photomultiplier tubes have been employed to reduce the noise rate. Even pulse-shape discrimination has been used; this has the virtue of reducing noise and discriminating against γ-ray events in the scintillator.

Unfortunately these methods are complicated and/or awkward to implement. Thomas[12] fabricated a ^{10}B loaded liquid scintillator assembly coupled to a single photomultiplier tube which is usable without any of the special refinements mentioned above. The pulse-height distribution for that detector is shown in Fig. 16. The pulse-height resolution is about 50% and photomultiplier tube noise is still a small problem; but, this represents the best results obtained to date with ^{10}B scintillators without the special techniques mentioned above.

Though in the past ^{10}B has been loaded into liquid, glass and plastic scintillators and a number of different experimental techniques have been tried, very little work has been done recently on ^{10}B scintillators. Some of the problems noted by Bollinger[11] were a result of non-uniform efficiency of photocathodes for the photomultiplier tubes employed. It seems reasonable that with the improvements in photomultiplier tubes and electronics in general in the past 15 years and the possibility of improved scintillators, more work in this general area could yield a satisfactory detector.

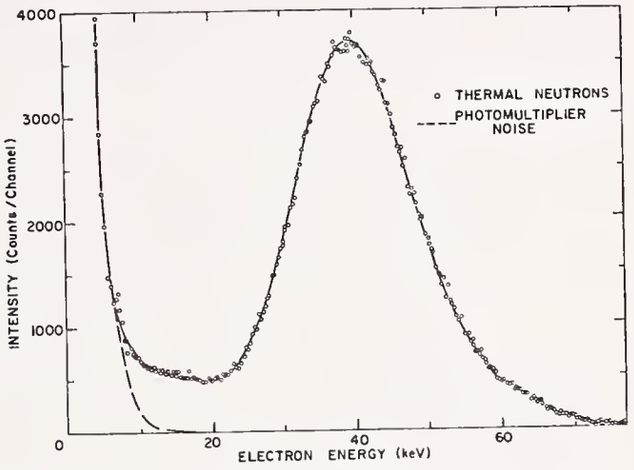

Figure 16. Pulse height distribution of a boron loaded liquid scintillator for thermal neutrons.

Conclusion

A number of techniques are available at the present time for implementing the ^{10}B(n,α)^{7}Li cross sections to an accuracy satisfactory for most cross section measurements. Further developmental work may improve the utilization of this standard. Improvement of the standard cross sections themselves is needed at the higher neutron energies, however, the rapid fall of the cross sections above $\sim$500 keV may introduce fundamental limitations to the use of this cross section for some experiments.

References

1. M. S. Coates, G. J. Hunt, C. A. Uttley and E. R. Rae, Proc. Symp. Neutron Standards and Flux Normalization, CONF-701002, p. 401, U.S.A.E.C. (1971).

2. R. A. Schrack, G. P. Lamaze, and O. A. Wasson, to be published.

3. S. J. Friesenhahn, A. D. Carlson, V. J. Orphan and M. P. Fricke, "Measurements of the $^{10}B(n,\alpha_{1\gamma})$ and $^{10}B(n,\alpha)$ Cross Sections," U.S.A.E.C. Report Gulf-RT-A12210 (1972).

4. G. P. Lamaze, A. D. Carlson and M. M. Meier, Nucl. Sci. Eng. 56 (1975) 94.

5. I. L. Fowler, Rev. Sci. Instrum. 34 (1963) 731.

6. O. K. Harling, Nucl. Instrum. Methods 34 (1965) 141.

7. L. W. Weston, private communication (1977).

8. R. W. Peelle, L. W. Weston, R. W. Ingle, J. H. Todd and F. E. Gillespie, Neutron Phys. Div. Ann. Progr. Rep. May 31, 1972, ORNL-4800, p. 10 (1972), and R. W. Peelle, private communication (1977).

9. C. Wagemans and A. J. Deruytter, Annals of Nucl. Energy 3 (1976) 437.

10. G. I. Anisimova, L. S. Danelyan, A. F. Zhigach, V. R. Lazarenko, V. N. Siryatskaya and P. Z. Sorokin, Pribory i Tekhnika, Eksperimenta 1 (1969) 49.

11. L. M. Bollinger and G. E. Thomas, Rev. Sci. Instrum. 28 (1957) 489 and L. M. Bollinger and G. E. Thomas, Nucl. Instrum. Methods 17 (1962) 97.

12. G. E. Thomas, Nucl. Instrum. Methods 17 (1962) 137.

EVALUATION AND USE OF CARBON AS A STANDARD.

J.C. Lachkar
Service de Physique Nucléaire - Centre d'Etudes de Bruyères-le-Châtel
B.P. n° 561 - 92542 Montrouge-Cedex, France.

Available data on the carbon total and elastic scattering cross sections are reviewed. Major emphasis is placed on two neutron-energy regions below 5 MeV and between 8.5 and 15 MeV. The overall consistency of the recommended values has been established with the aid of previously performed theoretical analyses. It is concluded that carbon elastic data below 5 MeV can be adopted as a standard except at the location of resonances. It is also suggested that the present need for high energy neutron standards could be satisfied by carbon data.

(Standard ; evaluation ; carbon ; total cross section ; elastic scattering cross section ; R-function analysis ; optical model).

Introduction

Carbon cross-section data are of interest in a number of areas of applied physics. Detailed knowledge of differential cross sections for neutrons scattered by carbon is required for calculations of neutron transport in materials for fusion and fission reactors. These needs have justified a large number of measurements, the earliest ones being performed 30 years ago. Since reasonably accurate sets of data were available, neutron data on carbon have been proposed as standards. Carbon is a good candidate since it is a light nucleus and then the level density of the compound n + carbon system is small ; also the threshold for inelastic scattering is high. In 1970, at the Argonne Symposium on Neutron Standards and Flux Normalization, it was suggested that carbon is suitable as a transmission standard up to 1.5 MeV but is marginal in angular distribution applications [1,2]. Since that time new measurements and more complete analyses have been performed in several laboratories ; consequently it has been conjectured that, by including all the presently available experimental informations on the total cross section, differential elastic cross sections and polarization in a R-matrix fit, a complete and consistent set of evaluated data could be generated up to 5 MeV [3,4]. At higher energies, where the presence of resonances in the ^{13}C compound nucleus and competing reactions do not allow carbon to be considered as a standard scatterer, differential scattering cross sections for carbon are still of interest. In scattering experiments, absolute normalization is generally made by replacing the sample by a polyethylene scatterer : moreover, emitted neutrons usually are detected using plastic scintillators. Thus neutron data for carbon, are needed for those two parts of the measurements. This need is more and more pronounced as the energy increases since the relative importance of the neutron data of carbon to the (n,p) scattering data increases with energy as shown in fig.1. In addition it is likely that a measurement of scattering from a secondary standard such as carbon, from which good samples are easy to prepare, would allow easier comparison of data obtained at various laboratories.

Also, neutron induced reactions on ^{12}C produce mainly one γ-ray corresponding to the de-excitation of its first excited level at 4.44 MeV. This line may be a good candidate to determine the detector efficiency at high energy or to be a reference for γ-ray production cross sections for neutron induced reactions at high energy [5].

Finally the neutron cross sections for carbon exhibit several well defined and sharp resonances and thus carbon may be considered as an energy-scale standard in both white and monoenergetic source measurements [3,6].

Here, we shall review the data on the carbon total and elastic scattering cross sections. We shall concentrate on the most recent available data, mainly in the low-energy range. Contributions from ^{13}C also will be considered along with radiative capture cross sections. We shall then discuss the theoretical models used in the analysis of the data. By comparing theoretical values to the experimental ones we shall give some error estimates.

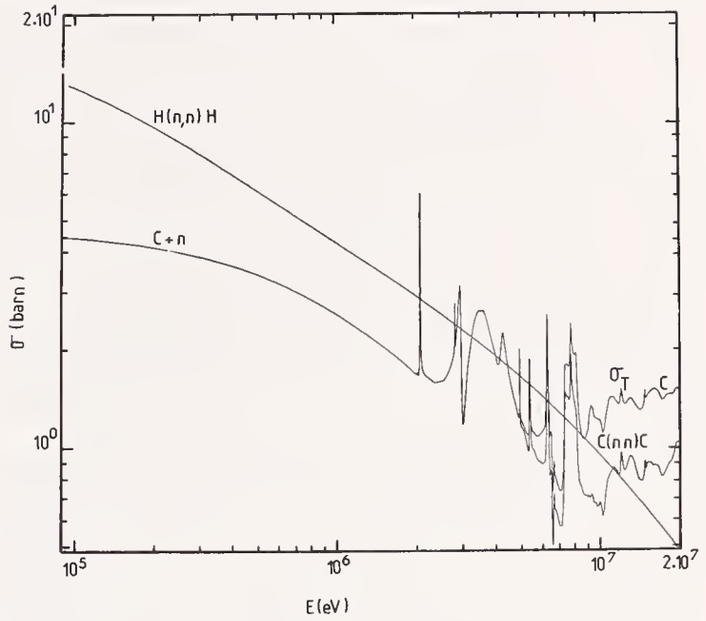

Fig.1. Energy dependence of the carbon total and elastic cross sections compared to the H(n,p) scattering cross section.

Neutron-induced reactions on carbon

The Q-values and thresholds of the neutron-induced reactions corresponding to the n + ^{12}C system are derived from ref.[7]. The $^{12}C(n,\gamma)$ reaction has a Q value of 4.947 MeV. The threshold energy for the inelastic scattering is 4.812 MeV.

Natural carbon consists of 98.892% of ^{12}C and 1.108% ^{13}C, so we have to consider the contribution of the ^{13}C content. Neutron data for ^{13}C have to be taken into account if a precision of 0.5% or better is required. The (n,γ) reaction for ^{13}C has a Q value of 8.177 MeV and the threshold energy for the inelastic scattering is 3.323 MeV.

Analysis of the data

The analysis of the data will be divided into three parts. In the first one, from the thermal value up to 2.0-MeV neutron energy, the total cross section for ^{12}C exhibits no resonance structure. The second part extends from 2.0 MeV up to 4.8 MeV which corresponds to the threshold of inelastic scattering for ^{12}C. The

third one is up to 15 MeV. For each part, total and differential elastic scattering cross sections will be discussed.

From 0 to 2 MeV neutron energy.

The total cross section for natural carbon has been measured and evaluated by many groups; we have analysed most of these studies and used the data to propose evaluated total cross sections [8]. Our recommended values are shown in fig. 2. The most complete data considered in our analysis are listed in table 1. They can be seen in fig.3 which plots versus neutron energy the percent difference between each data set and our recommended values. The data of Cierjacks et al. [9] from KFK are characterized by a good energy resolution and a precise energy calibration ; however they have been found to be higher by about 1%. On the other hand, the data from RPI [10] seem to be low by about 1.5%. Finally nearly all the data from NBS [11], Harwell [12], ORNL [13] and ANL [14] lie in a band of total width approximately 1% of the average cross section.

The thermal value of the total cross section has been evaluated by Leonard et al. [15] and Story et al. [16] These two evaluations were based on all the available carbon thermal cross section measurements from the year 1946 to 1970. Their adopted values are given in table 2. More recently, Mughabghab and Garber [17] have proposed the value of 4.750 ± 0,02 barn. This value is very consistent with that (4.756 ± 0.036 b) deduced by Heaton et al. [11] from their data above 1 keV by assuming that the total cross section is constant between 10 keV and thermal energy. Our recommended value, 4.728 ± 0.008 b, is consistent with all the previous ones.

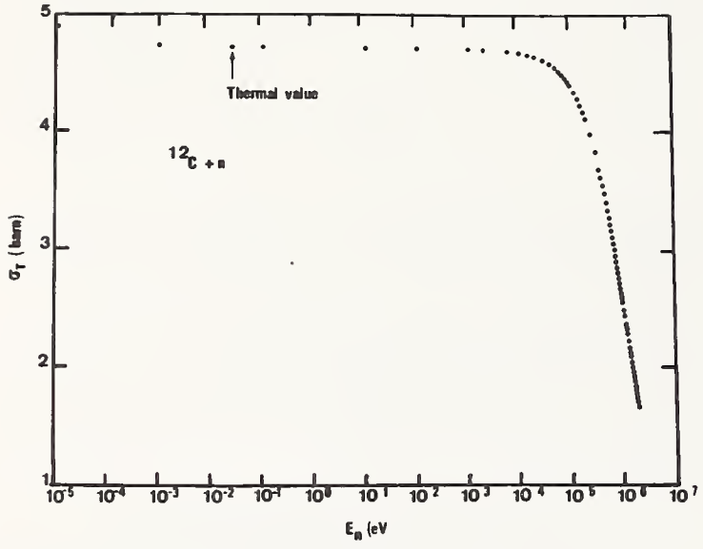

Fig.2. Recommended carbon total cross section below 2 MeV.

Between 10 eV and 2.0 MeV, the variation of the total cross section with neutron energy has been expressed by a polynomial in energy which was fitted to the averaged data by minimizing χ^2. The proposed values are given by the expression:

$\sigma(E) = 4.725 - 3.251\ E + 1.316\ E^2 - 0.227\ E^3$ (barn)

where E is the neutron energy in MeV. The accuracy of the total cross section is believed to be 0.5% below 1 keV and less then 1% up to 2 MeV. Such an analytical expansion does not take into account resonances in ^{14}C which will be discussed below.

Various and detailed measurements on differential elastic cross sections have been reported below 2 MeV. Most of them, listed in table 3, have been presented or discussed at the Argonne Symposium on Neutron Standards and Flux Normalization in 1970. All these data have been also considered to propose

TABLE 1

Available total cross section data.

Authors	Year	Lab	Energy-range (MeV)	Remarks	Ref
Bockelman	1951	WIS	1.25-3.35	exp.data	20
Fossan	1961	WIS	3.30-16	"	23
Uttley	1968	HAR	7.10^{-5}-1.5	"	12
Cierjacks	1968	HFK	0.3 - 30	"	9
Clements	1970	RPI	0.9 - 30	"	10
Foster	1971	BNW	2.3 - 15	"	22
Nishimura	1971	JAE	10^{-2}-0.3	"	46
Perey	1972	ORL	0.2 - 20	"	13
Meadows	1970	ANL	0.5 - 1.5	"	14
Holt	1975	ANL	1.5 - 5.0	"	18
Heaton	1975	NBS	10^{-3}-15	"	11
Auchampaugh	1976	LAS	1.5 - 14	preliminary data	35
Francis	1970	KAP	10^{-10}- 15	evaluated data	1
Nishimura	1971	JAE	≤ 2	"	46
Perey	1974	ORL	10^{-10} - 20	ENDF B/IV	19
Lachkar	1975	BRC	10^{-10} - 20	evaluated data	8

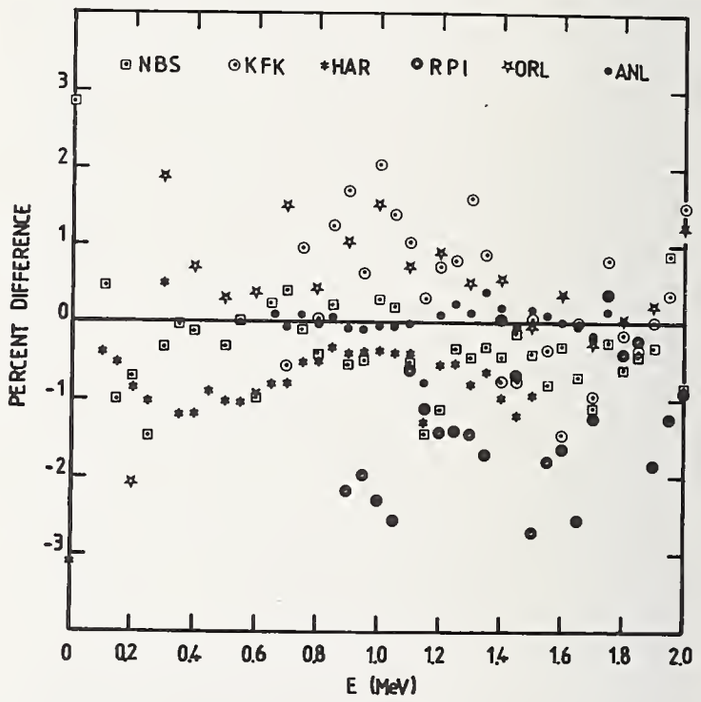

Fig.3. Ratios of carbon σ total experimental data to recommended curve. NBS data are from ref.[11], KFK from ref.[9], HAR from ref. [12], RPI from ref. [10], ORL from ref. [13] and ANL from ref. [14].

TABLE 2

Thermal neutron total cross section for carbon

Authors	Year	Recommended σ_T for thermal energy	Ref
Leonard	1970	4.730 ± 0.008 b	15
Story	1970	4.723 ± 0.0125 b	16
Mughabghab	1973	4.750 ± 0.02 b	17
Lachkar	1975	4.728 ± 0.008 b	8

TABLE 3

Summary of neutron elastic scattering measurements from 0.05 MeV up to 15 MeV.

Authors	Year	Lab	Ref	Neutron-Energy range (MeV)	Number of measured energies	Measurement angles (deg)	Remarks
Lane	1961	ANL	47	0.05 - 2.20	56	25 - 145	Ang. Distr.
Lane	1969	ANL	42	0.10 - 2.0	30	22 - 145	Ang. Distr. Pol.
Ahmed	1970	GEL	48	0.5 - 2.0	31	20 - 160	Ang. Distr.
Wills	1958	ORL	27	1.45 - 4.10	12	35 - 145	Ang. Distr.
Holt	1975	ANL	18	1.8 - 4.0	12	20 - 160	Ang. Distr.
Meier	1954	LAU	26	2.2 - 3.8	8	35 - 145	"
Galati	1972	KTY	24	3.0 - 7.0	32	15 - 160	"
Knox	1973	OHO	39	2.63	1	17 - 118	Ang.Distr. Pol.
Fasoli	1973	PAD	25	2.1 - 4.7	29	20 - 160	Ang.Distr. Total X sect.
Perey	1969	ORL	28	4.5 - 8.5	13	15 - 140	Ang.Distr.
				5.2 - 8.7	40	15 - 140	
Velkley	1973	ABD	29	7.0 - 9.0	5	10 - 150	"
Haouat	1974	BRC	30	8.5 - 11.0	4	30 - 160	"
				8.0 - 14.5	14	10 - 160	"
Glasgow	1976	DKE	31	9 - 15	14	25 - 160	"

evaluated data in ENDF/B IV [19]. The new results since that time are from ANL where Holt et al. [18] have measured angular distributions at 1.8 and 2.0 MeV. Their data have been found consistent with the recommended angular distributions from ENDF/B IV except at forward angles. This deviation might suggest that some changes would be necessary in the existing evaluations at least above 1.8 MeV.

Above 0.1 eV the integrated elastic scattering cross section can be taken equal to the total cross section. This results in a (n,γ) cross section that is too small. The deviations between the integrated elastic cross section, determined from polynomial fits to the measured angular distributions, and the recommended total cross section are less than the experimental uncertainties which are about 3%. Differential cross section are generally quoted with a precision of less then 5%.

From 2- to 4.8-MeV neutron energy.

At the neutron energy of 2.077 ± 0.002 MeV, the ^{12}C + n reaction reaches the resonance at 6.863 MeV in ^{13}C ; the total width of this resonance is 6 keV and the value of the total cross section at the peak is 6.020 b taken from ref. [13]. The narrowness of this resonance implies that a good energy resolution is needed in the vicinity of 2.077 MeV. This may be a severe constraint in the extension of the use of carbon as a standard above 2 MeV.

Between 2.1 and 2.7 MeV, the total cross section show no resonance (fig.4) and, here, carbon still could be used as a standard. In this energy range, three sets of data from NBS [11], ORNL [13] and the older ones from the University of Wisconsin [20] have been found very consistent. The accuracy is of the same order as below 2 MeV, i.e. not greater than 1%. Recently reported data from ANL [18] were also found to be in good agreement. The major interest in these measurements lies in a very good energy resolution which was obtained with the aid of monoenergetic source techniques.

At E_n = 2.816 ± 0.004 MeV, most of the recent data exhibit a maximum associated with the resonance at 7.545 MeV in ^{13}C. This resonance was ignored in the evaluation file ENDF/B III but was included in the ENDF/B IV file. The total width of less than 5 keV reported by Ajzenberg-Selove [21] for this resonance is consistent with the data of ref. [9,11,13,18].

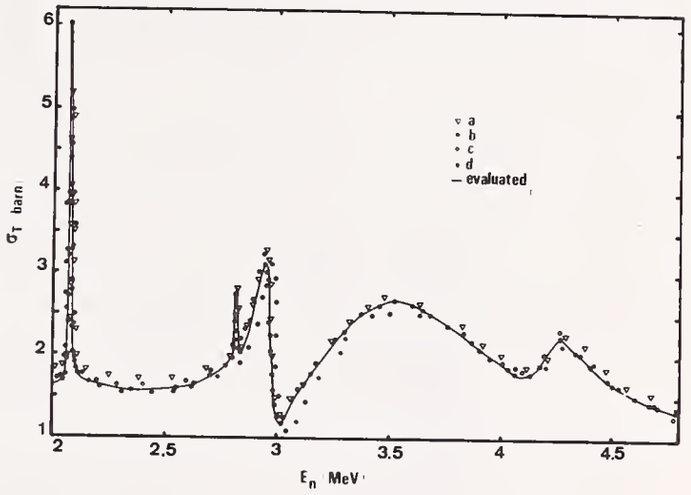

Fig.4. Comparison of neutron total cross sections of carbon between 2 and 5 MeV (a = ref.[9], b = ref.[20,23], c = ref.[11], d = ref.[13], the evaluated curve is from ref.[8]).

Large discrepancies appear at the 3.05 MeV interference dip due to differences in the resolution and energy calibration precision. Our adopted values were based on the data of KFK [9] and ORNL [13]. The results of Foster and Glasgow [22] present a significant shift to lower energies and those from Fossan et al.[23] are subtantially shifted to higher energies. Above 3.05 MeV up to 4.8 MeV no other fine structure is expected and only some smooth variations such as the broad 3.58 MeV resonance and the 4.261 MeV one are encountered. The proposed values, obtained by smoothing the composite results of ref. [9,11,13] in the energy range 2.84-4.8 MeV are given with 2% accuracy.

Three recent sets of elastic scattering data are available from the University of Kentucky [24], from the University of Padoua[25] and from ANL [18]. They are higher accuracy repetitions of older ones from Meier et al.[26] and Wills et al.[27]. Average relative uncertainties of the measured differential cross sections vary from 5 to 7 %. The adopted values are then quoted with an accuracy of less than 5 %. The angle-integrated cross sections deviate from the recommended total cross sections by 3 to 5 %.

High resolution neutron scattering experiments are in progress at ORELA from 2 to 3.2 MeV but the data are not yet available.

From 4.8 to 15 MeV.

Between 4.8 and 8.5 MeV neutron energies as many as 12 resonances in ^{12}C are reached, some of them being good candidates for energy-scale standards. But, for our purposes, they make this energy range of limited value. In addition two exit channels are open by the inelastic scattering and the (n,α) reaction. The data from KFK [9], NBS [11], ORNL [13] and University of Wisconsin [23], which are in good agreement for the resonances energies have been considered. Between the sharp resonances the recommended total cross section values are very close to those of Heaton et al. [11] and the uncertainty is about 2%. The values at the resonances are taken from Perey et al. [13] and the accuracy is better than 4%.

Above 4.8 MeV and below 8.5 MeV, elastic angular distributions σ(θ) have been extensively measured mainly by Galati et al. [24] up to 7 MeV, by Perey et al. [28] from 4.5 to 8.7 MeV and by Velkley et al. [29] above 7.2 MeV. The data expressed in the center of mass system were fitted to a Legendre polynomial expansion using the least squares method. The coefficients are plotted versus energy in fig.5, they show large variations at the location of the various structures observed in the total cross section.

Fig.5. Recommended F_ℓ Legendre coefficients for elastic scattering below 15 MeV. The coefficients are defined by :

$$\frac{d\sigma}{d\Omega}(\theta) = \frac{\sigma_{int}}{4\pi} \sum_{\ell} (2\ell + 1)\, F_\ell\, P_\ell\, (\cos\theta_{CM}).$$

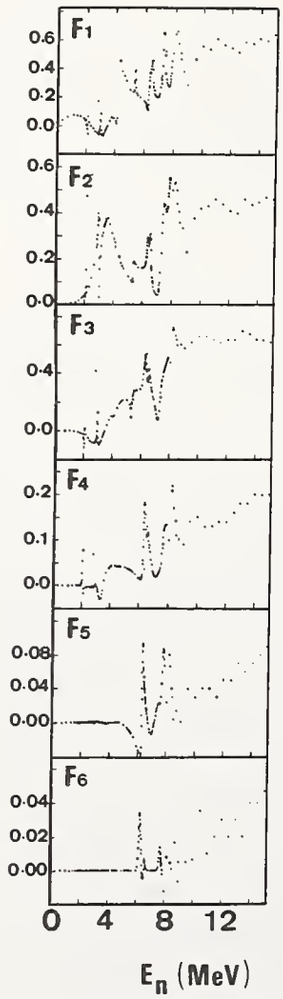

In the region extending from 8.5 to 15 MeV the resonances reached in the ^{13}C compound system become broader than in the lower energy range. Moreover they are generally overlapping so that the cross section variations with neutron energy are rather smooth. The data from KFK [9], NBS [11], ORNL [13], BNW [22] and from the University Of Wisconsin [23] are in satisfactory agreement. Nearly all of them lie in a band of total width approximately 8% of the average cross section. The recommended values are very close to those from ref. [13] and they are given with 4% accuracy.

In this energy range, differential elastic scattering cross sections are well known. Evaluated data have been mainly based upon the time of flight measurements performed at Bruyères-le-Châtel by Haouat et al. [30] between 8 to 14.5 MeV. Two independant sets of data were obtained in two measurements periods and they were found consistent with each other. The normalization used was the n-p scattering cross section near 0°. Glasgow et al. [31] have measured the elastic angular distributions between 9 and 15 MeV. Their data are in overall good agreement with those from ref. [30]. All these data compare favorably with the previous measurements below 9 MeV from Perey et al. [28] and Velkley et al. [29]. The integrated elastic cross sections are given with an accuracy varying from 6 to 8%. The adopted values are then taken within a global uncertainty of less than 7%. The comparison of these values with those from ENDF/B III and ENDF/B IV shows significant deviations by about 7 to 15%. The recommended values from the previous evaluations are too high at about 11.0 MeV and systematically low between 12 and 14.5 MeV.

The evaluated Legendre coefficients of the elastic angular distributions have been deduced with a reasonable accuracy due to the overall consistency of the available data. The degree of confidence in the evaluated data was increased when they were compared to the data of Bucher et al. [32] from forward angle elastic scattering measurements and those of Morgan et al. [33] from backward angle measurements made at ORELA.

Competing reactions

Reactions in ^{13}C

Now we have to consider the contribution of the 1.1% of ^{13}C present in natural carbon.

The existing data of Cohn et al. [34] from 0.112 to 22.8 MeV and those of Auchampaugh et al. [35] from 1.5 to 14 MeV show that the cross section of this isotope is very close to the corresponding one for ^{12}C except in the vicinity of the ^{14}C resonances observed at neutron energies of 0.153, 1.751, 2.432 and 2.454 MeV [17]. The first one at 153 keV has been observed in the total cross section measured by Heaton et al. [11] using natural carbon sample. This is mainly due to the large value of the total cross section (σ = 21 ± 2 b) and to the small width of the resonance (Γ = 3.7 ± 0.7 keV). This example shows clearly that good ^{13}C data, including differential elastic cross sections which have never been measured, are needed for a good knowledge of carbon data.

Radiative capture in carbon

The recommended values for the (n,γ) cross section for thermal neutrons are for the two isotopes of natural carbon :

^{12}C $\quad \sigma(n,\gamma)_{th} = 3.36 \pm 0.3$ mb

^{13}C $\quad \sigma(n,\gamma)_{th} = 0.9 \pm 0.2$ mb.

These recommended values taken from ref. [17] have been strongly influenced by the data of Jurney and Motz [36]. At low energy, i.e. $E_n < 100$ keV, the (n,γ) cross section has been assumed to vary with neutron energy according to the 1/v law.

The radiative capture is the inverse of the nuclear photo-effect ; by applying the reciprocity

theorem, the (n,γ) cross sections can be deduced from the (γ-n) data. The excitation function for the ^{13}C (γ, n) reaction has been measured by Cook [37]; using these data we have obtained the (n,γ) cross sections from 0.2 to 20 MeV [8]. The radiative capture cross section from thermal energy up to 20 MeV is very low and does not exceed 0.07% of the total cross section.

Theoretical analysis

In order to confirm the overall consistency of the evaluated values deduced from the review of all the available experimental data a theoretical analysis is required. Such an analysis would lead to accurate knowledge of the scattering phase shifts.

The phase-shift analysis of differential cross sections can be performed in a rather simple way since the ground-state spin of ^{12}C is 0^+ and then the channel spin has only the value $S = 1/2^+$. In this formalism, the center of mass differential cross section can be written as [38] :

$$\frac{d\sigma}{d\Omega}(\theta) = \lambda^2 \left(|f_c|^2 + |f_i|^2 \right)$$

where :

$$f_c = \sum_{\ell=0}^{\infty} P_\ell(\cos\theta)\left[(\ell+1)e^{i\delta\ell^+}\sin\delta\ell^+ + \ell e^{-i\delta\bar{\ell}}\sin\delta\bar{\ell}\right],$$

$$f_i = \sin\theta \sum_{\ell=0}^{\infty} P'_\ell(\cos\theta)\left[e^{i\delta\ell^+}\sin\delta\ell^+ - e^{i\delta\bar{\ell}}\sin\delta\bar{\ell}\right].$$

$\delta\ell^{\pm} = \delta(\ell, J = \ell \pm 1/2)$ is the phase-shift of the partial wave of total angular momentum $J = \ell \pm 1/2$. $P_\ell(\cos\theta)$ and $P'_\ell(\cos\theta)$ are the ℓ^{th} - order Legendre polynomial and its derivative, λ is the incident wave length.

For E below 4.8 MeV when only the elastic scattering channel is open, if the radiative capture process is supposed negligible, the phase shift can be expressed as the sum of two real quantities, the first one being the contribution from hard-sphere scattering, the second being due to scattering from compound - nucleus resonances. When nonelastic channels are open the phase shifts become complex quantities.

Phase-shift analyses have been carried out by several groups. Some sets of parameters were obtained by fitting a limited set of measured angular distribution data [26,27], and the others were obtained by simultaneously fitting the total cross section, the differential elastic scattering cross sections and polarization data [18, 24, 25, 39, 40] over a large energy range. In addition to direct fits, R-matrix calculations and coupled channel calculations were used to derive the phase shifts.

R-matrix calculations.

In the low energy part below 4.8 MeV, extensive R-matrix calculations have been performed at Ohio University [39], at Yale University [41] and ANL [18], and at University of Padoua [25]. Some other calculations are in progress at LASL and at ORNL. In this energy range, the application of R-matrix theory is relatively easy since the R-matrix reduces to a R function. This function has an explicit energy dependence given by :

$$R_{\ell J} = \sum_{\lambda} \frac{\gamma^2_{\lambda \ell J}}{E_{\lambda \ell J} - E} + R^{\infty}_{\ell J}.$$

$\gamma^2_{\lambda \ell J}$ is the reduced width and $E_{\lambda \ell J}$ is the level energy. The sum over λ denotes the number of levels which are explicity considered, while $R^{\infty}_{\ell J}$ is the contribution to the R-function from distant levels. This last contribution has been treated either as a constant [39] ($R^{\infty}_{\ell J} = R^{\ell J}_{o}$) or expanded as follows [18 41]:

$$R^{\infty}_{\ell J} = R^{\ell J}_{o} + R^{\ell J}_{1} \cdot E.$$

All the levels in ^{13}C up to an excitation energy of about 10 MeV except the ones at 0 and at 7.545 MeV have been considered in the various analyses. The scattering in carbon below 2-MeV neutron energy, is strongly influenced by the -1.86-MeV, $1/2^+$, state. Two other bound states have been included specifically : the -1.09-MeV, $5/2^+$, state in the calculation of ref. [39] and the -1.27-MeV, $3/2^-$, state in the calculations of ref. [41] and [18]. The two strongly interfering $3/2^+$ states at 2.95 and 3.58 MeV influence both the cross sections and polarizations.

The R-function is defined from the boundary condition for the radial part of the wave function $u_\ell(r)$ at the channel radius a :

$$\left(\frac{1}{u_\ell}\frac{du_\ell}{dr}\right)_{r=a} = (1 + B_{\ell J}) / R_{\ell J}.$$

The $B_{\ell J}$ quantity is the boundary condition factor chosen to cancel the level shift factor at the resonance energy.

In the different analyses, two distinct values were adopted for the channel radius a. Holt et al. [41] have taken a equal to the interaction radius which is 4.61 fm. Then they determined the reduced width of the $s_{1/2}$ bound state at - 1.86 MeV by fitting the expected cross section to the data below 2 MeV. They found $\gamma^2_{o\ 1/2} = 0.69$ MeV. The $p_{3/2}$ bound state reduced width was deduced from polarization data. On the other hand, Lane et al. [42] have assumed that low-energy data are dominated by the contribution from only the above mentioned $s_{1/2}$ bound state. The s-wave phase shift was obtained from the analysis of the data for σ(θ) below 0.8 MeV. The deduced parameters were a = 3.72 fm , $E_{o\ 1/2} = -6.0$ MeV, $\gamma^2_{o\ 1/2} = 4.0$ MeV. The last one is large and close to the single particle estimate which is 4.87 MeV [42]. In this analysis other fits also led to higher values of a as large as 4.9 fm.

The comparison of the adopted R-function parameters derived from these analyses is given in table 4. Although they are different, up to 3 MeV they give equally good fits to all the data.

The corresponding phase shifts are given by the relation :

$$\delta_{\ell J}(E) = -\phi_\ell + \arctan\left[P_\ell R_{\ell J} / \left(1 - (S_\ell - B_{\ell J}) R_{\ell J}\right)\right].$$

where ϕ_ℓ, P_ℓ and S_ℓ are hard-sphere phase shift, penetration factor and level-shift factor respectively. Such a description provides a simple tool for predicting neutron scattering data.

Phase-shift analysis up to 7 MeV.

Phase shift analysis of the elastic scattering data from 3 to 7 MeV has been carried out by Galati et al. [24]. The real part of the phase shifts was deduced at 32 energies. In the region of overlap they are in good agreement with those from ref. [41]. The data show large variations at the location of the resonances at 3.58 MeV ($d_{3/2}$), 4.26 MeV ($p_{1/2}$), 5.37 MeV ($p_{3/2}$), 6.29 MeV ($f_{7/2}$) and 6.56 MeV ($s_{1/2}$). The 2.95-MeV, resonance which interferes strongly with that at 3.58 MeV was not considered. In addition this analysis led to an ambiguous assigment for the exited state of ^{13}C at 9.52 MeV (4.936-MeV resonance). Above 4.8 MeV the phase shift is a complex quantity and the imaginary part γ^J_ℓ is needed. Except at few energies, these parameters could not be determined with a sufficient accuracy to show non-zero values.

This analysis was characterized by an excel-

lent agreement with the measured angular distributions (within the experimental uncertainties) and with the total cross section between 3 and 4.35 MeV and from 4.7 to 5.4 MeV. Also polarization were calculated from the derived phase shift and compared to the existing data. The predicted values agree fairly well with most of the polarization measurements below 4.2 MeV.

Coupled channel calculations at low energy (below 5 MeV)

The low-energy resonances in the nucleon $-^{12}C$ interaction can be interpreted as single-particle states and doorway states originated from the coupling between the incoming nucleon and the low-lying target levels. Calculations have been made in the frame of a phenomenological collective description of the target. Coupled channel calculations using a deformed shell model for the ^{12}C nucleus were performed by Reynolds et al. [40,1] and Leung and Koshel [43]. Emphasis was placed by the former on calculations of neutrons cross sections. The method used there and the results were presented at the Argonne Symposium on Neutron Standards and Flux Normalization and thus they will be mentioned just for completeness.

From their coupled-channel calculations Reynolds et al. [40] were able, with suitable potential wells, to account for all the observed resonances below 5 MeV except for the 2.82 MeV one. The measured total cross section was well represented at all energies between 0 and 5 MeV. Also the calculated differential elastic cross sections agreed quite well with the data throughout the entire energy region. Finally, the agreement between calculated polarizations and the data was good up to 4.2 MeV but above this energy large discrepancies appeared.

Coupled-channel calculations at high energy (above 8.5 MeV)

At neutron energies above 8.5 MeV, coupled-channel calculations can be used to predict elastic and inelastic angular distributions. In this energy range the nuclear structure effects may be assumed to be sufficiently averaged and thus described conveniently within the framework of the optical model. Several attempts have been made to find a set of monotonically energy-dependent potential parameters that would describe at least the overall features of neutron-carbon elastic cross sections above 8.5 MeV. Differential cross sections from ref. 30 and 45 have been analysed in 1 MeV steps by Delaroche [44]. The potential parameters deduced from this analysis are given in table 5 and compared to those obtained at Duke University [45]. The potential parameters are similar to those found to describe the nucleon scattering from heavier nuclei with one exception : the small diffusenesses. Such small values were also used by Reynolds et al.[40] at low energy. Further improvements could be made by adding Breit-Wigner resonance amplitudes to the optical-model scattering amplitude.

TABLE 4

R - function parameters

Levels in ^{13}C				ANL[18] a = 4.61 fm					OH10[39] a = 3.72 fm			
l_J	E_{ex} keV	E_{lab} keV	E_{cm} keV	E_λ keV	γ_λ^2 keV	B_{lJ}	R_o	R_l (MeV^{-l})	E_λ keV	γ_λ^2 keV	B_{lJ}	R_o
s 1/2	3086	-	- 1861	- 1860	690	0	0.40 (0)	0	- 1860	4000	- 1.035	0.075
p 1/2	0	-	- 4947	-	-	-	-	-	-	-	-	-
	8879	4261	3932	4200	700	- 0.2	0.16	0.02	3911	83.4	- 0.293	0.1
p 3/2	3680	-	- 1270	- 1270	500	- 0.18	0.34	0.055	-	-	-	-
	9503	4936	4556	-	-	-	-	-	4560	2	- 0.247	0.25
	9900	5367	4954	-	-	-	-	-	4940	10.3	- 0.247	0.25
d 3/2	7665	2946	2718	2920	170	- 1.00	0.15	0.02	2734	212	- 1.368	0.107
	8250	3580	3300	3500	870	- 1.00	0.15	0.02	3537	2500	- 1.368	0.107
d 5/2	3854	-	- 1093	-	-	-	-	-	- 1093	1800	- 2.213	0.0
	6863	2077	1915	2076	14	- 1.30	0.05	0.0	1959	75	- 2.213	0.0
f 5/2	7545	2816	2598	-	-	-	-	-	-	-	-	-

TABLE 5

Potential parameters used in coupled channel calculations above 8.5 MeV.

Ref	Real Part			Imaginary part			Spin Orbit part			Deformation Parameter
	R_R	a_R	V_R	R_I	a_I	V_I	R_{so}	a_{so}	V_{so}	β_2
44	1.25	0.40	51.50 - 0.3 E	1.25	0.30	0.74 + 0.38 (E - 8.5)	1.25	0.40	5.0	- 0.60
45	1.25	0.35	58 - 0.9 E	1.25	0.20	0.28 E	1.25	0.35	5.0	- 0.64

R and a are in fm, V and E are in MeV.

Conclusion

In conclusion, it appears that accurate neutron data for carbon can be obtained from comparison of several experimental values. The best accuracy is attained below the threshold of the inelastic scattering for ^{12}C except at the location of resonances which are of little interest for our purposes. For the total cross section the uncertainties vary from 0.5% below 1 keV up to 2% at 4.8 MeV. A large number of elastic scattering data have been reported and the recommended values which are derived are given with 7% accuracy. This accuracy could be improved by considering the last data from ANL in 1.8 MeV region. Accurate polarization data also cover the whole energy range.

The consistency of all the data below 5 MeV has been confirmed by theoretical analyses based on R-matrix calculations or coupled channel calculations. It has been shown that very accurate phase shifts have been derived by fitting simultaneously the total, differential, and polarization cross sections. The reason is that the total cross section gives rather weak constraints on the parameters while differential elastic cross sections and polarization data are sensitive to small phase shifts in addition to the dominant ones because of interference effects.

A source of difficulty for the coupled-channel calculations in predicting the observed neutron polarization from neutron elastic scattering occurs above 4.4 MeV. Good agreement with measured polarization is found from R-matrix calculations throughout the entire region and hence these calculations are prefered for neutron cross section prediction. Values of σ_t predicted by the R-function calculations performed concurrently in two laboratories agree with the recommended values to within less than 2 %. An overall agreement, within the experimental uncertainties, is obtained for elastic angular distributions by using mainly the ANL parameters.

We may definitely conclude that carbon elastic data below 5 MeV can be adopted as a standard. Evaluated data could be achieved by a R-matrix analysis including all the observed resonances. It is likely that no precision improvements could be attained by further measurements on ^{12}C. As a consequence, the analyzing power of ^{12}C is proposed as a calibration standard for neutron polarization studies which is technically more convenient to use than ^{4}He.

The discussion of carbon data above 8.5 MeV is warranted by the need for high energy neutron standards. If the accuracies are not as good as at lower energy, the overall consistency of the data which could be confirmed by further theoretical analyses would suggest that the present lack of adequate neutron standards in this energy range can be fulfilled by carbon data.

Acknowledgements

The author is very grateful to A. Michaudon and S. Cierjacks for their encouragements. He is very indebted to G. Haouat and M. Cates who contributed to the preparation of this work. He acknowledges J.P. Delaroche for providing results in advance of publication.

References

1. N.C. Francis, C.R. Lubitz, J.T. Reynolds, C.J. Slavik and R.G. Stieglitz, Proc. of Neutr. Standards and Flux Normalization Argonne Nat. Lab. (Oct. 1970) AEC Symp. Series 23 p. 166.

2. E. Rae, Proc. of Neutr. Standards and Flux Normalization - Argonne Nat. Lab. (Oct. 1970), AEC Symp. Series 23 p. 505.

3. A.B. Smith, Report of the NEANDC Subcommittee on Standards and discrepancies INDC 24/G (1977) p.12.

4. H. Liskien, Proc. of the Intern. Conf. on the interactions of Neutrons with nuclei, Lowell (March 1976). Conf. 760 715 P2 p. 1110.

5. J.D. Brandenberger, Associated gamma-ray techniques. This Conference.

6. G.D. James, Neutron Energy Standards. This Conference.

7. A.H. Wapstra and N.B. Grove , Nucl. Data Tables 9 (1971) 267.

8. J. Lachkar, F. Coçu, G. Haouat, P. Le Floch, Y. Patin and J. Sigaud, NEANDC(E) 168 "L", INDC (FR) 7/L (Nov. 1975).

9. S. Cierjacks, P. Forti, D. Kopsch, L. Kropp, J. Nebe and H. Unseld, EANDC (E) "U" (1968) - KFK 1000.

10. J.C. Clements et al. USAEC Report RPI 328.200 (1970) 24 Reusselaer Polytechnic Institute.

11. H.T. Heaton, II, J.L. Menke, R.A. Schrack and R.B. Schwartz Nucl. Sci. and Eng. 56 (1975) 27.

12. C.A. Uttley and K.M. Diment, Proc. of Neutr. Standards and Flux Normalization. Argonne Nat. Lab. (Oct. 1970) AEC Symp. Series 23 p.201.

13. F.G. Perey, T.A. Love and W.E. Kinney, Report ORNL 4823 (ENDF 178) 1972.

14. J.W. Meadows and J.F. Whalen, Nucl. Sci. and Eng. 41 (1970) 351.

15. B.R. Leonard Jr. Evaluation of the Standard Carbon cross sections and ENDF/BII. (Sept. 1970) (unpublished).

16. J.S. Story - Nuclear data for Reactors - Proc. Conf. Helsinki - IAEA - CN - 26/110 (1970) 721.

17. S.F. Mughabghab and D.I. Garber - B.N.L. 325 3° ed. Vol. 1 EANDC (US) 183/L - INDC (USA) 58/L (1973).

18. R.J. Holt, A.B. Smith and J.F. Whalen, Proc. Conf. on Nuclear cross sections and Technology NBS SP 425 Vol. 1 (1975) 246.

19. F.G. Perey and C.Y. Fu : ENDF/BIV - Mat 1274 (1974),

20. C.K. Bockelman, D.W. Miller, R.K. Adair and N.H Barschall, Phys. Rev. 84 (1951) 69.

21. F. Ajzenberg-Selove, Nucl. Phys. A152 (1970) 1.

22. D. Foster and D.W. Glasgow Phys. Rev. C3 (1971) 576.

23. D.B. Fossan, R.L. Walter, W.E. Wilson and N.H. Barschall, Phys. Rev. 123 (1961) 209.

24. W. Galati, J.D. Brandenberger and J.L. Weil, Phys. Rev. C5 (1972) 1508.

25. U. Fasoli, A. Metellini, D. Toniolo and G. Zago, Nucl. Phys. A205 (1973) 305.

26. R. Meier, P. Scherrer and G. Trumpy, Helv. Phys. Acta 27 (1954) 577.

27. J. Wills, J. Blair, H. Colin and H. Willard, Phys. Rev. 109 (1958) 891.

28. F.G. Perey and W.E. Kinney, Report ORNL-4441 (1969).

29. D.E. Velkley, J.D. Brandenberger, D.W. Glasgow, M.T. Mc Ellistrem, J.C. Manthuruthil and C.P. Poirier, Phys. Rev. C7 (1973) 1736.

30. G. Haouat, J. Lachkar, J. Sigaud, Y. Patin and F. Coçu, CEA Report R.4641 (1975).

31. D.W. Glasgow et al. Nucl. Sci. and Eng. 61 (1976) 521.

32. W.P. Bucher, CE. Hollandworth, A. Niiler, D. Mc Natt and J.E. Youngblood - B.R.L. Report R 1652 (1973).

33. G.L. Morgan, T.A. Love and F.G. Perey, Nucl. Inst. Meth. 128 (1975) 125.

34. H.O. Cohn, J.K. Bair and H.B. Willard Phys. Rev. 122 (1961) 534.

35. G.F. Auchampaugh, S. Plattard, R. Extermann and G.E. Ragan III. Proc. of the Intern. Conf. on the Interactions of Neutrons with Nuclei Lowell Conf. 760 715.P2 (1976) 1389.

36. E.T. Jurney and H.T. Motz Report ANL 6797 (1963) 236.

37. B.C. Cook, Phys. Rev. 106 (1975) 300.

38. A.M. Lane and R.G. Thomas, Rev. Mod. Phys. 30 (1958) 257.

39. H.D. Knox, J.M. Cox, R.W. Finlay and R.O. Lane, Nucl. Phys. A217 (1973) 611.

40. J.T. Reynolds, C.J. Slavik, C.R. Lubitz and N.C. Francis, Phys. Rev. 176 (1968) 1213.

41. R.J. Holt, F.W.K. Firk, R. Nath and H.L. Schultz, Nucl. Phys. A213 (1973) 147.

42. R.O. Lane, R.D. Koshel and J.E. Monahan, Phys. Rev. 188 (1969) 1618.

43. T.T. Leung and R.D. Koshel, Ann. of Phys. 75 (1973) 132.

44. J.P. Delaroche (to be published).

45. F.O. Purser et al. BNL - NCS 21501 (1976) 274.

46. K. Nishimura, S. Igarasi, T. Fuketa and S. Tanaka, JAERI 1218 (1971).

47. R.O. Lane, A.S. Langsdorf Jr, J.E. Monahan and A.J. Elwyn, Ann. of Phys. 12 (1961) 135.

48. N. Ahmed, M. Coppola and H.H. Knitter, Proc. of Neutr. Standards and Flux Normalization. Argonne Nat. Lab. (Oct. 1970) AEC Symp. Series 23 p. 208.

NEED FOR IMPROVED STANDARDS IN NEUTRON PERSONNEL DOSIMETRY*

John A. Auxier
Health Physics Division
Oak Ridge National Laboratory
Oak Ridge, TN 37830

There is a continuing need for standards in neutron monitoring. A discussion of special problem areas and the benefits of intercomparisons is given. The RBE for leukemia induction in the survivors of the nuclear bombings of Hiroshima and Nagasaki is greater than ten for absorbed doses in the bone marrow of less than 100 rads; this may have an important impact on neutron standards preparation.

(Standards; criteria, performance; dose equivalent; neutrons, low energy; neutrons, high energy; non-uniform exposures; elements, transuranic; quality factor; glove box; intercomparison; criteria, accuracy)

More than a quarter century has elapsed since quantitative measurements of absorbed dose became feasible, at least on a laboratory scale.[1,2] Several steps have been taken to establish the bases for standards on an international level, including meetings and documents sponsored by the International Commission on Radiological Protection, the International Commission on Radiological Units and Measurements, the World Health Organization, and the International Atomic Energy Agency. Also, there is an approved standard entitled "Personnel Neutron Dosimeters (neutron energies less than 20 MeV," by the American National Standards Institute.[3] This standard gives performance criteria, use factors, and dosimetry system calibration criteria for neutron dosimetry systems. However, accuracy criteria are not included.

Clearly, there remains a definite need for attainable standards for minimum accuracy in the determination of neutron energy fluence or dose equivalent. In addition to standards requirements, we must remember that there are a number of problems for which there is still no technologically suitable answer. Fortunately, the number of persons to be monitored for neutron exposure in most installations is small, and special effort may sometimes make possible a dose determination that is not feasible with simple monitoring devices.

There are several categories of neutron monitoring, each with special technological problems to be solved, which must be considered in standards preparation. These include low energy neutrons (thermal to about 0.5 MeV), high energy neutrons (greater than 20 MeV), and highly non-uniform exposures (such as those from transuranic elements to be handled in glove boxes). Each of these has associated difficulties in both measurement and calibration; though fast-neutrons in the range of 0.5 MeV< E<20 MeV cannot always be measured accurately, there are fewer instrumental and calibration problems than in the other categories.

Further, there are three generic aspects of the dosimetry problem of consequence in all the above categories and which are independent of the instrumentation used: (1) recent heightened concern over the appropriate quality factor for neutrons, (2) calibration of instruments as a function of energy, and (3) expertise and care in the use of instruments and interpretation of results.

Technological problems are most apparent in the energy range below 0.5 MeV. Because of the rapid variation of neutron non-elastic cross sections and the low recoil energies resulting from elastic reactions, no satisfactory solution to measurement problems, especially for personnel monitoring, is apparent.

For neutron energies greater than 20 MeV, the problems depend on the range under study, e.g., 20 MeV < E < 50 MeV, 50 MeV < E < 300 MeV, etc. However, by a combination of various track detectors, activation/spallation detectors, ionization chambers, and calculation, the health physicist can generally assess the dose with confidence that protection is assured without a huge penalty in conservatism.

Highly non-uniform fields frequently present a combination of problems, including those associated with low energy neutrons, coexistent soft x-rays, the need for small detectors for hands and forearms such that glove box work can be performed, etc.

More research and development is needed in each of these categories, but no federal agency has accepted the responsibility for solving them. Many who should be concerned believe that the problems of dosimetry have been resolved adequately. This does not appear to be entirely prudent in today's trend toward "super-safety" in all things.

Let us now examine the more generic aspects of neutron monitoring. Recent work by Jones[4] has indicated that if one considers the energy absorbed in bone for the survivors of the nuclear bombings of Hiroshima and Nagasaki, the leukemia induction RBE of neutrons approaches 30 for low dose levels. For many years, depth dose distributions have been reported which indicate that neutrons in the fission range are attenuated in tissue more rapidly than gamma rays from the fission process or gammas produced by neutron interactions in air. These different attenuation rates become even more important in the case of the Japanese leukemia data, because RBE is markedly dose dependent. This dose dependence stems from the fact that risk from the gamma component appears to be quadratic with dose while risk from the high LET recoil ion component seems to vary linearly with dose. In no case, involving people or large animals, is there evidence that QF should be greater than 10 for neutron dose measured either in air or on the surface of the body, so applied health physicists

*Research sponsored by the Energy Research and Development Administration under contract with Union Carbide Corporation.

prefer to use QF=10 for protection purposes. In any event, the magnitude of RBE or renormalization of risk to remove the quadratic behavior of the denominator should be a decision of standards setting groups.

The omission of accuracy criteria in the ANSI N319 standard is primarily because of the lack of a simple neutron dosimeter which responds accurately over the range of energies which may be encountered at a given facility. For example, if simple track counting in nuclear emulsions is used as the basis of dosimetry, then for any given number of grains used to identify a track, the average dose per track is dependent on neutron energy. Consequently, if a Pu-Be or Pu-B source is used in calibration and the wearer of the dosimeter is exposed to neutrons of energy less than 1 MeV, the accuracy can be very poor. In some cases the measured dose may be an order of magnitude too low.[5] Professional health physicists would, of course, recognize the circumstances and make corrections; but the accuracy is seldom as good as for gamma ray measurements, all other parameters constant. Calibration is an important aspect of neutron monitoring and one which has an important bearing on standards setting.

Finally, the generic aspect of competence and care must rank high in considerations of standards. Without a basic understanding of the physical mechanisms of a detector and its associated apparatus, results are apt to be unsatisfactory. In addition, some experience under field conditions is certainly desirable and probably essential. It is under field conditions that all generic aspects must be handled properly, and testing in the field can provide the impetus to improve the results of a monitoring program.

One series of field tests that demonstrates the wide variability of results and the capability to improve systems as a result of testing is the ORNL Health Physics Division's Nuclear Accident Intercomparison series which has included at least one major workshop per year for nearly 15 years. Tables 1, 2, and 3 show typical results of these studies; most of these participants, usually about ten institutions are represented, took part in each of the sessions shown here. Similar results were obtained for other groups, i.e., range of reported results was nearly always wide for first-time participants but improved with experience. These are all high exposures of nuclear accident systems. More recent studies of routine monitoring systems show similar trends though there are insufficient data as yet to ascertain the ultimate improvements to be expected in performance. Table 4 shows clearly that uncertainties of up to a factor of two must be expected under first test conditions. For routine monitoring conditions, especially where detector response may fade or otherwise change during long periods of use, uncertainties could be much greater. It is disturbing that the gamma ray dosimetry was subject also to such wide variation. Table 5 shows marked improvement by the same group of dosimetrists for the second intercomparison of personnel dosimetry systems. Although the gamma ray measurements were made in a coexistent neutron field, the percentile error is much greater than for the neutrons under these test conditions.

Because of the success of the national and international intercomparisons of nuclear accident systems initiated at ORNL, the IAEA began sponsoring a series of intercomparisons of a similar nature. Table 6 lists studies which have been conducted to date.

It is apparent that standards for neutron monitoring are needed and, in my opinion, accuracy criteria are needed as well. However, accuracy criteria would be of little value without some test and evaluation procedures pertinent to field applications. It appears that an important aspect of tests or intercomparisons is that of training; using a routine monitoring system without such tests is analogous to solving problems in textbooks without knowledge of whether the answers are correct. At present, accuracy criteria would have to be quite loose in order to be met by most monitoring groups for the most simple applications.

References

1. G. S. Hurst, R. H. Ritchie and H. N. Wilson, Rev. Sci. Inst. 22:981 (1951).

2. G. S. Hurst, J. Radiol. 27:353 (1954).

3. Personnel Neutron Dosimeters (neutron energies less than 20 MeV), American National Standards Institute.

4. T. D. Jones, A CHORD Simulation for Insult Assessment to the Red Bone Marrow, ORNL-5191 (1976).

5. Richard L. Lehman, Energy Response and Physical Properties of NTA Personnel Neutron Dosimeter Nuclear Track Film, UCRL-9513 (1961).

TABLE 1

INTERCOMPARISON OF AREA DOSIMETERS
IN SIMULATED NUCLEAR ACCIDENTS
HPRR UNSHIELDED

DATE	CALCULATED* NEUTRON DOSE (rad)	AVERAGE NEUTRON† DOSE REPORTED (rad)	RANGE OF DOSE REPORTED (rad)
MARCH 1965	324	377 ± 65	300 – 468
JULY 1970	319	310 ± 16	287 – 335
AUGUST 1973	343	338 ± 25	310 – 386
JULY 1974	388	362 ± 40††	308 – 430

*Based on Absolute Proportional Counter

†One Standard Deviation

††Included Several First-Time Participants

TABLE 2

INTERCOMPARISON OF AREA DOSIMETERS
IN SIMULATED NUCLEAR ACCIDENTS
HPRR — LUCITE MODERATOR

DATE	CALCULATED* NEUTRON DOSE (rad)	AVERAGE NEUTRON† DOSE REPORTED (rad)	RANGE OF DOSE REPORTED (rad)
DECEMBER 1967	26	29 ± 9	18 – 48
JULY 1970	37	42 ± 7	31 – 52
AUGUST 1973	51	56 ± 10	44 – 100
JULY 1974	51	60 ± 11	56 – 77

*Based on Absolute Proportional Counter

†One Standard Deviation

TABLE 3

INTERCOMPARISON OF AREA DOSIMETERS
IN SIMULATED NUCLEAR ACCIDENTS
HPRR — 13-cm STEEL MODERATOR

DATE	CALCULATED* NEUTRON DOSE (rad)	AVERAGE NEUTRON† DOSE REPORTED (rad)	RANGE OF DOSE REPORTED (rad)
MAY 1967	105	109 ± 36	30 – 154
JULY 1970	104	106 ± 15	73 – 134
AUGUST 1973	138	135 ± 30	105 – 180
JULY 1974	144	133 ± 45	60 – 175

*Based on Absolute Proportional Counter

†One Standard Deviation

TABLE 4

PERSONNEL DOSIMETER INTERCOMPARISON
DOSAR FACILITY — MAY 1974

EXPOSURE CONDITION	NEUTRON DOSE EQUIVALENT (mrem)	GAMMA DOSE EQUIVALENT (mrem)
UNSHIELDED	453 ± 213	24.6 ± 5.9
STEEL-SHIELDED	554 ± 346	18.1 ± 4.3
LUCITE-SHIELDED	675 ± 687	75.1 ± 14.2
14-MEV NEUTRONS	587 ± 501	384 ± 151

TABLE 5

PERSONNEL DOSIMETER INTERCOMPARISON
DOSAR FACILITY — FEBRUARY 1976

EXPOSURE CONDITION	NEUTRON DOSE EQUIVALENT (mrem)	GAMMA DOSE EQUIVALENT (mrem)
UNSHIELDED	550 ± 217	35 ± 29
STEEL-SHIELDED	753 ± 226	31 ± 30
LUCITE-SHIELDED	532 ± 154	86 ± 46

TABLE 6

IAEA-SPONSORED DOSIMETRY INTERCOMPARISON STUDIES

DATE	COUNTRY	TYPE RADIATION FIELDS USED
JUNE 1970	FRANCE	^{235}U SOLUTION IN CYLINDRICAL TANK – BARE ^{235}U SOLUTION SHIELDED WITH CONCRETE
MAY 1971	USA	HPRR UNSHIELDED REACTOR HPRR REACTOR SHIELDED WITH STEEL HPRR REACTOR SHIELDED WITH LUCITE
MAY 1973	YUGOSLAVIA	RB–REACTOR
APRIL 1975	ENGLAND	VIPER REACTOR

STANDARDS IN MEDICAL NEUTRON DOSIMETRY

J.J. Broerse
Radiobiological Institute TNO,
Rijswijk, The Netherlands

Clinical and radiobiological experience has shown that differences in absorbed dose of less than 10 percent can be recognized for tumour eradication probability as well as for normal tissue damage. These observations determine the degree of precision and overall accuracy required in medical neutron dosimetry. Standard neutron fields are available only for restricted conditions; the feasibility of a number of detectors as standard dosimeters will be considered. Uncertainties in basic physical parameters will be discussed and recommendations for future research in neutron dosimetry for biology and medicine will be included.

(Standards, medical, neutron dosimetry, mixed n-γ fields, basic physical data)

Introduction

To estimate the risk of mixed n-γ radiation fields and to predict the responses of irradiated biological systems, it will be essential to obtain a quantitative description of the radiation field or of the energy deposition processes. For purposes of radiation protection, a rough characterization of the radiation field in terms of type, energy, direction and number of particles is in most cases sufficient. For medical and biological applications generally the absorbed dose and the radiation quality have to be determined. The absorbed dose is defined[1] as the quotient of the mean energy imparted by ionizing radiation to the matter in a volume element and the mass of the matter in that volume element (the special unit of absorbed dose is the rad and the SI unit is the gray, 1 Gy = 1 Jkg^{-1} = 100 rad). The radiation quality can be related to the neutron energy spectrum, lineal energy (y) spectra or the linear energy transfer (LET) spectrum and is an essential concept in view of the dependence of the relative biological effectiveness (RBE) on these interrelated parameters.

Changes in the quality of initially monoenergetic neutrons by scattering processes can modify the biological effects to a considerable extent. This has been illustrated by studies on the survival of colony forming units (CFU) in mouse spleen after irradiation with d+T neutrons in two different experimental arrangements; in free air and inside a steel collimator[2]. The survival curves presented in fig. 1 show a considerable difference in the radiation response of bone marrow stem cells, resulting in a difference of 25 percent in the RBE for CFU survival. For the irradiations in the steel collimator 20 percent of the neutron absorbed dose was delivered by scattered neutrons of lower energy. The contribution of these low energy neutrons increases the RBE according to the general tendency as observed for effects on various biological systems. Even larger differences in RBE values have been demonstrated for mortality studies in mice after fission neutron irradiations at two installations where the fission spectra were produced by exposing converter plates with thermal neutrons[3]. These biological results clearly indicate the need for quality specification; at present quality can most unambiguously be characterized in terms of the neutron energy spectrum.

The selection of methods for neutron dosimetry and the precision (i.e. the reproducibility) and accuracy to be achieved will depend on the object irradiated and on the endpoint observed[4]. In studies of effects of fast neutrons on mammalian systems, doses will range from 100 to 1000 rad (1 to 10 Gy); in fast neutron radiotherapy the neutron dose will be administered in fractions e.g. in daily fractions of 100 rad (1 Gy) at a dose rate of approximately 10 rad/min (0.1 Gy/min). In radiotherapy applications, differences of 10 percent in absorbed dose have shown significant differences in local control of tumours[5] and in the incidence of late radiation sequelae, e.g. fibrosis[6]. For radiobiological studies, maximum variations over the biological object should be restricted to a ratio of 1.10 and preferably 1.06, in order to avoid significant changes in biological responses over the object[7]. Based on these considerations, it is now generally recognized that, for biological and medical applications, the dose in the biological object should be determined with a precision of at least 2 percent and an overall uncertainty of not more than 5-6 percent. Some authors are even more stringent and aim for an overall uncertainty of less than 2 percent in the statement of the absolute total absorbed dose[8]. It must be stressed that the above mentioned requirements are more severe than generally encountered in radiation protection, where the dose effect relations for radiation-induced late effects are not yet well known. Although, higher accuracy and

Fig. 1. Survival curves for bone marrow stem cells after irradiation with d+T neutrons in two different experimental arrangements[2].

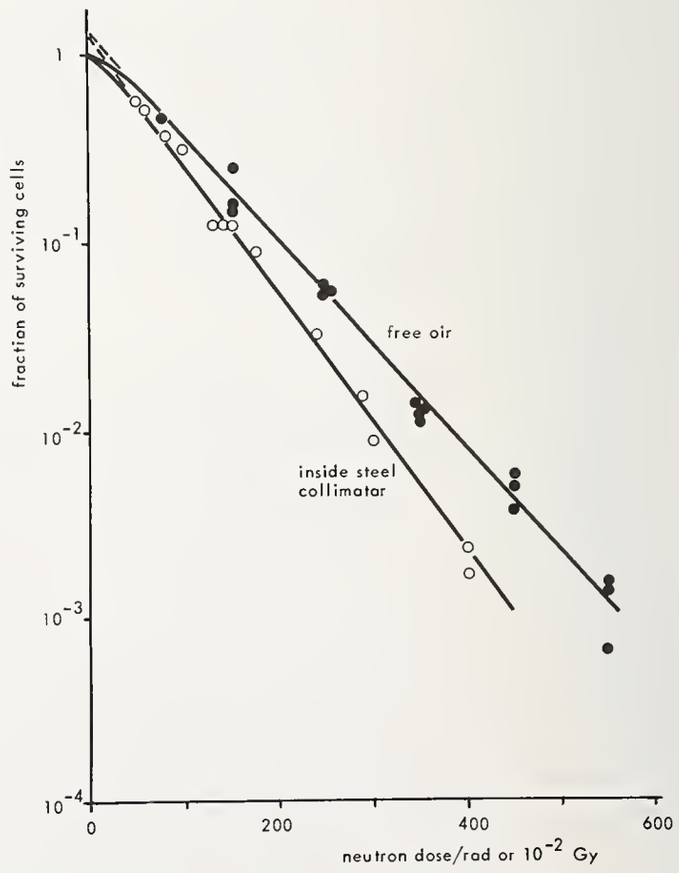

precision in dosimetry are required for the medical applications, the doses and dose rates under these conditions are higher than in the protection situation, which facilitates the measuring techniques.

In the present contribution the principles of dosimetry in mixed fields will be discussed. The absorbed dose, D, can generally be derived from the response, R, of the dosimeter:

$$D = \alpha R \qquad (1)$$

where α is the response function of the instrument and the reciprocal of α is the sensitivity. The response function, α, can be calculated from known constants and measured parameters or can be determined by calibration in a standard neutron field or by comparison of the response of the instrument with that of a standard dosimeter. In the context of this presentation a neutron field is regarded as "standard" when the spatial and temporal distribution of absorbed dose rate for both neutrons and accompanying photons and the neutron and photon energy spectrum are known. A dosimeter is regarded as "standard" or "absolute" if it can be constructed and subsequently used to measure the absorbed dose without the necessity of calibrating its response in a known radiation field[9].

The different medical applications include fast neutron radiotherapy, capture therapy with thermal and epithermal neutrons, neutron radiography and in vivo neutron activation analysis. The availability of standard neutron fields for these different situations will be discussed and the usefulness of different instruments as standard dosimeters will be analyzed. The uncertainties in basic physical parameters to be employed for the conversion of instrument response to neutron and gamma absorbed dose will be discussed. Some common values will be recommended, however, future measurements of some basic parameters are highly necessary for improvement of internationally acceptable standards.

Principles of mixed-field dosimetry

Neutron fields are always accompanied by gamma rays originating from the neutron producing target, the shielding and other materials surrounding the target as well as from the biological object or phantom material irradiated. It is necessary to determine the neutron absorbed dose, D_N, as well as the gamma ray absorbed dose, D_G, at a certain position in a material of specified composition, because of the differences in relative biological effectiveness (RBE) of these two radiation components.

Generally, two instruments are used for the evaluation of the separate absorbed dose of neutrons and photons in a mixed field. One device (T) is usually constructed to have approximately the same sensitivity to neutrons and to photons, whereas the construction of the second instrument (U) results in a lower sensitivity to neutrons than to photons. For the same mixed field, the quotients of the responses of the dosimeters and their sensitivities to gamma rays used for calibration are given by:

$$R'_T = k_T D_N + h_T D_G \qquad (2)$$

$$R'_U = k_U D_N + h_U D_G \qquad (3)$$

where D_N and D_G are absorbed doses of neutrons and of photons in tissue in the mixed field; k_T and k_U are the sensitivities of each dosimeter to neutrons relative to its sensitivity to the gamma rays used for calibration and h_T and h_U are sensitivities of each dosimeter to the photons in the mixed field relative to its sensitivity to the gamma rays used for calibration.

Most detectors used in neutron dosimetry have approximately the same sensitivity to neutrons and photons, e.g. tissue equivalent (TE) ionization chambers and TE calorimeters. The response of one of the above mentioned detectors must be combined with that of a detector which is relatively insensitive to neutrons to determine D_N and D_G. It will be generally advantageous to reduce k_U to minimize overall uncertainties in the neutron and photon absorbed doses[1].

A common procedure in neutron dosimtery is the use of TE, CH or CH_2 ionization chambers, as the neutron sensitive device, in combination with nonhydrogenous ionization chambers (Al/Ar, Mg/Ar, C/CO_2) or GM counters. The principle of the use of ionization chambers in neutron dosimetry does not differ from their use in photon dosimetry. It can be shown that:

$$k_T = \frac{\bar{W}_c}{\bar{W}_N} \cdot \frac{(s_{w,g})_c}{(s_{w,g})_N} \cdot \frac{(K_t/K_m)_c}{(K_t/K_m)_N} \qquad (4)$$

$\bar{W}$ is the average energy expended to create an ion pair; $s_{w,g}$ is the ratio of the average mass stopping power of the wall relative to the gas and K_t/K_m is the ratio of the kerma in tissue to that in the dosimeter material[1]. The subscript c denotes values applicable to the calibration situation, for which gamma rays are commonly used. Although photon spectra in neutron fields are generally not known, h_T is usually taken to be equal to one. However, this is not necessarily always the case; calibration at more than one photon energy is indicated when there is a possible dependence of h_T and h_U on photon energy.

Availability of standard neutron fields

For specific medical applications such as in vivo activation analysis[10] and neutron capture therapy[11,12] it will be sufficient to perform the calibrations in a neutron field of known fluence. Standard neutron fluence fields are available for radioactive sources such as Am-Be, Sb-Be and Pu-Be, spontaneous fission sources such as ^{252}Cf and reactors[13]. Monoenergetic neutron beams with energies between 60 eV and 120 keV can be produced with sets of matched filters and scattering foils located in the beam tube of high flux reactors[14,15].

Accelerator neutron sources which can serve as primary standards for neutron fluence measurements involve nuclear interactions where a neutron is emitted in coincidence with a charged particle. The most important of these standard reactions are H(n,n)H, D(γ,n)H, D(d,n)^{3}He and T(d,n)^{4}He. In the first reaction, the fluence can be derived from the number of recoil protons counted and the scattering cross section σ (n,n). For the other reactions associated particle counting can be employed. Considering the reaction kinematics, the energy and direction of emission of the neutron can be derived from the measurement of the charged particle which is emitted in coincidence. In principle accelerator neutron sources can also be used as fluence standards by measuring the induced activities in materials with well-known reaction cross sections.

By definition dosimetry includes those measurements (or calculations) which secure information on the energy deposition processes and the resulting absorbed dose. For purposes of calibration and intercomparison of neutron dosimeters, standard neutron fields have to be established where the absorbed dose (or dose rate) is known with regard to its spatial and temporal distribution and the neutron energy spectrum. In fast neutron radiotherapy and radiobiology, the contribution of thermal and intermediate energy neutrons to the total dose is generally limited. This can be seen from table 1, where the kerma due to thermal and intermediate neutrons (neutrons with energies between the Cd cut-off

TABLE 1.

KERMA OF THERMAL AND INTERMEDIATE NEUTRONS RELATIVE TO TOTAL DOSE FOR A COLLIMATED 15 MeV NEUTRON BEAM

(SSD 45 cm, field size 6 cm x 8 cm)

depth in phantom (cm)	$\frac{K_{th}}{D_{total}}$ (percent)	$\frac{K_{int}}{D_{total}}$ (percent)
0.9	0.17	0.031
3.0	0.23	0.031
5.0	0.23	0.027
10.0	0.21	0.019
20.0	0.20	0.018
29.4	0.18	0.017

energy, 0.5 eV, and 10 keV) is given for a 15 MeV neutron beam[16].

The ^{252}Cf spontaneous fission source has been suggested as a standard for neutron dosimetry delivering soft tissue kerma rates per microgram of ^{252}Cf at 1 meter in free air of 0.199 mrad h^{-1} μg^{-1} (1.99 $\mu Gy\ h^{-1}$ μg^{-1}) and 0.108 mrad h^{-1} μg^{-1} (1.08 $\mu Gy\ h^{-1}$ μg^{-1}) for the neutrons and gamma-rays respectively[17]. In fig. 2 the absorbed dose rate factor is shown as a function of distance for a 1.5 cm active length ^{252}Cf source encapsulated by 0.7 mm Pt + 10 percent Ir[1]. It should be realized that the relative dose contributions from beta rays emitted by the ^{252}Cf equilibrium fission product mixtures can not be neglected near the source when the encapsulation thickness is less than about 0.5 mm Pt + 10 percent Ir. It can be seen from fig. 2 that in a tissue-equivalent phantom the relative contribution from gamma rays increases with increasing distance from the source. Provided that source encapsulation and scattering conditions are normalized, californium with a minimum source mass of 1 mg can be considered to be a reasonably good source for calibrating and checking the proper operation of the instruments to be used for mixed-field dosimetry.

Monoenergetic neutrons with energies ranging between a few tenths of a MeV and 20 MeV can be produced with accelerators by bombarding targets with beams of protons and deuterons (examples are the d+T, d+D and p+T reactions). A number of factors may influence the composition of the neutron field[1]. In case of deuteron bombardment, competing reactions can become important e.g. with carbon layers originating from organic vapors in the vacuum system and deposited on the target. For the d+T reaction, the target will become increasingly contaminated with deuterium, resulting in a low energy neutron component from the d+D interaction. Furthermore, gamma rays can result from fast neutron interactions with the target assembly. Extraneous deuterons striking this assembly or components of the beam transport system will also generate gamma rays and spurious neutrons. Target thickness determines the energy spread of the emitted neutrons and the neutron yield. During ion bombardment the target deteriorates which results in lower neutron yields for equal ion currents. These factors make it difficult to predict the spatial and temporal distribution of absorbed dose rate for both neutrons and accompanying photons and the neutron energy spectrum. The d+D reaction, using pressurized gaseous deuterium targets, should be considered for standardization purposes, in as much as the neutron yield is only dependent on the reaction cross section and the number of target atoms. A recent inventory[18] has shown that accelerator standard fields with well defined levels of absorbed dose are not yet available at the national standards laboratories, although at some institutions including NBS, NPL and PTB such facilities are in preparation.

In three instances (RARAF Brookhaven, GSF Neuherberg, and TNO Rijswijk) accelerator produced neutron fields have been employed for neutron dosimetry intercomparison projects (the International Neutron Dosimetry Intercomparison, INDI, sponsored by the ICRU and the European Neutron Dosimetry Intercomparison Project ENDIP, promoted by the Commission of the European Communities) and considerable effort has been devoted to the monitoring of the radiation field, to obtain a continuous indication of total absorbed dose, gamma-ray absorbed dose and radiation quality[19,20,21]. Analysis of the monitoring results indicates that the total absorbed dose can be delivered to the participants' dosimeters with a reproducibility within 2 percent. Larger variations (with a maximum of 20 percent) have been observed in the relative dose contribution of photons, which might be attributed to instabilities in the ion beam geometry. At one institute two disc type tissue equivalent transmission ionization chambers have been employed to monitor total absorbed dose; the use of this dual monitoring system has proved to be of great value for a continuous check on the reliability of the system[21]. It must be stressed that the radiation fields for INDI and ENDIP have been established only for purposes of intercomparison and not for calibration. Although the objective of these intercomparisons was to understand differences in dosimetry, much was learned about how to do an intercomparison and how to do calibrations in a reliable manner[22]. This will be of great value for the laboratories concerned and perhaps also for the standards laboratories if they have to offer calibrations in this field at some time in the future.

Standard neutron dosimeters

For photon dosimetry only three devices are generally accepted as being accurate enough to serve as

Fig. 2. Comparison of the attenuation in a tissue equivalent phantom for radiation from a 1.5 cm active length ^{252}Cf source (0.7 mm Pt + 10 percent Ir) with the attenuation in water for photons from ^{226}Ra (0.5 mm Pt + 10 percent Ir) and ^{192}Ir sources[1].

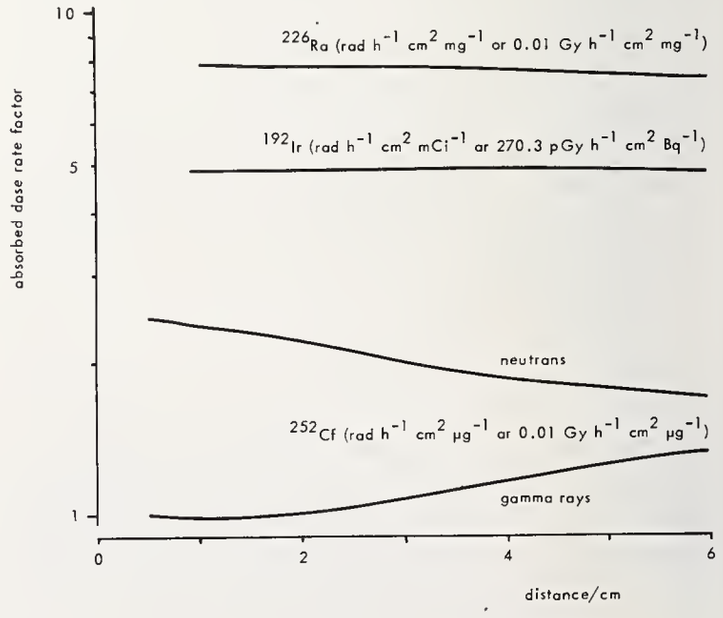

dosimetry standards: calorimeters, ionization chambers and Fricke chemical dosimeters[9]. It should be realized that for the latter two dosimeters, the response function in a neutron field will be different from that in the photon field used for calibration, because of differences in basic physical parameters determining instrument response for these two types of radiation. Consequently, it might be more appropriate to qualify ionization chambers and chemical dosimeters as secondary standards for neutron dosimetry.

The proportional counter lined with polyethylene and filled with ethylene as designed by Hurst[23] is still considered to be an absolute device for the measurement of neutron absorbed dose. However, measurements with proportional counters have to be performed at beam intensities which are considerably reduced with respect to the situation under which biological and clinical irradiations are performed[24]. These reduced beam intensities involve different operational conditions of the accelerator and consequently the radiation fields can show differences with regard to geometry and radiation quality, including the relative contribution of photons to the total absorbed dose.

The calorimeter is a fundamental instrument for measuring absorbed dose and in principle its response is independent of neutron energy[1]. The method is too insensitive and cumbersome for routine use; rather it should serve as a dosimetry standard for the calibration of secondary instruments. The calorimeter can only measure the total amount of heat produced and so determines the total absorbed dose due to neutrons plus accompanying photons. A separate measurement, usually of the gamma ray component, is needed to assess the separate absorbed doses. The choice of absorbing material is more critical for neutrons than for photons, ideally the material should have the same atomic composition as tissue. In addition the thermal defect, defined as that fraction of the energy absorbed from the beam which does not appear as heat, but is stored in the form of chemical changes or lattice defects, should be zero. The overall uncertainty in the determination of neutron absorbed dose can be estimated to be about 4.5 percent; the principal sources of uncertainty being the ratio of kerma in tissue to that in calorimeter material (3 percent), the thermal defect (2 percent) and the uniformity of absorbed dose in the calorimeter element (1 percent), whereas the random uncertainty can be taken as 1 percent.

With great care one can construct ionization chambers capable of measuring exposure with an uncertainty of about 1 percent. Ionometric determinations of the absorbed dose of photons using the Bragg-Gray principle will entail overall uncertainties of ± 2.3 percent which arise mainly from uncertainties in $\bar{W}$ (1 percent) and stopping power ratios (2 percent). The principle of the use of ionization chambers in neutron dosimetry does not differ from that in photon dosimetry. In order to make the ratio of kerma in the dosimeter material to that in soft tissue as close to one as possible, conducting tissue equivalent plastic, designated A-150, is often used for the construction of ionization chambers. As can be seen from table 2 the principal compromise in the formulation of A-150 is the substitution of carbon[25] for much of the oxygen required to match muscle tissue. An approximately homogeneous chamber can then be obtained by flushing the chamber with a mixture of gases with comparable composition (TE gas). Use of ionization chambers for the determination of the neutron absorbed dose involves a major systematic uncertainty since equation (4) must be evaluated to determine k_T. The systematic uncertainties in $\bar{W}$ ratio, stopping power ratio and neutron kerma ratio can be estimated to be equal to 5, 3 and 3 percent, respectively. Additional factors such as failure to meet Bragg-Gray conditions equally for photon and neutron irradiations (with a systematic uncertainty of 2 percent) result in an overall uncertainty of 7 percent for the determination of neutron absorbed dose with an ionization chamber[4].

TABLE 2.

ELEMENTAL COMPOSITION IN PERCENT BY WEIGHT OF A-150 MUSCLE EQUIVALENT PLASTIC COMPARED TO ICRU MUSCLE TISSUE

element	ICRU muscle	A-150 plastic
H	10.2	10.2 ± .1
C	12.3	76.8 ± .5
O	72.9	5.9 ± .2
N	3.5	3.6 ± .2
Ca	.007	1.8 ± .1
F	not listed	1.7 ± .1
total	98.9	100 ± .5

The ferrous sulfate (Fricke) dosimeter has been extensively studied using photons and electrons. Due to its good reproducibility, linearity of response and relatively small energy dependence, the system is suitable for photon, electron and neutron dosimetry. A disadvantage of the system is the rather low sensitivity requiring long irradiation times at sources having relatively low output e.g. 15 MeV neutron sources. Recent improvements in the optical density measurements have resulted in higher sensitivities of the Fricke system[26]. For fast neutrons, there are few determinations of G (the number of ferric ions produced by an energy dissipation of 100 eV). The G value for mixed neutron and gamma ray fields has a systematic uncertainty of 7 percent. If the low dose technique is used, the random uncertainties are between 2 and 3 percent, which implies that with, the Fricke dosimeter, an overall uncertainty of 8 percent can be attained for the determination of the total absorbed dose in mixed neutron and gamma ray fields[1].

Uncertainties in basic physical parameters

In order to compare the results obtained by various groups in performing dosimetry in mixed fields with systems generally encountered in neutron radiotherapy and neutron radiobiology, two international neutron dosimetry intercomparisons have been performed. The International Neutron Dosimetry Intercomparison (INDI) was conducted at Brookhaven National Laboratory in 1973, the analysis of the results is completed and will be published in the near future[27]. A European Neutron Dosimetry Intercomparison Project (ENDIP) was conducted in 1975 at two locations: the Institut für Strahlenschutz GSF, Neuherberg and the Radiobiological Institute TNO, Rijswijk. The analysis of the ENDIP results is near to completion, preliminary results of ENDIP can be found elsewhere[28].

The quantities to be measured in INDI and ENDIP were the neutron and gamma tissue kerma in free air for neutron beams of different energies and the neutron and gamma tissue dose at various depths in a water phantom. Analysis of the calculations of the participants showed that, for the same experimental conditions, the various groups employed divergent basic parameters characterizing the detector response, such as the ratio of kerma values in dosimeter material and tissue, the energy required to produce an ion pair in a gaseous detector and the neutron sensitivity of photon dosimeters.

a. Ratio of kerma in dosimeter material and soft tissue

A considerable number of participants in INDI and ENDIP employed tissue equivalent ionization chambers, thus a conversion from kerma in TE dosimeter material to kerma in soft tissue (ICRU muscle approximation) was necessary. The kerma conversion factors adopted by the participants in INDI and ENDIP are summarized in table 3. It can be seen that the values employed show differences of up to 8 percent for the same neutron energy. Information was available from two groups on the set of parameters employed for the evaluation of the INDI and the ENDIP results. Apparently, these groups had to change their parameters on the basis of additional experimental or theoretical information.

New kerma factors (products of mass energy transfer coefficient and neutron energy) have recently been calculated by Caswell[1], Coyne and Randolph for neutron energies up to 30 MeV. In the energy region below 20 MeV, overall uncertainties less than 2 percent and usually less than 1 percent have been estimated for hydrogen. For other elements, the estimated overall uncertainties would nearly always be less than 10 percent and usually less than 5 percent. Overall uncertainties in kerma factors for tissue and tissue like material may be estimated to be about 3 percent. For energies above 20 MeV kerma factors except for hydrogen, have a much higher uncertainty due to the lack of neutron cross section measurements in this energy region. Other groups have also performed kerma calculations[29,30] and it will be very useful to compare the different calculational procedures and to adopt one common set of kerma factors.

b. $\bar{W}$ values

Relatively large discrepancies are also observed in the ratio $\bar{W}_N/\bar{W}_G$ as employed by the participants in INDI and ENDIP for TE gas consisting of methane, carbon dioxide and nitrogen (see table 4). The main difference among the various groups is due to the fact that in some cases, the $\bar{W}$ ratio was taken to increase with decreasing neutron energy, while other groups employed a constant $\bar{W}$ ratio. These discrepancies lead to a maximum difference of 11 percent in the case of the lower neutron energies.

For photons and electrons extensive measurements of $\bar{W}$ values in air have been performed, resulting in a relatively small uncertainty of about 1 percent in $\bar{W}$ for electrons in air[31]. $\bar{W}$ values for electrons in other gases are less well known, while for protons and other charged particles only limited information is available. Until recently only the experimental results of Larson[32] and Leonard and Boring[33] on $\bar{W}_P/\bar{W}_G$ were available for protons in methane-based TE gas. In fig. 3, lines 1 and 2 show the relationships used by Dennis[34] and Bewley[35], respectively, for the calculations of $\bar{W}_N/\bar{W}_G$ for neutrons of different energies. New experimental results of Chemtob et al.[36] and Rohrig and Colvett[37] show that the energy dependence of $\bar{W}$ for protons is small. It can be concluded that the dependence of $\bar{W}_N$ on neutron energy needs further experimental verification. Until this is done it is recommended that $\bar{W}_N/\bar{W}_G$ for tissue equivalent gas be taken to be 1.05. It is estimated that the systematic uncertainty in this value is about 5 percent for neutron energies above 1 MeV and that the systematic uncertainty increases at lower energies.

c. Stopping power ratios

If the gas and the wall of an ionization chamber have the same composition, it is generally assumed that they have the same stopping power. There is some experimental evidence[38] that the mass stopping power for protons and alpha particles in vapour could be higher than that in the condensed phase. However, in other experiments no difference in stopping power has been observed and the measured difference of about 5-10 percent is not much higher than the experimental uncertain-

TABLE 3.

RATIO OF KERMA IN ICRU MUSCLE TISSUE TO KERMA IN TE DOSIMETER MATERIAL ADOPTED BY PARTICIPANTS IN TWO INTERNATIONAL NEUTRON DOSIMETRY INTERCOMPARISONS

Participant	Neutron Energy (MeV)				
	15.1	5.5	2.1	0.67	^{252}Cf
AFF	0.926	0.962	0.917	0.962	0.962
ANL	0.9666	0.9835	0.9749	0.9880	0.9847
CHRI	0.925	0.962	0.950	0.950	0.950
CNEN	0.969	0.963	0.956	0.970	0.959
FON	0.988	0.976	0.981	0.982	0.981
GSFF (1)	0.971	0.990	0.971	0.971	--
GSFF (2)	0.935	0.980	0.971	0.976	0.971
GSFM	0.969	0.963	0.956	0.970	0.959
IAEA	1.00	1.00	1.00	1.00	1.00
NIRS	0.99	0.95	0.97	0.97	0.97
RAR	0.956	0.960	0.956	0.960	0.956
TNO (1)	0.972	0.935	0.951	0.951	0.951
TNO (2)	0.94	0.98	0.96	0.97	--
WWD	0.948	0.950	0.940	0.940	0.946

(1) Values used for INDI

(2) Values used for ENDIP

TABLE 4.

RATIO OF $\bar{W}_N/\bar{W}_G$ FOR TE GAS EMPLOYED BY PARTICIPANTS IN INDI AND ENDIP

Participant	Neutron Energy (MeV)				
	15.1	5.5	2.1	0.67	^{252}Cf
AFF	1.01	1.02	1.03	1.05	1.04
ANL	1.04	1.04	1.04	1.04	1.04
CHRI	1.04	1.05	1.09	1.10	1.10
CNEN	1.038	1.058	1.106	1.158	1.110
EUR	1.03	--	1.098	1.151	--
FON	1.037	1.037	1.037	1.037	1.037
GSFF (1)	1.042	1.042	1.042	1.042	1.042
GSFF (2)	1.053	1.053	1.053	1.075	1.053
GSFM	1.037	1.059	1.105	1.161	1.110
NIRS	1.055	1.055	1.055	1.055	1.055
RAR	1.05	1.05	1.05	1.05	1.05
TNO (1)	1.055	1.055	1.055	1.055	1.055
TNO (2)	1.05	1.05	1.05	1.05	1.05
WWD	1.05	1.05	1.05	1.05	1.05

(1) Values used for INDI

(2) Values used for ENDIP

Fig. 3. Ratio of $\bar{W}$ for protons and photons in methane-based TE gas. Lines 1 and 2 show the relationships used for calculations of $\bar{W}_N/\bar{W}_G$ for neutrons of different energies.

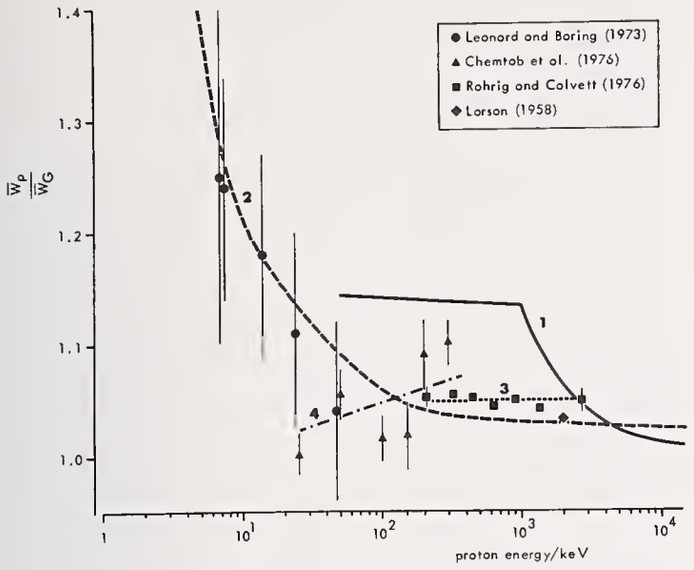

ty. Until further experimental data become available, no firm conclusions can be drawn. The use of a recommended relative mass stopping power of unity[1] may result in an overestimate of the neutron dose in the wall of a hydrogenous ionization chamber by about 5 percent.

The good agreement observed[39], between absorbed dose in a 14 MeV neutron field measured with a polythene calorimeter and a polythene-ethylene ionization chamber using a stopping power ratio of one, indicates that the error introduced by taking equal stopping power at all neutron energies will probably be less than about 3 percent. Decreasing the overall uncertainty attainable with ionization chambers requires better data on the relative mass stopping powers, particularly for TE plastic and TE gas.

d. Relative neutron sensitivity, k_U

In table 5 the values for the relative neutron sensitivity, k_U, as employed by the groups participating in INDI and ENDIP are tabulated for three different devices, notably C/CO_2 chamber, Al/Ar chamber and Geiger-Müller counter. In two cases, where groups employed either relatively high or relatively low values of k_U the reported gamma ray contributions were found to be lower or higher respectively than the mean value observed.

For a number of neutron insensitive devices, the relative neutron sensitivity has been derived from calculations[1], from measurements made in neutron fields with minimal gamma ray contamination and by calibration with a proportional counter. In table 6, relative neutron sensitivities are given for relatively small non-hydrogenous ionization chambers and a GM counter[40]. It can be seen that the relative neutron sensitivities for Al-Ar are considerably less than for the C/CO_2 combination. Using a lead-filter technique[41,42], k_U values of 0.32 and 0.28 have been observed for a C/CO_2 chamber for neutrons from the d(35)+Be reaction (mean energy approximately 15 MeV) and for collimated 14 MeV neutrons, respectively. Kuchnir et al.[43] employed a difference method to determine the relative neutron sensitivity of ionization chambers as a function of neutron energy for the wall and gas combinations indicated in fig. 4. The difference technique utilizes accelerator target reactions for which the neutron flu-

TABLE 5.

RELATIVE NEUTRON SENSITIVITY, k_U, EMPLOYED BY PARTICIPANTS IN INDI AND ENDIP

Detector	Porticipont	Neutron Energy (MeV) 15.1	5.5	2.1	0.67	^{252}Cf
C/CO_2 chamber	AERE	--	0.105	0.0751	0.0677	0.106
	ANL	0.351	0.097	--	--	0.099
	CHR	0.356	0.114	0.089	0.074	0.086
	CNEN	0.373	0.106	0.077	0.073	0.094
	EUR	0.39	--	--	0.058	--
	GSFF (1)	0.33	0.13	--	--	--
	GSFF (2)	0.32	0.10	0.02	0.02	0.02
	GSFM	0.341	0.096	0.070	0.065	0.086
	NIRS	0.365	0.102	0.090	0.083	0.090
	NRPB	0.361	0.104	0.068	0.053	0.090
Al/Ar chamber	EUR	0.046	--	0.020	0.011	--
	FON	0.127	0.029	0.017	0.017	0.017
	IAEA	0.13	0.011	0.012	0.014	0.02
	RAR	0.132	--	--	--	--
Geiger-Müller counter	ORNL	0.005	0.005	0.005	0.005	0.005
	RAR	0.015	0.005	0.002	0.002	0.003
	TNO (1)	0	0	0	0	0
	TNO (2)	0.004	0.002	0.001	0.001	--
	WWD	0.004	0.002	0.001	0.001	0.001

(1) Volues used for INDI

(2) Volues used for ENDIP

TABLE 6.

RELATIVE NEUTRON SENSITIVITIES AND THEIR OVERALL UNCERTAINTIES FOR NON-HYDROGENOUS IONIZATION CHAMBERS (CAVITY GAS AT ATMOSPHERIC PRESSURE) AND GM COUNTER

neutron energy MeV	percent energy spread	relative neutron sensitivity, k_U: $C-CO_2$ chamber computed[o]	$C-CO_2$ chamber observed[b]	Al-Ar chamber observed[c]	GM counter measured[c]
0.7	25	0.05	0.07 ± 0.006	0.014 ± 0.004	0.001 ± 0.0005
2	5	0.07	0.08 ± 0.01	0.012 ± 0.002	0.001 ± 0.0005
5	6	0.07	0.11 ± 0.01	0.011 ± 0.003	0.002 ± 0.0005
15	7	0.31	0.32 ± 0.02[d]	0.13 ± 0.01	0.004 ± 0.001
^{252}Cf	fission spectrum	0.08	---	0.02 ± 0.015	0.001 ± 0.0005

o: Goodmon, 1974; b: Greene, 1974; c: Goodman and Colvett, 1974; d: Broerse, 1974.

Fig. 4. Relative neutron sensitivity with respect to ^{60}Co gamma rays as a function of neutron energy for a magnesium-wall and graphite-wall chamber with a variety of filling gases at atmospheric pressure[43].

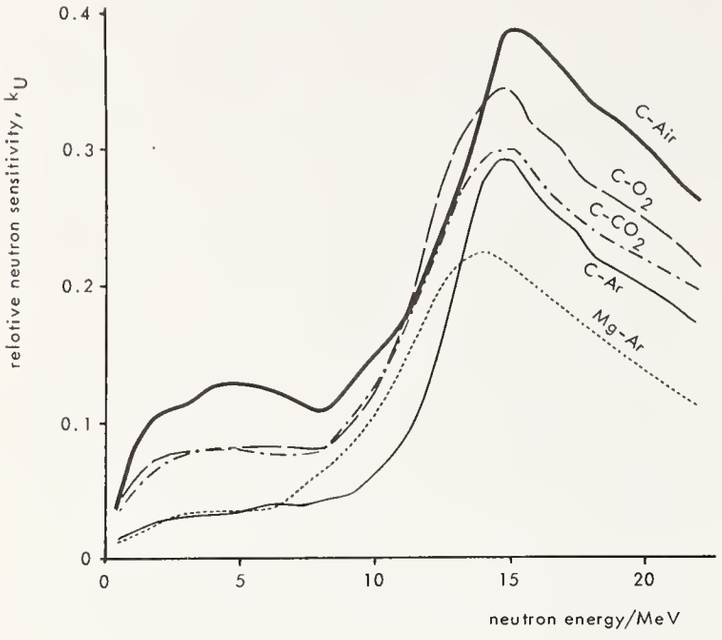

ence rate and neutron energy are functions of the angle with respect to the target but for which the accompanying photon production is isotropic. The data in fig. 4 have been obtained for a Mg chamber with a 0.5 cm^3 cylindrical cavity and for a C chamber with a 2 cm^3 spherical cavity. Below 15 MeV the overall uncertainty in k_U was estimated to be about 10 percent; above 15 MeV the values of k_U are less reliable. There is fairly good agreement between the C/CO_2 and C/air data of fig. 4 and the corresponding values discussed above. The values given in table 6 can be used as a guideline for relative neutron sensitivity, k_U. However, these data should be handled cautiously since ionization chambers constructed with the same wall and gas materials, but of markedly different size, configuration or gas pressure, may have different relative neutron sensitivities. Recent studies of Lewis et al.[44] indicate slightly higher values of k_U for energy-compensated GM counters than indicated in the table, however, these results need to be confirmed by complementary experiments.

Conclusions and recommendations

For medical and radiobiological applications there is certainly a need for standard neutron fields where the absorbed dose is known with regard to its spatial and temporal distribution and the neutron energy spectrum. If calibration of absorbed dose with fission spectrum neutrons would prove to be satisfactory, ^{252}Cf can be considered to be an acceptable standard neutron source, provided that source encapsulation and scattering conditions are normalized.

Standard neutron fields produced by accelerators are not yet available at national standards laboratories, however, facilities for calibration of neutron dosimeters are under construction. At present, the most preferable standard field will be deliverd by a photon source e.g. ^{60}Co or ^{137}Cs, with subsequent adjustment of the response function to the neutron field concerned. Regarding the preparation of standard fields for medical neutron dosimetry, the characteristics of the neutron field should be relevant to the clinical situation. This implies that the possibility of irradiations with collimated beams at reasonably high dose rates of e.g. 5-10 rad/min (0.05-0.1 Gy/min) should be provided.

For standardization purposes, the instruments having the lowest overall uncertainty for measuring total absorbed dose are the TE calorimeter and the homogeneous TE ionization chamber. In both cases, a separate measurement with a dosimeter having a relatively low neutron sensitivity is required to evaluate the partial absorbed dose of photons. Relatively bulky and complicated equipment is needed for calorimetry. The ionization chamber has many advantages including greater sensitivity, lower random uncertainty and smaller size[1].

The two international neutron dosimetry intercomparisons have provided information on the present adequacy of neutron dosimetry and on the advantages, corrections and systematic errors involved in the various methods used[27]. The groups participating in these two intercomparison projects have employed for the same experimental conditions, sets of basic physical data which showed considerable variations. General agreement on the most accurate parameters will be an essential requirement to accomplish consistency in neutron dosimetry results obtained at different institutes. For a specific type of instrument such as the TE ionization chamber, which was employed by the majority of participants in both INDI and ENDIP an analysis for uniform parameters was performed. For INDI it was shown that the differences between reported values could not be attributed solely to differing factors used to convert instrument response to neutron kerma or absorbed dose[27]. For ENDIP, the standard deviations of kerma and absorbed dose values were in the same order as the standard deviation of the instrument responses reported by the participants. These analyses clearly indicate that other factors such as incomplete charged particle equilibrium, insufficient saturation of the ionization chambers, and choice of effective measurement point tend to overshadow inconsistencies in ratios of $\bar{W}$, kerma and mass stopping power applied. Although adoption of uniform basic physical parameters is desirable, it seems of more importance to agree to use the same dosimeter type, preferably a TE ionization chamber of standardized construction[45]. The measurement and correction procedures for this common type of dosimeter should be standardized, e.g., the calibration with photons, the gas flow rate, the collecting potential, polarity and the correction for wall thickness. An alternative would be that a standards laboratory maintain a reference dosimeter which could be used for calibration of other dosimeters. At the moment, however, none of the standards laboratories is prepared to offer such a service. Different specifications should be applied for the interpretation of instrument response at different energies. General agreement on the neutron energy dependence of parameters such as $\bar{W}$ and corrections for wall attenuation will obviously be necessary, but will only be needed for one type of dosimeter. A thimble type homogeneous TE ionization chamber with a set of TE build-up caps to achieve complete charged particle equilibrium would be a useful standard dosimeter.

It must be realized that for medical applications the quantity of interest is the absorbed dose in the patient. In general, this value is derived from in phantom measurements, with separate corrections for tissue inhomogeneities. For the various centers in Europe co-operating in the Fast Neutron Therapy Project Group sponsored by the EORTC (European Organization for Research on Treatment of Cancer), a second draft of a protocol for medical neutron dosimetry is available[45].

Interest in the use of fast neutrons for biological and medical applications has increased considerably in the past decade. These applications introduced requirements for precision and accuracy in dosimetry methods which are more demanding than generally encoun-

tered in radiation protection. The following recommendations for future research in neutron dosimetry in biology and medicine have been formulated[1]:

1. It is recommended that standards laboratories develop and establish standard instruments and/or radiation fields which will be directly applicable to absorbed dose calibrations for the neutron energies applied in the life sciences.

2. The results of neutron dosimetry should be reported by giving the following values:

(a) The absorbed dose of neutrons in the region of interest and its time dependence or fractionation schedule.

(b) The absorbed dose of photons or the magnitude of this component relative to either the neutron or total absorbed dose in the region.

When the spatial variation of absorbed dose in the region of interest can affect the biological response, it is important to describe the variation.

Meaningful comparisons of biological data and therapeutic results require that radiation quality be specified, for example, by means of neutron energy spectra or by lineal energy spectra. These data should be supplied at more than one point when quality changes significantly in the region of interest.

3. Knowledge of neutron energy spectra is important not only for correlation with biological effects but also for determining the corrections and systematic uncertainties to be applied to measurements with neutron and photon dosimeters. Neutron spectrometers of small size which can operate over a broad range of neutron energies, say from about 1 keV to at least 50 MeV, are needed. The low-energy capability is needed mainly for radiobiological research; the high-energy capability is necessary for the spectra encountered in radiotherapy. The instrument(s) should be small and nondirectional to permit spectral studies with good spatial resolution to be made in phantoms and across collimated beams. The data available on radiation quality need to be expanded to include effects on spectra caused by variations in the design of collimators, filters and accelerator target structures.

4. The data on cross sections and related mass energy transfer coefficients for neutron-produced secondaries in the elements constituting tissue and for elements employed in dosimeters should be expanded to improve the values presently available above 20 MeV and to provide necessary information above 30 MeV. These data are required to compute kerma factors for various tissues, dosimeter materials and tissue-substituting materials, particularly for use in radiotherapy.

5. In order to decrease the overall uncertainty of neutron absorbed doses determined with ionization chambers, it is essential that further measurements of W for the gases used in these chambers should be made, especially for protons and heavy charged particles with energies between 0.01 and 10 MeV. This will permit effective values of W for neutrons to be calculated more reliably.

6. Decrease of the overall uncertainty attainable with ionization chambers also requires better data on the relative mass stopping powers with regard to the physical state (solid or gaseous) of the chamber materials, particularly for low energy secondaries.

7. In order to decrease the systematic uncertainty of the measurement of neutron absorbed doses with calorimeters, further measurements of the thermal defect for the materials used in these instruments should be made.

8. The overall uncertainty of measurements of photon absorbed doses in mixed fields can be decreased by more reliable determinations of relative neutron sensitivities of photon dosimeters as a function of neutron energy than has heretofore been available. In particular, this should include neutron energies above 15 MeV. Evaluation of the effects of dosimeter size and configuration on relative neutron sensitivities should be made.

In addition to improving data presently available, many of these recommendations call for a substantial extension of our knowledge into both higher and lower regions of neutron and charged particle energies than have previously been the focus of study.

Acknowledgements

This review contains specific conclusions reached by a number of scientists preparing the ICRU report 26 on Neutron Dosimetry for Biology and Medicine (1977) and is also based on the discussions during a workshop on Basic Physical Data for Neutron Dosimetry (1976). The stimulating discussions with my colleagues Drs. B.J. Mijnheer, H. Schraube and J. Zoetelief in the final preparation of this paper are gratefully acknowledged.

References

1. ICRU report 26, Neutron Dosimetry for Biology and Medicine (1977).
2. Broerse, J.J., Engels, A.C., Lelieveld,P., Putten, L.M. van, Duncan, W., Greene, D., Massey, J.B., Gilbert, C.W., Hendry, J.H. and Howard, A., Int. J.Radiat.Biol. 19, 101 (1971).
3. Rossi, H.H., p. 129 in Proc. Symp. on Neutrons in Radiobiology, Oak Ridge, CONF-691106 (1969).
4. Broerse, J.J. and Mijnheer, B.J., in Proc. VIII Int. Congress on Radiation Protection, Saclay (1976).
5. Shukovsky, L.J., Amer.J.Roentgenol. 108, 27 (1970).
6. Hussey, D.H., Fletcher, G.H. and Caderao, J.B., Cancer 34, 65 (1974).
7. Sinclair, W.K., p. 617 in Radiation Dosimetry, Vol. III, Academic Press, New York (1969).
8. Bichsel, H., Eenmaa, J., Weaver, K. and Wootton, P.B., p. 71 in Proc. Int. Workshop on Particle Radiation Therapy, American College of Radiology, Philadelphia (1976).
9. Roesch, W.C. and Attix, F.H., p. 1 in Radiation Dosimetry, Vol. I, Academic Press, New York (1968).
10. Proc. of a Panel on In Vivo Neutron Activation Analysis, IAEA, Vienna (1973).
11. Murray, B.W., Deutsch, O.L., Zamenhof, R.G., Pettigrew, R.I., Rydin, R.A. and Brownell, G.L., p. 179 in Proc. Symp. Biomedical Dosimetry, IAEA, Vienna (1975).
12. Hatanaka, H. and Sweet, W.H., p. 147 in Proc. Symp. Biomedical Dosimetry, IAEA, Vienna (1975).
13. ICRU report 13, Neutron Fluence, Neutron Spectra and Kerma (1969).
14. Harvey, J.R. and Mill A.J., in Proc. 3rd Symp. on Neutron Dosimetry in Biology and Medicine, Neuherberg/München, to be published.
15. Alberts, W.G. and Knauf, K., in Proc. 3rd Symp. on Neutron Dosimetry in Biology and Medicine, Neuherberg/München, to be published.
16. Mijnheer, B.J., Broers-Challiss, J.E. and Broerse, J.J., p. 423 in Proc. 2nd Symp. on Neutron Dosimetry in Biology and Medicine, Neuherberg/München, EUR 5273 (1975).
17. Colvett, R.D., Rossi, H.H. and Krishnaswamy, V., Phys.Med.Biol. 17, 356 (1972).
18. Goodman, L.J., p. 65 in Basic Physical Data for Neutron Dosimetry, EUR 5629 (1976).
19. Goodman, L.J., Colvett, R.D. and Caswell, R.S., p. 627 in Proc. 2nd Symp. on Neutron Dosimetry in Biology and Medicine, Neuherberg/München, EUR 5273 (1975).
20. Schraube, H., Morhart, A., Schraube, G. and Burger, G., p. 243 in Basic Physical Data for Neutron Dosimetry, EUR 5629 (1976).

21. Zoetelief, J., Bouts, C.J., Engels, A.C. and Broerse, J.J., p. 249 in Basic Physical Data for Neutron Dosimetry, EUR 5629 (1976).
22. Coppola, M., p. 271 in Basic Physical Data for Neutron Dosimetry, EUR 5629 (1976).
23. Hurst, G.S., Brit.J.Radiol. 27, 353 (1954).
24. Broerse, J.J., p. 197 in Basic Physical Data for Neutron Dosimetry, EUR 5629 (1976).
25. Smathers, J.B., Otte, V.A., Smith, A.R., Almond, P.R., Attix, F.H., Spokas, J.J., Quam, W.M. and Goodman, L.J., Med.Phys., in press.
26. Law, J., Int.J.Appl.Radiat. and Isotopes 22, 701 (1971).
27. ICRU, An International Neutron Dosimetry Intercomparison, in press.
28. Broerse, J.J., Burger, G. and Coppola, M., p. 257 in Basic Physical Data for Neutron Dosimetry, EUR 5629 (1976).
29. Alsmiller, R.G. and Barish, J., Neutron Kerma Factors for H, C, N, O, and Tissue in the Energy Range of 20 to 70 MeV, ORNL/TM-5702 (1976).
30. Bassel, R.H. and Herling, G.H., Radiat.Res, in press.
31. ICRU report 14, Radiation Dosimetry: X-rays and Gamma Rays with Maximum Photon Energies Between 0.6 and 50 MeV (1969).
32. Larson, H.V., Phys.Rev. 112, 1927 (1958).
33. Leonard, B.E. and Boring, J.W., Radiat.Res. 55, 1 (1973).
34. Dennis, J.A., Phys.Med.Biol. 18, 379 (1973).
35. Bewley, D.K., p. 5 in Proc. 2nd Symp. on Neutron Dosimetry in Biology and Medicine, Neuherberg/München, EUR 5273 (1975).
36. Chemtob, M., Lavigne, B., Noel, J.P., Chary, J., Nguyen, V.D., Parmentier, N. and Fiche, C., p. 95 in Basic Physical Data for Neutron Dosimetry, EUR 5629 (1976).
37. Rohrig, N. and Colvett, R.D., p. 99 in Basic Physical Data for Neutron Dosimetry, EUR 5629 (1976).
38. Williamson, J. and Watt, D.E., Phys.Med.Biol. 17, 486 (1972).
39. Greene, D., Major, D. and Redpath, T., Phys.Med. Biol. 20, 244 (1975).
40. Goodman, L.J. and Colvett, R.D., p. 24 in Annual Report on Research Project, USAEC Report C00-3243-3 (1974).
41. Attix, F.H., Theus, R.B. and Rogers, C.C., p. 329 in Proc. 2nd Symp. on Neutron Dosimetry in Biology and Medicine, Neuherberg/München, EUR 5273 (1975).
42. Cleland, M.R. and Wells, N., p. 397 in Proc. 2nd Symp. on Neutron Dosimetry in Biology and Medicine, Neuherberg/München, EUR 5273 (1975).
43. Kuchnir, F.T., Vyborny, C.J. and Skaggs, L.S., p. 107 in Int. Symp. on Advances in Biomedical Dosimetry, IAEA, Vienna (1975).
44. Lewis, V.E., Rossiter, M.J., Wood, J.W. and Young, D.J., p. 133 in Basic Physical Data for Neutron Dosimetry, EUR 5629 (1976).
45. Broerse, J.J. and Mijnheer, B.J., p. 275 in Basic Physical Data for Neutron Dosimetry, EUR 5629 (1976).

NBS FACILITIES FOR STANDARDIZATION OF NEUTRON DOSIMETRY FROM 0.001 TO 14 MeV

O. A. Wasson
National Bureau of Standards
Washington, D.C. 20234

The neutron sources available at NBS for use in neutron dosimetry are described in terms of fluence, beam size, and background contamination. Operational details and neutron fluence monitoring of the recently installed standardized beam line of the 3 MV Van de Graaff Laboratory are given for the 200 keV to 1 MeV energy region along with plans for measurements at 14 MeV. Measurements of the response of typical laboratory dose rate meters and films to monoenergetic neutrons of accurately known fluence in the 250 keV to 1 MeV energy region are given. The problem of the neutron fluence to dose equivalent conversion is discussed.

(Calibration; dosimetry; detection; facilities; fluence; flux; moderation; monitor; neutron; shielding; sources; standardization)

Introduction

A large variety of calibrated neutron sources and flux monitors exist at the National Bureau of Standards which are useful for studies of neutron dosimetry. These sources and associated energy regions are shown in Fig. 1. The 140 MeV electron linear accelerator is used to produce a pulsed neutron source at a rate of approximately 1×10^{13} n/sec. The neutron spectrum is continuous from thermal energies to over 14 MeV and can be tailored for different experiments. Various evacuated drift tubes with lengths from 2m to 200m permit the measurement of neutron energies by the time-of-flight method. Beam sizes are variable, depending upon the collimation used.

The next group of sources are associated with the NBS reactor. The filtered beam facility produces monoenergetic beams by transmission of the reactor fission spectrum through selected filtering materials. The three beams in operation include a 2 keV beam from a scandium filter, a 24.3 keV beam from an iron-aluminum filter, and a 144 keV beam from a silicon filter. The investigation of the response of various detectors and dosimeters to various energy neutrons is aided by a scanning table and human phantom. A detailed presentation of the neutron dosimetry measurements on this facility are given in a paper in this symposium by R. B. Schwartz[1] and will not be given here.

There is also a cavity source located in the graphite thermal column of the reactor which produces a fission spectrum with a strength of approximately 3×10^{11} n/sec which is useful for studies of materials dosimetry. The details of another source (ISNF) in this column which produces a neutron spectrum similar to that of the Liquid Metal Fast Breeder Reactor are given in papers by D. M. Gilliam[2] and C. M. Eisenhauer[3] at this symposium. The neutron field has a mean energy of 0.8 MeV and flux of $\sim 10^{9}$ n/cm^2 sec.

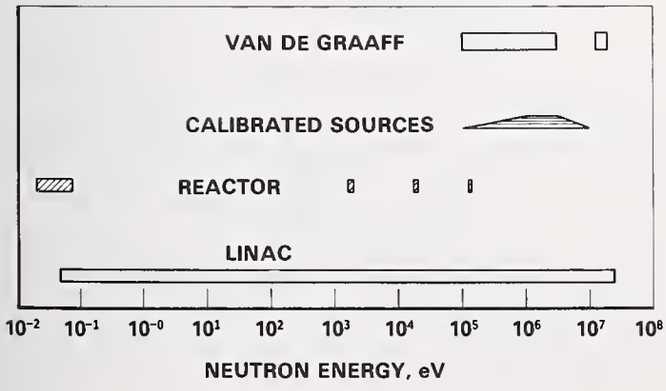

Fig. 1 Neutron Sources in Standards Program

The next class of neutron sources are those produced from radioactive decay. The national standard Ra-Be source (NBS-I) has a source strength of 10^{6} n/sec with an uncertainty of $\pm$ 1%. This is the primary standard for all fast neutron source and field strength measurements. There are also several ^{252}Cf spontaneous fission sources with strengths between 1 and 7×10^{9} n/sec which can be calibrated within an uncertainty of $\pm$ 1.2% based on NBS-I. These sources emit a broad energy spectrum in the 0.2 to 5 MeV region.

Other neutron sources are obtained at the NBS 3 MV positive ion Van de Graaff laboratory. Monoenergetic neutron beams in the 0.1 to 2.2 MeV energy region are produced by means of the ^{7}Li(p,n)^{7}Be and ^{3}H(p,n)^{3}He reactions. The 14 MeV region is covered by the ^{3}H(^{2}H,n)^{4}He reaction. Production of 144 keV neutrons allows a comparison with experiments done with the silicon filtered beam at the reactor. The remainder of this paper is devoted to the properties of the recently installed standard neutron beam line and to the results of the first measurements of the response of several neutron personnel monitors to low level neutron exposures.

Van de Graaff Experimental Geometry

The layout of the three beam lines at the Van de Graaff Laboratory is shown in Fig. 2. The beam to the right is used for other testing and physics measurements. The center beam line is used for the calibration of the Black Detector neutron flux monitor by means of the associated particle technique. The standard neutron beam line shown on the left side of the figure became operational in November of 1976. A more detailed view of this beam line is shown in Fig. 3.

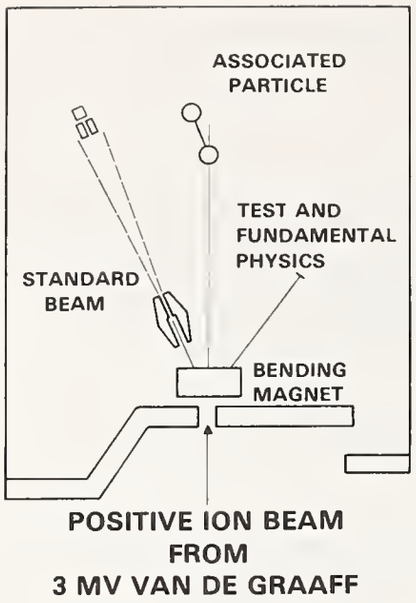

Fig. 2 Van de Graaff Experimental Area

Our initial experiments have been limited to the neutron energy region from 200 keV to 2 MeV. The neutron sources were the $^{7}Li(p,n)^{7}Be$ and $^{3}H(p,n)^{3}He$ reactions. The neutron source is surrounded by a large neutron shield in order to reduce room background. The shield is mounted on an air table in order to produce easy access to the end of the beam pipe for target charges. The neutron beam is collimated to a cone with a 4.5^{o} half angle by means of a removable lithium loaded polyethylene insert. This angle provides a 19 cm diameter neutron beam at a distance of 120 cm from the target. The primary neutron flux monitor is the Black Detector located in a shield approximately 6 meters from the target. The beam size incident on this monitor is determined by a precision machined collimator 30 cm long with a 4.445 ± 0.010 cm diameter cylindrical hole. This shield is also mounted on an air table for easy movement. The proton beam energy is calibrated by measuring the $^{7}Li(p,n)^{7}Be$ and $^{3}H(p,n)^{3}He$ thresholds and checked by measurements of carbon transmission near the 2077 keV resonance.

The neutron flux at the dosimeter position, r, is determined from the yield of the Black Detector by the expression

$$\varphi(r) = \frac{R^2}{r^2} \frac{Y_{BD}}{\epsilon\, T(R - r)\, A}$$

where $\varphi(r)$ is the neutron flux at distance r
R is the distance from source to exit of collimator
Y_{BD} is the Black Detector counting rate
ϵ is the Black Detector efficiency
A is the effective area of the collimator
$T(R - r)$ is the air transmission between the Black Detector and the position r.

For thick dosimeters which absorb a large fraction of the beam, it is necessary to use secondary monitors placed outside the direct beam for neutron flux monitoring. The monitors include a long counter placed at 90^{o} to the beam direction and a BF_3 counter located inside the shield at approximately 180^{o} to the beam direction. Tests have shown that the back angle detector is the better arrangement. The secondary monitors are calibrated by means of the Black Detector using a pulsed proton beam. Continuous beam operation is used for dosimetry measurements in order to increase the neutron flux by a factor of 5.

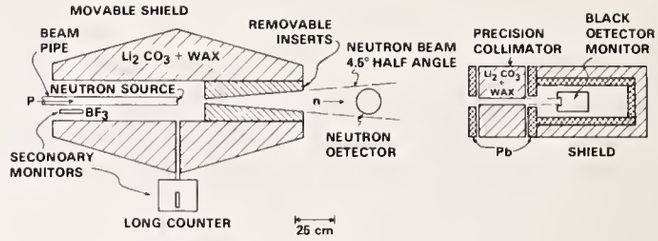

Fig. 3 Standard Neutron Beam Line

Black Detector Neutron Flux Monitor

The Black Detector is a cylindrical shaped plastic scintillator viewed by a single photomultiplier tube as is shown in Fig. 4. The scintillator is 12.5 cm in diameter with a length of 15 cm and a 5 cm diameter reentrant hole 2.5 cm deep. The purpose is to completely absorb the incident neutron in the scintillator so that the light output is proportional to incident neutron energy. Hence the name, Black Detector, as christened by Poenitz[4]. A detailed presentation of the operation and calibration of this monitor is given in another contribution to this symposium by M. M. Meier[5].

The neutron detection efficiency is measured by means of the associated particle method and also calculated by means of a Monte-Carlo type program. The results for 500 keV and 750 keV neutrons are shown in Fig. 5. The points represent the measurement while the solid curves are from the calculation. Since the two methods agree within $\pm$ 1%, the efficiency is taken from calculation for intermediate energies. The detector efficiency is greater than 90% for neutron energies between 200 keV and 1 MeV.

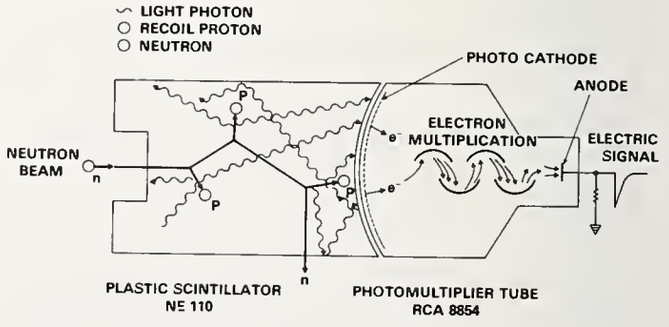

Fig. 4 Black Detector Operation

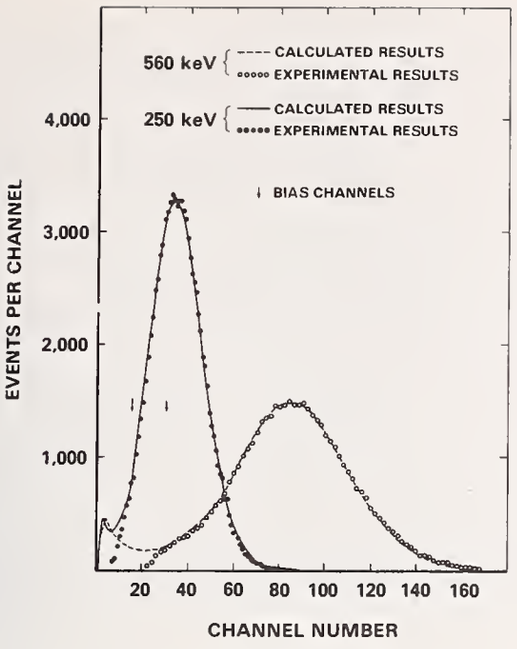

Fig. 5 Black Detector Response

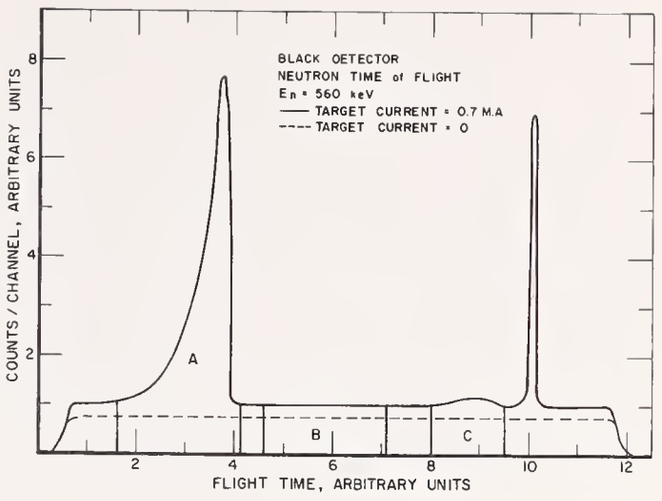

Fig. 6 Black Detector Time of Flight Yield

In addition to detecting neutrons, the monitor is also an efficient detector of γ rays, as is shown in Fig. 6. Here is displayed a time of flight spectrum with the Van de Graaff operating in the pulsed mode. The narrow peak is due to the X-rays from the proton beam hitting the Ta beam stop, while the broad peak is from 560 keV neutrons. The width of the neutron peak is determined by the energy spread of the neutron beam. This gives us a means of measuring the thickness of the target as well as the neutron energy. Most of the flat part of the spectrum, showed by the dashed line, is the ambient room background which is present with the beam off. Because of the strong X-ray peak, the monitor is used in the pulse mode of operation in order to separate neutrons from γ rays and to calibrate the secondary monitors which are relatively insensitive to γ rays.

After corrections for the effective area of the collimator beam hole and air transmission the neutron flux is determined within $\pm$ 2% at the dosimeter position for neutron energies between 200 keV and 1 MeV. The uncertainty increases outside of this region.

For operation at 14 MeV, we plan to calibrate the same detector by using the associated particle technique with the $^{3}H(^{2}H,n)^{4}He$ reaction and by extending the Monte-Carlo calculations to higher energies. The detector efficiency will decrease to approximately 30%. The shield around the target will be replaced by a more massive shield which is under construction.

Neutron Beam Parameters

Most of the dosimeter measurements to be reported in this paper were done at a distance of 120 cm from the neutron target. The beam diameter is 19.5 cm with a uniformity of $\pm$ 1%. The neutron flux and dose equivalent for a 5μA proton beam on a 20 keV thick ^{7}Li target are given in Table 1 for several energies.

Table 1

Measured neutron flux at a distance of 120 cm for a 5μA proton beam incident on a 20 keV ^{7}Li target

En, keV	φ, n/cm^2 sec	DE, millirem/hr*
250	600	30
500	2100	195
1000	1200	155

*National Council on Radiation Protection and Measurements Report No. 38, Table 2 (1971)

The dose equivalent in units of millirem per hour is taken from the NCRP report[6]. The measured γ ray background dose equivalent is 1.5 millirem/hr. The low energy (E_n < 1 keV) neutron background flux is less than 0.8% as measured with a ^{3}He gas proportional counter. The neutron fluxes are low so that a practical upper limit to irradiations is approximately 10 rem.

At 14 MeV neutron energies the expected rates for a 5μA deuteron beam on a tritium target are a flux of approximately 6 x 10^3 n/cm^2 sec and a dose equivalent of approximately 1.4 rem/hr.

The first use of the calibrated neutron fluence of this facility for dosimetry purposes is to study the response of typical personnel type neutron monitors to monoenergetic neutron fluences of 250, 500, and 1000 keV energy at low dose rates.

Measurements with Moderating Detectors

The first type of detector consisted of a hand held paraffin moderating cylinder with a BF_3 counter in the center arbitrarily selected from the group of instruments on hand. The output of the device consisted of a current meter calibrated in units of neutrons per cm^2 per sec. The results of the measurements are shown in Fig. 7. The cadmium covered cylinder was 12 cm in diameter and 12 cm in length with the neutron beam incident on the front face. The neutron flux varied between 10 and 100 n/cm^2 sec for various positions and neutron energies. The ratio of the meter flux reading to the incident flux is shown for incident neutron energies of 250, 500, and 1000 keV. The detector was calibrated by means of an Am-Be neutron source. The error bars indicate the statistical fluctuation of the current meter dial. The response at 1 MeV is approximately 30% less than that claimed by the manufacturer who states that the response should vary less than 10% throughout this energy region.

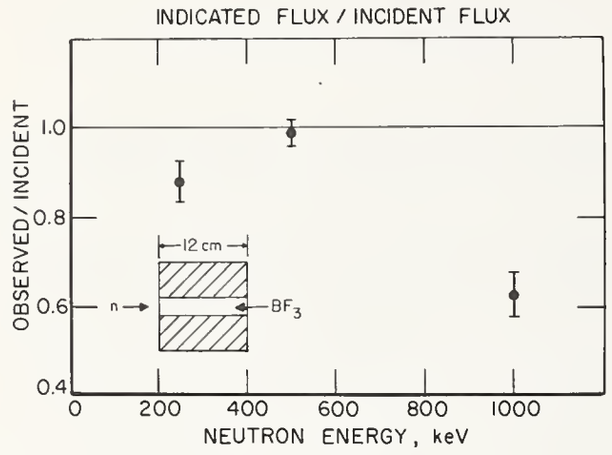

Fig. 7 Ratio of observed neutron flux to incident flux for moderating cylinder

The next measurements were done with larger moderating cylinders from two different manufacturers as shown in Fig. 8. These are the Andersson-Braun[7] type detectors which are supposed to have a uniform dose equivalent response from thermal to 10 MeV neutron energies. The detectors are composed of polyethlyene cylinders 21 cm in diameter and a length of 24 cm with a small BF_3 proportional counter in the middle. The moderated flux is tailored by means of a boron absorber with holes in order to produce a response which approximates the neutron dose equivalent in tissue. The neutron beam was incident on the front, flat end of the counter as is shown in the figure. Both detectors were calibrated by an Am-Be neutron source at a distance of 1.5 m using a dose equivalent to flux constant of 3.49×10^{-8} rem/(n/cm^2) as given by Nachtigall[8].

The results of the measurements are shown in Fig. 9. The ratio of the observed dose equivalent to that calculated from the incident neutron fluence, is plotted as a function of neutron energy for the two detectors. The response of both detectors follows the same general shape, although they differ in absolute calibration by 25%. Two values are shown for each detector at 250 keV. These result from different extrapolations of the neutron fluence to dose equivalent relationship at that energy.

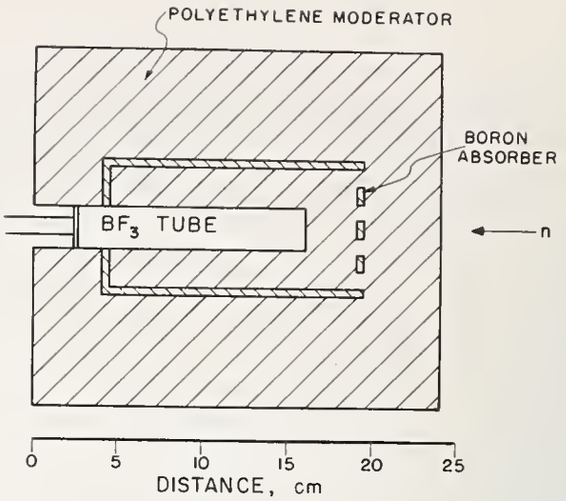

Fig. 8 Diagram of larger moderating neutron rem counter

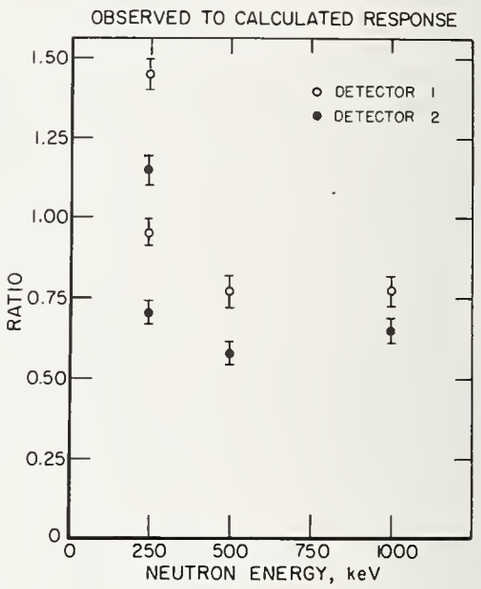

Fig. 9 Ratio of observed to calculated response for two rem counters

Figure 10 shows the dependence of dose equivalent on neutron fluence as a function of neutron energy. The points connected by the solid lines are from the 1971 report by the National Council on Radiation Protection and Measurements[6] while those connected with the dashed line are from the 1957 NBS Handbook No. 63[9]. These recent results differ by nearly 50% from the earlier results which were in use at the time of the Andersson-Braun detector invention and the Am-Be source calibration. Since no values are given for 250 keV, the value at this energy is obtained by extrapolation from the points at 100 and 500 keV. Due to the rapid variation in this region, the value obtained is, of course, dependent on the method of extrapolation and can easily vary by a factor of two. The circle on the graph is a result of logarithmic extrapolation which produces a better fit to the measurements as is shown by the lower datum points at 250 keV in Fig. 9. The higher values result from a linear extrapolation. Thus logarithmic extrapolation should be used in the 100 to 500 keV interval for the data in the NCRP report[6] and not linear extrapolation as recommended in the report.

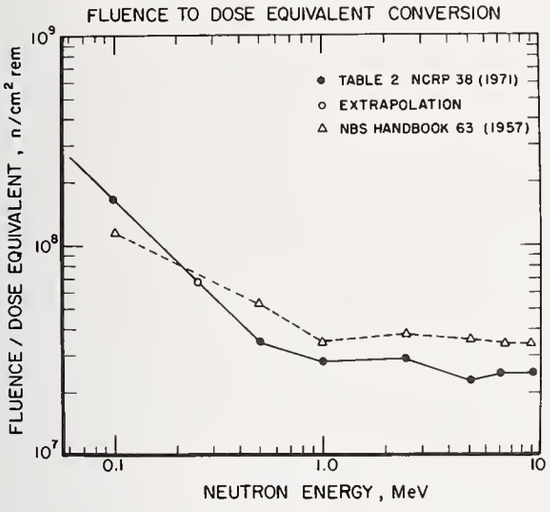

Fig. 10 Fluence to Dose-equivalent conversion factor

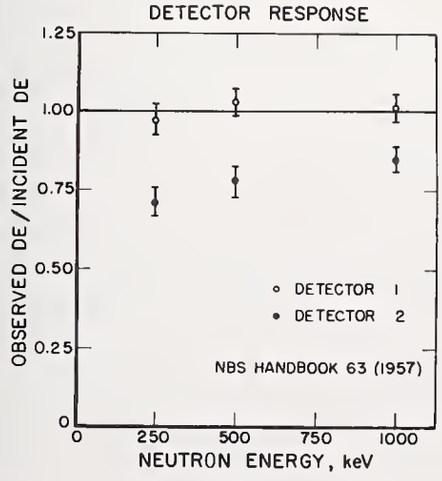

Fig. 11 Ratio of observed to calculated dose equivalent for two rem counters. Conversion factor is taken from ref. 9

Part of the difference between observed and incident dose equivalent in Fig. 9 is due to the use of different values of the neutron fluence to dose equivalent conversion factor for the detector calibration and the incident fluence. The older 1957 results were used for the former while the 1971 results were used for the latter. Figure 11 shows the results obtained if the older fluence to dose equivalent conversion is used for both the calibration and the fluence measurement. For detector No. 1 the response agrees with that predicted from the incident fluence while the response of detector No. 2 is approximately 25% low. Since the error bars indicate the statistical errors only, the 25% difference between the responses of the two similar detectors is an indication of the systematic errors involved in neutron dose equivalent measurements with typical neutron dose meters.

Measurements with Nuclear Test Films

The Nuclear track film used in dosimeters has an energy threshold at approximately 500 keV and an exposure threshold of approximately 100 mrem. As a check of these limits, film dosimeters were exposed to 250 keV, 500 keV, and 1 MeV beams with exposures ranging from 7 to 120 mrem. The films were exposed in groups of six in both free air and while mounted on the chest of a plastic phantom. The films were then treated in the usual manner by the processing laboratory.

The processing laboratory scanned the film visually and observed no exposure for the 250 keV and 500 keV beams. This is as expected for a 500 keV energy threshold. Since the results for 1 MeV neutrons were the same, within statistical error, for both the phanton and free air film backing, only the results observed with the phantom are shown in Table 2. The first column indicates the incident dose equivalent in units of millirem determined from the fluence measurement, the second column lists the total number of observed tracks in each group of 6 films, while the final column lists the exposure deduced by the processing laboratory. The listed error is only that from the finite number of observed tracks.

The observed dose agrees, within the ± 12% statistical error, with the exposure at the 110 mrem level but is systematically high for the lower exposures. These results confirm the observation that the typical film dosimeters used in personnel monitoring do not function for neutron energies below approximately 500 keV and for exposure levels less than approximately 100 mrem. Different type monitors are required for these regions

Table 2. Film irradiation results for 1 MeV neutrons

Incident Dose Equivalent mrem	Observed Tracks	Observed Dose Equivalent mrem
7.7	36	56 ± 9
15.4	28	43 ± 8
30.3	43	66 ± 10
110	77	119 ± 14

Summary

A calibrated neutron fluence beam is available at the NBS Van de Graaff with an accuracy of ± 2% in the energy region from 200 keV to 1.0 MeV with low background. This large sized beam is ideal for testing of instruments at low flux levels which is becoming more important as permissable personnel dose levels are lowered. Examples of the use of this beam for checking the response of typical radiation monitoring equipment, including the Andersson-Braun type monitor, were given. This facility along with the other neutron sources available at NBS offers a unique opportunity for standardization of neutron dosimetry for neutron energies below 15 MeV.

References

1. R. B. Schwartz, Proceedings of International Specialists Symposium on Neutron Standards and Applications, Paper G7, (1977).

2. D. M. Gilliam, Op. Cit., Paper H4.

3. C. M. Eisenhauer, Op. Cit., Paper 12.

4. W. P. Poenitz, Nucl. Instr. and Meth. 109, 413 (1973).

5. M. M. Meier, Proceedings of International Specialists Symposium on Neutron Standards and Applications, Paper G2, (1977).

6. "Protection Against Neutron Radiation", National Council on Radiation Protection and Measurements Report Number 38, Table 2, (NCRP Publications, Washington, D. C., 1971).

7. I. O. Andersson and J. Braun, "A Neutron rem Counter With Uniform Sensitivity from 0.025 eV to 10 MeV", Neutron Dosimetry, Vol 2, p. 87 (International Atomic Energy Agency, Vienna, 1963), Proceedings of a Symposium, Harwell, 1962.

8. D. Nachtigall, "Average and Effective Energies, Fluence-Dose Conversion Factors and Quality Factors of the Neutron Spectra of Some (α,n) Sources", Health Physics 13, 213 (1967).

9. "Protection Against Neutron Radiation up to 30 Million Electron Volts", National Bureau of Standards Handbook 63, (Superintendent of Documents, Washington, D. C., 1957).

INTERNATIONAL NEUTRON DOSIMETRY INTERCOMPARISONS

R. S. Caswell
National Bureau of Standards
Washington, D.C. 20234

Three recent international neutron dosimetry intercomparisons are discussed: the International Neutron Dosimetry Incomparison (INDI) sponsored by the International Commission on Radiation Units and Measurements (ICRU); the European Neutron Dosimetry Intercomparison Project (ENDIP) sponsored by EURATOM; and the intercomparison carried out by the centers doing neutron radiotherapy. Physical dosimetry to an accuracy of two or three percent is desired in order to achieve a generally-accepted 5% accuracy in dose to the tumor. In general it is found that 3% accuracy has not been achieved by the intercomparison participants; however, the radiotherapy centers agree on an arbitrary (but not absolutely known) scale within this uncertainty.

(Standards, medical, neutron dosimetry, intercomparisons, radiation effects).

Introduction

Perhaps the first question one might ask is: Why do intercomparisons at all? Some of the chief reasons are: (1) to verify the international measurement scale; (2) to obtain information on systematic errors; (3) to compare measurement methods or instruments; (4) to compare corrections used by different laboratories; (5) to evaluate the state-of-the-art in measurement; and (6) to motivate scientists to make better measurements. In reference to the first reason above, it is very important that 500 rads of absorbed dose to a tumor be the same in one hospital as in another so that comparison of clinical results is on a uniform basis, and one hospital may benefit from the experience of another hospital. It is also important to a national standards laboratory to verify that errors have not been made in the laboratory's own absolute measurements--comparison with one or more other standards laboratories gives some degree of assurance that no blunder has been made, and that the international measurement system is uniform, even though it may not be known absolutely to the accuracy to which uniformity can be established. If national standards laboratories do not offer standards for a particular kind of measurement, then intercomparisons represent a way of testing the uniformity of those institutions that constitute the international measurement system.

Evaluation of systematic errors, unlike random errors for which there is a good theory, is very difficult and is usually done by an estimate or guess. Intercomparison provides a way for getting at systematic errors. If all laboratories using independent methods get the same result we gain confidence that the systematic errors of each method are small. On the other hand, if one laboratory using a particular method is 20% higher than all other laboratories which are in agreement to, say, 3%, we tend to look for errors in this one method or in this laboratory's procedures.

A scientist participating in an intercomparison to some extent has his vulnerabilities exposed. He is therefore likely to try to do the best possible job of measurement to make sure that his numbers stand up well in the comparison with his peers.

Three international neutron dosimetry intercomparisons will be discussed here, although there have been a number of others: (1) The INDI (International Neutron Dosimetry Intercomparison) comparison was sponsored by the International Commission on Radiation Units and Measurements (ICRU) and was carried out by Leon Goodman and collaborators at the RARAF Accelerator facility at Brookhaven National Laboratory in 1973 with 14 international participating groups.[1,2,3] (2) The ENDIP (European Neutron Dosimetry Intercomparison Project) comparison was sponsored by EURATOM and carried out at TNO Rijswijk, Netherlands for dosimetry for neutron therapy, and at GSF Neuherberg (Munich) for neutron protection, in 1975.[4,5,6] The Radiotherapy Centers' intercomparisons have been carried out on a bilateral basis with participants from two laboratories performing measurements at a common radiotherapy facility.[7,8]

INDI Comparison

The physical arrangement for the INDI intercomparison is shown in Figure 1. The ion beam from the accelerator

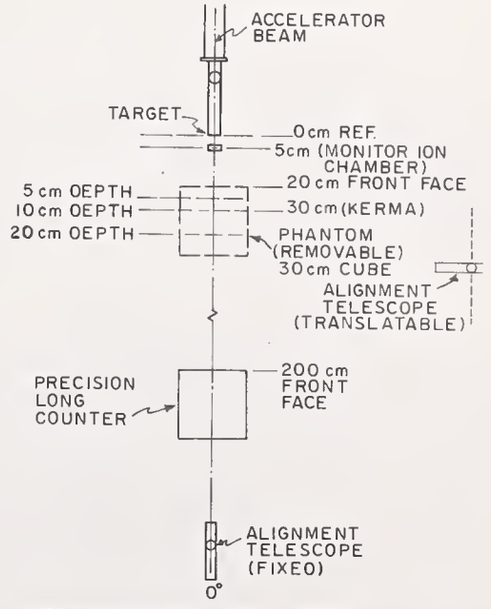

Fig. 1. Arrangement for the INDI intercomparison.

was incident upon the target where the neutrons were produced. At 5 cm downstream from the target was a transmission ionization chamber which monitored the total radiation (predominantly neutrons) in the experiments. Air measurements were carried out at 30 cm from the target. A 30 cm x 30 cm acrylic box filled with distilled water served as a phantom and could be located with its front face 20 cm from the neutron-producing target. Water was used, rather than tissue-equivalent liquid, to avoid problems of change of composition with time. Multiple monitoring was carried out, including a Precision Long Counter along the beam line at 200 cm, and 3 BF_3 counters at various depths in moderators, which were sensitive to changes in neutron spectrum. Positioning was done optically using an alignment telescope with such accuracy that errors due to position could be neglected. A photograph of the experimental area is shown in Figure 2.

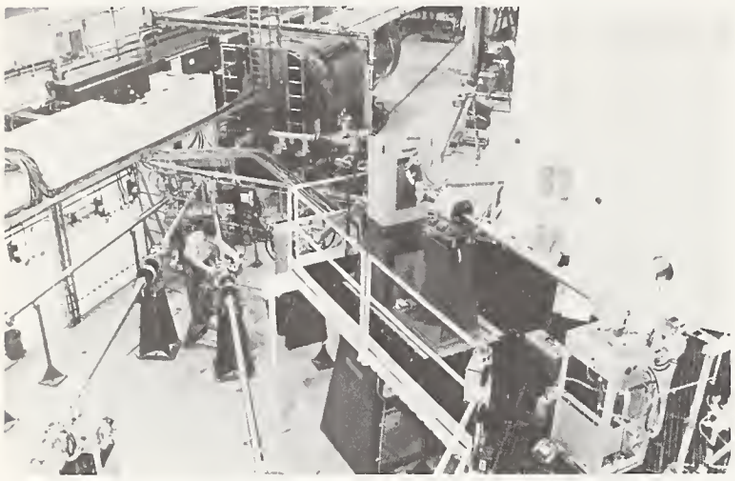

Fig. 2. Photograph of the experimental area used for the INDI intercomparison at the Brookhaven National Laboratory RARAF facility.

The principal monitor for the experiment is shown in Figure 3 and is a parallel-plate tissue-equivalent-wall

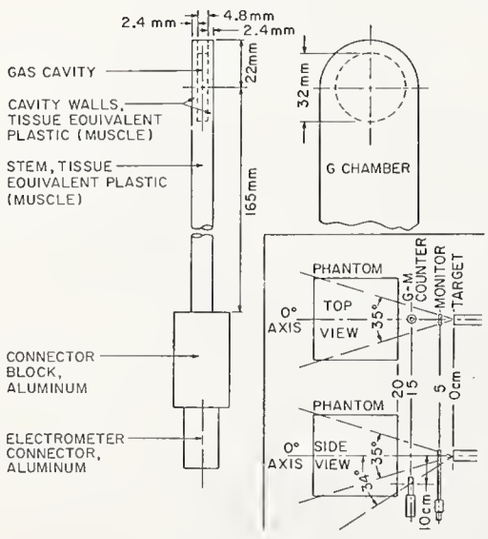

Fig. 3. Transmission ionization chamber monitor and location of phantom and GM counter used as a gamma-ray monitor in the INDI comparison.

transmission chamber. The principal gamma-ray monitor is a GM counter[9], also shown in Figure 3, and is located below the beam line at a horizational distance of 15 cm. A photograph of the transmission ionization chamber is shown in Figure 4.

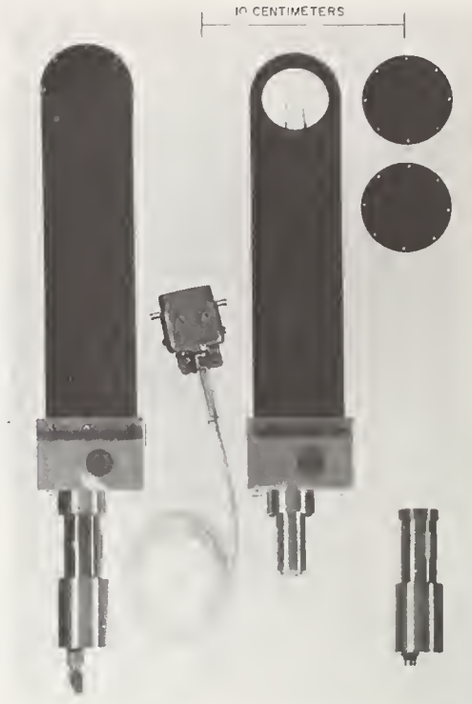

Fig. 4. Photograph of transmission ionization chamber monitor used in INDI experiment.

Measurements were carried out by participating groups for 11 measurement conditions. Five measurement conditions were in air: 15.1 MeV, 5.5 MeV, 2.1 MeV, 0.67 MeV and for Cf-252 neutrons. In addition measurements were made at three depths in the phantom for each of the two higher neutron energies, 15.1 and 5.5 MeV. The measurement conditions and reactions are summarized in Table 1. A summary of the INDI results in air is given in Figure 5. Note the larger spread in the results at 0.67 MeV where the dose was low. Results are grouped tightly at the two higher energies. At the lower energies the tendency of the C_2H_4 counter and the C_2H_4 ionization chamber to read low is evident. This is believed to be due to the necessity of applying a conducting film, usually graphite, to the polyethylene to make the chamber wall conducting. Secondary particles ejected by neutrons may be absorbed in this conducting coating of the chamber wall. The tissue-equivalent ionization chambers and acetylene-polystyrene equivalent chambers (C_2H_2) are intrinsically conducting, so this problem does not exist. The silicon diode and the precision long counter are calibrated independently, but do not yield results very different from those of the tissue-equivalent ionization chambers.

A more detailed look at the measurements at 15.1 MeV in air is given in Figure 6. Note that measurements were made over a period of roughly a year, requiring very good Van de Graaff accelerator radiation field stability. The stability of the calibration fields used in the experiment is believed to be good to 2%. Note that RARAF made measurements at 4 times during the procedures, and these all agree within a spread of 2%. One can see that the measurements are generally in agreement with the uncertainty quoted by the experimentalist. However, one should not be content with this situation, because the absolute uncertainties are relatively large, typically

Table 1.
Neutron energies and kerma rates

Reaction	Neutron energy MeV	Percent energy spread (±)	Nominal maximim total tissue kerma rate in air at 30 cm Gy h^{-1} (100 rad h^{-1})	Approximate percent gamma-ray tissue kerma, relative to total tissue kerma in free air
$T(d,n)^4He$	15.1	4	0.40	5
$D(d,n)^3He$	5.5	7	0.80	5
$T(p,n)^3He$	2.1	5	0.20	5
$T(p,n)^3He$	0.67	20	0.05	5
fission	^{252}Cf spectrum		0.06[a]	40

[a]About 2 mg.

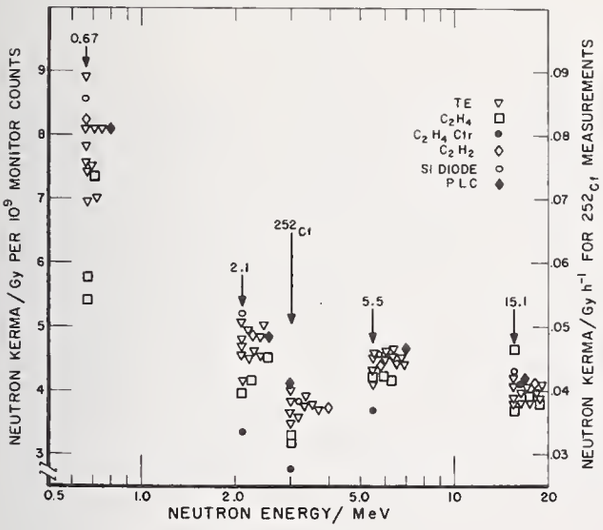

Fig. 5. Summary of INDI comparison results in air.

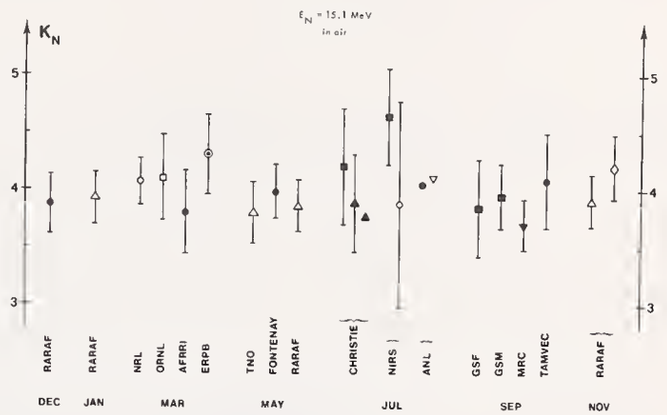

Fig. 6. Summary of INDI measurements at 15.1 MeV from December 1972 to November 1973. Solid circles, solid squares, erect hollow triangles and open circles all refer to tissue-equivalent ionization chambers with different systems for measuring the gamma-ray component of the mixed neutron and gamma-ray radiation field. Inverted open triangle is for C_2H_2 ionization chamber, erect and inverted solid triangles are for C_2H_4 ionization chambers. Open square is for the C_2H_4 proportional counter, diamond is for the Precision Long Counter, and the circle with dot in the center is for the Si diode.

7% or 8%. Since many of the measurers used similar systems, for example the tissue-equivalent ionization chamber, one might expect that these methods would agree to much better than the quoted uncertainty. However, this is not the result of the present comparison.

Figure 7 shows the results of the measurement of gamma-rays in the presence of neutrons, expressed as a percentage of the neutron kerma in air. Several different systems of gamma-ray measurement were used, the GM counters and the film having generally the lowest neutron sensitivity. Some negative results are shown particularly at 15.1 MeV which indicate that the neutron sensitivity assumed for the gamma-ray detector was probably too high. Note that for Cf-252 (for which one should read the right hand scale on the figure) the gamma rays are a much larger fraction of the neutron dose than in the other cases, and the agreement of the various measurement methods for the gamma rays is in fact much better. Measurements at 15.1 MeV in air and in phantom are summarized in Figure 8. Note that this is not a depth dose curve, since the phantom is not present during the measurements in air. A tendency for the polyethylene-ethylene dosimeters to read low in the lower neutron energy spectra associated with depth in the phantom is evident. Finally, in Figure 9, are shown measurements in air and phantom at 5.5 MeV. Notice the spread in results at 20 cm depth, where the dose rates are rather low, making it difficult to make accurate measurements with the ionization chambers (which

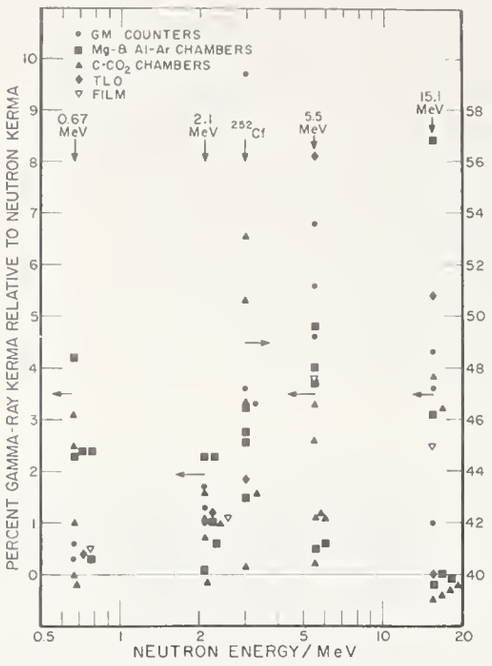

Fig. 7. Results of gamma-ray measurements in the mixed radiation field. For Cf-252 read right-hand scale, for all other energies read the left-hand scale.

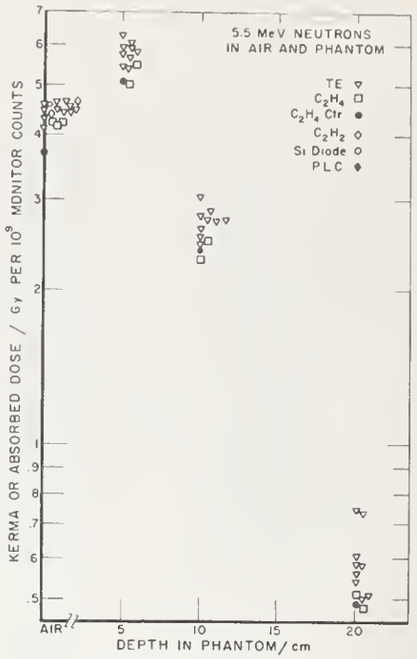

Fig. 9. INDI measurements in air and at 5, 10, and 20 cm depths in the phantom for 5.5 MeV neutrons.

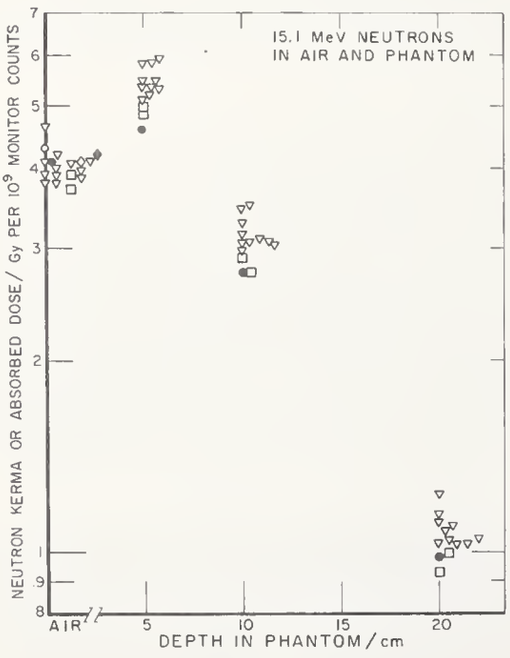

Fig. 8. INDI measurements in air and at 5, 10, and 20 cm depths in the phantom for 15.1 MeV neutrons. Symbols are the same as in Figure 5.

are mostly used in this experiment).

Some of the conclusions of the experiment were: (1) the spread in results is greater than the desired three percent, is roughly 10%, but no methods are in extreme disagreement with the others. (2) Uniform corrections for tissue equivalent ionization chambers were tried in an analysis by a statistical expert, J. W. Müller of the Bureau International des Poids et Mesures (International Bureau of Weights and Measures) in Sèvres, France. The essential result of this analysis was that uniform corrections, for example uniform $W_n/W_{(3)^Y}$ ratios, helped very little. This was a surprise. Ranking analysis (ranking in the sense of determining which laboratory tends to read high on all eleven measurements conditions, and which laboratories tend to read low) was tried by Goodman[10] and showed groups of 11 laboratories with similar results containing 1,2,6,2 laboratories in the sense from high reading to low reading. That is, one laboratory tended to read significantly higher than all others, then a group of two read somewhat lower, etc. This analysis was carried out on the response of the chamber with the correction factors removed, and showed that there are systematic procedure differences between laboratories--that is the laboratories do not get the same "dial reading" for similar instruments in a given radiation field.

ENDIP Intercomparison

Some preliminary results for the ENDIP Intercomparison, are shown in Figure 10.[4] These measurements were carried out at GSF-Neuherberg in 1975, the example here being for 15.1 MeV. An analysis of these results is shown in Table 2. Note in this case the better agreement in air at the low neutron energies, and also that the 3% spread has not been achieved. Table 3 compares the results by 3 participants, TNO, GSFM, and CENF who par-

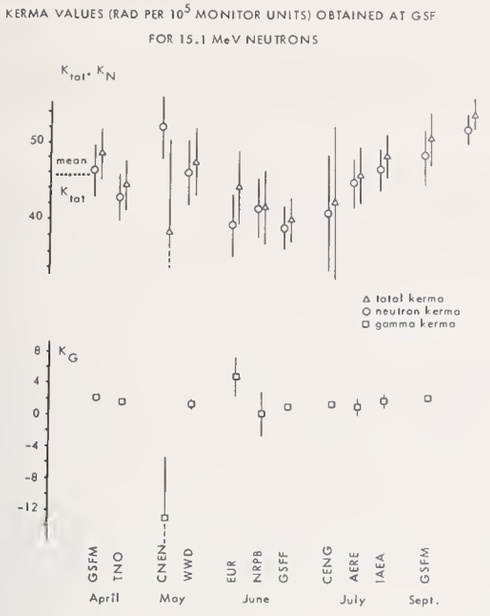

Fig. 10. Results of ENDIP comparison measurements for 15.1 MeV neutrons carried out at GSF-Neuherberg, West Germany in 1975.

TABLE 2
NUMBER OF GROUPS ENDIP-GSF WITH RELATIVE DIFFERENCE, Δx, FROM THE MEAN

Neutron energy		$\Delta x \leq 5\%$	$5\% < \Delta x \leq 10\%$	$\Delta x > 10\%$
15.1 MeV	K_N	5/11	3/11	3/11
	K_{tot}	5/11	3/11	3/11
5.25 MeV	K_N	7/10	2/10	1/10
	K_{tot}	8/10	2/10	0/10
2.1 MeV	K_N	9/11	0/11	2/11
	K_{tot}	9/11	1/11	1/11
0.57 MeV	K_N	9/11	0/11	2/11
	K_{tot}	9/11	1/11	1/11
^{252}Cf neutrons	K_N	7/8	1/8	0/8
	K_{tot}	8/8	0/8	0/8

TABLE 3
VALUES OF ABSORBED DOSE AND KERMA (RELATIVE TO THE MEAN) AS DETERMINED BY THREE PARTICIPANTS AT GSF AND TNO FOR 15 MeV NEUTRONS

Conditions		TNO	GSFM	CENF
GSF, free in air	K_N	0.97	1.08	1.17
	K_{tot}	0.97	1.08	1.17
TNO, free in air	K_N	0.99	1.05	1.05
	K_{tot}	1.00	1.06	1.05
TNO, 5 cm depth	D_N	0.94	1.06	1.11
	D_{tot}	0.94	1.08	1.10
TNO, 10 cm depth	D_N	0.94	1.05	1.11
	D_{tot}	0.94	1.07	1.10
TNO, 20 cm depth	D_N	0.91	1.05	1.17
	D_{tot}	0.94	1.07	1.14

ticipated at both radiation facilities. The apparent difference between these three laboratories, which is consistent throughout the measurements, has not been resolved satisfactorily to my knowledge.

Radiotherapy Center Comparison

The Radiotherapy Center comparison was carried out in the Spring of 1974 between three U. S. Radiotherapy Centers and the Medical Research Council-Hammersmith Hospital facility in London. The results are given in Table 4.[8] Note the high degree of agreement between the three U. S. therapy centers (University of Washington, U of W; Naval Research Laboratory, NRL; and M.D. Anderson Hospital - Texas A&M Variable Energy Cyclotron, TAMVEC). The lower reading of MRC was later adjusted upward by 8% in January 1975. The measurements at depths in phantom are largely consistent with the measurements in air. Further laboratories were brought into this intercomparison in the Autumn 1975 and February 1976. (See Table 5). These laboratories were CHHRI (Christie Hospital-Holt Radium Institute in England); Louvain, Belgium; and Chiba, Japan. Allowing for uniform parameters in the case of CHHRI, one can see that these laboratories are on a very closely uniform measurement system.

Conclusion

The Radiotherapy Centers, following the intercomparisons, are now largely on the same measurement scale which is well-known relatively, but not absolutely. It is the author's belief that more efforts in the laboratory are needed to correct possible systematic errors and to understand these consistent differences that appear from laboratory to laboratory throughout many different measurement conditions, before further international comparisons will be worthwhile. However, following an effort at eliminating systematic errors, international comparison would be justified to see if the attempted corrections of systematic errors have in fact worked. In view of the importance of this problem, it seems appropriate that the National Standards Laboratories should be developing standards and providing calibration services for neutron dosimetry. Such calibrations could follow three largely independent routes to see if the same calibration is achieved following each route. These routes are: (1) calibration of neutron dosimeters with known fluences of monoenergetic neutrons using kerma factors to obtain the dose (a subject very dependent on the work being discussed at this conference); (2) using a gamma-ray calibration of an ionization chamber and appropriate ratios of W, stopping power and kerma factors to determine the dose; and (3) use of a tissue-equivalent calorimeter with appropriate corrections for calorimetric defect to determine the dose or kerma in the radiation field.

Table 4. Intercomparison results: ratios of measurements with respect to TAMVEC measurements during the Spring of 1974.[8]

Participants	MRC / TAMVEC	U of W / TAMVEC	NRL / TAMVEC	U of W / TAMVEC	NRL / TAMVEC
Location	MRC	U of W	NRL	TAMVEC	TAMVEC
Beam	16 MeV d+Be	21.5 MeV d+Be	35 MeV d+Be	50 MeV d+Be	50 MeV d+Be
Tissue kerma in air	0.89[b]	1.04[a]	0.99	0.99	1.00
Dose at depth	0.86[c] @ d_{max} 0.86[d] @ 10 cm	1.01 @ d_{max} 1.02 @ 10 cm	0.99 @ d_{max} 0.99 @10 cm	0.99 @ 2 cm 0.99 @10 cm	0.99 @ 2 cm 0.98 @10 cm
Photon Calibration	1.01 (8 MeV)	1.01 (^{60}Co)	1.03 (^{137}Cs)	1.00 (^{60}Co)	0.99 (^{60}Co)

a Data suspicious owing to leakage problems.
b MRC excludes 3% gamma component
c MRC excludes 6% gamma component
d MRC excludes ~9% gamma component

Table 5. Intercomparison results: ratios of measurements with respect to TAMVEC measurements during the Autumn of 1975 and February 1976.[8]

Participants	CHHRI / TAMVEC	MRC / TAMVEC	NRL / TAMVEC	Louvain / TAMVEC	Chiba / TAMVEC	Chiba / TAMVEC
Location	CHHRI	MRC	NRL	Louvain	TAMVEC	TAMVEC
Beam	15 MeV d+T	16 MeV d+Be	35 MeV d+Be	50 MeV d+Be	30 MeV d+Be	16 MeV d+Be
Tissue kerma in air	0.95[a]	1.01	1.00		1.01	1.01
Dose at depth		0.97 @ 1 cm 0.96 @ 5 cm 0.97 @10 cm		1.02 @ 2 cm 1.02 @ 10 cm	0.97 @ 5 cm 0.96 @10 cm 0.97 @15 cm 0.96 @20 cm	
Photon Calibration			1.00 (^{137}Cs)	1.00 (^{60}Co)	0.99[b] (^{60}Co)	

a Choice of parameters account for 4% of the 5% difference (see text).
b Ratio of calbration made in Japan to calibration made at M.D. Anderson Hospital.

References

1. ICRU Report 29, An International Neutron Dosimetry Intercomparison, International Commission of Radiation Units and Measurements, Washington, D.C. 20014, U.S.A., to be published (1977).

2. R. S. Caswell, L. J. Goodman, and R. D. Colvett, International Intercomparison of Neutron Dosimetry, in Radiation Research, Biomedical, Chemical, and Physical Perspectives, O. F. Nygaard, H. I. Adler, and W. K. Sinclair, eds., Academic Press, New York (1975), p. 532.

3. L. J. Goodman, R. D. Colvett, and R. S. Caswell, An International Neutron Dosimetry Intercomparison, Proceedings of the Second Symposium on Neutron Dosimetry in Biology and Medicine, Commission of the European Communities, Luxembourg (1975), p. 627.

4. J. J. Broerse, G. Burger, and M. Coppola, Basic Physical Data for Neutron Dosimetry, J. J. Broerse, ed., Commission of the European Communities, Luxembourg (1976), EUR 5629e, p. 257.

5. Basic Physical Data for Neutron Dosimetry, (op. cit.), p. 243.

6. Basic Physical Data for Neutron Dosimetry, (op. cit.), p. 249.

7. A. R. Smith, P. R. Almond, J. B. Smathers, V. A. Otte, F. H. Attix, R. B. Theus, P. Wootton, H. Bichsel, J. Eenmaa, D. Williams, D. K. Bewley, and C. J. Parnell, Medical Physics, 2, 195 (1975).

8. Basic Physical Data for Neutron Dosimetry, (op. cit.), p. 267.

9. E. B. Wagner and G. S. Hurst, Health Physics 5, 20 (1961).

10. Basic Physical Data for Neutron Dosimetry, (op. cit.), p. 219.

REACTOR CORE DOSIMETRY STANDARDS

Willem L. Zijp
Netherlands Energy Research Foundation, ECN
1755-ZG Petten (NH), The Netherlands

Reactor neutron metrology serves to determine directly flux densities, fluences, spectra, and indirectly effects like burn-up, depletion and displacements. There are tendencies to require an accuracy of 2 to 5%. This gives requirements for the accuracy of nuclear data, of which the cross section data are most important.
Average fission neutron cross sections for many reactions of interest are at present not accurate enough, owing to inadequacy of the spectral cross section data and to inadequacy of the knowledge of the fission neutron spectrum of ^{235}U above about 8 MeV.
More experiments in benchmark fields, performed in interlaboratory experiments and in international collaboration are necessary to arrive at accuracies specified in reactor development programs.

(Comparative evaluation; cross sections; fission spectra; integrals; neutrons; radioactivation; resonance integrals; spectral functions)

Purpose of in-core reactor metrology

Reactor neutron metrology performed inside research and power reactors provides numerical information on flux density values, fluence values and spectrum data for many purposes. This information is of the primary type. Information which can be derived from these source data are e.g. burn-up values, displaced atoms, helium production, and transmutation rates.
For providing these secondary data one often needs full information of the primary type, and a theoretical model for the way of interaction under consideration. Since often the interaction of interest (e.g. displacements) is a spectrum dependent function, one then needs spectrum information. The interest in in-core metrology data can be categorized with respect to the materials.

1. Fuel material: Of importance is here the fission rate density (i.e. the number of fissions per unit volume) and its distribution axially (vertically) along the fuel rods (or plates), and radially (horizontally) within these rods (or plates), and its distribution over a cluster of fuel rods (or a fuel assembly), and from cluster to cluster (or assembly to assembly).
Flux density mapping over the fuel core is needed to:
- check the assumed flux density pattern macroscopically over the fuel region;
- check the assumed flux density pattern microscopically in a restricted region;
- locate the positions with peak values of the flux density (detection of possible hot spots);
- calculate the heat dissipation in specified fuel regions.

Localized flux density measurements are required to provide information on local flux density values (e.g. for radionuclide production, in irradiation facilities, or any other accessible location).
Apart from these interests, from the point of view of smooth and optimized reactor operation, there are the interests from the point of view of research and development of new types of fuels.
Here measurements are desired to determine the changes in the characteristics of fuel samples (due to irradiation under severe test conditions).

2. Fuel cladding material: Of main importance is here the determination of radiation damage effects in fuel cladding after long irradiations, i.e. after large incident neutron fluences.
Results of irradiation of test samples are used to predict the radiation damage occurring when the sample material is irradiated at an other location (often a longer irradiation in a smaller flux density) in a comparable neutron spectrum.

3. Structural materials: This category comprises reflector materials (such as graphite in a HTGR) and materials for reactor tanks and reactor pressure vessels. Here one needs to know how long the materials can be positioned at a certain location in a reactor of given type, before deleterious radiation induced property changes prohibit further use.
Nowadays much money and effort is spent to reactor pressure vessel surveillance programs, since the useful lifetime of such a vessel is an economic issue of first importance.
The damage effects in graphite and steels are mainly induced by fast neutrons, i.e. neutrons with energies larger than say 10 keV.
Since thermal nuclear reactors are being sold by many vendors to utility companies, there is a need for a good surveillance metrology and for national and international standards for execution of such a dosimetry at an internationally accepted level.

Accuracies required

In practical applications of reactor neutron metrology the neutron spectrum is not a goal in itself; it serves as a tool to calculate integral effects (reaction rates, burn-up, radiation damage effects) which in general are not directly measurable.
The accuracies in neutron metrology are set by the accuracies for the integral quantities of final interest. The 1973 Consultants Meeting[1] mentioned that in special cases like fuel irradiations and graphite irradiations in high temperature gas cooled reactors, accuracies to 5% or better may be needed.
The following remarks are based on the conclusions of the IAEA Consultants Meeting in 1976[2]. For most applications at present the reached accuracies are in the range from 5 to 10%. In some cases, required accuracies have recently been re-evaluated to more stringent specifications, partly also as consequence of improved understanding of the damage functions. These requirements are reflected in target accuracies to be set for neutron field determination for the three categories of benchmark fields discussed further on.
At the 1975 Petten Symposium these accuracy requirements were stated[3] to be in the range from 2 to 5% for fast breeder reactor, and somewhat less stringent for light water reactors and controlled thermonuclear reactors.
Present state-of-the art accuracies are estimated to be in the range of 2 to 30%. The 2 to 5% goal objective may be considered ambitious for some applications, it is nevertheless reasonable.

At least on the long term most reactor fuel and materials development programs will not accept an uncertainty larger than 5%. In order to achieve such an accuracy routinely, however, it is necessary to work towards a better level of accuracy, namely 2 to 5%.

Role of nuclear data

Threshold reactions commonly used to determine fast neutron fluences are $^{58}Ni(n,p)$, $^{54}Fe(n,p)$, $^{46}Ti(n,p)$, $^{63}Cu(n,\alpha)$. If the neutron spectrum is unknown, one cannot define effective cross sections to arrive at fluences of neutrons with energies above 0.1 or 1 MeV (or any other energy bound). One can only define an equivalent fission neutron fluence, by using a cross section averaged over the fission neutron spectrum.
The accuracy of the average cross section values determine directly the accuracy of the equivalent fission neutron fluences. Activation detectors with cross section curves approximating a step function with the step at 1 or 0.1 MeV are not readily available.
The most interesting reaction in this respect is $^{93}Nb(n,n')$, but there are still some practical problems with this reaction[4]. It has been recognized that for radiation damage studies reporting of equivalent fission neutron fluences only is often not sufficient. More information is required, either in the form of spectrum information, or in the form of displacements per atom, calculated using an assumed spectrum and an accepted damage model.
Neutron spectrum measurements using activation techniques and unfolding programs have been reviewed elsewhere[5]. For this purpose accurate energy dependent cross section data for a series of detectors must be available.
Displacements can easily be calculated when so-called damage cross sections are available, derived from such an accepted displacement model[29].

Damage cross sections

At an IAEA Specialists Meeting on Irradiation Damage Units, held in Harwell, November 2-3, 1976 the present status of damage cross sections was discussed. Comparison has shown that two sets of damage energy cross sections for Fe, Cr and Ni (and hence steels) based on the UKNDF file and the ENDF/B-IV file agree within adequate accuracy, when applied to fission reactor spectra.
The agreement for Ni and Fe is within a few per cent; the agreement for Cr is somewhat poorer, but the discrepancy is negligible in applications to stainless steels.
Direct integral measurements of damage effects in graphite are possible with the so-called GAMIN detectors[28]. These detectors consist essentially of a small graphite cylinder between two nickel activation detectors. By determining after irradiation the change in electrical resistivity in the graphite cylinder, and the incident neutron fluence on the nickel foil, one can derive an index Φ_G/Φ_{Ni} (=graphite damage fluence/nickel fluence). Using the GAMIN technique the damage-to-activation ratio has been determined experimentally in many research reactors in the Euratom Community. Available experience show that within roughly 10% these measured integral effects agree with calculated effects using damage cross sections and available spectrum information.

Thermal and intermediate energy regions

Much attention has been paid in the past few years to develop neutron metrology methods related to fast reactor neutron spectra.
Apart from this development work there remain still problems related to improvement of techniques for measurements of thermal and intermediate neutrons with capture reactions (selfshielding effects; flux perturbation effects; resonance structure studies; gamma sensitivity of self powered neutron detectors; influence of cadmium or boron carbide covers of activation foils).
Also in these studies the cross section data play an important role.

Fast energy region

The main uncertainties in nuclear data are in general related to the fast neutron cross section data.
At the 1975 Petten Symposium Paulsen and Magurno[6] concluded that the situation in the field of spectral cross section data for reactor radiation measurements is still unsatisfactory with respect to accuracy and completeness. As reasons for this unsatisfactory situation the 1973 Consultants Meeting[1] recognized the following reasons:

a. The lack of agreement for a limited set of reactions on which all measuring efforts should be concentrated;
b. The failure to concentrate the differential measurements on the most sensitive energy region for dosimetry purposes;
c. The lack of a sufficient number of laboratories equipped with accelerators which can produce monoenergetic neutrons in the 6 to 12 MeV region, and which are used for neutron measurements.

Since then much attention was paid to the development of a consistent set of cross section data and to the set-up of benchmark experiments.

Reference set of cross sections

The ENDF/B-IV dosimetry file[7,8] is now generally available and has been adopted for international comparisons as a reference cross section set. All users are requested to communicate their experience with this data file, so that future improvements aid to the aim of arriving at one generally accepted, internally consistent and extended dosimetry data file.
The dosimetry reactions have been classified in two categories[2]. Category I reactions are defined as reactions:

a. for which the energy dependent cross sections are well known over their response ranges in standard neutron fields;
b. for which calculated reaction rates in the standard neutron fields are consistent with the measured reaction rates.

The following reactions belong to category I:
$^{197}Au(n,\gamma)^{198}Au$, $^{239}Pu(n,f)$, $^{237}Np(n,f)$, $^{238}U(n,f)$, $^{56}Fe(n,p)^{56}Mn$, $^{27}Al(n,\alpha)^{24}Na$, $^{63}Cu(n,2n)^{62}Cu$ and $^{58}Ni(n,2n)^{57}Ni$. (Remark: for the (n,2n) reactions with very high threshold energies, accuracies of about 10% are presently acceptable).
A number of other reactions are considered category I candidates: $^{59}Co(n,\gamma)^{60}Co$, $^{238}U(n,\gamma)^{239}U$, $^{115}In(n,n')^{115}In^{m}$, $^{58}Ni(n,p)^{58}Co$, $^{32}S(n,p)^{32}P$, $^{54}Fe(n,p)^{54}Mn$ and $^{59}Co(n,\alpha)^{56}Mn$.
All other reactions used for neutron metrology are category II reactions.

Decay data

Apart from neutron cross section data, also other nuclear data play an important role in neutron detection: half-lives, decay schemes, gamma abundances, fission product yields etc.

Role of benchmark fields

The 1976 Consultants Meeting[2] identified three types of benchmark neutron fields for reactor dosimetry:

1. Standard field: A permanent and reproducible neutron flux intensity, energy spectra and angular flux density distributions characterized to state-of-the art accuracy (Examples: thermal Maxwellian spectrum; epithermal 1/E spectrum; ^{252}Cf spontaneous fission neutron spectrum).

2. Reference field: A permanent and reproducible neutron field, less well characterized than a standard field, but accepted as a measurement reference by a community of users. (Examples: ^{235}U thermal fission neutron spectrum; the spectra in facilities like ΣΣ, ISNF, Big Ten, Tapiro, CFRMF; shielding benchmarks using a Fe-block or a Na-block).

3. Controlled environment field: A neutron field, physically well-defined and with some spectrum definition, employed for a restricted set of validation experiments. (Examples: HFIR; BSR; BR-2 Cd loops; HFR; reactor pressure vessel mock-ups; cores of ECEL, EBR-II).

In reactor neutron metrology benchmark fields serve three general objectives[2]:
- validation and/or calibration of experimental techniques;
- validation and/or improvement of cross section data and other nuclear data for proper application of experimental techniques;
- validation and/or improvement of analytical methods needed to extrapolate dosimetry data from a monitoring or surveillance position to the location of interest.

The highest priority is given to the second purpose, which includes more specifically[9]:
- establishment of high accuracy, consistent cross section data for basic integral detectors;
- spectrum dependence of fission yields;
- validation of resonance and threshold detectors for use in neutron fields where differential microscopic data may be inadequate;
- activation detectors for which energy dependent cross section data are uncertain.

Fission spectrum representation

For the calculation of equivalent fission neutron fluences one needs the values for the cross sections of the activation (or fission) detectors used, and in particular the cross section averaged over a fission neutron spectrum.
For the fission neutron spectrum of ^{235}U several analytical representations have been used in the past years.
In the following expressions, which have been normalized to a value of unity, E denotes the neutron energy, expressed in MeV:
- the formula proposed by Watt[10]
  $X_1(E) = 0.48395 \exp(-E).\sinh\sqrt{2E}$
- the formula proposed by Cranberg, Frye et al.[11]
  $X_2(E) = 0.45274 \exp(-E/0.965).\sinh\sqrt{2.29E}$
- the formula of Maxwellian type proposed by Leachman[12]
  $X_3(E) = 0.76985 \exp(-E/1.29).\sqrt{E}$
- the modified Watt-Cranberg formula proposed by Wood[13]
  $X_4(E) = 0.5827 \exp(-0.992E).\sinh(1.27\sqrt{E})$

The IAEA Consultants Meeting on prompt fission neutron spectra[14], held in 1971, concluded that a simple Maxwellian form does not satisfactorily fit all observed fission spectra.
It was felt then that for the present a purely numerical representation of experimental results would be best. Magurno and Ozer[7] tested the data on the ENDF/B-IV dosimetry file also by calculating spectrum averaged cross section using the Maxwellian spectrum function:
$X_5(E) = 0.770.\sqrt{E}.\exp(-E/T)$
using
T = 1.29 MeV and T = 1.32 MeV.

Recently Grundl and Eisenhauer[15,16] from the National Bureau of Standards made a new evaluation, based on 16 documented differential spectrometry measurements of the thermal neutron induced ^{235}U fission neutron spectrum, and of the ^{252}Cf spontaneous fission neutron spectrum. Their results can be described in three forms:
- A reference Maxwellian representation, obtained from a weighted least squares fit in the energy range from 0.25 MeV to 8 MeV.
  For ^{235}U : $M(E) = 0.7501.\sqrt{E}.\exp(-1.50E/1.97)$.
  For ^{252}Cf: $M(E) = 0.6672.\sqrt{E}.\exp(-1.50E/2.13)$.
- A seven-group spectrum of adjusted Maxwellian segments, which fit the data over all energies. Estimated uncertainties are 1% to 4% for both spectra between 0.25 and 8 MeV and between 5 and 15% outside this energy range.
- A continuous line segment correction to the reference Maxwellian, which establishes a final fit to the experimental data:
  $X(E) = \mu(E).M(E)$
  Below 6 MeV the correction function $\mu(E)$ is linear, above 6 MeV it is exponential. The correction functions for the two spectra are as follows:

energy interval (in MeV)	$\mu(E)$ for ^{235}U	$\mu(E)$ for ^{252}Cf
0 to 0.25	1+0.800E-0.153	1+1.200E-0.237
0.25 to 0.8	1-0.140E+0.082	1-0.140E+0.098
0.8 to 1.5	1+0.040E-0.062	1+0.024E-0.0332
1.5 to 6.0	1+0.010E-0.027	1+0.0006E+0.0037
6.0 to ∞	1.043{exp-0.06× (E-6.0)/1.043}	1.0 exp{-0.03× (E-0.60)/1.0}

Similar representations have been tried for the spontaneous fission neutron spectrum of ^{252}Cf:
- A formula proposed by Knitter et al[17], using a Maxwellian function with an average energy <E>=2.13 MeV;
- A more complicated function used by Green[18], based on a detailed evaporation model, and yielding an average energy <E>=2.105 MeV.

The choice of the representation of the fission spectrum may not be so important for activation reactions with low thresholds, but it becomes important when reactions with very high threshold (say about 10 MeV) are considered.
As can be seen from table 1 the different representations of the ^{235}U fission neutron spectrum give clearly different results for reactions with very high threshold energy. The Euratom Working Group on Reactor Dosimetry noted that the fission neutron spectrum in the energy region above 8 MeV is only known with an accuracy of the order of 25%.
For the application of reactions with high thresholds and for the prediction of helium production by (n,α) reactions the knowledge of the fission neutron spectrum should be improved.

Quality of integral cross section data

Integral experiments to determine σ_o (the 2200 m/s value), I (the resonance integral) and $\langle\sigma_f\rangle$ (the cross section averaged over the fission neutron spectrum) have been performed by experienced people in recognized laboratories.

The values for σ_0, I and $\langle\sigma_f\rangle$ which can be derived from the ENDF/B-IV dosimetry file[8] have been compared in tables 2, 3, 4 and 5 with evaluated or experimental data in recent compilations.
For the fission neutron spectra of ^{235}U and ^{252}Cf the NBS evaluations of Grundl and Eisenhauer[15,16] were used.
A rough estimation on the quality can be based on three aspects: the uncertainty in the measurement, and the accuracy (or bias) and the consistency of the evaluated values. As a measure for the experimental uncertainty serves the quoted fractional error, v. As a measure of the accuracy serves the absolute value of the fractional difference Δ between (evaluated) experimental error and the calculated value from the cross section file. As a measure of the consistency between (evaluated) experimental value and the calculated value serves the ratio of the fractional difference and its stated fractional error v.
The following indications are used in the tables:

category	uncertainty	accuracy	consistency
++	$0 < v < 2\%$	$0 < \Delta < 2\%$	$0 < \Delta/v < 1$
+	$2\% < v < 4\%$	$2\% < \Delta < 4\%$	$1 < \Delta/v < 2$
o	$4\% < v < 6\%$	$4\% < \Delta < 6\%$	$2 < \Delta/v < 3$
-	$6\% < v < 8\%$	$6\% < \Delta < 8\%$	$3 < \Delta/v < 4$
--	$10\% < v$	$10\% < \Delta$	$5 < \Delta/v$

The data for the fission neutron spectra are taken from recent reviews by Fabry et al[19,20].
The normalization adopted involves a so-called flux transfer, using the $^{239}Pu(n,f)$ reaction and the NBS ^{252}Cf source. This californium source was chosen because of its availability and its well known source strength (error 1.1%). The $^{239}Pu(n,f)$ reaction was chosen because of its relatively flat shape in the energy range of interest and its well known cross section.
It has been concluded by Fabry, McElroy et al[20] that integral cross section data for dosimetry reactions as measured in standard and reference benchmark neutron fields depart from computed ones, not only because of differential energy cross section inadequacies, but also because the spectral shapes characteristic of these benchmarks are usually inaccurate in the energy ranges not covered or poorly covered by differential neutron spectrum techniques, e.g.:
- below ≈250 keV and above ≈10 MeV for the fission neutron spectra of ^{235}U and ^{252}Cf;
- below ≈10 keV and above ≈2 MeV for ΣΣ, CFRMF, BIG-TEN.

The same authors conclude that even in the well covered energy ranges, the reliability remains questionable, as is presently the case for the ^{235}U fission neutron spectrum between 3 and 6 MeV, and for LFRMF between 100 and 400 keV.
The only benchmark whose spectral shape appears to be accurately established between ≈0.25 and ≈10 MeV is the ^{252}Cf neutron spectrum. The inconsistencies observed for some facilities like LFRMF and BIG-10 are mostly attributed to inaccurate spectral computations resulting from the inadequate ^{235}U fission spectrum, and the inelastic scattering cross section data in ENDF/B-IV. This effect is less pronounced for ΣΣ, because the spectral characterization from ≈10 keV up to ≈2 MeV mostly relies on differential spectrometry measurements and not on computations[20].
The 1976 Consultants Meeting recommended that efforts should be made to remove inconsistencies between integral measurements and differential evaluations at least as concerns the ^{235}U fission spectrum, the ΣΣ type facilities and the ISNF, and the cross sections for $^{58}Ni(n,p)$, $^{235}U(n,f)$, $^{59}Co(n,\gamma)$, $^{115}In(n,n')$, $^{54}Fe(n,p)$, $^{103}Rh(n,n')$, so as to qualify them as standard spectra and category I reactions respectively.

Improvement of consistencies

The consistency between measured and calculated reaction rates may be influenced by various effects or procedures:
- The group structure chosen for presentation of the final spectrum;
- The discontinuity or extrapolation at the lower and upper energy bounds of the spectrum;
- The group structure of the cross section libraries, and especially the detailed structure in the resonance region (e.g. important for (n,γ) reactions);
- The adjustments sometimes made to a spectrum from reactor physics calculations to obtain a better fit for experimental data;
- The accuracy and precision of the experimentally determined reaction rates;
- The perturbation of the neutron field by the presence of one or more activation and fission detectors, or their encapsulations;
- The uncertainty in the selfshielding effect in the activation and fission detector applied.

The present situation of the cross sections for reactor radiation measurements can be improved by a series of actions:
- Application of recommended evaluated cross section libraries, both in reactor physics calculations and in spectrum unfolding;
- Application of a reference group structure and application of recommended procedures for arriving at other group structures or a series of point values;
- Recalculation of neutron spectra using well established reactor physics computer programs under well defined and improved conditions;
- Selection of a few well known spectra (serving as benchmark spectra) with different shapes;
- Careful definition of the neutron spectra in the benchmark facilities;
- Accurate determination of experimental activities, using enlarged series of detectors;
- Adoption of agreed procedures for adjustment and extrapolation of neutron spectra based on reactor physics calculations;
- Intercalibration of counting equipment, based on distribution of calibrated radionuclide samples;
- Adoption of agreed nuclear data (half-lives, decay schemes, gamma abundances, fission product yields, etc.).

It will be clear that several parallel actions are necessary to arrive at the desired accuracies within a few years.

Current international efforts

The actions mentioned above are being discussed in several international meetings (the IAEA Consultants Meetings in 1973 and 1976; the regular meetings of the Euratom Working Group on Reactor Dosimetry; the annual meetings of the IAEA Working Group on Reactor Radiation Measurements; the IAEA Specialists Meeting on Radiation Damage Units in 1976; the ASTM-Euratom symposium on Reactor Dosimetry, held in 1975 at Petten, and the next one scheduled for October 1977 in the USA).
Owing to intensive international contacts the following progress results can be mentioned:
- the acceptance and the availability of the ENDF/B-IV dosimetry file as a reference data set for reporting and comparing obtained results;
- the acceptance of a list of dosimetry reactions in categories I and II;
- the acceptance of the IAEA program on Benchmark Neutron Fields Applications for Reactor Dosimetry;
- the recommendation for international interlaboratory studies like the Interlaboratory Reaction Rate Pro-

gram in the USA;
- the definition of a few selected standard neutron fields and revision of the list of category I reactions;
- the acceptance of a few radiation damage models for the calculation of the number of displaced atoms;
- the recommendation by the Euratom Working Group to apply the EURLIB 100 groups structure (very similar to the DLC 100 groups structure) as reference both for shielding and reactor metrology work;
- the exchange of technical information at the open biannual ASTM-Euratom symposia on Reactor Dosimetry;
- the quick exchange of items of interest through the Euratom Newsletter on Reactor Radiation Metrology;
- the intercomparison of some promising neutron spectrum unfolding codes;
- the IAEA intercomparison of computer programs for analyzing Ge(Li) gamma ray spectra;
- the international intercomparison of gamma emission rates of ^{152}Eu sources.

Conclusions

1. Different reactor development programs require accuracies in integral data (fission rates, burn-up, fluences, damage effects) of 2 to 5%.

2. An internationally accepted starting point for data treatment in neutron metrology work is the ENDF/B IV dosimetry file, which has been made available in a world-wide scale through the four nuclear data centres (Brookhaven, Saclay, Vienna, Obninsk).

3. Appreciable discrepancies exist between measured and calculated average cross section values in the ^{235}U fission neutron spectrum. The representation of the high energy tail (above ≈8 MeV) of this spectrum needs further study.

4. Dosimetry reactions in categories I and II, and classes of benchmark neutron fields have recently been reviewed by the IAEA 1976 Consultants Meeting. The accepted tables constitute the basis for a critical analysis of integral measurement data which is or becomes available.
The benchmark field approach can serve to detect discrepancies and inconsistencies, to arrive at a better quality of cross section data, and to improve spectrum determinations by the unfolding technique.
Many integral experiments in several benchmark fields, based on interlaboratory and international cooperation are needed to arrive at the requested accuracies of 2 to 5%.

References

1. VLASOV, M.; DUNFORD, C.: "Proceedings of a Consultants' meeting on nuclear data for reactor neutron dosimetry", held in Vienna, 10-12 September 1973. INDC(NDS)-56/U (IAEA, Vienna, 1974).

2. VLASOV, M.: "IAEA Consultants'Meeting on integral cross section measurements in standard neutron fields", held in Vienna 15-19 November 1976. Summary report, conclusions and recommendations, Report INDC(NDS)-81/L+DOS (IAEA, Vienna, 1977).

3. McELROY, W.N.; BENNETT, R.A.; JOHNSON, D.L.; DUDEY, N.D.: "Neutron environmental characterization requirements for reactor fuels and materials development and surveillance programs"
Proc. 1st ASTM-Euratom Symposium on Reactor Dosimetry, Petten, 22-26 September 1975.
HEDL-SA-911.

4. LLORET, R.: "Application de la réaction ^{93}Nb(n,n') à la dosimétrie des irradiations de matériaux"
Proc. 1st ASTM-Euratom Symposium on Reactor Dosimetry, Petten, 22-26 September 1975.

5. ZIJP, W.L.: "Review of activation methods for the determination of neutron flux spectra"
Report RCN-241 (Netherlands Energy Research Found., Petten, 1976).
Also proc. 1st ASTM-Euratom Symposium on Reactor Dosimetry, Petten, September 22-26 1975.

6. PAULSEN, A.; MAGURNO, B.A.: "Differential neutron data for reactor dosimetry"
Proc. 1st ASTM-Euratom Symposium on Reactor Dosimetry, Petten, 22-26 September 1975.

7. MAGURNO, B.A.; OZER, O.: "ENDF/B-IV file for dosimetry applications"
Nuclear Technology 25 (1975), 376.

8. MAGURNO, B.A.: "ENDF/B-IV dosimetry file"
BNL-NCS-50446 (April 1975).

9. GRUNDL, J.; EISENHAUER, C.: "Benchmark neutron fields for reactor dosimetry"
Paper presented at IAEA Consultants'Meeting on Integral Cross Section Measurements in Standard Neutron Fields for Reactor Dosimetry, Vienna, November 15-19, 1976.

10. WATT, B.E.: "Energy spectrum of neutrons from thermal fissions of ^{235}U"
Phys. Rev. 87 (1952), 1037.

11. CRANBERG, L.; FRYE, G.; NERESON, N.; ROSEN, L.: "Fission neutron spectrum of ^{235}U"
Phys.Rev. 103 (1956), 662.

12. LEACHMAN, R.B.: "Determination of fission quantities of importance to reactors"
Proc. Int. Conf. on Peaceful Uses of Atomic Energy, Geneva, 1955, Vol. 2 (1956), 193.

13. WOOD, J.: "The fission neutron spectrum of ^{235}U"
J. Nuclear Energy 27 (1973), 591-595.

14. "Prompt fission neutron spectra"
Proceeding of a Consultants'Meeting on prompt fission neutron spectra (IAEA, Vienna, 1972).

15. GRUNDL, J.A.; EISENHAUER, C.M.: "Fission spectrum neutrons for cross section validation and neutron flux transfer"
Conf. on Nuclear Cross Sections and Technology, Washington D.C. (March 1975).

16. GRUNDL, J.A.; EISENHAUER, C.M.: "Fission rate measurements for materials neutron dosimetry in reactor environments"
Proc. 1st ASTM-Euratom Symposium on Reactor Dosimetry, Petten, 22-26 September 1975.

17. KNITTER, H.H.; PAULSEN, A.; LISKIEN, H.; ISLAM, M.M.: "Measurements of the neutron energy spectrum of the spontaneous fission of ^{252}Cf"
Atomkernenergie 22 (1973), 84.

18. GREEN, L.; MITCHELL, J.A.; STEEN, N.M.: "The californium 252 fission neutron spectrum from 0.5 to 13 MeV"
Nucl. Sci. Eng. 50 (1973), 257.

19. FABRY, A.; CEULEMANS, H.; VAN DE PLAS, P.; McELROY, W.N.; LIPPINCOTT, E.P.: "Reactor dosimetry integral reaction rate data in LMFBR benchmark and standard neutron fields: status, accuracy and implications"
Paper presented at 1st ASTM-Euratom Symposium on Reactor Dosimetry, Petten, September 22-26, 1975.

20. FABRY, A.; McELROY, W.N.; KELLOGG, L.S.; LIPPINCOTT, E.P.; GRUNDL, J.A.; GILLIAM, D.M.; HANSEN, G.E.: "Review of microscopic integral cross section data in fundamental reactor dosimetry benchmark neutron fields"

Paper presented at IAEA Consultants'Meeting on Integral Cross Section Measurements in Standard Neutron Fields, Vienna, November 15-19, 1976.

21. SHER, R.: "2200 m/s neutron activation cross sections"
Contribution to "Handbook on Nuclear Activation Cross Sections"
Technical Reports Series No 156 (IAEA, Vienna, 1974)

22. MUGHABGHAB, S.F.; GARBER, D.I.; "Neutron cross sections, Vol. I, resonance parameters"
BNL-325, Third edition, Vol. I (NNCS-BNL, June, 1973).

23. BIGHAM, C.B.: "The slow-neutron fission cross sections of the common fissile nuclides (revised 1975)"
Nucl. Sci. Eng. 59 (1976), 50-52.

24. ZIJP, W.L.; NOLTHENIUS, H.J.: "Comparison of integral cross section values of several cross section libraries in the SAND-II format"
Report ECN-2 (Netherlands Energy Research Foundation, Petten, 1976).

25. ALBINSSON, H.: "Infinite-dilution resonance integrals"
Contribution to "Handbook on Nuclear Activation Cross Sections"
Technical Reports Series No 156 (IAEA, Vienna, 1974).

26. SMITH, D.L.: "Evaluation of the $^{115}In(n,n')^{115}In^{m}$ reaction for the ENDF/B-IV dosimetry file"
Report ANL/NDM-26 (December 1976).

27. PHILIS, C.; BERSILLON, O.; SMITH, D.; SMITH, A.: "Evaluated (n,p) cross sections of ^{46}Ti, ^{47}Ti and ^{48}Ti"
Report ANL/NDM-27 (January 1977).

28. CANCE, M.; GENTHON, J.P.; MICAUD, G.; SALON, L.: "Le détecteur neutronique au graphite G.A.M.I.N. Etudes et applications à la dosimétrie des dommages radio-induits"
Report CEA-N-1823 (Saclay, January 1975).

29. GENTHON, J.P.; HASENCLEVER, B.W.; SCHNEIDER, W.; MAS, P.; WRIGHT, S.B.; ZIJP, W.L.: "Recommendations on the measurement of irradiation received by the structural materials of reactors"
EUR-5274 e,n,d,f (C.E.C., Luxembourg, 1975).

Table 1: Influence of representation of fission neutron spectrum of ^{235}U on average cross sections

Based on cross sections from the ENDF/B-IV dosimetry file, and data reported by Fabry et al [19],[20]. Cross section values are given in $fm^2(=10^{-30}m^2)$.

reaction	effective threshold energy (in MeV)	integral measurement σ_m (in fm^2)	ratio σ_c/σ_m		
			Maxwellian <E>=1.97 MeV	NBS-eval. <E>=1.98 MeV	Watt <E>=2.00 MeV
$^{237}Np(n,f)FP$	0.6	131.2	1.006	1.006	1.019
$^{58}Ni(n,p)^{58}Co$	2.8	10.85	0.926	0.936	0.947
$^{54}Fe(n,p)^{54}Mn$	3.1	7.97	0.965	0.975	0.984
$^{27}Al(n,p)^{27}Mg$	4.4	0.386	1.078	1.067	1.062
$^{56}Fe(n,p)^{56}Mn$	6.0	0.1035	1.081	1.017	1.000
$^{59}Co(n,\alpha)^{56}Mn$	6.8	0.0143	1.140	1.035	1.021
$^{27}Al(n,\alpha)^{24}Na$	7.2	0.0705	1.106	0.983	0.970
$^{127}I(n,2n)^{126}I$	10.5	0.105	1.499	1.130	1.094
$^{55}Mn(n,2n)^{54}Mn$	11.6	0.0244	1.426	1.004	0.951
$^{58}Ni(n,2n)^{57}Ni$	≈13.5	5.77×10^{-4}	0.776	0.489	0.440

Table 2: Comparison of 2200 m/s cross section values

Cross section values are expressed in units of 100 fm^2 (in $10^{-28}m^2$)

reaction	compilation value, σ_m			uncertainty		calculated value, σ_c ENDF/B-III [24]	σ_c/σ_m	accuracy	consistency
	IAEA-TR-156 [21]	BNL-325 [22]	BIGHAM [23]	(in %)					
$^{6}Li(n,\alpha)^{3}H$		940±4		0.4	++	923	0.982	++	--
$^{10}B(n,\alpha)^{7}Li$		3837±9		0.2	++	3770	0.983	++	--
$^{23}Na(n,\gamma)^{24}Na$	0.528±0.005	0.530±0.005		0.9	++	0.524	0.989	++	+
$^{45}Sc(n,\gamma)^{46}Sc$	25±2	26.5 ±1.0		3.7	+	25.9	0.977	+	++
$^{58}Fe(n,\gamma)^{59}Fe$	1.14 ±0.05	1.15±0.02		1.7	++	1.16	1.009	++	++
$^{59}Co(n,\gamma)^{60}Co$	37.5 ±0.2	37.2 ±0.2		0.5	++	36.6	0.984	++	-
$^{63}Cu(n,\gamma)^{64}Cu$	4.4 ±0.2	4.5 ±0.1		2.2	+	4.42	0.982	+	++
$^{115}In(n,\gamma)^{116}In^{m}$	161±5	157 ±15		9.6	--	164	1.045	o	++
$^{197}Au(n,\gamma)^{198}Au$	98.8 ±0.3	98.8 ±0.3	98.7 0.2	0.2	++	97.1	0.983	++	--
$^{232}Th(n,\gamma)^{233}Th$	7.4 ±0.1	7.40±0.08		1.1	++	7.26	0.981	++	+
$^{235}U(n,f)FP$	580 ±2	582.2±1.3	576.9 3.4	0.6	++	573	0.993	++	+
$^{237}Np(n,f)FP$		0.019±0.003		15.8	--	0.0163	0.857	--	++
$^{238}U(n,\gamma)^{239}U$	2.720±0.025	2.70 ±0.02		0.7	++	2.65	0.981	++	o
$^{239}Pu(n,f)FP$	742 ±3	742.5±3.0	742.8 4.4	0.6	++	730	0.983	++	o

Table 3: Comparison of cross sections, averaged over a 1/E neutron spectrum

Values of resonance integrals refer to a cadmium cut-off equal to 0.5 eV, and are expressed in units of 100 fm^2 ($10^{-28}m^2$).

reaction	compilation value, σ_m		uncertainty		calculated value, σ_c ENDF/B-IV [8],[22]	σ_c/σ_m	accuracy	consistency
	IAEA-TR-156 [25]	BNL-325 [22]	(in %)					
$^{6}Li(n,total\ He)$	-	-	-		425.87	-		
$^{10}B(n,total\ He)$	-	1722	0.3	++	1722.17	1.000	++	++
$^{23}Na(n,\gamma)^{24}Na$	0.31	0.311	3.2	+	0.346	1.113	--	-
$^{45}Se(n,\gamma)^{46}Sc$	11	11.3	8.8	-	11.29	0.999	++	++
$^{58}Fe(n,\gamma)^{59}Fe$	1.2	1.19	5.9	o	1.58	1.328	--	--
$^{59}Co(n,\gamma)^{60}Co$	75.0	75.5	2.0	++	76.67	1.015	++	++
$^{63}Cu(n,\gamma)^{64}Cu$	5.0	4.9	6.2	-	5.55	1.133	--	o
$^{115}In(n,\gamma)^{116}In^{m}$	2600	3300	3.0	+	3242.74	0.983	++	+
$^{197}Au(n,\gamma)^{198}Au$	1550	1560	2.6	+	1564.70	1.003	++	++
$^{232}Th(n,\gamma)^{233}Th$	82	85	3.5	+	85.58	1.007	++	++
$^{235}U(n,f)FP$	275	275	1.8	++	282.00	1.025	+	+
$^{238}U(n,\gamma)^{239}U$	280	275	1.8	++	277.53	1.009	++	++
$^{239}Pu(n,f)FP$	310	301	3.3	+	303.90	1.010	++	++

Table 4: Comparison of cross sections, averaged over the fission neutron spectrum of ^{235}U

Cross section values are expressed in units of $fm^2 (=10^{-30} m^2)$. Calculated values refer to the ENDF/B-IV dosimetry file and the NBS spectrum evaluation. Table is based on data reported by Fabry et al [19], [20].

reaction	effective threshold (in MeV)	integral measurement σ_m (in fm^2)	uncertainty (in %)		calculated value σ_c (in fm^2)	σ_c/σ_m	accuracy	consistency
$^{115}In(n,\gamma)^{116}In^m$	-	13.45	4.5	o	13.59	1.010	++	++
$^{197}Au(n,\gamma)^{198}Au$	-	8.35	6.0	o	8.46	1.013	++	++
$^{63}Cu(n,\gamma)^{64}Cu$	-	0.930	15.0	--	1.099	1.182	--	+
$^{235}U(n,f)FP$	-	120.3	2.5	+	124.1	1.032	+	+
$^{239}Pu(n,f)FP$	-	181.1	3.3	+	178.1	0.983	++	++
$^{237}Np(n,f)$	0.6	131.2	3.8	+	132.0	1.006	++	++
$^{103}Rh(n,n')^{103}Rh^m$	0.8	73.3	5.2	o	-	-		
$^{115}In(n,n')^{115}In^m$	1.2	18.9	4.2	o	16.68[a]	0.883	--	o
					18.90[b]	1.000	++	o
$^{232}Th(n,f)FP$	1.4	8.1	6.7	-	6.90	0.852	--	o
$^{238}U(n,f)FP$	1.5	30.5	3.3	+	29.58	0.970	+	++
$^{47}Ti(n,p)^{47}Sc$	2.2	1.90	7.4	-	2.14	1.126	--	+
					2.138[c]	1.125	--	+
$^{31}P(n,p)^{31}Si$	2.4	3.55	7.6	-	3.245[d]	0.914	-	+
$^{58}Ni(n,p)^{58}Co$	2.8	10.85	5.0	o	10.16	0.936	-	+
$^{64}Zn(n,p)^{64}Cu$	2.8	2.99	5.4	o	-	-		
$^{32}S(n,p)^{32}P$	2.9	6.68	5.5	o	6.41	0.960	+	++
$^{54}Fe(n,p)^{54}Mn$	3.1	7.97	6.1	-	7.77	0.975	+	++
$Ti(n,x)^{46}Sc$	3.9	1.18	6.4	-	0.999	0.847	--	o
					1.088[c]	0.922	-	o
$^{27}Al(n,p)^{27}Mg$	4.4	0.386	6.5	-	0.412	1.067	-	o
$^{56}Fe(n,p)^{56}Mn$	6.0	0.1035	7.2	-	0.1053	1.017	++	++
$^{59}Co(n,\alpha)^{56}Mn$	6.8	0.0143	7.0	-	0.0148	1.035	+	++
$^{63}Cu(n,\alpha)^{60}Co$	6.8	0.0500	11.2	--	0.0352	0.704	--	o
$^{24}Mg(n,p)^{24}Na$	6.8	0.148	5.5	o	0.1518[d]	1.026	+	++
$^{27}Al(n,\alpha)^{24}Na$	7.2	0.0705	5.7	o	0.0693	0.983	++	++
$^{48}Ti(n,p)^{48}Sc$	7.6	0.0300	6.0	o	0.0173	0.577	--	--
					0.0303[c]	1.010	++	++
$^{93}Nb(n,2n)^{92}Nb^m$	10.2	0.0475	6.7	-	-	-		
$^{127}I(n,2n)^{126}I$	10.5	0.105	6.2	-	0.1186	1.130	--	o
$^{55}Mn(n,2n)^{54}Mn$	11.6	0.0244	6.1	-	0.0245	1.004	++	++
$^{63}Cu(n,2n)^{62}Cu$	12.4	0.0122	9.8	--	0.00915	0.750	--	o
$^{90}Zr(n,2n)^{89}Zr$	≈13	0.0247	6.9	-	0.008714	0.353	--	--
$^{58}Ni(n,2n)^{57}Ni$	≈13.5	5.77×10^{-4}	5.4	o	2.82×10^{-4}	0.489	--	--

a) Magurno [8] reports a calculated value of 16.68 fm^2; our calculations yield 16.72 fm^2. These two values are clearly different from the value of 18.22 reported by Fabry [20]

b) Based on a recent evaluation by D.L. Smith [26] using a Maxwellian spectrum with <E> = 1.98 MeV.

c) Based on a recent evaluation by C. Philis et al. [27].

d) Cross section data not present in ENDF/B-IV dosimetry file; listed value has been taken from SAND-II cross section file.

Table 5: Comparison of cross sections, averaged over the fission neutron spectrum of ^{252}Cf

Cross section values are expressed in units of $fm^2 (=10^{-30} m^2)$. Calculated values refer to the ENDF/B-IV dosimetry file and the NBS spectrum evaluation.
Table is based on data reported by Fabry et al. [19], [20]

reaction	effective threshold (in MeV) a)	integral measurement σ_m (in fm^2)	uncertainty (in %)		calculated value σ_c (in fm^2)	σ_c/σ_m	accuracy	consistency
$^{115}In(n,\gamma)^{116}In^m$		12.53	3.4	+	13.03	1.040	+	+
$^{197}Au(n,\gamma)^{198}Au$		7.99	3.6	+	7.99	1.000	++	++
$^{235}U(n,f)FP$		120.3	2.5	+	124.1	1.033	+	+
$^{239}Pu(n,f)FP$		180.4	2.5	+	178.9	0.992	++	++
$^{237}Np(n,f)FP$	0.6	133.2	2.8	+	135.1	1.014	++	++
$^{103}Rh(n,n')^{103}Rh^m$	0.8	75.7	7.0	-	- b)	- 0.886 b)	--	--
$^{115}In(n,n')^{115}In^m$	1.2	19.8	2.5	+	17.55 b)	0.886 b)	--	--
$^{238}U(n,f)FP$	1.5	32.0	2.8	+	31.54	0.986	++	++
$^{47}Ti(n,p)^{47}Sc$	2.2	1.89	2.1	+	2.384 c)	1.261 c)	--	--
					2.422 c)	1.281 c)	--	--
$^{58}Ni(n,p)^{58}Co$	2.8	11.8	2.5	+	11.50	0.975	+	++
$^{54}Fe(n,p)^{54}Mn$	3.1	8.46	2.4	+	8.91	1.053	o	o
$^{46}Ti(n,p)^{46}Sc$	3.9	1.38	2.2	+	1.252 c)	0.907 c)	-	--
					1.381 c)	1.001 c)	++	++
$^{27}Al(n,p)^{27}Mg$	4.4	0.51	9.8	--	0.514	1.008	++	++
$^{56}Fe(n,p)^{56}Mn$	6.0	0.145	2.4	+	0.1475	1.017	+	++
$^{27}Al(n,\alpha)^{24}Na$	7.2	0.1006	2.2	+	0.1059	1.053	-	o
$^{48}Ti(n,p)^{48}Sc$	7.6	0.042	2.4	+	0.265 c)	0.630 c)	--	--
					0.0446 c)	1.062 c)	-	o
$^{55}Mn(n,2n)^{54}Mn$	11.6	0.058	10.3	--	0.0528	0.910	-	++
$^{59}Co(n,2n)^{58}Co$		0.057	10.5	--	0.0379	0.665	--	--
$^{63}Cu(n,2n)^{62}Cu$	12.4	0.030	10.0	--	0.02415	0.715	--	--

a) Threshold values are valid for a ^{235}U fission neutron spectrum.
b) Based on a recent evaluation by D.L. Smith [26].
c) Based on a recent evaluation by C. Philis et al [27].

STANDARDS FOR DOSIMETRY BEYOND THE CORE

Frank J. Rahn, Karl E. Stahlkopf and T. U. Marston
Electric Power Research Institute
Palo Alto, CA 94304

and

Raymond Gold and James H. Roberts*
Hanford Engineering Development Laboratory
Richland, WA 99352

Introduction

The need for well understood, standardized neutron dosimetry techniques is increasingly evident for several applications in thermal and fast reactors beyond the core region.[1] This need for dosimetry comes mainly from separate but related interests, namely: pressure vessel surveillance, materials testing, design and shielding requirements. The needs of the controlled thermo-nuclear program are addressed in another session of this symposium.

Objectives of Dosimetry

The problem of dosimetry for use in reactors (damage studies, irradiation experiments, shield assessment, reactor studies) is a very critical one that may influence the development of nuclear power. The self-consistency of calculated and dosimetrically derived flux and spectrum is of prime importance to the development of validated techniques for design, testing and licensing purposes.[2]

Dosimetry measurements serve the following objectives:

1) Surveillance of the safety and integrity of the pressure vessel of a nuclear steam supply (NSS) system.

2) Knowledge of the neutron fluence and spectrum for correlation with changes in properties in a materials test program.

3) Validation and/or calibration of experimental techniques.

4) Verification of analytical methods for predicting fluxes far from the core (in terms of a neutron's mean free path) for shielding purposes, sensitivity analyses,[3] channel theory,[4] etc.

There are many additional uses of dosimetry results.[5] Among these are:

1) choosing between two or more data sets,
2) identifying discrepancies and
3) improving (i.e., adjusting) cross sections.

These latter uses are generally controversial, and split the engineering and physics community. One hopes to identify discrepancies between integral and differential data and, if necessary, make adjustments in a self-consistent way. It is of prime importance to obtain the sensitivity of the integral results to uncertainties in the nuclear data.

To reach these objectives it is important that the cross section data for dosimetry reactions be integrally consistent and well-known.[6] Benchmark neutron fields are now classified according to guidelines first established at the Petten Symposium (1975):

> Standard: a permanent and reproducible neutron field with neutron flux intensity, energy spectra and angular flux distributions characterized to state-of-the-art accuracy. The main characterizations must be verified by interlaboratory measurements and calculations.
>
> Reference: a permanent and reproducible neutron field, less well-characterized than a standard, but accepted as a measurement reference by a community of users.
>
> Controlled Environment: a neutron field, physically well-defined and with some spectrum definition, employed for a restricted set of validation experiments.

Dosimetry and Benchmark Experiments

A conclusion of the recent IAEA Consultants' Meeting of Integral Cross Section Measurements in Standard Neutron Fields[1] is that spectrum averaged cross section data as measured in standard and reference benchmark neutron fields differ from computed ones, not only because of absolute flux and cross section inadequancies, but also because of uncertainties in observed spectra in most of these benchmarks. Uncertainties in spectral measurements stem from limitations in the energy range coverage in differential neutron spectra techniques.

In controlled environments, a combination of calculations, neutron differential spectrometry and integral measurements will be required for the determination of the spectra. The development of improved unfolding codes to handle the results of these techniques is desired.[8] The success of such techniques, however, will depend on the availability of data and analytical methods for handling errors and their correlation, i.e., not only cross section data files but also for spectrometry and reaction rate data. The total flux and spectral shape uncertainties for the important energy regions are currently estimated in the ± 5 to 15% (1σ) and ± 5 to 30% (1σ) range.[9] The current best estimates of the accuracy required for support of experimental out-of-core flux and spectral measurements are given in Table 1.

There is no current experimental technique which allows the determination of the entire spectrum to accuracy of $\pm 10\%$ (1σ) or better. Proton recoil, ^{6}Li and ^{3}He results, taken together, can approach the required accuracy in the energy range of a few keV to > 5 MeV. The state-of-the-art determination of spectrum requires the combined use of calculations, good unfolding techniques, and data from differential spectrometry and integral measurements.

*On leave from Macalester College, St.Paul, MN 55105.

Dosimetry Requirements for Design and Shielding

Dosimetry requirements for reactor applications can be quite stringent. The nature of the problems can be quite diverse and complex and is often related to specific designs. Situations can arise in which the uncertainties in calculations can lead to unacceptable constraints. If in an LWR, for example, the diameter of the pressure vessel is increased to mitigate radiation embrittlement of the steel, then the effects of dosimetry uncertainties can have a rather dramatic effect on the cost of the plant. If, in an existing plant, the dosimetry has unduly large uncertainties, then licensing and safety considerations may result in premature plant life and/or operating constraints. Many other examples exist. For instance, possible radiation effects on support plates and grids, fuel assemblies, and other core internals, especially in the design of fast reactors, can impact on the size of the pressure vessel required, pressure drop across the core, and in-vessel configuration.[10] Good dosimetry can also lead to the optimum location of low and intermediate power flux monitors and instrumentation.

There is presently a fairly disparate range of opinions as to the accuracies required for the dosimetry measurements. In part, this is due to the lack of consensus on the quantification of the design/experimental criteria and the diversity of the problems encountered. In addition to knowledge of the magnitude of the flux in some region outside the core, spectral information is usually required. This is true, for instance, of activation rates in control rod, drive mechanisms or for pressure vessel irradiation where both the flux and the spectrum (as related to either the activation cross section or some pseudo-damage cross sections) are required. Some typical target accuracies (2σ) required in power and experimental reactors[11] are:

1) Radiation Heating $\pm$20%
   a) thermal shields
   b) support plate
   c) control rods

2) Displacement Rates $\pm$15%
   a) reflector region
   b) support plate
   c) internal shields

3) Instrument & Control Tubes $\pm$15%

4) Activation $\pm$30%
   a) structural members
   b) coolant and coolant circuit
   c) components

5) Radiation Streaming $\pm$30%

Dosimetry Requirements in Operating Reactors

The reference experimental measurements planned on operating reactors generally fall into the category of controlled environment fields. An integral part of a dosimetry program is the comparison of the data with results from computer codes so as to produce a validated analytic method of estimating the flux and spectrum for streaming, damage, or activation purposes. There are also a series of computational benchmarks available which are intended to check the methodology, data and adequacy of the models used to calculate quantities of interest.

The purpose of reactor dosimetry programs outside the core is to obtain high accuracy and precision quantities which can be related to physical quantities of interest and which can be used to validate the calculational methodology.[12] This mandates that the neutron flux and spectrum be measured as the intermediary between the radiation exiting the core and the various quantities to be determined. One of the greatest needs for good dosimetry is for use in correlating material effects occurring in the pressure vessel of LWR's under irradiation.

The requirements for dosimetric measurements on operating and experimental reactors are:

(a) A relatively complete flux and spectrum mapping starting at the edge of the core through the outside edge of the pressure vessel. This should include detectors in the coolant gap radially outward from the core, and in a sufficient number of axial and azimuthal positions within the coolant region in order to assure complete knowledge of the neutron field at the pressure vessel. In addition, detectors should be positioned on both sides of the pressure vessel to measure the transmission and the change in spectrum in the steel. Such complete knowledge is required to validate the computational methods and to establish a self-consistent set of experimental points.

(b) The principal energy range of interest for dosimetry purposes is the range $0.1 \leq E \leq 10$ MeV. It is the neutrons in this energy range which are the greatest contributors to radiation embrittlement in steels. However, information on the spectra in the energy region $1 \leq E \leq 100$ keV is important for shielding problems due to the high transmission of neutrons through steel and sodium for these energies. The most important location for spectral measurements in this energy range is at the exit surface of the pressure vessel. At this point the usual calculational approach is to interface the 2D finite difference transport calculations used inside the pressure vessel with the 3D Monte Carlo and albedo scattering techniques used in the reactor cavity region. Flux and spectral measurements, then, in the 1 to 100 keV range are necessary to verify the deep penetration predictions and establish the source for the Monte Carlo simulations. Thermal flux measurements are usually required for activation considerations, and for corrections of the various detector responses to the fast flux.

    Using an LWR as an example for fast neutrons, the water gap is approximately 7 mean free paths (mfp) wide. For neutrons much below 1 MeV, the concept of spatial distances in terms of mean free paths is somewhat misleading, because the neutron density of these energies is due to high energy neutrons, undergoing collision and rapidly thermalizing. The pressure vessel is about 1.5 mfp wide for BWR's and 2.0 mfp wide for PWR's. At the inside edge of the pressure vessel, the expected flux (< 0.1 Mev) is approximately 3.6×10^9 n/cm^2/sec for a BWR and 1.4×10^{10} n/cm^2/sec for a PWR, for plants producing 3400 MWth and 3600 MWth, respectively.

(c) Practical considerations which determine the proper balance between desired accuracy and what is actually obtainable on commercial operating reactors. On such plants, operational considerations, accessibility and instrument locatability require very precise planning to

Table 1

Energy Range	Accuracy Required* (2σ) Standard** Radiation Field	Reference** Neutron Fields	Controlled Radiation Environment
thermal	>4% (4%)	≥10% (6%)	≥10% (10%)
0.414 eV - 1.0 keV	>10% (10%)	≥10% (≥20%)	≥20% (30%)
1.0 keV - 100 keV	↓	↓	≥10% (20%)
0.1 MeV - 1.0 MeV	↓	≥6% (≥20%)	≥6% (20%)
1.0 MeV - 4.5 MeV	↓	↓	≥6% (20%)
4.5 MeV - 10 MeV	↓	≥10% (≥20%)	≥10% (30%)

*the first number is what is ultimately needed, the second is what is believed to be currently achievable with state-of-the-art techniques for measuring integral flux over the energy interval.

**for standard and reference fields, the accuracy is specified for LWR, LFMBR and CTR requirements, reflecting the overall requirements for all of these systems.

Table 2

COMPARISON OF SELECTED DIFFERENTIAL REACTOR NEUTRON SPECTROSCOPY METHODS

	Method	E_L[a]	E_u[b]	Resolution	Accuracy % (1σ)	
1.	(n,p) Emulsions					
	° Collimated Source	3×10^{-1}	20		5-10%	0.3<E<10 Mev
					10-20%	10<E<20 MeV
				Fair		
	° Non-Collimated Source	3×10^{-1}	10		10-15%	0.3<E< 3 Mev
					15-25%	3<E<10 Mev
					10-50%	0.001<E<0.03 Mev
2.	(n,p) Proportional Counters	1×10^{-3}	2.5	Good	5-10%	0.03<E<1.0 MeV
					10-25%	1.0<E<2.5 MeV
					15-40%	0.01<E<0.5 MeV
3.	$^6Li(n,t)^4He$	1×10^{-2}	6.5	Fair	15%c	0.5<E<2.0 MeV
					20-30%	2.0<E<6.5 MeV
4.	Time-of-Flight (TOF)				10-15%	0.00001<E<0.001 Mev
	° $^H(d,n)^He$ Source	5×10^{-5}	0.2		15-20%	0.001<E<0.02 Mev
					20-30%	0.02<E<0.5 MeV
				Good	10-15%	0.00001<E<0.001 Mev
	° LINAC Source	5×10^{-5}	5		15-20%	0.001<E<0.02 Mev
					10%	0.02<E<0.5 Mev
					15%	0.5<E<1.0 MeV
					20%	1.0<E<5.0 Mev

a) Approximate lower energy limit of applicability, MeV.

b) Approximate upper energy limit of applicability, MeV.

c) The current accuracy of $^6Li(n,t)^4He$ spectroscopy is mainly dominated by the uncertainty in the angular and total reaction cross sections.

bring off a successful experimental program. These various considerations, and especially the problem of equipment installation, almost in themselves require that the experiment be performed during a reactor start up. It is essential that a set of precalculations exist to bracket the fluxes and fluences expected.

(d) The detectors should be chosen with some care, and should have overlapping energy ranges. Redundancy is important in achieving a self-consistent set of measurements. There are several different classes of detectors, each of which has particular virtues and disadvantages for use in operating and experimental reactors. They are:

(1) Activation Foils - provide good coverage of the thermal range and energies between 0.5 and 8.0 MeV. Since these are passive detectors and have a long history of use they are ideally suited to in-vessel measurements. When using such detectors care must be given to the quality assurance of the foil materials, and multilaboratory intercomparison of the activation counting is recommended.[13,14,15] One must also exercise care that flux perturbations due to the detectors themselves do not influence the results.

(2) Proton Recoil Proportional Counters - give good resolution spectra from a few keV to a few MeV and are capable of covering the range from 0.1 to 1 MeV where activation foils have difficulties. The proton recoil detectors are usually H_2 or Ch_4 filled at various pressures. Experimental devices are being tested using ^4He. Proton recoil detectors are not operable in neutron fluxes higher than about 10^6 n/cm^{2}sec. When used in an operating reactor environment, they are not suitable for use inside the pressure vessel and can be used outside the pressure vessel only during low or zero power operation. At low power, the fission distribution within the core may be appreciably different and influence the axial distribution total flux in the cavity.

(3) Special and Experimental Detectors[16] - In pressure vessel surveillance (PVS) applications, highly specialized miniature proportional counters will be required. Consequently, accurate treatment of proportional counter finite size effects will be mandatory.

A proton recoil method which introduces less perturbation and possesses considerably reduced finite size effects is emulsion-photographic track plate proton recoil spectrometry. The emulsion technique possesses the advantages of passive monitoring; however, just as for active spectrometry, low power clean environments are mandatory. Hence, it is appropriate to combine the emulsion method with active neutron spectrometry techniques wherever possible.

For actual experiments in operating reactors, it is only possible to utilize passive multiple foil flux-fluence spectrometry. In such irradiations it is highly advantageous to use time integrative passive monitors. While the passive multiple foil spectrometry has utilized radiometric dosimeters in the main, in PVS applications the length of irradiation is often ill-defined and the power-time history of the reactor can also introduce considerable uncertainty. Hence, for more accurate data from such experiments, it will be necessary to exploit time integrative passive monitors, such as long-lived radiometric dosimeters (encapsulated fission foils providing long half-life fission products such as Cs) and, in particular, solid state track recorders (SSTR), and helium accumulation fluence monitors (HAFM). It is noted that the latter two passive methods possess higher sensitivity than radiometric dosimeters. Moreover, these two methods compliment each other in terms of the neutron sensitivity provided for the broad energy range of interest, 0.1 to 10.0 Mev. HAFM utilitizng ^6Li or ^{10}B will provide good sensitivity in the low energy region, whereas SSTR incorporating fission threshold nuclides such as ^{232}Th, ^{238}U, or ^{237}Np, will provide good complimentary sensitivity at higher energy.

For longer term irradiations where the fast fluence exceeds 10^{18} neutrons/cm^2, another time integrative passive neutron dosimeter that can be used is crystalline quartz. Physical changes in the crystalline quartz can be examined such as changes in density and in the refractive index of the medium. These properties can provide sensitive indicators of fast fluence that accrues during irradiations.

Differential Neutron Spectroscopy

A "state-of-the-art" comparison of differential reactor neutron spectroscopy that is available for dosimetry measurements is presented in Table 2. This comparison is not exhaustive, but has been confined to those selected techniques which have generally found world-wide acceptance.[17,18,19] All of these techniques possess limitations, in that no single spectroscopy method provides an ideal solution, i.e., possesses good sensitivity, accuracy, and resolution over the entire neutron energy region of interest in reactor applications, namely, from 4×10^{-7} MeV up to 15 MeV for fission reactors. In this regard, Table 2 contains the approximate lower and upper energy limits of applicability, E_L and E_u, for each of these selected methods. Consequently, many different methods of differential spectroscopy must often be used to cover the energy region of interest for a given benchmark neutron field.

Perhaps an even more unfortunate shortcoming of all current differential spectroscopy methods is the general inability to conduct measurements in high power reactor benchmark environs. The inapplicability of differential reactor neutron spectroscopy techniques in high power environs can be traced to inherent limitations, such as:

1) count rate limitations,
2) radiation damage (of detectors and/or electronic components),
3) sensitivity to background radiation components (principally the gamma-ray component), and

4) temperature sensitivity (of detectors and/or electronic components).

Although limitations frequently arise which are uniquely associated with a specific technique, different spectroscopy methods often share common shortcomings. As has been stressed in a recent review,[19] one such shortcoming is the need for unfolding which is apparently a universal necessity in all differential reactor neutron spectrometry methods. This universal requirement may well stem from one of the chief intrinsic characteristics of the neutron, namely, neutral charge. In neutral particle detection, one customarily uses interactions that produce charged particle reaction products which are, in turn, readily detected. Hence, the response of such a detector need not generally be in one-to-one correspondence with the energy of the incident neutrons. Any departure from this one-to-one correspondence automatically necessitates unfolding.

The discovery and validation of a differential neutron spectroscopy method which could be applied in high power reactor benchmark environs must necessarily be classified as a major breakthrough in research reactor technology. However, in assessing possible future directions and developments in differential reactor neutron spectroscopy less ambitious goals are obviously more prudent and realistic. Perhaps the major emphasis will occur in the higher region extending to 15 MeV. Here one can anticipate a re-emergence of the proton-recoil photographic emulsion technique, which possesses fundamental advantages for the high energy range for both fission and fusion reactor applications, such as small inexpensive passive detector packages of good energy sensitivity and negligible spectral perturbation.

In these higher energy neutron environs, increasing emphasis will also be placed on reactions which produce helium, i.e., alpha particles. The helium yield of many relevant reactions is vastly increased at high energy. Mass spectrometry techniques have already been perfected for measuring helium production in high power irradiations.[20] ^{4}He-recoil proportional counter spectroscopy has also been advanced[19] as a means of extending the current energy domain of applicability of proportional counter techniques (see Table 2). Perhaps the most appealing aspect of this latter technique is the adaptation of already existing hardware and instrumentation. By simply filling with helium instead of hydrogen or methane, proportional counters (already employed in the proton-recoil method) can be directly applied for α-recoil spectrometry. Estimates of $E_u \sim 15$ MeV have been forecasted, provided that proportional counters of high quality and helium of very high purity are employed. This estimate implies that just as with proton-recoil spectroscopy, accurate unfolding of finite-size effects in α-recoil proportional counters must be performed.

Two particularly important spectral characteristics, which have generally been neglected in differential reactor neutron spectroscopy, namely, absolute flux measurements and observation of angular flux anisotropy, will quite likely be singled out for emphasis in future work. Only very limited absolute spectral measurements have been carried out using proton recoil emulsions[21] and proportional counters.[22] On the other hand, additional information that can be obtained by means of nuclear emulsions is knowledge of the anisotropy of the neutron flux.[23] If, in the emulsion measurement of the proton spectrum[24,25] (which can be unfolded to give the neutron spectrum), the direction of the proton track is recorded, anisotropies in the neutron flux can be detected. For example, in a neutron spectrum in which the neutron flux is decreasing rapidly with increasing energy in the vicinity of 2 MeV, a significant fraction of the recoil protons with energies 2 MeV will be produced by neutrons of about this energy. For these events, the proton recoil direction is always forward. For protons > 2 MeV, the direction of the proton velocity can be determined with close to 100% certainty. This confidence factor decreases as proton tracks get shorter.

For neutrons of energy 250 keV, nuclear emulsions loaded with glass specks[26] and containing ^{6}Li can provide some knowledge of the anisotropy in neutron flux. For example, in the ^{6}Li(n,α) t reaction the sum of the ranges of the alpha particle and triton is significantly longer if the triton goes in a forward instead of a backward cone. Thus, there will be a strong correlation between the direction of the long tracks and the neutron direction. The ^{6}Li(n,α) t cross section resonance at 250 keV significantly increases the number of triton-alpha pairs and thereby provides improved statistical accuracies of angular observations in the vicinity of the resonance.

In hazarding one final projection for possible future directions of differential reactor neutron spectroscopy, one cannot ignore the virtual explosion of activity and developments which has occurred in the field of Solid State Track Recorders (SSTR) over the last decade or so.[27] In particular, the ability to extract relevant physical data such as mass, charge and energy from the shape of tracks formed in SSTR is a striking advance. This recent development, which is commonly referred to as track profile analysis, can only be considered to be in the very formative stages. This ability coupled with the vast improvements of α-particle sensitive SSTR, such as Cellulose Acetate Buterate (CAB) and Cellulose Nitrate (CN), augurs for the evolution of SSTR differential neutron spectroscopy methods. Advanced SSTR techniques for observing angular flux anisotropy should also become possible. Such methods would, of course, be direct descendants of emulsion techniques and thereby automatically possess many advantages. However, in contrast with emulsions, the insensitivity of SSTR to electrons would provide an enormous advantage for reactor applications. Moreover, the reduced α-particle range also implies improved high energy sensitivity with less attendant stress on the need for finite-size corrections.

The Importance of Good Dosimetry - A Specific Example

To put the value of good dosimetry into perspective, let us consider a specific example, relating to the materials test program and radiation embrittlement in LWR's.

There are presently 53 commercial nuclear reactors operating in the United States[28] which account for 10% of our nation's electricity requirements. Commercial nuclear power has been generating electricity in this country since 1959 with a safety record unmatched by any other heavy industry. Since the commissioning of Dresden I, the first commercial nuclear power plant, no fatalities and no substantial personnel contamination have resulted from the operation of the nuclear steam supply systems for electrical generation. One of the primary reasons for this excellent operating record is the very conservative design utilized in the building and operation of these plants.

A conservative design is necessary to account for unknowns in materials properties, operating stresses, and operating environments. As these factors are better defined through development of refined analytical techniques and measurements made on operating systems, it is possible to reduce overconservatism and still maintain safety, reliability, and availability.

Overly conservative design or regulatory action can result in substantial losses to the economy. If we assume a 7 mill/kWh difference in base loaded coal and nuclear electricity generation rates, and further assume that all electricity from nuclear outages is replaced by base loaded coal generation capacity, each percent of lost nuclear capacity represents a $16.6 million increase in cost of electricity per year. If each lost percent in nuclear capacity were replaced by oil the cost to the economy would be about $70 million per year.

The preceding remarks were presented to emphasize the economic consequences of overconservative definition of design and operating margins. The nuclear industry is presently faced with potential premature retirement or long forced outage for thermal anneal of a number of PWR plants due to irradiation embrittlement of reactor pressure vessel steels. The remainder of this paper will discuss the present regulatory and code requirements for irradiated materials properties and suggest research necessary to accurately define the proper irradiated materials properties requirements.

The Regulatory Position on Radiation Embrittlement

The prevention of brittle fracture of the pressure boundary of nuclear systems is assured by compliance with toughness requirements set forth in 10 CFR Part 50, Appendices G and H.[29] Recently the Nuclear Regulatory Commission has issued Regulatory Guide 1.99,[30] which describes procedures for predicting the effect of copper and phosphorous on transition temperature shift and upper shelf Charpy energy decrease of irradiated pressure vessel materials. The minimum upper shelf energy during the life of the plant is set at 50 ft-lb to insure sufficient toughness to prevent low energy ductile tearing. If the upper shelf level falls below the 50 ft-lb limit, the following actions may be required for continued licensability:

1. Extensive testing and analysis of existing surveillance specimens, where available.
2. Generation of irradiated fracture toughness data on relevant steels.
3. Extensive fracture mechanics analysis of the reactor vessel.
4. Extended outage to comply with nondestructive examination requirements.
5. In extreme cases, an in situ anneal with consequent prolonged outage or premature plant retirement could result.

It should be noted that such consequences could also result from inadequate data, even though the vessel may in reality be within safe limits. When credible surveillance data from a reactor are not available, prediction of radiation damage must be done in accordance with procedures given in Regulatory Guide 1.99.

Unfortunately, many installations do not have adequate surveillance data and thus must rely on Regulatory Guide 1.99 predictive methodology. The reasons for the lack of proper data include:

1. The materials incorporated in some vessel surveillance programs were selected on the basis of unirradiated materials properties and not on sensitivity to radiation embrittlement. This situation occurred because the deleterious effects of copper and phosphorous were not known at the time of the materials selection. Thus, these reactors have not included those radiation-sensitive materials, which will be controlling, in their surveillance programs
2. The surveillance capsules in some reactors were removed because of fretting fatigue damage resulting from flow-induced vibration. These plants presently have no active surveillance dosimetry programs.

Predictive Methodology of Regulatory Guide-1.99

The curves for prediction of transition temperature shift and shift in Charpy shelf energy are shown in Figure 1. These curves are based in large part, upon the data compiled by Bush[31] for all reported reactor surveillance capsules tested through 1973.

Serious questions have been raised about the appropriateness of the utilization of these curves for prediction of irradiated properties. Specific objections include:

1. The data base is incomplete and sometimes inapplicable. The inclusion of low exposure temperature Yankee Rowe surveillance data (irradiated at 450-525°F) results in prediction of greater than normal embrittlement.
2. The trend curves should be statistically developed, rather than simply bounding the available data.
3. Weld metal, base metal, and heat affected zone are unique materials (with different responses to irradiation), but the Guide requires that a single curve be used to predict property shifts for all materials.
4. The data base used to develop the shift curves includes data of doubtful accuracy. Source of possible errors include:
   a) Accuracy of dosimetry, particularly of older data, is in question. Estimates of possible error range as high as ±60%.[32]
   b) Calibration information for test machines is not available from much of the data; thus, testing errors could be significant.
5. The data base includes information from A302-B steel irradiations. This data may not be applicable for prediction of property shift for A533-B, Class 1 steel used in present-day vessels.
6. Hawthorne[33] has recently finished a preliminary assessment of the degree of conservatism in NRC Regulatory Guide 1.99. His data for A533-B plate and weld show the Guide to be extremely

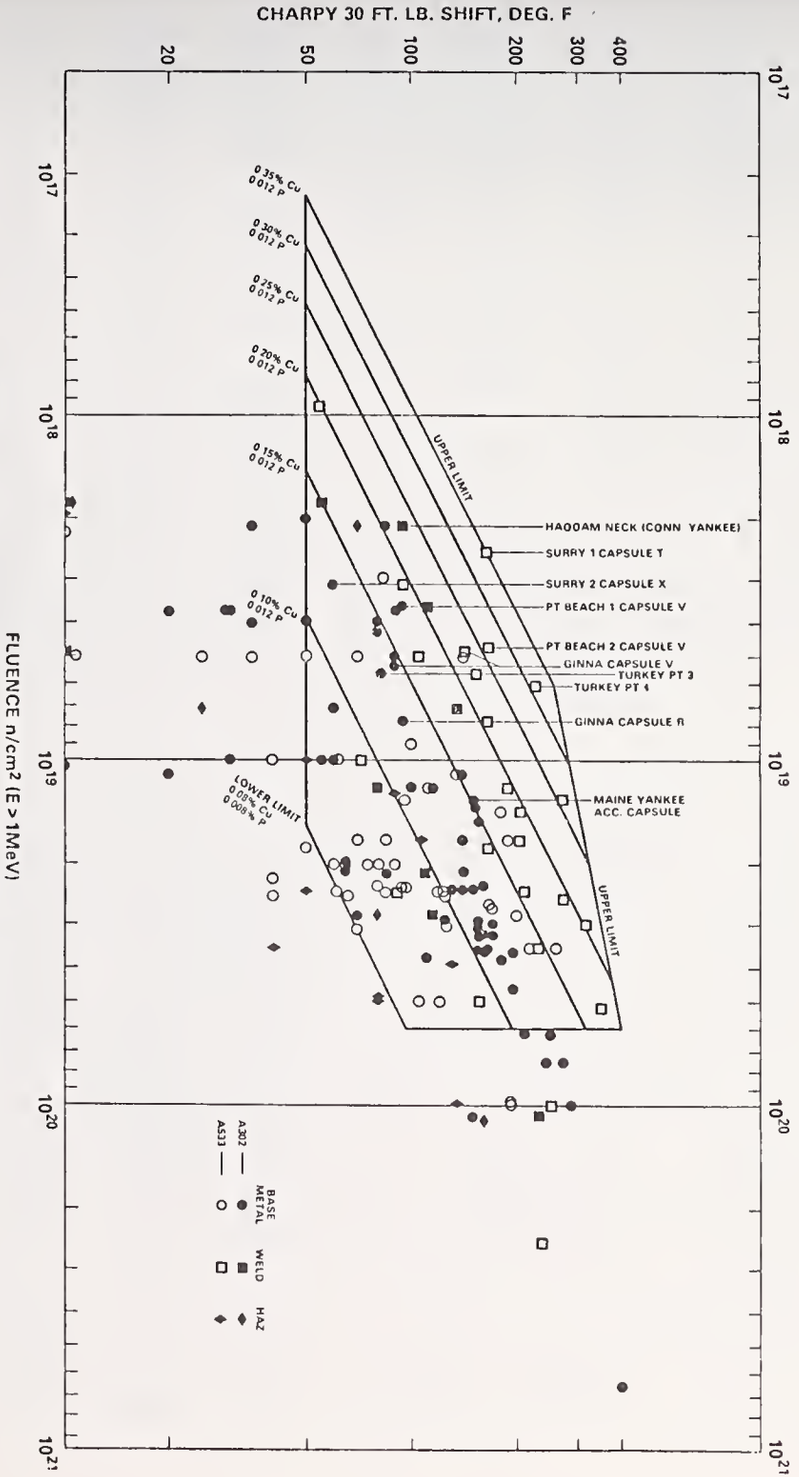

Figure 3. Data Used to Develop NRC Reg. Guide 1.99

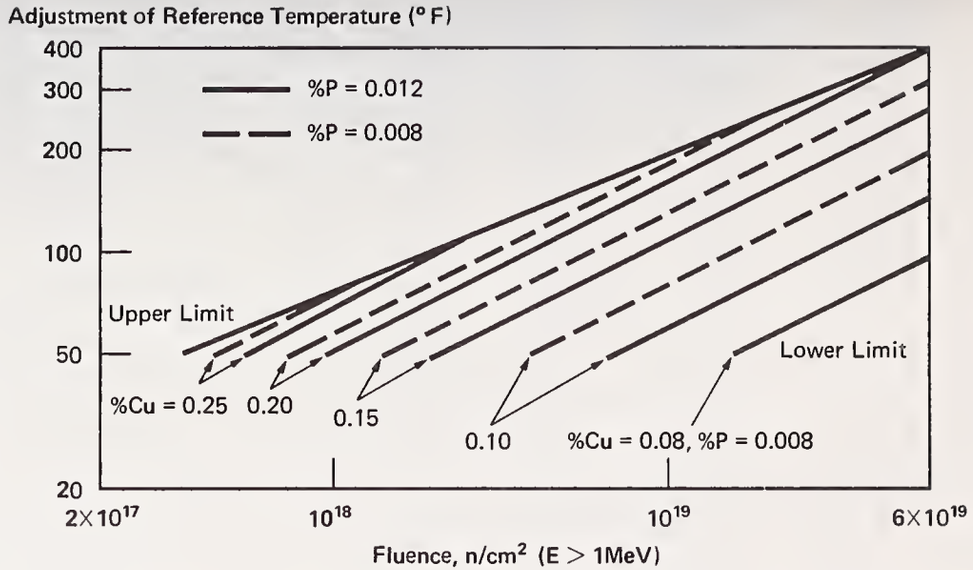

Figure 1 Adjustment of reference temperature as a function of Cu & P Content & Fluence

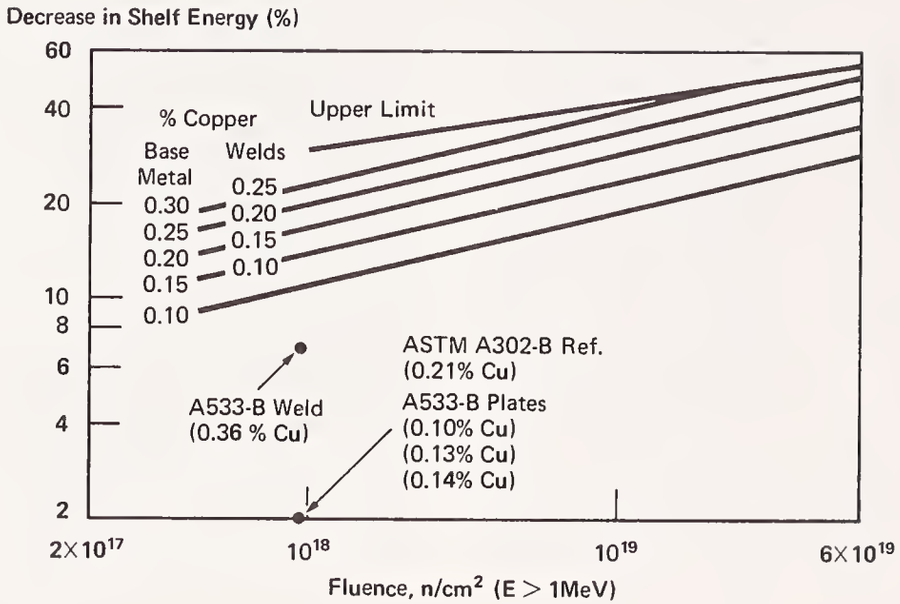

Figure 2 Measured upper shelf energy reduction with low fluence exposure.

conservative in the prediction of upper shelf Charpy energy drop at low fluence. A summary of these data is shown in Figure 2.

Because of the aforementioned problems and inaccuracies inherent in the present trend curves of Regulatory Guide 1.99, a new trend curve analysis should be formulated.

To demonstrate the impact of less than optimum dosimetry data, refer to Figure 3. This figure shows the correlation of a fracture toughness property as measured by the Charpy shift of various pressure vessel steels versus fluence. The large scatter in the data is evident. This data base impacts directly on the licensing of nuclear reactors in the U.S. The fluence limits for pressure vessel steels with various Cu and P content as given in Reg. Guide 1.99 is shown superimposed. The benefit of more precise and accurate dosimetry as well as the correlation of the data with spectral indices is evident.

Conclusion

Dosimetry beyond the core is an essential part of our reactor technology. In the materials test program, it is the link relating changes in the micro- and macroscopic material properties to neutron fluence and spectra. For pressure vessel surveillance programs, dosimetry is needed for the interpretation of actual or projected damage effects throughout reactor life and extrapolation from the surveillance testing positions to the pressure vessel wall itself. The dosimetry for shielding is a result of various problems receiving general attention for all types of reactors. These shielding requirements have given rise to interrelated programs of evaluation and benchmark experiments which coordinate closely with dosimetry benchmark programs.

References

1. M. Vlasov, "Proceedings of a Consultants' Meeting on Integral Cross Section Measurements in Standard Neutron Fields", Vienna, November 15-19, 1976, Report INDC(NDS)-81/L, IAEA (1977).

2. R. Odette, et al., "Application of Advanced Irradiation Analysis Methods to Light Water Reactor Pressure Vessel Test and Surveillance Programs", Proc. of the ASTM 8th International Symposium on the Effects of Radiation on Structural Materials, St. Louis, Mo., May 1976.

3. E. M. Oblow, "Reactor Cross Section Sensitivity Studies Using Transport Theory", ORNL-TM-4437, April (1974).

4. M. L. Williams and W. W. Engle, Jr., N.S.E 62, 92 (1977).

5. U. Farinelli, "Proc. of the Specialists' Meeting on Sensitivity Studies and Shielding Benchmarks", page 25, OECD, Paris, 7-10 October (1975).

6. J. Grundle and C. Eisenhauer, "Proceedings of a Consultants' Meeting on Integral Cross Section Measurements in Standard Neutron Fields, IAEA, Vienna, November 15-19, 1976.

7. Proceedings of the First International ASTM-EURATOM Symposium on Reactor Dosimetry, Petten, The Netherlands, September 22-26, 1975.

8. W. N. McElroy, et al., "Proceedings of a Consultants' Meeting on Integral Cross Sections Measurements in Standard Neutron Fields", Vienna, November 15-19, 1976.

9. M. Vlasov, op. cit.

10. A. F. Avery and S. D. Lympany, "Proc. of the Specialists' Meeting on Sensitivity and Shielding Benchmarks", OECD, Paris, October 7-10, 1975.

11. V. Herrnberger, et al., op. cit.

12. G. Hehn and P. Stiller, "Prediction of Radiation Damage in Structural Materials Outside the Reactor Core", Paper 32, Proc. of 1st ASTM-EURATOM Symposium, Petten, The Netherlands, September 22-25, 1975.

13. Nuclear Technology, 25, 1975.

14. Proc. of a Consultants' Meeting on Nuclear Data for Reactor Neutron Dosimetry, IAEA, Vienna, September 10-12, 1973.

15. Proc. of the ASTM-EURATOM Symposium on Reactor Dosimetry, Petten, The Netherlands, September 1975.

16. Private Communication, W. McElroy.

17. W. N. McElroy, et al., Special Series, Nucl. Techn. 25, 177-422 (1975).

18. G. DeLeeuw, "In-Pile Neutron Spectroscopy: Status", CEN/SCK Report (1976).

19. R. Gold, "Neutron Spectrometry for Reactor Applications: Status, Limitations and Future Directions", HEDL-SA 901 (1972) and in Ref. 2.

20. H. Farrar, E. P. Lippincott, and W. N. McElroy, "Dosimetry for Fluence Applications", HEDL-SA 939 (1975), and in Ref. 2 .

21. J. H. Roberts, "Absolute Flux Measurements of Anisotropic Neutron Spectra with Proton Recoil Tracks in Nuclear Emulsions", Rev. Sci. Instr. 28, 677 (1957).

22. R. Gold, "Energy Spectrum of Fast Cosmic Ray Neutrons Near Sea Level", Phys. Rev. 165, 1406 (1968).

23. T. Iijima and S. Momoto, "Measurements of Anisotropic Fast Neutron Spectrum with Nuclear Emulsions", Nucl. Sci, and Eng. 22, 102 (1965).

24. L. Rosen, "Nuclear Emulsion Techniques for the Measurement of Neutron Energy Spectra", Nucleonics 11, 7, 32 (1953).

25. J. H. Roberts and A. N. Behkami, "Measurements of Anisotropic Fast-Neutron Spectra with Nuclear Emulsion Techniques", Nuclear Applications 4, 182 (1967).

26. J. H. Roberts and F. E. Kinney, "Measurements of Neutron Spectra by Use of Nuclear Emulsions Loaded with ^{6}Li Glass Specks", Rev. Scien. Instr. 28, 510 (1957).

27. R. L. Fleischer, P. B. Price, and R. M. Walker, Nuclear Tracks in Solids, University of California Press, Berkeley, California (1975).

28. "Operating Unit Status Report." U.S. Nuclear Regulatory Commission, NUREG-0020-1, August 1976.

29. Title 10 - Chapter 1, Part 50, "Licensing of Production and Utilization Facilities", Federal Register, Vol. 38, No. 130, July 1973.

30. Regulatory Guide 1.99, "Effect of Residual Elements on Predicted Radiation Damage to Reactor Vessel Materials", U.S. Nuclear Regulatory Commission, July 1975.

31. S. H. Bush, "Structural Materials for Nuclear Power Plants", ASTM Journal of Testing and Evaluation, Vol. II, No. 6, November 1974.

32. R. Odette, N. Dudey, W. McElroy, R. Wullaert, A. Fabry, "Application of Advanced Radiation Analysis Methods to LWR Pressure Vessel and Surveillance Programs", ASTM 8th International Symposium on Effects of Radiation on Structural Materials, St. Louis, Mo., May 1976.

33. J. R. Hawthorne, "Radiation Effects on Vessel Steels and Welds with Varied Residual Element Content and Embrittlement Relief by Postirradiation Annealing", Fourth Water Reactor Safety Research Information Meeting, Nuclear Regulatory Commission, September 1976.

FISSION YIELDS: MEASUREMENT TECHNIQUES AND DATA STATUS

W. J. Maeck

Idaho National Engineering Laboratory
Allied Chemical Corporation
Idaho Falls, Idaho 83401

Techniques for the measurement of absolute and relative fission yields are reviewed. The preferred techniques are isotope dilution mass spectrometric measurement of the individual fission products, and the heavy element mass difference or the fission product summation method to establish the number of fissions. The accuracy of most thermal fission yields appears adequate, and the status of the various yield compilations is reviewed. For fast fission yields, the data are not nearly as well established. For many heavy nuclides, fast fission yield data are nearly nonexistent. Because fast fission yields change with neutron energy, it is imperative that fast yield data be evaluated as a function of neutron energy to generate the most complete and accurate compilation.

(Fission yield measurement techniques, counting, mass spectrometry; fission yields, thermal, fast, absolute, relative; data compilations; fission yields versus neutron energy)

INTRODUCTION AND HISTORY

Fission product yield data constitute one of the most important sets of basic information in the nuclear industry. Fission yield data are important in the measurement of nuclear fuel burnup; safeguards; neutron dosimetry and flux measurements; nuclear physics calculations; reactor design and operation (both from the physics and engineering standpoint); decay heat studies; shielding calculations; fuel handling and reprocessing; and environmental studies.

The measurement of fission yields is as old as the discovery of fission itself. Hahn and Strassman[1] performed the first yield measurements in their initial discovery of the fission process. Fission yield studies in the early 1940's established the asymetric mode of thermal fission; however, the shape of the mass yield curve was not well defined because of the rather large uncertainties associated with the data. In the 1950's, the shape of the mass yield curves for thermal fission, especially for ^{235}U, became reasonably well defined and the existence of "fine structure" was established. Similar data for ^{233}U and ^{239}Pu thermal fission became available in the early 1960's.

Up until the early 1960's the majority of the fission yield data had been obtained using radiochemical techniques. In the mid 1960's the demand for improved and new yield data increased. Radiochemical data lacked the desired accuracy because of uncertainties in the decay schemes, half-lives, and in-pile and out-pile decay corrections. These factors also tended to limit the applicability of the technique. A more accurate technique for the measurement of fission yields is mass spectrometry because concentration measurements for the stable isotopes using the isotope dilution technique are more accurate than counting of radioactive isotopes, and several isotopes of the same element can be measured simultaneously. Thus, several laboratories became involved in fission yield measurements using mass spectrometric techniques with the most extensive work being done at Idaho Falls[2]. The stable and long-lived isotopes of Rb, Kr, Sr, Zr, Mo, Ru, Cd, Xe, Cs, Ba, La, Ce, Nd, Sm, Eu, and Gd can now be routinely determined using the isotope dilution mass spectrometric technique.

Up to 1970, most nuclear energy laboratories had emphasized thermal fission yield measurements and over 500 literature references are available.

The shift from thermal yield measurement to fast yield measurement started about 1970. Present fast fission yield measurements being produced are based on radiochemical measurements for samples irradiated in low-flux fast reactor critical assemblies, radiochemical measurements for samples irradiated with beams of monoenergetic neutrons, and mass spectrometric measurements on samples irradiated in high flux fast reactors such as EBR-II. In this latter phase, the most extensive efforts are again being conducted at the Idaho National Engineering Laboratory (INEL) near Idaho Falls[3,4].

TYPES OF FISSION YIELD MEASUREMENTS

Fission yield data basically can be divided into two types, relative fission yields and absolute fission yields. Depending upon the specific application of the data, each have their merits; however, the most fundamental needs are for absolute data. Unfortunately, these are the most time consuming and difficult to obtain. In the following discussion, fission yields refer to cumulative or end-member chain yields after delayed neutron emission.

Absolute Fission Yields

Fission yield is defined by the following relationship:

$$\% \ FY_x = \frac{N_x}{F} \times 100$$

where FY_x is the fission yield of a given nuclide, x, N_x, is the number of atoms of the given nuclide formed, and F is the number of fissions that occurred. In the measurement of absolute yields, the most difficult measurement is the number of fissions. Generally, the number of the selected fission product atoms can be determined with smaller uncertainties.

Measurement of number of fissions - At least four techniques have been used to establish the number of fission events. These are: 1) heavy element mass difference, 2) fission product summation, 3) fission counting, and 4) calculational methods. A discussion

of each of these techniques and their associated uncertainties follows:

1. The number of fissions, F, based on the heavy element mass technique is derived from the relationship,

$$F = U^{\circ} - (U+U_{cp})$$

where U° is the accurately determined number of heavy element atoms being irradiated, U is the number of atoms of the heavy element remaining after the irradiation, and U_{cp} is the number of atoms of the heavy element which has been converted to another element by a capture or decay process. In this method, an amount of the well characterized (chemically and isotopically) heavy element is accurately weighed into the irradiation capsule and the capsule is sealed. Following irradiation, the capsule and its contents are dissolved and the amount of the heavy element and its isotopic composition are accurately measured, usually by mass spectrometry. Also measured, is the amount of other elements formed by capture and/or decay processes.
Heavy element mass difference is potentially the most accurate method for establishing the number of fissions, provided that the loss (ie, burnup) of the target element is 10% or greater. Using isotope dilution mass spectrometry, the pre- and post-irradiation content of the sample can be determined to at least 0.1%; however, even with a 0.1% absolute uncertainty, the error in the number of fissions is ∿1.5% relative for a burnup of 10% [(100±0.1) - (90±0.1) = 10±0.14]. Therefore, irradiation to 20% - 40% burnup is preferred, such that the number of fission can be determined to better than 1%.
The sources of error in this method are: a) the characterization (absolute number of atoms) of the heavy element target, b) the accuracy of the mass spectrometric analysis, including the spike isotope calibration, c) incomplete dissolution of the sample, and d) contamination. To minimize errors which might arise from changes in the response of the mass spectrometer or from unknown changes in the isotope dilution spike isotope concentration, it has been strongly recommended[5] that an archive sample of the heavy element be retained and analyzed when the post-irradiation heavy element analysis is performed.
2. A major advantage of the fission product summation technique[2], compared to the heavy element mass difference method for determining the number of fission is that it is especially applicable to samples having low burnup (1-10%). The summation technique is based on the fact that the sum of all of the fission products in one of the peaks in the mass yield curve is equal to the number of fissions. The success of this technique is directly dependent upon the fraction of the selected mass peak which is measured. The preferred peak for measurement is the heavy mass peak because the elements in this peak are more easily measured. The preferred measurement technique for the individual fission product atoms is isotope dilution mass spectrometry.
In our laboratory, approximately 90% of the fission product atoms[4] in the heavy mass peak (isotopes of Xe, Cs, Ba, La, Ce, Nd, and Sm) are measured to an uncertainty of better than 1% relative. The number of atoms of the unmeasured isotopes is obtained by interpolation and extrapolation, and an uncertainty of 10-20% relative is assigned to these values. This procedure only slightly increases the uncertainty in the total number of fissions. This technique is capable of establishing the number of fissions to an uncertainty of 1.0-1.5%.
A requirement of this method is that the number of fission events should approach 10^{18} such that sufficient quantities of fission products are available for measurement and the amount of natural contamination is minimized.
The principal sources of error in this technique are: a) measurement of the individual fission product atoms, including the uncertainties in the concentration of the various spike isotopes, b) incomplete dissolution of the target nuclide and all fission product nuclides, c) introduction of fission product element natural contamination from reagents and equipment, d) leakage of fission gases from the target assembly during and after irradiation, and e) incomplete collection of fission gases.
3. Two methods are used to measure the number of fission events directly. These involve use of fission counting chambers and solid-state track recorders (SSTR's). However, these methods do not measure the number of fissions which have occurred in the sample which is measured for fission products. In both of these methods two target foils are used. Both targets are adjacent and irradiated in the same neutron flux. One of the targets is a bare thin foil from which the fission fragments escape and are counted, and the other is a heavy target, usually wrapped in aluminum foil to contain the fission fragments. The heavy target is analyzed for the desired fission products. The number of fissions occurring in the thin foil is counted, and the number of fissions occurring in the heavy target is calculated from the relative amount of the target nuclide in each foil.
When fission chambers (ionization chambers) are used, the number of fissions occurring in the thin foil is established by direct counting of the fission fragments escaping from the foil. In the SSTR technique the thin foil is irradiated in direct contact with a material such as mica. The recoil fission fragments produce structural damage in the mica such that when the mica is etched with hydrofluoric acid, the damage is revealed in the form of individual tracks. The tracks are counted under a microscope, and the number of fissions is calculated by multiplying the number of tracks by an optical efficiency factor. An excellent detailed discussion of these techniques and their associated sources of error has been

presented by Grundel, Gilliam, Dudey, and Popek[6].

The use of these techniques is limited to low fluence and hence, a low number of fission events in the heavy foil. The heavy foil is dissolved and the desired fission products are separated and analyzed by counting, or the heavy foil is counted directly, preferably using a well calibrated high resolution Ge(Li) detector system. Accuracy in the measurement of certain nuclides is improved by counting at different time periods following the irradiation. Because the number of fission events is low, the use of mass spectrometry to determine the individual fission product abundances for fission yield measurements is not practical.

The two major sources of error in both techniques are: the measurement of the number of target atoms in the thin foil and the relationship between the number of recorded events and the number of fissions. Other common sources of error are: a) production of fission events from other nuclides in the target material, b) contamination in the foil backing or in the materials of construction, c) fission fragment adsorption in the thin foil deposit), and d) fission fragment scattering.

Sources of error distinct to the fission chamber technique are: a) efficiency and calibration factors for the chamber, b) correction for dead time losses in the fission rate measurement, c) background counting corrections, and d) scattering corrections. Based on very well controlled experiments, the number of fission events determined by use of a fission counting chamber can be established with an uncertainty of $\sim$1.5%[6].

The major distinct source of error for SSTR's is the optical efficiency factor for converting the number of tracks to fission. Other distinct sources of error are the counting of the number of fission tracks, the etching of the mica plate, and the identification of the tracks which result from fission fragments. Currently, the estimated uncertainty for the determination of the number of fissions by this technique is $\sim$3%[6].

4. The number of fissions also can be calculated using some measured quantity and an assumed value for a given factor, such as a cross section or the capture-to-fission ratio, α. For example, the number of ^{235}U fissions can be calculated from the measured pre- and post-irradiation isotopic composition of ^{235}U and an assumed value for α for ^{235}U. Because α varies with neutron energy and temperature, its true value is always in question. Other calculational methods based on neutron fluxes and cross sections also are subject to significant uncertainties. This is the least accurate of the various method discussed.

Measurement of fission product atoms - The oldest method for measuring fission product concentrations is based on counting of a given radioactive nuclide. Briefly, the irradiated target is dissolved, the desired nuclide is isolated by chemical means, and the activity of the separated product is measured. All of the early yield data were based on beta counting, because the gamma/disintegration values were unknown. In some cases, especially where the activity level is very low, beta counting is still used today.

Precise gamma ray spectrometry has minimized the need for exhaustive chemical separations because discreet gamma rays can be associated with a given nuclide. In some instances, no chemical separations are performed and the irradiated target is counted directly for selected radionuclides.The preferred counting technique is high resolution gamma ray spectrometry. Counting techniques are especially useful for the measurement of short-lived nuclides, or where the number of fissions is low.

Sources of error in converting gamma ray spectrometric data to atoms of the particular fission product are: a) the method for subtraction of the baseline or background activity, b) detector efficiency, c) the accuracy of the standards if a comparison counting technique is used, d) the nuclear constants, specifically the photon-to-disintegration ratios and the half-life values, e) the mass adsorption of the gamma rays by the material being counted, f) random coincidence summing, and g) interferences from other gamma rays.

In a limited number of cases, an uncertainty of 1-2% can be attained for the determination of the number of fission product atoms using high resolution gamma ray spectrometry. Uncertainties in the range of 3-10% are more common.

The most accurate method for the measurement of the concentration of stable and long-lived nuclides is isotope dilution mass spectrometry. In this technique, a known number of spike isotope atoms, preferably of an isotope not formed in the fission process, is added to a sample of the dissolved target and chemical identity of the spike isotope and sample is effected by chemical means. That element is separated chemically and the isotopic composition is measured using a mass spectrometer. The ratio of the spike isotope peak to the other mass peaks of that element is measured and the number of atoms of the other isotopes is determined relative to the number of spike isotope atoms added. A particular advantage of this technique is that quantitative recovery in the separation procedure is not required. It is imperative, however, that isotopic exchange be achieved.

The irradiated sample should have experienced about 10^{18} fissions so that a reasonable amount of material is produced for measurement. Because the ionization efficiency in the mass spectrometer varies from element to element, the minimum amount of a fission product required for a reliable mass spectrometric measurement also varies. For example, 100 nanograms of Rb or Cs on the mass spectrometer filament is more than adequate, while several micrograms of Ru are ideal for analysis.

Because the accuracy of any isotope dilution technique is controlled by the accuracy of the spike isotopes, great care must be taken in their preparation and standardization. In many cases, the occurrence of natural contamination can be corrected because one or more of the naturally occurring isotopes is not formed in fission. For those cases where all of the naturally occurring isotopes of the element also are fission product isotopes (eg, Rb, Cs) significant errors can occur. Spectral interference from an isotope of another element can also occur; however, this problem can usually be minimized by improved chemical separation techniques. Other factors which must be considered are mass fractionation, especially for the light elements, from the mass spectrometer filament, and mass discrimination corrections.

For most elements, the isotopic composition and atom abundances can be determined to an uncertainty of ∿0.25%.

Other techniques, although limited in scope, which have been used to measure selected fission product concentrations are spectrophotometry for ^{99}Tc[2], X-ray analysis for one or more rare earth elements[7], vapor phase chromatography for the fission gases[2], and volumetric determination of the fission gases[8].

Summary - Absolute Fission Yields - The preferred methods for the measurement of absolute fission yields is the isotope dilution mass spectrometric measurements of the individual fission products coupled with the heavy element mass difference or the fission product summation technique to establish the number of fissions. Based on state-of-the-art, more yield data with smaller uncertainties can be obtained from a well designed irradiation using this technique than from the others which have been discussed. A particular item of concern, however, is that while irradiations to high burnup can result in a more accurate value for the number of fissions, significant corrections for neutron capture on some of the fission product nuclides are required. This is especially true for irradiations conducted in thermal reactors. Although correction factors can be applied when sufficient information concerning the irradiation is available (for example, see Ref. 9) the existence of significant unknown cross sections can lead to biased fission yield data[10]. Because of this, it is believed that the more correct approach may be to irradiate a larger target to a low burnup, 1% or less, and to determine the number of fissions by the summation technique using isotope dilution mass spectrometry[10]. Yields with uncertainties in the 1-2% range are attainable using this approach.

Recent improvements in fission chamber counting coupled with direct gamma-ray spectrometry measurements have resulted in a limited number of absolute yields being reported with uncertainties of ∿2.5%[11]. This approach should be most valuable in the measurement of yields where irradiations are conducted in low flux critical assemblies or when mono energetic neutron beams are used.

A feature of any counting technique compared to the mass spectrometric techniques, is that in most cases, the yield of the nuclide being determined is generally displaced one or two Z units from the end-member of the chain. Thus, the yield may have a lower value than that determined on the stable end-member of the chain because of the independent yield contribution from the other non-measured members of the chain. This difference may be as large as 5% relative.

Relative Fission Yields

Relative fission yields, which constitute a major fraction of the reported yield data, are yields which have been measured relative to some other nuclide or normalized to some value. The basic assumption is that once the yield of one fission product is accurately known, from absolute yield measurements, is can be used as a monitor of the total number of fissions, or other yields can be measured relative to it. Nuclides which have been used as reference standards are ^{95}Zr, ^{97}Zr, ^{99}Mo, ^{137}Cs, ^{140}Ba, and ^{148}Nd. The bulk of the relative yield data is associated with radiochemical measurement.

Several variations of treating the data on a relative basis have been proposed over the years, but the one receiving the most attention is the R-value method. This method is based on the assumption that if the yield values for a given fissionable isotope, usually ^{235}U, are well known, that uncertainties in the radiochemical measurement, especially those associated with decay schemes and counting geometry, can be minimized. In practice, samples of two different fissionable isotopes are irradiated simultaneously, and each is chemically treated to obtain the same nuclides from each source. The reference monitor nuclides, for example ^{140}Ba, from each target isotope and the unknown from each source are then counted as close in time as possible. Assuming that the yield of the reference nuclide is known, the yield of the unknown can be determined. Various experimental techniques and prior references are given in a review by von Gunten[12].

The major obvious systematic source of error in any type of relative yield measurement is the accuracy of the reference standard. Because absolute thermal yield values are now reasonably well known, relative yield measurements for thermal yields is a viable option. It is especially useful in the measurement of the valley nuclides and those on the extreme wings of the mass yield curve where absolute mass spectrometric yields have not been determined. The application of this technique to fast yield measurements suffers from the fact that the yields are a function of the energy of the incident neutrons; hence, relative fast fission yield data must be carefully evaluated with respect to the assumed yield of the reference nuclide.

FISSION YIELDS - STATUS AND NEEDS

To date, approximately 1000 literature references relative to all types of fission yield measurements are in existence. Recognizing that it would be impossible for each user to evaluate and select the best value from this mass of data, several individuals have taken up the task of evaluating and compiling these data. As could probably be predicted, differences occur in these evaluated data sets which exceed the error assignment attached by the various evaluators. In attempting to clarify the situation, the

most used compilations of thermal and fast fission yields were reviewed by Walker[13] and Cuninghame[14], respectively, for the 1973 IAEA Panel Meeting on Fission Product Nuclear Data[15]. The current status of the yield data compilations and data requirements for thermal and fast yields are discussed below.

Thermal Fission Yields

The review, evaluation, and compilation of data from nearly a thousand individual literature references is a monumental task. Several individuals have undertaken this task with varying degrees of vigor and continuity. Of these, the most well documented and referenced are the works of Meek and Rider[16], E.A.C. Crouch[17], W. H. Walker[9], Lammer and Eden[18], and the U.S. Evaluated Nuclear Data File (ENDF/B-IV[19] task force group.

All of the compilations are based on some version of pooling and weighting techniques, plus the personal opinion and preferences of the individual evaluators. Briefly, Meek and Rider[16] attempt to include all reported data in a computerized data library and then assign various weighting functions to the reported data based upon the method of measurement. Crouch[17], whose work is sponsored by the U.K. Chemical Nuclear Data Committee, also uses a computer based library but tends to limit the input to well documented data. The errors are assigned by Crouch. Walker's[9] compilation is based primarily on mass spectrometric yield data, except where mass spectrometric data are not available and then radiochemical data are used. Lammer's and Eden's[18] compilation is not as extensive as the others and is primarily based on mass spectrometric data and the evaluation technique is similar to that of Walker[9]. Version IV of of the ENDF/B file is basically the same as the Meek and Rider[16] compilation.

For a more detailed discussion of these data sets and a comparison study of the data sets, it is strongly recommended that the reader consult Walker's excellent review[13] presented at the 1973 IAEA Bologna Fission Product Nuclear Data Conference.

Since that time, the primary emphasis in the U.S. has been an intensified effort to upgrade and update the ENDF/B data file. To this end, a task force group which includes, among others, B. F. Rider and W. H. Walker, has been formed under the auspices of U.S. ERDA to develop a preferred fission yield data file. This file is to be continually updated and Version V should be available for presentation at the Second IAEA Advisory Group Meeting on Fission Product Nuclear Data to be held in Petten, Netherlands, September 1977. Concurrent with the U.S. effort, the UK fission yield data file is in a continual upgrade under Crouch's direction. Rider and Crouch are continually exchanging information with respect to literature references. The update status of the Lammer and Eden compilation is uncertain at this time. A review of the current status of the various thermal fission yield compilations is being prepared by J. G. Cuninghame, UK, for presentation at the Petten Conference mentioned above.

At the Bologna IAEA meeting[15], it was concluded that the thermal yield data, except for certain isolated cases, generally satisfied the user's required accuracies, and no new extensive remeasurement program was justified. The exceptions are detailed in Volume II of Reference 15.

In 1975, we had the opportunity to remeasure a limited number of thermal fission yields for ^{235}U and ^{239}Pu. Although to date, only relative yields have been measured, the initial results of this study[20] show for several isotopes that there are large differences compared to previous measurement made in this laboratory[2] and compared to data in current fission yield compilations[15]. Particularly significant are 14% higher values for ^{138}Ba and 8.5% higher values for the Xe isotopes for ^{239}Pu thermal fission. The major impact is that all of the ^{239}Pu fission yields will have to be adjusted to preserve mass balance. Only minor differences were observed for ^{235}U thermal fission. It is expected that new absolute thermal yield data for about 40 different nuclides for ^{235}U and ^{239}Pu will be produced when this measurement program is completed in 1978.

Fast Fission Yields

Fission yield data for fast neutrons are not nearly as well developed as they are for thermal neutrons. Based on the fast fission yield compilations produced through 1973 and Cuninghame's review[14], the data are fragmentary and usually carry large uncertainties. The most complete fast yield compilations are for ^{235}U and ^{239}Pu which were produced by Meek and Rider[16] and Crouch[21]. The fast yield data for ^{232}Th, ^{233}U, ^{237}Np, ^{238}U, and ^{241}Am are limited and generally have large errors. No reliable fast yield data are given for the higher isotopes of plutonium.

This lack of data stems from several sources. Primary, is the lack of available irradiation facilities. Because fast reactor fission cross sections are low, prolonged high flux irradiations are required to generate a sufficient number of fission product atoms for mass spectrometric measurements. If this is not possible, irradiations can be made in experimental low power critical assemblies; however, normally only a limited number of radiochemical measurements can be obtained.

Another consideration is that accurate fast yields are more difficult to measure than thermal yields, because all of the heavy nuclides undergo fast fission, while thermal fission is only significant for ^{233}U, ^{235}U, ^{239}Pu, and ^{241}Pu. This is especially important in the measurement of fast fission yields for the even-even and odd-odd heavy nuclides (^{232}Th, ^{238}U, ^{237}Np, ^{240}Pu, ^{242}Pu, and ^{241}Am), because all have a high neutron energy threshold cross section for fission, a relatively high capture-to-fission ratio, and in some cases, a long-lived capture product which fissions with any energy neutron. For example, in a long-term fast

neutron irradiation of ^{238}U or ^{240}Pu, a large fraction of the fissions will result from ^{239}Pu and ^{241}Pu, respectively. While corrections for the fission from the capture product can be made if the fission yields for the fissioning capture product are well known, this correction can result in significant errors in the fission yields for the principal target nuclide.

Before going further, the term "fast fission yield" should be addressed. It is at best a relative term because it is well known that fast fission yields can vary with neutron energy. This one item has made it most difficult for the evaluators and compilers of "fast yields" to produce accurate compilations, because it prohibits use of the pooling techniques which have been applied to thermal yield data. Unfortunately, because most reported experimental fast yield data can not be associated with a known neutron spectrum, the compilers to date have had no choice other than to pool the data. Thus, it is not unreasonable that fast yield compilations show significant discontinuities for adjacent yields because the data were probably obtained from irradiations conducted in significantly different neutron spectra. It is appreciated that the early worker probably had little regard for the neutron spectrum effect on yields and that just obtaining fast yield data was of primary concern; however, it is strongly emphasized that all new measurements be associated with a known neutron spectrum.

The effect of neutron energy on fission yields is shown in Figure 1. In this presentation, the ratios of the fast to thermal yields[22] for ^{235}U are plotted as a function of mass number. The general result of fissioning with increasing energy neutrons is an increase in the yields on the wings of the mass yield curve, an increase in the valley yields, and a small depression in the peak yields. This effect appears to change systematically as the energy of the fissioning neutron increases. The discontinuities in the plotted data may be due to certain fine structure effects or the result of inaccuracies in data source[22].

An extensive fast yield measurement program is currently being conducted in our laboratory at the Idaho National Engineering Laboratory. Mass spectrometric yields are being measured for over 40 nuclides for ^{233}U, ^{235}U, ^{238}U, ^{237}Np, ^{239}Pu, ^{241}Pu, ^{242}Pu, and ^{241}Am which were irradiated in EBR-II[2,4]. Yield data for ^{233}U, ^{235}U, ^{238}U, and ^{239}Pu and neutron spectral data were published in 1975[4], and data for ^{240}Pu, ^{241}Pu, ^{242}Pu, and ^{237}Np should be available by the end of 1977.

Of primary concern in this program are the fast fission yields for the isotopes of Nd which are used for monitors for the determination of burnup in fast

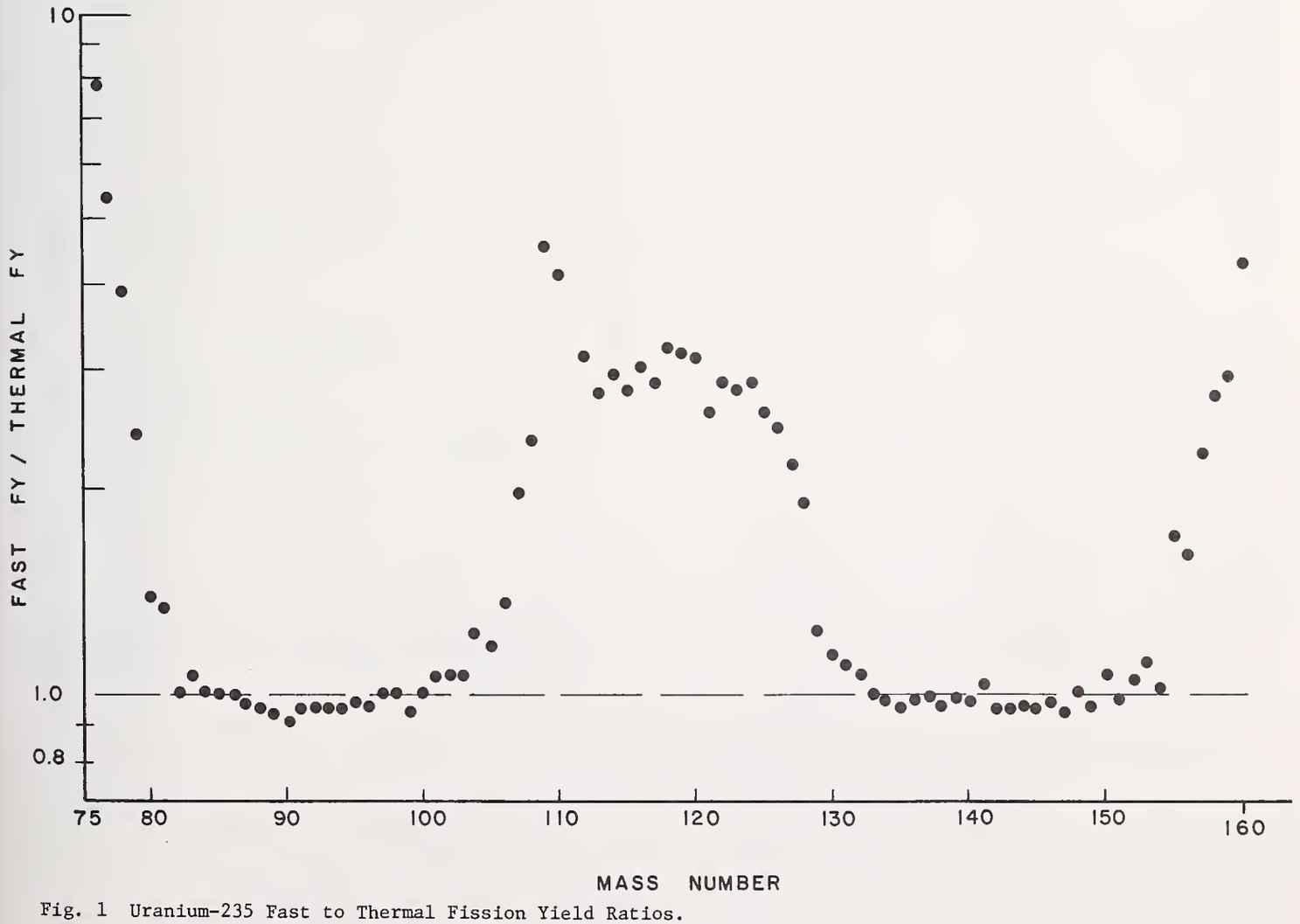

Fig. 1 Uranium-235 Fast to Thermal Fission Yield Ratios.

TABLE I. RELATIVE Nd ISOTOPIC COMPOSITIONS AND ISOTOPIC RATIOS FOR ^{235}U FISSIONING

	$\sigma_{f_8}/\sigma_{f_5}$ Spectral Index, Reactor, and Reference						
SI $\sigma_{f_8}/\sigma_{f_8}$	Thermal[10] 0.0	EBR-II[5] Axial Bl. 0.003	EBR-II[4] Row-8 0.02	DFR[23] 0.035	EBR-II[5] Row-4 0.06	OSIRIS[24] 0.089	EBR-I[4] Core 0.12
Isotopes							
^{143}Nd	0.3923	0.3898	0.3891	0.3870	0.3840	0.3836	0.3826
^{145}Nd	0.2583	0.2589	0.2563	0.2544	0.2545	0.2546	0.2544
^{146}Nd	0.1964	0.1975	0.1969	0.1981	0.1985	0.1962	0.1973
^{148}Nd	0.1101	0.1110	0.1126	0.1133	0.1149	0.1167	0.1161
^{150}Nd	0.0429	0.0429	0.0450	0.0472	0.0481	0.0489	0.0496
Isotopic Ratios							
150/143	0.1094	0.1101	0.1157	0.1220	0.1253	0.1275	0.1296
150/145	0.1661	0.1657	0.1756	0.1855	0.1890	0.1920	0.1950
148/143	0.2807	0.2848	0.2894	0.2928	0.2992	0.3042	0.3034

breeder reactor fuels. In the process of evaluating our Nd fast yield data and comparing it to data reported by other workers, the noted differences were considered to be too large to be attributed to measurement error. In lieu of comparing absolute yield values, we evaluated the relative isotopic data because systematic errors in the measured number of fissions used to calculate the absolute yields could be eliminated. A comparison of the relative Nd isotopic data is given in the top half of Table I. When the data are ordered by spectrum hardness, systematic changes in the Nd isotopic composition are apparent. To amplify these changes, selected isotopic ratios were calculated and are given in the bottom half of Table I. For ^{235}U, the change in the $^{150}Nd/^{143}Nd$ ratio between the thermal neutron values and the very hard EBR-I spectrum values is ∿20%.

As a result of the trends shown in Table I, several different forms of neutron energy indices were considered to provide a means for the possible correlation of yields with energy. Included were mean neutron energy, median neutron energy, mean and median neutron energy for fission of a given heavy isotope, fraction of neutrons in a given energy range, and the ratio of cross section values for two selected fissioning isotopes. Of these the ratio $^{238}U(n,f)/^{235}U(n,f)$ was selected because more yield data could be associated with this index than any of the others. This ratio gives a good indication of spectral hardness because ∿95% of the neutron energy response for $^{238}U(n,f)$ is above ∿1.4 MeV and ∿95% of the response for $^{235}U(n,f)$ is below 2 to 3 MeV.

The change in the isotopic ratio, $^{150}Nd/^{143}Nd$, for those ^{235}U and ^{239}Pu data which could be associated with the spectral index, $^{238}U(n,f)/^{235}U(n,f)$, is shown in Figure 2. The correlation of the isotopic composition of Nd with the selected spectral index is clearly demonstrated.

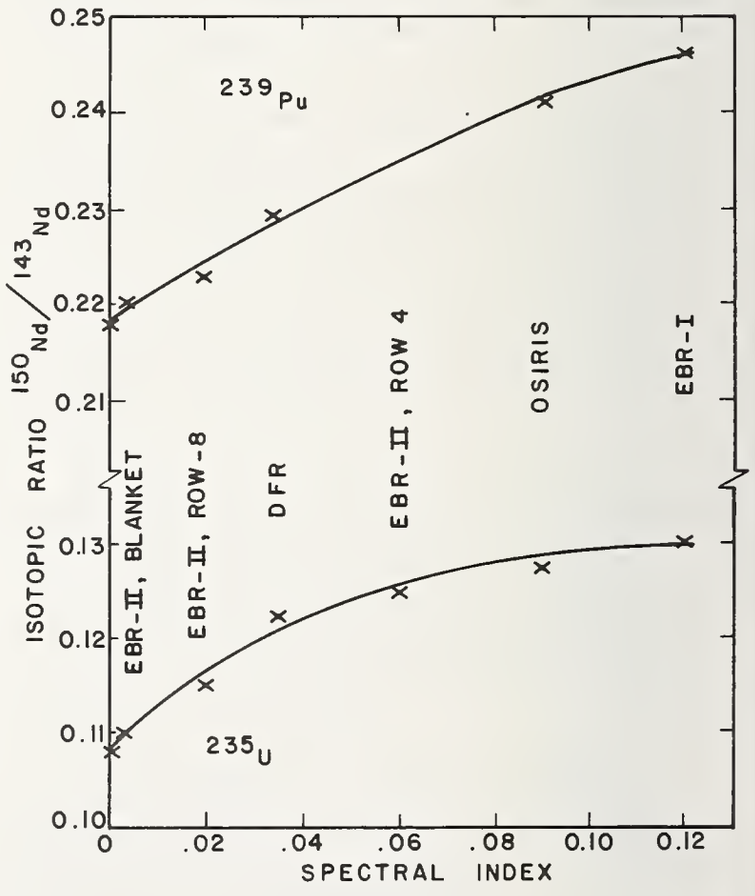

Fig. 2 Change in Isotopic Ratio of $^{150}Nd/^{143}Nd$ with Neutron Energy for ^{235}U and ^{239}Pu Fast Fission.

To extend the correlation of isotope ratios with neutron energy to other fission products, the extensive ^{235}U fission yield data obtained in the author's laboratory for thermal fission[2,10], fast fission in row-8 of EBR-II[4], and fast fission in the core of EBR-I[2] were evaluated. The respective spectral index values for these irradiations are zero, 0.02, and 0.124. Because little data are available between index values of 0.02 and 0.124, the correlations are not as accurate as those for the Nd isotopes.

Isotopic ratios were calculated for the various fission product elements using the isotope whose fission yield changed least with neutron energy as the reference isotope. For example, for the Kr isotopes, ^{86}Kr showed little change with neutron energy and was selected as the reference isotope.

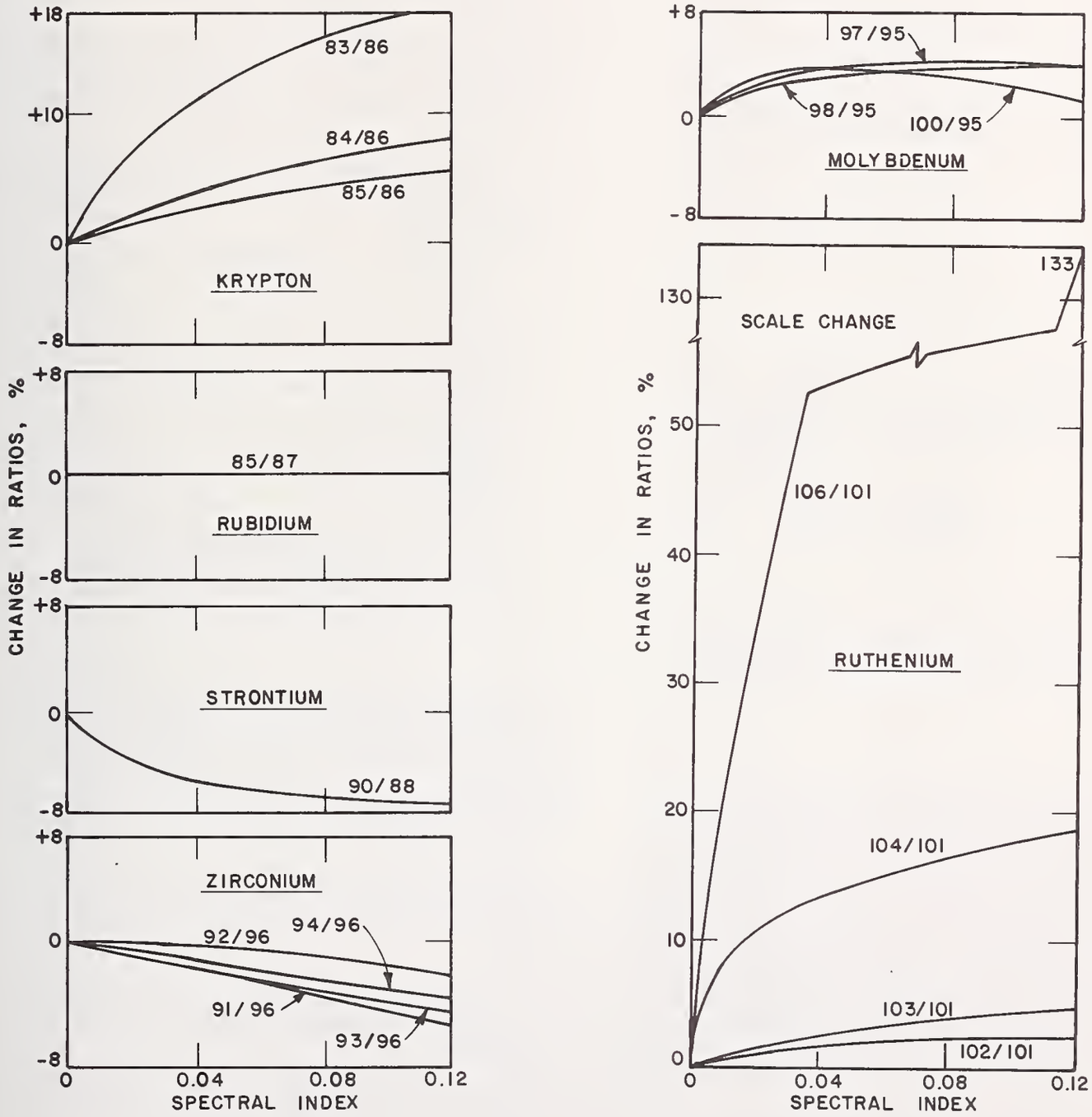

Fig. 3 Change in Fission Product Isotopic Ratios with Neutron Energy for the Isotopes of Krypton, Rubidium, Strontium, Zirconium, Molybdenum, and Ruthenium.

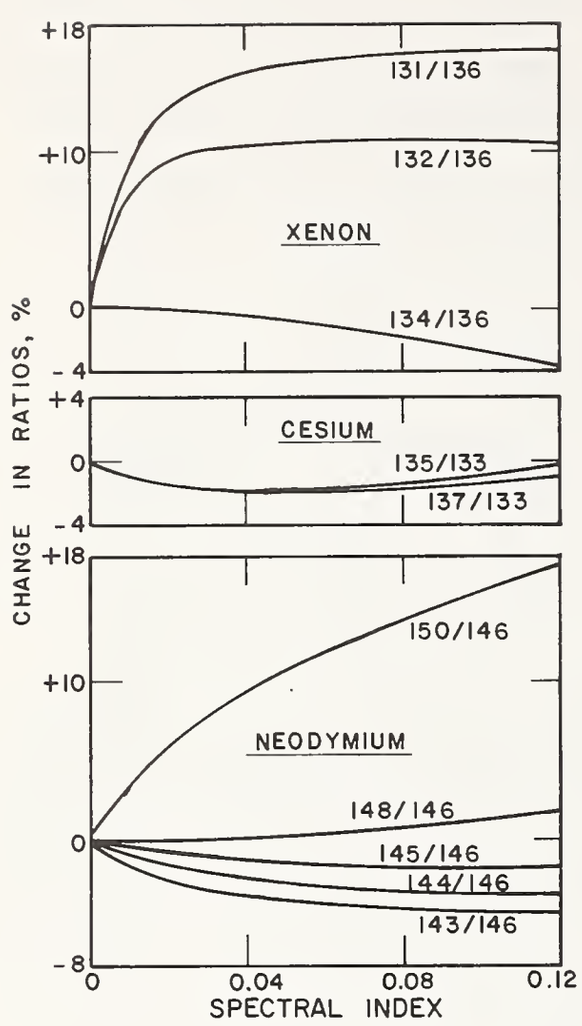

Fig. 4 Change in Fission Product Isotopic Ratios with Neutron Energy for the Isotopes of Xenon, Cesium, Neodymium, and Samarium.

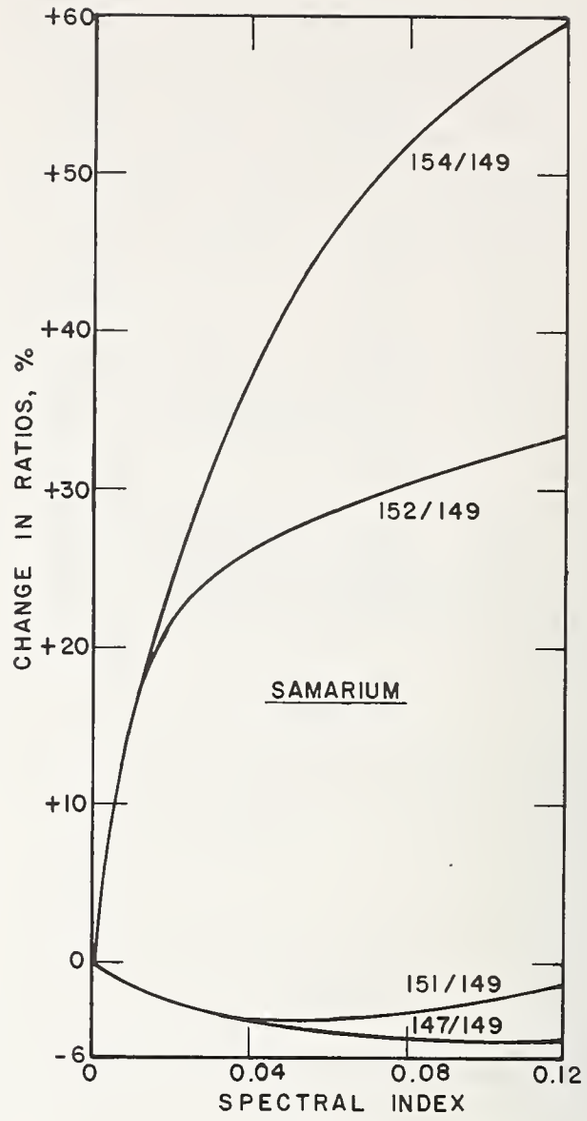

The percent changes in the ratios, relative to the thermal values are presented in Figures 3 and 4. The isotopic ratio changes in the light mass peak are reflected by counter isotopic ratio changes in the heavy mass peak. For example, the change of 15 to 20% for Kr isotopes 83 to 86 on light wing of the light mass peak is reflected by a like change in the mass region 148 to 151 on the heavy wing of the heavy mass peak. A second example is that the 86 to 88 mass region and its reflected 146 to 148 mass region, both change little. Another example, is similar changes for the light Xe isotopes and the light Ru isotopes. Little significant changes are seen for those isotopes on the peaks of each wing of the mass yield curve.

This study, of the changes in yields with neutron energy will be continued with the goal being the ability to predict a given yield for any neutron energy. To aid in the effort to quantify the changes in yields with neutron energy, it is imperative that every effort be made to define the neutron spectrum associated with fast fission yields being determined. For experiments currently in progress, the workers should attempt to obtain this information from the reactor physicist, or preferably, irradiate specific samples to define the neutron spectrum. For new experiments, the worker should make every effort to include a series of spectrum monitors in the irradiation assembly.

The compilers of fast fission yield data must use only well documented data and evaluate each set of yield data with respect to the neutron energy.

REFERENCES

1. Hahn, O., Strassman, F., Naturwiss. 27, 11,89 (1939).

2. Lisman, F. L., Abernathey, R. M., Maeck, W. J., Rein, J. E., Nucl. Sci. Eng. 42, 191 (1970).

3. Maeck, W. J., Larsen, R. P., Rein, J. E., USAEC Report, TID-26209 (1973).

4. Maeck, W. J., Editor, U.S. ERDA Report, ICP-1050-1 (1975).

5. Larsen, R. P., Argonne National Laboratory, Private Communication, 1973.

6. Grundal, J. A., Gilliam, D. M., Dudey, N. D., Popek, R. J., Nucl. Tech. 25 (2), 237 (1975).

7. Larsen, R. P., Schablaske, R. V., Oldham, R. D., Meyer, R. J., Homa, M. I., U.S. AEC Report, LA-4407, (1967).

8. Arrol, W. J., Chackett, K. F., Epstein, S., Can. J. Res, 27B, 757 (1949).

9. Walker, W. H., AECL Rept. 3037-II, (1973).

10. Maeck, W. J., U.S. ERDA Rept. ICP-1092 (1976).

11. Dudey, N.D., Popek, R. J., Greenwood, R. C., Helmer, R. G., Kellogg, L. S., Zimmer, W. H., Nucl. Tech. 25 (2), 294 (1975).

12. von Gunten, H. R., BNES Proceeding of the International Conference on Chemical Nuclear Data, Canterbury, UK (1971).

13. Walker, W. H., Review Paper 11a, IAEA-169 (1973).

14. Cuninghame, J. G., Review Paper 11b, IAEA-169 (1973).

15. IAEA Proceedings of a Panel on Fission Product Nuclear Data, Bologna, Italy, IAEA-169 (1973).

16. Meek, M. E., Rider, B. F., General Electric Co. Rept. NEDO-12154 (1972). Update NEDO-12154-1 (1974).

17. Crouch, E.A.C., Paper IAEA/SM-170/94 Symposium on Applications of Nuclear Data, Paris, (March 1973).

18. Lammer, M., Eder, O. J., Paper IAEA/Sm-170/13, Symposium on Applications of Nuclear Data, Paris (March 1973).

19. ENDF/B-IV Fission Yield Data File, National Nuclear Data Center, Brookhaven National Laboratory, USA.

20. Maeck, W. J., Emel, W. A., Delmore, J. E., Duce, F. A., Dickerson, L. L., Keller, J. H., Tromp, R. L., U.S. ERDA Rept. ICP-1092 (1976).

21. Crouch, E.A.C., UKAEA Rept., AERE-R 7394 (1973).

22. Rider, B. F., General Electric Co., Private Communication (1977).

23. Sinclair, V. M., Davies, W., International Conference on Chemical Nuclear Data, BNES, Univ. of Kent, Canterbury, England (1971).

24. Robin, M., Bouchard, J., Darrouzet, M., Frejaville, G., Lucas, M., Prost Marechal, F., ibid.

FISSION REACTION RATE STANDARDS AND APPLICATIONS

J. Grundl and C. Eisenhauer
National Bureau of Standards
Washington, D.C. 20234

Fission rate measurements in and around prototype and power reactors of all kinds, as well as in the criticals of reactor physics are vital elements in understanding nuclear energy generation rates, neutron transport, and the integrity of materials exposed to reactor radiation fields. Standardization and interlaboratory referencing for this historic measurement activity have improved significantly since the last neutron standards symposium in 1970. This advancement will be summarized along with a general orientation and description of fission detector response characteristics and interpretation. For the last, necessary analytic formulations and a brief treatment of error propagation are included. Also included is an updated look at observed versus predicted fission cross sections for fission spectrum neutrons and the related fast criticals of reactor physics.

(Cross sections; fission; neutron reactions; neutron spectrum; reactor fuels; reactor materials)

Introduction and Summary

The requirement to measure isotopic fission rates appears in a wide variety of technical-engineering problems associated with radiation effects in materials and reactor design and management. Looking only at physical changes in materials exposed to neutrons the array is bewildering. Some examples are swelling of reactor fuel claddings, fuel matrix rearrangements, integrity of pressure vessel weldments, activation of reactor service equipment, vaporization of liquid rocket propellant, and gain changes in transistors. In the management of these radiation effects problems, fission rate measurements are often used indirectly to derive neutron fluence and spectrum information. Direct application of fission rate measurements are also important and they arise most often, and with a longer history, in the area reactor design and nuclear fuels management. Examples are verification and guidance of reactor physics calculations; optimization of fission power gradients; relative fission rates among fissionable isotopes competing for neutrons in a reactor core; determination of fuel burn-up and burn-in rates in all types of power reactors including nuclear weapons.

Techniques of fission rate measurements are also diverse. Among active fission detectors there exist fission ionization chambers as small as a pencil tip and as large as a bread box; passive fission activation detectors can be as thin as a needle or as large as a sheet of paper. Among destructive analysis techniques, mass spectrometry for example, will measure total fissions in almost anything that can be dissolved.

Of primary concern perhaps for a neutron standards symposium, are fission rates that give rise to fundamental integral cross sections. These are the observables that stand as constraints for the evaluation of differential cross section data. A single review of integral results at the previous Neutron Standards Symposium in 1970 is matched at this meeting with a half dozen papers on integral measurement techniques, facilities, and results. The remarks in 1970 regarding differential and integral measurement as "areas of effort that do not always communicate so well," is now almost outdated.[1] The need by a much harassed nuclear energy industry for consistent design and operation parameters overwhelms the vestiges of mutual disrespect. Today, on one hand, an observed fission-spectrum-averaged fission cross section contributes to the setting of the ^{235}U fission cross section scale for ENDF/B-V, and on the other, reactor dosimetry spectrum characterizations routinely use the new ENDF/B dosimetry cross section file with only mild threats to "adjust."

Measurement Standards

Accuracy requirements for many of the direct applications of fission rates can be severe: as low as $\pm$ (2-5)%(1σ) for the determination of reactor fuel burn-up or in checks of reactor physics calculations. Neutron flux and fluence estimates for managing radiation effects problems typically are less severe and dependence upon neutron transport calculations with less experimental verification is common. The latter is true also, because in situ neutron flux measurements can be difficult for radiation effects surveillance. However, when optimum material performance is sought, and high-investment engineering or safety decisions are involved, stiff accuracy requirements appear. In this case, a measurement program in support of calculation assumes recognized importance. This is particularly true when critically evaluated spectrum characterization is sought and fission detectors coupled with other types of neutron energy sensitive activation detectors are employed (i.e., the familiar multiple foil spectrum unfolding techniques).

Standards and intermeasurement reference for all of this varied and decades-long effort of fission rate measurement are of two kinds: 1) artifacts, such as standard solutions or fissionable deposits; and 2) well-characterized neutron fields, such as thermal equilibrium, monoenergetic, and fission neutron spectra. The latter are most important when fission rates are used to derive neutron field characteristics.

Not all fission rates are standardized in the manner just stated, most in fact, are not. Measurements which depend upon extraneous instrument calibrations and various types of nuclear data are common (e.g., fission yields and alpha decay constants). Until recently, there existed no central repository of mass assayed fissionable deposits generally available for fission rate measurement calibration or referencing. Considering the vital role fission rates play in all branches of radiation effects and nuclear energy development, the deficiencies in standardization and interlaboratory comparisons is surprising. The introductory paper by R. Taschek at the 1970 Symposium referred to this odd circumstance in relation to the use of fission rate measurements as a standard for neutron flux determinations with accelerators.[2]

Improvements Since 1970

After 1970 notable concern and some improvements in referencing fission rate measurements have taken place. Recall first the operative distinctions set forth in References 1 and 3.

Mascroscopic Data. Experimental results from arrangements in which a dominating feature is neutron transport, i.e., multiple encounters of neutrons with nuclei which produce a series of velocity changes, and in important instances, new sources of neutrons.

Microscopic Data. Experimental results, generally energy dependent cross sections, from arrangements in which single encounters of neutrons with nuclei predominate.

Integral Measurements. Measurements that require for interpretation an integration of pointwise microscopic data over energy intervals and/or the neutron flux over space intervals that are not small compared to the range of interest.

Differential Measurements. Measurements for which energy or space integrations are not necessary for interpretation, only for corrections to data.

(1) In the area of macroscopic data from integral measurements, organized efforts are underway in the U.S. to achieve interlaboratory consistency in reactor physics and in reactor materials dosimetry.[4-6] Internationally, the IAEA has initiated a program of identifying benchmark neutron fields and evaluating their application. A Consultant's Meeting on Integral Cross Section Measurements in Standard Neutron Fields for Reactor Dosimetry was convened in November, 1976.[7] To prepare for this meeting a compendium of benchmark neutron fields was prepared within the context of the following characteristics:[9]

1. Simple and well-defined geometry;
2. Adequate neutron fluence and stable flux density;
3. Reproducible and accurately characterized neutron spectra based on spectrum measurements and/or reliable calculations;
4. Sustained availability for measurements.

(2) Both integral and differential measurements have benefitted from the development of a permanently available set of reference and working fissionable deposits at the National Bureau of Standards.[8] Isotopes presently represented in the set include ^{235}U, ^{239}Pu, ^{238}U, and ^{237}Np, with $^{240,241}Pu$ to be added within the next year. Traceability of fission rate measurements to these deposits may be established by direct alpha or fission comparison counting of deposit pairs, or by exposure in a relevant neutron field of a complete fission detector to be calibrated along with an NBS double fission ionization chamber operating with an NBS mass assayed deposit.[8]

(3) The situation regarding observed versus predicted fission-spectrum-averaged fission cross sections is better now than it was in 1970.[1] New absolute cross section measurements have been performed and the discrepancies with the differential microscopic data are no longer in excess of ten percent.[10-12] And most important for fast neutron standardization there exists now an evaluation of the fission neutron spectrum including uncertainty estimates based on all documented differential spectrometry.[9,13] The stubborn discrepancies surrounding fission rate ratios in simple macroscopic systems like the Big Ten Fast Metal Critical Assembly also have changed drastically following the inclusion of long-awaited changes in inelastic scattering cross sections into neutron transport calculations.[6]

This report will review briefly and largely by reference these various improvements in fission rate standardization and the associated advances in applied measurement. Preceding this and comprising the major portion of the paper will be an orientation regarding fission detector measurements and their use for neutron spectrum characterizations. This is appropriate, hopefully, and no more controversial than is beneficial on the occasion of a symposium devoted to neutron standards and applications.

Neutron Spectrum Response

The neutron energy dependence of fission detection falls neatly into two categories: 1) full-energy-range detectors with generally flat fission cross sections in the MeV range and increasing fission cross sections down to thermal equilibrium energies; and 2) threshold detectors with smooth cross sections that rise rather sharply in the energy range 0.5 to 2 MeV. There is not much distinction within these two categories and a small array of fission detectors are sufficient for illustration. Four are chosen for this review: $^{235}U(n,f)$, $^{239}Pu(n,f)$, $^{237}Np(n,f)$, and $^{238}U(n,f)$. Spectrum responses of these detectors will be summarized as an introduction to quantitative methods of interpretation.

Spectrum Characteristics

Five neutron spectra representative of much of nuclear technology are displayed in Figure 1. Included are two spectra associated with differential cross section verification and detector calibrations (the ^{235}U fission spectrum and the one-dimensional Intermediate-Energy Standard Neutron Field (ISNF)), two fast-breeder related spectra (the FTR and EBR-II core), and a typical light-water related spectrum (LWR pressure vessel environment).

Two ordinate scales are employed for this display: $\log [E\phi(E)]$ from 1 MeV down to the cadmium cut-off and $\log [\phi(E)/\sqrt{E}]$ versus a linear energy scale above 1 MeV. They were chosen in order to show the full spectrum energy range below 1 MeV, along with fission spectrum components as linear slopes proportional to average spectrum energy above 1 MeV. The neutron transport calculations represented in Figure 1 are from multigroup computations normalized to $\int\phi(E)dE = 1$ above 0.4 eV. As a first order approximation of the true shape of the spectra for this plot, the histogram spectra from the calculations were transformed to discontinuous linear segments which approximate slopes and preserve group fluxes.

Fission neutrons represent the top of the energy spectrum for fission reactors and their environments. Interestingly enough, the fission neutron energy distribution remains discernible in a number of these fission reactor environments. Measurements with threshold detectors have established that the fission spectrum component is well preserved above $\sim$ 1.5 MeV in fast metal criticals of ^{235}U and ^{239}Pu, and also in a zoned-core critical assembly with a spectrum typical of a fast breeder.[5,14] Reactor calculations appear to verify this spectrum characteristic showing it to be maintained in the cores of the U.S. Fast Test Reactor (FTR) and in EBR-II. Even for the LWR core shown in Figure 1 the fission spectrum component persists down to below 2 MeV. If transport calculations at LWR pressure vessels are to be believed, the spectrum there also resemble a fission spectrum shape over a significant part of the MeV

energy range. In fact, spectrum-averaged cross sections for $^{238}U(n,f)$ and Np(n,f), truncated at threshold, for all of these spectra are within 10% of the fission spectrum value - see Eq. (1) below.

Below the fission spectrum range a transition energy region exists between 10 keV and 1 MeV for the reactor spectra shown in Figure 1. This is the energy region where breeding occurs in fast reactors and relaxation to a 1/E equilibrium spectrum occurs in the light-water power reactor systems. This is a difficult energy range for neutron flux measurements, and for calculations as well, particularly in the decade above 10 keV. Below 10 keV the four energy decades down to thermal are characterized by a neutron slowing down spectrum, $E\phi(E) \sim$ constant.

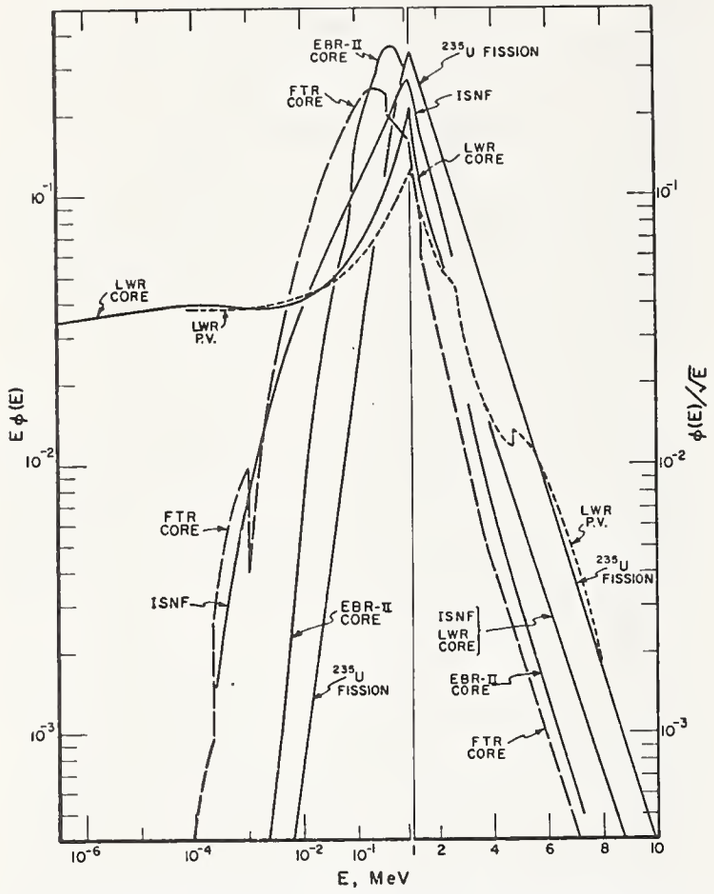

Fig. 1. Representative neutron spectra for materials dosimetry applications. For energies less than 1 MeV the quantity log [Eφ(E)] is plotted against log E. For energies greater than 1 MeV, the quantity log [φ(E)/√E] is plotted against E.

Fission Detector Response

Fission detection for the purpose of estimating neutron flux intensity and spectrum belongs to a class of integral measurements which in principle are simple to perform and interpret. As with all integral measurements, however, accuracy of measurement and the best possible understanding of detector response is essential if quantitative results are to be obtained. For two of the neutron fields shown in Figure 1, fission detector responses will be shown in cumulative spectrum response plots, Figures 2 and 3. In such plots the integral spectrum $\int_E^\infty \sigma(E)\phi(E)dE$, appear together. Energy-dependent cross sections for the display are from ENDF/B-IV.

For the ^{235}U fission spectrum in Figure 2, the ordinate gives the fraction of the response which is above the corresponding abscissa energy. The threshold fission reactions ^{237}Np and ^{238}U are seen to provide effective complementary coverage for the bulk of the spectrum. Near the 2 MeV average energy of the fission spectrum, the ^{238}U response fraction is ~ 0.8 while for ^{237}Np it has reached only ~ 0.5. Both threshold reactions cut off sharply providing a well-defined response range. The wide-energy-response fission detectors, ^{239}Pu, and ^{235}U, follow closely the fission spectrum shape. Thus, they are good total flux monitors for fission spectra, and in fact, ^{239}Pu is a good total flux monitor for all fast neutron spectra which do not have a significant spectrum component below ~ 10 keV.

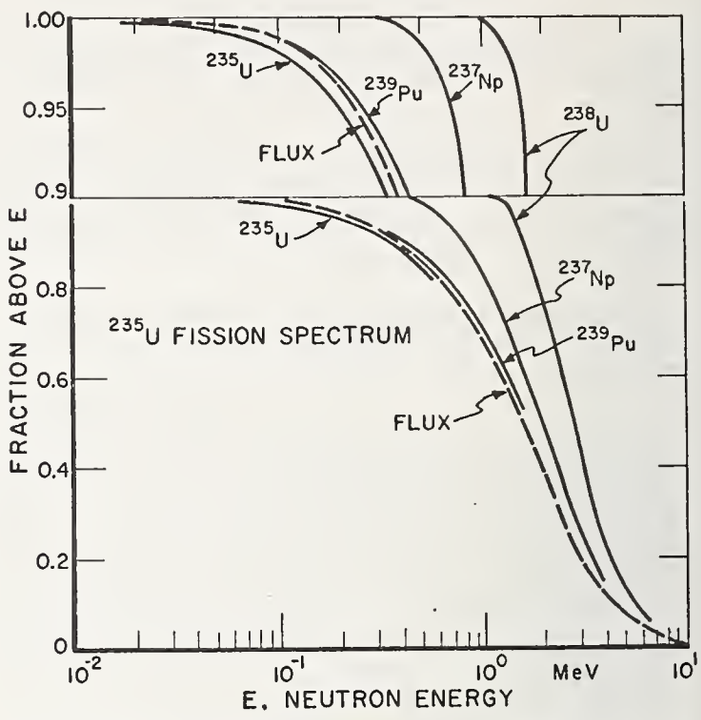

Fig. 2. Fraction of neutron flux and fission detector response above energy E in a ^{235}U fission neutron spectrum.

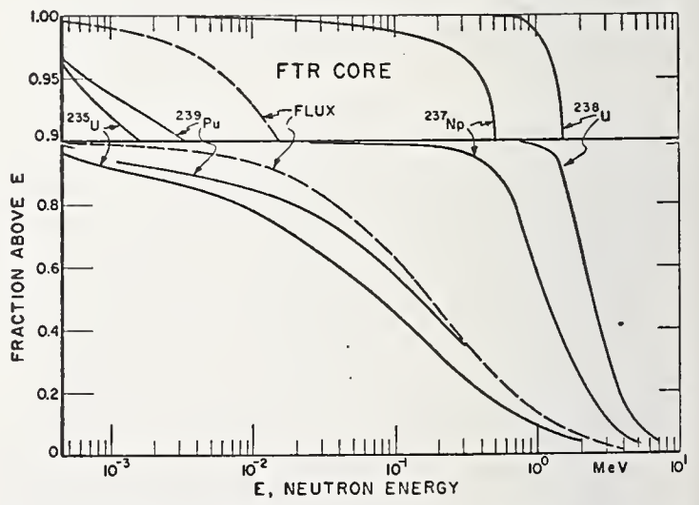

Fig. 3, Fraction of neutron flux and fission detector response above energy E in the FTR breeder core neutron spectrum.

Fission detector responses for the typical breeder reactor core spectrum of FTR are plotted in Figure 3. The ^{238}U response cut-off remains sharp, a result which remains in need of complete verification. Some recent measurements are helpful in this regard.[15] The complementary coverage of ^{237}Np and ^{238}U is even better than for fission spectra. The cumulative fraction 0.9 for ^{238}U corresponds to a cumulative fraction of less than

0.4 for ^{237}Np. A notable subthreshold tail for ^{237}Np extends to energies well below the 0.95 response fraction energy. This is a significant issue for spectrum characterizations and especially for checks of reactor physics calculations. The difficulty is that no satisfactory agreement exists regarding subthreshold fission for ^{237}Np.[16] The response functions for ^{235}U and ^{239}Pu in Figure 3 fall below the spectrum because of the rising cross sections which shift the detector responses to lower energies. Almost 10% of their response lies below 2 keV where transport calculation places less than 2% of the spectrum. Concerns for neutron self-shielding begin for activation fission foils when significant response below 10 keV occurs. In spite of this and similar measurement problems, the $^{239}Pu(n,f)$ detector is still an attractive total flux monitor. The maximum departure of the flux curve from ^{239}Pu response curve in Figure 3 is 15% and the average $^{239}Pu(n,f)$ cross section for this particular breeder core spectrum differs by less than 1% from the fission spectrum value. The possibility of neutron flux transfer which takes advantage of these small cross section differences is discussed in the next section.

The graphical displays just given indicate the general features of measured fission detector responses and their significance. In order to initiate quantitative interpretation of these observed fission rates, calculated spectrum-averaged fission cross sections must be available. Obtaining such computed cross sections is not always a straight-forward procedure because of the coarseness of multigroup spectra from reactor physics computations and because of rapidly changing cross sections in some energy regions. Nevertheless, a consistent set of calculated cross sections is essential for detector interpretation if arbitrary computational biases are not to render careful measurement worthless.

Some Principles of Neutron Field Characterization

The characterization of neutron fields in reactor physics criticals, and in and around the great variety of materials testing, prototype, and power reactors, depends very largely on passive integral detectors. Of these, fission detectors are the most essential. Among passive fission detectors, fission product activation is the dominant technique assisted in special situations by fission track recorders. Fission ionization chambers when applicable are important active detector complements. Neutron flux spectrum or intensity information may be derived from integral detectors based on absolute detection efficiencies and absolute fission cross sections, or upon a calibration carried out by exposure in a benchmark neutron field. A benchmark for calibration is a well-characterized neutron field which provides an adequate fluence of neutrons for detector calibration and which exhibits a spectrum that is relevant and better known than the spectra under study.

The choice between absolute detection methods and neutron field calibration is often one of convenience and custom more than an explicit evaluation of the relative effort and the errors involved. Absolute detection methods have taken precedence historically, a fact attributable in part to the minimal development and poor availability of well-characterized neutron fields for purposes of calibration. The latter situation has improved, although the recognition of it is delayed. For this reason the outline below of neutron field characterization with integral detectors will emphasize benchmark field calibration. The recognition that absolute measurements are also important is not set aside. Such complements are proper and "keep half an eye" on the claims of proponents of particular benchmark fields.

Response ratios among a set of integral detectors exposed to a benchmark field provide first and foremost a test of detector reaction cross sections over the energy range of the benchmark spectrum. If observed to predicted detector response ratios agree, field characterization may proceed with confidence and minimized uncertainties. If they disagree by more than the absolute detection errors and the assigned benchmark spectrum uncertainties, allowed adjustment of the cross sections may be justified. Alternatively, for detectors with reliable cross sections, allowed adjustments of some benchmark spectra may be undertaken. All in all, consistency of benchmark detector response should be established (forced somewhat, if necessary) in order to achieve unambiguous spectrum characterization in the neutron field under investigation.

Similarly, if the detection techniques employed in the benchmark exposure are the same as--or calibrated relative to--the techniques used in the field characterization exposure, observed and predicted ratios for the benchmark may be brought into agreement by ad hoc adjustment of the overall detection efficiency. Establishing detection efficiencies in this way removes a number of systematic errors associated with the detection scheme. Examples are errors of absolute cross section scales, activation counter calibrations, and nuclear parameters including branching ratios and fission yields. This error correlation in turn allows for a wider choice of integral detector types and of activation detection methods.

Beyond the matter of adjusting reaction cross sections, benchmark field spectra, or detection efficiencies--an issue for which agreement on systematics does not yet exist among experimenters--the benchmark exposure provides a basis for setting the accuracy and confidence for the entire spectrum characterization procedure. Often enough, it will point to inadequacies in cross sections or weaknesses in the experimental detection scheme.

Brief Formulations

Some analytic expressions for observed and derived integral detector responses are needed to move from the general assertions just given to specific applications. As noted, activation detectors are most typical for spectrum investigations, and therefore the formulations below are in terminology applicable for them. Modifications required for other types of integral detectors involve for the most part changes in time integrating quantities, e.g., flux-fluence, decay constants, etc., and do not affect the principles of integral detector calibration.

Spectrum and Cross Section Definitions

$(nv)_o$;$(nvt)_o$ = total energy-integrated flux and fluence, respectively.

$\psi(E)$ = neutron spectrum normalized to unity.

$\psi(>E_t)$ = fraction of spectrum above neutron energy E_t:

$\sigma(E)$ = detector reaction rate cross section vs. energy.

$\sigma(E) = \sigma_o \cdot s(E)$, where σ_o is the absolute cross section scale factor, and $s(E)$ the cross section shape normalized to unity over a relevant benchmark spectrum, $\psi_b(E)$:

$$\int_0^\infty s(E)\psi_b(E)dE = 1$$

$\bar{\sigma}$ = spectrum-averaged cross section:

$$\bar{\sigma} = \sigma_o \int_0^\infty s(E)\psi(E)dE$$

$\bar{\sigma}(>E_t)$ = spectrum-averaged cross section truncated at E_t:

$$\bar{\sigma}(>E_t) = \sigma_o \int_{E_t}^\infty s(E)\psi(E)dE / \int_{E_t}^\infty \psi(E)dE \quad (1)$$

$\frac{[\sigma(E)\psi(E)]}{\bar{\sigma}}$ = detector response function

E_p = truncation energy for defining a detector energy response range. For percentile P, the truncation energy is defined by

$$P = \frac{1}{\bar{\sigma}} \int_{E_p}^\infty \sigma(E)\psi(E)dE \quad , \quad (2)$$

where $E_p(P=0.5)$ = median energy, and for this paper $E_p(P=0) = 20$ MeV, $E_p(P=1) = 0.4$ eV.

Observed Reaction Rate

$$R = \varepsilon_\gamma \cdot \mu(\lambda, \bar{N}, Br, Y, I, \ldots) \cdot D \quad (3)$$

R = observed activation detector disintegration rate in disintegrations per second (dps) at end of irradiation.

D = observed gamma counting rate after neutron field exposure in counts per second (c/s).

ε_γ = gamma counting efficiency.

μ = composite factor for converting gamma counting rate of a detector to disintegration rate: decay constant (λ), effective number of detector atoms ($\bar{N}$), branching ratio (Br), fission yield (Y), γ-ctg losses and activation interference (I).

Derived Reaction Rate

$$R_e = G(\lambda,t) \cdot N \cdot \bar{\sigma} \cdot (nvt)_o \quad (4)$$

R_e = derived reaction rate (dps) from fluence $(nvt)_o$ received in a neutron field with spectrum $\psi(E)$.

$G(\lambda,t)$ = activation decay rate factor. At the end of an irradiation at constant flux and duration t, $G(\lambda,t) = [1 - \exp(-\lambda t)]/t$.

The neutron fluence greater than a given energy $[(nvt)_o \cdot \psi(>E_o)]$ is often used as a dosimetry parameter. For example, $\psi(>E_o = 1\ \text{MeV})$ in U.S. guides for surveillance of reactor pressure vessel fluence. Since detector reactions have various minimum response energies, it is useful to express a derived reaction rate in terms of a neutron fluence greater than E_o, and a detector cross section truncated at percentile P. This can be done by expressing $\bar{\sigma}$ in eq. (4) in terms of P using Eqs. (1 and 2):

$$R_e = G(\lambda,t) \cdot N \cdot \frac{1}{P} \cdot \bar{\sigma}\,(>E_p) \cdot \psi(>E_p) \cdot (nvt)_o \quad .$$

Thus,

$$R_e = G(\lambda,t) \cdot N \left[\frac{1}{P} \frac{\psi(>E_p)}{\psi(>E_o)}\right] \cdot \bar{\sigma}\,(>E_p) \cdot [\psi(>E_o)(nvt)_o] \quad . \quad (5)$$

This formulation has the advantage that it contains the cross section $\bar{\sigma}\,(>E_p)$ truncated at an energy E_p appropriate for the reaction, and the fluence truncated at another energy appropriate for dosimetry. The factor $\frac{\psi(>E_p)}{\psi(>E_o)}$ can be rewritten as

$$\frac{\psi(>E_p)}{\psi(>E_o)} = 1 - \frac{\int_{E_o}^{E_p} \psi(E)dE}{\int_{E_o}^\infty \psi(E)dE} \quad . \quad (6)$$

The departure of this quantity from unity is determined by the fraction of the spectrum between E_o and E_p, the energy region where the detector does not respond. Thus, for two different spectra with similar shapes above E_p but dissimilar between E_o and E_p, the truncated cross sections $\bar{\sigma}\,(>E_p)$ would be about equal and the dissimilarities would be expressed by the spectrum component ratio in eq. (6).

Uncertainty in Spectrum Average Cross Section

Spectrum and cross section errors are estimated in multigroup formats. The spectrum-average cross section as a discrete summation,

$$\bar{\sigma} = \sigma_o \sum_i s_i \psi_i \Delta E_i;\ \sigma_i \equiv \sigma_o s_i \quad , \quad (7)$$

is subject to an error propagation which must account for the normalization of the neutron spectrum:

$$\left(\frac{\delta\bar{\sigma}}{\bar{\sigma}}\right)^2 = \left[\frac{\delta\sigma_o}{\sigma_o}\right]^2 + \sum_i \left(\frac{\delta s_i}{s_i}\right)^2 \left(\frac{\sigma_i}{\bar{\sigma}}\right)^2 \psi_i^2 (\Delta E)_i^2 + \sum_i \left(1 - \frac{\bar{\sigma}_i}{\bar{\sigma}}\right)^2 \left(\frac{\delta\psi_i}{\psi_i}\right)^2 \psi_i^2 (\Delta E)_i^2 \quad (8)$$

Spectral Index Calibrations

The physical datum for spectrum characterization with integral detectors is a set of measured reaction rate ratios. Consideration of a single ratio suffices for an outline of calibration principles. For two detectors α and β, the observed disintegration rate ratio in a neutron field under study, R_α/R_β, obtained from a count rate ratio, D_α/D_β, according to eq. (3), can be set equal to the reaction rate ratio according to eq. (4) in order to obtain an observed cross section ratio or spectral index:

$$\frac{[\varepsilon_\gamma \cdot \mu]_\alpha}{[\varepsilon_\gamma \cdot \mu]_\beta} \cdot \frac{D_\alpha}{D_\beta} = \frac{[G \cdot N]_\alpha}{[G \cdot N]_\beta} \cdot \left(\frac{\bar{\sigma}_\alpha}{\bar{\sigma}_\beta}\right)_s \quad . \quad (9)$$

$[\bar{\sigma}_\alpha/\bar{\sigma}_\beta]_s$ = observed spectral index for the study spectrum. The spectral index expected on the basis of some presumed spectrum for the neutron field under study, (e.g., measured or computed, "apriori input", or derived from other integral results), is

$$\left(\frac{\bar{\sigma}_\alpha}{\bar{\sigma}_\beta}\right)_{s,exp.} = \frac{\left(\sigma_o\right)_\alpha \int_o^\infty s_\alpha(E)\psi_{exp}(E)dE}{\left(\sigma_o\right)_\beta \int_o^\infty s_\beta(E)\psi_{exp}(E)dE} \qquad (10)$$

ψ_{exp} = presumed spectrum of field under study,

$\sigma_o \cdot s(E)$ = energy dependent detector cross section.

The double ratio of observed to expected spectral indexes (eq. 9 and 10) is a measure of the adequacy of ψ_{exp} to describe the study spectrum. The departure from unity of the double ratio provides a basis for adjusting ψ_{exp} in two energy groups corresponding to the response ranges of the two detectors. With or without the help of unfolding codes (useful when more than a few detectors are employed), the uncertainty in the spectrum adjustment will include errors from all of the factors in eqs. (9) and (10):

$$\delta D,\ \delta\varepsilon_\gamma,\ \delta\mu(\gamma,\ \bar{N},\ Br,\ Y,\ I\ \ldots),\ \delta N,\ \delta G,\ \delta\sigma_o,\ \delta_s\ .$$

The propagation of these errors, further emphasized in the common case of detector pairs with large overlapping response ranges, can easily reduce a spectrum adjustment to one of qualitative significance.

Calibration of a spectral index in a benchmark neutron field can change the uncertainty dramatically. The similarity of the benchmark and study spectrum is not of primary importance, a substantial overlap of detector response ranges in the two spectra is sufficient to achieve most of the accuracy improvement. An observed spectral index obtained in a benchmark field irradiation may be set in ratio to the observed spectral index from the study field. Using eq. (9), the double ratio dosimetry to benchmark is,

$$\frac{[\bar{\sigma}_\alpha/\bar{\sigma}_\beta]_s}{[\bar{\sigma}_\alpha/\bar{\sigma}_\beta]_b} = \frac{[D_\alpha/D_\beta]_s}{[D_\alpha/D_\beta]_b} \ .$$

The spectral index can be specified for the benchmark from its known spectrum, ψ_b, and the expression,

$$\left(\frac{\bar{\sigma}_\alpha}{\bar{\sigma}_\beta}\right)_s = \frac{[D_\alpha/D_\beta]_s}{[D_\alpha/D_\beta]_b} \cdot \frac{\left(\sigma_o\right)_\alpha \int_o^\infty s_\alpha(E)\psi_b(E)dE}{\left(\sigma_o\right)_\beta \int_o^\infty s_\beta(E)\psi_b(E)dE} \ . \qquad (11)$$

This is the observed spectral index for the study field calibrated by means of a benchmark field exposure.

When this observed index is compared to the derived spectral index for the study spectrum, the uncertainty will involve only the gamma counting rates (c/s), the benchmark spectrum, and partially, the shapes of the detector cross sections:

$$\delta D,\ \delta s(E) \text{ partially},\ \delta\psi_b(E)\ .$$

For all situations, the detector calibration by exposure to neutrons in a benchmark field removes the errors due to detector efficiency δE_γ, the dps conversion factor $\delta\mu$, and absolute cross sections scale $\delta\sigma_o$. If the detector response functions for the study and benchmark spectra, $[s(E)\psi_s(E)]$ and $[s(E)\psi_b(E)]$ are poorly matched, the full uncertainty of s(E) remains in the error propagation. Fully consistent cross section shapes from interlaboratory measurements among benchmarks are required to reduce the latter error. This is generally seen as a two-step process, with a restricted set of well-known detectors (category I reactions) made consistent by fine adjustment of evaluated cross sections followed by more serious adjustment based on integral measurement results of less well understood dosimetry detectors (category II reactions).

Neutron Flux Transfer

When the total neutron flux and fluence, $(nv)_o$ and $(nvt)_o$, can be specified for the benchmark irradiation of an integral detector, it is sometimes possible to perform a direct neutron flux transfer to the neutron field under study. This is most successful when the integral detector cross section is largely energy independent over the study spectrum energy response range. or when the detector response function $[s(E)\psi(E)]$, for the benchmark and study fields are well matched. An example of the first circumstance is the $^{239}Pu(n,f)$ detector applied to fast reactor spectra, an example of the second is $^{238}U(n,f)$ applied to fields where the fission spectrum dominates the energy distribution above 1.5 MeV.

Observed reaction rates, eq. (3), obtained with experimental techniques matched in the benchmark and study field are set equal to the derived reaction rate, eq. (4), involving the computed average cross section and the neutron fluence in the two fields. Using the notation of eqs. (3) and (4),

$$\text{study field:}\quad \varepsilon_\gamma \cdot \mu \cdot D_s = G \cdot N \cdot \bar{\sigma}_s \cdot (nvt)_{os}$$

$$\text{benchmark field:}\quad \varepsilon\gamma \cdot \mu \cdot D_b = G \cdot N \cdot \bar{\sigma}_b \cdot (nvt)_{ob}$$

Dividing, the study field fluence $(nvt)_{os}$ is obtained in terms of the benchmark field fluence,

$$(nvt)_{os} = \frac{D_s}{D_b} \cdot \frac{\bar{\sigma}_b}{\bar{\sigma}_s} \cdot (nvt)_{ob} \ , \qquad (12)$$

and the only experimental quantities involved are the gamma counting rates.

To examine the influence of the cross section ratio on the fluence transfer, the alternative expression for the derived reaction rate given in eqs. (5) and (6) is appropriate. The flux transfer then in terms of cross sections truncated at the lower limit of their energy response range, $\sigma(>E_p)$, and neutron fluences above a given energy E_o, becomes

$$[\psi(>E_o) \cdot (nvt)_o]_s = \frac{D_s}{D_b} \cdot \frac{\left[1 - \int_{E_o}^{E_p} \psi_b(E)dE \Big/ \int_{E_o}^{\infty} \psi_b(>E_o)dE\right]}{\left[1 - \int_{E_o}^{E_p} \psi_s(E)dE \Big/ \int_{E_o}^{\infty} \psi_s(>E_o)dE\right]}$$

$$\cdot \frac{\bar{\sigma}_b(>E_p)}{\bar{\sigma}_s(>E_p)} \cdot \left[\psi(>E_o) \cdot (nvt)_o\right]_b \qquad (13)$$

where

$[\psi(>E_o) \cdot (nvt)_o]$ = neutron fluence greater than E_o,

$\psi(>E_o)$ = fraction of normalized spectrum above E_o,

$\bar{\sigma}(>E_p)$ = computed spectrum-averaged cross section truncated at percentile energy E_p near the lower limit of the detector response range - see Eq. (1).

The integrals in the brackets of eq. (13) give the spectrum fraction between E_o and E_p, an energy region where the detector does not respond. This spectrum fraction for the benchmark field will be known; for the dosimetry study spectrum, however, this fraction contributes an irreducible uncertainty which is common to any fluence measurement technique employing integral detectors. In multiple foil techniques, using unfolding codes for example, the corresponding problem is referred to as the energy range of poor detector coverage.

The cross section ratio in eq. (13) for appropriate detectors will be near unity. The absolute cross section scale cancels as with spectral index calibrations, and the remaining uncertainty in flux transfer due to cross section shape errors, $\delta s(E)$, propagates more nearly on the departure from unity of the cross section ratio rather than on the ratio itself. Thus, a ± 10% cross section shape error would affect a flux transfer involving a cross section ratio of 1.1 by about ± 1%. An exception to this occurs when the detector response ranges for the benchmark and dosimetry fields are very different. In this case spectrum uncertainties, presumably dominated by the study field, will propagate into the flux transfer according to the last term of eq. (8). This term, as applied to $\sigma_s(>E_p)$ in eq. (13), will not involve a sum over energies below E_p where $\sigma_i = 0$.

Fission Rate Measurement Standards

Fissionable Deposits

It is not difficult to achieve electronic pulse registration of a fission fragment as it emerges from a thin deposit of fissionable material with an absolute detection efficiency of better than 99.8%. Devices are simple to construct: ionization chambers and surface barrier detectors are examples. Thus, accuracy of fission rate measurements is primarily concerned with fissionable deposit mass determinations and the absorption of fission fragments in the deposit. The latter problem can be made small in many cases by obtaining effective masses of thicker working deposits (e.g., 0.4 to ~ 1 mg/cm^2) relative to thin deposits (e.g., ≤ 0.05 mg/cm^2) by means of low-geometry alpha counting or back-to-back fission counting. Well-studied and permanently maintained fissionable deposits then become the basic artifact standard for fission rate measurements.

A set of permanently maintained reference fissionable deposits generally available for interlaboratory comparisons has been established at NBS.[8] Characteristics of the deposits including interim errors for principle isotopic masses are given in Table I. The

TABLE I. REFERENCE FISSIONABLE DEPOSITS AT NBS

PRINCIPLE ISOTOPE:	^{239}Pu	^{235}U	^{238}U		^{237}Np
			NATURAL	DEPLETED	
DEPOSIT THICKNESS (MG/CM^2)	0.083	0.20	0.18	0.20	0.093
ISOTOPIC PURITY (AT %)	99.11	99.75	99.275	99.899	100 (NOMINAL)
INTERIM ERROR ASSIGNMENT FOR PRINCIPLE ISOTOPE MASS (1σ)	±1.2%	±1.2%	±1.5%	±1.5%	±1.7%
STANDARD DEVIATION OF INTER-LABORATORY COMPARISONS					
[A] EUROPE (1974-76)	±1.0%	±0.8%	±0.8%	---	---
[B] U.S. (1972-75)	±0.6%	±0.7%	---	---	---

ALL DEPOSITS ARE 1.27 CM DIAMETER OXIDE DEPOSITS ON POLISHED PLATINUM DISKS (19.0 MM DIA. X 0.13 MM THK)

[A] NORMALIZED FISSION RATE MEASUREMENTS AT THE SIGMA SIGMA FACILITY (MOL, BELGIUM) INVOLVING NBS (U.S.), GFK (GERMANY) AND RCN (NETHERLANDS) EACH USING THEIR OWN FISSION IONIZATION CHAMBERS TO RECORD FISSION RATES.

[B] INFORMAL FISSIONABLE DEPOSIT COMPARISONS INVOLVING LASL, ANL, ORNL, AND BCNM (GEEL, BELGIUM). THE FIRST TWO LABORATORIES PROVIDED RESULTS FOR BOTH ^{239}Pu AND ^{235}U.

imposed requirement for a systematic program of redundant mass assay, not yet complete, results in relatively high error assignments for these reference deposits. Some interlaboratory comparisons with NBS deposits have been performed. The last two lines of Table I indicate the standard deviations associated with some of these efforts: (1) a formal fission rate intercomparison involving two laboratories besides NBS; and (2) an informal grouping of results from four laboratories that have participated in joint measurements with NBS. The interlaboratory results suggest that the interim mass errors for the NBS reference deposits are conservative.

Natural Neutron Fields

Turning from artifact standards to well-characterized neutron fields as a reference for fission rate measurements, a natural focus is the upper and lower bounds of fission-driven reactor systems, namely fission neutron spectra and thermal neutron distributions. The latter are commonly employed for precise intercomparisons of fissile deposits or of fission rate detectors containing fissile materials. In addition, very useful cross checks among isotope species may be carried out at thermal based on well-studied nuclear parameters.

1. Mass ratios among fissile isotopes, e.g. ^{239}Pu: ^{235}U: ^{233}U, based on thermal fission cross sections. For high confidence levels, the comparison should be carried out also with monoenergetic neutrons near 0.025 eV in order to assure that the required non-1/v correction (e.g., Westcott g-factor) is correctly known for the thermal Maxwellian employed.

2. Mass ratio between ^{235}U and ^{238}U based on abundance of ^{235}U in natural uranium. A certified natural uranium base material should be used (e.g., NBS-SRM 950a, Colorado Plateau ore, 0.719 ± 0.0007 at.% ^{235}U) because the nominal natural abundance may differ slightly depending upon origin of the uranium ore.

High thermal fission cross sections for fissile isotopes along with the general availability of intense thermal flux intensities also makes these fields convenient for many interlaboratory comparisons and detector performance investigations, and for the mass assay of very light fissionable deposits, in the nanogram range for example.

Fission spectrum neutrons are the complement of thermal neutrons in the cycle of nuclear energy generation. Fission rate measurements in fission spectra are important for validating and normalizing differential fission cross sections, for measuring nuclear parameters needed for certain types of absolute fission rate detectors, and for direct neutron calibration of detectors used for reactor spectrum characterizations. The latter includes the so-called flux transfer technique outlined in the previous sections.

Fission-spectrum-averaged, fission cross section ratios have been particularly important for the issue of standardization and were the subject of the integral measurement paper given at the last Neutron Standards Symposium in 1970.[1] Measurement results obtained since 1970 and a review of the situation regarding observation vs. prediction are summarized in Table II.

Considerable progress in measurement has occurred with the advent of clean ^{252}Cf fission spectrum fluxes. Also, there are new ^{235}U fission spectrum measurements which employ large cavities and a traverse technique for establishing the contribution of wall-return neutrons[12]. Measured ratios among ^{235}U, ^{238}U, ^{237}Np (and for ^{239}Pu as well but not reported here) are accurate now to about ± 2% (1σ), and the fission rate

TABLE II

FISSION CROSS SECTION RATIOS FOR ^{235}U AND ^{252}Cf FISSION NEUTRONS

	$\sigma_f(^{238}U)/\sigma_f(^{235}U)$		$\sigma_f(^{238}U)/\sigma_f(Np)$	
	$\chi(^{235}U)$	$\chi(^{252}Cf)$	$\chi(^{235}U)$	$\chi(^{252}Cf)$
Observed				
Fission chbrs.				
1975 (Refs.10,11)	0.254 ± 2.2%	0.266 ± 1.6%	0.230 ± 3.0%	0.240 ± 2.2%
1972 (Ref. 3)	0.270 ± 4.6%	---	---	---
Activation				
1968 (Ref. 1)	0.260 ± 6%	---	0.238 ± 3½%	---
Track recorders				
1967 (Ref. 1)	0.265 ± 4.8%	---	---	---
Total spread	±3.2%		±1.8%	
Obs./Predicted				
*1976	1.065 ± 2.5%	1.047 ± 2.0%	1.026 ± 3.0%	1.031 ± 2.2%
1972	1.13	---	---	---
1967-68	1.20	---	1.11	---

*Predicted values are obtained by convolution of ENDF/8-IV cross sections and evaluated fission spectra from Ref. 9. Spectrum uncertainties are propagated according to Eq. 8.

component of the measurement has been subject to inter-laboratory verification -- see Table I. The observed-to-predicted ratios in Table II carry uncertainties for the first time based on an evaluation of fission neutron spectrum measurements that includes uncertainty assignments.[13] The spectrum uncertainty, adds little to the total uncertainty. The departures from unity for 1976 values vary between 1.026 to 1.065 with uncertainties between ± 2.0% to ± 3.0%. These discrepancies with the ENDF/B-IV evaluation are statistically significant but still in much better agreement than has been the case in previous years when they were the cause of much concern and speculation. The relative consistency of the integral measurement since 1967 indicates that the changes have occurred primarily in the differential microscopic cross section data.

Should integral ratio measurements be accepted uncritically without the associated absolute determinations as a systematic validation? Ratio data has been a feature of integral reaction rate measurements almost without exception; and, as has been noted on occasion, it is a feature much less common for differential microscopic data. Attention must be called, therefore, to the absolute fission-spectrum-averaged, fission cross sections that now exist. Published results for ^{252}Cf spontaneous fission neutrons provide integral microscopic data, namely fission cross sections, which are independent of any other nuclear cross section and to first order are independent of any other nuclear parameter as well.[10] Results are given in Table III. The comparison with ENDF/B-IV predicted values include a propagation of fission spectrum uncertainties so that departures from unity are a direct check of the differential-microscopic fission cross sections chosen for ENDF/B-IV. The agreement is generally good.

Critical Metal Spheres

Closely related to fission spectra are the unreflected critical spheres of ^{235}U and ^{239}Pu metal. Lady Godiva (^{235}U) and Jezebel (^{239}Pu), constructed more than two decades ago, sustain a strong fission spectrum component, some 60% for Lady Godiva and 80% for Jezebel. The remainder of the spectrum is largely determined by inelastic scattering. Fission cross section ratios for these systems provide vital checks of inelastic parameters presently on the evaluated files. They are also an example of integral macroscopic measurements nearly equivalent to their differential microscopic counterpart since inelastically scattered and fission neutrons are indistinguishable components in both types of experiments.

TABLE III

^{252}Cf FISSION-SPECTRUM – AVERAGED FISSION CROSS SECTIONS

Isotope	Observed	*Obs./Pred.
U235	1205 ± 2.2%	0.971 ± 2.2%
U238	321 ± 2.4%	1.018 ± 2.6%
Pu239	1808 ± 2.2%	1.010 ± 2.2%
Np237	1332 ± 2.6%	0.986 ± 2.7%

*Predicted values are obtained by convolution of ENDF/B-IV cross sections and the evaluated ^{252}Cf fission spectrum from Ref. 9. Spectrum uncertainties are propagated according to Eq. 8.

Fission cross section ratios for the ^{235}U and ^{239}Pu critical metal spheres are presented in Table IV. Ratio measurement results listed in the upper section of the Table were obtained separately with fission chambers and with activation detectors, both calibrated by means of exposures to monoenergetic neutrons with energies close to 2.5 MeV.[14] Uncertainties for the 1967 measurements on Godiva and Jezebel were ± 2.5% (fiss. chbr.) and ± 3% (activation) exclusive of fission cross section errors at the calibration energies. This is an early example neutron field calibration of fission rates undertaken in order to reduce errors. The errors given for average values, ± 2.5% for all four ratios, do not include fission cross section uncertainties at the calibration energy. The actual values in the Table have been adjusted to be consistent ENDF/B-IV cross section ratios at the calibration energies. The 1976 absolute values for BIGTEN were obtained with high resolution double fission chambers and include, as do the Godiva and Jezebel results, small corrections for cavity flux pertubations. Observed-to-ENDF/B-IV predicted ratios are relatively good for the uranium systems, Lady Godiva and BIGTEN. The average deviation from unity for the four obs/pred. ratios, 1.003, 1.043 (Godiva), and 0.976, 1.031 (BIGTEN),

TABLE IV. FISSION CROSS SECTION RATIOS FOR CRITICAL METAL SPHERES

	$\sigma_f(^{238}U)/\sigma_f(^{235}U)$			$\sigma_f(^{238}U)/\sigma_f(Np)$		
	^{235}U (GODIVA)	^{239}Pu (JEZEBEL)	10%^{235}U-90%^{238}U (BIG TEN)*	^{235}U (GODIVA)	^{239}Pu (JEZEBEL)	10%^{235}U-90%^{238}U (BIG TEN)*
	MONOENERGETIC CALIBRATION (1967)**		ABSOLUTE (1976)	MONOENERGETIC CALIBRATION (1967)**		ABSOLUTE (1976)
FISSION CHAMBERS	0.166_4	0.215_3	0.0372 ±.0006	0.196	0.2190	0.117_2 ±.0026
ACTIVATION	0.164	0.218_1	-	0.199	0.229	-
AV.	0.165 ±2.5%	0.217 ±2.5%	0.0372 ±1.7%	0.198 ±2.5%	0.224 ±2.5%	0.117_2 ±2.2%
OBSERVED PRED. (ENDF/B-IV)	1.003	1.12	0.976	1.043	1.084	1.031
FISSION SPECTRUM CALIBRATION						
FISSION CHAMBERS (1976)	-	-	0.147±1.4%	-	-	0.510 ±1.2%
ACTIVATION (1967)	0.617 ±3.2%	0.803 ±3.2%		0.816 ±2.0%	0.907 ±1.5%	-
OBSERVED PRED. (ENDF/B-IV)	0.887	1.03_1	0.918	0.964	0.993	1.007

*A LARGE CYLINDRICAL CRITICAL ASSEMBLY WITH A HOMOGENEOUS METAL CENTRAL REGION. THE CENTRAL SPECTRUM IS LITTLE EFFECTED BY A DISTANT REFLECTOR AND CYLINDER-SHAPED BOUNDARIES.

**DETECTORS CALIBRATED WITH MONENERGETIC NEUTRONS: 2.43 MeV (FISS. CHBR.), 2.75 MeV (ACTIVATION).[14] VALUES REPORTED IN 1967 ADJUSTED TO CORRESPOND TO ENDF/B-IV CROSS SECTION RATIOS AT THESE ENERGIES.

is 2.5% with a standard deviation of ± 1.7. This compares with an observed-to-predicted average deviation from unity of 6.0% for Lady Godiva reported in 1970 when calculations were based on the earliest version of ENDF/B.[1] The departures from unity for the ^{239}Pu critical sphere are large, 1.12 and 1.084, far beyond the uncertainties of the measurements. This is indicative of inadequate ^{239}Pu inelastic transfer cross sections in the calculations if the detector fission cross sections and the ^{239}Pu fission spectrum are correctly known.

A more proper neutron field for calibration of cross section ratio measurements intended to check neutron transport calculations is the fission spectrum. It is the strong fission spectrum component in the critical metal spheres that computation transforms into the respective spectra of these systems. A fission spectrum calibration, therefore, circumvents fission cross section scale errors and fission spectrum uncertainties.

The lower section of Table IV shows results of ratios based on experimental calibration with fission neutrons. For Godiva and Jezebel, this was carried out by the activation method alone and the ^{235}U and ^{239}Pu fission spectra experiments were performed in difficult geometry.[14] However, the same results, derived in an alternative manner by taking the values based on monoenergetic calibration (upper section of Table IV) and dividing by the 1975 ^{235}U fission spectrum ratios (Table II), do not differ by more than 4%. The BIGTEN measurements carried out in 1976 were performed with fissionable deposits related by alpha and fission comparison counting to those used in the 1975 ^{235}U cavity fission spectrum measurements.[6] The resulting spectral indexes for BIGTEN relative to the fission spectrum driving source (0.147 ± 1.4% and 0.510 ± 1.2%) are particularly accurate checks of neutron energy transfer for reactor physics.

The observed-to-predicted ratios now show a very different pattern from those in the upper section of Table IV. The ^{239}Pu system now is in agreement with calculation and the uranium systems are not. The obs/pred. ratios all are uniformly lower, a result consistent with but not fully accounted for by the latest obs./predicted ratios for fission spectra - see 1976 values in Table II.

It is not the purpose of this paper to evaluate the implications of the results displayed in Table IV. It is a purpose however to illustrate how reference neutron field calibrations of experiments designed to check reactor spectrum computations may reveal features not otherwise apparent. The critical metal spheres are particularly apt for this purpose because they involve little or no complexities of geometry. This ambiguity for many reactor physics criticals can, and probably has, obscured the desirability of reference neutron field calibrations.

References

1. Grundl, J. A. "Fission-Neutron Spectra: Macroscopic and Integral Results," Proc. Symp. on Neutron Standards and Flux Normalization, P. 417, Conf-701002, ANL (August, 1971).

2. Taschek, R. F., ibid. 1.

3. Grundl, J. A. "Brief Review of Integral Measurements with Fission Spectrum Neutrons," and "Measurement of Av. Fiss. Cross-Section Ratio, ^{235}U/^{238}U For ^{235}U and ^{239}Pu Fission Neutrons;" Prompt Fission Neutron Spectra, Panel Proceedings Series, IAEA (1972).

4. Pinter, M., Scholtyssek, W., Fehsenfeld, P., Van der Camp, H. A. J., Quaadvliet, W. H. J., Fabry, A., DeLeeuw, G. and S., Cops, F., Grundl, J., Gilliam, D., and Eisenhauer, C., "Interlaboratory Comparison of Absolute Fission Rate and Uranium-238 Capture Rate Measurements in the MOL-ΣΣ Secondary Intermediate-Energy Standard Neutron Field," Conf. on Nucl. Cross Sections and Technology, Washington, D.C. (March 1975).

5. McElroy, W. N. and Kellogg, L. S., "Fuels and Materials Fast-Reactor Dosimetry Data Development and Testing," Nuclear Technology 25, 180-223 (1975).

6. McElroy, W. N., ed. ILRR Progress Reports, Nos. 9-11, HEDL-TME 75-130 (1973-1977).

7. Vlasov, M., "IAEA Program on Benchmark Neutron Fields Applications for Reactor Dosimetry," INDC(SEC)-54/L+DOS. (July, 1976).

8. Grundl, J. A., Gilliam, D. M., Dudey, N. D. and Popek, R. J., "Measurement of Absolute Fission Rates," Nuclear Technology 25, 237-257 (1975).

9. Grundl, J., Eisenhauer, C., "Benchmark Neutron Fields for Reactor Dosimetry," Consultants Meeting on Integral Cross Section Measurements in Standard Neutron Fields for Reactor Dosimetry, IAEA (Nov. 1976). Manuscript copies available from authors at National Bureau of Standards.

10. Heaton II, H. T., Grundl, J. A., Spiegel Jr., V. Gilliam, D. M., and Eisenhauer, C., "Absolute ^{235}U Fission Cross Section for ^{252}Cf Spontaneous Fission Neutrons," Conf. on Nucl. Cross Sections and Technology, Washington, D.C. (1975).

11. Gilliam, D. M., Eisenhauer, C., Heaton II, H. T., and Grundl, J. A., "Fission Cross SEction Ratios in the ^{252}Cf Neutron Spectrum (^{235}U: ^{238}U: ^{239}Pu: ^{237}Np)," Conf. on Nucl. Cross Sections and Technology, Washington, D.C. (1975).

12. Fabry, A., Grundl, J., and Eisenhauer, C., "Fundamental Integral Cross Section Ratio Measurements in the Thermal-Neutron-Induced Uranium-235 Fission Neutron Spectrum," Conf. on Nucl. Cross Sections and Technology, Washington, D.C. (March, 1975).

13. Grundl, J. A., and Eisenhauer, C. M., "Fission Spectrum Neutrons for Cross Section Validation and Neutron Flux Transfer," Conf. on Nucl. Cross Sections and Technology, Washington, D.C. (March 1975).

14. Grundl, J. A., and Hansen, G. E., "Measurement of Average Cross Section Ratios in Fundamental Fast-Neutron Spectra," in Nuclear Data for Reactors, Vol. I, pp. 321-336, IAEA, Vienna (1967). Also see Nucl. Sci. and Eng., 8, 598-607 (1960).

15. Behrens, J. W., Carlson, G. W., and Bauer, R. W., "Neutron-Induced Fission Cross Sections of ^{233}U, ^{234}U, ^{236}U and ^{238}U with Respect to ^{235}U," Conf. on Nucl. Cross Sections and Technology, Washington, D.C. (1975). See also M. S. Coates, D. B. Gayther and N. J. Pattenden, "A Measurement of the ^{238}U/^{235}U Fission Cross Section Ratio," same conference.

16. Private communication from ENDF/B-IV cross section evaluators (1975).

UTILITY AND USE OF NEUTRON CAPTURE CROSS SECTION STANDARDS AND THE STATUS OF THE Au(n, γ) STANDARD

A. Paulsen
Central Bureau for Nuclear Measurements
B-2440 Geel, Belgium

The main application of a neutron capture cross section standard should be found in ratio measurements using the prompt γ-ray detection method. A review of neutron capture cross section measurements in the last six years shows that the Au(n, γ) standard is increasingly used for this purpose. But the majority of all measurements is still based on other normalization methods than ratio measurements, although the accuracy established for the Au(n, γ) cross section below 3 MeV competes now well with that of other normalization methods. On the other hand this accuracy has scarcely reached the accuracy of necessary corrections associated with prompt γ-ray detection measurements below 3 MeV neutron energy, and is completely insufficient above 3 MeV. Below 200 keV the cross section fluctuations due to level statistics in the compound system ^{198}Au are seriously disturbing measurements aiming at high accuracy and high resolution.

(Review ; neutron capture cross section ; measurement ; normalization ; reference standard ; accuracy ; Au(n, γ) cross section ; cross section fluctuations)

Introduction

A standard cross section for neutron capture measurements is of quite different importance in the three neutron energy regions :

- -thermal and resonance region
- -unresolved resonance region
- -high energy region.

Thermal and resonance region

In the thermal and resonance region many thermal cross sections and resonance parameters (e.g. for ^{55}Mn, ^{59}Co, ^{103}Rh, ^{107,109}Ag, ^{113,115}In, ^{197}Au) have been determined to a rather high degree of accuracy[1]. These data have been often used to normalize neutron capture cross section measurements in the thermal or resonance region. Therefore, with good reasons these thermal capture cross sections and resonance parameters could be named "capture standards". Something similar is valid for certain capture resonance integrals (e. g. for Mn and Au) which have been used as reference standards for the measurement of resonance integrals. The relative large amount of existing data is responsible for today's relative small interest in thermal and resonance capture standards.

Unresolved resonance region

A standard cross section in its unresolved resonance region is in principle of no use unless the measurement averages over a sufficiently broad energy interval to arrive at a smooth cross section shape. This implies that one capture reaction chosen as a reference standard can never be suited for the whole neutron energy range.

High energy region

Due to the required smoothness of the cross section curve a capture standard cross section is of sufficient versatility in application only in the high energy region. Therefore the main region of interest in the Au(n, γ) reaction, which is up to now the only one recognized as capture standard[2], can be only in the energy region above about 100 keV.

The Measurement of Cross Section Ratios

In the thin sample approximation the reaction cross section σ can be calculated from the number of counts C of a capture detector with efficiency ε, the number of sample atoms N and the neutron fluence density Φ according to Fig. 1. In a similar way the neutron fluence density can be deduced from a known standard cross section σ_o .

C : number of counts — N : number of atoms
ε : detection efficiency — Φ : neutron fluence density

$$\sigma = \frac{C}{\varepsilon \cdot N \cdot \Phi}$$

$$\Phi = \frac{C_o}{\varepsilon_o \cdot N_o \cdot \sigma_o}$$

index 'o' corresponds to standard reaction

$$\sigma = \frac{C \cdot \varepsilon_o \cdot N_o}{C_o \cdot \varepsilon \cdot N}\,\sigma_o$$

standard used to measure neutron fluence

if $\varepsilon = \varepsilon_o$

$$\frac{\sigma}{\sigma_o} = \frac{C \cdot N_o}{C_o \cdot N}$$

standard used to perform ratio measurement (ε is unknown, Φ can not be evaluated)

Fig. 1 : Explanation of the term "ratio measurement".

If the standard reaction requires another detector than the capture reaction to be measured, then the efficiencies will not cancel from the equation for σ. In this situation the measurement of the neutron fluence density could also be done with any other suitable standard which has not at all to be a capture cross section. In this case all detector efficiencies have to be known and the neutron fluence density can be calculated.

However, if the standard reaction can be detected in completely the same way than the capture reaction under study, then due to $\varepsilon = \varepsilon_o$ the standard is used for a ratio measurement for which no efficiency has to be known and Φ can not be evaluated. A neutron capture standard is therefore characterized by the fact that it permits capture cross section determinations by ratio measurements.

The Prompt Gamma-Ray Detection Method

Neglecting here measurement techniques based on neutron absorption (shell transmission and pile reactivity measurements) only the detection of the prompt capture γ-rays fulfils approximately the condition for ratio measurements, whereas the activation method is faced with characteristic radiations changing completely from radioisotope to radioisotope. For the prompt γ-ray detection method the condition $\varepsilon = \varepsilon_o$ is only approximately fulfilled because the capture γ-ray spectra (and possibly also the angular distributions) are changing from isotope to isotope. This has to be corrected for.

It is a principal question whether the prompt γ-ray detection method measures the full capture cross section also at higher neutron energies. To discriminate against γ-rays from inelastic scattering one is obliged to use only the upper part ($E_n \leq E_\gamma$) of the capture spectra. Therefore cascade passages through unbound states could be missed. For this reason it is interesting to compare prompt γ-ray detection results σ_{gamma} with activation results $\sigma_{activ.}$. This is done for Au(n,γ) in the 1 to 3 MeV energy range[3,4,5] in Fig. 2 and for several reactions at 14 MeV in Fig. 3. For the latter only activation results were taken into account which passed a critical examination[6] in view of corrections for scattered neutrons of degraded energy. Within today's experimental accuracy there is no indication that capture γ-ray cascades are passing partially through unbound states.

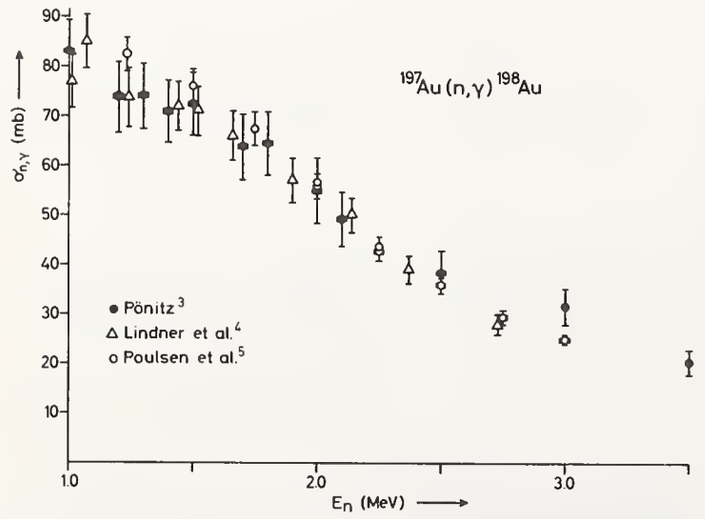

Fig. 2 : Comparison of prompt γ-detection (full symbols) and activation (open symbols) results for Au(n,γ).

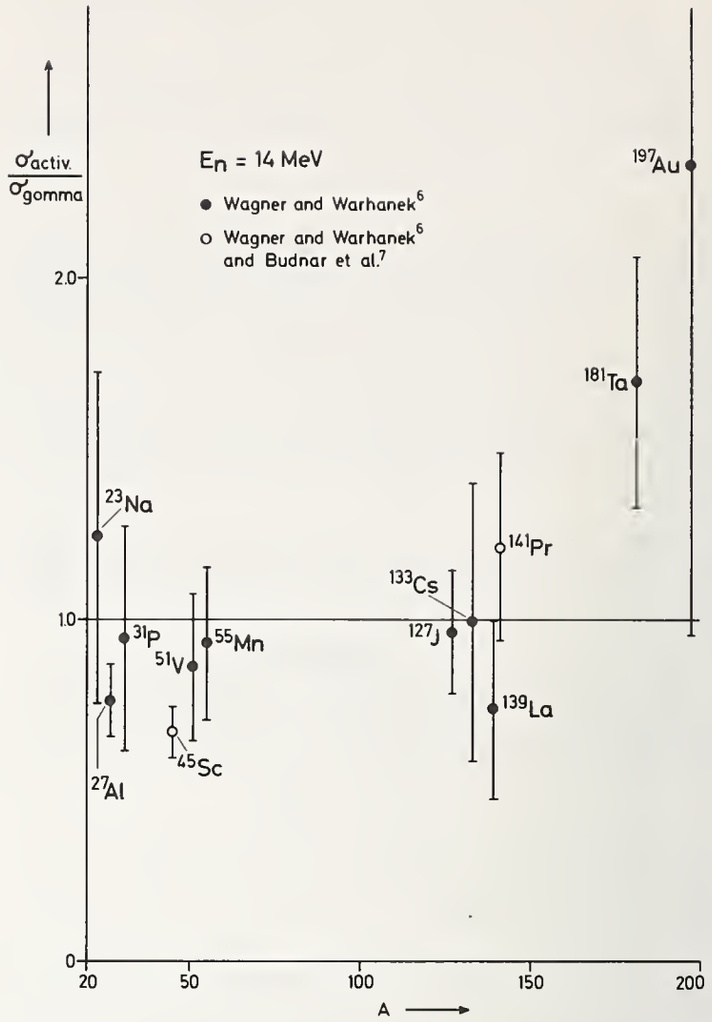

Fig. 3 : Ratio of activation results σ_{activ} to prompt γ-ray detection results σ_{gamma} at 14 MeV.

Actually used Normalization Methods of Neutron Capture Measurements

A review was made concerning the used standards and normalization methods for capture cross section measurements in the neutron energy range above 20 keV by the prompt γ-ray detection technique. This review covers all measurements for which numerical results have been compiled at one of the four cooperating Neutron Data Centers between 1971 and 1976. The result is shown in Table 1 where the measurements are counted per studied isotope or element (Au excluded). The number of ratio measurements relative to gold (at least at one neutron energy) is increasing from the 71/73 to the 74/76 period, indicating that the gold standard is now indeed increasingly used. All the ratio measurements relative to gold were performed at electrostatic accelerators, whereas at linear accelerators a normalization in the eV range by saturated resonances is preferred. However, an additional normalization at the high energy end ($E_n > 100$ keV) by a gold ratio measurement could probably improve the accuracy of the results produced at linear accelerators. It has to be kept in mind that these ratio measurements can be renormalized at any time.

Table 1: Normalization Methods of Neutron Capture Measurements.*

Period	Separ. Determ. of ε and φ	Sotur. Reson. + ϕ_{rel}	Therm. Cross Sect. + ϕ_{rel}	Ratio Measurements			Total
				Au	In	Ag	
1971 - 1973	30	15	4	10	10	3	72
1974 - 1976	7	23	7	23	—	—	60

* per isotope or element
prompt γ-ray detectian method only
for neutron energies abave 20 keV only

Comparison of Normalization Methods

Most probably the preference given to other normalization methods than the gold ratio measurement is due to the fact that experimentalists believe to assess better accuracies that way. Therefore a comparison is made between the estimated accuracy of the Au(n, γ) cross section and that one of other normalization methods used for measurements above 20 keV neutron energy. This comparison is shown in Table 2. The uncertainties are estimated at the confidence level of one standard deviation and contain the principal uncertainty of the neutron fluence and the γ-ray detector efficiency. The total error was obtained from the individual uncertainty components by quadratic summation. The table contains further the upper energy limit for the validity of the quoted error and the reference to the corresponding publication.

Table 2: Uncertainties of Normalization Methods.

Method	ε_{abs} or $(\varepsilon \cdot \phi)_{abs}$			ϕ_{abs} or ϕ_{rel}			Capture Standard			Total Uncertainty
	Method	Acc. Ref	Energy Limit	Method	Acc. Ref	Energy Limit	Cross Section	Acc. Ref	Energy Limit	
Separ. Determ. of ε and φ	Radioac. Sources	2% (27)	1 MeV	Ass.part.	2% (9)	15 MeV	—	—	—	3 - 10%
				Long C.	2% (10)	1 MeV				
	(p,γ) Reactions	10% (16)	15 MeV	H (n,n)	3% (9)	15 MeV				
				$^{235}U(n,f)$	4% (12)	6 MeV				
Determ. of $(\varepsilon \cdot \phi)$	Satur. Resonances	1-2% (11,22)	100 eV	$^{6}Li(n,t)$	4% (13)	0.1 MeV	—	—	—	3 - 5%
				$^{10}B(n,\alpha)$	3% (13)	0.1 MeV				
Normaliz. at Therm. Energy	—	—	—	$^{10}B(n,\alpha) + H(n,n)$	4% (13)	1 MeV	Therm. Cross Section	1-2% (1)	0.025 eV	3 - 5%
				$^{235}U(n,f)$	3% (14)	6 MeV				
Ratio Measurem. with Gold	—	—	—	—	—	—	Au (n,γ) Cross Section	4% (29)	0.2 - 3.5 MeV	4 - 5%
								5% (18)	0.1 - 3 MeV	

The comparison of these uncertainties with today's accuracy of the gold capture cross section (last line of Table 2) is not at all unfavourable for the latter. But it is also not yet convincing to give preference to ratio measurements with gold. However, the accuracy of the gold capture cross section could finally surpass that one of the competing normalization methods, because many measurements and all experimental measuring techniques for neutron capture can principally contribute to it.

Up to now measurements carried out with high efført and using a normalization method according to the first two lines of Table 2 can be still superior to gold ratio measurements with respect to resulting accuracy. Here the influence of the simultaneously progressing standards $^{6}Li(n,t)$, $^{10}B(n,\alpha)$ and $^{235}U(n,f)$ has to be mentioned. Of course, this comparison is only valid for measurements in or ranging up to the indicated energy range for the Au(n, γ) cross section. Comparable measurements belonging to the third line of Table 2 are nearly not existing : there is no experimental technique to cover neutron energies from thermal energy up to several hundreds of keV (slowing-down time measurements just reach 100 keV). The relative simplicity of ratio measurements and the readjustibility of their results justify further efforts for an amelioration of the accuracy of the gold capture cross section.

Uncertainties of Ratio Measurements

There are certain sources of error inherent to all capture cross section measurements performed by the prompt γ-ray detection technique. It is interesting to compare the accuracy of the gold capture cross section with these 'inherent' uncertainties. This is done in Table 3 by comparing uncertainties which have been quoted in literature as average values.

Table 3: Uncertainties of Ratio Measurements.

Source of Uncertainty	Pulse Height Weighting Techn.	Maxon-Rae Detectors	Liquid Scint. Tonks	Spectrometers NaI(Tl), Ge(Li), Pair
Variation of γ-ray Spectrum	± 1% Ref. 8, 15	± 3% Ref. 19, 20	± 5% Ref. 21, 22	± 10% Ref. 16, 17
Multiple Scattering	± 2 - 3% Ref. 22, 23			
Neutron Scatt into γ-detector	for $\frac{\sigma_n}{\sigma_\gamma} = 10^2$ ± 0.5 - 3% Ref. 24, 25			
Background Subtraction	± 1 - 3% Ref. 23, 24			
Au (n,γ) Cross Section	± 4 - 5% Ref. 18, 29			

There is a detector-dependent error due to variations of the capture γ-ray spectra. This error is minimized for detectors having the least spectrometric response and is a maximum for the true spectrometers. The pulse height weighting technique in conjunction with C_6F_6 or C_6D_6 γ-detectors results in a remarkable independence from the shape of the γ-spectrum. It is the clear predominance of the Compton γ-scattering process in these detectors with its smooth and relative weak energy dependence which is responsible for this independence as well as for a good reliability of efficiency calculations. This type of detector should be also applicable in the MeV neutron energy range because the spectrum fraction above threshold can be well calculated. For the pulse height weighting technique and for Moxon-Rae detectors there are difficulties in the data evaluation if the sample is a compound of elements or a mixture of isotopes with unknown capture cross sections and strongly differing neutron binding energies. Uncertainties originating from these difficulties have not been considered in Table 3. For tank measurements the spectrum fraction uncertainty is astonishingly high due to the relative high thresholds which have to be used for background reasons with such detectors. Cross section measurements performed with spectrometers are mainly done in the high MeV range where the accuracy of the Au(n, γ) cross section is anyway

not yet defined. Variations of the γ-ray angular distributions with increasing neutron energy seem to be negligibly small[26].

Uncertainties due to corrections for multiple scattering, response of γ-detector to scattered neutrons and general background can vary considerably and are depending on several experimental conditions. The average uncertainties of these corrections quoted in Table 3 are smaller than the normalization and γ-detection uncertainties.

In conclusion Table 3 demonstrates that further efforts for an improvement of the accuracy of the gold standard seem to be justified.

Status of Au(n, γ) Standard

Below 0.2 MeV

Recent measurements[11,27] have confirmed that considerable cross section fluctuations are extending up to 200 keV. These fluctuations are the high energy extension of the unresolved resonance region and are caused by the statistical distribution of the capturing levels in the ^{197}Au + n system. The amount of observable fluctuations does not only depend on the neutron energy but also on the energy resolution. Fig. 4 shows the relative neutron energy resolution which would permit the observation of ± 3 and ± 5 % deviations for capture in gold and tantalum as a function of neutron energy. These data have been produced[28] by Monte Carlo calculation assuming level distances and reduced level widths according to a Wigner and a Porter-Thomas distribution, respectively. Fig. 4 demonstrates that due to the higher level density Ta(n, γ) would be in this respect a much better standard in the 50 to 200 keV energy range. As these fluctuations could strongly influence high resolution ratio measurements ENDF/B-V[29] will no longer support the gold standard below 200 keV. Furtheron one can read from Fig. 4 that gold activation measurements with Sb-Be neutron sources at 22.8 ± 1.3 keV can deviate up to 5 % from the smooth average cross section curve.

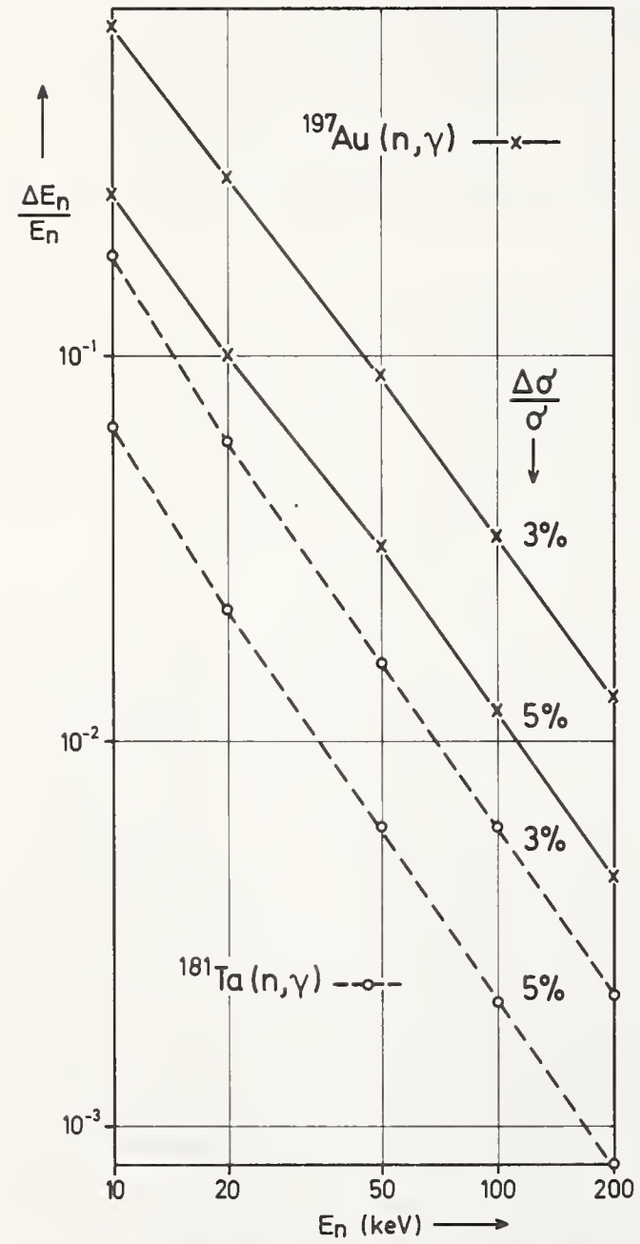

Fig. 4 : The relative neutron energy resolution necessary for the observation of ± 3 and ± 5 % relative cross section fluctuation for the neutron capture in Au and Ta (acc. to ref. 28).

Between 0.2 and 3 MeV

In this energy region the accuracy of the Au(n, γ) cross section is estimated to be ± 5 %[18] for the ENDF/B-IV data or ± 4 %[29] for the ENDF/B-V data in preparation.

Above 3 MeV

In the energy region above 3 MeV the available Au(n, γ) cross sections are very scarce. Fig. 5 shows all available cross section data together with the ENDF/B-IV curve and the proposed ENDF/B-V data. It is in this energy region from 3 to 14 MeV where new Au(n, γ) cross section measurements would be very valuable in view of checking the validity of interpolations by model calculations.

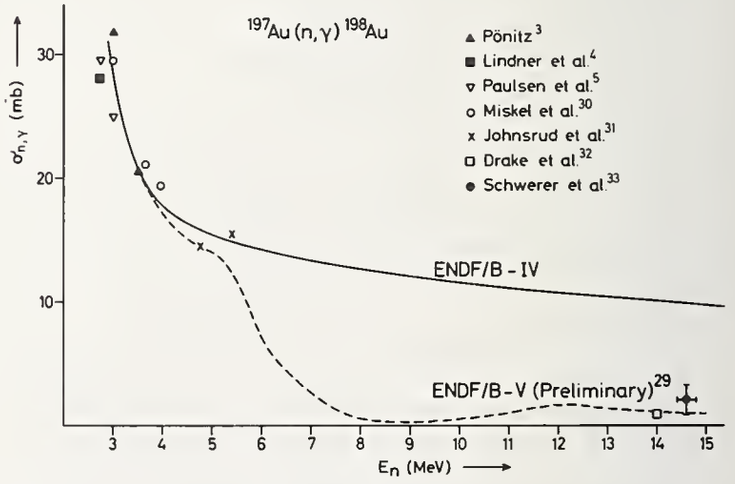

Fig. 5 : Cross section data for the neutron capture in Au above 3 MeV.

Conclusions

Since the introduction of a capture standard cross section is aiming at the performance of ratio measurements, more measurements of that type should be done, especially at the high energy limit of linear accelerator facilities. Results of ratio measurements can be easily renormalized afterwards. But already

today the accuracy of the gold standard can well compete with other normalization methods in the 0.2 to 3 MeV energy range. Also the problem of the influence of cross section fluctuations seems to be clarified. With respect to these cross section fluctuations the Ta(n,γ) reaction is a much more suited standard in the 50 to 200 keV energy range. Above 3.5 MeV neutron energy the existing cross section data are completely insufficient for any reference purpose. This reflects of course the data needs for fission reactors. Further measurements in this energy range could help to extend considerably the applicability of this standard for developments in fusion technology and nuclear safeguards[34].

References

1. S. F. Mughabghab and D. I. Garber, Neutron Cross Sections, Volume I, Resonance Parameters, Report BNL 325 Third Edition (1973)

2. Proc. Neutron Standard Reference Data, Vienna 1972, Recommendations p. 360

3. W. P. Pönitz, Nucl. Sci. Eng. 57 (1975) 300

4. M. Lindner, R. J. Nagle and J. H. Landrum, Nucl. Sci. Eng. 59 (1976) 381

5. A. Paulsen, R. Widera and H. Liskien, Atomkernenergie 26 (1975) 80

6. M. Wagner and H. Warhanek, to be published

7. M. Budnar, F. Cvelbar, A. Kikar, R. Martincic, M. Potokar and V. Ivkovic, Measurements of 14 MeV Neutron Radiative Capture γ-Ray Spectra and Integrated Cross Sections in Sc, Y, Pr, and Ho, Report INDC(YUG)-5/L (1977)

8. C. Le Rigoleur, A. Arnaud, Proc. NEACRP/NEANDC Specialists Meeting Karlsruhe May 1973, Report KFK 2046/NEANDC-U-98, p. 33

9. A. Paulsen, H. Liskien and M. Cosack, Nucl. Instr. Meth. 105 (1972) 103

10. J. L. Leroy, J. L. Huet and J. Gentil, Nucl. Instr. Meth. 88 (1970) 1

11. R. L. Macklin, J. Halperin and R. R. Winters, Phys. Rev. C11 (1975) 1270

12. M. Lindner, R. J. Nagle and J. H. Landrum, Report UCRL-75838 (1974)

13. H. Liskien, Neutron Standards and their Application, Proc. Intern. Conf. on the Interaction of Neutrons with Nuclei, Lowell 1976, p. 1110

14. V. A. Konshin, Review and Evaluation of the ^{235}U Fission Cross Section in the 0.1 keV to 15 MeV Energy Range, Report INDC(CCP)-94/U (1976)

15. J. B. Czirr and M. L. Stelts, Nucl. Sci. Eng. 52 (1973) 299

16. I. Bergqvist, D. M. Drake and D. K. McDaniels, Nucl. Phys. A191 (1972) 641

17. M. Stamatelatos, B. Lawergren and L. J. Lidofsky, Nucl. Sci. Eng. 51 (1973) 113

18. A. B. Smith, The Contemporary Status of the ^{197}Au (n,γ) Cross Section, status report to the 8th INDC Meeting, Vienna October 1975

19. M. C. Moxon, thesis London University 1968

20. R. L. Macklin, J. H. Gibbons and T. Inada, Nucl. Phys. 43 (1963) 353

21. D. Kompe, Nucl. Phys. A133 (1969) 513

22. R. E. Chrien, Neutron Capture Cross Section Measurement Techniques, Proc. Nucl. Cross Sections and Technology, Washington D. C. 1975, NBS Spec. Publ. 425, Vol. I (1975) 139

23. R. C. Block and R. W. Hockenbury, The Precision of Tank Capture Cross Section Measurements, Proc. Neutron Standards and Flux Normalization Argonne 1970, AEC Symposium Series 23 (1971) 355

24. M. C. Moxon, D. B. Gayther and M. G. Sowerby, NEANDC Topical Conf. on Capture Cross Section Measurements, Report AERE-R 8082, Harwell 1975, p. 12

25. R. L. Macklin and B. J. Allen, Nucl. Instr. Meth. 91 (1971) 565

26. D. M. Drake, E. D. Arthur and I. Halpern, Proc. Sec. Intern. Symp. on Neutron Capture Gamma-Ray Spectroscopy, Petten 1974, p. 227

27. C. Le Rigoleur, A. Arnaud and J. Taste, Report CEA-N-1662 (1973)

28. H. Liskien and H. Weigmann, Annals Nucl. Energy in press

29. S. F. Mughabghab, Informal Report BNL-NCS-21774 (1976)

30. J. A. Miskel, K. V. Marsh, M. Lindner and R. J. Nagle, Phys. Rev. 128 (1962) 2717

31. A. E. Johnsrud, M. G. Silbert and H. G. Barshall, Phys. Rev. 116 (1959) 927

32. D. Drake, I. Bergqvist and D. K. McDaniels, Phys. Lett. 36B (1971) 557

33. O. Schwerer, M. Winkler-Rohatsch, H. Warhanek and G. Winkler, Nucl. Phys. A264 (1976) 105

34. R. M. Lessler, WRENDA 76/77 World Request List for Nuclear Data, Report INDC(SEC)-55/URSF (1976)

REMARKS ON THE 2200 m/s and 20° C MAXWELLIAN NEUTRON DATA FOR U-233, U-235, Pu-239 and Pu-241 †

H.D. Lemmel
Nuclear Data Section
International Atomic Energy Agency
A-1011 Vienna, Austria

Abstract: Attention is drawn to the still existing systematic discrepancy between experimental cross-sections for 2200 m/s neutrons and those for a 20° C Maxwellian neutron spectrum for U-235 and U-233.
(Keywords: Neutron nuclear data evaluation. Fission standards. U-233, U-235, Pu-239, Pu-241, thermal neutron cross-sections, fission-neutron yields. Pu-239 half-life.)

Introduction

In 1965 [1], 1969 [2] and 1975 [3] the IAEA Nuclear Data Section, in cooperation with external specialists, published consistent sets of recommended best values of the thermal neutron data of the main fissile nuclides.

The method of evaluation was a multi-parameter least-squares fit of all available experimental data, after reviewing and, where feasible, reassessing the authors' quoted values and errors, usually in consultation with the authors or other experts.

In the present paper I would like to demonstrate which discrepancies still exist for these important data.

Discrepancies

Although the thermal neutron data of the fissile nuclides are basic parameters and reference standards for the data at higher energies as well as for data of other nuclides, it has not yet been possible to issue a final set of recommended values, due to the existence of systematic uncertainties.

In 1965 the situation looked still fine. The accuracy of experimental data was not yet as good as today, and possible discrepancies did not significantly exceed the experimental errors.

In 1969 it became obvious that there were, among the experimental data, some unexplained discrepancies. For example, experimental U-235 fission cross-section data were discrepant; data for the neutron-yield per fission, $\bar{\nu}$, were discrepant; the mean energy values of the fission neutron spectra, which influence the $\bar{\nu}$ values, were uncertain; the Westcott g-factors and their temperature dependence were uncertain; half-life values, which influence the fission cross-section values, were discrepant; and some of them, for example the experimental values of the Pu-239 half-life, were consistent but turned out later to be all together wrong. In particular the neutron yield data, $\bar{\nu}$ and η, appeared to be inconsistent with the Chalk River irradiation experiments which yielded a capture-to-fission cross-section ratio $\hat{\alpha}$ with high accuracy. The equation

$$1 + \hat{\alpha} = \bar{\nu}_t / \hat{\eta}$$

(where the sign $\hat{}$ denotes the 20° C Maxwellian spectrum average) was not fulfilled within the error limits of the experimental data. At that time, the weakest parameter within this equation seemed to be $\bar{\nu}$, since all $\bar{\nu}$ values had been measured relative to the spontaneous $\bar{\nu}$ of Cf-252, of which experimental values existed in two distinct groups around 3.7 and around 3.8 respectively. We then concluded that, considering the Chalk River $\hat{\alpha}$ value, a high value of $\bar{\nu}$ (Cf-252) should be correct rather than a lower one. - Soon after, this conclusion turned out to be wrong.

This wrong prediction of 1969 was a good illustration of the limited value of a least-squares fit, when systematic discrepancies are present, and in particular when several different sources of discrepancies interfere within the same fit.

Today, this limitation is no longer as serious as previously, but it seems advisable to remember that the results of a least-squares fit are subject to certain limitations which I shall discuss briefly.

Treatment of correlated data

The thermal cross-sections and neutron yield data for one fissile isotope are all interrelated, and the data of different fissile isotopes are also interrelated due to ratio measurements. Thus there are about 200 interrelated experimental input data, thereof about 50 independent variables, which are simultaneously treated in the least-squares fit.

The main problem in such a fit is the treatment of experimental input data which have correlated error sources. It would lead to wrong results if such correlated data would be treated in the fit in the same way as uncorrelated data. Several methods were used to take care of such correlations.

In 1965 a mathematical procedure [1] was used by which certain types of data correlations can be represented in the fit by appropriate down-weighting of the correlated input data and their ratios. This method applies when, e.g., the fission cross-section is measured in one experiment for three nuclides; the three results are then correlated due to the uncertainties of all those corrections which they have in common.

For a number of input data this method was still applied, but in 1975 an additional, more flexible method was introduced, by which error sources common to several input data are formulated in the fit as independent parameters.

For example, most measurements of the fission-neutron yield $\bar{\nu}$ depend on assumptions about the energy-spectrum of fission neutrons. Therefore, the mean energy values $\bar{E}$ of the fission neutrons of each of the nuclides considered, were treated as independent parameters in the fit, thus adjusting automatically the experimental $\bar{\nu}$ data for changes in the values of the mean fission neutron energies $\bar{E}$.

† Since the author was unable to attend, this paper was summarized by B. R. Leonard, Jr. at the Symposium.

Another example are the fission cross-section measurements which mostly depend on half-life values, when the sample assay was done by alpha-counting. Therefore, the half-lives for the nuclides considered were entered as independent parameters in the fit, thus adjusting automatically the experimental fission cross-section data for changes in the half-life values.

A special problem is the treatment of the Westcott g-factors, which relate the cross-sections for monoenergetic neutrons at the reference velocity of 2200 m/s to the cross-sections for a thermal Maxwellian neutron spectrum. The g-factors are strongly dependent on the exact cross-section curve shape $\sigma(E)$ in the thermal neutron energy range, in particular in the not very well known range below 0.0253 eV [3].

In the fit, experimental values of 2200 m/s cross-sections, of Maxwellian average cross-sections corrected to a spectrum temperature of 20° C, and g-factor values as obtained from curve shape studies, are all entered as parameters to be fitted. However, these data show a correlation which is difficult to formulate.

Firstly, the absorption cross-section curve $\sigma_a(E)$ is derived from measurements of the total cross-section. Thus, the g-factor computed from the curve $\sigma_a(E)$ is dependent on the scattering cross-section assumed. Secondly, if in the course of the least-squares fitting procedure, the value of the absorption cross-section σ_a (0.0253 eV) is adjusted, then this adjustment will affect the cross-section curve-shape $\sigma_a(E)$ and, as a consequence, will change the g-factor g_a.

Consequently, the absorption cross-section, the scattering cross-section, and the g-factor for absorption are correlated in the fit. Whereas in the earlier IAEA evaluations this correlation had been ignored, it had been considered, at least in a good approximation, in the 1975 evaluation.

These examples are mentioned here, in order to illustrate that the more important complications inherent in the least-squares fitting method have been taken care of, and that the results of the least-squares fit should therefore be reliable.

The improved fitting procedure by B.R. Leonard Jr.et al

Nevertheless, this way of a least-squares analysis leaves the evaluator in a difficult situation. If the g-factors are adjusted in the fit, as a result of simultaneous fitting of monoenergetic and spectrum average cross-sections, the evaluator is faced with the problem , that he has to construct, subsequently, a best cross-section curve which exactly reproduces the g-factor resulting from the least-squares fit. Obviously, this is a tedious, if not impossible job.

B.R. Leonard Jr. et al, therefore, achieved a considerable progress in the evaluation method of the thermal cross-sections, by considering in the least squares fit not only the monoenergetic and thermal Maxwellian experimental cross-sections but also the entire low-energy cross-section curves $\sigma(E)$ in a formulation using multilevel resonance parameters [4]. The results for U-235 were published in February 1976, and I am not informed at the moment when writing this, whether this work continues for the other fissile nuclides. But it would certainly be most useful, if this work by B.R. Leonard et al could be continued as a simultaneous fit for the four main fissile nuclides.

The recommended U-235 data obtained by B.R. Leonard et al deviate partly by more than a standard deviation from the 1975 IAEA recommended values. However, this deviation is only an expression of the still existing disturbing discrepancies among the existing experimental data.

The last (?) discrepancy to be solved

Despite of the more powerful fitting method developed by B.R. Leonard, the less powerful IAEA fit still serves a good purpose, because it may give us a hint about the source of the, perhaps last, disturbing discrepancy which remains to be solved for the thermal fission data.

In 1969 the results of the least-squares fit were somewhat unsatisfactory, since a number of different sources of discrepancies were interfering, thus making the interpretation of the results difficult. It was obvious that there were disturbing discrepancies among the experimental data, but it was not evident which of the many input data may be responsible for the discrepancies.

In the 1975 evaluation, the situation had so much improved, that one could well localize the origin of the discrepancies encountered. The one of the discrepancies has meanwhile found its solution, after a new more reliable value of the Pu-239 half-life has been established in a number of parallel experiments [5].

Hence it seems that there is only one discrepancy left which will hopefully be the last one: the systematic discrepancy between 2200 m/s cross-sections and thermal Maxwellian cross-sections for the uranium isotopes.

This is illustrated in Table 1.

The data given in Table 1 were obtained from least-squares fits of exactly the same input data as in 1975 [3] except for two items: a lower value of the Pu-239 half-life (24130 $\pm$ 50 years) was tentatively adopted, which seems to be the consensus of several independent experiments being performed at present [5]; and the final values of J.R. Smith's η experiment [6] were used instead of the somewhat lower values reported in 1974 [7].

When trying to localize the origin of the discrepancies encountered, several least-squares fits were made with different subsets of the experimental data, and the internal consistency of each subset was studied. As a result it became obvious that one can devide the experimental data into two subsets, where each subset has a very good internal consistency, but both subsets are inconsistent with each other.

The one subset comprises all monoenergetic 2200 m/s data together with the $\bar{\nu}$ data, see column 1 Table 1. The other subset comprises all data measured in a thermal Maxwellian neutron spectrum, see column 3 Table 1. Both of these subsets show an internal consistency which is striking and by far better than can be statistically expected. (Within each of both subsets only 4% of the input data deviate from the fitted value by more than the quoted, or re-assessed, experimental error.)

Column 2 in Table 1 shows the thermal Maxwellian data as deduced from the 2200 m/s data as given in column 1 using g-factor values as determined from curve-shape studies (see Table 2 column 1).

	1.	2.	3.	4.	
	Fit of experimental 2200 m/s data incl. $\bar{\nu}$ data	20°C Maxwellian data deduced from col 1. with 20°C g-factors of Table 2 col.1.	Fit of experimental 20°C Maxwellian data	Difference between columns 2. and 3.	
U-233 σ_a	573.8 ± 1.8	573.1 ± 2.1	574.3 ± 3.7	+0.8	
σ_f	533.2 ± 3.0	531.4 ± 3.1	526.9 ± 3.4	-4.5	(0.9%)
σ_γ	40.6 ± 2.5	41.7 ± 2.7	47.4 ± 0.4	+5.7	(13%)
α	0.076 ± 0.005	0.079 ± 0.005	0.090 ± 0.001	+0.012	(15%)
η	2.294 ± 0.009	2.289 ± 0.010	2.296 ± 0.019	+0.007	
$\bar{\nu}_t$	2.469 ± 0.008				
U-235 σ_a	680.0 ± 1.8	665.1 ± 2.0	663.6 ± 4.5	-1.5	
σ_f	588.1 ± 1.9	574.9 ± 2.0	566.0 ± 3.8	-8.9	(1.5%)
σ_γ	91.9 ± 2.3	90.3 ± 2.3	97.5 ± 0.8	+7.2	(8%)
α	0.156 ± 0.004	0.157 ± 0.004	0.172 ± 0.001	+0.015	(10%)
η	2.079 ± 0.008	2.077 ± 0.008	2.090 ± 0.016	+0.013	
$\bar{\nu}_t$	2.404 ± 0.006				
Pu-239 σ_a	1014.1 ± 4.3	1091.7 ± 7.0	1095.5 + 7.5	+3.8	
σ_f	748.1 ± 2.8	787.8 ± 3.7	787.8 ± 5.3	0.	
σ_γ	265.9 ± 4.1	304.0 ± 7.1	307.7 ± 2.6	+3.7	
α	0.355 ± 0.006	0.386 ± 0.010	0.391 ± 0.002	+0.005	
η	2.110 ± 0.008	2.064 ± 0.014	2.060 ± 0.019	-0.004	
$\bar{\nu}_t$	2.860 ± 0.009				
Pu-241 σ_a	1377. ± 13.	1431. ± 14.	1432. ± 13.	+1.	
σ_f	1023. ± 11.	1069. ± 13.	1059. ± 10.	-10.	
σ_γ	355. ± 8.	362. ± 11.	373. ± 8.	+11.	
α	0.347 ± 0.009	0.339 ± 0.012	0.352 ± 0.008	+0.013	(4%)
η	2.165 ± 0.013	2.177 ± 0.019	2.192 ± 0.032	+0.015	
$\bar{\nu}_t$	2.915 ± 0.010				
Cf-252 $\bar{\nu}_t$	3.740 + 0.009				

Table 1. Discrepancies between experimental 2200 m/s cross-sections and experimental 20°C Maxwellian cross-sections.

When comparing the directly measured 20° C Maxwellian data with those derived from monoenergetic data and g-factors, one finds:

1. Discrepancies exist for the uranium isotopes and, to a much lesser extent, for Pu-241. The data for Pu-239 are consistent. (Some authors, e.g. [4], quote that the data for Pu-239 are also inconsistent. However, this is correct only for the Pu-239/U-235 cross-section ratios, where however the discrepancies seem to come rather from U-235 than from Pu-239.)

2. For the uranium isotopes, systematic discrepancies exist for the fission and capture cross-sections and their ratio α, but not for the neutron yield η. Consistent are also the absorption cross-sections, where the discrepancy contributions from capture resp. fission seem to cancel.

3. The order of magnitude of the discrepancies is 1 - 2% for the uranium fission cross-sections and 8 - 15% for the uranium capture cross-sections and the ratio α.

These discrepancies are well known since long. But their origin is still unknown.

Since our 1969 evaluation all important experimental data have been carefully remeasured or reanalyzed: the fission cross-sections, the half-lives involved, the scattering cross-sections, the Chalk

River thermal irradiation data, the fission-neutron yields η and $\bar{\nu}$, the fission-neutron spectra, etc. Although one can never be sure of unexpected surprises, the striking consistency of the experimental data within the two subsets suggests that all these values are reliable within their quoted errors.

The only area which has not been reinvestigated with comparable scrutiny, is the lowest energy region around and below 0.01 eV, which significantly contributes to the 20° C Maxwellian cross-sections.

In 1975 [3], I thought that the lowest-energy cross-section curve shapes and thus the Westcott g-factors may be responsible for the discrepancies, but the analysis of B.R. Leonard et al [4] showed that the g-factors as obtained from the curve shapes, are rather accurately known, at least for U-235, not so much for U-233. However, a re-examination or re-measurement of the few existing data in the lowest energy region still seems to be advisable.

		1. $g = \int \sigma\sqrt{E}\,\mathrm{Maxw}\,dE/\sigma_o\sqrt{E_o}$	2. $g = \hat{\sigma}/\sigma_o$
U-233	absorption	0.999 ± 0.003 [8]	1.001
	fission	0.9965 ± 0.002 [8] (or 1.000 for different extrapolation of σ(E) to zero energy)	0.988
	capture	(1.03 ± 0.02)	1.17
U-235	absorption	(0.978 ± 0.002)	0.976
	fission	0.9775 ± 0.0015 [4]	0.963
	capture	0.982 ± 0.002 [4]	1.06
Pu-239	absorption	1.077 ± 0.005 [10]	1.081
	fission	1.053 ± 0.003 [9]	1.053
	capture	(1.14 ± 0.02)	1.16
Pu-241	absorption	1.039 ± 0.003 [10]	1.039
	fission	1.045 ± 0.006 [11]	1.035
	capture	(1.02 ± 0.02)	1.05

Table 2. 20°C Westcott g-factors

col. 1: g-factors calculated from the curve shape σ(E) according to

$$g = \int \sigma(E)\sqrt{E}\,\mathrm{Maxw}(E)\,dE/\sigma_o\sqrt{E_o}$$

The values in () were deduced from the other two g-factors quoted for the same isotope using cross-sections of col. 1 in Table 1.

col. 2: g-factors calculated from 20°C Maxwellian and 2200 m/s experimental cross-sections according to

$$g = \hat{\sigma} / \sigma_o$$

using the values from columns 3. resp. 1. in Table 1.

It is however evident, that the lowest-energy curve shapes and thus the g-factors derived from them, cannot be responsible for the full amount of the discrepancies. The g-factors

$$g = \hat{\sigma}/\sigma_o$$

obtained from comparison of experimental data $\hat{\sigma}$ in a 20° C Maxwellian neutron spectrum with σ_o for 2200 m/s neutrons, cannot be brought into agreement with the g-factors obtained from curve shapes

$$g = \int \sigma(E)\sqrt{E}\,\mathrm{Maxwellian}\,(E)\,dE/\sigma_o\sqrt{E_o}$$

This is illustrated in Table 2. One must suspect that there exists a still unknown physical effect in the lowest energy range.

Scientists at NBS are considering whether this unknown effect may be related to phonon transitions between cold neutrons and the sample [12]. Not knowing any details of these considerations, I believe that they may go into the right direction, although I cannot judge whether such effects may give a quantitative explanation of the discrepancies encountered. I can only conclude that the energy range around 0.01 eV will require further investigations before the thermal cross-sections of the fissile nuclides can be established as reliable standards.

References

[1] Westcott C.H., Ekberg K., Hanna G.C., Pattenden N.S., Sanatani S., Attree P.M., Atomic Energy Review 3 2 (1965) 3.

[2] Hanna G.C., Westcott C.H., Lemmel H.D., Leonard Jr. B.R., Story J.S., Attree P.M., Atomic Energy Review 7 (1969) No. 4 p. 3.

[3] Lemmel H.D., Proceedings of the Conference on Nuclear Cross-Sections and Technology, Washington D.C., 3-7 March 1975, NBS Special Publication 425 (Oct. 1975) Vol. 1 p. 286.
Note that the more detailed report announced as Lemmel H.D., Axton E.J., Deruytter A.J., Leonard Jr. B.R., Story J.S., INDC(NDS)-64 has not yet been issued.

[4] Leonard Jr. B.R., Kottwitz D.A., Thompson J.K., EPRI/NP-167 (Feb. 1976).

[5] Vaninbroukx R., ANL/ND-77-1 (Nov. 1976) p. 29.

[6] Smith J.R., Proceedings of the Conference on Nuclear Cross-Sections and Technology, Washington D.C., 3-7 March 1975, NBS Special Publication 425 (Oct. 1975) Vol. 1 p. 262.

[7] Smith J.R., USNDC-11 (June 1974) 12.

[8] Primarily based on Steen N.M., WAPD-TM-1052 (Sept. 1973).

[9] Deruytter A.J., Becker W., Annals of Nucl. Sci. and Eng. 1 (1974) 311, and Deruytter A.J., Wagemans C., J. of Nucl. En. 26 (1972) 293.

[10] Westcott C.H. AECL-3255 (April 1969), value increased due to revised scattering cross-section.

[11] Lemmel H.D., Westcott C.H., J. of Nucl. En. 21 (1967) 417, corrected for revised scattering cross-section.

[12] Bowman C.D., private communication 1977.

AN ASSESSMENT OF THE "THERMAL NORMALIZATION TECHNIQUE" FOR MEASUREMENT OF NEUTRON CROSS SECTIONS *vs* ENERGY*

R. W. Peelle and G. de Saussure
Oak Ridge National Laboratory
Oak Ridge, Tennessee 37830

Refined knowledge of the thermal neutron cross sections of the fissile nuclides and of the (n,α) reaction standards, together with the reasonably well-known energy dependence of the latter, have permitted resonance-region and low-keV fissile nuclide cross sections to be based on these standards together with count-rate ratios observed as a function of energy using a pulsed "white" source. As one evaluates cross sections for energies above 20 keV, optimum results require combination of cross section shape measurements with all available absolute measurements. The assumptions of the "thermal normalization method" are reviewed and an opinion is given of the status of some of the standards required for its use. The complications which may limit the accuracy of results using the method are listed and examples are given.

For the ^{235}U(n,f) cross section, the option is discussed of defining resonance-region fission integrals as standards. The area of the ∿9 eV resonances in this nuclide may be known to one percent accuracy, but at present the fission integral from 0.1 to 1.0 keV is known to no better than about two percent. This uncertainty is based on the scatter among independent results, and has not been reduced by the most recent measurements. This uncertainty now limits the accuracy attainable for the ^{235}U(n,f) cross section below about 50 keV.

Suggestions are given to indicate how future detailed work might overcome past sources of error.

[^{10}B(n,α); cross section; ^{6}Li(n,α); neutron; normalization; resonance; shape; standards; thermal; ^{235}U(n,f)]

Introduction

Since the earliest days of neutron cross section measurements using pulsed "white" neutron sources, workers have utilized the simple (1/v) shape of the (n,α) cross sections of ^{6}Li and ^{10}B to exploit the relatively well known absorption cross sections of the thermal energy range.[1] Through the last decades our knowledge of the requisite data has become successively more refined, and the existence of more powerful sources has allowed this "thermal normalization method" to be extended over an extremely broad energy range of ∿8 decades. In this talk the authors explore the definition of the method, identify some practical problems which have prevented this method from dominating all others, show some measure of the success so far obtained, and suggest where the cross section community might labor in its quest to exploit this technique to the extent many have dreamed should be possible. This talk is pertinent to the present meeting because the thermal normalization technique provides a prime requirement for the shapes of the standard (n,α) reactions and for the 2.2 km/s cross section standards. For ^{235}U(n,f), the technique is used to aid the definition of a secondary standard of great utility, so many of the examples below are from work on that nuclide. The recent papers of Leonard[2] and of Bhat[3] give forceful examples of the effort required to apply the method to this nuclide in a more correct way than earlier was possible for a present author.[4] Carlson and Czirr[5] have discussed the status of the thermal normalization for this cross section from a somewhat different point of view.

One reason for the ascendancy of the technique is that with it a linac or other white-source laboratory can provide an in-house cross section result which is complete over a very large energy range. All this can be done without direct measurements of sample mass which would otherwise generate a minimum uncertainty of 1-2 percent. Therefore, many cross section sets are normalized at thermal energies, although segments of the results could as well have been normalized in another way; therefore, more of the experimental literature seems to be based on this method than in fact is the case.

From a more global point of view, which requires that all existing data be combined, one sees at once that the use of a normalization based on thermal cross sections is conceptually separate from the use of relative measurements of count ratios between a counter based on the unknown and one based on a cross section of known shape. (This distinction is nicely emphasized by evaluation techniques such as those of Poenitz[6] in which shape and normalization decisions are separated.) In fact, nearly all sets of cross sections *vs* energy, in whatever energy range, are based on count ratios to the output of a detector with smooth and presumably known energy response, and it is a matter of detail whether or not this response follows the values of a known cross section. One can expect a typical synthesized result from a linac lab to consist of one or more segments of relative σ(E) data, the lowest segment reaching the thermal energy region and providing one normalization. This normalization has peculiar status only because it may be tied directly to applications through thermal critical experiments and when it provides a normalization with smaller uncertainty than others available to an evaluator. Other means of absolute normalization are available, especially in the MeV range, so that for sufficiently high energy some absolute measure other than the thermal normalization is likely to dominate. Whether this crossover of relative importance occurs at 20 keV or at 1 MeV or above will depend on the nuclide and the opportunities provided to the experimenters at the several laboratories. However, in every case a thermal normalization can be applied, it is important and could not be ignored below ∿10 keV even if ±1% absolute normalization data were available at scattered energy points above 20 keV.

In the special case of ^{235}U(n,f), one may be tempted in evaluating the standard cross section to ignore data based on normalization at thermal energies because the presence of fluctuations prevents this fission standard from being recommended for use at energies below 200 keV, and because there is such a wealth of experimental absolute data at the higher energies. Such a reaction would be hasty for three reasons: 1) the weight of measurements based largely on normalization at thermal energies is far from null, and independent methods must always be compared for mutual

consistency if we are ever to achieve the correct cross sections, 2) average cross sections of "standards" quality are needed in the region of fluctuations if one is to take advantage of clean integral fission-rate experiments in which the lower-energy neutrons play a significant role, and 3) when the approximate shape of the flux is known and is smooth, one may make use of the ^{235}U fission rate to fix the normalization of the flux even if one cannot be sure enough of energy scale alignment to use directly the ratio observed to $^{235}U(n,f)$ within each experimentally defined energy cell. The question of the importance of $^{235}U(n,f)$ below 0.2 MeV is actually moot because this cross section must anyhow be known well because of its direct practical applications.

What the Thermal Normalization Method Requires

For now, assume a restricted definition of the thermal normalization method. The method requires use of a standard cross section known well as a function of energy and at thermal energy (2.2 km/s), and it may be applied to an unknown whose cross section is also well known in the thermal energy region. Figure 1 exhibits the standard relation between unknown, known, and observed quantities, and quotes the restrictions on the method's applicability. One must previously have subtracted any backgrounds from the observed rates. Understood departures from the required energy independence of flux ratio or detector efficiencies may be corrected. The beauty of the technique is that neither neutron fluxes nor sample masses or areal densities appear in the equation of Figure 1.

The Thermal Normalization Method Requires No Mass Measurements and Only Relative Count Rates *vs* Energy

If $R_{x/s}(E)$ = Reaction Rate Ratio $\frac{\text{x-sample}}{\text{standard sample}}$,

$$\sigma_x(E) = \sigma_x(th)\left(\frac{\sigma_s(E)}{\sigma_s(th)}\right)\left(\frac{R_{x/s}(E)}{R_{x/s}(th)}\right), \text{ if}$$

ratio of flux between two samples is not a function of energy.

Count-rate ratios may be used for $R_{x/s}(E)$ whenever efficiency for detecting reactions is also not a function of energy.

Figure 1.

To sense whether the necessary standards data are available to apply this method, one may look at an example consisting of the thermal cross sections of the fissile materials and the evaluated results for the light-element (n,α) reactions. Table 1 compares several evaluations of the 2.2 km/s fission cross sections of some important materials. Evaluations will differ until data inconsistencies are removed. The sometimes-quoted uncertainties of ∿0.2 percent may be too ambitious, but one senses that half-percent uncertainties suffice for fission. Achieving such an accuracy in a single absolute measurement involving sample masses involves very great care.[7] The 2.2 km/s cross sections of ^{6}Li and ^{10}B are typically quoted to 0.4 and 0.2 percent,[8] and Table 2 exhibits the stability of the evaluated energy dependence of these cross sections through the last three ENDF/B evaluations. Since measured data for these cross sections at any one energy

Table 1.

Evaluations of 2.2 km/s Fission Cross Sections for Uranium Have Varied By More Than the Uncertainties Quoted

^{233}U	^{235}U	^{239}Pu	Reference
530.6 ± 1.9	580.2 ± 1.8	741.6 ± 3.1	Hanna (IAEA) 1969[a]
	585.7 ± 1.8	742.5 ± 3.1	De Volpi, 1971[b]
526.3 ± 0.8	577.5 ± 1.1		Steen, 1972[c]
533.7 ± 2.7	585.7 ± 2.3	742.0 ± 4.2	ENDF/B-IV, 1973[d]
529.9 ± 1.4	583.5 ± 1.3	744.0 ± 2.5	Lemmel, 1975[e]
	583.5 ± 1.7		Leonard, 1976[f]

[a] G. C. Hanna *et al.*, Atomic Energy Review 7, No. 4, p. 3 (1969).

[b] A. de Volpi, Conference on Neutron Cross Sections and Technology, CONF-710301 (Vol. 2), p. 564 (1971).

[c] N. M. Steen, WAPD-TM-1052 (Sept. 1972).

[d] J. R. Stehn, BNL, private communication to Cross Section Evaluation Working Group members on final fit Q4 (Dec. 13, 1973).

[e] H. D. Lemmel, Conference on Nuclear Cross Sections and Technology, NBS Special Publication 425, p. 286 (1975).

[f] B. R. Leonard, D. A. Kottwitz, and J. K. Thompson, "Evaluation of the Neutron Cross Sections of ^{235}U in the Thermal Energy Region," Report EPRI-NP-167-Project 512 (1976).

Table 2. Evaluated ENDF/B Cross Sections for the ^{6}Li and $^{10}B(n,\alpha)$ Reactions.[a]

(Values of $\sigma\sqrt{eV}/(\sigma_o\sqrt{0.0253})$ are Tabulated)

	$^{6}Li(n,\alpha)$			$^{10}B(n,\alpha)$		
E(kev)	III	IV	V	III	IV	V
0.1	0.999	1.001	0.999	0.995	0.994	0.994
1.0	0.987	0.998	0.987	0.985	0.982	0.983
10.0	1.000	1.009	1.004	0.963	0.965	0.963
30.0	1.027	1.054	1.042	0.958	0.970	0.963
50.0	1.078	1.121	1.099	0.971	0.984	0.972
100.0	1.379	1.460	1.386	1.035	1.016	1.000
σ_o in barns						
	940.3	940.0	935.9	3836.5	3836.5	3836.6

[a] Values for Versions III and IV were obtained from the files of the National Neutron Cross Section Center at BNL. The ENDF/B-III standards are also described in BNL 17188 (ENDF-179), M. K. Drake, editor (1972). Version IV was documented by Hale, Stewart, and Young in LA-6518-MS (1976). The preliminary evaluation for Version V was obtained from G. M. Hale et al., LASL (1976) and also included in the Minutes of the CSEWG Normalization and Standards Subcommittee, May 17-20, 1976.

in the tens of keV region spread widely (10 percent), the stability shown could be illusory if surprises develop in proper representation of the data using reaction theory.[9] Though complete evaluated uncertainty information for the energy dependence of these cross sections has not been given, one can see why confidence in the cross sections through 10 keV to 1 percent has been gained from the stability of the result and the closeness to a (1/v) response. (These authors are concerned whether one can at present have confidence in

either reaction cross section at 50 keV to 2 percent or at 100 keV to 3 percent, but the doubt arises from casual rather than detailed studies.)

These (n,α) reactions and the $^{10}B(n,\alpha\gamma)$ reaction have been used as standards to much higher energies, so it seems important that work continue to establish the underlying cross sections. Fortunately, other flux detectors based on the hydrogen cross section become available above about 10 keV, but counters based on ^{6}Li and ^{10}B can have much better time response than the hydrogen proportional counter which becomes useful at this energy. As additional smooth-response detector systems, not applicable at thermal energies, become available at energies above 10 keV, the simple thermal-normalization technique discussed above gradually loses its pre-eminence. In weighing the data or planning an experiment, one must balance the niceness of a fresh detector system against the need to internormalize results if the new system can no longer "see" the thermal-energy guidepost.

Of course, the thermal normalization method need not depend on an (n,α) reaction, and need not depend on a cross-section shape standard at all if a detector of calculable response with adequate time resolution can be used over a broad energy range down to thermal energies.

Experience with the Thermal Normalization Technique for $^{235}U(n,f)$

While thermal normalization may be employed by a single group to give results covering a broad energy range, its most important application is in cross section evaluation. An evaluator quickly finds that there are few individual measurements which span the region of interest without significant changes of apparatus, so one must combine the results from a number of individual experiments covering the energy range in patchwork fashion. Moreover, each reported data set may be referred to a different value of the 2.2 km/s cross section using a different technique for establishing this normalization, and be based on a different shape for the standard (n,α) reaction used to determine the energy dependence of the flux. With great effort, and the help of the data center system, it is possible to unravel the variations of data treatment.

Leonard has recently described his efforts to renormalize on a common basis a number of measurements covering portions of the energy range below 1 eV; most of the examples in this section depend on his work.[2] Through such consistency studies it is sometimes possible to uncover systematic difficulties not suspected by the original authors. The tables of Ref 2 imply renormalization requirements ranging from 0.3 to 1.5 percent, not counting the effect of differences in the 2.2 km/s cross section used.

For reasons given by Deruytter and Wagemans[10] and suggested in the next section, and because some of the more careful measurements do not in any case reach to energies above the resonance region, it is convenient to define the fission integral of the resonances near 9 eV as an intermediate standard. Table 3 gives the data for this integral using two popular choices for the energy bounds. Most of the listed data follow the renormalizations given by Leonard[2] and the uncertainties on these values reported by Bhat,[3] but the first line came directly from Ref 10 renormalized to σ_f^o = 583.5 b, and the Gwin data on the last line came from newly analyzed data sets.[11] The uncertainties on the Deruytter and Wagemans data were taken from Ref 10, and the uncertainties given on the last two data sets were assigned by this author without much analysis. The weighted average integrals at the bottom of the table indicate that the decision, whether to include Leonard's re-evaluation of Ref 10 or the original results, alters the output average by as much as the uncertainty assigned by expanding the propagated output uncertainty to make $\chi^2/df = 1$. In the presence of the observed inconsistency and conflict, it is difficult to accept the small 0.6 percent output uncertainty given. Pending more detailed uncertainty analysis, and including an uncertainty for the 2.2 km/s value, the overall uncertainty on this integral is judged to be about 1 percent. Based on more study, Leonard has estimated a 2.8% uncertainty in the 7.8-11.0 eV integral.[2]

Table 3.

DATA ARE INCONSISTENT FOR THE FISSION AREA[a] OF THE ∿ 9 eV RESONANCES IN ^{235}U.

$\int_{7.4}^{10.} \sigma_f\, dE$ (barn-eV)	$\int_{7.8}^{11.} \sigma_f\, dE$ (barn-eV)	Reference
221 ± 2	238 ± 2	Deruytter & Wagemans (1971).
(226 ± 2)	(243 ± 2)	Deruytter, per Leonard (1976).
227 ± 2[b]		Czirr & Sidhu (1976). Private communication (Feb. 1977). Leonard (June 1976) gives 224 b-eV for this value and 241 b-eV for Czirr's 7.8-11.0 eV integral.
219 ± 3[b]	236 ± 3[b]	Gwin et al. (1976), per Leonard (1976).
225 ± 4[b]	241 ± 5[b]	de Saussure et al. (1966), per Leonard (1976).
234 ± 7[b]	252 ± 7[b]	Bowman (1966), per Leonard (1976).
216 ± 6		Shore & Sailor (1958), per Leonard (1976).
226 ± 3	245 ± 3	Gwin (1977). Private communication. These two integrals come from separate new measurements.
$\bar{\sigma}(7.4\text{-}10.0) = 223.7 \pm 1.5 (225.2 \pm 1.4)$ b-eV, $\chi^2_6 = 11.8(9.5)$[c]		

a. Normalized to σ_f^o = 583.5 b. Table follows that of Leonard (1976).
b. Uncertainties as reported by Bhat (1976).
c. Values in parentheses use the Deruytter data renormalized by Leonard using only the data above 0.21 eV.

The energy intervals used in Table 3 which are commonly chosen for study are plausible ones, but if normalization or the relative behavior of various data sets are to be considered seriously, it is highly desirable to compare the areas of two or more resonances. In this way shape differences can be sensed which might place an evaluation procedure at an appropriate level of doubt.

If the fission integral of the ∿9 eV resonances is considered given, then the chosen value can be used to normalize experiments which did not reach to thermal energies or for some reason should not be trusted in that regime. Table 4 shows most of the independent data for the 0.1-1.0 keV $^{235}(n,f)$ fission integral which can be normalized at thermal energy or in this resonance.

Table 4.

THE MOST MODERN VALUES OF THE 0.1-1.0 keV ^{235}U FISSION INTEGRAL DIFFER BY 7 PERCENT. Details depend somewhat on evaluation technique.

Listed by Bhat[a]	Listed by Wagemans[b]	Original Author
12.4	12.3	de Saussure (1967)
11.8	11.8	Gwin (1976)
11.4	11.5	Czirr and Sidhu (1976)
12.2	12.3	Wagemans (1976)
11.8		Wasson (1976)
$\bar{I} \tilde{=}$ (11.9 ± .2) b-keV		

[a] M. R. Bhat, ANL-76-90, p. 307 (1976). Normalized to σ_o^f = 583.5 b and using the ENDF/B-V (n,α) shapes. Wagemans and Wasson data were normalized to I(7.8-11) = 241.2 b-eV.

[b] C. Wagemans and A. J. Deruytter, Annals of Nucl. Energy 3, 437 (1976). This table is based entirely on data and standard shapes utilized by the respective authors.

The data sets of Wagemans[12] and of Wasson[13] were normalized in the resonance while the other three sets retain the thermal normalization. The left column lists the results as renormalized by Bhat,[3] while the right column lists the values given in the original papers. Bhat's reworked values are to be preferred because they were obtained in a consistent way, but in this particular case the distinction is not great compared to the large scatter of results. The scatter will appear little less than disastrous for anyone having strong hope for early use of thermal normalizations for precision work; the range of values is 6 to 8 percent depending on whether one includes only the newer measurements which were optimized for the goal of obtaining precise fission cross sections. In fact there seems to be no reason to downweight the older results, since the uncertainty based on the scatter of the last three values is just as large as that based on all five. Simply put, the data base to date does not define the 0.1 to 1 keV fission integral, relative to the thermal cross section, to better than about 2 percent.

The particular energy interval displayed in Table 4 was chosen for convenience, but experience shows that such comparisons for normalization purposes are needlessly confused if comparison intervals much narrower than two lethargy units are used. As noted by Carlson and Czirr,[5] it is important that a normalization interval be chosen above ~0.2 keV because below this energy the shapes of the various measurements seem more discrepant. Also, as treated in the evaluation of Bhat,[3] many additional measurements are available above about 0.1 keV. It is puzzling that prior to the experiments of Refs 12-14 so few measurements spanned the range from 7 eV to 1 keV.

From the scatter indicated in Tables 3 and 4, and from the additional similar difficulties encountered at higher energies,[3,4] one must conclude that the application of the thermal normalization technique to ^{235}U(n,f) through the resonance and on into the keV region is more difficult than has been assumed. More care will be required than has already been expended. Much concern is relieved by recognizing that many of the studies were not optimized for the fission cross section alone, but as seen above there is important scatter among the most recent measurements performed with only this goal in mind. Considering the dispersion among results and uncertainties in the shapes of the (n,α) standards above 30-50 keV, it is remarkable that an evaluation task force was able to determine that an alteration as small as 1 percent to the results obtained by this method for the 0.01 to 0.2 MeV region would be all that would be necessary to bring the results into better agreement with experiments performed using monoenergetic sources and other normalization techniques.[3]

Complexities in Application of the Thermal Normalization Method

Given the apparent adequacy at least through 10 keV of the data which underlie the use of the thermal normalization method, why might various investigators obtain conflicting results? Figure 2 lists some possibilities.

The ratio data proving the consistency of the ^{6}Li and ^{10}B(n,α) standards are quite limited, the work of Sowerby *et al.*[15] being most quoted though some indications are given in papers by Perez *et al.*[16] and by Wagemans and Deruytter.[12] Since the ratio of these cross sections is presumably easier to measure than the absolute value of either one, and since any inconsistency between these standards is causing serious confusion, a significant effort would be worthwhile to establish beyond doubt the ratios of these cross sections.

Why Don't All Authors Get the Same Answers?

- The (n,α) standards may be inconsistent.
- Efficiencies of detectors for flux and unknown may not be proportional to reaction rates.
- Conflicting requirements on sample thickness, flight-path length, source pulse rate, and run time inhibit optimization for accuracy.
- Assessment of counting backgrounds and resolution functions is beset with hazards.
- Time pressure often curtails complete evaluation and intercomparison of results.

Figure 2.

Detectors for the light element (n,α) reactions are usually designed to have uniform efficiency for the reaction products, independent of neutron energy at least to first order. Not often, however, does one see a detailed demonstration that this assumption is valid for a particular detector. The reaction Q-values are sufficiently large that one would not expect significant effects on detector performance from reaction kinematics for energies up to at least 10 keV, but at higher energies the energy dependence should be worked out for each detector design. Nonisotropy of reaction cross sections in the c.m. system also requires consideration; we have seen from the work of Raman *et al.*[17] that a measurable fore-aft asymmetry is confirmed even for 10 eV neutrons when the detector subtends π solid angle! The observed energy dependence of this asymmetry to 10 keV had the form $1 + 0.005x\ E(eV)^{0.54}$, so the effect is strong. This finding again suggests that for precision work the energy dependence of flux detectors based on the (n,α) reactions should be analyzed with considerable care.

The reason that a thermal normalization must so often be carried out through successive renormalization of partially overlapping data sets is that the experimenter using a pulsed white source cannot simultaneously optimize all the experimental variables which affect data accuracy; it is mandatory to compromise other values as one extends the energy range of an individual data run to minimize the number of successive normalizations. Gwin *et al.*,[18] in their paper describing very broad-range experiments, discuss some of the problems to be handled in such measurements.

One set of compromises involves sample thickness: to obtain adequate counting rate one may use a sample so thick that self-absorption is serious in the unknown or in the flux detector, and in some cases a thick sample in a fission ion chamber may complicate timing and make less sure a constant efficiency for the detection of fission products. The sample-thickness conflict might be resolved by establishing precision average cross sections using a thin sample, while filling in the short-range detailed energy dependence using a detector with more material; a disadvantage of this solution would be that backgrounds are more difficult to assess using the black resonance technique when the counting rates are low.

Assuming that the repetition rate and the thickness of anti-overlap filters may be changed at will when using a pulsed white neutron source, another set of compromises involves choice of flight-path length and neutron pulse repetition rate. Short flight paths (5-20 m) minimize overlap problems but may not permit satisfactory time resolution for flux detectors and may place any effect of "gamma flash", or of the electrical noise associated with neutron pulse production, too close in time to the interesting data. Assuming the flight-path length has been chosen, Figures 3 and 4 illustrate the shape of the count rate from a (1/v) flux detector with two different arrangements to reduce the low-energy sensitivity enough to avoid time-frame overlap. In Figure 3 the experiment could cover energies to about one-half electron volt, but there is need

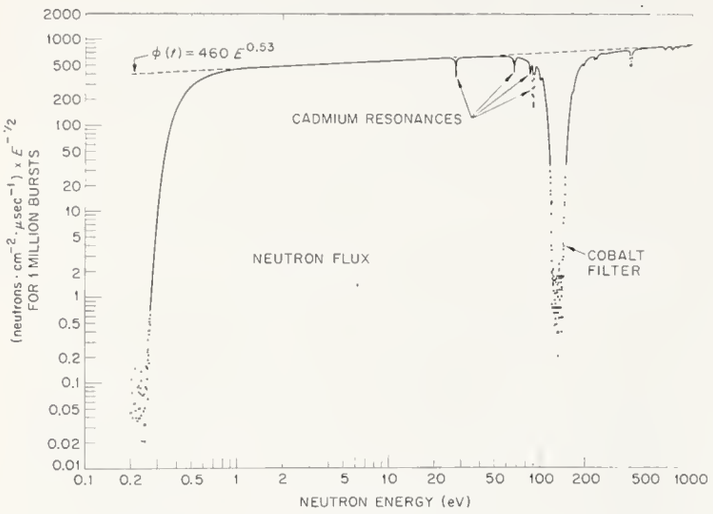

Figure 3. The time spectrum in a ^{10}B-based flux monitor when a cadmium filter was used to eliminate time-frame overlap. The cobalt filter was used for background estimation. From Ref 19.

to work hard to correct for the effect of the cadmium resonances which may be resolved to different extents in detectors for the flux and for the unknown. For Figure 4 a boron filter was used to cut the flux off at

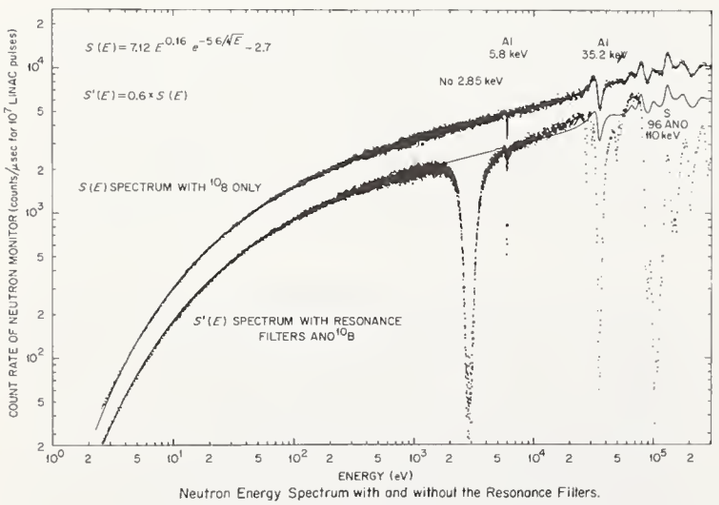

Figure 4. Time spectra in a ^{10}B-based flux monitor when a boron filter was used to avoid overlap. The lower curve illustrates the use of resonance filters to help estimate backgrounds. From Ref 20.

∿1 eV, but the counting rate at about 4 eV is only one percent of what it would have been if a clean cutoff-mechanism had been available to eliminate all neutrons with energies below 1 eV. If more boron is used, a faster repetition rate is possible and vice versa; in the case of Figure 4 the net counting rate was optimized at about 3 keV, and counting rates could have been improved by decreasing boron thickness and repetition rate had the experimenters wished to improve performance for energies below 3 keV. A point of this discussion is that lowering repetition rates to increase the energy range of an experiment may increase counting rates through a large share of the dynamic range.

Backgrounds in pulsed neutron experiments are usually determined by inserting into the beam "filters" designed to remove all the neutrons at the resonance energies of these absorbers. If the filter can be thin, one assumes that the filter does not affect the shape of the overall spectrum of higher-energy neutrons which normally cause all the troublesome backgrounds. Between the well-spaced energies of the filter resonances, the experimenter must interpolate a shape based on auxilliary data or an assumption of smoothness. Rarely has it seemed possible to understand the shape of the background based on calculation of the transport of beam neutrons through the regions surrounding the neutron source and detector. Figures 3 and 4 illustrated this background estimation method for boron-based flux detectors. Note that the backgrounds seem very low. In Figure 4, where a boron filter was used to roll off the flux, one senses that the background ratio was not so favorable at lower energy since the boron filter attenuated relatively less the higher-energy neutrons inducing the background. Figure 5 from an earlier experiment[19] shows that measured relative backgrounds have not always been so low; one can see that the average cross sections and the valleys between resonances would have been markedly affected by an error in the assumed

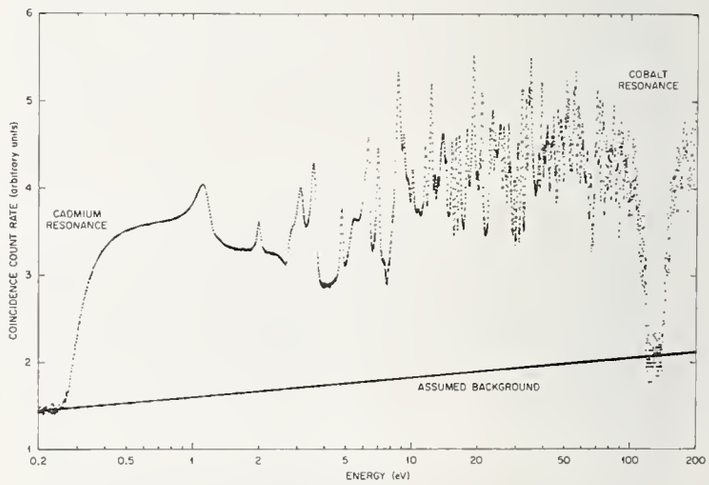

Figure 5. An example of background determination in a fission cross section measurement, from Ref 19. Coincidences were recorded between a fission chamber and a liquid scintillator tank which surrounded it.

background shape. Figure 6 is a more favorable example at higher energy where the background level appears to be about 1 percent.

When the background level estimated by the above technique is not small, more detailed analysis is required. Gayther *et al.*[21] have suggested one way to

proceed using data obtained using several filter thicknesses. The difficulties arise partly because one struggles to differentiate sharply between a neutron-induced background and a "tail" on the experimental

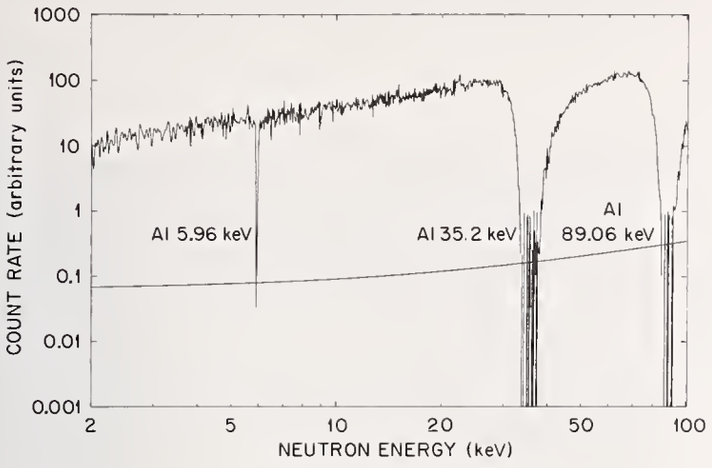

Figure 6. A background determination in the keV energy range using the black resonance technique, from Ref 16.

resolution function. The only difference is one of degree. Figure 7, though from a transmission experiment, shows the effect of a close-range asymmetry in a resonance chosen by Olsen[22] to facilitate analysis.

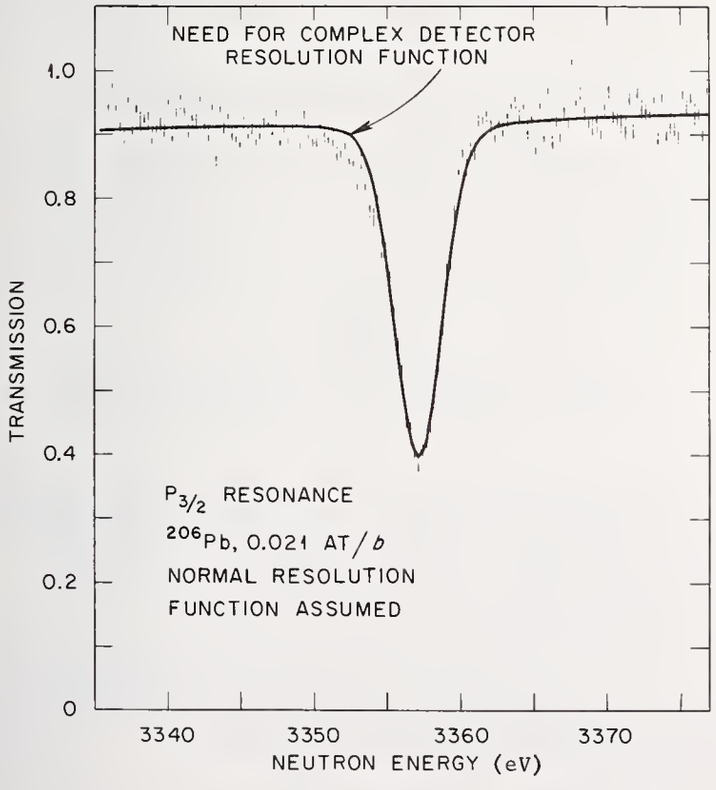

Figure 7. Discrepancy between observed and expected shapes of a transmission dip when the skew distribution of neutrons from a moderator and detector distortions were neglected.

The small discrepancy on the low energy side of the peak was subsequently explained by taking into account neutron diffusion in the thick ^{6}Li-glass detector and the skew shape expected for the time distribution of neutrons leaking from the target moderator.[23]

As the thickness of a resonance filter is increased, one typically obtains evidence that the flux at a given energy is affected a little by that at nearby energies far beyond the nominal system resolution width. Figure 8 illustrates this effect. The third-thinnest filter would be computed "black", with less than 0.001 transmission, yet increasing the sample

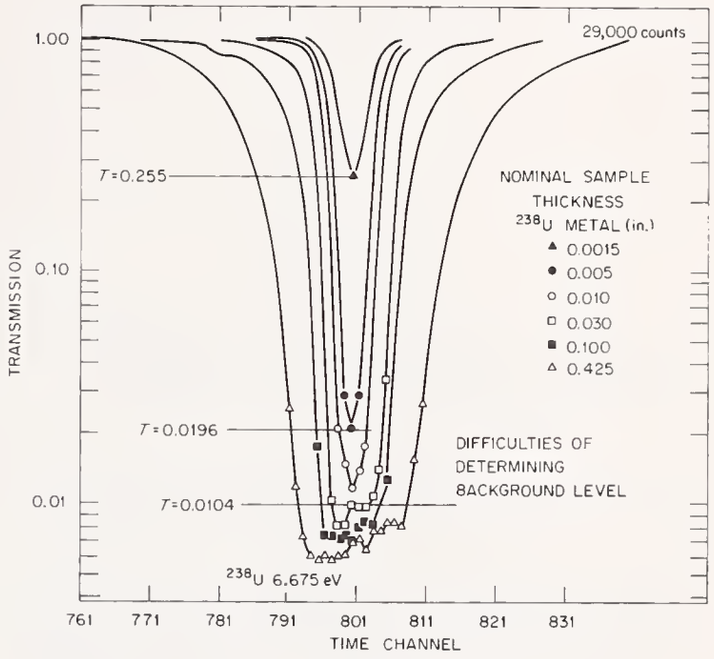

Figure 8. Neutron intensity near 6.7 eV observed through a broad range of ^{238}U absorbers. From the work of Ref 24.

thickness continued to reduce the counting rate near the minimum as the energy region of low transmission broadened. At any time after the neutron burst there are neutrons present at low intensity from a very broad energy range. The intensity and spectral distribution of these neutrons depends on the source, collimator, and detector construction and their environs. Improving accuracy of measurement through background reduction depends on identifying the sources of these off-energy neutrons, reducing their intensity, and learning to correct more precisely for the presence of those which cannot be removed. Given the difficulty of knowing the precise content of neutron beams, it seems preferable that the neutron flux shape be measured at the same time and place as the count spectrum from the sample under study.

Figure 9 is adapted from a very old comparison among preliminary sets of ^{235}U(n,f) data in the resonance region.[25] Much of the discrepancy was ascribed to detection of neutrons scattered from aluminum and concrete structures in the beam near the detector, and we believe that subsequent final data did not suffer so much from this difficulty.

Some of the error sources discussed above relate to counter design, some to beam production and collimation, and some may be inherent to pulsed-source methods.

Most have not been investigated and minimized with all the tenacity and ingenuity which would be possible, partly because practical experiments are beset by recurrent crises originating in electrical noise, counter decay, electronic malfunction, and sometimes the need to suffer suboptimal beam conditions to meet the needs of other experimenters.

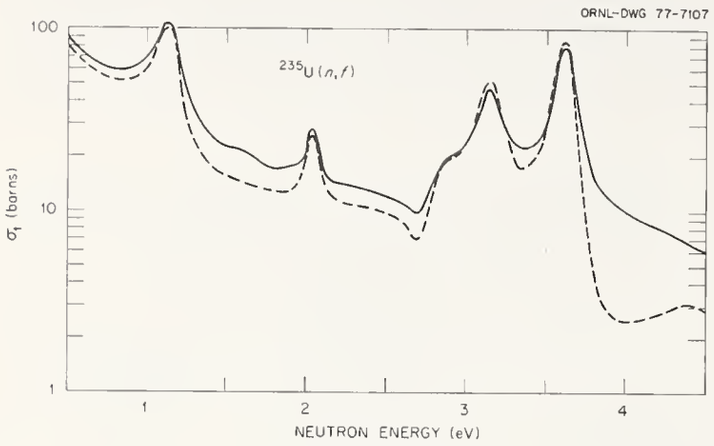

Figure 9. Two sets of preliminary observations of the $^{235}U(n,f)$ cross section, illustrating effects ascribed to return of neutrons scattered from structures in the beam.

How Precise Extrapolation from Thermal Cross Sections May Yet be Achieved

Experience shows that accuracy improvements are iterative, and depend on improved sources and instruments as well as the broad shoulders of those who have labored before. Figure 10 lists some major areas of effort which require attention. In the second point

WE KNOW SOME DIRECTIONS TO LOOK FOR IMPROVING ACCURACY USING THE THERMAL NORMALIZATION METHOD

- Improved analysis of backgrounds and resolution functions will be needed for most detectors.
- To cover 7-8 energy decades, important overlap of several data sets will often be required. Full evaluation of results through this range is required to establish credibility of normalization.
- Hasty exhibition of final results must be resisted, if haste will prevent full analysis and exhibition of data uncertainties and correlations.

Figure 10.

we mean by evaluation not only the intercomparison of results on the same cross section but thorough joint evaluation including the total cross section and other partial cross sections. It is customary to advise against the release and use of preliminary results, but the third point indicates that the present authors are more concerned about the apparently increasing pressures to issue final results before the necessary technical work has really been completed. The requirements on final reporting are substantial if evaluators are to have all the needed information.[26]

The main standard cross section efforts called for in this paper are listed in Figure 11; substantial progress toward these goals has already been made in this decade.

MORE WORK ON STANDARDS IS REQUIRED TO ENABLE THE FULL POTENTIAL OF THE THERMAL NORMALIZATION METHOD

- Perform measurements to prove compatibility of the $^{6}Li(n,\alpha)$, $^{10}B(n,\alpha)$, and $^{10}B(n,\alpha\gamma)$ reactions.
- Press hard to reach 100 keV with (n,α) cross sections accurate to one percent.
- For $^{235}U(n,f)$, try harder to establish two resonance-region fission integrals to 0.5 percent accuracy. A standard integral over a broad region between 0.1 and 1 keV is probably also needed.
- Continue work to achieve thermal-neutron cross section standards with credible 0.3 percent uncertainties. (Data inconsistencies now confuse uncertainty analysis.)

Figure 11.

With improved techniques and underlying standards, the goal of precise extrapolation to high energies based on thermal-region normalization can yet be reached. This goal, qualified by the recognition that absolute measurements at energies above ~20 keV will also be important, indeed must be achieved if there is to be a ^{235}U fission standard "for all seasons" and a knowledge of other cross sections sufficiently precise to satisfy all needs of developing technologies.

Acknowledgements

The authors gratefully acknowledge discussions on this topic with colleagues the world over, and particularly with R. Gwin, L. W. Weston, R. B. Perez, and D. K. Olsen. We are indebted to J. Gentry and E. Plemons for expedited production of the typescript.

References

*Research sponsored by the Energy Research and Development Administration under contract with the Union Carbide Corporation.

1. For example, J. F. Raffle and B. T. Price, Proceedings of the International Conference on the Peaceful Uses of Atomic Energy, paper P/422, Vol 4 p 187 (1955). Equally, papers by B. R. Leonard, ibid, paper P/589, p 193 (1955); V. L. Sailor, ibid, paper P/586, p 199 (1955).

2. B. R. Leonard, Jr., in ANL-76-90, Proceedings of the NEANDC/NEACRP Specialists Meeting on Fast Neutron Fission Cross Sections of ^{233}U, ^{235}U, ^{238}U, and ^{239}Pu, p 281 (1976).

3. M. R. Bhat, in ANL-76-90, op. cit., p 307 (1976). Also, related private communications (1976).

4. R. W. Peelle, ORNL-4955, An Evaluation for ENDF/B-IV of the Neutron Cross Sections for ^{235}U from 82 eV to 25 keV, (1976).

5. C. W. Carlson and J. B. Czirr, in ANL-76-90, op.cit. p 258 (1976).

6. W. P. Poenitz and P. Guenther, in ANL-76-90, op.cit. p 154 (1976).

7. A. J. Deruytter, in CONF-701002, Neutron Standards and Flux Normalization, p 221 (1971).

8. S. F. Mughabghab and D. I. Garber, BNL 325 Third Edition, Vol 1 (1973).

9. G. M. Hale, NBS Special Publication 425, Proceedings of a Conference on Nuclear Cross Sections and Technology, p 302 (1975). See also G. M. Hale, in proceedings of December 1975 Trieste IAEA consultant's meeting on Use of Nuclear Theory in Neutron Nuclear Data Evaluation. Lane, Hausladen, and Monahan, in CONF-701002, op.cit. p 107 (1971). Uttley, Sowerby, Patrick, and Rae, in CONF-701002, op.cit. p 80 and p 151 (1971).

10. A. J. Deruytter and C. Wagemans, J. Nucl. Energy 25, 263 (1971).

11. R. Gwin, ORNL, private communication (1977).

12. C. Wagemans and A. J. Deruytter, Annals of Nucl. Energy 3, 437 (1976).

13. O. A. Wasson, in ANL-76-90, op.cit. p 183 (1976).

14. J. B. Czirr and G. S. Sidhu, Nucl. Sci. Engr. 60, 383 (1976). See also Ref 5.

15. Sowerby, Patrick, Uttley, and Diment, in CONF-701002, op.cit. p 151 (1971).

16. Perez, de Saussure, Silver, Ingle, and Weaver, Nucl. Sci. Eng. 55, 206 (1974).

17. Raman, Hill, Halperin, and Harvey, CONF-760715-P2, International Conference on the Interactions of Neutrons with Nuclei, p 1340 (1976).

18. Gwin, Silver, Ingle, and Weaver, Nucl. Sci. Eng. 59, 79 (1976). See particularly sections IV.A. and IV.D.

19. G. de Saussure et al., ORNL-TM-1804 (1967). Also, with A. Lottin, Proc. Conf. Nucl. Data for Reactors, Paris, 2, 233 (1967). (The values given in the ORNL report are to be preferred.)

20. de Saussure, Silver, Perez, Ingle, and Weaver, Nucl. Sci. Eng. 51, 385 (1973).

21. D. B. Gayther et al., Proc. of a Panel on Neutron Standard Reference Data, p 201 (1974). IAEA, Vienna. Also, D. B. Gayther, AERE Harwell, private communication (1972).

22. D. K. Olsen, ORNL, private communication (1977).

23. A. Michaudon, J. Nucl Energy Parts A/B, 17, 165 (1963).

24. D. K. Olsen et al., Nucl. Sci. Eng. 62, 479 (1977).

25. F. D. Brooks, EANDC(UK)28 (1964).

26. R. W. Peelle, in ANL-76-90, op.cit., p 421 (1976).

REVIEW OF $\bar{\nu}$ FOR ^{252}Cf AND THERMAL NEUTRON FISSION

J. W. Boldeman
Australian Atomic Energy Commission Research Establishment
Private Mail Bag, Sutherland, NSW 2232, Australia

A review is presented of absolute measurements of $\bar{\nu}$ for the spontaneous fission of ^{252}Cf and of relative measurements for thermal neutron induced fission of $^{233,235}U$ and $^{239,241}Pu$. The discussion includes the consideration of a number of sources of revision that have been suggested for some of the measurements. No evidence is found in the revised data of any experiment-dependent systematic error. A set of recommended values is given.

{Neutron standards, $\bar{\nu}$, ^{252}Cf, $^{233,235}U(n,f)$, $^{239,241}Pu(n,f)$}

1. Introduction

Absolute values of $\bar{\nu}$, the average number of neutrons emitted per fission*, for the thermal neutron fission of ^{233}U, ^{235}U, ^{239}Pu and ^{241}Pu have been requested by reactor designers to accuracies approaching $^1/_4$ to $^1/_2$%. For experimental reasons, the most convenient way of performing such measurements is relative to a spontaneously fissioning standard and, for a number of years now, $\bar{\nu}$ for the spontaneous fission of ^{252}Cf has been the accepted standard. Consequently, an equivalent or better level of accuracy is required for this standard.

In view of the precision which has been requested, the presence of a number of discrepancies in the measurements over the last 10 years or so has been the cause of considerable concern. Historically, the difficulties began following the publication of $\bar{\nu}$ for ^{252}Cf as measured by the Boron Pile[1]. The value obtained [3.713±0.015] differed from the average of the two liquid scintillator determinations[2,3] [3.793±0.023] by an amount uncomfortably larger than the comparative error. Subsequently, preliminary values of $\bar{\nu}$ for ^{252}Cf obtained using manganese sulphate baths[4,5] for the neutron counting also supported a value lower than the liquid scintillator average. Alternatively, indirect values of $\bar{\nu}$ for ^{252}Cf calculated using the 2200 ms^{-1} constants (≈3.78) were in agreement with the liquid scintillator values. The 1969 IAEA review[6] of the 2200 ms^{-1} constants, therefore, recommended compromise figures in which both $\bar{\nu}$ and η values were shifted slightly from their experimental averages. For example, the average experimental value of $\bar{\nu}$ for ^{252}Cf of 3.743±0.016 compared with the recommended value of 3.765±0.012.

However, as the precision of the $MnSO_4$ bath determinations of $\bar{\nu}$ for ^{252}Cf improved, the support for the lower values increased. A third liquid scintillator measurement[7] obtained an intermediate value. Furthermore, it became apparent that some minor corrections were required for the two early liquid scintillator measurements[8]. Thus the 1972 Neutron Standards Reference Panel was able to conclude that within the direct measurements the spread of the different values was statistically acceptable. The 1972 Panel recommended a value of 3.733±0.008 for $\bar{\nu}$ for ^{252}Cf. The implications of this recommendation were either that there existed some error in the other 2200 ms^{-1} parameters or, alternatively, the error assignments were too optimistic. In particular, the η values used to provide indirect values of $\bar{\nu}$ were questioned. Subsequent revisions[9,10,11,12] of two η measurements[13,14] for ^{233}U and ^{235}U have failed to attribute the discrepancy to any specific factor. Although Leonard[15] and Lemmel[16] have questioned the α measurements, the entire explanation does not seem to lie here either.

*In this review, the symbol $\bar{\nu}_p$ will be used for the average prompt neutron emission, while $\bar{\nu}$ will be used for the total neutron emission, including the delayed neutrons.

The unresolved nature of this discrepancy has stimulated considerable activity in the revision of previous $\bar{\nu}$ measurements. At least two new absolute measurements are in progress[17,18], in addition to a re-examination[19] of the $\bar{\nu}$ ratios, all of which aim to achieve high accuracy. In the present report, all documented $\bar{\nu}$ measurements of reasonable accuracy have been reviewed, including subsequent revisions to these measurements and consideration is given to further corrections that are now appropriate. In section 2, absolute measurements of $\bar{\nu}$ for the spontaneous fission of ^{252}Cf are examined, while section 3 is devoted to the $\bar{\nu}$ ratios. A set of recommended values is presented in section 4.

2. Absolute $\bar{\nu}$ Measurements

Absolute $\bar{\nu}$ measurements may conveniently be subdivided into two categories:

(a) Delayed coincidence experiments (e.g. liquid scintillators and Boron Pile) in which a neutron counting gate is opened for a finite time after each fission event. The technique to a first approximation is independent of the absolute fission rate.

(b) Direct measurements (e.g. manganese sulphate baths) in which the absolute fission and neutron emission rates are compared from separate determinations.

Liquid Scintillator Measurements

The large liquid scintillator technique was first developed for the measurement of $\bar{\nu}$ by Diven et al.[20] The neutron detector consists of a large liquid scintillator [100-1000 ℓ in volume] which is loaded with a high neutron capture cross section material such as gadolinium or cadmium. A fission counter containing the appropriate target is placed at the centre of a tube which runs axially through the scintillator tank and allows entry and exit of a neutron beam. Neutrons produced by fission in this counter enter the scintillator, are moderated there and, after a mean lifetime generally of the order of 10 μs, are captured by the gadolinium or cadmium. The capture gamma rays so produced cause scintillations which may be observed by photomultiplier tubes mounted on the outside of the scintillator tank. By this method a multiplicity of neutrons produced in the fission event may be counted individually. Excellent discrimination against background radiation can be obtained by gating the output of the photomultiplier tubes with the fission pulse and only counting scintillation pulses for several neutron lifetimes.

The neutron detection efficiency of the liquid scintillator is proportional to the probability of neutron capture in the hydrogen and gadolinium or cadmium loading (and the structural materials), ε_c, and to the probability of the subsequent detection of the capture gamma rays, ε_γ. The efficiency is a function

of the original neutron source energy (mostly because of the variation in leakage) and, because of the asymmetry introduced by the axial tube, it is also a function of the neutron emission angle with respect to the scintillator axis θ. To determine the neutron detection efficiency of the scintillator for ^{252}Cf spontaneous fission neutrons requires a knowledge of $\varepsilon_c(E_n,\theta)$ and $\varepsilon_\gamma(E_n,\theta)$ for E_n = 0-15 MeV. These functions cannot be determined entirely experimentally. The normal procedure of calibration in the past has been as follows:

(i) The probability of neutron capture in the scintillator as a function of neutron energy and emission angle $\varepsilon_c(E_n,\theta)$ has been calculated with a Monte Carlo code.

(ii) It was assumed that ε_γ is independent of E_n and θ.

(iii) By measuring the probability of neutron detection of neutrons of specific energy and with a particular emission angle into the scintillator, a value of ε_γ was obtained.

(iv) The calibration of the scintillator efficiency was checked by repeating the efficiency measurement for a number of other values of E_n and θ.

Four sources of revision have been considered in the present review.

(a) Fission Neutron Spectra

Because of the neutron energy dependence of the scintillator tanks, it is necessary to make regular revision of all measurements to take advantage of the improvement in the precision of fission neutron spectra. Unfortunately, recommended values for the fission neutron spectra from Johansson[21] were not available for this review, which used the data listed in Table 1. For neutron fission of ^{235}U and ^{239}Pu the data were taken from the evaluation of Adams[22]. The spectrum for neutron fission of ^{233}U was taken to be Maxwellian with an average energy 1.025 times that for ^{235}U from the review of Smith[23]. The neutron spectrum for neutron fission of ^{241}Pu was related to that for ^{239}Pu using the expression of Terrell[24] and $\bar{\nu}$ values from the present paper. Because the experimental data for ^{252}Cf show a wide distribution of values[23], the spectrum normally assumed, namely Maxwellian with $\bar{E}$ = 2.15 MeV, has been retained.

TABLE 1

FISSION NEUTRON SPECTRA

Reaction	Shape	T (MeV)	A (MeV)	B (MeV)
$^{233}U(n,f)$	Maxwellian	1.37		
$^{235}U(n,f)$	Watt		0.9878	2.1893
$^{239}Pu(n,f)$	Watt		0.9723	2.7005
$^{241}Pu(n,f)$	Maxwellian	1.40		
$^{252}Cf(s,p)$	Maxwellian	1.43		

Watt spectrum: $P(E) = C \exp(-E/A)\sinh\sqrt{BE}$

Maxwellian: $P(E) = C\sqrt{E}\exp(-E/T)$

(b) Delayed Gamma Rays from Fission

Because of the gamma ray sensitivity of the liquid scintillators, the delayed gamma rays which arise from the decay of isomeric states among the fission products contribute to the apparent neutron count rate. Table 2 lists the delayed gamma ray cascades which can make a significant contribution. Some gamma ray yields have not been obtained experimentally. Fortunately, in all cases (bracketed yields in Table 2), it has been possible to estimate the missing yield using relative fission fragment yields of the identified parent from the experimental data of Unik et al.[29] Attention is drawn, in particular, to the isomer with a half life of 162 ns, where the yield in the spontaneous fission of ^{252}Cf is fairly large and the estimated yields for ^{235}U and ^{239}Pu show that it can make a serious contribution to $\bar{\nu}$ measurements. This contribution can be minimised in future measurements by introducing a delay of at least 500 ns before initiating neutron counting.

No experimental data are available for neutron fission of either ^{233}U or ^{241}Pu. For ^{233}U, I have used the ^{235}U yield data and for ^{241}Pu, the ^{239}Pu data.

TABLE 2

DELAYED GAMMA RAY DATA

$T_{½}$ (μs)	Energy of Cascade (MeV)	Parent	% Yield per Fission		
			$^{252}Cf(sp)$	^{235}U	^{239}Pu
0.020	0.614	A=100	0.34	(0.93)	(0.85)
0.100	1.723	A=134	0.22	(0.51)	(0.49)
0.162	1.692	^{134}Te	1.15	(2.7)	(2.5)
0.62	1.505	A=135	0.28	(0.51)	(0.51)
3.1	1.891	A=137 or ^{136}Xe	0.60	0.63	1.30
26.7	1.710		0.38	0.45	0.73
54.0	1.110	^{93}Rb	0.50	0.85	0.72
80.0	1.710		0.64	0.32	0.46

Data taken from refs. 7,25-28)

(c) Improved Monte Carlo Calculations

All liquid scintillation measurements of $\bar{\nu}$ are dependent on the accuracy of the calculation of the neutron leakage. Improved input data, and particularly the ability to specify more exactly the geometry of the detector systems, have afforded some recent improvement.

(d) Dependence of the Capture Gamma Detection Efficiency on E_n and θ

It has normally been assumed that the capture detection efficiency is independent of the original properties of the neutron. This assumption was questioned at the 1972 Panel Meeting. Since then, Poitou and Signarbieux[30] have investigated the validity of this assumption by also following the history of the capture gamma rays in a Monte Carlo calculation. They find a small variation in neutron capture detection efficiency with neutron energy which depends on the size of the scintillator. More specific calculations have been made by Ullo[31] with particular reference to the liquid scintillator measurement[7].

Particular application of these four sources to individual liquid scintillator measurements follows.

Spencer[18)]

A new absolute determination is in progress at Oak Ridge National Laboratory. No details or data are yet available.

Boldeman[7)]

The liquid scintillator in this measurement was spherical, 76 cm in diameter, and contained a loading of 0.5% by weight gadolinium. The axial hole through the scintillator had a diameter of 7.62 cm. The absolute calibration of the system was made as follows.

(a) The relative neutron capture efficiency of the scintillator was calculated as a function of neutron energy and angle of emission with respect to the beam tube, using a Monte Carlo method.

(b) The calculated efficiency values were normalised at the low energy end of the fission neutron spectrum in a measurement in which 2 MeV neutrons were scattered from a hydrogen gas target. Essentially, the normalisation was based on the detection efficiency for 0-1 MeV neutrons emitted at angles of 90-45^{0} respectively, with respect to the scintillator axis.

(c) It was assumed that there was no energy dependence of the neutron capture gamma ray detection efficiency.

(d) The shape and absolute calibration of the energy dependence of the efficiency curve were checked in a second experiment in which 16 MeV neutrons were scattered from a polythene target. The detection efficiency of the system was verified within 1.5% to 8.73 MeV.

In the original work, the fission neutron spectrum assumed for ^{252}Cf was the same as the present and therefore no correction is necessary. The effects of delayed gamma rays from fission were also adequately taken into account.

An extensive re-analysis of items (c) and (d) has been carried out by Ullo[31)]. Most of the structural details of the scintillator were included in a Monte Carlo calculation of the neutron energy dependence of the scintillator, in which the histories of the capture gamma rays were also followed. The variation in leakage with neutron energy and angle from the original calculation was confirmed. However, an energy dependence for the probability of neutron capture detection was determined.

The relative probability of neutron capture detection for isotropic ^{252}Cf spontaneous fission neutrons to that for isotropic 0-1 MeV neutrons was computed to be 0.9972. Furthermore, the relative probability of capture detection of 0-1 MeV isotropic neutrons to those of the calibration, 0-1 MeV between 90^{0} and 45^{0}, was estimated to be 0.9997. Thus this work estimates a total difference of 0.31% between the calibration neutrons and those for ^{252}Cf, compared with a +0.10% correction in the original paper. For the present paper, the analysis of Ullo[31)] has been accepted and a further correction of +0.21% has been applied to the measured value.

A further modification suggested by Ullo concerns the reliability of the estimate of the effect on neutron leakage caused by the axial hole. His somewhat pessimistic contribution of 0.3% to the experimental error compares with a value of 0.1% used in the original paper. A compromise figure of 0.2% has been used in this review.

Table 3 lists the revised corrections for this measurement and all identified sources of error. The final value obtained for the prompt neutron emission is 3.746±0.016 and 3.755±0.016 for the total neutron emission after the addition of the delayed neutron fraction.

TABLE 3

CORRECTIONS TO EXPERIMENTAL DATA AND SOURCES OF ERROR FOR REF. 7)

Effect	Correction (%)	Contribution to Accuracy (%)
Statistical accuracy		0.24
Dead-time correction:		
(a) ^{252}Cf	+1.107	
(b) Low energy proton recoil	+0.279	
(c) Relative	+0.828	0.10
Delayed gamma rays	-0.28	0.07
Fission neutron spectra:		
(a) Accuracy of $\bar{E}$		0.12
(b) Accuracy of energy calibration		0.17
French Effect	-0.10	0.10
Effect of hole through scintillator on neutron leakage		0.20 (0.10)[a)]
Background error in proton recoil counter	-0.33	0.10
Variation in neutron capture detector efficiency for ^{252}Cf fission neutron and calibration neutrons[b)]	+0.31 +0.05[a)] +0.05	0.10 0.05[a)] 0.05

[a)] Value used in original paper

[b)] Two separate effects considered in original paper

Asplund-Nilsson et al.[2)]

In this experiment the liquid scintillator was 60 cm in diameter with a 6 cm diameter axial hole. The tank contained 110 ℓ of liquid scintillator with a Cd/H atom ratio of 0.002. The absolute calibration of the neutron detector efficiency was carried out as follows:

(i) For four incident energies (3.0, 4.3, 4.5 and 14.9 MeV) neutrons were scattered from an anthracene crystal at the centre of the scintillator and the neutron detection probability was determined for 28 values of (E_n,θ). The highest energy for which the efficiency was determined was 10.75 MeV.

(ii) It was assumed that there was no angular dependence for the neutron detection efficiency. Thus the detection efficiency for a ^{252}Cf fission neutron spectrum (T = 1.40 MeV assumed) was obtained by integrating over the measured energy dependence.

(iii) The efficiency figure so obtained was corrected for the effect of the axial hole using a Monte Carlo calculation.

This measurement was down-weighted in the review by Axton[8] partly because assumption (ii) was shown to be inappropriate. However, because the neutron detection efficiency was measured for such a large number of neutron energies and emission angles, it seemed reasonable to try to correct this deficiency in the original analysis.

For the exact scintillator geometry, the probability of neutron capture in both hydrogen and cadmium was calculated using the code of ref. 7) to be 0.9035 for an isotropic source of ^{252}Cf spontaneous fission neutrons [$\bar{E}$ = 2.15 MeV]. For each of the 28 efficiency measurements at a specific neutron energy and emission angle the probability of capture was also determined. Comparison of the experimental data with the calculated leakage, yields 28 values for the probability of neutron capture detection. The relevant data are listed in Table 4.

TABLE 4

CALIBRATION DATA FROM ASPLUND-NILSSON ET AL.[2]

Scattered Neutron Energy (MeV)	Scattered Angle (degrees)	Detection Probability (%)	Calculated Capture (%)	Effective ε_γ (%)
0.24	73.6	72.6±1.5	99.25	73.1
0.65	62.3	74.7±1.2	98.92	75.5
1.07	53.3	74.8±1.1	97.75	76.5
0.15	79.5	70.9±1.5	99.46	71.3
0.50	70.5	72.9±1.4	98.97	73.7
0.97	62.3	73.1±1.5	98.34	74.3
1.40	56.1	73.4±1.5	96.79	75.8
1.86	50.0	71.5±1.4	94.01	76.0
2.43	42.7	72.0±1.4	90.18	79.8
2.75	38.6	67.3±1.2	87.30	76.9
2.93	36.2	67.7±1.4	88.15	76.8
0.21	77.2	73.2±1.6	99.27	73.7
0.58	68.5	73.9±1.6	99.00	74.6
1.00	61.2	72.7±1.7	98.19	74.0
1.82	49.4	72.1±1.6	94.79	76.1
3.17	30.8	65.4±2.0	83.75	78.1
0.48	79.7	71.6±1.7	99.21	72.2
1.65	70.6	72.3±1.7	96.02	75.3
1.79	69.7	72.8±1.8	95.48	76.2
2.18	67.5	70.2±1.6	93.22	75.3
2.49	65.9	72.4±1.8	91.49	79.1
3.01	63.3	69.9±1.7	88.86	78.7
3.46	61.2	66.8±2.1	88.47	75.5
4.27	57.6	62.9±1.8	84.51	74.4
5.42	52.8	57.5±1.7	74.47	77.2
6.69	47.9	51.5±1.8	68.04	75.7
7.94	43.1	51.3±1.7	66.67	76.9
10.75	31.9	40.1±1.6	48.83	82.1

It will be noted that the capture detection probability is fairly constant, although there is a suggestion of a small drop at low neutron energies, while the value at 10.75 MeV seems slightly large. An average value for the capture detection efficiency was obtained by weighting the numbers in Table 4 according to a fission neutron spectrum. The value obtained, 0.7595, when combined with the probability of neutron capture gives a value of 0.6862 for the overall neutron detection efficiency.

Since the publication of the original paper, it has been reported[32] that a correction of -0.6±0.3% is necessary in this experiment to account for the French Effect[33]. This is the bias that can be introduced into $\bar{\nu}$ measurements by the use of a coincidence between the fission counter pulse and a scintillator pulse from fission gamma ray detection and neutron induced proton recoils, to initiate the neutron counting gate. There are many experimental advantages in utilising this coincidence in liquid scintillator measurements. It was assumed that those fissions without a coincident pulse had the same average neutron emission as those with a coincident pulse. In the original identification of this problem, the data suggested a possible correction of the order of 1% or so. Subsequent work has shown the French Effect to be very small and it is only in this experiment that the effect is really significant.

No correction was applied in the original paper for the contribution to the neutron count rate of the delayed gamma rays from fission. This was estimated for the 1972 Panel Meeting to be -0.20±0.20%[34]. This correction has been re-evaluated. The threshold on the neutron detector was set at the equivalent of approximately 600 keV from gamma ray sources. Furthermore, the neutron counting gate began 160 ns after fission. With these parameters, the revised correction is -0.43±0.2%.

The final revised value from this experiment for the prompt neutron emission is 3.783±0.040 and 3.792±0.040 for the total neutron emission. A full list of the experimental errors is given in Table 5.

TABLE 5

SOURCES OF ERROR (ASPLUND-NILSSON ET AL.[2])

Cause	Error
Statistical accuracy (^{252}Cf)	0.15
Statistical accuracy calibration	0.30
Corrections for proton recoil	0.20
Dead time correction	0.30
Delayed gamma rays	0.20
Fission neutron spectra (±0.03 in $\bar{E}$)	0.15
Accuracy of energy calibration	0.75
French Effect	0.30
Effect of hole through scintillator	0.30
Variation in neutron capture detection efficiency	0.20

Hopkins and Diven[3]

This experiment used a cylindrical liquid scintillator, 1 m long and 1 m diameter. The 1000 ℓ of liquid scintillator had a cadmium to hydrogen atom ratio of 0.002. For the absolute calibration of this detector, 3.9 MeV neutrons were scattered in a plastic

scintillator located at the centre of the 7 cm diameter axial tube. Neutrons within the energy range 0-1.3 MeV at an average emission angle of 72^{o} were selected for the actual calibration by the bias on the plastic scintillator. The energy dependence of the neutron leakage was based, as before, on a Monte Carlo calculation. In a second experiment to confirm the calculated energy dependence, 14.5 MeV neutrons were scattered in the plastic scintillator. The efficiency scale was confirmed for two energy groups, 0-2 MeV and 6-8 MeV.

A number of queries regarding the accuracy of the calculated leakage probabilities were raised by Axton[8] at the 1972 Panel Meeting. The authors subsequently confirmed the relative accuracy of their leakage calculation. Prior to the present paper, the leakage calculations were checked using the Monte Carlo code of ref. 7). Our calculations would require the $\bar{\nu}$ value from this experiment to be adjusted downwards by 0.15%. This adjustment has not been made, as our calculations included none of the structural details of the scintillator.

The original value of 3.771±0.031 was obtained using Bonner's[35] measurement of the ^{252}Cf fission neutron spectrum. An adjustment of +0.11% is required to correct the efficiency for the assumed fission neutron spectrum of Table 1.

No correction was applied in the original work for the effect of delayed gamma rays from fission. The threshold was set at approximately 1 MeV and it would appear that the neutron gate began approximately 300 ns after fission. Thus, relative to experiment 7), the efficiency for detection of delayed gamma rays compared to that for neutron capture gamma rays will be smaller. On the other hand, the earlier neutron gate increased the contribution. A reasonable estimate would appear to be 0.2±0.1%.

There are unfortunately no data on which to base a correction for the variation in neutron capture detection between ^{252}Cf spontaneous fission neutrons and those used in the calibration (0-1.3 MeV neutrons). Poitou and Signarbieux[30] indicate that the variation of gamma ray detection with neutron energy is flatter for a 50 cm radius scintillator than for the 38 cm radius scintillator in experiment 7). Therefore, the effect should be smaller than the total effect of +0.31% calculated by Ullo[31] for experiment 7). Of course, the higher threshold in experiment 3) increases the effect relative to 7), although this will be counter-balanced by the higher gamma ray energy emitted in cadmium capture versus that in gadolinium. In fact, if all the gamma ray energy is deposited in the scintillator, it is possible to conceive of a negative magnitude for this effect. Because of these considerations, it has been decided to make no correction at all. However, a contribution of 0.1% has been included in the experimental error of $\bar{\nu}_p$ for the spontaneous fission of ^{252}Cf.

The final value obtained from the revision of this experiment is 3.768±0.031 or 3.777±0.031 for the total neutron emission.

The Boron Pile (Colvin and Sowerby[1])

In this experiment, the neutron detector was a 220 cm cube of graphite surrounded by a 35 cm thick reflector of graphite. The pile contained a lattice of 240 BF_3 counters to detect the thermalised neutrons.

The energy dependence of the leakage from the pile and therefore the relative efficiency of the system, was calculated by Pendlebury[36] using the Carlson S_n technique (Fig. 1). For the calculation, the pile was idealised to a homogeneous sphere of graphite, ^{10}B and aluminium, with aluminium being used to simulate the copper bodies of the BF_3 counters. The calculated energy dependence was normalised using four measurements in which the absolute detection efficiency was obtained for four different essentially monoenergetic sources. For the Boron Pile the reaction used to produce the neutrons was the photo-disintegration of the deuteron. Four different product neutron energies were obtained using four different gamma ray energies. The data are listed in Table 6. It will be noted that the calculated efficiency curve does not reproduce particularly well the variation of the calibration values.

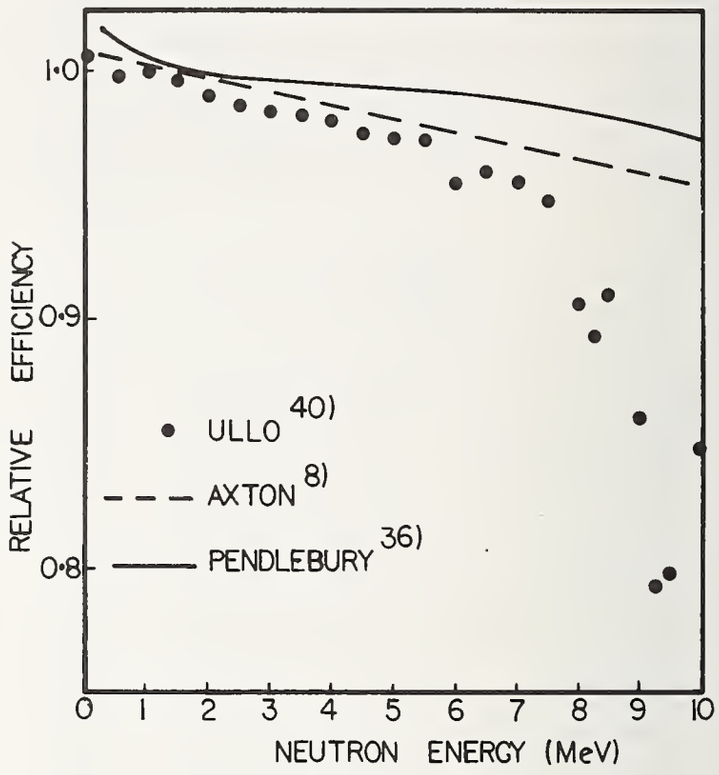

Fig. 1: Efficiency calculations for the Boron Pile

TABLE 6

CALIBRATION MEASUREMENTS FOR BORON PILE[1]

Measurement	Neutron Energy (MeV)	Efficiency	Error (%)
D(γ,n)p with Th C" γ-rays	0.19	0.6440	0.60
D(γ,n)p with ^{24}Na γ-rays	0.265	0.6457	0.21
D(γ,n)p with ^{19}F (p,α,γ) γ-rays	2.0	0.6433	0.25
D(γ,n)p with ^{27}Al (p,γ) γ-rays	4.9	0.6500	1.24
Ra-γ-Be*	≡0.25	0.6475	0.74

*Source calibrated by N.P.L. $MnSO_4$ bath[38]

Because the $\bar{\nu}$ value obtained, 3.713±0.015, was so different from existing measurements, the Boron Pile was subjected to close scrutiny. Colvin et al.[37] have answered a number of criticisms that have been made. Furthermore, a number of independent checks of the efficiency of the Boron Pile were made. For example, an independent measurement was made using a Ra-γ-Be source calibrated by N.P.L. using a $MnSO_4$ bath[38]. This value, effectively for neutrons at 250 keV, has been included in Table 6. Some recent objections have been voiced by

Leonard[15].

(a) The error assigned to the correction for the proportion of neutrons detected outside the gate period should be increased from the original assignment of 0.1%. The proportion of neutrons outside the 4 ms gate period is given by Colvin et al.[37] as 4.3±0.3%. From the data in Table V of ref. 37), the correction would appear to be at least as accurate as this. Thus, for the comparison of the Ra-γ-Be source measurement of the neutron detection efficiency with that from the D(γ,n) reaction, this correction must be applied and the full error in the correction included in the list of errors. However, for the comparison of ^{252}Cf fission neutrons and D(γ,n) reaction neutrons, it is the relative difference in the correction which is important. It is difficult to see how this could be any larger than the error of 0.1% assigned for this effect. It should be noted that a similar effect exists in all liquid scintillator measurements (1-2% loss outside the gate). In these cases, no contribution to the experimental error has been included.

(b) Loss of neutrons in the Boron Pile caused by Cu(n,p), Cu(n,α) and C(n,α) reactions was neglected in the efficiency calculations. Certainly the first two reactions were ignored; however Sowerby[39] estimates their effect as less than 0.1%. The effect of the third reaction has also been estimated by Sowerby to be 0.15±0.05%. It is thought that the effect of this reaction was included in the original calculations; however it has not been possible to verify this.

(c) Because the measured values of the efficiency calculations do not fit the calculated energy dependence, some subjective judgement is involved in choosing the best method of normalisation of the curve. In fact, it is fairly obvious that a recalculation of the energy dependence of the neutron detection efficiency of the Boron Pile is required, especially when the age of the original calculation is considered. A new calculation would also eliminate any objection on account of (b) above.

For the 1972 Panel Meeting, Axton[8] recalculated the energy dependence of the Boron Pile using a Monte Carlo calculation. His calculated efficiency curve is shown in Fig. 1, together with the original calculation. Use of this efficiency curve, rather than the Pendlebury calculation, leads to a value for the detection efficiency of the Boron Pile for ^{252}Cf spontaneous fission neutrons of 0.64145 versus the original value of 0.6428. Also shown in Fig. 1 is a more recent Monte Carlo calculation of the relative neutron energy dependence of the Boron Pile neutron detection efficiency by Ullo[40]. This work has not yet been published, but some details are available. For neutron transport the energy range from 5 keV to 10 MeV was spanned by 3000 energy points and inelastic scattering was handled implicitly. The angular distribution for elastic scattering in carbon was described with four Legendre components in the centre of mass. The cross sections for Cu(n,p), Cu(n,α) and C(n,α) were included in the calculation. Finally, some structural details of the Boron Pile were included. The calculated efficiency curve is also shown in Fig. 1.

There is a most unfortunate lack of agreement between the three different calculations. The two Monte Carlo calculations give the most similar dependence. In fact, it is likely that the difference between them can be partly attributed to slightly incomplete data sets employed in the calculation of Axton[8]. The difference between the original efficiency curve and that of Ullo is quite marked. The latter calculation does not show the rapid rise in efficiency at low energies, but shows a much more dramatic fall in efficiency at high neutron energies than does the Pendlebury calculation. The overall effect of the use of the Ullo efficiency curve is to increase the measured value of $\bar{\nu}$. For this review the Ullo efficiency curve has been used for two reasons. Firstly, the input data set was considerably more comprehensive. Secondly, in the calculation of the energy dependence of the liquid scintillator of ref. 7) the Ullo code produced values in substantial agreement with two other Monte Carlo calculations[7,39] and in agreement with the experimental data. However, it is important to resolve this question of the energy dependence of the Boron Pile as soon as possible.

For the normalisation of the calculated efficiency curve, a weighted value has been obtained from the experimental values at 0.190, 0.265, 2.0 and 4.9 MeV from the D(γ,n) measurements, plus the value at 0.250 MeV from the Ra-γ-Be source measurement. The weighted efficiency obtained for a ^{252}Cf fission neutron spectrum is 0.6379±0.0010. The error here is the direct experimental error. Because of the failure of the experimental data to reproduce satisfactorily the calculated energy dependence of the efficiency curve, some contribution to the experimental error is necessary. Unfortunately, this contribution is somewhat subjective. A value of ±0.3% has been used which compares with an effective value of 0.25% used by Colvin and Sowerby[1].

Colvin and Sowerby have indicated that they are prepared to accept, provisionally, the recalculated efficiency curve for the Boron Pile, pending an examination of the details of the calculation. The revised (provisional) value of $\bar{\nu}_p$ for ^{252}Cf from the Boron Pile is therefore 3.732±0.016 and 3.741±0.016 for the total neutron emission. All contributions to the experimental error are listed in Table 7.

TABLE 7

SOURCES OF ERROR (BORON PILE[1])

Cause	Contribution to Experimental Error (%)
Statistical accuracy of calibration[a]	0.15
Statistical accuracy[a] ^{252}Cf	0.11
Anisotropy in pile efficiency	0.20
Beam modulation	0.05
Electrical pick-up	0.03
Neutrons after gate	0.10
Fission spectrum (error in $\bar{E}$)	0.05
Lack of agreement of calculated and experiment shape of energy dependence of efficiency	0.30

[a] Includes contribution from error in correction for loss of neutrons caused by chamber materials

One objection that might be levelled at any revision of the Boron Pile $\bar{\nu}$ value for ^{252}Cf is that the old value was in agreement with values obtained using calibrated neutron sources to determine the efficiency of the pile. Colvin et al.[37] lists these measurements in Table II of that reference. Three different neutron sources were employed, namely, the AERE and AWRE ^{240}Pu sources and a Ra-γ-Be source. The latter source, which was calibrated using the N.P.L. $MnSO_4$ bath, has already been included in the absolute normalisation of the efficiency scale.

For the calibration of the Boron Pile using the ^{240}Pu sources, it is necessary to make a correction for the energy difference between ^{252}Cf spontaneous fission neutrons and those for spontaneous fission of ^{240}Pu if the efficiency curve of Ullo is appropriate. A correction of 0.25% is required in this case. For these source calibrations three independent efficiency values can be derived for the Boron Pile based on three independent methods of source calibration, namely,

(a) the revised original calibration[41] of the AERE ^{240}Pu source;

(b) the AWRE oil bath[42] calibration of the AWRE ^{240}Pu source;

(c) the calibration of the AWRE ^{240}Pu source using the N.P.L. $MnSO_4$ bath.

After applying the 0.25% correction referred to above, the efficiency of the Boron Pile for ^{252}Cf fission neutrons derived using the source calibrations (a) and (b) are

$0.6417^{\pm 0.0006 \text{ random}}_{\pm 0.0104 \text{ systematic}}$ and $0.6396^{\pm 0.0006 \text{ random}}_{\pm 0.0087 \text{ systematic}}$.

The average of these two values leads to a value of $\bar{\nu}$ for ^{252}Cf of 3.726±0.039. The error was derived assuming the original errors were independent. This is probably not the case, and the actual error may be fractionally larger. It is evident that the value of $\bar{\nu}$ derived using these two source calibrations is consistent with the revised $\bar{\nu}$ value from the Boron Pile experiment itself.

Finally, the value of $\bar{\nu}$ for ^{252}Cf derived using the N.P.L. calibrated value for the AWRE ^{240}Pu source is 3.697±0.034. The difference between this value and the revised Boron Pile value (slightly larger than one standard deviation) is not sufficient to raise any objections to the present revision. This third source value is more appropriately incorporated with the N.P.L. band measurements.

Manganese Sulphate Bath Measurements

The absolute measurement of neutron source strengths with manganese sulphate baths will be discussed in considerable detail at this conference by Axton[43]. Consequently, few of the details of the actual neutron counting will be given here and more attention will be devoted to the fission counting.

Bozorgmanesh[17]

A new $MnSO_4$ bath determination of $\bar{\nu}$ for the spontaneous fission of ^{252}Cf has apparently been completed at the University of Michigan. No details have been published as yet. The reported value, 3.744±0.023 for the total neutron emission, has been accepted for this review, together with the nominated error.

Measurements based on N.P.L. $MnSO_4$ bath[5,8,44,45]

Two separate absolute determinations[8,45] of $\bar{\nu}$ for ^{252}Cf have been made in which the neutrons were counted in the N.P.L. $MnSO_4$ bath, but the method of fission counting varied. Each is discussed separately below.

Axton et al.[5,8]

In this experiment a series of thin ^{252}Cf spontaneous fission sources were aliquotted from a stock solution of californium chloride and the absolute fission rates were counted in a pill box type gas flow proportional counter. The method employed to provide a satisfactory correction for fragment losses in the foils was discussed in detail in ref. 5). The neutron emission rate of the remaining californium chloride solution was then determined in the N.P.L. $MnSO_4$ bath. This process was repeated a number of times for four separate californium samples. A total of 20 separate neutron sources and 200 fission sources were prepared. The final value for the total neutron emission obtained in this experiment was 3.725±0.019 where the experimental error includes only the error on the fission counting.

White and Axton[45]

For this determination, the fission and neutron emission rates were obtained for the same source. The neutron emission rate was measured in the N.P.L. $MnSO_4$ bath and the fission rate was determined using a low geometry fission counter at Harwell. At the 1972 Panel Meeting, Axton[8] revised the accuracy of the fission counting. For the present review the revised value is retained. The value for $\bar{\nu}$ obtained was 3.797±0.038 where the error, as before, includes only that for the fission counting.

Other N.P.L. $MnSO_4$ bath dependent measurements

A number of other measurements of $\bar{\nu}$ for ^{252}Cf are generally included in the list of N.P.L. dependent measurements. One of them was the calibration of the Boron Pile with a Ra-γ-Be source and the AWRE ^{240}Pu source, both of whose activities were calibrated in the N.P.L. $MnSO_4$ bath. In the present report, the first has been included as part of the absolute calibration of the efficiency curve for the Boron Pile. Only the second source measurement, revised previously to 3.697±0.034, is included here with the N.P.L. dependent measurements.

Another addition was a measurement from Moat et al.[46] in which the neutron emission rate of a californium sample was determined using two cylindrical wax detectors of different dimensions, each containing several BF_3 counters for the detection of thermalised neutrons. The efficiency of the detector was determined using the Harwell ^{240}Pu source which was calibrated using the N.P.L. $MnSO_4$ bath, the Boron Pile and the Aldermaston oil bath. The original value of 3.77±0.07 for $\bar{\nu}$ for ^{252}Cf was corrected by Fieldhouse et al.[41] to 3.685±0.040 in a revision of the Harwell ^{240}Pu source and then to 3.727±0.056 by Hanna et al.[6] to account for an improved estimate of the difference in the ^{240}Pu and ^{252}Cf fission neutron spectra. Because of the very strong dependence of this measurement on the "softened" ^{240}Pu spontaneous fission neutron spectrum, it has not been included in the final list of values.

Average value from N.P.L.

The average of the three N.P.L. dependent measurements is 3.731±0.015 for $\bar{\nu}$ for ^{252}Cf. The error here includes only that from the fission counting. The error for the neutron source calibration in the N.P.L. bath was given by Axton[8] as 0.33%. Thus the total error becomes ±0.020.

A small revision to the N.P.L. value of $\bar{\nu}$ for ^{252}Cf has been recommended by Smith et al.[47] following their accurate measurement of the σ_H/σ_{Mn} ratio. They used the variable manganese concentration technique developed by Axton et al.[44]; but for the neutrons employed a Bragg reflected beam of approximately 0.02 eV. Thus corrections required for the $^{16}O(n,\alpha)^{13}C$ and $^{32}S(n,p)^{32}P$ are eliminated, together with any dependence on resonance capture data for ^{55}Mn. Recent experimental work[48] can be used to predict considerable intermediate structure in the $^{55}Mn(n,\gamma)$ cross section and specifically a strong valence component which could lead to a radiative width for the 2.375 keV resonance as large as 2 eV. The value they obtained, 0.02503±0.23%, compares with the revised value from Axton et al.[44] of 0.02495±0.35%. Use of the Smith et al.[47] value would lead to a positive adjustment of 0.15% in the N.P.L. $\bar{\nu}$ value.

For the purposes of this review, the N.P.L. $\bar{\nu}$ value has provisionally been adjusted by +0.15% to 3.737±0.020.

De Volpi and Porges[4,49,50]

For this experiment the experimental procedure was as follows. Three separate fission counters were prepared in which the californium sources, all yielding approximately 10^6 neutrons/s, were deposited in three different ways on one electrode of a fast ionisation chamber with a plate spacing of 1-2 mm and operated in the current mode. The neutron emission rates were measured by inserting the fission chambers in the A.N.L. manganese sulphate bath. Subsequently, the absolute fission rates for each of the three fission counters were determined in a coincidence system in which the fission fragments were counted in coincidence with prompt fission neutron detection in a Hornyak button[51]. The coincidences were recorded as a function of the angle (θ) between the fission counter normal and the neutron detection axis. The fission rate was given by NF/C where N is the neutron count rate, F is the fission rate and C the coincidence rate. The angular anisotropy of the effective fission rate was removed by averaging the four measurements at θ = ±37.4 and ±79.2. Although three different counters were employed, the final value of $\bar{\nu}$ was essentially based upon one counter (parallel plate) which had a fission fragment detection efficiency >99%. In addition to the coincidence method, the fission rate was also measured in a variety of other ways, including low geometry counting and simple extrapolation of the bias curve. Despite the considerable care that has been taken in arriving at the absolute fission rates, the estimated error for the third fission counter, 0.13%, appears optimistic. From Table 6 of ref. 4), the two sources of error for fission counter 3, namely the error of 0.13 for counter 3 in particular and that for the error common to the three detectors, appear not to have been added. Furthermore, two of the entries in the common errors, those for neutron detection efficiency dependence on $\bar{\nu}$ and fission detection efficiency dependence on $\bar{\nu}$, could each be increased to 0.1%. In addition, there does not appear to be any component added for the distribution in nodal values listed in Table III of ref. 4). The error has provisionally been expanded to 0.23%. This compares to an effective fission counting error in the summed N.P.L. measurements of 0.42%.

Axton[8] in his 1972 review recommended the introduction of an additional 0.5% error into the neutron source calibration in the $MnSO_4$ bath to account for aliquotting errors. De Volpi, in a private communication to the 1972 Panel Meeting, answered criticisms on this score, and the 0.5% error has therefore not been included in the list of errors in this review. However, from the text of ref. 8) and De Volpi's reply, there appears to be a number of small unresolved differences between A.N.L. and N.P.L. Finally, it should be noted that the measured value of σ_H/σ_{Mn} from A.N.L. of 0.2531±0.00003 differs significantly from the measurement of 0.02503±0.00006 by Smith et al.[47]. The explanation proposed by the authors[49] to explain their high value, impurities in the solution, could introduce an unknown correction as would any densimetric error. No error has been introduced here on this account. The final value obtained using the A.N.L. $MnSO_4$ bath is therefore 3.729±0.017.

Summary of Absolute $\bar{\nu}$ Measurements for ^{252}Cf

The revised values of $\bar{\nu}$ for the spontaneous fission of ^{252}Cf from the eight measurements are listed in Table 8. The average of these measurements, weighted according to the experimental error, is 3.745±0.008. The errors are not all independent and the accuracy should be expanded to ±0.010 to include various common errors. This revised value represents an increase of 0.32% in the value recommended by the 1972 Panel Meeting.

TABLE 8

RE-EVALUATED VALUES OF $\bar{\nu}$ FOR ^{252}Cf

Measurement	Total Neutron Emission Original	Total Neutron Emission Revised
Liquid Scintillator Measurements:		
Boldeman[7]	3.747±0.015	3.755±0.016
Asplund-Nilsson et al.[2]	3.808±0.034	3.792±0.040
Hopkins and Diven[3]	3.780±0.031	3.777±0.031
Boron Pile:		
Colvin and Sowerby[1]	3.713±0.015	3.741±0.016
Fieldhouse et al.[41]		3.726±0.039
Manganese Sulphate Baths:		
Bozorgmanesh[17]		3.744±0.023
Axton et al.[8,45]	3.728±0.019	3.737±0.020
De Volpi and Porges[49,50]	3.729±0.015	3.729±0.017

The most important question to decide is whether the weighted error represents the true error of the summed eight measurements, or whether there is any evidence within the final numbers for a possible experiment-dependent systematic error. Of the eight measurements, only that from Asplund-Nilsson et al.[2] lies more than one standard deviation from the mean and certainly the external error of ±0.006 is less than the internal error. The weighted average of the three liquid scintillator measurements is 3.763±0.014 which is approximately one and a half standard deviations of the comparison displaced from the average of the three manganese sulphate bath measurements [3.735±0.011]. Alternatively, the average of the four gated measurements, 3.754±0.010, compares satisfactorily with the four source measurements. Thus any suggestion in the original data of an experiment dependent systematic error has now disappeared. Therefore it is considered that the error of ±0.010 represents a legitimate estimate of the accuracy of the standard.

The recommended value for the total neutron emission from the spontaneous fission of ^{252}Cf is 3.745±0.010

3. The $\bar{\nu}$ Ratios

Most previous reviews of the ratios of neutron emission for neutron fission of ^{233}U, ^{235}U, ^{239}Pu and ^{241}Pu to that for the standard, spontaneous fission of ^{252}Cf, e.g. refs. 6 and 16) have concluded that the different measurements were in satisfactory agreement. However, it will always be necessary to effect those small revisions that become apparent with the general improvement in nuclear data.

The principal revisions made in this paper include those for improvements in the measured fission neutron spectra (Table 1) and in the delayed gamma ray from fission data (Table 2). The correction, considered for the standard, to account for variation in the neutron capture detection efficiency with emitted neutron source energy can be safely ignored as it will be at least an order of magnitude smaller here (i.e. $\leq$0.01%).

A new correction that must be considered for all of the $\bar{\nu}$ ratio measurements arises from the resonance dependence of $\bar{\nu}$. None of the measurements that are generally included in the evaluation of the $\bar{\nu}$ ratios were made with monoenergetic neutrons and thus the measured value has some small sensitivity to the exact shape of the incident neutron spectrum. Since the existing experimental data on the resonance dependence of $\bar{\nu}$ is neither complete for the four important isotopes nor always consistent, a brief review is included here of the data and the likely character of the effects which are contributing to the variation.

Resonance Dependence of $\bar{\nu}$

Work on the resonance dependence of $\bar{\nu}$ was stimulated by the conflicting evidence presented at the second IAEA Symposium on the Physics and Chemistry of Fission. For the neutron fission of ^{239}Pu, Weinstein et al.[52] found that $\bar{\nu}$ values for 20 resolved resonances below 100 eV fell into two groups strongly correlated with the resonance spin. The average value of $\bar{\nu}$ for resonances with spin J = 0 was 3% higher than the average for resonances with spin J = 1. A smaller resonance effect was noted for ^{235}U. Ryabov et al.[53] observed the opposite effect. For resonances in ^{239}Pu they found $\bar{\nu}$ for J = 1 resonances was 5% larger than that for J = 0 resonances. A subsequent experiment by Weston and Todd[54] confirmed neither experiment. They found that $\bar{\nu}$ for the two spin classes was similar within $^1/_4$%. However, they observed a fluctuation in the different $\bar{\nu}$ values outside the statistical accuracy of the measurements. Two later measurements[55,56] in substantial agreement with ref. 54) gave rise to an explanation[57] of most of the fluctuations in $\bar{\nu}$ values in terms of the (n,γf) process. Essentially, they found that the $\bar{\nu}$ values for the ^{239}Pu resonances were inversely correlated with the fission widths. Fairly clearly, $\bar{\nu}$ is smaller for the (n,γf) reaction than for direct fission. Furthermore, because the (n,γf) process is a multichannel process, its width is fairly constant. Thus $\bar{\nu}$ for resonances with small fission widths should also be small because of the increased relative importance in these cases of the (n,γf) process.

The relevance of the resonance energy dependence of $\bar{\nu}$ to the evaluation of the thermal value will be apparent from Fig. 2 from Leonard[58] where the $\bar{\nu}$ energy dependence near thermal neutron energies has been plotted from the data of refs. 52,59-61). The resonance at 0.296 eV has a considerable impact on the energy dependence. The value of $\bar{\nu}$ for this resonance is approximately 0.029 neutrons less than that for thermal fission. From the data in ref. 56), 0.011 of this depression can be expected because of the (n,γf) process. The remainder, 0.018, is similar in magnitude to the difference, 0.014±0.007, found by Frehaut and Shackleton[56] for the difference in $\bar{\nu}$ for $J = 0^+$ and $J = 1^+$ resonances with the effects of the (n,γf) process removed.

Two effects can be expected to contribute to this difference. Cowan et al.[62] have shown that the symmetric fission yields for $J = 1^+$ resonances are about $^1/_3$ those for $J = 0^+$. Since symmetric fission fragments emit more neutrons[24], $\bar{\nu}$ for $J = 0^+$ resonances should be larger than that for $J = 1^+$. However, this effect is likely to be extremely small. For ^{235}U, Howe et al.[63] have found no correlation between resonance $\bar{\nu}$ values and the measured mass asymmetry[61]. A second contribution arises because of the considerable difference in the fission barrier for $J = 0^+$ compound states relative to that for $J = 1^+$ states. It has been shown that the fine structure in the $\bar{\nu}_p(E_n)$ dependence between 0-1 MeV for neutron fission of ^{233}U[64] can be explained if the collective energy at the fission saddle point is weakly coupled to the nuclear degrees of freedom at scission, and appears predominantly in the fission fragment kinetic energies. The fission barrier for $J = 1^+$ compound states ($K\pi = 1^+$) is displaced by at least 1.2 MeV with respect to the ground state fission band ($K\pi = 0^+$). Thus one might expect the average total fission fragment kinetic energy for the fission of a $J = 1^+$ compound state to be as much as 1.2 MeV larger than that for the fission of a $J = 0^+$ compound state. From energy conservation, this is equivalent to a difference of approximately 0.15 neutrons. In fact, the measured effect is very much less than this. The reduction is readily explained. The measurements of Bach et al.[65] have shown that the inner peak of the fission barrier is the higher for the ^{240}Pu compound nucleus. Thus the difference in the average collective energy for the two J states is a property of the first barrier. It is well established that mixing of K states occurs in crossing the intermediate well and the outer peak of the fission barrier[66]. Thus only a small component of the original effect survives.

Possible resonance effects can now be evaluated for neutron fission of the other fissile nuclei. For ^{233}U, the (n,γf) process should have a width similar to that in the neutron fission of ^{239}Pu. Here, however, there are fully open fission channels for both $J = 2^+$ and $J = 3^+$ compound states and the (n,γf) process for both spin populations is only a minor effect. Similarly, it can be expected that any effect caused by the variation in the mass distribution is extremely small. However, using the data of ref. 64) it can be shown that $\bar{\nu}(J = 2^+)-\bar{\nu}(J = 3^+)$ should be approximately 0.009. Thus it is expected that there should be a difference of $\lesssim$0.0045 between $\bar{\nu}$ at 0.0253 eV and that for the resonance at 0.19 eV where the spin has not been identified.

For the neutron fission of ^{235}U, the fission barrier for both the 3^- and 4^- spin states is considerably higher relative to the neutron binding energy than that for neutron fission of either ^{233}U or ^{239}Pu. Thus on these grounds alone, the width for the (n,γf) process is extremely small. As indicated previously, Howe et al.[63] have shown that $\bar{\nu}$ is also uncorrelated with the resonance mass asymmetry. The data from ref. 64) can also be used to show that collective effects give rise to a difference in $\bar{\nu}$ for the two spin states of less than 0.001.

Similar arguments can be used to show that resonance effects in $\bar{\nu}$ for neutron fission of ^{241}Pu are also very small, in agreement with the experimental data from Simon and Frehaut[67]. Thus the only case where care must be exercised is in the evaluation of $\bar{\nu}$ for thermal neutron fission of ^{239}Pu.

$\bar{\nu}$ Ratios

In the consideration of the $\bar{\nu}$ values for thermal neutron fission there are a number of different approaches that may be adopted. In all cases, the values have been measured relative to ^{252}Cf, but for a number of experiments, e.g. 1 and 7) in particular, it is possible to eliminate the standard altogether and refer the neutron counting rate for thermal fission directly to the absolute calibration. This procedure has been adopted in the past because of the apparent disagreement between different absolute measurements for ^{252}Cf. However, since the revised $\bar{\nu}$ data for ^{252}Cf show a very acceptable level of consistency, it is more appropriate to evaluate the ratios and refer these values to the average experimental value of $\bar{\nu}$ for ^{252}Cf. A brief discussion follows of the corrections that have been made for specific experiments.

Boldeman and Dalton[68)]

The adjustments applied to the measured $\bar{\nu}$ ratios are listed in Table 9. For the evaluation of the delayed gamma ray correction, the measured delay of 585 ns between the fission event and the opening of the neutron counting gate was used. The listed delayed gamma ray corrections are those relative to the correction for ^{252}Cf. The correction for the resonance dependence of $\bar{\nu}$ corrects the measured result to the equivalent 2200 ms^{-1} value. For the only case where this correction was necessary, neutron fission of ^{239}Pu, the correction was based on the data of Fig. 2 and a calculated neutron leakage spectrum from a well thermalised graphite system at 300 K. The estimated correction is +0.10%.

TABLE 9

REVISION OF $\bar{\nu}_p$ RATIOS

		^{233}U	^{235}U	^{239}Pu	^{241}Pu
Boldeman and Dalton[68)]					
Fission spectra	(%)	+0.27	+0.21	+0.21	+0.21
Delayed γ-rays	(%)	-0.16	-0.16	-0.43	-0.43
Resonance dependence	(%)			+0.10	
Mather et al.[69,70)]					
Fission spectra	(%)	-0.04	-0.12	+0.01	
Delayed γ-rays	(%)	-0.20	-0.20	-0.54	
Colvin and Sowerby[1)]					
Fission spectra	(%)	-0.06	-0.06	-0.03	-0.03
Resonance dependence	(%)			+0.10	
Condé[71)]					
Fission spectra	(%)		+0.06		
Delayed γ-rays	(%)		-0.25		
Hopkins and Diven[3)]					
Fission spectra	(%)	-0.08	-0.10		
Delayed γ-rays	(%)	-0.10	-0.10	-0.30	

Mather et al.[69,70)]

The liquid scintillator used in these experiments was identical with that of ref. 7). The adjustments for the fission neutron spectra differences were based on the data from this experiment. There is not sufficient data in the original papers to make an accurate estimate of the contribution of the delayed gamma rays from fission. However, the correction will be slightly larger than that for ref. 7) because of the earlier (undefined) opening of the neutron counting gate. Corrections 1.25 times those applied for ref.68) have been used. The corrections are listed in Table 9.

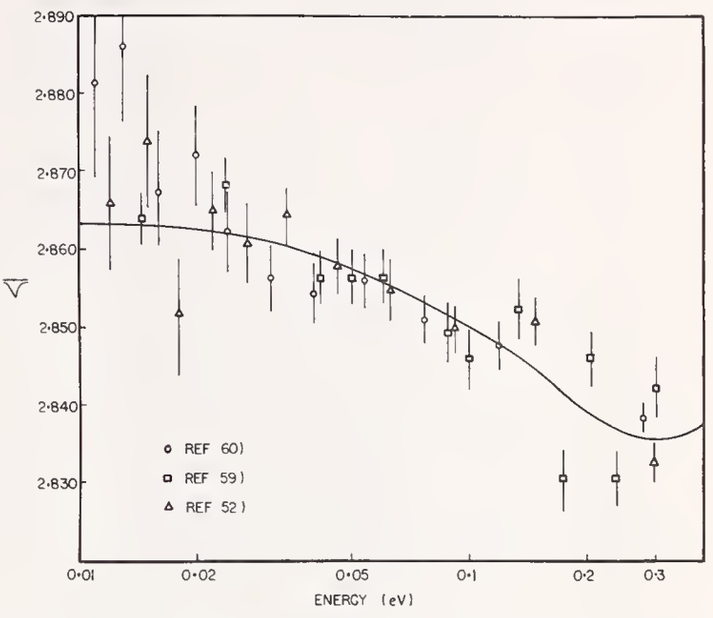

Fig. 2: Energy dependence of $\bar{\nu}$ for ^{239}Pu from Leonard[58)]

Colvin and Sowerby[1)]

A very small correction for fission neutron spectra differences is necessary if the Ullo efficiency curve is used. The thermal $\bar{\nu}$ measurements were made using a beam of thermal neutrons from GLEEP. For ^{239}Pu an identical correction to that applied in ref. 68) has been used for the resonance variation of $\bar{\nu}$.

Condé[71)]

The fission neutron spectra difference correction has been revised using the calculated energy dependence referred to in the section dealing with the absolute measurement of Asplund-Nilsson[2)]. The delayed gamma ray correction is also based on the data from this section.

Hopkins and Diven[3)]

The adjustments applied in this experiment for fission spectra differences were based on the assumption that the original corrections were derived using the fission neutron spectra measurements of Bonner[35)]. The thermal neutron measurements were made using a 400 keV neutron beam moderated by a polyethylene plug in the neutron collimator. A correction was applied for fission by neutrons above a cadmium filter cut-off. The correction for the resonance dependence of $\bar{\nu}$ is therefore extremely small.

Comparison of Ratios

Table 10 lists the revised ratios from the above experiments. The listed ratios are those for prompt neutron emission. The consistency noted in previous evaluations still exists and there is no evidence within the sets to suggest any systematic error.

4. Recommended Values

Table 11 lists the recommended values and their errors from the revision above. The delayed neutron components have been taken from Lemmel[16)]. The conclusion to be drawn from this review of existing $\bar{\nu}$ data is that there is no evidence within the data of any significant systematic error.

TABLE 10

$\bar{\nu}_p$ RATIOS

Experiment	^{233}U	^{235}U	^{239}Pu	^{241}Pu
Boldeman and Dalton[68]	0.6593±0.0015	0.6388±0.0012	0.7662±0.0021	0.7771±0.0019
Mather et al.[69,70]	0.668 ±0.008	0.6357±0.0032	0.771 ±0.009	
Colvin and Sowerby[1]	0.6547±0.0039	0.6392±0.0029	0.7598±0.0051	0.7746±0.0071
Condé[71]		0.6388±0.0053		
Hopkins and Diven[3]	0.6546±0.0058	0.6418±0.0053	0.7485±0.0074	
Average	0.6587±0.0013	0.6386±0.0010	0.7647±0.0018	0.7769±0.0018

TABLE 11

RECOMMENDED $\bar{\nu}$ VALUES

Isotope	$\bar{\nu}_p$	$\bar{\nu}$
^{233}U	2.461±0.008	2.468±0.008
^{235}U	2.386±0.007	2.402±0.007
^{239}Pu	2.857±0.010	2.863±0.010
^{241}Pu	2.902±0.010	2.918±0.010
^{252}Cf	3.736±0.010	3.745±0.010

Acknowledgements

I wish to acknowledge the contributions to this report of many authors too numerous to mention. I am particularly indebted to J. J. Ullo, B. R. Leonard Jr., E. J. Axton and J. R. Smith for permission to use unpublished data.

References

1) D. W. Colvin and M. G. Sowerby, Proc. IAEA Symp. Physics and Chemistry of Fission, Salzburg (1965) Vol. 2, p. 25.

2) I. Asplund-Nilsson, H. Condé and N. Starfelt, Nucl. Sci. and Eng. 16 (1963) 124.

3) J. C. Hopkins and B. C. Diven, Nucl. Phys. 48 (1963) 433.

4) A. De Volpi and K. G. Porges, Phys. Rev. C1 (1970) 683.

5) E. J. Axton, A. G. Bardell and B. N. Audric, J. Nucl. Energy A/B 23 (1969) 457.

6) G. C. Hanna, C. H. Westcott, H. D. Lemmel, B. R. Leonard Jr., J. S. Story and P. M. Attree, Atomic Energy Review 7 (1969) No. 4, p. 3.

7) J. W. Boldeman, Nucl. Sci. and Eng. 55 (1974) 188.

8) E. J. Axton, Proc. IAEA Panel Neutron Standard Reference Data, Vienna (1972) p. 261.

9) J. R. Smith, Proc. Conf. Nuclear Cross Sections and Technology, Washington (1975) Vol. 1, p. 262.

10) J. A. Mitchell and G. J. Emert, Proc. 3rd Conf. Neutron Cross Sections and Technology, Knoxville (1971), Vol. 2, p. 605.

11) J. J. Ullo and M. Goldsmith, Nucl. Sci. and Eng. 60 (1976) 239.

12) M. Goldsmith and J. J. Ullo, Nucl. Sci. and Eng. 60 (1976) 251.

13) J. R. Smith, S. D. Reeder and R. G. Fluharty (1966) Phillips Petroleum IDO-17083.

14) R. L. Macklin, G. de Saussure, J. D. Kington and W. S. Lyon, Nucl. Sci. and Eng. 8 (1960) 210.

15) B. R. Leonard Jr., Proc. Conf. Nuclear Cross Sections and Technology, Washington (1975) Vol. 1, p. 281.

16) H. D. Lemmel, Proc. Conf. Nuclear Cross Sections and Technology, Washington (1975) Vol. 1, 286.

17) H. Bozorgmanesh, private communication to B. R. Leonard Jr.

18) R. R. Spencer, private communication.

19) R. Gwin, private communication.

20) B. C. Diven, H. C. Marlin, R. F. Taschek and J. Terrell, Phys. Rev. 101 (1956) 1012.

21) P. I. Johansson, these proceedings.

22) J. M. Adams, NEANDC(E)-172, (1976).

23) A. B. Smith, Proc. Meeting Prompt Fission Neutron Spectra, Vienna (1971) p. 3.

24) J. Terrell, Symp. Physics and Chemistry of Fission, Salzburg (1965) Vol. 2, p. 3.

25) F. W. Guy, Laurence Radiation Laboratory report, UCRL-50810 (1970).

26) N. N. Ajitanand, Nucl. Phys. 164 (1971) 300.

27) R. B. Walton and R. E. Sund, Phys. Rev. 178 (1969) 1894.

28) J. W. Grüter, K. Sisternick, P. Armbruster, J. Eidens and H. Lawn, Phys. Rev. Lett. 33B (1970) 474.

29) J. P. Unik, J. E. Gindler, L. E. Glendenin, K. F. Flynn, A. Gorski and R. K. Sjoblom, Proc. 3rd. IAEA Symp. Physics and Chemistry of Fission, Vienna (1973) Vol. 2, p. 19.

30) J. Poitou and C. Signarbieux, Nucl. Instr. and Methods 114 (1974) 113.

31) J. J. Ullo, Bettis Atomic Power Laboratory report WAPD-TM-1232 (1976).

32) H. Condé, J. Hansén and L. Widén, Proc. Conf. Neutron Standards and Flux Normalisation, Argonne (1970) 481.

33) M. Soleilhac et al. - refer D. W. Colvin, Proc. Conf. Neutron Data for Reactors, Helsinki (1970) Vol. 2, p. 195.

34) H. Condé, Proc. Panel Neutron Standard Reference Data, Vienna (1972) p. 277.

35) T. M. Bonner, Nucl. Phys. 23 (1961) 116.

36) E. Pendlebury, private communication to Colvin and Sowerby[1]

37) D. W. Colvin, M. G. Sowerby and R. I. MacDonald, Proc. Conf. Nuclear Data for Reactors, Paris (1966) Vol. 1, p. 307.

38) E. J. Axton, private communication to Colvin et al.[37)]

39) M. G. Sowerby, private communication.

40) J. J. Ullo, private communication.

41) P. Fieldhouse, E. R. Culliford, D. S. Mather, D. W. Colvin, R. I. MacDonald and M. G. Sowerby, J. Nucl. Energy A/B 20 (1966) 549.

42) P. Fieldhouse, E. R. Culliford and D. S. Mather, (1966), private communication to 37).

43) E. J. Axton, Proc. this conference.

44) E. J. Axton, P. Cross and J. C. Robertson, J. Nucl. Energy A/B 19 (1965) 409.

45) P. White and E. J. Axton, J. Nucl. Energy 22 (1968) 73.

46) A. Moat, D. S. Mather and M. H. McTaggart, J. Nucl. Energy A/B 15 (1961) 102.

47) J. R. Smith, S. D. Reeder, B. M. Cawsey and V. Spiegel, private communication.

48) J. R. Bird, B. J. Allen, J. W. Boldeman, M. J. Kenny and A. R. de L. Musgrove, Proc. Int. Conf. Interaction of Neutrons with Nuclei, Lowell (1976) Vol. 1, p. 77.

49) A. De Volpi and K. G. Porges, Metrologia 5 (1969) 128.

50) A. De Volpi, J. Nucl. Energy 26 (1972) 75.

51) W. F. Hornyak, Rev. Sci. Instr. 23 (1952) 264.

52) S. Weinstein, R. L. Reed and R. C. Block, Proc. 2nd IAEA Symp. Physics and Chemistry of Fission, Vienna (1969) p. 447.

53) Yu. V. Ryabov, So Don Sirk, N. Chikov and N. Yaneva, Sov. J. Nucl. Phys. 14 (1972) 519.

54) L. W. Weston and J. H. Todd, Proc. 3rd Conf. Neutron Cross Sections and Technology, Knoxville (1971) Vol. 2, p. 861.

55) D. Shackleton, J. Trochon, J. Frehaut and M. Le Baro, Phys. Lett. 42B (1972) 344.

56) J. Frehaut and D. Shackleton, Proc. 3rd IAEA Symp. Physics and Chemistry of Fission, Vienna (1972) Vol. 2, p. 201.

57) Yu. V. Ryabov, J. Trochon, D. Shackleton and J. Frehaut, Nucl. Phys. A216 (1973) 395.

58) B. R. Leonard Jr. (1976), private communication.

59) B. R. Leonard Jr., E. J. Seppi and W. J. Friesen, HW-4344.

60) R. W. Hockenbury, private communication to B. R. Leonard Jr.

61) R. Gwin, R. Ingle, R. R. Spencer, J. H. Todd and L. W. Weston, private communication to B. R. Leonard Jr.

62) G. A. Cowan, B. P. Bayhurst, R. J. Prestwood, J. S. Gilmore and G. W. Knobeloch, Phys. Rev. 144 (1966) 979.

63) R. E. Howe, T. W. Phillips and C. D. Bowman, Phys. Rev. C13 (1976) 195.

64) J. W. Boldeman, W. K. Bertram and R. L. Walsh, Nucl. Phys. 265 (1976) 337.

65) B. B. Bach, O. Hansen, H. C. Britt and J. D. Garrett, Proc. 3rd IAEA Symp. Physics and Chemistry of Fission, Rochester (1973) Vol. 1, p. 25.

66) V. M. Strutinsky and H. C. Pauli, Proc. 2nd IAEA Symp. Physics and Chemistry of Fission, Vienna (1969) p. 155.

67) G. Simon and J. Frehaut, Proc. 3rd National Soviet Conf. Neutron Physics, Kiev (1975) Vol. 5, p. 337.

68) J. W. Boldeman and A. W. Dalton, AAEC/E172 (1967).

69) D. S. Mather, P. Fieldhouse and A. Moat, Phys. Rev. 133 (1964) 1403.

70) D. S. Mather, P. Fieldhouse and A. Moat, Nucl. Phys. 66 (1965) 149.

71) H. Condé, Ark. f. Fysik 29 (1965) 293.

MEASUREMENT OF THE ^{252}Cf SPONTANEOUS FISSION NEUTRON SPECTRUM

M. V. Blinov, V. A. Vitenko, V. T. Touse
V. G. Khlopin Radium Institute
Leningrad, USSR

The neutron energy spectrum of ^{252}Cf spontaneous fission has been measured by the time-of-flight method using two neutron detectors -- a $^{6}LiI(Eu)$ crystal and a fast ionization chamber with ^{235}U layers. The influence of scattered neutrons and fission neutron emission time on the spectrum shape was studied. In the range from 10 keV to 7 MeV, the neutron energy spectrum is satisfactorily described by a Maxwellian distribution within the experimental errors with T = 1.41 ± 0.03 MeV.

(Fission neutron spectrum; neutron detectors; neutron standard; time-of-flight; ^{252}Cf)

Introduction

It is known that the neutron energy spectrum of spontaneous fission of ^{252}Cf has been recommended as a standard. Such important role of this neutron spectrum demands high precision of its shape measurement over the whole energy region from several keV up to 10 - 15 MeV. The experimental data for the energy interval above 1 MeV are in agreement,[1-5] however the measurement accuracy is desired to be improved. As to the neutron energies below 1 MeV, there is a significant difference between the data; the discrepancies between the results attain 30-40% and more.[4-10] That makes much more precise measurements necessary.

The difficulties of measurements in this low energy region are first of all due to the absence of suitable detectors, which could be used in a wide energy region, including the keV range. Plastic and liquid scintillators permit neutron spectra measurements only in a limited part of this region. In the past few years, lithium scintillation glasses have come into use for neutron detection at energies below 1-2 MeV. But they present some serious difficulties in the experiment. Hence we have developed a technique of $^{6}LiI(Eu)$ crystal use for time-of-flight neutron spectrum measurements. This crystal was used earlier as a neutron detector in experiments which did not demand high time resolution. The ionization chamber with ^{235}U layers is a neutron detector with smooth spectral efficiency and practically unlimited energy sensitivity region. In order to use it in this experiment, it was necessary to solve the problem of ensuring the necessary efficiency and high time resolution simultaneously. Such a chamber has not yet been used for fission neutron spectrum measurements.

In this report we present the results of ^{252}Cf fission neutron spectrum measurements, done by time-of-flight method using a $^{6}LiI(Eu)$ crystal, and also the preliminary data on spectrum shape, which was measured with a multiplate ^{235}U ionization chamber. Thus, we have used two detectors, which detect neutrons by means of $^{6}Li(n,\alpha)$ and $^{235}U(n,f)$ reactions. Both reactions are standards.

Experimental

Method and Instrumentation

The time-of-flight method was chosen, since at present it gives the highest accuracy in neutron energy measurements.

The fragments of ^{252}Cf spontaneous fission were detected by a gas scintillation counter or by a fast ionization chamber. Californium layers were deposited on platinum backings 0.2 mm thick; 0.3 x 10^5, 0.6 x 10^5 and 1.2 x 10^5 fissions per second occurred in the layers. A $^{6}LiI(Eu)$ crystal was used for neutron detection below 2 MeV. This crystal was chosen because of its higher γ-equivalent in comparison with that for lithium glass (3.5 MeV as compared to 0.8 MeV). This reduces considerably the danger of spectrum distortion due to γ-quanta detection. Besides, the lithium glasses contain large amounts of oxygen and silicon, total neutron cross sections of which exhibit large resonances. The main difficulty of the work with lithium crystals is their large decay time (about 1.2 microseconds), which even at their high light yield, leads to the emission of a small number of photons per nanosecond time interval. Thus, it was necessary to select crystals according to their light output and photomultipliers according to their quantum yield of photocathode. In order to obtain a high time resolution, the electronics were constructed, taking into account the specifics of light emission features of $^{6}LiI(Eu)$ crystal. A short description of the procedure for the use of this crystal in a time-of-flight spectrometer was given in our publication.[11] The time resolution of 1.5 ns was obtained for low-energy neutrons. It must be noted, though, that the large decay time of the crystal in case of insufficient quality of electronics adjustment may lead to the erroneous spectrum -- intensity rise for low neutron energies. The correct adjustment was controlled by the symmetry of a gamma peak.

The second detector was the fission chamber. Its low efficiency requires the use of multilayer construction. In our chamber ten layers of uranous-uranic oxide (^{235}U), 10 cm in diameter and deposited on both sides of the electrodes were mounted (the total ^{235}U amount was 1.5 grams). The distance between electrodes was 3 mm. The chamber was filled with methane to atmospheric pressure. All the chamber electrodes were connected to the same fast current amplifier. The time resolution of the spectrometer with this chamber was about 2 ns.

Investigation of the Effects Caused by Scattered Neutrons

Scattered neutrons usually cause considerable difficulties at low neutron energies, when continuous neutron spectra are being measured. We paid special attention to this problem and made several control experimental setups. At first we tried fission fragment detectors and neutron detectors of the types currently used in similar experiments. We found the scattering effects were rather large, which could give a neutron intensity increase at the low energy part of the spectra about 30-50% or more. Then we measured neutron spectra, using detector setups of different weight. The constructions, which caused no noticeable spectrum deformation within experimental errors, were chosen in that way. Two spectra, which show the detector scattering mass influence on the spectrum shape, are presented in Fig. 1.

The gas counter after several modifications was made of a steel tube (diameter 40 mm, wall thickness

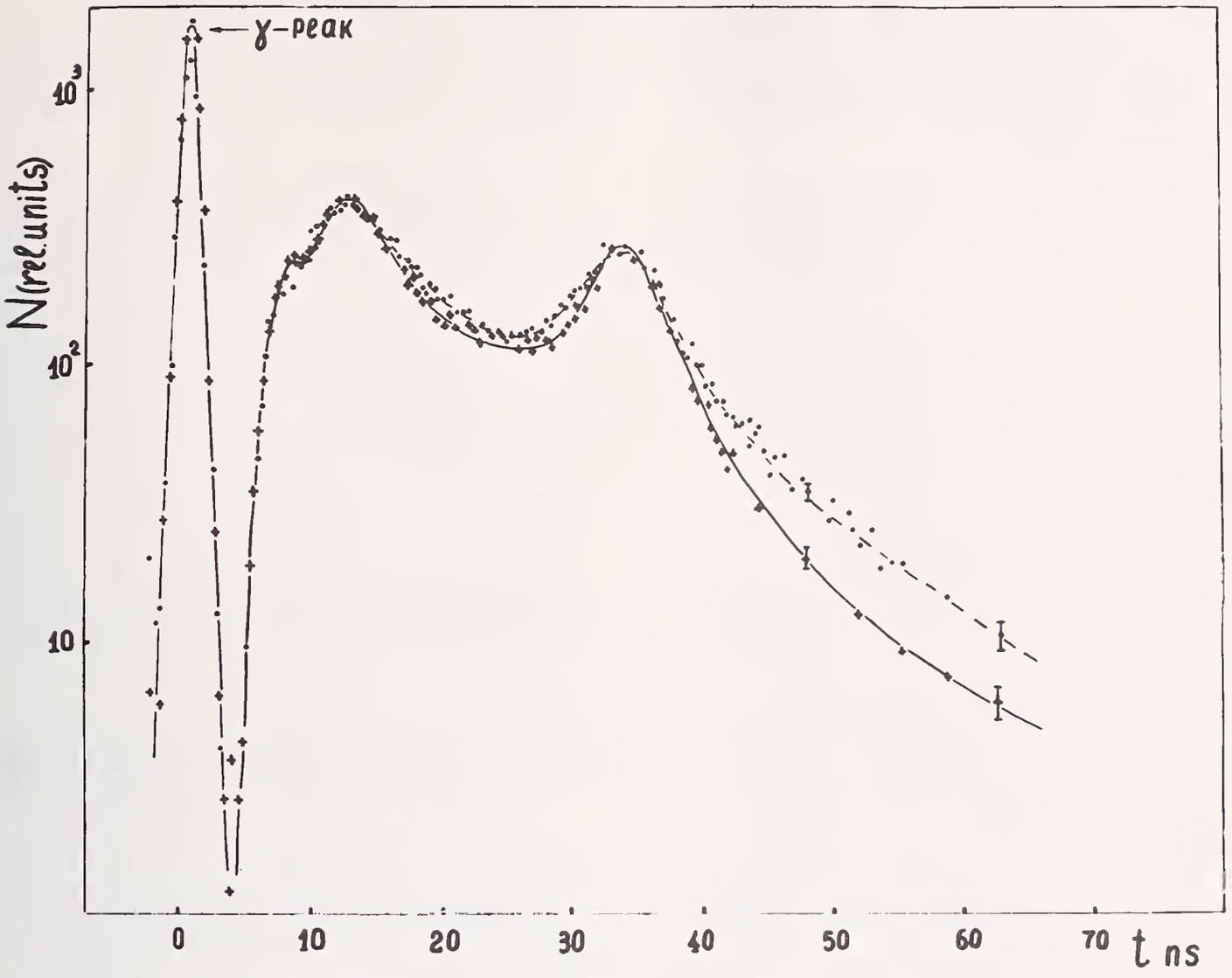

Figure 1. Time-of-flight spectra of ^{252}Cf neutrons, measured with the $^{6}LiI(Eu)$ crystal on 25 cm flight path in two different setups: (o) - Setup with usual neutron scattering probability (the gas counter with quartz window, the californium layer 6 cm from the window, model 30 PMT in the neutron detector). (+) - The modified setup with significantly lower neutron scattering probability (the gas counter without a quartz window, the californium layer 15 cm from the photocathode, model 71 miniature PMT in the neutron detector).

0.2 mm, length 150 mm) without the usual quartz window. It was mounted directly on the photomultiplier (PMT). The californium layer was placed at the far end of the tube.

The scattering effects of PMT mass and of crystal protective capsule were observed for $^{6}LiI(Eu)$ detector. Multiple scattering in the crystal more than 6 mm thick caused a noticeable change in spectrum shape. For measurements a crystal 4 mm thick and 15 mm in diameter was used. It was glued directly to a miniature model 71 PMT. The crystal container was made of aluminum 0.5 mm thick. The last modification of multilayer uranium chamber was made of a brass foil 0.2 mm thick. Uranium was deposited on thin nickel foil.

The measurements taken to decrease (or remove) the scattering masses of neutron and fission fragment detectors permitted a decrease in scattering effects (more than 10 times in comparison with currently used experimental setups).

On Fission Neutron Emission Time

In ^{252}Cf fission neutron spectrum measurements, it is necessary to take into account the neutron emission time in case it is more than 1×10^{-14} second. Such intervals between fission events and the emission of some part of the neutrons are possible because of large fission fragment angular momentum. A time interval of 10^{-13} to 10^{-14} sec is large enough to allow the fragment to slow down noticeably in the backing, on which the californium layer is deposited. In such a case the energies of neutrons, emitted by a slowed-down and by a free-moving fragment, may differ considerably. Due to this fact the backing material and thickness may influence the spectrum shape. In Refs. 12 and 13 it has been shown that the upper limit of neutron emission time in ^{235}U fission induced by thermal neutrons is about 4×10^{-14} to 10^{-13} seconds. But in the case of the ^{252}Cf spectrum shape measurement, which must be used as a standard, a much more accurate determination of emission time must be made, to permit a clearer interpretation of results.

We made a precise comparison of fission spectra of neutrons, which were emitted by fragments, moving in vacuum and in a dense medium.[14] The measurements were made in wide neutron energy region from 20 keV to 7 MeV. It was found that spontaneous fission neutrons are emitted earlier than 1×10^{-14} sec after fission event. The neutrons emitted about 10^{-13} sec and more after fission event are less than 2 to 3% from the total number of neutrons.

Neutron Spectra Measurements

^{252}Cf fission neutron spectra were measured at flight distances of 12.5, 25, 37.5 and 50 cm with a $^{6}LiI(Eu)$ crystal and at 25 and 50 cm with a uranium chamber.

The results obtained at four flight distances with a lithium crystal were compared and found to be identical within the experimental errors. A small discrepancy was observed only in the region of the 240-keV peak, especially for 12.5 cm flight path, due to the influence of energy resolution. These data contradict the results of the work,[9] where it was found that the neutron spectra for various flight distances differ significantly in the low energy part of the spectra. The authors of Ref. 9 came to the conclusion that below 1 MeV a considerable yield of neutrons with emission times 10^{-9} to 10^{-7} sec exists, and that at 100 keV the yield of degraded neutrons is comparable to the yield of prompt ones. Our experiments[15] did not lead to such a conclusion even at 10% level of the value, published by the authors of Ref. 9. Fig. 2 shows the experimental time-of-flight distribution, obtained with $^{6}LiI(Eu)$ crystal, measured in one of the runs with a 25 cm flight path. It can be seen that for a 25 cm path a complete separation of the gamma-peak from neutron distribution is observed, the gamma-peak full width being 1.2 ns at half maximum and 5 ns at 0.1% of its height. This is evidence of the absence of any "tailing" effects of the gamma-peak in the region of neutron flight times. The intensity ratio of the 240-keV peak to the valley between the peak and the rest of the neutron distribution was 2.4 to 2.5, which also characterizes the time resolution obtained. In Refs. 8 and 16 "fine structure" of the ^{252}Cf fission neutron spectra was reported for a wide energy region. We did not find it below 1 MeV in this experiment, and also in the measurements with stylbene crystal for neutron energies between 1 and 5 MeV.

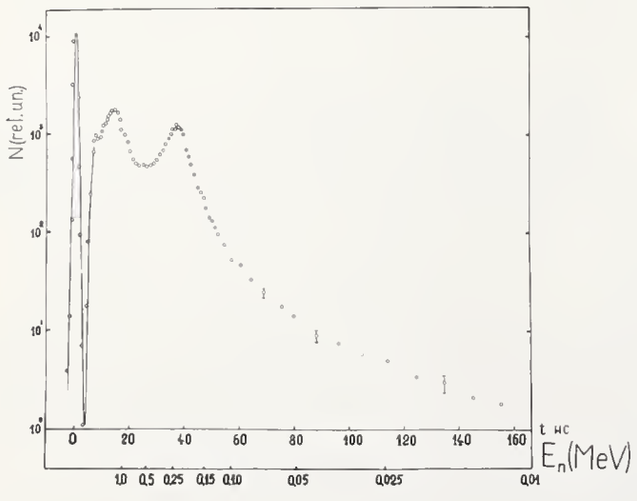

Figure 2. Time-of-flight ^{252}Cf fission neutron spectrum [$^{6}LiI(Eu)$ neutron detector, flight path 25 cm].

To determine the influence of iodine and of ^{7}Li, which were present in our detector, and also the influence of our crystal capsule, the same measurements were repeated with a $^{7}LiI(Eu)$ crystal of the same size and light output. The background was found to be 3% for 1 MeV, 2% for 0.5 MeV and 0.3% for 0.25 MeV. Measurement runs with $^{6}LiI(Eu)$ were done round-the-clock for one month and for 15 days with a uranium chamber.

Discussion of Experimental Results

Fig. 3 presents the energy spectrum of neutrons from ^{252}Cf fission, which was measured by us with $^{6}LiI(Eu)$ crystal.

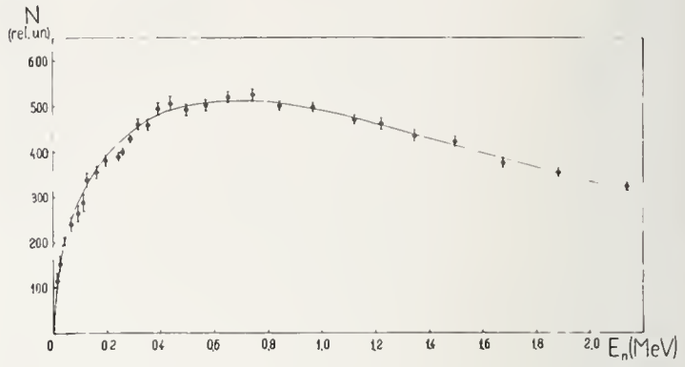

Figure 3. Energy spectrum of ^{252}Cf fission neutrons (o) - Data obtained with $^{6}LiI(Eu)$ detector at 12.5, 25 and 37.5 cm flight paths. The smooth curve is a Maxwellian distribution with T = 1.38 MeV. The errors plotted are statistical, only.

In calculating crystal efficiency we used the estimated values of the $^{6}Li(n,\alpha)$ cross sections from the ENDF/B-IV file. No correction was made for multiple scattering in the crystal. In Fig. 3 a Maxwell distribution curve for T = 1.38 MeV is also plotted. The experimental points lie within ±5% from this curve. Taking into account the errors in the $^{6}Li(n,\alpha)$ reaction cross sections, one should note that there is satisfactory agreement between the Maxwell distribution and the experimental data.

Our preliminary data,[10] after correction for new values of cross sections, agree with the present data within the experimental errors. Further precision spectrum measurements using the $^{6}Li(n,\alpha)$ reaction depend greatly on more accurate cross section data for this reaction.

In the calculation of the spectra, obtained with the uranium chamber, we used the estimated fission cross section for ^{235}U from Ref. 17. The energy spectrum measured in this way is presented in Fig. 4. The results of these preliminary measurements in a wide energy interval can be approximated by a Maxwell distribution with T = 1.41 ± 0.03 MeV, which is in good agreement with the data obtained by the lithium technique.

Thus, we may say that our experimental data agree in the region above 1 MeV with the data.[2-5] In the low energy region (below 1 MeV) we did not find any noticeable neutron excess over the Maxwellian, which does not confirm earlier Refs. 6, 8, 9 and 18. Considering the importance of knowledge of the precise

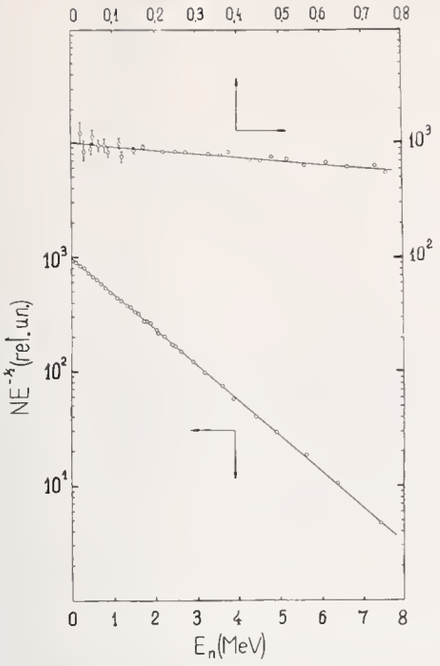

Figure 4. Energy spectrum of ^{252}Cf fission neutrons. Points - experimental data obtained with uranium chamber at flight paths 25 and 50 cm. Continuous line - Maxwellian distribution with T = 1.41 MeV.

shape of the ^{252}Cf spontaneous fission neutron spectrum as an international standard, we plan to continue the measurements of this spectrum with higher accuracy and in a wider energy region.

Along with the measurements of ^{252}Cf fission neutron spectrum at the Radium Institute, the determination of the average number of neutrons per fission, $\bar{\nu}$, is being performed in the spontaneous fission of ^{252}Cf. The work is being done in the laboratory, headed by K. A. Petrzhak.

The method of separate determination of neutron emission rate and fission events of californium source is used. The samples of about 0.5 microgramm ^{252}Cf have been prepared by vacuum evaporation on stainless steel backings. The absolute fission rate is measured by a surface barrier detector with a small level of low energy "tail" of the fission-fragment spectrum in low geometry, the solid angle being calculated. The neutron yield is measured by manganese sulphate bath techniques. The manganese solution is pumped continuously from the spherical tank 1 m in diameter through the counting system. To calibrate the counting system, a $4\pi\beta$-γ-coincidence set-up was made.

At present the value of $\bar{\nu}_t(^{252}Cf) = 3.738$ is obtained with estimated total error about 0.5%. The work is still in progress.

Acknowledgments

The authors wish to thank S. S. Kovalenko and M. A. Bak for discussion of the results, and also O. I. Batenkov, I. T. Krisyuk, N. M. Kazarinov, A. S. Veshchikov, V. I. Yourevich, B. M. Alexandrov, G. G. Verbitskaya for their help at different stages of this work.

References

1. A. B. Smith, Prompt Fission Neutron Spectra (Proc. Conf. Meeting Vienna 1972) IAEA, Vienna (1972), 3.

2. G. V. Kotelnikova, B. D. Kuz'minov, G. N. Lovchikova, O. A. Sal'nikov et al., Neitronnaya fizika (Proc.3rd National Conference on Neutron Physics, Kiev, USSR, 1975) Moskwa (1976), 5, 109.

3. L. Green, I. A. Mitschel, N. N. Steen, Nucl. Sci. Eng. 50 (1973), 257.

4. H. H. Knitter, A. Paulsen, H. Liskien, M. M. Islam, Atomkernenergie 22 (2) (1973), 87.

5. H. Werle, H. Bluhm, I. Nucl. Energy 26 (1972), 165.

6. J. W. Meadows, Phys. Rev. 157 (1967), 1076.

7. L. Eki, D. Kluge, A. Laitaj, P. P. Dyachenko, B. D. Kuz'minov, Atomnaya Energia 33 (1972), 784.

8. Yu. S. Zamyatnin, N. I. Krochkin, A. K. Mel'nikov, V. N. Nefedov, Nucl. Data for Reactors (Proc. Int. Conf. Helsinki 1970) IAEA, Vienna 2 (1970), 183.

9. V. N. Nefedov, B. I. Starostov, Neitronnaya fizika (Proc.2nd Nat. Conf. on Neutron Physics, Kiev, USSR, 1973) Obninsk 4 (1974), 163.

10. O. I. Batenkov, M. V. Blinov, V. A. Vitenko, I. T. Krisjuk, V. T. Touse, Neitronnaya fizika (Proc. 3rd Nat. Conf. on Neutron Physics, Kiev, USSR, 1975) Moskwa 5 (1976), 114.

11. M. V. Blinov, V. A. Vitenko, Nietronnaya fizika (Proc. 3rd Nat. Conf. on Neutron Physics, Kiev, USSR, 1975) Moskwa 6 (1976), 252.

12. Yu. S. Zamyatnin, Phyzika delenia tyazhelykh jader (Fission Physics of Heavy Nuclei) Moskwa (1957), 75.

13. I. S. Fraser, Phys. Rev. 88 (1952), 536.

14. M. V. Blinov, V. A. Vitenko, I. T. Krisjuk, Neitronnaya fizika (Proc.3rd Nat. Conf. on Neutron Physics, Kiev, USSR, 1975) Moskwa 5 (1976), 131.

15. M. V. Blinov, V. A. Vitenko, I. T. Krisjuk, DAN 224 (1975), 802.

16. V. N. Nefedov, Preprint, NIAR (Atomic Reactor Research Institute, Melekess) (1969), 52.

17. G. V. Antsipov, A. R. Benderskii, V. A. Kon'shin et al., Jadernye konstanty (Nuclear constants) 20 (1975), 3.

18. A. M. Andreichuk, V. A. Korostylev, B. G. Basova, V. N. Nefedov et al., Neitronnaya fizika (Proc. 3rd Nat. Conf. on Neutron Physics, Kiev, USSR, 1975) Moskwa 5 (1976), 120.

PROMPT FISSION NEUTRON SPECTRA*,†

Leona Stewart
University of California
Los Alamos Scientific Laboratory
Los Alamos, NM 87545

and

Charles M. Eisenhauer
National Bureau of Standards
Washington, D.C. 20234

Recent measurements of the spectra of prompt neutrons emitted from neutron-induced fission in ^{235}U and ^{239}Pu are reviewed. Results are discussed in terms of departures of the data from a simple Watt representation. An evaluation of the neutron spectrum from neutron-induced fission in ^{235}U and spontaneous fission in ^{252}Cf, made by NBS in 1975, is also reviewed. Recent measurements on the fission spectra of ^{235}U and ^{239}Pu seem to indicate a harder energy spectrum than indicated by the earlier data available for the NBS evaluation. Possible reasons for this trend in the experimental data are discussed.

(Californium-252; Maxwellian spectrum; plutonium-239; prompt fission spectrum; uranium-235; Watt spectrum)

I. Introduction

The prompt neutrons emitted in the fission process have been studied for more than three decades. It is interesting to note, however, that the prompt neutron spectra for many important fissile and fertile isotopes have not been measured and the data available on other isotopes show significant discrepancies. Recent experimental measurements of the spectra of emitted neutrons have reduced some of these discrepancies. However, since experiments have been limited to incident energies of less than 2 MeV, the dependence of the spectra upon incident neutron energy for neutron-induced fission is still virtually unknown, even for ^{235}U and ^{239}Pu.

The differential fission spectrum $\phi_E(E')$, for an incident energy E and final energy E', of neutrons arising from neutron-induced fission has been the subject of many measurements. An alternate approach to obtaining information on the spectrum is that of integral measurements of the form $R(E) = \int \sigma(E')\phi_E(E')dE'$, where $\sigma(E')$ is the cross section for a reaction such as $^{238}U(n,f)$, often used for reactor dosimetry studies.

Apparent discrepancies between differential fission spectral measurements and integral cross sections and/or reaction-rate ratios have existed for several years. These discrepancies were discussed at a Consultants' Meeting[1] in August 1971 and recommendations for measurements were made. In order to better define the differential spectrum $\phi_E(E')$ for neutron-induced fission, a Specialists Meeting[2] was called at Harwell in April 1975 to present and discuss recent experimental data from Cadarache (France), Geel (Belgium), Harwell (United Kingdom) and Studsvik (Sweden) on ^{235}U and ^{239}Pu. These results are described in the next section.

The spectrum of ^{252}Cf fission neutrons is very similar to that for neutron-induced fission of ^{235}U and ^{239}Pu. Furthermore, small near-point sources of ^{252}Cf can be used as absolute flux standards. Therefore, integral detectors with broad energy responses, such as the $^{239}Pu(n,f)$ fission reaction, can be used to relate the flux in a ^{235}U fission environment to an absolute flux determination using a ^{252}Cf fission source.

Historically, both integral and differential measurements predicted a "harder" spectrum, that is, higher average neutron energy, for ^{239}Pu than for ^{235}U. For ^{252}Cf, the spontaneous fission spectrum is even harder than for ^{239}Pu. However, the difference in average energy between ^{235}U and ^{252}Cf is only ~ 5%, and all of the spectrum determinations available today are "similar" in shape. Figure 1 shows a typical time-of-flight spectrum by Johansson[2] for ^{235}U neutron-induced fission. Also shown are best fits of his data to the following forms:

Maxwellian Distribution:

$$\phi_E(E') \sim \sqrt{E'}\, \exp(-E'/T); \qquad \bar{E}' = \frac{3}{2} T$$

Watt Distribution:

$$\phi_E(E') \sim \exp(-AE')\, \sinh(\sqrt{BE'});$$

$$\bar{E}' = \frac{3}{2A} + \frac{B}{4A^2}$$

In general, good fits to either of these analytic functions are obtained from all of the experimental data available, except for small systematic deviations which will be described in more detail in Sections II and III. For more than a decade, however, the Maxwellian with T = 1.29 to 1.30 MeV was most often the recommended representation for low-energy neutron-induced fission on ^{235}U.

A complete review of the measurement and theoretical contributions on fission spectra cannot be given here -- this subject, alone, could command an entire symposium. Instead, only a few of the more recent contributions to the field are discussed.

II. Neutron-Induced Fission: ^{235}U and ^{239}Pu:

Since the Consultants' Meeting[1] on "Prompt Fission Spectra" in 1971, much effort has been expended in studies on the differential and integral spectra for several important nuclei.

---

*Work performed partially under the auspices of the United States Energy Research and Development Administration.

†This paper was presented in place of a paper by P. I. Johansson of Sweden, who was unable to attend the Symposium.

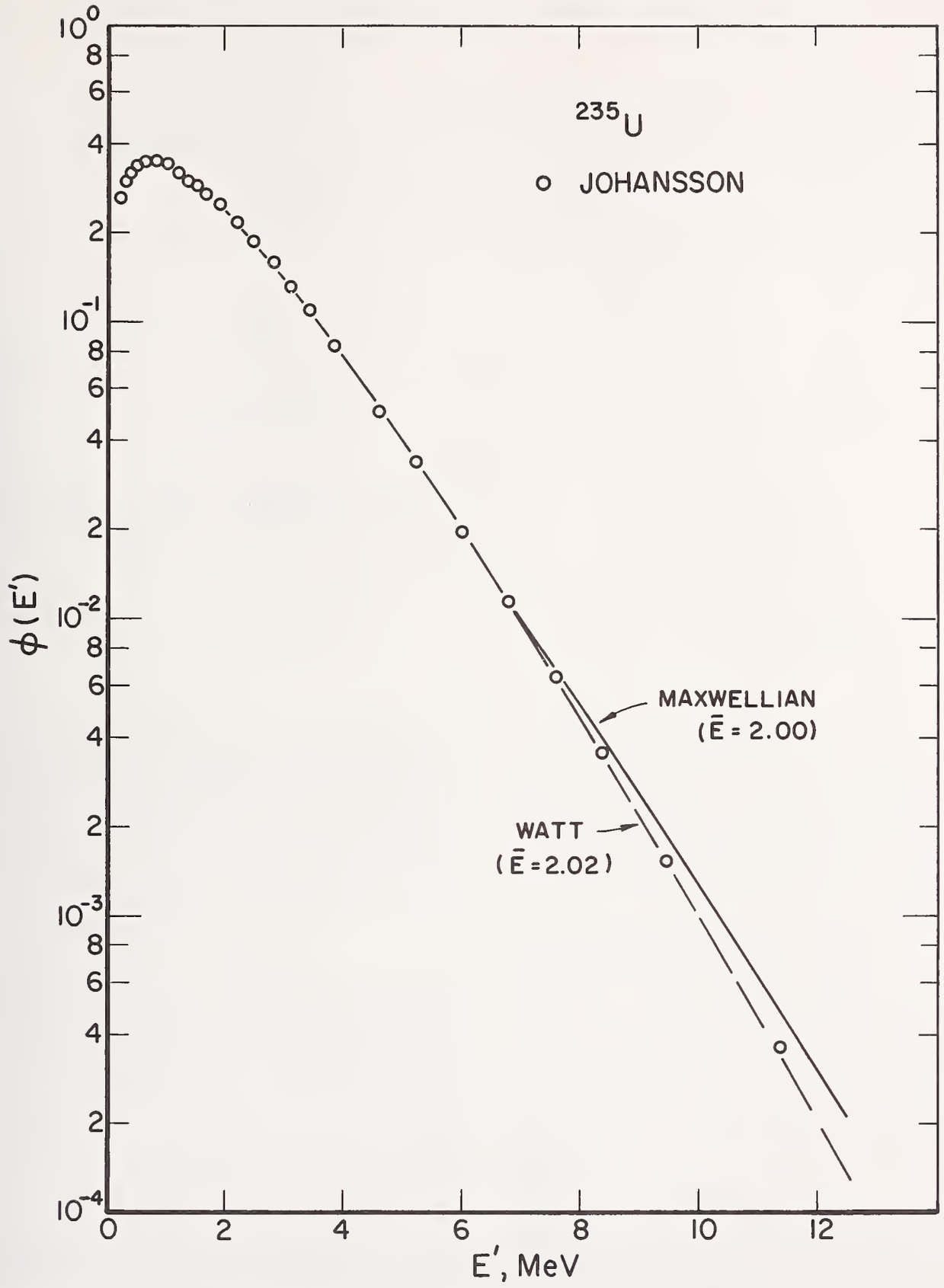

Figure 1. Comparison of Measured and Calculated Spectra of Emitted Neutrons from Neutron-Induced Fission in ^{235}U.

The experiments described at the Specialists Meeting at Harwell are listed in Table I along with other pertinent information. All of the experiments were performed using time-of-flight, and Monte Carlo corrections[3] were applied for scattering and secondary fission in the scattering samples. These corrections, which were not applied in most of the earlier experiments, tend to harden the spectra; that is give a slightly higher average energy. In addition, all but one of the newer measurements record the neutron spectrum out to energies greater than 13 MeV. As a result, the spectrum can now be predicted with more confidence for neutrons emitted with energies up to 10 MeV.

TABLE I. Experimental Data for Neutron-Induced Fission of ^{235}U and ^{239}Pu

Target	Incident Neutron Energy (keV)	No. Pts.	Range of Emitted Neutrons (MeV)	Authors	
^{235}U	10 - 58	96	0.5 - 13.946	D. Abramson C. Lavelaine	Cadarache
	400^{+33}_{-39}	91	0.575 - 6.87	M. M. Islam (Dacca), H. H. Knitter	Geel
	520 ± 20	90	0.625 - 15.629	J. M. Adams P. I. Johansson (Studsvik)	Harwell
	100 180 530 ± 32 2070	62	0.225 - 14.4	P. I. Johansson B. Holmqvist T. Wiedling L. Jeki (Budapest)	Studsvik
^{239}Pu	10 - 58	95	0.55 - 14.253	D. Abramson C. Lavelaine	Cadarache
	215 ± 32	183	0.28 - 13.87	H. -H. Knitter	Geel
	100 180 530 ± 32 2070	60	0.325 - 14.4	P. I. Johansson B. Holmqvist T. Wiedling L. Jeki (Budapest)	Studsvik

Many attempts have been made to obtain analytic representations of the fission spectra in order to satisfy the requests of the reactor designer. The two most often recommended are mentioned in the Introduction, namely the Maxwellian and the Watt distributions. Furthermore, since it is impossible to compare the experiments point-by-point, ratios of the experimental data to analytic expressions permit one to compare trends in the data.

The ^{235}U data shown in Figure 2 are plotted as ratios of the experimental spectra to a Watt distribution with A = 1.0193; B = 2.3075; and $\bar{E}'$ = 2.027 MeV. The ^{239}Pu experimental data are presented in the same manner in Figure 3 with A = 1.0364; B = 2.8728; and $\bar{E}'$ = 2.116 for the Watt distribution. The excess of neutrons below one MeV in the Cadarache results are said to be due to instrumental effects. Figures 2 and 3 were obtained by averaging over groups of emitted neutron energies for each set of data listed in Table I. Data for all incident energies measured by Johansson et al were combined in one set.

It should be noted that the experiments outlined in Table I also included a study of the angular dependence of the fission spectra. For example, the Geel spectra of ^{235}U were observed at 45°, 90°, and 130°. Cadarache made measurements on both ^{235}U and ^{239}Pu with acceptance angles of ± 30° and ± 60°. All other spectra were observed at 90°. These data indicated that the shape of the observed spectra were not dependent upon the angle of the emitted neutrons.

Since the Maxwellian shape has been the recommended distribution for fission-reactor analyses for many years, the Johansson data on ^{235}U were chosen to compare the Watt and Maxwellian parametrizations. The ratios of the experimental points[2] to these analytic representations† are plotted in Figure 4. While the Cadarache and Geel results do not show as clearly the preference for the Watt distribution over the Maxwellian as do the Studsvik (Figure 4) and Harwell data, all of the measurements individually and collectively indicate slightly better agreement with a Watt distribution. Therefore, the Proceedings of the Specialist Meeting[2] include recommended Watt distributions for ^{235}U and ^{239}Pu. Considering these results and recent data on ^{252}Cf, perhaps the Watt distribution should be the recommended parametrization for all important isotopes on ENDF/B.

III. Comparison with NBS Evaluations

In 1975 Grundl and Eisenhauer[4] described their evaluation of differential neutron fission spectra for ^{235}U and ^{252}Cf, based on all available experimental data for these two isotopes. Tabulated data were obtained and least-squares fits were made to a Maxwellian form by consistent procedures for each data set. The goodness-of-fit was generally of the quality of the ^{235}U spectrum shown in Figure 1. However, the average energy deduced for each fit varied by as much as 10% - considerably greater than the quoted uncertainties of less than 5%. The main purpose of the analytic representation was to obtain a consistent procedure for normalizing the data. Reference Maxwellians for ^{235}U and ^{252}Cf were determined from a weighted average of individual data sets for each isotope. Seven energy intervals were chosen and departures of the data from the reference Maxwellian shape were averaged. Uncertainties in the small but systematic

† It is interesting to note that the "best fit" to the Johansson data using the Watt representation gives an average energy of 2.020 MeV while the Maxwellian fit gives 2.001 MeV. These average energies were obtained by fitting over limited energy regions while Johansson obtained the same average energy (2.027 MeV) for both shapes when fits were made over the entire energy range.

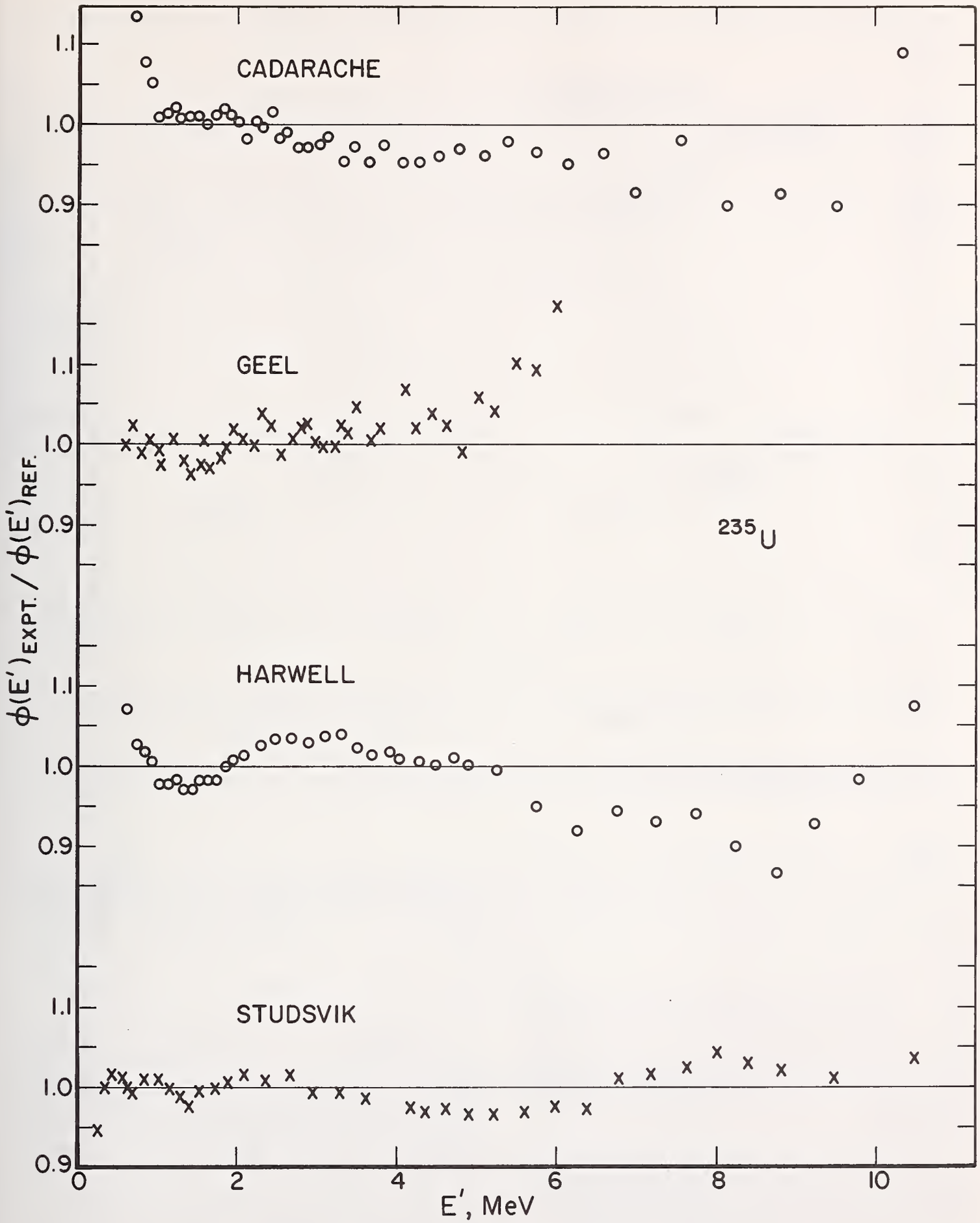

Figure 2. Ratio of Experimental Data for Neutron-Induced Fission in ^{235}U to a Reference Watt Spectrum[2] with A = 1.0193, B = 2.3075 and $\bar{E}'$ = 2.027 MeV.

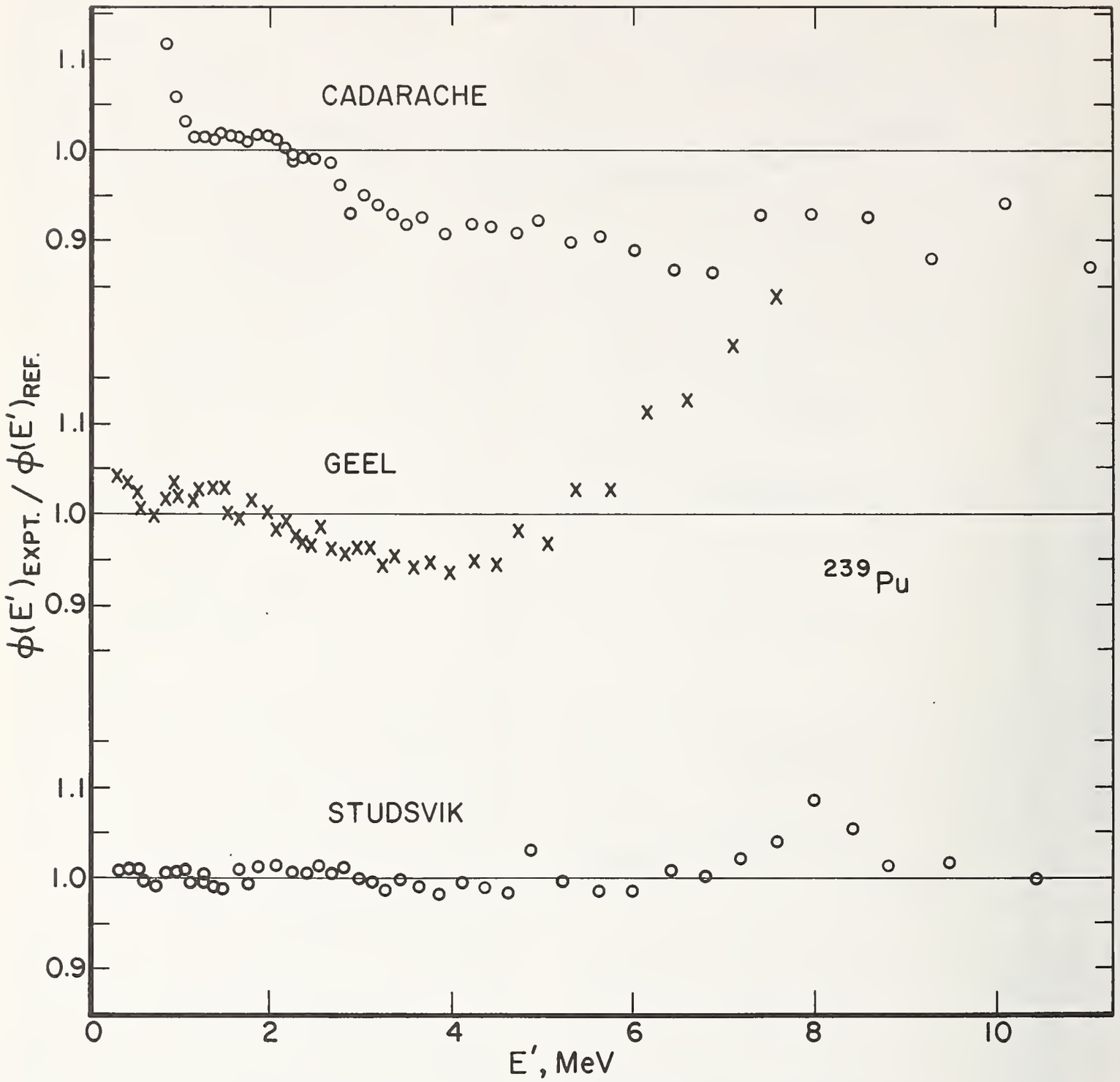

Figure 3. Ratio of Experimental Data for Neutron-Induced Fission in ^{239}Pu to a Reference Watt Spectrum[2] with A = 1.0364, B = 2.8728, and $\bar{E}'$ = 2.116 MeV.

departures, based on the spread of the data, were calculated and found to be statistically significant. The NBS reference Maxwellian[4], together with departures from this Maxwellian and assigned uncertainties, constituted the evaluation.

Specification of the departures in seven energy intervals had the disadvantage that the evaluated spectra were discontinuous. Therefore, subsequent to the published evaluation, the same average departures of the data from the Maxwellian were reanalyzed in finer energy groups. This procedure resulted in a continuous analytic representation of the fission spectrum. This NBS representation, which is called the "segment-adjusted Maxwellian," was described in a recent paper at the Vienna Consultants Meeting[5].

The departures of the NBS evaluated spectra from a Maxwellian with $\bar{E}$ = 1.97 MeV for ^{235}U and from a Maxwellian with $\bar{E}$ = 2.13 MeV for ^{252}Cf are shown in Figures 5 and 6. Some of the departures of the measurement of Green[6] for the ^{252}Cf spectrum shown in Figure 6 give an indication of variations from the mean values. The average energies of the evaluated spectra are 1.98 MeV for ^{235}U and 2.12 MeV for ^{252}Cf.

Both figures show a deficiency of neutrons, compared with the Maxwellian shape, above 6 MeV and below 0.3 MeV. This behavior, which is consistent with a Watt distribution, suggests that the reference spectrum is closer to a Watt rather than to a Maxwellian. However an integral measurement reported by McElroy *et al*[7] in a ^{235}U fission spectrum indicates that the

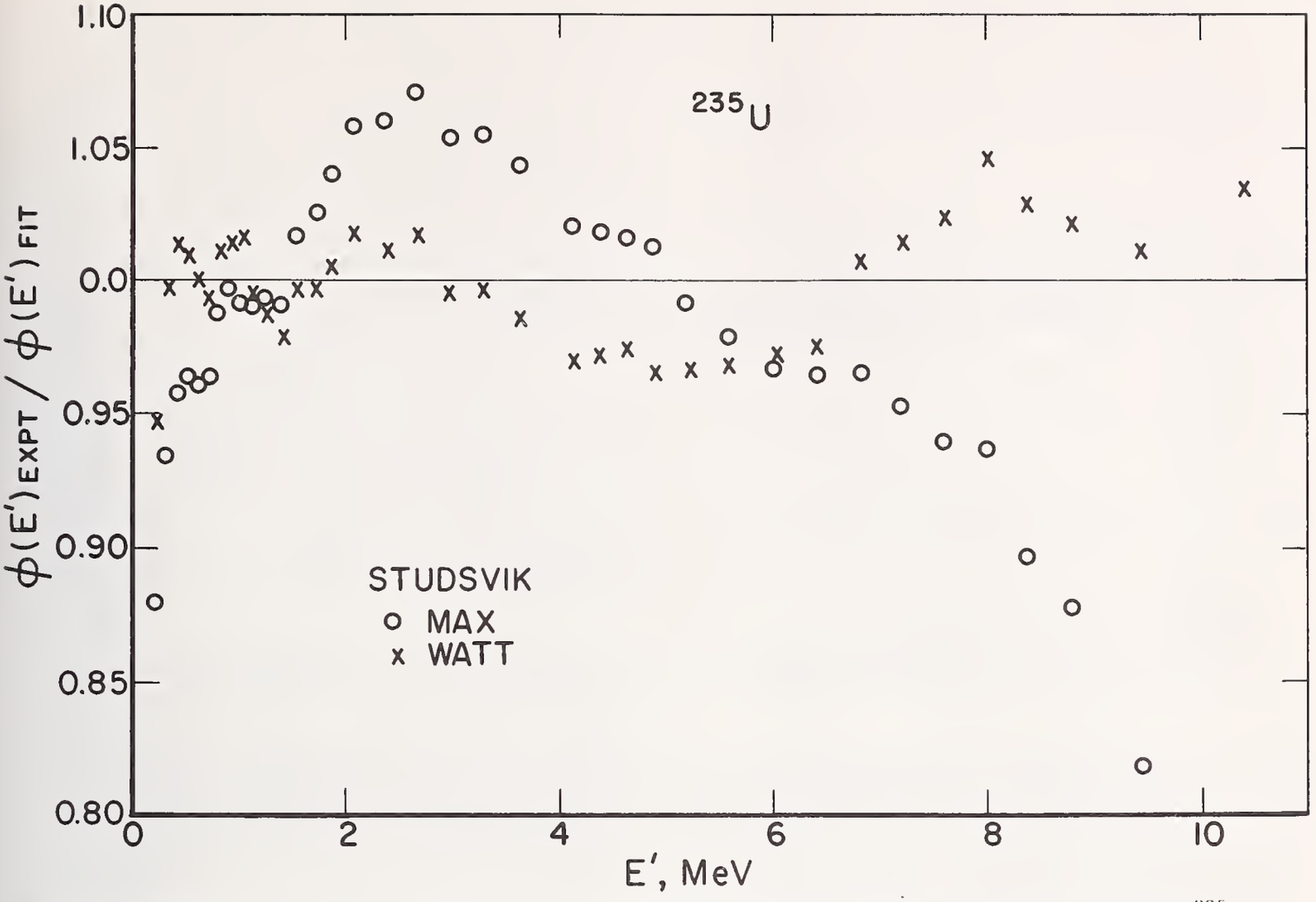

Figure 4. Comparison of Ratios of Measured Spectrum of Neutrons Emitted from Neutron-Induced Fission of ^{235}U to Analytic Fits of a Maxwellian and a Watt Shape. For the Maxwellian; $\bar{E}'$ = 2.001 MeV. For the Watt; A = 1.0172, B = 2.2553 amd $\bar{E}'$ = 2.020 MeV.

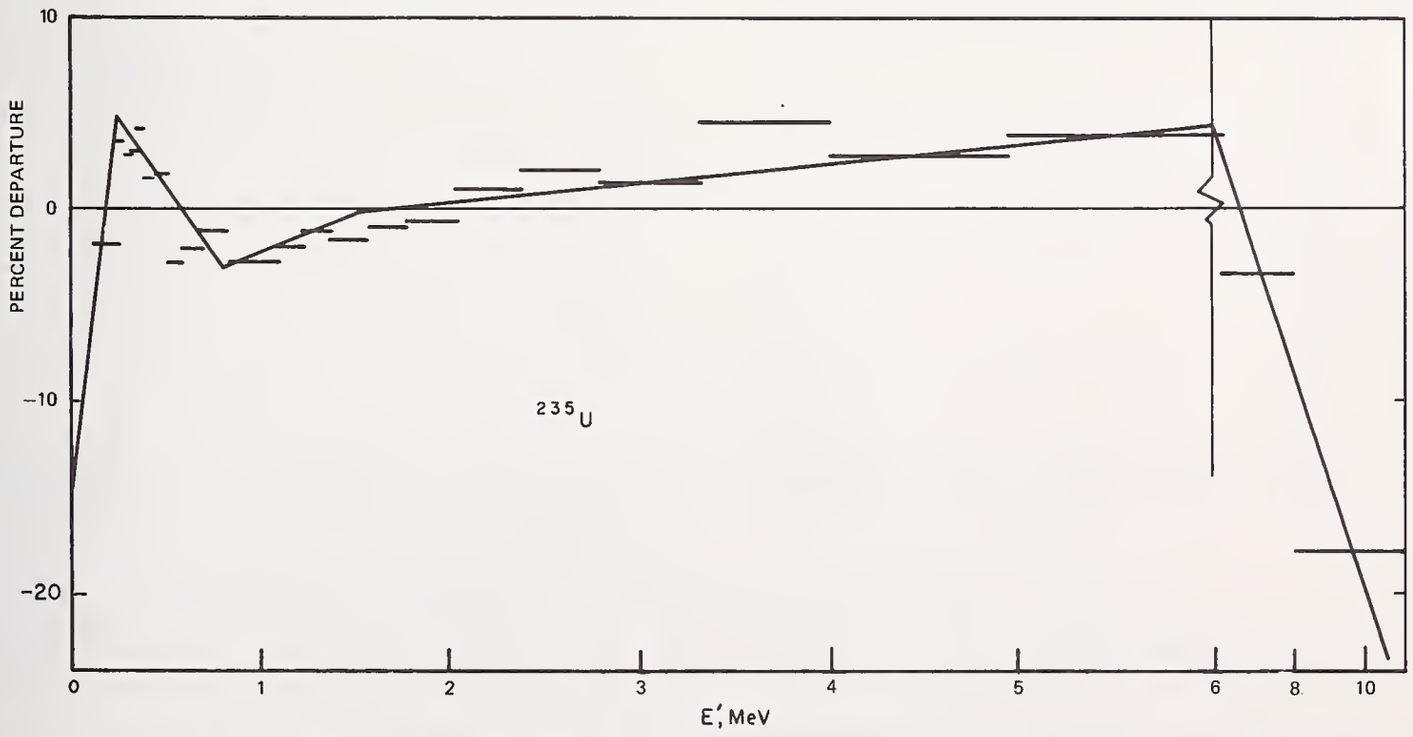

Figure 5. Percent Departures of the NBS Evaluated Spectrum of Neutrons Emitted from Neutron-Induced Fisssion in ^{235}U. Horizontal lines are average departures of the data in 28 energy groups; linear segments are piecewise continuous approximations to these departures.

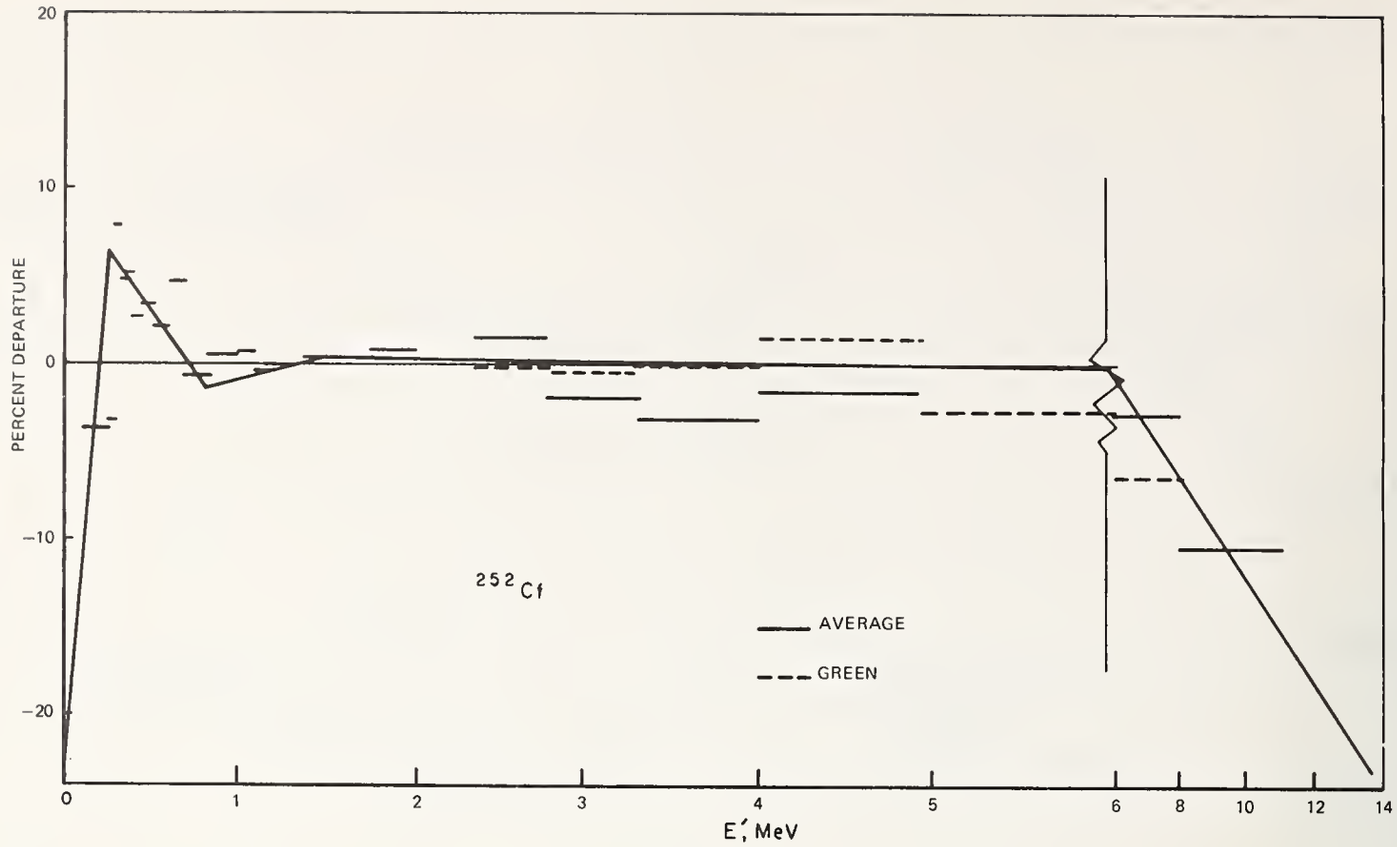

Figure 6. Percent departures of the NBS Evaluated Spectrum for Neutrons Emitted from Spontaneous Fission of ^{252}Cf. Solid horizontal lines are average departures of the data in 28 energy groups; dashed horizontal lines are departure of Green's data; linear segments are piecewise continuous approximations to the average departures.

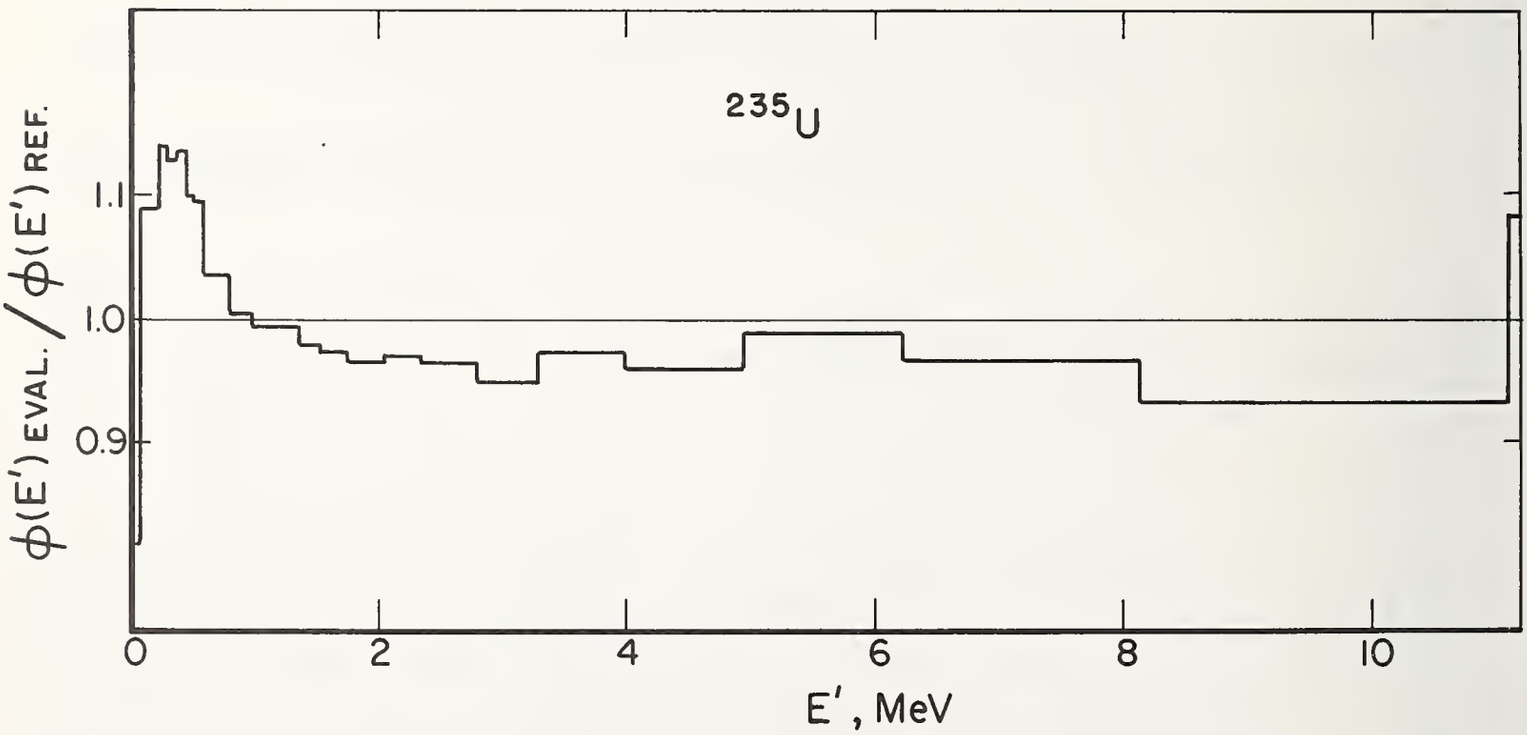

Figure 7. Ratio of NBS Evaluated Spectrum for Neutron-Induced Fission in ^{235}U to a reference Watt spectrum[2] with A = 1.0193, B = 2.3075 and $\bar{E}'$ = 2.027 MeV.

spectrum at about 10 MeV may be closer to a Maxwellian than a Watt. Finally, both figures indicate an excess of neutrons around 0.5 MeV, which is inconsistent with either of the representations discussed here.

For ^{235}U, the apparent excess of neutrons has been eliminated in more recent data by scattering corrections in the ^{235}U sample. For example, when Knitter's correction for this effect was applied to Johansson's

data, the average energy of the experimental spectrum increased from 1.99 MeV to 2.02 MeV. Since Johansson's data represented only one of six experiments included in the NBS evaluation, the impact of this change on the NBS evaluation is small, increasing the average energy of the evaluated spectrum of ^{235}U fission neutrons from 1.98 MeV to 1.99 MeV. It is suggested that the average energy would increase still further if the older data sets of Cranberg and Rosen[8], Barnard et al[9] and Werle and Bluhm[10] were corrected for scattering effects in the ^{235}U sample. However, Johansson's sample was considerably thicker than many of those used in earlier work. Therefore the effect of scattering in the sample would probably be much less than the effect calculated for Johansson's data.

In order to permit a direct comparison, the NBS-evaluated spectrum for ^{235}U is plotted in Figure 7 as ratios to the same reference Watt spectrum assumed in Figure 2. In general, the magnitude of the ratios shown in Figure 7 is comparable to those shown in Figure 2. However, the ratios are systematically greater than unity between 0.2 and 1 MeV and less than unity between 1 and 10 MeV. This follows from the fact that the average energy of the evaluated spectrum ($\bar{E}$ = 1.98 MeV) is lower than that of the reference spectrum ($\bar{E}$ = 2.03 MeV) obtained from the most recent measurements.[2]

For ^{252}Cf, the excess of neutrons in the region around 0.5 MeV is still not understood. Green[6] has formulated a model based on experimentally determined parameters which predicts an excess of neutrons over the Maxwellian below about 0.75 Mev. On the other hand, in the previous paper presented at this Symposium, Blinov noted that an apparent component of low-energy neutrons disappeared when the thickness of the Li-glass detector was reduced. His statistics are not good enough, however, to determine the excess over a Maxwellian to better than 5%.

IV. Summary and Conclusions

Recent experiments have served to establish with greater confidence the fission neutron spectrum for low-energy neutron-induced fission of ^{235}U and ^{239}Pu and for the spontaneous fission of ^{252}Cf. Average energies of emitted spectra inferred from experiments on neutron induced fission have tended to increase with time. Since the scattering corrections[3] applied to the recent measurements slightly harden all of the spectra, better agreement with the older data might be obtained if such corrections had been applied.

While these data, when considered separately, show a slight increase in the average energy of the emitted neutron, the highest incident neutron energy investigated was only 2.07 MeV. Therefore, the trend is indistinguishable from a fission spectrum independent of incident neutron energy and the dependence of the shape of the prompt fission spectrum upon the incident neutron energy remains an enigma.

The fission spectral shape is considered to be well determined over the range of emitted neutron energies from about 1-8 MeV. Below one MeV, some experimentalists see a large excess of neutrons over the Watt or the Maxwellian shape; while above 8 MeV, the statistical errors are often large due to the extremely low flux in that region. In many reactor physics applications it could be important to know about an excess of low-energy neutrons.

REFERENCES

1. "Prompt Fission Neutron Spectra", Proceedings of a Consultants' Meeting on Prompt Neutron Spectra; organized by the International Atomic Energy Agency and held in Vienna, 25-27 August 1971, IAEA, Vienna, 1972.

2. B. H. Armitage and M. G. Sowerby, ed, "Inelastic Scattering and Fission Neutron Spectra," AERE-R 8636, Proceedings of a Specialist Meeting; sponsored by the Joint Euratom Nuclear Data and Reactor Physics Committee and held at AERE, Harwell, April 14-16, 1975, Harwell, U.K., January 1977.

3. M. M. Islam and H. -H. Knitter, "The Energy Spectrum of Prompt Neutrons from the Fission of Uranium-235 by 0.40 MeV Neutrons", Nuc. Sci. Eng. 50, 108 (1973).

4. J. A. Grundl and C. M. Eisenhauer, Proc. Conf. Neutron Cross Sections and Technology, Washington, D.C. (1975). NBS Special Publication 425, p. 250. Edited by R. A. Schrack and C. D. Bowman.

5. J. Grundl and C. Eisenhauer, "Benchmark Neutron Fields for Reactor Dosimetry," IAEA Consultant's Meeting on Integral Cross Section Measurements in Standard Neutron Fields for Reactor Neutron Dosimetry; International Atomic Energy Agency, Vienna, Nov. 15-19, 1976 (to be published).

6. L. Green, J. A. Mitchell, and N. M. Steen, "The Californium-252 Fission Neutron Spectrum from 0.5 to 13 MeV," Nuc. Sci. Eng. 50, 257 (1973).

7. W. N. McElroy, R. Gold, E. P. Lippincott, A. Fabry, and J. H. Roberts, "Spectral Characterization by Combining Neutron Spectroscopy, Analytical Calculations and Integral Measurements", Consultants Meeting on Integral Cross-Section Measurements, IAEA, Vienna, Nov. 15-19, 1976.

8. L. Cranberg, G. Frye, N. Nereson, and L. Rosen, "Fission Neutron Spectrum of ^{235}U", Phys. Rev. 103, 662 (1956).

9. E. Barnard, A. T. G. Ferguson, W. R. McMurray, and I. J. van Heerden, "Time-of-Flight Measurements of Neutron Spectra from the Fission of ^{235}U, ^{238}U, and ^{239}Pu", Nuc. Phys. 71, 228 (1965).

10. H. Werle and H. Bluhm, "Fission-Neutron Measurements of ^{235}U, ^{239}Pu, and ^{252}Cf", Jour. Nuc. Energy 26, 165 (1972).

ON QUANTITATIVE SAMPLE PREPARATION OF SOME HEAVY ELEMENTS*

A. H. Jaffey
Chemistry Division, Argonne National Laboratory,
Argonne, Illinois 60439

A discussion is given of some techniques that have been useful in quantitatively preparing and analyzing samples used in the half-life determinations of some plutonium and uranium isotopes. Application of these methods to the preparation of uranium and plutonium samples used in neutron experiments is discussed.

(Absolute counting, aliquotting, α-activity, analysis (plutonium, uranium), isotope dilution, sample preparation, specific activity)

Introduction

In an experiment which measures such properties of heavy element isotopes as fission cross-sections and the like, it is usually necessary to know the sample's content of the isotope of interest with some accuracy. For some experiments, for example those involving fission fragment counting, it is also desirable to have thin uniform deposits of the isotope. Unfortunately, the two desiderata are often partially incompatible.

I shall not review the various methods that may be applied to this problem. A cursory examination of the literature indicates that there have been many papers on this and related subjects, and there have even been a number of conferences. I would like to describe some techniques that my colleagues and I have used extensively in a series of half-life measurements of some uranium and plutonium isotopes. These methods may be directly used for preparing certain kinds of samples for fission and neutron measurements, and, using the same principles, the methods may also be modified for preparing a wider range of sample types.

Measurement of Heavy Element Half-Lives by Specific Activity

After a period of relative dormancy, there has been a flurry of activity in this field in the last five or six years. Our group has measured and published results on ^{238}U, ^{235}U, ^{236}U, and ^{233}U,[1-3] and on ^{238}Pu and ^{239}Pu.[4,5] The techniques used have gone through several stages of development, but they have some common features throughout. In these experiments, we used absolute alpha counting to measure the alpha particle emission rate from known masses of the isotope considered. We have examined many published experimental reports on the results of absolute counting as applied to half-life measurements. When two experimenters, each making absolute measurements to 0.2% error or less, get results differing by over 1%, it is clear that some "absolute" measurement is less than absolute. In examining our own work, we checked all the possible sources of error that we could think of; there nevertheless remained the possibility that some important point was overlooked. However, in our last measurement,[5] which involved ^{239}Pu, the half-life was evaluated by two methods: one, using our usual absolute counting technique; the other, using isotopic dilution (mass spectrometric) to determine the mass of ^{235}U grown into a known mass of ^{239}Pu in a given time. That the two results agreed within a statistical error <0.1% gave us confidence that our absolute counting method was rightly named.

This method stands on three legs: (1) measurement of the mass of the element used (e.g., uranium or plutonium), (2) accurate dilution and aliquotting for sample preparation, and (3) counting the samples in an alpha counter of precisely known geometry factor.

Mass Measurement of Plutonium and Uranium Samples

Since it is desired to transform weights to moles or inversely, a mass spectrometric analysis is necessary to provide the correct atomic weight of the element. In most cases, one isotope dominates, so only a modest accuracy is needed in the analysis.

For accurate mass measurement of good accuracy (in the tenth percent range) two primary methods are useful: (a) preparation of a compound of known composition and purity or (b) oxidation-reduction titration. A secondary method is that of mass spectrometric isotope dilution; secondary, in the sense that the spike itself must ultimately be standardized by a primary method.

The compound preparation technique has been widely used in the half-life field. Among the compounds used for uranium have been the pure metal and the oxide U_3O_8. A wider variety has been used for plutonium, including the pure metal, the dioxide PuO_2, the disulfate $Pu(SO_4)_2$, cesium plutonium chloride Cs_2PuCl_6, and the halides PuF_3, $PuCl_3$ and $PuBr_3$. For accurate determination of the element's weight from the weight of the compound, it is necessary to know that the compound is really stoichiometric, i.e., that the material as formed actually contains the ratio of atoms described by the simple chemical formula (e.g., that, to a high decree of accuracy, prepared $PuCl_3$ indeed has three times as many chlorine atoms as plutonium atoms). The metal is simplest in that no stoichiometry is involved, but it is harder to make without impurities, which tend to be mostly oxides or materials coming from the reduction process or from the crucible material.

For uranium it has been found that heating the oxide carefully at 900°C in air for at least one hour yields a composition very close to U_3O_8. Hence, the NBS finds it feasible to provide natural uranium oxide with a warranteed composition as a primary standard. There has been less satisfaction with the stoichiometry of the various plutonium compounds, hence the wide variety of compounds used.

With suitable experience and use of a large mass of metal, the impurities in metal formation can be adequately segregated. Plutonium is harder to make, one of the reasons being the handling problem caused by its high radioactive toxicity. For the same reason, it is harder to analyze for small amounts of impurities, the methods used generally requiring volatilization (e.g., optical spectra). Nevertheless, the problems have been sufficiently well solved so that the Bureau also offers uranium and plutonium metal samples of warranteed purity. No plutonium compounds are so offered. The U content in the metal is known better than the Pu content, the NBS setting a 1 σ error of 0.009% for U and 0.025% for Pu.

Since both plutonium and uranium form well-defined and stable (+6) and (+4) states in water solution, it is feasible to measure the amount of oxidant or reductant required to change the element completely from one form to the other. For example, the method we used for analyzing plutonium[6] involved oxidizing it completely to Pu(VI) and then reducing it quantitatively with standardized ferrous ion solution according to the reaction:

$$Pu(VI) + 2Fe(II) \rightarrow Pu(IV) + 2Fe(III)$$

The concentration of Fe(II) is determined by oxidizing it with pure standard potassium dichromate, whose composition is warranteed by NBS. In the titration, the point of exact equivalence is observed as a sudden change in the current passing through the solution (hence, an amperometric endpoint). Uranium can be completely reduced to U(IV) and then quantitatively oxidized with standard dichromate, with an endpoint detected through a sudden potential change.[7] The NBS standard uranium or plutonium can be used as the primary standard instead of potassium dichromate; such a procedure serves to protect against possible uncertainties in the stoichiometry of the endpoint. Experience, however, shows that this uncertainty is very small for uranium (<0.02%) and quite small for plutonium (∿0.05%).

The uranium and plutonium provided by NBS are excellent chemical standards, but the isotopic composition is usually not that desired by the experimenter. The titration method, can then serve as a means of transferring knowledge about the exact mass of an NBS sample to the experimenter's material.

The titration method for uranium can be made more precise than that for plutonium. For uranium titrations, the standard deviation per sample can be <0.02%, whereas that for plutonium titrations is ∿0.05%. For most purposes, such precision suffices. Such accuracies are attainable only through the use of relatively large samples. The precision values described were attained when 60 mg U and 20 mg Pu samples were used, and smaller samples yield poorer precision. It may also be noted that other precision titration methods are available for both uranium and plutonium, but we do not have experience with their use.

Aliquotting, Dilution and Sample Spreading

After the solution concentration has been evaluated, sample preparation requires that a known fraction of the solution be appropriately transferred to a backing plate. Frequently the amount of isotope needed for the experiment is so small that an intermediate dilution is required. This was, indeed necessary for the half-life measurements of such highly radioactive nuclides as ^{239}Pu or ^{233}U.

That an intermediate dilution might be necessary is due to the fact that accuracy requirements set a lower limit on the sample size which may be transferred. In our experiments, we use a Mettler semi-micro single-pan balance which could weigh to 100 g and had a random weighing error of ∿0.02 mg. Since all weight measurements were made by difference, the expected error was $0.02\sqrt{2} \cong 0.03$ mg. We required our minimum sample size to be ∿200 mg, which should yield ∿0.015% net weighing error.

If, for example, there were 400 g of solution, then 200 mg would represent 1/2000 of the total amount. If the sample required was larger than this limit, then the sample could be prepared by direct transfer from the stock solution. However, for samples which were a smaller fraction of the stock solution, an intermediate dilution would be needed. In the ^{239}Pu measurement, for example, requirements for weighing out titration samples resulted in a concentration of ∿40 mg Pu/g solution. Since counting samples were to contain 3-4 μg Pu, intermediate dilution was necessary, and by a factor of ∿2000, i.e., diluting the transferred volume (aliquot) containing ∿8 mg Pu with 400 g of acid solution. Where dilution is required, we have found it feasible to dilute only once, by choosing the dilution volume as large as necessary.

The technique used for accurately transferring an aliquot to a dilution flask is the same as that used for sample transfer to a backing plate. It involves the use of a polyethylene pycnometer of the type described briefly by Janet Merritt in Ref. 8 and more fully in Ref. 9. The pycnometer is made from a small polyethylene vial whose top is pulled out in the form of a long, thin snout. Solution is sucked up into the vial, the vial is weighed, some drops are delivered into a dilution bottle or onto a plate (as in Fig. 1), and the vial is reweighed. The weight delivered in the aliquot is the difference in vial weights. The technique is not quite this simple; some refinements are necessary for good results, and these are described in Refs. 4 and 9. After some practice an operator can achieve quite good precision in the aliquotting process.

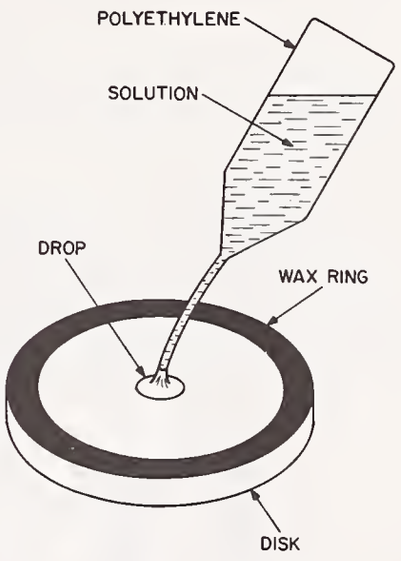

Fig. 1. Use of Polyethylene Pycnometer
The snout on a polyethylene vial is pulled out into a long capillary, the vial cleaned, dried and weighed. The vial is carefully handled, the capillary inserted into the stock solution, and liquid drawn up. The capillary is wiped, the end cut off. Droplets are delivered with pressure, preferably with a mechanical jig, and with no free-fall (with its potential of splashing) when sample plates are prepared as in the figure. Reweighing the vial gives the aliquot weight with great accuracy.

The data of Table I and II show examples, the first representing the results in an earlier phase of developing the technique. Table I shows the counts of samples taken from a dilution bottle and prepared as in Fig. 1. The final result represents the activity concentration of the original stock solution. Table II corresponds to a different stock solution. $\underline{s}$ is the usual estimate of the standard deviation per sample and ε_{av} is the average counting error. We may take $\delta^2 = s^2 - \varepsilon_{av}^2$, where δ represents the error of

Table I. Aliquotting Precision - 1

No.	Ct/min	Min	Dis/min per g soln $\times 10^{-7}$	Ct error ε_i
1	26996.5	400	523.883	±0.159
2	31768.9	400	523.441	0.147
3	34580.1	1000	523.917	0.089
4	30425.8	900	523.441	0.100
5	28880.3	1000	523.547	0.097
6	39130.4	400	523.658	0.132
7	28887.3	1000	523.652	0.097
8	29806.8	1000	523.453	0.096

$s = 0.192$; $\varepsilon_{av} = 0.115$

Table II. Aliquotting Precision - 2

No.	Ct/min	Min	Dis/min per g soln $\times 10^{-7}$	Ct error ε_i
1	40534.3	3800	419.978	±0.034
2	48980.3	400	419.821	0.095
3	34436.1	900	419.913	0.075
4	41628.5	400	419.814	0.103
5	38192.6	1000	420.042	0.068
6	42040.3	400	419.830	0.105

$s = 0.095$; $\varepsilon_{av} = 0.080$

aliquotting, sample preparation and positioning it in the counter. In Table I, $\delta = 0.153$ (0.029%); in Table II, $\delta = 0.051$ (0.012%).

For sample plates prepared as in Fig. 1, the distribution of the activity over the place is made more uniform by evaporating with a spreading agent such as tetraethylene glycol.[4] Better uniformity, however, is achievable by electrodeposition. We have used the method of molecular plating,[10] a high voltage deposition from an isopropyl alcohol solution, using the plating cell in Fig. 2. In this case, the aliquot

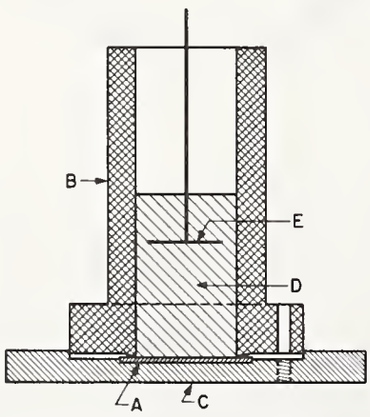

Fig. 2. Molecular Plating Cell
A: Aluminum sample plate and cathode. B: Teflon wall. C: Base plate. D: Isopropyl alcohol solution. E: Platinum anode.

is delivered into a temporary transfer tube or directly into the plating cell. The deposition gives quite a uniform distribution, the range of density variation being up to 20%, but generally <10% (for example, see Ref. 1). Such uniformity makes practical the deposition of thicker samples than can be usefully prepared by the method of Fig. 1. We have prepared samples of uranium up to 500 $\mu g/cm^2$ in thickness. Plutonium samples have not been made to such thickness.

The molecular deposition method is not quantitative, part of the element remaining in the isopropyl alcohol. The amount, however, is generally a small fraction of the total, and it can be accurately accounted for by washing the plating cell, evaporating the isopropyl alcohol and depositing the residue for counting with an α-counter.[1] We have gotten higher deposition yields more consistently with uranium, the residual being generally <1%; with plutonium, residuals of <1% are achievable, but 2 or 3% are not uncommon.

Absolute Alpha Counting

Various methods can be used for absolute counting, including coincidence techniques, liquid scintillation counting and 4π proportional counting. We have used the defined geometry technique, in which the α-particle source is placed at a known distance from an aperture of known dimensions. On the assumption of isotropic emergence from the source, the fraction of particles passing through the aperture is the same as the fractional solid angle subtended by the aperture at the source. The major factor limiting the accuracy of this assumption lies in the scattering of α-particles either from the sample mount or from the counter walls. With suitable care in the counter's construction, a negligible fraction of the scattered α-particles reach the aperture. The limit on the accuracy of the method is then set by the accuracy of measuring the dimensions which define the subtended solid angle.

In our half-life work we have used IGAC,[1] an intermediate geometry alpha counter (Fig. 3). With a

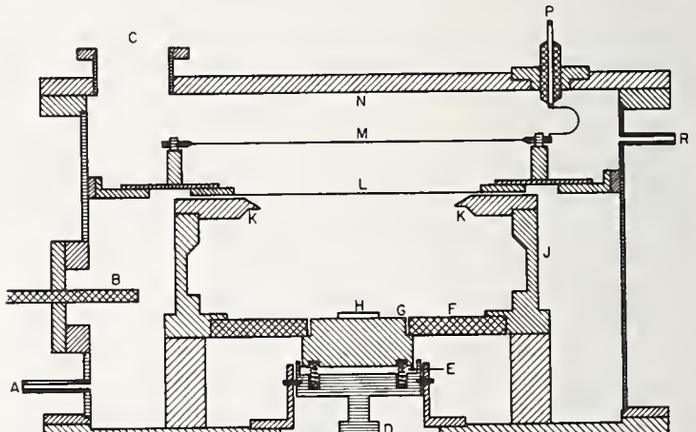

Fig. 3. The Intermediate Geometry α-Counter (IGAC) Operated with flowing argon (10% CH_4) gas filling entire chamber, 35 to 50 torr pressure (depending upon α-energy). Geometry defined by accurately machined and measured circular aperture K (with 0.025 mm thick edge) and by measured distance between aperture plane and sample surface H. Proportional counter chamber above thin window L ($\sim$0.6 mg/cm^2, plastic with evaporated gold layer) with wires M spanning circular area.

relative solid angle G $\sim$1/11, it is *intermediate* in solid angle between the 2π counter (G $\sim$0.5) and the low geometry counter, for which G is generally <0.01. By reducing G well below 0.5, we avoid the well-known back-scattering from the sample mount and severe sample self-absorption at oblique angles. Further, the large

aperture makes for accurate dimensional measurement and negligible slit-edge scattering, and the relatively large value of G allows counting of low specific activity isotopes. At a given distance from the aperture plane (Fig. 3), the relative solid angle G subtended by an elementary area dS on the source is a function G(r) of the distance r from the axis (defined by the circular aperture) to dS.[11] The average relative solid angle for a particular sample is evaluated by counting the sample in a 2π counter with a series of collimators. Each collimator contains annularly-distributed orifices at a given r-value, hence corresponds to the relative solid angle G(r).[1,11]

By counting the same sample in both counters, we have checked the IGAC geometry factor against that of a low geometry counter (G ~1/100) with a 2 cm aperture and a surface barrier detector; the two counters agreed within counting statistics (0.05%).

One of the most important features of IGAC is that it has a very flat plateau. This means that the pulses at levels below the discriminator level constitute <0.005% of the total, even for quite thick samples. Figure 4 shows a pulse distribution for a relatively thick ^{238}U sample, Fig. 5 for a thinner sample. In both cases, the number of pulses smaller than the pulse selector level is negligible.

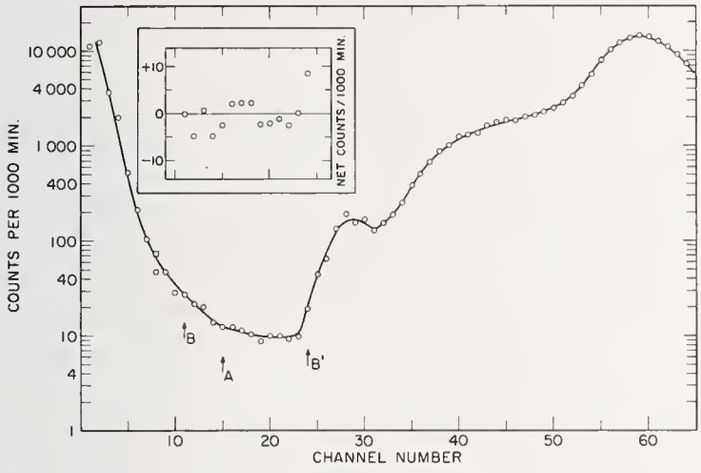

Fig. 4. Pulse Height Distribution from IGAC Proportional Counter for ^{238}U Source
Discriminator setting is A. Inset shows the plateau region BB' on expanded scale. Subtracting background, the net counts over the whole plateau is -4.6 ± 10.6 counts/1000 min, compared to 2 x 10^5 counts/1000 min for the sample.

It is common practice to extrapolate α-counter plateaus to zero pulse height and to assume that the extrapolated counting rate, when corrected for the geometry factor, corresponds to 100% counting efficiency. It has been our experience that when an extrapolation to zero pulse height is necessary due to a sloping plateau, then the extrapolated result is generally too low. In using IGAC, the pulse distribution (as in Figs. 4 or 5) is routinely used as a diagnostic. Net counts in the plateau region (i.e., a sloping plateau) usually correspond to low results, so such samples are automatically discarded. We usually ascribe entry of small pulses into the distribution as due to poor sample spreading, with some clumping.

A continuum of small pulses has also been observed with liquid scintillation α-counting and with a faulty surface-barrier detector used with a low

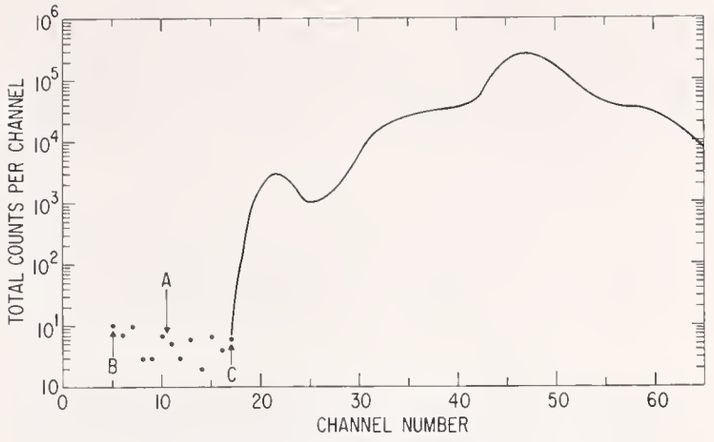

Fig. 5. Pulse Distribution from a Thinner and More Active Source
Discriminator setting at A. Within counting error, the background accounts for all counts between B and C, so the plateau is flat in this region. Even without subtracting background, the counts of pulses smaller than A (extrapolating to zero pulse height) is <2 x 10^{-5} of the total number of counts.

geometry counter. For the liquid scintillator, the pulse distribution showed α-particle pulses down to the noise level, and extrapolation to zero pulse-height yielded results 0.15-0.20% lower than that derived from IGAC. Replacement of the surface barrier detector did not sensibly change the peak half-width, but decreased the number of small pulses and restored the correct counting rate. This effect may have been due to a small defective region in the large area detector.

While IGAC (or other counters) may be used to determine the disintegration rate of an α-emitting source, the experimenter generally wishes to determine the rate for a specific isotope. Auxiliary information is then required, usually supplied by a mass spectrometric analysis and an α-pulse analysis with a solid state detector. In certain cases, however, the pulse analysis does not help, because it cannot discriminate between certain nuclide pairs which have overlapping α-energies. The most important of these are: (^{240}Pu, ^{239}Pu), (^{238}Pu, ^{241}Am) and (^{233}U, ^{234}U). The members of the pair must be distinguished by the mass spectrometric analysis or by other radiometric methods, such as detection of the prolific ^{241}Am 60 keV γ-ray with a Ge(Li) detector. With the mass spectrometric and pulse analysis data, the fraction of the measured disintegration rate ascribable to the nuclide of interest may be evaluated.

When some component in the sample gives rise to relatively short-lived decays, it is important that the disintegration rate measurement be made at close to the same time that the auxiliary measurements are made. The most common cases in which such problems arise are those in which samples of uranium contain ^{232}U (73.6 yr) or samples of plutonium contain ^{241}Pu (14.5 yr). The latter decays to ^{241}Am (432 yr) and the former decays to ^{228}Th (RdTh, 1.91 yr) and then in turn to an entire chain of very short-lived decays giving four more α-particles. Depending upon the fraction of ^{232}U (or ^{241}Pu) present, neglecting the possibility of these activity-growths can, and, indeed, has, caused serious errors.

Consider the following examples:

1. A sample of ^{233}U contains 0.0005% ^{232}U; hence, the ^{232}U provides 1.072% of the total uranium α-activity. Just after the uranium has been chemically separated from thorium, the ^{233}U α-activity is 98.928%

of the total activity, a fact that is readily determined by α-pulse analysis. Immediately after such separation, the thorium daughter starts growing and the subsequent decay chain is in almost immediate equilibrium with the ^{228}Th. Then, as a function of time (T yr) after chemical separation, the α-activity is expressed as

$$A(T) = A_0[1 + 5(0.01072)(1-e^{-0.363\ T})],$$

where A_0 is the activity of the sample just after purification. For short times, approximately,

$$A(T) = A_0[1 + 0.01946\ T]$$

The ^{233}U α-activity is a decreasing fraction of the total activity. Thus, in six months, the sample activity has increased by about 0.9%, so the ^{233}U fraction has correspondingly decreased. Clearly, for longer times or larger concentrations of ^{232}U, the growth of α-activity is more serious.

2. A plutonium sample contains 97.1% ^{239}Pu, 2.5% ^{240}Pu and 0.4% ^{241}Pu. After separation from Am, the sample activity is A_0 and after T yr, it is

$$A(T) = A_0[1 + 0.010\ T]$$

Analysis by Isotope Dilution

Into a sample containing isotope A of an element, we add a known amount of isotope B of the same element. After the two isotopes are chemically equilibrated, the measurement of the ratio of A to B yields a determination of the amount of A in the sample. This type of measurement is called *isotope dilution* and the added isotope is the *spike*. The procedure is most commonly carried out mass spectrometrically, yielding an A/B mole ratio, or by pulse analysis, yielding an A/B α-activity ratio.

Either method is valid only when care is taken to correct for inherent isotopic biases in the ratio measurement. Such correction may be made, but high accuracy (0.1% or better) requires a skilled operator. The mass spectrometric method requires calibration for inherent mass discrimination; pulse analysis requires a valid correction for the fact that the high energy peak has a tail which overlaps the low energy peak, hence gives the lower peak an apparent higher intensity.

Recent examples from our work:

1. In a determination of the ^{239}Pu half-life,[5] we measured the amount of ^{235}U grown in a given time. Solutions of ^{233}U and ^{238}U were standardized as described above, and precise aliquotted spikes were added to the ^{239}Pu solution. Uranium was extracted and the (^{233}U, ^{235}U, ^{238}U) mixture was mass-spectrometrically analyzed. The linear bias was evaluated by comparing the observed ^{233}U/^{238}U mole ratio to the known spike ratio.

2. In an evaluation of the ^{238}Pu half-life,[4] we measured the amount of ^{238}Pu grown from the decay of a known α-activity of ^{242}Cm during a given time. A known α-activity of ^{240}Pu was added as a spike, the plutonium was extracted, and the ^{240}Pu/^{238}Pu α-activity ratio was determined by pulse analysis. The most serious potential error source arose from the need to subtract the low energy tail of the ^{238}Pu peaks (5.491, 5.448 MeV) from the apparent intensity of the ^{240}Pu peaks (5.159, 5.114, 5.01 MeV). A "template" for subtraction was derived from pulse analysis of a pure ^{238}Pu sample.

In both cases, we tested the correction methods by analyzing known artificial mixtures. Mass spectrometrically, samples made from mixed aliquots of titrated ^{233}U, ^{235}U and ^{238}U were tested. For pulse analysis, we analyzed samples prepared from standardized solutions of pure ^{238}Pu and ^{240}Pu. The half-life measurements were made when the calibration techniques were found to be satisfactory.

The first experiment was made somewhat more complex because a ^{238}U spike was used. The ubiquitous presence of natural uranium contamination in reagents, dust, glassware, etc., required that super-clean techniques be used in all handling and chemical manipulations. It would be possible to avoid such meticulous handling by using only one spike (usually ^{233}U) and to calibrate the mass discrimination bias with a separate source containing a known mass ratio (generally, an NBS ^{235}U/^{238}U source). However, one then loses an internal calibration based upon spike ratios taken under the identical conditions used for the experimental ratio. For the bias calibration with external source to be valid, it must be shown that the bias calibration of the mass spectrometer remains constant to the accuracy required over a number of succeeding runs.

Mass spectrometric isotope dilution analysis of plutonium isotopes may be similarly used. Enriched ^{242}Pu is most commonly used for plutonium, because it is generally in low concentration in the plutonium samples of most interest.

The General Sample Problem

The techniques described above have the virtue that they allow preparation of samples containing known amounts of material, when analyzed solutions of the desired isotopes are available. Samples prepared as in Fig. 1 are suitable when small masses are needed or for heavier samples, when sample self-absorption is not important. Molecular plating may be used when heavier samples are needed and uniformity is important.

When heavier samples of good uniformity are needed, other preparation techniques must be used. These, unfortunately, are generally not quantitative. For example, the well-known electrospraying technique can be used to prepare thick, quite uniform samples, but quantitative deposition is not possible. In many cases, however, it is feasible to calibrate the samples, either by counting or by destructive analysis.

If the samples are not too thick, they may be counted either in a low or intermediate geometry counter, depending upon specific activity. In either case, the quality of the plateau must be carefully examined, as mentioned above. If the isotopic half-lives and the mole- or activity-ratios are known, the isotopic masses can be calculated.

If the samples are not good enough for direct counting, they may be dissolved after the experiment is completed. Analysis may then be carried out either by α-counting an aliquot as described above or by analyzing through one or the other form of isotope dilution.

References

*Work performed under the auspices of the Division of Physical Research of the U. S. Energy Research and Development Administration.

[1] A. H. Jaffey, K. F. Flynn, L. E. Glendenin, W. C. Bentley and A. M. Essling, *Phys. Rev. C*, 4, 1889 (1971).

[2]K. F. Flynn, A. H. Jaffey, W. C. Bentley and A. M. Essling, *J. Inorg. Nucl. Chem.*, 34, 1121 (1972).

[3]A. H. Jaffey, K. F. Flynn, W. C. Bentley and J. O. Karttunen, *Phys. Rev. C*, 9, 1991 (1974).

[4]H. Diamond, W. C. Bentley, A. H. Jaffey and K. F. Flynn, *Phys. Rev. C*, 15, March (1977). In press.

[5]A. H. Jaffey, H. Diamond, W. C. Bentley, K. F. Flynn, D. J. Rokop, A. M. Essling and J. Williams (to be published).

[6]C. A. Seils, Jr., R. J. Meyer and R. P. Larsen, *Anal. Chem.*, 35, 1673 (1963).

[7]A. R. Eberle, M. W. Lerner, G. C. Goldbeck and C. J. Rodden, *"Titrimetric Determination of Uranium in Product Fuel and Scrap Materials after Ferrous Ion Reduction in Phosphorous Acid; Manual and Automatic Titration,"* Proc. Sympos. on Safeguards and Techniques (Karlsruhe, July 6-10, 1970), Vol. II, p. 27, IAEA, 1970. Also New Brunswick Laboratory Report NBL-252 (1970).

[8]Janet S. Merritt, *Nucl. Instrum. Methods*, 112, 325 (1973).

[9]J. S. Merritt and J. G. V. Taylor, *"Gravimetric Sampling in the Standardization of Solutions of Radionuclides,"* Atomic Energy of Canada, Ltd. Report AECL-2679, 1967 (unpublished).

[10]W. Parker, H. Bildstein and N. Getoff, *Nucl. Instr. Methods*, 26, 55 (1964).

[11]A. H. Jaffey, *Rev. Sci. Instr.*, 25, 349 (1954).

BLACK AND GREY NEUTRON DETECTORS*

F. Gabbard
University of Kentucky
Lexington, Kentucky 40506

Recent progress in the development and use of "black" and "grey" detectors is reviewed. Such detectors are widely used for counting neutrons in (p,n) and (α,n) experiments and in neutron cross section measurements. Accuracy of each detector is stressed.

(Review; black & grey neutron detectors; neutron flux measurement.)

Introduction

Comprehensive early reviews of methods of neutron flux measurement and associated standard cross sections have been given by Barschall, et al.[1] Larsson[2] and Perry[3]. Advances in neutron flux measurement techniques have been discussed in Conferences on Neutron Cross Sections and Technology in 1968 and 1970.[4,5] Reviews were given at these conferences by Batchelor, Gibbons[4] and Landon.[5] The symposium on Neutron Standards and Flux Normalization,[6] held at the Argonne National Laboratory in October, 1970, treated, rather extensively, the whole subject of neutron flux measurement as practiced at that time. Further work has been reported at the Conference on Nuclear Cross Sections and Technology[7] held at the National Bureau of Standards in 1975 and at the International Conference on the Interactions of Neutrons with Nuclei[8] held at the University of Lowell in July, 1976. Papers at the Lowell Conference by H. Liskien and B. Zeitnitz deal with detectors and standards.

The basic techniques for neutron flux measurement are well known and advances have been largely in the refinement of these methods toward easier use and higher accuracy. There are some five (5) basic methods in current use for the measurement of neutron flux. These are:

(1) Associated particle methods;
(2) Proton recoil methods;
(3) Neutron moderation methods;
(4) Associated radioactivity methods; and
(5) Methods of reaction cross section comparison.

One obvious point to be emphasized[6] is that there is no "best" method for measuring neutron flux which works at all energies and in all geometries; the "best" technique depends on the neutron energy and the geometrical configuration of source and detector.

Since the advent of time-of-flight methods of neutron spectroscopy, the time response of fast neutron detectors has become an important consideration in neutron-flux-standards applications. Properties of an IDEAL neutron detector include the following:

(1) Variable detection sensitivity;
(2) An efficiency independent of neutron energy, i.e., a "flat" response;
(3) Insensitivity to background radiations; and
(4) Fast time response.

The advantage of variable detection sensitivity is that different experiments require the use of different intensity levels in the neutron flux. Fast time response is important in time-of-flight applications.

Such an ideal detector does not exist and it appears unlikely that any single detector can have the optimum characteristic in all of these properties. Nevertheless, these are important criteria for selection of a real detector.

The objective here is a review of recent developments in the use of "black" and "grey" neutron detectors for the measurement of neutron flux. The detectors which I shall describe are of two types; proton-recoil detectors and moderated neutron detectors. The recoil detectors use liquid or plastic scintillators as the active medium and moderated detectors utilize hydrocarbons, LiH, or carbon as the moderating medium.

Selection of detectors for description was based on personal knowledge of recent development and/or new uses. Among the "black" or "grey" neutron detectors or classes of detectors which will not be discussed in any detail are the Large Liquid Scintillators and the Activated Bath Detectors. These are covered by Dr. Axton in this session and by others at other sessions of the Symposium.

The time period covered in this review is roughly from 1970 until now. During this time there have been no startling breakthroughs in the neutron counting game; however, there has been steady progress on all fronts.

The Macklin Sphere

First, I want to recall, or call as the case may be, your attention to the Graphite Sphere Detector,[9] or Macklin Sphere designed and built by R.L. Macklin at the Oak Ridge National Laboratory. Although this detector is not new, there have been important developments in its use. This detector is a sphere of reactor grade graphite with a radius of 78 cm. Neutrons originating at the center are moderated in the graphite and counted by eight (8) BF_3 counters near the surface of the sphere. The detector is covered with cadmium to reduce the effect of room scattered neutrons. Figure 1 shows a picture of the detector with Cleland Johnson in the laboratory at Oak Ridge.

An attractive feature of this detector is that its simple construction makes it feasible to calculate its relative efficiency as a function of neutron energy through application of age-diffusion theory.[9] Figure 2 shows the calculated efficienty of the detector as a function of neutron energy. To be noted is the

Fig. 1. The Macklin Graphite Sphere neutron Detector with C.H. Johnson at the Oak Ridge National Laboratory.

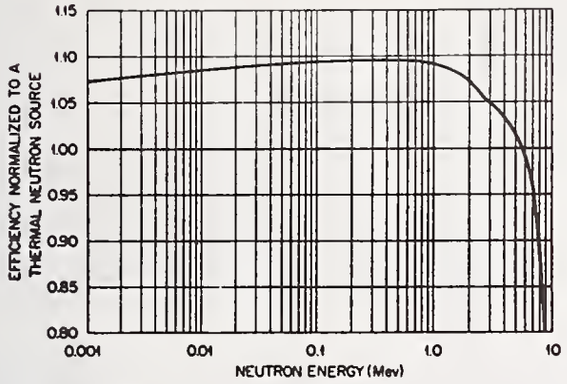

Fig. 2. The calculated efficiency of the Macklin Sphere as a function of neutron energy.

flat response curve at low energy in the keV region. This feature makes the detector particularly well suited for use in measuring total neutron yields from sources placed at the center. The detector has been used extensively for neutron production cross-section measurements and continues to be used, most recently by Johnson, Bair and co-workers[10] for highly accurate measurements of cross sections for neutrons produced in (p,n) and (α,n) reactions.

Bair, Johnson and co-workers have recently recalibrated the Macklin Sphere using NBS II[11] as the calibrating source. At the time of calibration, the detector efficiency for Ra-Be neutrons was measured to be (0.003149 ± 0.000011). A local source was made by placing 492.2 mg of radium in a Be can. This source was compared to NBS II and is used as a local calibration source in the continued use of the Macklin Sphere. Johnson estimates that recent measurements of (p,n) cross sections are accurate to better than 1%.[10]

In addition to its continued importance for measurement of neutron production cross sections, the Macklin Sphere as a prototype has good potential as a secondary standard. Source comparison with this detector can be made quick and precise since the BF_3 detectors make measurements of neutron emission rate simple and in "real" time as compared to Activated Bath methods. The efficiency can be raised to about 3% through use of $^{10}BF_3$ counters in place of the natural BF_3 detectors. The response curve for the detector is well understood. The response can be quantitatatively checked with high precision in the keV neutron energy range through the use of the associated activity method with $^{7}LI(p,n)^{7}Be$, $^{51}V(p,n)^{51}Cr$ and $^{57}Fe(p,n)^{57}Co$ as neutron sources.

I also want to mention in passing a second detector designed by R.L. Macklin and co-workers[8,12] at Oak Ridge. This detector can be made flat through appropriate tuning of the position of BF_3 counters in the moderator assembly. This detector has an efficiency of ∿30% and will be useful in applications where very high sensitivity is needed.

The Poenitz Detectors

1. The Grey Detector

An important group of black and grey neutron detectors has been developed and used by Poenitz.[13,15] The first of these detectors which Poenitz has called the "Grey Neutron Detector" consists of a homogeneous hydrogeneous material such as water, paraffin, or polyethylene with an entrance channel for a collimated neutron beam. The neutrons are thermalized in the moderator and subsequently captured in the moderator material. The capture γ- rays are detected at the surface of the moderator. Figure 3 shows a schematic diagram of a typical experimental setup for the use of this detector.

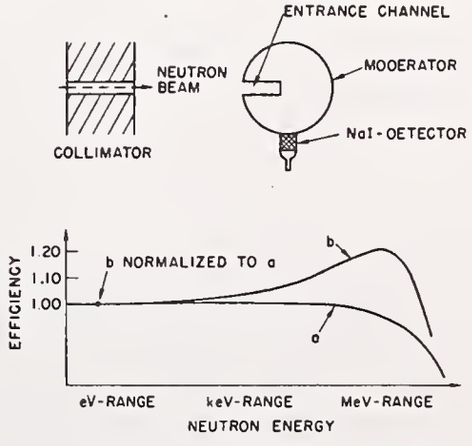

Fig. 3. Schematic diagram of the Grey Neutron Detector and a comparison of the efficiency response curve (b) with that of a manganese bath (a).

Poenitz has calculated the relative efficiency for the "Grey Detector" which exhibits a flat energy response over a wide range of energies. Comparisons of the relative efficency of this detector with that of a manganese bath are shown in the lower part of Figure 3.

The relative efficiency of the "Grey Detector" was measured by two different methods,[13] the associated activity method and a flux integration technique. Results showed agreement with calculated efficiency to within 2% for neutron energies below 1 MeV and showed somewhat larger deviations toward higher neutron energy.

The detector reported by Coates, et al.[14] uses the same operating principle, i.e. the ^{10}B-vaseline detector is a "grey" detector. In this latter case, the 478 keV γ-rays from the $^{10}B(n,\alpha\gamma)^{7}Li$ were detected. The time response of this detector is about 0.7 μ sec which is sufficiently fast for work with linac sources.

The energy range for which the Grey Neutron Detector appears to be most useful is the keV range. This detector has been used by Poenitz in several experiments for measurement of relative cross sections.[13,16] The precision of these measurements ranges around (2-3)% for keV neutrons.

2. The Black Neutron Detector

The "Black Neutron Detector" is a fast time-response detector (designed by W.P. Poenitz) for absolute neutron flux measurements.[15,17] The detector consists of a hydrogeneous scintillator material in the shape of a cube, cylinder or sphere. The neutron beam enters the detector system through a channel which terminates near the center of the detector volume. The light produced in the scintillation material is detected by several photo-multiplier tubes. A neutron entering the detector undergoes several successive collisions and loses most of its energy to hydrogen or carbon nuclear recoil energy. The comparison in the concept and energy response of a conventional scintillation detector and the Black Neutron Detector is illustrated in Figure 4. A very important difference is in the light pulse spectra in the two detectors. The energy spectrum for the Black Neutron Detector allows accurate extrapolation to zero pulse height because most of the energy of all neutrons is lost in the detector. Pulses counted above a low-set bias will account for almost all (90-95)% of the neutrons losing energy in the detector.

A monte-carlo computer code, Carlo Black,[17] for the purpose of evaluating a Black Neutron Detector of cylindrical shape was used by Poenitz. The parameters in the evaluation were the length of the cylinder, H, the radius of the cylinder, R, and the length of the re-entrant hole, H_C, the radius of the re-entrant hole, R_C, and the detection threshold, E_C. The prototype detector is filled with a scintillator having atomic densities of hydrogen and carbon of N_H and N_C, respectively. The calculated efficiency of this detector is shown in Figure 5. The structure in the calculated

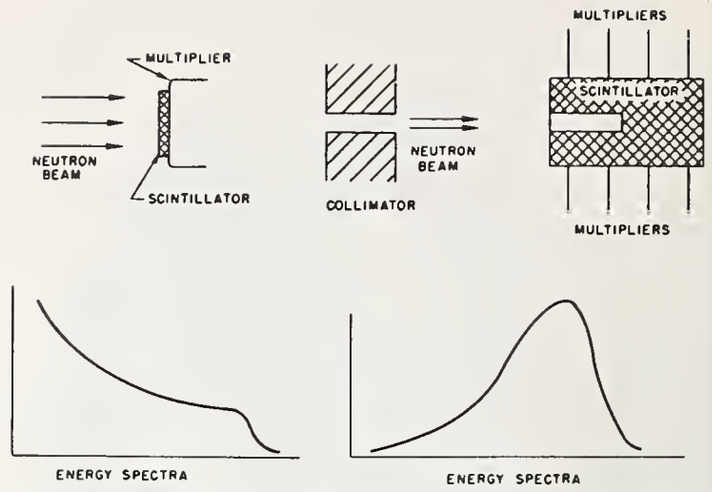

Fig. 4. Schematic comparison of a conventional scintillator detector (left) and the Black Neutron Detector (right).

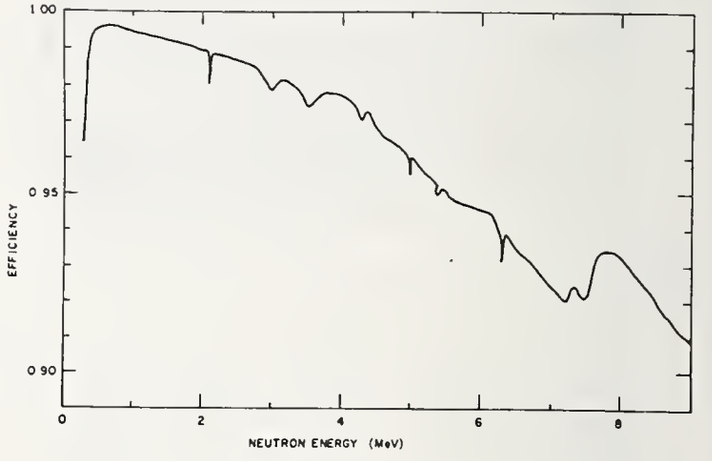

Fig. 5. The calculated efficiency of the Black Neutron Detector versus energy. The calculation was done with Carlo-Black with H = 40 cm, R = 13 cm, H_C = 15 cm, R_C = 1.26 cm, E_C = 200 keV, N_C = 4.2 x 10^{22} / cm^3, N_H - 7.04 x 10^{22} / cm^3.

efficiency curve is due to scattering resonances in carbon and gives fluctuations of 1% or so.

Figure 6 shows examples of calculated energy spectra at neutron energies of 1 MeV, 2.5 MeV, and 4 MeV. The important features are the low background counting rates at pulse heights below 20. Figure 7 shows experimental spectra obtained with the Black Neutron Detector. The two spectra at 1.5 MeV and 2.5 Mev show the desirable features of low background and good peak definition. The energy resolution spreading of the detector system causes the shape of the spectra to be smoother than the calculated curves of Figure 6.

The Black Neutron Detector has high sensitivity, flat response as a function of energy and a fast time response (~4-5 ns). This detector with a well known energy response can be used in time-of-flight experiments with pulsed or associated particle-tagged sources.

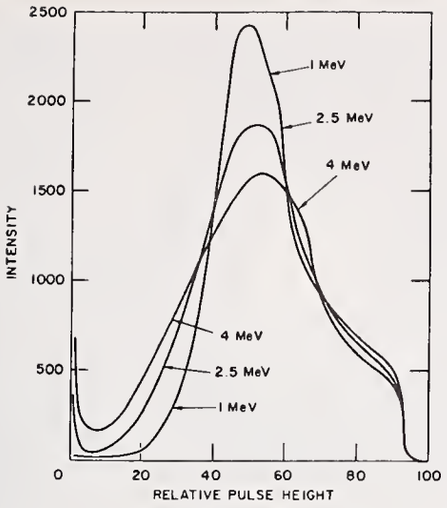

Fig. 6. Calculated (Carlo-Black) pulse-height spectra evaluated for three different monoenergetic neutron beams.

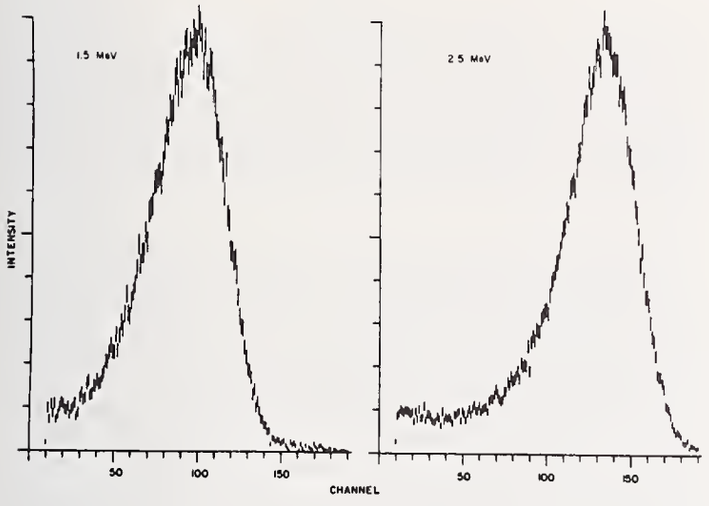

Fig. 7. Experimental pulse-height spectra for 1.5 and 2.5 - MeV neutrons.

The detector, designed for use with collimated beams, must be carefully shielded against stray neutrons and γ-radiation. Absolute measurements[15] with the Black Neutron Detector have been made to an accuracy of $\sim$2%.

3. The NBS Black Detector

Lamaze, Meier and Wasson[18] at the National Bureau of Standards have constructed a detector of a plastic scintillator after the Black Neutron Detector design of W.P. Poenitz.[15] This detector consists of a cylinder of NE 110 plastic scintillator 12.7 cm in diameter by 17.78 cm long with a re-entrant hole having a diameter of 2.54 cm and a depth of 5.08 cm. The scintillator is optically coupled to an RCA 8854 photomultiplier tube. A schematic diagram of the detector is shown in Figure 8.

The program Carlo-Black[17] was used to provide design criteria for the NBS Black Detector.

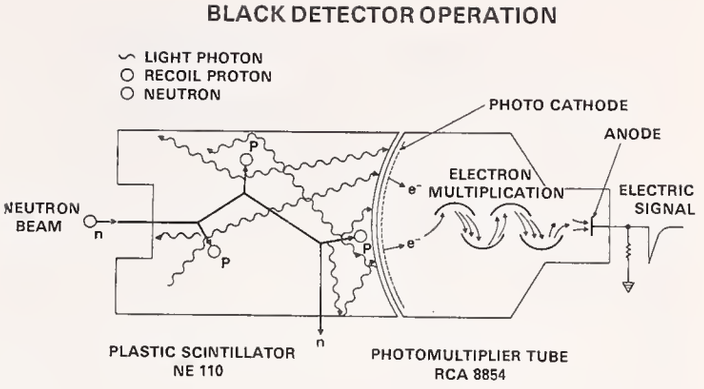

Fig. 8. Schematic of the NBS Black Detector showing the scintillator and the electron multiplier.

Fig. 9 shows the efficiency of this detector as a function of neutron energy for three different bias settings. It is seen that the response curves are very nearly flat on the energy interval between 200 keV and 1000 keV.

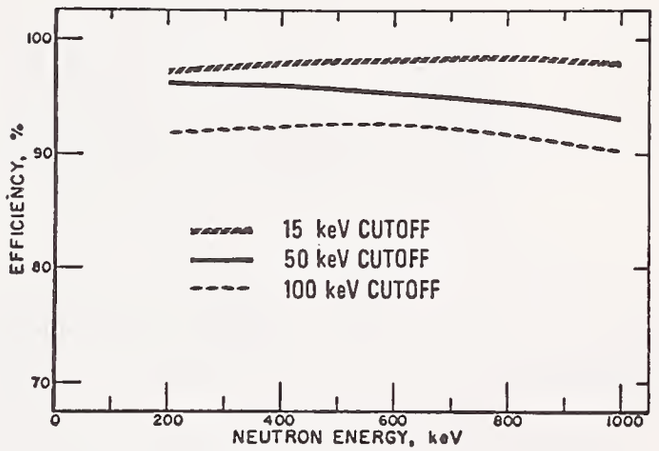

Fig. 9. Calculated efficiencies of the NBS Black Detector for different lower level cutoffs. Calculations were done with the computer program Carlo-Black.

At low neutron energies (<250 keV), only a small number of photons are produced in the scintillator and only a fraction of these produce photoelectrons. Therefore, the photoelectron statistics are important in the determination of the response below 300 keV or so. This effect is illustrated in Figure 10 which shows comparison of a calculated and experimental spectrum at E_n = 250 keV and 560 keV. The calculated curves were obtained using Carlo-Black[17] as modified by M. Meier[19] to calculate the spectral distributions at the two neutron energies. The modification is the explicit treatment of the Poisson statistics when N,

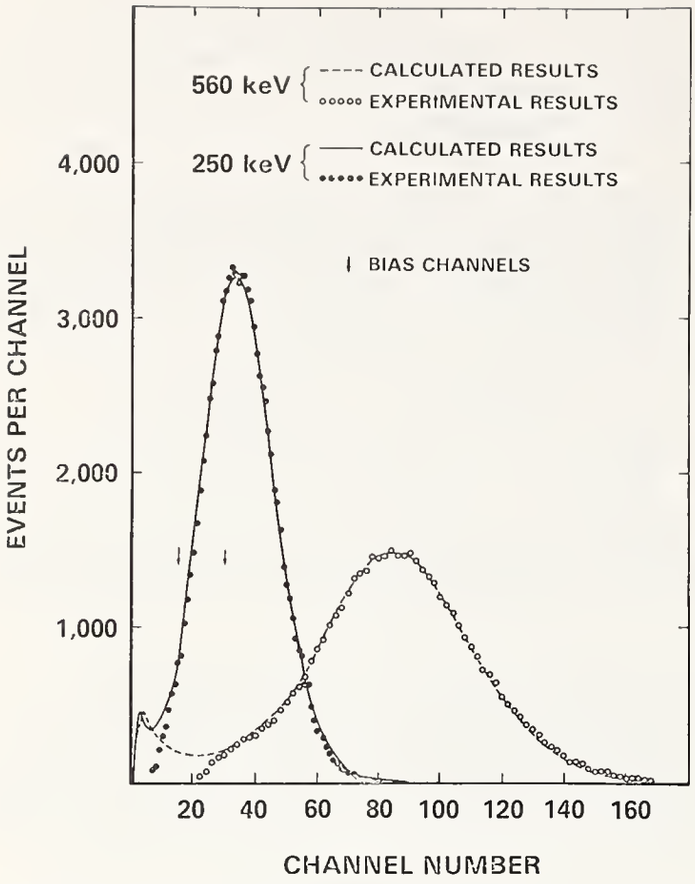

Fig. 10. Comparison of calculated and experimental recoil spectra from the NBS Black Detector at incident neutron energies of 250 keV and 560 keV. Calculations were done with Carlo-Black as modified by M.M. Meier for use with small N in the Poisson statistics.

the number of photoelectrons, is small. The result of Meier that the photoelectron production at low energies corresponds to about 15 keV/photoelectron is consistent with Cranberg's[20] findings.

The NBS Black Detector has an efficiency near 100% and has very fast time response (~5 ns). As is the case with the Black Neutron Detector built by Poenitz, this detector is designed for use with a collimator or beam defining device and must be well shielded. The detector is being used in both the Linac and Van de Graaff laboratories at NBS.

The Kentucky Polyethylene Sphere

The nuclear physics group at the University of Kentucky has developed a detector for use in the keV region. This detector has been briefly described in the Conference on Neutron Cross Sections and Technology held at NBS in 1975.[7,21] This detector was constructed primarily for the accurate measurement of total neutron production cross sections. The detector consists of a polyethylene sphere with a radius of 30 cm in which 8 $^{10}BF_3$ counters are radially installed. A picture of this detector is shown in Figure 11. The detector is designed so that it may be opened up for insertion of targets into a chamber at the center of the detector. The charged-particle beam from a Van de Graaff accelerator can be passed through the target and the resulting neutrons counted. The counter is covered with 1 mm of cadmium to reduce neutron background from the room.

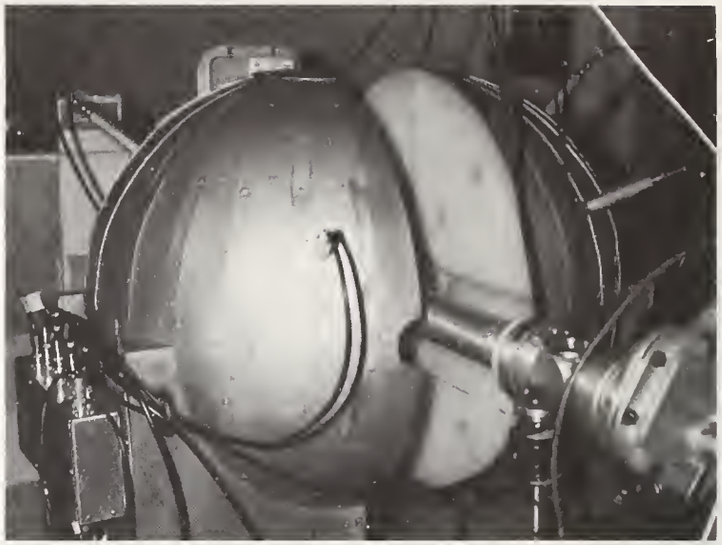

Fig. 11. The Kentucky polyethylene sphere detector. The two hemispheres are drawn apart. In operation the counter is closed.

The efficiency of this detector has been measured in the neutron energy range from 30 keV to 2.5 MeV. The resulting energy response curve is shown in Figure 12. Absolute efficiency measurements were made near 300 keV and 1.35 MeV. The results gave (0.55 ± 0.017)% and (0.56 ± 0.016)% respectively for the efficiency of the detector. The associated activity method was used in these efficiency measurements. A 35 cm^3 Ge(Li) detector was used to compare the gamma-ray yield from the residual ^{51}Cr and ^{57}Co produced in the calibrating

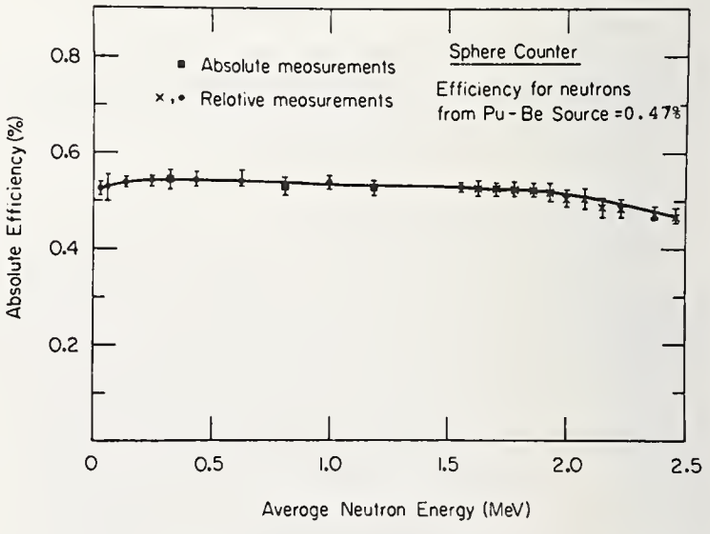

Fig. 12. The absolute efficiency of the polyethylene sphere counter as determined by the associated activity method.

targets of ^{51}V and ^{57}Fe, with standard sources of ^{51}Cr and ^{57}Co obtained from the National Bureau of Standards. Accuracy of the standards was ± 1.7%. The estimated accuracy of our measurements was ± 3%. Relative efficiency was measured using the $^{7}Li(p,n)^{7}Be$ reaction. In the energy range below an average of 1.5 MeV, the relative neutron yield as a function of neutron energy was determined using the ^{7}Be decay as observed from observation of the 478 keV γ-ray from ^{7}Li.[22]

Figure 13 shows a comparison of the $^{7}Li(p,n)^{7}Be$ excitation function as measured by Gibbons and Macklin[23] with the cross section measured with the polyethylene sphere detector. Agreement is very good up to a proton energy of 4.2 MeV. Toward higher energies, the yield observed with the polyethylene detector falls off relative to the yield observed with the graphite sphere counter. This fall-off of efficiency of the polyethylene counter relative to the graphite sphere is shown as a function

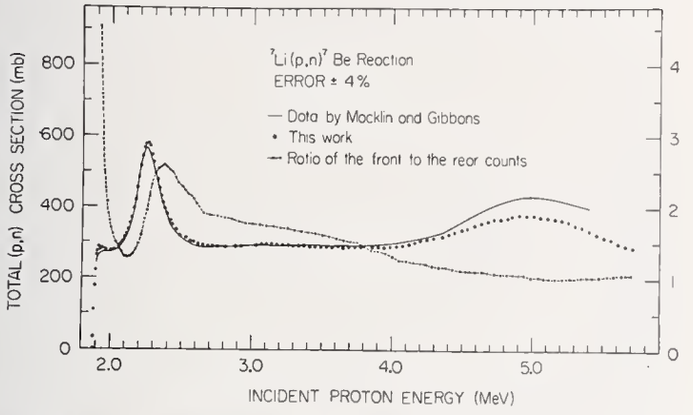

Fig. 13. Comparison of the total (p,n) cross section as determined with the polyethylene sphere and by Gibbons and Macklin in the Macklin Sphere.

of neutron energy in Figure 12. The decrease in counting efficiency for the polyethylene sphere is quite rapid above 2 MeV.

The falloff of efficiency toward higher energies is primarily a geometrical effect resulting from the radial placement of the $^{10}BF_3$ counters; this means that the fraction of the volume filled with detector decreases inversely as the square of the distance from the detector center. The average thermalization distance increases with neutron energy and the spatial distribution of thermal neutrons spreads radially. This latter effect partially compensates for the detector geometry. The key to the energy response (Fig. 12) is the placement of the $^{10}BF_3$ counters in their radial channels. Figure 14 shows counting rate as a function of counter position for three different average neutron energies. The three lines come very near to intersecting at the same point. If the counters are placed at 1.2 cm, the apparent difference in efficiency is about 1% for the three energies shown. Figure 12 shows that the flat response extends nearly to 2 MeV.

In addition to reasonably high sensitivity and flat response, the polyethylene sphere is quite insensitive to gamma-ray background. It has moderate sensitivity to neutrons coming

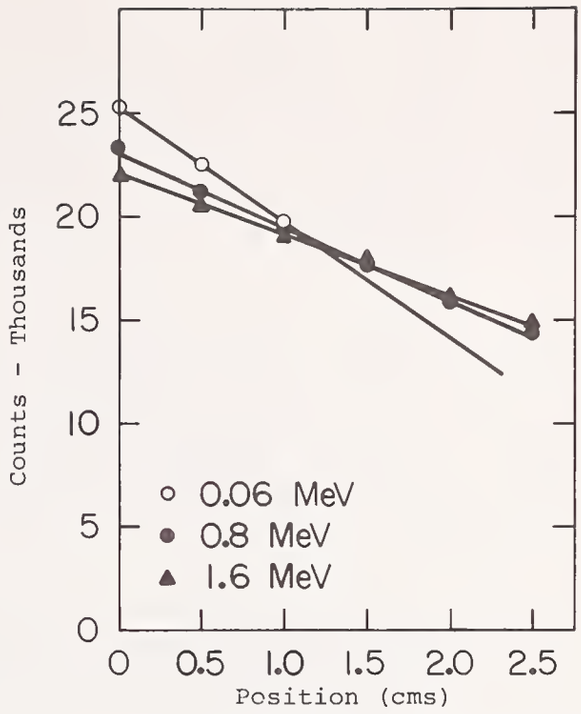

Fig. 14. The counting rate in the polyethylene counter as a function of counter position for three different average neutron energies. The detectors were placed at 1.2 cm for operation.

from surroundings. The time response is a few microseconds.

Now I want to turn briefly to the performance of the detector as a device for measuring total neutron production cross sections from nuclear reactions, such as (p,n)and (α,n), of interest in stellar nucleosynthesis and nuclear reactor design problems.

The detector and the γ-ray counter, Ge(Li), were used to measure the neutron yield for γ-ray count[21] from ^{51}Cr for the $^{51}V(p,n)^{51}Cr$ reaction at incident proton energies of 3 and 5 MeV. This ratio was constant to a precision of 0.5% indicating that a precise neutron count is given by the polyethylene sphere even though the ground state neutrons at a proton bombarding energy of 5 MeV is 3.4 MeV (Q = -1.534); and, the sphere efficiency is decreasing with energy above a neutron energy of 2 MeV. This precise result is obtained primarily because the neutron spectrum emitted in (p,n) and (α,n) reactions roughly follows a lumpy Maxwellian distribution.[24] The lumps correspond to individual excited states and groups of states. Such a spectrum is illustrated schematically by the dashed curve in Fig. 15. This dashed curve was derived from the time-of-flight spectrum shown, corrected for scintillator efficiency, and the assumption that the peak of the Maxwellian falls at about 0.5 MeV.[24] The time-of-flight spectrum was taken with a 1.3 cm plastic scintillator. Fewer than 10% of the neutrons emitted have energies higher than 2 MeV.

The energy range in which the efficiency of the polyethylene sphere is flat can be increased by the insertion of trimmer counters into the sphere. For the present applications, this has not been necessary.

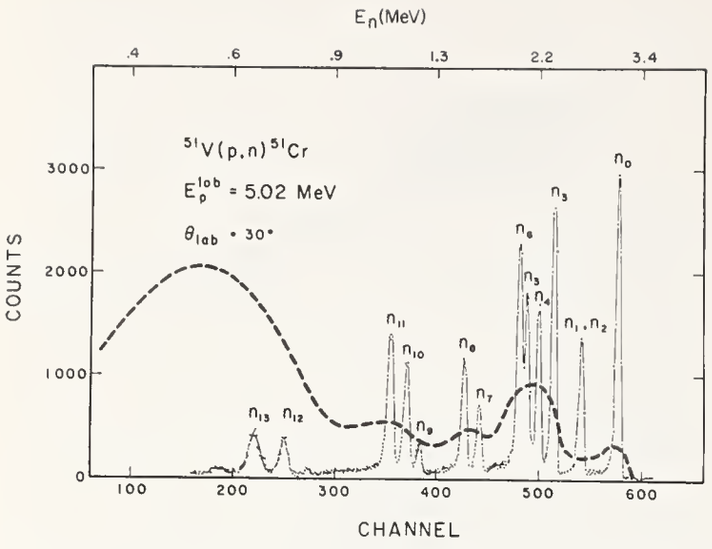

Fig. 15. Time-of-flight spectrum for neutrons from $^{51}V(p,n)^{51}Cr$. The dashed curve is a schematic representation of the neutron spectrum emitted at a proton bombarding energy of 5 MeV.

The LLL ^{6}Li Detector

A neutron detector for time-of-flight measurements in the 1 keV to 1 MeV energy range has been designed by Czirr and Shosa[25] at the Lawrence Livermore Laboratory. The design concept is an outgrowth of the detector designs of W.P. Poenitz.[15] Neutrons incident through a channel are moderated and captured in a 4 m^3 of compressed ^{6}LiH and the capture distribution is sampled with thin slabs of ^{6}Li glass scintillator. The mean capture time is approximately 100 nsec.

Figure 16 shows a schematic diagram of this detector. The outer dimensions of the detector were determined primarily by the available lengths of Li-glass slabs. Slabs 165 mm long can be reliably produced so the detector length was fixed at 320 mm. The design provides for use of two pieces of glass to sample each longitudinal detection zone. Photomultiplier tubes view the glass slabs end on. The radius of the sampled region used in the design model was 200 mm. The glass

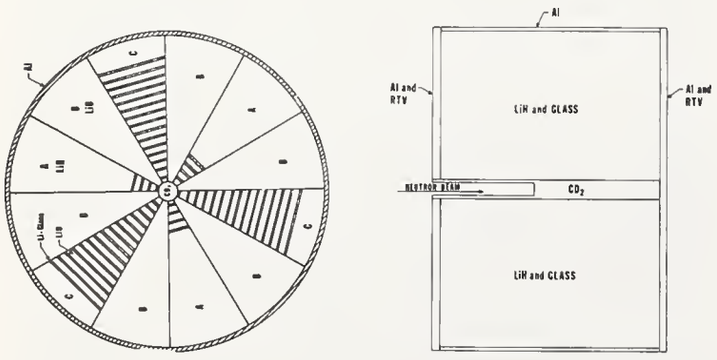

Fig. 16. Schematic diagram of the totally absorbing detector showing end-on and side views.

slabs were taken to be 2 mm in an effort to compromise between requirements of strength and good counting statistics and the requirement of small flux perturbations. The glass slabs were separated by 10 mm in the model. The radius of the entrance hole was chosen to be 10 mm in a deuterated-polyethylene, $(CD_2)_n$ scatterer with a radius of 14 mm. The optimum depth of the re-entrant hole in the $(CD_2)_n$ scatterer was found to be 115 mm.

The TARNP Monte Carlo transport code[26] which access the LLL cross-section library was used for the design calculations.

Figure 17 shows the calculated efficiency for the model detector. The efficiency is flat over the energy range from 1 keV to 1 MeV. The error flags are an estimate of the computational uncertainty at each point. The error in the shape of the efficiency curve is estimated as 0.7%. The computational accuracy is about 2% as shown in Fig. 17.

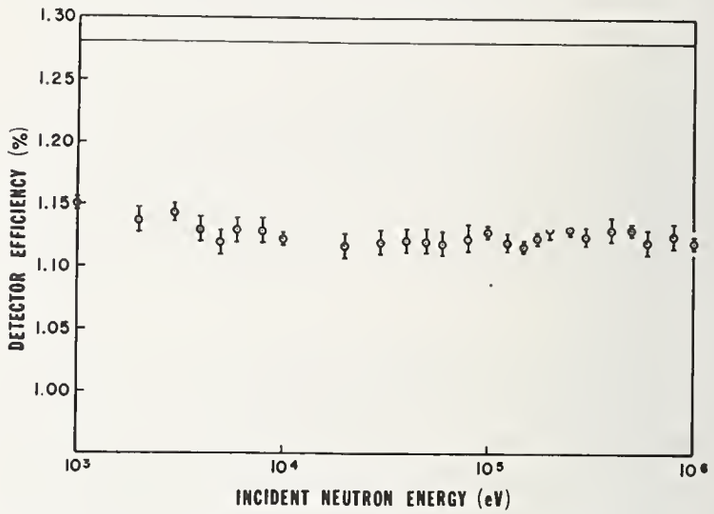

Fig. 17. Calculated efficiency of the LLL totally absorbing Time-of-Flight neutron detector. Calculation was done with computer program TARNP.

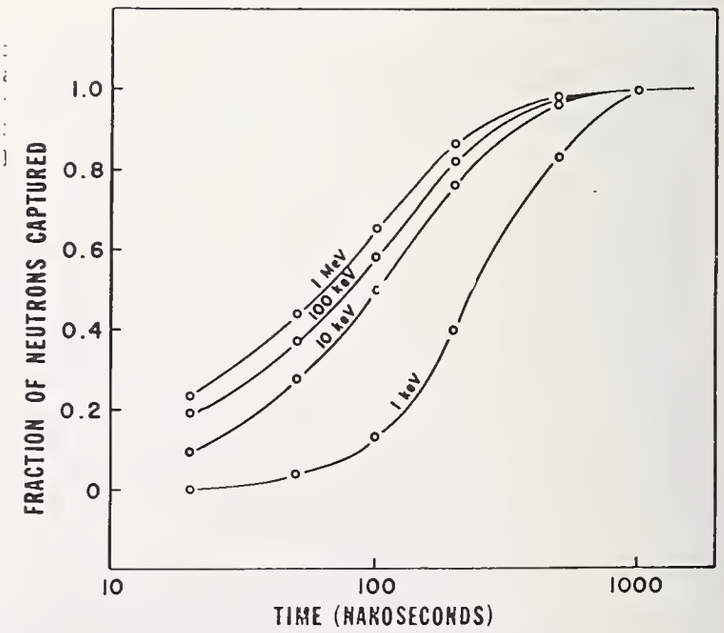

Fig. 18. Time response of LLL detector as a function of incident neutron energy.

The time response of the detector is shown in Fig. 18. Essentially all of the neutrons are captured in 1 μsec and about half are captured during the first 100 nsec. This time response is quite satisfactory for long flight paths such as encountered at Linacs.

This detector is novel and exhibits good characteristics. It should be well suited for use at linac neutron sources. The materials required for its fabrication tend to be expensive.

A Word About Collimators

The black and grey neutron detectors which have been discussed are capable of ultimate accuracy of better than 1% for measurement of neutrons originating in a target at the center. Usage of these detectors with collimated neutron beams has been extensive.[13-18] In the first use mode, the neutrons detected are the primary nuclear reaction products; in the second, neutrons produced in a neutron source are collimated and caused to react with a target. The neutron flux is measured with the black or grey neutron detector. These detectors can accurately count all neutrons which reach the central region of the counter near the end of the re-entrant channel. One of the largest potential sources of error is the perturbation of the neutron "beam" by the material between the neutron source and the detector. When collimation is used this perturbation takes two forms; first, the resolution function or energy definition is broadened and made less precise through energy losses in scattering from air, the target and the collimator material; and, second, a general background may be produced in the collimator materials which affects accuracy. An example of this is the production of 2.225 MeV γ-rays in hydrogen containing collimators which will affect detectors sensitive to γ-rays. Most of these γ-rays are emitted after the neutrons are moderated.

Spencer and Woolf[27] provide important guidelines for the construction of neutron collimators. Langdorf's[28] work remains as the most complete treatment of neutron collimation. Figure 19 shows a collimator for use at a Van de Graaff accelerator. As has been emphasized by Langsdorf,[28] one very important region in a collimator is the throat which is the most narrow part where neutrons are strongly scattered. The heavy shielding material near the center of the collimator (Fig. 19) serves two purposes. It is useful to have strong attenuation in the collimator throat; and, this material serves as a detector shield for the 2.225 MeV γ-rays produced by the neutron capture in hydrogen. The intensity of such γ-rays is large near the neutron source in hydrogen containing collimators.

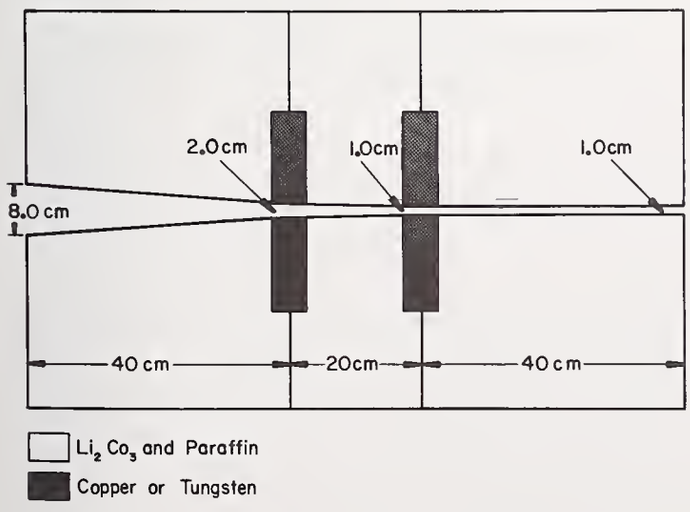

Fig. 19. A neutron collimator designed for keV neutrons.

Tests of a collimator 1 m long at the University of Kentucky by Cochran[29] have shown that excellent geometrical definition of the neutron beam can be achieved for neutrons with energies in the range of 250 - 750 keV. This work also shows that fewer than 5% of the neutrons in the collimated beam have energies differing from the primary beam by more than 25 keV. With proper design, it should be possible to further reduce this fraction. Detectors such as the Black Neutron Detector and the NBS Black Detector with fast time response reject all but a fraction of a percent of the wrong-energy neutrons by the time-of-flight discrimination. Even so these "background" neutrons remain a problem since their effect will depend on the target and reaction studied.

Further work on the transmission and beam quality of neutrons passing through such collimators is needed.

Summary

As counting devices for neutrons in the energy range between 1 - 1000 keV, the black and grey neutron detectors show high potential for ultimate accuracy. High accuracy levels can also be achieved in the MeV energy range. Such detectors are useful in two operational modes. First, they may be used to detect neutrons originating in their center. Second, they may be used to count the neutrons in a collimated beam.

With current techniques, the accuracy of such detectors can be made better than 1% for neutrons originating at the center of the detector. The accuracy limit with a collimated beam of neutrons is less well established. It is known that long, thin collimators provide neutron beams of high quality; both with respect to their geometrical definition and with respect to energy definition. Ultimate accuracy of measurement of the flux of collimated neutrons in the keV energy range with current techniques is estimated at 2%.

In the neutron energy range between 1 keV and 250 keV, the moderated detectors even with their corresponding slow time response are among the best detectors for measurement of neutron flux.

Acknowledgments

I want to express gratitude for the opportunity to make this presentation. Thanks go to J.B. Czirr, C.H. Johnson, R.L. Macklin, M.M. Meier, and W.P. Poenitz without whose help the review would not have been possible. Special thanks go to W.P. Poenitz.

*Work supported in part by the National Science Foundation and U.S.E.R.D.A.

References

1. H.H. Barschall, L. Rosen, R.F. Taschеck and J.H. Williams, Rev. Mod. Phys. 24, 1 (1952).
2. K.E. Larsson, Ariv. for Fysik 9, 287 (1954).
3. J.E. Perry, Jr., Fast Neutron Physics, Part I, J.B. Marion and J.L. Fowler, eds.; Interscience Publisher, New York, p. 623 (1960).
4. R. Batcherlor, in Proceedings of the Conference on Neutron Cross Sections and Technology NBS Special Pub. 299, Vol. 1, Wash., D.C. (1968), p. 89; J.H. Gibbons, Ibid. p. 111.
5. H.H. Landon, in Proceedings of the Conference on Neutron Cross Sections and Technology, Knoxville, Tennessee, U.S. A.E.C., Conf. 710301, p. 528 (1971).
6. Proceedings of the Symposium on Neutron Standards and Flux Normalization, October 21-23, 1970. Available as CONF-701002 from National Technical Information Service, U.S. Department of Commerce, Springfield, Virginia 22161.
7. Proceedings of the Conference on Nuclear Cross Sections and Technology, National Bureau of Standards, NBS Special Publication 425 (1975). Available from U.S. Government Printing Office, Washington, D.C. 20402.
8. Proceedings of the International Conference on the Interactions of Neutrons with Nuclei, University of Lowell, Lowell, Massachusetts (1976). CONF-760715-P2.
9. R.L. Macklin, Nucl. Instr. 1, 335 (1957).
10. R.L. Macklin and J.H. Gibbons, Phys. Rev. 109, 105 (1958); J.H. Gibbons and R.L. Macklin, Phys. Rev. 114, 571 (1959); C.H. Johnson and R.L. Kernell, Phys. Rev. C 2, 639 (1970); C.H. Johnson, J.K. Bair, C.M. Jones, S.K. Penny, and D.W. Smith, Phys. Rev. C 15, 196 (1977).
11. C.H. Johnson, Private Communication, (1977).
12. R.L. Macklin, F.M. Glass, J. Halperin, R.T. Roseberry, H.W. Schmitt, R.W. Stoughton, and M. Tobias, Nucl. Instr. and Meth. 102, 181 (1972).
13. W.P. Poenitz, Nucl. Inst. and Meth. 58, 39 (1968); W.P. Poenitz et al., J. Nucl. Energy 22, 505 (1968); H.O. Menlove and W.P. Poenitz, Nucl. Sci. Eng. 33, 24 (1968); W.P. Poenitz, Nucl. Instr. and Meth. 72, 120 (1969).
14. M.S. Coates, G.J. Hunt, C.A. Uttley, and E.R. Rae, Reference 6, p. 401 (1970).
15. W.P. Poenitz, "Neutron Standard Reference Data", International Atomic Energy Agency, Vienna (1974); W.P. Poenitz, Nucl. Inst. and Meth. 109, 413 (1973).
16. W.P. Poenitz, Nucl. Sci. and Eng. 53, 370 (1974).
17. W.P. Poenitz, ANL-7915, Argonne National Laboratory (1972).
18. G.P. Lamaze, M.M. Meier, and A.O. Wasson, Reference 7, p. 73 (1975).
19. M.M. Meier, Private communication (1977).
20. L. Wishart, R. Plattner and L. Cranberg, Nucl. Instr. and Meth. 57, 237 (1967).
21. K.K. Sekharan, H. Laumer, B.D. Kern,and F. Gabbard, Nucl. Inst. and Meth. 133, 253 (1976).
22. M. Mutterer, Reference 6, p. 452 (1970).
23. J.H. Gibbons and R.L. Macklin, Phys. Rev. 114, 571 (1959).
24. J.M. Blatt and V.F. Weisskopf, Theoretical Nuclear Physics, John Wiley, New York (1952), p. 365 ff.
25. J.B. Czirr and D.W. Shosa, "A Totally-Absorbing Time-of-Flight Neutron Detector." Lawrence Livermore Laboratory, Livermore, California 94550. Preprint UCRL-79089.
26. Ernest F. Plechaty and John R. Kimlinger, TARNP: A Coupled neutron-photo Monte Carlo transport code, UCRL-50440, Vol.14 (1976).
27. L.V. Spencer and S. Woolf, Nucl. Instr. and Meth. 97, 567 (1971).
28. Alexander Langsdorf, Jr., in Fast Neutron Physics, Part I, J.L. Fowler and J.B. Marion, eds. (Interscience Publishers, Inc., New York, (1960) p. 721.
29. J.L. Cochran, M.S. Thesis, University of Kentucky (unpublished).

ASSOCIATED PARTICLE METHODS

Michael M. Meier

Developments in the associated particle method for the last ten years are summarized with emphasis on the reactions $^{3}H(d,n)^{4}He$, $^{2}H(d,n)^{3}He$ and $^{3}H(p,n)^{3}He$. Recent progress on the associated particle calibration of a black detector in the energy range 250 to 1000 keV is reported. Current accuracies for the time uncorrelated and time correlated approaches are noted and prospects for future improvement are estimated.

(calibration; efficiency; neutrons; neutron beams; neutron flux; ^{3}H, ^{2}H, ^{4}He, ^{3}He, protons)

Introduction

The associated particle technique (APT) has been used as a monitor of neutron flux for about thirty years and has been discussed in several reviews of neutron flux monitoring techniques.[1-3] This survey includes major developments in the method utilizing the $^{3}H(d,n)^{4}He$, $^{2}H(dn)^{3}He$ and $^{3}H(p,n)^{3}He$ reaction from 1970 to the present. These reactions have been used for flux monitoring at energies between about 200 keV and 25 MeV.

The APT has been used in two rather different ways and there are distinct advantages associated with each. In the first, the charged particle reaction products are collimated and counted in a detector, and the neutron flux is then calculated for the corresponding neutron angle. This method has the advantage that the electronics can be rather simple, needing only to identify the charged particles with which the neutrons are associated. Also, if the neutron flux does not change rapidly with angle, or if its angular behavior is well known, then the neutron detector or sample can subtend a large solid angle. This approach is also useful when the neutron detection system is not amenable to fast timing techniques or when high count rates associated with large solid angle are necessary.

Essential to the success of the method is accuracy in measuring the effective solid angles for both the neutron detector and the charged particle collimator. Angle measurement is also critical, since the differential ratio of solid angles enters into the calculation and may be a rapidly varying function of angle. If the neutron detector subtends an appreciably larger solid angle than the one associated with charged particle detection a correction dependent on the differential cross section may be necessary. A further problem is the correction for background neutrons which are not associated with the direct flux.

The second technique correlates the detected neutron with the charged particle of interest by coincidence or time of flight methods. One is restricted obviously to detectors which have fast response, although in principle they need only be fast relative to the data acquisition rate. The neutron detector must also be larger than the associated neutron cone, which normally implies that the extent of this beam must be experimentally determined.

This usually restricts the size of the charged particle solid angle and with it the associated neutron production rate. It is also clear that this is a calibration of only a part of the detector and uniformity may be a problem. Advantages which accrue are the elimination of geometry determination and suppression of neutron backgrounds by coincidence or time of flight. Once the experiment is properly set up there is a minimum of calculation and correction to the data. The efficiency of a detector is simply the ratio of the correlated rate in the neutron detector to total associated particle counts. In the following, these two methods will be referred to as the "time-uncorrelated" and "time correlated" methods respectively.

$^{3}H(d,n)^{4}He$ Reaction

Several properties of this reaction make it attractive to use for absolute flux monitoring. The + 17.6 MeV Q value provides a source of 14 MeV neutrons and associated 4 MeV alpha particles which are therefore well separated in energy from scattered deuterons at bombarding energies of only a few hundred keV. The attractiveness of this technique to a laboratory with a low energy accelerator is enhanced by the 110 keV resonance with a peak value of about 400 mb sr^{-1}. Also other (d, charged particle) reactions in target components, e.g. titanium or zirconium and backing materials, which would provide background for the alpha particles are strongly suppressed by the Coulomb barrier. There are also serious difficulties encountered in the use of low bombarding energies and thick tritiated targets. First, the identification of alpha particles is complicated by the presence of an intense Coulomb scattered deuteron background which is inversely proportional to E_d^2. If detected, these deuterons can cause saturation of electronics, baseline shifts due to pulse pileup and other problems associated with high rates. One simple technique[4] to eliminate this problem has been to interpose a metal foil between target and detector. The foil thickness is selected to be slightly greater than the deuteron range, permitting the alpha particles to pass through with slightly increased straggling.

Another problem arising from Coulomb scattering is the broadening of the neutron cone beyond the limits kinematically defined by the alpha detector. At low bombarding energies this effect is largest and predominately due to deuteron scattering. For experiments in which the neutron beam must be smaller than the detector, this effect must be taken into account.

Another set of problems arises because of the time dependence of the tritium distribution in a solid target. For these targets, where the total beam power is dissipated in the target and substrate, tritium is depleted from the surface layer and the effective mean deuteron energy is decreased. For a fixed charged particle detection angle, the associated neutron angle increases (see, for example Figure 2, Ref. 4) and thereby causes misalignment of the neutron detector relative to the beam center. This problem is not usually important for a time uncorrelated experiment, since the laboratory (d,n) cross section varies by less than a percent for a typical five degree change in neutron angle.

Finally, for time uncorrelated experiments, background neutrons may result from scattering in the target and beam line structures and from production via (d,n) reactions. In particular, drive in deuterons are always a source of background for experiments using a solid target. References 5, 6 and 7 are recent examples of the APT with low energy deutrons for measurement of fission cross sections, (n, charged particle) spectrometry and for evaluation of collimetor design.

If one wishes to extend the energy range of neutrons away from 14 MeV the use of higher bombarding

energies becomes necessary. Although the Coulomb scattering effects are thereby reduced, other difficulties become important. Specifically, beam power is usually increased, accelerating the tritium loss and the consequent neutron angle change. Also, other (d, charged particle) and (d,n) reactions contaminate the alpha particle and neutron spectrum respectively. A unique scheme employed by Cookson et al.[8] utilizes a tritium gas target chamber to obtain neutron energies between 14 and 25 MeV. Many experimental difficulties are eliminated by utilizing such a system. First, problems associated with the target backing disappear. The Coulomb scattering, neutron beam broadening and neutron angle migration are all essentially eliminated. Background in the charged particle spectrum is reduced since the alpha particle collimation shields the surface barrier detector from reactions in the entrance and exit foils and from the beam dump where (d charged particle) reaction products would be produced. This apparatus has been used to obtain an absolute calibration for the efficiency of a 2.5 cm thick by 10 cm diameter NE-213 scintillator. Neutron background originating in foils and beam defining slits is small and easily corrected since the experiment uses the time-of-flight method for obtaining the detector efficiency.

$^{2}H(d,n)^{3}He$ Reaction

Many of the remarks concerning the $^{3}H(d,n)$ reaction at low bombarding energies apply to the $^{2}H(d,n)$ reaction as well. For acceleration voltages lower than 500 keV monoenergetic neutrons spanning the energy range 2 to 3.5 MeV can be produced with appreciable yield. In at least two important respects this is a less favorable reaction. First, the competing $^{2}H(d,p)^{3}H$(Q = 4.033 MeV) complicates the spectrum of ^{3}He from the (d,n) reaction (Q = 3.269 MeV), the triton and ^{3}He differing in energy by only a couple hundred keV for energies below 500 keV bombarding energy. Second, the ^{3}He energy is usually less than 1 MeV, giving rise to Coulomb scattering problems for the recoiling particles as well as the bombarding deutrons. Apart from the degradation of energy resolution in the ^{3}He peak, this effect also contributes to the cone broadening and migration. Finally, the cross section for this reaction is only 20 mb sr^{-1} at 500 keV and increases with increasing energy, becoming 90 mb sr^{-1} at 10 MeV bombarding energy.

Use of a deuterium gas target for this reaction has been employed with the chamber discussed above. The benefits of a gas target and higher bombarding energies are the same as those discussed for the $^{3}H(d,n)$ reaction plus the fact that the yield increases with increasing energy. A transmission surface barrier detector is used in this experiment in order to detect the ^{3}He particles in the presence of tritons with almost identical energy. The thickness of the detector is selected to stop ^{3}He particles and allow the tritons to pass through, losing only a fraction of their energy. Breakup and other reactions that produce neutrons are not a problem since the experiment time correlates charged particles and neutrons.

Applications of the APT have been made at bombarding energies below 500 keV by employing electrostatic[9] and magnetic[10] analysis of the reaction products to eliminate scattered deuterons and tritons. Foils were used to stop the scattered deuterons for an experiment[11] at 150 keV bombarding energy although background in the charged particle spectrum is a difficult problem under these conditions.

Bartle and Quin have used a surface barrier detector ΔE - E pair.[12] The ΔE detector has a thickness equal to the range of the ^{3}He particles. Tritons and elastically scattered deuterons are transmitted and detected in the E detector which produces a veto for data accumulation. To reduce the Coulomb scattering a deuterated polyethylene target 0.5 μm thick is used in a transmission position. Target rotation extends the lifetime to about 100 hrs with a 0.5 μA beam collimated to a 2 mm diameter. Background in the charged particle spectrum becomes a problem when the $^{12}C(d, \alpha_0)\ ^{10}B$(g.s.) alpha particles begin to interfere with the ^{3}He peak. This background can be reproduced by using a carbon film of similar thickness in place of the polyethylene. A simple stripping technique is then sufficient to separate the ^{3}He peak. This system has been used to produce calibrated neutron beams from 2 to 10 MeV.

Other applications of the $^{2}H(d,n)$ reaction include a calibration[13] of a neutron detector in the energy range 25 to 60 MeV. Also, a novel approach to the time uncorrelated method has been used by Ryves and Sharma.[14] Here the $^{2}H(d,p)$ protons are monitored at an angle where (d,p) and (d,n) cross sections are comparable.

$^{3}H(p,n)^{3}He$

This reaction has been used extensively in the past decade, its attractiveness stemming largely from the possibility of monitoring flux at energies as low as 100 keV. To obtain energies this low the associated ^{3}He particles must be detected at angles on the order of 10^{0}, where the ratio of Coulomb to (p,n) cross section is 10^{5}. It is necessary to cope with these conditions in order to obtain ^{3}He particles with sufficient energy to escape the tritiated target and be detected unambiguously. Under these "favorable" conditions the energy spread of 1 MeV ^{3}He's is 15% for a 100 $\mu g/cm^{2}$ titanium layer. Again, the neutron cone is broadened, this time almost exclusively on account of the recoil particle scattering. Apart from the large elastic proton background, inelastic protons from the target and collimating surfaces and tritons from elastic scattering $^{3}H(p,t)$ are present in the charged particle spectrum.

Fort and co-workers[15] have used this technique for measurements in the range 100 to 500 keV. Transmission targets 200 $\mu g/cm^{2}$ thick are used and by employing sequential electrostatic and magnetic fields the separation of ^{3}He particles from background is very clearly accomplished. The solid angle for this technique is rather small, limiting the count rate, but providing a consequent advantage. The apparatus can be turned to accept a very limited band of ^{3}He energies and in this way actually select those ^{3}He particles which have undergone a minimum of Coulomb scattering in the target. By operating in this fashion the angular and energy spread of the neutron cone can be minimized.

This system has been used to calibrate the efficiency of a ^{6}Li - loaded glass scintillator. The measurement was complicated by the necessity for making a large multiple scattering correction in the glass to extract the ^{6}Li cross section. This calculation included a Monte Carlo calculation of the Coulomb scattering of the ^{3}He and its effects on the energy spread and angular broadening of the associated neutron beam. The largest uncertainty in this measurement was for the conversion of the efficiency as measured at a distance of 5 cm from a point source to that which would result in a parallel beam.

Liskien, Paulsen and co-workers[16,17,18] have combined an electrostatic deflector and a pulsed beam time of flight system to produce calibrated beams between 250 keV and 1 MeV. The deflection is used to suppress the elastic proton rate by sweeping the

$^3He^{++}$ into an offset surface barrier detector. A gate is generated by particles which have the source to detector flight time appropriate for a ^3He particle. This logic signal is then used to generate gated pulse height spectra for the surface barrier detector.

Experiments done with this apparatus have been done using the time uncorrelated approach. As previously mentioned, the calculation of flux for this case involves determination of the effective solid angle for charged particle collimation, solid angle of neutron detection and $(d\Omega_{^3He}/d\Omega_n)$. That careful measurement of these quantities is essential is illustrated by the fact that $(d\Omega_{^3He}/d\Omega_n)$ varies by 5% for a one degree change in the ^3He detection angle. The use of deflection complicates the time uncorrelated measurement in two ways. First, assurance must be obtained that all the $^3He^{++}$ which are collimated into the deflection system are, in fact, detected by the solid state detector. This can be ascertained by varying the deflection voltage and operating on the plateau of counting rate. Also, since neutral and singly-ionized ^3He are associated with the flux at the neutron detector, a correction of order 10% must be made. The latter can be partially checked by experiment. By varying the deflecting field and using a 2 mm collimator Paulsen, Liskien and Cosack[18] have measured the relative $^3He^+$ to $^3He^{++}$ yields with their associated particle system. These measurements agree well with calculation and give an added measure of confidence to the correction. Excellent agreement was obtained using this method to calibrate a proton recoil proportional counter.

Leroy has used the associated particle apparatus described earlier in the time uncorrelated way.[22] By properly tuning the electrostatic - magnetic analyser, it is possible to eliminate to first order the effects of spatial spread of the $^3He^{++}$ beam which is due to its energy dispersion. Because of this, the effective solid angle of the ^3He beam can be increased and a larger corresponding solid angle of neutron flux can be measured. Count rates a factor of 50 to 100 higher than with the time correlated technique are possible with this method. The system has been used to check the calibration of a long counter which had been previously calibrated with a $MnSO_4$ bath. The calibrations are in good agreement within the $\pm$ 2% error bars.

At NBS we have used a setup similiar to Liskien's, employing pulsed beam and electrostatic deflection to identify the ^3He particles. Two chambers for detection of recoil particles at 10° and 25° are used to cover the range of neutron energies 250 keV to 900 keV. The Coulomb scattering is not severe at 25°, and no electrostatic deflection is used there. A two parameter data analysis system is now used for obtaining the ^3He data, providing an easy to use method for background determination. Figure 1 shows such a spectrum from an experiment where electrostatic deflection is used. Each of the 32 time channels has a width of about 7ns and is comprised of a 128 channel pulse height spectrum. The background under the peak is about 5% of the ^3He rate and can be very accurately determined by gating the spectrum with a logic signal generated by neutron detection. This method provides a powerful technique for determining the ^3He lineshape. It is especially useful in cases where no deflection is used and the ^3He peak can be incompletely resolved from tritons from proton elastic scattering, T(p,T).

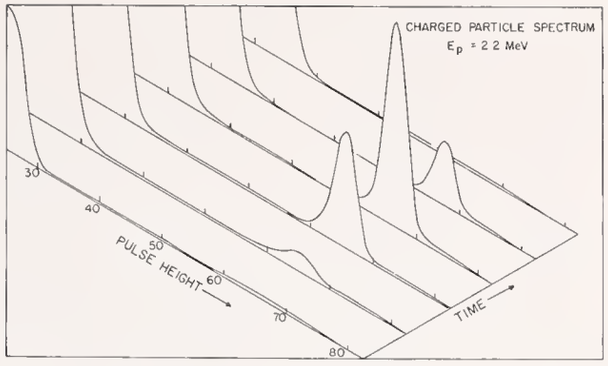

Figure 1. Charged particle spectrum for 2.2 MeV protons. The resolved group is ^3He from $^3H(p,n)^3He$

The system has been used to calibrate a black detector[19] which has a response calculable by Monte Carlo technique. For the calibration the detector is placed at the appropriate angle with the front face 11 cm from the target. The anode signal from the photomultiplier is supplied to two linear gates which are gated by logic signals generated by ^3He events. The first gate operates normally, opening for 200 ns to permit the neutron event to be analysed when an associated ^3He event occurs. The second gate opens one microsecond earlier corresponding to the preceding proton pulse and thereby measures accidental background that is not physically correlated with true ^3He events.

After subtracting this background, the reduced spectrum is normalized in area and channel width so as to be directly comparable to the Monte Carlo calculation. The program used is "CARLO BLACK"[20] by W. P. Poenitz modified to include the effects of Poisson statistics for photoelectron production at the photocathode. Figure 2 shows data taken at 250, 500, 700 and 880 keV and the corresponding Monte Carlo calculations. The data were all obtained under the same conditions and in particular no gains or bias voltages were changed in the neutron electronics. In reducing the data, the same bin width conversion factor was used for all energies so that the agreement between experiment and calculation could be compared as a function of energy. The Monte Carlo generated response functions are shown as smooth curves for each energy in the figure. Two curves are shown for each energy, corresponding to levels of photoelectron production which differ by 50% for a given light output.

These comparisons are very encouraging in that calculation and experiment qualitatively agree for a single set of parameters for all energies. The spreading of the peak seems to be well described by a single Poisson parameter between the two shown here and the peak amplitude shifts as calculated. This latter indicates that the light tables used are valid in a relative sense over this energy region. The efficiencies for the detector when a bias corresponding to channel 20 is chosen are compared for calibration and calculation in Figure 3. The agreement seems acceptable at the 2.5% level.

The black detector is now being used as a flux monitor in absolute cross section measurements and for dosimetry at the NBS Van de Graaff. Our confidence in the system is enhanced by the understanding we have obtained in bringing experiment and calculation into the detailed agreement shown above.

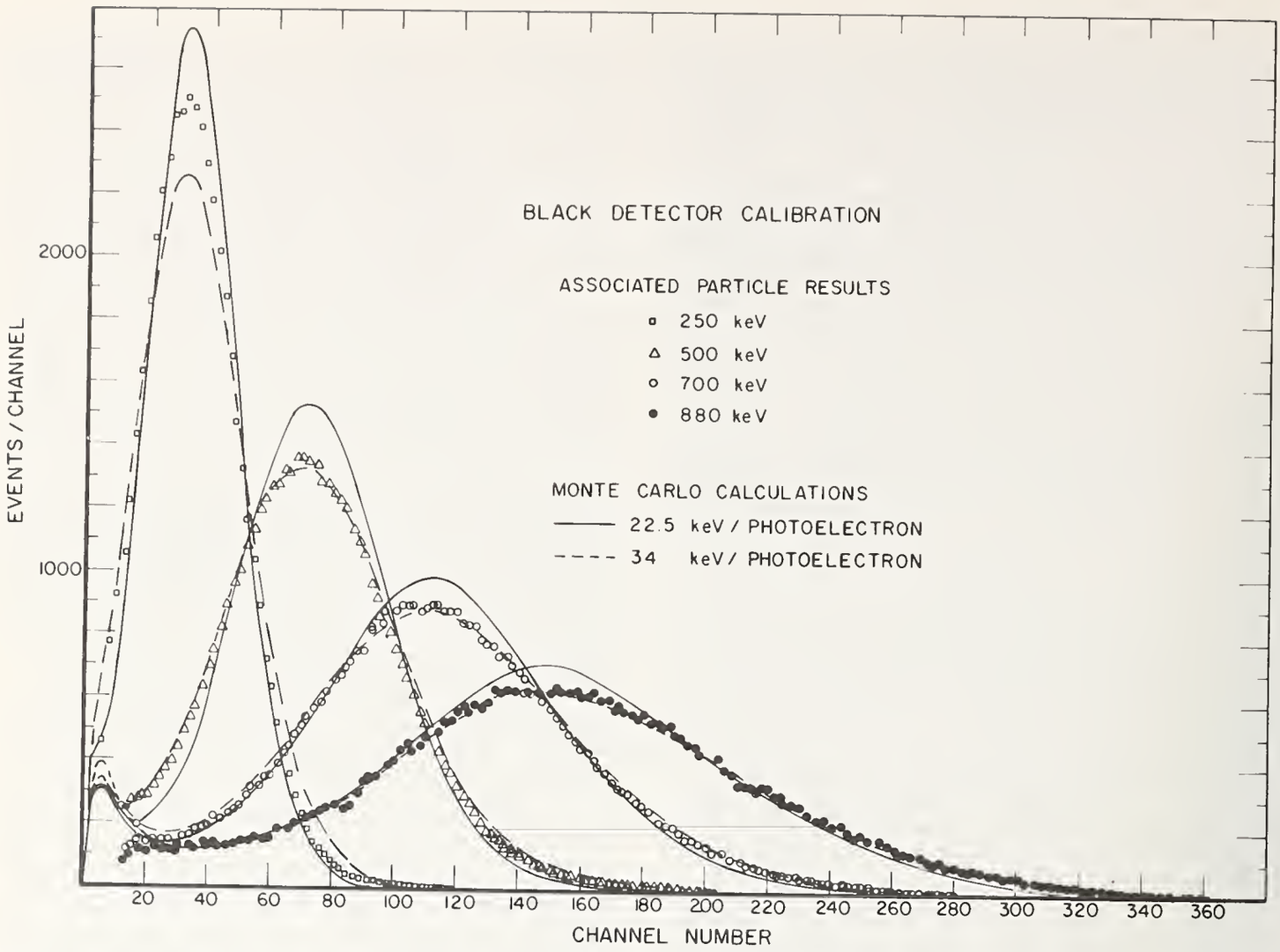

Figure 2. Experimental and calculated response functions for the black detector

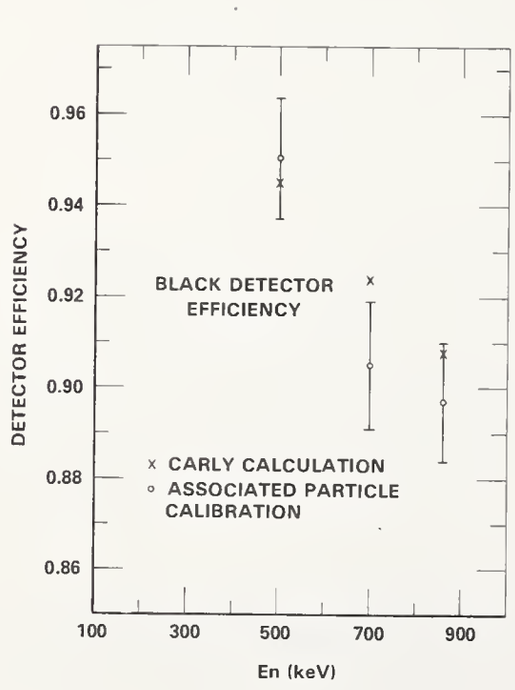

Figure 3. Measured and calculated detector efficiencies for the black detector

Conclusion

It is perhaps worthwhile to summarize by reviewing the present APT accuracy and to speculate on future improvements. The best accuracies obtainable with the time uncorrelated method have been on the order of 3%. A major limitation of this method, as mentioned previously, is the difficulty in determining the solid angles for neutron and charged particle detectors. Uncertainties for the latter are quoted to be 0.5%. A neutron detector in a divergent beam with finite source dimension may be even more difficult. Without some breakthrough in this area it is unlikely that accuracies much better than 1% overall will be obtained.

For the time correlated method the accuracy is limited by the details of the particular reaction considered. For $^{3}H(d,n)$ Cance and Grenier estimate their uncertainty in the APT to be 0.1%, only dependent on counting statistics of the alpha particles. This impressive accuracy is a good bit better than can be expected for sample assay or efficiency calculation in the near future. It is probable that experimenters will therefore attack these latter problems rather than improve this accuracy level.

The $^{2}H(d,n)$ reaction with a gas target has the potential for a very high ultimate accuracy. ^{3}He identification is quite unambiguous with detectors that transmit the competing tritons. Also, the Coulomb scattering which disperses the neutron beam is due only to the tritium and not to any intervening foils. The accuracies obtained in a scintillator calibration have

been about 2%, due mostly to uncertainties in extending the calibration over the complete surface of the detector. Presumably the accuracy could be considerably improved in the calibration of a detector with a re-entrant hole or in a cross section measurement where sample assay and uniformity were well known.

The $^{3}H(p,n)$ reaction has a current accuracy of 1 - 3% using the time correlated approach. Some of this uncertainty is due to problems not inherent to APT, but to sample and geometric difficulties. A good example is the non-trivial problem of converting an efficiency in a divergent beam back to the normal parallel beam situation. APT measurements will, as a rule, have such detector or sample problems and it would be inappropriate to attempt a listing of all of them here. There are two areas of concern specific to the APT which are common to all $^{3}H(p,n)$ applications (and to some extent the other two reactions) and which now limit our use of the method. First is the identification of charged particles. This has been done with an accuracy of 0.1% using very sophisticated deflection systems[15] but at a large sacrifice in count rate. At NBS we now cope with a 5% background known to 20% accuracy and can obtain with some effort 1% ± 0.5%.[21] The technique of using the neutrons to gate the charged particle spectrum and thereby determine the lineshape has been mentioned above. We plan to combine this method with a computer data collection system that utilizes "tagging" for very accurate determination of background. It is likely that we can obtain better than 0.2% accuracy in charged particle background in this way.

A second problem is somewhat less tractable. Figure 4 shows the angular profile of our neutron beam for two different targets with a ^{3}He energy of 1.2 MeV

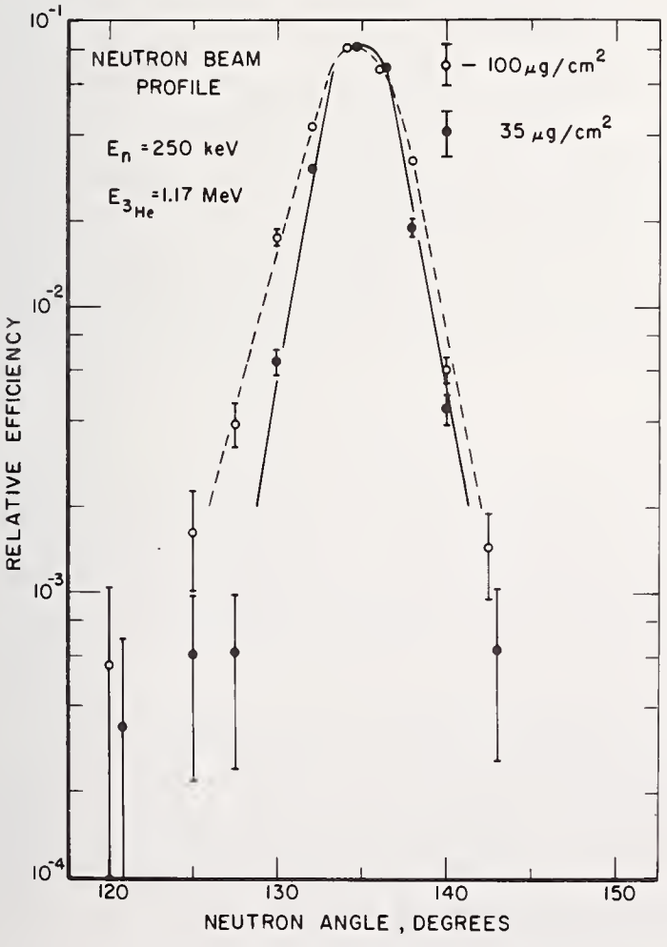

Figure 4. Spatial profile of associated neutron beam for two targets of different thickness

where the Coulomb scattering is rather severe. A problem that ultimately limits accuracy is the question of how many associated neutrons are found outside the cone defined by a given detector or sample. Such neutrons arise from scattering by the chamber walls and by cone broadening due to Coulomb scattering. The former are usually calculable, although for our 0.8 mm aluminum wall the correction is on the order of one percent.

One way to experimentally check on the Coulomb scattering problem is to perform the measurement with differing target thicknesses. We have checked our black detector calibration and do not find differences at the 2% level for the targets represented in the figure. Tuning the electrostatic analyser to select ^{3}He's which have undergone different amounts of Coulomb scattering might also provide some measure of this effect. It is clear that both the above problems could be diminished by the development of new targets, for example, tritium gas with very thin windows or tritiated polyethylene.

References

1. H. H. Barschall, L. Rosen, R. F. Tascek and J. H. Williams, Rev. Mod. Phys. 24, 1 (1952).

2. J. E. Perry, Fast Neutron Physics, Vol. 1, J. B. Marion and J. L. Fowler, Interscience Publisher, New York (1960).

3. R. Batchelor, Neutron Cross Sections and Technology, NBS Special Pub. 299, Vol. 1, Washington, D. C. (1968).

4. H. Marshak, A. C. B. Richardson and T. Tamura, Phys. Rev., 150, No. 3, 996-1010 (1966).

5. M. Cance and G. Grenier, Trans. Am. Nucl. Soc. 22, 664-665, Nov. 1975.

6. C. Sellem, I. D. Perroud and J. F. Loude, Nuclear Instruments and Methods 128, 495 (1975).

7. K. M. Jones, E. P. Cytacki and C. S. Kelsey, Phys. Med. Biol., 20 (1), 131-135 (1975).

8. J. A. Cookson, M. Hussian, C. A. Uttley, J. L. Fowler and R. B. Schwartz, Neutron Cross Sections and Technology, Vol. 1, pp. 66-68 (1975).

9. R. B. Galloway and A. Waheed, Nucl. Instr. and Methods 128, 505 (1975).

10. P. B. Johnson, J. E. Callaghan, C. M. Bartle and N. G. Chapman, Nucl. Instr. and Methods, 100, 141-148 (1972).

11. A. Greil and K. Trützschler, Kernenergie, 12, 68-70 (1969).

12. C. M. Bartle and P. A. Quin, Nucl. Instr. and Methods 121, 119-127 (1974).

13. R. A. J. Riddle, G. H. Harrison, P. G. Rose, M. J. Saltmarsh, Nucl. Instr. and Methods 121, 445 (1974).

14. T. B. Ryves and D. Sharma, Nucl. Instr. and Methods 128, 455 (1975).

15. E. Fort, Nuclear Data for Reactors (Proc. Conf. Helsinki: 1970) 1, IAEA, Vienna (1970); E. Fort, J. L. Leroy and J. P. Marquette, Nucl. Instr. and Methods 85, 115-123 (1970).

16. H. Liskien and A. Paulsen, Nucl. Instr. and Methods 69, 70-76 (1969).

17. A. Paulsen, R. Widera, A. Berlin and A. Trapani, Nucl. Instr. and Methods 91, 589-593 (1971).

18. A. Paulsen, H. Liskien and M. Cosack, Nucl. Instr. and Methods 105, 103-107 (1972).

19. G. P. Lamaze, M. M. Meier and O. A. Wasson, Nuclear Cross Sections and Technology, Vol. 1, pp. 73-74 (1975).

20. W. P. Poenitz, ANL-7915, Argonne National Laboratory (1972).

21. M. M. Meier, A. D. Carlson and G. P. Lamaze, Nuclear Cross Sections and Technology, Vol. 1, 75-77 (1975).

22. J. L. Leroy, I. Szabo and J. Y. Tocquer, Neutron Standard Reference Data, IAEA, pp. 63-73 (1972).

ASSOCIATED GAMMA-RAY TECHNIQUE FOR NEUTRON FLUENCE MEASUREMENTS

by

J. D. Brandenberger
University of California
Los Alamos Scientific Laboratory
Los Alamos, New Mexico 87545

The use and development of the $^{7}Li(p,n_1\gamma)^{7}Be$ reaction as an example of the associated gamma-ray technique for neutron fluence and detector efficiency measurements are described. Present limits on energy range and accuracy are stated for this method, and current extensions of this work are discussed.

(Neutron fluence; detector efficiency; cross sections)

Introduction

Associated gamma-ray techniques have been used extensively in nuclear physics. Two examples are the gamma-gamma coincidence method that has been used for decades in analyzing gamma-ray cascades of excited nuclei in nuclear spectroscopic studies, and coincident measurement of annihilation radiation to study the interaction of positrons with matter. Several years ago, with the advent of high resolution Ge(Li) detectors, it became convenient and enhanced experimental precision to monitor particle induced neutron producing reactions by a gamma-ray associated with a neutron group. With respect to neutron measurements, the 431-keV gamma-ray from the $^{7}Li(p,n_1\gamma)^{7}Be$ reaction has been used at Lowell University to monitor the relative fluence from the $^{7}Li(p,n_o)^{7}Be$ reaction.[1] While this gamma ray is not actually associated with the n_o neutrons, the principle is similar because at a given proton energy, the branching ratio of n_1/n_o neutrons is constant. The closest example to the technique described here is the use by Presser and Bass[2] in determining both the $^{7}Li(p,n_1\gamma)^{7}Be$ to $^{7}Li(p,p_1\gamma)^{7}Li$ branching ratio and the integrated cross sections by observing the 431- and 478-keV gamma rays, respectively. That work, however, required proton fluence and target thickness measurements in order to obtain the absolute total reaction cross sections. The present work uses associated gamma-ray techniques in conjunction with a neutron source reaction to measure angular distributions which for simplicity and accuracy can be used to measure the neutron fluence and detector efficiencies while avoiding target thickness and proton beam current measurements.

Use of the Method

For the moment, let us assume that a set of $^{7}Li(p,n_1\gamma)^{7}Be$ angular distributions as a function of proton energy are known with good precision either on an absolute or relative scale. The measurement of these angular distributions must be made before the associated gamma-ray method can be used with this reaction. This subject is left for later discussion because of its critical relation to the accuracy of the method.

Figure 1 shows the spectroscopic information involved in the example reaction. The n_1 neutron leaves ^{7}Be in the $1/2^-$, 431-keV level, which promptly decays to the $3/2^-$ ground state. Because of the spin values involved, the decay of the level is by the isotropic emission of the 431-keV gamma ray, and the ratio of the number of these gamma-rays to n_1 neutrons is unity from threshold until the 4.5-MeV level is reached. Thus, from $0 \leq E_{n_1} \leq 4$ MeV one may monitor the n_1 neutrons by observing the 431-keV gamma ray. If the absolute efficiency of the gamma-ray detector has been determined for the 431-keV gamma ray by comparison to gamma-ray standards that are now available from, for example, the National Bureau of Standards (NBS), the absolute n_1 neutron fluence may be determined at each proton energy and detector angle. A high-resolution gamma-ray detector must be used in order to resolve the 431-keV gamma rays.

If the objective is to determine the absolute fluence of n_1 neutrons, the above measurements are all that is necessary. To calibrate a neutron detector with this reaction, it is necessary to make time-of-flight measurements of the n_1 neutrons because of the presence of n_o neutrons, gamma rays, and room-scattered background. Subsequently, a second detector may be calibrated for monoenergic neutrons by direct comparison with the first if only monoenergetic neutrons are present. The method was developed to measure detector efficiencies as a function of energy with a combination of ease and precision that has not previously been possible in this energy region ($E < 4.1$ MeV). The ultimate motivation, of course, is the measurement of neutron differential cross sections normalized to the n-p cross section at laboratory angles of about 40°.

Figure 2 shows a set of $^{7}Li(p,n_1)^{7}Be$ angular distributions,[3] which are considered for the present to be precise. We can use these angular distributions, or we can use the information[3] in Fig. 3 to generate angular distributions from interpolated polynominal coefficient ratios.

Each angular distribution can be expressed as

$$W(\theta,E_p) = \sum_{\ell=0}^{\ell=\ell_{measurable}=\ell_{max}} A_\ell(\theta,E_p)P_\ell(\cos\theta).$$

$$A_\ell = A_o\left(\frac{A_\ell}{A_o}\right)$$

where A_ℓ/A_o is known, and

$$W(\theta,E_p) = A_o(E_p) \sum_{\ell=0}^{\ell_{max}} \left(\frac{A_\ell}{A_o}\right) P_\ell.$$

The total number of n_1 neutrons N emitted by the source is obtained by dividing the number of detected 431-keV gamma rays, N_γ, by the gamma-ray detector's absolute efficiency, ε_γ. Thus,

$$N = N_\gamma/\varepsilon_\gamma$$

or $$N = K\int W(\theta,E_p)\,d\Omega = N_\gamma/\varepsilon_\gamma.$$

The fluence at a particular energy and angle is

$$F(\theta,E_p) = N\,\frac{KW(\theta,E_p)}{K4\pi\,A_o}\left(\frac{\Omega_d}{S_d}\right)$$

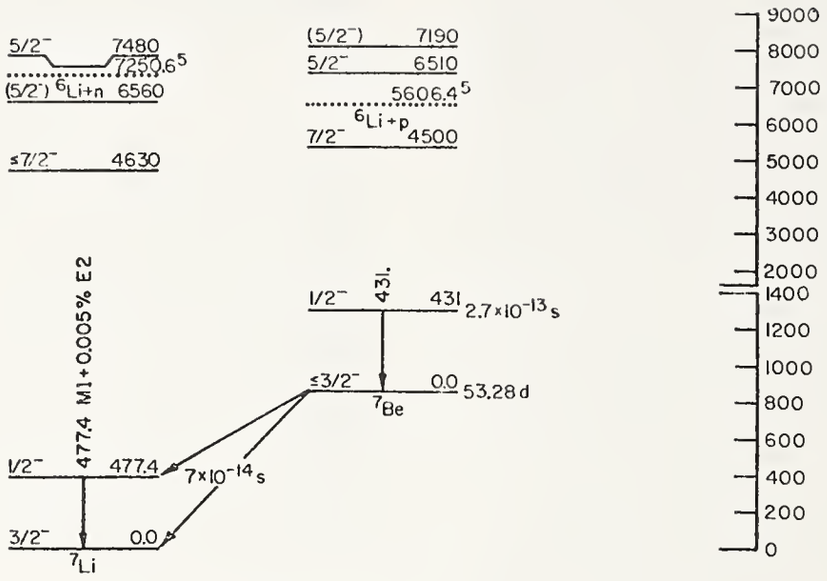

Fig. 1

The level and decay schemes of ^{7}Li and ^{7}Be.

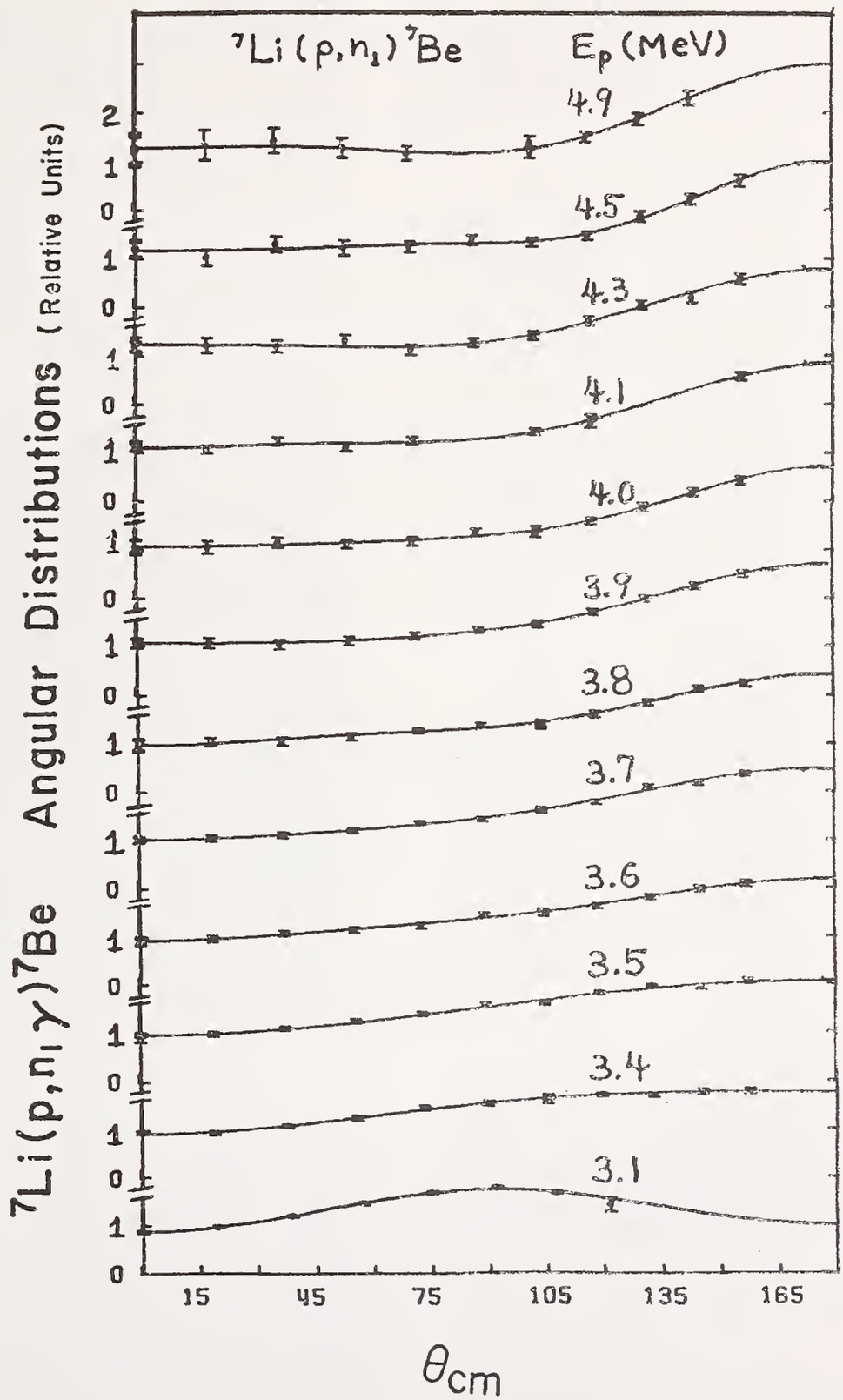

Fig. 2

The ^{7}Li(p,n$_1$)^{7}Be angular distributions from E_p = 3.1 MeV to E_p = 4.9 MeV. Units are relative.

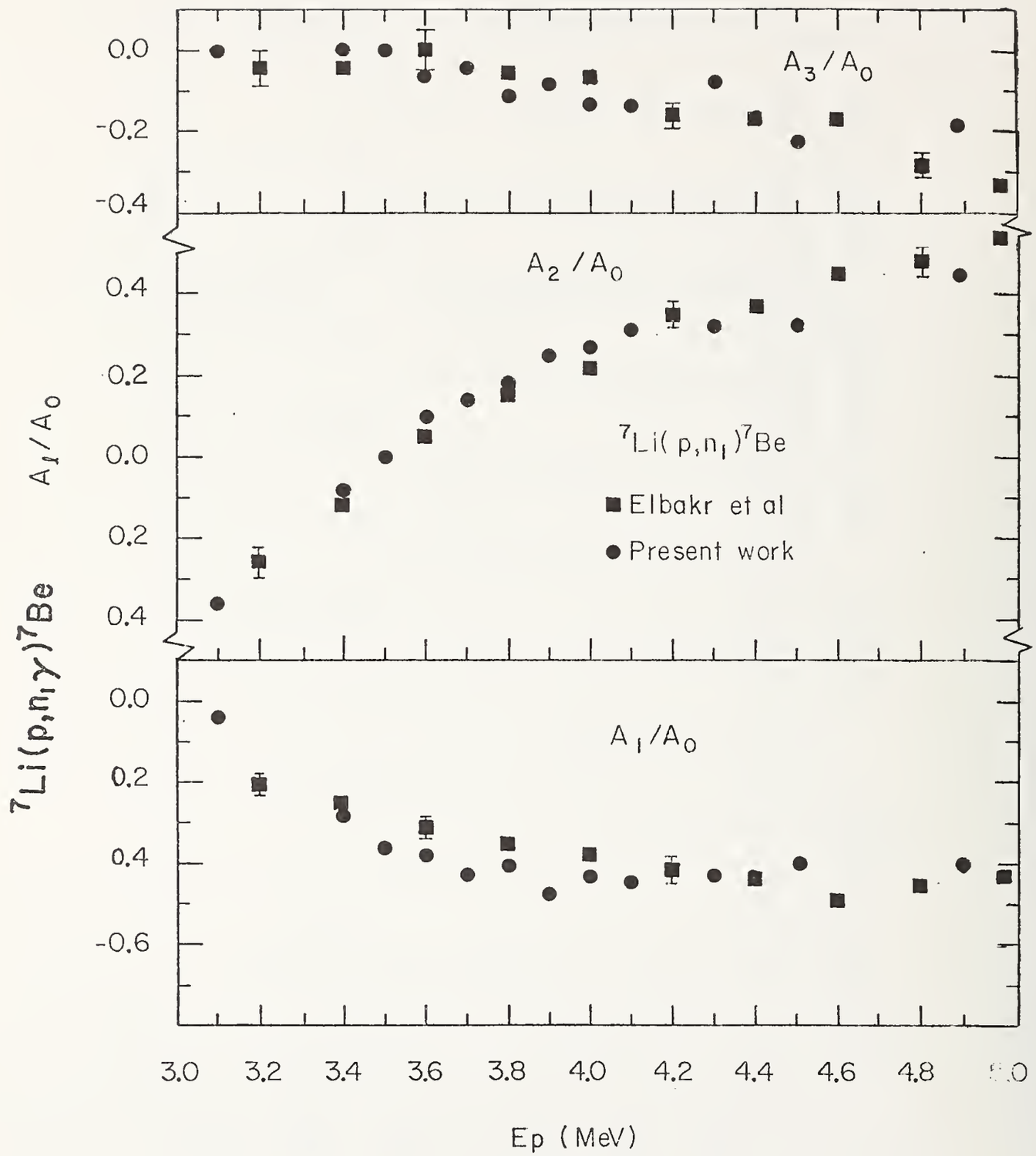

Fig. 3

The Legendre Polynominal ratios that fit the angular distributions of Fig. 2. The dots are from Ref. 3 and the squares from Elbakr et al.

where Ω_d and S_d are the solid angle subtended by the detector and its effective area, respectively. Thus, we simply have

$$F(\theta,E_p) = N_\gamma/\varepsilon_\gamma \frac{W(\theta,E_p)}{4\pi \cdot A_o L^2}$$

where the distance from the source is L. Note that ε_γ is a property of the gamma-ray detector that has been measured, L^2 appears as the $1/R^2$ dependence of the flux, and W/A_o is determined by the known ratios of the polynominal coefficients. The only quantities measured for each fluence determination are N_γ and θ, which are extremely easy to determine.

To bring us to a final result, the absolute efficiency of a neutron detector whose yield is $Y(E_n)$ is

$$\varepsilon = Y(E_n)/F(\theta,E_p)xS$$

for a detector with effective (or nominal) area S, and the relative efficiency is

$$\varepsilon_{rel} = Y(E_n)/N_\gamma xW(\theta,E_p).$$

For determining Y and N_γ, it is assumed that corrections for attenuations by the target, target backing, and target assembly have been made appropriately as the experimental arrangement requires. To obtain a detector efficiency in the range of applicability of the method with the $^7Li(p,n_1\gamma)^7Be$ reaction, i.e. 0 to 4 MeV, typically two or three angular distributions of the $^7Li(p,n_1\gamma)^7Be$ reaction are necessary. This can be seen in Fig. 4, where the angular distributions denoted by A, F, and L have overlapped nicely in energy to give an efficiency curve. By knowing the efficiency ε, both elastic and inelastic neutron cross sections can be normalized to the n-p cross sections. If the absolute efficiency is determined as outlined, (p,n), (α,n), (d,n) and in general all neutron source reactions below 4 MeV can be determined provided target thicknesses and appropriate particle currents are known. It is important to realize (1) that the standard deviation of the points from a smooth curve (and probably also the correct efficiency curve) is <2%, which is probably indicative of the accuracy as well as precision of the results, and (2) that the results are independent of detailed knowledge of (a) the gamma-ray detector's position and effective area, (b) the proton current or target thickness, or (c) the neutron detector's area.

Method of Establishment of the Primary Standard

To establish the standard for neutron flux determination using the $^7Li(p,n_1\gamma)^7Be$ reaction, it has been shown in the previous section that a set of angular distributions is required for use with the associated gamma-ray method. These angular distributions may be relative with respect to angle, but each angular distribution must have the same normalization factor to the absolute value. Such a set of angular distributions must be established concurrently with the neutron detector's efficiency by measuring a large set of such angular distributions and demanding that the gross redundancy in measurements at the same or very nearby neutron energies be consistent with a single detector efficiency curve. The method is outlined in detail by Brandenberger *et al.*[3] In principle the establishment of these angular distributions is simple, in practice it is very time consuming. Each point on all the angular distributions is normalized to a constant associated gamma-ray count, assuring that each point on an angular distribution is monitored to a constant integral fluence of n_1 neutrons. If an efficiency curve is found which fits both the data points of each angular distribution and each of the integral cross sections, it is assumed to be correct. This assumes that the efficiency curve is smooth or that enough data are taken to establish any fine structure in the efficiency curve. The precision of the efficiency curve is taken to be not much greater, say 1.5 times greater, than the standard deviation of the data points from the assumed efficiency curve. There is no obvious means to determine a valid statistical uncertainty in the usual sense for this method.

Present Status

Figures 2 and 3 indicate the sole source of completed measurements using the associated gamma-ray method. These are from Ref. 3. A statistical analysis indicates that the standard deviation of the set of data points from the assumed efficiency curve derived by the fitting and normalizing procedure is 1.9% in the region above E_n = 0.4 MeV. Many alternate efficiency curves have been considered and have been rejected as being erroneous or at least inferior to that shown. Thus, considering the average and individual errors as 1.5 times the standard deviation over most of the energy range gives an uncertainty of about 3% from 0.6 MeV to 2.75 MeV. The higher energy region, where only one angular distribution is represented, may have slightly larger errors, but this angular distribution is required to be compatible with a large number of points from several angular distributions at lower energies and is consistent with the behavior of efficiency curves well past the maximum.

Further Developments in Energy Range and Accuracy

Further work is underway by Ron Harper, E. C. Hagen, B. D. Kern and the author to extend the energy range and accuracy of the method. Data have been taken, and continue to be taken by Harper and Kern, to extend the range from 70 keV to 4.1 MeV with an accuracy of 1-2%. The difficulties are (1) maintaining a very low detector threshold at a constant value, (2) maintaining appropriately thin targets for energies near the neutron threshold that are uniform, and (3) integrating the n_1 neutron time-of-flight peaks in a consistent and precise manner. These difficulties may become real obstacles as the work is extended to lower energies.

Conclusions

It appears that the present work is accurate to $\cong$ 3% for energies above 600 keV. Such accuracy as indicated by the data cannot be accepted without equally rigorous substantiation by independent observers. In any case, the method, *per se*, opens the possibility of measuring differential cross sections in the 0.1 to 4.1 MeV energy range to accuracies heretofore not attained, say 1.5 to 3%. Several other uses quickly come to mind. It should be possible to:

1. further develop secondary standards such as the C(n,n)C reactions,

2. make more precise measurements of neutron-producing reactions, such as the $T(p,n)^3He$ reaction, using a calibrated detector,

Fig. 4

The efficiency curve of the neutron detector used in Ref. 3. Each set of letters represents a 12 or 13 point angular distribution at a given E_p.

3. calibrate other detectors including counters of the McKibben long counter type, the moderating sphere type, ^{3}He and ^{4}He counters, etc., as well as scintillation counters operated in the time-of-flight mode.

References

1. A. Mittler, Lowell University, private communication, April 1973.

2. G. Presser and R. Bass, Nucl. Phys. A182 (1971) 321.

3. J. D. Brandenberger, F. D. Snyder, J. D. Dawson, T. W. Burrows, and F. D. McDaniel, Nucl. Instr. Methods 138 (1976) 321.

4. S. A. Elbakr, I. J. Van Heerden, W. J. McDonald, and G. C. Neilson, Nucl. Instr. and Methods 105 (1972) 519.

ASSOCIATED ACTIVITY METHOD

K. K. Sekharan
Cyclotron Institute
Texas A&M University
College Station, Texas 77843

A brief description of the associated activity method is given and its application for the calibration of flat response neutron detectors in three laboratories is described. The uncertainties involved in the associated activity method have been discussed and suggestions for improving the accuracy of the efficiency for neutron detection have been made.

(Description of Method; Possible Improvements; Uncertainties in Efficiency)

Introduction

A neutron has to be detected always by some nuclear process such as $^{10}B(n,\alpha)^{7}Li$ reaction or (n,p) scattering. As the nuclear processes are energy dependent the efficiency of the neutron detector for detection of neutrons also tend to be energy dependent. Hence the efficiency of a neutron detector has to be determined experimentally and/or by theoretical calculations as a function of the neutron energy. The "Associated Activity Method" is a precise experimental method for determining the efficiency of a neutron detector. A survey of the literature shows that this method has been employed for detector calibration in at least three laboratories. Recently, K. K. Sekharan, H. Laumer, F. Gabbard and B. D. Kern have determined the efficiency of a spherically shaped 4π neutron detector[1] using associated activity method. They have used $^{51}V(p,n)^{51}Cr$ and $^{57}Fe(p,n)^{57}Co$ reactions for the determination of the absolute efficiency of the detector. W. P. Poenitz has calculated the efficiency of the grey neutron[2] detector by calculating the intensity of the 2.2 MeV capture gamma rays. However, he has used the associated activity technique[3] to determine the relative efficiency of this detector as a function of neutron energy. Another group to use this technique to calibrate their long counter was J. M. Adams, A. T. Ferguson, and C. D. McKenzie.[4] They have also used ^{51}Cr and ^{57}Co for the activity measurement. Taschek and Hemmendinger[5] employed the associated activity method to measure the total cross section of $^{7}Li(p,n)^{7}Be$ reaction.

Description of the Method

There are many (p,n) reactions in which the residual nucleus decays back, at least partly, to an excited state of the target nucleus by positron emission or electron capture which results in the emission of a gamma ray when the nucleus is de-excited to the ground state. Some of these residual nuclei decay with long half lives whereas others are short lived. As one residual nucleus is produced for every neutron produced during the (p,n) reaction the gamma rays associated with the decay of the residual nucleus have a definite relationship to the total number of neutrons produced in the nuclear reaction. Hence it is possible to determine the efficiency of a neutron detector by counting the neutrons (with the detector whose efficiency is to be determined) for the entire length of time for which the target is bombarded with the proton beam and then determining the gamma ray activity of the bombarded target. From the ratio of the neutron yield to the gamma ray yield the efficiency of the neutron detector can be determined.

It turns out that the (p,n) reactions which can be conveniently used for the associated activity method are $^{7}Li(p,n)^{7}Be$, $^{51}V(p,n)^{51}Cr$ and $^{57}Fe(p,n)^{57}Co$ although possibilities of employing some of the other (p,n) reactions cannot be ruled out. Available information[6,7] about the residual nuclei of the above reactions (^{7}Be, ^{51}Cr and ^{57}Co) are tabulated in Table 1. It can be observed from the table that the half lives of these residual nuclei are very long compared to the time required to activate the target by proton bombardment or the time required to measure the gamma ray activity. Appropriate corrections can always be applied for the finite time required for the proton bombardment of the target, the counting of the gamma rays from the residual nucleus and also for the time elapsed between proton bombardment and gamma ray counting.

Table 1

Half lives of residual nuclei and the associated gamma ray energies.

Residual Nucleus	Half Life (days)	Activation Time (hours)	Associated Gamma Ray Energy (keV)
^{7}Be	53	2	477.4
^{51}Cr	27.704±.002	3 to 4	319.8
^{57}Co	270.9 ±.6	6	121.94 136.31

However, one should remember that the charged particle accelerators are not a source of constant current. Therefore, the rate of build up of the radioactive residual nucleus will not be constant and it is advisable to make the bombarding time as small as possible compared to the half life of the residual nucleus. A brief description of the techniques employed in the three laboratories in calibrating the detectors is given below.

$^{7}Li(p,n)^{7}Be$ reaction was used to determine the relative efficiency of the 4π neutron detector[1] at the University of Kentucky in the neutron energy range 30 keV to about 1600 keV. Neutron yield was measured from LiF targets at several energies using a fresh target for proton bombardment lasting one to two hours at each energy. 478 keV gamma ray yield was measured

from each target immediately after the proton bombardment. For the absolute efficiency calibration a vanadium metal target was bombarded with protons corresponding to an average neutron energy of 300 keV. Similarly, an isotopically enriched ^{57}Fe target ($^{57}Fe_2O_3$ evaporated on to a carbon backing) was bombarded with protons to produce neutrons of average energy 1350 keV. The gamma ray detector was calibrated using ^{51}Cr and ^{57}Co sources (standard sources supplied by the National Bureau of Standards) which enabled the determination of the absolute efficiency of the neutron detector at 300 and 1350 keV. The relative efficiency in the energy range 30 keV to 1600 keV was then normalized to the absolute efficiencies at 300 and 1350 keV to obtain the efficiency for the entire energy range. The efficiency of the detector as a function of the neutron energy is shown in Fig. 1. The efficiency of the detector for neutrons form a Po-Be source was found to be 0.47%. $^{7}Li(p,n)^{7}Be$ reaction cross section was measured with this detector and compared to the cross section published by R. L. Macklin and J. H. Gibbons.[8] In Fig. 2, the dots are the present measurements and the dashed lines are cross section data published by Macklin and Gibbons. The detector is being used extensively for measurement of (p, n) and (α, n) cross sections, some of which are important for astrophysical calculations.

The grey neutron detector[3] is applicable in the neutron energy range thermal to several MeV. Fast neutrons incident at the center of the detector, are slowed down in a moderating medium such as water or paraffin and a fraction of these neutrons are captured in the hydrogen medium emitting 2.2 MeV gamma rays which are detected by a NaI (Tl) detector mounted at the surface of the moderating medium. Assuming that the detector is large enough to prevent leakage of neutrons from the moderating medium the efficiency of the detector as a function of neutron energy has been calculated taking into account the gamma ray absorption in the medium. The relative efficiency of the grey neutron detector was determined by the associated activity method and compared to the calculated efficiency in the energy range 30 to 1000 keV. The $^{7}Li(p,n)^{7}Be$ and the $^{51}V(p,n)^{51}Cr$

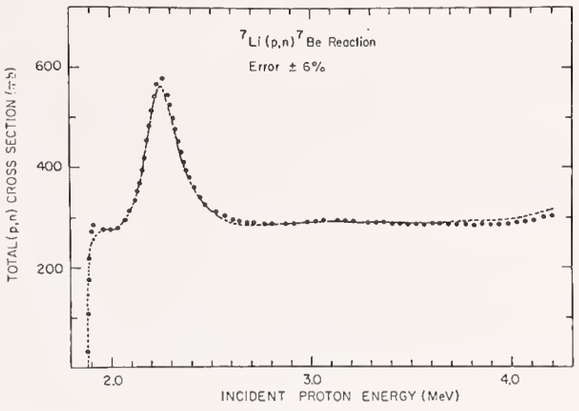

Fig. 2. $^{7}Li(p, n)^{7}Be$ reaction cross section. Dashed lines are cross sections published by Macklin and Gibbons.

reactions were the neutron sources for the calibration. The activities of ^{7}Be and ^{51}Cr in the irradiated targets were counted by measuring the yield in the photopeak of the 478 and 320 keV gamma rays from ^{7}Be and ^{51}Cr respectively. The results are shown in Fig. 3. The performance of the detector was also checked by measuring the $^{7}Li(p,n)^{7}Be$ cross section.[8] The grey neutron detector has been used for measurement of cross sections of neutron producing reactions important for fast reactor calculations.[9,10]

The conventionally determined efficiency of the long counter was compared to the efficiency determined by the associated activity method by J. M. Adams, A. T. G. Ferguson and C. D. McKenzie[4] in the neutron energy range 50 to 1300 keV. They measured the angular distribution of the neutrons from $^{51}V(p,n)^{51}Cr$ and $^{57}Fe(p,n)^{57}Co$ reactions and compared the neutron yields from these reactions to the activities of the bombarded targets. A NaI (Tl) detector was used to measure the yield in the photopeak of the 320 keV gamma ray from ^{57}Fe. They observed deviations in the efficiency of the long counter from that determined by the conventional method.

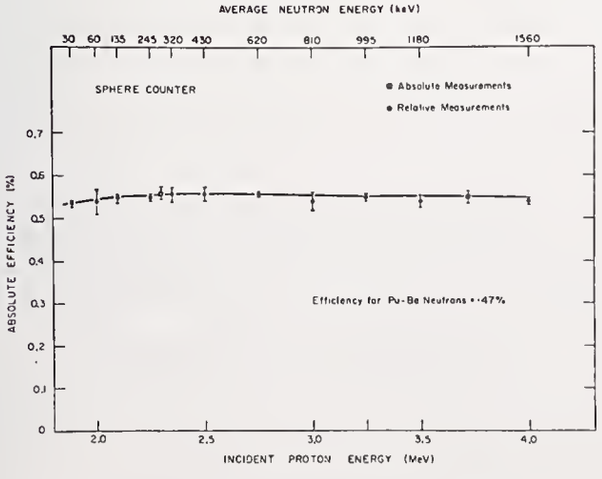

Fig. 1. The absolute efficiency of the 4π neutron detector. The error flags are an estimate of the standard error at each point.

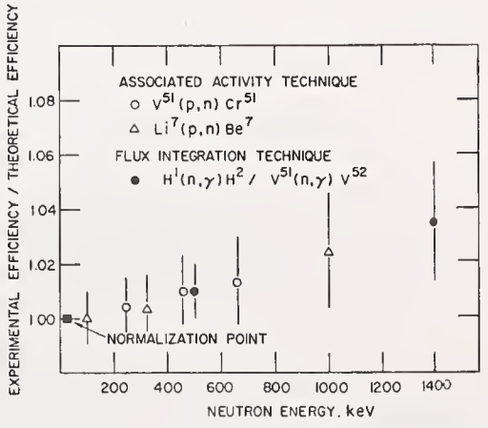

Fig. 3. The ratio of the experimental efficiency to the theoretically calculated efficiency of the grey neutron detector.

Uncertainties in the Determination of the Efficiency of the Detector

The important factors in the determination of the efficiency of the detector using the associated activity method are (1) the knowledge of the half life of the radioactive target whose activity is to be measured after bombarding the target with charged particles and (2) the knowledge of the strength of the sources used to calibrate the gamma ray detector. The beauty of the associated activity method is that the accuracy of the efficiency determination is independent of the target uniformity and errors in the target thickness determination which are, in general, two difficult factors in efficiency calibration. Even the absolute efficiency of the gamma ray detector need not be known. One needs to know only the relative efficiency of the particular geometry in which gamma ray counting from the bombarded targets and the standard sources are done. However, one should exercise great caution to avoid uncertainties arising from geometrical factors in the placement of bombarded targets and calibrated gamma ray sources.

The easiest method to determine the absolute number of gamma rays from the irradiated targets is to compare the gamma ray yield from the target to that of the standard sources of the same radioactive element. As several days may be elapsed between the time of the determination of the strength of the standard sources and the determination of the relative efficiency of the gamma ray detector used for gamma ray activity measurement, the half lives of the standard sources must be known as accurately as possible. The half lives of ^{7}Be, ^{51}Cr and ^{57}Co have been reported extensively in the literature.[6,7] Various methods have been used to determine the half lives of these nuclei. Any improvement in the accuracy of the values of the half lives of these or similar radioactive nuclei will be useful for improving the accuracy of the efficiency of the neutron detector. Hence it is necessary to obtain consistent values for the half lives of those radioactive nuclei from several different methods. Improvements in the accuracy of the knowledge of the strength of the gamma ray sources employed for the calibration work will also reduce the overall uncertainty in the efficiency of the neutron detector.

The effect of strongly anisotropic angular distribution of neutrons on the efficiency of the flat response 4π neutron detector has been studied[1,3] and found to be less than 1% in the case of the strongly forward peaked resonance[11] at 2.28 MeV in the $^{7}Li(p, n)^{7}Be$ reaction. However, for the development of a neutron detector whose efficiency is known to an accuracy of about 1%, the effect of the angular distribution on the detector should not be neglected.

Possible Improvements in the Efficiency Determination

The efficiency of the above mentioned detectors as a function of the neutron energy is known to about 1300 keV. It will be useful to determine the efficiency of the detectors for somewhat higher energies though complications may arise due to flux leakage from the moderating medium. A Monte Carlo type calculation can be used for this purpose. In fact, W. P. Poenitz has calculated the efficiency of a black neutron detector[12] using Monte Carlo method.

A practical method for extending the energy range over which the efficiency of the 4π neutron detector[1] is known, will be to compare the calculated efficiency to the experimentally determined efficiency in the energy range 30 to 1300 keV and then extend the calculation to higher energies. Good agreement between the calculated and experimental efficiencies in the energy region 30 to 1300 keV will be adequate justification for using calculated efficiencies at higher energies. The Monte Carlo method can also be used to investigate the effect of strongly anisotropic angular distributions of a nuclear reaction on the efficiency of the 4π detector. Thus better knowledge of the half lives, improvements in the uncertainty of the source strength of standard sources used in associated activity method and theoretical calculation of the neutron efficiency are major factors which will improve the accuracy of the neutron detector efficiency.

References

[1] K. K. Sekharan, H. Laumer and F. Gabbard, Proc. Int. Conf. Nuc. Cross Sec. Tech., NBS SP 425, 108(1975); K. K. Sekharan, Ph.D. Dissertation, Unpublished; K. K. Sekharan, H. Laumer, B. D. Kern and F. Gabbard, Nucl. Instr. and Meth., 133, 253(1976).

[2] W. P. Poenitz, Nucl. Instr. and Meth., 58, 39(1968).

[3] W. P. Poenitz, Nucl. Instr. and Meth., 72, 120(1969).

[4] J. M. Adams, A. T. G. Ferguson and C. D. Mckenzie, Activation Technique for the Absolute Calibration of a Long Counter, A. E. R. E.- R.6429(1970).

[5] E. F. Taschek and A. Hemmendinger, Phys. Rev. 74, 373(1948).

[6] Nuclear Decay Data for Selected Radionucleides, ed. M. J. Martin, ORNL - 5114(1976).

[7] E. De Roost and F. Lagoutine, Atomic Energy Review, 11, 642(1973).

[8] R. L. Macklin and J. H. Gibbons, Phys. Rev., 114, 571 (1959).

[9] H. O. Menlove and W. P. Poenitz. Nucl. Sci. Eng., 33, 24(1964).

[10] W. P. Poenitz, J. Nucl. Energy, 22, 505(1968).

[11] J. H. Gibbons and H. W. Newson, Fast Neutron Physics Part I, ed. J. B. Marion and J. L. Fowler, Interscience Publishers Inc., New York, 164(1960).

[12] W. P. Poenitz, Nucl. Instr. and Meth., 109, 413 (1973).

ACCURACIES AND CORRECTIONS IN NEUTRON BATH TECHNIQUES

E.J. Axton
National Physical Laboratory
Teddington, Middlesex, United Kingdom

The corrections and currently attainable accuracy in the neutron source emission rate measurements with the manganese sulphate bath technique are discussed in detail, followed by a review of other bath techniques and their adaptation for neutron flux measurement.

1. Introduction

Over the last 25 years much has been written about the use of bath techniques for neutron measurements and it would be impossible to review all this work in the space of 15 minutes. Probably of greatest interest is the use of manganese sulphate baths to measure neutron source strengths, particularly with respect to fission yield measurements. Therefore, in spite of the title of this session, it is proposed to begin by assessing the ultimate accuracy attainable with an ideal system and if there is time left to discuss the limitations of practical systems, and some other applications of the bath technique.

2. Design

Figure 1 is a schematic diagram of a typical system. This shows some of the features which are essential to the attainment of high accuracy. Some of the design features are necessarily compromises. For example the bath has to be large to reduce neutron escape but the specific activity goes down with the cube of the radius. The presence of the central cavity increases the neutron escape but reduces the capture of neutrons returning to the source. Spherical geometry maximises the specific activity whilst minimising the escape. It also eases the problems of calculation and measurement of the corrections. The bath should not be shielded unnecessarily, but if it is shielded provision should be made for the insertion of detectors to assess the neutron escape. Provision should also be made to measure the thermal neutron flux at the cavity boundary. The solution should have a high concentration to minimize the effect of uncertainties in the cross section ratios, and should be circulated through the activation detectors so that they can be operated whilst the source is in the bath in order to improve the counting statistics. Two independent detection systems should be employed so that a change or failure in one of them is instantly detected. A further advantage is that twice as much data is acquired. The bath detectors are calibrated by the insertion of calibrated samples of ^{56}Mn which have been measured by the $4\pi\beta\gamma$ coincidence method. A very stable high pressure ionisation chamber system is essential to check the consistency of the coincidence counting. Standard sources in fixed geometry should be used regularly to check the stability of the bath detectors. The concentration of the solution should be measured regularly by at least two methods. Two bath sizes should be used to check the validity of the evaluated corrections. Finally a standard neutron source should be measured periodically to check the whole system.

3. Source strength determination

The source strength Q is derived from the following equation:

$$Q = \frac{A}{f\,E\,(1 - O)(1 - S)(1 - L)} .$$

The fraction f of neutrons captured by manganese is

$$f = 1 + \frac{\sigma_S}{\sigma_{Mn}(1 + G\,\bar{r}\,s)} + \frac{NH}{NMn}\,\frac{\sigma_H}{\sigma_{Mn}(1 + G\,\bar{r}\,s)}$$

Where A is the saturation manganese counting rate measured by the bath detector system with efficiency E, O is the fraction of neutrons which are captured in the n,α and n,p reactions in sulphur and oxygen, S is the fraction of neutrons recaptured by the source, and L is the fractional neutron escape from the boundaries of the bath. σ_H, σ_S and σ_{Mn} are the thermal neutron capture cross sections of hydrogen, sulphur, and manganese respectively, and NH/NMn is the hydrogen to manganese atom ratio in the solution. s is the normalised above 1/v resonance activation integral of manganese, $\bar{r}$ is the epithermal flux parameter averaged over the bath, and G is the resonance self shielding factor. In the following sections the components of this equation will be examined in detail.

3.1 Measurement of bath efficiency E

The difficulties associated with this apparently simple operation are almost invariably underestimated as there are so many things which can go wrong. Basically a quantity of radioactive ^{56}Mn of high purity is divided into portions by weight, some of which are used to activate the baths and others are measured in the $4\pi\beta\gamma$ coincidence equipment to determine the specific activity. Differences in the specific activity of these solutions can be caused by sticking of activity to glassware and by evaporation of water during the weighing of small liquid samples either in the bath loading or counting operations. In absolute measurement of ^{56}Mn solutions, an international comparison revealed differences in apparent activity depending on whether a liquid scintillator or gas flow proportional counter is used for the β channel. In the proportional counter the wrong result can be obtained if the plastic source mount becomes non-conducting. If a liquid scintillator is used it is necessary to check experimentally that no significant after pulsing occurs. Both methods require a correction for the fact that the β counter is not 100% efficient (the decay scheme correction). In the case of the liquid scintillator this correction is larger and more difficult to derive. Unsuspected radioactive contamination can occur in which case the measurement will be time dependent. Inevitably the time will come when the bath efficiency will appear to have changed. This could be due to a fault in the bath counting or in the coincidence counting, or in the dispensation of the sample or its purity, or to a simple mistake. A third party is then required to arbitrate. This is the role of the high pressure ionisation chamber referred to in section 2. The calibration figure for the ion chamber based on the coincidence equipment should remain constant, a typical standard deviation for a large number of calibrations being about $\pm$ 0.15%. Only if this reproducibility is

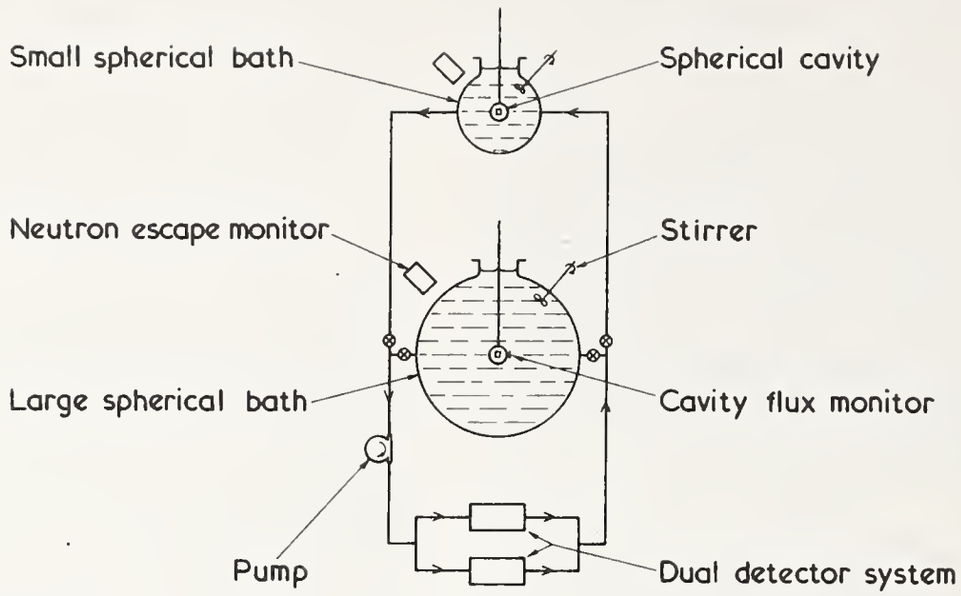

Fig. 1. Schematic arrangement for a typical bath system.

achieved, and the resultant calibration figure is in agreement with that obtained using a standard from an appropriate national laboratory can there be confidence in the measurements, and their relationship to those of other laboratories throughout the world. For the actual bath efficiency measurements, if precautions are taken to prevent loss of activity on the way e.g. along the walls of entrance pipes, or by splashing, and no electronic drifts or faults have occurred a typical standard deviation of ± 0.3% can be obtained and sufficient repetitions of the calibration may be carried out to reduce the standard error of the mean to an acceptable level. Ultimately one is left with an additional systematic uncertainty ~ ± 0.2% for the bath calibration. This is the current level of agreement obtained by national laboratories in international comparisons, de Volpi[1] and is attributable in part to the difficulties of weighing small quantities of liquids.

3.2 The H/Mn atom ratio

This may be determined by three methods.

(1) The volumetric method by titration with EDTA.

(2) The gravimetric method by drying and weighing weighed samples of solution both as the monohydrate after drying at 100 °C and as the dehydrate after drying at 300 °C.

(3) Determination of solution density.

The third method is not absolute but has to be calibrated by one of the first two, both of which are capable of reproducibility ~ 0.05% standard deviation. In the absence of impurities the two methods should give identical results. In the presence of impurities the volumetric method should give the correct specific manganese concentration provided there are no other titratable ions present, whilst the difference between the results of the two methods gives a guide to the impurity level. Needless to say, impurities should be avoided wherever possible. The H/Mn ratio can be determined sufficiently accurately to make a negligible contribution to the overall uncertainty.

3.3 The manganese to hydrogen thermal neutron cross section ratio

This is the dominant factor in the computation of the fraction of neutrons captured by manganese. The ratio of the individual cross sections taken from Mughabghab and Garber[2] is 0.02496 ± 1.62%. However the ratio can be determined more acurately by variation of the concentration of the solution. Equation (1) is rearranged as follows to form a straight line equation.

$$\frac{A}{E\,(1-0)(1-S)(1-L)} = \frac{NH}{NMn}\,(1 + G\,\bar{r}\,s)\,\cdot \frac{\sigma_H}{\sigma_{Mn}} + \frac{1}{Q}\left[1 + \frac{\sigma_s}{\sigma_{Mn}\,(1 + G\,\bar{r}\,s)}\right]$$

Measurements are made for a variety of values of NH/NMn from say 30 to 300 and the source strength is derived from the intercept of the line and the cross section ratio from the ratio of the slope to the intercept. All the quantities on the left hand side are concentration dependent and therefore have to be

evaluated for each concentration. By suitable choice of source energy and the bath size O can be made zero and L very small. Nevertheless L can vary by a factor of 2 over the range of concentration used so provision must be made to measure and calculate L at each point if it is significant. A typical uncertainty in the cross section ratio which can be obtained by this method would be ± 0.3% to 0.4%. The NPL value is 0.02495 ± 0.34% standard error[3]. A measurement in progress[4] indicates agreement between this value and the BNL 325 3rd edition value. A further value of 0.02531 ± 0.12% has been published, but this is qualified as an effective ratio for the particular bath and solution used to measure it[5]. The sign of the change of efficiency with concentration can be positive or negative depending on the type and mode of operation of the bath counters. In principle a different bath and counting system could be used for each point provided the appropriate corrections were made. Thus if the same source were used, all available data could be analysed in one global fit.

3.4 The effect of the impurities

The effects of the impurities are rather complex. Impurities which absorb neutrons and produce measurable activity would introduce a time dependent bias to the result which would be very difficult to interpret. Assuming that no measurable activity is produced, the linearity of the fit should be unaffected if the impurity concentration is proportional either to that of the Mn or to that of the H. Neglect of an impurity in the supply of the solid $MnSO_4$ would produce a low value for the H/Mn cross section ratio, but if the atom ratio was determined by a gravimetric method it too would be too low and this would tend to cancel the error in the cross section ratio. However, an impurity in the water would produce the correct source strength but a high value of the cross section ratio. The latter situation is unlikely in practice because the initial concentrated solution is probably made up from $Mn\,SO_4\,4H_2O$, in other words 25% of the water is already present, and an impurity in the added water would produce a non-linear situation.

4. Corrections

4.1 Fast neutron capture in oxygen and sulphur

This correction is both concentration and spectrum dependant. Its evaluation is almost entirely dependant on calculations. The oxygen loss in water for a Ra Be source was measured by de Troyer and Tavernier[6] as (2.25 ± 0.3)%. Ryves and Harden[7] using the same type of source obtained (1.69 ± 0.25)% in water and (3.05 ± 0.3)% for the oxygen and sulphur loss in concentrated manganese sulphate solution. Agreement is obtained between the NPL manganese bath and the AERE boron pile[8,9] if a correction of (3.0 ± 0.5)% is applied to the bath measurements. This information could be interpreted as another measurement of the correction. Unfortunately the Ra Be source is not a very good source for this experiment from the point of view of comparison with calculations as one is dependent on assumptions regarding the intensity of the low energy component in the spectrum, which is fairly large and known to vary from source to source. Finally one should mention the experimental method developed by de Volpi[5] whereby the correction is derived from the change in slope of the line obtained in a dilution experiment. Unfortunately the method is not very sensitive. Nearly 80% of the oxygen effect in a concentrated solution is due to the oxygen in water. Thus the change in the slope registers only the sulphur effect plus 20% of the oxygen effect, which varies from about 1.4% for AmBe source down to 0.35% for a californium spectrum. Thus a change in the slope of only 1 to 4 times the uncertainty in the slope can be expected. Calculations have been published for a number of source spectra by Ryves and Harden[7] and by Louwrier[10] based on standard slowing down theory and by Murphey[11] using Monte Carlo techniques. In the case of Ryves and Harden, and Murphey the oxygen cross sections used are now thought to be too high particularly in the energy range above 7 MEV. Likewise the oxygen cross sections used by Louwrier are thought to be too low. Table 1 shows a comparison of calculations based on both methods for a number of source spectra using cross sections obtained from the data centre at Saclay at the end of 1972 and are believed to be up to date. The calculations are for concentrated manganese sulphate solution with NH/NMn = 30.

Table 1

Oxygen and Sulphur correction (%)

Source	Mean E	Monte Carlo	Slowing down theory
Am Be	4.46	3.09	3.17
Ra Be	3.94	2.20	2.45
Cf-252	2.09 (ET=1.39)[a]	0.53	0.73
Cf-252	2.15 (ET=1.43)	0.62	0.79
Am B	2.76	0.49	0.64

[a] Maxwellian temperature in MeV.

The agreement seems to become progressively worse as the neutron energy decreases. The only other calculations known to have been performed with up to date cross sections are those of Ullo and Goldsmith[12,13] in their re-appraisal of the η measurements. Table 2 compares their results with recent calculations at NPL.

Table 2

	Axton			Ullo			Macklin	Steen
	O	S	O+S	O	S	O+S	O+S	O+S
Smith et al. NH/NMn= 77.7	0.30	0.09	0.39	0.19	0.03	0.22		
Macklin et al. NH/NMn= 192.6	0.24	0.04	0.28			0.25		

So it appears that even calculations by the same technique, using the same cross section data do not agree. Whatever cross section data is used the oxygen effect should follow the O/H atom ratio, and the sulphur effect should follow the S/H atom ratio. The figures on the right of the table do not appear to do this. There is no way of assessing the absolute validity of these results other than by agreement between different calculations. These programs are necessarily complex and it seems almost impossible to be certain that no hidden faults exist in them. It would be a good idea to hold an international comparison of Monte Carlo calculations to resolve the point.

4.2 Neutron Escape

As with the oxygen and sulphur loss correction the escape correction is dependent on the concentration of the solution and on the source spectrum. In addition it depends on the size and geometry of both the bath and the central cavity. It is also varied by the

presence of shielding materials. There are so many variables that it is difficult to produce a comprehensive correction set which would suit all occasions, and it is equally difficult to compare corrections which have been evaluated for different systems. Many authors have used expressions of the type $A\,e^{-Br}$ [31] to evaluate their escape corrections using constants derived for other systems by other authors. Whilst such expressions give a good estimate of the order of magnitude of the correction, they are not transferable when the geometry of the bath or the central cavity are changed, or if the concentration of the solution or the shielding is changed. On the other hand the correction may be checked by measurement. In principle the escape correction can be derived from measurements in different bath sizes and extrapolated to infinite radius [31]. This is not very practicable, but the use of two bath sizes provides a valuable bench mark for testing measurement and calculation procedures. For day to day monitoring at NPL a flat response detector (long counter) is used to monitor the neutron flux at the surface of the bath, which is then integrated over the bath surface. The counter efficiency is chosen empirically for each source spectrum to give agreement between the two bath sizes. Although there are many reasons why the long counter would appear to be unsuitable for this purpose it seems to give satisfactory results for the two baths. Table 3 compares these measurements with Monte Carlo calculations at NPL which are only in a preliminary state. The fast neutron program records fast neutron escape and records the position of neutrons which become thermalised. Shell sources of thermal neutrons so produced can be used to determine thermal escape either by diffusion calculations (M/C + Diff) or by a Monte Carlo program (M/C). The programs are still being developed so that the results must be regarded as provisional. Agreement becomes progressively worse as the source energy decreases, and the thermal fraction increases. Part of the problem is due to the uncertainty in the source spectrum. Some Am B and Am Li sources are believed to be contaminated with Be.

At the present state of the art, a systematic uncertainty of ± 10% of the correction for an Am Be source and 20% for a Californium source seems reasonable.

Table 3

Neutron escape from an unshielded sphere with a 8.9 cm. dia. cavity and NH/NMn = 30

	Total leakage (%)			Thermal fraction		
	Meas.	M/C	M/C + Diff.	Meas.	M/C	M/C + Diff.
98 cm. tank						
Am Be	1.46	1.49	1.41	17	18	13
Ra Be	1.15	1.14	1.07	9	15	10
Am B	0.33	0.33	0.34	35	28	19
Cf (ET=1.39)	0.30	0.32	0.30	23	22	17
Cf (ET=1.43)		0.42	0.38		20	12
Am F	0.05	0.05	0.05		19	
25 cm. tank						
Am Be	23.2	23.4	21.2	21	12	20
Ra Be	19.7	18.8	15.8	22	22	13
Am B	14.6			29		
Cf (ET=1.39)	10.0	12.1	10.0	32	34	20

Table 4

Comparison of neutron escape calculations with Ullo and Goldsmith evaluations

	Total escape		
	M/C	M/C + Diff.	Ullo
Smith et al bath	0.16	0.13	0.23 ± 0.11
Macklin	0.28	0.21	0.26 ± 0.03

4.3 Source capture of moderated neutrons

This correction is both concentration and source spectrum dependent. In all cases it is necessary to know accurately the amount and geometry of each material in the source assembly and the appropriate reaction cross sections. There are two approaches to this problem. One can derive the cavity boundary thermal and epithermal neutron flux in terms of the Wescott parameters either by measurement with foils or by diffusion calculations [14] or by Monte Carlo calculations. It is then necessary to evaluate an effective cross section for the source assembly with appropriate flux depression and self shielding corrections for each region of the source assembly. Spiegel and Murphey [15] describe a method of treating the problem. Alternately sufficient detail can be programmed into the Monte Carlo calculation to reproduce the source interactions directly. In either case a convenient test of the calculation is the ability to determine the cavity boundary flux, which can be measured to about ± 2% with foils. Table 5 compares the result of Monte Carlo and diffusion calculations with sub-cadmium thermal neutron flux measurements by Bardell [16] using gold foils. Again the agreement gradually worsens as the energy decreases. The low value for Am B is due to flux depression in the absence of which these results would lie on a smooth curve as a function of neutron energy.

Table 5

Thermal neutron flux at cavity boundary for unit source (%)

	Measured with gold foils	Monte Carlo/ Diffusion calculations
Am Be	0.139	0.134
Ra Be	0.180	0.178
Am B	0.140	0.128
Cf (ET=1.39)	0.223	0.218
Cf (ET=1.43)	0.223	0.214
Am F	0.249	0.208
Smith et al HH/NMn=77 ET=1.323		0.175
Macklin et al NH/NMn=192 ET=1.323		0.204

4.4 The manganese resonance correction

This correction can be obtained by deriving an effective cross section for manganese in terms of the Wescott[17] parameters G, $\bar{r}$, and s. Calculations by this method have been published by Axton and Ryves[18]. Alternately one could enter the detailed manganese resonance data directly into a Monte Carlo calculation.

Both methods depend on knowledge of the manganese activation integral. If the resonance parameters are put into a Monte Carlo calculation it is necessary to choose the γ width so as to give the preferred resonance integral. The value given in BNL 325 edition 3 is 8 barns. Recent measurements at NPL in terms of the gold resonance integral[19] indicate a value of about 7.6 barns. There are some much higher values elsewhere in the literature. The derived source strength is not very sensitive to the precise value of the integral. With concentrated solutions (H/Mn = 30) a change of 10% in the integral would alter the source strength by about 0.07%. Table 6 gives examples of the magnitude of the correction. The difference between the Axton, and Ullo and Goldsmith values is almost entirely accounted for by the difference in the value of the resonance integral used. Ullo and Goldsmith used 9.15 barn. The details of their calculation are not given in their paper.

Table 6

Manganese resonance corrections

	NH/NMn	NPL	Ullo and Goldsmith
NPL	30	1.0071	
Smith et al	77.7	1.0083	1.0100
Macklin et al	192.6	1.0093	1.0111

4.5 Photoneutron production

In some cases a small correction is necessary to allow for photoneutron production from deuterium in the solution. This correction is usually negligible with light water baths except in the case of high energy high intensity γ emitting sources such as Na Be.

5. Uncertainties

Provided all the necessary precautions are taken and all the ohecks* are successful, typical uncertainties would be estimated as shown in Table 7. Uncertainties are evaluated for two concentrations and two source spectra. The figures shown are for a 98 cm. diameter bath with an 8.9 cm. diameter cavity. The random uncertainties are quoted at the 68% confidence level. Five measurements of the bath efficiency, and five irradiations of the bath by the source are assumed. The existence of the second counting channel, in addition to providing internal consistency checks, also doubles the amount of data for analysis. It is assumed in all cases that the source is sufficiently strong to provide adequate counting statistical accuracy and that the background uncertainty is negligible even for the dilute solution.

*see Appendix

Table 7

Typical estimates of uncertainties

Systematic Uncertainties (%)	NH/NMn=30 Am Be	NH/NMn=30 Cf	NH/NMn=192 Am Be	NH/NMn=192 Cf
Bath efficiency	0.2	0.2	0.2	0.2
Cross section ratios				
σ_H/σ_{Mn}	0.145	0.145	0.287	0.287
σ_s/σ_{Mn}	0.122	0.122	0.039	0.039
Manganese resonance	0.07	0.07	0.09	0.09
Oxygen and sulphur	0.3	0.1	0.18	0.060
Leakage	0.15	0.03	0.20	0.04
Source capture	0.015	0.020	0.02	0.03
Random uncertainties				
Bath efficiency	0.13		0.13	
Source activation of bath	0.10		0.10	

6. Other baths used for source strength measurements

6.1 Noyce et al[20] introduced heavy water into their manganese bath in order to reduce the cross section dependence. It was necessary to introduce a proportion of light water into the mixture to prevent excessive neutron escape. In addition to the usual corrections, a correction for the photoneutron production in the bath was necessary. To minimise this correction an intermediary Sb-Be source was calibrated instead of the NBS standard Ra Be photoneutron source. In a subsequent comparison measurement ± 1% accuracy was achieved for the standard source.

6.2 de Troyer and Tavernier[6], Jaritsina et al[21], Van der Eijk[22] and Michikawa[23] used a water bath in which the neutron density as a function of distance from the source was integrated numerically. The neutron density at each point was measured by gold foil activation. The necessary corrections are similar to those described for the manganese bath. The method is time consuming and less amenable to automation but provides a valuable check on $MnSO_4$ bath calibrations. In principle it might be possible to develop the method to the same accuracy. Present uncertainty in the gold/hydrogen cross section ratio is ± 0.7%.

6.3 Fieldhouse et al[24] used a cylindrical bath in which the neutron density as a function of distance was determined from BF_3 counter measurements. The system was calibrated by associated particle counting of α particles from the T(dn) reaction. The experiment did not achieve its aimed accuracy of ± 1%.

6.4 Smith et al[25] and Macklin et al[26] used cylindrical manganese sulphate baths for their η measurements. In these experiments only ratio's of source strength are involved so none of the uncertainties associated with the absolute calibration of the bath detectors are relevant. On the other hand the problem of calculating the correction for neutron

absorption and multiplication in the complex source assembly are correspondingly greater and it seems difficult to believe that these effects can be calculated to the accuracy quoted. For example in the Goldsmith and Ullo[13] re-evaluation of the Oak Ridge measurement, the correction quoted for cadmium absorption is (1.85 ± 0.04)%.

7. The use of baths with accelerators

7.1 Scott[27] used a spherical manganese sulphate bath to determine the thick target yield from the $^{7}Li(p,n)$ reaction, the source in this case being the accelerator target situated at the centre of the bath. In addition to the usual corrections it was necessary to allow, in the continuous flow detector system, for time dependent fluctuations in the neutron emission rate. Overall accuracy of 2-3% was achieved.

7.2 Poenitz[28] used a spherical manganese sulphate bath to measure the neutron flux at zero degrees at energies close to the threshold of the endothermic reactions $^{7}Li(p,n)$ and $T(p,n)$. By careful control of the accelerator energy the neutron production was limited to a forward cone of half-angle 9 degrees, thereby removing the need to collimate the bath with bulk shielding. The largest contribution to the uncertainty in the neutron flux was ± 1.3% due to neutron escape.

7.3 The use of 3.8 minute. ^{52}V speeds up the measurement cycle considerably compared with 155 minute ^{56}Mn. However, the short half-life introduces problems in the absolute measurement of the activity and its comparison with other laboratories. Furthermore, the uncertainty in the V/H cross section ratio of ± 1% enters into the source evaluation with greater weight as the V cross section is only 5 barns. For these reasons, if an absolute system is required it is preferable to calibrate the system with standard neutron sources.

7.4 Robertson et al[29] used a collimated vanadyl sulphate bath to measure the relative zero degree neutron yield from the $^{7}Li(p,n)$ reaction. It was necessary to shield the bath from room scattered neutrons and to admit the direct neutrons into the bath through a collimator. An important feature of the experiment was the demonstration by Monte Carlo calculation supported by inverse square measurements that the collimator could be taken as having, for each energy, a fixed entrance aperture at a fixed position over the energy range considered. The system was used to measure relative neutron flux with a standard deviation of ± 2%.

7.5 Leroy et al[30] used a small shielded and collimated manganese sulphate bath to measure the neutron flux from an accelerator in the energy range from 10 keV to 1 MeV.

The bath detector system was calibrated by means of a Ra Be neutron source which had been calibrated by BIPM. Neutron capture in the neutron source assembly and neutron escape into the reflector were obtained by Monte Carlo calculations as was the effective solid angle subtended by the bath aperture. An additional correction was necessary for air attenuation of the neutrons and the overall precision was reported to be + 1.8%. Above 1 MeV the neutron escape fraction became unacceptably large.

8. Conclusion

With sufficient care, the manganese sulphate bath can be used to achieve an uncertainty estimated at + 0.35% for a Californium neutron source at the 68% confidence level or + 0.7% at the 99% confidence level. Adapted for the measurement of neutron flux density, typical uncertainties of + 1.8-2.0% at the 68% confidence level have been achieved with bath detectors.

9. References

1. de Volpi, A., 1973, Metrologia, 6, 65.
2. Mubhabghab, S.L. and Garber, D.I., 1973, BNL 325, Edition 3.
3. Axton, E.J., Cross, P.,and Robertson, J.C., 1965, J. Nucl. Energy, 19, 409.
4. Smith, J.R., 1977. Private communication.
5. de Volpi, A. and Porges, K.G., 1969, Metrologia, 5, 128.
6. de Troyer, A. and Tavernier, G.C., 1954, Acad. Roy. Belg. Bull. Class. Sci., 40, 150.
7. Ryves, T.B. and Harden, D., 1965, J. Nucl. Energy A/B, 19, 607.
8. Colvin, D.W. and Sowerby, M.G., 1965, Physics and Chemistry of Fission, (Proc. Symp. Salzburg, 1965), 2, 25. IAEA Vienna.
9. Colvin, D.W., Sowerby, M.G. and Macdonald, R.I., 1967, Nuclear Data for Reactors, (Proc. Symp. Paris, 1966), 1, 307. IAEA Vienna.
10. Louwrier, P.F., 1964, PhD Thesis, Institute for Nuclear Physics Research (IKO) Rototype, Amsterdam.
11. Murphey, W.M., 1965, Nucl. Inst. Meth., 37, 13.
12. Ullo, J.J. and Goldsmith, M., 1976, Nucl. Sci. Eng., 60, 239.
13. Goldsmith, M. and Ullo, J.J., 1976, Nucl. Sci. Eng., 60, 251.
14. Ryves, T.B., 1964, J. Nucl. Energy A/B, 18, 49.
15. Spiegel, V. Jr. and Murphey, W.M., 1971, Metrologia, 7, 34.
16. Bardell, A.G., 1977, to be published.
17. Wescott, C.H., Walker, W.H. and Alexander, T.K., 1958, Proc. 2nd. Conf. The Peaceful Uses of Atomic Energy, Geneva. 15/P/202 United Nations N.Y.
18. Axton, E.J. and Ryves, T.B., 1967, J. Nucl. Energy, 21, 543.
19. Ryves, T.B. and Axton, E.J., to be published.
20. Noyce, R.H., Mosburg, E.R. Jr., Garfinkel, S.B. and Caswell, R.S., 1963, J. Nucl. Energy A/B, 17, 313.
21. Jaratsina, I.A., Constantinos, A.A. and Forminikh, V.I., 1964, Energie Atomique, 16, 253. Jaratsina, I.A., Andreev, O.L., Katchine, A.E. and Stukov, S.M., 1964, Energie Atomique, 16, 255.
22. Van der Eijk, see Naggiar, V., 1967, Metrologia, 3, 51.
23. Michikawa, T., Teranishi, E., Tomimasu, T. and Inoue, Y, 1959, Bull. Electrotechnical Laboratory, Japan, 23, 223.

24. Fieldhouse, P., Culliford, E.R. and Mather, D.S., 1967, J. Nucl. Energy, 21, 131.

25. Smith, J.R., Reeder, S.D. and Fluharty, R.G., 1966, IDO 17083, Phillips Petroleum.

26. Macklin, R.L., de Saussure, G., Kington, J.D. and Lyon, W.S., 1960, Nucl. Sci. Eng., 8, 210.

27. Scott, M.C. and Ashraf Atta, M., 1973, Nucl. Inst. Meth., 106, 465.

28. Poenitz, W., 1966, J. Nucl. Energy, 20, 825.

29. Robertson, J.C., Ryves, T.B. and Hunt, J.B., 1972, J. Nucl. Energy, 26, 507.

30. Leroy, J.L., Huet, J.L. and Gentil, J., Nucl. Inst. Meth., 88, 1.

31. Davy, D.R., 1966, J. Nucl. Energy, 20, 277.

Appendix

The following internal checks give valuable insight into the behaviour of the system and can save time being wasted on abortive irradiations. If any check fails the cause should be ascertained and rectified.

1. The product of bath efficiency (E) and total volume of bath and detector system should be constant for all bath sizes.

2. Fixed geometry γ source checks on the bath detectors should yield a constant count rate for each channel.

3. Results should be processed for both growth (source in bath) measurements and decay (source removed) measurements, growth/decay ratios should be constant and equal to unity for both channels. Channel 1/channel 2 ratios should be the same for growth, decay, and efficiency measurements. Deviations in the early stages of growth or near the changeover point immediately reveal faults due to change in pumping speed, timing errors or inadequate mixing.

INTERNATIONAL COMPARISON OF FLUX DENSITY MEASUREMENTS FOR MONOENERGETIC FAST NEUTRONS

V.D. Huynh
Bureau International des Poids et Mesures
Pavillon de Breteuil, F-92310 SEVRES, France

An international flux density intercomparison of fast neutrons has been organized by the Bureau International des Poids et Mesures during the past three years. Nine laboratories have carried out measurements. Three neutron energies were selected (250 keV, 2.5 MeV and 14.8 MeV), to which two optional energies were added (565 keV and 2.2 MeV). A polyethylene sphere with a small BF_3 counter at the center was used as a transfer instrument at all energies except for 14.8 MeV. A ^3He proportional counter was used at the two lower energies as the second transfer instrument. At 14.8 MeV a fission chamber (^{238}U) and the iron foil activation method using $^{56}Fe(n,p)^{56}Mn$ reaction were used. The results concerning the sensitivity of each transfer instrument measured by all the participating laboratories are summarized.

(International comparison; fast neutron flux density)

Introduction

At the request of Section III (Mesures neutroniques) of the Comité Consultatif pour les Etalons de Mesure des Rayonnements Ionisants, the Bureau International des Poids et Mesures decided in 1972 to organize an international comparison of flux density measurements for monoenergetic fast neutrons. Nine laboratories have carried out measurements. Table 1 lists the neutron energies chosen, the transfer instruments used and the participating laboratories with their responsible physicists. V.D. Huynh of the BIPM took part in the measurements performed in all the participating laboratories in order to control the good functioning of the transfer instruments and to ensure the homogeneity of the comparison.

Three neutron energies were selected, namely 250 keV, 2.50 MeV and 14.8 MeV, to which two optional energies (565 keV and 2.20 MeV) were added.

Three transfer instruments were used: a Bonner sphere (polyethylene sphere with a small BF_3 counter at the centre), a ^3He counter and a fission chamber (^{238}U). The polyethylene sphere was used at all energies (except for 14.8 MeV), the ^3He counter for the two lower energies and the fission chamber at 14.8 MeV. Another method was used at 14.8 MeV also, namely the activation of iron foils by the $^{56}Fe(n,p)^{56}Mn$ reaction.

Transfer instruments

1. Bonner sphere

The BIPM studied and supplied the polyethylene sphere + BF_3 counter (Fig. 1). This counter is placed at the center of the sphere, the diameter of which is 20.3 cm. The active part of the counter has a diameter of 1 cm and is 3 cm long. The threshold and the stability of the counter are checked by means of a 100 mCi Am-Be source which can be introduced into the sphere and placed near the counter.

Table 1

Conditions of the international comparison of flux density measurements for monoenergetic fast neutrons (neutron energies, transfer instruments and participating laboratories)

Neutron energies	Transfer instruments	Participating laboratories*
250 keV	polyethylene sphere + BF_3	NRC, CEN, BCMN, NPL, ETL, PTB, NBS
	^3He counter	NRC, CEN, NPL, ETL, PTB, NBS
565 keV (optional)	polyethylene sphere + BF_3 / ^3He counter	NRC, CEN, NPL, ETL, PTB, NBS
2.20 MeV (optional)	polyethylene sphere + BF_3	CEN, BCMN, NPL, PTB
2.50 MeV	polyethylene sphere + BF_3	BIPM, NRC, CEN, BCMN, NPL, ETL, PTB
14.8 MeV	fission chamber (^{238}U)	CEN, BCMN, NPL, ETL, BIPM
	$^{56}Fe(n,p)^{56}Mn$	NPL, BCMN, IMM, ETL, BIPM

* given in chronological order of participation; the acronyms stand for:

BCMN : Bureau Central de Mesures Nucléaires, Euratom, Geel, Belgium (H. Liskien and A. Paulsen)
BIPM : Bureau International des Poids et Mesures, Sèvres, France (V.D. Huynh)
CEN : Centre d'Etudes Nucléaires, Cadarache, France (I. Szabo)
ETL : Electrotechnical Laboratory, Tokyo, Japan (E. Teranishi and T. Michikawa)
IMM : Institut de Métrologie D.I. Mendéléev, Leningrad, USSR (I.A. Jaritzina and V.T. Stchebolev)
NBS : National Bureau of Standards, Washington, D.C., USA (M.M. Meier and O.A. Wassan)
NPL : National Physical Laboratory, Teddington, Great Britain (E.J. Axton, J.B. Hunt and A.G. Bardell)
NRC : National Research Council of Canada, Ottawa, Canada (K.W. Geiger and L. Van der Zwan)
PTB : Physikalisch-Technische Bundesanstalt, Braunschweig, Federal Republic of Germany (R. Jahr and M. Cosack).

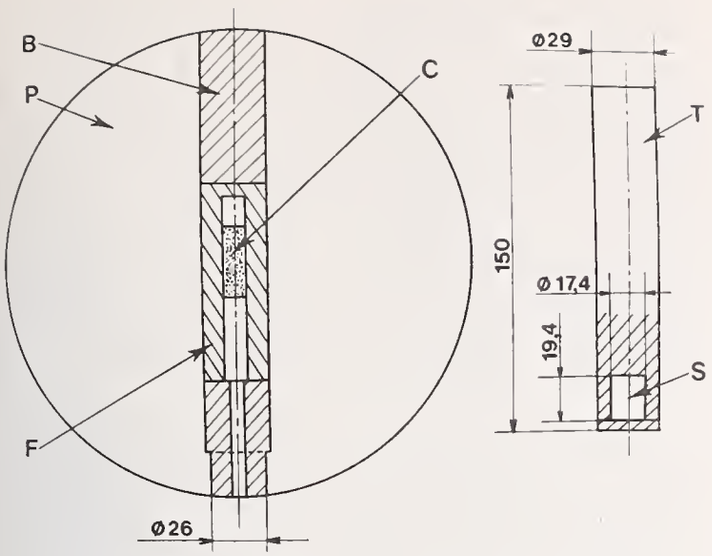

Figure 1 - BIPM polyethylene sphere with BF_3 counter (all dimensions in mm)

P - polyethylene sphere, Ø 203
F - polyethylene sheath containing the BF_3 counter, type 0,2NE3/1 F (LMT)
B - polyethylene plug which can be removed to place the source
C - active part of the counter, Ø 10, l 30
T - polyethylene plug containing the source
S - 100 mCi Am-Be(a,n) source, 2.2×10^5 n/s

2. ^{3}He proportional counter

The ^{3}He counter was supplied by NRC. It has an active length of 10.2 cm and a diameter of 2.44 cm. It is filled with helium-3 at a pressure of 10^6 Pa. Figure 2 gives an example of the response of the counter to 565 keV neutrons. In the comparison the bias was set at a pulse height which corresponds to

$$764 \text{ keV} + (0.6 \times E_n),$$

where E_n is the neutron energy considered (in keV).

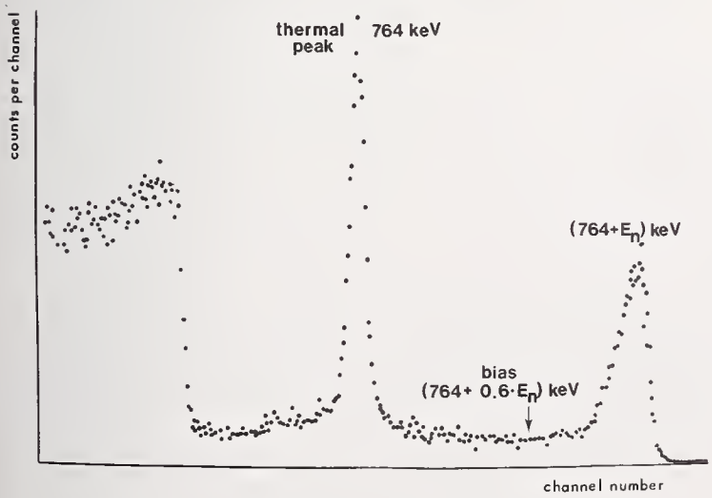

Figure 2 - ^{3}He counter spectrum far E_n = 565 keV

3. Fission chamber (^{238}U)

The fission chamber was constructed and supplied by NBS. It consists in fact of twa chambers called chamber T ("top") and chamber B ("battam") (Fig. 3). The supports are twa platinum foils set back to back and having each a ^{238}U deposit of 1 mg/cm^2 over an area of 1.3 cm^2. The gas circulating through the chamber is pure methane.

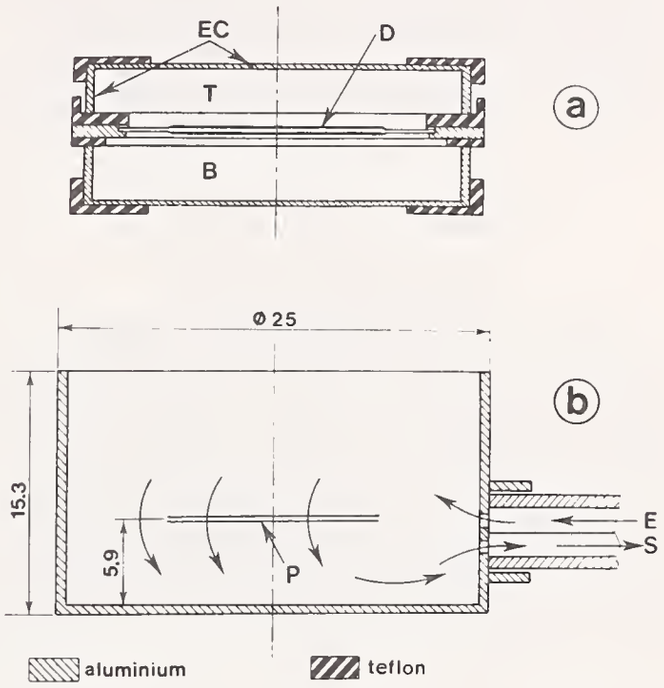

Figure 3 - Fission chamber constructed by NBS (all dimensions in mm)

a - fission chamber:
T - top chamber
B - battom chamber
EC - collecting electrodes
D - ^{238}U depasits, 1 mg/cm^2, surface 1.3 cm^2, on platinum foils (ground potential)

b - envelope af the fissian chamber:
P - position of the deposits
E - entrance af methane
S - exit "

Figure 4 - Respanse of the fissian chamber

Figure 4 shows the extrapolation method used for the low energy counts of the spectrum: a straight line is drawn between the point corresponding to the minimum of the "valley" and the one corresponding to zero amplitude ("true zero") of the multichannel analyzer.

4. Iron foil activation method

Iron foils are irradiated in the 14.8 MeV neutron beam and the induced "saturated" β activity according to the $^{56}Fe(n,p)^{56}Mn$ reaction is measured. This comparison was organised by E.J. Axton (NPL). Before the real comparison started, ^{60}Co foils were circulated among the participating laboratories to enable them to compare the results of β counting measurements. In the light of the agreement obtained the method may be considered valid.

Determination of the sensitivity of the transfer instruments

Let us recall that the comparison consisted in measuring the sensitivity $\mathcal{E}$ of each instrument defined as the quotient of the count rate of the detector to the neutron flux density. In practice, all laboratories measured the neutron flux density by means of a quantity Ψ_n which is the number of neutrons emitted by unit of solid angle in the direction of the detector; therefore, it is easier to compare directly the ratio $\mathcal{E}_\Omega = N_c/\Psi_n$ for a chosen source-detector distance d, where N_c is the number of counts of the transfer instrument. This gives the relation

$$\mathcal{E} = \mathcal{E}_\Omega \times d^2 \ .$$

For the sake of convenience, $\mathcal{E}_\Omega$ will be called the sensitivity of the transfer instrument in what follows.

Results

The results obtained in the various participating laboratories are summarized in Tables 2a, b, c, d, e and f. The Bonner sphere, the ^3He counter and the fission chamber were placed at 1.50 m, 50 cm and 10 cm from the target, respectively. The $1/d^2$ law was used to estimate the contribution of scattered neutrons for the Bonner sphere. The statistical and systematic uncertainties given in the tables were obtained by a quadratic sum of the various contributions as given by each laboratory. These results are also indicated in Figures 5 to 12.

It appears that there exists in general a reasonable agreement among the results (within 5% or better), except for 250 keV (Bonner sphere) where the discrepancy ranges from 10 to 20%. At 250 keV the corrections for the contributions of scattered neutrons are inconsistent: the $1/d^2$ law was used by all laboratories to estimate the contribution of scattered neutrons, but some laboratories (NPL, ETL and PTB) used also a shadow bar which gave practically the same correction, except for the cases where the contribution of scattered neutrons was high, in particular for 250 keV where a difference turned up in all laboratories (Table 3). Moreover, this difference is more important in the cases where the contribution of scattered neutrons is larger. One can see in Fig. 5 that for the 250 keV energy there are two groups of results, one for the laboratories having a higher correction for scattered neutrons and the other for those having a smaller correction (Table 2a). In addition, it happens that the group with the larger correction obtains also a higher value for the sensitivity of the Bonner sphere. Consequently, if for each laboratory we correct the contribution of scattered neutrons by means of the value determined by the shadow bar, the discrepancy between the two groups of laboratories should be reduced.

As a matter of fact, the $1/d^2$ law for the determination of the contribution of scattered neutrons is valid only if the variation of the scatter with distance is known or constant. Since this is not true, we should use the shadow bar. Table 4 summarizes the results obtained in the laboratories which used a 50 cm long shadow bar to estimate the contribution of scattered neutrons for the Bonner sphere.

In conclusion, we can say that, on the one hand, a great effort is still necessary to improve the absolute measurement of flux density for reaching an accuracy of 1% and, on the other hand, a new suitable transfer instrument has to be found which has a reasonable efficiency and a low sensitivity to scattered neutrons and γ rays.

Table 2a

Results of the comporison for the 250 keV neutron energy

Loboratory ond tronsfer instrument		"Absolute" detector*	Correction for scottered neutrons (%)	Sensitivity [counts/(n/sr)]	Uncertointy syst. (%)	Uncertointy stot. (1σ) (%)
sphere + BF_3 at 1.50 m	NRC	PC	11.3	5.71×10^{-6}	3.5	1.0
	CEN	DC	6.9	4.81×10^{-6}	2.3	0.4
	BCMN	PC	20.7	5.31×10^{-6}	2.8	0.5
	NPL	LC	9.1	4.71×10^{-6}	3.2	0.6
	ETL	PC	10.2	5.24×10^{-6}	2.5	0.6
	PTB	PC	6.4	4.71×10^{-6}	3.1	0.4
	NBS	BD	1.0	4.76×10^{-6}	3.7	0.8
^3He counter at 50 cm	NRC	PC	-	3.35×10^{-6}	3.2	1.7
	CEN	DC	-	3.05×10^{-6}	2.2	0.1
	NPL	LC	-	2.90×10^{-6}	3.1	0.5
	ETL	PC	-	3.05×10^{-6}	2.5	0.4
	PTB	PC	-	3.09×10^{-6}	3.1	0.6
	NBS	BD	-	3.20×10^{-6}	3.6	0.8

* PC - recoil proton proportionol counter
DC - directionol counter
LC - long counter
BD - block detector

Table 2b

Results of the comporison for the 565 keV neutron energy

	Loboratory ond transfer instrument	"Absolute" detector*	Correction for scottered neutrons (%)	Sensitivity [counts/(n/sr)]	Uncertointy syst. (%)	Uncertointy stot.(1σ) (%)
sphere + BF_3 at 1.50 m	NRC	PC	8.9	5.96×10^{-6}	1.9	0.4
	CEN	DC	3.5	6.21×10^{-6}	2.2	0.1
	NPL	LC	6.0	5.88×10^{-6}	3.1	0.4
	ETL	PC	9.0	5.84×10^{-6}	2.3	0.6
	PTB	PC	4.6	5.84×10^{-6}	3.1	0.2
	NBS	BD	1.0	5.97×10^{-6}	3.6	0.7
^3He counter at 50 cm	NRC	PC	-	2.19×10^{-6}	2.6	1.4
	CEN	DC	-	2.20×10^{-6}	2.2	0.1
	NPL	LC	-	2.17×10^{-6}	3.1	0.5
	ETL	PC	-	2.08×10^{-6}	2.2	0.6
	PTB	PC	-	2.08×10^{-6}	3.1	0.3
	NBS	BD	-	2.21×10^{-6}	3.5	1.0

* PC - recoil proton proportional counter
DC - directionol counter
LC - long counter
BD - black detector

Table 2c

Results of the camparison of the 2.20 MeV neutron energy

(palyethylene sphere + BF_3 counter at 1.50 m)

Labaratary	"Absolute" detectar*	Carrection far scattered neutrans (%)	Sensitivity [counts/(n/sr)]	Uncertainty syst. (%)	Uncertainty stat.(1σ) (%)
CEN	DC	3.9	6.88×10^{-6}	3.1	0.1
BCMN	T	6.1	7.61×10^{-6}	2.7	0.7
NPL	LC	6.0	7.24×10^{-6}	3.2	0.4
PTB	T	4.0	7.24×10^{-6}	2.2	0.8

* DC - directianal caunter
T - telescope
LC - long caunter

Table 2d

Results af the camparisan far the 2.50 MeV neutran energy

(palyethylene sphere + BF_3 caunter at 1.50 m)

Laboratary	"Absalute" detectar*	Correctian for scattered neutrans (%)	Sensitivity [caunts/(n/sr)]	Uncertainty syst. (%)	Uncertainty stat.(1σ) (%)
BIPM	AP	15.8	7.16×10^{-6}	1.8	0.1
NRC	SS	8.7	7.23×10^{-6}	4.2	0.8
CEN	DC	4.0	6.58×10^{-6}	3.2	0.1
BCMN	PC	8.5	6.90×10^{-6}	2.6	0.4
	T	8.5	7.15×10^{-6}	2.7	1.0
NPL	LC	6.5	6.97×10^{-6}	3.2	0.5
ETL	SD	48.5	8.07×10^{-6}	8.6	1.0
PTB	T	3.6	7.13×10^{-6}	2.2	0.7

* AP - assaciated particle
SS - stilbene spectrameter
DC - directianal caunter
PC - recoil pratan prapartional caunter
T - telescope
LC - long caunter
SD - semiconductar detector + hydragen radiatar

Table 2e

Results of the camparison for the 14.8 MeV neutran energy

(Fission chamber at 10 cm)

Laborotary	Neutron energy (MeV)	"Absalute" detector*	Sensitivity [counts/(n/sr)]	Uncertainty syst. (%)	Uncertainty stat.(1σ) (%)
CEN	14.8	AP	6.33×10^{-8}	3.3	0.5
BCMN	14.8	T	6.50×10^{-8}	3.1	1.0
NPL	14.67	PR	6.68×10^{-8}	2.9	0.6
ETL	14.75	AP	6.55×10^{-8}	2.8	0.3
BIPM	14.68	AP	6.36×10^{-8}	2.0	0.3

* AP - associated particle
T - telescope
PR - single stage protan recail device

Table 2f

Results of the comparison far the 14.8 MeV neutron energy

($^{56}Fe(n,p)^{56}Mn$ reoctian)

	Loborotory	Neutran energy (MeV)	"Absolute" detector*	Sensitivity [counts/(n/cm²)]	Uncertainty syst. (%)	Uncertainty stat.(1σ) (%)
iron foil n° 44	NPL	14.67	PR	3.23×10^{-4}	2.6	0.4
	BCMN	14.8	T	3.22×10^{-4}	2.5	0.8
	ETL	14.75	AP	3.21×10^{-4}	2.8	0.3
	BIPM	14.68	AP	3.17×10^{-4}	2.5	0.1
iron foil n° 45	NPL	14.67	PR	3.21×10^{-4}	2.6	0.3
	BCMN	14.8	T	3.22×10^{-4}	2.5	0.9
	ETL	14.75	AP	3.14×10^{-4}	2.8	0.3
	BIPM	14.68	AP	3.11×10^{-4}	2.5	0.2
iron foil n° 48	NPL	14.67	PR	3.22×10^{-4}	2.6	0.3
	BCMN	14.8	T	3.18×10^{-4}	2.5	0.9
	ETL	14.75	AP	3.17×10^{-4}	2.8	0.3
	BIPM	14.o8	AP	3.13×10^{-4}	2.5	0.2
iron foil n° 47	NPL	14.67	PR	3.25×10^{-4}	2.6	0.5
	IMM	14.8	AP, CM, NP	3.24×10^{-4}	0.8	0.3
iron foil n° 49	NPL	14.67	PR	3.22×10^{-4}	2.6	0.3
	IMM	14.8	AP, CM, NP	3.17×10^{-4}	3.1	0.4
iron foil n° 57	NPL	14.67	PR	3.19×10^{-4}	2.6	0.4
	IMM	14.8	AP, CM, NP	3.19×10^{-4}	1.0	0.4

* AP - ossociated porticle
T - telescope
CM - n-a coincidence method
NP - method bosed on n-p scottering cross section
PR - single stoge proton recoil device

The results of the comparison are given in graphical form in Figures 5 to 12

systematic uncertainty statistical uncertainty

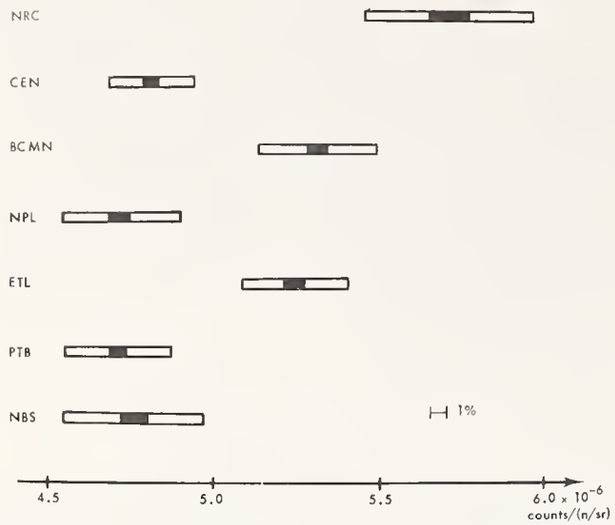

Figure 5 - E_n = 250 keV, sphere + BF_3 counter at 1.50 m

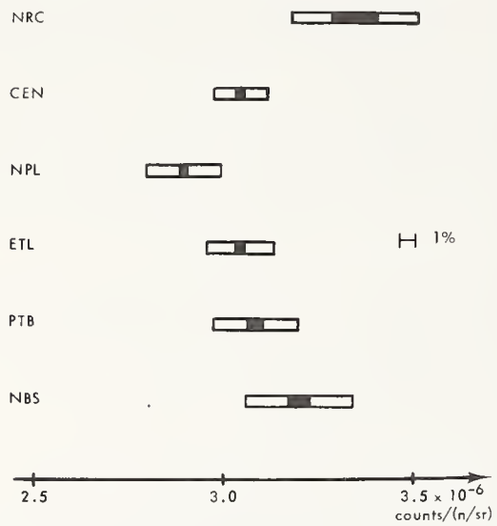

Figure 6 - E_n = 250 keV, ^{3}He counter at 50 cm

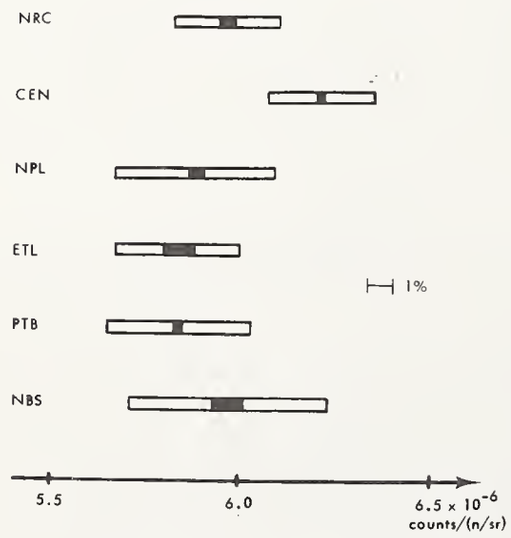

Figure 7 - E_n = 565 keV, sphere + BF_3 counter at 1.50 m

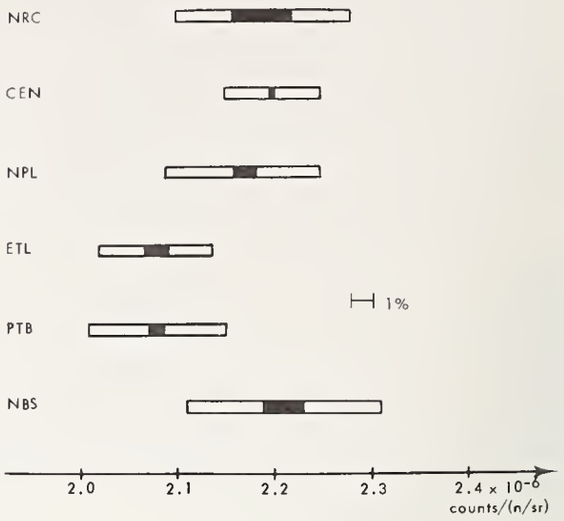

Figure 8 - E_n = 565 keV, ^{3}He counter at 50 cm

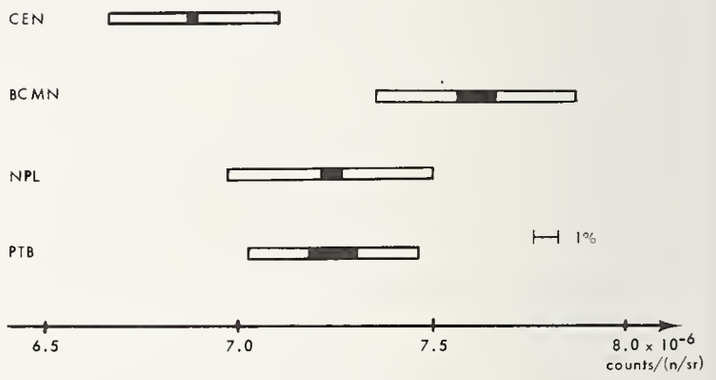

Figure 9 - E_n = 2.20 MeV, sphere + BF_3 counter at 1.50 m

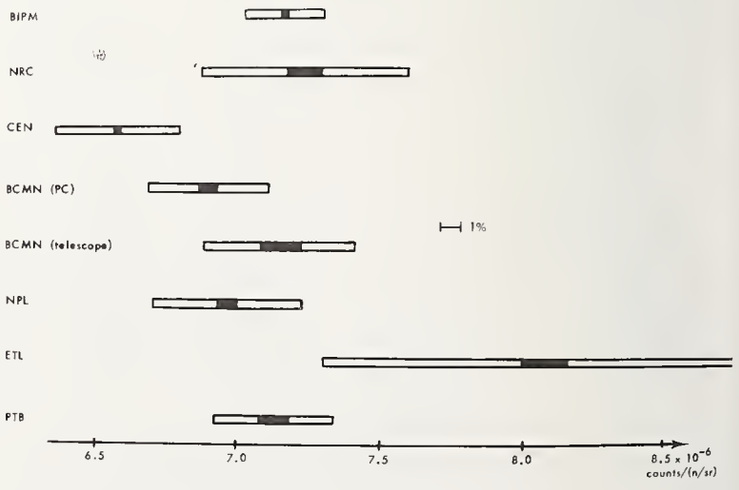

Figure 10 - E_n = 2.50 MeV, sphere + BF_3 counter at 1.50 m

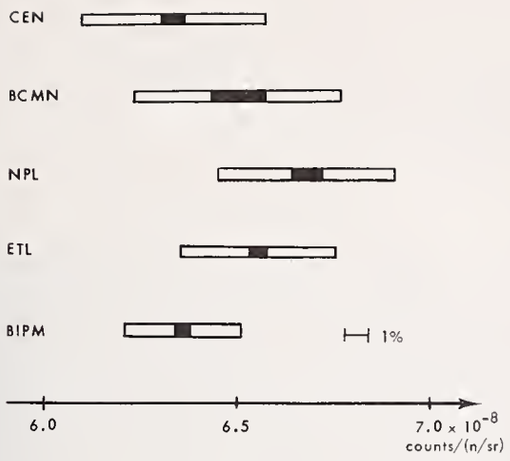

Figure 11 - E_n = 14.8 MeV, fission chamber at 10 cm

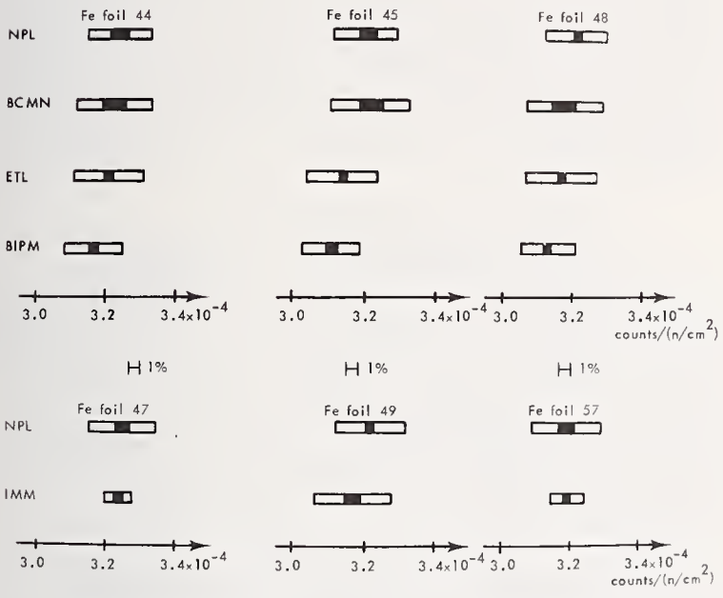

Figure 12 - E_n = 14.8 MeV, $^{56}Fe(n,p)^{56}Mn$ reaction

Table 3

Contribution of scattered neutrons (%)
(polyethylene sphere + BF_3 counter at 1.50 m)

Laboratory	250 keV		565 keV		2.20 MeV		2.50 MeV	
	(a)	(b)	(a)	(b)	(a)	(b)	(a)	(b)
BIPM	-	-	-	-	-	-	15.8	17.8
NPL	9.1	11.2	6.0	6.3	6.0	6.2	6.5	5.8
ETL	10.2	17.1	9.0	11.2	-	-	48.5	58.1
PTB	6.4	9.3	4.6	4.8	4.0	5.3	3.6	5.2
NBS	1.0	1.0	1.0	1.0	-	-	-	-

a) according to the $1/d^2$ low

b) measured with a shadow bar

Table 4

Results of the comparison. Polyethylene sphere + BF_3 counter at 1.50 m.
(Correction for scattered neutrons measured with a shadow bar)

Neutron energy (MeV)	Laboratory	Correction for scattered neutrons (%)	Sensitivity [counts/(n/sr)]	Uncertainty syst. (%)	Uncertainty stot. (1σ) (%)
0.250	NPL	11.2	4.60×10^{-6}	3.2	0.6
	ETL	17.1	4.84×10^{-6}	2.5	0.6
	PTB	9.3	4.56×10^{-6}	3.1	0.4
	NBS	1.0	4.76×10^{-6}	2.8	0.8
0.565	NPL	6.3	5.86×10^{-6}	3.1	0.4
	ETL	11.2	5.70×10^{-6}	2.3	0.6
	PTB	4.8	5.83×10^{-6}	3.1	0.2
	NBS	1.0	5.97×10^{-6}	2.8	0.7
2.20	NPL	6.2	7.22×10^{-6}	3.2	0.4
	PTB	5.3	7.14×10^{-6}	2.2	0.8
2.50	BIPM	17.8	6.99×10^{-6}	2.5	0.1
	NPL	5.8	7.02×10^{-6}	3.2	0.5
	ETL	58.1	6.57×10^{-6}	4.0	1.0
	PTB	5.2	7.01×10^{-6}	2.2	0.7

CALIBRATION AND USE OF FILTERED BEAMS †

R. B. Schwartz
National Bureau of Standards
Washington, D.C. 20234

Using a combination of resonant scatterers and filters, very pure beams of 2 keV, 24 keV, and 144 keV neutrons are produced at the NBS reactor. The calibration of these beams and their application to dosimeter calibration will be discussed.

(Dosimeter calibration; monoenergetic neutrons; neutrons; neutron beams; resonant scatterer.)

Introduction

The existence of "windows" in neutron cross sections has made possible the development of filters which transmit neutrons in relatively narrow energy bands, starting from a continuous reactor spectrum. These "windows" are, of course, just minima in the total cross section arising from destructive interference between s-wave resonance and potential scattering, and, as such, have been known and understood for many years. In fact, the 24 keV minimum in iron is rather infamous, since it has long been known that a fast neutron shield made of iron becomes a copious source of 24 keV neutrons. It remained for the MTR group,[1] however, to turn this "infamous" behavior into a virtue, when Simpson and his co-workers produced an intense 24 keV neutron beam by passing a reactor beam through an iron filter. They also produced beams of 2 and 144 keV, by using scandium and silicon filters, respectively. Unfortunately, the MTR was shut down before this work could be completed, and the filters themselves were transferred to NBS. Several other laboratories subsequently also developed filtered beams and Table I, taken from the compilation of Tsang and Brugger,[2] lists the current filtered beam facilities.

Table I. Filtered Beam Facilities. The numbers are neutron flux in neutrons/cm^2-sec.

Filter Material	^{238}U	Sc	Fe-Al	Si	O_2
Energy	186 eV	2 keV	24 keV	144 keV	2.35 MeV
FWHM	∿ 2 eV	700 eV	2 keV	25 keV	500 keV
BNL		3.5×10^6	1.3×10^6		
BOMBAY			1.5×10^4		
KYOTO			T.O.F.		
MTR		5×10^6	6×10^5	$\sim 10^7$	
MURR	$\sim 1 \times 10^5$		1.2×10^6	2.5×10^6	1.7×10^4
NBS		2.6×10^5	2×10^5	4.5×10^5	
RPI			T.O.F.		
USSR		5×10^4	2×10^4	8×10^4	

(The data for the original MTR beams are also listed, for the sake of nostalgia.) The numbers are the reported fluxes for the appropriate beams, in n/cm^2-sec. The entries for the RPI and Kyoto 24 keV beams indicate that these are used in conjunction with a pulsed linac neutron time-of-flight facility, and hence the fluxes are not comparable with the other beams, which are all from reactors.

†Work supported in part by U.S. ERDA.

The "Filter Material" refers to the principal component of the filter. Small amounts of additional materials may be added to suppress secondary peaks; some examples of this will be discussed later. Additionally, lead or boral may be added to reduce gamma ray or thermal neutron contamination. "Energy" is the nominal energy of the beam so produced and "FWHM" is the full width at half-maximum of the beam. The values for FWHM for the 186 eV, 2 keV, and 24 keV beams are calculated from the appropriate cross sections; the 144 keV and 2.35 MeV results are measured values. The values given are typical, but may vary from facility to facility depending upon the actual filter construction.

As we see, there are now several sets of filtered beams, each with its own reason for existence. In this paper we shall very briefly discuss some of the other beams, but shall primarily be concerned with the development and use of the NBS filtered beams. This is because: a) I know more about the NBS beams than any of the others, and b) the principal applications of the NBS beams are, possibly, closer to the general theme of this Symposium than the others.

Applications of Filtered Beams

For studying the properties of neutron capture gamma rays (as opposed to using capture gamma ray spectroscopy as a tool for studying the capturing states), a neutron source with a moderately broad (but well defined) energy spread may be preferable to the high resolution approach afforded by time-of-flight techniques. Such a broad source, encompassing many capturing states, will average over the Porter-Thomas fluctuations and allow the average properties of the gamma rays to be seen without the complications of resonance-to-resonance fluctuations.

Filtered beams are ideal for these experiments and, in fact, one of the first complete sets of high-quality keV neutron capture γ-ray data was obtained with the 2 keV beam at the MTR. This type of work is now being carried on using 2 keV and 24 keV beams by Bob Chrien and his group[3] at BNL; the study of capture γ-ray spectra also provides part of the motivation for the Bombay effort.[4] The Kyoto[5] and RPI[6] groups use iron filters in time-of-flight systems to essentially eliminate background and gamma-flash. This allows very precise total and capture cross section measurements at the iron windows. (The similarity of these two programs is not entirely accidental, since Bob Block seems to have carried the Wisdom of the Occident with him on his sabbatical journey to the East.) The MURR group[2] seems to have been most innovative, using the well-known minimum in (liquid) oxygen at 2.35 MeV, and the less well-known minimum at 186 eV in ^{238}U to produce beams at these high and low energies, as well as the more usual 24 and 144 keV beams.[7]

At NBS, the principal motivation for the development of the filtered beams has been for use in the calibration and development of neutron dosimeters, both "active" types such as remmeters and Bonner spectrometers, and "passive" devices such as albedo dosimeters. The lower energy beams are of particular importance, since typically 30% to 40% of the dose in the working environment around a reactor is due to neutrons below 30 keV,[8] but there are few (if any) suitable neutron calibration sources anywhere in this range. Preliminary data have been given earlier:[9] These will now be brought up to date.

NBS Filtered Beams

2 keV (Scandium) Beam

The problem with scandium as a filter material is that in addition to the window at 2 keV, there are several other windows at higher energies, which can give a relatively high transmitted flux in the energy region between 8 and 800 keV. Since a remmeter should give a higher response to high energy neutrons, the presence of a significant high energy background would be disastrous for the calibration of such instruments. Specifically, for the BNL Sc-Ti filtered beam[3] the higher energy neutron flux is listed as 25% of the 2 keV flux; the rem dose due to these higher energy neutrons is almost twice the dose due to the 2 keV neutrons. This type of background which is very difficult to avoid in any facility in which a scandium filter looks at a reactor core, is essentially eliminated in the NBS installation by the use of a through-tube in conjunction with a resonant scatterer. The through-tube passes 10 cm outside of the edge of the reactor core, and the collimating system containing the filter only sees a scatterer at the center of the tube (see Fig. 1). We use manganese to scatter

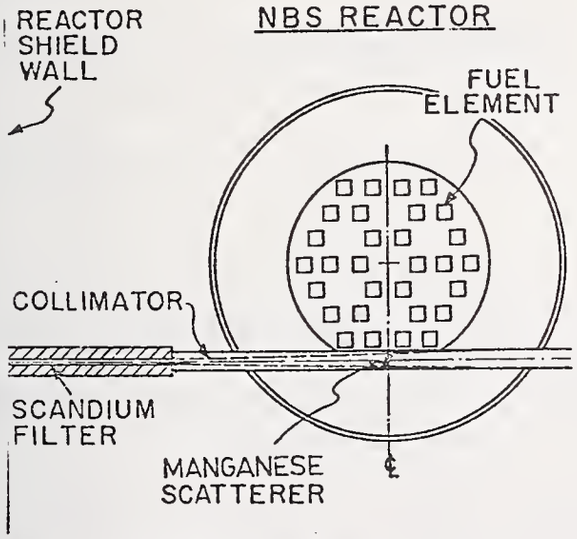

Fig. 1. Schematic representation of the NBS Reactor showing the filter, collimater, and scatterer in the through tube (not to scale).

the neutrons, making use of the scattering resonance at 2.375 keV. Although the resonant energy does not exactly match the energy of the 2 keV window, the resonance is sufficiently broad (Γ = 400 eV) that at 2 keV the scattering cross section is still >100 barns.[10] Physically, the scatterer is a 3 mm thick Mn-Al alloy containing 57 atomic percent manganese. This design eliminates unwanted core neutrons and gammas. The advantage of this design can be inferred from Table II,

Table II. Comparison of 2 keV filtered Beams

Lab.	2 keV Flux	% of Other Energy Neutrons	γ-Intensity (mR/hr)
BNL	3.5×10^6	25%	340
MTR	5×10^8	40%	~ 1
NBS	2.6×10^5	3%	8

which compares 2 keV beams. We note that the NBS beam has a considerably lower intensity than the other two, but also a much lower fraction of higher energy neutrons and a much lower gamma ray background than the BNL beam. For our purposes, this is a very advantageous trade-off. (Greenwood and Chrien,[3] BNL, describe a scandium-cobalt-titanium filter which they estimate would have 9% higher energy neutrons, and a 2 keV flux of 2×10^6 neutrons/(cm^2-sec). This filter does not appear to have been actually used for any experiments, however.) The spectrum of the NBS 2 keV beam is shown in Fig. 2. These data were taken with a 1 atm. hydrogen proton-recoil counter. The solid line shows the spectrum obtained with a 110 cm long Sc filter; the dashed curve shows the effect of adding one cm of Ti to the Sc. Even without the Ti,

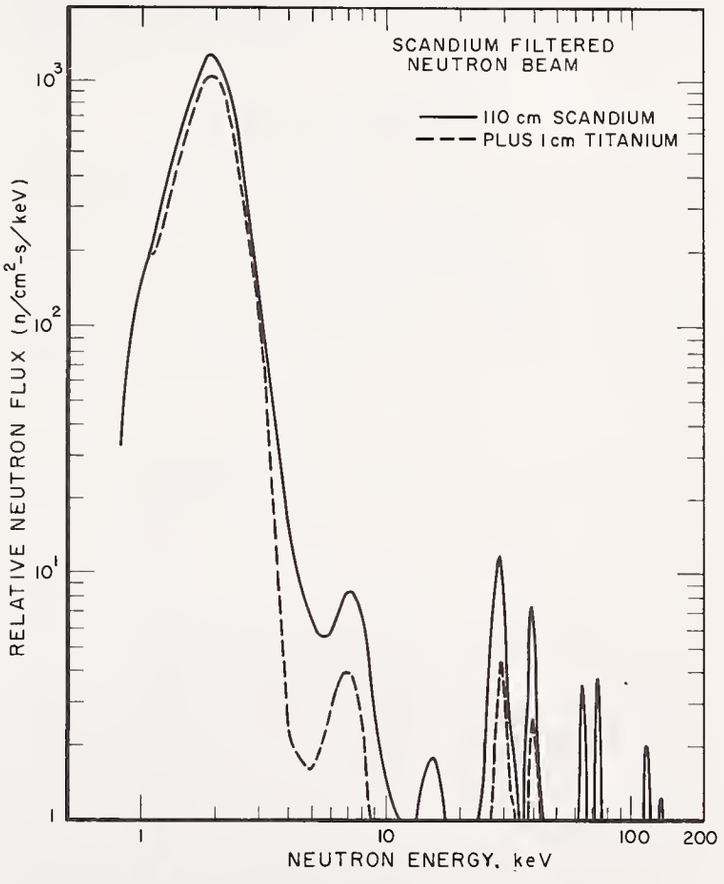

Fig. 2. Neutron spectrum through scandium filter. The solid curve represents the spectrum with a 110 cm scandium filter alone, and the dashed curve the spectrum with the addition of 1 cm of titanium.

the main secondary peak at 29 keV has an area of only 3% of the 2 keV peak. The addition of the Ti reduces this peak (as well as the ones at 7, 15, and 40 keV) by a factor of about 2-1/2, at the cost of only 17% of the 2 keV peak.

In terms of total flux, the higher energy contaminants amount to approximately 6% of the 2 keV flux without the titanium; the addition of the titanium reduces their contribution to 3% of the 2 keV flux.

Before leaving the matter of 2 keV beams, it must be pointed out that the value of the cross section minimum in scandium of 50 mb originally reported[1,11] is almost certainly wrong. A very careful combined BNL-RPI measurement[12] gives a total cross at the minimum of 700 mb, rather than 50. This higher value is consistent with a very rough transmission measurement made with the NBS filter, and suggests that the optimum filter thickness for a scandium filter may be rather thinner than heretofore believed.

24 keV Beam

The NBS 24 keV beam is produced by an iron-aluminum filter in another through tube, using a graphite scatterer. Both iron and aluminum have broad cross section minima near 24 keV, but their other minima do not, in general, overlap. Hence, it is not too difficult to produce reasonably clean 24 keV beams by judicious choice of the thickness of iron and aluminum, and since iron is a good gamma-ray absorber, these beams generally do not have serious gamma ray background problems. In this instance, therefore, the use of the through tube does not seem to be any great advantage. Our iron-aluminum 24 keV spectrum is shown in Fig. 3. The magnitude of the higher energy components is typical of the other 24 keV beams listed in Table I.

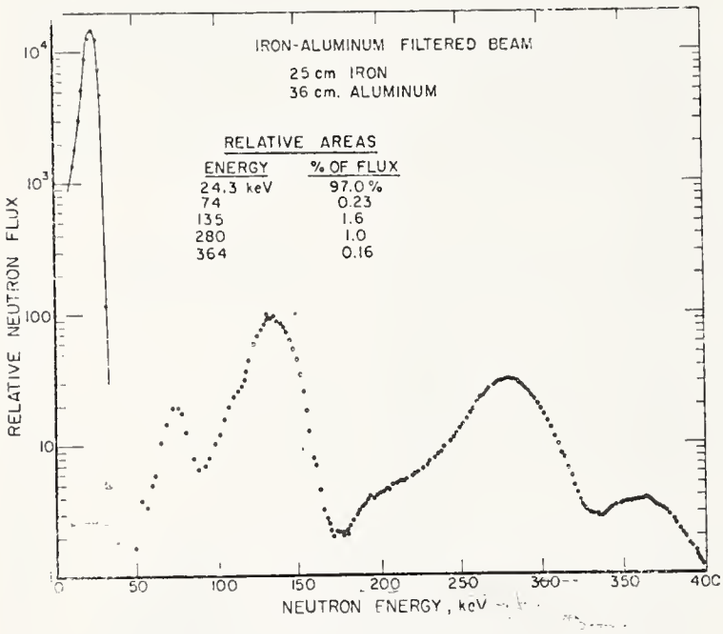

Fig. 3. Neutron spectrum through the iron-aluminum filter.

144 keV Beam

Other than the 144 keV window, the only window in silicon is at 54 keV, and the effect of this window can easily be minimized by an additional thin titanium filter. The main problem with silicon-filtered beams is the γ-ray background. In our case, the silicon filter is on the other side of the through tube from the iron-aluminum filter and, hence views the same graphite scatterer. Table III compares the 144 keV beams; we see that the use of the through tube-plus-scatterer greatly reduces the γ-background, but at the expense of a loss in neutron intensity.

Table III. Comparison of 144 keV Filtered Beams

Lab.	144 keV Flux	γ-Intensity (mR/hr)
MTR	$\sim 10^7$	~ 500
MURR	2.5×10^6	~ 450
NBS	4.5×10^5	~ 40

Our silicon filtered 144 keV spectrum is shown in Fig. 4.

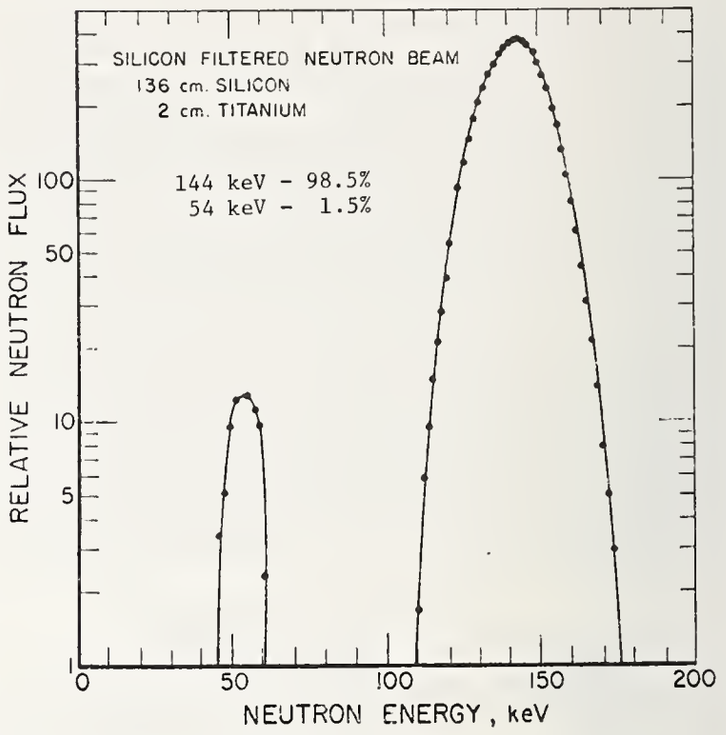

Fig. 4. Neutron spectrum through the silicon filter.

Beam Intensity Measurements

The 2 keV and 24 keV beam intensities are determined by counting with a one-atmosphere $^{10}BF_3$ counter. We use standard commercial counters, 5 cm diameter, varying in sensitive length from 6 to 33 cm, and employing a thin ceramic end window. The beam is brought in through the center of the ceramic window, parallel to the center wire. Since the beams are 2-1/2 cm diameter or less, there is minimum wall effect, and it is only necessary to know the ^{10}B density and the sensitive length to determine the counter efficiency. The ^{10}B density was determined by measuring the transmission of the counter along a diameter, using beams of 3.86 and 54.4 millivolt neutrons produced by NBS crystal spectrometers. The transmission was measured relative to an identical, but empty, counter to take into account the effect of the 0.9 mm thick stainless steel walls. At these low neutron energies, the ^{10}B absorption dominates the transmission, and thus the ^{10}B content can be determined quite accurately. The sensitive length of the counter was determined by scanning along its length with a finely collimated thermal beam. The small correction for losses in the 2 mm ceramic window was determined by an explicit measurement using a dummy window. We thus end up with counters whose absolute efficiencies are known in terms

of the ^{10}B cross section and the explicitly measured physical properties of the counter. Measurements of the 2 keV beam intensity, using 3 counters of lengths 6.4, 31, and 33 cm, showed a spread in values of less than ± 1%, which suggests at least internal consistency in our use of these counters. In the absence, however, of any cross checks on these measurements (e.g., foil activation) we feel that we can only quote an accuracy of ± 5% for the 2 keV beam intensity.

This technique is better suited to the 2 keV than the 25 keV beam, since the $^{10}B(n,\alpha)$ cross section is ∿ 3-1/2 times higher at the lower energy. However, a proton recoil counter can also be used for the 25 keV beam, as well as for the 144 keV beam. In this case, we use a counter which is physically similar to the 31 cm long BF_3 counter, but filled with hydrogen to an accurately known pressure. Since the hydrogen cross section is very well known, the area under the proton recoil spectrum is a direct measure of the beam intensity.

The 25 keV beam intensity measurements performed with the two different types of detectors differed by 7%. We consider this to be satisfactory agreement at this stage, although we are working to understand, and reduce, this difference. The flux quoted in Table I is the mean of these two values and ± 7% is probably a reasonable measure of the uncertainty in this flux, as well as for the uncertainty in the 144 keV flux.

Use of the Beams for Calibration

The first extensive use of the beams for dosimeter calibrations was by Dale Hankins of Livermore. Some of his results are shown in Fig. 5.[13] The circles are the

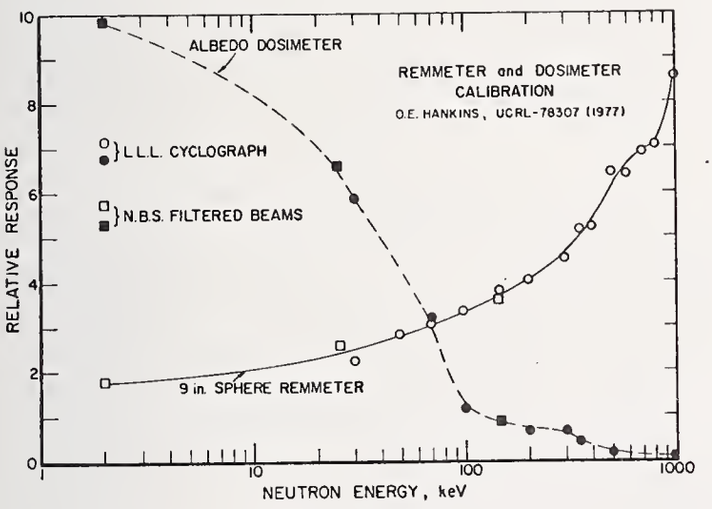

Fig. 5. Energy response of 9-inch sphere and of albedo dosimeter.

data obtained with the L.L.L. cyclograph; the squares are the data taken with the NBS beams. While the ordinate is in arbitrary units, there has been no normalization between the two sets of data. The line is an eye-guide only. We note that the NBS 144 keV point is in excellent agreement with the data taken with the cyclograph. The 30 keV cyclograph data represent the low energy limit of that device; the beam quality is rather poor at this energy and, for some of Hankins' runs, there was a suspicion that the data were systematically somewhat low.[14] This is borne out by comparison of the 30 keV cyclograph and 25 keV NBS datum for the 9 inch sphere calibration. The 2 keV NBS data then allow the calibrations to be extended a decade lower in energy. The importance of this can be judged from the albedo dosimeter calibration curve; without the NBS 2 keV datum, there would simply be no way of knowing the low energy response of the dosimeter.

Future Development

We feel that "Phase I" of the NBS filtered beam facility is complete: we have three clean beams whose intensities are well enough known for the initial uses to which they are being put. "Phase II" will consist first, of optimizing the filter configurations, and, second improving the calibrations. We feel that the 2 keV beam intensity can probably be increased with no appreciable loss in beam purity, and that the 24 keV beam purity can be further improved. More careful work on the corrections associated with the counter calibrations (e.g., end effects, backgrounds, etc.) together with alternate calibration methods (foil activation, counting with standard fission chambers) will reduce the uncertainty in our intensity measurements. We feel that accuracies in the 2%-3% range are a reasonable goal for the near future.

Conclusion

At the conclusion of his talk at the 1970 Neutron Standards Symposium,[1] Orval Simpson predicted that "... one fine day a reactor will offer standard neutron sources of 2, 24.5, and 144 keV produced from filtered neutron beams." We should like to suggest that perhaps that fine day has arrived.

Acknowledgements

The importance of using the resonant scatterer technique to clean up the 2 keV beam was first pointed out by Ivan Schröder, and we are grateful for his continued advice, assistance, and close collaboration.

It is a pleasure to thank E. D. McGarry and C. Heimbach for making the proton recoil spectra measurements shown in Figs. 2, 3, and 4.

References

1. O. D. Simpson, J. R. Smith, and J. W. Rogers, Proc. Symp. Neutron Standards and Flux Normalization, Argonne, Illinois (1970). CONF-701002, p. 362.

2. F. Y. Tsang and R. M. Brugger, private communication.

3. R. C. Greenwood and R. E. Chrien, Nucl. Instr. and Meth. 138, 125 (1976).

4. E. Kondaiah, R. P. Anand, and D. Bhattacharya, Proc. Int. Conf. Photonuclear Reactions and Applications, Asilomar, California (1973), CONF-730301, paper 2D11-1.

5. R. C. Block, Y. Fujita, K. Kobayashi, and T. Oovaki, J. Nucl. Sci. and Technology, 12, (1975).

6. R. C. Block, N. N. Kaushal, and R. W. Hockenbury, Proc. Nat. Topical Meeting on New Develop. Reactor Phys. and Shielding, CONF-72091, 1107 (1972).

7. F. Y. Tsang and R. M. Brugger, Nucl. Instr. and Meth. 134, 441 (1976).

8. J. R. Harvey and S. Beynon, Proc. First Symposium on Neutron Dosimetry in Biology and Medicine, Neuherberg/Munchen (Germany), (1972) p. 955.

9. I. G. Schröder, R. B. Schwartz, and E. D. McGarry, Proc. Conf. Neutron Cross Sections and Technology, Washington, D.C. (1975). NBS Special Publication 425, p. 89; E. D. McGarry and I. G. Schröder, loc. cit., p. 116.

10. M. D. Goldberg, S. F. Mughabghab, B. A. Magurno, and V. M. May, "Neutron Cross Sections, Vol. IIA, Z=21-40," BNL 325, Second Edition, Supplement No. 2 (Physics TID-4500) Feb. 1966.

11. W. L. Wilson, "Neutron Cross Section Measurements and Gamma Ray Studies of ^{45}Sc;" M. S. Thesis, University of Idaho Graduate School, Dec. 1966 (unpublished.)

12. H. I. Liou, R. E. Chrien, K. Kobayashi, and R. C. Block, Bull. Am. Phys. Soc 22, 53 (1977).

13. D. E. Hankins, UCRL-78307 (1977).

14. D. E. Hankins, private communication.

MUCH ADO ABOUT NOTHING: DEEP MINIMA IN ^{45}SC AND ^{56}FE TOTAL NEUTRON CROSS SECTIONS*

R. E. Chrien and H. I. Liou
Brookhaven National Laboratory, Upton, New York 11973

R. C. Block and U. N. Singh
Gaerttner Linac Laboratory, Rensselaer Polytechnic Institute, Troy, New York 12181

and

K. Kobayashi
Kyoto University Research Reactor Institute, Kumatori-cho, Osaka-fu, Japan

The deep minima in ^{45}Sc and ^{56}Fe neutron total cross sections have been measured at the Gaerttner Linac Laboratory by using thick, ultra-pure samples in transmission experiments. The samples are used to produce quasi-monoenergetic beams at the BNL High Flux Beam Reactor. For the ^{45}Sc minimum near 2.05 keV we obtain $\sigma_{total} = 0.71 \pm 0.03$ barns, in sharp contrast to a previously reported value of ~ 0.05 barns. The ^{56}Fe measurement was carried out with a 6 kg, 68.58-cm-long sample of 99.87% isotopically pure sample of ^{56}Fe; a minimum cross section of 0.0085 ± 0.004 barns at 24.39 keV is inferred. This may be compared to a value of 0.420 barns for natural iron.

(Neutron total cross sections, ^{45}Sc measured from 0.4 to 22 keV; deduced neutron resonance parameters; ^{56}Fe measured from 0.4 to 1000 keV)

I. Introduction

Many elements exhibit deep neutron total s-wave cross section minima due to the interference between resonance and potential scattering amplitudes. These minima are of considerable interest in shielding applications and in the design of transmission filters for the production of quasi-monoenergetic neutron beams. For the latter application both steady state reactors[1,2,3] and pulsed sources[4,5] have been used. The use of such filters for dosimetry measurements has been discussed by Schwartz[6] at this meeting. Scandium and iron-aluminum filters have been also rather widely used for capture γ-ray and cross section studies. The empirical optimization of scandium and iron filters has been discussed by Greenwood and Chrien.[3] A summary of known filter facilities has recently been prepared by Tsang and Brugger.[7]

In spite of the wide applicability, the total neutron cross sections of ^{45}Sc and ^{56}Fe, in particular, are ratherly poorly known. In the installation of the HFBR scandium filter, it became obvious that the flux measured at this filter could not be reconciled with the accepted cross sections. Furthermore no accurate measurement of ^{56}Fe total cross sections has been published. For these reasons we carried out experiments to establish the cross sections at the 2.05 and 24.4 keV minima in ^{45}Sc and ^{56}Fe. Thick metallic samples of Sc (99.9% pure) and separated Fe (enriched to 99.87% in ^{56}Fe) were obtained from the HFBR Tailored Beam Facility. Neutron transmission measurements were carried out at RPI's Gaerttner Linac Laboratory, and the data subsequently were analyzed at BNL.

II. Method

A full description of the RPI Linac Facility has been reported, and only a brief description is given here.

The standard water-cooled Ta and CH_2-moderated neutron TOF target and the ^{10}B-NaI neutron detector at the 28.32-m flight path were used for these measurements. The linac was operated at a repetition rate of 500 sec^{-1}, an electron energy of $\simeq$ 70 MeV, a peak electron current of $\simeq$ 1 A, and an electron pulse width of either 19, 35, or 66 ns. The counting data were recorded vs. TOF with the 31.25-ns TOF clock interfaced to the PDP-7 on-line computer. The transmission samples were cycled automatically into and out of the neutron beam by the programmed computer, and a cycle was repeated every 10 to 20 minutes to average out neutron source intensity fluctuations.

The composition of the ^{45}Sc and ^{56}Fe samples are listed in Table 1. The ^{45}Sc samples were prepared by vacuum sublimation onto a cooled Ta plate, and the sublimed metallic material was subsequently pressed into steel containers 2.54 cm in diameter. The H and O impurities were determined by the vacuum fusion method, and the heavier elements by mass spectrometry,

Table 1
Sample Properties

(A) Scandium Samples

Sample No.	Dimensions (cm)	1/N (barn/atom)
1	2.54 diameter x 10.2	2.738
2	2.54 diameter x 15.2	1.844
3	2.54 diameter x 30.5	0.922
4	2.54 diameter x $\simeq$0.2	152.5
5	2.54 diameter x 0.55	50.8
6	2.54 diameter x 2.4	11.7

Impurity	Atom Per Cent
H	0.49
O	0.18
Ta	0.037

(B) ^{56}Fe Sample

Dimensions (cm)	1/N (barn/atom)
3.22 x 3.85 x 68.6	0.175

Isotope	Wt. Per Cent
^{54}Fe	0.05
^{56}Fe	99.87
^{57}Fe	0.07
^{58}Fe	0.006

Impurity	Atom Per Cent	Impurity	Atom Per Cent
O	.617	Cr	.011
Cu	.120	W	.010
H	.059	Ni	.005
C	.020	Si	.002
N	.012	P	.002

for both samples, at the Ames Laboratory Analytical Center. In addition the Ta content of the Sc was checked by emission spectrography, by resonance x-ray fluorence, by neutron activation, and by neutron transmission. This wide variety of methods for Ta analysis was necessitated by the discovery of a sharply inhomogeneous distribution of Ta impurity throughout the bulk of the Sc filter. Both activation and transmission methods were able to sum over large sections of the filter and thus produce a more reasonable average impurity content than was the case for the other techniques, which were applied to small samples of the filter material.

The ^{56}Fe sample was prepared at Oak Ridge National Laboratory from electromagnetically enriched iron in the form of iron oxide. The metallic sample was obtained by reducing the oxide in a hydrogen atmosphere. The isotopes and impurities listed in Table 1 were determined from measurements of the iron oxide and metal respectively.

In the final analysis, these cross section measurements are only as reliable as the impurity content determination. At the Sc minimum, the impurity correction is about 112 mb out of a measured 822 mb; while in the ^{56}Fe, the correction is about 51.5 mb out of a measured $\sim$ 60 mb. In each case ENDF/B IV evaluated cross sections were used in the correction.

Two sets of ^{45}Sc transmission measurements were carried out. In one measurement the 10.2-cm-long scandium sample No. 1 was placed in the neutron beam to produce a TOF-filtered spectrum of neutrons which is peaked near the interference minimum in scandium. This removes most of the neutrons from the beam and results in a very low background of neutrons with energies far from the minimum. Then samples No. 2 and 3 were cycled into the filtered beam to obtain an accurate measurement of the cross section near the interference minimum. The other measurement was a conventional transmission measurement. The 10.2-cm-long scandium filter was removed from the beam and samples No. 4, 5 and 6 were cycled into the beam. This latter measurement enabled the cross section to be determined near the peaks of the resonance as well as near the minima.

For the ^{56}Fe measurements a 20.3-cm-long filter of pure Armco iron was placed in the neutron beam to produce a TOF-filtered spectrum peaked near the iron minimum. The 68.6-cm-long ^{56}Fe sample was then cycled into and out of the filtered neutron beam. The filtering effect in iron is illustrated in Fig. 1 near the 24 keV minimum. Here the ^{10}B-NaI detector relative counting rate is shown for Armco iron filters varying in thickness from 5.1 cm(2") to 50.8 cm(20"). For this experiment the 20.3 cm(8") thickness was used, and from Fig. 1 we see that the peak transmission through the filter is 48% and that most of the neutrons at energies several keV away from the peak are removed from the beam.

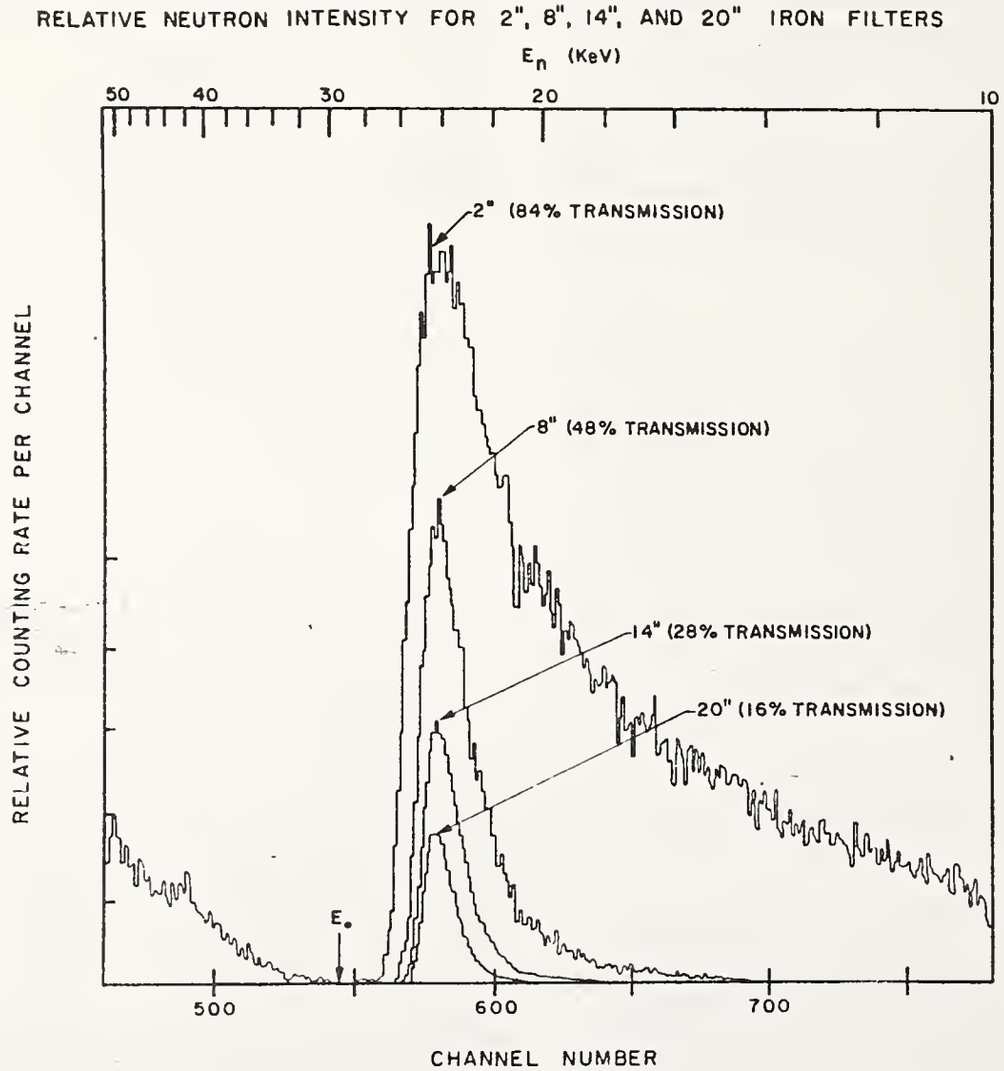

Fig. 1: The ^{10}B-NaI detector counting rate vs. TOF with Armco iron filters 5.1-cm(2"), 20.3-cm(8"), 35.6-cm(14") and 50.8-cm(20") thick. The peak transmission through each filter is shown in parentheses.

The TOF counting data were corrected for dead-time losses in the electronics and for background, and the neutron transmission was then determined. The total cross section σ_t was obtained from the neutron transmission with the following equation

$$\sigma_t = -(1/N)\ \ln T - (N_{air}\sigma_{air})/N \qquad (1)$$

where N is the thickness of the scandium or ^{56}Fe sample, T is the neutron transmission, N_{air} is the thickness of air displaced by the sample, and σ_{air} is the neutron total cross section of the air. The cross section of air was obtained from the oxygen and nitrogen cross sections plotted in BNL-325.[10]

III. Results

A. ^{45}Sc

The ^{45}Sc total cross section obtained from equation (1) is plotted in Fig. 2 over the neutron energy range from $\simeq$ 0.4 to 22 keV. This plot is a "blend" of all the ^{45}Sc data, where the data near the peaks in the cross section are from the thinnest sample and the data near the deep minima are from the thickest sample. The data have been corrected for the presence of the contaminants listed in Table 1.

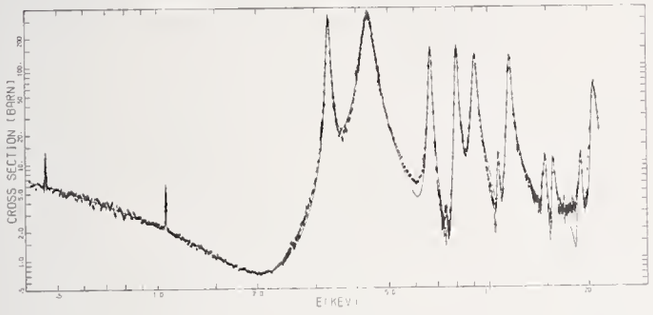

Fig. 2: The neutron total cross section of ^{45}Sc. The experimental data are shown as solid points with error bars (standard deviations determined from the counting statistics). The solid curve is a resolution-broadened "R-matrix" fit to the data using the resonance parameters listed in Table 2.

The measured minimum cross section of ^{45}Sc near 2 keV is (0.71 $\pm$ 0.03)b, where the error is derived from a combination of the counting statistics and the uncertainties in the H and O corrections. The minimum occurs at an energy of (2.05 $\pm$ 0.02) keV. This minimum cross section of (0.71 $\pm$ 0.03)b is in serious disagreement with earlier measurements reported by Wilson[11] of $\sim$ 0.05 b, and it is also in disagreement with the evaluated minimum cross section[12] of $\sim$ 0.085 b which was based on these older measurements. Our result of 0.71 b has serious implications for the effective use of expensive scandium for filtered beams. The 0.71 b cross section at 2.05 keV is comparable to, or larger than, the cross sections in the higher energy ^{45}Sc minima, and thus the length of the ^{45}Sc filter should be limited to enhance the transmitted neutron flux near 2 keV relative to that transmitted at higher energies.

The ^{45}Sc total cross section has been fit by an approximate R-matrix formalism,[13] and the solid curve through the experimental points in Fig. 2 is a "best fit" to the data. The curve has been resolution broadened; the resolution FWHM is approximately 3 channels near the 2 keV minimum. In Table 2 are listed the resonance parameters derived from this fit.

Table 2

^{45}Sc Resonance Parameters

s-wave level parameters: Γ_γ = 0.4 eV

E_o (eV)	Γ_n (eV)	J	E_o (eV)	Γ_n (eV)	J
-500	4.0 (Γ_n^o)	3	11575	290	4
-220	0.67 (Γ_n^o)	4	14525	20	3
3295	75	3	14740	26	4
4330	340	4	15560	28	4
6684	130	3	15850	5	3
8023	145	4	18580	32	3
9092	300	3	18870	62	4
10625	10	3	20500	80	4
10735	6	4	20780	710	3

p-wave level parameters

E_o (eV)	$g\Gamma_n$ (eV)
460.6	0.0022
1060.4	0.0050
7377.0	0.4
7458.0	0.4
7548.0	0.25

Resonance parameters for ^{45}Sc derived from shape fits to the total cross section.

This fit was determined by the following procedure:

(a) The spins of the positive energy resonances were obtained by fitting the peak cross sections and the shape of the interference between resonances.

(b) Negative energy levels were introduced to fit the cross sections at thermal and in the low energy region.

(c) The neutron widths were obtained for all the resonances such that (i) the calculated R-matrix cross section curve produced an acceptable overall fit to the data, and (ii) the R-matrix minimum total cross section near the 2 keV minimum equaled the observed value of 0.71 b.

(d) A single radiation width was then determined for all the resonances such that the thermal capture cross section resulting from the sum of contributions from all the resonances equaled the evaluated value[12] of (26.5 $\pm$ 1.0) b.

The best fits to the data are obtained when the J=3 channel spin contributes significantly to thermal capture. The "best fit" parameters listed in Table 2 produce a thermal capture cross section which has approximately equal contributions from J=3 and J=4 channel spins.

Thermal neutron capture γ-ray spectral measurements by Bolotin[14] favor a significant J=3 channel spin contribution. He observed a primary gamma-ray transition to the 1^- state in ^{46}Sc at an excitation energy

of 142 keV. Thermal capture in scandium consists of a mixture of capture into 3^- or 4^- states and Bolotin's observed transition strength of 1.3 gammas per 1000 captures indicates that this gamma ray is an E2 transition from a 3^- to a 1^- state. The partial radiation width for this E2 transition can be calculated from the observed transition strength and the resonance parameters deduced from the R-matrix fit to the total cross section. The E2 width calculated from the "best fit" parameters in Table 2 is about 6 times larger than the typical E2 width observed in this mass and energy range, and this is reasonable considering the fluctuations of the observed E2 widths. However, when the E2 width is determined from the R-matrix parameters which produce predominantly J=4 channel spin thermal capture, the E2 width is about 500 times larger than the typical E2 width.

Such a 500 times larger E2 width is very unlikely, and thus Bolotin's measurements favor thermal capture which has a significant J=3 channel spin contribution. We have independently confirmed Bolotin's observation in a separate experiment to be reported elsewhere.

A polarized neutron experiment by Roubeau et al.[15] claims to have measured the difference in scattering lengths at thermal between the (I + 1/2) J=4 and (I - 1/2) J=3 spin states. They report a value of $(a_+ - a_-) = +1.2 \times 10^{-12}$ cm. The implication of their result is that a J=4 state dominates thermal scattering. This result is inconsistent with our present result, since it would mandate a deep minimum near 2 keV, as a result of interference between the dominant J=4 resonance at 4.330 keV and a strong J=4 bound state. An attempt to fit our data subject to this constraint results not only in a poor fit, but requires absurd R-matrix parameters, (e.g., $R^{I-\frac{1}{2}}_{I-\frac{1}{2}}/R^{I+\frac{1}{2}}_{I+\frac{1}{2}} \approx 8$). We conclude that the experiment of Roubeau et al. is in error.

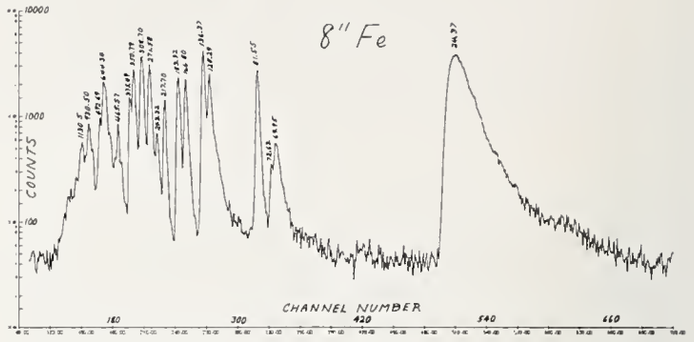

Fig. 3: The ^{10}B-NaI detector counts vs. TOF channel number for a 20.3-cm(8") Fe filter placed in the neutron beam. The TOF channel width is 31.25 ns.

B. ^{56}Fe

The ^{10}B-NaI detector counts per TOF channel are plotted in Fig. 3 for the 20.3-cm (8") Armco iron filter in the neutron beam, and in Fig. 4 for the 20.3-cm Armco iron filter plus the 68.6-cm (27") ^{56}Fe sample. The 68.6-cm ^{56}Fe sample produces a quasi-monoenergetic peak of neutrons which peaks near an energy of 24 keV.

The total cross section of ^{56}Fe near the 24 keV minimum is plotted in Fig. 5. For iron both impurity cross section corrections and resolution corrections are very important, which was not the case for scandium. The total correction for impurities amounted to 51 mb in the region of the minimum; and we infer a minimum observed cross section of $\sim$ 15 mb at an energy of 24.39 $\pm$ 0.04. This cross section is, however, seriously affected by our resolution function, which has a FWHM of about 200eV at the minimum ($\sim$ 2.1 channels). Using the parameters of Pandey and Garg[16] we fitted a series of resolution broadened cross section curves to the minimum, using the radiation width of the major s-wave resonance near 27 keV as a parameter. We find the best fit for a radiation width of about 2.2 eV, which provides an independent measurement of that important parameter. We also include a p-wave potential scattering contribution in this calculation. From the best fit, we infer a minimum cross section of 8.5 $\pm$ 4 mb, of which 1.3 mb is due to ℓ=1 scattering, and the balance is due to the (n,γ) reaction.

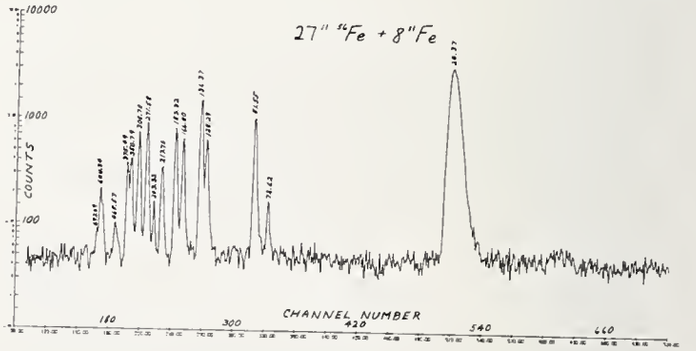

Fig. 4: The ^{10}B-NaI detector counts vs. TOF channel number for a 20.3-cm(8") Fe filter plus a 68.8-cm(27") ^{56}Fe sample placed in the neutron beam. The TOF channel width is 31.25 ns.

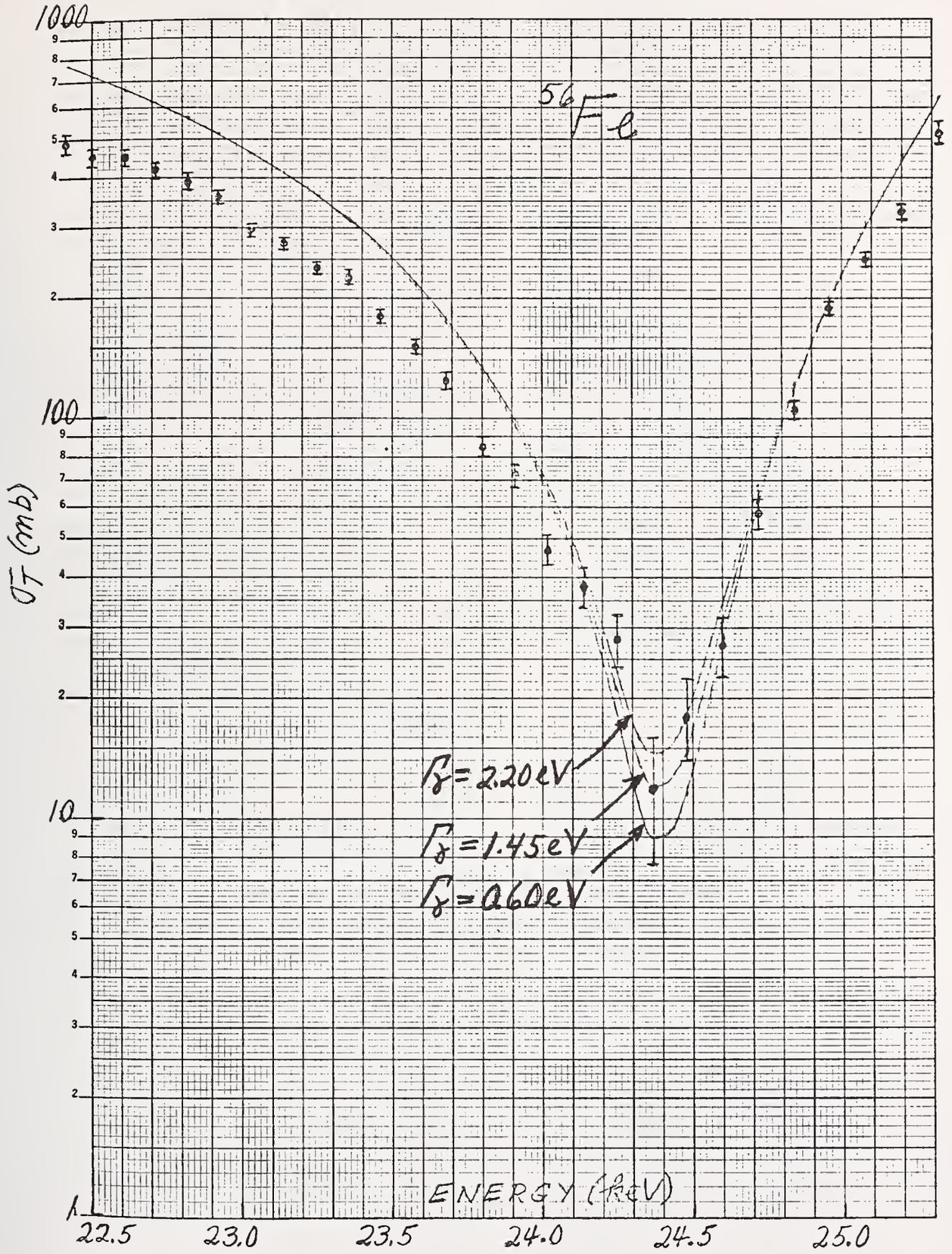

Fig. 5: The neutron total cross section of ^{56}Fe near the 24.37 keV minimum. The solid curves are resolution-broadened "R-matrix" calculations using the resonance parameters shown in the figure.

The minimum cross section measured for this ^{56}Fe sample is almost two orders of magnitude smaller than the $\simeq$ 420 mb cross section measured for elemental Fe.[17,18] This results in a much more intense beam of quasi-monoenergetic $\simeq$ 24 keV neutrons from this filter than from a filter of Fe of the same length. For example, for the 68.6-cm long filter with 1/N = 0.175 b/a, the transmission through the ^{56}Fe filter at 24.4 keV is 72% (allowing for impurities), whereas the transmission through the same thickness of Fe is only 9%. Thus a quasi-monoenergetic beam of $\simeq$ 24 keV neutrons can be obtained with a ^{56}Fe filter which has excellent transmission through the 24.4 keV minimum. The filter can be used in very thick configurations to reduce unwanted fast neutrons and gamma rays.

Summary

The neutron total cross section has been measured for ^{45}Sc and ^{56}Fe with particular emphasis upon measuring the cross section in the minima. The ^{45}Sc cross section has a prominent minimum at (2.05 $\pm$ 0.02) keV which is (0.71 $\pm$ 0.03) b. This cross section is an order of magnitude larger than estimated from earlier measurements, and this has serious implications in the design of a ^{45}Sc filter for reactors. Although the design of a ^{45}Sc filter system depends upon the application of the system (e.g., for neutron capture spectra, dosimetry, etc.), this higher cross section of 0.71 b should lead to the selection of a thinner ^{45}Sc filter than one based on the former $\sim$ 0.05 b value.

The ^{56}Fe cross section has a prominent minimum at 24.4 keV which is (8.5 $\pm$ 4.0) mb. This is considerably smaller than the $\simeq$ 420 mb minimum in elemental iron, and thus thick filters of ^{56}Fe can provide intense quasi-monoenergetic beams of $\simeq$ 24 keV neutrons with a very small contamination of gamma rays and fast neutrons.

Acknowledgements

The authors wish to acknowledge the valuable contribution of B. Beaudry in arranging for the vacuum fusion and mass spectrographic analyses of the samples at Ames Laboratory. Valuable discussions were held with Larry Passell, Harvey Marshak, Wally Koehler, Marty Blume and Said Mughabghab. The able assistance of Frederick Paffrath in the sample preparation is much appreciated.

References

*Work supported by the Energy Research and Development Administration.

[1] O. D. Simpson and L. G. Miller, Nucl. Instr. and Meth. 61, 245 (1968); and U.S. Atomic Energy Commission Report I N-1218 (1968).

[2] R. B. Schwartz, contribution to this conference.

[3] R. C. Greenwood and R. E. Chrien, Nucl. Instr. and Meth. 138, 125 (1976).

[4] R. C. Block, N. N. Kaushal and R. W. Hockenbury, Proc. of New Devel. in Reactor Phys. and Shielding, CONF-720901, Book 2, 1107 (1972).

[5] R. C. Block, Y. Fujita, K. Kobayashi and T. Oosaki, J. of Nucl. Sci. and Tech. 12, 1 (1975); Y. Fujita, K. Kobayashi, T. Oosaki and R. C. Block, Nucl. Phys. A258, 1 (1976).

[6] R. B. Schwartz, contribution to this conference.

[7] F. Y. Tsang and R. M. Brugger, private communication, University of Missouri.

[8] R. W. Hockenbury, Z. M. Bartolome, J. R. Tatarczuk, W. R. Moyer and R. C. Block, Phys. Rev. 178, 1746 (1969).

[9] Z. M. Bartolome, R. W. Hockenbury, W. R. Moyer, J. R. Tatrczuk and R. C. Block, Nucl. Sci. and Eng. 37, 137 (1969).

[10] D. I. Garber and R. R. Kinsey, BNL-325, 3rd Ed., Vol. 2, (1976).

[11] W. L. Wilson, M.S. Thesis (Univ. of Idaho, 1966), unpublished.

[12] B. A. Magurno and S. F. Mughabghab, Proc. Conf. on Nuclear Cross Sections and Technology, NBS Spec. Pub. 425, Vol. 1, 357 (1975).

[13] R. G. Thomas, Phys. Rev. 97, 224 (1955); F.W.K. Firk, J. E. Lynn, M. C. Moxon, Proc. Phys. Soc. 82, 477 (1963).

[14] H. Bolotin, Phys. Rev. 168, 1317 (1968).

[15] P. Roubeau, A. Abragam, G. L. Bacchella, H. Glaetti, A. Malinovski, P. Meriel, J. Piesvaux and M. Pinot, Phys. Rev. Lett. 33, 102 (1974).

[16] M. S. Pandey, J. B. Garg, J. A. Harvey and W. M. Good, Proc. of Conf. on Nuclear Cross Sections and Tech., NBS Special Publ. 425, Vol. 2, 748 (1975).

[17] J. A. Harvey, Proc. of New Devel. in Reactor Phys. and Shielding, CONF-720901, Book 2, 1075 (1972).

[18] K. A. Alfieri, R. C. Block and P. J. Turinsky, Nucl. Sci. and Eng. 51, 25 (1973).

THE U-235 NEUTRON FISSION CROSS SECTION FROM 0.1 TO 20.0 MEV

W. P. Poenitz

Argonne National Laboratory, Argonne, Illinois 60439

The status of the U-235 fast neutron fission cross section is discussed based primarily on material contributed and considered at the NEANDC/NEACRP Specialists Meeting on Fast Neutron Fission Cross Sections held at Argonne National Laboratory in June 1976. However, some newer measurements and evaluations are discussed as well. Specifically, recent measurements at ANL over the energy range 0.2-8.2 MeV, using several BND's, are reported. Data from the last 10 years are found to be in good agreement with an evaluated average of these data. Suggested problem areas are investigated in terms of their actual significance. It is found that the presently suggested version of ENDF/B-V for the U-235 (n,f) cross section does not represent the data base well and a reconsideration is recommended.

(U-235 (n,f), 0.1-20.0 MeV, Status, Data, Evaluations)

Introduction

An NEANDC/NEACRP Specialists Meeting on Fast Neutron Fission Cross Sections of U-233, U-235, U-238 and Pu-239 was held at Argonne National Laboratory in June, 1976[1]. One of the major sessions dealt with the absolute U-235 cross sections. A workshop on absolute cross sections considered essentially U-235 and presented conclusions and recommendations. The material presented at this meeting, and considered by the workshop, forms the base for the present investigations. However, additional data were included and further extensive analysis was carried out. This has led to the present status report and recommendations which go beyond those of the above meeting.

Recent Experiments

Most of the experiments considered here have been described in detail in the literature, and some of the detectors were discussed in other sessions of this symposium. Thus, the present account will be extremely short.

Wasson ('76 ANL, Ref.2)

This was a very important and extensive contribution on U-235 (n,f) at the '76 ANL Meeting. Though the actual normalization of the data was in the 7.8-11.0 eV interval, the experiment follows a suggestion by C. Bowman[32] that all cross sections be measured as shape data and then normalized at thermal energy. This would utilize the well known thermal cross section.

The measurements were carried out at the NBS-Linac using the time-of-flight technique and a "white neutron-source" spectrum. First, the ratio U-235 (n,f)/Li-6(n,α) was measured from 7.8 eV to 30 keV using a multiple layer ionization chamber and a Li-glass detector. Secondly, the ratio of U-235(n,f)/H(n,n) was measured with the same ionization chamber and a recoil detector. The U-235 (n,f) cross section was obtained from the U5/Li-measurements using an R-Matrix fit[33] for the Li-6 cross section and normalizing in the 7.8-11.0 eV interval to an absolute value reported by Deruytter and Wagemans[3]. The U-235 (n,f) cross section obtained from these measurements in the 10-20 keV interval was then used to normalize the cross section obtained from the U5/H-measurements. The two sets of data differed in the remaining overlap-range below 10 keV by ∿ 5% but agreed rather well in the 20-30 keV range (better than 1%). The quoted uncertainty of the results is typically 1.6%, not including normalization uncertainties.

Leugers et al. ('76 ANL, Ref.4)

The shape of the ratio U-235 (n,f)/H(n,n) was measured between 1.2 MeV and 20 MeV. A multiple gas-scintillation chamber was used and both fission fragments were detected in coincidence. The neutron flux was measured with a special proton recoil telescope. Both detectors were positioned at a 59 m flight-path in the white neutron-source spectrum obtained from the KFK-Cyclotron. The systematic uncertainties of these measurements are between 4 and 8%.

Szabo and Marquette ('76 ANL, Ref.5)

An extension of previous measurements to the 2.3-5.5 MeV energy range was reported. The efficiency of the directional neutron monitor was determined relative to the D(d,n) reaction cross section and normalized below 2.2 MeV where it was known from two previous independent calibrations. The paper also contains a listing of all previously reported data in its finalized form.

Barton et al. ('76 ANL, Ref.6)

A summary of the previously reported data was presented and some time was devoted to considering the possibility of an energy shift around 6 MeV between the data from LASL and LLL. It was shown that the suggestion of an energy shift results from insufficient consideration of statistical uncertainties. The experimenters have in the meantime extensively investigated their energy scale calibration using threshold reactions, resonances in carbon, and the Aℓ(p,γ) reaction. The largest difference which could be found was 20 keV, but under more realistic operation conditions the estimated uncertainty would be much less.

U. of Michigan ('ANL, Ref.7)

These measurements will be reported later in this session. Four values were obtained using calibrated photo neutron sources and one value was obtained with a Cf-252 source. The uncertainties are ∿ 2% for the former and 1.6% for the latter.

Cancé and Grenier ('76 ANL, Ref.8)

An absolute value was obtained at 14 MeV using the associated particle technique and the T(d,n)α-reaction. The experiment was carried out in time-of-flight and in coincidence with the associated α-particle. The result has an uncertainty of 1.9%.

Heaton et al. ('76 ANL, Ref.9)

This experiment will be reported later in this session. A value was obtained for a calibrated Cf-252 source with 2.2% uncertainty.

Zhuravlev et al. ('76 Lowell, Ref.10)

Several values were measured relative to the B-10(n,α) cross section using filtered reactor neutron beams. One of the values falls in the energy range considered here and was obtained at 144 keV using a Si-filter.

Poenitz [Ref. 11]

Previous measurements with a Black Neutron Detector were extended to lower and higher energies using various sized detectors. The basic experimental set-up was similar to that previously reported. An ionization chamber with two U-235 samples back-to-back was placed ∿ 8 cm from the neutron source (Li-7 (p,n) below 4.5 MeV and D(d,n) above). The neutron flux was measured with a BND positioned behind a collimator at a distance of ∿ 5 m. At low energies, a small BND with only one photo-multiplier was used and the modification of the code "Carlo Black" by G. Lamaze from NBS for the Poisson statistics of photo electrons was utilized. At higher energies, a 16 multiplier-detector was used. An additional shape measurement with improved resolution was made by detecting the higher energy (> 6 MeV) γ-rays associated with the fission process in a metallic sample with a large-liquid scintillator. The energy resolution of this experiment was ∿ 6 keV in the 200-300 keV range. Data were grouped in 10-keV intervals and normalized using the absolute values. The latter have a typical uncertainty of 2%, but are larger at higher energies.

Data Consideration

General Overview

It was noted at the '76 ANL Meeting that all more recent data can be found in a ± 3% band. Though statistics or systematic errors cause some points to scatter outside this band, the general systematic trends are with few exceptions within this band.

Some Specific Problems

As a result of the '76 ANL Workshop on absolute cross sections, it was stated that the ±3% band would have to be replaced with a ±5% band in a local region from 200 to 400 keV. Another notable difference appears to be between the data by Szabo and other sets above 3 MeV. Fig. 1 shows the relevant data sets. The difference at 280 keV between the data by Wasson[1] and those by Szabo[5] and by Poenitz[13] is about 13%. The systematic difference between the data by Szabo[5] and by Barton et al.[6] and Czirr and Sidhu[12] is about 6% around 4 MeV.

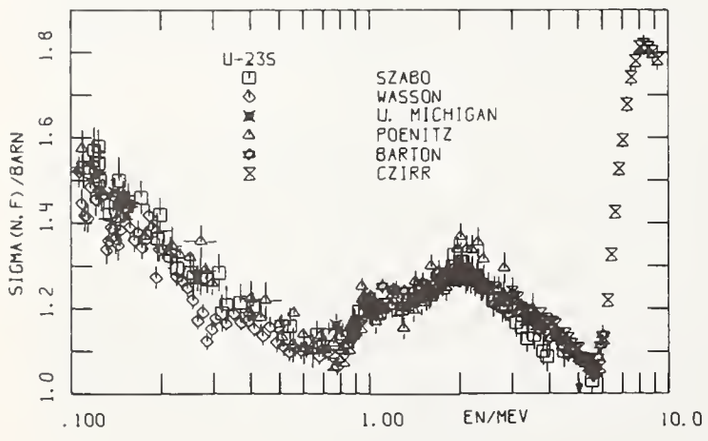

Fig. 1. Comparison of some data in the 0.1-10 MeV energy range. The difference between the data by Wasson and those by Poenitz and by Szabo is about 13% at 280 keV. The difference between the data by Szabo and those by Barton et al. and by Czirr and Sidhu is about 6% at 4 MeV.

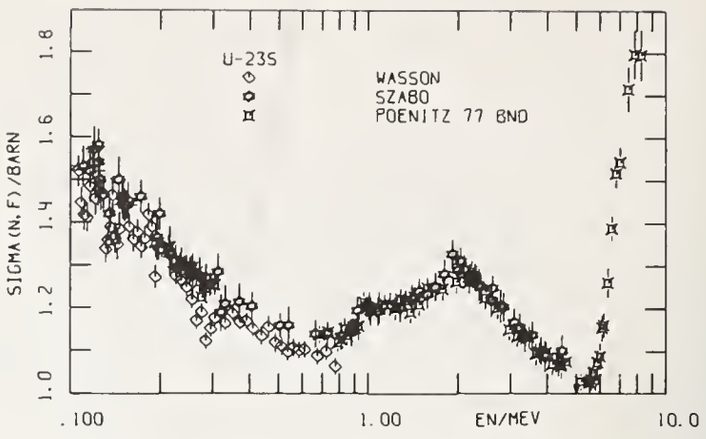

Fig. 2. Comparison of the data by Szabo with new results by Poenitz.

Fig. 2 shows the results from the new ANL measurements which support the data by Szabo in both areas under question. Structure around 270 keV may be construed from the new data set but the dip would be only ∿ 4% and ∿ 10 keV wide based on the ANL measurements compared with ∿ 9% and ∿ 30 keV for the Wasson data. A better comparison can be made for the ratio of the 250-300 keV interval vs. the 200 - 250 keV interval:

Poenitz (13) GND '72	.958
Szabo (5) '70-'73	.967
Gaythe r (14) '75	.940
Wasson (2) '76	.907
Poenitz (11) BND '77	.955

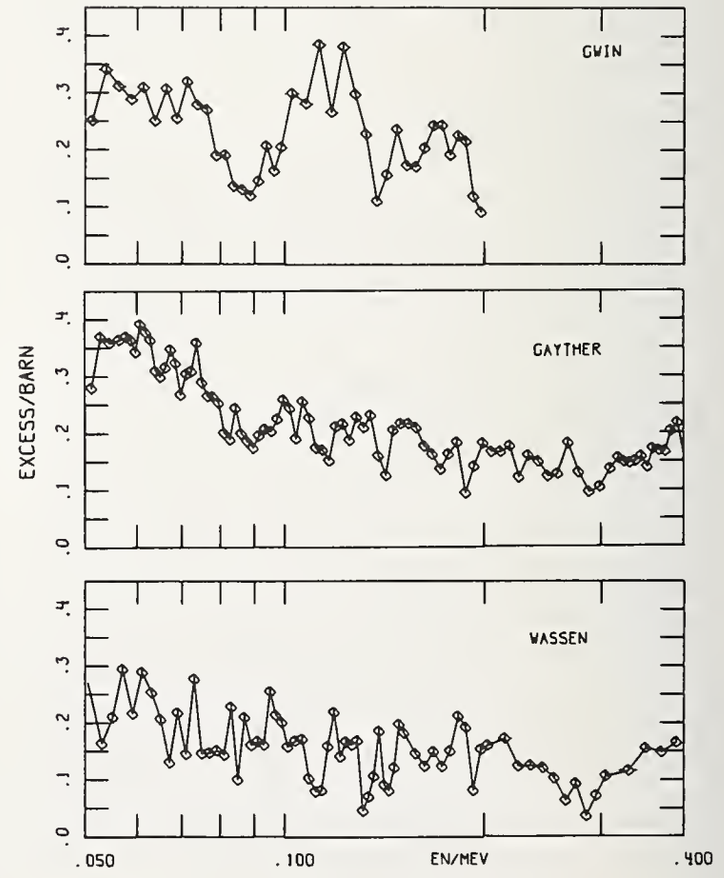

Fig. 3. Comparison of fluctuation in the U-235 (n,f) cross section obtained in the 50-400 keV energy range.

The applicable uncertainties for these values are unknown but presumably are ∿ 2%. The problem around 280 keV suggests a comparison of structure in other energy ranges, in order to consider the possible influence of such structure on cross section averages. Fig. 3 shows the three available data sets[2,14,15] (a smooth cross section, 0.7585-0.26356 · ℓn (E), was subtracted). Some structure is common to all three sets, but some dips or peaks occur only in one or two of the three data sets. Correlations with the Aℓ-scattering cross section could not be found.

A Basis for Status, Problem Analysis and Data Comparison

Many problems, including some discussed during the '76 ANL Meeting, appear to be based on a poor understanding of the result of an experiment on the part of "data interpreters". This situation is most vividly demonstrated in the still continuing practice of displaying or discussing differences in data without displaying or taking into account the uncertainties of these data sets or the uncertainty in the knowledge of the considered quantity. It is imperative to judge the significance of existing differences by relating them to their uncertainties. Another important criterion for determining the significance of a suggested problem is the magnitude of its practical implication.

For further investigation of the status of U-235 (n,f), an evaluated cross section is desirable. The comparison of individual data sets and conclusions about possible problem areas should be done using such an evaluated "best value set". For practical purpose we restrict the data base here to values reported since the experiment by White[16] (∿ 12 years ago), thus all discussion is restricted, by definition, to this data base. Following standard procedures and previously described techniques[17] an evaluated "best value set" was determined. It represents practically a weighted average of the data base (which was, with one exception, not altered).

An extensive display of existing data sets was made in the supplements of the proceedings of the '76 ANL Meeting[1]. Here we consider instead the quantity

$$D/U = \frac{\sigma_i - \sigma_{ev}}{\sqrt{(\Delta\sigma_i)^2 + (\Delta\sigma_{ev})^2}}$$

where $\sigma_i \pm \Delta\sigma_i$ is an individual measured cross section and $\sigma_{ev} \pm \Delta\sigma_{ev}$ the evaluated "best data set" cross section at the same energy. In other words, D/U represents the deviation of a measured value from the best value in terms of the uncertainties of both, the measurement and the knowledge of the measured quantity. The above definition of D/U permits us to define criteria for the existence or non-existence of significant problems:

1. Fluctuations of D/U values should be expected to follow a normal distribution. This applies to both, individual point-scatter and larger range, systematic variations. Fluctuations must be expected for statistical and for many systematic uncertainties.

2. Average D/U-values should be within ± 1. The cause is most likely an error of the normalization which should not exceed the estimated total uncertainty.

Data Comparison

Figs. 4 and 5 show the D/U values for the data which contributed to the U-235 (n,f) evaluation. The shape data by Czirr and Sidhu[12], and by Leugers et al.[4], were normalized to the absolute 14 MeV value by Cancé and Grenier[8]. The shape data by Gayther et al.[14] were normalized to the absolute values from the U. of Michigan[7]. We can conclude that, for the high energy range (E>1 MeV), no significant problem exists for U-235 as a whole nor for individual data sets. However, it may be noted that all data but those by Czirr and Sidhu[12] tend to suggest lower values between 2 and 5 MeV. It should also be noted that the suggestion of an energy shift of the data by Barton et al.[6] cannot be supported by the present analysis as significant.

At lower energies (< 1 MeV) the data set by Kaeppeler[18] fails to follow anything close to a normal distribution. The 100 keV-averaged data by Wasson[2] still reflect the influence of the structure previously discussed but, in general, follow the shape measured by Gayther et al.[14], Poenitz[11,13] and Szabo[5]. The data by Wasson appear to be inconsistent with the evaluated result as they are systematically lower by a D/U of 2 or more. However, a proper normalization and accounting of normalization uncertainties (which will be discussed later) shift these data into a satisfactory D/U range.

In Table 1, the average deviations of all absolute values which contributed to the normalization of the evaluated cross section are listed. The average uncertainty and the D/U values are also listed. Again, there is no indication of any major problem after adjustments of the data by Wasson were made. The uncertainty of the normalization of U-235 (n,f), based on the values given in the Table, is 0.6%. This uncertainty covers the unweighted average normalization factor. A check for a dependence of the results on the time of the measurements, which in a similar analysis was shown at the '70 ANL Symposium[19], may still indicate some trend, however, exclusion of pre-1975 data would change the average normalization by no more than its uncertainty.

TABLE I. Average Difference of Absolute Cross Section Values from the Evaluated Data Set of U-235(n,f). All Data Since and Including the Experiment by White. Dependent Data were Lumped Together.

First Author	Ref.	Average Deviation %	Average Uncertainty %	D/U*
Smith	22	-7.5	6.3	-1.3
White	16	+2.6	2.6	+0.9
Kaeppeler	18	+3.0	3.0	+1.0
Kuks	23	+5.5	3.6	+1.4
Poenitz (W/O BND)	13	-1.0	3.6	-0.3
Szabo	5	-0.2	3.0	-0.1
Barton	6	+0.4	1.5	+0.2
U. Michigan	7	-0.2	2.0	-0.1
Cance	8	-1.5	1.9	-0.8
Adamov	24	+3.6	1.6	+2.0
Heaton	25	-1.3	2.2	-0.6
(Wasson	2	-4.0	1.7	-2.3) not used
Wasson (revised)	See text	-2.8	3.8	-0.9
Poenitz(BND)	See text	-1.3	2.4	-0.5
Data rel.B10	10,15	-3.2	3.1	-1.0
Data rel.Li6	26	-4.8	5.2	-1.0

*Values of D/U < ± 0.7 are expected with 50% Probability.

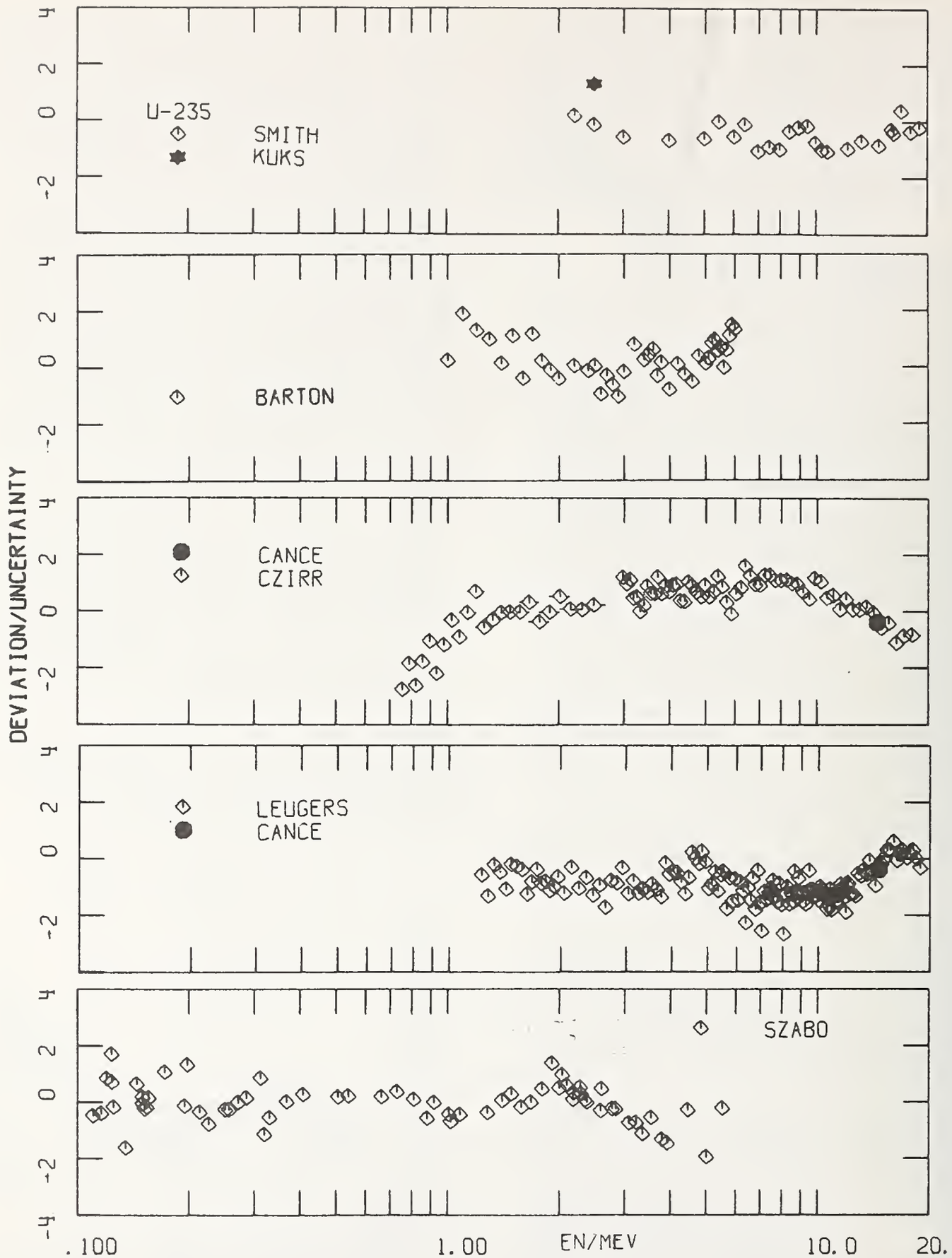

Fig. 4. Comparison of experimental data with an evaluated cross section. The difference relative to the uncertainty is shown.

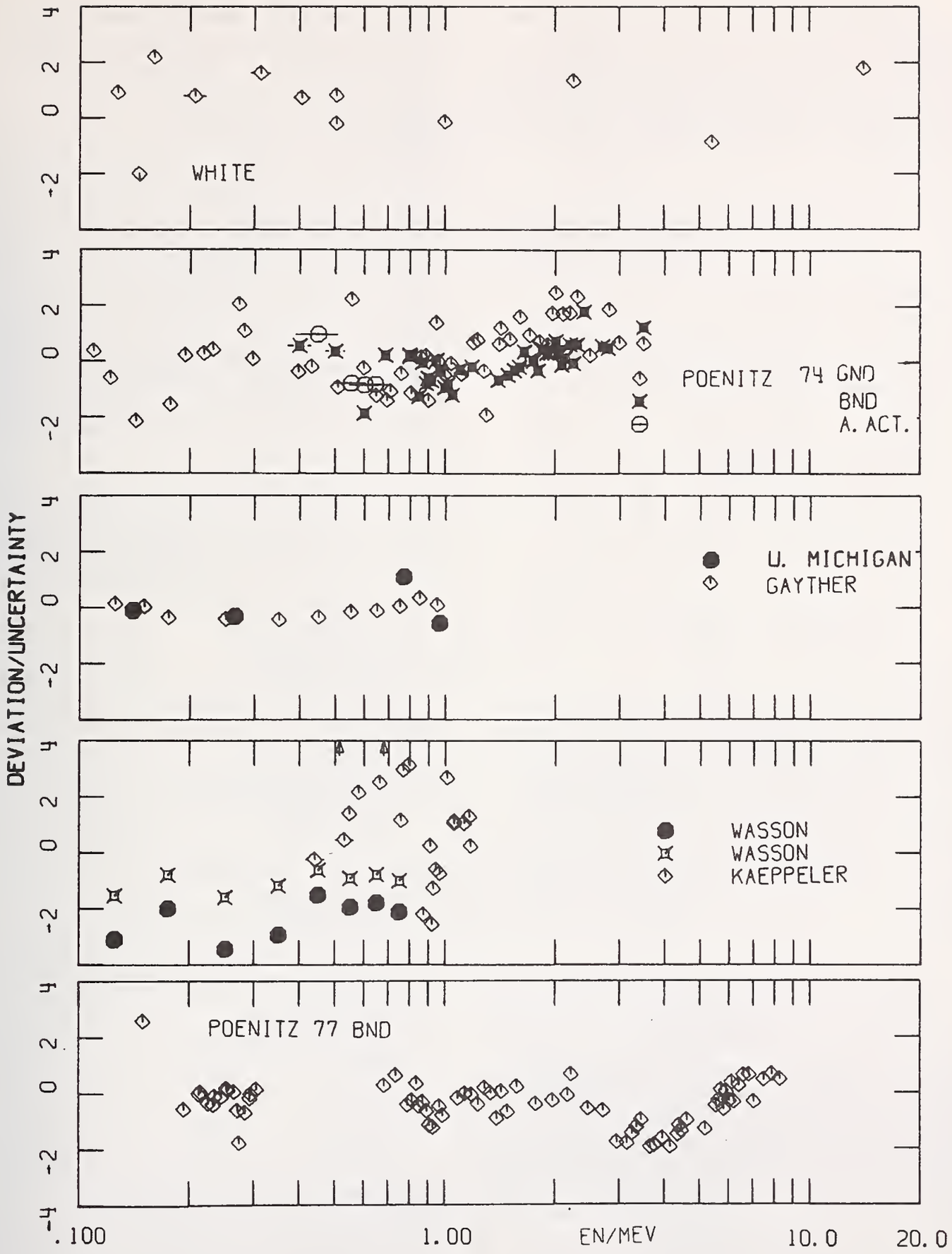

Fig. 5. Comparison of experimental data with an evaluated cross section. The difference relative to the uncertainty is shown.

The only data which were changed for the present evaluation were those by Wasson. The original normalization, which was based on one specific experimental value, was replaced by the normalization to an average value obtained from a large number of experiments for the 7.8 eV-11.0 eV interval (obtained by the '76 ANL Workshop[27]). The uncertainty for the normalization consists of several components which are listed in Table 2.

TABLE II. Accounting of Uncertainties Associated with the Wasson Data Above 100 keV.

Source	Ref.	Uncertainty %
1. Average Stated Uncertainty (Statistical + Systematic)	2	1.6
2. Added Uncertainties Related to the Normalization		
Uncertainty of Norm. Integral	27	2.4
Statistical, 7.8-11.0 eV	2	0.8
Statistical, 10-20 keV, U5/Li	2	0.8
Statistical, 10-20 keV, U5/H	2	0.6
Systematic, U5/Li, eV-keV	2	1.0
Systematic, U5/H, 10-20 keV	2	1.6
Li-6 Cross Section, eV-keV	34	0.5
H Cross Section, Tens to Hundreds keV	34	0.7
Systematic Discrepancy in Overlap Range		None Added
Total Uncertainty (1. and 2.)		3.8 %

Comparison with Other Evaluations

In Fig. 6 two other evaluations are compared with the present evaluation result. The recent evaluation by Konshin[20] represents the data base very well. The proposed ENDF/B-V[21] is generally lower below 1 MeV and higher above 1 MeV than the existing data base would require. The deviation is substantial below 1 MeV and caused in part by placing unjustified emphasis on a preliminary data set. It was specifically suggested by the '76 ANL Workshop that the use of preliminary data should be restricted or avoided. The upper part of the figure shows a comparison with the ±3% band considered at the '76 ANL Meeting.

Conclusions

Changes of the U-235(n,f)Cross Section

At the panel discussion of the 1970 Helsinki Conference, R. F. Taschek pointed out[28] that one can draw a fine line between the data by White[16] and other English[29] and LASL measurements[30] which would be consistent with all but one data set. The presently evaluated average cross section is ∿ 7-8% lower in the hundreds of keV range and a further lowering by ∿ 1% might be expected.

Status of U-235 (n,f) Above 100 keV

The fact that no data exist which conflict with the weighted evaluated data set for U-235 (n,f) suggests that the evaluated uncertainty represents a reasonable estimate of the real uncertainty. The evaluated uncertainty is less than 2% below 2 MeV, less than 3% below 8 MeV, and increases to 5% at 20 MeV. Fluctuations superimposed on the average cross section are probably less well established but should have little practical importance beyond their implications in high resolution differential measurements[31]. The knowledge of U-235 (n,f) is backed by a sufficient number of independent techniques and results.

Requirements for Future Measurements, Choice of Techniques

A sensitivity study based on the present level of uncertainty and the number of independent techniques and experiments involved, lead to the requirement that any new measurement should have an uncertainty of less than 2%. Any difference which is found in respect to the average of presently available data should be backed up by an absolute D/U of at least 2 in order to be significant. Table 3 summarizes the status of present techniques for obtaining absolute values above 100 keV. The table suggests that the preferable techniques will be those involving the determination of absolute masses and efficiencies rather than the reliance on normalization at low energies. The present status and expectations for future improvements of techniques indicate that improvements in the cross section can only be expected from a large number of independent measurements.

TABLE III. Present Status of Experimental Uncertainties for Absolute Values Above 100 keV.

Technique, Reference	Quoted Uncertainty %	Improvemnt %
Calibrated Bath, Absolute Mass Determination		
Poenitz(13) 1972,74	3.6	
Szabo(5) 1970,73	2.5	
Heaton(25) 1976	2.3	
Davis(7) 1976	1.7	
Associated Activity		
Poenitz(13) 1972,74	3.6	
Associated Particle, Absolute Mass Determination		
Szabo(5) 1970,73	2.5	
Kuks(23) 1973	3.8	
Cance(8) 1976	1.9	
Hydrogen Recoil, Absolute Mass Determination		
White(16) 1965	2.3	
Kaeppeler(18) 1972	2.1	
Barton(6) 1972,76	1.5	
Black Neutron Detector, Mass by α-Counting		
Poenitz(11) 1977	2.0	1.5
Low Energy Normalization		
Wasson 1976	3.8	2.8

The Question of the Need for Future U-235 Measurements

Nuclear data request lists usually state a 1% uncertainty requirement for U-235 (n,f) up to 14 MeV. In the light of these requests and the fact that the present uncertainty is ∿ 2-3%, the need for continued measurements is obvious. However, economics and the considerations mentioned above suggest that we look also at the limitations involved in the application of the U-235 (n,f) cross section at its present uncertainty level. The major application is its use to

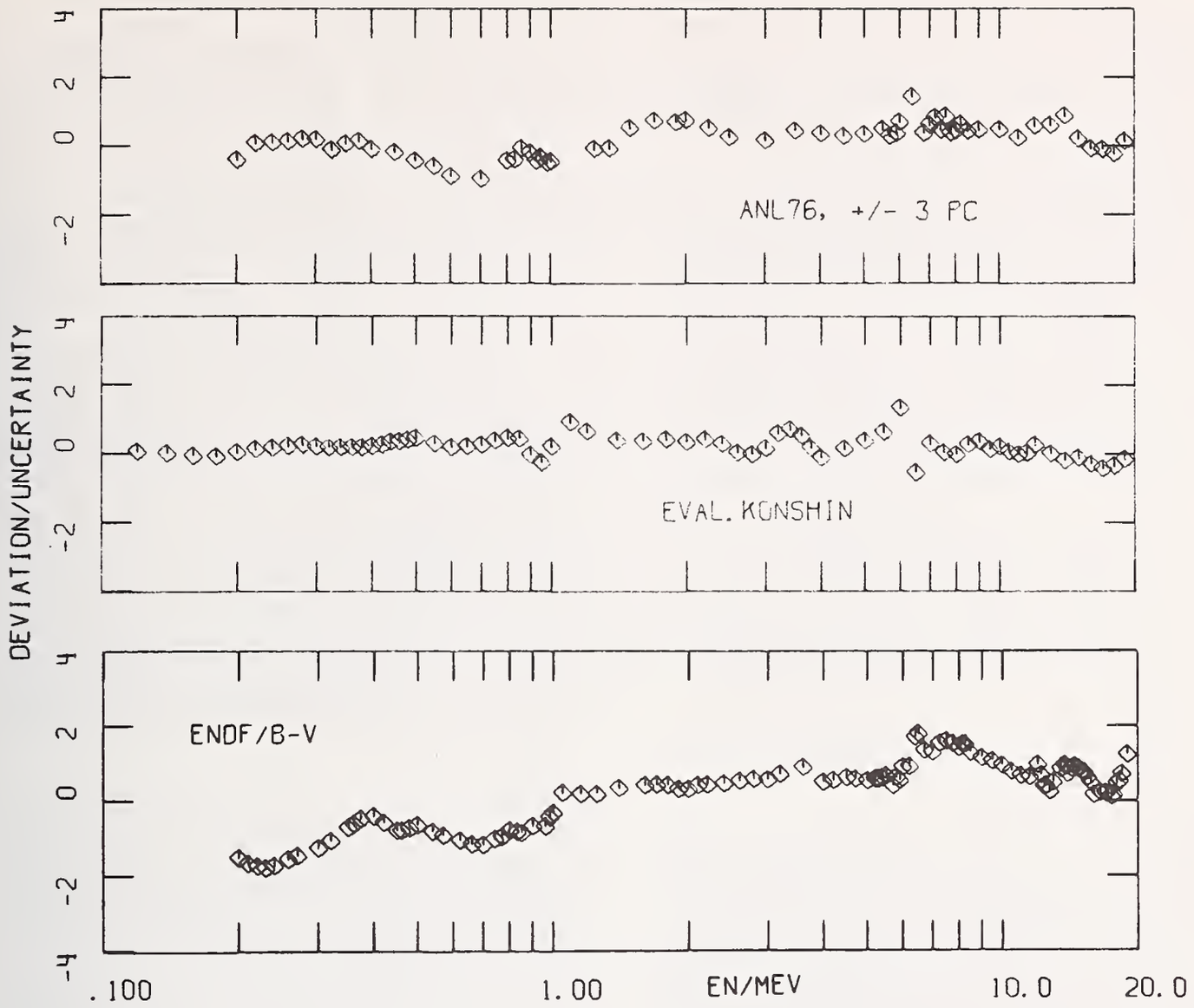

Fig. 6. Comparison of other evaluated cross sections with the present result. The difference relative to the uncertainty is shown.

convert measured ratios to cross sections. Such ratios, their present uncertainty and importance are

Ratio to U-235(n,f)	Uncertainty	Importance for k_{eff}
Pu-239(n,f)	$\gtrsim$ 3%	High
U-238(n,f)	< 2%	Medium
U-238(n,γ)	$\gtrsim$ 5%	Medium
U-233(n,f)	$\lesssim$ 3%	High
Th-232(n,f)		Medium
Th-232(n,γ)		Medium
Pu-240(n,f)		Low
Pu-241(n,f)		Low
Others		Low

This indicates that for U-238(n,f) and Pu-240, Pu-241 (n,f) the knowledge of U-235 (n,f) is sufficiently precise; and for other values, the uncertainty of the ratios is probably an equal or dominant factor. The workshop at the '76 ANL meeting considered the question whether absolute measurements should be made for Pu-239 (n,f) directly, rather than measuring U-235(n,f) and the ratio Pu9/U5. No conclusion was reached at that meeting, but considerations mentioned above suggest that absolute measurements of Pu-239 (n,f) are more profitable for the near future than further absolute U-235 (n,f) measurements.

Re-evaluation of U-235(n,f)

A re-evaluation of U-235 (n,f) for ENDF/B-V is recommended. This is based not so much on any new measurement but on the fact that ENDF/B-V does not represent the existing data base. The true cross section is unknown and the presently suggested version of ENDF/B-V may actually be closer to the true values than the weighted average of the data is. However, such assumption is purely speculation.

ACKNOWLEDGEMENT

This work was supported by the U.S. Energy Research and Development Administration.

References

1. Proc. of NEANDC/NEACRP Specialists Meeting on Fast Neutron Fission Cross Sections, Argonne National Laboratory, ANL-76-90 and Supplement, (1976).
2. O. A. Wasson, p. 183 of Ref.1, (1976).
3. A. J. Deruytter and C. Wagemans, J. Nucl. Energy 25, 263 (1971).
4. B. Leugers et al., p.246 of Ref.1, (1976).
5. I. Szabo and J. P. Marquette, p.208 of Ref.1, (1976); also see other references cited therein.
6. D. M. Barton et al., p.173 of Ref.1,(1976), Nucl. Sci. Eng. 60, 369 (1976).
7. M. C. Davis et al., p.225 of Ref.1, (1976).
8. M. Cancé and G. Grenier, p.237 of Ref.1, (1976).
9. H. T. Heaton II et al., p.333 of Ref.1, (1976).
10. K. D. Zhuravlev et al., Proc. of Int. Conf. on Interactions of Neutrons with Nuclei, U.Lowell, ERDA, CONF-760715 (1976).
11. W. P. Poenitz, to be submitted to Nucl.Sci.Eng., (1977).
12. J. B. Czirr and G. S. Sidhu, Nucl. Sci. Eng.57,18 (1975), Nucl.Sci.Eng.58, 371 (1975).
13. W. P. Poenitz, Nucl. Sci. Eng. 53, 370, (1974).
14. D. B. Gayther, Proc. of Conf. on Nuclear Cross Sections and Technology, Washington, NBS Spec. Pub. 425, (1975).
15. R. Gwin et al., Nucl. Sci. Eng.59, 79, (1976).
16. P. H. White, Nucl. Energy A/B 19, 325, (1965).
17. W. P. Poenitz and P. Guenther, p.154 of Ref.1, (1976).
18. F. Kaeppeler, Proc. of Panel on Neutron Standard Reference Data, Vienna, IAEA, p.213 (1974).
19. W. P. Poenitz, Proc. of Symposium on Neutron Standards and Flux Normalization, Argonne National Laboratory, AEC Symp. Series 23, p.331, (1970).
20. V. A. Konshin, Review and Evaluation of the U-235 Fission Cross Section, Intern. Nucl. Data Committee, INDC(CCP)-94/U, (1976).
21. M. R. Bhat, p.307 of Ref.1, (1976).
22. R. K. Smith et al., Bull. Am. Phys. Soc. 2, 196 (K4), 5704, revised by G.E. Hansen et al. (1969).
23. I.M. Kuks et al., Conf. on Neutron Physics, Kiev, Vol. 4, 18, (1973).
24. W. M. Adamov et al., Conf. on Neutron Physics, Kiev, Vol. 4, 21, (1973).
25. H. T. Heaton II, p.333 of Ref.1, (1976).
26. J. B. Czirr and G. S. Sidhu, Nucl. Sci. Eng. 60, 383 (1976).
27. B. R. Leonard and O. A. Wasson, p.452 of Ref.1, (1976).
28. R. F. Taschek, Sec. Int. Conf. on Nuclear Data for Reactors, Helsinki, IAEA Vol.II, Panel Discussions, p. 929, (1970).
29. W. D. Allen and A.T.G. Ferguson, Proc. Phys. Soc. A70, 573 (1957).
30. R. L. Henkel, LA-2122 (1957), B.C. Diven, Phys. Rev. 105, 1350, (1957).
31. C. D. Bowman et al., p.270 of Ref.1, (1976).
32. C. D. Bowman, Proc. of Symp. on Neutron Standards and Flux Normalization, Argonne National Laboratory, p.246, AFC Symp. Series 23, (1970).
33. G. R. Hale, priv. communication to G.Lamaze (1976).
34. G. R. Hale and L. Stewart, private communication (1977).

Appendix I: Evaluated Data

The evaluation of a best value cross section should include all absolutely measured cross sections and all ratios in an "consistent data set" evaluation procedure (Ref.19). It also should extend to average cross sections at lower energies. Such evaluation is in progress and will be published elsewhere. The evaluation for the present purpose was restricted to recent data, to energies above 100 keV and to U-235(n,f), thus the validity of the values given below is restricted as well.

E/MeV	σ/b	E/MeV	σ/b	E/MeV	σ/b
0.100	1.587	0.900	1.178	5.800	1.050
0.125	1.510	0.940	1.215	5.900	1.073
0.150	1.454	0.960	1.230	6.000	1.096
0.175	1.412	1.000	1.226	6.200	1.180
0.200	1.346	1.050	1.209	6.400	1.255
0.225	1.326	1.100	1.210	6.800	1.484
0.250	1.297	1.200	1.213	7.000	1.550
0.275	1.274	1.400	1.221	7.400	1.671
0.300	1.256	1.500	1.233	7.800	1.742
0.350	1.225	1.700	1.254	8.000	1.758
0.400	1.200	1.900	1.271	8.500	1.758
0.450	1.178	2.000	1.274	9.000	1.744
0.500	1.156	2.250	1.263	10.000	1.734
0.550	1.149	2.500	1.242	12.000	1.741
0.600	1.143	2.750	1.220	13.000	1.892
0.650	1.135	3.000	1.206	14.000	2.054
0.700	1.130	3.500	1.160	15.000	2.111
0.750	1.128	4.000	1.147	16.000	2.117
0.800	1.129	4.500	1.110	17.000	2.051
0.820	1.134	5.000	1.079	18.000	2.004
0.850	1.147	5.500	1.039	20.000	1.967

Appendix II: Criteria for D/U-Limitations

Establishing criteria for the existence or nonexistence of problems of any cross section can be obtained by simulation techniques (as for example used in testing and comparing economic or technical models). This approach is presently under investigation and the results will be published elsewhere. The two criteria stated in the text are crude approximations based on the more commonly expected behavior of experimental variables.

Appendix III: Recent ANL BND Results

The recent experimental values shown in Fig. 2 are listed below. Until their final publication these values must be considered preliminary, though no change is anticipated at the present time.

E/MeV	σ/b	Δσ/mb	E/MeV	σ/b	Δσ/mb	E/MeV	σ/b	Δσ/mb
0.215	1.342	50	0.929	1.158	35	3.756	1.096	25
0.225	1.311	38	0.969	1.214	25	3.955	1.095	27
0.235	1.309	34	0.988	1.203	25	4.153	1.069	29
0.245	1.297	29	1.088	1.201	38	4.351	1.068	30
0.255	1.294	27	1.138	1.209	25	4.449	1.065	31
0.265	1.283	27	1.185	1.209	29	4.396	1.083	23
0.275	1.225	26	1.236	1.199	29	4.618	1.075	22
0.285	1.246	27	1.288	1.221	26	5.179	1.028	22
0.295	1.257	27	1.336	1.217	26	5.536	1.026	24
0.305	1.255	26	1.388	1.190	25	5.618	1.033	28
0.193	1.354	37	1.433	1.225	26	5.714	1.049	27
0.213	1.342	30	1.486	1.208	26	5.809	1.032	27
0.233	1.304	26	1.578	1.247	26	5.898	1.073	30
0.253	1.297	26	1.778	1.245	29	6.006	1.087	33
0.271	1.261	23	1.978	1.262	28	6.107	1.154	32
0.293	1.254	28	2.178	1.262	28	6.185	1.161	31
0.684	1.138	23	2.222	1.286	28	6.384	1.260	36
0.735	1.144	23	2.472	1.224	28	6.579	1.387	30
0.793	1.119	22	2.718	1.201	26	6.803	1.515	35
0.814	1.126	22	2.968	1.150	26	7.025	1.541	37
0.835	1.151	28	3.162	1.134	26	7.478	1.713	54
0.850	1.135	23	3.262	1.137	25	7.875	1.795	59
0.871	1.151	24	3.360	1.134	26	8.275	1.793	62
0.893	1.155	24	3.463	1.133	26			
0.909	1.154	24	3.658	1.093	27			

PROPAGATION OF UNCERTAINTIES IN FISSION CROSS SECTION STANDARDS IN THE INTERPRETATION AND UTILIZATION OF CRITICAL BENCHMARK MEASUREMENTS[a,b]

C. R. Weisbin and R. W. Peelle
Oak Ridge National Laboratory
Oak Ridge, Tennessee 37830
USA

This work explores the constraints imposed on the $^{235}U(n,f)$ standard (proposed ENDF/B version V) by information deduced from clean integral measurements and demonstrates how uncertainties in fission cross section standards propagate in an uncertainty analysis and interpretation of those experiments. The question of what a significant improvement in the accuracy of the $^{235}U(n,f)$ standard would accomplish is addressed in the limited context of analyses of GODIVA and JEZEBEL measurements.

The CSEWG integral benchmark results and uncertainties were updated in accordance with more recent information. Sensitivity coefficients were developed and used to estimate calculated results which should be obtained using the subsequent release of $^{238}U(n,f)$, $^{235}U(n,f)$, and $^{239}Pu(n,f)$ at version V status. Covariance files were evaluated and processed for all important cross sections with the sole exception being inelastic scattering for all levels and the continuum. Uncertainties due to the $^{235}U(n,f)$ standard were estimated to comprise more than half of the calculated uncertainty for criticality and $\langle {}^{28}\sigma_f/{}^{25}\sigma_f \rangle_c$ spectral index in JEZEBEL as well as GODIVA; though the JEZEBEL assembly contained no ^{235}U. We are not able at this time, to predict criticality or $\langle {}^{28}\sigma_c/{}^{28}\sigma_f \rangle_c$ to anywhere near the accuracy obtained by direct measurements, and therefore the integral results are significant to our analysis capability. Inclusion of integral information from GODIVA and JEZEBEL in an adjustment procedure was effective in reconciling all parameters other than $\langle {}^{28}\sigma_f/{}^{25}\sigma_f \rangle_c$ measurement in JEZEBEL for which current calculation and measurement are in disagreement. The adjustment procedure made changes of less than one standard deviation in the cross sections for $^{235}U(n,f)$, $^{235}U(n,\gamma)$, $^{238}U(n,f)$, $^{238}U(n,\gamma)$, and $^{239}Pu(n,f)$ including an increase of $\sim$1.5% for the $^{235}U(n,f)$ cross section above 1.3 MeV. This specific adjustment result could change with inclusion of inelastic covariance files and must be viewed cautiously at this time.

(criticals, cross section, ENDF/B, fission, standards, uncertainties)

I. Introduction

It is well known that if uncertainties in fast reactor performance parameters were to be developed solely from consideration of uncertainties in differential nuclear data, and even assuming all methods approximations to be negligible, the resulting uncertainties in predicted fast reactor performance would still be significantly larger than those required by designers.[1] Thus, in addition to the customary calculation/experiment comparison, data adjustment schemes have been developed[2-4] which can incorporate information from both evaluated differential data and relatively clean geometry, fast integral data. The latter generally lacks energy resolution but provides bounds within which the reactor performance predictions should lie. In general, the cross section adjustment schemes minimize a quadratic function of the weighted difference between the measured and computed values of the performance parameters and between the reference and adjusted cross section values. The fitting procedure provides an estimate of the accuracy of the adjusted cross sections and of the reactor properties calculated using them.[2-4] Although the standard deviations of the adjusted cross sections may not be significantly smaller than those assumed for the unadjusted cross sections, performance parameter predictions can be significantly improved because of the large effect the adjustment has in altering the off-diagonal elements of the cross section covariance matrix.[2-4] It is important to note, however, that the adjusted covariance matrices depend upon the initial estimated accuracy for both the differential and integral measurements.

Adjustment of the nuclear data base, and associated uncertainty analysis, for improvement of performance parameter prediction has sometimes been received with considerable skepticism. In part, this was because adjustments have been made without detailed consideration of the differential data covariance information.[3] This was not at all a simple error of omission. The evaluation of differential cross section covariance matrices is a formidable task[5] involving correlations of evaluated cross sections with cross sections in other energy ranges and reaction types. Evaluated data which is derived (e.g., by deducing the elastic cross section from the total and non-elastic data) or evaluated through measurements relative to standard cross sections introduce additional complexity. Although the level of effort required is considerable, the rational assessment of uncertainty information for ENDF/B files was considered of high urgency[6] to improve upon existing analyses by permitting systematic sensitivity investigations to propagate uncertainties in a credible fashion.

In a recent paper, we presented the first results of our uncertainty analysis for fast reactor benchmarks.[7] The FORSS system[7] was employed to compute sensitivities[8] in 126 energy groups using transport theory. Multigroup covariance files were developed for $^{238}U(n,f)$, $^{238}U(n,\gamma)$, $^{239}Pu(n,f)$, $^{239}Pu(n,\gamma)$, and $^{239}Pu(\bar{\nu})$ using evaluations generated at ORNL[9] and formats and procedures established for the ENDF/B

[a]Research performed at Oak Ridge National Laboratory for Union Carbide Corp. under contract with U. S. Energy Research and Development Administration.
[b]Notice: By acceptance of this article, the publisher or recipient acknowledges the U. S. Government's right to retain a non-exclusive, royalty-free license in and to any copyright covering the article.

system[10] for the definition and processing of evaluated and correlated energy dependent uncertainty information. Using the measurements in ZPR-6/7 for k and central ^{238}U capture/^{239}Pu fission with assigned uncorrelated one standard deviation (1σ) uncertainties of 1 and 2 percent resulted in (1σ) predictions for the same parameters of 0.8% and 1.8% when the integral data was included in a cross section adjustment procedure which made changes of less than one standard deviation to the basic multigroup file. This technique was subsequently applied[11] to a realistic two-dimensional model of an LMFBR, including several reaction rate ratios measured in ZPR-6/7 and ZPR-3/56B. The (1σ) uncertainties in predicted multiplication factor and breeding ratio of a 1200 MWe LMFBR were reduced from 3% and 7.2% (differential nuclear data only) to 0.9% and 3.2% after inclusion of the information from CSEWG benchmark assemblies. In all cases, the cross section covariance files referred to the average cross sections in an infinitely dilute situation. The only cross section reaction correlation considered was for $^{239}Pu(n,f)$ and $^{239}Pu(n,\gamma)$ as developed from measurements of their ratio. Later work[12] in the analysis of the TRX-2 thermal lattice required covariance file evaluations for the four low energy resonances of ^{238}U (i.e., covariance of Γ_n and Γ_γ), and the thermal region. However, even with this expanding data base, none of the studies above gave detailed consideration to the effects of correlated uncertainties resulting from measurements relative to standards. (It should be noted that a more comprehensive covariance file is expected with the 1978 release of ENDF/B-V.)

A file of cross section uncertainty information for use in reactor performance uncertainty analysis should take into account the propagated effects of uncertainties in the standard cross sections used.[13] In particular, this applies to the $^{235}U(n,f)$ standard above a few hundred keV; the $^{239}Pu(n,f)$ and $^{238}U(n,f)$ cross section measurements, among others, are often made relative to $^{235}U(n,f)$. The purpose of this paper is to explore the constraints imposed on the $^{235}U(n,f)$ standard by information deduced from clean integral measurements and to demonstrate how uncertainties in fission cross section standards propagate in an uncertainty analysis and interpretation of those experiments. The question of what a significant improvement in the accuracy of the $^{235}U(n,f)$ standard would accomplish is addressed in the limited context of analyses of GODIVA and JEZEBEL measurements.

II. Data Testing Assemblies Description

The CSEWG Benchmark Specifications[14] contain a recommended calculational model as well as pertinent experimental results for the GODIVA and JEZEBEL assemblies.[15,16] The GODIVA model is a bare sphere of enriched uranium metal, having a core radius of 8.74 cm and atomic densities of .045/.002498/.000392 atoms/barn-cm for $^{235}U/^{238}U/^{234}U$, respectively. Similarly, the calculational model for JEZEBEL is a bare sphere of plutonium metal, having a core radius of 6.385 cm and atomic densities of .03705/.001751/.000117 atoms/barn-cm for $^{239}Pu/^{240}Pu/^{241}Pu$, respectively.

The experimental results for the performance parameters studied are given in Table I; the bracketed quantities refer to reaction rate ratios measured at the center of the sphere and are effective microscopic quantities, densities divided out.

It should be noted that the experimental values for the $\langle {}^{28}\sigma_f/{}^{25}\sigma_f\rangle_c$ ratios have been modified from the CSEWG recommendations (0.205 for JEZEBEL and 0.156 for GODIVA) in accordance with the recent recommendations of Hirons.[17] The uncertainties in the $^{49}\sigma_f/^{25}\sigma_f$ have been increased from ∿2% to ∿5% (1σ) due to revised uncertainty estimates[18] associated with the deduction of the number of fissions through β-counting of ^{99}Mo.

Table I. Accurate Measurements and Associated Uncertainties Have Been Reported for GODIVA and JEZEBEL

GODIVA		JEZEBEL	
k	1.00±0.003	k	1.00±0.003
$\langle {}^{28}\sigma_f/{}^{25}\sigma_f\rangle_c$	0.16±0.005[a]	$\langle {}^{28}\sigma_f/{}^{25}\sigma_f\rangle_c$	0.21±0.008[a]
$\langle {}^{49}\sigma_f/{}^{25}\sigma_f\rangle_c$	1.42±0.071[b]	$\langle {}^{49}\sigma_f/{}^{25}\sigma_f\rangle_c$	1.49±0.075[b]
$\langle {}^{28}\sigma_c/{}^{28}\sigma_f\rangle_c$	0.47±0.02		

[a] The experimental values for the $\langle {}^{28}\sigma_f/{}^{25}\sigma_f\rangle_c$ ratios have been modified from the CSEWG recommendations (0.205 for JEZEBEL and 0.156 for GODIVA) in accordance with recent recommendations of Hirons.[17]

[b] The uncertainties in the $\langle {}^{49}\sigma_f/{}^{25}\sigma_f\rangle_c$ ratios have been increased[18] from ∿2% to ∿5% (1σ) due to revised uncertainty estimates associated with the deduction of the number of fissions through the β-counting of ^{99}Mo.

[c] Macroscopic central reaction rates, denoted by $\langle\ \rangle_c$, have been divided by respective densities; i.e., all ratios are "microscopic" reaction rate ratios. σ_c is the capture (n,γ) cross section; σ_f is the fission (n,f) cross section.

III. Analyses of GODIVA and JEZEBEL: Generation of Sensitivity Coefficients

The cross section library employed in these calculations was a 126 group processed MINX/SPHINX library[19] generated from ENDF/B-IV data at ORNL. Group constants were developed simultaneously in CCCC,[20] AMPX,[21] and MATXS[22] formats to allow for self shielding, preparation of user libraries for transport codes and creation of a data base for the FORSS sensitivity profile modules. The ANISN code[23] was used to generate regular and generalized fluxes and adjoints in the S_{16}, P_3, 40 spatial mesh interval description provided in the CSEWG specifications[14] and to compute the desired responses. The volume integrated flux spectrum for GODIVA is illustrated in Fig. 1. Previously determined correction factors[24] to account for higher order transport approximations were applied and the results are

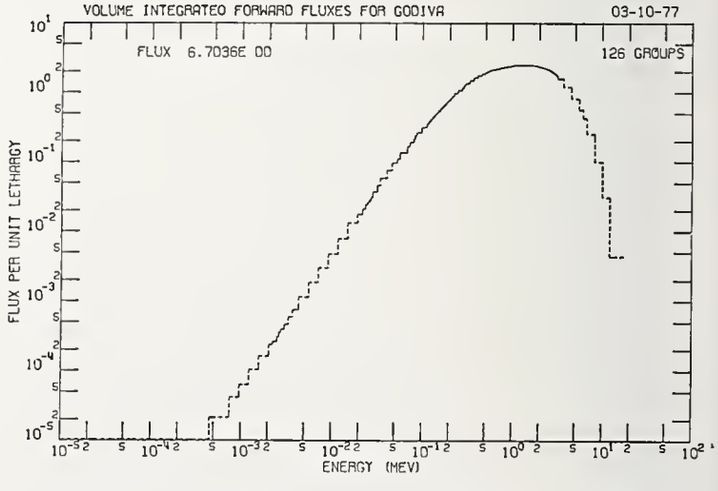

Fig. 1. The Flux Spectrum in GODIVA Is Applicable for Testing $^{235}U(n,f)$ Cross Sections in the Fission Source Energy Range.

listed in Table II along with results of other laboratories participating in the CSEWG data testing effort[24] and the experimental uncertainties from Table I. It is important to note that the revised recommendations for the $\langle {}^{28}\sigma_f/{}^{25}\sigma_f \rangle$ experimental results[17] change previous GODIVA overprediction into reasonable agreement but makes the JEZEBEL discrepancy even worse. The plutonium fission ratio is underpredicted in the JEZEBEL assembly consistent with underprediction of criticality there. This somewhat complicated series of results is not the final picture. With the coming issue of ENDF/B-V, several of the principal cross sections are due for revision. We assess this effect in a subsequent section by making use of the sensitivity profiles developed from ENDF/B-IV as discussed below.

Table II. Calculation/Experiment Data Testing with ENDF/B-IV Indicates Discrepancies Particularly for JEZEBEL

	BNL	LASL	ORNL	Experimental Uncertainties (%: 1σ)
		JEZEBEL		
k_{eff}	0.992	0.996	0.992	0.3
$\langle {}^{28}\sigma_f/{}^{25}\sigma_f \rangle$ C/E[a]	0.908	0.922	0.905	3.8
$\langle {}^{49}\sigma_f/{}^{25}\sigma_f \rangle$ C/E	0.934	0.936	0.933	5.0
		GODIVA		
k_{eff}	1.005	1.007	1.003	0.3
$\langle {}^{28}\sigma_f/{}^{25}\sigma_f \rangle$ C/E	1.031	1.035	1.031	3.1
$\langle {}^{49}\sigma_f/{}^{25}\sigma_f \rangle$ C/E	0.971	0.970	0.972	5.0
$\langle {}^{28}\sigma_c/{}^{28}\sigma_f \rangle$ C/E		0.937	0.954	4.2

[a] C/E is the ratio of calculation to experiment for the quantity in brackets. The (C/E)'s for $\langle {}^{28}\sigma_f/{}^{25}\sigma_f \rangle_c$ are relative to the experimental values in Table I which updates the CSEWG recommendations changing previous GODIVA overprediction into reasonable agreement but making the JEZEBEL discrepancy even worse.

Energy dependent sensitivity profiles were calculated with the JULIET module[7] of the FORSS system. Space-energy-and angle integrated sensitivities for each of the performance parameters in GODIVA and JEZEBEL are presented in Tables III and IV for many of the cross sections of interest. Comprehensive libraries[8] of energy dependent coefficients in a computer retrievable format[22,8] have been documented and released for distribution by RSIC and NNCSC. As examples, Fig. 2 illustrates

Table III. Relative Sensitivity of GODIVA Performance Parameters to Various Cross Section Reaction Types

k		$\langle {}^{28}\sigma_f/{}^{25}\sigma_f \rangle_c$		$\langle {}^{49}\sigma_f/{}^{25}\sigma_f \rangle_c$		$\langle {}^{28}\sigma_c/{}^{28}\sigma_f \rangle_c$	
Reaction[b]	Relative Sensitivity[a]	Reaction[b]	Relative Sensitivity[a]	Reaction[b]	Relative Sensitivity[a]	Reaction[b]	Relative Sensitivity[a]
$^{25}\bar{\nu}$	0.983	$^{28}\sigma_f$	0.998	$^{49}\sigma_f$	1.00	$^{28}\sigma_c$	0.998
$^{25}\sigma_f$	0.660	$^{25}\sigma_f$	-0.819	$^{25}\sigma_f$	-0.979	$^{28}\sigma_f$	-0.997
$^{25}\sigma_{n,n}$	0.113	$^{25}\sigma_{n,n',d}$	-0.269	$^{25}\sigma_{n,n',d}$	-0.031	$^{25}\sigma_{n,n',d}$	0.385
$^{25}\sigma_{n,n',d}$	0.062	$^{25}\sigma_{n,n',c}$	-0.164	$^{25}\sigma_{n,n',c}$	-0.013	$^{25}\sigma_f$	-0.266
$^{25}\sigma_c$	-0.037	$^{25}\sigma_{n,n}$	-0.087	$^{25}\sigma_{n,n}$	-0.011	$^{25}\sigma_{n,n',c}$	0.230
$^{25}\sigma_{n,n',c}$	0.014	$^{25}\bar{\nu}$	0.068	$^{25}\sigma_c$	+0.0059	$^{25}\sigma_{n,n}$	0.126
$^{28}\bar{\nu}$	0.0097	$^{25}\sigma_c$	0.034	.	.	$^{25}\bar{\nu}$	-0.096
$^{25}\sigma_{n,n',2}$	0.0083	$^{28}\sigma_{n,n',d}$	-0.026	.	.	$^{25}\sigma_c$	-0.054
$^{24}\bar{\nu}$	0.0083	$^{25}\sigma_{n,n',2}$	-0.009	.	.	$^{28}\sigma_{n,n',d}$	0.037
$^{28}\sigma_{n,n}$	0.0073	$^{28}\sigma_{n,n',c}$	-0.009	.	.	$^{25}\sigma_{n,n',2}$	0.016
$^{28}\sigma_f$	0.0068	$^{28}\sigma_{n,n}$	-0.006	.	.	$^{28}\sigma_{n,n',c}$	0.013
$^{24}\sigma_{n,f}$	0.0057	.	.	.	.	$^{28}\sigma_{n,n}$	0.009
.	.	.	.	.	.	$^{25}\sigma_{n,n',3}$	0.007
.	.	.	.	.	.	.	.

[a] This is percent change in response per percent change in cross section uniformly over all energy.

[b] σ_f is fission [(n,f) MT=18]

σ_c is capture [(n,γ) MT=102]

$\sigma_{n,n',x}$ is total discrete inelastic when x=d (MT=4); discrete inelastic to level n when x=n (MT=51-90); total continuum cross section when x=c (MT=91).

The fission spectrum temperature is not included in this list; otherwise ranking of reactions is in order of importance.

Table IV. Relative Sensitivity of JEZEBEL Performance Parameters to Various Cross Section Reaction Types

k		$\langle {}^{28}\sigma_f/{}^{25}\sigma_f \rangle_c$		$\langle {}^{49}\sigma_f/{}^{25}\sigma_f \rangle_c$	
Reaction[b]	Relative Sensitivity[a]	Reaction[b]	Relative Sensitivity[a]	Reaction[b]	Relative Sensitivity[a]
$^{49}\bar{\nu}$	0.967	$^{28}\sigma_f$	1.0	$^{49}\sigma_f$	1.011
$^{49}\sigma_f$	0.729	$^{25}\sigma_f$	-1.0	$^{25}\sigma_f$	-1.0
$^{49}\sigma_{n,n}$	0.082	$^{49}\sigma_{n,n',d}$	-0.192	$^{49}\sigma_{n,n',d}$	-0.022
$^{40}\bar{\nu}$	0.031	$^{49}\sigma_{n,n',c}$	-0.151	$^{49}\sigma_{n,n',c}$	-0.014
$^{49}\sigma_{n,n',d}$	0.027	$^{49}\sigma_f$	0.101	$^{49}\sigma_{n,n}$	-0.011
$^{40}\sigma_f$	0.023	$^{49}\sigma_{n,n}$	-0.078	.	.
$^{49}\sigma_{n,n',c}$	0.012	$^{49}\bar{\nu}$	0.054	.	.
$^{49}\sigma_c$	-0.008	$^{49}\sigma_c$	0.012	.	.
.	.	$^{40}\sigma_{n,n',d}$	-0.010	.	.
.	.	$^{40}\sigma_{n,n',c}$	-0.007	.	.
.	.	.	.	.	.
.	.	.	.	.	.

[a] This is percent change in response per percent change in cross section uniformly over all energy.

[b] σ_f is fission [(n,f) MT=18]

σ_c is capture [(n,γ) MT=102]

$\sigma_{n,n',x}$ is total discrete inelastic when x=d (MT=4); discrete inelastic to level n when x=n (MT=51-90); total continuum cross section when x=c (MT=91).

The fission spectrum temperature is not included in this list; otherwise ranking of reactions is in order of importance.

the sensitivity profile of k for GODIVA with respect to the ^{235}U fission cross section. Figure 3 presents the sensitivity profile for the ^{238}U capture/fission ratio with respect to the ^{235}U fission cross section. The dashed line is positive, i.e., an increase in $^{235}U(n,f)$ at high energies effectively competes with the $^{238}U(n,f)$ cross section, thus increasing the $\langle {}^{28}\sigma_c/{}^{28}\sigma_f \rangle_c$ ratio [the solid line is negative; it peaks near $^{238}U(n,f)$ threshold and at all energies below, competes only with the ^{238}U capture rate]. Figure 4 presents the sensitivity of $\langle {}^{28}\sigma_f/{}^{25}\sigma_f \rangle_c$ in GODIVA with respect to the ^{238}U fission cross section. Increases in $^{238}U(n,f)$ clearly have a positive direct effect on this performance parameter since the cross section appears explicitly in the performance parameter definition. The net contribution to the flux

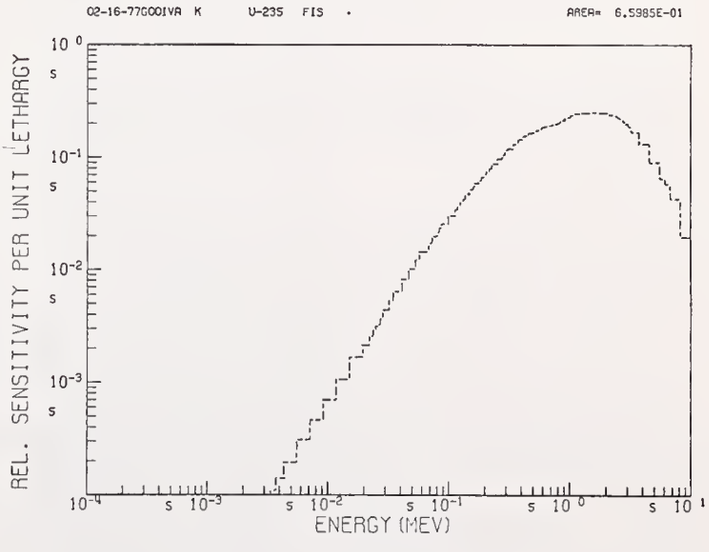

Fig. 2. Relative Sensitivity Per Unit Lethargy of k_{eff} in GODIVA with Respect to the $^{235}U(n,f)$ Cross Section.

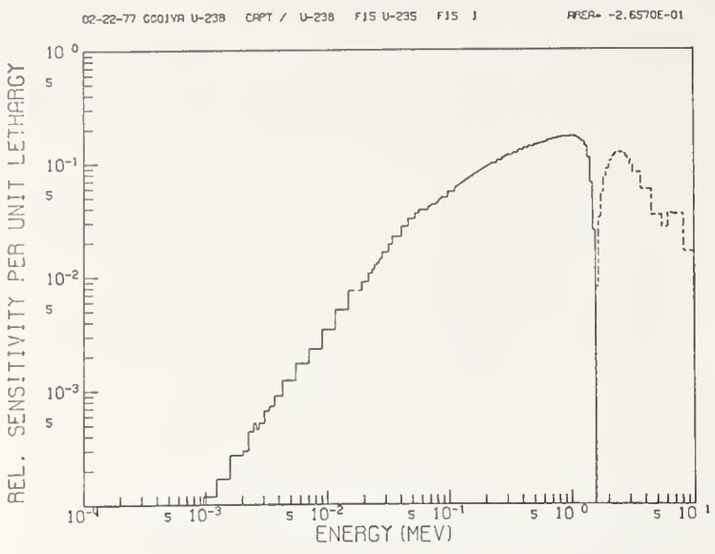

Fig. 3. Relative Sensitivity per Unit Lethargy of $\langle {}^{28}\sigma_c/{}^{28}\sigma_f\rangle_c$ in GODIVA with Respect to the $^{235}U(n,f)$ Cross Section.

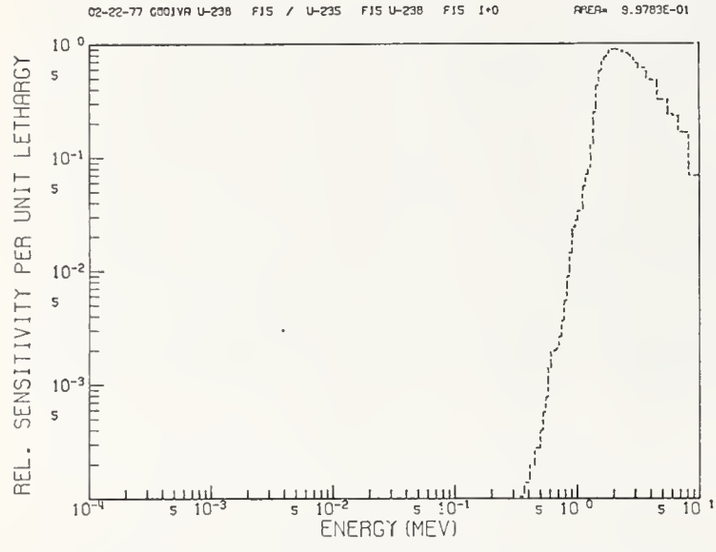

Fig. 4. Relative Sensitivity Per Unit Lethargy of the $\langle {}^{28}\sigma_f/{}^{25}\sigma_f\rangle_c$ in GODIVA with Respect to the ^{238}U Fission Cross Section.

effect is essentially negligible with additional fission neutrons increasing both relative ^{238}U and ^{235}U fission rates in roughly the same proportion.

IV. Changes to GODIVA and JEZEBEL Calculated Performance Associated with ENDF/B Re-Evaluation to Version V

At the May, 1976, ENDF/B-V Task Force meeting, evaluators made "first cut" estimations for what changes might be made in the cross sections for the principal isotopes [$^{235}U(n,f)$, $^{238}U(n,\gamma)$, $^{239}Pu(n,f)$] for Version V relative to ENDF/B Version IV. The Data Testing Subcommittee then made projections based upon available sensitivity coefficients of the possible impact on fast reactor criticals analysis (e.g., ref. 7, p. 71). Subsequently, McKnight and Poenitz[25] re-examined this question with alternative evaluations discussed at the 1976 ANL Fast Neutron Fission Cross Section Meeting. For the present study, we've taken McKnight's five group estimated cross section changes[25] for $^{235}U(n,f)$ and $^{239}Pu(n,f)$ and have projected the impact on all of the GODIVA and JEZEBEL performance parameters considered in this work. The cross section changes proposed were +1.44, -0.24, -2.57, -3.32, -2.13 percent change in $^{25}\sigma_f$ relative to ENDF/B-IV for 3.679-10.000, 1.353-3.679, 0.498-1.353, 0.183-0.498, 0.067-0.183 MeV energy regions. Similarly, the per cent changes for $^{49}\sigma_f$ in the same energy ranges were -1.07, +0.83, +1.02, -0.30, and -2.13, respectively. In addition to McKnight's tabulation[25] we have included the proposed changes associated with $^{238}U(n,f)$ for ENDF/B-V. For the three highest energy groups, we estimate -2.5, -3.5, and +12% respectively (highest energy group first).

As a result of lowering the $^{235}U(n,f)$, the $^{238}U(n,f)$, and raising (slightly) the $^{239}Pu(n,f)$ cross section, the results on the whole are brought into much better agreement. Criticality, for both systems, is underpredicted as is the $\langle {}^{28}\sigma_f/{}^{25}\sigma_f\rangle_c$ ratio in JEZEBEL. Other performance parameters are close to or within one standard deviation of the experimental value. Table V summarizes the projected calculated results (ENDF/B-V ^{235}U, ^{238}U, and ^{239}Pu fission) and measurements for GODIVA and JEZEBEL.

Table V. ENDF/B-IV, Projected ENDF/B-V and Measured GODIVA and JEZEBEL Performance

	ENDF/B-IV	"ENDF/B-V" (Updating ^{238}U, ^{235}U, ^{239}Pu Fission)	Experimental Uncertainty (%: 1σ)
		JEZEBEL	
k_{eff}	0.9920	0.9944	0.3
$\langle {}^{28}\sigma_f/{}^{25}\sigma_f\rangle_{C/E}$	0.905	0.892	3.8
$\langle {}^{49}\sigma_f/{}^{25}\sigma_f\rangle_{C/E}$	0.933	0.949	5.0
		GODIVA	
k_{eff}	1.0033	0.9937	0.3
$\langle {}^{28}\sigma_f/{}^{25}\sigma_f\rangle_{C/E}$	1.031	1.010	3.1
$\langle {}^{49}\sigma_f/{}^{25}\sigma_f\rangle_{C/E}$	0.972	0.990	5.0
$\langle {}^{28}\sigma_c/{}^{28}\sigma_f\rangle_{C/E}$	0.954	0.991	4.2

V. Evaluated "Pointwise" Covariance Files

Covariance files have been evaluated for $^{235}U(n,f)$, $^{238}U(n,\gamma)$, $^{235}U(\bar{\nu})$, $^{238}U(n,f)/^{235}U(n,f)$ ratio, $^{238}U(n,n',1st)$, $^{238}U(n,\gamma)$, $^{238}U(\bar{\nu})$, $^{239}Pu(n,f)/^{235}U(n,f)$ ratio $^{239}Pu(n,\gamma)/^{239}Pu(n,f)$ ratio, $^{239}Pu(\bar{\nu})$, $^{240}Pu(n,\gamma)$, $^{240}Pu(\bar{\nu})$, $^{241}Pu(n,f)$, and $^{241}Pu(n,\gamma)$. The evaluations were based primarily on "external" methods of analysis which examine the scatter among existing data sets. These sets are assumed to represent fairly the statistical ensemble of hypothetical sets of measurements which could have been obtained in the experiments which form our present data base. The "pointwise" covariance files were represented on convenient energy grids believed to be adequately fine to reproduce the broad range behavior important for estimation of uncertainties in integral quantities.

The source of data for new uncertainty files evaluated for $^{28}\sigma_f/^{25}\sigma_f$ and $^{49}\sigma_f/^{25}\sigma_f$ was the recent compilation prepared by W. Poenitz.[26] In the method used, weights were assigned to each experiment which were estimated to reflect the reciprocal variance of a typical point from the data set. Since uncertainties

in most sets are a function of energy, an overall judgement was used. The evaluated ratio for $^{28}\sigma_f/^{25}\sigma_f$ was taken to be the proposed evaluated fission ratio for ENDF/B-V;[27] i.e., the ratio was used which, when multiplied by the ^{235}U fission cross section for ENDF/B-V gives the proposed ^{238}U fission cross section for ENDF/B-V. For the $^{49}\sigma_f/^{25}\sigma_f$ fission ratio, the ENDF/B-V evaluated ratio was not in hand early enough so the evaluated ratio had to be taken from ENDF/B-IV. Only in these two recent fission ratio evaluations was a distinction made between the ensemble of hypothetical measurements and the ensemble of evaluations based upon these measurements. Accounting for this apparently straightforward difference introduced calculational complexities because of the varied pattern of measurements made by individual authors and because of unequal weights assigned. In practice, these files for the ratios were group averaged and subsequently combined with multigroup covariance files based upon existing ^{235}U data[12] (properly weighted).

In general, the remaining files were obtained as indicated in the SUR report,[9] essentially applying the definition of the covariance matrix directly to compiled sets of experimental cross sections. Additional information relating to the pointwise covariance files can be found in ref. 7. In cases for which only a few data sets exist or could be compiled, the ensemble variances were statistically poorly determined by the small sample; however, variance fluctuations over small energy regions may be unimportant after averaging over the assembly spectrum. It is also important to recognize that such "external" covariance evaluation methods do not include any systematic bias; for example, the possibility that the ^{239}Pu half life may be uncertain to 2% could systematically affect all "absolute" ratio measurements requiring exact foil weights. Finally, in all cases, the uncertainty files refer to the infinitely dilute average cross section.

VI. Multigroup Covariance Files

The differential covariance files developed in the preceding sections were put into ENDF/B- IV format[10] and processed with the PUFF covariance file processing code.[28] The complete covariance matrix used is illustrated in Fig. 5.

The ^{238}U and ^{239}Pu fission ratios relative to ^{235}U combined with the ^{239}Pu capture/fission measurements introduce several off-diagonal components that are directly related to the $^{235}U(n,f)$ standard. For example, if the ^{239}Pu fission cross section is measured relative to ^{235}U ($^{49}\sigma_f = r\ ^{25}\sigma_f$; r being the $^{239}Pu/^{235}U$ fission ratio) and the ^{239}Pu capture cross section is measured relative to the ^{239}Pu fission data (i.e., $^{49}\sigma_c = \alpha\ ^{49}\sigma_f$; α is the Pu capture/fission ratio). Then it follows that:

(1) The relative covariance matrix for ^{239}Pu fission is the sum of the relative covariance matrices of r and $^{25}\sigma_f$.

(2) The relative covariance matrix of ^{239}Pu fission and capture is the sum of the relative covariance matrices of r and $^{25}\sigma_f$.

(3) The relative covariance matrix of ^{239}Pu fission and ^{235}U fission is the relative covariance matrix for $^{25}\sigma_f$.

(4) The relative covariance matrix of ^{239}Pu capture is the sum of the relative covariance matrices for α, r, and $^{25}\sigma_f$.

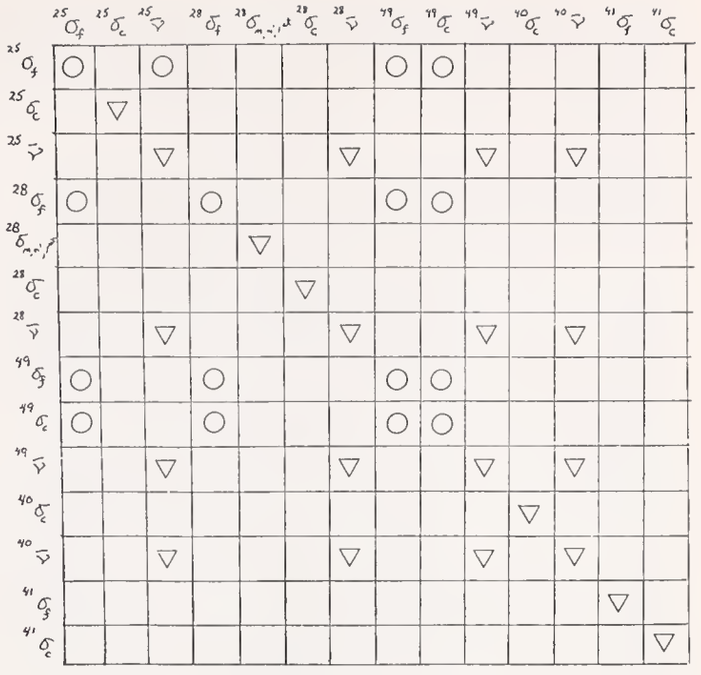

Fig. 5. The $^{235}U(n,f)$ Covariance Matrix Impacts Several Sub-Matrices of the Complete Multigroup Uncertainty Matrix.

1. Each box contains a 6x6 energy group covariance matrix. The blank boxes contained null elements.
2. ▽ indicates evaluation used in this study.
3. ◯ indicates representation includes a processed ^{235}U component.

(5) The relative covariance matrix of ^{239}Pu capture and ^{235}U fission is the relative covariance matrix for $^{25}\sigma_f$.

Similarly arguments can be made to deduce relative covariance matrices between ^{238}U fission and ^{235}U fission and between ^{238}U fission and ^{239}Pu capture cross sections. Additional off-diagonal components are introduced due to the uncertainty in ^{252}Cf $\bar{\nu}$ affecting a $\bar{\nu}$ evaluation. Perey has shown[29] that when the covariance matrix for a cross section is to be determined from the covariance matrices of ratios and other cross sections, it is necessary in the reduction to group form to weight the error files with the cross section whose covariance is being determined. This was implemented properly in this work for the matrices which required only one reaction type for weighting. However, off-diagonal group matrices [e.g., $\langle\ ^{239}Pu(n,\gamma),\ ^{239}Pu(n,f)\rangle$] for which the ^{235}U covariance file should have been weighted bilinearly [e.g., by the $^{239}Pu(n,f)$ cross section at one energy and by the $^{239}Pu(n,\gamma)$ cross section at the other] were approximated by weighting with the ^{235}U cross section itself.

It is important to note that each block of Fig. 5 is, in fact, a 6x6 energy group covariance matrix. Tables VI-XI present several of the important covariance files in the form of relative standard

Table VI. Relative Standard Deviation and Correlation Matrices for ^{235}U Fission

Energy Range (eV)	% Rel. Std. Dev.	Group	1	2	3	4	5	6
2.000E+07-3.679E+06	3.1	1	1000					
3.679E+06-1.353E+06	2.3	2	545	1000				
1.353E+06-4.979E+05	2.7	3	184	516	1000			
4.979E+05-1.832E+05	2.8	4	49	243	749	1000		
1.832E+05-4.087E+04	2.7	5	9	72	311	515	1000	
4.087E+04-1.000E-05	3.3	6	0	0	0	282	609	1000

Table VII. Relative Standard Deviation and Correlation Matrices for ^{235}U Capture

Energy Range (eV)	% Rel. Std. Dev.	Group	1	2	3	4	5	6
2.000E+07-3.677E+06	61.8	1	1000					
3.679E+06-1.353E+06	60.0	2	729	1000				
1.353E+06-4.979E+05	39.7	3	592	762	1000			
4.979E+05-1.832E+05	24.1	4	358	417	727	1000		
1.832E+05-4.087E+04	10.9	5	148	193	291	501	1000	
4.087E+04-1.000E-05	8.4	6	96	99	150	247	663	1000

Table VIII. Relative Standard Deviation and Correlation Matrices for ^{238}U Fission

Energy Range (eV)	% Rel. Std. Dev.	Group	1	2	3	4	5	6
3.000E+07-3.679E+06	3.1	1	1000					
3.679E+06-1.353E+06	2.5	2	542	1000				
1.353E+06-4.979E+05	2.6	3	272	620	1000			
4.979E+05-1.832E+05	3.1	4	52	241	352	1000		
1.832E+05-4.087E+04	7.8	5	-2	32	40	474	1000	
4.087E+04-1.000E-05	107.0	6	0	0	0	6	7	1000

Table IX. Relative Standard Deviation and Correlation Matrices for ^{238}U Capture

Energy Range (eV)	% Rel. Std. Dev.	Group	1	2	3	4	5	6
2.000E+07-3.679E+06	51.8	1	1000					
3.679E+06-1.353E+06	17.8	2	921	1000				
1.353E+06-4.979E+05	19.8	3	448	611	1000			
4.979E+05-1.832E+05	12.7	4	402	547	856	1000		
1.832E+05-4.087E+04	7.6	5	326	427	618	769	1000	
4.087E+04-1.000E-05	9.6	6	67	149	402	404	500	1000

Table X. Relative Standard Deviation and Correlation Matrices for $^{239}Pu(n,f)$

Energy Range (eV)	% Rel. Std. Dev.	Group	1	2	3	4	5	6
2.000E+07-3.679+06	3.1	1	1000					
3.679E+06-1.353E+06	2.4	2	543	1000				
1.353E+06-4.979E+05	2.7	3	184	510	1000			
4.979E+05-1.832E+05	2.8	4	50	242	748	1000		
1.832E+05-4.087E+04	2.8	5	9	74	310	508	1000	
4.087E+04-1.000E-05	3.4	6	0	0	0	271	569	1000

Table XI. Relative Standard Deviation and Correlation Matrices for $^{239}Pu(\bar{\nu})$

Energy Range (eV)	% Rel. Std. Dev.	Group	1	2	3	4	5	6
2.000E+07-3.679E+06	1.3	1	1000					
3.679E+06-1.353E+06	0.7	2	891	1000				
1.353E+06-4.979E+05	0.5	3	-277	57	1000			
4.979E+05-1.832E+05	0.8	4	-664	-458	793	1000		
1.832E+05-4.087E+04	0.8	5	-664	-458	793	1000	1000	
4.087E+04-1.000E-05	0.8	6	-664	-458	793	1000	1000	1000

deviations and correlation matrices (matrix elements multiplied by 1000 for ease of reading) in the six group structure selected for analysis. The GODIVA spectrum (Fig. 1) was used as the weighting function. Note that the energy dependent correlation matrix for a specific reaction is symmetric

VII. Uncertainty Analysis

The GODIVA and JEZEBEL sensitivity profiles calculated in Section III were collapsed to the six-group structure used in multigroup covariance file generation (Section VI) and folded[7] with the nuclear data covariance files for each of the performance parameters analyzed. The computation was then repeated assuming that the $^{235}U(n,f)$ cross section was known exactly. The results are indicated below in Table 12. It is vitally important to note that the evaluated uncertainty files which form the basis of Table 12 included only those represented in Fig. 5. It is clear from Tables III and IV that the uncertainty

Table 12. Increased Precision in $^{235}U(n,f)$ Could Significantly Impace Our Interpretation of k and $\langle^{28}\sigma_f/^{25}\sigma_f\rangle$ Measurements in GODIVA and JEZEBEL

	ENDF/B-V "Calculation"	Uncertainty (%: 1σ) All Nuclear Data	Uncertainty (%: 1σ) [$^{235}U(n,f)$ Assumed Known Exactly]
		JEZEBEL	
k_{eff}	0.9944	1.5	0.5
$\langle^{28}\sigma_f/^{25}\sigma_f\rangle_c$	0.188	1.3	0.3
$\langle^{49}\sigma_f/^{25}\sigma_f\rangle_c$	1.414	0.4	0.3
		GODIVA	
k_{eff}	0.9937	1.7	1.0
$\langle^{28}\sigma_f/^{25}\sigma_f\rangle_c$	0.163	1.5	0.7
$\langle^{49}\sigma_f/^{25}\sigma_f\rangle_c$	1.401	0.4	0.3
$\langle^{28}\sigma_c/^{28}\sigma_f\rangle_c$	0.466	14.3	14.0

in discrete and continuum inelastic scattering could add significantly to the projected uncertainties in Table 12. This is particularly true for the threshold reaction rate ratios, $\langle^{28}\sigma_f/^{25}\sigma_f\rangle_c$ and $\langle^{28}\sigma_c/^{28}\sigma_f\rangle_c$, and is also important for the uncertainties in k_{eff}. In addition to the lack of covariance file data for inelastic interactions in ^{235}U and ^{239}Pu, covariance files were not constructed for the fission spectrum shape. This might also have made a significant contribution. Clearly, the uncertainties listed in Table 12 are probably lower estimates. However, the numbers presented are themselves quite interesting.

The most startling result obtained is probably the 0.4% uncertainty for the $\langle^{49}\sigma_f/^{25}\sigma_f\rangle_c$ ratios, particularly in view of the ∿3% uncertainties for each of the reactions (Table VI and Table X). However, there is good reason for this low number. Recall that the $^{239}Pu(n,f)$ was evaluated through a ratio measurement relative to $^{235}U(n,f)$. Thus, the direct component of the $^{235}U(n,f)$ uncertainty vanishes to first order. The large number of rather independent measurements tend to reduce the estimated uncertainty on the evaluated ratio to ∿0.5%. In addition, combining uncorrelated data over the spectrum of the assembly reduces the uncertainty further.

For the $\langle^{28}\sigma_f/^{25}\sigma_f\rangle_c$ ratio, the situation is not as clean. As shown in Table III, the indirect effect of $^{235}U(n,f)$ on the GODIVA $\langle^{28}\sigma_f/^{25}\sigma_f\rangle_c$ spectral index is considerable. [The $^{235}U(n,f)$ uncertainty would cancel if the sensitivity for $^{238}U(n,f)$ and $^{235}U(n,f)$ were equal and of opposite sign.] In addition to the direct effect, which would correspond to a sensitivity of -1, there is an approximate +0.2 indirect effect so that the sensitivity to $^{238}U(n,f)$ [0.998] is not equal in magnitude to the sensitivity to $^{235}U(n,f)$ [-0.819]. Thus, a component of the $^{235}U(n,f)$ covariance remains. In the case of JEZEBEL where the sensitivities to $^{238}U(n,f)$ and $^{235}U(n,f)$ are +1 and -1 respectively (and thus, the ^{235}U contribution should cancel) there is a reasonably large sensitivity to $^{239}Pu(n,f)$ which in turn depends strongly on $^{235}U(n,f)$. The resulting uncertainty in $\langle^{28}\sigma_f/^{25}\sigma_f\rangle_c$ in JEZEBEL is then comprised largely of the uncertainty in $^{238}U/^{235}U$ fission ratio (small) and the uncertainties arising from ^{239}Pu from $^{235}U(n,f)$. The nuclear data uncertainties in k_{eff}, approximately 1-2 percent, depend on many factors but $^{235}U(n,f)$ is important. Finally $\langle^{28}\sigma_c/^{28}\sigma_f\rangle_c$ cannot be computed with high confidence due primarily to the large uncertainties assigned to ^{235}U capture at fission spectrum energies.

The third column of Table 12 indicates that eliminating all uncertainty in the $^{235}U(n,f)$ cross section could significantly improve our confidence in calculated criticality and $\langle ^{28}\sigma_f/^{25}\sigma_f\rangle_C$. This remark must be qualified until such time as uncertainties in ^{235}U and ^{239}Pu inelastic and in imprecision in the fission spectrum temperature have been included in the analysis. Hence, the significance of increased precision in the $^{235}J(n,f)$ cross section on our analysis capability for GODIVA and JEZEBEL is limited by the lack of covariance file components for other cross sections in the system and, of course, on the reliability of our estimates of uncertainties in cross sections evaluated for this analysis.

Inclusion of the measurements (and their uncertainties) in GODIVA and JEZEBEL, listed in Table I, in a data adjustment scheme[2] which included simultaneously the seven integral parameters led to the new set of calculated results (and uncertainties) listed in Table 13. The integral measurements have a pronounced effect on the resulting uncertainties for k_{eff} and $\langle ^{28}\sigma_c/^{28}\sigma_f\rangle_C$ since in these cases the assigned integral experiment uncertainties are considerably smaller than those projected to be due to nuclear data. It is interesting to note that the optimal adjustment could do little to resolve the

Table 13. The Adjusted Data Set Combines Information from Both the Differential and Integral Data

	ENDF/B-V "Calculation" Reported Measurement	Adjusted Data Set Reported Measurement	Uncertainty (%: 1σ) on Calculated Result Using Adjusted Set
	JEZEBEL		
k_{eff}	0.9944	0.9999	0.3
$\langle ^{28}\sigma_f/^{25}\sigma_f\rangle_{C/E}$	0.892	0.901	1.1
$\langle ^{49}\sigma_f/^{25}\sigma_f\rangle_{C/E}$	0.949	0.950	0.3
	GODIVA		
k_{eff}	0.9937	0.9999	0.3
$\langle ^{28}\sigma_f/^{25}\sigma_f\rangle_{C/E}$	1.010	1.019	1.2
$\langle ^{49}\sigma_f/^{25}\sigma_f\rangle_{C/E}$	0.990	0.991	0.3
$\langle ^{28}\sigma_c/^{28}\sigma_f\rangle_{C/E}$	0.991	0.998	4.0

$\langle ^{28}\sigma_f/^{25}\sigma_f\rangle_C$ in JEZEBEL; increases in this ratio tended to disturb the current agreement of the same ratio for GODIVA. (This might not have been true had the ^{239}Pu and/or ^{238}U inelastic files or the covariance of the fission spectrum shape been included.) Since the experimental ratio of ratios $[(^{28}\sigma_f/^{25}\sigma_f]_{GODIVA}/(^{28}\sigma_f/^{25}\sigma_f)_{JEZEBEL}]$ is more surely well known,[18] the discrepancy in one of these ratios would appear to be real and of necessity be related to the calculated flux spectrum. The adjustment was characterized by a χ^2/degree of freedom of 1.55; there is a ~20% probability that χ^2/degree of freedom is at least that large if the assigned integral and differential errors are correct. This minor overall inconsistency cannot be given much weight until uncertainties are included for all important quantities.

The actual adjustments made in this study are less significant since the adjustment is very sensitive to additional degrees of freedom which would be provided with the inclusion of the fissile material inelastic covariances (which may be difficult to estimate) and the uncertainty on the fission spectrum shape. For the record, however, only the cross sections for $^{235}U(n,f)$, $^{235}U(n,\gamma)$, $^{238}U(n,f)$, $^{238}U(n,\gamma)$, and $^{239}Pu(n,f)$ were modified in any significant way, and at most, these adjustments were 0.4-0.6 of one standard deviation. This particular adjustment would suggest that the $^{235}U(n,f)$ cross section above ~1.3 MeV be increased by ~1.5%; below 500 keV an additional 0.4% reduction was suggested. These suggested adjustments cannot be divorced from associated adjustments to the other four cross section type reactions; the adjustments must yet be confirmed by review and extension of the current covariance files before use in associated analysis.

Conclusions

Uncertainties due to the $^{235}U(n,f)$ standard were estimated to comprise more than half of the calculated uncertainty for criticality and $\langle ^{28}\sigma_f/^{25}\sigma_f\rangle_C$ spectral index in JEZEBEL as well as GODIVA, though the JEZEBEL assembly actually contains no ^{235}U. We are not able, at this time, to predict criticality or $\langle ^{28}\sigma_c/^{28}\sigma_f\rangle_C$ to anywhere near the accuracy obtained by direct measurements, and therefore the integral results are significant to our analysis capability and, particularly in the case of criticality, could eventually lead to improvement in our knowledge of the $^{235}U(n,f)$ cross section. Inclusion of integral information from GODIVA and JEZEBEL in an adjustment procedure was effective in reconciling all parameters other than the $\langle ^{28}\sigma_f/^{25}\sigma_f\rangle_C$ measurement in JEZEBEL. The adjustment procedure made changes of less than one standard deviation for the ^{239}Pu and ^{235}U fission and capture cross sections including an increase of ~1.5% for the "ENDF/B-V" $^{235}U(n,f)$ cross section above 1.3 MeV. This specific adjustment, as well as the strength of the JEZEBEL $\langle ^{28}\sigma_f/^{25}\sigma_f\rangle_C$ discrepancy, could change with inclusion of inelastic covariance files and must be viewed cautiously at this time.

Acknowledgements

The authors take pleasure in acknowledging the significant contributions of R. Q. Wright and J. L. Lucius in the generation of cross sections, transport results, and sensitivity profiles. E. M. Oblow and J. H. Marable offered valuable insight on the validity of the sensitivity profiles. The guidance of F. G. Perey in the generation of multigroup covariance files was essential as was the efforts of J. D. Drischler in processing of such data and in carrying forth the data adjustment calculated. The authors appreciate the advice of G. Hansen with respect to the measured uncertainties in GODIVA and JEZEBEL. Many of the original covariance files generated by F. Defillipo were developed from information generated by R. B. Perez, G. deSaussure, R. Gwin, and L. Weston. The authors gratefully appreciate the careful review of this paper performed by J. H. Marable, G. deSaussure, and E. M. Oblow. Timely information important to this study pertaining to the proposed ENDF/B-V evaluations was graciously provided by L. Stewart and W. Poenitz prior to its formal general release. Finally, this paper would not be nearly as readable without the careful typing and organization provided by Virginia Glidewell and would probably not exist at all without the financial and moral support of P. B. Hemmig and F. C. Maienschein.

References

1. See, for example, the review of E. Kiefhaber, "Evaluation of Integral Physics Experiments in Fast Zero Power Facilities," Advances in Nuclear Science and Technology, Vol.8 (1975).

2. A. Gandini, "Nuclear Data and Integral Measurements Correlation for Fast Reactors," Parts I, II, and III, RT/FI(73)5, RT/FI(73)22, and RT/FI(74)3 (1973 and 1974).

3. C. G. Campbell and J. L. Rowlands, "The Relationship of Microscopic and Integral Data," Nuclear Data for Reactors, Proc. Int. Conf. 2nd, Vol. II, p. 391 (June 1970).

4. J. B. Dragt, J. W. M. Dekker, H. Gruppelaer, and A. J. Janssen, "Methods of Adjustment and Error Evaluation of Neutron Capture Cross Sections: Application to Fission Products," Nucl. Sci. Eng., 62, 117-129 (1977).

5. S. M. Zaritsky, M. N. Nikovaev, and M. F. Troyanov, "Nuclear Data Requirements for the Calculation of Fast Reactors," INDC(CCP)-17U, Int. Nucl. Data Committee, IAEA Nucl. Data Sect., Karntner Ring 11.A-1010, Vienna (1971).

6. W. H. Hannum, "Projections for the Future of Reactor Physics," Luncheon address at the ANS National Topical Meeting on New Developments in Reactor Physics and Shielding (September 1972).

7. C. R. Weisbin, J. H. Marable, J. L. Lucius, E. M. Oblow, F. R. Mynatt, R. W. Peelle, and F. G. Perey, "Application of FORSS Sensitivity and Uncertainty Methodology to Fast Reactor Benchmark Analysis," ORNL/TM-5563 (ENDF-236) (December 1976).

8. J. H. Marable, J. L. Lucius, and C. R. Weisbin, "Compilation of Sensitivity Profiles for Several CSEWG Fast Reactor Benchmarks," ORNL-5262 (ENDF-234) (March 1977).

9. F. C. Difillipo, "SUR, A Program to Generate Error Covariance Files," ORNL/TM-5223 (March 1976). The data in this report were derived from discussions with G. deSaussure, R. B. Perez, R. Gwin, L. W. Weston, and R. W. Peelle; the principles behind the procedures described are discussed in F. G. Perey, G. deSaussure, and R. B. Perez, "Estimated Data Covariance Files for Evaluated Cross Sections - Examples for ^{235}U and ^{238}U," Advanced Reactors: Physics, Design, and Economics, Edited by Kallfelz and Karam, Pergamon Press, p. 578 (1975).

10. F. Perey, Format Modifications 73-7, minutes of the CSEWG Meeting, December 1973 (Enclosures 6 and 12), S. Pearlstein, Editor, Brookhaven National Laboratory; see also, F. G. Perey, "Estimated Uncertainties in Nuclear Data - An Approach," Proceedings of a Conference on Nuclear Cross Section and Technology, Vol. II, edited by R. A. Schrack and C. D. Bowman, p. 842 (October 1975).

11. J. H. Marable and C. R. Weisbin, "Performance Parameter Uncertainties for a Large LMFBR," Trans. Am. Nucl. Soc., June 1977 (to be published).

12. E. T. Tomlinson, G. deSaussure, and C. R. Weisbin, "Sensitivity Analysis of TRX-2 Lattice Parameters with Emphasis on Epithermal ^{238}U Capture," Research Projecy 612 (EPRI) Final Report (March 1977).

13. R. W. Peelle, "Uncertainties and Correlations in Evaluated Data Sets Induced by Use of Standard Cross Sections," Nuclear Cross Sections and Technology, Vol. II, p. 173, edited by R. A. Schrack and C. D. Bowman, Proceedings of a Conference, Washington, D.C. (March 1975).

14. "ENDF-202 Cross Section Evaluation Working Group Benchmark Specifications," BNL-19302 (ENDF-202) (November 1974).

15. G. E. Hansen and H. C. Paxton, "Reevaluated Critical Specifications of Some LASL Fast Neutron Systems," LA-4208 (1969).

16. G. E. Hansen, "Status of Computational and Experimental Correlations for Los Alamos Fast Neutron Critical Assemblies," Proc. of Seminar on Physics of Fast and Intermediate Reactors, Vol. I, IAEA, Vienna (1962).

17. T. J. Hirons and R. E. Seamon, "Calculations of Fast Critical Assemblies Using ENDF/B-IV Cross Section Data," Trans. Am. Nucl. Soc., 22, 722 (1975).

18. G. Hansen, private communication (March 1977).

19. C. R. Weisbin, R. W. Roussin, J. E. White, and R. Q. Wright, "Specifications for Pseudo-Composition Independent Fine-Group and Composition-Dependent Fine- and Broad-Group LMFBR Neutron-Gamma Libraries at ORNL," ORNL-TM-5142 (ENDF-224) (December 1975); see also, J. E. White, R. Q. Wright, L. R. Williams, and C. R. Weisbin, "Data Testing of the 126/36 Neutron-Gamma ENDF/B-IV Coupled Library for LMFBR Core and Shield Analysis," Trans. Am. Nucl. Soc., 23, 507 (June 1976).

20. B. M. Carmichael, "Standard Interface Files and Procedures for Reactor Physics Codes, Version III," LA-5486-MS (February 1974).

21. N. M. Greene, J. L. Lucius, L. M. Petrie, W. E. Ford, III, J. E. White, and R. Q. Wright, "AMPX: A Modular Code System for Generating Coupled Multigroup Neutron-Gamma Libraries from ENDF/B," ORNL/TM-3706 (March 1976).

22. Committee on Computer Code Coordination, Working Group Meeting, Los Alamos Scientific Laboratory (May 1976).

23. W. W. Engle, Jr., "A User's Manual for ANISN, A One-Dimensional Discrete Ordinates Transport Code with Anisotropic Scattering," K-1693, Computing Technology Center, Oak Ridge Gaseous Diffusion Plant (1967).

24. E. M. Bohn, R. Maerker, B. A. Magurno, F. J. McCrossen, and R. E. Schenter, editors, "Benchmark Testing of ENDF/B-IV," ENDF-230, Vol. I (March 1976).

25. R. D. McKnight and W. P. Poenitz, "The Effect of $^{235}U(n,f)$ and $^{239}Pu(n,f)$ Changes on CF-252 and ZPR6-6A and -7 Averages," ANL memorandum to participants on the CSEWG Meeting. Oct. 27-28, 1976, illused October 27, 1976.

26. W. P. Poenitz and A. B. Smith, Editors, "Proceedings of the NEANDC/NEACRP Specialists Meeting on Fast Neutron Fission Cross Sections of ^{233}U, ^{235}U, ^{238}U, and ^{239}Pu," ANL-76-90 (June 1976).

27. W. Poenitz, Argonne National Laboratory, private communication (March 1977).

28. C. R. Weisbin, E. M. Oblow, J. Ching, J. E. White, R. Q. Wright, and J. D. Drischler, "Cross Section and Method Uncertainties: The Application of Sensitivity Analysis to Study Their Relationship in Radiation Transport Benchmark Problems," ORNL-TM-4847 (ENDF-218) (August 1975); see also, RSIC Code Collection PSR-93.

29. F. G. Perey, "Final Draft of the Formats Manual for Files 31, 32, and 33 for ENDF/B-V," letter to R. J. LaBauve, March 1, 1977.

^{237}Np AND ^{238}U AS POSSIBLE STANDARDS FOR THE MeV REGION

S. Cierjacks

Institut für Angewandte Kernphysik
Kernforschungszentrum Karlsruhe, F.R. Germany

The aspects of using the fission cross sections of ^{237}Np and ^{238}U as possible standards in the MeV region are considered. In comparison to other neutron standards their application is particularly advantageous for experiments involving white-source techniques. Major distortions in fast neutron measurements due to frame-overlap problems and contributions from slow neutrons events can be avoided by spectrum cut-off at threshold energies. The present data basis for both nuclei is discussed and critically examined. Some suggestions are made of how to achieve an ultimate accuracy of 2 % with measurements employing ^{237}Np or ^{238}U as secondary standards.

(^{237}Np, ^{238}U(n,f) as neutron standards, summary of experimental results, E_n = 0.1 - 20 MeV)

Introduction

Recent developments in fast reactor design, fast reactor safety, waste disposal projects and in fusion reactor technology have turned the interest in accurate neutron data to a substantial extent towards neutron cross sections in the MeV region. As experienced largely in the eV and the keV-range absolute flux measurements necessary for absolute cross section determinations are difficult to perform, so that the use of a cross section standard turnes out to be most preferable also in this range. Among the presently internationally recommended six standard cross section of H(n,n), ^{6}Li (n,α), ^{10}B (n,α), ^{12}C (n,n), ^{197}Au (n,γ), and ^{235}U (n,f) there are only two, H (n,n) and ^{235}U (n,f), which are suitable for general application in the MeV region. For the other four reactions either a resonance structure of increasing complexity occurs or cross sections drop-off very rapidly with increasing energy ; both facts excluding them as useful standards. The use of the two remaining neutron reactions, though acceptable in principle, is also not fully satisfactory in this range. The difficulty for the application of the H(n,n) cross section is mainly connected with the fact, that the use of pure hydrogen is difficult and that the use of solid radiator foils creates either threshold problems and/or background problems if no telescope-like flux counters are used, or suffer from counting statistics due to the low efficiency of counter telescopes. Involving the fission cross section of ^{235}U instead, causes complications due to the appearance of structure in the cross section up to the several hundred keV range or due to background problems occurring from small impurities of slow neutrons. The latter fact is mainly of importance in experiments with white neutron sources and high pulse repetition rates. In the present paper, therefore, two possible new standards for the MeV region are proposed. In connection with such a proposal the recent assessments in determining accurate cross sections for these nuclei are discussed.

Possible Standards in the MeV-Region

In general an ideal standard reaction should meet the following requirements:

i. The cross sections of the reactions should be large and accurately known over the energy interval of interest.

ii. The cross section should smoothly vary with neutron energy.

iii. Good samples should easily be preparable, target material with the required chemical and isotopic purity ought to be readily available.

iv. A suitable neutron detector based on the standard reaction should have good overall properties, such as high efficiency, high stability, low sensity against other than neutron irradiations. For use with time-of-flight devices also a good timing characteristic is important.

In addition the above general requirements another property becomes highly desirably if a standard is to be used in the MeV range and/or with white neutron sources and broad continuous energy spectra.

v. The reference cross section process should be a threshold reaction, since MeV cross sections are typically small compared with eV- but also keV-cross sections. Small admixtures of slow-neutrons thus may introduce large distortions from small impurities of slow neutrons. Another favourable aspect in this context is that such a standard could directly be used in connection with the threshold method. The latter has favourably been employed in a number of recent fission cross section ratio measurements[1].

In relation to our criterion (i) fission cross sections are reasonably high compared with other partial cross sections in the MeV-range. From the large number of fissile isotopes only a small number of nuclei is of interest for our purpose, since highly radioactive material and isotopes occuring with low abundance in the isotopic mixture are to be excluded from the consideration. On this basis there remain except from ^{235}U mainly three nuclei and their fission reactions: ^{232}Th, ^{238}U and ^{237}Np. From these ^{232}Th turned out to be less suitable in view of the pronounced structure effects observed recently at Saclay in most of the energy range between 1 - 2 MeV as a consequence of isomeric fission in this nucleus. In how far structure effects to a lesser extent play also a role in the fission cross section of the remaining two isotopes will be discussed in the next paragraph. Considering the criterion iii, ^{237}Np and ^{238}U favourably fulfill this requirement. The monoisotopic element ^{237}Np is nowadays widely used in medicine as an energy source for heart pace-makers. Thus ^{237}Np material with high chemical purity is easily available. Likewisely highly enriched ^{238}U can easily be obtained from nuclear industry. Suitable fission foils and fission detectors are standard production of various laboratories in different countries.

From the viewpoint of detector availability, fission reactions have several advantages in the sense mentioned under item iv: Gas scintillation chambers as well as ionization chambers have high efficiencies, good stability and good timing characteristics to be used for measurements in the 1 nsec range. Their sen-

sitivity against γ-rays and charged particles can be largely reduced. Since suitable detectors can be run in approximately 2π or 4π-geometry, their sensitivity against anisotropy effects is small as long as sufficiently thin fission foils are employed.

Structure and Fluctuations in ^{237}Np, ^{238}U

As mentioned in the previous paragraph a pronounced structure in the fission cross section can occur in nuclei exhibiting subthreshold neutron fission. To a lesser extent fluctuations can also be observed as a consequence of statistical fluctuations of average level spacings and level widths in an energy range of strongly overlapping resonances. Structure of the first type can be caused by vibrational levels in the second wall of the double humped fission barrier, where the total width might be smaller than the spacing of class-II states. Since the damping width increases rapidly with excitation energy, gross structure effects should be minimum for nuclei having about the same barrier height for the first and the second well with a deep minimum within between. An inspection of the systematics of fission barrier parameters - e.g. that given by Michaudon[2] - shows that the above condition is best fulfilled for the uranium isotopes and neptunium. The thorium isotopes have about the same height for the inner and outer well, but only a rather shallow minimum within between. For nuclei starting from plutonium, the height of the outer barrier is systematically lower than that of the inner one; this effect increases with increasing target mass. Structure effects connected with isomeric fission should therefore be minimum in the range of ^{238}U and ^{237}Np. Fluctuation due to statistical effects in the matrix elements determining the neutron reaction can also be observed provided the fission cross section is measured in a sufficiently high resolution experiment. As demonstrated by Bowman[3] such random fluctuations can be predicted with resonance parameters obtained from measurement in the resolved resonance region. Bowman has also shown that the well documented fluctuations in ^{235}U in the several hundred keV region can be well understood in terms of Adler-Adler[4] or R-matrix resonance parameters.

For ^{237}Np and ^{238}U very high resolution measurements have recently been carried out at the Saclay laboratory. The result for ^{237}Np obtained by Plattard et al.[5] with a resolution of 0.3 ns/m in the range from 25 keV - 2 MeV is shown in Fig. 1. The data exhibit over the whole energy range a structureless fission cross section. All oscillations are purely due to counting statistics of the measurement. The data show also that no intermediate resonance occurs near 0.3 MeV as assumed by Brown et al.[6]. In Fig. 2 a new unpublished measurement for ^{238}U of Blons and coworkers[7] is shown. This measurement which was also carried out at the Saclay linac with a 0.3 ns/m resolution reveals substantial fluctuation in the whole energy region from threshold to $\sim$ 4 MeV. Unexpectedly large fluctuation amplitudes exceeding partially 10 % of the average fission cross sections are being observed. These fluctuations might have a significant influence on many of the past and future measurements in this range because the resolution and point spaces become important factors in the measurements. If this observed structure turns out to be real it becomes doubtful to some extent, whether ^{238}U would be a good standard, since one of the major requirements, that a standard should possess a smooth excitation function, is no longer fulfilled.

Status of Present Data

^{238}U Fission Cross Sections

Ratios Relative to ^{235}U.

The status of the cross section ratio relative to ^{235}U has only recently been reviewed at the 1976 ANL Specialists Meeting on Fast Neutron Fission Cross Section of U and ^{239}Pu[6]. Since only little new informations was obtained in addition during the meantime, mainly a brief summary of the conclusions from the Argonne Meeting will be given here. Present data available for this nucleus have been summarized in the Proceedings of the Meeting[8]. In Fig. 3 the more recent data sets obtaind since - say about 1970 - are shown. Some new data not available at the ANL Meeting have been included. Fig. 4 shows a selection of most of the older data available from CCDN Saclay. In these graphs several relative measurements have been renormalized at 2.5 MeV to the corresponding Pönitz[9] value. With respect to the ratio data the Working Group on Ratios concluded at the time of the Argonne Meeting, that a large number of experiments can be brought now into what one would consider an excellent agreement in the energy region from threshold to 10 MeV. This is achieved after some energy changes and after some adjustments for possible mass changes. It was expected by the Group that a new evaluation of the ratio data would yield ratio numbers of as good as 2 %. Above 10 MeV data becomes more sparce. There appear to be discrepancies in the white source data. Here are presently two cyclotron and two linac measurements extending to 20 MeV and beyond. Between cyclotron and linac measurements there occurs a divergence above $\sim$10 MeV, showing increasingly higher ratios for the cyclotron measurements with increasing energy. The difference approaches about 10 % at 20 MeV. This discrepancy is not yet well understood, in particular since the agreement below 10 MeV is so well in the same measurements. One possible source of the discrepancy might be due to the use of both ion chambers and gas scintillation chambers in cyclotron and linac measurements.

Absolute Fission Cross Section of ^{238}U

Figs. 5 and 6 compare the fission cross sections presently available from the NEA Nuclear Cross Section Centre at Saclay. In Fig. 5 the more recent data sets are shown, while Fig. 6 contains mainly a collection of all old cross section measurements. The data in both figures are shown together with the newest evaluated curve of KEDAK 3[10]. No adjustments of energy scales and absolute values were made, although several measurements were arbitrarily normalized at particular neutron energies. A more detailed inspection of the data shows that a large portion of the data is in rather good agreement over most of the energy range between 2 and 13 MeV, an exception being the threshold region below 2 MeV.

Also after adjustment of energies due to the obvious energy shifts in several data sets there seem to exist further significant differences in the overall shape in the threshold region. Excluding the threshold region it can be expected that a simultaneous evaluation of ratio and shape measurements would produce fission cross sections with an accuracy of better than 3 %. in the range below about 10 MeV. Above this energy fission cross section measurements are more scarce than ratio determinations relative to ^{235}U. Excluding discrepant very old measurements of Katase and keeping in mind that the measurements of Wilson were not inten-

ded to be precise determinations of the ^{235}U fission cross section, there exist only two cyclotron measurements in addition which agree rather favourably with each other within 5 % (compare Figs. 5 and 6). Unfortunately, however, this agreement is misleading since no linac measurements are available in this range.As long as we do not know the sources for the discrepancy between the linac and the cyclotron measurements in the ratio determinations we cannot exclude that the absolute cross sections have systematic uncertainties of as much as 10 % between 10-15 MeV as well as the ratios+.

^{237}Np Fission Cross Sections

Ratios Relative to ^{235}U.

There have only very few ratio measurements of ^{237}Np relative to ^{235}U been made in the past. Only two data sets are presently available from CCDN-Saclay. These values together with a new measurement of Behrens et al.[11]) from the Lawrence Livermore Laboratory are shown in Fig. 7. The latter data which have been obtained with the threshold method agree favourably with the 1967 White data by better than 2 % below 10 MeV. The additional data point given for 14 MeV deviates from the LLL results by as much as 10 %. The third data set of Stein turns out to be on average 4 % higher than Behrens' ratios. Despite the general good quality of the Livermore results for fission cross section ratios, only restricted conclusions might be drawn from these ^{237}Np ratio measurements. To judge the present data basis, one has to rely also on the numerous absolute fission cross section determinations.

Absolute Fission Cross Sections of ^{237}Np

In contrast to the few ratio measurements a large number of absolute or shape measurements exists for ^{237}Np. The latter fact reflects its importance as a threshold detector. Existing data contained in the CCDN library are shown in Figs. 8 and 9. As in the case of ^{235}U the data are plotted separately with respect to new and old results. Here the END-FBIV curve is included in both graphes as a reference for interrelations of measurements in the figures. It should be noted that the fission data are given on a double logarithmic scale. No adjustments of possible energy and mass changes were made .This spread is mainly due to the fact, that some rather discrepant 14 and 2-3 MeV values exist for this nucleus. The absolute fission cross section measured in the 14 MeV range are listed in Table I. On a first view these data appear to have very large scattering. But, if we exclude the 1960 Pankratov results but take his new 1963 values instead, and remove all old data with unassigned uncertainties (Rago, Henkel), there remains only a severe discrepancy with Iyer's value . All remaining determination are then consistent with the newest and most accurate σ_f-value of Adamov (2.43 ± 0.043 b). A similar, only slightly better situation exists in the 2-3 MeV region (Table II).If we exclude for the same reasons Henkel's measurements and the very old Klema data, all remaining results are consistent with the most accurate values of Jiacoletti of 1.59 ± 2 %. Even Plattard's high value is not discrepant, considering the large error in the absolute cross section determination. Due to the scatter in the normalization cross section data in Fig. 9 deviate in a broad band of ± 10 %. But also if one restricts consideration to more recent data sets as given in Fig. 8 data scattering exceeds by far the 3 % limit necessary to justify its use as a fast neutron standard cross section.

Table I. Absolute fission cross sections of ^{237}Np in the 14-15 MeV range

Author,Lab.	Year	E_n(MeV)	σ(b)	Flux Stand.
Henkel,LAS	1957	14.0	2.6	no information
Pankratov, KUR	1960	14.5 15.0	2.6 ± 5 % 2.62± 5 %	σ_f(7)
Pankratov, KUR	1963	14.0 14.7	2.4 ± 5 % 2.54± 5 %	σ_f(7)
White, ALD	1966 1967	14.1	2.33± 0.1	σ_f(5)
Rago, NRD	1968	14.0 14.2	2.31± ? 2.27± ?	σ_f(8)
Protopopov, USSR	1958	14.6	2.4 ± 0.2	-
Iyer, TRM	1969	14.1	2.98± 0.3	σ_f(8)
Adamov,LEN	1977	14.8	2.43± 0.047	ass. particle

Table II. Absolute fission cross sections of ^{237}Np in the 2-3 MeV range

Author, Lab.	Year	E_n(MeV)	σ(b)	Flux. Stand.
Klema, LAS	1948	2.5 3.0	1.45±3 % 1.48±3 %	σ_f(5),σ_f(8), σ_f(9)
Henkel, LAS	1957	2.0-2.5 2.5-3.0	1.48 1.45	no inform.
Schmitt, ORL	1959	2.82	1.65±10 %	σ_f(8)
White, ALD	1966 1967	2.25	1.67±0.1	σ_f(5)
Grundl,LAS	1967	2.0-2.5 2.5-3.0	1.652±0.05 1.575±0.05	σ_f(8)
Jiacoletti, LAS	1967	2.75	1.59 ±2 %	σ_f(5)
Brown, LAS	1970	2.0-2.5	1.62 ±10 %	σ_f(5) Davey
Kobayashi, KTO	1973	3.5	1.65 ±0.17	In^{115}
Plattard, SAC	1976	2.0-2.1	1.79±12 %	σ_f(5)

Proposal for Additional Measurements

It has been demonstrated that the availability of ^{237}Np and ^{235}U as additional neutron standards for the MeV range would be desirable. Furthermore it was shown that the fission cross sections for these data are not yet sufficiently known to carry out precise flux measurements in the accuracy region of ≤ 2 %. In order to reach this long-term goal, further experimental and

+Note added in proof: at the time of the Conference a preliminary evaluation of Pönitz[12]) became available, which is consistent with above accuracy estimates. A comparison of "absolute" and (U8/U5)*U5(ENDF-B/IV) results showed that a consistent-data-fit would have lowered the present U5 (ENDF-B/V) data between 2-13 MeV. This would support the data of Hansen et al. and the recent data of Szabo (both above 3 MeV). The difference between the "two" sets could also be resolved by lower U8/U5 values in the above energy range. This assumption would support the ratio measurements of Stein and recent data by Cancé.

evaluational effort is necessary. In this context the following measurements are suggested:

i. Ratio measurements for Np relative to ^{235}U over the whole energy region from threshold to 20 MeV employing the threshold method. Resolutions might be moderate of the order of 5 %. A high accuracy for the absolute neutron energy of 1 % should be obtained. Useful measurements must aim a statistical accuracy of better than 2 %. Measurements can rather easily be carried out with a cyclotron or some of the existing linacs.

ii. Additional absolute measurements of the fission cross section of ^{237}Np at~14 MeV and at an energy point between 2-3 MeV. The measurements at both energies would serve as a cross check of good normalizations at either one or the other energy point.

iii. Accurate shape measurements for ^{237}Np and ^{238}U between about 10 and 20 MeV with moderate resolution but good statistics to establish a reliable shape curve in this range.

iv. Extended high resolution cross section measurements for ^{238}U above 4 MeV and for ^{237}Np above 2 MeV with resolutions better than 0.3 ns/m. Measurements should be made relative to a smooth cross section such as H(n,n) and should extend to an energy for U at which the percent standard deviation of the cross section fluctuation decreases below 2 %. For Np the measurements should cover at least the plateau region between about 2-5 MeV. For the absolute values a 10 % accuracy should be adequate. Such investigations are necessary for U to investigate the existence and the extent of the cross section fluctuations in the few MeV range. For Np such measurements serve to verify that the smooth shape of the fission cross section curve continues above 2 MeV as would be most likely. Such measurements can in principle by carried out with most of the white-source neutron facilities.

Summary

To summarize, the ^{237}Np (n,f) and the ^{238}U(n,f) reactions have several favourable characteristics which justify their use as fission standards for fast neutron cross section measurements. An inspection of the ^{238}U (n,f) data indicate that the numbers might already be as accurate as 3 % in the range from threshold to 10 MeV. But care must be taken with respect to fluctuations at least below 4 MeV.

From this point of view ^{237}Np is much more favourable, since it experiences a smooth behaviour as demonstrated in a recent very high resolution measurement. Unfortunately the fission data for this nucleus are not yet accurate enough, to permit precise cross section determinations. Above 10 MeV the data situation is unsatisfactory for both, Np and U. In this range, which gains increasing importance in connection with fusion data needs further experimental effort is necessary to achieve the ultimately desired accuracy of ≤ 2 %.

Acknowledgements

The author is indebted to Dr. L. Edvardson from the NEA Neutron Data Compilation Centre at Saclay for supplying renormalized cross section data for ^{235}U and for providing graphs for almost all cross sections shown in this paper. The cooperation of Drs. J. Behrens, J. Blons, M. Cancé, G. Grenier and S. Plattard of readily providing their data for this survey partially even before publication is gratefully acknowledged. The author wishes also to thank Dr. Derrien from CCDN Saclay for his assistance in the collection of lacking data sets.

References

1. J.W. Behrens, G.W. Carlson, NSE, to be published, Preprint UCRL-78704.
2. A. Michaudon, Neutrons and Fission, Invited Paper Int. Conf. on the Interactions of Neutrons with Nuclei, Lowell, Mass., July 1976.
3. C.D. Bowman, Nuclear Data for Reactors, Conf. Proc. Helsinki, IAEA, 1970, Paper CN-26/41.
4. D.B. Adler, F.F. Adler, USAEC Report, ANL-6792, p. 695, 1963.
5. S. Plattard, J. Blons, D. Paya, Nucl. Sci.Eng.61 (1976) 477.
6. W.K. Brown,D.R.Dixon,D.M.Drake,Nucl.Phys.A156(1970)609.
7. J. Blons, private communication.
8. Proc. NEADNC/NEACRP Specialists Meeting on Fast Neutron Fission Cross Sections, ANL 28-30 June, 1976, ed. by W.P. Pönitz and A.B. Smith.
9. W.P. Pönitz, J. Nucl. Energy 26, (1972) 683.
10. B. Goel, F. Weller, KEDAK-Evaluation File, KFK-Report 2386, Part II.
11. J.W. Behrens, J.W. Magana, C.J. Browne, Report, UCID-17370 (1977).
12. W.P. Pönitz, private communication, 1977.
13. V.M. Adamov et al., Contribution to this Symposium.

Data Basis Used in the Graphs

Figs. 3,4 U-238 / U-235

Name, Symbol		Reference	Source
COATES	Har 75	75 Wash GB 7	CCDN,energy scale revised
CIERJACKS	KFK 76	76 ANL 2 KFK	Listing
BEHRENS	LLL 75	75 Wash 2 591	CCDN
DIFILIPPO	ORL 76	76 ANL ORL	CCDN
FURSOV	FEI 73	73 Kiev 3 73 FEI	CCDN
CONDE	ULL 76	76 ANL UPP	CCDN
POENITZ	ANL 72	JNE 26 483	CCDN
POENITZ	ANL 72	JNE 26 483	CCDN
POENITZ	ANL 72	JNE 26 483	CCDN
POENITZ	ANL 72	JNE 26 483	CCDN
POENITZ	ANL 72	JNE 26 483	CCDN
MEADOWS	ANL 75	Meadows 75 D	CCDN
MEADOWS	ANL 72	NSE 49 310	CCDN
MEADOWS	ANL 72	NSE 49 310	CCDN
MEADOWS	ANL 75	Meadows 75 D	CCDN
CANCE	BRC 76	76 ANL 1 BRC	Paper
CANCE	BRC 75	75 Kiev 1 BRC	CCDN
CANCE	BRC 77	Grenier P.C. 77	Listing
WHITE	ALD 67	JNE 21 671	Paper

Name, Symbol		Reference	Source
PANKRATOV	KUR 60	AE 9 399	CCDN
PANKRATOV	KUR 63	AE 14 177	CCDN
VOROTNIKOV	KUR 71	71 MOSCOW	CCDN
KALININ	KUR 58	58 GEN 16 136	CCDN
ADAMS	ALD 61	JNAB 1485	CCDN
NETTER	SAC 56	Wetter PC	CCDN
GRUNDL	LAS 67	NSE 30 39	CCDN
LAMPHERE	ORL 56	PR 104 1654	CCDN
KATASE	KYO 61	KATASE PC 61	CCDN
BATCHELOR	ALD 65	NP 65, 236	CCDN

Fig. 7 Np-237/U-235

BEHRENS	LRL 76	77 UCID-17370	Report
WHITE	ALD 67	JNE 21, 671	CCDN
STEIN	LAS 68	68 Wash 1 627	CCDN

Fig. 8,9 Np-237

ENDFB/IV			CCDN
KOBAYASHI	KTO 73	EANDC(J)-26	CCDN
KOBAYASHI	KTO 73	EANDC(J)-26	CCDN

Figs. 5,6 U-238

KEDAK 3		Ged. KFK-2386(77)Report	
ALKHAZOV	RI 74		
VOROTNIKOV	KUR 71	YFI 20 9	CCDN
VOROTNIKOV	KUR 75	75 Kiev FEI	CCDN
CIERJACKS	KFK 76	76 ANL 2 KFK	Listing
BLONS	SAC 77	BLONS PC 77	Computer-cards
WILSON	LAS 67	WASH 1074	CCDN
GRUNDL	NBS 72	ANS 15 945	CCDN
FLEROV	USSR 58	AE 5 657	CCDN
JIACOLETTI	LAS 70	NSE 48 412	CCDN
GRUNDL	LAS 67	NSE 30 39	CCDN
PLATTARD	SAC 75	NSE 61, 477	Journal
KALININ	KUR 58	58 GEN 16 136	CCDN
SCHMITT	ORL 59	PR 116 1575	CCDN
BROWN	LAS 70	NP A 156 609	CCDN
RAGO	NRD 68	HP 14 595	CCDN
PROTOPOPOV	USSR 58	AE 4 190	CCDN
HOCHBERG	KUR 59	LA-1495, 52	CCDN
PANKRATOV	KUR 60	AE 9 399	CCDN
WHITE	ALD 66	EANDC(UK)-77	Report
HENKEL	LAS 57	LA-1495, 52	CCDN
IYER	TRM 69	BARC-474, 1	CCDN
KLEMA	LAS 47	PR 72 88	CCDN

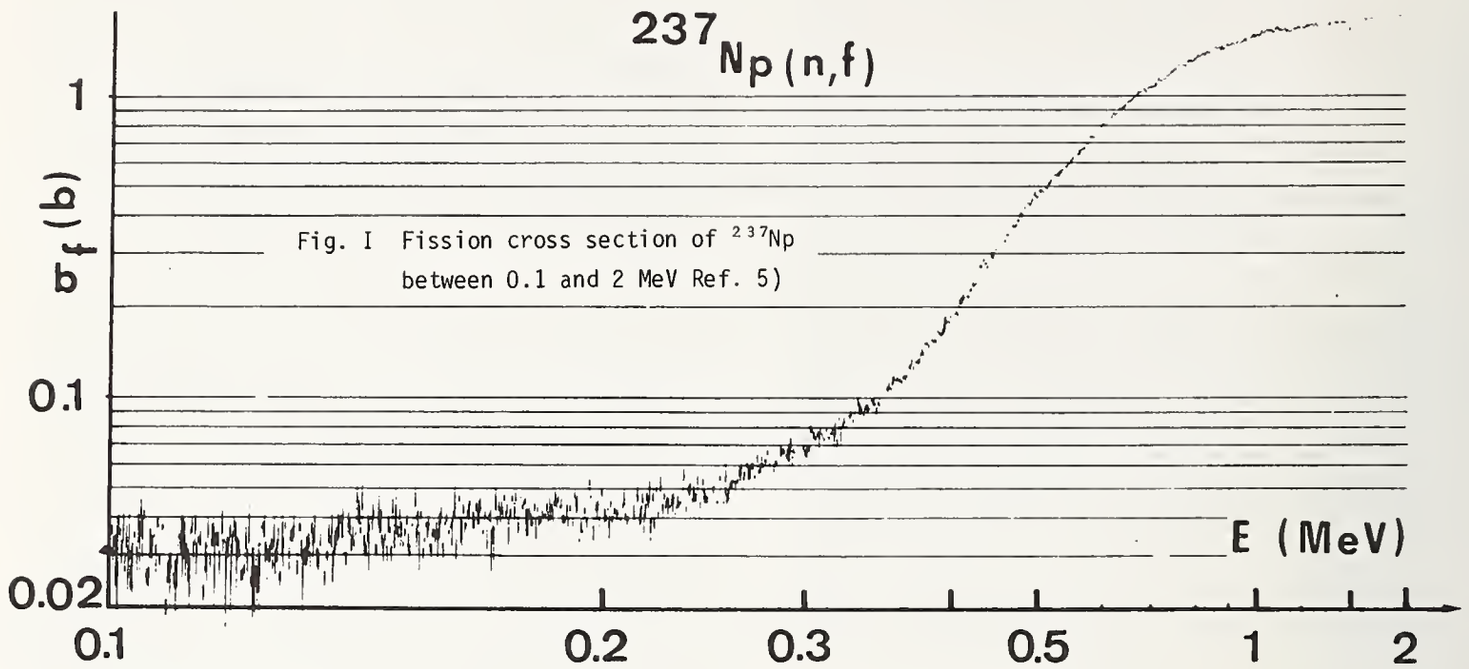

Fig. I Fission cross section of ^{237}Np between 0.1 and 2 MeV Ref. 5)

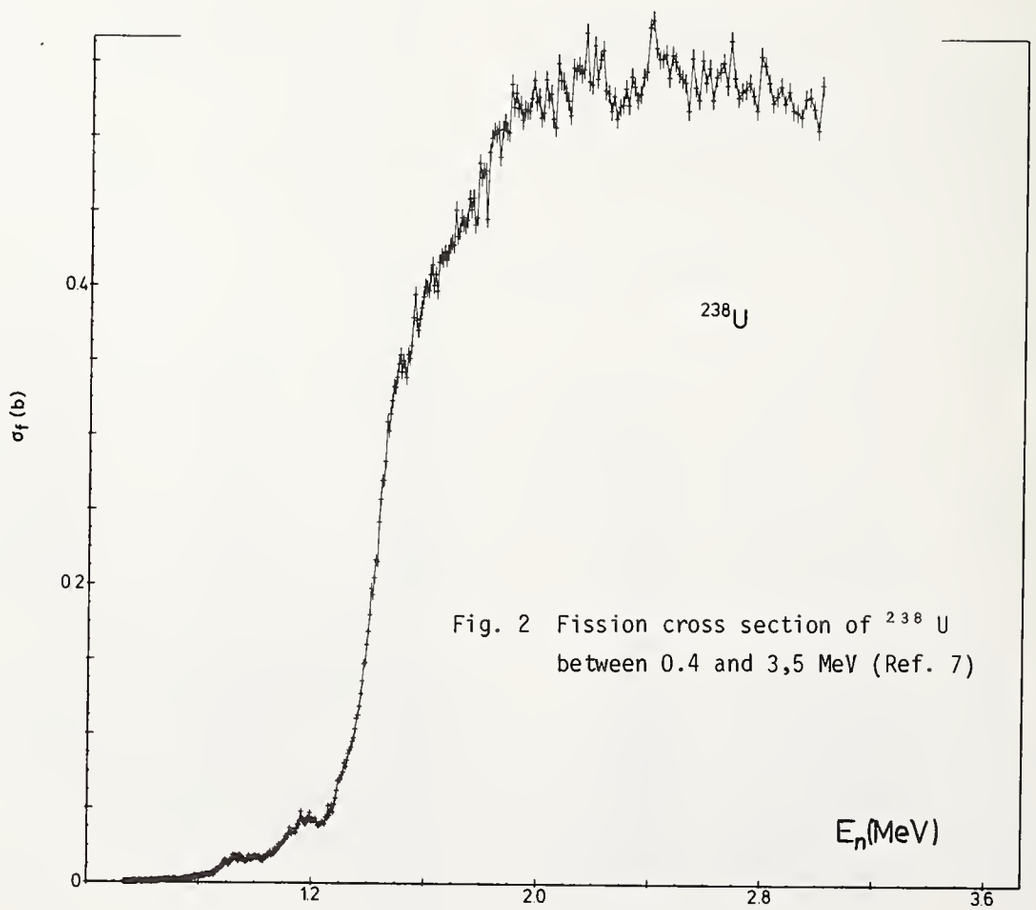

Fig. 2 Fission cross section of ^{238}U between 0.4 and 3,5 MeV (Ref. 7)

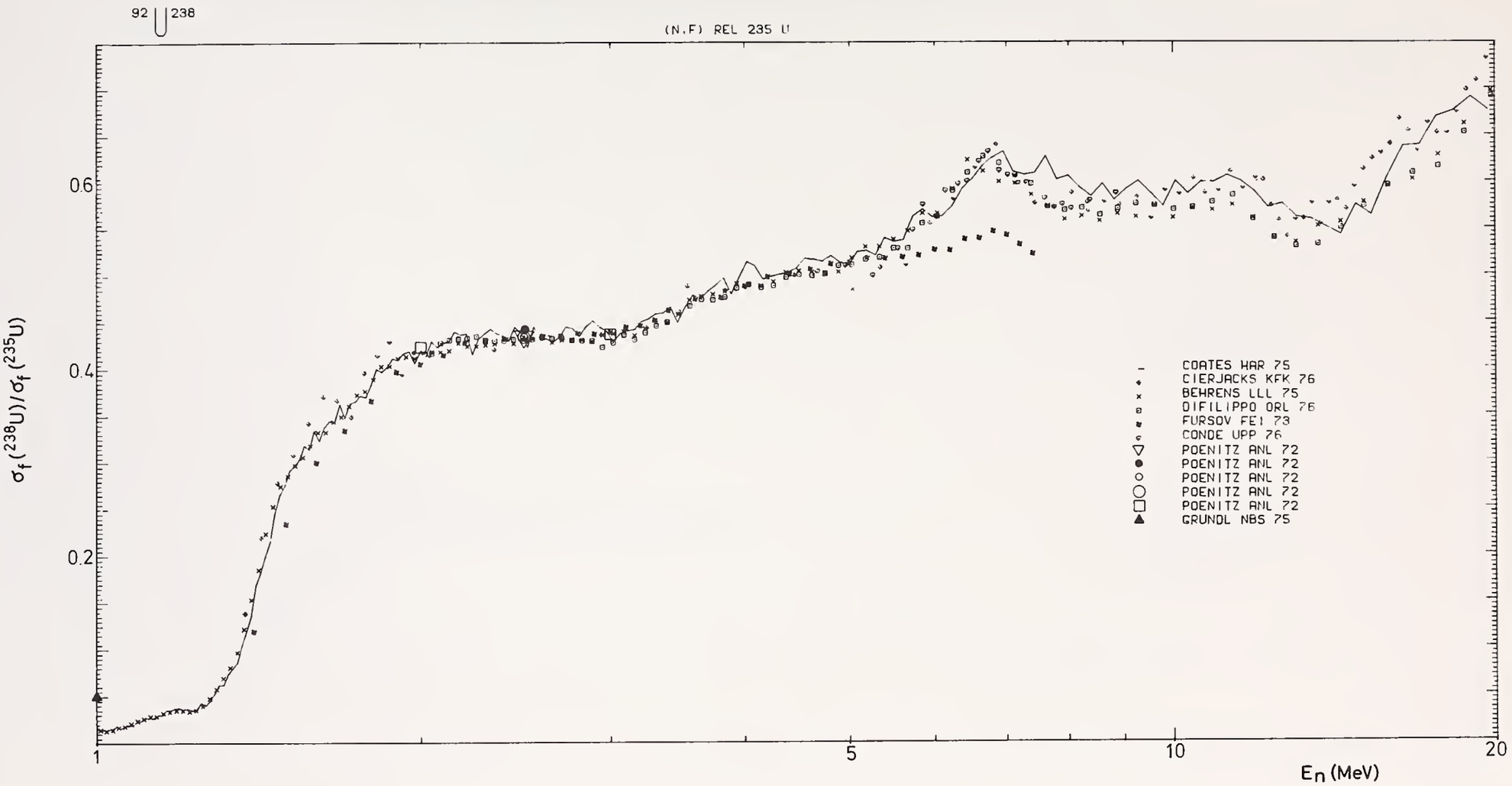

Fig. 3 Fission cross section ratios $^{238}U/^{235}U$. Comparison of recent measurements I

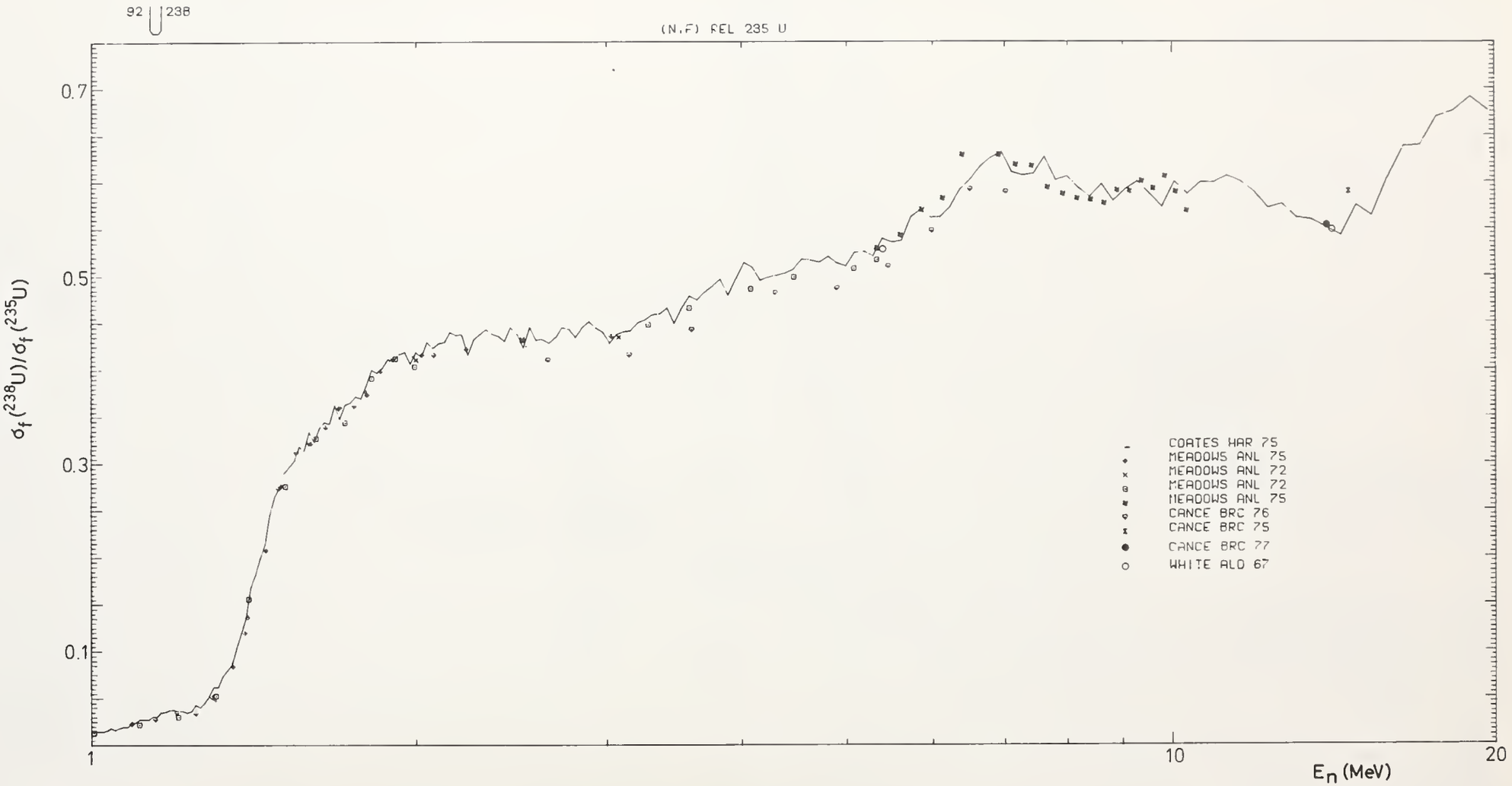

Fig. 4 Fission cross section ratios $^{238}U/^{235}U$. Comparison of recent measurements II

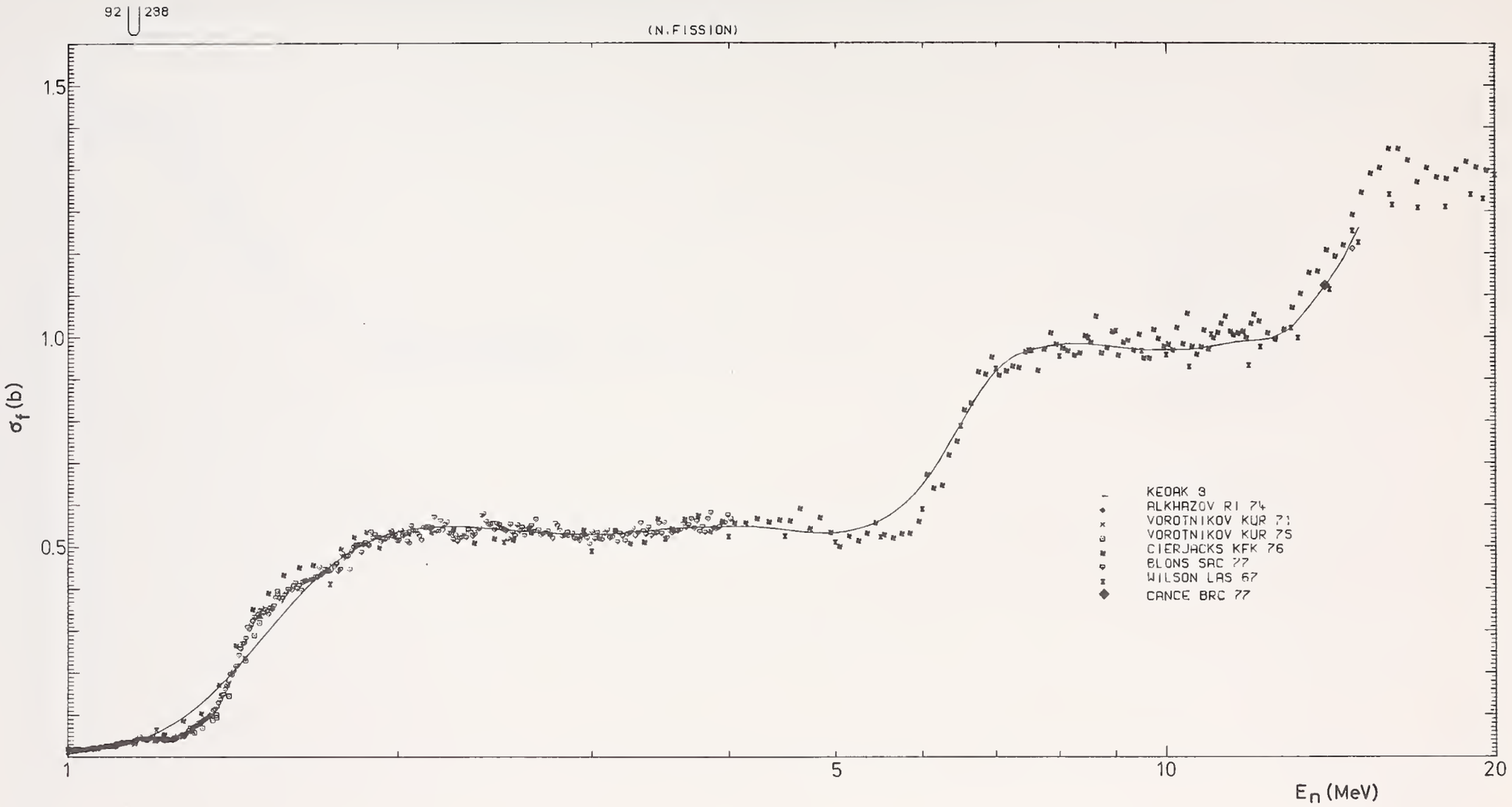

Fig. 5 Fission cross section of ^{238}U. Comparison of recent measurements

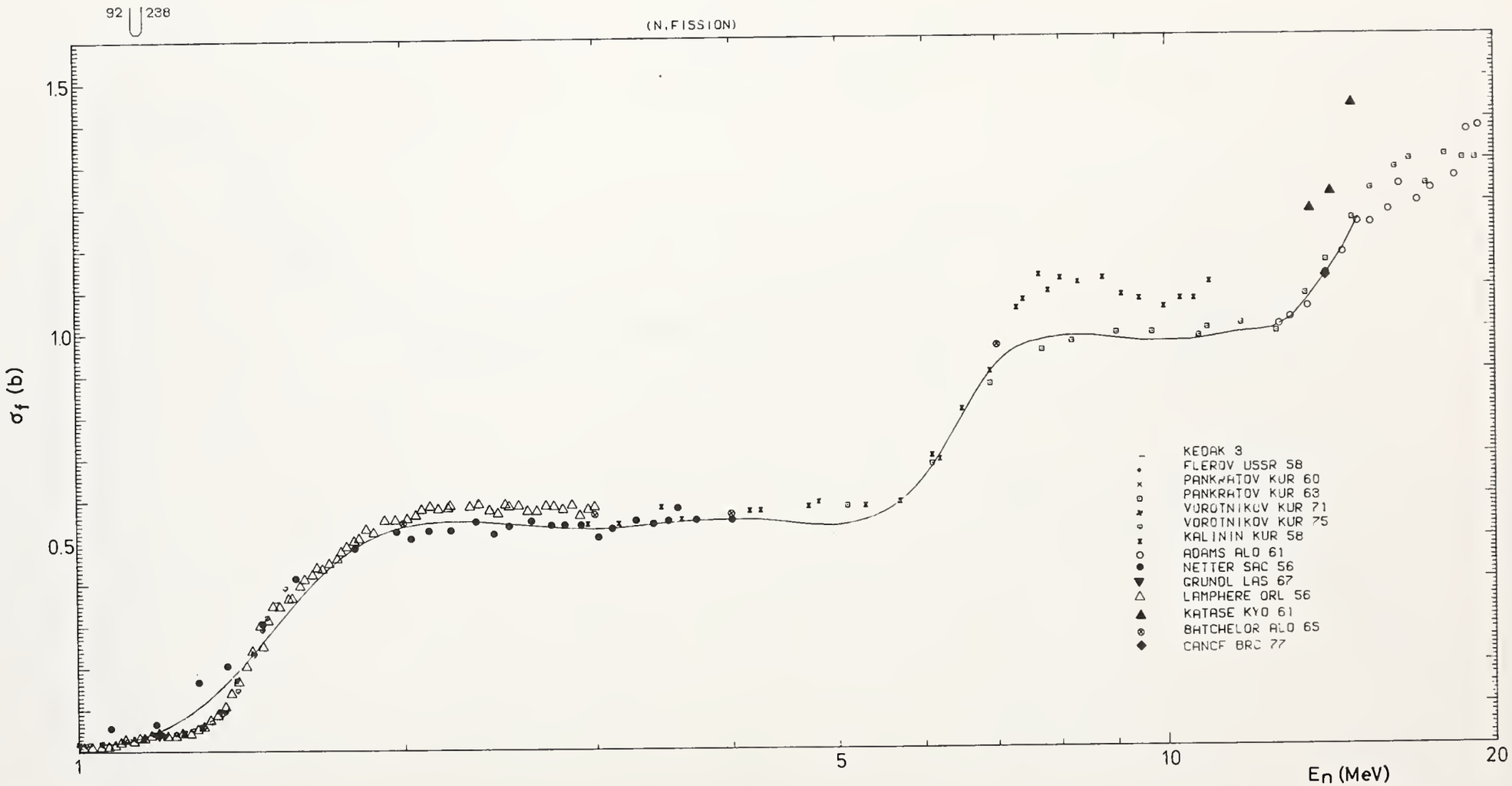

Fig. 6 Fission cross section of ^{238}U. Comparison of older results

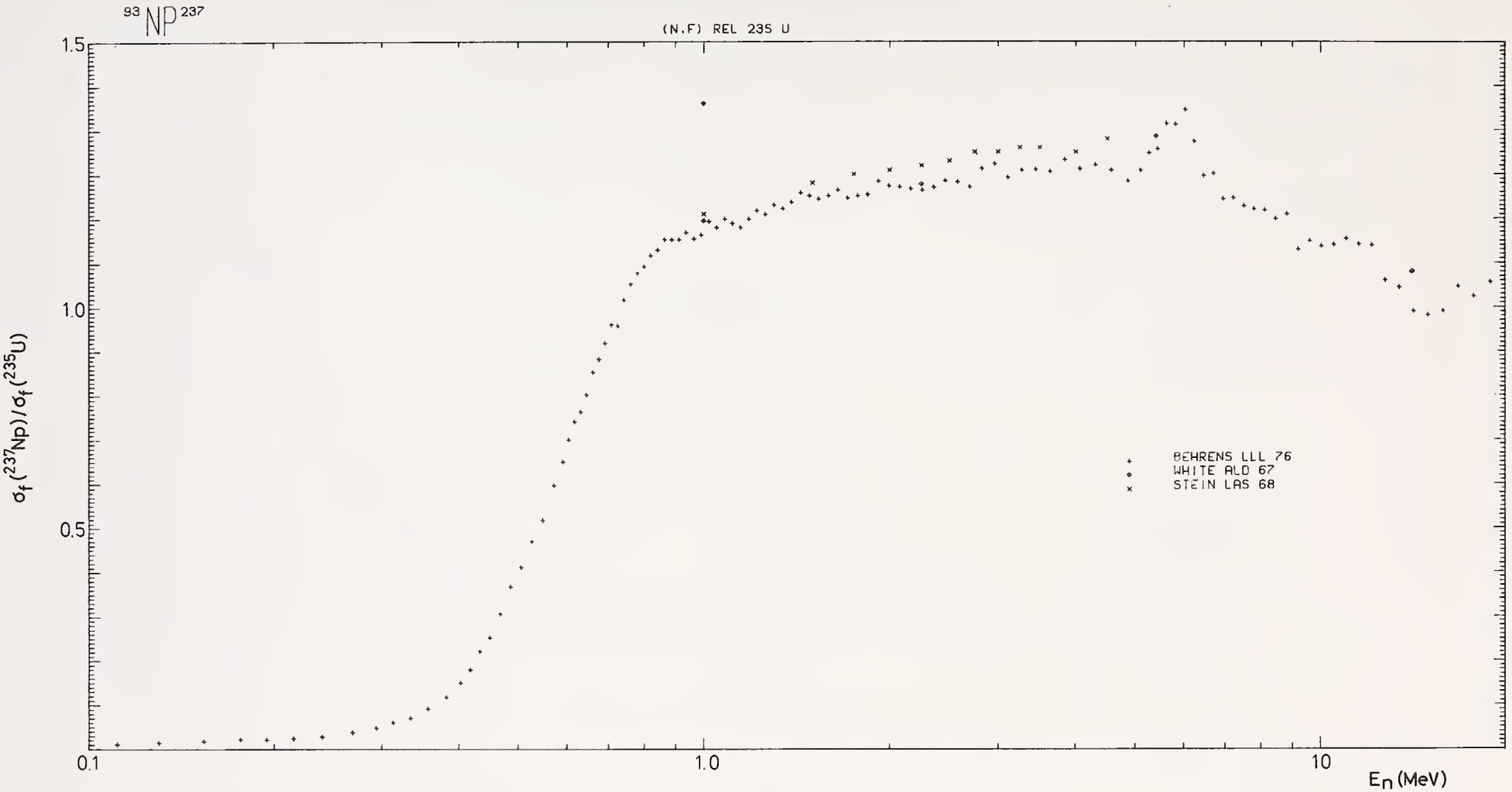

Fig. 7 Fission cross section ratios $^{237}Np/^{235}U$

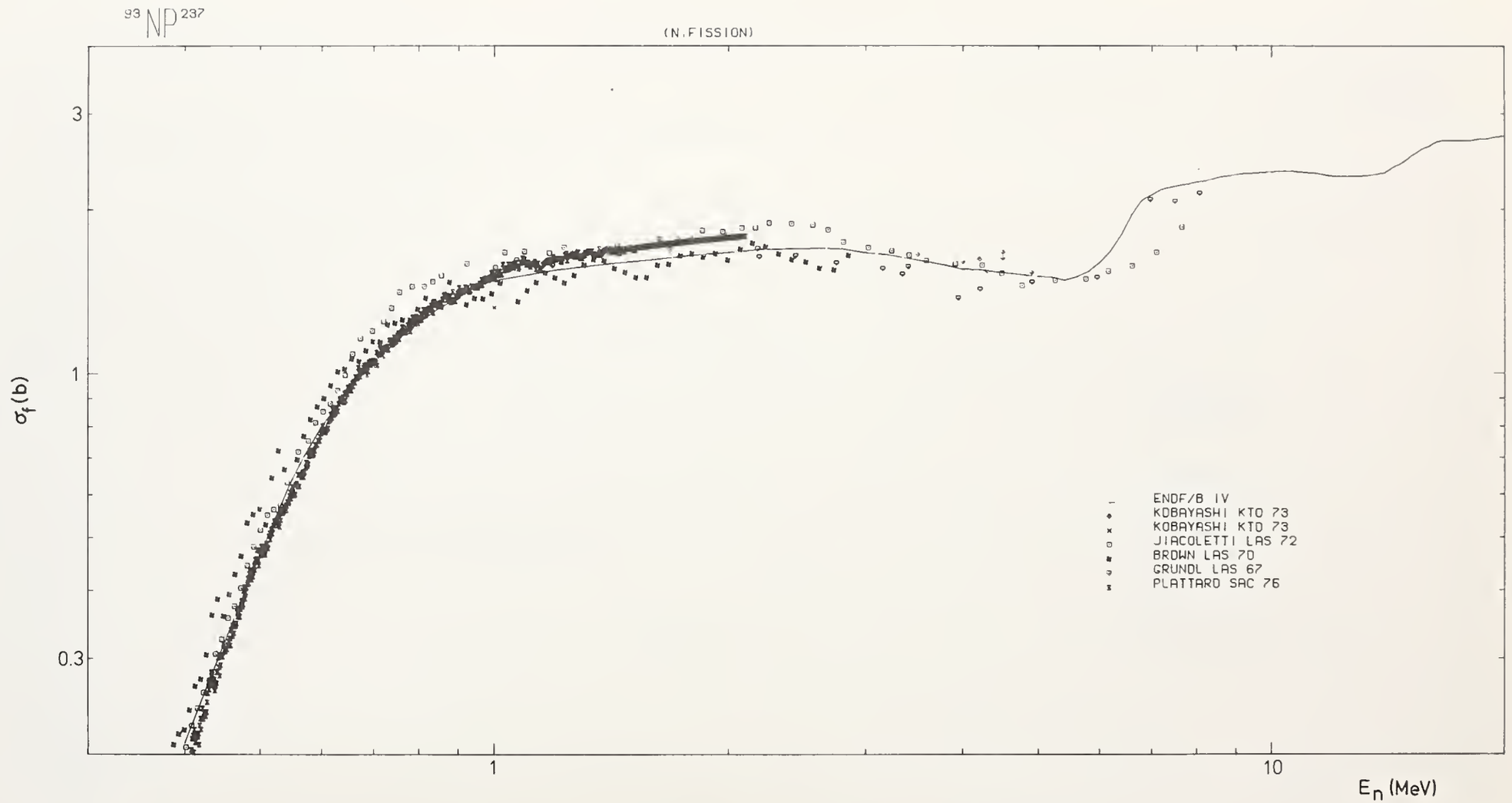

Fig. 8 Fission cross section of ^{237}Np. Comparison of recent measurements

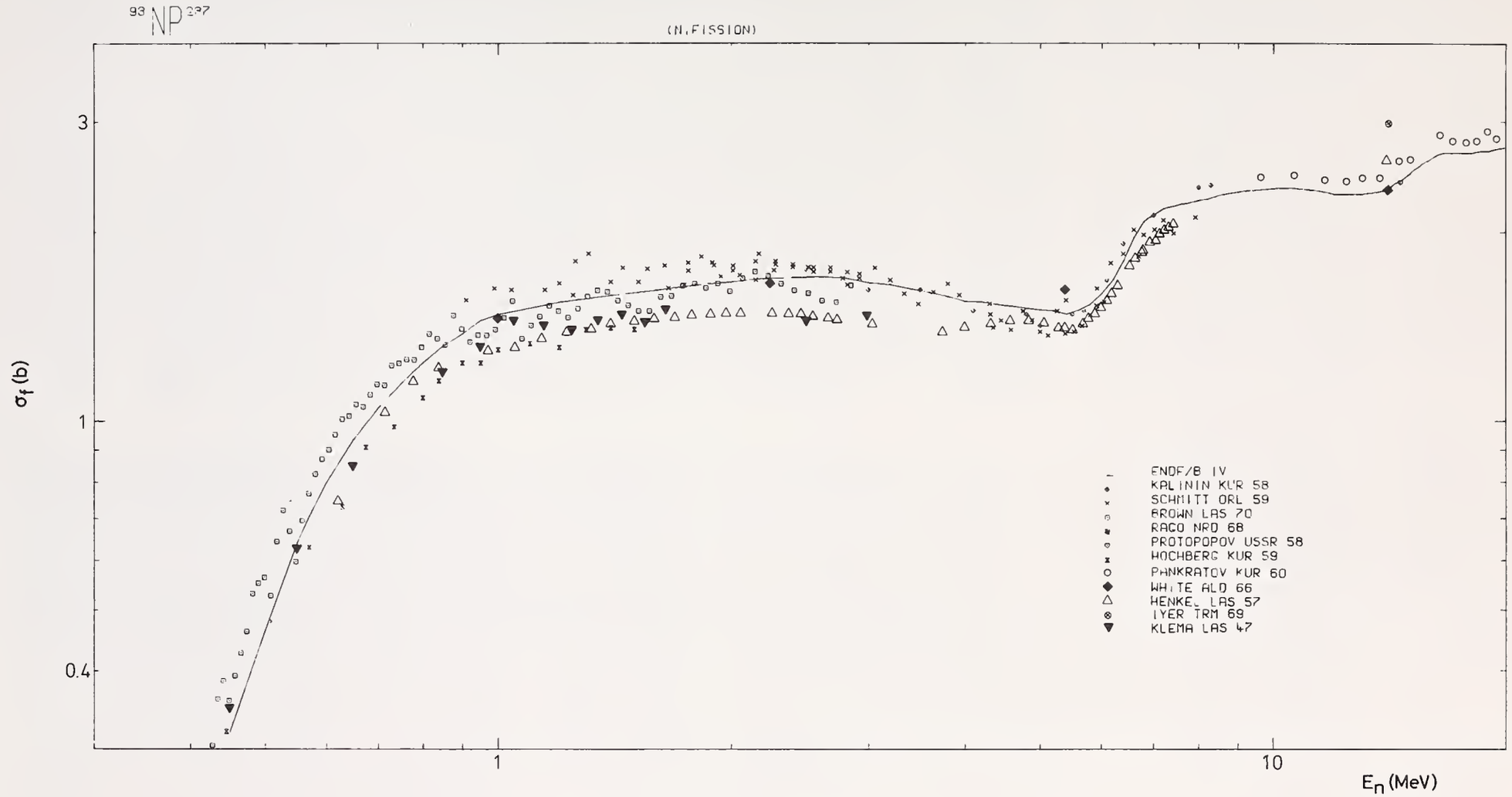

Fig. 9 Fission cross section of ^{237}Np. Comparison with older results

STANDARD INTEGRAL MEASUREMENT FACILITIES

A. Fabry
C.E.N./S.C.K., Mol, B-2400
Belgium

The usefulness of integral measurements in standard and reference neutron fields is examined in terms of the validation of microscopic differential-energy neutron fission cross section standards needed for fission reactor technology. This synthesis encompasses a summary description of the identified neutron fields and of the status of their spectral characterization, discussion of the corrections and uncertainties involved in such experiments, and an appraisal of the accuracy of integral fission cross sections, in particular at the light of interlaboratory comparisons. The significance of such integral measurements to the testing and improvement of evaluated nuclear data is illustrated by a limited confrontation with the ENDF/B IV cross section file.

(Cross sections, ENDF/B, fission, integral measurements, standard neutron fields)

1. Introduction

The aim of this paper is to examine how far integral measurements in standard neutron fields may contribute to obtain accurate microscopic differential-energy neutron fission cross section standards. Other important applications of standard neutron fields to fission reactor technology are discussed elsewhere[1-4]. A standard radiation field is tentatively defined[5] as a permanent, stable and reproducible radiation field (neutron or gamma or mixed) that is characterized to state-of-the-art accuracy in terms of flux intensity and energy spectra, and spatial and angular flux distribution. Important field quantities must be verified by interlaboratory measurement.

The concepts of microscopic and macroscopic integral measurements have been delineated satisfactorily in reference[6]. In particular, a microscopic integral neutron cross section $\bar{\sigma}$ is simply the convolution of a microscopic differential-energy neutron cross section $\sigma(E)$ and of an energy distributed neutron field or spectrum, $\Phi(E)$. All quantities of relevance to the design, operation and safety of nuclear reactors are macroscopic integral ones : critical masses or enrichments, reactivity worths, fuel pin power and burn up, damage in structural-components, ...; all directly relate to integral reaction rates, e.g. microscopic integral cross sections of various types, in different neutron spectra. Because differential-energy neutron cross sections are not known well enough to afford sufficiently accurate predictions of reactor macroscopic properties, it has been current practice to adjust them within their uncertainties[7,8,9,10] so as to match the results of a variety of microscopic and macroscopic integral measurements - critical masses, fission rate ratios, central reactivity worths, material bucklings, ... - performed in zero-power "clean" [11] critical or exponential assemblies and even mock-up[11] of actual reactors. Differential neutron spectrum measurements[12], mostly by time-of-flight, $^{6}Li(n,\alpha)$ and proton recoil techniques, are also done in such "controlled environments" (terminology as defined in[5]); they are sometimes taken into account[13] in the automated cross section adjustment procedures. Neutron spectra are predominantly sensitive to elastic and inelastic scattering cross sections; such nuclear data are often tested in separate neutron spectrometry experiments on simple source-driven one-material macroscopic arrangments[14,15,16].

All in all, this semi-empirical approach leads to adjusted multigroup cross section sets associated to appropriate reactor physics computational codes. It is not generally claimed that such adjusted cross sections are more accurate than unadjusted ones but they have proven successful and necessary in establishing in a timely manner design parameters for specific demonstration power plants such as LMFBRs in the 300 MWe range[17].

In the long term however, the nuclear industry will have to keep a flexible perspective relatively to various competitive reactor and fuel cycle options. Adjusted cross section sets developed in the frame of such specific projects as the LMFBR need thus to be validated for wider applicability; this is because the type of approach briefly evocated above may introduce various fictitious correlations between the many differential nuclear data and the integral observables simultaneously analyzed : though the accuracy of predicted reactor integral quantities is improved, this is likely to result of compensating errors which are propagated in a consistent way. As far as fission cross section standards are concerned, accuracy requirements are and will remain severe, whatever the nuclear strategy. The potential shortcomings of cross section adjustment procedures can in this case be largely alleviated if accurate integral data sensitive only to fission cross sections are considered and given adequate weight. Integral microscopic fission cross section measurements in standard neutron fields serve this purpose. Such measurements provide straightforward, relevant and general integral constraints that must be satisfied by differential data.

In this paper, standard neutron fields are identified, the status of their spectral characterization is briefly discussed as well as the quality of integral fission cross section measurements.

Some ratios of integral fission cross sections are largely insensitive to neutron spectral shapes and can be considered as standard integral observables, even if not obtained in standard neutron fields : this review consequently encompasses also some reference[5] neutron fields less well characterized than the standard ones. Finally a quick outlook at selected integral results in the various considered facilities reveals a few interesting trends relatively to the ENDF/B IV cross section file.

2. Identification of Standard Neutron Fields

The definition of standard neutron fields given in the introduction does not specify what is meant by a state-of-the-art accuracy characterization in terms of the space, angle and energy dependent absolute flux spectrum $\Phi(E, \vec{r}, \vec{\Omega})$[a]. To a large degree, this vague qualification stems from the fact that the accuracy level at which a neutron field may be considered as a standard depends on the application and energy range considered.

For instance, if the field is used to calibrate or validate an instrument aimed at measuring scalar reactor neutron spectra with an energy resolution of 5% to a requested accuracy of ± 5% in the energy range 10 keV - 1 MeV, there is no need for the standard to be characterized much better than according to these specifications; in this example nevertheless, the accuracy of the flux spectrum above 1 MeV and below 10 keV should be sufficient to allow adequate corrections for the eventual sensitivity of the instrument to higher and lower energy neutrons; furthermore, the gamma dose to neutron flux ratio should not be excessive (typically, 10^{-6} rad $hr^{-1}/cm^{-2}sec^{-1}$ constitutes an upper bound). Thus, a number of more or less subtle considerations are involved in deciding whether a particular permanent, stable and reproducible neutron field is indeed a standard in terms of a given application.

For the integral testing and potential improvement of differential-energy cross sections, it is the shapes of the cross sections and of the flux spectrum as a function of energy that determine the sensitivity of the integral cross sections to flux spectral uncertainties. The less rapid is the variation of a cross section, or flux spectrum, or both, with energy over the reaction response range (e.g. over the energy range contributing to 90% or so of the reaction rate) and the less stringent is the accuracy with which the spectral shape must be known. Although a ± 1 - 2% accuracy goal for differential-energy fission cross sections means as well a ± 1 - 2% target for the integral fission rate measurements and for the determination of the total absolute flux in the standard neutron fields, the corresponding needed accuracy for the flux spectral characterization is generally much less severe, of the order of ± 5% over the energy response range; this is still a difficult target to meet, but it is manageable provided the standard flux spectrum displays little or no energy structure. A neutron field can thus be standard relatively to a given type of nuclear reaction and not relatively to another : for example, the thermal-neutron induced uranium-235 fission neutron spectrum is presently a standard for the validation of fission cross sections, but it is not for the validation of (n, 2n) cross sections of relevance to fusion reactor technology.

In the context of this paper - fission cross section standards needed for fission reactor technology - five types of neutron fields only have been identified as standard.

They are, in order of decreasing spectral average energy :

1. the californium-252 spontaneous fission neutron spectrum χ_{82}
2. the thermal-neutron induced uranium-235 fission neutron spectrum, χ_{25}
3. the intermediate energy standard neutron fields, ISNF, a family of boron-10 tailored, carbon moderated neutron spectra driven by fission neutrons ; the spectral hardness is variable within some limited energy range and the gross spectral shapes are comparable to LMFBRs
4. 1/E or near $^1/E$ shape neutron spectra
5. Maxwellian thermal neutron spectra

3. Appraisal of Standard Neutron Fields

Californium-252 Fission Spectrum Facilities

Intense spontaneous fission sources of ^{252}Cf provide a close approximation to an isolated point neutron source. Typically, this involves simply a small aluminium-steel capsule containing a few mgr of $Cf_2O_2SO_4$ and associated, lightweight detecting instruments suspended in a low scatter environment (a large room or outdoor). Such facilities have been developed in recent years by a few laboratories, most noticeably NBS (USA)[18], PTB (Germany)[19] and IEP (Hungary)[20]. Integral fission cross section measurements in the ^{252}Cf fission neutron spectrum have been performed at NBS[21,22] to an accuracy level suitable for standard integral data.

The absolute source strength is determined to ± 1 %[b] by total absorption techniques (the manganese sulfate bath at NBS) ; current international comparisons of ^{252}Cf source strengths support so far this accuracy assessment. The total absolute free field neutron flux intensity at carefully established distances from such source is deemed known to within ± 1.4 %.
The error component due to distance assessment is typically as low as ± 0.6 % ; this is achieved[18] by simultaneous exposure of two nearly identical detectors on opposite sides of, and equidistant from, the source : the first-order distance error is then associated with the separation of the detectors. The maximum error component related to intrinsic neutron field perturbation by scattering in the source capsule and supports is ± 0.7 %.

(a) In all neutron fields discussed in this paper, $\Phi(E, \vec{r}, \vec{\Omega})$ is separable and space-angle variations are well understood.

(b) All uncertainties in this paper are quoted for a 68.3 % confidence interval (1σ).

The fraction of the neutrons that undergo one inelastic scatter in the source capsule is indeed as low as (0.7 ± 0.3) %.
The only other component of error in such measurements relates to neutron return from the environment : albedo from boundaries, irradiation support structures, source capsule and air scatter. These corrections and their uncertainties are very small : for a source-to-detector distance of 5 cm, (1.4 ± 0.6) % for ^{235}U fission with cadmium enclosure and (0.4 ± 0.7) % for ^{238}U fission.
The uncertainties in the determination of absolute fission rates themselves are discussed in a subsequent section.
Integral fission cross sections in the ^{252}Cf fission neutron spectrum are reported with an overall combined uncertainty of ± 2.2 - 2.8 %, depending on the isotope.

The spectral characterization of the californium-252 spontaneous fission neutron spectrum is excellent over the bulk of the energy range. A recent evaluation[23] of eight documented spectrometry measurements indicates an accuracy of ± 1 to 2 % between 250 keV and 8 MeV. This is by far the best known distributed energy neutron field to-day. If spectral uncertainties are weighted by differential-energy cross sections, they can be expressed as uncertainty components of the corresponding integral cross sections : for ^{235}U and ^{238}U fission, these components are 0.24 % and 0.95 % respectively[23]. This is a satisfactory situation from the viewpoint of the differential-energy fission cross section validation by integral measurements.

Uranium-235 Fission Spectrum Facilities

Integral cross section measurements in the thermal neutron induced uranium-235 fission neutron spectrum represent an effort covering almost two decades [6,24,25,26], but few fission cross section data have been reported and most of them are ratios. This is because the generation of pure uranium-235 fission neutron spectra is not straightforward and the determination of the absolute flux is difficult.
Four facilities are in operation to-day : at KYOTO University (Japan)[27], LJUBLANA (Yugoslavia)[28], NBS (USA)[29] and CEN-SCK (Belgium)[30]. Background responses in the two first ones prevent their application to non-threshold fission cross section work. The CEN-SCK facility is the most versatile and extensively investigated one ; it will thus be briefly discussed.

This facility involves a one-meter diameter spherical cavity within the vertical graphite thermal column of the BR1 reactor at MOL. Two types of arrangments have been developed to produce fission neutron spectra :

1. central coaxial source disc assemblies[31] for passive measurements (solid state track recorders, activation foils) : two bare discs of ^{235}U, typically diameter 19 x 0.1 mm, surround coaxially a cadmium box containing the samples to be exposed (Fig. 1) ; this type of arrangment is also used at NBS (30 cm diameter graphite cavity)
2. central cylindrical source shell[30] concentric to an extruded cadmium sleeve extending from

TABLE I. CORRECTION FACTORS FOR BACKGROUND RESPONSES AND NEUTRON FIELD PERTURBATIONS IN THE CAVITY URANIUM-235 FISSION SPECTRUM NEUTRON FIELD MEASUREMENTS : STANDARD CYLINDRICAL SOURCE SHELL

TYPE OF CORRECTION	NUCLIDE						TYPICAL ASSOCIATED UNCERTAINTY
	^{235}U	^{233}U	^{239}Pu	^{241}Pu	^{237}Np	^{238}U	
Wall return background	0.8636	0.7810	0.8923	0.7995	0.9975	0.9978	± 0.1 to ± 0.3 %
Photofission, epithermal and thermal neutron penetration	0.9907	0.9939	0.9840	0.9939	0.9967	0.9935	± 0.1 %
Impurity isotopes[(a)]	0.999	0.997	0.999	1.000	1.000	0.998	± 0.1 %
Cadmium sleeve perturbation	0.991	0.991	0.991	0.991	1.001	1.010	± 1.0 %
Instrumental perturbation	1.000	1.000	1.000	1.000	1.003	1.006	± 0.3 %
Net correction	0.8472	0.7668	0.8693	0.7875	0.9982	1.0056	± 1.05 % to ± 1.10 %

[(a)] For typical fissionable deposits

cavity bottom to reactor top : this allows fission rate traverses with a variety of active (fission chambers) and passive detectors.

Arrangement 1 is currently applied for absolute cross section measurements. The source strength is derived[27] from ^{140}Ba-^{140}La absolute radiometric counting of the uranium-235 discs, using literature values for the fission yield and the number of neutrons per fission ; the accuracy is of ± 2 %. The flux follows by straighforward geometry calculations[32]. This arrangement has been chosen for international radiometric integral fission cross section measurements for ^{235}U and ^{238}U. Selected high quality sources and samples will be assembled and exposed at CEN-SCK by end 1977, will be transferred to IAEA for dismantling, inspection and geometry control, and will be subsequently shipped for counting by various laboratories in Europe, the U.S. and Japan.

Table I presents, for the standard cylindrical source shell (diameter 33 x 77 x 0.1 mm ^{235}U) in arrangement 2, an inventory of all corrections an uncertainties involved in cross section measurements for six important fissionable isotopes[33] (excluding uncertainties in the determination of absolute fission rates, to be discussed separately). The dominating correction is for non-threshold reactions and relates to the background responses to neutrons returning from the cavity walls ; these fractional responses, of 15 to 20 % in the table, can be varied easily by modifying the diameter and height of the shell source, in a range as large as from 2 % (using miniature fission chambers[30]) to 100 %. These responses can be measured directly by moving the instruments from cavity center up to half its radius : this is because the fission flux decays rapidly with distance to the source while the cavity wall return neutron flux in the energy range of response for non-threshold fissionable isotopes (< 1 keV) displays the remarkable property of a relatively great space-angle uniformity[34]. Indeed, the return neutron spatial and angular distribution within the cavity would be perfectly flat if the angular flux at the vacuum-moderator boundary was perfectly isotropic. The actual patterns can be parametrically vizualized by considering the reciprocal configuration : a central point detector and a source shell of increasing radius R_s in a cavity of arbitrary radius R_c. Figure 2 displays the relative central wall return neutron flux ratio $\phi_w(\bar{E}, \rho_s)/\phi_w(\bar{E},0)$ as a function of the reduced source radius $\rho_s = R_s/R_c$ for three cavity sizes and various neutron energy groups of approximate mid energy E.

The short history of neutron cross section technology presents here an amusing paradox : years ago, measurers of differential-energy cross sections, alert to struggle with room return neutrons in their experiments, tended to feel that integral measurers applying fission neutron sources in moderating cavities might well mishandle their corrections for wall return backgrounds ; to-day, integral measurers do not hesitate to use such background neutrons as one of the primary spectral components of intermediate-energy standard neutron fields, as outlined in the next section. The dominating uncertainties of the corrections needed in ^{235}U fission spectrum integral experiments are actually the ones due to intrinsic neutron field perturbation by the materials close to the source and detectors, as shown by Table I.

The spectral characterization of the ^{235}U thermal fission neutron spectrum is not comparable in quality to the californium case. The previously considered evaluation[23] of spectrometry data lists uncertainties of ± 3 % to ± 5 % in the energy range 250 keV - 8 MeV, and these propagate into computed integral cross section errors of 0.24 % and 1.7 % for ^{235}U and ^{238}U fission respectively, e.g. about twice the ^{252}Cf error for ^{238}U fission. This evaluation however does not include finite sample size corrections which are important in some spectrometry experiments[35]. Although the long-standing inconsistencies[6] between differential and integral data in the thermal neutron induced ^{235}U and ^{239}Pu fission neutron spectra tend to be generally resolved[25], there are still some discrepancies affecting nuclear reactions of importance to reactor dosimetry. These suggest[26,36,37] a slightly harder ^{235}U fission spectrum than presently evaluated[23] and close to the fits of pulsed Van de Graaffs spectrometry measurements[35]. Nevertheless, the impact of these differences is small insofar as the validation of fission cross sections is concerned and χ_{25} may be considered a good standard to this particular respect ; the fact that it is a less accurate standard than χ_{82} is balanced by its greater practical importance as basic source of neutrons in chain reacting systems, an argument whose weight is obvious at the light of the introductory section.

Intermediate-energy Standard Neutron Fields

The concept of primary intermediate-energy standard neutron field, contemplated since about a decade, has become reality in 1976 only when the ISNF-1 assembly was put into operation at NBS (USA), as the result of a cooperation between NBS, CEN-SCK (Belgium) and LOS ALAMOS SCIENTIFIC LABORATORY (USA). The first ISNF fission cross section measurements are reported at this conference[38] ; the NBS-ISNF facility is also described and analyzed to some extent[39]. In this section, a brief and somewhat general discussion of the concept and its physics is done.

ISNF does not designate a specific standard neutron field, but a family of standards derived from the same fundamental principle : controlled moderation and absorption of fission spectrum neutrons in a one-dimensional macroscopic arrangment of materials with differential-energy cross sections known to the accuracy of primary standards - at least over the energy range where they significantly participate to the mechanisms of spectral generation. The last condition is crucial to the definition of primary intermediate-energy standard neutron fields, as opposed to secondary ones[2] (exemplified by ΣΣ). This condition bears upon a theoretical predictability argument : it is required that the ISNF space, angle and energy neutron flux density be fully and accurately characterized by solution of the stationary Boltzmann linear integro-differential transport equation ; neutron spectrometry techniques are consequently not mandatory for spectral characterization purposes, but can be validated usefully by measurements in the ISNF and contribute to the certification of the fields. Other conditions of ISNF definition such as adequate simulation of LMFBR neutron spectra, reproducibility, ... are outlined elsewhere[2]. A parametric investigation has resulted into some specialization of the concept : selection of boron-10 and carbon as major

material constituants of the systems, and restriction to the class of spherical geometry arrangements specified by Fig. 3. Thus the ISNF fields involve a fission spectrum source shell of radius R_S concentric to a boron-10 shell (the absorber) of outer radius R_A ($< R_S$) and thickness χ_A ($\ll R_A$), centered in a spherical cavity of radius R_C within a graphite moderator (the reflector).

In practice, the infinite reflector thickness is 50 cm, but 35 cm is satisfactory for most applications, and the source shell can be replaced by a few adequately distributed point sources, either thin uranium-235 discs driven by thermal neutrons or californium-252 capsules.

As illustrated by Fig. 4, ISNF neutron fluxes (full line) are formed as the superposition of fission neutrons (dotted line) and cavity wall return neutrons (dashed line minus dotted line, not shown) tailored by the boron-10 absorber. This superposition can be formulated semi-analytically in terms of reduced radii and thicknesses $\rho_A = R_A/R_C$, $\rho_S = R_S/R_C$ and $\delta_A = \chi_A/R_C$. Consider first a configuration in which the boron shell is replaced by a thin cadmium absorber, the so-called ISNF/CV standard field[3]. The central scalar neutron flux spectrum $\Phi(E,\rho_S,R_C)$ for a fission shell source of unit total strength may be expressed as :

$$4\pi R_C^2\,\Phi(E,\rho_S,R_C) = \frac{\chi(E)}{\rho_S^2} + \left[\varphi_W(E,R_C)\,g(E,\rho_S)\frac{\Psi_o}{(1+\lambda/R_C)^2}\right]$$

where $\chi(E)$ is the normalized fission spectrum, $\varphi_W(E,R_C)$ is the wall return neutron flux spectrum for a central point fission source in a cavity of radius R_C normalized so that $\int_{0.5eV}^{\infty}\varphi_W(E,R_C)dE = 1$ and the function $g(E,\rho_S)$ is displayed on figure 2. The constant Ψ_o and the relaxation length λ are characteristic of the moderator (11.37 and 8.75 cm respectively for carbon). This equation quantifies the superposition of an uncollided source spectrum and the collided component associated to the reflector, these two basic spectral shapes being weighted by the intensity scaling factors $1/\rho_S^2$ and $\Psi_o/(1+\lambda/R_C)^2$. This relates the ISNF to the properties of carbon wall return neutrons, which are accurately predictable by discrete-ordinates transport theory approximations[34] and MONTE CARLO methods. The parametric survey calculations for the ISNF have shown that detailed design criteria are optimized if $\rho_S \simeq 1$ and $\rho_A/\rho_S \leq 0.5$. Under these conditions, insertion of the boron-10 absorber modifies the above equation as follows :

$$4\pi R_C^2\,\Phi(E,\rho_S,\rho_A,\delta_A,R_C) = \left[\frac{\chi(E)}{\rho_S^2}\right] T_A^{\infty}(\delta_A) + \left[\varphi_W(E,R_C)\,g(E,\rho_S)\frac{\Psi_o}{(1+\lambda/R_C)^2}\right] T_A^{\infty}(E,\delta_A)\,C_{AS}\left(\frac{\rho_A}{\rho_S}\right)\,C_{AR}(\rho_A,T_A^{\infty}(E,\delta_A))$$

The function $T_A^{\infty}(E,\delta_A)$ is the intrinsic neutron transmission of the boron-10 shell in infinite vacuum ; deep physical insight has been brought into this type of macroscopic neutron interaction by the famous analytical work of Bethe, Beyster and Carter[40]. It is this tailoring exponential-like term that drastically shapes the neutron spectrum at intermediate and low energies while the other terms essentially result in relatively small rescalings of the intensity factors for the two superposed spectral components as identified by the previous equation. For the uncollided flux, the rescaling is a transmission factor $T_A^{\infty}(\delta_A) \simeq 0.97$, almost energy-independent from a practical standpoint. For the collided flux, the rescaling involves two coupling functions : a) the source-absorber coupling $C_{AS}(\rho_A/\rho_S) = 0.99$ to 1.0 for $\rho_A/\rho_S = 0.5$ to zero : this is a simple shadowing effect related to the decrease of the first collision source density in the carbon wall caused by the intensity rescaling of the uncollided flux ; b) the absorber-reflector coupling $C_{AR}(\rho_A,T_A^{\infty}(E,\delta_A))$, that varies smoothly with energy between ~ 0.7 and unity, depending on ρ_A (for $\rho_A \leq 0.15$, the deviation from unity is less than 5 % over the whole energy range); this expresses the fact that the probability of neutron absorption by the boron-10 shell is enhanced by multiple cavity crossings of the collided component neutrons ; this may also be seen as a shadowing effect, but the important point is that it is governed by the intrinsic shell transmission itself.

Summarizing, the ISNF physics is dominated by simple and well understood mechanisms acting in a largely decoupled way and amenable to almost textbook formulation : streaming of virgin fission neutrons in vacuum, reflective scattering of neutrons from a point source at the center of a spherical moderating cavity and transmission of neutrons by a spherical absorbing shell.

1/E and near 1/E Standard Neutron Fields

The slowing-down of fission neutrons from point sources homogeneously distributed in a non-absorbing infinite moderator generates a collided neutron spectral flux that varies as the inverse of the neutron energy above the thermalization range. Such idealized way of creating 1/E neutron fields has unfortunately no direct implementation able to compete with californium facilities when they meet the challenge of materializing a free field point source fission flux ! Measurers of resonance integrals, e.g. of $\int_{E_C}^{\infty}\sigma(E)\frac{dE}{E}$, not only have to be careful in assessing what their cadmium cut-off energy E_C actually is[41], how accurate their neutron self-shielding corrections are - to list only two major uncertainty components - but most importantly, they have to ascertain that their integral measurements are indeed performed in a pure 1/E standard field, e.g. place realistic bounds on errors due to spectral shape deviations from the ideal law. Such deviations may be small, but it does not matter if they are not, provided they are accurately known. Carbon cavity wall return neutron flux spectra do not obey the 1/E law, but generally speaking, and most certainly in terms of integral fission cross sections, the deviations are excessively well known, e.g. ISNF/CV type fields as defined in the previous section are relevant. They do not seem necessary from the standpoint of this review because fission resonance integrals[42] are usually considered as well known for standard isotopes and they also agree generally with differential data. This section could thus have been limited to such statement. But even keeping out of mind the various technological applications of ISNF/CV standard fields, it seems valuable to report here the integral-versus-differential cross section comparison displayed in Table II ; $\bar{\sigma}_\chi$ and σ_W denote cross sections averaged over the spectra

TABLE II. $\bar{\sigma}_W/\bar{\sigma}_\chi$: INTEGRAL CROSS SECTION RATIO FOR FISSION BY GRAPHITE WALL RETURN(*) AND URANIUM-235 FISSION SPECTRUM NEUTRONS

NUCLIDE	MEASURED	COMPUTED	DIFFERENCE
^{235}U	9.07(± 4%)	9.37	- 3.3 %
^{239}Pu	6.93(± 4%)	6.67	+ 3.9 %
^{233}U	16.1 (± 5%)	15.9	+ 1.3 %
^{241}Pu	14.4 (± 5%)	14.8	- 2.8 %

(*) 1 meter spherical cavity, central fission source

$\chi(E)$ and $\varphi_W(E,R_C)$ entering the ISNF equations, previous section. The measured integral data are the by-product of a careful fission spectrum average cross section study[33], and state-of-the art accuracy was consequently not searched for, so that error estimates are largely conservative. The confrontation is most gratifying.

Thermal Maxwellian Standard Neutron Fields

Maxwellian thermal neutron spectra in moderators have been used extensively to measure microscopic integral fission cross sections. The data have been compiled and evaluated[43]. They can be expressed as the product $g_f(T)\sigma_{f_o}$ of the 2200 m/sec fission cross section σ_{f_o} and the Westcott $g_f(T)$ factor, equal to $\int_o^\infty \sigma_f(E)(\sqrt{E}/\sqrt{E_o})$ $M(E,T)dE$ where E_o = 0.0253 eV and $M(E,T)$ is a Maxwellian distribution of temperature T (usually 20° C).

Comparisons of integral versus differential $g_f(T)\sigma_{f_o}$ values reveal consistency within mutual uncertainties for ^{233}U (~ 0.8 %), ^{239}Pu (~ 0.6 %) and ^{241}Pu (~ 0.9 %), but an unexplained bias of 1.5 % for ^{235}U, outside of experimental errors of 0.4 to 0.7 %.

Maxwellian thermal neutron spectra are often used for normalization of integral fission cross section ratio measurements in other neutron fields. Not surprisingly, a critical source of uncertainty in such procedure lies in the thermal field flux spectral characterization : this can be achieved by chopper time-of-flight measurements, spectral index comparisons to monochromatic beams (using lutetium, europium and dysprosium activation foils) and by transport theory computations.

4. Accuracy of Integral Fission Rate Measurements

Differential and integral measurers of microscopic fission cross sections face the same stringent accuracy requirements and very similar difficulties regarding a major component of their experiments : the determination of absolute fission rates and of their uncertainties. Careful experimenters apply independent approaches at the two major steps, mass assay of fissionable deposits and detection of the fission events. Nevertheless, interlaboratory comparisons are and will remain of utmost importance to realistically assess the uncertainties. It must be regretted that such comparisons have generally not brought together the differential and integral communities, who seem to more or less ignore each other - but not always[44] fortunately - to this very practical respect. Interlaboratory comparisons of fission rate measurements have been organized from time to time by integral experimenters, usually for specific programmatic reasons. The most ancient and extensive effort of this type, reported in 1966, involved the Idaho Division of Argonne National Laboratory, the Zebra reactor group at Winfrith, the Vera team at Aldermaston, the Los Alamos fast criticals group and, to a modest extent, the Cadarache fast reactor group ; most of the measurements have been done in ZEBRA and FLATTOP-25 using parallel plate fission chambers ; the isotopes were ^{233}U, ^{235}U, ^{238}U and ^{239}Pu. Another exercice of this type took place in the frame of the SCHERZO 556 unit k-infinity lattice benchmark[45] realized at Winfrith, Karlsruhe, Fontenay and Cadarache, but this was limited to the $^{238}U/^{235}U$ fission rate ratio. More recently, the Karlsruhe, Petten, Mol and NBS groups have published[46] the results of intercomparisons performed in the MOL-ΣΣ secondary standard neutron field[2] and encompassing the absolute fission rate of ^{235}U, ^{239}Pu, ^{238}U and ^{237}Np ; further data have been obtained since, including for higher plutonium isotopes, and the $^{239}Pu/^{235}U$ fission rate results have been updated as shown in Table III. In general, it seems that integral measurers may be conservative in their error estimates. The combined interlaboratory uncertainties are quoted[46] as ± 1.3 %, ± 1.6 % and ± 1.8 % for the absolute fission rates of ^{235}U, ^{238}U and ^{239}Pu in ΣΣ, which is consistent with the estimates[48] of the US Interlaboratory LMFBR Reaction Rate (ILRR) program[4], but further, currently planned intercomparison work and on-going mass assay efforts may well lead to the conviction that the actual uncertainties are rather of the order of ± 1 %.

TABLE III. INTERCOMPARISON OF ^{239}Pu to ^{235}U FISSION RATE RATIO MEASUREMENTS IN THE MOL-ΣΣ FACILITY

Laboratory	$^{239}Pu/^{235}U$ (a)	Departure from recommendation(b)
Petten[46]	1.162(.7/1.8)	- 0.4 %
Karlsruhe[46]	1.161(.5/1.5)	- 0.5 %
Karlsruhe, mass renormalized[47]	1.169(.5/1.5)	+ 0.2 %
NBS-MOL[46]	1.178(.5/2.0)	+ 0.9 %
Mol[33]	1.173(.6/1.5)	+ 0.5 %

(a) Number in parentheses are respectively the random and systematic errors in percent

(b) 1.167(± 2 %)

TABLE IV. INTEGRAL TESTING OF ENDF/BIV : FUNDAMENTAL FISSION CROSS SECTION RATIOS IN STANDARD AND REFERENCE NEUTRON FIELDS

NEUTRON FIELD	$\frac{^{239}Pu(n,f)}{^{235}U(n,f)}$		$\frac{^{237}Np(n,f)}{^{238}U(n,f)}$		$\frac{^{235}U(n,f)}{^{238}U(n,f)}$		$\frac{^{239}Pu(n,f)}{^{238}U(n,f)}$
	MEASURED[d]	MEASURED / COMPUTED	MEASURED[d]	MEASURED / COMPUTED	MEASURED[d]	MEASURED / COMPUTED	MEASURED / COMPUTED
λ_{82}[a]	1.500 (±1.6%)	1.040	4.16 (±2.5%)	0.972	3.76 (±1.7%)	0.955	0.993
λ_{25}[a]	1.505 (±2.2%)	1.049	4.30 (±3.0%)	0.964	3.94 (±2.0%)	0.939	0.985
JEZEBEL[b]	1.49 (±5.0%)[f]	1.068	4.59 (±3.0%)[e]	0.950	4.74 (±3.2%)[e]	0.917	0.980
GODIVA[b]	1.42 (±5.0%)[f]	1.030	5.19 (±3.0%)[e]	0.985	6.21 (±3.2%)[e]	1.033	1.064
$\Sigma\Sigma$[c]	1.167 (±2.0%)	1.025	6.92 (±2.5%)	(0.926)[g]	17.8 (±1.5%)	0.948	0.972
CFRMF[b]	1.145 (±1.5%)	1.025	7.29 (±2.3%)	0.967	20.6 (±1.4%)	0.993	1.018
BIG-10[b]	1.199 (±1.5%)	1.023	8.52 (±2.3%)	0.965	26.8 (±1.7%)	1.014	1.037

(a) $\phi(E)$ for computation : NBS evaluation[23]

(b) $\phi(E)$ for computation : transport theory, ENDF/B-IV cross sections

(c) $\phi(E)$ for computation : reference[2]

(d) All experimental data taken from reference[37], unless otherwise indicated

(e) Reference[49]. The data relate to monoenergetic calibrations at ~ 2.5 MeV where absolute ratio measurements were performed for the normalization ; they are backed by interlaboratory comparisons in Flattop[44]

(f) Reference[50]

(g) In the energy range of major response, the neutron spectrum is to be significantly revised

5. Integral data testing of selected ENDF/BIV fission cross sections

The $^{239}Pu/^{235}U$ fission cross section ratio belongs to the category of data qualified in section 1 of standard observables for reference neutron fields. This is maybe true also for the $^{237}Np/^{238}U$ ratio, but not for the $^{235}U/^{238}U$ ratio. Nevertheless, all three ratios are gathered in Table IV for an array of standard and reference neutron fields ; the Los Alamos bare metal critical spheres GODIVA and JEZEBEL are well known and the other reference fields[4] are the ones investigated by the already mentionned ILRR program. The ENDF/BIV cross section file was used to obtain the computed integral values. This table represents a state-of-the art confrontation between differential and integral fundamental fission cross section data and illustrates clearly the major and most interesting trends. This deserves an extensive discussion which lies outside the scope of the present paper.

References

1. A. FABRY, P. VANDEPLAS - Fast Reactor Physics I, 389, IAEA (1968)
2. A. FABRY, G. and S. DE LEEUW - Nucl. Techn. 25, 349 (1975)
3. J.A. GRUNDL, C. EISENHAUER - "Benchmark Neutron Fields for Reactor Dosimetry" in IAEA Consultants' Meeting on Integral Cross Section Measurements in Standard Neutron Fields for Reactor Neutron Dosimetry, November 15-19 (1976)
4. W.N. McELROY et al. - Special Issue, Nucl. Techn. 25 n° 2 (Feb. 1975)
5. J.A. GRUNDL, A. FABRY - "Report of Workshop Session on Reactor Dosimetry Benchmarks" in First ASTM-EURATOM Symp. on Reactor Dosimetry, Petten, Netherlands (1975)
6. J.A. GRUNDL - Proc. Symp. on Neutron Standards and Flux Normalization, p. 417, Conf-701002 (1971)
7. The Physics of Fast Reactor Operation and Design, Proc. Int. Conf. BNES, June 24-26 (1969)
8. Proc. IAEA Helsinki Conf. "Nuclear Data for Reactors" (1970)
9. Third Conf. Neutron Cross Sections and Technology, CONF-710301 (1971)
10. Proc. Int. Symp. on Physics of Fast Reactors, Tokyo, October 16-19 (1973)
11. W.G. DAVEY, W.C. REDMAN - Techniques in Fast Reactor Critical Experiments. Gordon and Breach Science Publ.
12. Y.A. KAZANSKIJ, A.A. VAN'KOV, E.I. INYUTIN - Atom. En. Rev. 13, 807 (1975)

13. E.D. PENDLEBURY - CONF-710301, p. 1 (1971)

14. A. PARVEZ, M. BECKER - Nucl. Sci. Eng. 62, 571 (1977)

15. G. and S. DE LEEUW - in Report BLG 495, p.1-44 (1974)

16. H. BLUHM, G. FIEG, H. WERLE - Nucl. Sci. Eng. 54, 300 (1974)

17. J.L. ROWLANDS et al. - ibid. 10, 1133

18. J.A. GRUNDL et al. - Nucl. Techn. 32, 315 (1977)

19. W.G. ALBERTS et al. - NBS Spec. Publ. 425, I, 273 (1975)

20. M. BUCZKO et al. - Int. Symp. on Californium-252 Utilization, Paris, April 26-28 (1976)

21. H.T. HEATON II et al. - NBS Spec. Publ. 425, I, 266 (1975)

22. D.M. GILLIAM et al. - NBS Spec. Publ. 425, I, 270 (1975)

23. J.A. GRUNDL, C. EISENHAUER - NBS Spec. Publ. 425, I, 250 (1975)

24. A. FABRY - Report BLG 465 (1972)

25. A. FABRY - Report NEACRP-L-140, also in AERE-R8636 (1977)

26. A. FABRY et al. - "Reactor Dosimetry Integral Reaction Rate Data in LMFBR Benchmark and Standard Neutron Fields : Status, Accuracy and Implications" ibid. 5

27. I. KIMURA et al. - J. Nucl. Sci. Tech. 10, 574 (1973)

28. M. NAJZER et al. - Proc. Conf. Nuclear Data for Reactors, II, 571 (1970)

29. J.A. GRUNDL - Proc. of "Prompt Fission Neutron Spectra" p. 107, IAEA (1972)

30. A. FABRY, J.A. GRUNDL, C. EISENHAUER - NBS Spec. Publ. 425, I, 254 (1975)

31. A. FABRY, K.H.CZOCK - Report IAEA/RL/27 (1974)

32. J.A. GRUNDL - Nucl. Sci. Eng. 31, 191 (1968)

33. A. FABRY, I. GIRLEA - "Quality control and calibration of miniature fission chambers by exposure to standard neutron fields. Application to the measurement of fundamental integral cross section ratios" ibid. 3

34. A. FABRY, J.D. JENKINS - Trans. ANS 15, 940 (1972)

35. J.M. ADAMS - "Comparison of ^{235}U and ^{239}Pu Fast Neutron Fission Spectra" Appendix A in AERE-R8636 (1977)

36. M.F. VLASOV, A. FABRY, W.N. McELROY - Proc. Int. Conf. on Interactions of Neutrons with Nuclei, Lowell, Mass. (1976)

37. A. FABRY et al. - "Review of Microscopic Integral Cross Section Data in Fundamental Reactor Dosimetry Benchmark Neutron Fields" ibid. 3

38. D.M. GILLIAM - "Integral Measurement Results in Standard Fields" this conf.

39. C.M. EISENHAUER et al. - "Transport Theory Applications in Neutron Standards" this conf.

40. H.A. BETHE, J.R. BEYSTER, R.E. CARTER - J. Nucl. En. 3, 207 ; 3, 273 ; 4, 3 ; 4, 147 (1956)

41. S. PEARLSTEIN, E.V. WEINSTOCK - Nucl. Sci. Eng. 29, 28 (1967)

42. S.F. MUGHABGHAB, D.I. GARBER - Report BNL 325 (1973)

43. H.D. LEMMEL - NBS Spec. Publ. 425, I, 290 (1975)

44. P.I. AMUNDSON et al. - Report ANL 7320, 679 (1966)

45. M. DARROUZET et al. "Studies of Unit k Lattices in Metallic Uranium Assemblies ZEBRA 8H, SNEAK 8, ERMINE and HARMONIE UK" - ibid. 10

46. M. PINTER et al. - NBS Spec. Publ. 425, I, 258 (1975)

47. D. GILLIAM, National Bureau of Standards - Private communication (1976)

48. J.A. GRUNDL et al. - Nucl. Techn. 25, 237 (1975)

49. J.A. GRUNDL, G.E. HANSEN - Proc. Nuclear Data for Reactors, vol.I, 321, IAEA (1967)

50. H. ALTER et al. - Report ENDF-202 (1974)

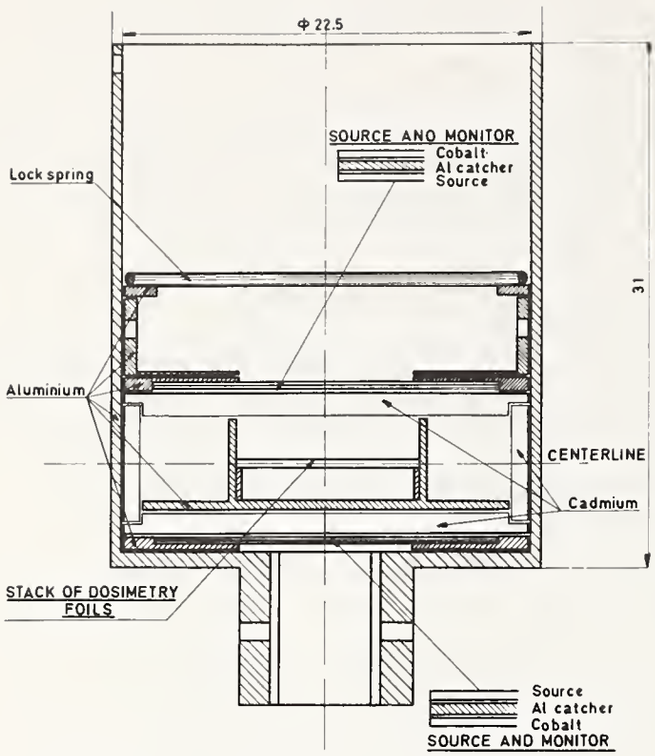

Fig.1. TYPICAL SOURCE-DETECTOR ASSEMBLY FOR ACTIVATION MEASUREMENTS IN THERMAL-NEUTRON INDUCED FISSION NEUTRON SPECTRA

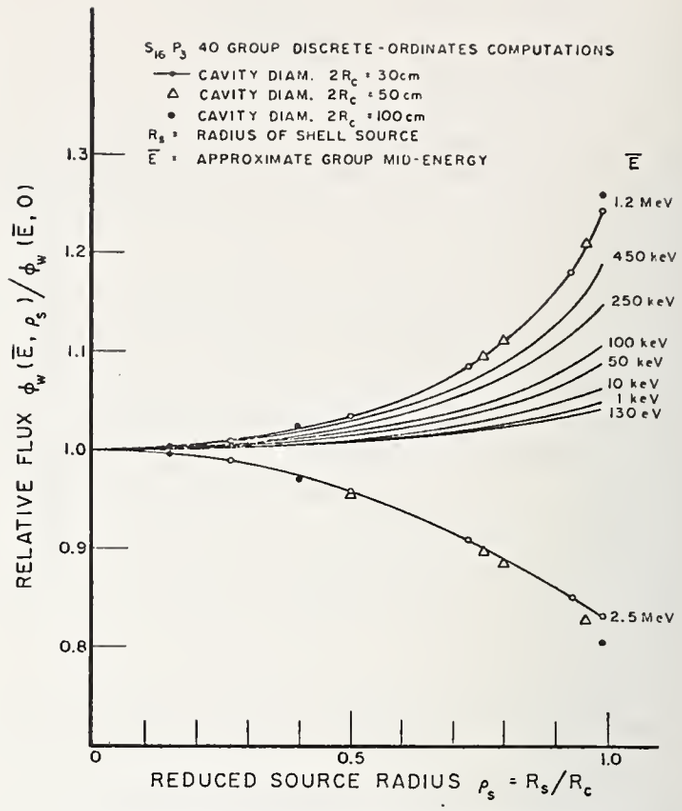

Fig 2. SPATIAL DISTRIBUTION OF CARBON WALL RETURN NEUTRON FLUXES

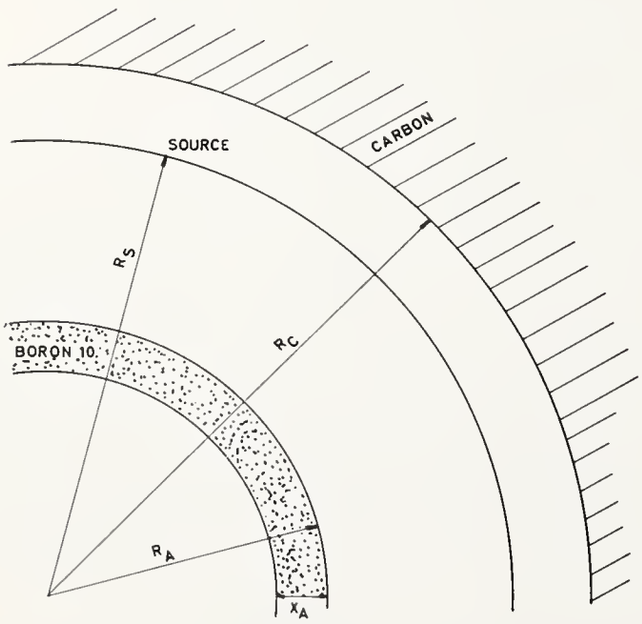

Fig.3. GEOMETRICAL PARAMETERS OF THE ISNF

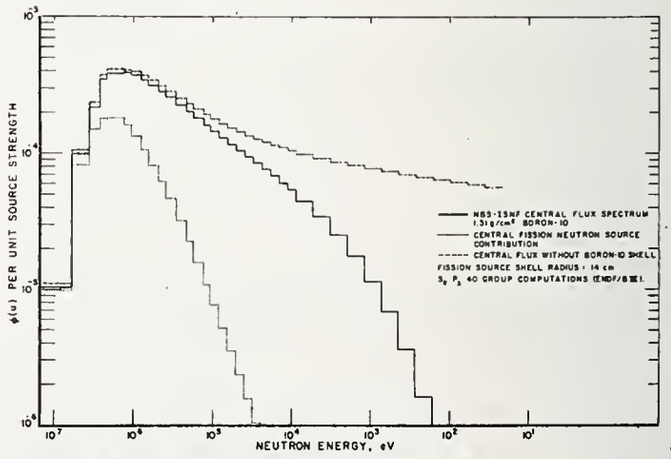

Fig.4. NEUTRON SPECTRUM COMPONENTS OF THE ISNF

INTEGRAL MEASUREMENT RESULTS IN STANDARD FIELDS

D. M. Gilliam
National Bureau of Standards
Washington, D.C. 20234

Measured spectrum-averaged fission cross sections are reported for several benchmark fast neutron fields. For the Cf-252 spectrum, absolute cross section measurements at NBS and the University of Michigan are compared. Cross section ratios (relative to Pu-239) are reported for U-235, U-238, and Np-237 for the following fields: U-235 fission spectrum, BIG-10, CFRMF, SIGMA SIGMA, and the Intermediate-Energy Standard Neutron Field (ISNF) at NBS.

Fission product yields measured by the Interlaboratory LMFBR Reaction Rate Program (ILRR) are reported in two categories: (1) Consensus Yields from thorough interlaboratory studies and (2) Subsidiary Yields for isotopes studied less intensively (usually by a single laboratory). All measured yields were determined by Ge(Li) counting of fission activation foils, with specific fission rates determined by counting fissions from a separate light deposit in an ionization chamber. The fission product yields for the CFRMF and BIG-10 fields are reported first separately and then combined, to provide a single set of yields for a Fast Reactor Spectrum.

(Nuclear data; neutrons; standard fields; cross sections; fission yields)

Introduction

The preceding paper by A. Fabry has discussed facilities employed in standardization of measurement of neutron doses for reactor fuels and materials research. The present paper summarizes results from tests in many of these facilities in which there has been a direct NBS involvement in the past five years. Most of the NBS involvement in this area has been through the USERDA Interlaboratory LMFBR Reaction Rates (ILRR) program, centered at the Hanford Engineering Development Laboratory.

Spectrum-Averaged Fission Cross Sections

Absolute Cross Sections

The availability of small Cf-252 neutron sources and manganese bath facilities has made it possible to determine the neutron flux in a fission-spectrum neutron field so that absolute spectrum-averaged cross section measurements can be made. Table I shows the results of absolute fission cross section measurements made in Cf-252 neutron fields at NBS and at the University of Michigan. The results for U-235 and Pu-239 agree within 1.0%, well within the total uncertainty estimates of either laboratory. At both laboratories, the neutron irradiations were performed with two counters positioned symmetrically about the source in order to avoid sensitivity to the positioning of the highly radioactive source. The calibration of the manganese baths at both laboratories is based on the same standard neutron sources, NBS-I and NBS-II. The mass assay of fissionable deposits at the two laboratories have been intercompared by both fission and alpha counting methods; and in the case of Pu-239, the mass of the University of Michigan deposit was based almost entirely on comparison with the NBS reference deposit by alpha counting. The good agreement of the results is not so surprising in view of the several areas of collaboration between the two laboratories, and yet there are also significant areas of independence in the separate measurements. The fission counting methods were entirely different. At NBS miniature fission ionization chambers were employed; while at the University of Michigan, track-etch detectors were used. The scattering perturbations from the source capsule, the experiment support structures, and the laboratory walls were all very different at the two sites. The averages of the experimental results are compared with calculated values in Table I, also. The calculated values for U-235 and Pu-239 are not very sensitive to the assumed neutron energy spectrum. Thus the discrepancy of 2.5% for U-235 is primarily a disagreement of the integral measurements with the ENDF/B-IV data. Since the total estimated uncertainty in the integral result for U-235 is 2.0%, the disagreement cannot be considered a strong one. The measured cross sections for U-238, Pu-239, and Np-237 agree with calculated values within 1.4%, indicating a generally satisfactory situation in terms of both the ENDF/B data and the evaluated neutron energy spectrum for Cf-252.

TABLE I

ABSOLUTE FISSION CROSS SECTIONS IN A Cf-252 NEUTRON FIELD (mb)

	U-235	U-238	Pu-239	Np-237
NBS (Refs. 1,2)	1205 ± 27	319 ± 8	1808 ± 41	1332 ± 37
University of Michigan (Ref. 3)	1215 ± 17	--	1790 ± 34	--
Average of Measurements	1210 ± 2.0%	319 ± 2.5%	1800 ± 2.2%	1332 ± 2.8%
Calculated Spectrum-Averaged Cross Section*	1241	315	1789	1351
Measured/ Calculated	0.975	1.013	1.006	0.986

*Calculated cross sections were derived from ENOF/B-IV data and the neutron energy spectrum given in the NBS evaluation (Ref. 4).

Cross Section Ratios

The Intermediate-Energy Standard Neutron Field (ISNF)

Table II presents the results of initial measurements in the Intermediate-Energy Standard Neutron Field (ISNF) which has recently become operational at NBS. The fission cross section ratios for U-235, U-238, and Pu-239 were measured by back-to-back fission counting in an NBS double fission ionization chamber at the center of the ISNF facility. The most accurate measurement of the ratio $\bar{\sigma}_f$(U-238)/$\bar{\sigma}_f$(U-235)

was achieved by use of a natural enrichment uranium sample which allowed the deposit mass ratio and counter efficiencies to be determined by observing the fission rate ratio in a thermal neutron beam prior to the ISNF run. (The isotopic ratio of the U-235 and U-238 in the natural uranium sample is known to better than 0.5%.) In all, U-238 deposits with three different depletion levels were used, giving results that had a spread of only 1.2%. The ratio $\bar{\sigma}_f$(Pu-239)/$\bar{\sigma}_f$(U-235) was determined using two Pu-239 deposits from two separate batches. The spread of these results was only 0.3%. In Table III, the thermal neutron "background" and other background contributions are shown to range from 1.3% to 2.8% of the fission rate due to the ISNF spectrum. A description of the ISNF system may be found in the compendium by Grundl.[7] The intermediate-energy field is formed in a spherical cavity within the thermal column of the NBS reactor by exposing disks of U-235 to the high thermal flux and then using a spherical shell of B-10 to cut off the low-energy end of the resulting degraded fission neutron spectrum. The background component shown in Table III is residual count rate within the B-10 shell when the driving disks of U-235 are removed. This background arises from leakage of thermal and epithermal neutrons through penetrations in the shell and from other effects, probably mostly fission induced by capture gammas.

TABLE II

ISNF MEASUREMENTS:
FISSION CROSS SECTION RATIOS

$\bar{\sigma}_f$(U-238)/$\bar{\sigma}_f$(U-235)	Comments on Separate Measurements and Averages
0.0914 ± 0.7%	Natural uranium vs. 99.75% enriched U-235
0.0921 ± 2.0%	1600/1 depleted uranium vs. 99.75% enriched U-235
0.0925 ± 3.0%	Thick U-238 deposit, 250,000/1 depletion; same U-235
0.0918 ± 1.1%*	Average in situ without correction for scattering in the detector
0.0923 ± 1.1%*	Corrected average for unperturbed ISNF field
$\bar{\sigma}_f$(Pu-239)/$\bar{\sigma}_f$(U-235)	Comments on Separate Measurements and Averages
1.155 ± 1.8%	99.98% enriched Pu-239, same U-235
1.152 ± 1.9%	99.12% enriched Pu-239, same U-235
1.155 ± 1.8%*	Average (the scattering correction is nil in this case)

*The error estimate given here does not include any allowance for epithermal neutron perturbations. These perturbations are expected to be small, based on Fabry's experience with SIGMA-SIGMA (Ref. 12). However, these ISNF results cannot be considered as final until the epithermal neutron perturbations have been determined experimentally.

TABLE III

THERMAL-NEUTRON-INDUCED FISSION RATES
IN THE ISNF

Fissionable Isotope	Fission Rate in ISNF Spectrum (s^{-1} mg^{-1})	Fission Rate Due to Thermal Neutrons plus Background (s^{-1} mg^{-1})	Background and Thermal-Induced Fission Rate/ Fast-Induced Fission Rate
U-235	3170	45 ± 11	1.4%
U-238	290	8 ± 0.5	2.8%
Pu-239	3660	47 ± 10	1.3%

Other Dosimetry Benchmark Fields

Table IV summarizes the spectrum-averaged fission cross section ratio results from measurements in dosimetry benchmark fields. The results are given in terms of cross section ratios, because it is not possible to determine the absolute neutron flux precisely for most of these fields. The choice of $\bar{\sigma}_f$(Pu-239) as the normalizing cross section was made because this cross section varies the least (± 6.5%) over the set of fields considered. Table V compares the ratios given in Table IV to calculated ratios derived from ENDF/B-IV cross section data and the spectra compiled by Grundl and Eisenhauer.[7] The ratio of measured to calculated results for U-235 are clustered within ± 1.7% about a mean value of 0.97, underscoring the result seen previously in Table I - that the integral measurements give lower fission rates for U-235 than those calculated from ENDF/B IV data. The measured/calculated values in Table V for the threshold reactions U-238(n,f) and Np-237(n,f) show much larger fluctuations: ± 4.8% and ± 3%, respectively. These discrepancies are more suggestive of errors in the tabulated neutron energy spectra than of consistent cross section biases. Of course, one expects to find the calculated threshold detector responses to be very sensitive to the neutron enery distribution, since these isotopes see only a small part of the total spectrum.

TABLE IV

MEASURED FISSION CROSS SECTION RATIOS
IN DOSIMETRY BENCHMARK FIELDS

$\bar{\sigma}_f(x)/\bar{\sigma}_f$(Pu-239)

Field and References	x:U-235	x:U-238	x:Np-237
Cf-252 fission neutrons (1,2,3,7)	0.672 ± 1.6%	0.177 ± 1.7%	0.740 ± 2.2%
U-235 fission neutrons (10,7)	0.664 ± 2.2%	0.169 ± 2.2%	0.734 ± 3.0%
B1G-10 (5,7)	0.835 ± 1.5%	0.0311 ± 1.9%	0.265 ± 2.2%
CFRMF (6,7)	0.873 ± 1.6%	0.0428 ± 1.9%	0.309 ± 2.3%
SIGMA-SIGMA (7,8,9)	0.857 ± 2.1%	0.0483 ± 2.5%	0.333 ± 2.8%
ISNF (7; Table II above)	0.866 ± 1.8%	0.0799 ± 1.8%	---

TABLE V

FISSION CROSS SECTION RATIOS IN DOSIMETRY BENCHMARK FIELDS--MEASUREMENT VS. CALCULATION

$\{\bar{\sigma}_f(x)/\bar{\sigma}_f(\text{Pu-239})\}/\{\bar{\sigma}_f(x)/\bar{\sigma}_f(\text{Pu-239})\}$

Measured Calculated*

	x:U-235	x:U-238	x:Np-237
Cf-252 fission neutrons	0.970	1.007	0.981
U-235 fission neutrons	0.953	1.016	0.991
BIG-10	0.979	0.960	0.930
CFRMF	0.978	0.993	0.951
SIGMA-SIGMA	0.986	1.034	0.957
ISNF	0.964	1.055	---

*Calculated cross section ratios are derived from folding together the ENDF/B-IV cross section data and the neutron energy spectra as tabulated in the compendium by Grundl (Ref. 7).

Fission Product Yields

Consensus Fission Yields

Table VI summarizes the ILRR Consensus Fission Yields results. The term Consensus Fission Yields is used to denote the very satisfactory agreement which was achieved after an intensive interlaboratory effort in which the absolute fission product gamma activities were determined by three independent Ge(Li) counting laboratories. In eighteen cases of yield measurements for fission of U-235, U-238, and Pu-239, the spread of the three individual results about their mean exceeded ± 1.9% in only two instances. The uncertainties quoted for these radiometric fission yield data are about twice as small as some evaluators were willing to concede to be possible until very recently.[14] The gamma counting laboratories participating in this effort were from EG&G Idaho at the Idaho National Engineering Laboratory, Argonne National Laboratory, and the Hanford Engineering Development Laboratory. The specific fission counts (fissions/unit mass of a given isotope) for the fission activation foils were determined by NBS by means of a double fission ionization chamber. In Table VI the separate interlaboratory averages for BIG-10 and CFRMF are first given separately and then combined to provide a single ILRR recommendation to ENDF/B under the Fast Reactor Spectrum Category. Table VII shows the differences in yields measured in the two separate fields. These differences are generally comparable to or smaller than the estimated uncertainties of the measurements, despite the somewhat harder spectrum of CFRMF.

TABLE VI

ILRR CONSENSUS FISSION YIELDS

Fission Product/ Principal Isotope of Foil	ILRR Mean and Combined Errors (exclusive of decay-scheme errors)		ILRR Average for a Fast Reactor Spectrum and Total Error
	Fast Neutron Field		
	BIG-10	CFRMF	
Zr-95/U-235	0.0646 ± 1.9%	0.0644 ± 2.0%	0.0645 ± 2.2%
Ru-103/U-235	0.0337 ± 1.9%	0.0330 ± 2.0%	0.0333 ± 2.3%*
Ba-140/U-235	0.0607 ± 1.9%	0.0607 ± 2.0%	0.0607 ± 1.9%
Zr-95/U-238	0.0520 ± 2.5%	0.0516 ± 2.4%	0.0519 ± 2.6%
Ru-103/U-238	0.0635 ± 2.2%	0.0631 ± 2.4%	0.0634 ± 2.5%
Ba-140/U-238	0.0601 ± 2.2%	0.0597 ± 2.4%	0.0600 ± 2.2%
Zr-95/Pu-239	0.0479 ± 2.0%	0.0480 ± 2.1%	0.0480 ± 2.3%
Ru-103/Pu-239	0.0709 ± 2.0%	0.0705 ± 2.1%	0.0708 ± 2.3%
Ba-140/Pu-239	0.0529 ± 2.0%	0.0532 ± 2.1%	0.0530 ± 2.0%
Zr-95/Np-237	0.0597 ± 3.4%	0.0570 ± 3.7%	0.0593 ± 4.0%
Ru-103/Np-237	0.0591 ± 4.1%	0.0588 ± 3.7%	0.0589 ± 4.3%
Ba-140/Np-237	0.0566 ± 4.0%	0.0574 ± 3.4%	0.0571 ± 3.6%

*Significant neutron energy dependence has been observed in the yield of Ru-103 from fission of U-235. The measured yields in the BIG-10 and CFRMF spectra differ by (2.1 ± 1.0)%. These fast reactor yields are about 10% higher than the ILRR average for well-thermalized neutrons. The error stated does not account for deviations due to energy dependence.

TABLE VII

COMPARISON OF FAST FISSION YIELDS: CFRMF/BIG-10

$\frac{\text{CFRMF Yield}}{\text{BIG-10 Yield}} - 1$		Principal Isotope of Fission Foil			
		U-235	U-238	Pu-239	Np-237
Fission Product Nuclide	Zr-95	-0.3 %	-0.8 %	0.2 %	-4.5 %
	Ru-103	-2.1 %	-0.6 %	-0.6 %	-0.5 %
	Ba-140	0.0 %	-0.7 %	0.6 %	1.4 %

However, the Ru-103 yield from U-235 has shown significant energy dependence in the ILRR measurements (See the footnote of Table VI).

Table VIII gives the decay scheme data used in deriving the yields given in Table VI. To get the most accurate results in using the yields of Table VI to get fission counts from fission activation foils, one should use the same decay scheme data assumed in deriving the yields. If one does use the data of Tables VI and VIII together in subsequent fission counting, the errors in gamma ray intensities will cancel out exactly and there can be considerable cancellation of errors in the half-lives.

TABLE VIII

DECAY SCHEME DATA AND ERRORS

Fission Product Nuclide	Half-life* (days)	Gamma-Ray Energy* (keV)	Gamma-Ray Intensity* (%)	Resultant Yield Uncertainty (%)
Zr-95	64.1 ± 0.3	724.179 756.710	44.1 ± 0.5 54.6 ± 0.5	1.1
Ru-103	39.43 ± 0.10	497.08	89.0 ± 1.0	1.2
Ba-140	12.789 ± 0.006	537.35	24.4 ± 0.3	0.2
La-140	1.6775 ± 0.0008	1596.18	95.40 ± 0.08	

*These data (in columns 2, 3, and 4) were given in a private communication from R. G. Helmer, Nuclear Physics Branch, EG&G Idaho, Inc., Idaho National Engineering Laboratory, Feb. 23, 1977. An earlier review by Helmer and R. C. Greenwood was published in Nuclear Technology, 25, No. 2, February 1975, p. 258.

†In equilibrium, the ratio of the La-140 to Ba-140 activities is

$$T_{\frac{1}{2}}(\text{Ba})/\left[T_{\frac{1}{2}}(\text{Ba}) - T_{\frac{1}{2}}(\text{La})\right] = 1.15097 \pm 0.00012$$

Table IX compares the ILRR radiometric results with mass spectrometric results from yield measurements at EBR-II.[13] No comparison is made for Ru-103 data because there is no high precision mass spectrometric data available for this chain; a plating-out problem is known to exist in the destructive analysis procedure, preventing accurate results for this case. The Zr-95 and Ba-140 yields from the EBR-II and ILRR tests agree within 2% in five of six cases. The 4.8% discrepancy for Zr-95 yield from U-238 is beyond the 1σ error limits. There is no EBR-II data on Np-237 yields for comparison.

TABLE IX

COMPARISON OF ILRR RADIOMETRIC YIELD DATA WITH E8R-II MASS SPECTROMETRIC DATA*

Fission Product Nuclide/ Principal Isotope of Fuel Specimen	ILRR Radiometric Result	EBR-II Mass Spectrometric Result	$\frac{\text{Maeck}}{\text{ILRR}} - 1$ x 100%
Zr-95/U-235	0.0645 ± 2.2%	0.0642 ± 0.9%	-0.5%
Ba-140/U-235	0.0607 ± 1.9%	0.0618 ± 0.8%†	1.8%
Zr-95/U-238	0.0519 ± 2.6%	0.0494 ± 1.6%	-4.8%
Ba-140/U-238	0.0600 ± 2.2%	0.0592 ± 2.0%	-1.3%
Zr-95/Pu-239	0.0480 ± 2.3%	0.0471 ± 1.3%	-1.9%
Ba-140/Pu-239	0.0530 ± 2.0%	0.0538 ± 1.1%†	1.5%

*W. J. Maeck, Ref. 13.

†The mass spectrometric data from Ref. 13 has been adjusted slightly for differences in the yields of the radioactive fission products observed in the ILRR measurements and the stable fission products observed in the mass spectrometric measurements.

Table X gives some subsidiary ILRR fission yield results. There are two distinctions between the "subsidiary" yields and the "consensus" yields. The gamma counting for the subsidiary yields was usually done by only one laboratory rather than three, and the decay scheme uncertainties for the subsidiary yields isotopes are generally larger than the decay scheme uncertainties for the consensus yields. Table XI lists the decay scheme data for the subsidiary yields. Some comments were made previously about using the yield data and decay scheme data together for the most accurate results. These comments are all the more important in the case of the subsidiary yields, because the errors in the gamma ray intensities are so much larger in these cases.

TABLE X

ILRR SUBSIDIARY FISSION YIELDS

Fission Product/ Principal Isotope of Foil	Cumulative Fractional Fission Yield		Comparison of Results from Two Fast Neutron Fields	ILRR Average for a Fast Reactor Spectrum and Total Error
	Fast Neutron Field		$\frac{\text{CFRMF}}{\text{BIG-10}} - 1$ x 100%	
	BIG-10	CFRMF		
Zr-97/U-235	0.0600	0.0606	1.0	0.0603 ± 2.4%
I-131/U-235	0.0334	0.0328	-1.8	0.0331 ± 4.3%
Te-132/U-235	0.0481	0.0486	1.0	0.0483 ± 6.1%
Cs-137/U-235	0.0628	0.0623	- .8	0.0626 ± 5.8%
Ce-143/U-235	0.0514	0.0521	1.4	0.0517 ± 8.7%
Ce-144/U-235	0.0596	0.0569	-4.5	0.0583 ± 4.5%
Zr-97/U-238	0.0568			0.0568 ± 3.0%
I-131/U-238	0.0328	0.0324	-1.2	0.0326 ± 4.3%
Cs-137/U-238		0.0600		0.0600 ± 4.5%
Ce-143/U-238	0.0424	0.0418	-1.4	0.0421 ± 8.7%
Ce-144/U-238		0.0495		0.0495 ± 4.3%
Zr-97/Pu-239	0.0541	0.0547	1.1	0.0544 ± 2.5%
Te-132/Pu-239	0.0537	0.0551	2.6	0.0544 ± 6.1%
Cs-137/Pu-239		0.0676		0.0676 ± 2.6%
Ce-143/Pu-239	0.0390			0.0390 ± 8.7%
Ce-144/Pu-239		0.0379		0.0379 ± 5.5%
Zr-97/Np-237	0.0644	0.0632	1.9	0.0638 ± 3.8%
Cs-137/Np-237		0.0650		0.0650 ± 5.2%

TABLE XI

DECAY SCHEME DATA AND ERRORS FOR SUBSIDIARY YIELDS

Fission Product Nuclide	Half-life*	Gamma-Ray Energy* (1eV)	Gamma-Ray Intensity* (%)
Zr-97	16.88(6)† h	743.3(1)†	92.9(3)†
I-131	8.05 d	364.5	82.(3)‡
Te-132	77.9(5) h	228.16(6)	89.(5)
Cs-137	30.03(15) yr	661.647(12)	85.3(4)
Ce-143	33.0(2) h	293.26(2)	47.(4)
Ce-144	284.4(4) d	133.53(3)	11.0(2)

*Except for the I-131 data, these data were given in a private communication from R. G. Helmer, Nuclear Physics Branch, EG&G Idaho, Inc., Idaho National Engineering Laboratory, Feb. 23, 1977.

†The number in parentheses is the uncertainty in the least significant digit.

‡Arbitrary error assignment.

References

1. H. T. Heaton II, D. M. Gilliam, V. Spiegel, C. Eisenhauer, and J. A. Grundl. Proceedings of the NEANDC/NEACRP Specialists Meeting on Fast Neutron Fission Cross Sections of U-233, U-235, U-238, and Pu-239, June, 1976, Argonne, Illinois. ANL-76-90, ERDA-NDC-5/L, NEANDC(US)-199/L. p. 333.

2. D. M. Gilliam, C. Eisenhauer, H. T. Heaton II, and J. A. Grundl. Proceedings of a Conference on Nuclear Cross Sections and Technology, March, 1975, Washington, D. C. NBS Special Publication 425, Vol. I, p. 270.

3. M. C. Davis, Absolute Measurements of Fast Fission Cross Sections for U-235 and Pu-239, Ph.D. Thesis, University of Michigan, Ann Arbor, Michigan, 1976.

4. J. A. Grundl and C. M. Eisenhauer. Proceedings of a Conference on Nuclear Cross Sections and Technology, March 1975, Washington, D. C. NBS Special Publication 425, Vol. I, p. 250.

5. D. M. Gilliam, J. A. Grundl, G. E. Hansen, and H. H. Helmik, LMFBR Reaction Rate and Dosimetry 10th Progress Report, (Hanford Engineering Development Laboratory Report) HEDL-TME 75-130, UC 79 b,d. 1976. p. NBS-15.

6. J. A. Grundl, D. M. Gilliam, N. D. Dudey, and R. J. Popek. Nuclear Technology, 25 (1975), p. 237.

7. J. Grundl and C. Eisenhaur, "Benchmark Neutron Fields for Reactor Dosimetry," Proceedings of the IAEA Consultant's Meeting on Integral Cross Section Measurements in Standard Neutron Fields for Reactor Neutron Dosimetry, Vienna, November, 1976.

8. M. Pinter, W. Scholtyssek, et al., Proceedings of a Conference on Nuclear Cross Sections and Technology, March, 1975, Washington, D. C., NBS Special Publication 425, Vol. I, p. 258.

9. A. Fabry, et al., "Review of Microscopic Integral Cross Section Data in Fundamental Reactor Dosimetry Benchmark Neutron Fields," Proceedings of the IAEA Consultant's Meeting on Integral Cross Section Measurements in Standard Neutron Fields for Reactor Neutron Dosimetry, Vienna, November, 1976.

10. A. Fabry, J. A. Grundl, and C. Eisenhauer, Proceedings of a Conference on Nuclear Cross Sections and Technology, March, 1975, Washington, D. C., NBS Special Publication 425, Vol. I, p. 254.

11. C. M. Eisenhauer "Neutron Transport Calculations for the Intermediate-Energy Standard Neutron Field (ISNF) at the National Bureau of Standards," Proceedings of this Conference.

12. A. Fabry, G. de Leeuw, and S. de Leeuw, Nuclear Technology, Vol. 25 (1975), p. 349.

13. W. J. Maeck, editor, "Fact Reactor Fission Yields for U-233, U-235, U-238, and Pu-239 and Recommendations for the Determination of Burnup on FBR Mixed-Oxide Fuels: An Interim Project Report," Allied Chemical Corporation Report, Idaho National Engineering Laboratory, ICP-1050-1, UC-79c, (1975).

14. D. M. Gilliam, "Interlaboratory Consensus Fission Yields and Subsidiary Fission Yields," LMFBR Reaction Rate and Dosimetry 11th Progress Report, Hanford Engineering Development Laboratory Report, HEDL-TME to be published, 1977.

ABSOLUTE FISSION CROSS SECTION MEASUREMENTS USING FIXED ENERGY NEUTRON SOURCES

G. F. Knoll
The University of Michigan
Ann Arbor, Michigan 48109

Quasi-monoenergetic neutron sources of fixed energy can permit generation of absolute cross section data at well-known and isolated neutron energies. These data can serve as independent normalization points for cross section shape measurements made using other techniques. Several examples of their application to fission cross section measurements are given.

(absolute cross sections, neutron sources)

Introduction

Most of the cross section data discussed at this symposium have been generated using techniques in which the neutron energy either covers a continuum of values or is arbitrarily chosen by the experimenter. In particular, time-of-flight experiments carried out using white neutron sources are capable of closely reproducing the shape of cross sections over extended energy ranges. Other experiments make use of nearly monoenergetic neutrons generated in thin targets by charged particle beams from accelerators. The neutron energy can be varied over wide ranges and, with the use of a flux monitor with known efficiency variation, the cross section shape can also be determined through repeated measurements at different neutron energies. In either case, however, the determination of the neutron flux in an absolute sense is a separate problem generally involving more difficult procedures than are required for a simple shape determination.

This paper deals with a different category of neutron sources in which the energy is fixed by fundamental nuclear parameters. They are monoenergetic to first approximation, but all show some energy spread about the average neutron energy. In some cases, the neutron spectrum may also contain one or more contaminant groups of neutrons whose energy differs widely from the primary yield. With the application of corresponding corrections, however, these fixed energy neutron sources allow the measurement of cross sections at well-defined energies and can serve as "spot checks" on cross section shapes deduced from other methods. The principal merit of this approach is that it is often simpler to determine the absolute neutron yield from fixed energy sources, and the resulting absolute cross section values can be used for normalization purposes in conjunction with other shape data.

Correction for the finite energy spectrum width requires information on both the shape of the neutron energy spectrum emitted by the source and the shape of the measured cross section over the same energy range. These neutron sources are therefore best suited for the measurement of cross sections which do not change greatly across the source energy spectrum. However, any fluctuation in the cross section on an energy scale which is fine compared with the inherent source width will be averaged out. It is conventional to make these spectrum corrections relative to the median or average energy of the source, and thus to reduce the data to a single cross section value at this energy.

Commonly used neutron sources which fall into the fixed energy classification are:

A. Nuclear reactions with a large Q-value compared with the energy of the incident particle.

B. Filtered beams in which sources with a broad energy spectrum are transmitted through thick samples of absorbers with cross section minima.

C. Nuclear reactions with negative Q-value in which the incident particle energy is just above threshold.

D. Neutrons produced by photodisintegration of target nuclei.

In the first category, the primary examples are the D-D and D-T reactions produced in low energy accelerators. The corresponding neutrons at about 3 and 14 MeV have been widely used in fast neutron cross section measurements. Since data of this type are involved in many of the discussions presented at this symposium, further elaboration will not be given here. Filtered beams are also discussed in a preceding paper by R. B. Schwartz in this symposium. Associated particle methods are commonly used to determine the absolute neutron yield in the first case, but it is somewhat more difficult to gain absolute information about the neutron flux provided by filtered beams.

Topics C and D listed above are the major subjects of this paper. In both cases, circumstances can be created in which the absolute neutron yield can be determined to a high precision. These methods are therefore most applicable to the measurement of absolute neutron cross sections which are not dependent on other cross section data or assumptions about the efficiency of flux monitor detectors.

Endothermic Reactions Near Threshold

If a neutron producing reaction with a negative Q-value is observed using an incident particle beam below the threshold energy, no neutrons are produced. If the energy of the particle beam is raised, neutrons first appear when the particle beam just reaches the threshold energy. Because of the motion of the center-of-mass of the incident particle and target, neutrons at threshold are emitted only in the extreme forward direction. Their energy can easily be calculated from the center-of-mass motion, and typically amounts to several tens of keV. As the incident particle energy is raised further, the neutrons observed in the laboratory frame of reference are emitted within a forward-directed cone with ever widening apex angle. For particle energies sufficiently above threshold, the cone broadens into a full sphere and neutrons are observed in all directions.

If the energy of the incoming particle beam can be sufficiently well regulated, conditions can be maintained in which the entire neutron yield is confined within a cone of small apex angle. For example, using the $^{7}Li(p,n)^{7}Be$ reaction with a proton energy 2 keV above threshold, the neutron yield is confined to

within a 12° cone. Under these conditions, the neutron energy at the cone edge is approximately 30 keV and is between 43.2 and 18.7 keV along the cone axis. The neutron energy spectra have been calculated for this reaction by Poenitz and Brudermueller[1] for cone angles of 5 and 10 degrees for which the energy spread is somewhat reduced.

As illustrated in Fig. 1, it is possible to conduct a cross section measurement under these conditions in which all neutrons, since they are confined to the narrow cone, pass through the sample target. This type of geometry can then greatly simplify calculation of the incident neutron flux. In the example given above, the total neutron yield can be determined from a fresh target through the use of the associated activity technique (see preceding paper in this symposium by K. K. Sekharan). Since each of these neutrons passes through the sample target, the integrated neutron flux can be easily determined from the sample thickness.

In addition to the ^{7}Li(p,n) reaction with a threshold neutron energy of 30 keV, other endothermic neutron-producing reactions can be employed in the same way. A lighter target nucleus increases the center-of-mass motion energy and consequently raises the neutron energy at threshold. For example, the ^{3}H(p,n)^{3}He reaction provides threshold neutrons at 64 keV.[2]

Photoneutron Sources

Neutrons produced by photodisintegration of deuterium or beryllium can also be used in cross section measurements. If the incident gamma rays are monoenergetic above the photodisintegration threshold energy, the neutron spectrum will also be nearly monoenergetic, subject only to slight broadening due to kinematic and scattering effects. The examples of their application to cross section measurements given here will be drawn from recent experience at The University of Michigan.[3,4,5] However, extensive application of photoneutron sources in other cross section work has previously been made by Perkin et al.[6], Robertson et al.[7,8], and several other groups.

The advantages of photoneutron sources in cross section measurements are summarized below:

1. The sources are "quasi-monoenergetic" in that the neutron spectrum in most cases consists of a single kinematically-broadened peak with a low energy tail due to neutron scattering within the source (see Fig. 2). The absolute energy scale can be accurately predicted from the high-precision nuclear data available on neutron binding energies and gamma ray photon energies. Because of the simple geometry of the sources, the energy spectrum can be calculated with a reasonable degree of reliability. Some data are also available from direct spectrum measurements.[9,10] The degree of low-energy tailing can be reduced at the expense of a lower absolute neutron yield by decreasing source dimensions.

2. Because of the small physical size of these sources, they can be readily calibrated by total absorption bath measurements. If the sources are constructed in simple spherical geometry, a straightforward neutron transport calculation gives the absolute neutron flux at any distance from the source surface. Since these geometric calculations can be carried out to high precision, an absolute neutron flux can be accurately generated for cross section measurements.

3. Using readily available gamma ray sources produced by reactor activation, neutrons ranging in energy from 24 keV to 964 keV can be conveniently produced. This is an energy region in which competing methods of monoenergetic neutron source generation often have some difficulties.

The use of such sources also has some significant drawbacks:

1. In order to produce neutron yields in the 10^{6} to 10^{7} per second range, gamma ray activities of the order of tens of curies are typically required (see Table I). Therefore, all manipulation and handling of the sources must be done under remote conditions within heavily shielded working areas. Furthermore, targets and detectors used for cross section measurements are subjected to high gamma ray exposure rates (as large as 10^{4} R/hr). These high gamma fluxes preclude the use of many conventional detectors for reaction product counting. Therefore, most photoneutron cross section measurements have been carried out using foil activation or particle track-etch methods which are inherently insensitive to gamma rays.

2. With the exception of ^{124}Sb, useful gamma ray sources have half-lives of no more than several days. Therefore, sources must be reactivated immediately prior to each use requiring close proximity to a reactor if elaborate handling and transportation schemes are to be avoided.

Fission Cross Section Measurements at The University of Michigan

Source Description

The five photoneutron sources currently in routine use at The University of Michigan are listed in Table I. In all cases, the source consists of a spherical gamma ray emitting core surrounded by a 3 mm thick spherical shell of either beryllium or deuterated polyethelene. For most of the sources, the shells are detachable and can be fitted to a number of different cores. This modularity allows separate reactor irradiation of the core to prevent radiation damage to the deuterated polyethelene shells, and also permits maximal use of each set of shells. Physical dimensions of the sources are standardized (36 mm OD) to simplify their handling during the irradiation and calibration phases.

Table I

Properties of Photoneutron Sources

Source-Target	Median Neutron Energy (keV)	Source Half-Life	Initial Neutron Yield (n/sec)
^{24}Na-Be	964	15.00 hr.	5×10^{7}
^{140}La-Be	770	40.23 hr.	2×10^{6}
^{24}Na-D	265	15.00 hr.	2×10^{7}
^{72}Ga-D	140	13.95 hr.	6×10^{6}
^{124}Sb-Be	23	60 days	5×10^{7}

Target Irradiation

A typical cross section irradiation geometry is shown in Fig. 3. Virtually all our measurements have employed the dual target or "compensated beam" geometric arrangement in which nearly-identical targets are positioned on either side of the spherical

photoneutron source. The summed reaction rate from both targets is then a much less sensitive function of the exact source location than if a single target geometry were used. It is then necessary to measure only the distance between target foils to high precision, a measurement which can be carried out in the absence of the highly radioactive source. Dimensional uncertainties typically result in uncertainties in the flux of several tenths of a percent.

To minimize the effect of thermalized neutrons on the measurements, the irradiations are carried out within a cadmium enclosure which is located at the center of a laboratory in which all walls, ceiling, and floor have been covered with three inches of anhydrous borax. Despite these low albedo conditions, a measurable reaction rate is induced in samples with high thermal fission cross sections by neutrons which have been moderated in the room structures. We therefore routinely carry out multiple measurements in which the spacing between targets and source is varied. A plot of the apparent cross section measured under these conditions is shown in Fig. 4. We eliminate the effect of room return neutrons by extrapolating these plots to zero spacing.

All our fission cross section measurements are carried out with detectors located behind limited solid angle apertures. The efficiency of this detector geometry must then be calculated from geometric data and assumed anisotropy of fission fragments with respect to the incident neutron direction. When using track-etch detectors, the limited solid angle geometry prevents difficulties arising from fragments incident at low angles relative to the film surface which may not give rise to etchable tracks. We also avoid complications arising in 2π geometry due to fission fragments emitted near the plane of the target foil. We are, however, dependent on angular distribution data and the associated uncertainties are one of the dominant sources of error in our fission cross section measurements.

Source Calibration

We have relied exclusively on the manganese bath technique to provide calibration of our photoneutron sources. Methods for the absolute calibration of such baths are the subject of a preceding paper in this symposium by E. J. Axton. At The University of Michigan, we have carried out all source calibrations relative to the secondary national neutron standard, NBS-II. We therefore avoid many of the uncertainties associated with absolute bath calibration, but are dependent on prior calibrations carried out on NBS-II. Based on an evaluation by Gilliam[3], we currently assume this uncertainty to be 0.5%.

The activity of the manganese bath is continuously sampled and counted by a sodium iodide scintillation detector. Multiscaler data are recorded over the entire cycle of activity build-up, saturation, and decay after source removal. After appropriate calculations are made to account for source decay, bath dynamics, and mixing delays, we normally obtain data over the entire cycle which is self-consistent to within statistical uncertainties. A single best value for the neutron induced activity is then obtained by statistical weighting methods.

Small corrections (< 1%) must then be made in the manganese bath data to account for differences in source self-absorption and activation of the bath by photoneutrons produced from the natural deuterium contact of the bath. The self-absorption was directly measured by noting the decrease in saturated bath activity as additional absorber was placed at the source position. The photoactivation of the bath was simply determined for each source by removing the target shells from the core. Since the uncertainties in these corrections are small, our overall calibration uncertainty is dominated by the uncertainty in the NBS-II emission rate.

Fission Fragment Recording

All fission fragments are recorded on polyester track-etch films and are manually counted using a projection microscope. In order to reduce counting errors, all important films are counted twice by independent observers and any discrepancies resolved by a third count. With proper etch conditions, visual discrimination against alpha-induced pits and other background is relatively simple.

Fission Cross Section Results

Results obtained to date using four of the photoneutron sources with targets of ^{235}U and ^{239}Pu are given in Table II. Some of these values are slight revisions of previously-reported results, reflecting improved counting data and updated values for some corrections. Additional data are currently being generated from the same target foils using the Sb-Be source. After these measurements are completed, we plan to apply the set of photoneutron sources to measurements of the ^{233}U and ^{237}Np fission cross sections. Since many of the same techniques are common to all these measurements, additional data should help establish the validity of the entire set of cross sections.

Table II

Fission Cross Section Results Obtained with Photoneutron Sources

En (keV)	^{235}U (barns)	^{239}Pu (barns)
140	1.471 ± .024	1.469 ± .041
265	1.274 ± .020	1.515 ± .035
770	1.162 ± .022	1.670 ± .037
964	1.195 ± .025	1.643 ± .033

References

1. W. P. Poenitz and G. Brudermueller, Report EANDC-33"U" (1963).
2. L. W. Weston and W. S. Lyon, Phys. Rev. 123, 948 (1961).
3. D. M. Gilliam and G. F. Knoll, Annals of Nucl. Energy 2, 637 (1975).
4. J. C. Robertson, M. C. Davis, J. C. Engdahl, and G. F. Knoll, Trans. Am. Nucl. Soc. 21, 503 (1975).
5. M. C. Davis, J. C. Robertson, J. C. Engdahl, and G. F. Knoll, Trans. Am. Nucl. Soc. 22, 663 (1975).
6. J. L. Perkin, P. H. White, P. Fieldhouse, E. J. Axton, P. Cross, and J. C. Robertson, J. Nucl. Energy 19, 423 (1965).
7. J. C. Robertson, Nucl. Phys. 71, 417 (1965).

8. J. C. Robertson, T. B. Ryves, E. J. Axton, I. Goodier, and A. Williams, J. Nucl. Energy 23, 205 (1969).

9. K. Mueck and F. Bensch, J. Nucl. Energy 27, 857 (1973).

10. T. B. Ryves and J. C. Robertson, J. Nucl. Energy 25, 557 (1971).

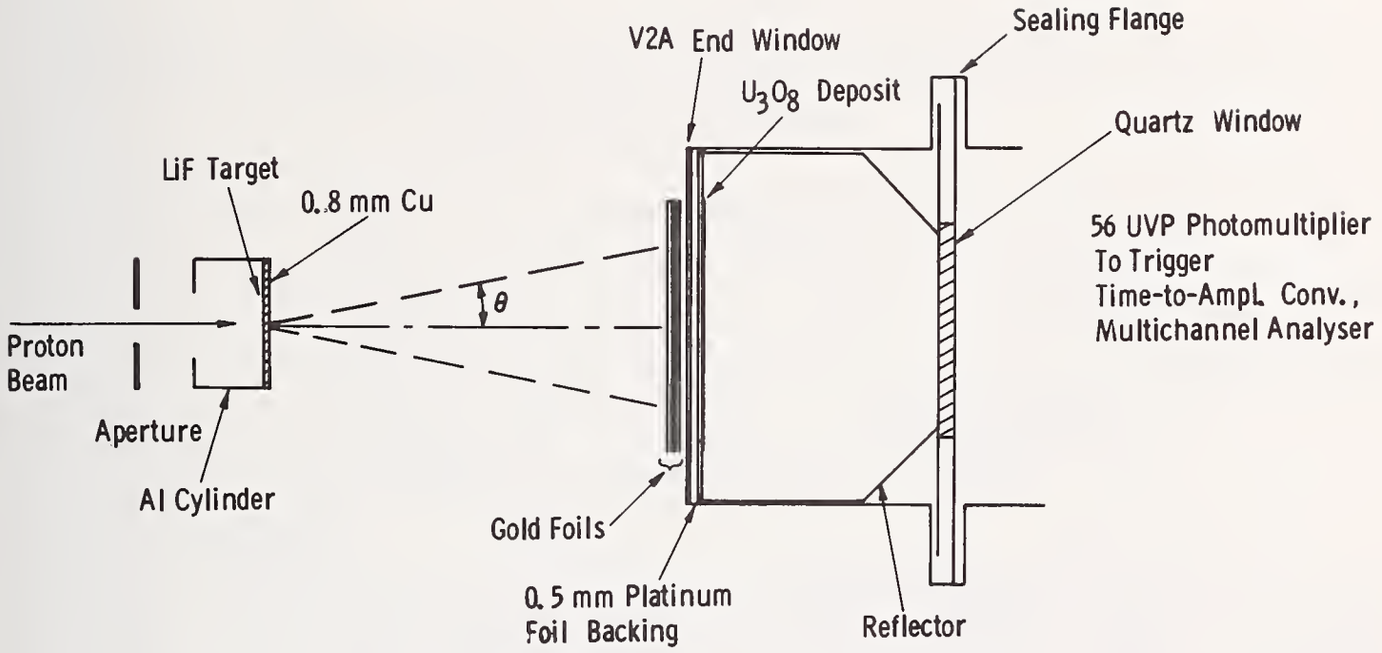

Fig. 1 Kinematic collimation provided by operating the $^{7}Li(p,n)$ reaction 2 keV above threshold (from G. F. Knoll and W. P. Poenitz, J. Nucl. Energy 21, 643 (1967)).

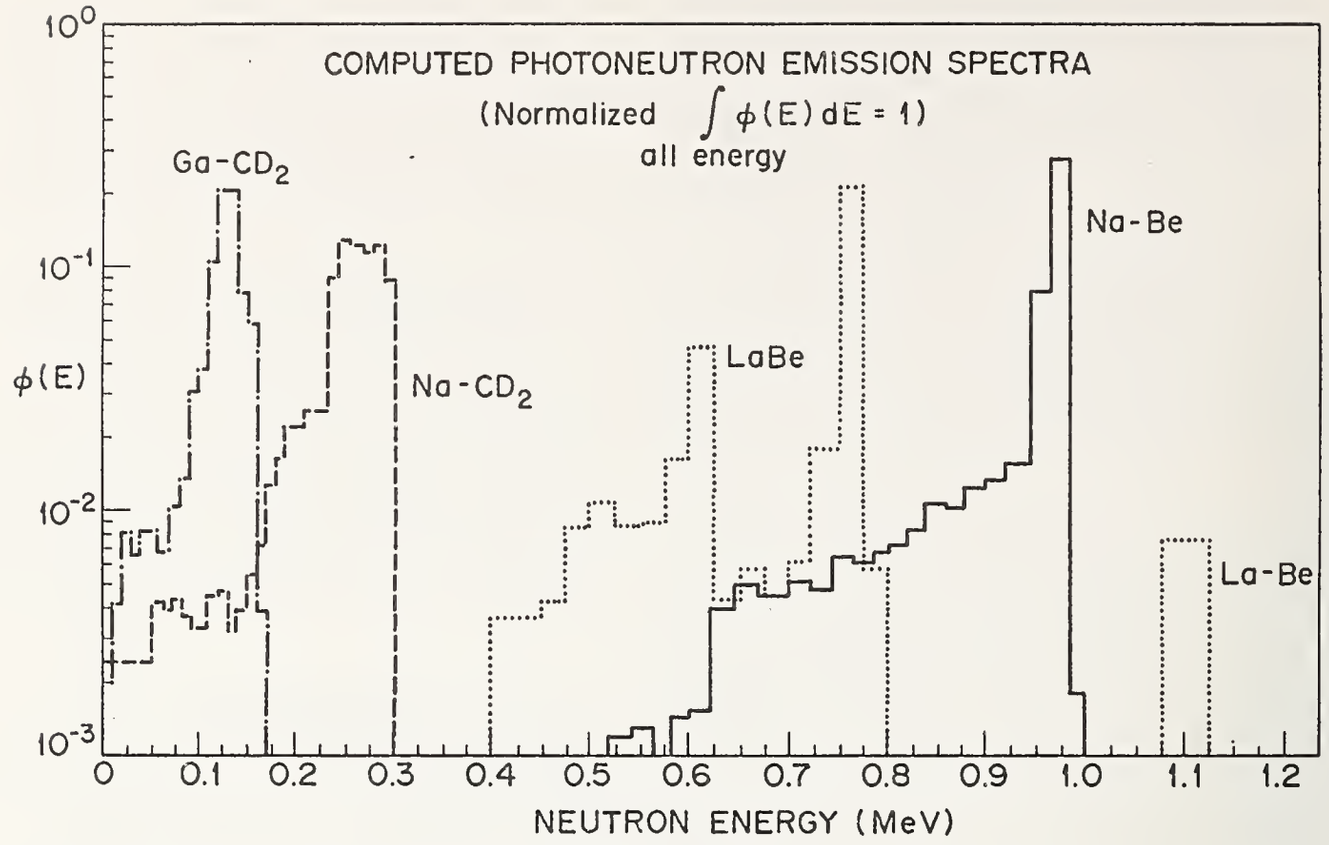

Fig. 2 Neutron spectra produced by several photoneutron sources as calculated by Monte Carlo.

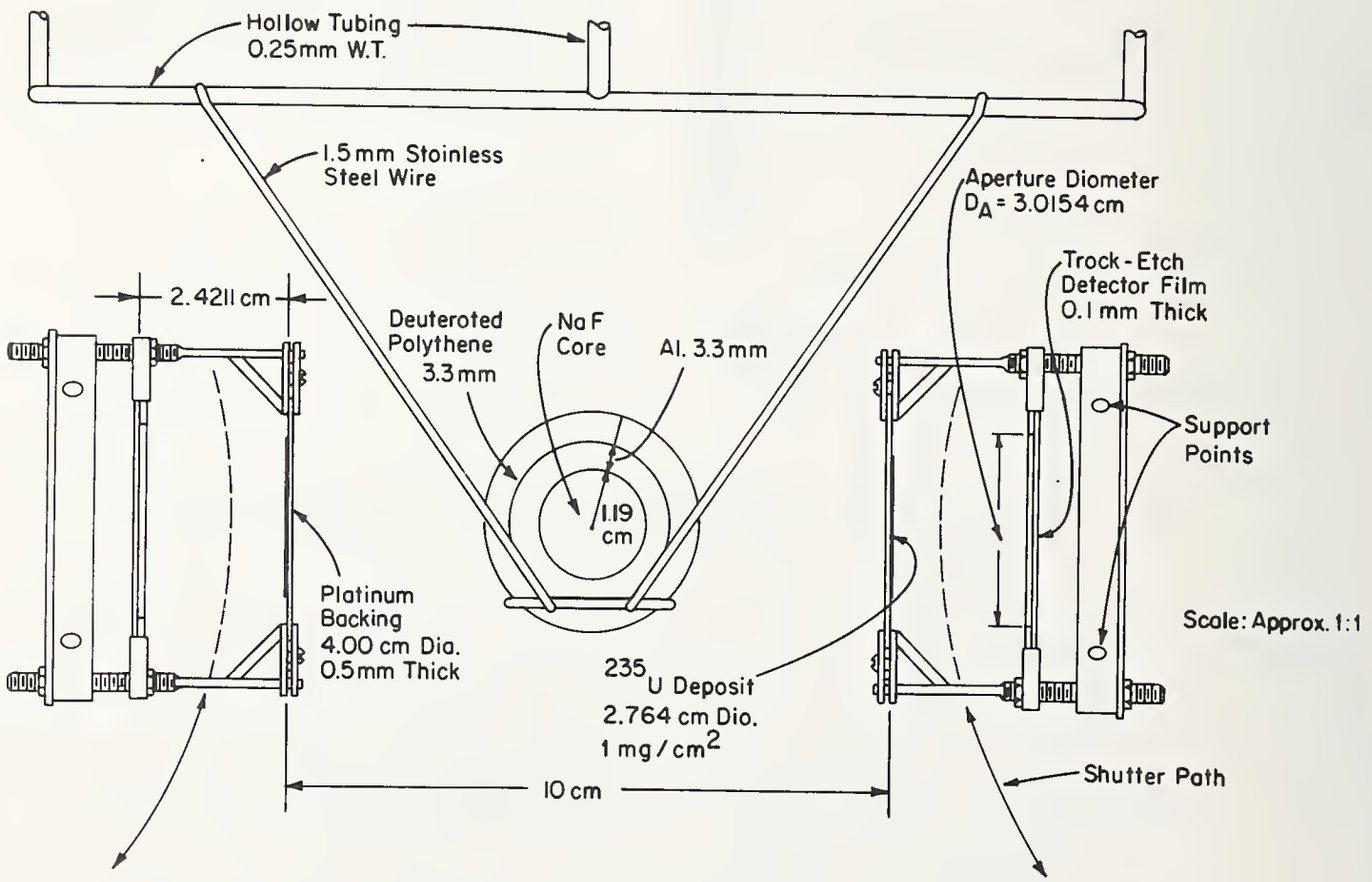

Fig. 3 Dual foil "compensated beam" geometry used for fission cross section measurements.

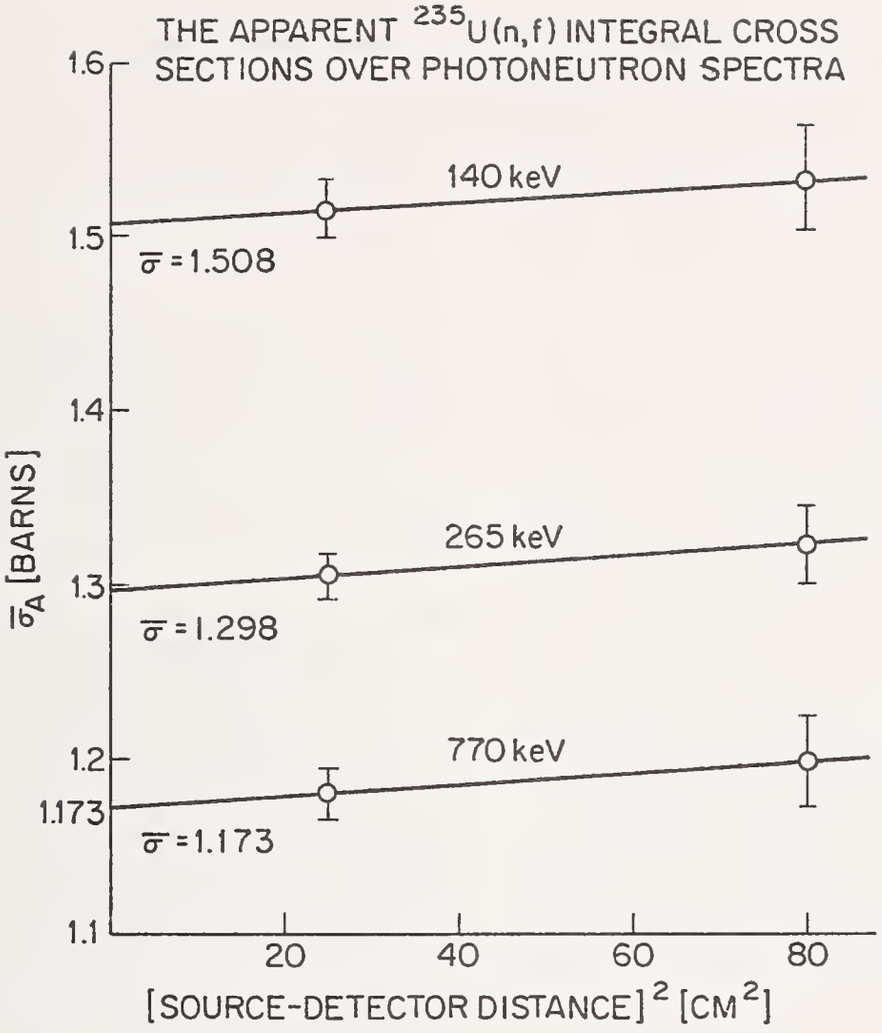

Fig. 4 Plots of the apparent fission cross section vs. the square of the source-target spacing showing extrapolation to eliminate the contribution of room-return neutrons.

IMPACT OF ENDF STANDARDS ON FAST REACTORS

Ugo Farinelli
Comitato Nazionale Energia Nucleare
C.S.N. Casaccia, Roma, Italy

ENDF/B is widely used throughout the world by fast reactor designers, either directly or as a basis for adjustment procedures. Neutron standards have at least potentially a value that goes beyond their intrinsic function in the production of evaluated nuclear data files; they could be used as standards also for integral measurements, especially in connection with benchmark experiments, and could provide a reference set for adjustment procedures. The conditions under which this new use of the standards would be possible are briefly reviewed in the paper.

(Adjustment; benchmark; cross-sections; fast reactors; integral experiments; standards)

Introduction

When I was asked to prepare a paper discussing what was the impact of ENDF standards on fast reactors, my first reaction was to answer by a four letter word - please don't misunderstand me, the four letter word was just NONE. Cooler thinking convinced me that this was perhaps not the case, that the question deserved closer scrutiny and that even a negative answer would have to be amply qualified. In any case, asking a European to report on this subject is either meant to be provocative or to invite provocation -and I decided to interpret it in this second way.

The question does of course not concern ENDF/B as a whole: anybody connected with fast reactor design, in any part of the world, will share grateful appreciation and due respect for the virtues of ENDF/B-IV in dealing with fast reactor problems. If ENDF standards help measure and evaluate nuclear data and prepare END Files, God bless them. But this is an indirect and somewhat trivial consideration; the real problem is, does the concept of neutron standards - in the sense meant in this Conference - have a more direct bearing on the real world, I apologize for the professional bias, I mean on the macroscopic world to which nuclear reactors belong?

I believe that it does - or at least that it might. But before discussing these possible impacts, at least from a European point of view, I have to venture on very slippery ground and refer to a subject which is very touchy on this side of the Atlantic: cross section adjustment, a procedure that may meet here with an adverse environment.

The Utopia of the IDAlists

In Europe we do not believe in the Happy Utopia of IDA - the Ideal Differential Approach. According to the tenets of this faith, there shall come a day (the Day of the Final Evaluation) in which all the relevant cross sections will be known to any desirable detail and degree of accuracy. By using the highly sophisticated calculational methods then available on the Utoputer (Utopian Computer) it will be possible to obtain results as accurate as needed, and an estimate of the errors to go with. Although tremendous progress has been made in nuclear data measurement and evaluation, notwithstanding the development of powerful codes, despite the fact that new breeds of bigger and faster computers appear every day on the shelves, I do not think that IDA is any closer now than it was some years ago /1/.

There are mainly two reasons behind this. The first is that reactors are not waiting for IDA to be built. Light Water Reactors are now designed and operated with methods and data that make IDAlists frown their brows. It is an upside-down world that of commercial reactor design, where diffusion performs better than transport and old data better than new ones. Still, reactors are built and do work, although basic data and methods are still unable to account for the observed temperature coefficient, to name but one.

Adjusting to Adjustment

A similar situation applies to fast reactors. Here the different time-scale, and emphasis, in Europe and in the United States may account at least partially for the difference in philosophical approach. With two demo reactors in operation and advanced work on the commercial plants, hardware is obviously attracting most of the attention and of the effort, and little space is left for fundamental research. Our reactor physicists are hardly pressed for numbers that have to go into the design, and they would become highly unpopular should answer something like "Wait a minute, I need a better cross section for hafnium, let me file it into WRENDA". We have to make use of anything that is available, which often means integral experiments. In this way one makes mistakes (who doesn't anyway?) but one also makes reactors.

Incidentally, something like this might conceivably repeat itself for fusion reactors in a not too far future, with an exchange of roles, due to the more relaxed time-scale and fundamental approach prevailing in Europe, as compared with the faster and more technologically-oriented CTR program in the United States.

The second reservation on IDA is more basic. As time goes, the amount of detail that is available on nuclear data grows tremendously, and to the reactor designer who has to use them the situation may well seem to run out of hand. We had difficulties in adjusting to the idea of 5 000 energy points for the elastic cross section of iron, when Francis Perey comes up and tells us that this is oversimplified, the cross section is much more complex and structured than that, and the amount of detail available (and needed) is one order of magnitude greater, or more. At this point of course we are unable to deal with such a hyperfine structure and the first thing we do is straightforward summation to bring the number of points down to an amenable few thousands at most. Why should then one go to such a resolution in the first place if all this information is going to be thrown away? Somebody might compare this situation with that of the designer of a capacitor for routine circuitry who is given a detailed account of the electronic levels, including Lamb shifts, of his dielectric to come out with his capacity.

A Hundred Ways to Cook a Reactor

How does all this connect with the problem of standards? Just a moment of patience. I will first disclose to you a Party Secret: the Party of Adjusters is not monolitic in Europe as it would appear from the outside. There are hidden contrasts and diverging points of view. Incidentally, our intelligence reports speak of similar divergences in the Non-Adjusters' Party of North America, but this is a different question.

European adjusters exhibit a very wide range of behavioural schemes, the extremes of which can be exemplified by the Italian Consistent Approach on one side and the Formulaire à la Française on the other (the two extremes co-existing more or less peacefully within the same joint fast reactor program). The Consistent Approach /2/ tries to take into account all the information available from the differential measurements and the theoretical models by using the results of integral experiments only to make corrections that are consistent with the original information, and therefore preserve all the physical meaning. This method implies the use of calculations for neutron diffusion or transport that are sophisticated enough not to introduce any bias. In this case, I believe one can really talk of cross-section improvement rather than adjustment (or "fudging").

The other extreme - the French formulaire or Book of Recipees /3/ - follows a route close to that used for thermal reactors. It boldly faces the fact that errors are likely to be introduced by the calculational methods commonly used in design as much as by the nuclear data, and uses integral experiments - as well as a limited set of sophisticated calculations with basic data - to generate multigroup cross-sections that are applicable to a certain range of compositions and problems to yield, by low-cost, simple calculational methods, a final result that has an accuracy estimated to be adequate for the design needs. In this context, there have been two different cross section sets for sodium according to the amount of steel or other materials present with the sodium /4/. Obviously in this case you cannot talk about improvement of cross-sections - the only thing you can say in favour of this approach is that it appears that you can design, build and operate fast reactors with it.

Standards as Fixed Points...but How Fixed?

This distinction of a variety of positions in the adjusters' front is important in order to discuss the role of neutron standards It is clear that brute-force approaches correcting for limitations in calculational methods at the same time as for uncertainties in the nuclear data have little, if any, interest in neutron standards. On the other hand, standards may play a preeminent role in the more fundamental methods. The role of standards with respect to these methods could be twofold. On one side, they could be standards for integral cross sections or reaction rates much in the same way as they are for differential measurements. On the other side, they could provide a basis for the evaluation of errors in the nuclear data, a process which is essential for sensitivity studies and uncertainty determination, and for any adjustment procedure.

Let us consider these two aspects separately. The idea of establishing a set of international standards for integral measurements has been proposed for instance by the IAEA Consultants on Reactor Dosimetry Cross Sections /5, 6/. According to the recommendations of this group the cross sections of interest for reactor dosimetry should be subdivided into two categories. Category 1 reactions are a limited set with better known cross sections, covering all the energy range of interest, and for which differential and integral measurements in the standard neutron fields are consistent within acceptable margins. Category 2 includes all the other reactions important for reactor dosimetry. The basic idea is that Category 1 cross sections should be extracted from differential measurements and evaluation, and that integral experiments in benchmark fields should only assess the validity of these evaluations - much along the classical lines of CSWG and ENDF/B in the United States; for Category 2 reactions, on the other hand, a more "European"approach is suggested. The original draft conclusions of the IAEA Consultants predicted that for most Category 2 reactions "the improvement of cross sections is expected to derive essentially from integral measurements in benchmark fields". Strong opposition from US differentialists prompted a milder formulation of improvements being "expected to derive from a combination of integral and differential measurements which should yield internally consistent data". What if they don't?
Whichever the formulation, Category 1 reactions hold a preeminent position in the procedure, and it is suggested that integral experiments in benchmark fields are aimed at measuring the ratio between Category 2 and Category 1 average cross sections in a given neutron field rather than the absolute values of the cross sections themselves. In this sense, Category 1 reactions have the role of standards.

I believe that this approach is fruitful and represents a reasonable compromise between differentialists' and integralists' points of view and that it could be usefully extended to other areas of reactor physics (and not only reactor physics: think for instance of damage cross sections) where integral experiments play an important role. The situation would be still more promising if the same standards could be used in differential and in integral experiments. This would make it much easier to reach consistency. Unfortunately, this seems impossible at least at the present time and for various reasons.

The first reason is that most, if not all, of ENDF standards are very difficult to use in an integral experiment. In most such experiments, only activation measurements are made. This rules out the use of Li, B, C and H. Even fission standards are used only indirectly with activation detectors, since energy-dependent yields must be known or assumed. The situation could be improved by the development of sufficiently precise and standardized techniques such as alpha-sensitive solid state track detectors, or helium production assay, but at the moment these are not simple, reproducible and precise enough to be used in connection with standards. Even if it were possible to measure these standards in integral experiments, it would certainly not be possible to restrict their use to the energy range for which they are defined as standards in differential measurements.

Finally, in my personal appreciation, the word "standard" carries with it some implication of stability; one would very much like to measure a length with a ruler that does not stretch and shrink during the operation. The desire to improve continuously the quality of the standards, however, implies frequent revisions of the standard cross sections, in contrast with the stability. This contrast is particularly evident for the U-235 fission cross section: the extreme direct usefulness of this cross section in

reactor calculations (as distinct from its use as a standard) on one hand results in more frequent and more accurate measurements of this cross section, on the other hand it pushes the use of new values as soon as they become available; or in other cases it encourages the adjustment procedures in order to force agreement with integral results. I know of many calculations carried out now that use recent values for this cross section, that will no doubt be reflected in ENDF/B-V but that could not be considered the standard values at the present time.

The Role of Standards in Error Evaluation

Standards also have a crucial role in the assessment of uncertainties in the integral results of calculations and in all adjustment procedures. I think this aspect has been covered in detail in the preceding paper /7/. I just want to stress the importance of an accurate assessment of the errors and of the covariance of errors in any consistent adjustment procedure. The splitting of this error in the part pertinent to the measurement relative to the standard, and in the part inherent to the standard itself, greatly helps in arriving at a consistent formulation of the errors and the correlations.

References

/1/ U.FARINELLI, "The Role of Integral Experiments in the Production of Nuclear Data for Reactor Core and Shield Design and for Irradiation Experiments", in Nuclear Data in Science and Technology, Vol.II, p.103-119, I.A.E.A., Vienna (1973)

/2/ A.GANDINI, M.PETILLI and M.SALVATORES, "Nuclear Data and Integral Measurements Correlation for Fast Reactors. Statistical Formulation and Analysis of Method: The Consistent Approach", International Symposium on Physics of Fast Reactors, Vol.II, 612, Tokyo (1973)

/3/ J.C.MOUGNIOT et al., "Review of Neutronic Considerations arising from Studies for a Proposed 1200 MWe Fast Reactor", ibid. Vol.I, paper A 44

/4/ P.BOUTEAU et al., "Formulaire de Propagation de Neutrons dans les Milieux Acier-Sodium pour les Protections de la Filière Rapide", Proceedings of the Specialists' Meeting on Sensitivity Studies and Shielding Benchmarks, p.148, Nuclear Energy Agency, Paris (1975)

/5/ Proceedings of a Consultants' Meeting on Nuclear Data for Reactor Neutron Dosimetry held at Vienna, 10-12 September 1973; I.A.E.A., Nuclear Data Section INDC (NDS)-56/6, Vienna (1973)

/6/ Proceedings of a Consultants' Meeting on Integral Cross-Section Measurements in Standard Neutron Fields for Reactor Dosimetry held at Vienna, 15-19 November 1976, I.A.E.A., Nuclear Data Section (to be published)

/7/ C.R.WEISBIN, "Propagation of Uncertainties in Fission Cross Section Standards in the Interpretation and Utilization of Critical Benchmark Measurements", this Symposium.

ABSOLUTE ^{235}U, ^{238}U, ^{237}Np FAST NEUTRON FISSION CROSS-SECTION MEASUREMENTS* †

V. M. Adamov, B. M. Alexandrov, I. D. Alkhazov,
L. V. Drapchinsky, S. S. Kovalenko, O. I. Kostochkin,
G. Yu. Kudriavzev, L. Z. Malkin, K. A. Petrzhak,
L. A. Pleskachevsky, A. V. Fomichev, V. I. Shapakov

V. G. Khlopin Radium Institute,
Leningrad, USSR

The fission cross sections of ^{235}U, ^{238}U and ^{237}Np for ^{252}Cf fission spectrum neutrons and 14.8-MeV neutrons have been absolutely measured. Coincidence method fission fragment - associated particle was used. Measurement accuracy is better than 2%. Error sources are discussed.

(Fission cross sections; absolute measurements; ^{252}Cf; fission spectrum neutrons; 14.8-MeV neutrons; ^{235}U; ^{238}U; ^{237}Np)

Absolute measurements of induced fission cross sections of ^{235}U, ^{238}U and ^{237}Np for both ^{252}Cf fission spectrum neutrons and 14.8-MeV neutrons have been made. The method of coincidence between fission events in the target of the nuclide and the particles associated with neutrons, inducing fissions, was used. For the fission spectrum neutron measurements, the neutron source was ^{252}Cf, and the associated particles were ^{252}Cf spontaneous fission fragments. Each ^{252}Cf fission fragment corresponds to $\bar{\nu}$ neutrons - a value known to a precision[1] of tenths of 1%. For the measurements on 14.8-MeV neutrons, the $T(d,n)^4He$ reaction from a neutron generator was used and the associated particles were α-particles.

The main advantages of the coincidence method are as follows: there is no need for either direct neutron flux determination or 100% efficiency of associated particle detection; the influence of slowed-down and scattered neutrons can be minimized. Additionally, in the case of 14.8-MeV neutron measurements, effects due to neutrons from other reactions are eliminated, and there is no need to determine the solid angles and other geometrical factors.

In the fission spectrum neutron measurements, the experimental set-up was used, where a flat target of a fissionable nuclide was irradiated by neutrons from a ^{252}Cf source of the smallest possible dimension. Source and target were fixed 4 mm apart with an accuracy ± 10 microns. The mass of structural materials was negligible (Fig. 1 and 2).

The double ionization current pulse chamber was used as a fission fragment detector.

The following expression was derived for calculation of fission cross sections for the ^{252}Cf fission neutrons:

$$\sigma_f = \frac{2\pi A R^2 N_f}{N_o P \bar{\nu} G K_T N_{Cf}} , \qquad (1)$$

where: σ_f - fission cross section of the measured nuclide,

N_f - number of fissions of the measured nuclide,

A - atomic weight of the measured nuclide,

N_o - Avogadro constant,

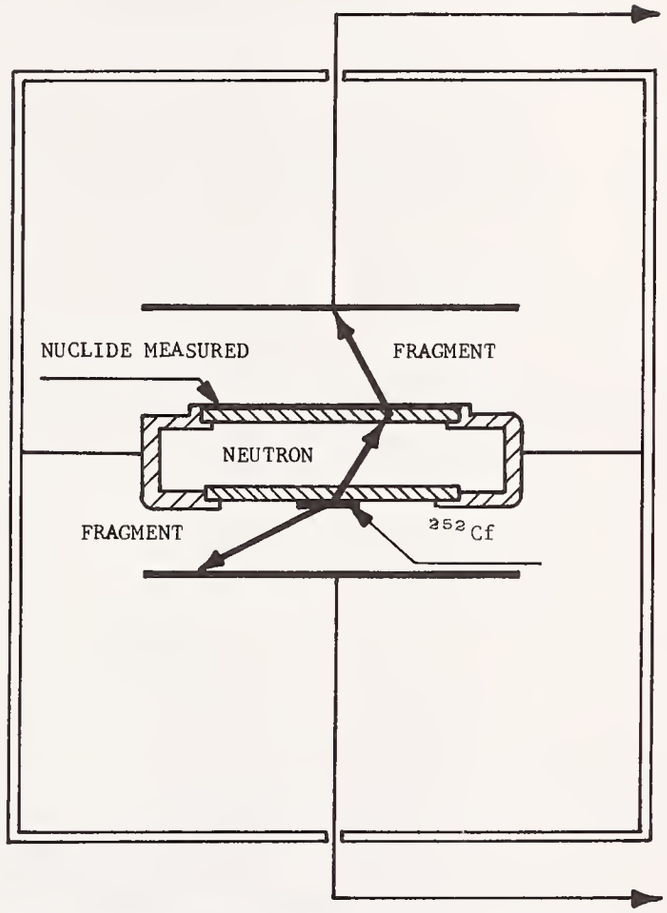

Fig. 1. Experimental geometry in the cross-section measurements for ^{252}Cf fission-spectrum neutrons.

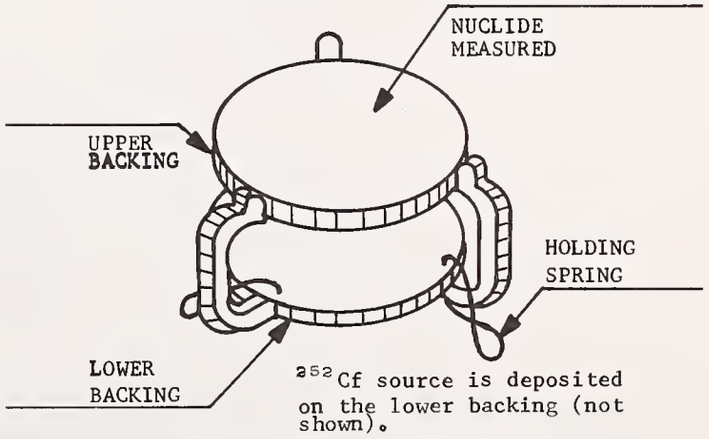

Fig. 2. Assembly for holding the ^{252}Cf source and fissionable nuclide target.

*Work supported by the International Atomic Energy Agency (Research Contract No. 1718/RB)

†This paper was not presented orally at the Conference.

P - mass of fissionable nuclide,

$\bar{\nu}$ - ^{252}Cf prompt neutrons average number,

N_{Cf} - number of ^{252}Cf fission events,

G - geometrical factor,

R - fissionable nuclide layer radius,

K_T - the correction for overlapping in the ^{252} f fission fragments channel.

The neutron flux is introduced in Eq (1) through the value of $\bar{\nu}$ (^{252}Cf) and the geometrical factor which takes into account the mutual position of the ^{252}Cf neutron source and the target.

An exact calculation of the geometrical factor requires:

(a) the fissile layer radius, the distance between ^{252}Cf layer and that of the fissile nuclide, and the thicknesses of the backing material have to be accurately determined, the layers of ^{252}Cf and of the fissile nuclide have to be strictly parallel;

(b) the layer of fissile nuclide be uniform to better than 1%;

(c) the backings be as thin as possible and their surfaces - mirror-polished;

(d) the mass of structural materials be minimized in the vicinity of the ^{252}Cf source and target.

For present experimental geometry

$$G = I_1 + I_2 + I_3 \quad , \tag{2}$$

where: I_1 - the main term, taking into account fissions by neutrons, not scattered in the backings, in case of a "point" ^{252}Cf source;

I_2 - the correction term, taking into account the ^{252}Cf source real size;

I_3 - the correction term, taking into account fissions, induced by neutrons, scattered in the backings.

Expressions for I_1, I_2, I_3 are multidimensional integrals and were calculated by numerical integration.[11] The factors in the geometrical error estimation were made by varying of formulae parameters in their error limits.

The experimental geometry in case of neutron generator is shown in Fig. 3. Associated α-particles were detected by a thin plastic scintillator. The detection angle was 165°. The fission-fragment detector was an ionization current pulse chamber. As mentioned above, there was no direct neutron flux determination. The associated alphas were detected in the solid angle defined by the input diaphragm of the detector.

Provided the two main geometrical constraints are met, 1) the solid angle of the cone of neutrons, associated with the detected alphas, is sufficiently smaller than that subtended by the fissionable deposit, and 2) the fission target nonuniformity is less than

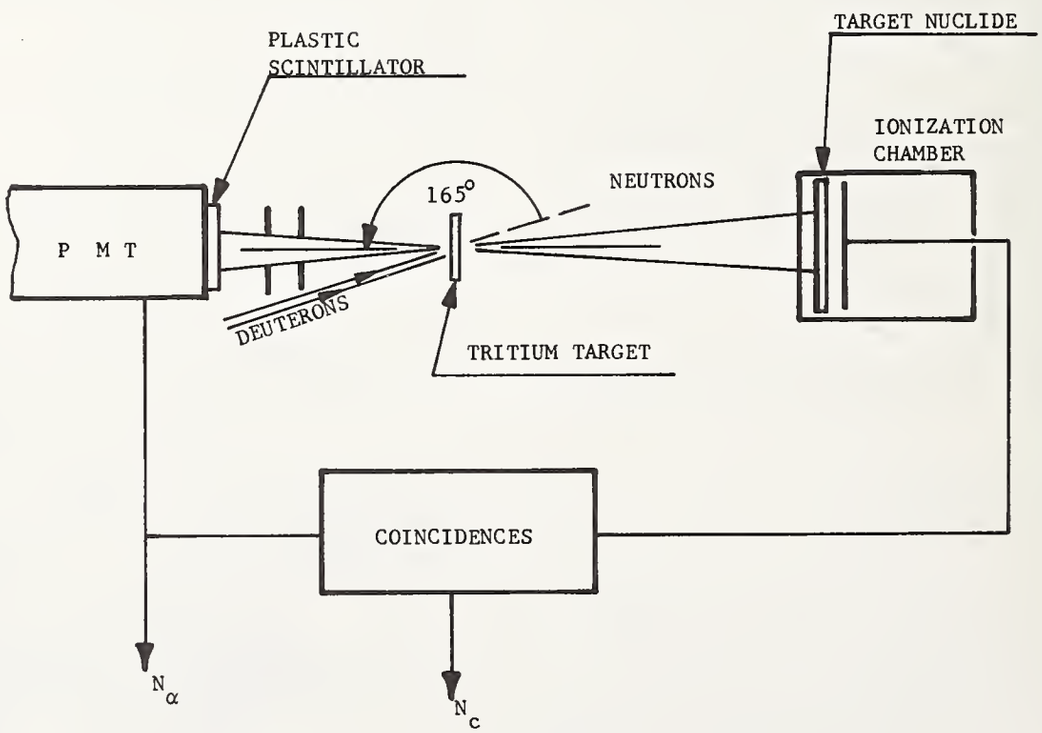

Fig. 3. Experimental geometry in 14.8-MeV neutron fission cross-section measurements.

1%; the induced fission cross section, for 14.8 MeV neutrons, σ_f is determined from the expression:

$$\sigma_f = \frac{N_c}{N_n N_\alpha (1 - \beta)(1 - \delta)} \qquad (3)$$

where: N_c - number of coincidences (without random ones),

N_α - number of associated alphas,

N_n - number of fissile nuclei per 1 cm^2,

β - correction for undetected fission fragments in 2π-geometry,

δ - neutron flux attenuation correction.

The fission-fragment detection efficiency decrease in 2π-geometry is due to counting plateau slope of ionization chamber and fission fragment absorption in the target layer. The plateau slope was determined using fragment pulse-height spectrum analysis. The fission fragment losses were calculated, taking into account fission anisotropy.

The neutron flux attenuation due to scattering and absorption on structural materials was determined both experimentally (the materials thicknesses being doubled) and by calculation in the same way as in the preceding case.

To ensure the main geometrical constraints, the ratio N_c/N_α was measured at the different distances between tritium and fission targets. These ratios were found to be constant within the errors limits for the distances used.

Two special channels for time and pulse-height spectra analysis were included in electronic equipment to distinguish the true coincidences and to improve the pules-height extrapolation to zero.

The fission targets were prepared by high frequency sputtering. The deposit nonuniformity had been checked by means of α-counting scanning and was found to be less than 1%. The masses of fissionable deposits were determined by α-counting in a 2π-ionization chamber, and with a low geometry surface-barrier detector. All the dimensions for low geometry were determined by optical methods; errors were found to be a few microns (the solid angle calculation accuracy being 0.2%). Moreover, the solid angle calculation was checked experimentally with an ^{241}Am standard source, the latter had been calibrated by the α-γ coincidence method to an accuracy 0.1%.

Isotopic analysis was carred out for all the fissionable deposits, using a semiconductor spectrometer with energy resolution 27 keV. For ^{235}U, which had impurities undistinguishable with α-spectrometry, mass-spectrometric analysis was carried out.

The following α-decay half-lives were used to calculate deposits masses:

T_α 1/2 (^{235}U) = (7.0381 ± 0.0048) x 10^8 y.[2]

T_α 1/2 (^{238}U) = (4.4683 ± 0.0029) x 10^9 y.[2]

T_α 1/2 (^{237}Np) = (2.11 ± 0.01) x 10^6 y.[3]

The sources and values of errors, associated with fission cross sections determinations, are listed in Tables 1 and 2. The fission cross sections, determined in the present work, are listed in Table 3 along with the results of other authors.

To compare the data obtained with differential measurement results, numerical calculations of ^{235}U and ^{238}U cross sections had been made for ^{252}Cf fission-spectrum neutrons, compiled differential ^{235}U and ^{238}U cross sections data being taken from ref. 4. The fission neutron spectrum had been approximated by a Maxwellian distribution with parameter, T = 1406 keV. Calculated values obtained are in a good agreement with our data. One should keep in mind, however, in this comparison, that the accuracy of compiled data is much less than that of our results.

References

1. Second IAEA Panel Meeting on Neutron Standard Reference Data, 20-24 November, 1972, IAEA, Vienna, 1972, IIIC 3.

2. A. H. Jaffey, K. F. Flynn, L. E. Glendenin, W. H. Bentley, A. M. Essling, Phys. Rev. C4, 1889 (1971).

3. F. P. Brauer, R. V. Stromatt, J. D. Ludwick, F. P. Roberts and W. L. Lion, J. Inorg. Nucl. Chem. 12, 234 (1960).

4. I. Laigner, J. J. Schmidt, D. Woll, Tables of evaluated cross sections for fast reactor materials, Karlsruhe, 1968.

5. H. T. Heaton II, J. A. Grundl, V. Spiegel, Jr., D. M. Gilliam, and C. Eisenhauer, Nuclear Cross Sections and Technology, Proc. of a Conference, Washington, D. C., March 3-7, 1975. Vol. I, p. 266.

6. J. A. Grundl, V. Spiegel, Jr., C. Eisenhauer, Trans. Amer. Nucl. Soc. 15, 945 (1972).

7. J. B. Czirr, G. B. Sidhu, Nucl. Sci. Eng. 57, 18 (1975).

8. M. G. Sowerby, B. H. Patrick, Annals of Nucl. Sci. and Eng. 1, 409 (1974).

9. M. Cancé, G. Grenier, Proc. of the NEANDC/NEACRP Specialists Meeting on Fast Neutron Fission Cross Sections of U-233, U-235, U-238 and Pu-239, June 28-30, 1976, at Argonne National Laboratory, p. 237.

10. W. Hart, UKAEA, ANS(S)R, 169 (1969).

11. V. M. Adamov, L. V. Drapchinsky, G. Yu. Kudriavzev, S. S. Kovalenko, K. A. Petrzhak, L. A. Pleskachevsky, A. M. Sokolov, Preprint Radievogo Instituta, RI - 52, Leningrade, 1976.

Table 1. The errors of data, associated with determination of fission cross sections for ^{252}Cf fission spectrum neutrons (%)

Error Sources		Nuclides		
		^{235}U	^{238}U	^{237}Np
$\bar{\nu}$ (^{252}Cf)		0.35	0.35	0.35
Geometrical factor		0.71	0.71	0.71
Mass determination at low geometry	Solid angle	0.30		0.30
	Statistics	0.35		0.45
	Part of measured isotope α-activity	0.41		0.10
	Half-life	0.20		0.47
Mass determination in 2π - geometry	Statistics		0.55	
	Extrapolation to zero pulse height		0.51	
	Absorption and scattering correction		0.30	
	Part of measured isotope α-activity*		0.30	
Number of fissions of isotope measured	Statistics	0.80	1.11	0.95
	Extrapolation to zero pulse height	0.40	0.37	0.41
	Correction for absorption in layer	0.30	0.25	0.28
	Fissions in other isotopes	0.30	0.14	
Total fission cross section error		1.44	1.68	1.59

* ^{238}U half-life error is taken into account in determination of a part of the measured isotope α-activity.

Table 2. The errors of data, associated with determination of 14.8 MeV neutron induced fission cross sections (%)

Error sources		Nuclides		
		^{235}U	^{238}U	^{237}Np
Mass determination at low geometry	Solid angle	0.35		0.35
	Statistics	0.35		0.45
	Part of measured isotope α-activity	0.41		0.10
	Half-life	0.20		0.47
Mass determination in 2π - geometry	Statistics		0.55	
	Extrapolation to zero pulse height		0.51	
	Absorption and scattering correction		0.30	
	Part of measured isotope α-activity		0.30	
Number of fissions	Statistics	1.0	1.0	1.4
	Number of random coincidences	0.20	0.20	0.20
	Neutron flux attenuation	1.0	1.0	1.0
	Extrapolation to zero pulse height	0.40	0.20	0.30
	Correction for absorption in layer	0.30	0.30	0.30
	Fissions in other isotopes	0.20	0.12	
Number of associated particles		0.05	0.05	0.05
Total fission cross section error		1.60	1.70	1.94

Table 3. Results of absolute fission cross section measurements (and comparison with other authors)

Nuclides	Fission cross sections (mb)				
	^{252}Cf fission spectrum neutrons			14.8 MeV neutrons	
	This work		Other authors	This work	Other authors
	Experiment	Calculation			
^{235}U	1266 ± 19	1281	1204 ± 29[5]	2188 ± 37	2075 ± 40 (14.6 MeV)[7] 2191 ± 40 (14.6 MeV)[8] 2063 ± 39 (14.6 MeV)[9]
^{238}U	347 ± 6	352	324 ± 14[6]	1207 ± 20	1193 ± 20 (14.6 MeV)[8] 1149 ± 25 (14.6 MeV)[9]
^{237}Np	1442 ± 23	-	-	2430 ± 47	2360 ± 90 (14.1 MeV)[10] 2500 ± 70 (14.0 MeV)[10]

NEUTRON ENERGY STANDARDS

G. D. James
UKAEA, Atomic Energy Research Establishment,
Harwell, England.

In recent years there have been several examples of discrepancy between the neutron energy scales from different spectrometers. Some of the work undertaken to review and improve neutron energy determination is noted and some suggestions on how errors can be reduced are listed. The view advocated by Youden that the only worthwhile estimates of systematic error are those made experimentally is presented. Comparison of energy determinations for a few resonances show that at best resonance energies can be quoted to an accuracy of about one in 10 000. A list of 41 narrow resonances, over the energy range 0.6eV to 12.1MeV, which should prove suitable as energy standards is given. At present, not all the energies listed are known to the highest accuracy attainable.

(Accurate neutron energy determination, energy standards)

1. Introduction

Neutron energy standards are required to help ensure that all neutron spectrometers produce data on energy scales that agree to within the estimated errors of measurements. Discrepancies in neutron energy scales, of which there have been several examples in recent years, present additional problems for evaluators and compilers, for the users of data, for example those who wish to use transmission data for the calculation of neutron shielding, and for analysts who wish to undertake a combined study of partial and total cross section data. The work required to revise and correct energy scales could be saved if a set of accurately measured resonance energies became available. These could then be checked on each spectrometer, preferably during each experiment. At least one such list has been published[1] but improvements in neutron spectrometer resolution demand that this should be revised or supplemented by much narrower resonances.

As energy measurements become progressively more accurate, several examples of energy discrepancies have arisen some of which have been successfully removed but some of which are still outstanding. A discrepancy of 20keV at 6MeV between measurements made using the $^{2}H(d,n)$ reaction compared with those made using the $^{3}H(p,n)$ reaction was explained by Davis and Noda[2] in terms of a field dependent calibration factor. More recently, a discrepancy of 25keV at 1.5MeV in the energy scale of $^{238}U/^{235}U$ fission cross section measurements as measured on white source spectrometers[3-6] was removed when inadequacies in the method of calibrating one of the spectrometers by the resonance technique were revealed and the results were revised using a direct calibration in terms of measured flight path length[7]. Measurements of the same ratio[8] using a mono-energetic Van de Graaff neutron source give results which are about 20keV above the mean of the broad spectrum measurements. A discrepancy of 7keV, again indicating that data from mono-energetic sources tend to lie higher than white sources, is presented by data on the energy of the peak of the resonance in the total cross section of ^{6}Li near 250keV. The data available on this cross section are presented in sect. 5.1. This resonance is very broad and neither it nor the ^{238}U threshold are suitable for accurate energy comparison. Nevertheless they easily reveal discrepancies which amount to about 1%. Within the group of white source spectrometers the discrepancies are not so large. Böckhoff et al.[9] have shown, however, that the energies of ^{238}U resonances below 2.7keV as measured at Geel and Columbia[10] differ by 0.1%. This difference is almost independent of energy and is equivalent to a 10cm discrepancy in the lengths of the 200m flight paths used in each experiment. This is far greater than the errors of measurement which are about 1cm or less.

As a framework for considering how to improve the measurements and comparison of neutron energies, the methods in use on three spectrometers and the random and systematic errors in each of the methods are briefly reviewed in sect. 2. Some considerations which can help to reduce inaccuracies are described in sect. 5 and the important concept of making experimental measurements of systematic errors, so ably advocated by Youden[11], is presented in sect. 4. Examples of the accuracies which are achieved in energy measurements at present are discussed in sect. 5 where the results available from transmission measurements for ^{6}Li, ^{23}Na, ^{238}U and ^{12}C are discussed. In sect. 6 a list of forty-one resonances over the energy range 0.6eV to 12.1MeV is presented. This list was drawn from examples of narrow resonances kindly suggested to me by members of an INDC sub-group on neutron energies*. It does not yet carry the imprimatur of the sub-group but it is likely that the list finally adopted will contain most if not all the resonances given in sect. 6. The establishment of a recognised list of resonances is important in that it will encourage the measurement and intercomparison of the energies of these resonances by scientists who recognise the need to establish accurate energy scales for their spectrometers. The conclusions that can be drawn from the studies presented in this paper are discussed in sect. 7.

2. Neutron resonance energy determination

Two methods of neutron energy determination are in use; those based on neutron time-of-flight and those based on the uses of mono-energetic charged particles to produce mono-energetic neutrons. The

*J. Boldeman, F. Corvi, J.A. Harvey, G.D. James, J. Lachkar, A.B. Smith and F. Voss

former require pulsed sources and spectrometers based on electron linear accelerators, cyclotrons, synchrocyclotrons and pulsed Van de Graaff machines are in operation. The latter method is based exclusively on Van de Graaff machines which alone can produce charged particle beams with energies known to sufficient accuracy. In this section the methods used to determine energy on three spectrometers which are typical of the range of instruments in use are presented so that the relative magnitudes of random and systematic errors can be more readily appreciated.

2.1 Neutron energy determination at ORELA

In the ORELA neutron time-of-flight spectrometer, short bursts of 140MeV electrons of minimum width 5ns strike a water cooled tantalum target to produce bursts of fast neutrons which are moderated in water to produce a pulsed source of neutrons covering the energy range from several MeV down to the Maxwellian spectrum at thermal neutron energy. Neutrons are detected by a detector set at a known distance from the source. Part of the interval between the time when the neutrons are produced and the time when neutrons are detected is measured and recorded by a time digitizer in units of timing channel width which have a minimum value of 2ns. Another part of the interval is determined by the delay between the electron pulse and the opening of the first timing channel - the so called initial delay. As an example[12] to illustrate the contribution of systematic and random errors, in an experiment to measure the transmissions at a path length of 155441 ± 10mm, the following equations are used to derive neutron energy E_c and the relativistically corrected energy E_R

$$E_c = \frac{72.2977(155441\text{-}10mm)}{t\text{-}(2695 \pm 2ns)}^2 \quad \ldots 1(a)$$

$$E_R = E_c(1 + 1.5965\ 10^{-9}E_c) \quad \ldots 1(b)$$

Here 2695 ± 2ns is the initial delay and t is the part of the flight time recorded on the time digitizer. Examples of the results obtained for a few selected resonances in Pb, Al, S, Na and ^{238}U are given in table 1 which gives the contribution to the quoted uncertainty made by dE_{ch}, the error in locating the peak of the resonance, dE_t the error in energy due to the 2ns uncertainty in the initial delay and dE_L the error in energy due to the 10mm uncertainty in the neutron flight path. Below the Al resonance at 5903.5eV the error is dominated by the uncertainty in flight path length. Above this energy the error is dominated by the error in locating the peak of the resonance by the fitting programme SIOB.

2.2 Neutron energy determination on the Harwell Synchrocyclotron

In the Harwell synchrocyclotron neutron time-of-flight spectrometer, pulses of protons are accelerated to an energy of 140MeV and deflected downwards to strike a 2cm thick tungsten target to produce fast neutrons by spallation. The salient features of the target and detector system are illustrated in fig. 1. Fast neutrons from the proton target reach a 2cm thick beryllium faced water moderator tank from which a pulse of moderated neutrons travels towards the detector.

Table 1

ORELA 150m Neutron Energies

Isotope	Resonance Energy (eV)	dE_{ch} (eV)	dE_t (eV)	dE_L (eV)	BNL-325[13] (eV)
^{206}Pb	3357.4 ±0.5	0.1	0.07	0.43	3360 ±10
^{27}Al	5903.5 ±0.8	0.3	0.16	0.76	5903 ± 8
^{32}S	30378 ±6	4	2	4	30350 ±90
^{23}Na	53191 ±27	26	4	7	53150 ±30
^{206}Pb	71191 ±18	14	6	9	71000 ±100
^{32}S	97512 ±28	22	10	13	96600 ±500
^{32}S	112186 ±33	27	12	14	111400 ±500
^{27}Al	257.3 ±0.3*	276	41	33	257.5 ±1.8*
^{238}U	1419.76±0.18	0.04	0.02	0.18	1419.5 ±0.3
^{238}U	2489.18±0.32	0.03	0.04	0.32	2488.4 ±0.7

*keV

Since late 1973 transmission measurements have generally been carried out using either a 2.5cm thick Li-glass detector at 50m or using a 1.2cm thick NE110 detector at 100m. The 50m measurements give results over the energy range 100eV to 100keV and the 100m measurements give results over the energy range 10keV to 10MeV. During 1974 the distances between reference marks at 1m, 4m, 13m, 49m and 98m from the neutron source were measured to better than 0.5mm accuracy by a tellurometer*. The equations used to determine neutron energy are set out in Appendix 1 where the symbols used have the following meaning. L is the distance from the face of the moderator to the point in the detector where a neutron interacts to give a detectable pulse. It is made up of the moderator face to detector face distance P and the distance D traversed inside the detector. The neutron time-of-flight is the difference between the time t_{no} when a neutron leaves the face of the moderator and the time t_n when it is detected. Using $t_{\gamma o}$, the time when γ-rays and fast neutrons leave the proton target, and t_γ when the γ-flash is detected, t can be re-stated in terms of t_1, the recorded time between the detected γ-flash in channel Xo and a neutron in channel X, t_2 the γ-ray time-of-flight over a distance L_γ, t_3 the transit time of fast neutrons from the proton target to the water moderator and t_4 the neutron slowing down time delay. The channel width is denoted by w, D_γ is distance travelled by γ-rays in the detector and S_γ is the distance travelled by γ-rays to reach the face of the moderator from which they emerge. In calculating the transit time of fast neutrons it is assumed that detected neutrons of energy E are produced by neutrons of energy 2E. The slowing down time delay is calculated from the formulae of Groenewold and Groendijk[14]. In an experiment to determine the energy of the peak of the resonance near 250keV in the total cross section of ^6Li carried out in 1974, the Li-glass detector was used, exceptionally, at 100m. In the same experiment the energies of three peak cross sections in ^{23}Na and ^{27}Al were also determined. A careful assessment of the errors arising in the measurement have been made[15] and are presented in table 2.

*Tellurometer(U.K.) Ltd., Roebuck Rd., Chessington, Surrey, England K19 1RQ
Tellurometer-U.S.A.,89 Marcus Blvd, Hauppauge,NY11787

Table 2

Harwell Synchrocyclotron 100m Neutron Energies

Isotope	Resonance Energy (keV)	dE_{ch} (eV)	dE_t (eV)	dE_L (eV)
Al-27	119.753±0.042	3	18	28
Li-6	242.71 ±0.34	330	68	58
Al-27	257.16 ±0.13	90	74	62
Na-23	299.19 ±0.12	15	97	72

2.3 Energy measurements at the Argonne Fast Neutron Generator.

Recently, Meadows[16] has undertaken a close scrutiny of the techniques involved in energy determination at the Argonne FNG when used as a source of mono-energetic neutrons. Yield curves and neutron energy spectra were calculated for some (p,n) reactions commonly used as neutron sources for energy calibration purposes. These calculations take into account the energy spread of the incident proton beam and the statistical nature of the proton energy loss. Meadows shows that when thresholds are observed by detecting neutrons at 0 deg. to the proton beam direction, the best results are obtained by plotting the square of the yield against proton energy and extrapolating to zero yield. A linear plot of neutron yield against proton energy can be in error by 1 - 2keV if the energy spread of the proton beam is large. A calibration was established by locating the $^{7}Li(p,n)^{7}Be$ threshold (1880.60 ± 0.07keV) and the $^{11}B(p,n)^{11}C$ threshold (3016.4 ± 1.6keV). Using this calibration a measurement of a carbon resonance gave the value for a mean over five target thicknesses of 2078.2 ± 2.8keV. This error allows for systematic uncertainties. The error in the mean derived from the spread of the five readings is 0.67keV. The calibration was also confirmed by a neutron time-of-flight measurement which at E_n= 2.7739 ± 0.0046MeV gives E_p = 4.4624 ± 0.0046MeV to be compared with the value E_p = 4.466 ± 0.004MeV derived from the analysing magnet calibration.

3. Reduction of uncertainties

Several techniques are available which can be used to reduce uncertainties in some of the quantities involved in the determination of neutron energy. Five of these are discussed in this section.

3.1 Effect of resolution on s-wave resonance energies

In total cross section and transmission measurements, s-wave resonances show a marked asymmetry caused by resonance-potential interference which causes a minimum on the low energy side of the resonances. With worsening energy resolution, the energy at the observed peak of the cross section, E_M, shifts to higher energy and the energy difference between the peak and the interference minimum, observed at E_m, increases. This effect is illustrated for the 299keV resonance in Na, in fig. 2 which is taken from a paper by Derrien[17]. Derrien shows that provided both E_M and E_m are known, the effects of spectrometer resolution can be allowed for to derive E_r, the energy at the resonance peak observed with perfect resolution. Values of E_r derived from six measurements of different resolution are illustrated in fig. 3. The mean of the six values of E_r is 298.65 ± 0.32keV. Even after carrying out the correction, however, only the three measurements with the best energy resolution agree within the error in the mean. Taking these three values only, the mean value of E_r is 298.550 ± 0.082keV which corresponds to an error of one in 3650. This effect of energy resolution on asymmetric s-wave resonances makes them less suitable for accurate energy comparison than symmetric resonances.

3.2 Cumulative probability plot

Fitting programmes such as SIOB in use at Oak Ridge[18] are not always available for the determination of the position of the peak of a resonance in energy or time. When the observed shape of a resonance is Gaussian, or at least close to symmetric, the error in deducing the position of the resonance peak can be considerably reduced by the use of a cumulative probability plot (ogive curve) in which, after the subtraction of a suitable background representing the neighbouring value of the data, the data (cross section, transmission or observed counts per timing channel) are treated as probability values and plotted on probability graph paper against timing channel number. The linear portion of the graph is fitted by the least squares method to derive the timing channel corresponding to the centre of the resonance at 50% probability. Half a channel must be added to the result obtained because of the binning of data into channels. This technique readily allows peak positions to be estimated to within an error of 0.1 channels or less and an example is shown in fig. 4. The extent to which the resonance shape is not normal is immediately apparent. Only the linear portion of the curve is fitted and the error derived reflects any departure from normality.

3.3 The $\Delta L/\Delta t$ method

In deriving neutron energies by the direct method set out in sect. 2.2 and in Appendix 1, it will be seen that several of the quantities involved can only be estimated with relatively large uncertainties. These quantities are the distance D traversed by a neutron within the detector before detection, the energy, transit distance and transit time, t_3, of the fast neutrons which generate the neutrons under consideration, the slowing down time delay t_4 and any difference δ, caused by differences in pulse shape, between the detection of neutrons and coincident gamma rays. It is shown in Appendix 1 that all these quantities can be removed from the equations used to determine energy if the neutron flight times t_1 and t_2 are measured with the same detector at two path lengths L_1 and L_2. However, a disadvantage of the method is that the effective path length is reduced to $\Delta L = L_1 - L_2$. In principle the method allows $(t_3 + t_4)$ to be measured but only at the expense of re-introducing the poorly known quantities D, $L_{\gamma 1}$, $L_{\gamma 2}$ and δ. However, by careful design, such as the use of thin detectors to reduce D, improved measurements of $(t_3 + t_4)$ could be made.

3.4 Y^2 - H Method

This method, described by Meadows[16], for reducing the error in determining the energy at the threshold of a (p,n) reaction has been described in sect. 2.3.

3.5 Effect of counting statistics on the energy uncertainty

In their measurement of the ^{6}Li total cross section peak energy, the statistical quality of the data was not good but James et al.[15] were able to

derive accurately the error in determining the peak energy caused by the errors in the counts per timing channel. This was done using random number (Monte Carlo) techniques to vary each measured transmission datum by an amount controlled by the normal law of errors and by the standard deviation of each datum. The data set obtained in this way was fitted and another estimate of peak cross section energy obtained. This process was repeated ten times to get a measure of the spread of the values derived. In this numerical experiment, uniform pseudo-random variates were converted to normal variates using the simple but exact Box-Müller transformation[19]. It was found that even for the broad resonance near 250keV in ^{6}Li the peak could be located to an error of 0.33keV.

4. Experimental determination of systematic errors

When a constant has been measured in several independent studies, it becomes necessary to undertake some data evaluation with the aim of determining a best value and of setting some limit to the error in this best value. In a series of papers which are models of clarity, W.J. Youden[11] has shown that the aim should be to establish 'enduring values' which are best values with an error range within which future best values will lie. By examining fifteen values of the astronomical unit measured between 1895 and 1961 and 21 measured values of the velocity of light, Youden shows that, as so often happens, the data differ from one another by more than would be expected from the ascribed estimates of uncertainty. He attributes this to a poor assessment of systematic errors and argues that the only worthwhile estimates of systematic errors are those which are made experimentally. To achieve this it should be noted that when an experiment is done at another laboratory everything gets changed whereas an investigator at one laboratory makes only minor changes to his equipment. Youden argues elegantly for making a direct experimental assessment of systematic errors by planning experiments in which everything which could make a difference to the experiment, and even a few things which are regarded as not affecting the measurement, is changed. Often the things or quantities changed will have only two descriptions or values but the benefit in bringing systematic errors to light will be immense. The time devoted to the experiments need not increase inordinately. Clearly, more will be learnt by making six changes and accumulating data for a sixth of the time after each change than if no changes are made. Youden also clearly shows that if the changes are properly planned a large reduction in the error in the mean can be achieved by changing more than one thing at a time. Many papers on the way such experiments should be planned are now available, some in the collection of Ku[20].

5. Comparison of data for certain resonances

In this section the data available on single resonances in Li, Na and C and five resonances in ^{238}U are presented. Average values derived by taking the best value from each laboratory are given and used to produce a comparison factor G which equals the mean value divided by the error in the mean. The resonances selected differ markedly from one another. The resonance near 250keV in ^{6}Li is broad and will not be used as an energy standard but it is interesting to note the accuracy achieved for the quoted peak cross section energy. This resonance also shows the importance of measuring a well defined quantity such as the energy at the maximum of the cross section rather than the value of the 'resonance energy' which appears in the theoretical expression for the cross section. The resonances in Na and ^{238}U are s-wave resonances, which in the case of Na have been corrected by Derrien for the effects of instrumental resolution, whereas the resonance in carbon has $l = 2$ and is symmetric.

5.1 The resonance in ^{6}Li total cross section near 250keV

Values of the energy at the maximum of the ^{6}Li total cross section near 250keV are available from four white source time-of-flight measurements and from four mono-energetic measurements on Van de Graaff accelerators. The data are presented in table 3 and illustrated in fig. 5 in chronological order. The data of Harvey and Böckhoff have been reanalysed using the formulae used initially by Uttley and then by James so that there is no difference in the method of analysis for the four time-of-flight values quoted. The average of these values is 244.0 ± 0.5keV corresponding to G = 488. This contrasts with the four mono-kinetic beam Van de Graaff measurements all of which lie at or above 246keV. In fairness to the early measurers it must be stated that the energy at the peak was not a prime consideration in these papers and no errors are quoted on the values given. The errors of ±1keV given in the table are judgements made by experienced workers. The value of 0.33keV given by James et al.[15] is derived from a careful assessment of all the errors involved in their measurement including, as described in sect. 3.5 above, the effect of limited counts per timing channel on the energy derived. It is likely that an experimental determination of systematic errors as advocated in sect. 4 above would lead to an upward revision of this error.

Recently a value, given preliminarily as 242 ± 2keV, has been measured by time-of-flight on a Van de Graaff in an experiment which allows the succeeding gamma flash to fall at the peak of the ^{6}Li resonance. If confirmed, this would reduce the average of all measurements made by the time-of-flight method of 243.60 ± 0.58keV.

Table 3

Neutron energy at the maximum of the ^{6}Li total cross section

Author	Year	E(max) (keV)
Hibdon & Mooring[21]	1968	246
Farell & Pineo[22]	1968	250.6
Meadows & Whalen[23]	1972	252.5
Uttley[24]	1975	*243.5 ± 1
James et al.[15]	1975	*242.71 ± 0.33
Harvey et al.[25]	1975	246 ± 1
Harvey (James)	1975	*244.8 ± 1
Böckhoff et al.[9]	1975	245.0 ± 1
Böckhoff (James)	1975	*245.0 ± 1
Knitter[26]	1976	247.0 ± 3
Average of values marked *		244.0 ± 0.5

5.2 The resonance in ^{23}Na at 298.550 ± 0.082keV

As discussed in sect. 3.1, the data available on the observed peak energy E_M for the s-wave resonance near 299keV in ^{23}Na have been corrected by Derrien[17] for the effects of instrumental resolution. The values of E_M and the values of E_r which would be observed with perfect resolution are illustrated in

fig. 3 and listed in table 4. The mean of the three values with the best energy resolution corresponds to G = 3640

Table 4

Observed and corrected peak energy values for the 298.55keV resonance in Na

Origin	E_M(keV)	E_r(keV)
Saclay II	298.94 ± 0.37	*298.39 ± 0.37
Karlsruhe	299.26 ± 0.20	*298.66 ± 0.20
Columbia	298.5 ± 1.0	297.35 ± 1.0
Harwell S.C.	299.2 ± 0.2	*298.6 ± 0.34
Cadarache	302 ± 4	299.4 ± 4.0
Saclay I	303 ± 3	299.5 ± 3.0
Average		298.65 ± 0.32
Average of values marked *		298.550 ± 0.082

5.3 Five resonances in ^{238}U

It is suggested in sect. 6 that resonances in ^{238}U could be selected for use as standard over the energy range 6eV to 3keV. The data available on five of these resonances are presented in table 6. All the measurements made at the Harwell synchrocyclotron used a Li-glass detector. A 50m measurement was made in August 1976. For other reasons, the flight path was then raised by 3cm and the source geometry was altered so that the water moderator stood in front of the proton target instead of underneath it. Energy measurements of ^{238}U resonances were then made, in November 1976, both at 50m and at 100m. Results were also derived using the $\Delta L/\Delta t$ method discussed in sect. 3.3. The $\Delta L/\Delta t$ method is based on the same data as the two other results obtained in November and the correct method of deriving the best value and an error in this best value remains to be formulated. For the present, the four results obtained for each resonance are regarded as independent and the average value is given. However, the error quoted in the average value is that for an individual reading derived from the spread of the measurements. Results from Oak Ridge for three of the resonances were not available to me when the table was prepared. An unweighted average from all laboratories together with an error in the mean derived from the spread is also given. The agreement between Harwell and Oak Ridge is well within the quoted errors and all the Harwell values are within the quoted range of the average from all laboratories. The discrepancy between Geel and Columbia has already been noted[27]. The results for the resonance at 2489.47 ± 0.5eV are illustrated in fig. 6.

5.4 The resonance in carbon at 2078.05 ± 0.32keV

The data available on the energy of the resonance in the total cross section of carbon near 2078keV are presented in table 5. Two measurements were made on the Harwell synchrocyclotron in August 1976 one using a Li-glass detector at 50m and one using an NE110 detector at 100m. The value obtained from the measurements by the $\Delta L/\Delta t$ method are also given although, with two dissimilar detectors, the distances D travelled by neutrons within the detectors are not eliminated from the equations. Source distance uncertainties are, of course, still eliminated. The measurements of Heaton et al. and of Meadows were made on Van de Graaff accelerators by the mono-energetic beam technique. All the other measurements are made by neutron time-of-flight. The excellent agreement between the two methods is clear. The three central values are quoted more precisely than the others. Taken alone these values have an average of 2078.11 ± 0.16keV corresponding to G greater than 10 000.

Table 5

Measured peak energy for the resonance in carbon at 2078.05 ± 0.32keV

Reference	Date	Energy - keV
Harwell 50m	Aug 1976	2079.2 ± 1.1
" 100m	Aug 1976	2078.31 ± 0.44
" $\Delta L/\Delta t$	Aug 1976	2077.45 ± 0.84
" Average*		2078.33 ± 0.89
Davis & Noda[2]	1969	2079 ± 3
Heaton et al.[28]	1975	2079 ± 3
James	1977	2078.33 ± 0.89
Meadows[16]	1977	2078.2 ± 2.8
Perey et al.[29]	1972	2077.8 ± 1.5
Bockhoff et al.[9]	1976	2077 ± 1
Cierjacks et al.[30]	1968	2077 ± 1
Average**		2078.05 ± 0.32

*Error in individual reading derived from spread of the data
**Error in the mean derived from spread of the data

6. Resonances for use as energy standards - a selected list

To compare the energy scales of different spectrometers and thereby help to establish accurate energy standards it is necessary that those concerned with this task should all make measurements on the same set of resonances. To promote this development the INDC set up a sub-group with the task of producing a list of suitable resonances. Seventy-six narrow resonances were suggested in the energy range 0.6eV to 12.1MeV. This list is probably too long and I have reduced it by selecting about six resonances in each decade which have the smallest value of $(\Gamma + \Delta)/E$. Here Γ is the resonance width, Δ is the Doppler width and E is the resonance energy. The reduced list of forty-three resonances is presented in table 7. The resonances are all in the total cross section of the eleven elements listed. Apart from sodium and iridium, all the elements are commonly occurring, readily available and easily fabricated into suitable transmission samples. The energies given are listed as nominal energies to emphasise the fact that they do not represent evaluated data. Nevertheless the best values of energy available are given wherever possible. No errors are given for the U-238 resonances of ref.(12) but it is known that the errors are likely to be of the order of 1 in 5000. The distribution of the resonances listed is shown in fig. 7. It will be seen that the largest gaps on a logarithmic energy scale are between 0.6eV and 6eV and between 6keV and 30keV. It may be necessary to augment the list within these ranges.

As more data become available more stringent evaluation of the energies of the resonances listed in table 7 will be possible. Evaluators may then reasonably demand that the only data to be considered are those for which full details of all steps in the

Table 6

Measured peak energies for five resonances in ^{238}U

Origin	Energy - eV				
Harwell 50m Aug 1976	145.634 ± 0.037	463.23 ± 0.12	708.44 ± 0.19	1420.12 ± 0.045	2490.16 ± 0.40
" 50m Nov 1976	145.578 ± 0.051	462.93 ± 0.15	708.62 ± 0.27	1419.56 ± 0.35	2489.96 ± 1.1
" 100m Nov 1976	145.593 ± 0.033	463.09 ± 0.12	708.09 ± 0.13	1419.80 ± 0.34	2489.26 ± 0.79
" ΔL/Δt Nov 1976	145.606 ± 0.071	463.24 ± 0.25	707.59 ± 0.29	1420.02 ± 0.46	2488.61 ± 1.54
Harwell average*	145.603 ± 0.024	463.12 ± 0.14	708.18 ± 0.45	1419.88 ± 0.25	2489.50 ± 0.71
Oak Ridge[12]				1419.76 ± 0.19	2489.18 ± 0.43
Geel[27]	145.68 ± 0.10	463.62 ± 0.20	708.59 ± 0.25	1420.7 ± 0.3	2490.8 ± 0.4
Columbia[10]	145.57 ± 0.15	462.8 ± 0.4	707.9 ± 0.4	1419.2 ± 0.3	2488.4 ± 0.7
Average**	145.617 ± 0.033	463.18 ± 0.24	708.22 ± 0.20	1419.88 ± 0.32	2489.47 ± 0.5
G	4412	1929	3541	4437	4978

*Error quoted here is that in an individual reading derived from the spread of four values
**Error in the mean derived from the spread is quoted

energy determination are published. At present, such a demand would mean that almost no resonance energy data could be evaluated.

7. Conclusion

This report has reviewed the methods of neutron energy determination in such a way as to indicate the sources of error, and methods whereby some of the errors can be reduced have been described. The errors quoted on published energy values are often derived from reasoned judgements by experienced scientists. Better estimates of the systematic errors would clearly be derived by adopting the suggestion made by Youden that as many experimental components as possible should be deliberately varied preferably more than one at a time in a planned way. From a comparison of the data available on certain resonances it appears that at best energy measurements from different laboratories agree to a fraction approaching one in 10 000. Furthermore, the work of Meadows has shown that with the development of careful methods there is no discrepancy between monoenergetic and white source measurements. A list of forty-three narrow resonances suitable for energy comparison and calibration has been drawn up which may encourage experimentalists to measure the energies of the resonances listed both as a means of improving energy standards and also as a means of keeping a continual check on the energy scales of their spectrometers. The confirmation of at least one energy from a list such as that in sect. 7 should be encouraged whenever changes are made which could result in a changed energy scale. Very few papers have been published giving the full details of energy determination which could reasonably be demanded by an evaluator. It is hoped that this situation will change and that soon energy values from fully documented published sources will be available for all the resonances used in energy intercomparisons.

Acknowledgements

I am grateful to the members of the INDC subgroup on Neutron Energy Calibration, J. Boldeman, F. Voss, F. Corvi, J. A. Harvey, J. Lachkar and A. B. Smith, for their invaluable advice, for their suggestions on suitable narrow resonances and for many of the energy values quoted in this paper. However, the sub-group has had no opportunity to comment on the reduced list presented in sect. 7 and it does not carry their imprimatur. Both J. A. Harvey and K. H. Böckhoff readily sent me their data on the total cross section of ^{6}Li so that all white source measurements could be analysed by the same method. The help given by D. K. Olsen in selecting suitable resonances in ^{238}U is greatly appreciated. His list was, however, augmented slightly and the responsibility for this rests with me.

It is a pleasure to acknowledge the interest taken in this work by Basil Rose who in the course of lively discussions suggested the use of the ogive curve method and stimulated the development of the ΔL/Δt method. Experiments on the synchrocyclotron enjoy the unstinting support of Colin Whitehead and the active participation of P. H. Bowen, A. D. Gadd, D. B. Syme and I. L. Watkins. Many of the energy calculations were carried out by A. D. Gadd.

References

1. S. Wynchank, F. Rahn, H. S. Carmada, G. Hacken, M. Slagowitz, H. I. Liou, J. Rainwater and W. W. Havens, Jr. Nucl. Sci. & Engng. 51 (1973) 119

2. J. C. Davis and F. T. Noda. Nucl. Phys. A134 (1969) 361

3. M. S. Coates, D. B. Gayther and N. J. Pattenden. Proc. 4th Conf. on Neutron Cross Sections and Technology, Schrack and Bowman (Eds.) NBS Spec. Pub. 425 Vol. 2 (1976) 568

4 J. W. Behrens and G. W. Carlson. Proc. NEANDC/NEACRP Specialist Meeting on Fast Neutron Fission Cross Sections, ANL-76-90 (ANL, Argonne, 1976) 47

5. S. Cierjacks, B. Leugers, K. Kari, B. Brotz, D. Erbe, D. Gröschel, G. Schmalz and F. Voss. Ibid. 94

Table 7

Narrow resonances suitable for use as energy standards

Energy Range (eV)	Isotope	Nominal Energy	Order*	Reference
0.1 - 1	Ir-191	0.6551 ± 0.0014	1	13
1 - 10	U-238	6.672	1	12
10 - 100	U-238	10.236	5	12
	U-238	20.864	4	12
	U-238	36.671	3	12
	U-238	66.015	2	12
	U-238	80.729	1	12
100 - 1000	U-238	145.617 ± 0.033	7	Table 5
	U-238	189.64	8	12
	U-238	311.18 ± 0.25	5	13
	U-238	397.58	4	12
	U-238	463.18 ± 0.24	3	Table 5
	U-238	619.95	2	12
	U-238	708.22 ± 0.20	1	Table 5
	U-238	905.03	6	12
1000 -	U-238	1419.88 ± 0.32	7	Table 5
10 000	U-238	1473.8	5	12
	U-238	2489.47 ± 0.5	3	Table 5
	U-238	2672.2	4	12
	Pb-206	3360 ±10	8	13
	U-238	3458.1	6	12
	U-238	4512.0	2	12
	U-238	5650.6	1	12
	Al-27	5903 ± 8	9	13
(keV)		(keV)		
10 - 100	S-32	30.378 ± 0.006	3	12
	Na-23	53.191 ± 0.027	6	12
	Si-28	67.73 ± 0.02	5	31
	Pb-206	71.191 ± 0.018	4	12
	Fe-56	90.134 ± 0.016	2	32
	S-32	97.512 ± 0.028	1	12
100 - 1000	S-32	112.186 ± 0.033	3	12
	Fe-56	266.347 ± 0.053	2	32
	S-32	412.3	1	31
	S-32	818.7	6	31
1000 - 10 000	O-16	1651 ± 2	6	13
	C-12	2078	5	33
	C-12	2818 ± 4	3	13
	O-16	3211.1 ± 1.5	1	13
	C-12	6293 ± 5	2	13
10 000 - 100 000	C-12	12100 ± 100	1	

*Order of $(\Gamma+\Delta)/E$ within an Energy Range

6. P. A. R. Evans, G. B. Huxtable and G. D. James, Ibid. 149

7. M. S. Coates - private communication 1975

8. J. W. Meadows, Ibid. 73

9. K. H. Böckhoff, F. Corvi and A. Dufrasne, NEANDC(E) 172 "U" Vol.III- EURATOM (1976) 17

10. F. J. Rahn, H. Camarda, G. Hacken, W. W. Havens, Jr., H. I. Liou, J. Rainwater, M. Slagowitz and S. Wynchank, Phys. Rev. C6 (1972) 1854

11. W. J. Youden, Technometrics 14 (1972) 1

12. D. A. Olsen, Unpublished data communicated by J. A. Harvey

13. S. F. Mughabghab and D. I. Garber, BNL325, Third Ed. Vol. 1 (1973)

14. H. J. Groenewold and H. Groendijk, Physica 13 (1947) 141

15. G. D. James, D. B. Syme, P. H. Bowen, P. E. Dolley, I. L. Watkins and M. King, Report AERE-R7919 (1975)

16. J. W. Meadows, Report ANL/NDM-25 (1977)

17. H. Derrien, Report NEANDC(E)-164-L

18. G. de Saussure, D. K. Olsen and R. B. Perez, (unpublished)

19. G. E. P. Box and M. E. Müller, Ann. Math. Statistics 29 (1958) 610

20. H. H. Ku, NBS Special Pub. 300 (1969)

21. C. T. Hibdon and F. P. Mooring, Neutron Cross Sections and Technology, NBS Special Publication 299 Vol. 1 (1968) 159

22. J. A. Farell and W. F. E. Pineo, Ibid. 153

23. J. W. Meadows and J. F. Whalen, Nuc. Sci. & Engng. 41 (1970) 351, 48 (1972) 221

24. C. A. Uttley - private communication

25. J. A. Harvey and N. W. Hill, Nuclear Cross Sections and Technology, NBS Special Publication 425 (U.S. Dept. of Commerce, NBS, Washington, 1975) 244

26. H. H. Knitter , C. Budtz-Jørgensen, M. Mailly and R. Vogt Report EUR-5726e (1977)

27. F. Corvi - private communication and ref. (9)

28. H. T. Heaton II, J. L. Menke, R. A. Schrack and R. B. Schwartz, Nucl. Sci. & Engng. 56 (1975) 27

29. F. G. Perey, T. A. Love and W. E. Kinney, Report ORNL-4823 (ENDF-178). The value quoted is derived from the data described in this report.

30. S. W. Cierjacks et al. Report KFK-1000 (1968). The value communicated by F. Voss is based on the data in this report.

31. J. A. Harvey - private communication and Report ORNL/TM-5618

32. Unpublished results from the Harwell synchro-cyclotron to be regarded as preliminary.

33. H. Weigmann, R. L. Macklin and J. A. Harvey, Phys. Rev. C 14 (1976) 1328, with errors provided by J. A. Harvey - private communication.

Appendix 1

DETERMINATION OF NEUTRON ENERGY

DIRECT METHOD

$$L = P + D$$

$$t = t_n - t_{n_o}$$

$$= (tn - t_\gamma) + (t_\gamma - t_{\gamma_o}) - (t_{n_o} - t_{\gamma_o})$$

$$= t_1 + t_2 - (t_3 + t_4)$$

$$= (x - x_o)\, w + L_\gamma/0.29979 - (\text{fast transit time} + \text{slowing down time delay})$$

$$L_\gamma = P + D_\gamma + S_\gamma$$

$$\beta = L/(t \times 0.29979)$$

$$E = 469776.3\ (\beta^2 + 0.75\beta^4)$$

$\Delta L/\Delta t$ METHOD

Perform experiment at L_1 and L_2

$$L_1 = P_1 + D$$

$$t_1 = (X_1 - X_{O1} + \delta)w + L_{\gamma 1}/0.29979 - (t_3 + t_4)$$

$$L_2 = P_2 + D$$

$$t_2 = (X_2 - X_{O2} + \delta)w + L_{\gamma 2}/0.29979 - (t_3 + t_4)$$

$$L_{\gamma 1} = P_1 + D_\gamma + S_\gamma \quad ; \quad L_{\gamma 2} = P_2 + D_\gamma + S_\gamma$$

$$\Delta L = P_1 - P_2$$

$$\Delta t = (X_1 - X_{O1})\, w - (X_2 - X_{O2})\, w + (P_1 - P_2)/0.29979$$

$$\beta = \Delta L/(\Delta t \times 0.29979)$$

$$E = 469776.3\ (\beta^2 + 0.75\beta^4)$$

Note: δ D D_γ S_γ and $t_3 + t_4$ are removed

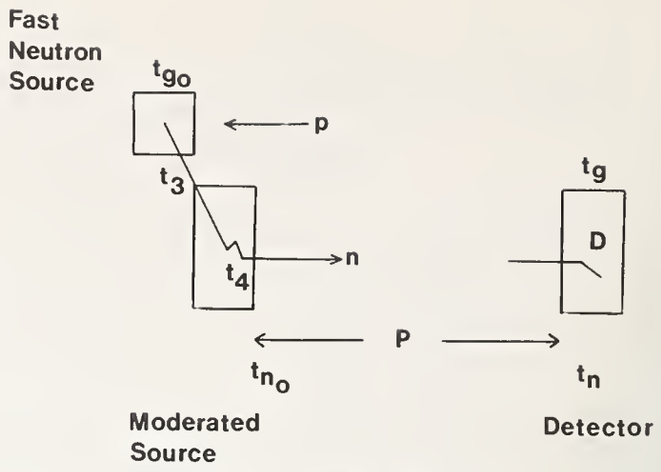

Fig. 1 Arrangement of target and detector in the Harwell synchrocyclotron neutron time-of-flight spectrometer illustrating some of the symbols used in Appendix 1.

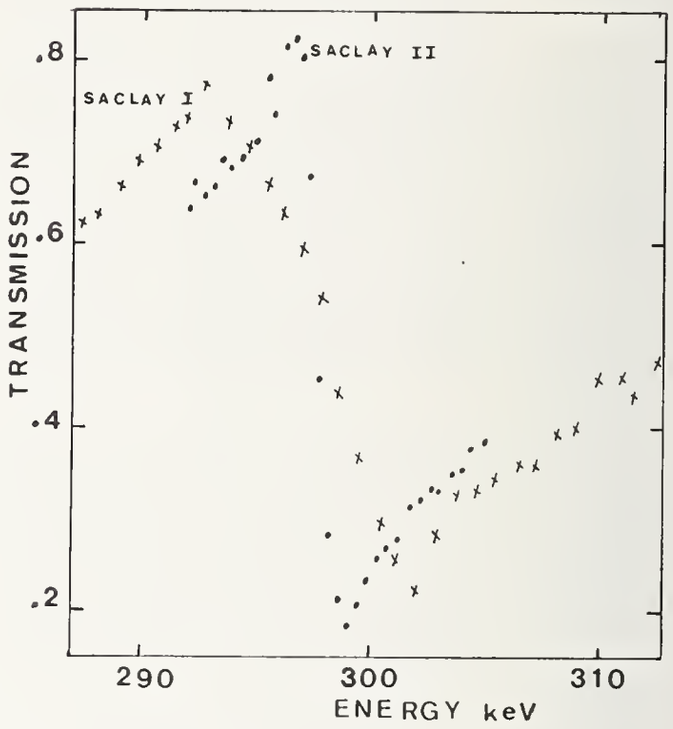

Fig. 2 The transmission of sodium near the resonance at 299keV measured with good resolution, Saclay II, and poor resolution, Saclay I, as presented by Derrien[17]. It illustrates the effect of resolution on the observed energy of the transmission maximum and minimum.

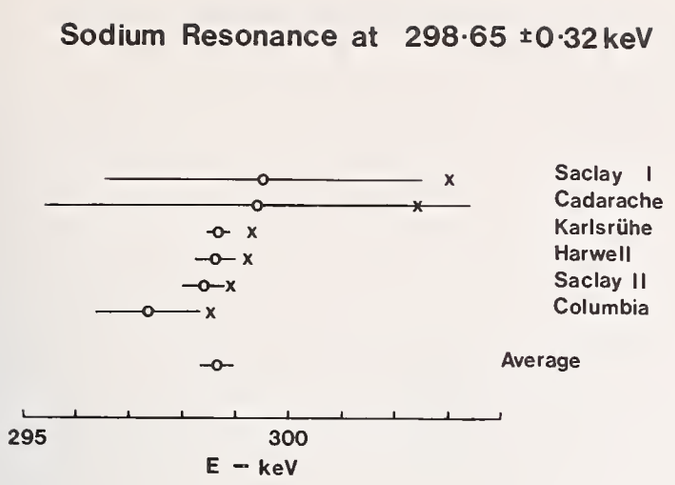

Fig. 3 The energy of the sodium resonance at 298.65 ± 0.32keV as measured in six laboratories (X) and the values obtained by Derrien[17] after correcting for the effect of spectrometer resolution (O).

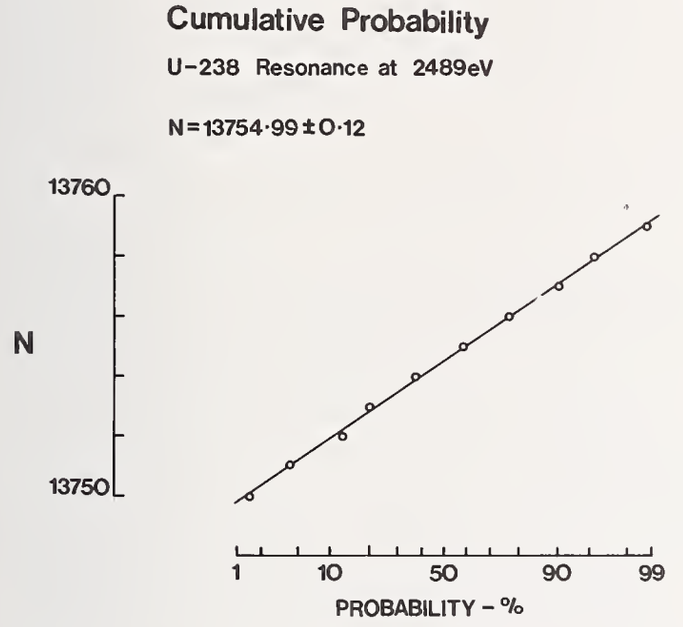

Fig. 4 Cumulative probability distribution for the transmission of a resonance in U-238 at 2489eV. A least squares fit to the data plotted on probability graph paper enables the resonance timing channel N to be located to 0.12 units.

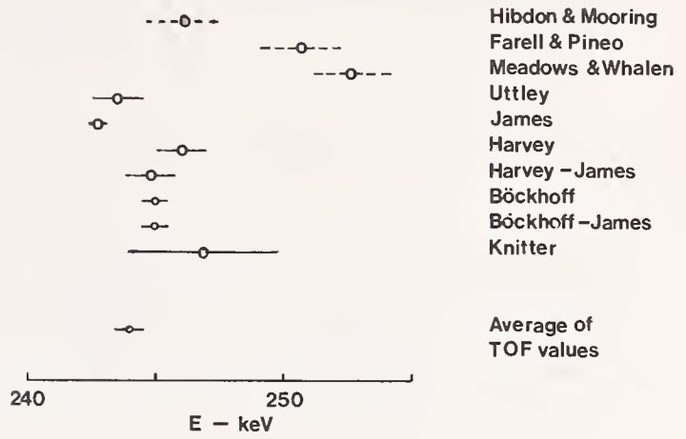

Fig. 5 Energies at the peak of the ^{6}Li total cross section near 250keV. (James) denotes results obtained after fitting the data by the formulae used by Uttley and by James. The average of results obtained by time-of-flight experiments is 244.0 ± 0.5keV

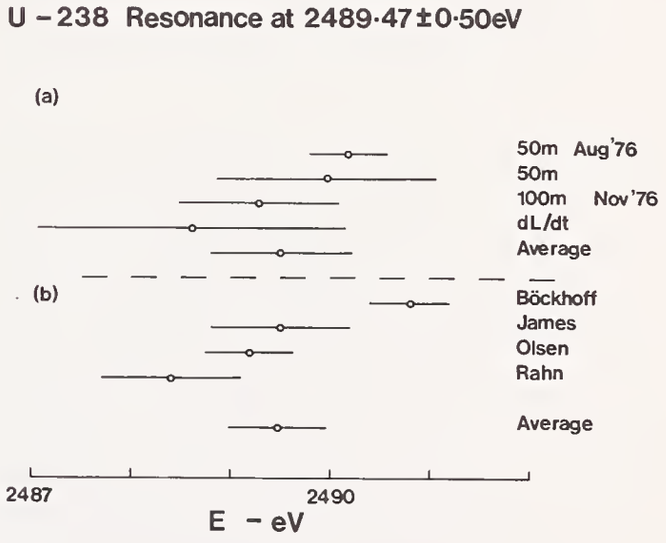

Fig. 6 An illustration of the data for the resonance in the total cross section of ^{238}U at 2489.47 ± 0.5eV presented in table 6.

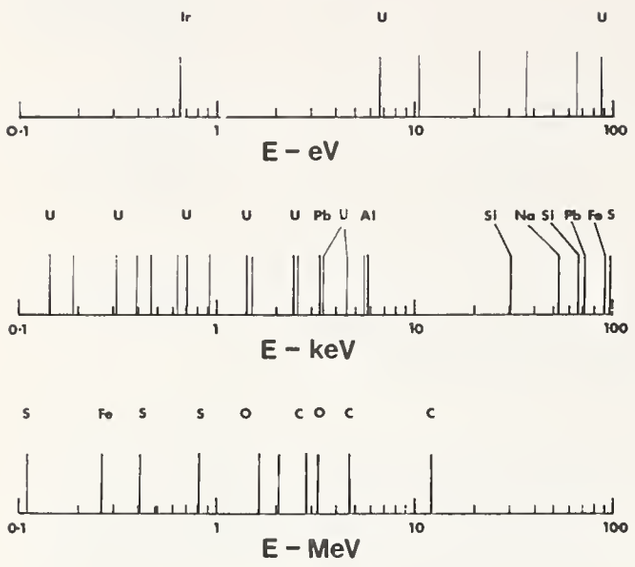

Fig. 7 Energy distribution of narrow resonances selected as suitable for use as standards. The largest relative gaps are between 0.6eV and 6eV and also between 6keV and 30keV.

NEUTRON TRANSPORT CALCULATIONS FOR THE INTERMEDIATE-ENERGY STANDARD NEUTRON FIELD (ISNF) AT THE NATIONAL BUREAU OF STANDARDS

C. M. Eisenhauer and J. A. Grundl
National Bureau of Standards
Washington, D.C. 20234

and

A. Fabry
C.E.N. - S.C.K.
2400 Mol, Belgium

The intermediate-energy standard neutron field (ISNF) established in the thermal column of the NBS reactor is designed to produce a benchmark neutron spectrum concentrated between 10 keV and 3 MeV. Design principles and physical description of the spherically-symmetric system are summarized. Neutron transport calculations of the ISNF spectrum at the center of the facility by the discrete-ordinates method are discussed and results are given for 40-group and 240-group computations. The sensitivity of the calculated spectrum to variations in important physical parameters such as material densities and carbon and boron-10 cross sections is explored.

(Benchmark spectrum; discrete ordinates; intermediate energy; measurement assurance; neutron standard; reaction rates)

Motivation and Design Principles

The Intermediate-energy Standard Neutron Field (ISNF) is an irradiation facility at NBS designed to produce a strong component of neutrons in the energy range of interest for fast neutron reaction rate technology. It is intended for use in the following measurement activities.

1. Measurement of integral fission and capture cross sections.
2. Long-term measurement assurance for neutron reaction rates required for the design and operation of power reactors.
3. Calibration of passive neutron detectors used in materials neutron dosimetry to characterize neutron fields associated with radiation effects testing.
4. Validation of neutron spectrometers and other energy-sensitive neutron detectors.

The ISNF arrangement is simple: a spherical cavity in the thermal column of the NBS reactor, a thin shell of ^{10}B lightly supported at the cavity center, and fission-source disks of ^{235}U placed symmetrically around the periphery of the cavity. The ISNF field at the center of the cavity consists of a fission-neutron component and a component of neutrons returned from the graphite, both of which are attenuated by the ^{10}B shell. The general properties of the neutron field at the center of the ISNF are as follows:

Total neutron flux	$\sim 7 \times 10^{8}$ n cm^{-2} sec^{-1}
Typical maximum fluence	$\sim 0.5 \times 10^{14}$ n cm^{-2}
Neutron field gradient	$\leq$ 2% over 4 cm
Spectrum:	
Average energy	1.0 MeV
Median energy	0.56 MeV
Energy range	90% between 8 keV and 3.5 MeV

Neutron transport in the ISNF is determined almost entirely by the ^{235}U fission neutron spectrum and by neutron scattering in carbon and neutron absorption in boron-10. In particular, the neutron spectrum at the center of the facility is governed by the kinematics of elastic scattering in carbon and by two accurately-known cross sections: σ_{tot} for carbon and σ_{abs} for boron-10. Moreover, only the energy dependence of the boron-10 absorption cross section is critical because the neutron transmission of the shells is checked experimentally with a 2-keV monoenergetic neutron beam. The one-dimensional geometry of ISNF permits calculation of the spectrum with an accuracy limited only by the uncertainties of input cross sections and densities of materials, and allows investigation of (1) sensitivity of the spectrum to variations in system parameters and (2) perturbation of the spectrum due to extraneous structural materials.

Physical Description of Facility

The initial ISNF facility has been set up in the graphite thermal column of the NBS reactor. A square opening, 30 cm x 30 cm provides access to the center of the graphite column. Split graphite blocks enclosing the ISNF cavity and containing cylindrical access penetrations may be inserted through the biological shield of the reactor and into the thermal column opening.

A detailed schematic cross section of the ISNF arrangement within the cavity is shown in Figure 1. Three levels of access are available: (1) instruments and/or irradiation samples may be inserted or removed through a 5 cm dia. cylindrical channel; (2) the boron-10 shell and the graphite pieces to which it is attached slide in a 20 cm dia. cylindrical access; and (3) the entire 30 cm x 30 cm cavity block may be withdrawn or inserted with the reactor at full power. Four of the eight ^{235}U fission source disks are indicated in symmetric array near the surface of the cavity in Fig. 1. Each disk is made of enriched uranium metal 16 mm dia. x 0.15 mm thick (93% enrichment, 0.476 or 0.511 gm each) and positioned at 1 cm from the surface of the 30 cm dia. cavity. Eight disks are used in normal operations producing a total fission neutron source strength of about 6×10^{11} sec^{-1}.

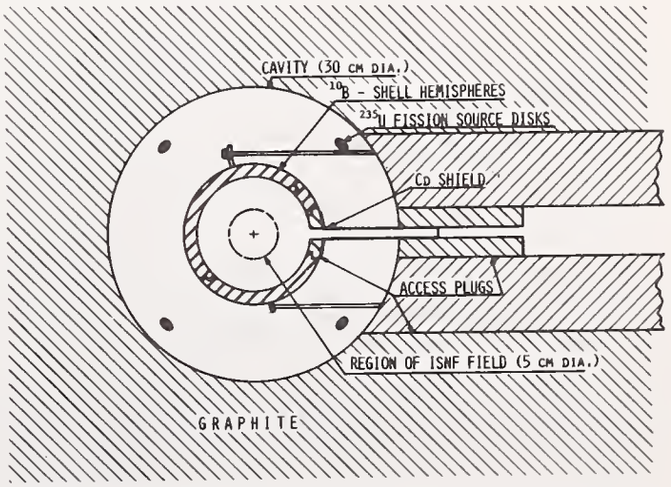

Figure 1. Intermediate-Energy Standard Neutron Field arrangement at the center of the NBS Reactor thermal column.

The crucial component of the ISNF is the boron-10 shell and serious difficulties were encountered in its fabrication. Two shells of different thickness, formed as stepped hemispheres at the Los Alamos Scientific Laboratory [1] by techniques of powder metallurgy, are now available. The shells are 14.26 cm outside diameter. The thick and thin shells have thicknesses of 1.293 cm and 0.638 cm. The mean boron-10 thickness of each shell is 1.26 and 0.61 g/cm^2. Fabrication of the shells required that a significant amount of aluminum be added to the 95%-enriched boron-10 metal powder.

TABLE I Chemical and Isotopic Analysis of Boron and Aluminum Powders [1]

Constituent	Concentration (weight%)	
	Boron-10	Aluminum
aluminum	-	99.65
boron-10	93.58	-
boron-11	4.87	-
carbon	0.6	-
silicon	0.4	0.15
iron	0.3	0.2
lead	0.1	-
uranium	0.15	-

(99.3% ^{238}U, 0.6% ^{234}U)

Table I presents an analysis of the boron and aluminum metal powders employed. Materials other than ^{10}B in and around the shell, including a protective shell of 0.7 mm thick spun aluminum metal, add up to 29 atom percent of aluminum and 4.8 atom percent of boron-11. Rings and support rods for mounting the shell in the cavity introduce another 1.4 atom percent of aluminum into the cavity. The uniformity and absolute absorber thickness of the shells is determined by means of neutron transmission measurements in the 2 keV filtered beam at the NBS reactor. Transmission measurements in the 2 keV beam for several orientations of the shell indicate that the thickness is uniform to better than 1%.

The flanged cadmium shield indicated in Figure 1, which fits over the stems of instruments placed inside the shell, prevents streaming of thermal neutrons through the hole in the shell access plug. Such streaming, particularly by epicadmium wall-return neutrons, is a characteristic problem for any driven, one-dimensional neutron field. Careful experimental investigation is required to demonstrate that the problem is under control. Shell access plugs without a hole are available to investigate this effect with passive detectors which do not involve instrument stems.

An inventory of ISNF components and their physical properties is given in Table II. Included are some characteristic nuclear parameters appropriate for the fission neutron transport problem.

TABLE II Inventory and Physical Properties of Principal ISNF Components

1. Graphite Thermal Column

--dimensions: 1.4 x 1.3 x 0.94 m^3
--graphite density: 1.71 g/cm^3
--cavity diameter: 29.8 cm

2. Boron-10 Shells [1]

--dimensions:	Thick	Thin
inside diameter:	11.68 cm	12.99 cm
outside diameter:	14.26 cm	14.26 cm
thickness	1.293 cm	0.638 cm
--densities:		
boron-10	0.975 g/cm^3	0.954 g/cm^3
boron	1.025 g/cm^3	1.002 g/cm^3
aluminum	0.992 g/cm^3	0.971 g/cm^3

--thickness in mean free paths $\Sigma_o t$ for neutrons (thick shell only; for thin shell multiply by 0.49)

	1 MeV	0.1 MeV	25 keV	2.7 keV
absorption	.025	.145	.29	.88
scattering	.30	.33	.20	.23

3. Fission Source Disks (93.5% Enriched ^{235}U Metal)

--dimensions: 16 mm dia. x 0.15 mm thick

total fission neutron source strength (8 disks, reactor at 10 MW)
$\sim 6 \times 10^{11}$ sec^{-1}

Calculation of Central Flux Spectrum (ISNF-1)

The main method for calculating the flux in the ISNF facility has been the discrete ordinates method. We have used the ANISNW version of this code which includes revisions by the Westinghouse Astro-nuclear Laboratory [2].

In making one dimensional discrete ordinates calculations of the ISNF system, certain schematizations must be made. Figure 2 gives the parameters which were used in the calculations for the thick shell. The linear diagram at the top shows the radial coordinates of ISNF-1. The ^{10}B-Aℓ shell has inner and outer radii

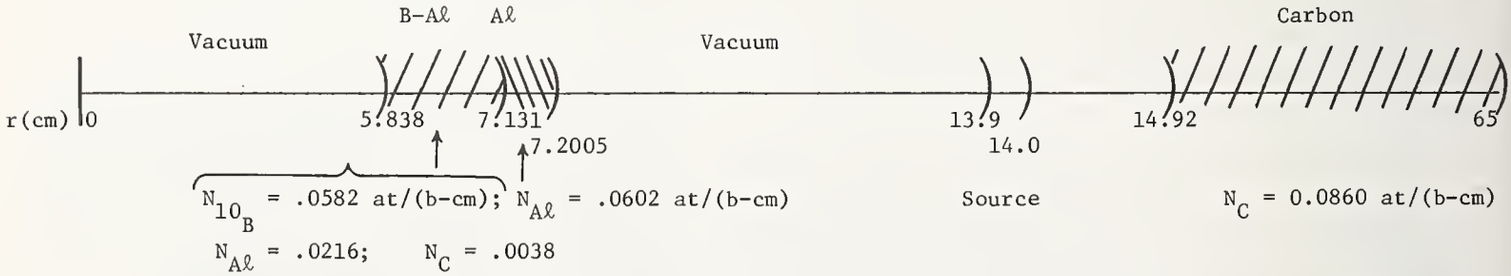

Adjustments made in Shell Composition to preserve Total Mass for Calculation in Spherical Geometry

ISNF-1 (thick ^{10}B shell)

Aℓ density = .0021 x .9916 = .9838 g/cm^3 (1.27 g/cm^2)
^{10}B density = .9747 x .9916 = .9665 g/cm^3 (1.25 g/cm^2)
Other = .0762 x .9916 = .0756 g/cm^3 (0.10 g/cm^2)

Total density 2.0259 g/cm^3
Volume = 4/3 π [(7.131)^3 - (5.838)^3] = 685.5 cm^3
Total Mass = 1388.8 g

Protective Aℓ Shell

Thickness t = 0.0695 cm
Inner Radius = 7.131 cm
Density = 2.70 g/cm^3
Mass = 4/3 π [(7.2005)^3 - (7.131)^3] 2.70 = 121 g

Figure 2. Parameters used in the one-dimensional discrete ordinates calculation of the ISNF-1 configuration.

of 5.838 cm and 7.131 cm. This is surrounded by an Aℓ protective shell with an outer radius of 7.2005 cm. The source was assumed to be distributed in a 1 mm annulus with inner radius of 13.9 cm. This assumption is justified by the fact that the field at the center of a spherically symmetric system is the same for a spherical shell source as for a number of point or thin disk sources placed at the same radius and having the same total source strength. The radius of the cavity is 14.92 cm and the carbon was assumed to extend out to a radius of 65 cm. Calculations show that neutrons reflected from graphite beyond 65 cm would add less than 0.2% to the flux above 8 eV.

The density of the various components in the B-Aℓ shell were adjusted from those provided by Los Alamos Scientific Laboratory in order to preserve the total mass (1389 g) of the two B-Aℓ hemispheres plus the heaviest of 3 access plugs. The outer radius of the protective Aℓ shell was adjusted to maintain the measured mass of 121 g.

Calculations with 40-group ENDF/B-III Cross Sections

Cross Sections

The cross sections used in calculations at NBS are based on ENDF/B-III data averaged in a 40-group energy structure. This library was derived from a 100-group set (the GAM-II structure) weighted by fine-group fluxes determined from one dimensional discrete ordinates calculations and averaged over spatial zones appropriate to the ISNF geometry.

Results

The three calculated spectra of interest at the center of the ISNF are shown in Figure 3. The quantity plotted is $E\phi(E)$ vs the log of the energy E. Thus the relative area under each histogram for any energy interval is proportional to the relative number of neutrons in that interval. The dotted histogram shows the ^{235}U fission neutron flux at the center of the ISNF. It dominates the ISNF spectrum above a few MeV.

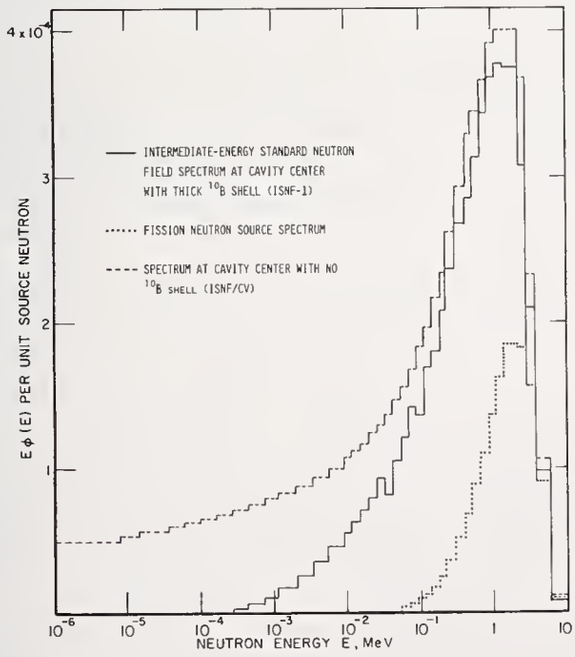

Fig. 3 Calculated central flux lethargy spectra for the intermediate-energy standard neutron field (ISNF-1), the fission neutron source spectrum, and the cavity spectrum with no ^{10}B shell (ISNF/CV).

The dashed curve shows the central spectrum (designated ISNF/CV) resulting from the addition of neutrons returned from the graphite. The spectrum below 1 MeV is greatly enhanced by the neutrons slowed down in the graphite, and below ~ 1 keV the spectrum extends smoothly down to thermal energies with a near-1/E behavior. This spectrum is realized for experiments by replacing the ISNF ^{10}B shell with a cadmium shell. The solid line shows the spectrum at the center of the ISNF facility, with the thick ^{10}B shell in place (designated ISNF-1). Here, neutrons below ~ 1 keV have been attenuated severely by absorption in ^{10}B. The corresponding group fluxes $\phi(E)\Delta E$ for the three spectra are given in Table III.

Detector responses in these three neutron spectra have been calculated with the DETAN [3] computer code. Calculated cross sections averaged over both ISNF spectra are given in Table IV for some fission detectors. Corresponding cross sections averaged over the fission spectrum are also shown. Experimental measurements are beginning to be made in the ISNF-1 configuration. Early results show an observed $^{235}U/^{238}U$ cross section ratio that is about 10% different from predictions of ENDF/B-IV tabulations. These measurements are discussed in another paper at this conference [4]. Similar discrepancies have been found for other fast reactor spectra.

Sensitivity Studies

Since the spectrum at the center of the ISNF is established by means of calculation, it is essential to assess the sensitivity of both the spectrum and integral detector responses to variations in physical and geometric parameters of the system.

^{10}B Absorption

The most important parameter for determining the shape of the ISNF spectrum below about 10 keV is the absorber thickness of ^{10}B in the B-Aℓ shell. A given uncertainty in either the ^{10}B cross section σ(b/at) or the mass thickness X(at/b) produces a larger uncertainty in the flux at low energies than at high energies because of the exponential nature of transmission of neutrons through the shell. In the calculation of ISNF-1 we have used a mass thickness of 1.25 g/cm^2 of ^{10}B and ENDF/B-III absorption cross sections. An uncertainty of 4% in the product of cross section and thickness produces an uncertainty of about 3% in the flux between 1 and 10 keV. With the 2 keV beam-transmission measurement as verification of shell thickness in mean free paths, the uncertainty in this quantity is judged to be less than $\pm$ 2%.

Graphite Density

Present measured values of the graphite density exist only for removable thermal-column stringers, because the bulk of the thermal column cannot be disassembled. Results vary from 1.67 to 1.71 g/cm^3, while the nominal value used in ISNF calculations is 1.71 g/cm^3. When the graphite density is increased by 3%, the flux in the cavity increases gradually from 0.1% at energies above 6 MeV to 2.7% at epithermal energies. This can be interpreted as a nearly uniform 2.7% increment in the cavity-return component of the flux. The corresponding increment in integral response of a ^{235}U fission foil is 1.4%, while that of a ^{238}U foil is 0.5%. Since a density change is equivalent to a change in total cross section, the error in the total cross section of carbon, presently set at $\pm$ 0.5%, would account for proportionately smaller uncertainties in flux and detector response.

TABLE III. Group Fluxes $\phi(E)\Delta E$ at Center of ISNF

Group	Upper Energy Bound (eV)	Fission Spectrum	ISNF/CV (no ^{10}B shell)	ISNF-1 (thick ^{10}B shell)
1	1.4918+07	1.03250-5	1.08436-5	9.81571-6
2	6.0653+06	4.47391-5	5.39036-5	4.89605-5
3	3.6788+06	4.68987-5	7.01945-5	6.30993-5
4	2.7253+06	3.64821-5	7.34228-5	6.66930-5
5	2.2313+06	9.21736-5	2.00399-4	1.86659-4
6	1.3534+06	3.22965-5	8.00682-5	7.60595-5
7	1.1080+06	4.04492-5	1.17128-4	1.10525-4
8	8.2085+05	2.18288-5	7.32631-5	6.86174-5
9	6.7206+05	2.61317-5	1.03554-4	9.41721-5
10	4.9787+05	1.34049-5	6.35855-5	5.70434-5
11	4.0762+05	1.51932-5	8.79786-5	8.00351-5
12	3.0197+05	1.04694-5	7.86573-5	7.08074-5
13	2.2371+05	4.84693-6	4.75933-5	4.16005-5
14	1.8316+05	5.01832-6	6.50756-5	5.39625-5
15	1.3569+05	2.27986-6	3.94921-5	3.39017-5
16	1.1109+05	2.03273-6	4.57084-5	3.39677-5
17	8.6517+04	1.39449-6	4.20754-5	3.54945-5
18	6.7380+04	9.57525-7	3.90805-5	3.02092-5
19	5.2475+04	6.54398-7	3.65123-5	2.62202-5
20	4.0868+04	4.51031-7	3.43059-5	2.02771-5
21	3.1828+04	3.08527-7	3.23951-5	2.32677-5
22	2.4788+04	2.12484-7	3.07273-5	1.98570-5
23	1.9305+04	1.45919-7	2.92581-5	1.76938-5
24	1.5034+04	9.99573-8	2.79549-5	1.57295-5
25	1.1709+04	6.87815-8	2.67891-5	1.40237-5
26	9.1188+03	7.96820-8	5.02952-5	2.28631-5
27	5.5308+03	3.75963-8	4.69476-5	1.78851-5
28	3.3546+03	1.77700-8	4.40797-5	1.31942-5
29	2.0347+03	8.38826-9	4.15821-5	9.28015-6
30	1.2341+03	3.96618-9	3.93778-5	6.11757-6
31	7.4852+02	1.87239-9	3.74039-5	3.68933-6
32	4.5400+02	8.84187-10	3.56270-5	1.97961-6
33	2.7536+02	4.17368-10	3.40149-5	9.11946-7
34	1.6702+02	1.97399-10	3.25422-5	3.42626-7
35	1.0130+02	9.31675-11	3.11880-5	9.82393-8
36	6.1442+01	4.40192-11	2.99415-5	1.95149-8
37	3.7266+01	3.06191-11	5.70116-5	1.43028-9
38	1.3710+01	4.64120-12	2.67281-5	6.66496-12
39	8.3153+00	4.10660-12	1.51313-4	2.32821-11
40	4.1400-01			

TABLE IV Spectral Indexes for ISNF and Fission Spectra

$\sigma(x)/\sigma(^{235}U)$

Reaction	^{235}U Fission	ISNF-1	ISNF/CV
$^{239}Pu(n,f)$	1.435	1.113	1.205
^{238}U (n,f)	0.238	0.0843	0.0111
$^{237}Np(n,f)$	1.064	0.480	0.0635

Source Radius

The flux at the center varies somewhat with source radius. The main sensitivity occurs at high energies where uncollided neutrons predominate. Flux changes at these energies are largely associated with the inverse-r^2 dependence. The variation below about 800 keV is generally less than 0.6% when the source radius of 13.95 cm is varied by $\pm$ 2 mm. The normal position of the sources is 1 cm from the cavity surface with an estimated uncertainty of less than 2 mm.

Scattering Anisotropy in Graphite

The effect of the angular distribution of scattering in graphite was examined by repeating the ISNF calculation with truncated P_ℓ scattering cross sections. The ratios of fluxes calculated by truncating after P_o rather than P_3, as in the usual ISNF calculations, indicate that the P_1 and P_2 components are important in determining the intensity of the scalar flux at the center. The ratio of fluxes with truncation after P_o vs. after P_3 remains constant at about 1.06 at low energies and does not reach 1.10 until a neutron energy of a few MeV is reached.

The ENDF/B-III Legendre harmonic coefficients for elastic scatter in carbon, in particular the P_1 component between 0.35 MeV and 1.35 MeV, which are responsible for lowering the flux of neutrons returned to the center of the ISNF, compared with that obtained for isotropic scatter, have not changed significantly in the ENDF/B-IV tabulation. For example, the elastic scatter in the backward direction $\sigma(-1)$ changed by only 1% at an energy of 2 MeV. Therefore difference in the ISNF central flux due to differences in scattering cross sections for carbon in ENDF/B-III and ENDF/B-IV are not expected to exceed 1%.

Aluminum in Boron Shells

The fabrication of the ^{10}B shells required that a significant amount of aluminum be included with the ^{10}B. In order to assess its effect a calculation of the spectrum at the center of the ISNF was performed with all aluminum removed. Fluxes with and without aluminum generally differ by less than 4% with the exception of energy groups where aluminum resonances scatter neutrons preferentially into an adjacent group. Variations of the spectrum due to uncertainties in the amount of aluminum actually present in the ISNF would be much smaller. The effect will be discussed in more detail in the next section.

Table V presents a summary of the effects of varying the parameters discussed above.

TABLE V. Summary of Sensitivity Studies

Parameter	Variation	Percent Effect: Group Fluxes 1-10 keV	10-100 keV	0.1-1.0 MeV	Total Flux 0.4 eV-18 MeV	Cross Section σ(n,f) ^{235}U	^{238}U
^{10}B Thickness	+ 4%	- 3.3	- 1.4	- 0.5	- 0.8	- 0.9	+ 0.8
Graphite Density	+ 3%	+ 2.4	+ 1.9	+ 1.2	+ 1.1	+ 0.3	- 0.4
Source Radius	+ 2 mm	- 0.3	+ 0.2	+ 0.0	- 0.2	- 0.1	- 0.6
Angular Distribution of Scatter in Carbon	$P_3 \rightarrow P_o$	+ 6.2	+ 6.7	+ 9.5	+ 8.3	- 0.6	- 0.3
Aluminum in ^{10}B Shell	29 → 0 atom%	+ 1.9	+ 1.8	+ 0.1	+ 1.0	+ 0.2	+ 1.2
Cross Sections and Group Structure	ENDF/B-III → IV 40 → 240	+ 1.1	+ 0.4	+ 1.5	+ 0.7	- 0.3	- 1.2

Results for 240-group Calculations

Two important limitations of the 40-group calculations are the accuracy of the ENDF/B-III cross sections and the coarse structure of the energy groups in which the cross sections and the resultant spectra are tabulated. In order to investigate these limitations calculations were performed by LaBauve and Muir [5], using ENDF/B-IV cross sections in a 240-group energy structure. They used exactly the same input parameters for dimensions and material concentrations as used in the 40-group ENDF/B-III based calculation. Table VI shows a comparison of the two calculated spectra in terms of the integral responses predicted for the total flux and several fission detectors. The largest discrepancy is 1.5% for a ^{238}U fission detector. This is a rather remarkable invariance since the 40-group calculation contains only 4 groups in the energy range in which 90% of the ^{238}U response occurs. One reason for the good agreement may be that the integral responses are calculated with the DETAN code, which transforms the histogram flux spectrum into a series of linear segments with interpolated slope in flux-vs.-lethargy.

This comparison of coarse and fine group structure is mainly a check on the group-averaging techniques used in discrete ordinates calculations, since the difference in the total cross sections of boron and carbon cross sections for ENDF/B-III and ENDF/B-IV is negligibly small. Significant differences in the angular distribution of scattering in carbon exist in the two data files, but they occur above 5 MeV where the impact on the ISNF spectrum is negligible.

Figure 4 shows the 240-group central ISNF-1 flux spectrum calculated by LaBauve and Muir. It is similar to the 40-group spectrum shown in Figure 3, except that the resonance structure due to the aluminum in the ^{10}B shell is now resolved. The effect of this structure

TABLE VI Comparison of Calculated Integral Cross Sections for 40-Group and 240-Group ISNF Spectra

	σ(b) ENDF/B-III NBS 40-Group	ENDF/B-IV LASL 240-Group	Percent Difference
Flux	.0013749	.0013850	+ .7%
$^{235}U(n,f)$	1.6362	1.6313	- .5%
$^{238}U(n,f)$	0.13798	0.13632	- 1.5%
$^{239}Pu(n,f)$	1.8176	1.8219	+ 0.2%
$^{237}Np(n,f)$	0.7834	0.7855	+ 0.3%

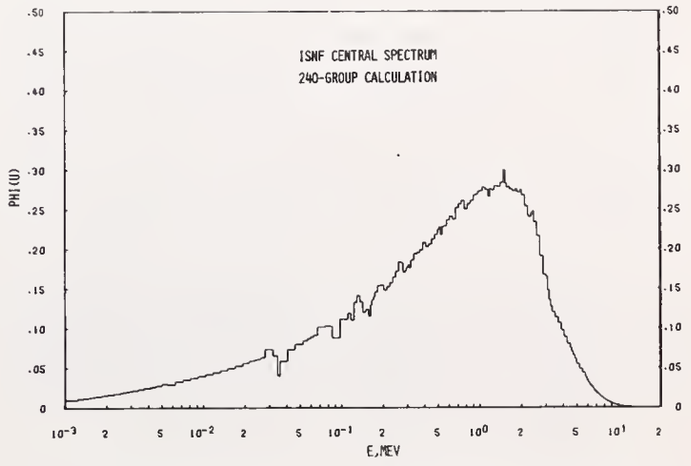

Fig. 4 Calculated Central flux lethargy spectrum for ISNF using 240-group cross sections.

on reaction rates whose energy dependence is smoothly varying in this region or for which only a small part of the response occurs in this region will be small. For example, the effect of the aluminum in the shell on the total flux is 1%; the effect on integral cross sections for wide-energy-range detectors such as $^{235}U(n,f)$ and $^{239}Pu(n,f)$ is less than 0.2%. The effect on threshold integral detectors such as $^{238}U(n,f)$ depends generally on the threshold energy. For $^{238}U(n,f)$. for which 95% of the response lies above 1.5 MeV, the effect of the shift in spectrum due to downscatter is 0.8%.

The effect of the aluminum on the flux spectrum can be interpreted almost entirely as a redistribution of elastically scattered neutrons in a localized energy range. In order to demonstrate this hypothesis, the detailed behavior of the ISNF spectrum near an aluminum resonance was calculated in a simple single scatter analysis. This was done by assuming that the effect of the aluminum could be approximated by concentrating it in an aluminum shell with an equivalent number of atoms per square cm placed just inside the boron shell. The scattering problem then is treated as resonance-energy removal of neutrons directed radially inward and inscatter of the others with a spectrum degraded in energy by the average logarithmic decrement for elastic scatter ($\xi = 0.072$). The expression for the ratio of the spectra with, and without, aluminum estimated by this procedure is

$$\frac{\text{ISNF } \omega/A\ell(\text{ISNF-1})}{\text{ISNF } \omega/o A\ell(\text{ISNF/NA})} = 1 - (1 - e^{-\Sigma_T t}) + e^{-\Sigma_T t}\,\Sigma_{el}\,t$$

Figure 5 shows the results of applying this single scattering analysis to the prominent resonance at 35 keV. [The region from 20 keV to 50 keV accounts for 6.5% of the ISNF flux.] In this figure we see the histogram representation of the smoothly varying ISNF/NA spectrum, the negative removal contribution and the positive inscatter contribution. The figure shows that the spectrum "ISNF(CALC)" obtained by single scatter analysis gives a very good representation of the ISNF-1 spectrum calculated by discrete ordinates method. The differences indicated by cross hatching in figure 5 account for about 1% of the ISNF flux between 20 keV and 50 keV.

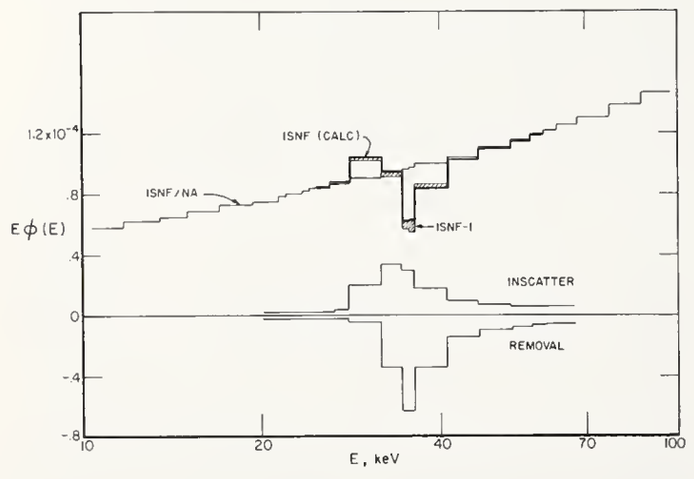

Fig. 5. Comparison of discrete-ordinates spectrum (ISNF-1) with spectrum (ISNF(CALC)) calculated by considering effect due to removal and inscatter in aluminum on slowly varying spectrum (ISNF/NA) for no aluminum. Hatched area indicated difference of two spectra.

Conclusions

The spectrum of the ISNF at NBS has been thoroughly studied by means of discrete ordinates transport calculations. Sensitivity of the spectrum and integral detector responses to variations of all significant physical parameters of the system has been investigated. For parameter variations considered realistic, spectrum changes in a coarse energy-group description are mostly less than 1% and never more than a few percent.

A quantitative assessment of the accuracy of the neutron spectrum calculated for the ISNF will be based on the sensitivity studies described in this paper, combined with a final estimate of uncertainties associated with the corresponding physical and nuclear parameters. The initial goal is to achieve a coarse (about 40 groups) specification of the spectrum that is accurate to better than $\pm$ 5% in the energy range 0.4 keV to 8 MeV. The lower bound corresponds to an energy below which the response of a 1/v-detector is less than 5% and the upper bound to the limit of good fission spectrum spectrometry data [6].

Acknowledgements

We wish to thank H. Scheinberg and J. Kostacopoulos for their efforts in the extremely difficult task of fabricating the boron-10 shell, and R. LaBauve and D. Muir for their 240-group discrete ordinates calculations of the ISNF spectrum.

References

[1] H. Scheinberg, Los Alamos Scientific Laboratory (Private Communication).

[2] R. G. Saltesz, "Revised WANL ANISN Program User's Manual", Westinghouse Astronuclear Laboratory Report WANL-TMI-1967, April, 1969.

[3] C. Eisenhauer and A. Fabry, "DETAN 74: Computer Code for Calculating Detector Responses in Reactor Neutron Spectra", available upon request from the National Bureau of Standards.

[4] D. Gilliam, et al., this conference.

[5] R. LaBauve and D. Muir, Los Alamos Scientific Laboratory (Private Communication).

[6] J. A. Grundl and C. M. Eisenhauer "Fission Spectrum Neutrons for Cross Section Validation and Neutron Flux Transfer", NBS Special Publication 425, October 1975.

STANDARDIZATION OF FAST PULSE REACTOR DOSIMETRY

A. H. Kazi
Army Pulse Radiation Facility, Aberdeen Proving Ground, Maryland 21005

E. D. McGarry
Harry Diamond Laboratories, Adelphi, Maryland 20783

D. M. Gilliam
National Bureau of Standards, Washington, D.C. 20234

A dosimetry method, developed at the National Bureau of Standards and known as the Flux Transfer Technique, is proposed for accurately determining the total fast flux in the vicinity of a fast-pulse reactor or bare-critical assembly. The method is to determine the fast flux from the comparison of free-field ^{239}Pu fission-rate measurements made at the reactor facility to calibration measurements made in a standard ^{252}Cf neutron flux. Use of the technique at the Army Pulse Radiation Facility shows that total fluxes can be measured in and near the reactor to a determinable accuracy of $\pm 5\%$. For comparison, but with less accuracy of $\pm 8\%$, the same total fluxes were verified using ^{237}Np, ^{234}U, ^{236}U and ^{238}U.

The technique has several important advantages. It uses a recognized standard neutron source for calibration. Accurate fission rates are measured and compared with dual-isotope fission chambers that are easily calibrated. The method is independent of errors in foil masses. The method does not require the use of an unfolding code and the effects of cross section errors are lessened because of the need to evaluate only cross section ratios. The method is simple and is readily amenable to absolute error analysis and interlaboratory calibrations.

(Pulse reactor calibration, neutron flux standard, dosimetry, Californium-252, radiation effects)

Introduction

Fast Pulse Reactors

Fast pulse reactors are bare, all-metal fuel critical assemblies that are operated either at steady state power or at super-prompt criticality to produce near-fission-spectrum neutrons in a microsecond time frame.[1-3] At present there are six such reactors operating in the US. They serve as sources of neutrons for a wide variety of DOD, ERDA and NASA programs, and are used extensively for TREE tests.[4] There are two non-US reactors which fall into this class: The French reactor CALIBAN[5] and a fast-pulse reactor in the USSR.[6] These reactors have the least complex physical structures of all the operating nuclear reactors, and their small sizes and lack of moderators enable them to be positioned far from neutron reflecting or moderating surfaces. Also, many of these reactors have simple geometry in-core irradiation facilities or "glory holes". All these conditions facilitate calculating spectra for direct comparison with measurement. Since most current fast pulse reactors are made of the same uranium-molybdenum fuel alloy, the in-core and free-field leakage spectra of these assemblies are expected to be nearly identical.

Neutron Dosimetry Requirements

There are three key neutron dosimetry requirements for fast-pulse reactors: (1) accurate measurement of the total neutron fluence that is delivered to a particular location; (2) high-resolution measurements of the neutron spectrum; (3) known energy dependence of the response functions characteristic of the particular phenomena being investigated.

The first two requirements are fundamental and the first is integrally related to the second through the spectrum-averaged cross sections of the neutron detectors. However, the third requirement encompasses more than neutron dosimetry, as discussed so far, and includes the response functions of the experiments of interest. Typical examples are neutron dose in tissue for biological experiments and atom-displacement damage effects in semiconductor electronics for experiments involving Transient Radiation Effects in Electronics (TREE experiments). For such experiments a spectrum measurement or calculation is required to determine a given response per unit neutron exposure. This is obtained by integrating the response function over the spectrum. For fast-pulse reactors a few reference spectrum determinations are adequate since for many response functions of practical interest the neutron fluence-to-response conversion factors are fairly weak functions of variations in fast-pulse reactor neutron spectra. This was confirmed in a sensitivity analysis performed at the Army Pulse Radiation Facility (APRF), which examined the sensitivity of various neutron response functions to realistic variations in neutron spectra encountered at fast pulse reactors.[7,8] Therefore, the key output characteristic of these reactors is the total neutron fluence which must be accurately determined for each exposure at each location. Present dosimetry is such that absolute errors in the fluence determinations are so dependent upon complex procedures and calibrations that accuracies are unknown. Furthermore, different dosimetry techniques give results that vary by 50% for the same exposure.[9,10] Obviously there is need for a standard calibration procedure. Such a standardization technique is described herein. The method was developed by the National Bureau of Standards (NBS),[11] and has been used at APRF[12] to measure total fluxes to an accuracy of $\pm 5\%$.

Flux Transfer Technique

Basic Method

Basically, the method uses a ^{239}Pu fission chamber as a flux-measurement standard after it has been calibrated against a ^{252}Cf source. The neutron-energy spectrum of a properly encapsulated ^{252}Cf deposit is the most accurately known neutron reference source available.[13,14] The fission cross section of ^{239}Pu is energy independent to within ±6% between 10 keV and 5 MeV.[15] In the absence of extraneous moderators, the fraction of neutrons with energies below 10 keV in and near a fast-pulse reactor is insignificant. Furthermore, greater than 97% of the neutrons in a fast-pulse reactor spectrum, like those in a ^{252}Cf spectrum, have energies between 10 keV and 5 MeV. All these factors, taken together, are the basis for the standardization technique.

Details of the Method

Let "r" refer to a reactor spectrum and "s" refer to the standard ^{252}Cf spectrum. For a given isotope the ratio of the fission rates, F_r/F_s is:

$$\frac{F_r}{F_s} = \frac{\sigma_r}{\sigma_s} \cdot \frac{\phi_r}{\phi_s}$$

where (σ_r/σ_s) is the ratio of the spectrum-averaged fission cross sections for the isotope of interest in the reactor and ^{252}Cf spectra, and ϕ is the flux. Note that the mass of the isotope has cancelled out of the ratio.

$$\text{Now let } K_s = \frac{\phi_s}{F_s}$$

The total flux, ϕ_r, at the reactor is therefore derived from the known ^{252}Cf flux, ϕ_s, by

$$\phi_r = K_s \cdot F_r \cdot \frac{\sigma_s}{\sigma_r}$$

Note that the equation for ϕ_r only involves the ratio of the spectrum-averaged cross sections. This ratio is more accurately known than the absolute value of either cross section, because errors in cross-section magnitudes tend to cancel from the ratio. Since the ^{239}Pu cross section is nearly flat (energy independent) over the energy range of interest, the ratio is very close to unity, typically 1.04 for a fast pulse reactor. This says that the ^{239}Pu Flux Transfer Technique is insensitive to the shape (energy dependence) of the spectrum between 10 keV and 5 MeV.

However, the cross section of ^{239}Pu is certainly not energy independent much below 10 keV. The method must therefore account for the presence of low-energy neutrons caused by structural or other extraneous material near the reactor. Herein, the technique is expanded to provide for several capabilities. First, by virtue of their dual-detector construction, the fission chambers can provide accurate ratios of various isotopic fission rates. Such ratios give information about the spectrum and are most useful in detecting spectral changes. Furthermore, the chambers may be covered with cadmium or boron-10 to demonstrate that the bare-chamber response has not been compromised by low-energy neutrons.

Fission Chambers

The fission rates are measured with dual fission chambers and a triple-scaler pulse-processing system developed by NBS. The chambers have been described in detail[11] and have been extensively evaluated at a variety of radiation sources.[16,17] Figure 1 shows a fission chamber with and without a boron-10 cover. Figure 2 shows an enlarged cross-sectional view of the chamber construction. To reduce neutron absorption and scattering effects, the electrodes and structural elements are made of aluminum and insulators are made of a hydrogen-free polymer (Teflon).

Five isotopes were used for the present measurements: ^{239}Pu; ^{237}Np; ^{234}U; ^{236}U; and ^{238}U. All deposits were 12.7mm-dia oxides vacuum evaporated on polished nickel or platinum disks of 19.1mm-dia and 0.33mm thickness. Isotope data and foil masses are summarized in Table I.

As seen in Fig. 2 the NBS double-fission chamber contains two independent fast-ionization chambers. The backings of the thin-fission deposits are back to back so that the deposits are only one millimeter apart. The chambers are operated at about 135 volts with continuous methane-gas flow. The electrical signals from the chambers have the voltage pulse height shown in Fig. 3. Note the very broad fission-fragment peak that is well separated by a low valley from the noise and alpha background, near zero pulse height. In the absence of undue electronic noise, the magnitude of the valley region is proportional to the thickness of the fission foils. The absolute efficiency of each fission chamber is near 100% for foils that are thin compared to the range of a fission fragment. Small corrections are described in Ref. 11.

Calibration

Use was made of the NBS ^{252}Cf Fission-Spectrum Irradiation Facility.[13,14] This ^{252}Cf neutron source is a 0.1-cm^3 deposit and singly encapsulated in a 0.34-cm^3 steel container. The location of the ^{252}Cf deposit in the capsule is known to within ±0.5mm relative to the surface. The source strength in February 1976 was 3.3×10^9 n/s ±1.3%. The ^{252}Cf neutron source strength was determined[18,19] with a manganous sulfate bath relative to the internationally compared radium-beryllium photoneutron source, NBS-I, presently known to ±1.1%.

For calibration, the fission chambers were mounted, two at a time, 106-mm apart on a light aluminum frame on opposite sides of the ^{252}Cf source. This is shown schematically in Fig. 4. By placing the source between two similar detectors in carefully controlled geometry, positioning errors were held to within 1.5% of the source-to-detector distance and, therefore, represent only 3% uncertainty in the ^{252}Cf calibration flux at the fission chamber. Repositioning of the source relative to the chambers can be accomplished to ±0.5mm. Prior to irradiation, all important distances can be measured without the source in place. Chamber-to-chamber distances are determined optically to ±0.5mm on a machinist's bench.

Fast Pulse Reactor Dosimetry Evaluation

The Army Pulse Radiation Facility (APRF)

The APRF reactor is representative of current generation fast-pulse, or as they are often called, fast-burst reactors. It consists of an unmoderated,

unreflected cylinder 22.6cm in diameter by 20cm high, made of 90% uranium (93.2% ^{235}U) and 10% molybdenum. The reactor is suspended from a transporter so that it can be located at floor level or as high as 14m above a borated concrete floor anywhere within, or 30m outside, a 30m dia by 26m high, low-scattering weather shield. Fig. 5 shows the reactor at 6m above the floor inside this reactor building. The APRF can be operated with two in-core irradiation facilities, called glory holes. The smaller glory hole is 38mm in useable diameter and 20cm long. The larger glory hole is 106mm in useable diameter and also 20cm long. When using the larger glory hole, the reactor is operated with reflector control.

Total Flux Measurements

The fluxes determined from ^{239}Pu fission-rate measurements are summarized in Table II. The errors quoted in the table result from a 1.3% error in the ^{252}Cf source strength, a 2.5% error in APRF power determination, a 3.3 to 3.9% combined error in the ^{252}Cf calibration factors and APRF fission-rate measurements, and a 0.7% error in effective cross-section ratio. This last error was determined from a sensitivity analysis in which the ^{252}Cf spectrum was shifted by $\pm$30 keV and the APRF spectra by $\pm$0.1 MeV and the corresponding effects on the spectrum-weighted cross-section ratios were calculated. The resultant error of 0.7% for ^{239}Pu is small, because the ^{239}Pu fission cross section is flat over the energy range of interest. As mentioned, this was the principal reason for selecting ^{239}Pu as the flux-standardization material.

Flux Measurements With Other Fissionable Isotopes

Flux measurements were also made using ^{237}Np, ^{234}U, ^{236}U and ^{238}U. The average fluxes obtained at the three locations were $1.22 \times 10^7 \pm 7.3\%$, $1.00 \times 10^8 \pm 7.3\%$ and $7.91 \times 10^7 \pm 7.3\%$ neutrons/cm^2-sec-watt respectively. The estimated errors in these measurements are based on data similar to the ^{239}Pu data, except that the cross-section ratio error is estimated at about $\pm$6%. This larger error is because approximately 40% of the neutrons in the APRF spectrum are in the energy range 600 keV to 1.5 MeV where the cross sections of these other fissionable isotopes are not energy independent like ^{239}Pu. Indeed, these other isotopes are nearly threshold functions with the ^{237}Np and ^{234}U thresholds near 600 keV, the ^{236}U threshold near 0.95 MeV and the ^{238}U threshold near 1.5 MeV. However, the total fluxes measured with all isotopes, including ^{239}Pu, agree to well within the estimated errors. This lends credence to the validity of the basic flux transfer data given in Table II. The implication is that the spectrum-averaged cross-section ratios and hence the calculated APRF spectra are satisfactory for use with detectors with threshold-type response functions.

Effects of Cadmium and $^{10}B_4C$ Shields

Fission-rate measurements were made with a 0.8mm thick cadmium-covered fission chamber containing ^{239}Pu and ^{237}Np at all three locations. The cadmium cover should eliminate any thermal neutron response of the ^{239}Pu. The measured fission rates differed by less than 0.2% from bare-chamber results, indicating the absence of any detectable thermal-neutron contribution.

Measurements were also made with a boron-covered $^{239}Pu/^{237}Np$ chamber (2.2 g/cm^2 thickness of ^{10}B). This boron shield should effectively remove all neutrons below 1 keV. The measured $^{239}Pu/^{237}Np$ fission-rate ratios were 2% below the bare chamber results. These data confirm that the APRF spectra at the selected locations have a very small low-energy (<10 keV) component. Additional verification of this fact is given in a later section.

Fission-rate measurements with boron-covered ^{237}Np in the 106mm dia glory hole are essentially a measurement of the attenuation of the flux due to the boron. This was determined to be 14.1%.

Spectral Indices

Table III compares measured and calculated spectral indices for ^{239}Pu relative to ^{237}Np and ^{237}Np relative to ^{238}U at three APRF exposure locations. Because of the close, fixed position of the two different isotopes in each fission chamber and simultaneous collection of fission rates on a dual-scaler counting system, one obtains accurate fission-rate ratios at the same time as measured fluxes. The APRF spectral indices were determined from the fission-rate ratios measured at APRF and two independent determinations of the spectral indices for $^{239}Pu/^{237}Np$ and $^{237}Np/^{238}U$ at the ^{252}Cf source. The indices for ^{252}Cf neutrons are $1.35 \pm 2.5\%$ and $4.16 \pm 2.7\%$, respectively.[20]

The data of Table III show that transport-calculated spectra and ENDF/B-IV cross sections give cross section ratios reasonably consistent with experimental data. The sensitivity of the ratios is, to first order, proportional to the difference in the low-energy thresholds of the two isotopes in the ratio. Thus agreement is expected to be better for the $^{237}Np/^{238}U$ ratio, with 600 keV and 1.5 MeV thresholds, than for the $^{239}Pu/^{237}Np$, which is primarily sensitive to spectrum behavior below 0.6 MeV. The $^{237}Np/^{238}U$ measured and calculated results are within the uncertainties of the measured results. The errors on the calculated ratios are not known as they involve absolute uncertainties in the cross sections as well as spectra.

The disagreement between measurement and calculation for the $^{239}Pu/^{237}Np$ ratio is not due to thermal neutrons, as indicated by measurements with cadmium and boron covers. For leakage-spectrum measurements, one could argue that the difference is due to the presence of neutrons scattered from external core-support structures. However, because the in-core ratios are also higher than calculated and not subject to spectral perturbations from external structures, the discrepancy is more likely to result from the calculational model.

Further Application

The evaluations, thus far, indicate that the procedures, when calibrated against a recognized-standard ^{252}Cf source, can provide a practical and acceptable technique for accurately determining total fluence and spectral indices at fast-pulse reactors. The fission chambers are not presently designed to operate in pulsed irradiations; however, there is no evidence of spectral differences between pulsed and steady-state reactor operations. In practice, fast-neutron pulsed fluence levels are determined from the ^{32}P beta radioactivity induced in sulfur. Because the sulfur reaction has a high-energy threshold, sulfur-monitored result is usually reported[21] as fluence with energy >3 MeV. The sulfur fluence is then multiplied by a previously determined (>10 keV/>3 MeV) flux ratio to yield the total fluence. In the absence of extraneous moderator, the number of neutrons with energies below 10 keV is insignificant. The required flux ratio is determined using a number of techniques including transport calculations, spectrum measurements, fission-foil analysis and spectral unfolding. The resulting flux ratios vary considerably, from 6.7 to 10.

This spread is not due to real differences in reactor spectra, but is the result of differences in measurement techniques. It is evident that there is also a need for a standard calibration procedure for sulfur-fluence monitoring.

Sulfur Fluence Measurements

For steady-state irradiations, ^{252}Cf can be used to provide a flux-transfer calibration for sulfur by the following:

$$\emptyset t_r = C_r \cdot \frac{\emptyset t_s}{C_s} \cdot \frac{\sigma_s}{\sigma_r}$$

where $\emptyset t_r$ is the fluence in spectrum "r" and C refers to the respective sulfur responses (e.g., counts/time on the beta counter used to measure the sulfur activity). The cross section ratio σ_s/σ_r refers to the ratio of the sulfur cross section integrated over the entire energy range of the spectrum.

A separate ^{252}Cf calibration of the sulfur resulted in fluxes of 8.0×10^7 n/cm^2·s·w, 1.0×10^8 n/cm^2·s·w and 1.2×10^7 n/cm^2·s·w, respectively, for the large- and small-glory hole and reactor-surface locations. There is very good agreement between these results and the total fluxes reported in Table II. The estimated error on the sulfur-monitored fluxes is ±7% and is composed of ±3.4% from the sulfur dosimetry, ±2.5% from power level normalization, and ±6% on the sulfur cross section ratio. The good agreement between the sulfur-flux values and the flux-transfer data suggest that the >3 MeV portions of the calculated APRF spectra are quite good.

Spectrum Measurement

Further confirmation of the quality of the calculated leakage spectrum is given by results of proton-recoil measurements, recently completed[22] and shown in Fig. 6. The uncertainties in the measured results in the 200 keV to 2 MeV range are approximately ±8%. Uncertainties below 200 keV increase from about ±15% at 100 keV to ±35% at the low-energy end. Assuming the calculated results (solid curve in Fig. 6) above 2 MeV, the measured-to-calculated total flux ratio above 30 keV is only 1.035. There is 21% more measured flux in the 30 keV to 200 keV interval but only 7% of the total flux is below 200 keV. This measured difference only accounts for half of the total difference in the previously discussed $^{239}Pu/^{237}Np$ spectral index.

>3 MeV Sulfur Dosimetry

Although it is not necessary for the sulfur-fluence measurement technique, it is of interest to extend the procedure to sulfur measurements of >3 MeV fluence to better evaluate the past history[10] of the 10 keV/3 MeV controversy.

Based on present knowledge of the ^{252}Cf spectrum, the fraction of ^{252}Cf flux >3 MeV is 0.237.[7] The present total-fluence sulfur-calibration results are corrected to reflect cross sections >3 MeV in the ^{252}Cf and APRF spectra. Such adjustments yield (>10 keV/>3 MeV) flux ratios for both glory holes and the leakage spectra of 8.8 ±0.6 and 7.4 ± 0.5, respectively.

Conclusions

The evaluations at APRF indicate that the procedures, when calibrated against a recognized standard ^{252}Cf source, can provide a practical, acceptable technique for accurately determining total fluence and spectral indices at fast pulse reactors. By calibrating with the ^{252}Cf source accurately positioned between two high-quality, thin-deposit fission chambers, the uncertainty in the ^{252}Cf calibration flux at the deposits can be held to ±2%. Subsequent measurements at the APRF, with ^{239}Pu fission deposits, show that free-field fluence at a fast-pulse reactor can be calibrated to an absolute accuracy of ±5%. Additional experiments with cadmium and $^{10}B_4C$ covers confirm the applicability of the Flux Transfer Technique for the situation where the neutron flux is free of low-energy neutrons. Also these results show that when the spectrum under investigation is similar to a fission spectrum, a direct neutron-flux transfer can be undertaken. For other classes of spectra, computed fission-spectrum-averaged cross sections are required to obtain a flux in the spectrum under investigation. In both cases, the neutron Flux-Transfer Technique relaxes the requirements to establish absolute activation detector efficiencies and uncertainties associated with absolute cross section scales.

Comparisons of the Flux Transfer Technique were made with ^{237}Np, several uranium isotopes and the $^{32}S(n,p)^{32}P$ reaction all calibrated against ^{252}Cf. Total fluxes from all measurements agree to within ±7%.

The technique provides several other capabilities. First, by virtue of their dual-deposit construction, the fission chambers give accurate ratios of various isotope fission rates at specified locations near reactors. Such ratios provide information about the neutron-energy spectrum and are most useful in detecting spectral changes that result from perturbations by structural materials or experiments. Second, the method may be used to establish secondary standarization of activation foils, which are suitable for neutron dosimetry during pulsed reactor operations. Such secondary standardization can be used to calibrate data obtained with unfolding codes.

Reactor neutron dosimetry includes questions of both the magnitude (total fluence) and the shape of the neutron spectrum. Sensitivity analyses, performed at APRF, indicate that for many applications the question of total fluence is paramount. This problem is satisfactorily solved with good accuracy by the present flux transfer technique. Since essentially all fast pulse reactors are similar in composition and construction, the method is proposed as a means of intercalibrating all fast-pulse reactor dosimetry. It has the tremendous advantage of being an easy task to repeat, thereby permitting periodic restandardization and interlaboratory comparison. The method is conceptually simple, accurate and readily amenable to absolute error analysis.

Acknowledgments

Credit is due to Dr. V. Spiegel for doing a large portion of the calibration work at the NBS ^{252}Cf source, Mr. Thomas Wright for assistance with data collection and computer analyses, and Lt George Davis for performing the sulfur calibrations. We also thank Mr. Charles Eisenhauer for obtaining ENDF/B cross section data and calculating the effects of energy shifts. We appreciate Mr. Robert Dallatore's careful fabrication of fission chambers and irradiation hardware and equally appreciate the many helpful suggestions given by Dr. James Grundl and the enthusiastic support of the APRF staff in operating the reactor.

References

1. Proceedings of the National Topical Meeting on Fast Burst Reactors, Albuquerque, N.M., January 1969, CONF-690102 (December 1969).

2. J. T. Mihalczo, "Superprompt-Critical Behavior of an Unmoderated, Unreflected Uranium-Molybdenum Alloy Reactor," Nuclear Science and Engineering 16:291-298 (July 1963).

3. A. H. Kazi, "Fast-Pulse Reactor Operation with Reflector Control and a 106mm Diameter Glory Hole," Nuclear Science and Engineering, 60:62-73 (May 1976).

4. R. W. Klingensmith et. al., "TREE Simulation Facilities," DNA-2432H, Defense Nuclear Agency (1973).

5. J. Cortella et. al., "Operational Characteristics of the CALIBAN Fast Pulse Reactor," pp 157-170, Proceedings of US/Japan Seminar on Fast Pulse Reactors, University of Tokyo, Takai, Ibaraki, Japan (January 1976).

6. G. G. Doroshenko et. al., "Spectra of Fast Neutrons from a Pulsed Reactor," Atomnaya Energiya, 40: 6, pp 460-464 (June 1976).

7. T. A. Dunn, A. H. Kazi, J. Saccenti, "Fluence-to-Dose Conversion Factors for APRF Fast Pulse Reactor Neutron Spectra," USA Ballistic Research Laboratory Report 1832 (September 1975).

8. A. H. Kazi, T. A. Dunn and J. C. Saccenti, "Sensitivity of Fluence-to-Dose Conversion to Changes in Fast Pulse Reactor Spectra," Proc. First ASTM-EURATOM Symposium on Reactor Dosimetry, Petten, Netherlands (September 1975).

9. F. N. Coppage, "The Influence of Dosimetry on Damage Equivalence Ratios," IEEE Trans. Nuc. Sci. NS-22, 6:2336 (December 1975).

10. J. L. Meason et. al., "The Neutron Spectral Distribution from a Godiva-Type Critical Assembly," IEEE Trans. Nuc. Sci. NS-22, 6:2330 (December 1975).

11. J. A. Grundl, D. M. Gilliam, N. D. Dudey and R. J. Popek, "Measurement of Absolute Fission Rates," Nuclear Technology 25: 237-257 (February 1975).

12. E. D. McGarry, A. H. Kazi, G. S. Davis and D. M. Gilliam, "Absolute Neutron-Flux Measurements at Fast Pulse Reactors with Calibration against Californium-252," IEEE Trans. Nucl. Sci., NS-23, 6:2002 (December 1976).

13. J. A. Grundl et. al., "A Californium-252 Fission Spectrum Irradiation Facility for Neutron Reaction Rate Measurements," Nuclear Technology 32 (3) (March 1977).

14. H. T. Heaton II, et. al., "Absolute ^{235}U Fission Cross Section for ^{252}Cf Spontaneous Fission Neutrons," Proc. of Conference, Nuclear Cross Sections and Technology, Vol I, NBS Special Publication 425:266 (October 1975).

15. J. A. Grundl and C. M. Eisenhauer, "Fission Spectrum Neutrons for Cross Section Validation and Neutron Flux Transfer," Proc. of Conference, Nuclear Cross Sections and Technology, Vol I, NBS Special Publication 425:250 (October 1975).

16. J. A. Grundl and J. W. Rogers, "Absolute Fission Chamber Measurements in CFRMF," LMFBR Reaction Rate and Dosimetry 7th Progress Report, HEDL-TME 73-31, Hanford Engineering Development Laboratory (1973).

17. D. M. Gilliam, "Integral Measurement Results in Standard Fields," paper #4. This conference.

18. R. H. Noyce, E. R. Mosburg, Jr., J. B. Garfinkel and R. S. Caswell, "Absolute Calibration of the National Bureau of Standards Photoneutron Source III Absorption in a Heavy Water Solution of Manganous Sulfate," Reactor Sci. Technol. (J. Nucl. Energy, Part A/B) 17:313 (1963).

19. V. Spiegel, Jr. and W. M. Murphy, "Calibration of Thermal Neutron Absorption in Cylindrical and Spherical Neutron Sources," Metrologia, 7:34 (1971).

20. D. M. Gilliam et. al., "Fission Cross Section Ratios in the ^{252}Cf Neutron Spectrum," Proc. of Conference, Nuclear Cross Sections and Technology, Vol I, NBS Special Publication 425:270 (October 1975).

21. T. A. Dunn, "APRF Reactor 3 MeV (Sulfur) Threshold Neutron Fluence Measurements," USA Ballistic Research Laboratories Report 1786 (May 1975).

22. E. D. McGarry, C. R. Heimbach, A. H. Kazi and G. W. Morrison, "Fast Pulse Reactor Neutron Spectrum Measurement and Calculation," IEEE Trans. Nuc. Sci. NS-24 (1977). To be published.

TABLE I

ISOTOPIC COMPOSITION AND NOMINAL MASSES
OF FISSIONABLE DEPOSITS

	TYPE OF DEPOSIT							
	Pu-239		Np-237	Np-237	U-234		U-236	U-238
MASS (MICROGRAMS)	427		265	170	30		37	175
PERCENTAGE OF ISOTOPES	Pu-239	99.978	Np-235	–	0.004	U-234	99.887	0.002	–
	Pu-240	0.002	Np-236	–	0.005	U-235	0.064	0.005	–
	Pu-241	0.005	Np-237	99.98	99.991	U-236	0.035	99.990	0.001
	Pu-242	0.005	(Pu-239)	0.02	–	U-238	0.014	0.003	99.999

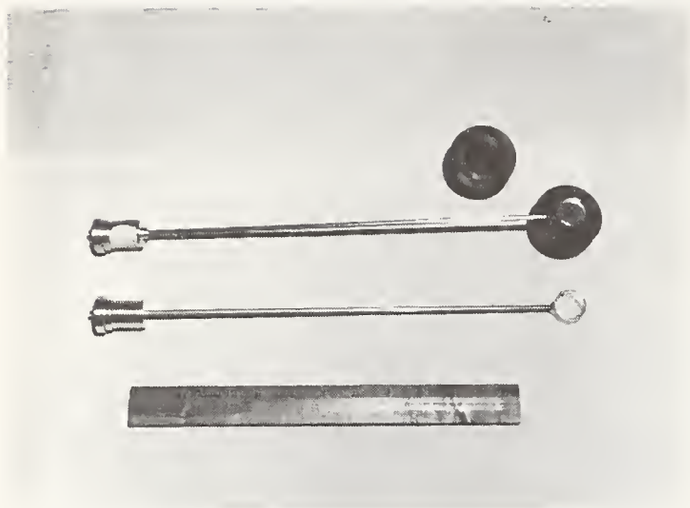

FIG. 1. NBS FISSION CHAMBER WITH AND WITHOUT BORON-10 COVER

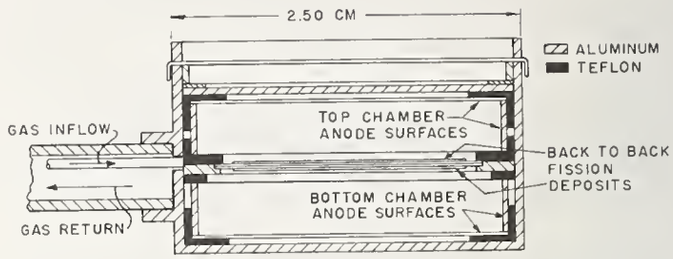

FIG. 2. CROSS-SECTIONAL VIEW OF NBS DUAL FISSION CHAMBER CONSTRUCTION

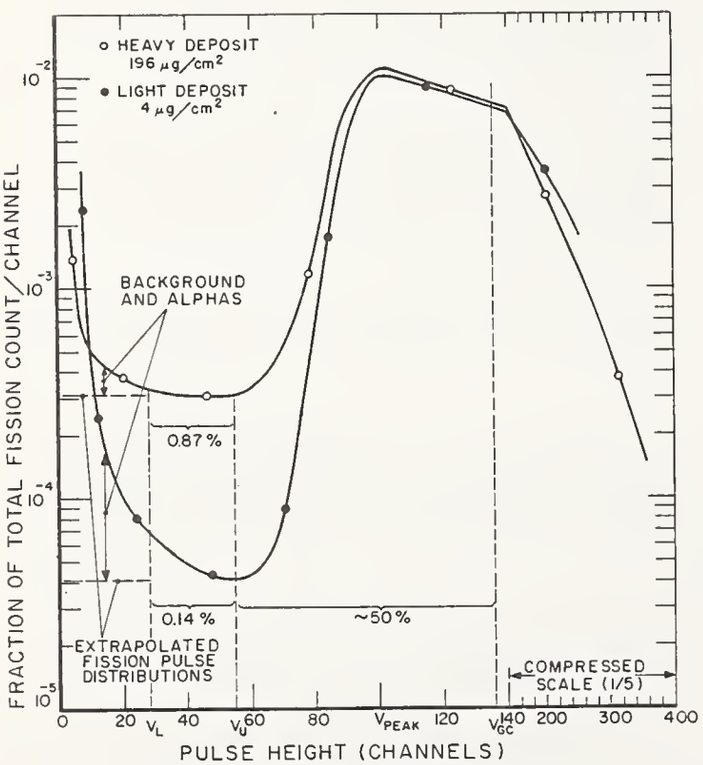

FIG. 3. FISSION FRAGMENT VOLTAGE PULSE HEIGHT DISTRIBUTION

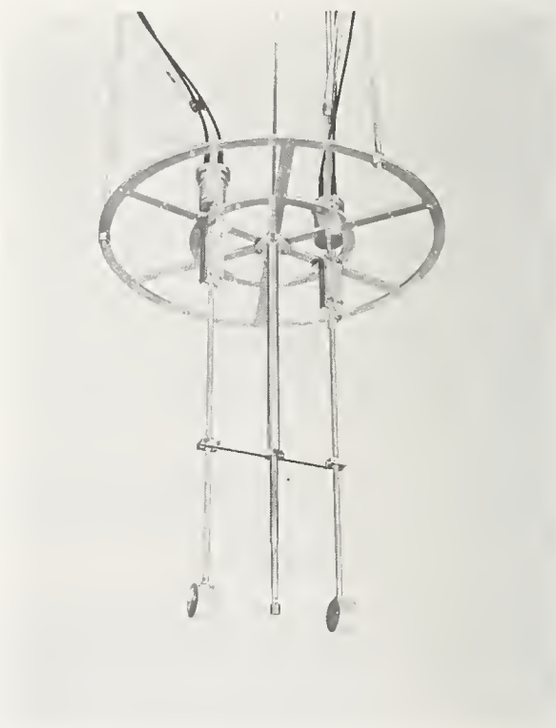

FIG. 4. GEOMETRY FOR FISSION CHAMBER CALIBRATION

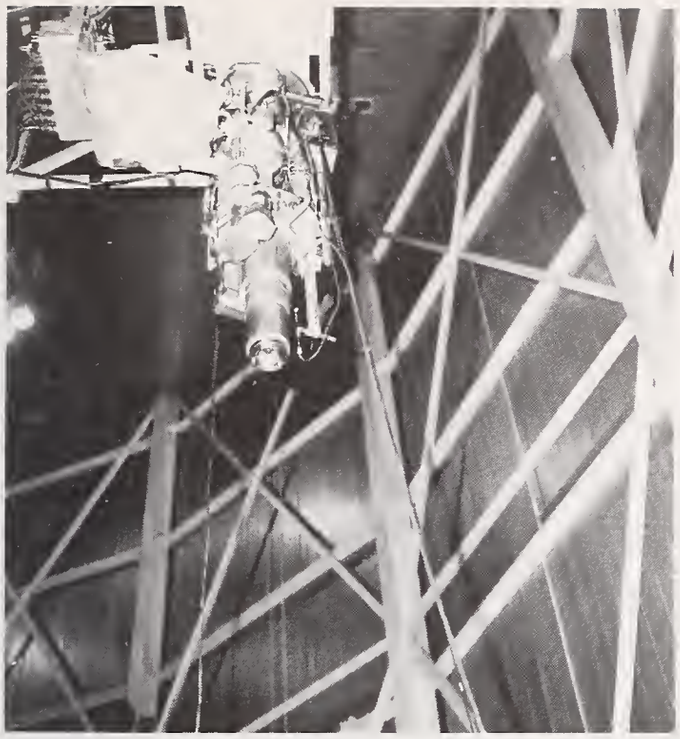

FIG. 5. APRF REACTOR POSITIONED 6 M ABOVE BORATED CONCRETE FLOOR FOR CORE SURFACE LEAKAGE FLUX MEASUREMENT

TABLE II

TOTAL APRF FLUXES MEASURED WITH PU-239 USING THE FLUX TRANSFER TECHNIQUE

EXPOSURE LOCATION	NEUTRONS /CM^2-SEC-WATT
67 MM FROM CORE SURFACE	$1.22 \times 10^7 \pm 4.4\%$
CENTER OF CORE INSIDE 38 MM GLORY HOLE	$1.04 \times 10^8 \pm 4.4\%$
CENTER OF CORE INSIDE 106 MM GLORY HOLE	$8.30 \times 10^7 \pm 4.9\%$

TABLE III - COMPARISON OF MEASURED AND CALCULATED SPECTRAL INDICES FOR THE APRF REACTOR

ISOTOPE RATIO	SPECTRUM-AVERAGED CROSS-SECTION RATIOS FOR:					
	67-MM FROM CORE SURFACE		38-MM GLORY HOLE		106-MM GLORY HOLE	
	MEASURED	CALCULATED / MEASURED	MEASURED	CALCULATED / MEASURED	MEASURED	CALCULATED / MEASURED
$\frac{^{237}NP}{^{238}U}$	5.39 ±3.4%	1.017	5.72 ±3.4%	1.000	5.77 ±3.4%	0.991
$\frac{^{239}PU}{^{237}NP}$	1.69 ±3.2%	0.929	1.78 ±3.2%	0.916	1.81 ±3.2%	0.901

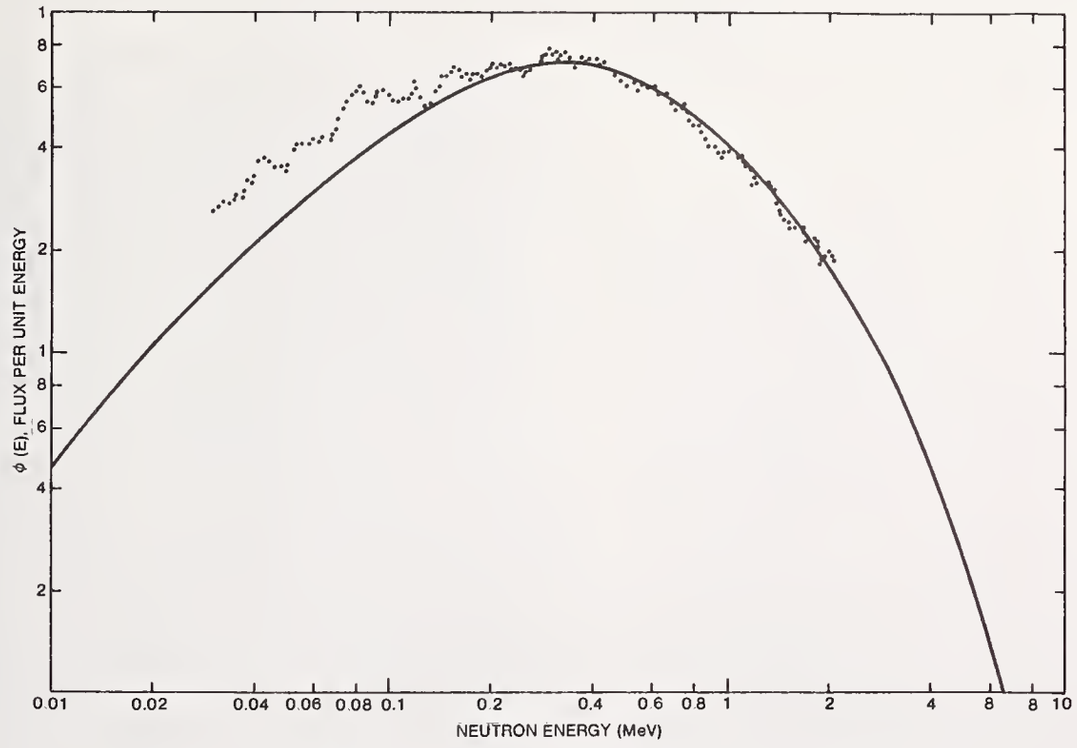

FIG. 6. MEASURED AND CALCULATED APRF NEUTRON LEAKAGE SPECTRUM

DOSIMETRY STANDARDS FOR NEUTRONS ABOVE 10 MeV

H.H. Barschall

University of Wisconsin, Madison, Wisconsin 53706

Dosimetry of neutrons in the energy range 10-50 MeV is needed for applications in radiation damage studies and in biomedical work. Dose determinations use either a fluence measurement or the Bragg-Gray principle. Better knowledge of activation cross sections, kerma factors, and energy per ion pair is needed to reduce uncertainties in dosimetry.

(Activation; Bragg-Gray; dosimetry; energy per ion pair; fluence; kerma factor; neutrons)

Introduction

This report discusses dosimetry standards for neutrons in the energy range 10-50 MeV with special emphasis on 14-MeV neutrons. Neutron dosimetry in this energy range is of importance for applications to studies of radiation damage in various materials and to biomedical work.

The effect of 14-MeV neutrons on materials is under intense study for the design of fusion reactors, in particular for the choice of a material for the first wall of the reactor.[1] Radiation damage problems are expected to be much more severe in fusion reactors than in fission reactors because of the much larger reaction cross sections for the neutrons of higher energy. Production of hydrogen and helium by nuclear reactions is likely to produce swelling, blistering, and embrittlement, and generally new elements produced in transmutations may affect the mechanical properties of the materials adversely.

In the biomedical area the interest in dosimetry used to be restricted to applications in radiation protection. More recently the interest has shifted to radiotherapy[2] where much higher accuracy is needed. If the dose administered to a tumor is 5% too low, the cure rate is greatly reduced, while a 5% too large dose may result in severe side effects.

Definitions

Both material scientists and radiobiologists wish to correlate observed effects and radiation dose. Dose is defined[3] as the energy imparted by ionizing radiation to the matter in a volume element, divided by the mass in that volume element. Dose differs in general from a similar quantity, kerma(K), which is defined[3] as the sum of the initial kinetic energies of all the charged particles liberated by indirectly ionizing particles in a volume element divided by the mass in that volume element. For neutrons kerma and dose differ primarily near the surface of the irradiated material within a distance of the order of the range of the secondary charged particles in the material. Both kerma and dose are measured in grays (1 Gy = 1 J/kg), although the older unit, the rad, is still more widely used (100 rad = 1 Gy). Another quantity related to the dose is the neutron fluence Φ. The neutron fluence is defined as the track length of all the neutrons in a volume element divided by the volume, and it determines the number of nuclear reactions in that volume. Kerma and fluence are related by the kerma factor, which is defined as the kerma per unit fluence. The kerma factor depends only on the nuclear constants of the material. For a single element of atomic weight A

$$K/\Phi = \frac{N}{A} \sum_i \sigma_i \bar{E}_i$$

where N is Avogadro's number and σ_i is the partial cross section for producing charged particles of average kinetic energy $\bar{E}_i$.

Neither dose, nor kerma, nor fluence are, however, good measures of either the radiation damage or of the biological effects induced by neutrons. As mentioned before, the radiation damage is strongly influenced by the gas production and transmutation cross sections which vary rapidly with neutron energy. When a material scientist says that a sample has been exposed to a certain neutron dose, he usually means fluence, not dose. If one looks at the Dosimetry File[4] published by the National Neutron Cross Section Center, one finds only neutron cross sections which might help to determine fluences, but there is no information in the Dosimetry File on how to get dose; in fact, the word dose appears only in the title. On the other hand, engineers who design fusion reactors need to know the dose in calculations of both nuclear heating and shielding.

For biomedical studies the dose is the quantity which is always quoted. In order to take into account the biological effect of the dose the radiobiologist multiplies the dose by the Relative Biological Effectiveness (RBE).

Measurement of Fluence

Neutron fluence can be measured most easily for a parallel beam of monoenergetic neutrons, for example, at a distance of, say, 50 cm from a small source of DT neutrons. In radiation damage studies the needed fluence is so high that small samples have to be placed as close to the neutron source as possible. In this geometry the neutrons are neither monoenergetic nor monodirectional, since the neutron energy varies with direction of emission, and the sample has a diameter equal to, or smaller than, the size of the source. In such experiments thin foils of an activation detector serve to determine neutron fluence and are placed around the sample that is under study.

The principal requirements for the activation detector are that it must have a half life longer than the time of bombardment, and that the resulting activity can be counted absolutely. In addition, the reaction that produces the activity should have a threshold not too far below the neutron energy being studied, and it should have a cross section that varies slowly with neutron energy in the energy range of interest. Three reactions which are frequently used are listed[5] in Table I. The (n,2n) reactions have thresholds around 10 MeV, the (n,p) reaction is exoergic, but has an effective threshold near 2 MeV. The Nb(n,2n) reaction is preferred for 14-MeV neutrons.

The absolute counting of the resulting activities does not introduce as much uncertainty as the lack of knowledge of the reaction cross sections.

The only neutron cross section that is accurately known for fast neutrons is the n-p scattering cross section, and most absolute reaction cross section measurements are comparisons with the n-p scattering cross section. The best known reaction cross section is probably the fission cross section of ^{235}U. Fig. 1, taken from a report on a specialists' meeting,[6] shows

TABLE I

Activation Reactions used in Dosimetry

Reaction	Q(MeV)	$T_{1/2}$(days)	γ(MeV)
$^{58}Ni(n,p)^{58}Co$	0.39	70.8	0.81
$^{59}Co(n,2n)^{58}Co$	-10.5	70.8	0.81
$^{93}Nb(n,2n)^{92}Nb^{m}$	-8.95	10.2	0.93

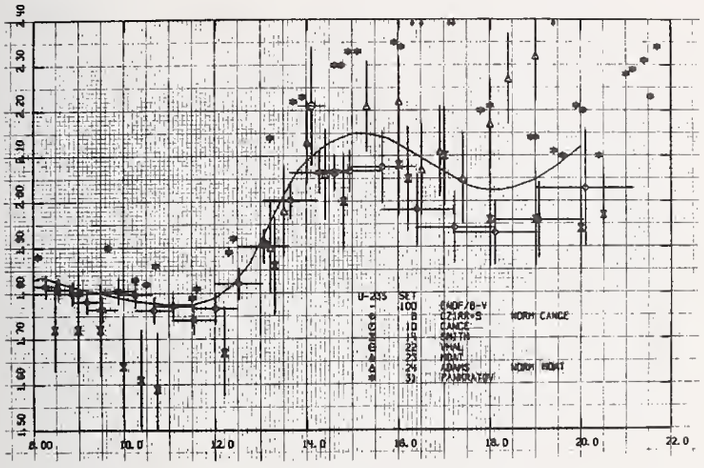

Fig. 1. Fission cross of ^{235}U between 8 MeV and 22 MeV. This figure is taken from ref. 6.

that measurements of this cross section at different laboratories differ by more than 10% although the experimenters quote much smaller errors. Activation cross sections are not as well known as the ^{235}U fission cross section; measurements at different laboratories often differ by an order of magnitude. The activation cross section that is reported to be best known for neutrons around 14 MeV is that for the reaction $^{27}Al(n,\alpha)^{24}Na$. Fig. 2 shows some values of this cross section as well as the ENDF/B-IV evaluation given in the dosimetry file.[4] The measurement quoted with the smallest uncertainty (less than 1%) is the absolute determination carried out in 1970 by Vonach et al.[7] by the associated particle method. This measurement is, however, ignored in the 1975 dosimetry file, and the ENDF/B-IV evaluation differs by 5% from this presumably most accurate measurement.

In most practical situations in which a foil serves to measure fluence in radiation damage studies, the variation of the activation cross section with neutron energy may introduce more uncertainty in the fluence determination than the error in the cross section at one energy. Fig. 3 shows the activation cross section as a function of neutron energy for the three reactions mentioned earlier. Experimental data on the Nb(n,2n) cross section are shown in Fig. 4. The two most recent extensive measurements[8,9] around 14 MeV differ by 10%. There are no measurements available above 20 MeV.

Even for D-T neutrons the energy spread is typically 1 MeV, and the energy distribution within this spread is usually poorly known and varies over the sample. Hence there is substantial uncertainty in the average neutron energy. If deuterons on Li or Be produce the neutrons, the energy spread is of the order of the bombarding energy. Hence activation of foils gives only a very rough measure of fluence. By using several reactions with different thresholds the contribution of

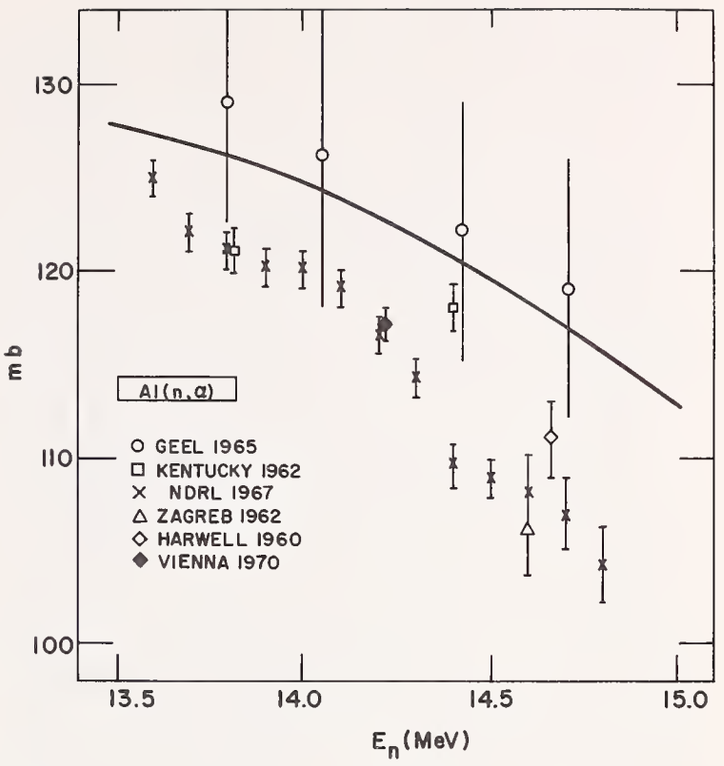

Fig. 2. Cross section of the reaction $^{27}Al(n,\alpha)^{24}Mg$ for neutrons between 13.5 and 15.0 MeV. Only experimental results which are quoted with small uncertainties are shown. The solid curve is the ENDF/B-IV evaluation given in reference 4. Additional measurements may be found in this reference.

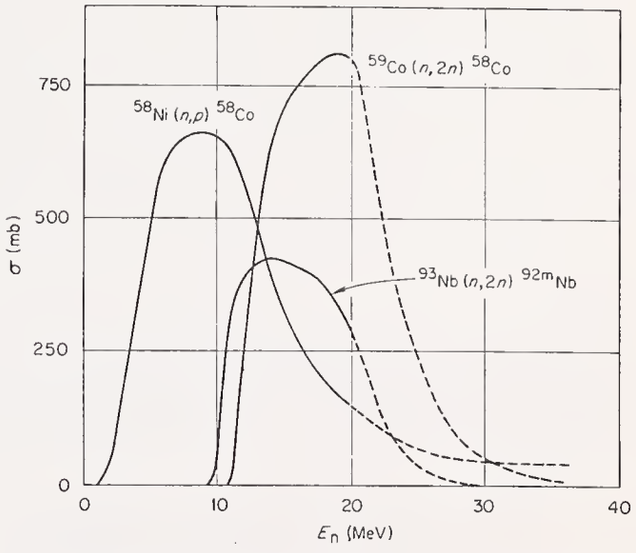

Fig. 3. Activation cross sections of three frequently used detectors as a function of neutron energy from ref. 5. The solid curves follow evaluated data sets, the dashed portion is an extrapolation based on theoretical considerations.

neutrons in different energy ranges can be estimated.

Dose and Kerma Determinations

If the fluence in a sample has been determined, the kerma can be calculated if the kerma factor is known. Again the only nuclide for which the kerma factor is accurately known is ^{1}H, since the only

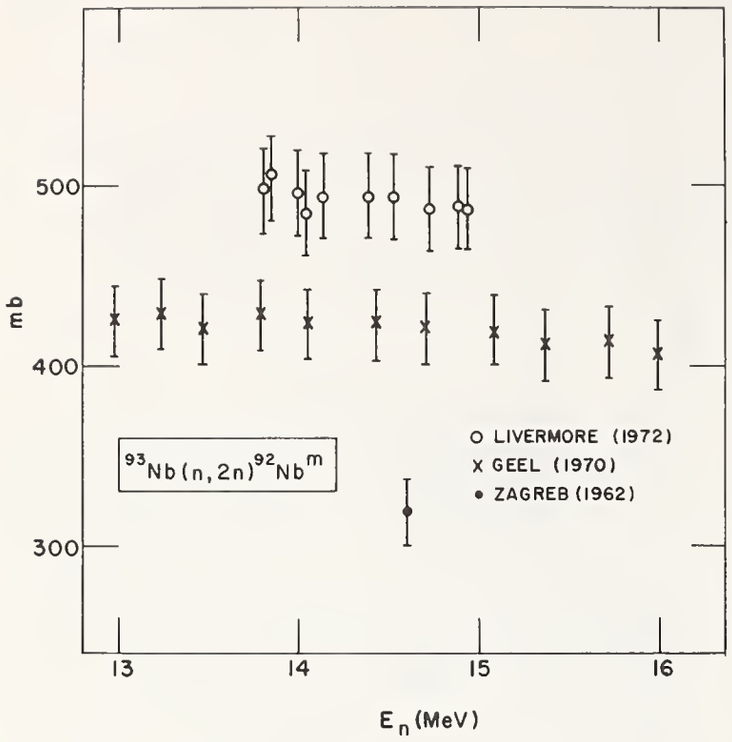

Fig. 4. Measured cross sections of the reaction $^{93}Nb(n,2n)^{92}Nb^{m}$ between 13 and 16 MeV. The most extensive recent measurements are given in ref. 8 and 9.

charged particles that are produced are recoil protons and their angular distribution is close to isotropic in the CM system. The kerma factors for ^{2}H and ^{4}He are also well known, but they are of smaller practical importance. For other nuclides the nuclear data needed for calculating kerma factors are not well known for neutrons above 10 MeV energy. Above 20 MeV there are hardly any measurements of the needed nuclear data, and kerma factors are calculated from nuclear models. Abdou has developed a computer code[10] for calculating kerma factors from the ENDF/B data file.

Because of their importance to the biomedical applications the kerma factors of the principal constituents of tissue, H, C, N, and O, have been calculated most carefully. The most widely used values are the kerma factors published by Bach and Caswell[11] in 1968. These have been revised recently by Caswell, Coyne and Randolph[12] on the basis of more recent nuclear data. Table II gives a comparison of the kerma factors of H, C, N, and O at 15.5 MeV according to the two evaluations by the NBS group, and also according to a recent evaluation by Howerton[13] at Lawrence Livermore Laboratory. The differences between these three evaluations indicate the uncertainties in the kerma factors for the most carefully studied nuclides.

TABLE II

Kerma Factors for 15.5-MeV Neutrons

(in 10^{-9} rad cm^2)

	H	C	N	O
Bach, Caswell (1968)	47.5	2.36	1.39	2.13
Caswell, Coyne, Randolph (1976)	47.1	3.02	2.68	2.07
Howerton (1976)	47.1	2.17	2.90	1.48

Bragg-Gray Approach to Dosimetry

In biological work dose in tissue is usually measured with a tissue-equivalent (TE) ionization chamber. According to the Bragg-Gray theory of cavity ionization, the ionization produced in a small gas-filled cavity in a solid material is related to the dose D at the position of the cavity by

$D = \frac{Q\ W\ S_{wall}}{e\ M\ S_{gas}}$, where Q is the collected charge, W the energy required to produce an ion pair in the gas, M the mass of the gas in the chamber, and S the mass stopping power. TE chambers were originally developed for measuring γ dose. The walls of the chamber consist of TE plastic, usually Shonka A-150 plastic,[14] in which most of the oxygen in tissue is replaced by carbon. Such plastic is, however, not exactly tissue equivalent for neutrons, since C and O have very different kerma factors for neutrons and the ratio of the two kerma factors varies with neutron energy by an order of magnitude. For 15-MeV neutrons the difference between tissue and TE plastic introduces a 5% correction.

TE chambers are usually calibrated with γ-rays. Such a calibration is not generally applicable for neutrons because W and S are likely to be different for the electrons produced by γ-rays, and for the protons, α particles, and ^{12}C and ^{16}O recoils, produced by neutrons. In the past data on the dependence of W on the mass and energy of the ionizing particle have been contradictory. During the last year two groups[15,16] have obtained new results which clearly indicate that W increases with increasing mass. There is also good evidence that for heavy ions W increases at low energies. Some of the recent results obtained for H^+, He^+, and C^+ in TE gas are shown in Fig. 5. Except for low energy C^+ ions these

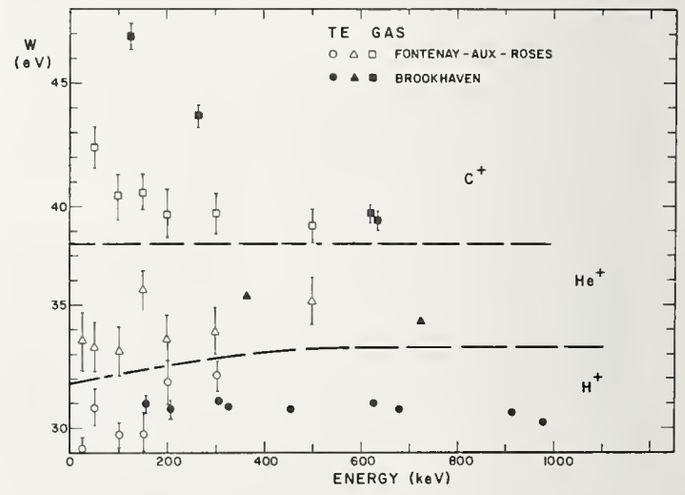

Fig. 5. Results of two recent determinations of the average energy loss per ion pair as a function of particle energy in methane-based tissue-equivalent gas for H^+, He^+, and C^+ ions. The data are from references 15 and 16.

data are consistent to within 3%. A calculation of an average value of W for the different type particles produced by energetic neutrons will, however, have an appreciably larger error.

Although there is also substantial uncertainty in the knowledge of the ratio of the mass stopping powers in solids and gases, the uncertainty has probably relatively little effect on the neutron calibration, because some of the errors will tend to cancel in taking the ratio of two ratios.

Comparison of Dose Measurement Based on Fluence and on Bragg-Gray Approach

Neutron dose in tissue can be measured by two independent methods, i.e., by measuring fluence or by measuring charge in a TE chamber. It is interesting to compare these two procedures for monoenergetic neutrons for which fluence can be measured fairly accurately. In an experiment[17] performed at the Rotating Target Neutron Source at Lawrence Livermore Laboratory a 1-cm^3-volume commercially obtained TE chamber was exposed to 15-MeV neutrons. Neutron fluence was measured both by foil activation and by proton recoil counters. Fluences were converted to dose using the kerma factors of ref. 12. Charge collected in the chamber was converted to dose on the basis of the γ-ray calibration with corrections for the difference in W for γ rays and neutrons. In separate experiments both air and TE gas served as chamber fillings. For air there is a small correction for the difference in stopping powers for electrons and protons. Table III

TABLE III

T-E Ion Chamber Conversion Factor (rad/nC)

(20°C, 760 Torr)

Radiation	Method	Material	Chamber Gas: Air	Chamber Gas: T-E Gas
^{60}Co γ's			3.19	2.78
15-MeV Neutrons	Bragg-Gray Approach	A-150	3.45	2.90
		Muscle	3.22	2.71
	Neutron fluence based calibration	A-150	3.31	2.81
		Muscle	3.09	2.62

lists the results of the comparison both for dose in muscle and A-150 plastic. The two procedures yield calibrations which differ by only 4%, which is much closer than would be expected on the basis of the uncertainties in the atomic and nuclear constants involved in the calculations.

Continuous Spectrum Neutron Sources

Since it is easier to obtain high neutron intensities by producing broad spectra than from the DT reaction, currently most neutron radiotherapy sources use Be targets bombarded by either protons or deuterons. For the materials applications there is a plan to build a large facility in which the reactions of deuterons with a thick lithium target serve as a high intensity neutron source. These sources produce a continuous neutron spectrum extending from very low neutron energies to the bombarding energy. Neutron dosimetry for such sources is very much more difficult than for D-T sources, and there is an almost complete lack of the required nuclear data. There are hardly any of the relevant cross sections known for neutron energies above 15 MeV so that neither the fluence nor the kerma can be determined if the bombarding energy is above 15 MeV.

In the biomedical application a tissue equivalent dosimeter yields fairly reliable information, but for the materials application there are large uncertainties. Since the sample is placed near the target, there is a wide variation of both neutron spectrum and intensity even over a small sample. The Li target has to be so thick compared to the distance to the sample that there is a significant difference in distance between source and sample for the more energetic neutrons, which are produced farther from the sample, from that for the lower energy neutrons, which are produced close to the sample. Hence the neutron spectrum at the sample is not the same as that observed at a distance from the sample by, say, time-of-flight measurements. In addition, the neutron spectrum varies rapidly with angle of emission with respect to the incident deuterons; the average neutron energy decreases rapidly with increasing angle. Before measurements with a D-Li neutron source can be interpreted meaningfully, more measurements of the neutron intensity and spectra are needed as a function of deuteron energy and emission angle. Furthermore, the charged-particle production cross sections in the materials to be studied and the activation cross section of the dosimeter materials need to be measured as a function of neutron energy up to the highest neutron energy that the source produces.

The uncertainty in the dose determination for radiotherapy with continuous-spectrum neutron sources is not as serious a problem because one does not know the RBE accurately either. Radiobiological experiments measure the product of dose and RBE. Uncertainties in dose produce corresponding uncertainties in RBE. While a better knowledge of the two factors separately would be of considerable interest, it is not essential for the therapy applications. Experiments are underway, however, which should improve the knowledge of kerma factors for tissue for neutron energies above 14 MeV. The results of such experiments will help in the understanding of the dependence of RBE as a function of average neutron energy.

References

1. Proceedings of the International Conference on Radiation Test Facilities for the CTR Surface and Materials Program. Report ANL/CTR-75-4 (1975).
2. H.H. Barschall, Am. Scientist 64, 668 (1976).
3. International Commission on Radiation Units and Measurements, Report 19 (1971).
4. ENDF/B-IV Dosimetry File, Report BNL-NCS-50446 (1975).
5. M.J. Saltmarsh, et al., Report ORNL/TM-5696 (1976).
6. Proceedings of the NEANDC/NEACRP Specialists Meeting. Report ANL-76-90 (1976).
7. H. Vonach, et al., Z. Physik 237, 155 (1970).
8. A. Paulsen and R. Widera, Z. Phys. 238, 23 (1970).
9. D.R. Nethaway, Nucl. Phys. A190, 635 (1972).

10. M.A. Abdou and C.W. Maynard, Nucl. Sci. Eng. 56, 360 (1975).

11. R.L. Bach and R.S. Caswell, Rad. Res. 35, 1 (1968).

12. R.S. Caswell, J.J. Coyne, and M.L. Randolph, Proc. Workshop on Physical Data for Neutron Dosimetry, Rijswijk, The Netherlands, EUR 5629e, Luxembourg, 1976, p. 69.

13. R.J. Howerton, private communication. E.F. Plechaty, D.E. Cullen, R.J. Howerton, and J.R. Kimlinger, Lawrence Livermore Laboratory Report UCRL-50400, Vol. 16 (1976).

14. F.R. Shonka, J.E. Rose, and G. Failla, Proc. Second U.N. Conf. on Peaceful Uses of Atomic Energy, 21, 184 (1958).

15. N. Rohrig and R.D. Colvett, Rad. Res. 67, 613 (1976).

16. M. Chemtob, B. Lavigne, J. Chary, V.D. Nguyen, N. Parmentier, J.P. Noel, and C. Fiche, Phys. Med. Biol. (to be published)

17. H.H. Barschall and E. Goldberg, Medical Physics 4 (to be published).

SUMMARY SESSION: W. W. Havens, Jr., Chairman

PANEL MEMBERS: R. Caswell, V. Farinelli, H. Liskien, H. Motz, R. Peelle, and L. Stewart

Introductory Remarks: Dr. Bowman

We now come to the final session - the summary of the Symposium. Bill Havens will be chairing this session and he has been charged with maintaining a tight schedule. Since we plan to incorporate the record of this session into the proceedings, I am required by federal government regulations to remind you that the discussion of this conference is being recorded. Now, I'll turn this session over to Bill Havens.

Prof. Havens: In the interest of time, we are not going to follow the format listed on the program. We are going to incorporate the summaries of the discussion groups into the appropriate portion of the summary of the program. And the format will be that the leader of the discussion group for the particular workshop will be allowed five minutes at maximum to present the summary of the workshop. Then Alan Smith will summarize that portion of the conference. Then we will go to the panel for discussion of that particular portion of the conference. Alan Smith and I put together a list of times which would be devoted to the particular subject matter of the conference, and we'll try to adhere rather rigidly to the allotted times. I don't know what I will do if somebody doesn't stop when I get up to cut them off but, hopefully, forcible means will not be necessary. So in the interest of time we'll start immediately.

The first session was on light nuclei and the nearest workshop to that was the one Bryan Patrick chaired, the Workshop on Li and B. So, I'll call on Bryan Patrick to give a five-minute summary of the workshop.

Dr. Patrick: I wonder if I'm allowed to take, as a foreigner, the Fifth Amendment to get around this recording business. No? We had a fairly lively discussion on ^{6}Li and ^{10}B in which a large number of people participated, and I hope this isn't too disjointed a representation of what went on.

The use of a large body of nuclear physics information in the form of angular-distribution, polarization and inverse-reaction data in addition to the direct measurements ($\sigma_{n,t}$, $\sigma_{n,\alpha}$, and $\sigma_{n,n}$) in the R-matrix calculation of Hale on the ^{7}Li system, although not a new idea, is a welcome development which should be encouraged. Most of the recent experimental work on ^{6}Li seems to have concentrated in the region of the 250-keV resonance. It's encouraging to note that the latest (n,α) measurements agree to the order of 3 percent with each other and that they also agree with the R-matrix calculation of Hale. However, we should not put too much emphasis on this. There have been many measurements over that resonance, and there has been much disagreement. The reasons for these problems are still not fully understood, and we should hesitate to conclude that the cross section is known to even 3 percent in that region. Before proceeding with further measurements using ^{6}Li glasses, we really need to know why the disagreements exist. Perhaps some of them are due to the problems of ^{6}Li concentrations and distribution in scintillation glasses that were discussed during the symposium. This is a situation that for a standard like ^{6}Li, which is used so much, is very disturbing, and I think really unacceptable if we're going to use this cross section as a primary standard. On the credit side, the agreement between the R-matrix calculation and the inverse reaction data of Brown et al. at $\Theta=0^{o}$ and 180^{o}, which were completed after the calculation was done and which were therefore not included as input to the calculation, is to be noted.

We spent some time considering the question, "Is ^{6}Li a suitable primary standard?" There are people who put forward the view that, with all the problems we have had measuring this cross section, it is not a good primary standard. It was concluded that for essentially, practical reasons, although for other reasons too, it is a good primary standard up to ∿150 keV. Above that energy it is questionable.

Now the problems with ^{6}Li and ^{10}B are bound up with detector technology. There have been few real advances in recent years, and this is an area which clearly needs improvement if higher accuracies are to be achieved in the cross sections. It was felt that we're probably fairly close to the limit of accuracy using present ^{6}Li glass techniques for measuring the cross section and maybe it is time that ^{10}B was investigated. Measurements have concentrated on ^{6}Li recently and ^{10}B has not had much attention, and perhaps it's time to look at ^{10}B again, particularly to cover the region above ∿150 keV where ^{6}Li becomes a poor standard, to ∿500 keV where hydrogen takes over. This region between is probably the most important problem at present. There was also some suggestion that ^{3}He detectors should be considered again, and maybe a fresh look would prove to be fruitful.

If you want some measurements, which are thought to be the most desirable, we've made a shopping list, mainly from Gerry Hale. The $^{6}Li(n,\alpha)$ and total cross sections at thermal energy are still important. We need to determine these more accurately if we are to know the 1/v part of the cross section better. In this connection, the levels in ^{7}Li responsible for the low-energy $^{6}Li(n,\alpha)$ cross section have not yet been clearly identified. This is not just an academic problem as their position determines the sign of the deviation from 1/v of that component. The minimum at about 80 or 90 keV in the region below the resonance is another important region where accurate (n,α) and $\sigma_{n,t}$ measurements would help to define the cross section over a wider energy interval and again the cross sections at the peak of the resonance are still relatively poorly known and must be more accurately defined. Elastic scattering over the resonance and angular distributions at low energies are also important. ^{6}Li above 500 keV to 1 MeV is used as a standard by certain groups and that's a region where the R-matrix calculation may be somewhat in error. And finally, it's felt that the $^{6}Li(n,\alpha)$ to $^{10}B(n,\alpha)$ cross section ratio measurements above 50 keV, extending up to at least several hundred keV would also be extremely useful. Thank you.

Prof. Havens: We'll have Alan's summary.

Dr. Alan Smith: I think before I start on the light nuclei which will include B, H, C and Li, I should outline my position here. I am somewhat awed by standing before you. I try to avoid making a precise measurement if at all possible, and there are those who say I never do. I think that maybe the best you can expect from me is an unbiased opinion, and one good sound reason is that the ultimate in unbiased judgment is complete ignorance in some cases. But I also think

I bring to it a look which maybe isn't as close. And I bring also some age, which is not anything but my biological credit; but I have gone to more of these standard conferences than have been mentioned in this proceedings. Somebody forgot the Oxford conference of 1963, he didn't count back that far. Well, that starts me off because I was reminded this morning by Bob Block that, at the '63 conference, Bob Batchelor had a little audit done by the Queen's exchequer, and his conclusion at that time was that one million pounds had been spent on the ^{6}Li(n,α) cross section to that date. We're still at it, and the pound has been devaluated, but even so I think it must be up to about 8 or 10 million dollars at least, and the question which I have now that really bothers me is, "Where are we, what do we want, and how much more effort is warranted?"

I looked at the new results, I counted crudely, and I see only a few new total cross section measurements that are really relevant to standards; maybe two. I see two new (n,α) measurements, and I believe they were both relative. I see two scattering measurements, several angular distributions of the α particle, and one study of inverse reactions. That's apparently in the last 10 years. I asked myself what the impact has been, and I think that the major effect is that we have perhaps a better knowledge of the (n,α) cross section below 150 keV. Beyond that I don't know. I concur with the Workshop's report that this is where we should focus our attention.

But looking at it from the pragmatic point of view, I asked myself why we're making all these measurements at higher energies. And I asked myself another question. Looking back in history, have we any evidence that perhaps we know it a good deal better than we think we do? I look back, for example, at an early measurement made 10 years ago by two English gentlemen who did a very good job using a simple-minded theory, and they came up with an (n,α) cross section. Bob Peelle plotted it on a slide here the other day. As near as I can figure out, it's within 1-1/4 percent to 1-1/2 percent of the current ENDF/B-V. So I wonder what we have gotten from these measurements. Have we got more confidence and to what degree? I have an uncertain feeling about how we improve that situation further.

Now, I am a little concerned at some of the statements that we see for what our needs are. You can look at some of the compilations of requests and you can see that you want the (n,α) cross section of ^{10}B to 1/2 percent from 0 to 3 MeV, and I think that's not a very rational request; I think that's what the workshop said. I think you may need it to that accuracy to 150 keV, but I think we should focus on what the range of interest is.

Some of you know that some years ago I wrote a memorandum extolling the virtues of physical interpretations and theoretical extrapolations for nuclear data purposes and some resistance to pragmatic adjustments. You also may know I took my knocks for that memo and I'm still black and blue in some places. So therefore I really welcome the outstanding work at Los Alamos to use established theory in a long-term way of knitting together this process. But I am a little concerned that apparently, if I understood correctly, after 10 years we are still looking for the positive parity state in the ^{7}Li system. That, I think, was Ernie Rae's search, too, in 1970. I also wonder about how far we extrapolate our fit. It is, I think, a parameterization and a theoretically sound one, if that's all it is.

I was interested particularly in Jack Harvey's statement, and his very nice experiments, and those here of Ivan Schröder at the Bureau, where we now have a different reaction mechanism proposed to account for the (n,α) angular distributions. I don't know, I'm not a theorist, but it bothers me that maybe we shouldn't get too hung up on one type of theory until we're sure we really understand it. And I think then if you take that approach maybe we shouldn't worry too much about the exact energy of that resonance. And I am certainly a guilty party for probing around in that thing, too.

I wonder if I should continue. I would be happy to do so, in fact I'd love to tickle some toes, but I would like some guidance. (Granted by Havens) I too share the workshop's opinion that ^{10}B is probably a more promising material. One of the reasons for this is that in my happy life I have not dealt either with B or Li, so after hearing Larry Weston's excellent talk on the difficulties with the Li detection system, I decided I never wanted to get involved. Maybe ^{10}B is easier. Somebody else mentioned something about the total cross section of ^{10}B. I think Bob Block needs that for correction procedures, and I think he's correct certainly. But that again reminds me of a statement made by Bob Batchelor, and I think I do have a positive suggestion there. Bob Batchelor in 1963 recommended the old shell transmission experiment as a way of getting the (n,α) cross section. And in fact some of the results were shown here. They didn't come out very good, but I think that was a mistake of the times in two ways: the correction procedures were poorly done and we didn't know the elastic-scattering angular distribution. Maybe it's worthwhile doing that one again, now using the calculated distributions which we have from our R-matrix theory. Maybe Batchelor's recommendation of 15 years ago is still a good one. The question I guess is "Do we have those Batchelor spheres in the AWRE vaults?"

There are two other light element cross sections, the hydrogen and carbon, that I would like to say a word about. Lovely experiments on (n-p) scattering from Harwell and their visitors; I was much impressed. I'm not a specialist in that area certainly, and it's been I guess five years since I even looked at that type of reaction at even lower energy. But I looked at the curves and so forth and I guess my question is, "Excellent and beautiful though the results are, do they really change our assumption of the Breit-Hopkins expression of the standard?" I didn't see a quantitative statement. Is there real doubt in that basic and most elemental standard? I'd like to see an answer to that question. I also think that we better give a little harder look at this n-p cross section at lower energies, and this is partly what the workshop said, but I'd go lower. And this impacts upon the ^{6}Li. I am impressed by Mr. Czirr's detector which is said to be flat to, I believe, 1 keV to a percent or so, and that I think takes much of the crunch out of the need for standards such as (n,α) of Li and B from say 150 to 500 or 600 keV. That was a very impressive detector.

My final light element comment has to do with carbon. I don't have any real serious objections, in fact none whatsoever on the paper presented. I particularly though wish to quote again the remark of one man from the audience who, yesterday I believe it was, said that, "If you are measuring angular distributions you better damn well measure carbon; if you can't get that you're in trouble". I strongly support that comment. I might also suggest that in my view the total and differential scattering cross section of carbon, probably from 1.8 MeV on down, is known to about 2 percent and that is very nearly as good as the hydrogen. That's also an energy standard which, we heard today, is well established. I will extend my remarks also from scattering from carbon to total

cross sections. And some of you may know that total cross sections are a mess in many areas. I would also suggest that those who measure total cross sections, even though self-normalizing, use carbon as a reference check point.

Prof. Havens: I would like to call on some of the panel members to comment on the summary and the workshop report. Lee Stewart.

Lee Stewart: Let me make one remark on hydrogen. Remember that Ugo Farinelli suggested the one thing he didn't like about ENDF standards was that we change them too often. Hydrogen has not changed since ENDF/B-III and yet I come to this symposium and I find very few people who use it; the answer is that hydrogen is too hard to implement. Well my comment, having been in this business for many, many years (26 to be exact), is we've done the easy experiments, now let's start and do the hard ones, because we have been measuring cross sections to standards other than hydrogen for many years. Hydrogen is the only standard in the MeV range that is both smooth and precisely known compared to all other standards; there is no structure. So let's do use it.

The only other comment I'll make refers to Alan's comment that we do not need further measurements in ^{6}Li. One problem has hurt us for a long time; there are two measurements on ^{6}Li elastic scattering at low energies. They differ by 30 to 40 percent; one comes from Harwell and one comes from Argonne, and we have never been able to resolve that 30 to 40 percent discrepancy. Therefore we cannot subtract the elastic from the total to get the (n,α). Thank you.

Prof. Havens: Unfortunately that's all the time we have allowed for this particular subject. The others will have to go more rapidly. Yes, it's a railroad job! The next session was Capture Standards, Fission Parameters, and Thermal Standards. And since there was no particular workshop which was associated with this, I'll call on Alan Smith to give the summary at this time.

Dr. Smith: Well I have ten minutes to cover this collection, and I will move very fast and try to catch up a bit. There was really only one capture standard discussed in detail and that was gold. It has its strong shortcomings in structure at low energies, and the results are poor at higher energies, but is really fairly well known, 4 percent or so from 200 keV to 3 MeV, and it was said there was no discrepancy between the direct detection and activation measurements. That, I think, is a change from the past. I guess my real problem with this general capture area is, "What happened to the other capture standards, Ho and Ta?" They have been proposed. Another question is, "Do we know some of the applied capture processes even better than our standard, and if so, should we neglect the standard? For example, "Is ^{238}U capture, in fact, better known than that of gold?" If I look in the same energy region between the ENDF/B-IV and ENDF/B-V, the changes are less than 4 percent.

I think then I should pass on to some of the other things that go under the general heading of fission physics, the fission neutron spectra. Here we had some new interesting results. One has been a question that's been in my mind for a long time. What is the energy distribution at very low energies? The Russian results seem to show it's a close fit to a Maxwellian. This gives me a bit of trouble in the context of some of the integral experiments which seem to show quite the opposite, an abundance of neutrons in the low-energy tail. I think that one must stress very importantly the acceptance of the ^{252}Cf fission spectrum as the standard fission spectrum as it already is accepted as a standard for $\bar{\nu}$. I think it is regrettable that in some past meetings the emphasis was put on ^{235}U and ^{239}Pu for pragmatic purposes. The basic standard should have been emphasized instead. Once you have that, the ratio obviously suffices for other isotopes.

Thermal standards I will not discuss to any great extent, the main authority on the subject unfortunately had to leave. I would only point out that there's one associated problem that bears on this and a number of other aspects of fission, and that's the foil assay in fabrication. I think that I have seen an order of magnitude difference in accuracy uncertainties in our standard foils. The Plutonium Subcommittee is working in the 0.1 percent range, while the rest of us are still at 1 percent. I think there's a transfer of technology problem here that will impact upon our precise thermal constants, our $\bar{\nu}$, and a number of other areas. I'm embarrassed to say that the speaker from the Plutonium Subcommittee comes from my own laboratory, and my foils aren't anywhere near as good as his.

Very carefully discussed was $\bar{\nu}$ for Cf. I think the thing that disturbs me a bit here is, "Are we at the end of the line with present techniques?" There was one new measurement as I understood it in the last 10 years. The rest are reassessments and recorrections. I understand another one which will combine η and $\bar{\nu}$ is in progress or planned. That might be welcomed, but I question whether we should continue those type of measurements with those existing techniques if we can't get a real breakthrough. And one thing that comes to mind, in which somebody with much more knowledge of the field should look at. You have an awfully intense and sensitive thermal column in the Lucas Heights reactor, it's an Argonaut reactor. What can you do with a few precise fissile foil assays *a la* the Plutonium Subcommittee and a good pile oscillator in that sensitive thermal column? Is that a new method? I know, for example, that very high accuracies are claimed for weighting of flux distributions in fast criticals. Perhaps this is some new technique that can be explored, maybe it's been looked at.

Prof. Havens: I understand that Dr. Boldeman had a rump session on $\bar{\nu}$, and I'd like to call on him. Could you take the microphone since this session is being recorded and give a very brief statement of the results of the discussions on $\bar{\nu}$?

Dr. Boldeman: Richard Smith with the eta bath is measuring $\bar{\nu}$ and, having seen the things that he's planning to do and the information that he's got already, I'd be very surprised in fact if he doesn't turn up with a particularly nice result, whatever that happens to be.

Bo Leonard suggested to me at one stage that when we combine the manganese sulphate bath measurements and the liquid scintillator measurements we should recognize that there are common errors in each of these. Measurements of a given type therefore should be first averaged together and then the systematic error applied to the average. The results from the different sets of measurements should then be averaged with weights according to their errors to get the final result. Well, I thought I would try that, so I did a bit of a quick calculation this morning. Using the conventional approach the result that I got was 3.745, $\pm$ 0.010. I expanded the error to this value because I thought there are lots of things like the uncertainties in the fission-neutron spectrum which really occur in every measurement. You might remember Ted Axton showed a slide for a manganese sulphate bath where, for average energies of 1.39 or 1.43 MeV; there's a 0.1 percent

change. So even in the manganese sulphate baths the spectrum matters. We expanded this error then to that. So then I thought we would assume that manganese sulphate baths have a common error and liquid scintillators have a common error. I therefore averaged all liquid scintillator measurements together and separately averaged all manganese sulphate baths together. These two values were then averaged with weights given by their uncertainties to the boron pile and the Fieldhouse measurements. The result now became 3.748 $\pm$ 0.01. So it doesn't strike me that anything you do with the measurements or the way which you write them will make very much difference. If I were to guess, as Lee Stewart sometimes thinks it's reasonable to do, I reckon the final answer is about 3.75.

Despite the very acceptable level of agreement between the different absolute measurement of $\bar{\nu}$ for ^{252}Cf, the question of a possible systematic difference between the $MnSo_4$ bath determinations and those obtained using liquid scintillators, and therefore the real accuracy of the mean of the measurements, continues to concern some evaluators. It should be reemphasized that of the eight absolute measurements only one lies more than one standard deviation away from the mean. Furthermore, the averages of the liquid scintillator and $MnSo_4$ bath values differ by only 1-1/2 standard deviations of the comparison. Consequently, their fears are unfounded and there is no evidence to postulate an experimental technique-dependent error.

I'd like to take up that thought of oscillating things in and out of reactors; maybe somebody can do something about that.

Prof. Havens: I'd like to then call on Dr. Liskien to comment on the summary and Dr. Boldeman's results.

Dr. Liskien: I think I have nothing to comment on this, but I would like to remind the Symposium that we had in this session and this group of subjects two potential newcomers as standards, namely ^{238}U and ^{237}Np. If a person asks me why we do need these cross sections, the answer is of course yes we want to conveniently measure fluxes. Then he will certainly answer yes, OK, so I understand you need one cross section for the whole energy range, but in fact I have to explain that we need perhaps more. Now comes the point that is suggested that we add again at least one of the two. Of course we all know the reason is that we don't want to have a thermal response in the standard. But my real point is that when I remember correctly that the interest for such a standard is coming from the reactor in-pile dosimetry, and I wonder if this is also true now for ^{235}U, if what is really wanted is not the total fission cross section for these isotopes, but, in fact, the partial production cross section for the production of a convenient fission product because many of these measurements are done not on-line by counting fission fragments but by off-line activity measurements. I would like to see in the future this point clarified; really, what is needed there?

Prof. Havens: Any other member of the panel like to comment on what is needed? Dr. Peelle.

Dr. Peelle: I'd like to comment in terms of another question which has concerned me. In my reading of many papers on the subject of the neutron spectrum from fission, I've never seen a really good analysis of what properties of the spectrum are actually required. Is the average energy enough? What parameters, what moments have sensitivity in the applications? And if we knew that, we might know better how to deal with, how to parameterize, and how to seek better accuracy in fission-spectrum measurements.

Prof. Havens: Would you like to comment on that?

Dr. Farinelli: I might make a comment on this last question. Well it depends very much on the problem. For instance, the high-energy tail of the fission spectrum is very important when you use threshold detectors with a high threshold. And why do you use these detectors? For instance, because you are interested in high-energy neutrons, if you have to simulate CTR conditions in a fast reactor. So this may explain why the status of the fission spectrum which was acceptable at high energies up to a certain time ago, perhaps a couple of years ago, is no longer satisfactory, and it's certainly one application for which you would need better resolution in the high-energy tail.

Prof. Havens: We have about one more minute. Lee.

Lee Stewart: Another remark is that Jud Hardy did some calculations in a thermal reactor and using the same average energy but just changing the shape, from a Maxwellian to a Watt, he got differences of 0.3 percent in k. So if you harden the spectrum, of course, you get a change in k. Just measuring the average energy in some configurations is certainly not enough; we need to know the shape and whether the shapes are different among the different isotopes.

Prof. Havens: I'm sure the problem is different for shielding than it is for k and therefore the answer to the question is you want to know as much detail as possible in the final analysis.

The next topic for which there is a workshop, which is closely related, that we divided the conference up into was Flux Intercomparisons. I will call on Dr. Axton to present the results of the workshop he conducted on the future of BIPM flux intercomparisons.

Mr. Axton: First let me state what the object of the intercomparison is and the criterion for judging whether or not it was a success. The object of the intercomparison is to identify systematic errors in absolute measurements of neutron flux density. There are two types of measurements involved in this comparison; firstly there are the absolute measurements of flux density made by different methods at different laboratories, and secondly there are the comparison measurements between those absolute measurements which are made directly as part of the comparison. The criterion for success is that the errors of comparison must be small compared with the absolute errors, otherwise you know nothing about the systematic errors in the absolute measurements. The intercomparison falls into ten subgroups because there were five intercomparison energies and there were two transfer methods for each energy. The conclusions of the discussion group were as follows: (1) Some transfer methods were good and other transfer methods were not so good; (2) When the transfer method is good the results are encouraging. Flux measurements by different methods agree and flux measurements at different laboratories agree. For example, associated-particle techniques and proton telescope techniques agree at 14 MeV. At 2.5 MeV, associated particle counting, the stilbene crystal spectrometer, proton telescope, the manganese bath and the proton proportional counter all give very good results. When the transfer method is bad, then the information we obtain is "that the transfer method is bad." Conclusion (3) is that we should carry on and improve the comparisons, in other words, do some more. (4)Future comparisons should satisfy both dosimetry interests and cross section measurement

interests. Conclusion (5): The energy range should be extended down to 144 keV to include reactors, and this energy is still feasible with Van de Graaffs. The range should also be extended up to 50 MeV for cross-section interests. Conclusion (6): There is a need to improve transfer methods. Conclusion (7): Cross section measurements should be included as transfer methods. This would allow participation from the white spectrum linacs and also those from the Van de Graaffs. There is need for a study period to iron out the problems involved in this particular aspect of the comparison. Thank you.

Prof. Havens: Alan, will you summarize this part of the comment of conference?

Dr. Smith: I only have a couple of remarks on this one. First of all, I'm happy to see that the concept of a transfer basic physical standard of cross section has entered the program. One of my problems with this type of measurement over many years is that the detectors tend to be environmentally associated or instrumentally associated, and therefore they're not suitable for many places. The second thing is that I am impressed by the real good agreement. I think it's quite good, and I think it was Caswell who pointed out that the similar dosimetry comparison was almost identical. I think they did quite a good job.

Prof. Havens: Dr. Caswell, will you comment?

Dr. Caswell: I would like to make a couple of comments, one of which might involve some interaction with the audience. The one question that the people who organized this have wondered about is that this has been essentially an intercomparison between Van de Graaffs and Cockcroft-Waltons. The white source machines have not been involved although there were earlier some expressed desires to have them involved. I think that people who are involved should be very interested to know to what extent the white-source people would want to participate and what is the mechanism envisioned. A very precise measurement of a specific cross section, preferably one that is not well known, could play the role of an intercomparison in this way.

Secondly, we have used the word "BIPM", and I'm not sure everyone in this audience knows what organization this is; but I thought I'd take a minute to explain. When you take an elementary physics course, in the old textbooks they would have a picture of the standard meter bar that sat in some institution near Paris, and also of the world standard kilogram that also sat in some institution near Paris. This institution is, in English, The International Bureau of Weights and Measures, in French the Bureau Internationale des Poids et Mesures, and it was set up originally by the Treaty of the Metre in 1875, at that time as the keeper of the artifact standards like the meter bar, the kilogram, and so on. There's only one artifact standard left. For example, the meter bar is passé; it's now a wavelength of light, and the one that's left is the kilogram. Incidentally, there have been some interesting troubles recently discovered in the transfer of information on the unit of mass where the effect of the density of the air on the balance was wrong. So even that field hasn't settled down.

Prof. Havens: Would any other panel member like to comment on the flux intercomparisons? No one. I'll proceed to the next sub-category, Personnel Dosimetry, Biomedical Needs. Prof. Barschall, would you give the results of the workshop on that subject?

Prof. Barschall: For biomedical applications, the quantity which one wants to know is the absorbed dose. Let me repeat from this morning what we mean by absorbed dose: the energy absorbed per unit mass. There are two types of instruments which can be used to measure directly absorbed dose. One is a tissue-equivalent ionization chamber and one is a calorimeter. There was agreement among those working in the area of personnel protection and those working in the area of therapy, that it would be extremely important to be able to have an ion chamber or calorimeter calibrated at the National Bureau of Standards and certified by the National Bureau of Standards as to the dose calibration for neutrons of these instruments. There was agreement that calibration should be available for two neutron energies; one in the energy range of the fission neutrons, and this might be done with a Cf source, but there's also a need for a calibration at higher energy. For this purpose, the most suitable source appears to be a 14 MeV d-T neutron source. I should like to emphasize once more that the interest is in the calibration in terms of dose per Coulomb rather than in terms of fluence per Coulomb, which is why perhaps the National Bureau of Standards might prefer to make the calibration. Now since actually most centers, especially those active in therapy, use continuous neutron spectra, if not fission spectra, they'll have to make corrections for the energy dependence of the kerma factor in order to apply the calibration which they might get from the Bureau to their particular spectrum. For this reason, there's an important need for a better knowledge of the energy dependence of the kerma factors, particularly of carbon, nitrogen and oxygen. It is not sufficient to know just the cross sections for various kinds of processes; what is more important to know is the charged-particle spectra which are the spectra of the charged particles produced by various kinds of processes, and so this is the quantity which should be measured. And this information is not only needed to evaluate the biological effects of the neutron; it is also needed to calculate the effective value of W, the energy per ion pair, for the mixture of charged particles that is produced by a given neutron spectrum. High priorities should be given to determining the charged-particle spectra for the 14-MeV neutrons, not only because the instrument should be calibrated at this energy, but also because it would be most desirable to tie down the kerma factors at a particular energy in the neutron energy range of interest in therapy. A knowledge of the kerma factor is also important to calculate the dose delivered in therapy to various organs which have different chemical composition.

Prof. Havens: Alan, would you comment on this?

Dr. Smith: I only have a few brief remarks because we had agreed that Randy is far more cognizant of this field than I ever hope to be. I, however, have had occasion to observe the Bureau's performance in this area for many years and I must say I am impressed by the magnitude of this problem and the impact on society and I don't think that's what comes through to people out here. It came through to me, sitting here watching the Bureau trying to handle it and its a very difficult problem and I think the problems in personnel protection for radiation dosimetry are fundamentally ones of public implementation, technology transfer and assurance and these are administrative management social problems but they are enormous in scope and I think this should be recognized. I don't think that there is really a basic standard need for that one. On the bio-med dosimetry problem I had some troubles, really. I was awestruck by the accuracies that are quoted. I am just glad that I'm not in a tumor hospital with someone probing into my innards with a 5% accuracy. What bothers me is, "Has anybody measured a kerma to

5% in an ideal laboratory situation of a dummy torso?" Can it be done with the current technology much less in a clinical application? I have trouble again with this debate that apparently is going on, what can we do with standards and how are we going to clinically utilize them? I think there is a great deal of ambiguity there and I have one final other remark. I think that from the point of view of my interests we should be rather specific in what we want. I saw these differences in calculated kermas which if I understood correctly were attributed to differences in carbon cross sections used at Livermore and the Bureau of Standards. What differences in the carbon cross section? What specifically is causing the trouble? I would like to see quite definitive lists if I could, of say the ten most wanted things to characterize the 14-MeV biological dosimetry problem. I agree the cross sections were bad. They've got to be determined and stated in the sense the physicists understand, not values like biological effective something or other but I would like to see a list. What is the specific set of ten cross sections? Then maybe I could do something about it.

Prof. Havens: Right now, Randy, would you care to comment on these?

Dr. Caswell: Well, first I'll send Alan a list in a few days and then I will go back to some observations I wanted to make earlier. First, I have had the good fortune I think to be at four out of five neutron standards meetings mentioned. I think this is the first time that any physicist or other representatives of the biomedical community have really been in attendance so I think we should recognize we are just beginning a dialogue between the neutron standards people and the biomedical people who are concerned with neutrons. We need to learn to speak each other's language and I would like to congratulate Prof. Barschall on the choice of elements that he presented which are really the essential guts you need to know to go from one to the other. So, his paper and Dr. Broerse's paper were both very nice from the standpoint of general introductions to the field. On the cross section question, I think that although there are problems in the values of the cross sections from time to time, the much bigger problem is that ENDF/B is an incomplete set. In general, it does not give you the charged-particle energies which are what you need for an energy deposition calculation. It is much more likely to give you neutrons than gamma rays so one way of playing the game is to take the energy available, subtract off the gamma-ray energy, subtract off an escaping or scattered neutron energy from a reaction and then say the rest has gone to charged particles. Well, how well you can do this depends on whether you are given both the neutron and gamma ray energy so for the kind of application we are talking about the biggest problem is really definitive secondary charged-particle energies. The elements in which the cross sections are needed are in carbon, nitrogen, and oxygen. An example that has come up several times in neutron dosimetry meetings is: There is a $^{12}C(n,n'3\alpha)$ reaction which is known and measured. You would think therefore there might be an $^{16}O(n,n'4\alpha)$ measurement and in fact it's got something like a 14- or 15-MeV threshold. To my knowledge, no one has ever measured it even once at one energy so that we are really in an area where there are lots of cross sections that are not known. I guess I'll make two more comments and then shut up. One is that in the personnel monitoring area I think accuracy is required which is easy for the neutron standards people. There is still an energy gap between thermal and 2 keV where there are lots of neutrons that people are interested in and where Auxier showed that successive intercomparisons improved performance. I think in his case that's true; it may not always be true in successive intercomparisons. It may be just that the field is getting better and intercomparison had nothing to do with the agreement but I think that the case shown by Auxier is clearly one where the existence of the intercomparisons improved the measurement performance in the field.

Prof. Havens: Any other member of the panel like to comment on it?

Lee Stewart: At Los Alamos, we have had some interest and expertise in calculating kerma factors and have found, in addition to the problems in the ENDF/B cross sections, problems in the calculational methods. Phil Young, who is in the audience, can perhaps tell you how not to calculate kerma factors. As far as the data files are concerned, we have found that some ENDF materials make very good refrigerators in that the calculated kermas are often quite negative for many of the individual reactions. I have asked other people about their calculations and the Livermore Group, for example, told me they just set a negative kerma to zero, wherever negativity occurs in the reaction calculation. Therefore, some of our problems are in the ENDF/B representation of the data and others may be traced to the calculational methods employed.

Prof. Havens: Shall I call on Phil Young to tell us how not to calculate kermas?

Dr. Young: Well, we looked at several elements in ENDF and tried to estimate what the kermas were by doing what Randy suggested. Taking differences between total energy, subtracting out neutron energy and gamma ray energy, and frequently we would get things like negative numbers. Energy is not conserved accurately enough in the files to get kermas by subtraction techniques for many of the elements, mainly for medium and heavy nuclei. That was the conclusion.

Dr. Peelle: I have formed an impression based on looking a little bit at the NASA work on this question some years ago as well as what's happened more recently. I think the personnel dosimetry problem, as one goes to higher neutron energies rising above successive reaction thresholds, is a very nice application of nuclear physics and related phenomena--related fields to some practical matter and a very difficult one especially as one gets above 15 or 20 MeV where I believe to do it right requires physics we haven't even figured out yet. So it's a challenging problem; its not just a matter of throwing off and transferring the information we really have to solve a practical problem. It's going to require some deep thought and is a very interesting as well as an important problem.

Prof. Havens: Any other comments?

Dr. Caswell: There were remarks made in some of the talks that the standards laboratories are not offering calibration services for biomedical application and therapy. I would like to say they are beginning now. NBS has been doing it for a little while. PTB and NBS are sort of in the status of beginning to offer known monoenergetic fluences for calibration. I think this is a step forward. I think doing the business for the therapy dosimeters at the high accuracy and following multiple methods to get the same answer has not been done and I might comment that we have two proposals which we had going for two years now neither of which has gotten anywhere to do that.

Prof. Havens: Well, we'll proceed now to the next subject which is "Benchmarks, Core Dosimetry"; Chuck Weisbin, would you report on the results of your workshop?

Dr. Weisbin: Let me apologize in advance to my colleagues if I misinterpret or leave out any of the comments. The discussion was quite lively on the interaction between differential and integral data. There seemed to be in our workshop essentially unanimous agreement that integral data must be considered in the process of cross-section standards definition. In order to achieve this worthwhile goal, important procedural issues must be addressed including which integral data, that is, what constitutes a standard integral benchmark and how is it to be included in the evaluation process. The methodology available for addressing the subject is fairly demanding in that it requires uncertainty information including correlations for both the integral and differential data and there I don't just mean standards, I mean all differential data. It expects quantitative estimates of possible methods bias as well as computed sensitivities of integral data to the various ENDF/B cross sections and their associated uncertainty files. Will they both represent only the differential data or will they both have to represent all available information? The characterization and definition of what is an uncertainty file may be difficult. It is clear that the methodology is becoming available but significant advances must be made in order to provide more credible input. The methods developed must be sophisticated enough to provide specific recommendations to an evaluator, for example, in distinguishing between modifications to the cross-section normalization and shape. In developing such methodology and data the very practical question is raised as to what kind of time frame would be required for an endeavor of this scope and indeed is it worth it. The process of assuring compatibility is clearly iterative and desperately needs documentation to improve best the communication between people, the real barrier, rather than fundamentally conflicting data. A strong driving force, perhaps much too strong in the direction of reconciliation of differential and integral data, would be to insist that a standard can only be so designated when it is judged to be consistent with all relevant information--both differential and integral.

Prof. Havens: Thank you. That may rule out all standards. Alan, would you summarize this?

Dr. Smith: I would like to back up a bit to the benchmark fields particularly those under the auspices, I believe, of the Inter-Laboratory LMFBR Reaction Rates (ILRR) program. I think this has been one of the best correlated national data efforts where people have really gotten together and through cooperation have come up with some very fine results. I heartily concur with what has just been said that these benchmarks in the real world of microscopic data are an essential part of the whole process. I don't think it's a goal in itself and I am worried that we have really not a measure of the sensitivity of the benchmark measurement in such things as the ISNF facility. It came out in the last paper this morning. There were some crude sensitivities, but it seems to me that's the first place to apply the sensitivity analysis. That's a first step toward the integral test and I also quarrel with an opinion which I've heard, and it wasn't expressed at this meeting, but I think I should express the view. A benchmark is a benchmark that tests some underlying principle; it is defined so in the dictionary. I think that you should never conceive of a benchmark as a method to measure microscopic data and I think that is something that is done periodically and I've had some words on that in the past and couldn't leave the opportunity go.

I think too that I could not, in this vein, quarrel with the Farinelli syndrome which is I guess to, "build it and try and fly it". If a cavity and testing it all out in the benchmarks is going to be the way to an engineering goal, then I don't think I am in a position to challenge but when you say that the benchmark is going to give you microscopic basic information, that it won't do.

I was impressed by the interest in core dosimetry both at and in the core and beyond the core but I was left a little bit with the feeling that the accuracies that are required are really not all that great. That the people that are involved in that work, particularly the commercial people--their needs are mostly met. There are some "fine structure" things remaining but there are no gross holes.

Quite a different area was the fission product, the burnup control, the analysis of core performance, and beautiful magnetic-spectrometry results from Idaho, and the excellent correlation of the chemical yield work here. Clearly the mass fields are changing violently with energy and I don't think it was fully appreciated what the impact of these, which I think really are proper fission-product standards, might be. I seem to recall that the way of monitoring the basic number of fissions in some of the best delayed-neutron experiments in the world was a counting of merely a hundred products. If that is true and they varied with energy, I question how good those delayed-neutron yields are now in view of these recent spectrometry results. The impact of those I think was very great. I think the Cf fission spectrum, as I mentioned earlier, should be accepted as a standard but, I got the general feeling that the averaged ratio rates given in various standard fission spectra, are running about two to three percent for Cf and that's probably not good enough. We are looking for another factor of two.

Now, again with the previous speaker, I concur with his error-file concept. It's a wonderful world, but there are several things that begin to bother me a little bit. I wonder if the sensitive things are not the standards. It seems to me that in some of the examples shown yesterday, the fission cross sections, which were the standards in the Godiva and Jezebel assemblies, they were not sensitive really. The other holes were those holes of uncertainty where we're guessing. What is the inelastic cross section of ^{235}U? Well I'd like to know and I guess some other people would like to know and that is a very sensitive item and how do I place an error on that aside from saying I don't know. I think that you've got to be a bit careful on how you specify these error files.

I also am a bit surprised that somebody hasn't given more emphasis to where you assign these uncertainties. Certainly the measurers and evaluators have simply got to give a great deal more attention to their error definition. Discrepancies are rampant throughout; people are just not representing things completely. It is a little like Ben Diven says, I guess, you correct it and put an error on everything you can think of but what do you do about the things you can't think of. Well you can't think of everything so people get ultra conservative but I think too that you might give consideration, particularly in the benchmark area, rather than assigning your discrepancies or your uncertainties and correlations to the microscopic data, follow the English course, as I understand it, and work with the correlated error files on the multigroup cross-section sets.

Prof. Havens: Dr. Farinelli would you comment on the subject?

Dr. Farinelli: Well, I think Randy Caswell mentioned before that this was the first Standards Meeting in which there was an attendance and the presence of biomedical people. To a certain extent I think it was the first meeting in which there was a fairly consistent representation of integral people as well. My opinion is that differentialists and integralists are much closer today than they were some years ago and that we are now starting to speak a common language. We seem to be able to understand and the fact that we have lively discussions is probably a representation of the fact that we have at least a common understanding - a common language. Otherwise, we couldn't even discuss. I think it is very important that we develop a common basis for understanding. It's quite clear that we must have some common way of looking, for instance, at errors, at error correlations if we want to assess what is the actual reliability of the data when they are applied to practical calculations.

I don't think it is the best procedure that differentialists and evaluators just well take their own responsibility to a certain point and then they leave the whole question to the others and say, "Well it's your business from now on." I think there should be some sort of hybridization of integral and differentialists to evaluate the final errors and so on and there are some other areas which we have not had time to mention but which are certainly interface areas and one of them I think is the area of how to make group cross sections, how to process the nuclear data. The way in which you process nuclear data involves both the way in which you have represented the nuclear data to start with and the way in which you are going to use the group cross sections and this is an in-between area which I think may be the cause of some of the discrepancy that we still observe.

Prof. Havens: I guess we have come full circle; when the reactor business first started it was the measurers who were the cross-section evaluators as well as the reactor theorists. In the Fermi group back in Columbia in 1940-1941, and then as time went on, we developed various specialities and were so interested in our specialities that we didn't talk to our nearest neighbor. We then find out that it is impractical and then come back again, but in the original days of the Manhattan project there was no need for communication because the people that did the measurements also used the measurements. They made them because they had to have them immediately to proceed to the next step, so I'm surprised sometimes at what the graduate students in both physics and nuclear engineering know and I'm also surprised sometimes at what they don't know. Would any other member of the panel care to comment on this subject?

Lee Stewart: I just might answer for some of the people here who have done the work. In CSEWG we have made many, many code comparisons to insure that we are processing the data in the same way or at least getting almost the same answers and I mean very close, depending on the methods that we use. There has been a great deal of work in this area in this country in CSEWG.

Prof. Havens: Any further comments from the panel?

Dr. Peelle: I have heard Chuck Weisbin give a talk on the subject of methods uncertainties and I'm sure Dr. Farinelli has made talks on that subject. Maybe we could hear just one comment which relates to this thing very clearly. How big are the uncertainties liable to be in calculated quantities, using the transport theory?

Dr. Weisbin: I don't know, Bob, if you're asking for a number or just a qualitative statement. Number one, they are not negligible. That's the first thing. I think I concur with Lee's comment that they are getting better, and there really are two types. There's the type of methods bias that we can know and pin down, for example P_3 versus P_4, or 50 groups versus 100 groups versus 200 groups. There are harder methods biases like taking a three-dimensional real problem and modeling it in 2-D, and saying what is the error due to our modeling when that is the best we can do. So now I go back to Al Smith's comment what do you do about the errors that you don't know about and of course those are harder. I would say that in general if you wanted a number though; well, let's take the number, k. I would say that methods errors today in the calculation of criticality are not less than three tenths of a percent.

Prof. Havens: Do you agree?

Dr. Farinelli: I concur.

Prof. Havens: I remember one time when there were about five measurements of the ^{235}U cross section at thermal, all of which were good to two percent and all of which varied by about 15%. They were poor measurements because the errors had been incorrectly determined.

Prof. Havens: We'll proceed on to the next subject which is rather a difficult subject to bring together, "Techniques and Methods." However, there was a workshop which is close to that although not exactly, that's the first on the list of the workshops, "Establishing Neutron Energy Standards," and would Dorien James please give a summary of that panel's discussion?

Dr. James: Perhaps I could say again that the work of the INDC subgroup in selecting a list of narrow resonances simply for use as energy standards could be regarded as complete and the list is given in Table 7 in my paper. The next stage is to evaluate the data available on all these resonances and establish the best values, and it is hoped that workers on each spectrometer will now and in the future publish their best values for these resonances. Mughabghab and Bhat have suggested to me that the list of best values should be published in the next addition of BNL-325. I've agreed to bring these results together. Now Joe Fowler suggested that someone should write a review article giving all the details of all the measurements involved in deriving the best values. He twisted my arm into doing this. He threatened to tell Basil Rose, if I didn't do it. You must wipe that out, Charlie. I guess you've got an expletive delete button on these federal tapes that you are producing. Now this would, I hope counter Alan Smith's strong objection to using any data as a standard which is not fully documented. I agree with that sentiment but I think that if we demand of all the measurers that they fully document their results, then maybe we would have to wait a long time. It looks from the evidence that white sources are now in fairly good agreement except perhaps the Geel-Columbia ^{238}U discrepancy which I mentioned this morning. The careful work of Meadows has shown that white sources and monokinetic sources can be brought into agreement also. Now many white sources have certain substances either always in the beam, for instance, ORELA bind the ^{10}B filter with sulfur so they always have sulfur in the beam and on the synchrocyclotron we use background filters so that our measurements can have silicon oxide in each run. These enable certain resonances on the list to be continually checked and it is suggested that the values obtained for these resonances should be included in the publication of any data. Anytime you

publish data you should also report your value for the resonances on the list, just to confirm that you are still checking. Finally, there might be a slight problem with poorer spectrometers because they may not see all the narrow resonances on the list, but in time of course they will be able to use the energies of broader resonances given by the laboratories which do quote their values for the narrow resonances.

Prof. Havens: Thank you. Alan, would you put together the summary?

Dr. Smith: I regret the action Dorien has taken because if he is going to write a comprehensive review with all the errors, I'm not going to see a good friend for 18 months, I guess. You're out of business, but I think it is certainly a proper thing to do and I encourage it. I think at the higher energies which I'm familiar with, the whole problem has essentially gone away. I think that the remarks this morning that there are discrepancies but with an exception of perhaps one fission cross section, for most practical reasons, they are negligible. What really bothers me is that for this example, and I think also one dealing with the fission neutron spectrum, considerable effort has been expended because of one or two measurements which turned out to be a little in error. I think one should be careful before you immediately take some action that you carefully review any standard measurement and try and find out if there is a problem or something. It is kind of a double-edged weapon. There was a great deal of effort put on fission cross sections and I include fission spectra and I think that was very warranted; we didn't know much. We know a lot more now. But in fact the disaster that we thought was there from some preliminary estimates was not there. I think there is a word of caution not to get carried away when somebody has a preliminary result on some of these standards that goes somewhere different. Take a good look at them, before everyone takes off and makes some measurements.

I would like to give justice particularly to all the people who talked about instruments. If I have any competence, it is didling with instruments, and I realize how difficult and how complex these things are. It was a very diverse discussion here with many contributions, and I can't begin to do justice to them. There were many of them that were very elegant and many of them were carried to very high degrees of accuracy; but if I recall, only two of the instruments were not described at the last standards conference. Really what is talked about is refinements - very hard to get and very well done but not a really new instrument with two exceptions which are really modifications of other schemes. One that I mentioned before was the flat counter from Livermore which has a tremendous potential for getting over this gap between the (n,α) resonance and one MeV. I think one of the great advances in the instrument area in the last 10 years which I never would have believed 10 or 15 years ago, is the ability to use the hydrogen recoil counter reliably at low energies. Just a technological achievement, but if somebody would have told me in 1970 that you could monitor a beam in a linac with precision at 50 keV, I would have laughed. It's done and I think that it is done well.

I think certainly that the sharp improvement in reference fields is a real key to the dosimetry problem particularly the very high purity fields which have the peculiar problems for dosimetry that they have here at the Bureau. I am not sure their impact was made clear; you may not find those so valuable for some research purposes, but it is clear that they are essential to the proper calibration of dose. I think we still have a big hole - the one thing which I have always been looking for - a flat detector with a high sensitivity. It's the crux of a lot of problems and I don't see it coming. For example, how do you solve the delayed-neutron issue which has been a very serious bottleneck for a number of years.

Prof. Havens: Thank you. That reminds me of one time a navy Admiral was trying to describe everything that was desirable in an anti-submarine detector, and I think it was Panofsky who got up and said, "Admiral, we can only use nature we can't coerce it." Seems to me that Alan is trying to coerce nature into getting the ideal detector. I don't know how we can do that.

Dr. Smith: I think that we should point out that one of our medical people wanted a spectrometer which would go from one kilovolt to 20 MeV with an absolutely determined response so they have their problems too.

Prof. Havens: We all have problems, but we can only use nature, we still can't coerce it. Dr. Motz would you take the lead on this?

Dr. Motz: Several other comments have been made about detectors and the fact that perhaps boron detectors deserve more attention and Lee has mentioned that hydrogen recoil isn't used as extensively as one would expect. Another detector that I think has hardly been mentioned is the ^{3}He counter. It has some disadvantages but it certainly has a good predictable response. It's a question of sensitivity and packaging but certainly one that deserves some attention as a standard reference.

I am very pleased to hear that Dorien is going to document the energy standards and I wish him luck. I hope he can come up with the enduring values that he was trying to explain to us during his talk. I would be especially interested in seeing that, Dorien, because I have some degree of scepticism about the high degree of accuracy that is claimed in the final results. I think that it does take a careful analysis to convince one that they are really known as well as you were indicating.

I wanted to make one comment about high-energy neutron sources. With respect to the presentation on associated-particle methods, it was mentioned that a lot of the defects which occur in neutron sources and associated-particle work are really associated with the solid targets that are used and many of these problems go away when one uses a gas target. There are in fact two recent reports out about purity of 8-14 MeV neutron sources considering most of the parameters that one could change such as beam stops and collimators defining beams and things of this sort. This work has been done at Los Alamos both for the t-P and the p-T sources and compared with d-D source and the second report is from Bruyéres-le-Châtel in France, similarly for p-T sources.

Prof. Havens: Would any other member of the panel like to comment on this subject?

Dr. Liskien: In the field of standards one has to use any occasion to check consistencies and I see a broad field where this is not fully exploited and I mean linac measurements which typically use shape monitors and then go from the eV to keV region to normalize, using hydrogen telescopes or similar devices as shape monitors. I could imagine that it must not be too difficult to go one step further from a shape monitor to absolute recoil counting and thereby provide additional information. I think nobody should be afraid that other inconsistencies could come out when you have two methods of normalization. Another point

is that I think in fact we have not really seen many new techniques in this symposium. I think one, not a new method, but at least a way of applying a technique has been demonstrated and I think it should be mentioned. I mean associated-particle counting, not the particle itself, via its activity or by counting but really by its gamma-deexcitation as Dr. Brandenberger has demonstrated. I think we should see the people that are doing absolute flux determination, and inquire what they really can do with this method with other sources.

Prof. Havens: Any further comments from members of the panel?

Dr. Peelle: I would like to just accent, another time the use of diverse techniques. We have heard in many contexts, that this is the key to long term success in the standards' field. One example is Dr. Knoll's paper in which he described the work he and his students have done at a few energies with γ-n sources. That's not a new idea but it appears that it is being pushed in a logical way to give highly credible results which seem very independent of most of the other work that is done, and therefore very valuable.

Prof. Havens: Lee Stewart do you have any comments?

Lee Stewart: If I may just mention a situation at Los Alamos many years ago; a young scientist started working with the n-p cross section and he accordingly calibrated his detector. Then he decided to measure the hydrogen cross section with this calibrated detector and he was quite discouraged when, at some angles he could not reproduce the hydrogen cross section better than approximately 15%. Naturally, he went back to the drawing board. Therefore, I believe the business of intercomparison is extremely important.

Prof. Havens: Any comments from the audience? Then we will proceed to a subject which has been controversial ever since this field started; that's the ^{235}U fission both at low and high energy. Now Dr. Cierjacks was the leader of a discussion group on the ^{235}U cross section. Would you give the summary, Dr. Cierjacks?

Dr. Cierjacks: The fission cross section of ^{235}U is in quite good shape presently, nevertheless there are a few problems left. As a result of the discussions we had in the working group, we came up with a few observations and recommendations which I should like to read to you.

Thermal Value: The group felt uncomfortable about the fact that evaluations gave about 0.3% accuracy for the actual thermal value while deviations are somewhat larger than the quoted values. Coming now to the situation of the 9-eV resonance region. Here we felt that more evaluations and more measurements are needed. The data in hand when published and evaluated could well result in a $\pm$1% accuracy of the fission integral in that resonance region. Let's go on to the remaining eV range; there we have two statements. First, another normalization point in the resonance region should be chosen to allow for a cross check of the data. A suitable resonance range would perhaps be between 33 and 41 or between 41 and 60 eV. Second, an additional reference band would be desirable in the range of perhaps 0.3 to 1 keV. With respect to the keV range, the following recommendation was made. Absolute white-source measurements with adequate accuracy ought to be encouraged in that region. Finally we had a recommendation for the MeV region which might not necessarily be limited to ^{235}U. Consideration should be given to fission reference cross sections in the range from about 10 to 40 MeV.

Prof. Havens: Alan, could you give your comments on this subject?

Dr. Smith: As many of you know, eight or nine months ago there was a special workshop conference at Argonne on fast fission cross sections of U-235, U-238, and Pu-239. All the available data were reviewed. There is a book over there in the coffee room. One of the outcomes was that certain areas were identified as being critical, other areas were in good shape, and we hoped that as a result some work could be done on those selected problem areas. In fact some was, and some is still in progress. I am pleased to say that I think that was an effective result of that conference, and some of it is reported here. I think as a result of this work, depending on how you want to view your various interpretations, the fission cross section of ^{235}U from a few keV to less than 2 MeV is known to about 2 percent. Up to 8 MeV I would estimate 3 percent, at 20 MeV I would estimate 5 percent. That puts it within the requirement, for example, of the biomedical people. One of the issues at the conference was structure in the fission cross section, it's there. There were examples shown at this meeting where careful search shows that it isn't particularly correlated in some cases, in some cases it is. I think the issue is not really important at the present time. I think that now the thing to do is to continue the work, which the previous speaker emphasized, to try and get a normalization of the white source measurements using an absolute calibration. I am very leery of this low-energy extrapolation. I think that the consistency with this and the higher-energy normalization has got to be achieved. A gap exists, and until you can get across it, I think you've got a real problem. The work is particularly going on here at the Bureau in that area, and I guess other places, and I suggest that these people get together and they keep in better contact with one another and that they attempt to put together a preliminary evaluation of these results in a better correlated manner. I agree with the opinion that was quoted at the conference at Argonne that I don't think any formal evaluation should use unfinalized or unpublished results. I think preliminary results are out. I'll extend that statement a bit farther, and I think I already made it today, that no evaluation should be distributed for final use or considered final until it is fully documented too. And I think a lot of the problems that are involved now are the interpretations of evaluations, how you want to interpret the data, and it's all rolling around in a ball of wax.

Now I think with this approach there are some other serious concerns. I think that you might, as I think it was expressed at this conference, wonder whether you need this cross section any better until you can master the ratio problem. I looked at those ratios again last night, and well, depending upon who you want to believe, it's one to three percent uncertainty in the ratio of ^{235}U to the other fission cross sections. It certainly is not an order of magnitude better and maybe not even a factor of two, or maybe even worse. I think before you push too hard on the problem of the absolute ^{235}U cross section, if it is correct to two percent over most of this range, you'd better master the ratio problem.

I also think that one should give far more attention to the weighting of the absolute source measurements; I believe it was Bob Peelle who just mentioned them here a minute ago. I think that there is an awful tendency in fission cross section measurements, both ratios and absolute ones, to look at the mass of points and to draw a line through them, and to ignore these highly precise and quite independent check points. I think that's a mistake that has been made in a number of contexts, and it's acute in this case. Only four or five points which appear to be

excellently done, and they get lost in the wilderness; but they're very essential normalization points. The same thing tends to be true of white-source versus monoenergetic-source machines.

I think that I would then like to go on to the problem of the high-energy fission standards. I certainly subscribe to the statements made by Siegfried Cierjacks a minute ago. Yes, we need a high energy fission standard from 14 MeV to 20 MeV, with perhaps 2 or 3 percent accuracy. What bothers me I think is the problem of structure in the ^{238}U cross section. The ^{238}U cross section has structure, I'm sure, and some very excellent measurements show it. Apparently it is not so prominent at all in ^{237}Np. But I think before we change standards one should be very careful to confirm the exact magnitude and nature of this structure. Furthermore, I had a little inspection of the data I could find last night, and I concluded that with any reasonable working experimental average you in fact could not be perturbed by that structure, and I am a little afraid that this is going to be a reflection of a syndrome, and I'm sure people will take exception to this, but a syndrome for resolutionmanship, as Henry Newson used to call it. In many of these things, let's not be possessed with the structure. I think Paulsen was right; gold's got structure, but when used with judgment, it's a good capture standard, and the same may be true for ^{238}U fission.

I think, too, that we should, of course, in this high energy range, before we put a big crunch on a new standard which does not have a direct application such as ^{238}U, always remember that this is a region, if nowhere else, where hydrogen should work. Do we really have a need for another reaction standard in this area? Well, that's where I'd like to stop on fission cross sections.

I'd like to make one more remark which is applicable to fission cross sections, but more generally applicable than that. It is aimed at our evaluators who, I must confess as my operating budget gets smaller and smaller and as I tend to spend more time in my office punching square holes in long cards, I seem to be joining. There seems to be an awful rigidity to evaluations. I don't think there's a sin in being smarter today than yesterday and that the result of new information or new thoughts ought to be incorporated into an evaluation - even a standard. I think we should be more adaptable in adjusting to changing conditions and changing knowledge. I guess that's in a direct opposition to the way the world is going, but I seem to have this feeling that we're awfully rigid in what we're doing. Even if somebody comes up today with a new standard result, it's going to be four years, if we're lucky, before anybody gets it out of their private files and used. And I think that's a very serious problem. There's a need for a great deal more responsiveness.

Prof. Havens: Thank you.

Dr. Peelle: There were many remarks in the last few days about the problem of normalizing cross sections near thermal energy, in addition to my own. One point I didn't make during my talk but which Dr. Bhat made at Argonne was, that in spite of the great discomfort with some of the intermediate results that one looks at in making such a normalization effort in ^{235}U, by the time the CSEWG Task Force with its imperfect understanding of everything got to about 100 keV, the seeming discrepancy on the average with the monoenergetic sources was of the order of one or two percent which is well within the uncertainty of the measurements. So perhaps the central limit theorem or law of averages has helped out. Perhaps it has not been so bad as it could possibly have been with the uncertainties along the way.

We were challenged to come up with an uncertainty on the request for a one percent ^{235}U cross section. Based on the evaluation of the statistics of the various request lists I've seen over the years, the answer is 1 ± 0.6 percent accuracy without any statement whatsoever as to what that means. I think it must mean, since most of the uses are somewhat integral in nature, that this kind of accuracy is needed in the integral over a substantial energy region including at least a few lethargy units. Now how we verify that as a desired accuracy, I don't really know. Most of those numbers were derived by people a decade or more ago that I didn't talk with. Since that time, in the case of ^{235}U, the cross section I think on the average has changed by several times that amount. But until we get stability somewhat near that value, I don't think we need to worry too much about the precise number.

But how do we know how well we must do? That's a question we'll have to face within a few years as the standards field becomes more mature. It seems to me that the work that Chuck Weisbin reported on, although of preliminary nature in a sense because all the necessary inputs that he said he needed were not present, does start to show in a fairly vigorous way what the impact of a change in a standard or an uncertainty in a standard really is. In the analysis of integral benchmarks, which are dear to the heart of the applications people, changes at the 1% level seem to have a significant impact, even in an integral experiment that contained no uranium. So the first tentative systematic study that I've seen suggests that there is a definite impact of knowing a standard to high accuracy perhaps better than the present knowledge.

I think that since 1970 there's been a dramatic improvement in the ^{235}U fission cross section. Dr. Poenitz suggested that indeed over some broad band it's something like 7 percent in seven years. Now I don't think it will do that in the next seven years, but who's to be sure, especially if we achieve the flexibility in using our knowledge that Dr. Smith asked us to show.

Prof. Havens: Would any other member of the panel like to comment on the ^{235}U cross section? Lee Stewart.

Lee Stewart: Well I suppose that you can plot data and, if you know what you want to show, you plot it that way to show it. But I believe I would find it very difficult to accept a 2 percent error on ^{235}U above a few keV, remembering the work that we've done for sometime now in CSEWG. In addition, if I remember correctly, and if people have not changed their data, the structure that we put into version IV in ^{235}U was based on a comparison of four separate experiments; one from Harwell, one by Charlie Bowman from Livermore, one from Los Alamos by Lemley, and Reg Gwin's from Oak Ridge. The structure did line up. We did find that they did not identically line up, but saw the same peaks and valleys in all four experiments. The main reason, however, we chose to put in the structure is because there are wide minima, there are 15 percent deviations, and therefore a person doing a monoenergetic experiment will measure a cross section depending upon his resolution, if you assume that those data are correct. Therefore I believe that we do need the structure in the cross section.

Prof. Havens: Further comments?

Dr. Poenitz: When structure shows up, I always take the practical point of view; I ask, what is the effect in a calculation? For example, what is the effect on a calculation using the ^{238}U capture cross section when the structure differs by an order of magnitude? While the structure may be interesting, I don't believe it has any practical implication, and the calculations agree with this.

The major comment I wanted to make is in regard to the question of the hydrogen cross section as a standard. First of all, there is no standard cross section anyway because standards can only exist for basic units, like length and time. I noticed you have the derived quantities, and so each new measurement necessarily changes that so-called standard; we should probably call it a reference. From that it follows immediately that there can be no difference among the standards. There is no primary standard. The argument that the hydrogen cross section, for example, is the best known, is a true argument or true statement, but it does not mean that the measurement using the hydrogen cross section is preferable to any other one because the cross section is not the only quantity involved. The efficiency of the detectors is the second one. So the absolute measurement of the fission cross section may bring us a much better reference cross section than the use of the hydrogen would permit us to do. As a matter of fact the question comes up now in the high energy range where we don't know the angular distribution of the hydrogen so well. It may be much better to use say a fission cross section where we have a very high precision in the efficiency of the counter.

Prof. Havens: Anyone care to comment on that?

Dr. Peelle: A small piece of it I'd like to comment on. It's true that we did one study for the unresolved resonance region in ^{238}U, looking at fast reactors, and found the fluctuations which have been seen there with indeed much less resolution than is available could not be shown to have an impact of any importance relative to the error in the average cross section. However, I think that one has to have a little reservation about that study and recognize that in any such question about the importance of fluctuations you have to ask about the particular situation. In general, I think we've gotten in trouble with our reactor engineer friends several times by having given them the impression that cross sections are smooth. They believed the graphs they saw in the book. Even though we know they weren't smooth, they didn't know they weren't smooth. It may be best to represent them to the extent that we know them.

Prof. Havens: Thank you.

Dr. Smith: What does Ugo Farinelli think about that?

Dr. Farinelli: This is I think a good example of the influence of the averaging procedure. It depends on whether you make the average from very detailed structure in the differential measurements, or whether it's the measurement itself that makes a certain average. I have always thought that it would be conceivable to make measurements that measured directly the average in the sense that it was to be used, especially when the detail is so great that even if theoretically you have the methods to weigh the structure differently according to the composition, which should be done, practically you don't do it because of the complexity. If you have say 100,000 points, you are not going to weight this over any spectrum; you're simply going to make a very straightforward average, independent of composition. So I think a measurement can yield the same result. Well, it may not be perfectly correct, but this is going to be the same value that is used by the integral man who is doing the calculations. So I agree that in principle the man who makes the measurements would like to give something which is perfect and then it's the responsibility of the man who uses his data if he fudges with them. But from a practical point of view I don't see the difference.

Dr. Peelle: I did make a quick effort to check that point on the question of thick-target transmission and self-indication measurements for ^{238}U, and to compare that to what one sees in a processed cross section taking into account what are thought to be the fluctuations. Even though the two studies are based on the same phenomena of the self-protection in the resonances, I could not demonstrate a direct correlation for either of those two types of measurements and the processed cross sections which are now found. Not only was there none, but I could not show there should be. I think I may have erred, but sometimes it will be necessary for the calculational expert to take the details in some form or another and deal with them.

Prof. Havens: Francis Perey.

Dr. Perey: I'm very much interested about the statement regarding structure details. As you know I've struggled with the problem, but you tell me that I must average the cross section in the measurement process or the evaluation process and give you a smaller number of points. We've tried to do that for years and never succeeded. I don't know how you're going to homogenize your calculations, whether you're going to use a couple of mm or one mm of fuel cladding or one meter of iron in your shield. Which average should I use to put into the file when I have structure, when I know the structure exists?

Prof. Havens: Do you want to answer that Ugo?

Dr. Farinelli: Yes. You don't know what to do, but you should not think that people who make the calculations know what to do. It's not really conceivable that somebody making the calculations for the reactor uses a different cross section if he moves from one point of the reactor to the other. Do you really think that somebody is going to take a different cross section for iron or nickel in the cladding or in the follower of the control rod, in the core or in just a little way off? I don't think so. It's common to have just one cross section for iron, at least in the core. You may have two if you go to the blanket or to the shield, but certainly in the core you have just one cross section. How are you going to calculate it? With an average composition over all the core or over a system of cores which are not too different from each other. From one point to the other there will be differences, but the differences will not be reflected in any set of cross sections used. So the problem is there.

Prof. Havens: Lee Stewart.

Lee Stewart: Let's get back to ^{235}U. It is a standard, and I dislike penalizing a monoenergetic experimentalist who does an experiment with very good resolution and therefore measures a cross section that is 10 percent lower than anybody else who does one with very poor resolution. And for that reason alone, if none other, I think we should be willing to put in the structure in ^{235}U that has been measured by at least four people. That was my primary reason for thinking that the structure should go in. It did bring in line, by the way, a lot of older experiments. It did show us where some of the problems are.

Prof. Havens: Chuck Weisbin.

Dr. Weisbin: I think this one study that we're talking about here in intermediate structure unfortunately can go back to something we did. This was one study, one case, not a large sampling. I think, however, in the future years we are going to see advanced techniques which can make use of the structure, Ugo, in the sense of the work that Red Cullen is doing on probability tables, where he tabulates the probability of a given cross section versus that cross section in a given energy range. This is a very efficient representation that can make use of the structure so that if evaluators did the smoothing ahead of time, and just gave us a single average, we could take advantage of that methodology. However, if we do have the access to the structure, we can put it in an efficient fashion, and I think we will find out we get different answers, at least in some cases, not yet shown, admittedly.

Prof. Havens: This problem of how much detail you should put in the cross section and then what you can use and what you assume and how you average has existed, I'm sure, ever since nuclear energy has existed in the form of reactors, and if you had seen some of the averages that Hans Bethe made in 1943 and 1944 you would be really flabergasted at some of the assumptions that went into the formulae. I remember very well when I first showed Neils Bohr a resonance in ^{235}U he said, "This can't happen". So, there are some problems with the detail you put in the cross section and the theoretical models, not only of the nucleus but of the reactor as well, and you're limited to what you can do in a practical sense.

Dr. Bowman: I think that's an interesting story because what you're saying is that as years have gone by and calculational techniques via computers have improved, that we've been able to handle more and more structure. It seems like a lot of the discussion here this afternoon assumes that we are at the end of that calculational development and calculational capability. But, if I read the latest issue of Science where they talk about what's coming in the speed of computers and so forth and assume that that's going to be implemented in the nuclear power industry, it would seem to me that there's quite a likelihood that we will develop these techniques. Maybe the technique that Chuck was referring to a minute ago is just the next of a series of steps into the future.

Prof. Havens: I think with the development of reactor design and reactor calculations over the years, the capability of computers has very often been the limitation of what you can do; and as that's improved, the calculational accuracy of what could be predicted has also improved and will continue to improve. However, I was asked to try to bring this session to a close shortly. Before we finish the session, I'd like to ask Alan Smith if he has anything further to say.

Dr. Smith: I do. I am brought back to Farinelli's point of view. I really think the greatest value of standards is the all-important ability to calculate the performance of the system within a measurable range. And if you can't do that, you could never expect to make the extrapolation of the calculation to an unmeasurable range which you'll have to do to prove acceptance in safety. So I think there's been a change in the values in my mind of standards from primarily economic now to safety and public acceptance. Now it may change back after you've passed a period to economic grounds, but I think that's the key. Your calculational ability is the thing that's important now. It's your ability to predict reliably and show that you can do it. Without that, I don't think your technology is going to fly.

Prof. Havens: Well the conference will be brought to a close, but before we do that I'd like to thank the panel members and Alan Smith for summarizing the conference. I'd also like to take this opportunity to thank Charlie Bowman for organizing the program, which, when he first said we're going to spend four days on standards, I said, "Oh, my God, not that." But certainly the interest of this conference has held up a lot more than many of the meetings that I have attended. The fraction of the audience here on Thursday afternoon to that here on Monday morning is very much higher than it is in most technical meetings that occur. The standards, someone said, only are needed after you've made several measurements and after a field has been pretty well developed. I think that's true if you only have one measurement. Then you don't need a standard, the one measurement is the standard. I don't want to get into a debate with Poenitz about standards because we have talked about standard reference data and there are various definitions of standards. I will suggest that you read the definitions of standards in some of the literature put out by the National Bureau of Standards, and you'll be surprised at what some of the standards are. Some of them are arbitrary, some of them are natural, in that they are physical measurements, but they vary all over the lot depending on the field that you're working in. But I think that Charlie and the Bureau have done an outstanding job. It's the first conference I have attended here at the Bureau, and I think that it has been a very well run conference, and the Bureau has excellent facilities which we've all enjoyed. I think we should give a vote of thanks to the Bureau, and we certainly appreciate the activity in this field that has been demonstrated here at this conference. Thank you, Charlie.

I now declare this meeting adjourned.

LIST OF PARTICIPANTS

Alberts, W. G.
Physikalisch-Technische Bundesanstalt
100 Bundesallee
D-3300 Braunschweig
WEST GERMANY

August, Leon S.
Naval Research Laboratory
Code 6643
Washington, D. C. 20375

Auxier, John A.
Health Physics Div., ORNL
Route 1, Jones Road
Lenoir City, Tennessee 37771

Awschalom, Miguel
Fermilab
P. O. Box 500
Batavia, Illinois 60510

Axton, E. J.
National Physical Laboratory
Teddington
Middlesex TWII OLW
UNITED KINGDOM

Barschall, H.
University of Wisconsin
Engineering Research Building
Madison, Wisconsin 53706

Bartholomew, G. A.
Atomic Energy of Canada Limited
Chalk River Nuclear Laboratories
Chalk River
Ontario, CANADA KOJ 1JO

Bartlett, William T.
Battelle, Pacific Northwest Labs.
Battelle Boulevard
Richland, Washington 99352

Bastian, C.
CEC, CBNM Euratom
Steenweg naar Retie
B-2440 GEEL
BELGIUM

Behrens, J. W.
Lawrence Livermore Laboratory
P. O. Box 808
Livermore, California 94550

Benjamin, Richard W.
E. I. du Pont de Nemours and Co.
Savannah River Laboratory
Aiken, South Carolina 29841

Bergqvist, I
Dept. of Physics,
University of Lund
14 Sölvegatan
S-22362 LUND
SWEDEN

Bhat, Mulki R.
Brookhaven National Laboratory
T197C
Upton, New York 11973

Blinov, Mickail
Chlopin Radium Institut
Leningrad
USSR

Block, Robert
Rensselaer Poly. Institute
Troy, New York 12181

Boldeman, John William
AAEC
Private Mailbag Southerland
N.S.W., AUSTRALIA

Bowman, Charles D.
Center for Radiation Research
National Bureau of Standards
Washington, D. C. 20234

Brandenberger, Jerry D.
Los Alamos Scientific Laboratory
Box 1663
Los Alamos, Nex Mexico 87545

Broerse, J. J.
Radiobiological Institute TNO
151 Lange Kleiweg
NL-RIJSWIJK
THE NETHERLANDS

Cancé, Michel
Commissariat à l Énergie Atomique
B.P. n° 561
F-92542 MONTROUGE CEDEX
FRANCE

Carlson, Allan D.
Center for Radiation Research
National Bureau of Standards
Washington, D. C. 20234

Carter, Robert E.
Institute for Resource Mgmnt. Inc.
9512 Edgeley Road
Bethesda, Maryland 20014

Caswell, Randall S.
Center for Radiation Research
National Bureau of Standards
Washington, D. C. 20234

Chemtob, M.
Dépt. de Protection SPS/LDS
Centre d'Etudes Nucléaires
de Fontenay-Aux-Roses
B.P. n° 6
F-92260
FONTENAY-AUX-ROSES, FRANCE

Chrien, Robert E.
Brookhaven National Laboratory
Physics Department, Bldg. 510A
Upton, New York 11973

Cierjacks, Siegfried W.
D-75 Karlsruhe, Weberstrasse
Karlsruhe 1
West Germany

Cosack, Martin
Physik Tech. Bundesanstalt
Bundesalle 100
33 Brannschweiz
WEST GERMANY

Czirr, John B.
Lawrence Livermore Laboratory
P. O. Box 808, L-280
Livermore, California 94550

Davis, Mark C.
Dept. of Engrg. Sciences
The Technological Institute
Northwestern University
2145 Sheridan Avenue
Evanston, Illinois 60201

Derrien, Hervé
CCDN/NEA OECD
B. P. n° 9
F-91190 GIF-SUR-YVETTE
FRANCE

Dierckx, Ronald
P.O. Box 1663
Los Alamos, New Mexico 87545

Diven, B. C.
Los Alamos Scientific Laboratory
P. O. Box 1663, MS 442
Los Alamos, New Mexico 87545

Duvall, Kenneth C.
Center for Radiation Research
National Bureau of Standards
Washington, D. C. 20234

Eisenhauer, Charles M.
Center for Radiation Research
National Bureau of Standards
Washington, D. C. 20234

Engdahl, John C.
Department of Physics
University of Michigan
Ann Arbor, Michigan 48109

Fabry, Albert
CEN-SCK (Belgium)
1900 Stevens Drive 214
Richland, Washington 99352

Farinelli, Ugo
CNEN-CSN CASACCIA
00060 Santa Maria Di Ualeria
Roma, ITALY

Farrar, Harry IV
Atomics International
8900 DeSoto Avenue
Canoga Park, California 91304

Flemming, Dale M.
Battelle, Pacific Northwest Labs.
Battelle Boulevard
Richland, Washington 99352

Fleming, Ronald F.
Center for Radiation Research
National Bureau of Standards
Washington, D. C. 20234

Fowler, Joseph L.
Oak Ridge National Laboratory
Oak Ridge, Tennessee 37830

Fuchs, Jean Eric
60 G rue Albert Garry
LIMEIL-BREVANNES, FRANCE 94450

Gabbard, Fletcher
Department of Physics & Astronomy
University of Kentucky
Lexington, Kentucky 40506

Geiger, Klaus W.
National Research Council of Canada
Division of Physics
Ottawa, Ontario
CANADA K1A OR6

Gilliam, David M.
Center for Radiation Research
National Bureau of Standards
Washington, D. C. 20234

Goldman, David T.
Institute for Basic Standards
National Bureau of Standards
Washington, D. C. 20234

Goodman, Leon J.
Radiological Research Accelerator Facility, Columbia University
Bldg. 902B, Brookhaven National Lab.
Upton, New York 11973

Green, Lawrence
Bettis-Westinghouse
P. O. Box 79
West Mifflin, Pennsylvania 15220

Greenwood, Lawrence
Argonne National Lab.
9700 South Cass Avenue
Argonne, Illinois 60439

Grundl, James A.
Center for Radiation Research
National Bureau of Standards
Washington, D. C. 20234

Hajnal, Ferenc
U.S. ERDA Health & Safety Lab.
376 Hudson Street
New York, New York 10014

Hale, Gerald M.
Los Alamos Scientific Laboratory
P.O. Box 1663
Los Alamos, New Mexico 87544

Harrison, George H.
Radiobiology Section
Univ. of Md. School of Medicine
660 W. Redwood Street
Baltimore, Maryland 21201

Harvey, J. A.
Oak Ridge National Laboratory
P. O. Box X
Oak Ridge, Tennessee 37830

Havens, William W. Jr.
Columbia University
520 West 120 Street
New York, New York 10027

Heaton, Henry T., II
Center for Radiation Research
National Bureau of Standards
Washington, D. C. 20234

Hemming, P. B.
U.S. ERDA
Washington, D. C. 20545

Hill, N. W.
Los Alamos Scientific Lab.
P.O. Box 1663
Los Alamos, New Mexico 87545

Howerton, R. J.
Lawrence Livermore Lab.
Box 808, L-71
Livermore, California 94550

Huynh, V. D.
Bureau International des Poids et Mesures
Pavillon de Breteuil
F-92310 SEVRES
FRANCE

Islam, M. Mizanul
Bangladesh Atomic Energy Commission
Atomic Energy Centre
P. O. Box 164, Dacca-2
Bangladesh

Jaffey, Arthur H.
Argonne National Laboratory
9700 S. Cass Avenue
Argonne, Illinois 60439

James, G. D.
Atomic Energy Res. Est.
HARWELL, Didcot, Oxon OX11 Ora
UNITED KINGDOM

Johnsen, S. W.
Crocker Nuclear Lab.
University of Calif., Davis
Davis, California 95616

Kazi, A. H.
Army Pulse Radiation Facility
STEAP-RF, Bldg. 860
Aberdeen Proving Ground, Md. 21005

Kellie, J. D.
Glasgow University
Kelvin Laboratory N.E.L.
East Kilbride, Lanarkshire
SCOTLAND

Knitter, H.-H.
CEC,CBNM Euratom
Steenweg naar Retie
B-2440 Geel
Belgium

Knoll, Glenn F.
2266 GGBL
University of Michigan
Ann Arbor, Michigan 48105

Knox, Harold
Physics Department
Accelerator Laboratory
Ohio University
Athens, Ohio 45701

Kuchnir, Franca T.
Dept. Radiology, Box 442
University of Chicago
950 E. 59th Street
Chicago, Illinois 60637

LaBauve, Raphael J.
Los Alamos Scientific Laboratory
MS-243, P. O. Box 1663
Los Alamos, New Mexico 87545

Lachkar, Jean C.
Commissariat à l'Energie Atomique
Centre d'Etudes de Bruyeres-le-Châtel
B. P n° 561 92542 Montrouge Cedex
FRANCE

Lamaze, George P.
Center for Radiation Research
National Bureau of Standards
Washington, D. C. 20234

Lane, Raymond O.
Physics Dept., Accelerator Lab.
Ohio University
Athens, Ohio 45701

Leiss, James E.
Center for Radiation Research
National Bureau of Standards
Washington, D. C. 20234

Leonard, Bowen R. Jr.
Battelle - Northwest
P. O. Box 999
Richland, Washington 99352

Lippincott, E. P.
Westinghouse Hanford Company
P. O. Box 1970
Richland, Washington 99352

Liskien, H.
CEC, CBNM Euratom
Steenweg naar Retie
B-2440 Geel
BELGIUM

Lisowski, Paul W.
Triangle Universities Nuclear Lab.
Dept. of Physics, Nuclear Bldg.
Duke University
Duke Station
Durham, North Carolina 27706

Lone, M. A.
Chalk River Nuclear Labs.
Chalk River, Ontario KOJ 1JO
CANADA

Lurie, Norman
IRT Corporation
7650 Convoy Court
San Diego, California 92111

McDonald, Joseph C.
Sloan-Kettering Institute
1275 York Avenue
New York, New York 10021

McElroy, William N.
Westinghouse Hanford Company
P. O. Box 1970
Richland, Washington 99352

McGarry, Emmert Dale
Harry Diamond Lab
2800 Powder Mill Road
Adelphi, Maryland 20738

Maeck, William J.
Allied Chemical Corp., INEL
550 2nd Street
Idaho Falls, Idaho 83401

Magurno, Benjamin A.
Brookhaven National Lab.
T-197
Upton, New York 11973

Marshak, Harvey
Heat Division
National Bureau of Standards
Washington, D. C. 20234

Meier, Michael M.
Center for Radiation Research
National Bureau of Standards
Washington, D. C. 20234

Moazed, Cyrus
Harry Diamond Laboratories
2800 Powder Mill Road
Adelphi, Maryland 20783

Moore, Michael S.
Los Alamos Scientific Lab.
P.O. Box 1663
Los Alamos, New Mexico 87545

Morgan, W. C.
Battelle-Northwest
Battelle Boulevard
Richland, Washington 99352

Motz, Henry T.
Los Alamos Scientific Lab.
Box 1663
Los Alamos, New Mexico 87544

Mughabghab, Said F.
Brookhaven National Lab.
Upton, Long Island
New York 11973

Navalkar, M. P.
Bhabha Atomic Research Centre
Neutron Physics Section
Trombay
Bombay, Maharasmtra
INDIA 400 085

Nelson, Charles E.
Triangle Universities Nuclear Lab.
Duke University
Durham, North Carolina 27706

Nelson, Ronald O.
Los Alamos Scientific Lab.
P.O. Box 1663
Los Alamos, New Mexico 87544

Nilsson, Leif
Tandem Accelerator Lab.
August Södermans väg 70
Uppsala, SWEDEN

Otroshenko, Gennady
Kurchatov Institute on the
Atomic Energy
Moscow, USSR

Ozer, Odelli
Electric Power Research Institute
P. O. Box 10412
Palo Alto, California 94303

Patrick, Bryan H.
U. K. Atomic Energy Authority
Harwell, Didcot
Oxon. OX11 ORA
ENGLAND

Paulsen, A.
CEC, CBNM Euratom
Steenweg naar Retie
B-2440 Geel
BELGIUM

Peelle, Robert W.
Oak Ridge National Laboratory
Building 6010
Oak Ridge, Tennessee 37830

Perey, F. G.
Oak Ridge National Laboratory
P. O. Box X
Oak Ridge, Tennessee 37830

Peters, Gerald J.
Naval Surface Weapons Center
White Oak Laboratory
Code WR41, Building 2-013
Silver Spring, Maryland 20910

Phillips, Leigh F.
Brookhaven National Laboratory
Building 535
Upton, New York 11973

Poenitz, W. P.
Argonne National Laboratory
9700 S. Cass Avenue
Argonne, Illinois 60439

Pullen, David
Dept. of Physics
University of Lowell
1 University Avenue
Lowell, Massachusetts 01854

Qazi, M. Nuruddin
Pinstech, P. O. Nilore
Rawalpindi, PAKISTAN

Quam, W. M.
E.G.&G.
P. O. Box 98
Goleta, California 93017

Rahn, Frank J.
Electric Power Research Inst.
Box 10412
Palo Alto, California 94303

Renner, Cleide
Oak Ridge National Laboratory
P. O. Box X
Oak Ridge, Tennessee 37830

Riel, Gordon K.
Naval Surface Weapons Center
Nuclear Branch
White Oak
Silver Spring, Maryland 20910

Robertson, James Craig
Dept. of Nuclear Engineering
University of Michigan
Ann Arbor, Michigan 48105

Rogers, J. W.
E.G.&G. Idaho
P. O. Box 1625
Idaho Falls, Idaho 83401

Rogosa, George L.
Division of Physical Research, J-309
U. S. Energy Research and Development
Administration
Washington, D. C. 20545

Rohrig, Norman
Brookhaven National Laboratory
Building 902B
Upton, New York 11973

Rosen, Mervine
Naval Research Lab.
Washington, D. C. 20370

Saltmarsh, M. J.
Oak Ridge National Laboratory
P. O. Box X
Oak Ridge, Tennessee 37830

Schell, Michael C.
Mid-Atlantic Neutron Ther.
6104 Breezewood Ct. # 304
Greenbelt, Maryland 20770

Schrack, Roald A.
Center for Radiation Research
National Bureau of Standards
Washington, D. C. 20234

Schwartz, Robert B.
Center for Radiation Research
National Bureau of Standards
Washington, D. C. 20234

Sekharan, K. K.
Cyclotron Institute
Texas A&M University
College Station, Texas 77840

Shapiro, Philip
Naval Research Laboratory
Code 6643
Washington, D. C. 20375

Shneiderov, Anatol
The Polycultural Inst. of America
1673 Columbia Road, N. W., Unit 309
Washington, D. C. 20009

Slater, William E.
Center for Radiation Research
National Bureau of Standards
Washington, D. C. 20234

Smith, Alan B.
Argonne National Laboratory
9700 South Cass Avenue
Argonne, Illinois 60439

Smith, Donald L.
Argonne National Laboratory
9700 South Cass Avenue
Argonne, Illinois 60439

Smith, J. Richard
E.G.&G. Idaho, INEL
Box 1625
Idaho Falls, Idaho 83401

Spiegel, Valentin
Center for Radiation Research
National Bureau of Standards
Washington, D. C. 20234

Stewart, Leona
Los Alamos Scientific Laboratory
P. O. Box 1663
Los Alamos, New Mexico 87545

Taschek, Richard F.
Los Alamos Scientific Lab.
P. O. Box 1663
Los Alamos, New Mexico 87545

Theus, Richard B.
Naval Research Lab.
Washington, D. C. 20375

Twining, Bruce
Division of Magnetic Fusion Energy
U. S. Energy Research & Dev. Admin.
Washington, D. C. 20545

Uttley, C. A.
Atomic Energy Res. Est.
Harwell
Didcot, Oxon OX11 ORA
United Kingdom

Vlasov, Mercury F.
Nuclear Data Section
International Atomic Energy
Agency
P. O. Box 590
Vienna, AUSTRIA

Wang, Joseph
Naval Surface Weapons Center
White Oak Laboratory
Code WR-Y1
White Oak
Silver Spring, Maryland 20910

Wasson, Oren A.
Center for Radiation Research
National Bureau of Standards
Washington, D. C. 20234

Wattecamps, E.
CEC, CBNM Euratom
Steenweg naar Retie
B-2440 Geel
BELGIUM

Weisbin, Charles R.
Oak Ridge National Laboratory
P. O. Box X
Oak Ridge, Tennessee 37830

Weston, Lawrence W.
Oak Ridge National Laboratory
Bldg. 6010, P. O. Box X
Oak Ridge, Tennessee 37830

Whetstone, Stanley L.
U. S. Energy Research & Dev. Admin.
MS J-309
Washington, D. C. 20545

White, Roger M.
Accelerator Laboratory
Ohio University
Athens, Ohio 45701

Yockey, Hubert P.
Army Pulse Rad. Facility
Aberdeen Proving Ground
Aberdeen, Maryland 21005

Yolken, H. Thomas
Nuclear Safeguards Meas., IBS
National Bureau of Standards
Washington, D. C. 20234

Young, Phillip G.
Los Alamos Scientific Laboratory
Los Alamos, New Mexico 87544

Zeitnitz, B.
Universität Bochum
Postfach 102148
D-4630 BOCHUM 1
WEST GERMANY

Zijp, W. L.
Netherlands Energy Dev. Agency
3 Westerduinweg
NL-PETTEN
THE NETHERLANDS

AUTHOR INDEX

ELEMENT S	A	QUANTITY	TYPE	ENERGY MIN	ENERGY MAX	DOCUMENTATION REF	VOL	PAGE	DATE	LAB	COMMENTS
H	001	DIFF ELASTIC	REVW-CONF	20+7	30+7	77NBS	47	477		HAR	UTTLEY.GRPHS,TBLS.EXPT CFD TH CALCS.
LI	006	EVALUATION	REVW-CONF	10-5	20+7	77NBS	30	477		LAS	HALE+R-MATRIX ENDFB5.GRPHS.CFD EXPTS
LI	006	TOTAL XSECT	REVW-CONF	10+0	10+7	77NBS	3	477		GEL	KNITTER.3 MEAS CFD.TOT CFD SEL GRPH.
LI	006	TOTAL XSECT	REVW-CONF	70+1	10+7	77NBS	10	477		SAC	DERRIEN+EXPTS CFD.TBL,GRPHS.REF TBL.
LI	006	ELASTIC SCAT	REVW-CONF	10+5	70+5	77NBS	3	477		GEL	KNITTER.INTEG DIFF CFD TOT CS GRPH
LI	006	ELASTIC SCAT	REVW-CONF	10+3	75+6	77NBS	10	477		SAC	DERRIEN+EXPTS CFD GRPH.REF TBL.
LI	006	DIFF ELASTIC	REVW-CONF	20+5	14+7	77NBS	3	477		GEL	KNITTER.4 MEAS CFD.ANG DIST,LEG COFS
LI	006	DIFF ELASTIC	REVW-CONF	10+3	50+6	77NBS	10	477		SAC	DERRIEN+ANG DISTR.NDG.TBL OF REFS.
LI	006	POLARIZATION	REVW-CONF	20+5	14+7	77NBS	3	477		GEL	KNITTER.ANAL,POL POWER MEAS.CFD.NDG
LI	006	POLARIZATION	REVW-CONF	20+6	50+6	77NBS	10	477		SAC	DERRIEN+ANAL PWR.NDG.TBL OF REFS.
LI	006	RES INT ABS	REVW-CONF	50-1		77NBS	128	477		RCN	ZIJP.TBL.1/E SPEC.FOR TOT HE PRODUCT
LI	006	N, TRITON	REVW-CONF	30+3	14+7	77NBS	3	477		GEL	KNITTER.INV NDG.INTEG,DIFF CS CFD.
LI	006	N, TRITON	REVW-CONF	10+0	10+5	77NBS	10	477		ORL	HARVEY+ANG ANISOTROPY.DIFF GRPHS.
LI	006	N, TRITON	REVW-CONF	25-2	18+7	77NBS	10	477		SAC	DERRIEN+INV NDG.DIRECT GRPHS.REF TBL
LI	006	N, TRITON	REVW-CONF	25-2		77NBS	128	477		RCN	ZIJP.TBL.COMPARISON OF 2200M/S CS.
LI	006	N, TRITON	REVW-CONF	10+2	10+5	77NBS	174	477		ORL	PEELLE+THR NORM TECH STUDY.TBLS,GRPH
LI	006	RESON PARAMS	EVAL-CONF	24+5	25+5	77NBS	319	477		HAR	JAMES.ALL FOR 250KEV RES CFD.TBL.
B	010	TOTAL XSECT	COMP-CONF	10+2	20+7	77NBS	67	477		GEL	WATTECAMPS.GRPHS,TBLS.TBL REFS GVN
B	010	ELASTIC SCAT	COMP-CONF	40+2	20+7	77NBS	67	477		GEL	WATTECAMPS.GRPHS,TBLS.TBL REFS GVN
B	010	DIFF ELASTIC	COMP-CONF	40+2	20+7	77NBS	67	477		GEL	WATTECAMPS.GRPHS,TBLS.TBL REFS GVN
B	010	RES INT ABS	REVW-CONF	50-1		77NBS	128	477		RCN	ZIJP.TBL.1/E SPEC.FOR TOT HE PRODUCT
B	010	N,ALPHA REAC	COMP-CONF	10+4	20+7	77NBS	67	477		GEL	WATTECAMPS.GND+1ST EXC CS GRPHS,TBLS
B	010	N,ALPHA REAC	REVW-CONF	25-2		77NBS	128	477		RCN	ZIJP.TBL.COMPARISON OF 2200M/S CS.
B	010	N,ALPHA REAC	REVW-CONF	10+2	10+5	77NBS	174	477		ORL	PEELLE+THR NORM TECH STUDY.TBLS,GRPH
C	012	TOTAL XSECT	EVAL-CONF	25-2	15+7	77NBS	93	477		BRC	LACHKAR.GRPHS,TBLS PHASE SHIFT ANAL.
C	012	DIFF ELASTIC	EVAL-CONF	50+4	15+7	77NBS	93	477		BRC	LACHKAR.GRPHS,TBLS PHASE SHIFT ANAL.
C	012	POLARIZATION	REVW-CONF	10+5	26+6	77NBS	93	477		BRC	LACHKAR.TBLS.CC,PHASE SHIFT ANAL.
C	012	N, GAMMA	REVW-CONF	25-2	20+7	77NBS	93	477		BRC	LACHKAR.THR VAL GVN.INV STUDY ALSO.
C	012	RESON PARAMS	EVAL-CONF	10+7	10+8	77NBS	319	477		HAR	JAMES.NARROW RES FOR E STANDARD GVN.
C	013	TOTAL XSECT	REVW-CONF	10+5	23+7	77NBS	93	477		BRC	LACHKAR.CS CONTRIBUTION TO NATURAL C
C	013	N, GAMMA	REVW-CONF	25-2	20+7	77NBS	93	477		BRC	LACHKAR.THR VAL GVN.INV STUDY ALSO.
O	016	RESON PARAMS	EVAL-CONF	10+6	10+7	77NBS	319	477		HAR	JAMES.NARROW RES FOR E STANDARD GVN.
NA	023	RES INT ABS	REVW-CONF	50-1		77NBS	128	477		RCN	ZIJP.TBL.AVG OVER 1/E SPECTRUM.
NA	023	N, GAMMA	REVW-CONF	25-2		77NBS	128	477		RCN	ZIJP.TBL.COMPARISON OF 2200M/S CS.
NA	023	RESON PARAMS	EVAL-CONF	10+4	10+5	77NBS	319	477		HAR	JAMES.NARROW RES FOR E STANDARD GVN.

ELEMENT S	A	QUANTITY	TYPE	ENERGY MIN	ENERGY MAX	DOCUMENTATION REF	VOL	PAGE	DATE	LAB	COMMENTS
MG	024	N, PROTON	REVW-CONF	FISS		77NBS	128	477		RCN	ZIJP.CS AVG OVER U235 FISS SPEC.CFD
AL	027	N, PROTON	REVW-CONF	FISS		77NBS	128	477		RCN	ZIJP.CS TBL.U235 FISS SPEC MDLS CFD.
AL	027	N, PROTON	REVW-CONF	FISS		77NBS	128	477		RCN	ZIJP.CS AVG OVER CF252 FISS SPEC CFD
AL	027	N,ALPHA REAC	REVW-CONF	FISS		77NBS	128	477		RCN	ZIJP.CS TBL.U235 FISS SPEC MDLS CFD.
AL	027	N,ALPHA REAC	REVW-CONF	FISS		77NBS	128	477		RCN	ZIJP.CS AVG OVER CF252 FISS SPEC CFD
AL	027	RESON PARAMS	EVAL-CONF	10+0	10+4	77NBS	319	477		HAR	JAMES.NARROW RES FOR E STANDARD GVN.
SI	028	RESON PARAMS	EVAL-CONF	10+4	10+5	77NBS	319	477		HAR	JAMES.NARROW RES FOR E STANDARD GVN.
P	031	N, PROTON	REVW-CONF	FISS		77NBS	128	477		RCN	ZIJP.CS AVG OVER U235 FISS SPEC.CFD
S	032	N, PROTON	REVW-CONF	FISS		77NBS	128	477		RCN	ZIJP.CS AVG OVER U235 FISS SPEC.CFD
S	032	RESON PARAMS	EVAL-CONF	10+4	10+6	77NBS	319	477		HAR	JAMES.NARROW RES FOR E STANDARD GVN.
SC	045	TOTAL XSECT	EXPT-CONF	40+2	22+4	77NBS	255	477		RPI	CHRIEN+LINAC.TRNS.GRPHS.CFD.
SC	045	RES INT ABS	REVW-CONF	50-1		77NBS	128	477		RCN	ZIJP.TBL.AVG OVER 1/E SPECTRUM.
SC	045	N, GAMMA	REVW-CONF	25-2		77NBS	128	477		RCN	ZIJP.TBL.COMPARISON OF 2200M/S CS.
SC	045	RESON PARAMS	EXPT-CONF	-5+3	21+4	77NBS	255	477		RPI	CHRIEN+S WAVE WN,J,WG.P WAVE G*WN.
TI		NXN REACTION	REVW-CONF	FISS		77NBS	128	477		RCN	ZIJP.TI(N,X)46SC.U235 FISS SPEC AVG.
TI		N, PROTON	REVW-CONF	FISS		77NBS	128	477		RCN	ZIJP.TI(N,X)46SC.U235 FISS SPEC AVG.
TI		N,N PROTON	REVW-CONF	FISS		77NBS	128	477		RCN	ZIJP.TI(N,X)46SC.U235 FISS SPEC AVG.
TI	046	N, PROTON	REVW-CONF	FISS		77NBS	128	477		RCN	ZIJP.CS AVG OVER CF252 FISS SPEC CFD
TI	047	N, PROTON	REVW-CONF	FISS		77NBS	128	477		RCN	ZIJP.CS AVG OVER U235 FISS SPEC.CFD
TI	047	N, PROTON	REVW-CONF	FISS		77NBS	128	477		RCN	ZIJP.CS AVG OVER CF252 FISS SPEC CFD
TI	048	N, PROTON	REVW-CONF	FISS		77NBS	128	477		RCN	ZIJP.CS AVG OVER U235 FISS SPEC.CFD
TI	048	N, PROTON	REVW-CONF	FISS		77NBS	128	477		RCN	ZIJP.CS AVG OVER CF252 FISS SPEC.CFD
MN	055	N2N REACTION	REVW-CONF	FISS		77NBS	128	477		RCN	ZIJP.CS TBL.U235 FISS SPEC MDLS CFD.
MN	055	N2N REACTION	REVW-CONF	FISS		77NBS	128	477		RCN	ZIJP.CS AVG OVER CF252 FISS SPEC.CFD
FE	054	N, PROTON	REVW-CONF	FISS		77NBS	128	477		RCN	ZIJP.CS TBL.U235 FISS SPEC MDLS CFD.
FE	054	N, PROTON	REVW-CONF	FISS		77NBS	128	477		RCN	ZIJP.CS AVG OVER U235 FISS SPEC.CFD
FE	054	N, PROTON	REVW-CONF	FISS		77NBS	128	477		RCN	ZIJP.CS AVG OVER CF252 FISS SPEC CFD
FE	056	TOTAL XSECT	EXPT-CONF	40+2	10+4	77NBS	255	477		RPI	CHRIEN+LINAC.TRNS.GRPHS.CFD.
FE	056	N, PROTON	REVW-CONF	FISS		77NBS	128	477		RCN	ZIJP.CS TBL.U235 FISS SPEC MDLS CFD.
FE	056	N, PROTON	REVW-CONF	FISS		77NBS	128	477		RCN	ZIJP.CS AVG OVER CF252 FISS SPEC CFD
FE	056	RESON PARAMS	EVAL-CONF	10+4	10+6	77NBS	319	477		HAR	JAMES.NARROW RES FOR E STANDARD GVN.
FE	058	RES INT ABS	REVW-CONF	50-1		77NBS	128	477		RCN	ZIJP.TBL.AVG OVER 1/E SPECTRUM.
FE	058	N, GAMMA	REVW-CONF	25-2		77NBS	128	477		RCN	ZIJP.TBL.COMPARISON OF 2200M/S CS.
CO	059	RES INT ABS	REVW-CONF	50-1		77NBS	128	477		RCN	ZIJP.TBL.AVG OVER 1/E SPECTRUM.
CO	059	N, GAMMA	REVW-CONF	25-2		77NBS	128	477		RCN	ZIJP.TBL.COMPARISON OF 2200M/S CS.

ELEMENT S	A	QUANTITY	TYPE	ENERGY MIN	ENERGY MAX	DOCUMENTATION REF	VOL	PAGE	DATE	LAB	COMMENTS
CO	059	N2N REACTION	REVW-CONF	FISS		77NBS	128	477		RCN	ZIJP.CS AVG OVER CF252 FISS SPEC.CFD
CO	059	N,ALPHA REAC	REVW-CONF	FISS		77NBS	128	477		RCN	ZIJP.CS TBL.U235 FISS SPEC MDLS CFD.
NI	058	N2N REACTION	REVW-CONF	FISS		77NBS	128	477		RCN	ZIJP.CS TBL.U235 FISS SPEC MDLS CFD.
NI	058	N, PROTON	REVW-CONF	FISS		77NBS	128	477		RCN	ZIJP.CS TBL.U235 FISS SPEC MDLS CFD.
NI	058	N, PROTON	REVW-CONF	FISS		77NBS	128	477		RCN	ZIJP.CS AVG OVER CF252 FISS SPEC CFD
CU	063	RES INT ABS	REVW-CONF	50-1		77NBS	128	477		RCN	ZIJP.TBL.AVG OVER 1/E SPECTRUM.
CU	063	N, GAMMA	REVW-CONF	25-2		77NBS	128	477		RCN	ZIJP.TBL.COMPARISON OF 2200M/S CS.
CU	063	N, GAMMA	REVW-CONF	FISS		77NBS	128	477		RCN	ZIJP.CS AVG OVER U235 FISS SPEC.CFD
CU	063	N2N REACTION	REVW-CONF	FISS		77NBS	128	477		RCN	ZIJP.CS AVG OVER U235 FISS SPEC.CFD.
CU	063	N2N REACTION	REVW-CONF	FISS		77NBS	128	477		RCN	ZIJP.CS AVG OVER CF252 FISS SPEC.CFD
CU	063	N,ALPHA REAC	REVW-CONF	FISS		77NBS	128	477		RCN	ZIJP.CS AVG OVER U235 FISS SPEC.CFD
ZN	064	N, PROTON	REVW-CONF	FISS		77NBS	128	477		RCN	ZIJP.CS AVG OVER U235 FISS SPEC.CFD
ZR	090	N2N REACTION	REVW-CONF	FISS		77NBS	128	477		RCN	ZIJP.CS AVG OVER U235 FISS SPEC.CFD.
NB	093	N2N REACTION	REVW-CONF	FISS		77NBS	128	477		RCN	ZIJP.CS AVG OVER U235 FISS SPEC.CFD
RH	103	TOT INELASTI	REVW-CONF	FISS		77NBS	128	477		RCN	ZIJP.CS AVG OVER U235 FISS SPEC.CFD
RH	103	TOT INELASTI	REVW-CONF	FISS		77NBS	128	477		RCN	ZIJP.CS AVG OVER CF252 FISS SPEC CFD
IN	115	TOT INELASTI	REVW-CONF	FISS		77NBS	128	477		RCN	ZIJP.CS AVG OVER U235 FISS SPEC.CFD
IN	115	TOT INELASTI	REVW-CONF	FISS		77NBS	128	477		RCN	ZIJP.CS AVG OVER CF252 FISS SPEC CFD
IN	115	RES INT ABS	REVW-CONF	50-1		77NBS	128	477		RCN	ZIJP.TBL.AVG OVER 1/E SPECTRUM.
IN	115	N, GAMMA	REVW-CONF	25-2		77NBS	128	477		RCN	ZIJP.TBL.COMPARISON OF 2200 M/S CS.
IN	115	N, GAMMA	REVW-CONF	FISS		77NBS	128	477		RCN	ZIJP.CS AVG OVER U235 FISS SPEC.CFD
IN	115	N, GAMMA	REVW-CONF	FISS		77NBS	128	477		RCN	ZIJP.CS AVG OVER CF252 FISS SPEC CFD
I	127	N2N REACTION	REVW-CONF	FISS		77NBS	128	477		RCN	ZIJP.CS TBL.U235 FISS SPEC MDLS CFD.
IR	191	RESON PARAMS	EVAL-CONF	10-1	10+0	77NBS	319	477		HAR	JAMES.NARROW RES FOR E STANDARD GVN.
AU	197	RES INT ABS	REVW-CONF	50-1		77NBS	128	477		RCN	ZIJP.TBL.AVG OVER 1/E SPECTRUM.
AU	197	N, GAMMA	REVW-CONF	25-2		77NBS	128	477		RCN	ZIJP.TBL.COMPARISON OF 2200 M/S CS.
AU	197	N, GAMMA	REVW-CONF	FISS		77NBS	128	477		RCN	ZIJP.CS AVG OVER U235 FISS SPEC.CFD
AU	197	N, GAMMA	REVW-CONF	FISS		77NBS	128	477		RCN	ZIJP.CS AVG OVER CF252 FISS SPEC CFD
AU	197	N, GAMMA	REVW-CONF	10+5	14+7	77NBS	165	477		GEL	PAULSEN.NORM.GRPHS.STANDARD STATUS.
PB	206	RESON PARAMS	EVAL-CONF	10+0	10+5	77NBS	319	477		HAR	JAMES.NARROW RES FOR E STANDARD GVN.
TH	232	N, GAMMA	REVW-CONF	25-2		77NBS	128	477		RCN	ZIJP.TBL.COMPARISON OF 2200 M/S CS.
TH	232	RES INT CAPT	REVW-CONF	50-1		77NBS	128	477		RCN	ZIJP.TBL.AVG OVER 1/E SPECTRUM.
TH	232	FISSION	REVW-CONF	FISS		77NBS	128	477		RCN	ZIJP.CS AVG OVER U235 FISS SPEC.CFD
U	233	ABSORPTION	EVAL-CONF	25-2		77NBS	170	477		IAE	LEMMEL.2200M/S VAL VS MAXW VAL.TBL.
U	233	N, GAMMA	EVAL-CONF	25-2		77NBS	170	477		IAE	LEMMEL.2200M/S VAL VS MAXW VAL.TBL.

ELEMENT S	A	QUANTITY	TYPE	ENERGY MIN	ENERGY MAX	DOCUMENTATION REF	VOL	PAGE	DATE	LAB	COMMENTS
U	233	FISSION	EVAL-CONF	25-2		77NBS	170	477		IAE	LEMMEL.2200M/S VAL VS MAXW VAL.TBL.
U	233	FISSION	EVAL-CONF	25-2		77NBS	170	477		IAE	LEMMEL.2200M/S VAL VS MAXW VAL.TBL.
U	233	FISSION	EVAL-CONF	25-2		77NBS	182	477		AUA	BOLDEMAN.RE-EVAL.TBL.RECOMMENDED VAL
U	233	FISSION	EXPT-CONF	NDG		77NBS	304	477		MHG	KNOLL.PHOTO N SOURCE TBD.NDG
U	233	ALPHA	EVAL-CONF	25-2		77NBS	170	477		IAE	LEMMEL.2200M/S VAL VS MAXW VAL.TBL.
U	233	ETA	EVAL-CONF	25-2		77NBS	170	477		IAE	LEMMEL.2200M/S VAL VS MAXW VAL.TBL.
U	233	NUBAR,(NU)	EVAL-CONF	25-2		77NBS	170	477		IAE	LEMMEL.2200M/S VAL VS MAXW VAL.TBL.
U	233	FISS YIELD	REVW-CONF	FAST		77NBS	146	477		INL	MAECK.MASS SPEC YLDS MEAS TBD
U	233	FISS YIELD	REVW-CONF	FISS		77NBS	299	477		NBS	GILLIAM.ILRR RESULTS.TBLS.
U	235	ABSORPTION	EVAL-CONF	25-2		77NBS	170	477		IAE	LEMMEL.2200M/S VAL VS MAXW VAL.TBL.
U	235	N, GAMMA	EVAL-CONF	25-2		77NBS	170	477		IAE	LEMMEL.2200M/S VAL VS MAXW VAL.TBL.
U	235	FISSION	REVW-CONF	25-2		77NBS	128	477		RCN	ZIJP.TBL.COMPARISON OF 2200 M/S CS.
U	235	FISSION	REVW-CONF	FISS		77NBS	128	477		RCN	ZIJP.CS AVG OVER U235 FISS SPEC.CFD
U	235	FISSION	REVW-CONF	FISS		77NBS	128	477		RCN	ZIJP.CS AVG OVER CF252 FISS SPEC CFD
U	235	FISSION	REVW-CONF	FISS		77NBS	156	477		NBS	GRUNDL+U235,CF252 FISS SPEC.TBLS.
U	235	FISSION	REVW-CONF	25-2	45+0	77NBS	174	477		ORL	PEELLE+THR NORM TECH STUDY.TBLS,GRPH
U	235	FISSION	EVAL-CONF	25-2		77NBS	182	477		AUA	BOLDEMAN.RE-EVAL.TBL.RECOMMENDED VAL
U	235	FISSION	EVAL-CONF	10+5	20+7	77NBS	261	477		ANL	POENITZ.TBL,GRPHS.MUST UPDATE ENDF5B
U	235	FISSION	REVW-CONF	FISS		77NBS	299	477		NBS	GILLIAM.CF252 SPEC AVG CS.TBL.CFD.
U	235	FISSION	REVW-CONF	FISS		77NBS	299	477		NBS	GILLIAM.REL PU239.DATA FOR 5 FIELDS
U	235	FISSION	EXPT-CONF	14+5	96+5	77NBS	304	477		MHG	KNOLL.PHOTO N SOURCE.4ES.TBL
U	235	FISSION	EXPT-CONF	FISS		77NBS	313	477		RI	ADAMOV+CF252 SPEC.TBL.ABSL CS.CFD
U	235	FISSION	EXPT-CONF	15+7		77NBS	313	477		RI	ADAMOV+ABSL CS.TBL.CFD OTH.
U	235	RES INT FISS	REVW-CONF	50-1		77NBS	128	477		RCN	ZIJP.TBL.AVG OVER 1/E SPECTRUM.
U	235	RES INT FISS	REVW-CONF	70+0	10+3	77NBS	174	477		ORL	PEELLE+2E RANGES.7-10EV,.1-1KEV.TBLS
U	235	ALPHA	EVAL-CONF	25-2		77NBS	170	477		IAE	LEMMEL.2200M/S VAL VS MAXW VAL.TBL.
U	235	ETA	EVAL-CONF	25-2		77NBS	170	477		IAE	LEMMEL.2200M/S VAL VS MAXW VAL.TBL.
U	235	NUBAR,(NU)	EVAL-CONF	25-2		77NBS	170	477		IAE	LEMMEL.2200M/S VAL VS MAXW VAL.TBL.
U	235	SPECT FISS N	REVW-CONF	10-3	10+7	77NBS	156	477		NBS	GRUNDL+DET SPEC RESPONSE.GRPHS.
U	235	SPECT FISS N	REVW-CONF	10+4	21+6	77NBS	198	477		LAS	STEWART+GRPH,TBLS.CFD WATT,MAXW SPEC
U	235	FISS YIELD	REVW-CONF	25-2		77NBS	146	477		INL	MAECK.REL YLDS MEAS IN PROGRESS.TBC
U	235	FISS YIELD	REVW-CONF	FAST		77NBS	146	477		INL	MAECK.GRPHS.MASS SPEC YLDS MEAS TBC
U	238	N, GAMMA	REVW-CONF	25-2		77NBS	128	477		RCN	ZIJP.TBL.COMPARISON OF 2200 M/S CS.
U	238	RES INT CAPT	REVW-CONF	50-1		77NBS	128	477		RCN	ZIJP.TBL.AVG OVER 1/E SPECTRUM.
U	238	FISSION	REVW-CONF	FISS		77NBS	128	477		RCN	ZIJP.CS AVG OVER U235 FISS SPEC.CFD

ELEMENT S	A	QUANTITY	TYPE	ENERGY MIN	ENERGY MAX	DOCUMENTATION REF	VOL	PAGE	DATE	LAB	COMMENTS
U	238	FISSION	REVW-CONF	FISS		77NBS	128	477		RCN	ZIJP.CS AVG OVER CF252 FISS SPEC CFD
U	238	FISSION	REVW-CONF	FISS		77NBS	156	477		NBS	GRUNDL+U235,CF252 FISS SPEC.TBLS.
U	238	FISSION	EXPT-CONF	10+5	20+7	77NBS	278	477		KFK	CIERJACKS.POSSIBLE STANDARD.DATA GVN
U	238	FISSION	REVW-CONF	FISS		77NBS	299	477		NBS	GILLIAM.CF252 SPEC AVG CS.TBL.CFD.
U	238	FISSION	REVW-CONF	FISS		77NBS	299	477		NBS	GILLIAM.REL PU239.DATA FOR 5 FIELDS
U	238	FISSION	EXPT-CONF	FISS		77NBS	313	477		RI	ADAMOV+CF252 SPEC.TBL.ABSL CS.CFD
U	238	FISSION	EXPT-CONF	15+7		77NBS	313	477		RI	ADAMOV+ABSL CS.TBL.CFD OTH.
U	238	SPECT FISS N	REVW-CONF	+6	60+6	77NBS	156	477		NBS	GRUNDL+DET SPEC RESPONSE.GRPHS.
U	238	FISS YIELD	REVW-CONF	FAST		77NBS	146	477		INL	MAECK.MASS SPEC YLDS MEAS TBD
U	238	FISS YIELD	REVW-CONF	FISS		77NBS	299	477		NBS	GILLIAM.ILRR RESULTS.TBLS.
U	238	RESON PARAMS	EVAL-CONF	10+0	10+4	77NBS	319	477		HAR	JAMES.NARROW RES FOR E STANDARD GVN.
NP	237	FISSION	REVW-CONF	FISS		77NBS	128	477		RCN	ZIJP.CS TBL.U235 FISS SPEC MDLS CFD.
NP	237	FISSION	REVW-CONF	25-2		77NBS	128	477		RCN	ZIJP.TBL.COMPARISON OF 2200 M/S CS.
NP	237	FISSION	REVW-CONF	FISS		77NBS	128	477		RCN	ZIJP.CS AVG OVER U235 FISS SPEC.CFD
NP	237	FISSION	REVW-CONF	FISS		77NBS	128	477		RCN	ZIJP.CS AVG OVER CF252 FISS SPEC CFD
NP	237	FISSION	REVW-CONF	FISS		77NBS	156	477		NBS	GRUNDL+U235,CF252 FISS SPEC.TBLS.
NP	237	FISSION	EXPT-CONF	10+5	20+7	77NBS	278	477		KFK	CIERJACKS.POSSIBLE STANDARD.DATA GVN
NP	237	FISSION	REVW-CONF	FISS		77NBS	299	477		NBS	GILLIAM.CF252 SPEC AVG CS.TBL.CFD.
NP	237	FISSION	REVW-CONF	FISS		77NBS	299	477		NBS	GILLIAM.REL PU239.DATA FOR 5 FIELDS
NP	237	FISSION	EXPT-CONF	NDG		77NBS	304	477		MHG	KNOLL.PHOTO N SOURCE TBD.NDG
NP	237	FISSION	EXPT-CONF	FISS		77NBS	313	477		RI	ADAMOV+CF252 SPEC.TBL.ABSL CS.CFD
NP	237	FISSION	EXPT-CONF	15+7		77NBS	313	477		RI	ADAMOV+ABSL CS.TBL.CFD OTH.
NP	237	SPECT FISS N	REVW-CONF	+5	40+6	77NBS	156	477		NBS	GRUNDL+DET SPEC RESPONSE.GRPHS.
NP	237	FISS YIELD	REVW-CONF	FAST		77NBS	146	477		INL	MAECK.MASS SPEC YLDS MEAS TBD
PU	239	ABSORPTION	EVAL-CONF	25-2		77NBS	170	477		IAE	LEMMEL.2200M/S VAL VS MAXW VAL.TBL.
PU	239	N, GAMMA	EVAL-CONF	25-2		77NBS	170	477		IAE	LEMMEL.2200M/S VAL VS MAXW VAL.TBL.
PU	239	FISSION	REVW-CONF	25-2		77NBS	128	477		RCN	ZIJP.TBL.COMPARISON OF 2200 M/S CS.
PU	239	FISSION	REVW-CONF	FISS		77NBS	128	477		RCN	ZIJP.CS AVG OVER U235 FISS SPEC.CFD
PU	239	FISSION	REVW-CONF	FISS		77NBS	128	477		RCN	ZIJP.CS AVG OVER CF252 FISS SPEC CFD
PU	239	FISSION	REVW-CONF	FISS		77NBS	156	477		NBS	GRUNDL+U235,CF252 FISS SPEC.TBLS.
PU	239	FISSION	EVAL-CONF	25-2		77NBS	170	477		IAE	LEMMEL.2200M/S VAL VS MAXW VAL.TBL.
PU	239	FISSION	EVAL-CONF	25-2		77NBS	182	477		AUA	BOLDEMAN.RE-EVAL.TBL.RECOMMENDED VAL
PU	239	FISSION	REVW-CONF	FISS		77NBS	299	477		NBS	GILLIAM.CF252 SPEC AVG CS.TBL.CFD.
PU	239	FISSION	EXPT-CONF	14+5	96+5	77NBS	304	477		MHG	KNOLL.PHOTO N SOURCE.4ES.TBL
PU	239	RES INT FISS	REVW-CONF	50-1		77NBS	128	477		RCN	ZIJP.TBL.AVG OVER 1/E SPECTRUM.

ELEMENT S	A	QUANTITY	TYPE	ENERGY MIN	ENERGY MAX	DOCUMENTATION REF	VOL	PAGE	DATE	LAB	COMMENTS
PU	239	ALPHA	EVAL-CONF	25-2		77NBS	170	477		IAE	LEMMEL.2200M/S VAL VS MAXW VAL.TBL.
PU	239	ETA	EVAL-CONF	25-2		77NBS	170	477		IAE	LEMMEL.2200M/S VAL VS MAXW VAL.TBL.
PU	239	NUBAR,(NU)	EVAL-CONF	25-2		77NBS	170	477		IAE	LEMMEL.2200M/S VAL VS MAXW VAL.TBL.
PU	239	SPECT FISS N	REVW-CONF	10-3	30+6	77NBS	156	477		NBS	GRUNDL+DET SPEC RESPONSE.GRPHS.
PU	239	SPECT FISS N	REVW-CONF	10+4	21+6	77NBS	198	477		LAS	STEWART+GRPH,TBLS.CFD WATT,MAXW SPEC
PU	239	FISS YIELD	REVW-CONF	25-2		77NBS	146	477		INL	MAECK.REL YLDS MEAS IN PROGRESS.TBC
PU	239	FISS YIELD	REVW-CONF	FAST		77NBS	146	477		INL	MAECK.GRPHS.MASS SPEC YLDS MEAS TBC.
PU	239	FISS YIELD	REVW-CONF	FISS		77NBS	299	477		NBS	GILLIAM.ILRR RESULTS.TBLS.
PU	240	FISS YIELD	REVW-CONF	FAST		77NBS	146	477		INL	MAECK.MASS SPEC YLDS MEAS TBD.
PU	241	ABSORPTION	EVAL-CONF	25-2		77NBS	170	477		IAE	LEMMEL.2200M/S VAL VS MAXW VAL.TBL.
PU	241	N, GAMMA	EVAL-CONF	25-2		77NBS	170	477		IAE	LEMMEL.2200M/S VAL VS MAXW VAL.TBL.
PU	241	FISSION	EVAL-CONF	25-2		77NBS	170	477		IAE	LEMMEL.2200M/S VAL VS MAXW VAL.TBL.
PU	241	FISSION	EVAL-CONF	25-2		77NBS	182	477		AUA	BOLDEMAN.RE-EVAL.TBL.RECOMMENDED VAL
PU	241	ALPHA	EVAL-CONF	25-2		77NBS	170	477		IAE	LEMMEL.2200M/S VAL VS MAXW VAL.TBL.
PU	241	ETA	EVAL-CONF	25-2		77NBS	170	477		IAE	LEMMEL.2200M/S VAL VS MAXW VAL.TBL.
PU	241	NUBAR,(NU)	EVAL-CONF	25-2		77NBS	170	477		IAE	LEMMEL.2200M/S VAL VS MAXW VAL.TBL.
PU	241	FISS YIELD	REVW-CONF	FAST		77NBS	146	477		INL	MAECK.MASS SPEC YLDS MEAS TBD.
PU	242	FISS YIELD	REVW-CONF	FAST		77NBS	146	477		INL	MAECK.MASS SPEC YLDS MEAS TBD.
AM	241	FISS YIELD	REVW-CONF	FAST		77NBS	146	477		INL	MAECK.MASS SPEC YLDS MEAS TBD.
CF	252	NUBAR,(NU)	EVAL-CONF	25-2		77NBS	170	477		IAE	LEMMEL.VAL FOR 2200M/S DATA FIT.
CF	252	NUBAR,(NU)	EVAL-CONF	SPON		77NBS	182	477		AUA	BOLDEMAN.RE-EVAL.TBL.RECOMMENDED VAL
CF	252	NUBAR,(NU)	EXPT-CONF	SPON		77NBS	194	477		RI	BLINOV+PRELIM VAL GVN.MEAS TBC.
CF	252	SPECT FISS N	EXPT-CONF	SPON		77NBS	194	477		RI	BLINOV+TOF.2 DETS.GRPHS.MAXW.TBC.
CF	252	SPECT FISS N	REVW-CONF	SPON		77NBS	198	477		LAS	STEWART+GRPH.CFD WATT,MAXW SPEC.

NBS-114A (REV. 7-73)

U.S. DEPT. OF COMM. BIBLIOGRAPHIC DATA SHEET	1. PUBLICATION OR REPORT NO. NBS SP-493	2. Gov't Accession No.	3. Recipient's Accession No.

4. TITLE AND SUBTITLE

NEUTRON STANDARDS AND APPLICATIONS

Proceedings of the International Specialists Symposium on Neutron Standards and Applications, Held at the National Bureau of Standards, Gaithersburg, MD, March 28-31, 1977

5. Publication Date October 1977

6. Performing Organization Code

7. AXXXXXXX Editors:
C. D. Bowman, A. D. Carlson, H. O. Liskien and L. Stewart

8. Performing Organ. Report No.

9. PERFORMING ORGANIZATION NAME AND ADDRESS

NATIONAL BUREAU OF STANDARDS
DEPARTMENT OF COMMERCE
WASHINGTON, D.C. 20234

10. Project/Task/Work Unit No.

11. Contract/Grant No.

12. Sponsoring Organization Name and Complete Address *(Street, City, State, ZIP)*
National Bureau of Standards; Central Bureau of Nuclear Measurements; U.S. Energy Research & Development Adm.; Electric Power Research Institute (U.S.A.); American Nuclear Society; American Physical Society; Nuclear Energy Agency (Europe); International Union of Pure & Applied Physics; with the cooperation of the International Atomic Energy Agency

13. Type of Report & Period Covered

14. Sponsoring Agency Code

15. SUPPLEMENTARY NOTES

Library of Congress Catalog Card Number: 77-14317

16. ABSTRACT *(A 200-word or less factual summary of most significant information. If document includes a significant bibliography or literature survey, mention it here.)*

These proceedings contain forty-seven papers, which were presented at the International Specialists Symposium on Neutron Standards and Applications held at the National Bureau of Standards on March 28-31, 1977. The topics addressed at the Symposium include light-element cross section standards, capture and fission cross section standards, integral neutron standards, flux measuring techniques, and medical and personnel dosimetry.

17. KEY WORDS *(six to twelve entries; alphabetical order; capitalize only the first letter of the first key word unless a proper name; separated by semicolons)*

Cross section standards; dosimetry; fission; flux; measuring techniques; neutrons; standards.

18. AVAILABILITY

[X] Unlimited

[ ] For Official Distribution. Do Not Release to NTIS

[X] Order From Sup. of Doc., U.S. Government Printing Office Washington, D.C. 20402, SD Cat. No. C13.10:493

[ ] Order From National Technical Information Service (NTIS) Springfield, Virginia 22151

19. SECURITY CLASS (THIS REPORT)	21. NO. OF PAGES
UNCLASSIFIED	379
20. SECURITY CLASS (THIS PAGE)	**22. Price**
UNCLASSIFIED	$8.50

USCOMM-DC 29042-P74

☆ U.S. GOVERNMENT PRINTING OFFICE : 1977 O—246-327